

SECOND EDITION

Water Resources Engineering



Larry W. Mays

Water Resources Engineering

This page intentionally left blank

Water Resources Engineering

Second Edition

Larry W. Mays

Professor

Civil, Environmental, and Sustainable Engineering Group

School of Sustainable Engineering and the Built Environment

Arizona State University

Tempe, Arizona



WILEY

John Wiley & Sons, Inc.

VP and Publisher	Don Fowley
Acquisition Editor	Jenny Welter
Editorial Assistant	Alexandra Spicehandler
Production Manager	Janis Soo
Assistant Production Editor	Elaine S. Chew
Senior Marketing Manager	Christopher Ruel
Marketing Assistant	Diana Smith
Media Editor	Lauren Sapira
Designer	RDC Publishing Group Sdn. Bhd.
Cover Image	© Larry W. Mays

This book was set in 9.5/12 Times Roman by Thomson Digital and printed and bound by Hamilton Printing Company. The cover was printed by Hamilton Printing Company.

This book is printed on acid free paper.

Copyright © 2011, 2005 John Wiley & Sons, Inc. All rights reserved. No part of this publication may be reproduced, stored in a retrieval system or transmitted in any form or by any means, electronic, mechanical, photocopying, recording, scanning or otherwise, except as permitted under Sections 107 or 108 of the 1976 United States Copyright Act, without either the prior written permission of the Publisher, or authorization through payment of the appropriate per-copy fee to the Copyright Clearance Center, Inc. 222 Rosewood Drive, Danvers, MA 01923, website www.copyright.com. Requests to the Publisher for permission should be addressed to the Permissions Department, John Wiley & Sons, Inc., 111 River Street, Hoboken, NJ 07030-5774, (201)748-6011, fax (201)748-6008, website <http://www.wiley.com/go/permissions>.

Evaluation copies are provided to qualified academics and professionals for review purposes only, for use in their courses during the next academic year. These copies are licensed and may not be sold or transferred to a third party. Upon completion of the review period, please return the evaluation copy to Wiley. Return instructions and a free of charge return shipping label are available at www.wiley.com/go/returnlabel. Outside of the United States, please contact your local representative.

Library of Congress Cataloging in Publication Data

Mays, Larry W.
 Water resources engineering / Larry W. Mays.—2nd ed.
 p. cm.
 Includes index.
 ISBN 978-0-470-46064-1 (cloth : alk. paper)
 1. Hydraulic engineering. 2. Hydrology. I. Title.

TC145.M383 2010
 627—dc22 2010005952

Printed in the United States of America

10 9 8 7 6 5 4 3 2 1

About the Author

Larry W. Mays is Professor in the Civil, Environmental, and Sustainable Engineering Group in the School of Sustainable Engineering and the Built Environment at Arizona State University (ASU), and former chair of the Department of Civil and Environmental Engineering. Prior to ASU he was Director of the Center for Research in Water Resources at the University of Texas at Austin, where he held an Engineering Foundation–endowed professorship. A registered professional engineer in several states, and a registered professional hydrologist, he has served as a consultant to many national and international organizations.

Professor Mays has published extensively in refereed journal publications and in the proceedings of national and international conferences. He was the author of the first edition of this book and *Optimal Control of Hydrosystems* (published by Marcel Dekker), and co-author of *Applied Hydrology* and *Hydrosystems Engineering and Management* (both from McGraw-Hill) and *Groundwater Hydrology* (published by John Wiley & Sons, Inc). He was editor-in-chief of *Water Resources Handbook*, *Water Distribution Systems Handbook*, *Urban Water Supply Management Tools*, *Stormwater Collection Systems Design Handbook*, *Urban Water Supply Handbook*, *Urban Stormwater Management Tools*, *Hydraulic Design Handbook*, *Water Supply Systems Security*, and *Water Resources Sustainability*, all published by McGraw-Hill. In addition, he was editor-in-chief of *Reliability Analysis of Water Distribution Systems* and co-editor of *Computer Methods of Free Surface and Pressurized Flow* published by Kluwer Academic Publishers.

Professor Mays developed the book, *Integrated Urban Water Management: Arid and Semi-arid Regions*, published by Taylor and Francis. This book was the result of volunteer work for the United Nations UNESCO-IHP in Paris. He recently was editor of the fourth edition of *Water Transmission and Distribution*, published by the American Water Works Association.

One of his major efforts is the study of ancient water systems and the relation that these systems could have on solving our problems of water resources sustainability using the concepts of traditional knowledge, not only for the present, but the future. His most recent book is *Ancient Water Technology*, published by Springer Science and Business Media, The Netherlands.

Among his honors is a distinguished alumnus award from the Department of Civil and Engineering at the University of Illinois at Champaign-Urbana and he is a Diplomate, Water Resources Engineering of the American Academy of Water Resources Engineering. He is also a Fellow of the American Society of Civil Engineers and the International Water Resources Association. He loves the mountains where he enjoys alpine skiing, hiking, and fly-fishing. In addition he loves photographing ancient water systems around the world and gardening. Professor Mays lives in Mesa, Arizona and Pagosa Springs, Colorado.

This page intentionally left blank

Acknowledgments

Water Resources Engineering is the result of teaching classes over the past 34 years at the University of Texas at Austin and Arizona State University. So first and foremost, I would like to thank the many students that I have taught over the years. Several of my past Ph.D. students have helped me in many ways through their review of the material and help in development of the solutions manual. These former students include Drs. Aihua Tang, Guihua Li, John Nicklow, Burcu Sakarya, Kaan Tuncok, Carlos Carriaga, Bing Zhao, El Said Ahmed, and Messele Ejeta. I would like to give special thanks to Professor Y.K. Tung of the Hong Kong University of Science and Technology. He has been a long time friend and was my very first Ph.D. student at the University of Texas at Austin. Y. K. was very gracious in providing me with some of the end of chapter problems for the hydrology chapters. I would like to acknowledge Arizona State University, especially the time afforded me to pursue this book.

I would like to thank Wayne Anderson for originally having faith in me through his willingness to first publish the book and now Jenny Welter who has worked to get this edition published.

During my academic career as a professor I have received help and encouragement from so many people that it is not possible to name them all. These people represent a wide range of universities, research institutions, government agencies, and professions. To all of you I express my deepest thanks.

Water Resources Engineering has been a part of a personal journey that began years ago when I was a young boy with a love of water. This love of water resources has continued throughout my life, even in my spare time, being an avid snow skier, fly-fisherman and hiker. Books are companions along the journey of learning and I hope that you will be able to use this book in your own exploration of the field of water resources. Have a wonderful journey.

Larry W. Mays
Mesa, Arizona
Pagosa Springs, Colorado

I would like to dedicate this book to humanity and human welfare.

Preface

AUDIENCE

Water Resources Engineering can be used for the first undergraduate courses in hydraulics, hydrology, or water resources engineering and for upper level undergraduate and graduate courses in water resources engineering design. This book is also intended as a reference for practicing hydraulic engineers, civil engineers, mechanical engineers, environmental engineers, and hydrologists.

TOPICAL COVERAGE

Water resources engineering, as defined for the purposes of this book, includes both water use and water excess management. The fundamental water resources engineering processes are the hydrologic processes and the hydraulic processes. The common threads that relate to the explanation of these processes are the fundamentals of fluid mechanics using the control volume approach. The hydraulic processes include pressurized pipe flow, open-channel flow, and groundwater flow. Each of these in turn can be subdivided into various processes and types of flow. The hydrologic processes include rainfall, evaporation, infiltration, rainfall-runoff, and routing, all of which can be further subdivided into other processes. Knowledge of the hydrologic and hydraulic processes is extended to the design and analysis aspects. This book, however, does not cover the water quality management aspects of water resources engineering.

HISTORY OF WATER RESOURCES DEVELOPMENT

Water resources development has had a long history, basically beginning when humans changed from being hunters and food gatherers to developing of agriculture and settlements. This change resulted in humans harnessing water for irrigation. As humans developed, they began to invent and develop technologies, and to transport and manage water for irrigation. The first successful efforts to control the flow of water were in Egypt and Mesopotamia. Since that time humans have continuously built on the knowledge of water resources engineering. This book builds on that knowledge to present state-of-the-art concepts and practices in water resources engineering.

NEW TO THIS EDITION

The *Second Edition* provides the most up-to-date information along with a remarkable range and depth of coverage. In addition to other changes, two new chapters have been added that explore water resources sustainability and water resources management for sustainability:

Chapter 2: Water Resources Sustainability, defines water resources sustainability, discusses challenges and specific examples of water resources systems, as well as examples of water resources unsustainability.

Chapter 19: Water Resources Management for Sustainability, introduces the idea of integrated water resources management, law related to water resources, methodologies for both arid and semi-arid regions, economics, systems analysis techniques, and uncertainty and risk-reliability analysis for sustainable design.

Principles of Flow in Hydrosystems, which was previously Chapter 2 in the *First Edition*, has now been integrated with Chapter 3 in the *Second Edition*.

Homework Problems: There are over 300 new problems in the *Second Edition*, resulting in a total of over 670 end-of-chapter problems, expanding the applications to which students are exposed.

New and updated graphics and photos: Over 50 new diagrams, maps and photographs have been integrated throughout the chapters to reinforce important concepts, and support student visualization and appreciation of water resources systems and engineering.

HALLMARK FEATURES

Breadth and Depth: The text includes a breadth and depth of topics appropriate for undergraduate courses in hydraulics, hydrology, or water resources engineering, or as a comprehensive reference for practicing engineers.

Control Volume Approach: Hydrologic and hydraulic processes are explained through their relationship to the control volume approach in fluid mechanics.

Visual program: Hundreds of diagrams, maps, and photographs illustrate concepts, and reinforce the importance and applied nature of water resources engineering.

CHAPTER ORGANIZATION

Water Resources Engineering is divided into five subject areas: Water Resources Sustainability, Hydraulics, Hydrology, Engineering Analysis and Design for Water Use, and Engineering Analysis and Design for Water Excess Management.

Water resources sustainability includes: Chapter 1 which is an introduction to water resources sustainability; Chapter 2 addresses water resources sustainability; and Chapter 19 water resources management for sustainability. Chapter 11 on water withdrawals and uses, Chapter 13 on water for hydroelectric generation, and Chapter 14 on water excess management also contain material related to water resources sustainability.

Hydraulics consists of five chapters that introduce the basic processes of hydraulics: Chapter 3 presents a basic fluid mechanics review and the control volume approach for continuity, energy, and momentum; and Chapters 4, 5, and 6 cover pressurized flow, open-channel flow, and groundwater flow, respectively. Chapter 18 covers the basics of sedimentation and erosion hydraulics.

Hydrology is covered in four chapters: Chapter 7 on hydrologic processes; Chapter 8 on rainfall-runoff analysis; Chapter 9 on routing; and Chapter 10 on probability and frequency analysis.

Engineering analysis and design for water use consists of three chapters: Chapter 11 on water withdrawals and uses; Chapter 12 on water distribution systems; and Chapter 13 on water for hydroelectric generation.

Engineering analysis and design for water excess management includes four chapters: Chapter 14 on water excess management; Chapter 15 on stormwater control using storm sewers and detention; Chapter 16 on stormwater control using street and highway drainage and culverts; and Chapter 17 on the design of hydraulic structures for flood control storage systems.

COURSE SUGGESTIONS

Several first courses could be taught from this book: a first course on hydraulics, a first course on hydrology, a first course on water resources engineering analysis and design, and a first course on hydraulic design. The flowcharts on the following pages illustrate the topics and chapters that could be covered in these courses.

This is a comprehensive book covering a large number of topics that would be impossible to cover in any single course. This was done purposely because of the wide variation in the manner in which faculty teach these courses or variations of these courses. Also, to make this book more valuable to the practicing engineer or hydrologist, the selection of these topics and the extent of coverage in each chapter were considered carefully. I have attempted to include enough example problems to make the theory more applicable, more understandable, and most of all more enjoyable to the student and engineer.

Students using this book will most likely have had an introductory fluid mechanics course based on the control volume approach. Chapter 3 should serve as a review of basic fluid concepts and the control volume approach. Control volume concepts are then used in the succeeding chapters to introduce the hydrologic and hydraulic processes. Even if the student or engineer has not had an introductory course in fluid mechanics, this book can still be used, because the concepts of fluid mechanics and the control volume approach are covered.

MOTIVATION

I sincerely hope that this book will be a contribution toward the goal of better engineering in the field of water resources. I constantly remind myself of the following quote from Baba Diodum: “In the end we will conserve only what we love, we will love only what we understand, and we will understand only what we are taught.”

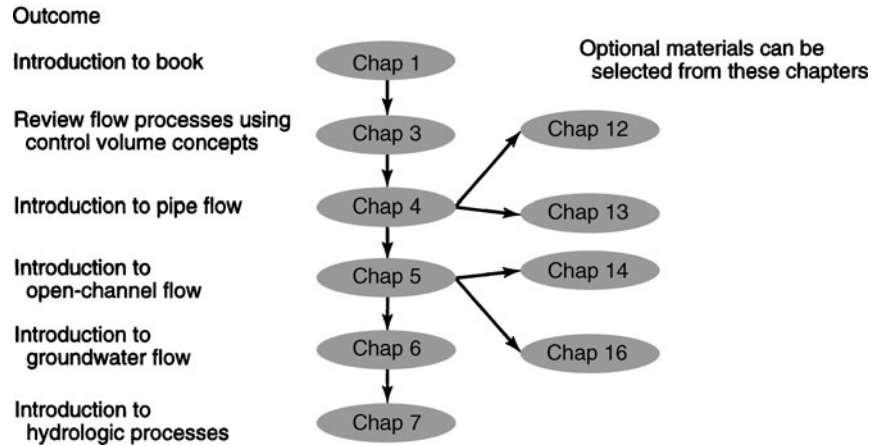
This book has been another part of a personal journey of mine that began as a young boy with an inquisitive interest and love of water, in the streams, creeks, ponds, lakes, rivers, and oceans, and water as rain and snow. Coming from a small Illinois town situated between the Mississippi and Illinois Rivers near Mark Twain’s country, I began to see and appreciate at an early age the beauty, the useful power, and the extreme destructiveness that rivers can create. I hope that this book will be of value in your journey of learning about water resources.

WEB SITE

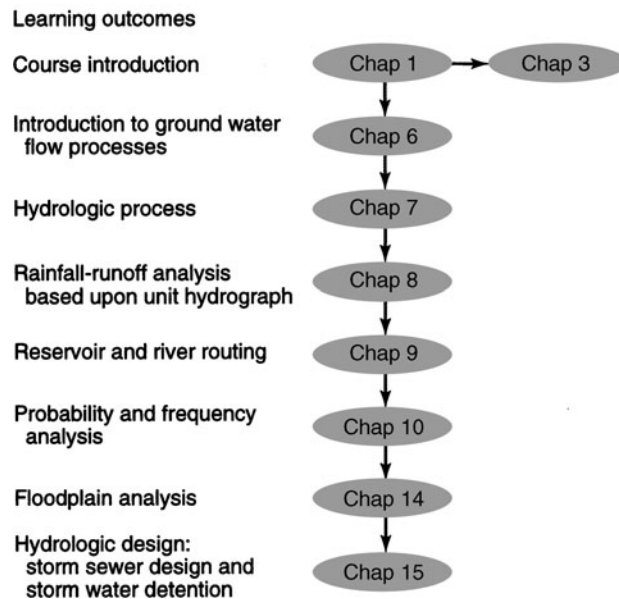
The Web site for this book is located at www.wiley.com/college/mays and includes the following resources:

- *Errata listing*: a list of any corrections that may be found in this book.
- *Figures from text*: non-copyrightable figures are available for making lecture slides or transparencies.
- *Solutions Manual for Instructors*: Includes solutions to all problems in the book. This resource is password-protected, and available only to instructors who have adopted this book for their course. Visit the Instructor Companion site portion of the Web site at www.wiley.com/college/mays to register for a password.

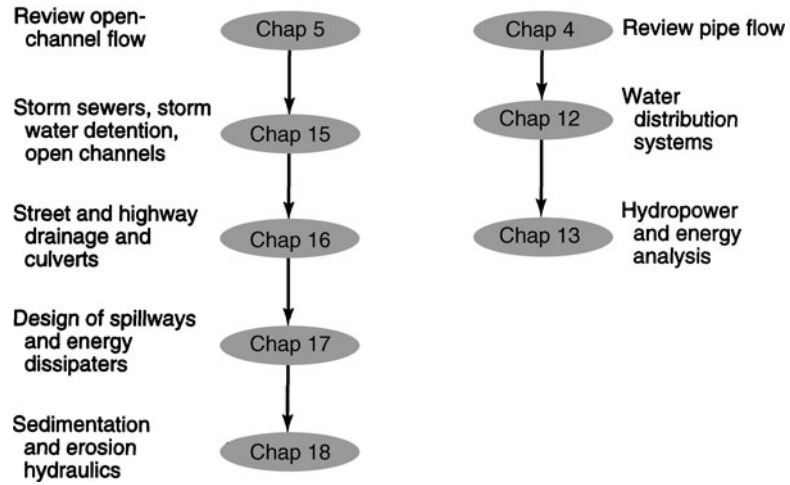
First Undergraduate Hydraulics Course



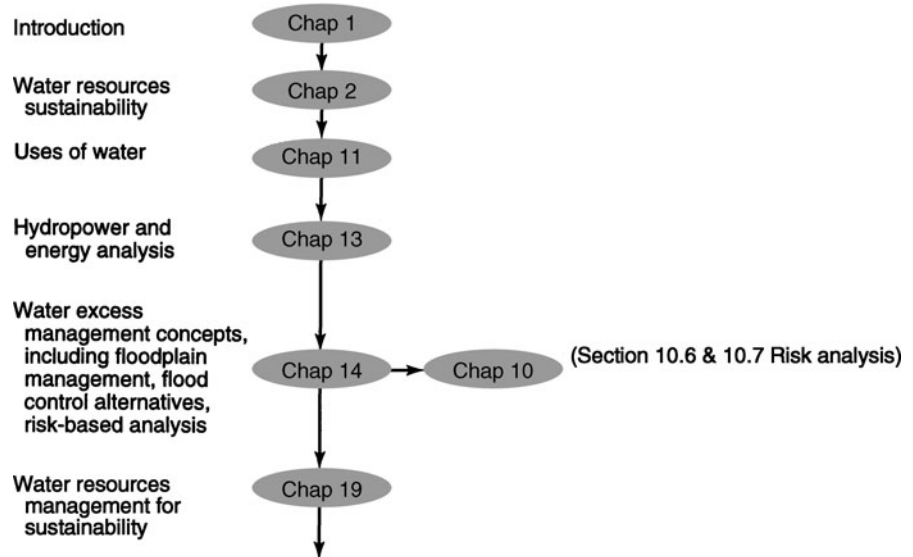
First Undergraduate Hydrology Course



Undergraduate Hydraulic Design Course



Water Resources Engineering and Sustainability



This page intentionally left blank

Brief Contents

Chapter 1	Introduction	1
1.1	Background	1
1.2	The World's Fresh Water Resources	4
1.3	Water Use in the United States	6
1.4	Systems of Units	8
1.5	The Future of Water Resources	10
Chapter 2	Water Resources Sustainability	13
2.1	What is Water Resources Sustainability?	13
2.2	Challenges to Water Resources Sustainability	16
2.3	Surface Water System – The Colorado River Basin	32
2.4	Groundwater Systems – The Edwards Aquifer, Texas	37
2.5	Water Budgets	41
2.6	Examples of Water Resources Unsustainability	47
Chapter 3	Hydraulic Processes: Flow and Hydrostatic Forces	57
3.1	Principles	57
3.2	Control Volume Approach for Hydrosystems	64
3.3	Continuity	66
3.4	Energy	68
3.5	Momentum	72
3.6	Pressure and Pressure Forces in Static Fluids	73
3.7	Velocity Distribution	78
Chapter 4	Hydraulic Processes: Pressurized Pipe Flow	83
4.1	Classification of Flow	83
4.2	Pressurized (Pipe) Flow	86
4.3	Headlosses	90
4.4	Forces in Pipe Flow	100
4.5	Pipe Flow in Simple Networks	103
Chapter 5	Hydraulic Processes: Open-Channel Flow	113
5.1	Steady Uniform Flow	113
5.2	Specific Energy, Momentum, and Specific Force	124
5.3	Steady, Gradually Varied Flow	134
5.4	Gradually Varied Flow for Natural Channels	141
5.5	Rapidly Varied Flow	152
5.6	Discharge Measurement	158
Chapter 6	Hydraulic Processes: Groundwater Flow	173
6.1	Groundwater Concepts	173
6.2	Saturated Flow	181

6.3	Steady-State One-Dimensional Flow	186
6.4	Steady-State Well Hydraulics	189
6.5	Transient Well Hydraulics—Confined Conditions	195
6.6	Transient Well Hydraulics—Unconfined Conditions	205
6.7	Transient Well Hydraulics—Leaky Aquifer Conditions	206
6.8	Boundary Effects: Image Well Theory	207
6.9	Simulation of Groundwater Systems	215
Chapter 7	Hydrologic Processes	227
7.1	Introduction to Hydrology	227
7.2	Precipitation (Rainfall)	237
7.3	Evaporation	260
7.4	Infiltration	266
Chapter 8	Surface Runoff	283
8.1	Drainage Basins and Storm Hydrographs	283
8.2	Hydrologic Losses, Rainfall Excess, and Hydrograph Components	287
8.3	Rainfall-Runoff Analysis Using Unit Hydrograph Approach	291
8.4	Synthetic Unit Hydrographs	294
8.5	S-Hydrographs	299
8.6	NRCS (SCS) Rainfall-Runoff Relation	301
8.7	Curve Number Estimation and Abstractions	303
8.8	NRCS (SCS) Unit Hydrograph Procedure	310
8.9	Kinematic-Wave Overland Flow Runoff Model	314
8.10	Computer Models for Rainfall-Runoff Analysis	320
Chapter 9	Reservoir and Stream Flow Routing	331
9.1	Routing	331
9.2	Hydrologic Reservoir Routing	332
9.3	Hydrologic River Routing	336
9.4	Hydraulic (Distributed) Routing	340
9.5	Kinematic Wave Model for Channels	346
9.6	Muskingum–Cunge Model	351
9.7	Implicit Dynamic Wave Model	352
Chapter 10	Probability, Risk, and Uncertainty Analysis for Hydrologic and Hydraulic Design	361
10.1	Probability Concepts	361
10.2	Commonly Used Probability Distributions	364
10.3	Hydrologic Design for Water Excess Management	367
10.4	Hydrologic Frequency Analysis	373
10.5	U.S. Water Resources Council Guidelines for Flood Flow Frequency Analysis	379
10.6	Analysis of Uncertainties	384
10.7	Risk Analysis: Composite Hydrologic and Hydraulic Risk	387
10.8	Computer Models for Flood Flow Frequency Analysis	393
Chapter 11	Water Withdrawals and Uses	399
11.1	Water-Use Data – Classification of Uses	399
11.2	Water for Energy Production	404
11.3	Water for Agriculture	411
11.4	Water Supply/Withdrawals	427

11.5	Water Demand and Price Elasticity	436
11.6	Drought Management	440
11.7	Analysis of Surface Water Supply	448
Chapter 12	Water Distribution	463
12.1	Introduction	463
12.2	System Components	475
12.3	System Configuration and Operation	492
12.4	Hydraulics of Simple Networks	495
12.5	Pump Systems Analysis	499
12.6	Network Simulation	514
12.7	Modeling Water Distribution Systems	525
12.8	Hydraulic Transients	527
Chapter 13	Water for Hydroelectric Generation	547
13.1	Role of Hydropower	547
13.2	Components of Hydroelectric Plants	552
13.3	Determining Energy Potential	561
Chapter 14	Flood Control	577
14.1	Introduction	577
14.2	Floodplain Management	579
14.3	Flood-Control Alternatives	585
14.4	Flood Damage and Net Benefit Estimation	595
14.5	U.S. Army Corps of Engineers Risk-Based Analysis for Flood-Damage Reduction Studies	600
14.6	Operation of Reservoir Systems for Flood Control	604
Chapter 15	Stormwater Control: Storm Sewers and Detention	611
15.1	Stormwater Management	611
15.2	Storm Systems	612
15.3	Stormwater Drainage Channels	639
15.4	Stormwater Detention	647
Chapter 16	Stormwater Control: Street and Highway Drainage and Culverts	671
16.1	Drainage of Street and Highway Pavements	671
16.2	Hydraulic Design of Culverts	693
Chapter 17	Design of Spillways and Energy Dissipation for Flood Control Storage and Conveyance Systems	713
17.1	Hydrologic Considerations	713
17.2	Dams	714
17.3	Spillways	725
17.4	Hydraulic-Jump-Type Stilling Basins and Energy Dissipators	748
Chapter 18	Sedimentation and Erosion Hydraulics	771
18.0	Introduction	771
18.1	Properties of Sediment	773
18.2	Bed Forms and Flow Resistance	781
18.3	Sediment Transport	786
18.4	Bed Load Formulas	792

18.5	Suspended Load	797
18.6	Total Sediment Load (Bed Material Load Formulas)	800
18.7	Watershed Sediment Yield	808
18.8	Reservoir Sedimentation	812
18.9	Stream Stability at Highway Structures	815
18.10	Bridge Scour	821
Chapter 19	Water Resources Management for Sustainability	827
19.1	Integrated Water Resources Management for Sustainability	827
19.2	Water Law: Surface and Groundwater Management Aspects	830
19.3	Sustainable Water Supply Methodologies for Arid and Semi-Arid Regions	836
19.4	Water Resources Economics	849
19.5	Water Resource Systems Analysis	856
19.6	Life Cycle Assessment (LCA)	862
Appendix A	Newton–Raphson Method	869
Index		873

Contents

About the Author	v	
Acknowledgments	vii	
Preface	ix	
Chapter 1	Introduction	1
1.1	Background	1
1.2	The World's Fresh Water Resources	4
1.3	Water Use in the United States	6
1.4	Systems of Units	8
1.5	The Future of Water Resources	10
Chapter 2	Water Resources Sustainability	13
2.1	What is Water Resources Sustainability?	13
2.1.1	Definition of Water Resources Sustainability	13
2.1.2	The Dublin Principles	14
2.1.3	Millennium Development Goals (MDGs)	14
2.1.4	Urbanization – A Reality of Our Changing World	15
2.2	Challenges to Water Resources Sustainability	16
2.2.1	Urbanization	16
2.2.2	Droughts and Floods	21
2.2.3	Climate Change	24
2.2.4	Consumption of Water – Virtual Water and Water Footprints	27
2.3	Surface Water System—The Colorado River Basin	32
2.3.1	The Basin	32
2.4	Groundwater Systems – The Edwards Aquifer, Texas	37
2.5	Water Budgets	41
2.5.1	What are Water Budgets?	41
2.5.2	Water Balance for Tucson, Arizona	44
2.6	Examples of Water Resources Unsustainability	47
2.6.1	Aral Sea	47
2.6.2	Mexico City	48
Chapter 3	Hydraulic Processes: Flow and Hydrostatic Forces	57
3.1	Principles	57
3.1.1	Properties Involving Mass or Weight of Water	57
3.1.2	Viscosity	57
3.1.3	Elasticity	59
3.1.4	Pressure and Pressure Variation	60
3.1.5	Surface Tension	61
3.1.6	Flow Visualization	61
3.1.7	Laminar and Turbulent Flow	62
3.1.8	Discharge	63

3.2	Control Volume Approach for Hydrosystems	64
3.3	Continuity	66
3.4	Energy	68
3.5	Momentum	72
3.6	Pressure and Pressure Forces in Static Fluids	73
	3.6.1 Hydrostatic Forces	73
	3.6.2 Buoyancy	77
3.7	Velocity Distribution	78

Chapter 4 Hydraulic Processes: Pressurized Pipe Flow 83

4.1	Classification of Flow	83
4.2	Pressurized (Pipe) Flow	86
	4.2.1 Energy Equation	86
	4.2.2 Hydraulic and Energy Grade Lines	89
4.3	Headlosses	90
	4.3.1 Shear-Stress Distribution of Flow in Pipes	90
	4.3.2 Velocity Distribution of Flow in Pipes	92
	4.3.3 Headlosses from Pipe Friction	94
	4.3.4 Form (Minor) Losses	97
4.4	Forces in Pipe Flow	100
4.5	Pipe Flow in Simple Networks	103
	4.5.1 Series Pipe Systems	103
	4.5.2 Parallel Pipe Systems	105
	4.5.3 Branching Pipe Flow	108

Chapter 5 Hydraulic Processes: Open-Channel Flow 113

5.1	Steady Uniform Flow	113
	5.1.1 Energy	113
	5.1.2 Momentum	116
	5.1.3 Best Hydraulic Sections for Uniform Flow in Nonerodible Channels	122
	5.1.4 Slope-Area Method	123
5.2	Specific Energy, Momentum, and Specific Force	124
	5.2.1 Specific Energy	124
	5.2.2 Momentum	129
	5.2.3 Specific Force	131
5.3	Steady, Gradually Varied Flow	134
	5.3.1 Gradually Varied Flow Equations	134
	5.3.2 Water Surface Profile Classification	137
	5.3.3 Direct Step Method	140
5.4	Gradually Varied Flow for Natural Channels	141
	5.4.1 Development of Equations	141
	5.4.2 Energy Correction Factor	143
	5.4.3 Application for Water Surface Profile	147
5.5	Rapidly Varied Flow	152
5.6	Discharge Measurement	158
	5.6.1 Weir	158
	5.6.2 Flumes	161
	5.6.3 Stream Flow Measurement: Velocity-Area-Integration Method	164

Chapter 6	Hydraulic Processes: Groundwater Flow	173
6.1	Groundwater Concepts	173
6.2	Saturated Flow	181
6.2.1	Governing Equations	181
6.2.2	Flow Nets	184
6.3	Steady-State One-Dimensional Flow	186
6.4	Steady-State Well Hydraulics	189
6.4.1	Flow to Wells	189
6.4.2	Confined Aquifers	191
6.4.3	Unconfined Aquifers	194
6.5	Transient Well Hydraulics—Confined Conditions	195
6.5.1	Nonequilibrium Well Pumping Equation	195
6.5.2	Graphical Solution	198
6.5.3	Cooper-Jacob Method of Solution	200
6.6	Transient Well Hydraulics—Unconfined Conditions	205
6.7	Transient Well Hydraulics—Leaky Aquifer Conditions	206
6.8	Boundary Effects: Image Well Theory	207
6.8.1	Barrier Boundary	208
6.8.2	Recharge Boundary	212
6.8.3	Multiple Boundary Systems	214
6.9	Simulation of Groundwater Systems	215
6.9.1	Governing Equations	215
6.9.2	Finite Difference Equations	216
6.9.3	MODFLOW	220
Chapter 7	Hydrologic Processes	227
7.1	Introduction to Hydrology	227
7.1.1	What Is Hydrology?	227
7.1.2	The Hydrologic Cycle	227
7.1.3	Hydrologic Systems	229
7.1.4	Atmospheric and Ocean Circulation	234
7.1.5	Hydrologic Budget	236
7.2	Precipitation (Rainfall)	237
7.2.1	Precipitation Formation and Types	237
7.2.2	Rainfall Variability	238
7.2.3	Disposal of Rainfall on a Watershed	240
7.2.4	Design Storms	241
7.2.5	Estimated Limiting Storms	257
7.3	Evaporation	260
7.3.1	Energy Balance Method	261
7.3.2	Aerodynamic Method	264
7.3.3	Combined Method	265
7.4	Infiltration	266
7.4.1	Unsaturated Flow	267
7.4.2	Green-Ampt Method	270
7.4.3	Other Infiltration Methods	276
Chapter 8	Surface Runoff	283
8.1	Drainage Basins and Storm Hydrographs	283
8.1.1	Drainage Basins and Runoff	283

8.2	Hydrologic Losses, Rainfall Excess, and Hydrograph Components	287
8.2.1	Hydrograph Components	289
8.2.2	Φ -Index Method	289
8.2.3	Rainfall-Runoff Analysis	291
8.3	Rainfall-Runoff Analysis Using Unit Hydrograph Approach	291
8.4	Synthetic Unit Hydrographs	294
8.4.1	Snyder's Synthetic Unit Hydrograph	294
8.4.2	Clark Unit Hydrograph	295
8.5	S-Hydrographs	299
8.6	NRCS (SCS) Rainfall-Runoff Relation	301
8.7	Curve Number Estimation and Abstractions	303
8.7.1	Antecedent Moisture Conditions	303
8.7.2	Soil Group Classification	304
8.7.3	Curve Numbers	307
8.8	NRCS (SCS) Unit Hydrograph Procedure	310
8.8.1	Time of Concentration	311
8.8.2	Time to Peak	313
8.8.3	Peak Discharge	313
8.9	Kinematic-Wave Overland Flow Runoff Model	314
8.10	Computer Models for Rainfall-Runoff Analysis	320
Chapter 9	Reservoir and Stream Flow Routing	331
9.1	Routing	331
9.2	Hydrologic Reservoir Routing	332
9.3	Hydrologic River Routing	336
9.4	Hydraulic (Distributed) Routing	340
9.4.1	Unsteady Flow Equations: Continuity Equation	341
9.4.2	Momentum Equation	343
9.5	Kinematic Wave Model for Channels	346
9.5.1	Kinematic Wave Equations	346
9.5.2	U.S. Army Corps of Engineers Kinematic Wave Model for Overland Flow and Channel Routing	348
9.5.3	KINEROS Channel Flow Routing Model	350
9.5.4	Kinematic Wave Celerity	350
9.6	Muskingum-Cunge Model	351
9.7	Implicit Dynamic Wave Model	352
Chapter 10	Probability, Risk, and Uncertainty Analysis for Hydrologic and Hydraulic Design	361
10.1	Probability Concepts	361
10.2	Commonly Used Probability Distributions	364
10.2.1	Normal Distribution	364
10.2.2	Log-Normal Distribution	364
10.2.3	Gumbel (Extreme Value Type I) Distribution	367
10.3	Hydrologic Design for Water Excess Management	367
10.3.1	Hydrologic Design Scale	368
10.3.2	Hydrologic Design Level (Return Period)	370
10.3.3	Hydrologic Risk	370
10.3.4	Hydrologic Data Series	371
10.4	Hydrologic Frequency Analysis	373
10.4.1	Frequency Factor Equation	373

	10.4.2 Application of Log-Pearson III Distribution	374
	10.4.3 Extreme Value Distribution	379
10.5	U.S. Water Resources Council Guidelines for Flood Flow Frequency Analysis	379
	10.5.1 Procedure	380
	10.5.2 Testing for Outliers	381
10.6	Analysis of Uncertainties	384
10.7	Risk Analysis: Composite Hydrologic and Hydraulic Risk	387
	10.7.1 Reliability Computation by Direct Integration	388
	10.7.2 Reliability Computation Using Safety Margin/Safety Factor	391
10.8	Computer Models for Flood Flow Frequency Analysis	393
Chapter 11	Water Withdrawals and Uses	399
11.1	Water-Use Data—Classification of Uses	399
11.2	Water for Energy Production	404
11.3	Water for Agriculture	411
	11.3.1 Irrigation Trends and Needs	411
	11.3.2 Irrigation Infrastructure	411
	11.3.3 Irrigation System Selection and Performance	420
	11.3.4 Water Requirements for Irrigation	424
	11.3.5 Impacts of Irrigation	427
11.4	Water Supply/Withdrawals	427
	11.4.1 Withdrawals	427
	11.4.2 Examples of Regional Water Supply Systems	432
11.5	Water Demand and Price Elasticity	436
	11.5.1 Price Elasticity of Water Demand	436
	11.5.2 Demand Models	438
11.6	Drought Management	440
	11.6.1 Drought Management Options	440
	11.6.2 Drought Severity	442
	11.6.3 Economic Aspects of Water Shortage	444
11.7	Analysis of Surface Water Supply	448
	11.7.1 Surface-Water Reservoir Systems	448
	11.7.2 Storage—Firm Yield Analysis for Water Supply	448
	11.7.3 Reservoir Simulation	457
Chapter 12	Water Distribution	463
12.1	Introduction	463
	12.1.1 Description, Purpose, and Components of Water Distribution Systems	463
	12.1.2 Pipe Flow Equations	470
12.2	System Components	475
	12.2.1 Pumps	475
	12.2.2 Pipes and Fittings	486
	12.2.3 Valves	488
12.3	System Configuration and Operation	492
12.4	Hydraulics of Simple Networks	495
	12.4.1 Series and Parallel Pipe Flow	495
	12.4.2 Branching Pipe Flow	498
12.5	Pump Systems Analysis	499
	12.5.1 System Head Curves	499

12.5.2	Pump Operating Point	500
12.5.3	System Design for Water Pumping	503
12.6	Network Simulation	514
12.6.1	Conservation Laws	514
12.6.2	Network Equations	515
12.6.3	Network Simulation: Hardy Cross Method	516
12.6.4	Network Simulation: Linear Theory Method	523
12.6.5	Extended-Period Simulation	524
12.7	Modeling Water Distribution Systems	525
12.7.1	Computer Models	525
12.7.2	Calibration	525
12.7.3	Application of Models	526
12.7.4	Water Quality Modeling	526
12.8	Hydraulic Transients	527
12.8.1	Hydraulic Transients in Distribution Systems	527
12.8.2	Fundamentals of Hydraulic Transients	528
12.8.3	Control of Hydraulic Transients	537
Chapter 13	Water for Hydroelectric Generation	547
13.1	Role of Hydropower	547
13.2	Components of Hydroelectric Plants	552
13.2.1	Elements to Generate Electricity	552
13.2.2	Hydraulics of Turbines	557
13.2.3	Power System Terms and Definitions	559
13.3	Determining Energy Potential	561
13.3.1	Hydrologic Data	561
13.3.2	Water Power Equations	561
13.3.3	Turbine Characteristics and Selection	563
13.3.4	Flow Duration Method	566
13.3.5	Sequential Streamflow-Routing Method	572
13.3.6	Power Rule Curve	573
13.3.7	Multipurpose Storage Operation	574
Chapter 14	Flood Control	577
14.1	Introduction	577
14.2	Floodplain Management	579
14.2.1	Floodplain Definition	579
14.2.2	Hydrologic and Hydraulic Analysis of Floods	579
14.2.3	Floodways and Floodway Fringes	582
14.2.4	Floodplain Management and Floodplain Regulations	583
14.2.5	National Flood Insurance Program	584
14.2.6	Stormwater Management and Floodplain Management	585
14.3	Flood-Control Alternatives	585
14.3.1	Structural Alternatives	586
14.3.2	Nonstructural Measures	593
14.4	Flood Damage and Net Benefit Estimation	595
14.4.1	Damage Relationships	595
14.4.2	Expected Damages	595
14.4.3	Risk-Based Analysis	599
14.5	U.S. Army Corps of Engineers Risk-Based Analysis for Flood-Damage Reduction Studies	600

	14.5.1 Terminology	600
	14.5.2 Benefit Evaluation	601
	14.5.3 Uncertainty of Stage-Damage Function	602
14.6	Operation of Reservoir Systems for Flood Control	604
	14.6.1 Flood-Control Operation Rules	604
	14.6.2 Tennessee Valley Authority (TVA) Reservoir System Operation	604
Chapter 15	Stormwater Control: Storm Sewers and Detention	611
15.1	Stormwater Management	611
15.2	Storm Systems	612
	15.2.1 Information Needs and Design Criteria	612
	15.2.2 Rational Method Design	613
	15.2.3 Hydraulic Analysis of Designs	621
	15.2.4 Storm Sewer Appurtenances	635
	15.2.5 Risk-Based Design of Storm Sewers	635
15.3	Stormwater Drainage Channels	639
	15.3.1 Rigid-Lined Channels	640
	15.3.2 Flexible-Lined Channels	641
	15.3.3 Manning's Roughness Factor for Vegetative Linings	646
15.4	Stormwater Detention	647
	15.4.1 Why Detention? Effects of Urbanization	647
	15.4.2 Types of Surface Detention	648
	15.4.3 Sizing Detention	650
	15.4.4 Detention Basin Routing	659
	15.4.5 Subsurface Disposal of Stormwater	660
Chapter 16	Stormwater Control: Street and Highway Drainage and Culverts	671
16.1	Drainage of Street and Highway Pavements	671
	16.1.1 Design Considerations	671
	16.1.2 Flow in Gutters	673
	16.1.3 Pavement Drainage Inlets	677
	16.1.4 Interception Capacity and Efficiency of Inlets on Grade	677
	16.1.5 Interception Capacity and Efficiency of Inlets in Sag Locations	685
	16.1.6 Inlet Locations	689
	16.1.7 Median, Embankment, and Bridge Inlets	692
16.2	Hydraulic Design of Culverts	693
	16.2.1 Culvert Hydraulics	694
	16.2.2 Culvert Design	705
Chapter 17	Design of Spillways and Energy Dissipation for Flood Control Storage and Conveyance Systems	713
17.1	Hydrologic Considerations	713
17.2	Dams	714
	17.2.1 Type of Dams	714
	17.2.2 Hazard Classification of Dams	715
	17.2.3 Spillway Capacity Criteria	717
	17.2.4 Examples of Dams and Spillways	719
17.3	Spillways	725
	17.3.1 Functions of Spillways	725
	17.3.2 Overflow and Free-Overfall (Straight Drop) Spillways	726

17.3.3	Ogee (Overflow) Spillways	728
17.3.4	Side Channel Spillways	735
17.3.5	Drop Inlet (Shaft or Morning Glory) Spillways	738
17.3.6	Baffled Chute Spillways	746
17.3.7	Culvert Spillways	748
17.4	Hydraulic-Jump-Type Stilling Basins and Energy Dissipators	748
17.4.1	Types of Hydraulic Jump Basins	748
17.4.2	Basin I	752
17.4.3	Basin II	752
17.4.4	Basin III	752
17.4.5	Basin IV	755
17.4.6	Basin V	755
17.4.7	Tailwater Considerations for Stilling Basin Design	756

Chapter 18 Sedimentation and Erosion Hydraulics 771

18.0	Introduction	771
18.1	Properties of Sediment	773
18.1.1	Size and Shape	773
18.1.2	Measurement of Size Distribution	775
18.1.3	Settling Analysis for Finer Particles	775
18.1.4	Fall Velocity	777
18.1.5	Density	781
18.1.6	Other Important Relations	781
18.2	Bed Forms and Flow Resistance	781
18.2.1	Bed Forms	781
18.2.2	Sediment Transport Definitions	782
18.2.3	Flow Resistance	784
18.3	Sediment Transport	786
18.3.1	Incipient Motion	786
18.3.2	Sediment Transport Functions	789
18.3.3	Armoring	790
18.4	Bed Load Formulas	792
18.4.1	Dubois Formula	793
18.4.2	Meyer-Peter and Muller Formula	794
18.4.3	Schoklitsch Formula	795
18.5	Suspended Load	797
18.6	Total Sediment Load (Bed Material Load Formulas)	800
18.6.1	Colby's Formula	800
18.6.2	Ackers-White Formula	803
18.6.3	Yang's Unit Stream Power Formula	805
18.7	Watershed Sediment Yield	808
18.8	Reservoir Sedimentation	812
18.9	Stream Stability at Highway Structures	815
18.9.1	Factors that Affect Stream Stability	815
18.9.2	Basic Engineering Analysis	815
18.9.3	Countermeasures (Flow Control Structure) for Stream Instability	817
18.9.4	Spurs	817
18.9.5	Guide Banks (Spur Dikes)	818
18.9.6	Check Dams (Channel Drop Structures)	820
18.10	Bridge Scour	821

Chapter 19	Water Resources Management for Sustainability	827
<hr/>		
19.1	Integrated Water Resources Management for Sustainability	827
	19.1.1 Principles of Integrated Water Resources Management (IWRM)	827
	19.1.2 Integrated Urban Water Management (IUWM): The Big Picture	828
	19.1.3 Water-Based Sustainable Regional Development	829
19.2	Water Law: Surface and Groundwater Management Aspects	830
	19.2.1 Water Law	830
	19.2.2 Surface Water Systems Management: Examples	831
	19.2.3 Groundwater Systems Management: Examples	835
19.3	Sustainable Water Supply Methodologies for Arid and Semi-Arid Regions	836
	19.3.1 Overall Subsystem Components and Interactions	836
	19.3.2 Water Reclamation and Reuse	836
	19.3.3 Managed Aquifer Recharge (MAR)	836
	19.3.4 Desalination	840
	19.3.5 Water Transfers	845
	19.3.6 Rainfall Harvesting	845
	19.3.7 Traditional Knowledge	847
19.4	Water Resources Economics	849
	19.4.1 Engineering Economic Analysis	849
	19.4.2 Benefit Cost Analysis	851
	19.4.3 Value of Water for Sustainability	854
	19.4.4 Allocation of Water to Users	855
19.5	Water Resource Systems Analysis	856
	19.5.1 Application of Optimization	856
	19.5.2 Example Applications of Optimization to Water Resources	858
	19.5.3 Decision Support Systems (DSS)	861
19.6	Life Cycle Assessment (LCA)	862
Appendix A	Newton–Raphson Method	869
<hr/>		
	Finding the Root for a Single Nonlinear Equation	869
	Application to Solve Manning’s Equation for Normal Depth	870
	Finding the Roots of a System of Nonlinear Equations	871
Index		873
<hr/>		

This page intentionally left blank

Chapter 1

Introduction

1.1 BACKGROUND

Water resources engineering (and management) as defined for the purposes of this book includes engineering for both *water supply management* and *water excess management* (see Figure 1.1.1). This book does not cover the *water quality management (or environmental restoration)* aspect of water resources engineering. The two major processes that are engineered are the *hydrologic processes* and the *hydraulic processes*. The common threads that relate to the explanation of the hydrologic and hydraulic processes are the fundamentals of fluid mechanics. The hydraulic processes include three types of flow: pipe (pressurized) flow, open-channel flow, and groundwater flow.

The broad topic of *water resources* includes areas of study in the biological sciences, engineering, physical sciences, and social sciences, as illustrated in Figure 1.1.1. Areas in the biological sciences range from ecology to zoology, those in the physical sciences range from chemistry to meteorology to physics, and those in the social sciences range from economics to sociology. Water resources engineering as used in this book focuses on the engineering aspects of hydrology and hydraulics for water supply management and water excess management.

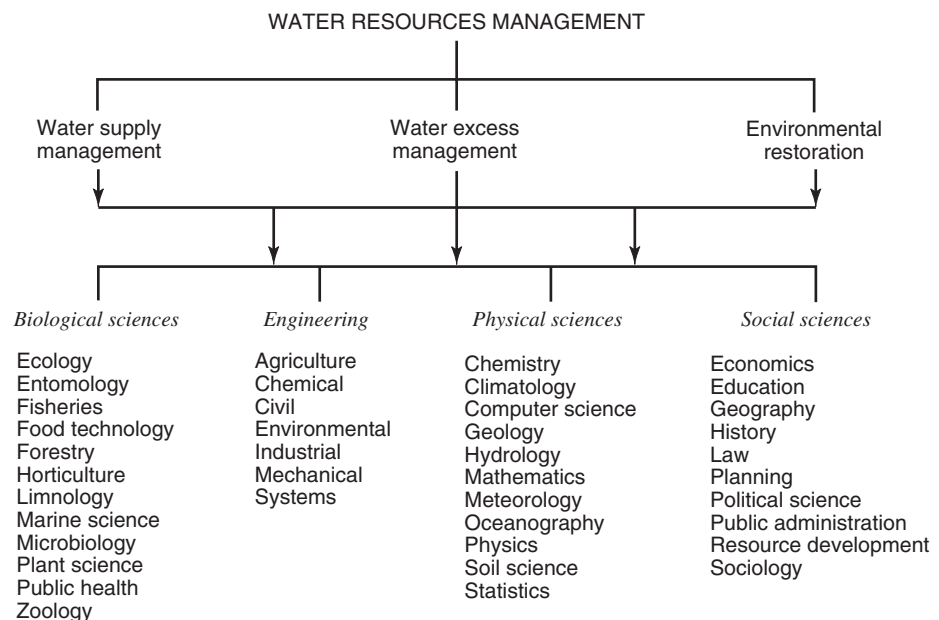


Figure 1.1.1 Ingredients of water resources management (from Mays (1996)).

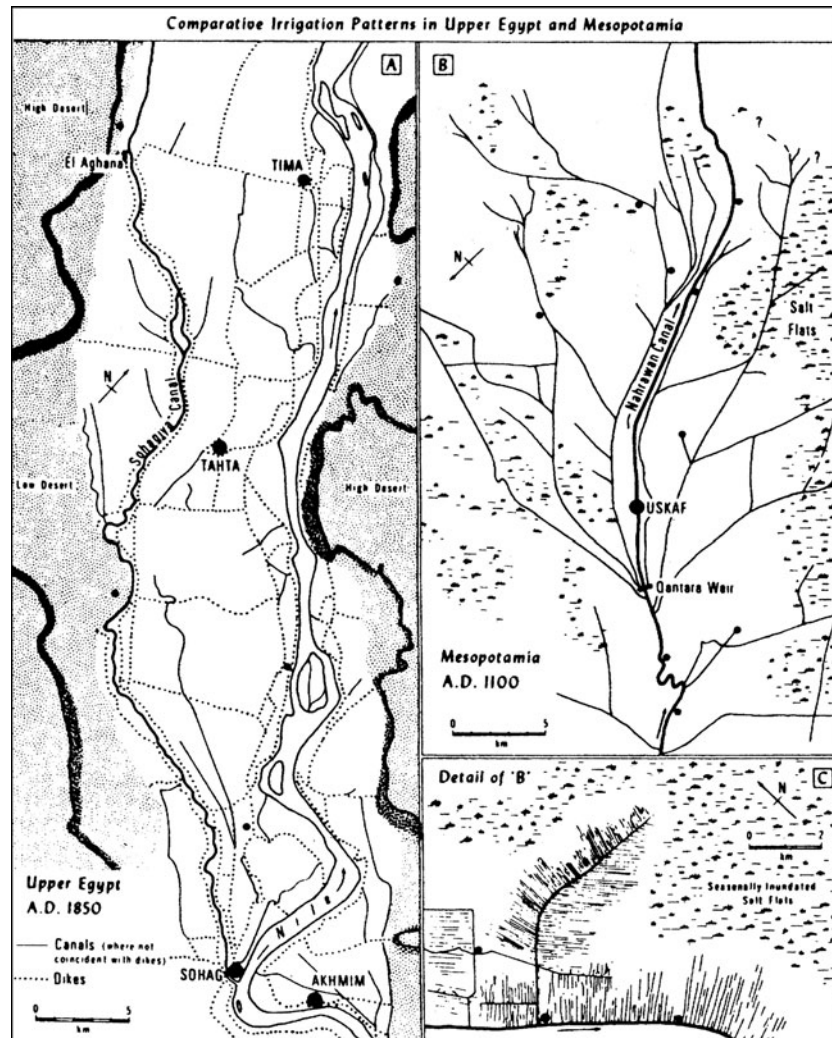


Figure 1.1.2 Comparative irrigation networks in Upper Egypt and Mesopotamia. (a) Example of linear, basin irrigation in Sohag province, ca. A.D. 1850; (b) Example of radial canalization system in the lower Nasharawan region southeast of Baghdad, Abbasid (A.D. 883–1150) (modified from R. M. Adams (1965), Fig. 9. Same scale as Egyptian counterpart); (c) Detail of field canal layout in (b) (simplified from Adams (1965), Fig. 10. Figure as presented in Butzer (1976)).

Water resources engineering not only includes the analysis and synthesis of various water problems through the use of the many analytical tools in hydrologic engineering and hydraulic engineering but also extends to the design aspects.

Water resources engineering has evolved over the past 9000 to 10,000 years as humans have developed the knowledge and techniques for building hydraulic structures to convey and store water. Early examples include irrigation networks built by the Egyptians and Mesopotamians (see Figure 1.1.2) and by the Hohokam in North America (see Figure 1.1.3). The world's oldest large dam was the Sadd-el-kafara dam built in Egypt between 2950 and 2690 B.C. The oldest known pressurized water distribution (approximately 2000 B.C.) was in the ancient city of Knossos on Crete (see Mays, 1999, 2000, for further details). There are many examples of ancient water systems throughout the world (see Mays (2007, 2008, 2010) and Mays et al. (2007)).

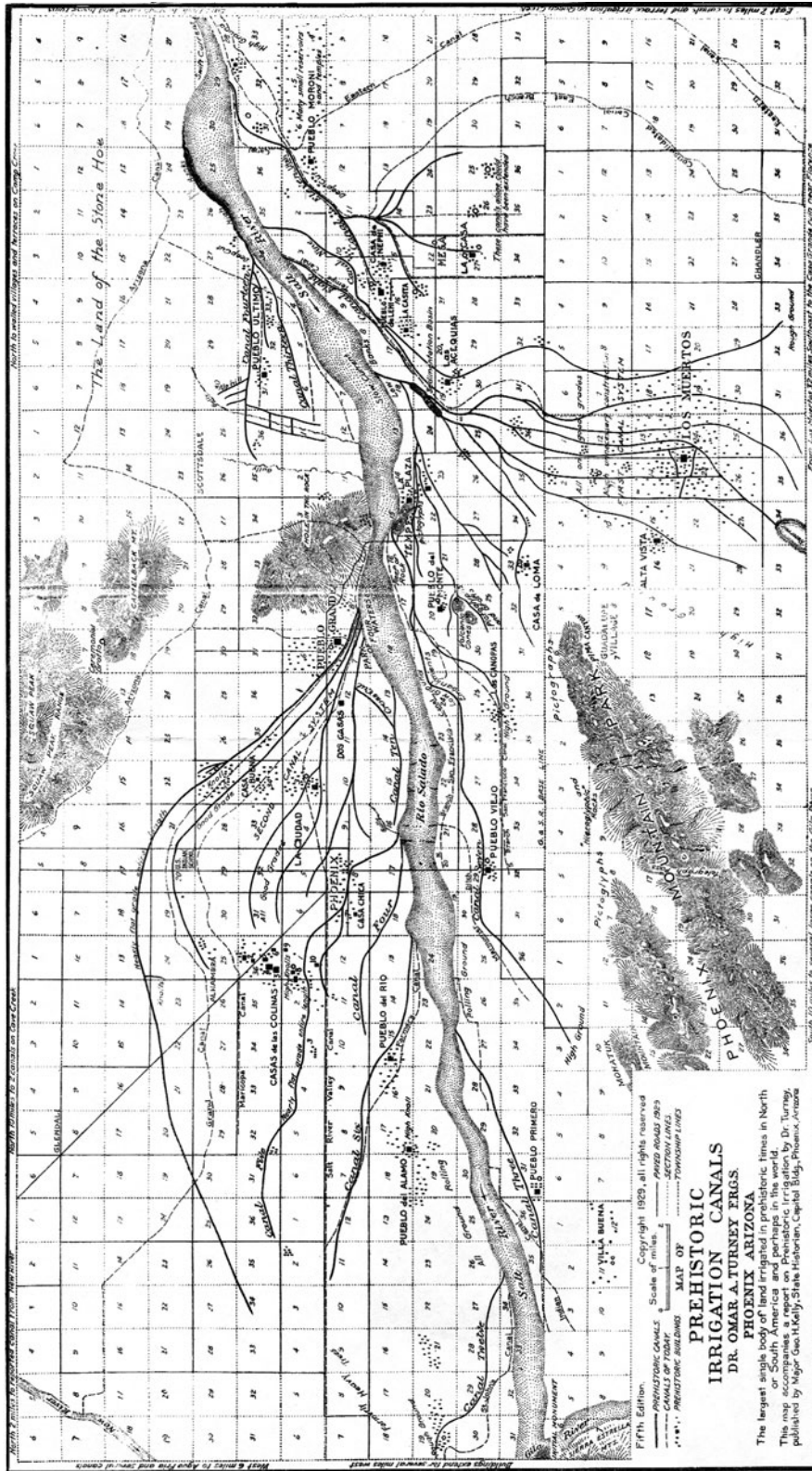


Figure 1.1.3 Canal building in the Salt River Valley with a stone hoe held in the hand without a handle. These were the original engineers, the true pioneers who built, used, and abandoned a canal system when London and Paris were clusters of wild huts (from Turney (1922)). (Courtesy of Salt River Project, Phoenix, Arizona.)

1.2 THE WORLD'S FRESHWATER RESOURCES

Among today's most acute and complex problems are water problems related to the rational use and protection of water resources (see Gleick, 1993). Associated with water problems is the need to supply humankind with adequate, clean freshwater. Data collected on global water resources by Soviet scientists are listed in Table 1.2.1. These obviously are only approximations and should not be considered as accurate (Shiklomanov, 1993). Table 1.2.2 presents the dynamics of actual water availability in different regions of the world. Table 1.2.3 presents the dynamics of water use in the world by human activity. Table 1.2.4 presents the annual runoff and water consumption by continents and by physiographic and economic regions of the world.

Table 1.2.1 Water Reserves on the Earth

	Distribution area (10^3 km ²)	Volume (10^3 km ³)	Layer (m)	Percentage of global reserves	
				Of total water	Of fresh- water
World ocean	361,300	1,338,000	3700	96.5	—
Groundwater	134,800	23,400	174	1.7	—
Freshwater		10,530	78	0.76	30.1
Soil moisture		16.5	0.2	0.001	0.05
Glaciers and permanent snow cover	16,227	24,064	1463	1.74	68.7
Antarctic	13,980	21,600	1546	1.56	61.7
Greenland	1802	2340	1298	0.17	6.68
Arctic islands	226	83.5	369	0.006	0.24
Mountainous regions	224	40.6	181	0.003	0.12
Ground ice/permafrost	21,000	300	14	0.022	0.86
Water reserves in lakes	2058.7	176.4	85.7	0.013	—
Fresh	1236.4	91	73.6	0.007	0.26
Saline	822.3	85.4	103.8	0.006	—
Swamp water	2682.6	11.47	4.28	0.0008	0.03
River flows	148,800	2.12	0.014	0.0002	0.006
Biological water	510,000	1.12	0.002	0.0001	0.003
Atmospheric water	510,000	12.9	0.025	0.001	0.04
Total water reserves	510,000	1,385,984	2718	100	—
Total freshwater reserves	148,800	35,029	235	2.53	100

Source: Shiklomanov (1993).

Table 1.2.2 Dynamics of Actual Water Availability in Different Regions of the World

Continent and region	Area (10^6 km ²)	Actual water availability (10^3 m ³ per year per capita)				
		1950	1960	1970	1980	2000
<i>Europe</i>	10.28	5.9	5.4	4.9	4.6	4.1
North	1.32	39.2	36.5	33.9	32.7	30.9
Central	1.86	3.0	2.8	2.6	2.4	2.3
South	1.76	3.8	3.5	3.1	2.8	2.5
European USSR (North)	1.82	33.8	29.2	26.3	24.1	20.9
European USSR (South)	3.52	4.4	4.0	3.6	3.2	2.4

<i>North America</i>	24.16	37.2	30.2	25.2	21.3	17.5
Canada and Alaska	13.67	384	294	246	219	189
United States	7.83	10.6	8.8	7.6	6.8	5.6
Central America	2.67	22.7	17.2	12.5	9.4	7.1
<i>Africa</i>	30.10	20.6	16.5	12.7	9.4	5.1
North	8.78	2.3	1.6	1.1	0.69	0.21
South	5.11	12.2	10.3	7.6	5.7	3.0
East	5.17	15.0	12.0	9.2	6.9	3.7
West	6.96	20.5	16.2	12.4	9.2	4.9
Central	4.08	92.7	79.5	59.1	46.0	25.4
<i>Asia</i>	44.56	9.6	7.9	6.1	5.1	3.3
North China and Mongolia	9.14	3.8	3.0	2.3	1.9	1.2
South	4.49	4.1	3.4	2.5	2.1	1.1
West	6.82	6.3	4.2	3.3	2.3	1.3
South-east	7.17	13.2	11.1	8.6	7.1	4.9
Central Asia and Kazakhstan	2.43	7.5	5.5	3.3	2.0	0.7
Siberia and Far East	14.32	124	112	102	96.2	95.3
Trans-Caucasus	0.19	8.8	6.9	5.4	4.5	3.0
<i>South America</i>	17.85	105	80.2	61.7	48.8	28.3
North	2.55	179	128	94.8	72.9	37.4
Brazil	8.51	115	86.0	64.5	50.3	32.2
West	2.33	97.9	77.1	58.6	45.8	25.7
Central	4.46	34.0	27.0	23.9	20.5	10.4
<i>Australia and Oceania</i>	8.59	112	91.3	74.6	64.0	50.0
Australia	7.62	35.7	28.4	23.0	19.8	15.0
Oceania	1.34	161	132	108	92.4	73.5

Source: Shiklomanov (1993).

Table 1.2.3 Dynamics of Water Use in the World by Human Activity

Water users ^a	1900	1940	1950	1960	1970	1975	1980		1990 ^b		2000 ^b	
	(km ³ per year)	(km ³ per year)	(km ³ per year)	(km ³ per year)	(km ³ per year)	(km ³ per year)	(km ³ per year)	(%)	(km ³ per year)	(%)	(km ³ per year)	(%)
Agriculture												
Withdrawal	525	893	1130	1550	1850	2050	2290	69.0	2680	64.9	3250	62.6
Consumption	409	679	859	1180	1400	1570	1730	88.7	2050	86.9	2500	86.2
Industry												
Withdrawal	37.2	124	178	330	540	612	710	21.4	973	23.6	1280	24.7
Consumption	3.5	9.7	14.5	24.9	38.0	47.2	61.9	3.2	88.5	3.8	117	4.0
Municipal supply												
Withdrawal	16.1	36.3	52.0	82.0	130	161	200	6.0	300	7.3	441	8.5
Consumption	4.0	9.0	14	20.3	29.2	34.3	41.1	2.1	52.4	2.2	64.5	2.2
Reservoirs												
Withdrawal	0.3	3.7	6.5	23.0	66.0	103	120	3.6	170	4.1	220	4.2
Consumption	0.3	3.7	6.5	23.0	66.0	103	120	6.2	170	7.2	220	7.6
Total (rounded off)												
Withdrawal	579	1060	1360	1990	2590	2930	3320	100	4130	100	5190	100
Consumption	417	701	894	1250	1540	1760	1950	100	2360	100	2900	100

^aTotal water withdrawal is shown in the first line of each category, consumptive use (irretrievable water loss) is shown in the second line.

^bEstimated.

Source: Shiklomanov (1993).

Table 1.2.4 Annual Runoff and Water Consumption by Continents and by Physiographic and Economic Regions of the World

Continent and region	Mean annual runoff		Aridity index (R/LP)	Water consumption (km ³ per year)					
	(mm)	(km ³ per year)		1980		1990		2000	
				Total	Irretrievable	Total	Irretrievable	Total	Irretrievable
<i>Europe</i>	310	3210	—	435	127	555	178	673	222
North	480	737	0.6	9.9	1.6	12	2.0	13	2.3
Central	380	705	0.7	141	22	176	28	205	33
South	320	564	1.4	132	51	184	64	226	73
European USSR (North)	330	601	0.7	18	2.1	24	3.4	29	5.2
European USSR (South)	150	525	1.5	134	50	159	81	200	108
<i>North America</i>	340	8200	—	663	224	724	255	796	302
Canada and Alaska	390	5300	0.8	41	8	57	11	97	15
United States	220	1700	1.5	527	155	546	171	531	194
Central America	450	1200	1.2	95	61	120	73	168	93
<i>Africa</i>	150	4570	—	168	129	232	165	317	211
North	17	154	8.1	100	79	125	97	150	112
South	68	349	2.5	23	16	36	20	63	34
East	160	809	2.2	23	18	32	23	45	28
West	190	1350	2.5	19	14	33	23	51	34
Central	470	1909	0.8	2.8	1.3	4.8	2.1	8.4	3.4
<i>Asia</i>	330	14,410	—	1910	1380	2440	1660	3140	2020
North China and Mongolia	160	1470	2.2	395	270	527	314	677	360
South	490	2200	1.3	668	518	857	638	1200	865
West	72	490	2.7	192	147	220	165	262	190
South-east	1090	6650	0.7	461	337	609	399	741	435
Central Asia and Kazakhstan	70	170	3.1	135	87	157	109	174	128
Siberia and Far East	230	3350	0.9	34	11	40	17	49	25
Trans-Caucasus	410	77	1.2	24	14	26	18	33	21
<i>South America</i>	660	11,760	—	111	71	150	86	216	116
Northern area	1230	3126	0.6	15	11	23	16	33	20
Brazil	720	6148	0.7	23	10	33	14	48	21
West	740	1714	1.3	40	30	45	32	64	44
Central	170	812	2.0	33	20	48	24	70	31
<i>Australia and Oceania</i>	270	2390	—	29	15	38	17	47	22
Australia	39	301	4.0	27	13	34	16	42	20
Oceania	1560	2090	0.6	2.4	1.5	3.3	1.8	4.5	2.3
Land area (rounded off)	—	44,500	—	3320	1450	4130	2360	5190	2900

Source: Shiklomanov (1993).

1.3 WATER USE IN THE UNITED STATES

Dziegielewski et al. (1996) define *water use* from a hydrologic perspective as all water flows that are a result of human intervention in the hydrologic cycle. The National Water Use Information Program (NWUI Program), conducted by the United States Geological Survey (USGS), used this perspective on water use in establishing a national system of water-use accounting. This accounting system distinguishes the following water-use flows: (1) water withdrawals for off-stream purposes, (2) water deliveries at point of use or quantities released after use, (3) consumptive use, (4) conveyance loss, (5) reclaimed wastewater, (6) return flow, and (7) in-stream flow (Solley et al., 1993). The relationships among these human-made flows at various points of measurement are illustrated in Figure 1.3.1. Figure 1.3.2 illustrates the estimated water use by tracking the sources, uses, and disposition of freshwater using the hydrologic accounting system given in Figure 1.3.1. Table 1.3.1 defines the major purposes of water use.

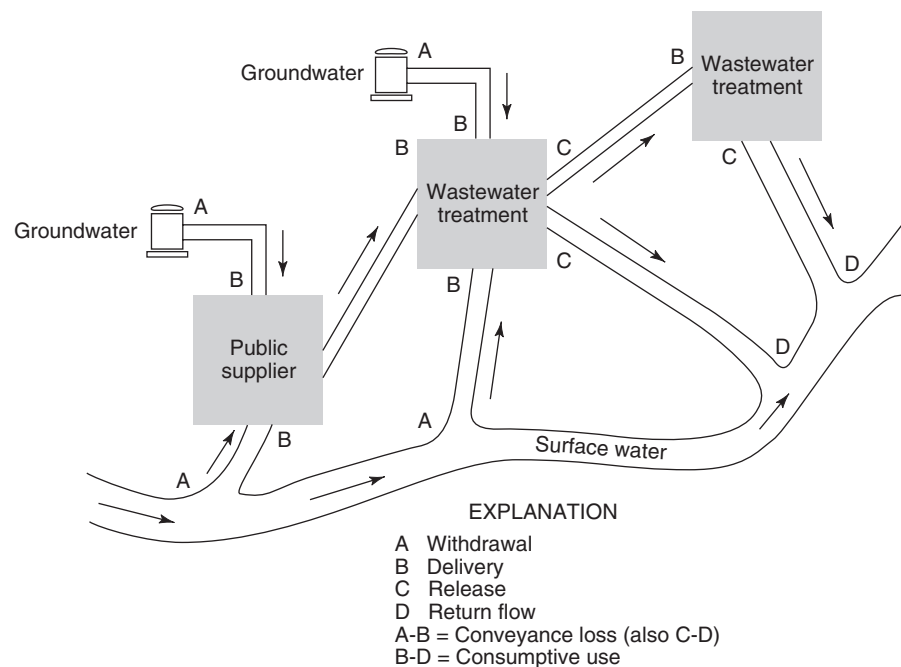


Figure 1.3.1 Definition of water-use flows and losses (from Solley et al. (1993)).

Table 1.3.1 Major Purposes of Water Use

Water-use purpose	Definition
Domestic use	Water for household needs such as drinking, food preparation, bathing, washing clothes and dishes, flushing toilets, and watering lawns and gardens (also called residential water use).
Commercial use	Water for motels, hotels, restaurants, office buildings, and other commercial facilities and institutions.
Irrigation use	Artificial application of water on lands to assist in the growing of crops and pastures or to maintain vegetative growth in recreational lands such as parks and golf courses.
Industrial use	Water for industrial purposes such as fabrication, processing, washing, and cooling.
Livestock use	Water for livestock watering, feed lots, dairy operations, fish farming, and other on-farm needs.
Mining use	Water for the extraction of minerals occurring naturally and associated with quarrying, well operations, milling, and other preparations customarily done at the mine site or as part of a mining activity.
Public use	Water supplied from a public water supply and used for such purposes as firefighting, street washing, municipal parks, and swimming pools.
Rural use	Water for suburban or farm areas for domestic and livestock needs, which is generally self-supplied.
Thermoelectric power use	Water for the process of the generation of thermoelectric power.

Source: Solley et al. (1993).

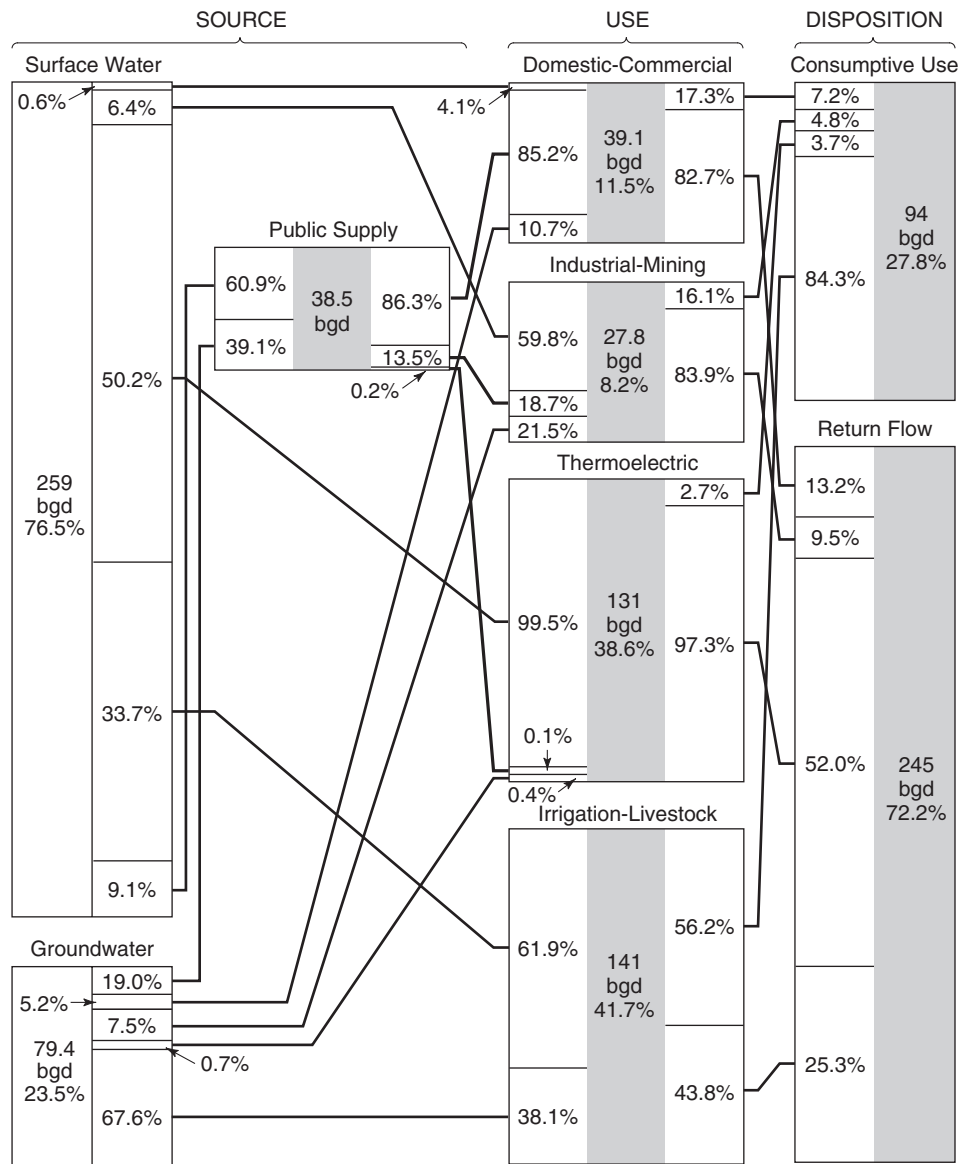


Figure 1.3.2 Estimated water use in the United States, 1990. Freshwater withdrawals and disposition of water in billion gallons per day (bgd). For each water use category, this diagram shows the relative proportion of water source and disposition and the general distribution of water from source to disposition. The lines and arrows indicate the distribution of water from source to disposition for each category; for example, surface water was 76.5 percent of total freshwater withdrawn, and, going from “Source” to “Use” columns, the line from the surface water block to the domestic and commercial block indicates that 0.6 percent of all surface water withdrawn was the source for 4.1 percent of total water (self-supplied withdrawals, public supply deliveries) for domestic and commercial purposes (from Solley et al. (1993)).

1.4 SYSTEMS OF UNITS

The analysis of pressurized (conduit) flow, open-channel flow, and groundwater flows requires an understanding of the elements of fluid mechanics (presented in Chapter 3). A review of the mechanics of materials is a prerequisite to the examination of fluid mechanics principles. Table 1.4.1

Table 1.4.1 Dimensions and SI Units for Basic Mechanical Properties

Property	SI unit	SI symbol	Dimension of unit	
			Derived	Basic
Mass	kilogram	kg		kg
Length	meter	m		m
Time	second	s		s
Area				m ²
Volume				m ³
Velocity				m/s
Acceleration				m/s ²
Force	newton	N		kg · m/s ²
Weight	newton	N		kg · m/s ²
Pressure	pascal	Pa	N/m ²	kg/m · s ²
Work	joule	J	N · m	kg · m ² /s ²
Energy	joule	J	N · m	kg · m ² /s ²
Mass density				kg/m ³
Weight density			N/m ³	kg/m ² · s ²
Stress	pascal	Pa	N/m ²	kg/m · s ²

lists the basic mechanical properties of matter with their dimensions and units in the SI system. In the United States much of the technology related to water resources engineering is still based upon the foot-pound-second (FPS) system of units, or what are referred to in this book as U.S. customary units. Table 1.4.2 provides a set of correction factors for converting U.S. customary units to SI units.

Table 1.4.2 Conversion Factors FPS (Foot-Pound-Second) System of Units to SI Units

	Multiply	By	To obtain
Length	ft	3.048×10^{-1}	m
	ft	3.048×10	cm
	ft	3.048×10^{-4}	km
	mile	1.609×10^3	m
Area	mile	1.609	km
	ft ²	9.290×10^{-2}	m ²
	mi ²	2.590	km ²
	acre	4.047×10^3	m ²
	acre	4.047×10^{-3}	km ²
Volume	ft ³	2.832×10^{-2}	m ³
	U.S. gal	3.785×10^{-3}	m ³
	U.K. gal	4.546×10^{-3}	m ³
	ft ³	2.832×10	ℓ
	U.S. gal	3.785	ℓ
	U.K. gal	4.546	ℓ
Velocity	ft/s	3.048×10^{-1}	m/s
	ft/s	3.048×10	cm/s
	mi/h	4.470×10^{-1}	m/s
	mi/h	1.609	km/h
Acceleration	ft/s ²	3.048×10^{-1}	m/s ²

(Continued)

Table 1.4.2 (Continued)

	Multiply	By	To obtain
Mass	lb _m	4.536×10^{-1}	kg
	slug	1.459×10	kg
	ton	1.016×10^3	kg
Force and weight	lb _f	4.448	N
	poundal	1.383×10^{-1}	N
Pressure and stress	psi	6.895×10^3	Pa or N/m ²
	lb _f /ft ²	4.788×10	Pa
	poundal/ft ²	1.488	Pa
	atm	1.013×10^5	Pa
	in Hg	3.386×10^3	Pa
	mb	1.000×10^2	Pa
Work and energy	ft-lbf	1.356	J
	ft-poundal	4.214×10^{-2}	J
	Btu	1.055×10^{-3}	J
	calorie	4.187	J
Mass density	lbm/ft ³	1.602×10	kg/m ³
	slug/ft ³	5.154×10^2	kg/m ³
Weight density	lb _f /ft ³	1.571×10^2	N/m ³
Discharge	ft ³ /s	2.832×10^{-2}	m ³ /s
	ft ³ /s	2.832×10	ℓ/s
	U.S. gal/min	6.309×10^{-5}	m ³ /s
	U.K. gal/min	7.576×10^{-5}	m ³ /s
	U.S. gal/min	6.309×10^{-2}	ℓ/s
	U.K. gal/min	7.576×10^{-2}	ℓ/s
Hydraulic conductivity (see also Table 2.3)	ft/s	3.048×10^{-1}	m/s
	U.S. gal/day/ft ²	4.720×10^{-7}	m/s
Transmissivity	ft ² /s	9.290×10^{-2}	m ² /s
	U.S. gal/day/ft	1.438×10^{-7}	m ² /s

1.5 THE FUTURE OF WATER RESOURCES

The management of water resources can be subdivided into three broad categories: (1) *water-supply management*, (2) *water-excess management*, and (3) *environmental restoration*. All modern multipurpose water resources projects are designed and built for water-supply management and/or water-excess management. In fact, throughout human history all water resources projects have been designed and built for one or both of these categories. A *water resources system* is a system for redistribution, in space and time, of the water available to a region to meet societal needs (Plate, 1993). Water can be utilized from surface water systems, from groundwater systems, or from conjunctive/ground surface water systems.

When discussing water resources, we must consider both the quantity and the quality aspects. The hydrologic cycle must be defined in terms of both water quantity and water quality. Because of the very complex water issues and problems that we face today, many fields of study are involved in their solution. These include the biological sciences, engineering, physical sciences, and social sciences (see Figure 1.1.1), illustrating the wide diversity of disciplines involved in water resources.

In the twenty-first century we are questioning the viability of our patterns of development, industrialization, and resources usage. We are now beginning to discuss the goals of attaining an equitable and sustainable society in the international community. Looking into the future, a new set of problems face us, including the rapidly growing population in developing countries; uncertain impacts of global climate change; possible conflicts over shared freshwater resources; thinning of

the ozone layer; destruction of rain forests; threats to wetland, farmland, and other renewable resources; and many others.

These problems are very different from those that humans have faced before. The fact that there are so many things undiscovered by the human race leads me to the statement by Sir Isaac Newton, shortly before his death in 1727:

I do not know what I may appear to the world, but to myself I seem to have been only like a boy playing on the sea shore, and diverting myself in now and then finding a smoother pebble or a prettier shell than ordinary, while the great ocean of truth lay all undiscovered before me.

REFERENCES

- Adams, R. M., *Heartland of Cities, Surveys of Ancient Settlement and Land Use in the Central Floodplain of the Euphrates*, University of Chicago Press, Chicago, 1965.
- Butzer, K. W., *Early Hydraulic Civilization in Egypt*, University of Chicago Press, Chicago, 1976.
- Dziegielewski, B., E. M. Opitz, and D. R. Maidment, "Water Demand Analysis," Chapter 23 in *Water Resources Handbook* edited by L. W. Mays, McGraw-Hill, New York, 1996.
- Gleick, P. H., *Water in Crisis*, Oxford University Press, Oxford, 1993.
- Mays, L. W., "Water Resources: An Introduction," in *Water Resources Handbook* edited by L. W. Mays McGraw-Hill, New York, 1996.
- Mays, L. W., "Introduction," in *Hydraulic Design Handbook* edited by L. W. Mays, McGraw-Hill, New York, 1999.
- Mays, L. W., "Introduction," in *Water Distribution Systems Handbook* edited by L. W. Mays, McGraw-Hill, New York, 2000.
- Mays, L. W., D. Koutsoyiannis, and A. N. Angelakis, "A Brief History of Urban Water Supply in Antiquity," *Water and Science Technology: Water Supply*, vol. 7, no. 1, pp. 1–12, IWA Publishing, 2007.
- Mays, L. W., "Water Sustainability of Ancient Civilizations in Mesoamerica and the American Southwest," *Water and Science Technology: Water Supply*, vol. 7, no. 1, pp. 229–236, IWA Publishing, 2007.
- Mays, L. W., "A Very Brief History of Hydraulic Technology during Antiquity," *Environmental Fluid Mechanics*, vol. 8, no. 5, pp. 471–484, 2008.
- Mays, L. W., (Editor-in-Chief), *Ancient Water Technology*, Springer, New York, 2010.
- Plate, E. J., "Sustainable Development of Water Resources: A Challenge to Science and Engineering," *Water International*, vol. 18, no. 2, pp. 84–94, International Water Resources Association, 1993.
- Shiklomanov, I., "World Fresh Water Resources," in *Water in Crisis* edited by P. H. Gleick, Oxford University Press, New York, 1993.
- Solley, W. B., R. R. Pierce, and H. A. Perlman, "*Estimated Use of Water in the United States in 1990*," U.S. Geological Survey Circular 1081, Washington, DC, 1993.
- Turney, O. S., Map of Prehistoric Irrigation Canals, Map No. 002004, Archaeological Site Records Office, Arizona State Museum, University of Arizona, Tucson, 1922.

This page intentionally left blank

Chapter 2

Water Resources Sustainability

2.1 WHAT IS WATER RESOURCES SUSTAINABILITY?

Traditionally, sustainability explores the relationships among economics, the environment, and social equity, using the three-legged stool analogy that includes not only the technical, but also the economic and social issues.

The term “sustainable development” was defined in 1987 by the World Commission on Environment and Development as “development that can meet the needs of the present generation without compromising the ability of future generations to meet their own needs. Some of the questions related to sustainable systems and sustainable design are:

- What are the characteristics of sustainable systems?
- How does the design process encourage sustainability?
- What is sustainable water resources development?
- What are the components of sustainable development?

2.1.1 Definition of Water Resources Sustainability

We live in a world where approximately 1.1 billion people lack safe drinking water, approximately 2.6 billion people lack adequate sanitation, and between 2 and 5 million people die annually from water-related diseases (Gleick, 2004). The United Nations Children’s Fund’s (UNICEF) report, “The State of the World’s Children 2005: Childhood under Threat,” concluded that more than half the children in the developing world are severely deprived of various necessities essential to childhood. For example, 500 million children have no access to sanitation and 400 million children have no access to safe water. One might ask how sustainable is this? The key to sustainability is the attention to the survival of future generations. Also important is the global context within which we must think and solve problems. The future of water resources thinking must be within the context of water resources sustainability.

The overall goal of water resources management for the future must be water resources sustainability. Mays (2007) defined water resources sustainability as follows:

“Water resources sustainability is the ability to use water in sufficient quantities and quality from the local to the global scale to meet the needs of humans and ecosystems for the present and the future to sustain life, and to protect humans from the damages brought about by natural and human-caused disasters that affect sustaining life.”

The Brundtland Commission's report, "Our Common Future" (World Commission on Environment and Development, WCED), defined sustainability as focusing on the needs of both current and future generations. A development is sustainable if "it meets the needs of the present without compromising the ability of future generations to meet their own needs."

Because water impacts so many aspects of our existence, there are many facets that must be considered in water resources sustainability including:

- Water resources sustainability includes the *availability of freshwater supplies* throughout periods of climatic change, extended droughts, population growth, and to leave the needed supplies for the future generations.
- Water resources sustainability includes having the *infrastructure*, to provide water supply for human consumption and food security, and to provide protection from water excess such as floods and other natural disasters.
- Water resources sustainability includes having the *infrastructure* for clean water and for treating water after it has been used by humans before being returned to water bodies.
- Water sustainability must have adequate *institutions* to provide the management for both the water supply management and water excess management.
- Water sustainability must be considered on a *local, regional, national, and international basis*.
- To achieve water resources sustainability, the principles of *integrated water resources management (IWRM)* must be implemented.

Sustainable water use has been defined by Gleick et al. (1995) as "the use of water that supports the ability of human society to endure and flourish into the indefinite future without undermining the integrity of the hydrological cycle or the ecological systems that depend on it." Seven sustainability requirements are presented in Section 11.1.

2.1.2 The Dublin Principles

The following four simple, but yet powerful messages, were provided in 1992 in Dublin and were the basis for the Rio Agenda 21 and for the millennium Vision-to-Action:

1. *Freshwater is a finite and vulnerable resource, essential to sustain life, development and the environment*, i.e. one resource, to be holistically managed.
2. *Water development and management should be based on a participatory approach, involving users, planners, and policy-makers at all levels*, i.e. manage water with people—and close to people.
3. *Women play a central role in the provision, management and safeguarding of water*, i.e. involve women all the way!
4. *Water has an economic value in all its competing uses and should be recognized as an economic good*, i.e. having ensured basic human needs, allocate water to its highest value, and move towards full cost pricing, rational use, and recover costs.

Poor water management hurts the poor most! The Dublin principles aim at wise management with focus on poverty.

2.1.3 Millennium Development Goals (MDGs)

The *Millennium Development Goals (MDGs)*, adopted in September 2000 during the Millennium Summit of the United Nations General Assembly, is comprised of eight goals (see Table 2.1.1). All of the goals can be translated directly or indirectly into water-related terms (Gleick, 2004). For example, Goal No. 1—"Eradicate extreme poverty and hunger"—and No. 7—"Ensure

Table 2.1.1 UN Millennium Development Goals and Targets for Goal 7

Goal 1 Eradicate Extreme Hunger and Poverty
Goal 2 Achieve Universal Primary Education
Goal 3 Promote Gender Equality and Empower Women
Goal 4 Reduce Child Mortality
Goal 5 Improve Maternal Health
Goal 6 Combat HIV/AIDS, Malaria, and Other Diseases
Goal 7 Ensure Environmental Sustainability
Target 9 Integrate the principles of sustainable development into country policies and programs and reverse the loss of environmental resources.
Target 10 Halve, by 2015, the proportion of people without sustainable access to safe drinking water and basic sanitation.
Target 11 Achieve by 2020 a significant improvement in the lives of at least 100 million slum dwellers.
Goal 8 Develop a Global Partnership for Development

Source: http://www.mdgmonitor.org/browse_goal.cfm

environmental sustainability” have direct relevance to water; whereas Goal No. 2—“Achieve universal primary education” and No. 3—“Promote gender equality and empower women” are water-related as millions of women and young girls spend many hours every day to fetch water. The health related Goals 4, 5, and 6 also have strong relevance to water, or the lack of it.

The MDG Goal 7, target 10 of halving, by the year 2015, the proportion of people without sustainable access (to reach or to afford) to safe drinking water seems unlikely to be met. The international community has made little progress to meet the similar part of target 10—to halve, also by 2015, the proportion of people without access to basic sanitation—adopted at the *World Summit on Sustainable Development* (WSSD), in Johannesburg in 2002 (United Nations,). An interesting fact is that this goal did not specifically emphasize wastewater treatment and disposal, because in many parts of the world wastewater treatment does not exist even though sanitation services exist and the sewage is used to irrigate agricultural crops. It is estimated that in Latin America 1.3 million hectares of agricultural land is irrigated with raw wastewater and has related health and disease issues. In countries with water shortages, the reuse of untreated wastewater will likely increase in the future.

2.1.4 Urbanization – A Reality of Our Changing World

Urban populations demand high quantities of energy and raw material, water supply, removal of wastes, transportation, etc. Urbanization creates many challenges for the development and management of water supply systems and the management of water excess from storms and floodwaters. Many urban areas of the world have been experiencing water shortages, which are expected to explode this century unless serious measures are taken to reduce the scale of this problem (Mortada, 2005). Most developing countries have not acknowledged the extent of their water problems, as evidenced by the absence of any long-term strategies for water management.

Changes Caused by Urbanization

Urbanization is a reality of our changing world. From a water resources perspective, urbanization causes many changes to the hydrological cycle including radiation flux, amount of precipitation,

amount of evaporation, amount of infiltration, increased runoff, etc. Changes brought about by urbanization can be summarized briefly as follows (Marsalek et al., 2006):

- Transformation of undeveloped land into urban land (including transportation corridors);
- Increased energy release (i.e., greenhouse gases, waste heat, heated surface runoff); and
- Increased demand on water supply (municipal and industrial).

2.2 CHALLENGES TO WATER RESOURCES SUSTAINABILITY

Urban populations are growing rapidly around the world with the addition of many mega-cities (populations of 10 million or more inhabitants). In 1975 there were only four mega-cities in the world and by 2015 there may be over 22 mega-cities in the world (Marshall, 2005). Other cities that will not become mega-cities are also growing very rapidly around the world. By 2010, more than 50% of the world's population is expected to live in urban areas (World Water Assessment Program, 2006).

Mega-cities mean mega problems of which urban water supply management and water excess management are among the largest. Mega-cities and other large cities will be a drain on the Earth's dwindling resources, while at the same time significantly contributing to the environmental degradation. Many of the large cities around the world are prone to water supply shortages, others are prone to flooding, and many are prone to both. A large number of the cities of the world do not have adequate wastewater facilities and most of the waste is improperly disposed or used as irrigation of agricultural lands. As the Earth's population continues to grow, so will the growth of cities continue across the globe, stretching resources and the ability to cope with disasters such as floods and droughts. These factors, coupled with the consequences of global warming, create many challenges for future generations.

There are many factors that affect water resources sustainability including: urbanization, droughts, climate change, flooding, and human-induced factors. Developed areas of the world such as the United States are not exempt from the need for water resources sustainability. Figure 2.2.1 shows areas in the western United States with potential water supply crisis by 2025.

2.2.1 Urbanization

The Urban Water Cycle

The overall urban water cycle is illustrated in Figure 2.2.2 showing the main components and pathways. How does the urbanization process change the water budget from predevelopment to developed conditions of the urban water cycle in arid and semi-arid regions? This change is a very complex process and very difficult to explain.

Urban Water Systems

Urban water system implies that there is a single urban water system and the reality of this is that it is an integrated whole. The concept of a single "urban water system" is not fully accepted because of the lack of integration of the various components that make up the total urban water system. For example, in municipalities it is common to plan, manage, and operate urban water into separate entities such as by service, i.e. water supply, wastewater, flood control, and stormwater. Typically there are separate water organizations and management practices within a municipality, or local or regional government because that is the way they have been historically. Grigg (1986) points out that integration could be achieved by functional integration

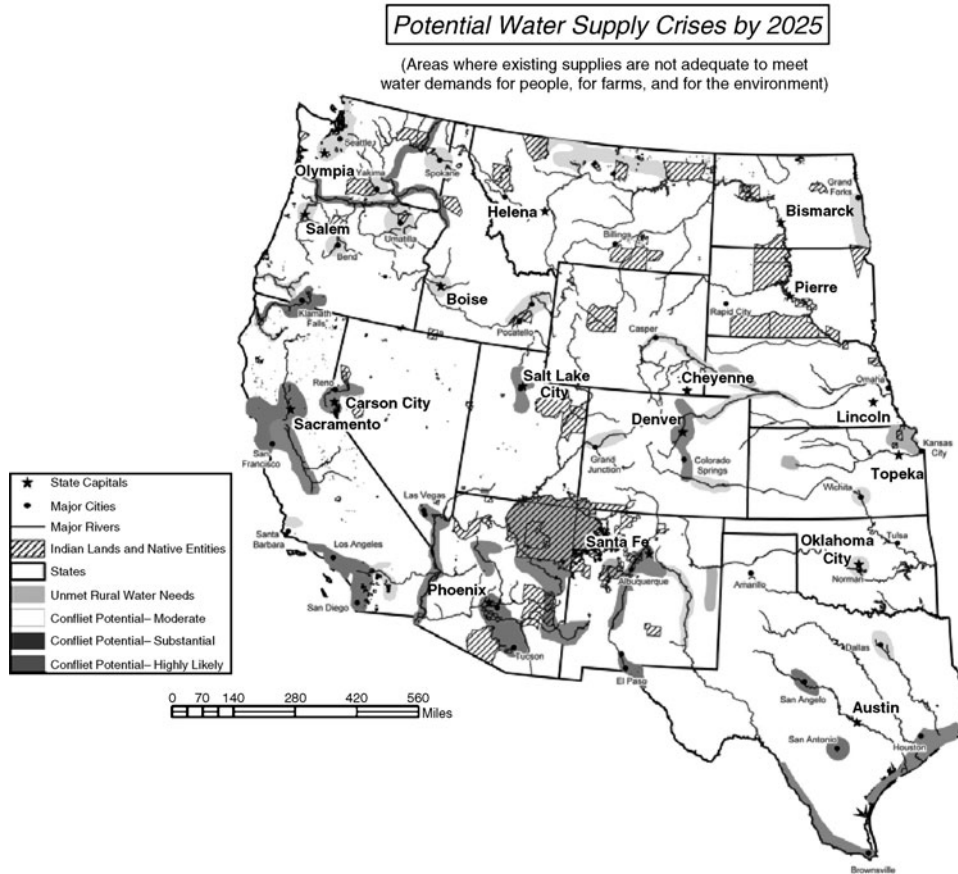


Figure 2.2.1 Areas in the western United States with potential water supply crisis by 2025. *Source:* U.S. Department of the Interior (2003).

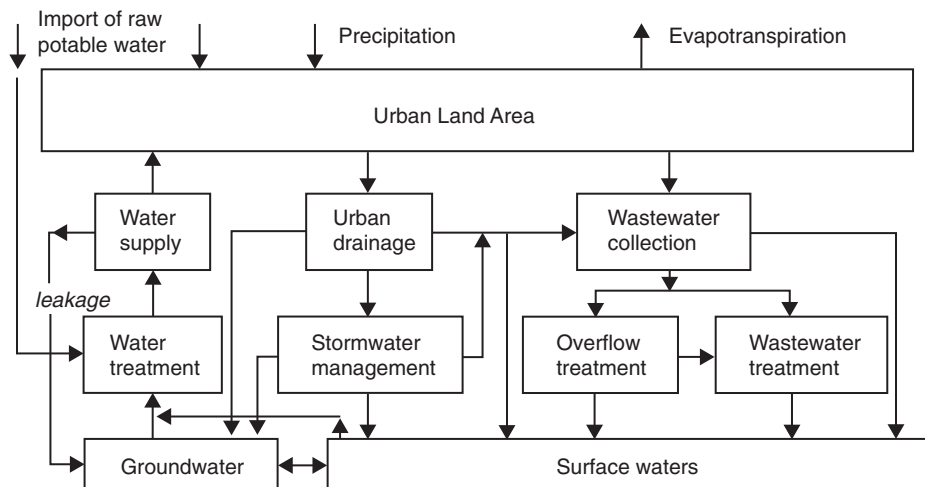


Figure 2.2.2 Urban water cycle: Main components and pathways (from Marsalek et al. (2006)).

and area-wide integration. There are many linkages of the various components of the urban water system with the hydrologic cycle being what connects the urban water system together. There are many reasons for considering the urban water system in an integrated manner. Two of the principal reasons are (a) the natural connectivity of the system through the hydrologic cycle and (b) the real benefits that are realized through integrated management rather than by independent action.

The urban water management system is considered herein as two integrated major entities, water supply management and water excess management. The various interacting components of water excess and water supply management in conventional urban water infrastructure are:

Water Supply Management

- Sources (groundwater, surface water, reuse)
- Transmission
- Water treatment (WT)
- Distribution system
- Wastewater collection
- Wastewater treatment (WWT)
- Reuse

Water Excess Management

- Collection/drainage systems
- Storage/treatment
- Flood control components (levees, dams, diversions, channels)

Sustainable Urban Water Systems

Sustainable urban water systems are being advocated because of the depletion and degradation of urban water resources coupled with the rapid increases in urban populations around the world. Marsalek et al. (2006) defined the following basic goals for sustainable urban water systems:

- Supply of safe and good-tasting drinking water to the inhabitants at all times.
- Collection and treatment of wastewater in order to protect the inhabitants from diseases and the environment from harmful impacts.
- Control, collection, transport, and quality enhancement of stormwater in order to protect the environment and urban areas from flooding and pollution.
- Reclamation, reuse, and recycling of water and nutrients for use in agriculture or households in case of water scarcity.

In North America and Europe many of the above goals have been achieved or are within reach. In many developing parts of the world these goals are far from being achieved. Climate change will be a major factor in both the developed and undeveloped parts of the world that has not been addressed for the future of water resources sustainability. The Millennium Development Goals put a strong emphasis on poverty reduction and reduced child mortality.

Urban Stormwater Runoff

Urban stormwater runoff includes all flows discharged from urban land uses into stormwater conveyance systems and receiving waters. Urban runoff includes both dry-weather, non-stormwater sources (e.g., runoff from landscape irrigation, dewatering, and water line and hydrant flushing) and wet-weather stormwater runoff. Water quality of urban stormwater runoff can be affected by the transport of sediment and other pollutants into streams, wetlands, lakes, estuarine

and marine waters, or groundwater. The costs and impacts of water pollution from urban runoff are significant and can include fish kills, health concerns of human and/or terrestrial animals, degraded drinking water, diminished water-based recreation and tourism opportunities, economic losses to commercial fishing and aquaculture industries, lowered real estate values, damage to habitat of fish and other aquatic organisms, inevitable costs of clean-up and pollution reduction, reduced aesthetic values of lakes, streams, and coastal areas, and other impacts (Leeds et al., 1993).

Increased stormwater flows from urbanization have the following major impacts (FLOW, 2003):

- acceleration of stream velocities and degradation of stream channels,
- declining water quality due to washing away of accumulated pollutants from impervious surfaces to local waterways, and an increase in siltation and erosion of soils from pervious areas subject to increased runoff,
- increase in volume of runoff with higher pollutant concentrations that reduces receiving water dilution effects,
- diminished groundwater recharge, resulting in decreased dry-weather flows; poorer water quality of streams during low flows; increased stream temperatures; and greater annual pollutant load delivery,
- increased flooding,
- combined and sanitary sewer overflows due to stormwater infiltration and inflow,
- damage to stream and aquatic life resulting from suspended solids accumulation, and increased health risks to humans from trash and debris which can also endanger, and
- destroying food sources or habitats of aquatic life (FLOW, 2003).

Groundwater Changes

Urbanization often causes changes in groundwater levels as a result of decreased recharge and increased withdrawal. In rural areas, water supplies are usually obtained from shallow wells, while most of the domestic wastewater is returned to the ground through cesspools or septic tanks. Thus the quantitative balance in the hydrologic system remains. As urbanization occurs many individual wells are abandoned for deeper public wells. With the introduction of sewer systems, stormwater, and (treated or untreated) wastewater are discharged to nearby surface water bodies. Three conditions disrupt the subsurface hydrologic balance and produce declines in groundwater levels.

1. Reduced groundwater recharge due to paved surface areas and storm sewers
2. Increased groundwater discharge by pumping wells
3. Decreased groundwater recharge due to export of wastewater collected by sanitary sewers

Groundwater quality is certainly another challenge to water resources sustainability resulting in many cases from urbanization. Groundwater quality can be affected by residential and commercial development as illustrated in Figure 2.2.3. The U.S. Geological Survey's National Water Quality Assessment (NAWQA) program (<http://water.usgs.gov/nawqa>) seeks to determine how shallow groundwater quality is affected by development (Squillace and Price, 1996). Residential developments have taken up very large tracts of land, and as a consequence, have widespread influence on the quality of water that recharges aquifers, streams, lakes, and wetlands. Liquids discharged onto the ground surface in an uncontrolled manner can migrate downward to degrade groundwater. Septic tanks and cesspools are another source of groundwater pollution. Polluted surface water bodies that contribute to groundwater recharge are sources of groundwater pollution.

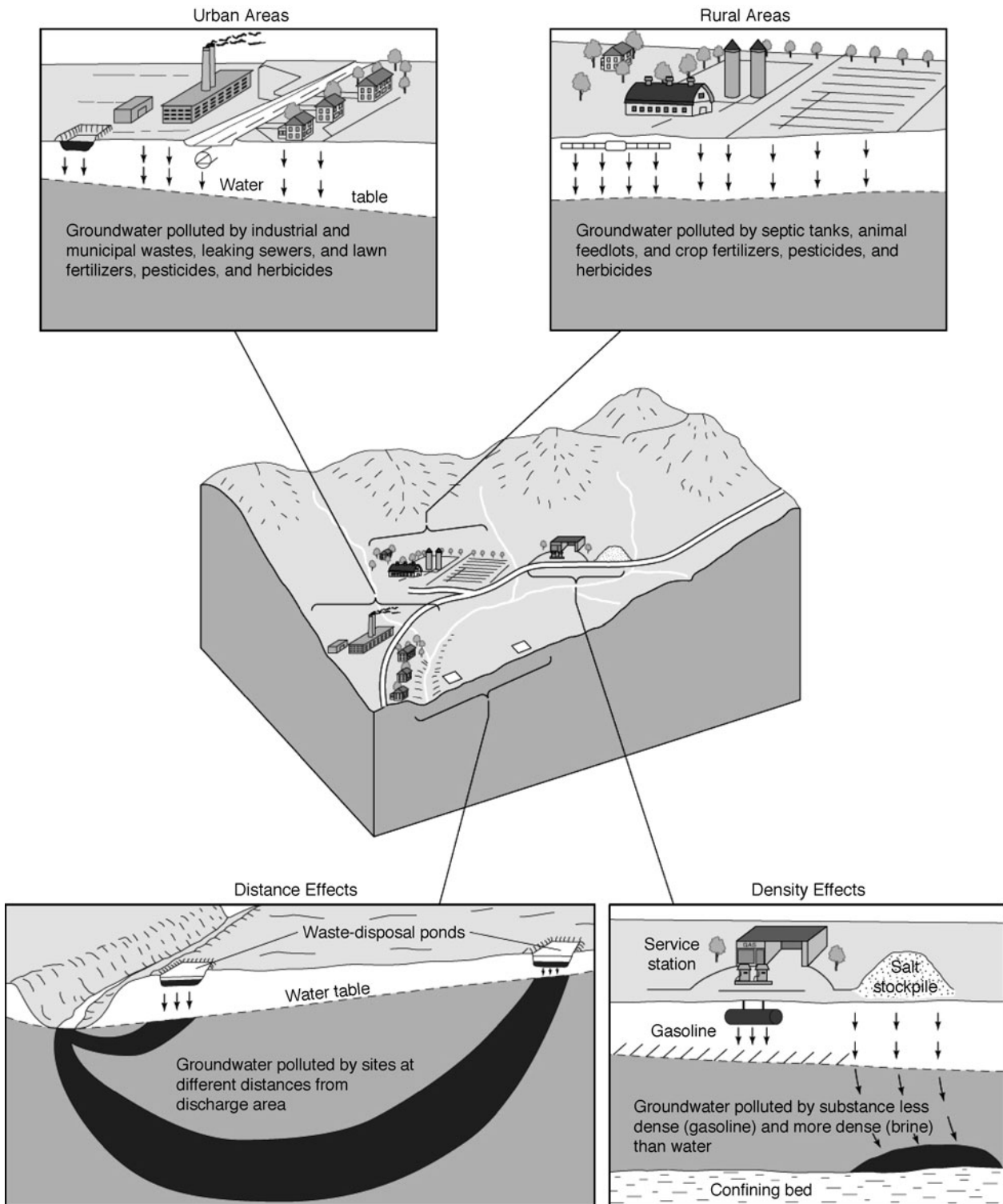


Figure 2.2.3 Groundwater pollution affected by differences in chemical composition, biological, and chemical reactions, and distance from discharge areas (from Heath, 1998).

There are many examples of urbanization effects around the world. One example is on Long Island, New York, where there was not only a decline in water tables but also groundwater pollution, seawater intrusion, and reduced streamflow.

2.2.2 Droughts and Floods

Droughts

Droughts continue to be one of the most severe weather-induced problems around the world. Droughts can be classified into different types: meteorological droughts refer to the lack of precipitation; agricultural droughts refer to the lack of soil moisture; and hydrological droughts refer to the reduced streamflow and/or groundwater levels. Figure 2.2.4 presents the progression of droughts and their impacts. Section 11.6 addresses drought management including management options, drought severity indices, and economic effects of water shortage. Figure 2.2.5 shows an example of the U.S. Drought Monitor.

The following is a definition of drought from the “Colorado River Basin Management: Evaluating and Adjusting to Hydroclimatic Variability” (from Water Science and Technology Board (2007)):

A basic concept invoked in understanding drought is that of a water budget. Water is held in storage buffers such as soil root zones, aquifers, lakes, reservoirs, and surface stream flows. These buffers act as water supplies, are subject to demands, and are replenished and lose water at varying rates. When losses exceed replenishment, impacts are experienced and, at

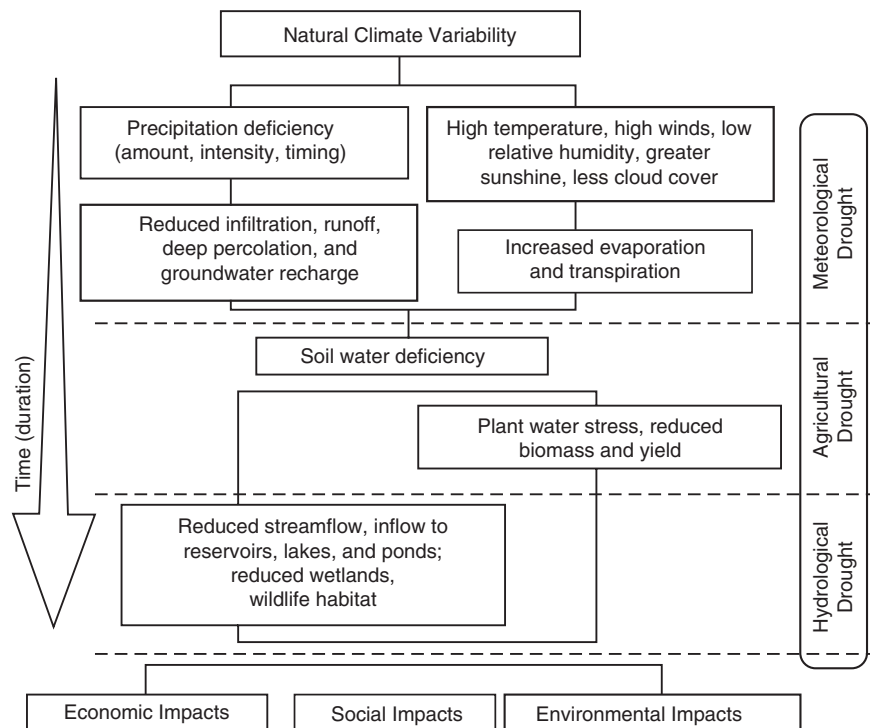


Figure 2.2.4 Progression of droughts and their impacts. (Source: National Drought Mitigation Center (<http://drought.unl.edu>))

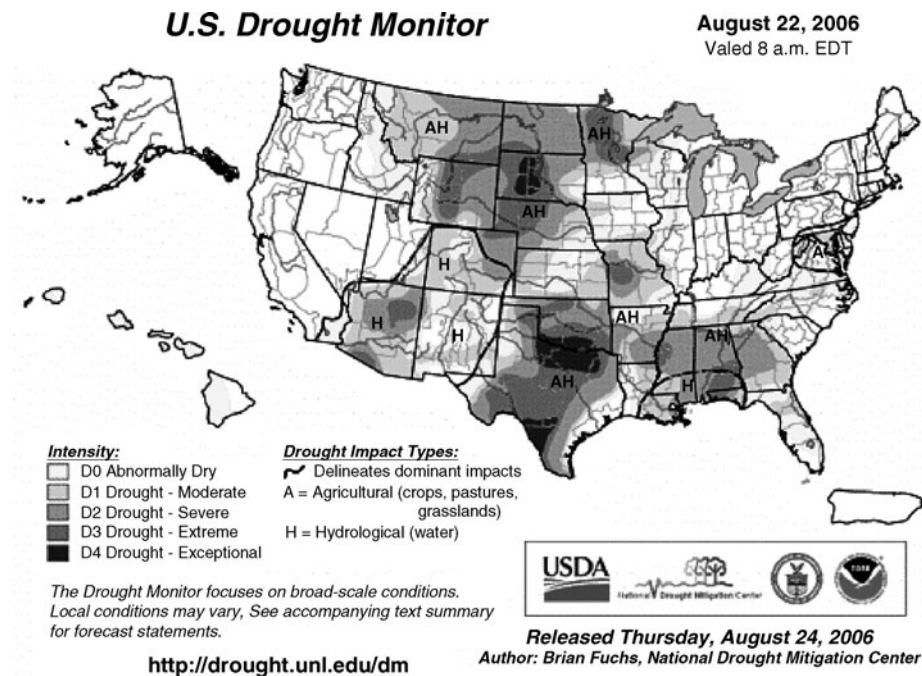


Figure 2.2.5 U.S. Drought Monitor. (Source: National Drought Mitigation Center (<http://drought.unl.edu>.)

lower storage levels, become increasingly severe. In essence, drought is defined by its impacts on both natural and manmade environments because without impacts there is no drought, no matter how dry it might be. Drought infers a relationship between supply rates and demand rates; drought is not simply a supply-side phenomenon, but also depends on water demands. Without demands, there is no drought, whether a given supply of water is big, small, or even zero.

Floods

Urban flood management (also referred to as water excess management herein) will be effected by the rapid urbanization and climate change among other factors and must be considered within the framework of water resources sustainability, which will require the principles of integrated urban water management. The impact of floods to cities can devastate national economies and industrial markets, even at the international level. Urban flood management must capture the following concepts that: (a) floods are part of the natural resources that should be considered within the scope of integrated urban water resources management (IUWRM); (b) water resources sustainability captures IUWRM; (c) and the realization that floods never can be fully controlled.

Urban flood management in developing countries is affected by development with little or no planning; high population concentration in small areas; lack of stormwater and sewage facilities; polluted air and water; difficulty of maintaining water supply with growing population; and poor public transportation among other things. The urban poor are often forced to settle in flood prone areas and they lack the adaptive capacity to cope with flood events. The unplanned urbanization and poverty are dramatically increasing the vulnerability to floods. Increase in vulnerability of cities to flood disasters arises predominantly from the systematic degradation of natural ecosystems, increased urban migration, and unplanned occupation, and unsustainable planning and building.

Urban flood disasters are not only prevalent in developing countries but have also impacted urban areas significantly in developed countries. In Europe, during the 10-year time period of 1973–1982, there were 31 flood disasters, and during the ten-year time period of 1993 to 2002, there were 179 flood disasters (Hoyois and Guha-Sapir, 2003).

The Mississippi River flooding (see photos in Figure 14.1.1) and particularly the St. Louis area (see Figure 2.2.6) are used as examples of flooding problems. The Mississippi River flood of 1993 caused major flood damage in nine Midwestern states in which 75 towns and millions of acres of

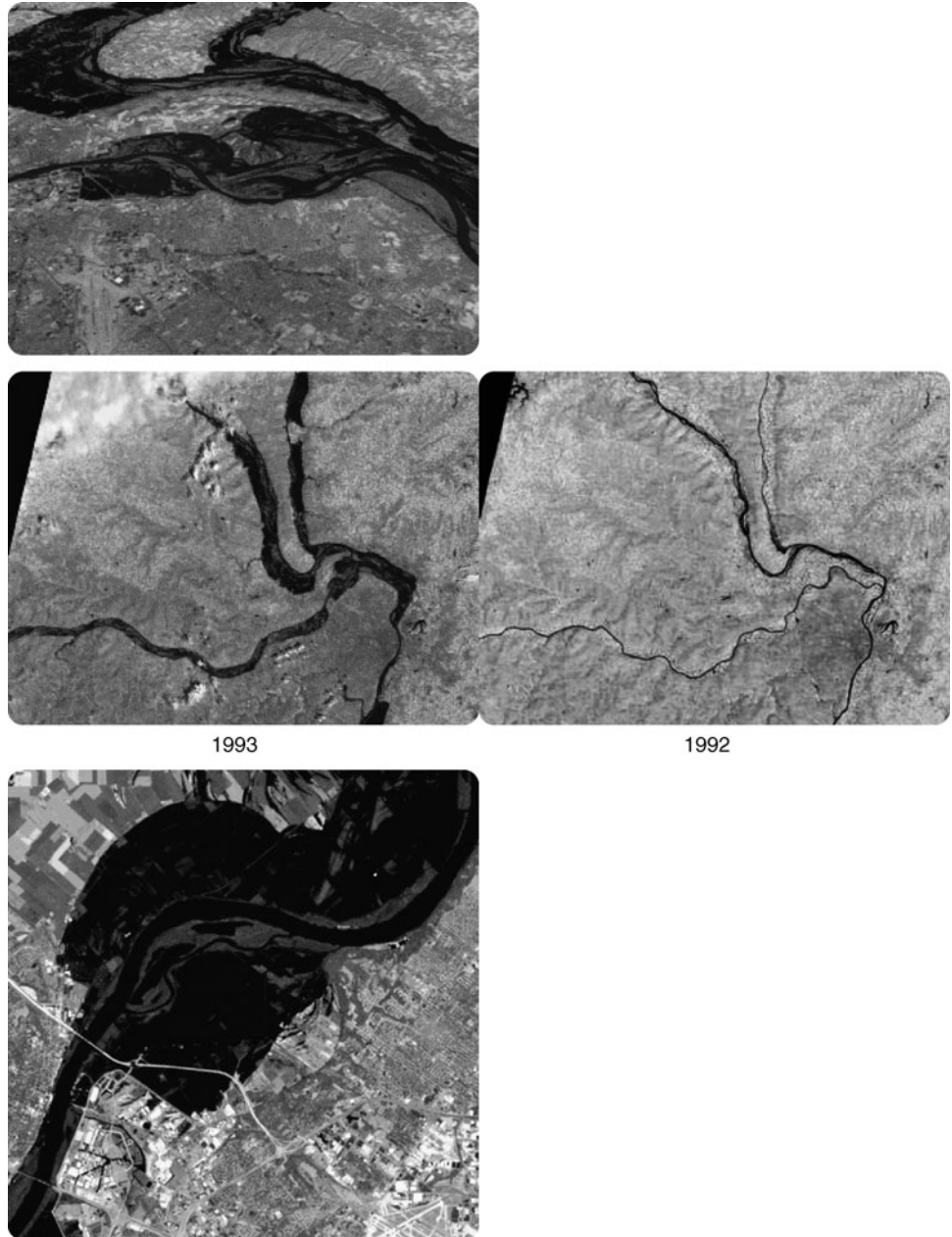


Figure 2.2.6 Mississippi River Flood of 1993 at the junctions of the Illinois and Missouri River with the Mississippi River and flooding in St. Louis, Missouri. (Courtesy of NASA.)

farmlands disappeared under the floodwaters. Approximately 50 people died, and tens of thousands of people were temporarily or permanently evacuated. Thousands of homes were completely destroyed and hundreds of flood levees failed. Flood damage estimates ranged from \$10 to \$20 billion.

Houston, Texas, is an example of poor urban flood management in a large city in a developed country. A combination of poor urban planning, poor floodplain management, poor stormwater management, and lack of integrated floodplain and stormwater management has caused billions of dollars of flood damage over the last couple of decades. Subsidence has been a factor, but minimal compared to the effects of poor floodplain and poor stormwater management in Houston. Tropical Storm Allison is one of the several examples with damage estimates of up to \$5 billion.

Hurricane Katrina in the Gulf of Mexico coastal region of the U.S. brought unprecedented death and destruction over a 90,000 m². Not only were the costs (estimates vary between \$100 and \$200 billion) and deaths (over 1200 lives) unprecedented, but a very large number of the residents who evacuated before the storm have not yet returned. Even to this date many of the essential city services have not yet been restored to pre-Katrina levels. Many lessons were learned (Kahan et al., 2006).

- Government officials need to consider policies and plans that are more robust against a wider range of disaster scenarios (e.g. on the Gulf of Mexico coast, storm surges had been anticipated, but not at the level of Katrina even though they had anticipated catastrophic flooding and levee failures).
- Failure to anticipate the widespread regional breakdown in infrastructure and services and the disabling of first-response and public safety programs was the biggest blind spot throughout the region (e.g. the planning for regional infrastructure and services must cover total catastrophic breakdown and must include secondary, contingency responses that can be invoked when primary responses are overwhelmed).
- Detection of the storm was adequate, but the detection of structural weakness, soil anomalies, and impending failure was not, as no monitoring was in place which was (remedied through extensive deployment of sensors on all structural features of the flood protection system).
- Reconstruction efforts are strongly influenced by the answer to the question, what will the level of protection be in the future? Complicating this is the fact that many flood victims have chosen not to return and economic recovery remains uncertain.
- Integrated urban water management from the perspective of flood control includes conceding land to the water from time to time (somewhat psychologically and politically difficult).

2.2.3 Climate Change

Definitions

The United Nations Intergovernmental Panel on Climate Change (IPCC) defines climate change as “a change in the state of the climate that can be identified (e.g. using statistical tests) by changes in the mean and/or the variability of its properties, and that persists for an extended period, typically decades or longer. It refers to natural variability or as a result of human activity.” The United Nations Framework Convention on Climate Change (UNFCCC) defines climate change as “a change in climate that is attributed directly or indirectly to human activity that alters the composition of the global atmosphere and that is in addition to natural climate variability observed over comparative time periods.” A schematic framework representing anthropogenic drivers, impacts of and responses to climate change, and their linkages, is shown in Figure 2.2.7.

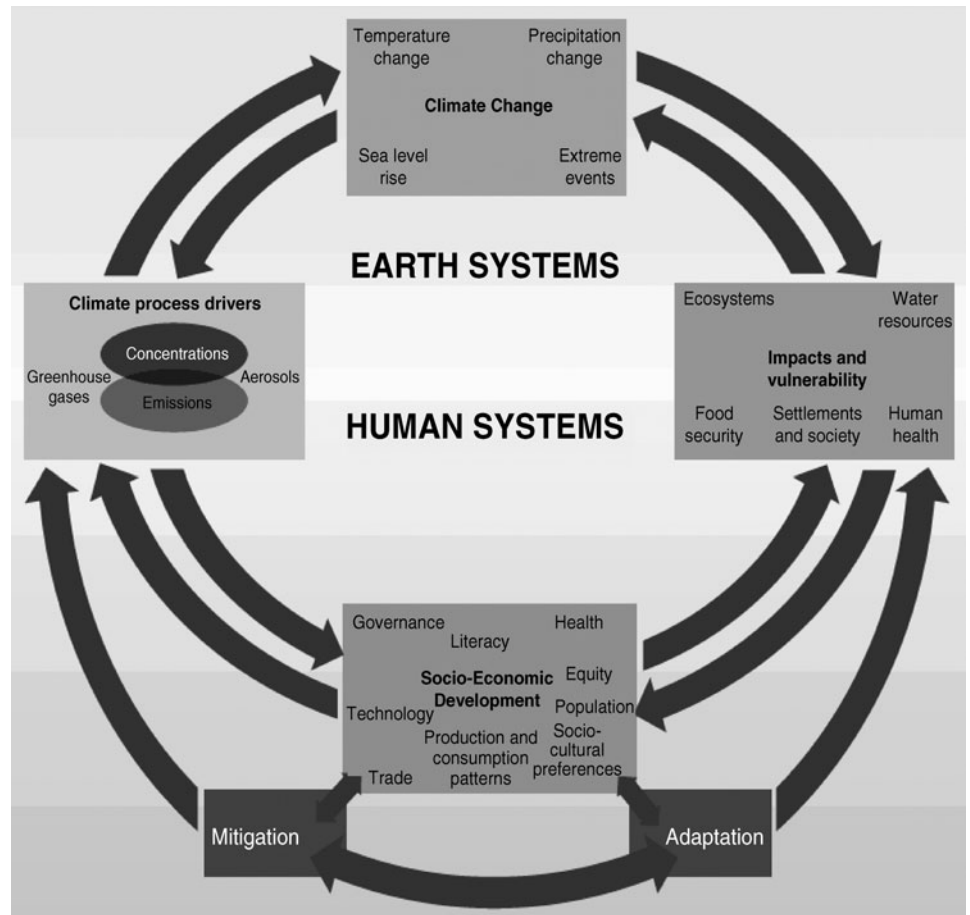


Figure 2.2.7 A schematic framework representing anthropogenic drivers, impacts of and responses to climate change, and their linkages (from IPCC, 2007).

In the last (fourth) assessment report of the United Nations Intergovernmental Panel on Climate Change (IPCC), the Working Group I states that “warming of the climate system is unequivocal, as is now evident from observations of increases in global average air and ocean temperatures, widespread melting of snow and ice and rising global average sea level.” The IPCC report also stated it is “very likely” that human activities are responsible for most of the warming of recent decades. The IPCC shared the 2007 Nobel Peace Prize with Al Gore.

The climate system is an interactive system consisting of five major components: the atmosphere, the hydrosphere, the cryosphere, the land surface, and the biosphere, forced or influenced by various external forcing mechanisms, the most important of which is the sun. The effect of human activities on the climate system is considered as external forcing. Climate change predictions are based on computer simulations using general circulation models (GCMs) of the atmosphere. The limitations of state-of-the-art climate models are the primary sources of uncertainty in the experiments that study the hydrologic and water resources impact of climate change. Future improvement to the climate models, hopefully resulting in more accurate regional predictions, should greatly improve the types of experiments to more accurately define the hydrologic and hydraulic impacts of climate change.

The impacts associated with global average temperature change will vary by the rate of temperature change, the extent of adaptation of humans, and the social-economic pathway. Water will be affected in general as follows:

- Increased water availability in moist tropics and high latitudes.
- Decreasing water availability and increasing droughts in mid-latitudes and semi-arid low latitudes.
- Hundreds of millions of people exposed to increased water stress.

Hydrologic Response

Future precipitation and temperature are the primary drivers for determining future hydrologic response. Because of the uncertainties of the predictions of the future precipitation and temperatures, the hydrologic responses of various river basins are uncertain, resulting in uncertainties of our future urban water resources, particularly in arid and semi-arid regions,

In general, the hydrologic effects are likely to influence water storage patterns throughout the hydrologic cycle and impact the exchange among aquifers, streams, rivers, and lakes. In arid and semi-arid regions, relatively modest changes in precipitation can have proportionately larger impacts on runoff, and higher temperatures result in higher evaporation rates, reduced streamflows, and increased frequency of droughts (Mays, 2007). The effects of climate change on groundwater sustainability include (Alley et al., 1999) (a) changes in groundwater recharge resulting from changes in average precipitation and temperature or in seasonal distribution of precipitation; (b) more severe and longer droughts (c) changes in evapotranspiration resulting from changes in vegetation; and (d) possible increased demands of groundwater as a backup source of water supply.

As an example, we can consider in general the hydrologic effects of climate change on the Pacific Northwest United States (e.g. the Columbia River) as summarized in Figure 2.2.8. Starting in the winter, changes in temperature and precipitation during the winter affects the snowpack during the winter. The winter snowpack in turn affects the stream flow during the spring and summer. The streamflow affects the quantity, quality, and timing of the water supply, which in turn affects

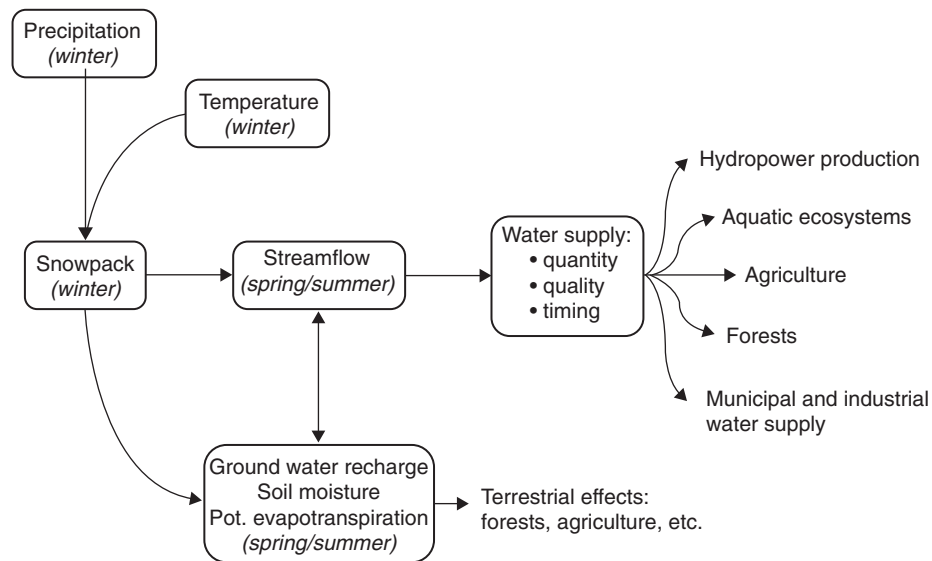


Figure 2.2.8 Dominant impact through which changes in regional climate are manifested in the Pacific Northwest (from Miles et al., 2000).

hydropower production, aquatic ecosystems, agriculture, forests, municipal and industrial water supply. Both the winter snowpack and the spring/summer streamflow affect the groundwater recharge, the soil moisture, and the evapotranspiration which have terrestrial effects on the forests, agriculture, etc. Hamlet and Lettenmaier (1999) and Miles et al. (2000) provide a more detailed discussion of the Columbia River Basin.

Some Realities of Climate Change

In the Fourth World Water Forum in March 2006, the Co-operative Programme on Water and Climate (CPWC) pointed to “the alarming gap between international recognition of the risks posed by climate change and the general failure to incorporate measures to combat those risks into national and international planning strategies (McCann, 2006). The CPWC findings and recommendations to cope with climate extremes were encompassed within the following five key messages:

- Strategies for achieving the 2015 Millennium Development Goals (MDG) do not account for the climate variability and change.
- Climate-related risks are not sufficiently considered in water sector development and management plans.
- Investment in climate disaster risk reduction is essential.
- The trend of increasing costs has to be reversed through the safety chain concept (prevention, preparation, intervention, risk spreading, recondition, reconstitution).
- Coping measures need to combine a suite of technical/structural and nonstructural measures.

The first message addresses the fact that climate impacts on hydrological systems and on livelihoods threaten to undo decades of development efforts. The second message relates to the fact that to meet MDG targets, there will need to be substantial long-term investments in structural and nonstructural approaches to water management. Structural measures include storage, control, and conveyance; and nonstructural measures include demand-side management, floodplain management, service delivery, etc. The third message relates to the fact that the costs of disasters, especially those related to water, are increasing and substantial efforts are needed in mainstream climate reduction. The fifth message advocates a combination of both structural and nonstructural measures. Structural measures include dams, dikes, and reservoirs; and nonstructural measures include early flood warning systems, spatial planning, “living with water” insurance, etc.

The reality is that climate change impacts are already with us and manifesting in increasing occurrences of and intensity of climate extremes such as droughts and floods, and climate variability. From the water supply perspective, there are both supply-side and demand-side options that could be considered for urban water supply. Table 2.2.1 summarizes some supply-side and demand-side adaptive options for the urban water-use sector.

2.2.4 Consumption of Water – Virtual Water and Water Footprints

In Section 1.2 we stated that some of today’s most acute and complex problems are related to the rational use and protection of water resources in order to supply humankind with clean freshwater. Table 1.2.3 presents the dynamics of water use in the world by human activity and Table 1.2.4 presents the annual runoff and water consumption by continents and by physiographic and economic regions. Chapter 11 discusses in detail water withdrawals and uses. Various types of uses include consumptive use, instream use, and offstream use. Tables 11.1.2 and 11.1.3 list water requirements for various industries; Table 11.1.4 lists the water requirements for municipal establishments; Table 11.1.5 lists typical household water use in the US; Table 11.2.1 and Table 11.2.2 list consumptive water use for energy production and electricity production, respectively; and Table 11.3.6 lists crop water requirements and crop evapotranspiration for agriculture.

Table 2.2.1 Supply-Side and Demand-Side Adaptive Options for Urban Water Supply (IPCC, 2001)

Supply side		Demand side	
Option	Comments	Option	Comments
Increase reservoir capacity	Expensive; potential environmental impact	Incentives to use less (e.g., through pricing)	Possibly limited opportunity; needs institutional framework
Extract more from rivers or groundwater	Potential environmental impact	Legally enforceable water standards (e.g., for appliances)	Potential political impact; usually cost-inefficient
Alter system operating rules	Possibly limited opportunity	Increase use of gray water turbines; encourage energy efficiency	Potentially expensive
Interbasin transfer	Expensive; potential environmental impact; may not be feasible	Reduce leakage	Potentially expensive to reduce to very low levels, especially in old systems
Desalination	Expensive; potential environmental impact	Development of non-water-based sanitation systems	Possibly too technically advanced for wide application

Consumptive use is defined in Table 11.1.1 as “that part of water withdrawn that is evaporated, transpires, incorporated into products or crops, consumed by humans or livestock, or otherwise removed from the immediate water environment”. It is difficult to imagine that to produce one cup of coffee requires 140 liters of water and to produce 1 kg of beef requires 16,000 liters of water. A discussion of the human consumption of water required to produce commodities and services follows.

The concepts of virtual water and water footprints are both important to the understanding of water resources sustainability. We are familiar with the concept of “ecological footprint” that quantifies the land area needed to sustain people’s living. The water footprint indicates the water required to sustain a population. To define the water footprint we must first discuss the concept of virtual water. Virtual water is the volume of water required to produce a commodity or service, as introduced by Allen (1993, 1994). The global average virtual water content of some selected products, per unit of product is listed in Table 2.2.2.

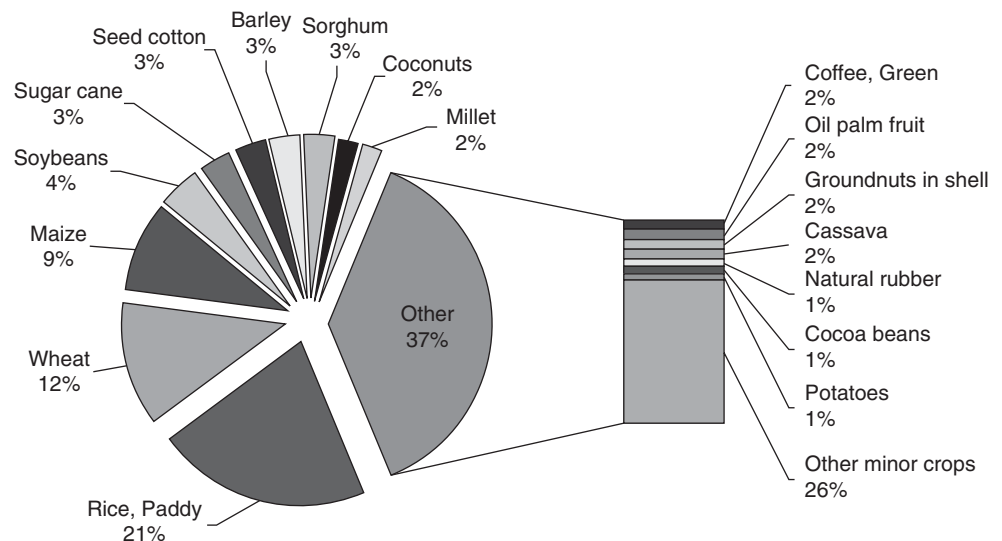
The water footprint concept was introduced by Hoekstra and Hung (2002) as a consumption indicator of water use in addition to the traditional production-sector indicators of water use. Figure 2.2.9 shows the contribution of some major crops to the global water footprint. Rice has the largest footprint, which is about 21%, and wheat has the second largest footprint, which is about 12%. The total volume of world rice production is approximately the same as wheat production, but with a much higher evaporative demand for rice production. Global average virtual water content of rice (paddy) is 2291 m³/ton, and wheat is 1334 m³/ton.

The water footprint of a nation is the total volume of freshwater that is used to produce goods and services consumed by the people of the nation (Hoekstra and Chapagain, 2007). Figure 2.2.10 shows the contribution of major consumers to the global water footprint. Obviously not all goods consumed in a country are produced in that country, so the water footprint consists of the use of domestic water resources of that country plus the water used outside the borders of that country. The water footprint indicates the water required to sustain a population, therefore the connection to water resources sustainability. The total water footprint of a nation is composed of the internal water footprint and the external water footprint. *Internal water footprint* is the volume of water used from domestic water resources. *External water footprint* is the volume of water used in other countries to produce

Table 2.2.2 Global Average Virtual Water Content of Some Selected Products, Per Unit of Product

Product	Virtual water content (liters)
1 glass of beer (250 ml)	75
1 glass of milk (200 ml)	200
1 cup of coffee (125 ml)	140
1 cup of tea (250 ml)	35
1 slice of bread (30 g)	40
1 slice of bread (30 g) with cheese (10 g)	90
1 potato (100 g)	25
1 apple (100 g)	70
1 cotton T-shirt (250 g)	2000
1 sheet of A4-paper (80 g/m ²)	10
1 glass of wine (125 ml)	120
1 glass of apple juice (200 ml)	190
1 glass of orange juice (200 ml)	170
1 bag of potato crisps (200 g)	185
1 egg (40 g)	135
1 hamburger (150 g)	2400
1 tomato (70 g)	13
1 orange (100 g)	50
1 pair of shoes (bovine leather)	8000
1 microchip (2 g)	32

Source: Hoekstra and Chapagain (2007).

**Figure 2.2.9** Contribution of different crops to the global footprint (from Hoekstra and Chapagain, 2007).

goods and services imported and consumed by the inhabitants of the country. Figure 2.2.11 shows the make-up of the water footprint of the US for 1997–2001.

Table 2.2.3 lists the composition of water footprint for some selected countries: 1997–2001. Figure 2.2.12 shows the national water footprint per capita and the contribution of different consumption categories for some selected countries. The study results indicate that the US

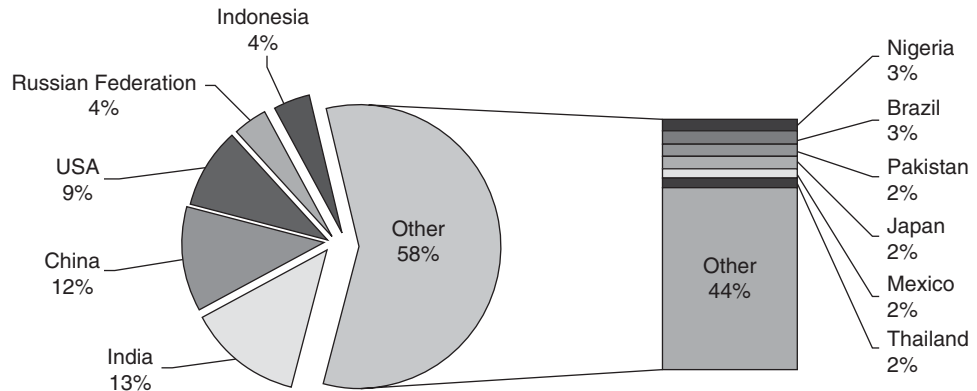


Figure 2.2.10 Contribution of major consumers to the global water footprint (Hoekstra and Chapagain, 2007).

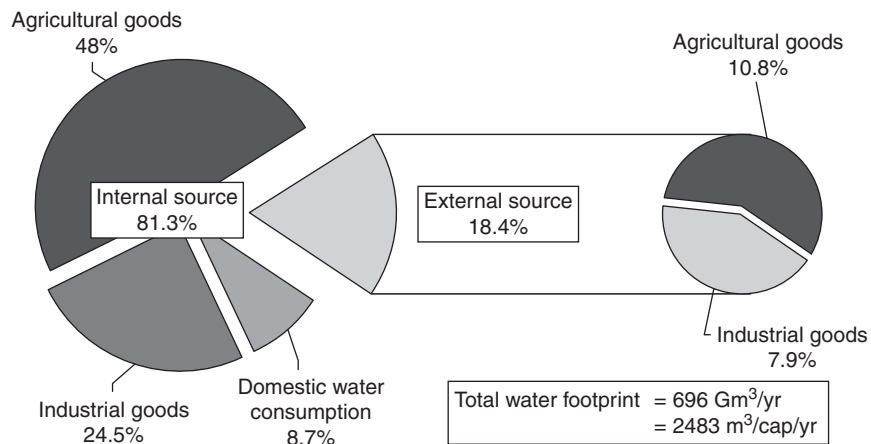


Figure 2.2.11 Water footprint of the US, 1997-2001 (from Hoekstra and Chapagain, 2007).

appears to have an average water footprint of 2480 m³/cap/yr, while China has an average footprint of 700 m³/cap/yr. The global average water footprint is 1240 m³/cap/yr.

Hoekstra and Chapagain (2007) defined four major direct factors that determine the water footprint of a country:

1. Volume of consumption (related to the gross national income)
2. Consumption pattern (e.g. high versus low meat consumption)
3. Climate (growth conditions)
4. Agricultural practice (water use efficiency)

Various aspects of water resources sustainability relate to virtual water flows between nations as a result of the trade of agricultural (crops and livestock) products and industrial products. We might ask the question, what water savings is there through the international trade of agricultural products? What effect does the globalization of water have on the water resources sustainability of various nations, or regions of the world?

For additional information refer to the book, *Globalization of Water: Sharing the Planet's Freshwater* by Hoekstra and Chapagain (2007) and the website www.waterfootprint.org.

Table 2.2.3 Composition of water footprint for some selected countries, 1997–2001

Country	Population	Use of domestic water resources						Use of foreign water resources				Water footprint by consumption category				
		Domestic water withdrawal (Gm ³ /yr)	Crop evapotranspiration*		Industrial water withdrawal		For national consumption		For re-export of imported products (Gm ³ /yr)	Water footprint		Domestic water footprint (m ³ /cap/yr)	Agricultural goods		Industrial goods	
			For national consumption (Gm ³ /yr)	For export (Gm ³ /yr)	For national consumption (Gm ³ /yr)	For export (Gm ³ /yr)	Agricultural goods (Gm ³ /yr)	Industrial goods (Gm ³ /yr)		Total (Gm ³ /yr)	Per capita (m ³ /cap/yr)		Internal water footprint (m ³ /cap/yr)	External water footprint (m ³ /cap/yr)	Internal water footprint (m ³ /cap/yr)	External water footprint (m ³ /cap/yr)
Australia	19071705	6.51	14.03	68.67	1.229	0.12	0.78	4.02	4.21	26.56	1393	341	736	41	64	211
Bangladesh	129942975	2.12	109.98	1.38	0.344	0.08	3.71	0.34	0.13	116.49	896	16	846	29	3	3
Brazil	169109675	11.76	195.29	61.01	8.666	1.63	14.76	3.11	5.20	233.59	1381	70	1155	87	51	18
Canada	30649675	8.55	30.22	52.34	11.211	20.36	7.74	5.07	22.62	62.80	2049	279	986	252	366	166
China	1257521250	33.32	711.10	21.55	81.531	45.73	49.99	7.45	5.69	883.39	702	26	565	40	65	6
Egypt	63375735	4.16	45.78	1.55	6.423	0.66	12.49	0.64	0.49	69.50	1097	66	722	197	101	10
France	58775400	6.16	47.84	34.63	15.094	12.80	30.40	10.69	31.07	110.19	1875	105	814	517	257	182
Germany	82169250	5.45	35.64	18.84	18.771	13.15	49.59	17.50	38.48	126.95	1545	66	434	604	228	213
India	1007369125	38.62	913.70	35.29	19.065	6.04	13.75	2.24	1.24	987.34	980	38	907	14	19	2
Indonesia	204920450	5.67	236.22	22.62	0.404	0.06	26.09	1.58	2.74	269.96	1317	28	1153	127	2	8
Italy	57718000	7.97	47.82	12.35	10.133	5.60	59.97	8.69	20.29	134.59	2332	138	829	1039	176	151
Japan	126741225	17.20	20.97	0.40	13.702	2.10	77.84	16.38	4.01	146.09	1153	136	165	614	108	129
Jordan	4813708	0.21	1.45	0.07	0.035	0.00	4.37	0.21	0.22	6.27	1303	44	301	908	7	43
Mexico	97291745	13.55	81.48	12.26	2.998	1.13	35.09	7.05	7.94	140.16	1441	139	837	361	31	72
Netherlands	15865250	0.44	0.50	2.51	2.562	2.20	9.30	6.61	52.84	19.40	1223	28	31	586	161	417
Pakistan	136475525	2.88	152.75	7.57	1.706	1.28	8.55	0.33	0.67	166.22	1218	21	1119	63	12	2
Russia	145878750	14.34	201.26	8.96	13.251	34.83	41.33	0.80	3.94	270.98	1858	98	1380	283	91	5
South Africa	42387403	2.43	27.32	6.05	1.123	0.40	78.18	1.42	2.10	39.47	931	57	644	169	26	33
Thailand	60487800	1.83	120.17	38.49	1.239	0.55	8.73	2.49	3.90	134.46	2223	30	1987	144	20	41
United Kingdom	58669403	2.21	12.79	3.38	6.673	1.46	34.73	16.67	12.83	73.07	1245	38	218	592	114	284
USA	280343325	60.80	334.24	138.96	170.777	44.72	74.91	55.29	45.62	696.01	2483	217	1192	267	609	197
Global total avg.	5994251631	344	5434	957	476	240	957	240	427	7452	1243	57	907	160	79	40

*Includes both blue and green water use in agriculture

Source: Hoestra and Chapagain (2007).

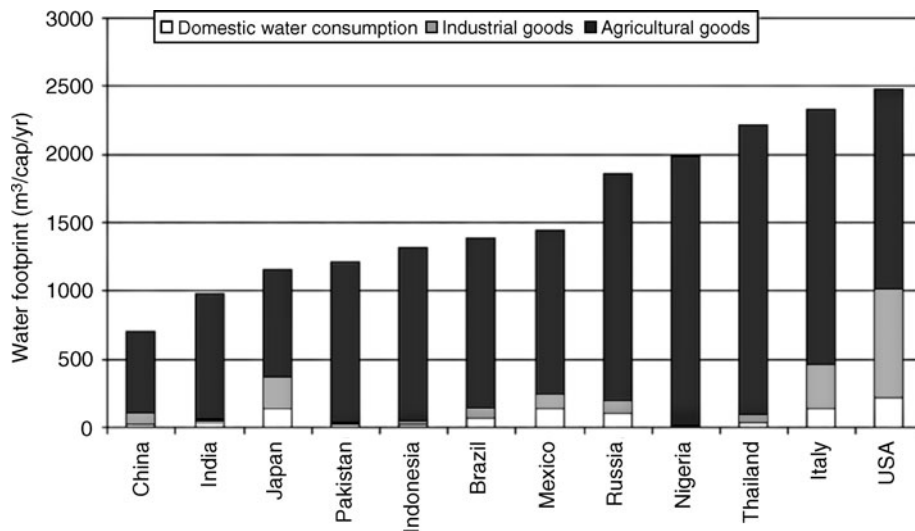


Figure 2.2.12 The national water footprint per capita and the contribution of different consumption categories for some selected countries (from Hoekstra and Chapagain, 2007).

2.3 SURFACE WATER SYSTEM—THE COLORADO RIVER BASIN

2.3.1 The Basin

Of the many river basins in the southwest, the Colorado River Basin has been the center of many controversies. The Colorado River Basin is divided into the upper and lower basins as shown in Figure 2.3.1. The upper Colorado River Basin includes areas of the states of Arizona, Colorado, New Mexico, Utah, and Wyoming; the lower Colorado River Basin includes areas of Arizona, California, New Mexico, and Utah. The drainage basin area is over 240,000 mi². The Colorado River and its main tributary streams originate high within the mountains of western Wyoming, central Colorado, and northeastern Utah. The Colorado River receives large amounts of snowmelt from several major tributaries with snowpack accumulating as high as 14,000 ft above sea level.

Annual average flow rate of the Colorado River is roughly 15 million ac-ft. The Colorado River is the most important source of water in the semi-arid and arid southwestern United States. It provides water for tens of millions of people from San Diego to Denver and a multitude of communities in between. Reservoirs of the Colorado River system have roughly 60 million ac-ft of storage capacity, approximately four times the Colorado’s average annual flow. The two largest and most significant reservoirs are Lake Mead and Lake Powell, which are impounded respectively by Hoover Dam, located near Las Vegas, Nevada, and Glen Canyon Dam, located 15 mi south of the Arizona–Utah border. With storage capacities of roughly 28 and 27 million ac-ft, including dead storage, each reservoir can store roughly 2 years of annual mean flow of the Colorado River (Water Science and Technology Board, 2007). Lake Mead and Lake Powell are major sources for water in southern California and Arizona. Figure 2.3.2 shows the storage in Lake Powell through December 1, 2006.

Most of the precipitation in the Colorado River Basin falls as winter snowfall in higher elevations of Colorado, Utah, and Wyoming. Approximately 20 percent of the basin’s precipitation falls in the highest 10 percent of the basin, and roughly 40 percent of the basin’s precipitation falls in the highest 20 percent of the basin (Water Science and Technology, 2007).



Figure 2.3.1 Colorado River Basin showing the upper and lower Colorado River Basins. (Courtesy of the U.S. Geological Survey.)

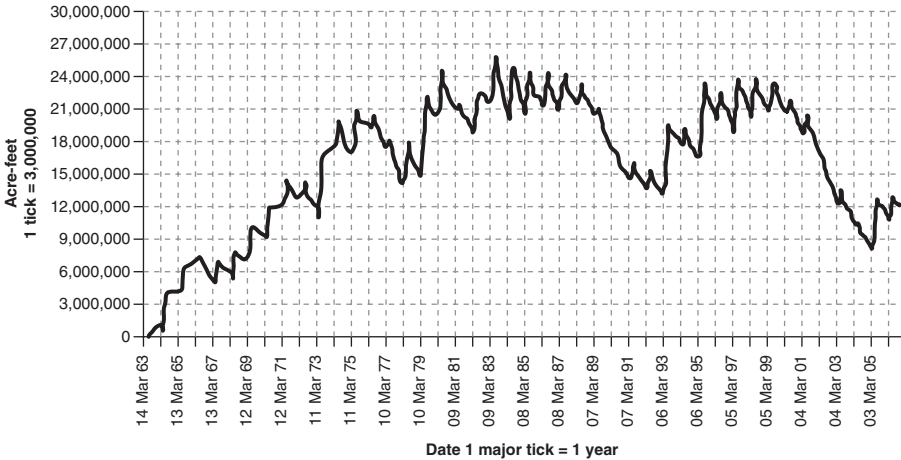


Figure 2.3.2 Storage in Lake Powell through December 1, 2006. Lake Powell’s capacity is 27 million ac-ft, including dead storage. Values shown do not include the volume of water in dead storage. (Source: <http://www.usbr.gov/uc/crsp/GetSiteInfo>.)

Figure 2.3.1 shows the potential water supply crisis areas in the western United States, noting the major areas in the Colorado River Basin.

Climate

Precipitation on the Colorado River Basin exhibits high year-to-year (interannual) variability, as illustrated in Figure 2.3.3 for the upper part of the basin. This figure is for spatially averaged precipitation over the basin upstream of Lees Ferry and aggregated to annual resolution (<http://ftp.ncdc.noaa.gov/pub/data/prism100>).

From Figure 2.3.4, it is evident that since the late 1970s there has been a steady upward trend in surface temperatures in the Colorado River Basin. The most recent 11-year average exceeds any previous values in the over 100 years of instrumental records. Notice how much warmer the basin has been in the drought of the early 2000s as compared to previous droughts. Temperatures across the basin today are at least 1.5°F warmer than during the 1950s drought. Increasing temperatures have

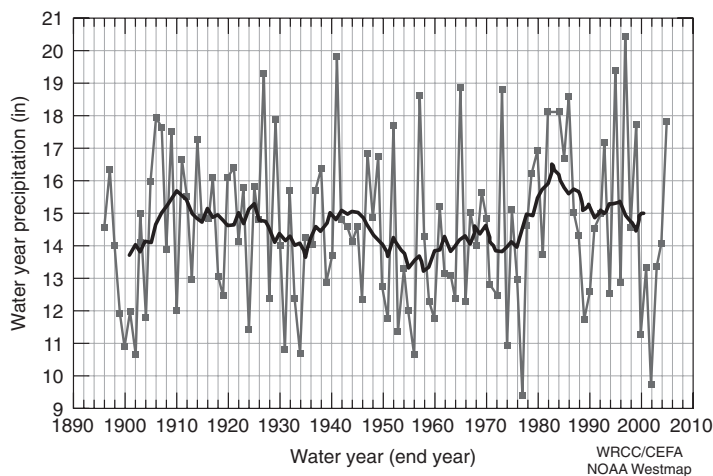


Figure 2.3.3 Annual precipitation for the Colorado River basin above Lees Ferry, 1895–2005. (Red: annual values. Blue: 11-year running mean)
 Source: Western Regional Climate Center.

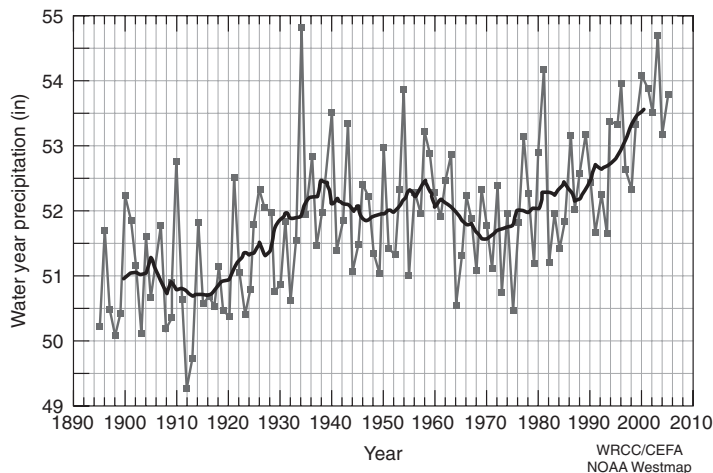


Figure 2.3.4 Annual average surface air temperature for entire Colorado River basin, 1895–2005. (Red: annual values; Blue: 11-year running mean)
 Source: Western Regional Climate Center.

many hydrologic implications related to evaporation, infiltration, snow melt, surface water runoff, aquifer recharge, and streamflows. One important result of these impacts is drought. The drought of the early 2000s has taken place in warmer conditions, comparing the temperature departures for the 6-year period (2000–2005) as compared to the 1895–2000 averages. Both in terms of absolute degrees and in terms of annual standard deviation, the Colorado River basin has warmed more than any region of the United States (Water Science and Technology Board, 2007).

Climate Change Affects the Basin

Climate change models have been used to project future precipitation and temperature changes for the Colorado River Basin. Long-term projections of precipitation are a greater modeling challenge than temperature projections. Precipitation projections for the Colorado River Basin using climate models suggest a wide range of potential changes in annual precipitation. Models have forecasted a slight decrease (less than 10 percent below current values) in annual precipitation in southwestern United States, with relatively little change in annual precipitation amounts forecast for headwaters regions of the Colorado River (Water Science and Technology Board, 2007). The changes in seasonality of precipitation or changes in the type of precipitation (rain or snow) can be just as important as changes in annual amounts of precipitation.

Future projections and past trends indicate a strong likelihood of a warmer future climate across the Colorado River Basin. Projected temperature increases across the Colorado River Basin have important direct and indirect implications for hydrology and streamflow, irrespective of the amount of the precipitation increases or decreases. The effects of warmer temperatures across the Colorado River Basin for hydrology include the following (Water Science and Technology Board, 2007):

- freezing levels at higher elevations, which means more winter precipitation will fall as rain rather than snow;
- shorter seasons of snow accumulation at a given elevation;
- less snowpack accumulation as compared to the present;
- earlier melting of snowpack;
- decreased baseflows from groundwater during late summer, and lowered water availability during the important late-summer growing season;
- more runoff and flood peaks during the winter months;
- longer growing seasons;
- reductions in soil moisture availability in the summer and increases in the spring and winter;
- increased water demand by plants; and
- greater losses of water to evapotranspiration.

A Short History of Water Development of the Basin

Due to the doctrine of prior appropriation (first in time, first in right, see Section 19.1), the states in the upper Colorado River Basin became worried that the rapidly developing California would obtain a large portion of the appropriated water, leaving them with a shortage in the future. As an attempt to settle the issues, the upper basin states agreed to support California on the Hoover Dam proposal that it needed to obtain Colorado River water for its growing development. In return, the states requested a guaranteed amount of water from the river for their own future development. This agreement between the states resulted in the Colorado River Compact in 1922, which Arizona did not ratify until 1944.

Under the Colorado River Compact, it was agreed that the upper and lower Colorado River Basin would each receive 7.5 maf. It was also agreed that the lower basin would have the right to increase its beneficial consumptive use by 1 maf annually. All of the states supported the compact except Arizona, which opposed the Compact and refused to sign it. The dispute over the water continued as the Boulder Canyon Project Act was passed on December 21, 1928 by

Congress, which authorized the construction of the Boulder Dam (now Hoover Dam). However, the one stipulation was that California must agree to limit its use of Colorado River water to an amount of 4.4 maf. Arizona and California fought over both the Colorado River Compact and the Boulder Canyon Act. Arizona was against the Act and did not want California to have any of their water.

In order to help in settling the dispute, the U.S. Congress made it clear to Arizona that, until they could settle the dispute of water allocation in the lower Colorado River Basin, the state would not receive any support for their water canal system, the Central Arizona Project (CAP), which would later become a controversy in itself. Arizona finally agreed to share its water with California in order to receive funding for the CAP. As a result of the case *Arizona v. California*, which took place in 1964, the Supreme Court decreed that California would receive 4.4 maf of Colorado River water, Arizona would receive 2.8 maf, and Nevada 0.3 maf.

The CAP is a 336-mi-long system of aqueducts, tunnels, pumping plants, and pipelines (Figure 2.3.5) that carries water from the Colorado River at Lake Havasu, through Phoenix, to the San Xavier Indian reservation southwest of Tucson. The main purpose of the CAP was to help Arizona conserve its groundwater supplies by importing surface water from the Colorado River. Figure 2.3.5 shows the layout and major features of the Central Arizona Project (CAP) system.

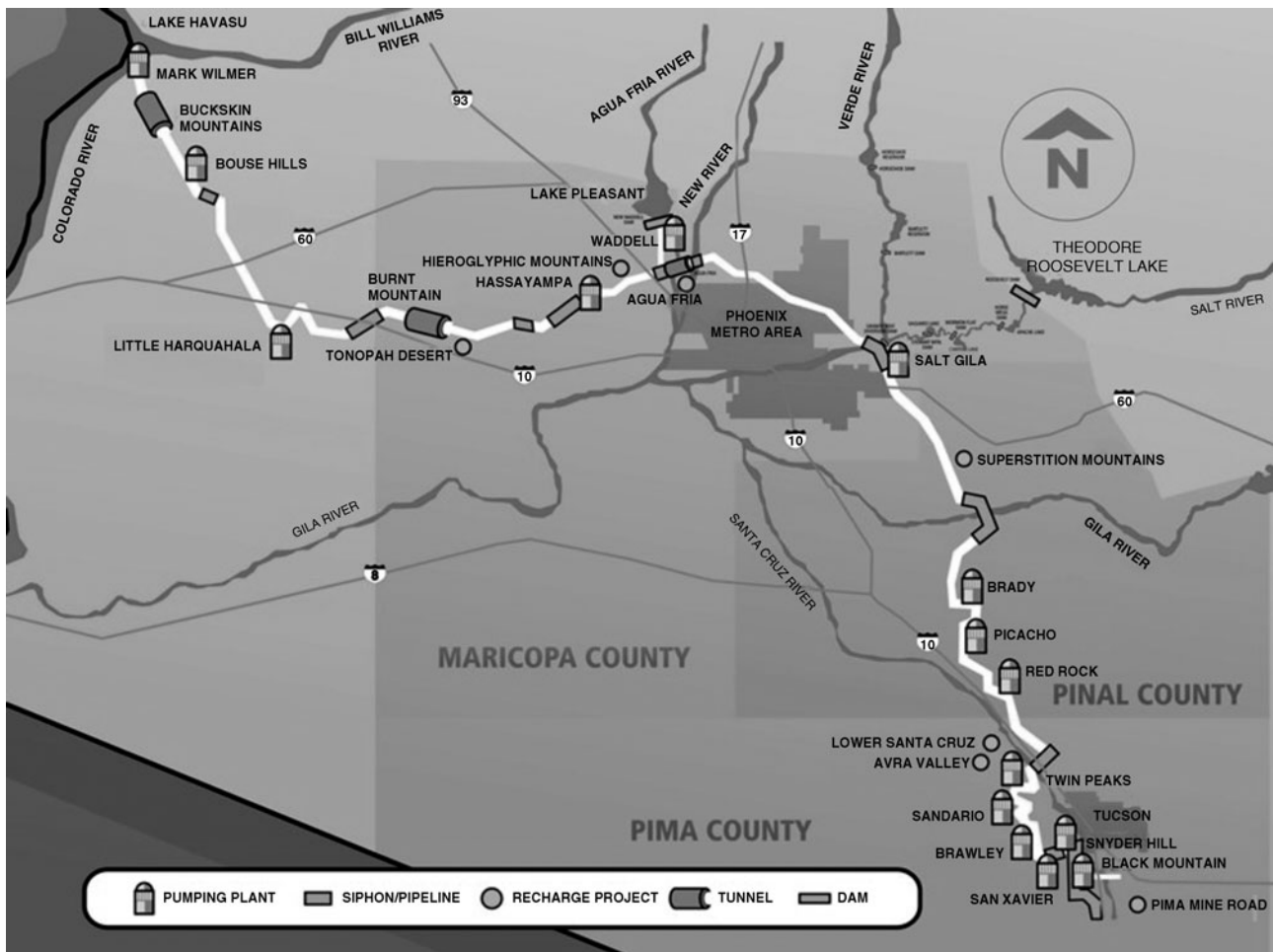


Figure 2.3.5 Layout and major features of the Central Arizona Project (CAP) system.

The CAP was the largest, most expensive, and most politically volatile water development project in U.S. history; it was also the most ambitious basin project that the bureau attempted (Espeland, 1998). Even early on in 1947, the strategy of CAP supporters was to paint CAP as a “rescue” operation. This was the project necessary to replace the “exhausted” groundwater supply in order to save the local economy. By 1963, the CAP was still justified as a “rescue” project; a doubling of the population over the previous 10 years supposedly made the project even more urgent. Economic development was assumed to be driven by agricultural development. The thought was that without more irrigated farmland, urban growth (which reduces irrigated farmland) would be stymied. How did the population grow so fast despite the previous prediction that water supply would limit economic growth?

In 1968, Congress authorized the construction of the CAP under the Colorado River Basin Project Act. The main purpose for the authorization was to assist Arizona in reducing its water deficiencies. By 1971, the first *environmental impact statement* (EIS) on the CAP was written and then finalized in 1972. The 1976 EIS was devoted solely to the Orme Dam, to become the beginning of a series of EISs in the major features of the CAP. In 1971, the *Central Arizona Water Conservation District* (CAWCD) was created to provide a means for Arizona to repay the federal government for the reimbursable costs of construction and to manage and operate the CAP once complete. The construction began in 1973 at Lake Havasu and was completed in 1993. The entire cost of the project was more than \$4 billion. Under the Colorado River Basin Project Act, the CAP would be the first to take shortages in the lower Colorado River Basin.

The users of the CAP water fall into three categories. The first category is municipal and industrial. These customers include cities and water utilities which are responsible for treating drinking water and delivering it to residences, commercial buildings, and industries. The next water use category is agricultural. These agricultural users are primarily irrigation districts. The last category is the Indian community. These communities receive water from the CAP under contracts with the federal government. Agriculture has been the main water user in the past; however, due to the increasing development of Arizona, cities will soon become the largest customer for the CAP.

The Future

A recent study at the Scripps Institution of Oceanography has shown that “under current conditions there is a 10% chance live storage in Lakes Mead and Powell will be gone by about 2013 and a 50% chance it will be gone by 2021 if no changes in water allocation from the Colorado River system are made.” These results are driven by climate change resulting from global warming, the effects of natural climate variability, and the current operation of the reservoir system. Water planners and managers at all levels have denied any knowledge that such a thing could happen, even though there have been a number of studies suggesting that there will be a decrease in runoff in the southwestern United States due to global warming.

As stated in the Water Science and Technology (2007) report, “Steadily rising population and urban water demands in the Colorado River region will inevitably result in increasingly costly, controversial, and unavoidable trade-off choices to be made by water managers, politicians, and their constituents. These increasing demands are also impeding the region’s ability to cope with droughts and water shortages.”

2.4 GROUNDWATER SYSTEMS – THE EDWARDS AQUIFER, TEXAS

The Edwards Aquifer, located in south-central Texas (Figure 2.4.1), is a large area of karst terrain. Limestone and dolomites are exposed at the land surface, referred to as the outcrop area or recharge area (see Figures 2.4.1 and 2.4.2). Figure 6.9.2 also points out the outcrop area of the aquifer. Recharge to the aquifer is derived mainly from streams that cross the outcrop area of the aquifer and from direct infiltration of precipitation on the outcrop. The watershed areas that provide recharge

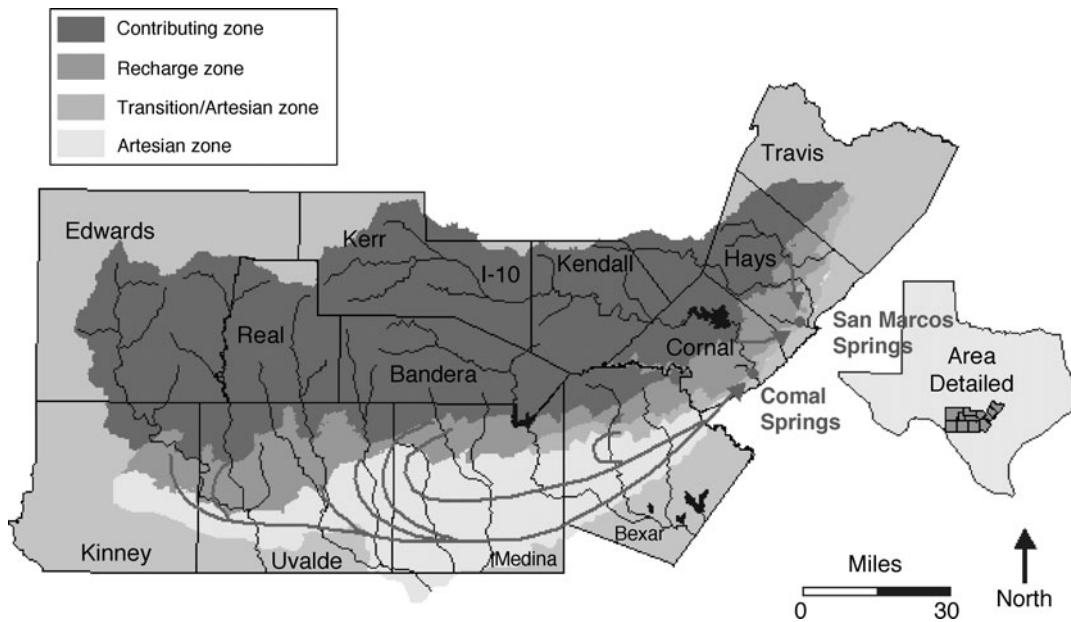


Figure 2.4.1 Edwards Aquifer in south-central Texas showing general flow paths of aquifer. (Courtesy of Greg Eckhardt.)

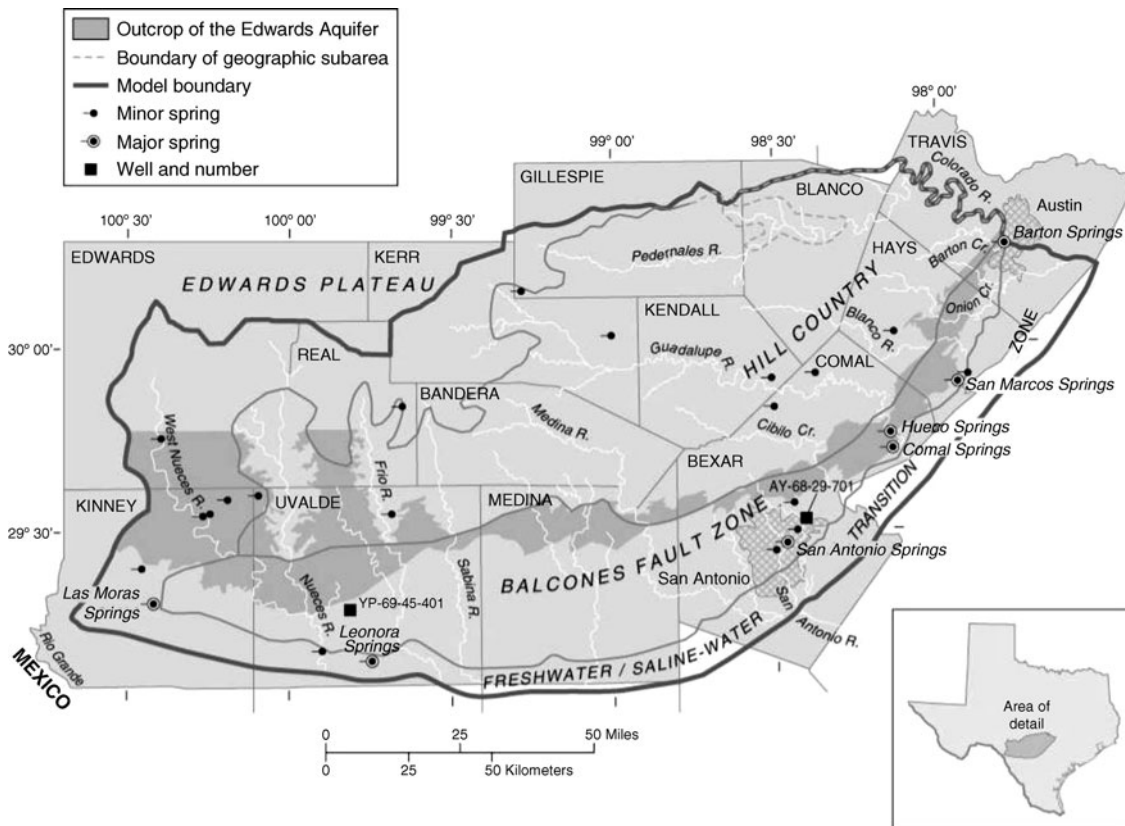


Figure 2.4.2 Edwards Aquifer showing springs (from Kuniansky et al., 2001).

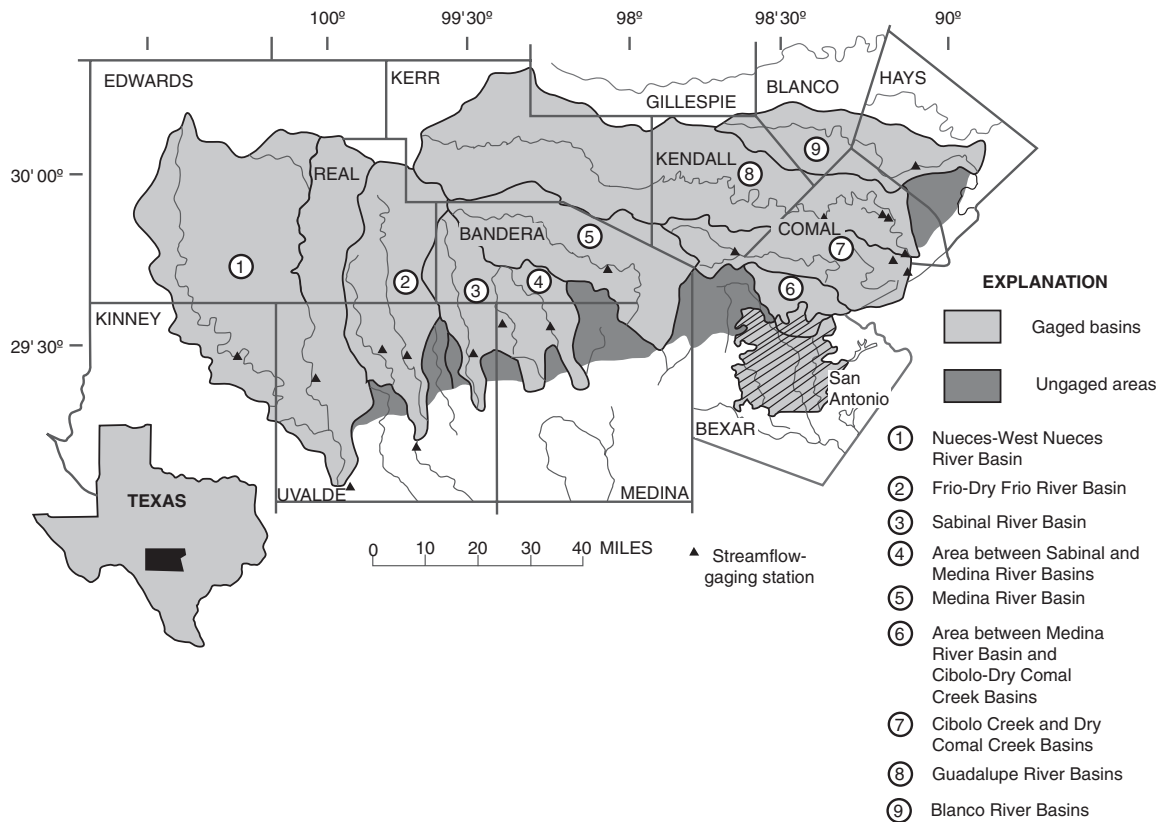


Figure 2.4.3 Map showing gaged basins and ungauged areas (modified from Puente (1978), Figure 1, as presented by Slattery and Thomas (2002)).

to the aquifer are shown in Figure 2.4.3. Estimated annual recharge to the aquifer by river basin is listed in Table 2.4.1.

Discharge from the Edwards Aquifer is from wells and springs. The major discharge from wells is in Bexar, Medina, and Uvalde Counties. The City of San Antonio, Texas obtains all of its water supply from the aquifer. Table 2.4.2 lists the estimated annual discharge from the Edwards Aquifer by county

Table 2.4.1 Estimated Annual Recharge to the Edwards Aquifer by Basin, 1980–2001 (thousands of ac-ft)

Calendar year	Nueces–West Nueces River Basin	Frio-Dry Frio River Basin ¹	Sabinal River Basin ¹	Area between Sabinal and Medina River Basins ¹	Medina River Basin ²	Area between Medina River Basin and Cibolo–Dry Comal Creek Basin ¹	Cibolo Creek and Dry Comal Creek Basins	Blanco River Basin ¹	Total ³
1980	58.6	85.6	42.6	25.3	88.3	18.8	55.4	31.8	406.4
1981	205.0	365.2	105.6	252.1	91.3	165.0	196.8	67.3	1448.4
1982	19.4	123.4	21.0	90.9	76.8	22.6	44.8	23.5	422.4
1983	79.2	85.9	20.1	42.9	74.4	31.9	62.5	23.2	420.1
1984	32.4	40.4	8.8	18.1	43.9	11.3	16.9	25.9	197.9
1985	105.9	186.9	50.7	148.5	64.7	136.7	259.2	50.7	1003.3
1986	188.4	192.8	42.2	173.6	74.7	170.2	267.4	44.5	1153.7
1987	308.5	473.3	110.7	405.5	90.4	229.3	270.9	114.9	2003.6

(Continued)

Table 2.4.1 (Continued)

Calendar year	Nueces–West Nueces River Basin	Frio–Dry Frio River Basin ¹	Sabinal River Basin ¹	Area between Sabinal and Medina River Basins ¹	Medina River Basin ²	Area between Medina River Basin and Cibolo Creek and Dry Comal Creek Basins			Total ³
						Cibolo–Dry Comal Creek Basin ¹	Cibolo Creek and Dry Comal Creek Basins	Blanco River Basin ¹	
1988	59.2	117.9	17.0	24.9	69.9	12.6	28.5	25.5	355.5
1989	52.6	52.6	8.4	13.5	46.9	4.6	12.3	23.6	214.4
1990	479.3	255.0	54.6	131.2	54.0	35.9	71.8	41.3	1123.2
1991	325.2	421.0	103.1	315.2	52.8	84.5	109.7	96.9	1508.4
1992	234.1	586.9	201.1	566.1	91.4	290.6	286.6	228.9	2485.7
1993	32.6	78.5	29.6	60.8	78.5	38.9	90.9	37.8	447.6
1994	124.6	151.5	29.5	45.1	61.1	34.1	55.6	36.6	538.1
1995	107.1	147.6	34.7	62.4	61.7	36.2	51.1	30.6	531.3
1996	130.0	92.0	11.4	9.4	42.3	10.6	14.7	13.9	324.3
1997	176.9	209.1	57.0	208.4	63.3	193.4	144.2	82.3	1134.6
1998	141.5	214.8	72.5	201.4	80.3	86.2	240.9	104.7	1142.3
1999	101.4	136.8	30.8	57.2	77.1	21.2	27.9	21.0	473.5
2000	238.4	123.0	33.1	55.2	53.4	28.6	48.6	34.1	614.5
2001	297.5	126.7	66.2	124.1	90.0	101.5	173.7	89.7	1069.4
Average	121.2	134.1	42.2	107.2	61.9	69.9	105.0	43.1	684.7

¹Includes recharge from ungaged areas.²Recharge to Edwards Aquifer from the Medina River Basin consists entirely of losses from Medina Lake (Puente, 1978).³Total might not equal the sum of basin values due to rounding.

Source: Slattery and Thomas (2002).

Table 2.4.2 Estimated Annual Discharge from the Edwards Aquifer by County, 1986–2001 (thousands of ac-ft)

Calendar year	Kinney–Uvalde Counties	Medina County	Bexar County	Comal County	Hays County	Total ¹	Well discharge	Spring discharge
1980	151.0	39.9	300.3	220.3	107.9	819.4	491.1	328.3
1981	104.2	26.1	280.7	241.8	141.6	794.4	387.1	407.3
1982	129.2	33.4	305.1	213.2	105.5	786.4	453.1	333.3
1983	107.7	29.7	277.6	186.6	118.5	720.1	418.5	301.6
1984	151.1	46.9	309.7	108.9	85.7	702.3	529.8	172.5
1985	156.9	59.2	295.5	200.0	144.9	856.5	522.5	334.0
1986	91.7 ²	41.9	294.0	229.3	160.4	817.3 ²	429.3	388.1 ²
1987	95.1 ²	15.9	326.6	286.2	198.4	922.0 ²	364.1	558.0 ²
1988	156.7 ²	82.2	317.4	236.5	116.9	909.7 ²	540.0	369.8 ²
1989	156.9	70.5	305.6	147.9	85.6	766.6	542.4	224.1
1990	118.1	69.7	276.8	171.3	94.1	730.0	489.4	240.6
1991	76.6	25.6	315.5	221.9	151.0	790.6	436.3	354.3
1992	76.5	9.3	370.5	412.4	261.3	1,130.2	327.3	802.8
1993	107.5	17.8	371.0	349.5	151.0	996.7	407.3	589.4
1994	95.5	41.1	297.7	269.8	110.6	814.8	424.6	390.2
1995	90.8	35.2	272.1	235.0	127.8	761.0	399.6	361.3
1996	117.6	66.3	286.8	150.2	84.7	705.6	493.6	212.0
1997	29.9 ³	7.0 ³	255.3 ³	243.3	149.2	684.7 ³	300.7 ³	384.0
1998	113.1	51.3	312.8	271.4	169.2	915.9	451.7	464.1

(Continued)

Table 2.4.2 (Continued)

Calendar year	Kinney-Uvalde Counties	Medina County	Bexar County	Comal County	Hays County	Total ¹	Well discharge	Spring discharge
1999 ⁴	99.8 ⁵	48.3	298.3	295.2	142.3	884.0	427.8	456.2
2000	89.1	45.1	283.6	226.1	108.4	752.3	414.8	337.5
2001	68.7	33.9	291.6	327.4	175.3	896.9	367.7	529.1

¹Total might not equal the sum of county values due to rounding.

²Differs from value to the *Edwards Underground Water District Bulletins*, pp. 46–48, table 3, due to correction of an error in the method of computing the Leona Formation underflow.

³Does not include irrigation discharge (Bexar, Medina, and Uvalde Counties).

⁴Does not include discharge for domestic supply, stock, and miscellaneous use.

⁵Does not include discharge from Kinney County.

Source: Slattery and Thomas (2002).

and lists the portion from wells and from springs. Note the relation of discharge from springs as compared to well discharge as a function of time. Discharge from the Comal Springs and San Marcos Springs for 2001 was 414,800 ac-ft, accounting for 78 percent of the discharge for that year.

There are many technical, legal, economic, and institutional issues concerning the Edwards Aquifer. Even though the Edwards Aquifer has been studied extensively over the years there are still no solutions or answers to many issues. These include technical, legal, economic, and institutional issues (<http://www.edwardsaquifer.net/>).

2.5 WATER BUDGETS

2.5.1 What are Water Budgets?

The use of water budgets is very important in the evaluation of water resources sustainability. A water budget, hydrologic budget, or water balance is a measurement of the continuity of the flow of water through a system or control volume. The budget holds true for any time interval and applies to any size area ranging from local-scale areas to regional scale areas or from any drainage area to the earth as a whole. An open system is usually considered for which quantification is a mass balance equation in which the change of storage of water (ΔS) over a time period within the system equals the inputs (I) to the system minus the outputs (O) from the system.

A common application of the water budget (hydrologic budget) is to geographical areas to establish hydrologic characteristics of the area. A watershed or drainage basin or catchment is defined as the area that contributes, on the basis of topography, all the water that flows through a given location of the stream. The water budget for a watershed (Figure 2.5.1) includes the precipitation (P) onto the watershed, the groundwater inflow (G_{in}), the evaporation (E), the evapotranspiration (T), the stream outflow (Q), and the groundwater outflow (G_{out}) from the watershed, all in terms of volume over a time period. Change of storage, ΔS , is then expressed as

$$\Delta S = P + G_{in} - E - T - G_{out} - Q \quad (2.5.1)$$

EXAMPLE 2.5.1

Determine the net groundwater flow to a lake (which is the groundwater inflow to the lake minus the groundwater outflow) using a water budget for a particular year in which the precipitation was 43 in, the evaporation was 53 in, the surface water inflow was 1 in, the surface outflow was 173 in, and the change in storage was -2 in.

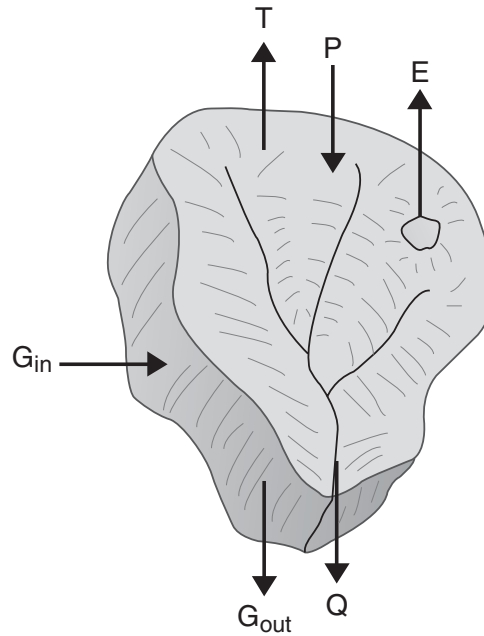


Figure 2.5.1 Watershed showing components of the water budget (hydrologic budget: P = precipitation, G_{in} = groundwater flow inflow, E = evaporation, T = evapotranspiration, Q = streamflow and G_{out} = groundwater outflow, all in terms of volume. Change of storage, ΔS , is $\Delta S = P + G_{in} - E - T - G_{out} - Q$).

SOLUTION

The water budget equation to define the net groundwater inflow to the lake neglecting evapotranspiration is

$$\begin{aligned}
 G &= G_{in} - G_{out} = \Delta S - P + E - Q_{in} + Q_{out} \\
 &= -2 - 43 + 53 - 1 + 173 \\
 &= 180 \text{ in for the year}
 \end{aligned}$$

Figure 2.5.2 illustrates a simple water budget for a groundwater system for predevelopment conditions and development conditions. The possible sources of water entering (recharge) a groundwater system under natural conditions could be (a) the areal recharge from precipitation that percolates through the unsaturated zone to the water table and (b) recharge from losing streams,

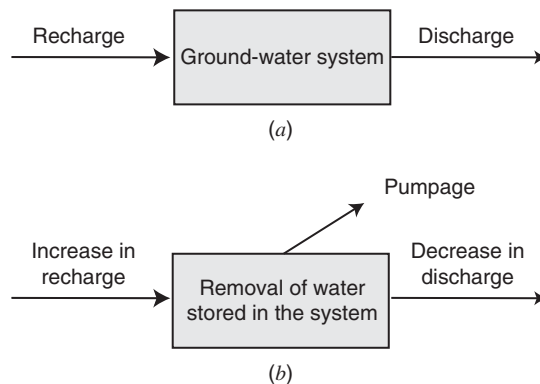
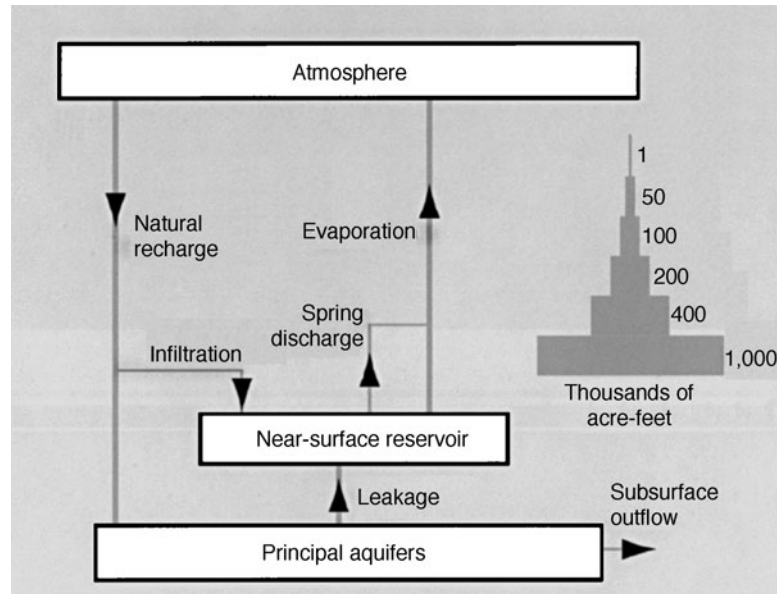


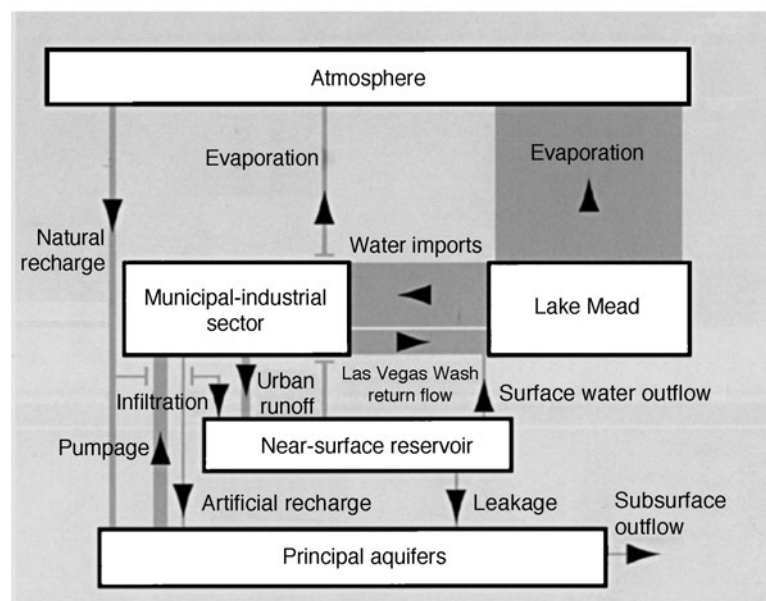
Figure 2.5.2 Diagrams of water budgets for a groundwater system for predevelopment and development conditions. (a) Predevelopment water-budget diagram illustrating that inflow equals outflow; (b) Water-budget diagram showing changes in flow for a groundwater system being pumped. The sources of water for the pumpage are changes in recharge, discharge, and the amount of water stored. The initial predevelopment values do not directly enter the budget calculation (from Alley et al., 1999).

lakes, and wetlands. The discharge leaving a groundwater system under natural conditions could be (a) discharge to streams, lakes, wetlands, saltwater bodies (bays, estuaries, or oceans), and springs; and (b) groundwater evaporation.

Figure 2.5.3 illustrates the difference in water budget components for predevelopment times and the present for Las Vegas, Nevada. Figure 2.5.4 illustrates the groundwater budgets for predevelopment and development conditions for a part of Nassau and Suffolk Counties, Long Island, New York. Both budgets assume equilibrium conditions with little or no change in storage.



(a)



(a)

Figure 2.5.3 Comparison of water budgets for (a) predevelopment period and (b) the present for Las Vegas, Nevada (from Galloway et al., 1999).

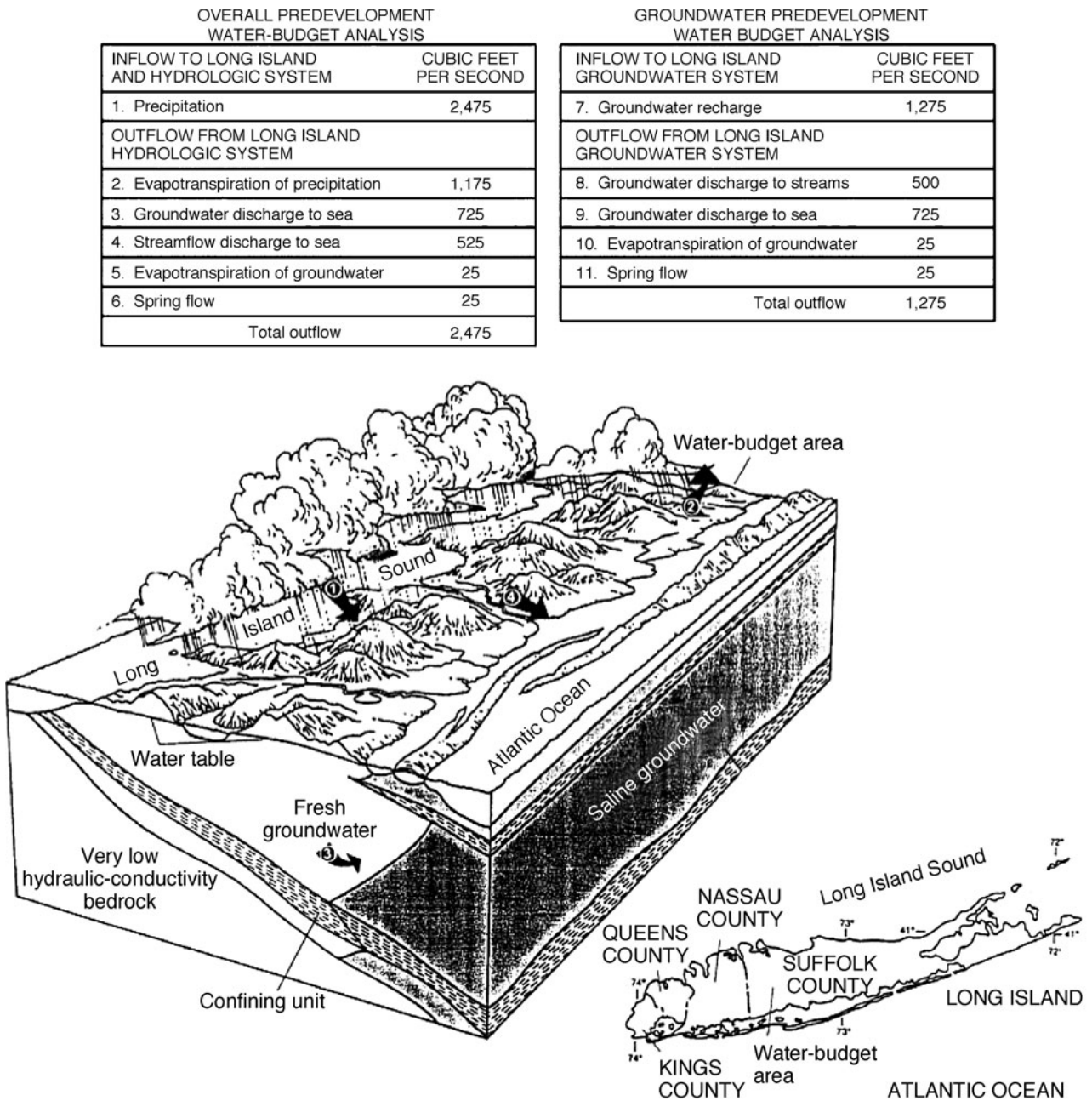


Figure 2.5.4 Groundwater budget for part of Nassau and Suffolk Counties, Long Island, New York. Block diagram of Long Island, New York, and tables listing the overall water budget and groundwater budget under predevelopment conditions. Both water budgets assume equilibrium conditions with little or no change in storage (from Alley et al., 1999).

2.5.2 Water Balance for Tucson, Arizona

To further illustrate the water balance procedure and its importance in water resources sustainability evaluations, Tucson, Arizona, is used. In 1989, Arizona’s Groundwater Management Act (GMA) was passed creating five Active Management Areas (AMAs). These AMAs encompassed Arizona’s most populous, water-stressed regions. One of these AMAs is the Tucson Active Management Area

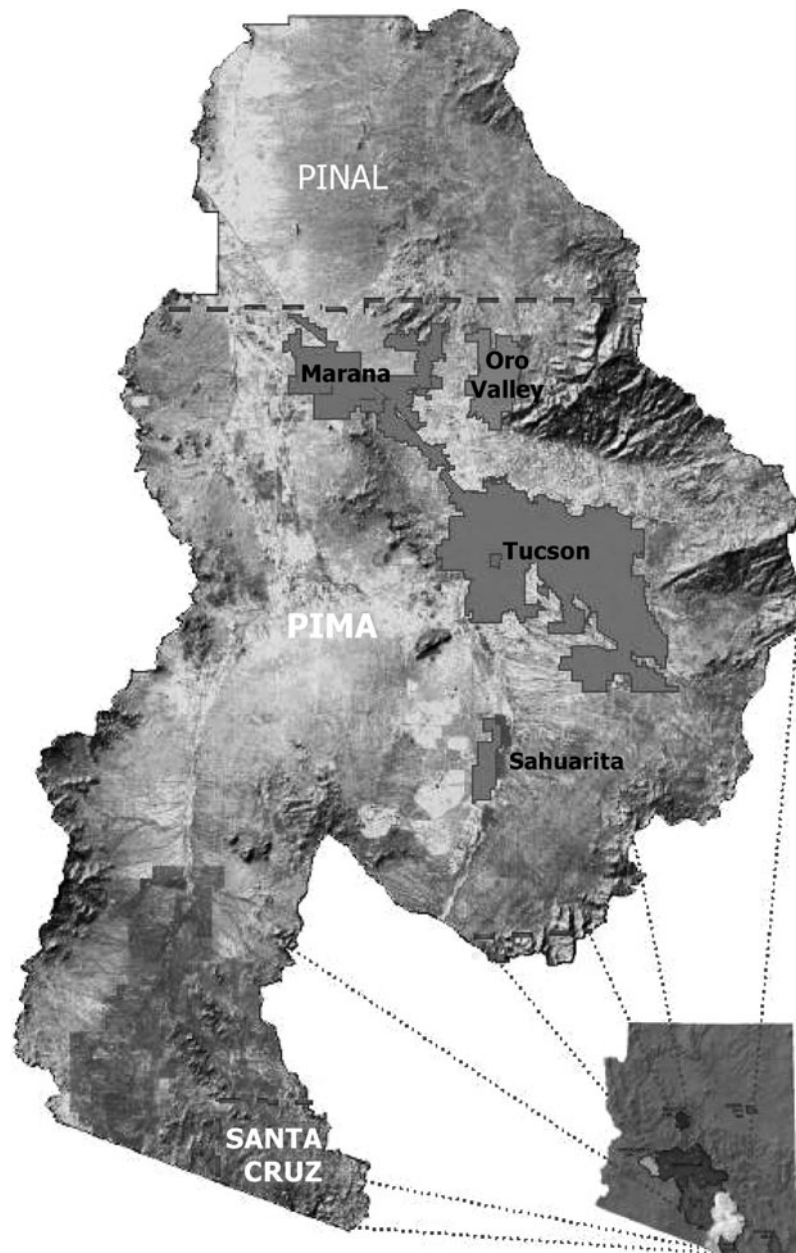


Figure 2.5.5 The Tucson Active Management Area (TAMA).

Source: Arizona Department of Water Resources.

(TAMA), illustrated in Figure 2.5.5, covers 3866 mi². Prior to 2001, the Tucson, Arizona metropolitan area relied entirely on groundwater to satisfy the potable water demand. Because there was no engineered effort to replenish the groundwater resources, the groundwater levels declined up to 4 ft per year in major Tucson wells. Agricultural, industrial, and municipal water are the three primary water use categories. Water demand in the TAMA has outgrown the local renewable groundwater supply, so that sustained growth is possible only because Colorado River water is delivered to the Tucson area via the CAP canal (Figure 2.3.2). However, it must be pointed

Table 2.5.1 The Year 1995 TAMA Water Budget (Demand and Supply)

Demand ($10^6 \text{ m}^3/\text{year}$)	Supply ($10^6 \text{ m}^3/\text{year}$)		
	CAP water	Effluent	Groundwater
Municipal sector	191.8	9.50	182.2
Agricultural sector	120.9	2.22	118.7
Industrial sector	74.3	0.99	73.3
Loss due to evaporation	4.56	0	4.56
Totals:	392	12.7	378.7
Groundwater use			378.7
(Less) Net natural recharge			-75.0
(Less) Incidental recharge ¹			-101.5
Groundwater overdraft			202.2

¹Incidental recharge arises from fractional infiltration of water demands in municipal, agricultural, and industrial sectors. *Source:* Arnold and Arnold (2009).

out that Arizona has the lowest priority use of CAP water, making it the state most vulnerable to shortages. Table 2.5.1 shows the TAMA water budget for 1995.

Referring to Figure 2.5.6, a detailed water balance for the TAMA groundwater resource has the following form:

$$G = S_{gs} + S_c + (RD_m - W) + I_a D_a + I_i D_i + I_m D_m + I_e W - D_a - D_i - D_m \quad (2.5.2)$$

where G is the net annual accumulation of groundwater in the TAMA; S_{gs} is the natural rate of groundwater replenishment ($75 \times 10^6 \text{ m}^3/\text{yr}$); S_c is the volume of CAP water supplied to the TAMA

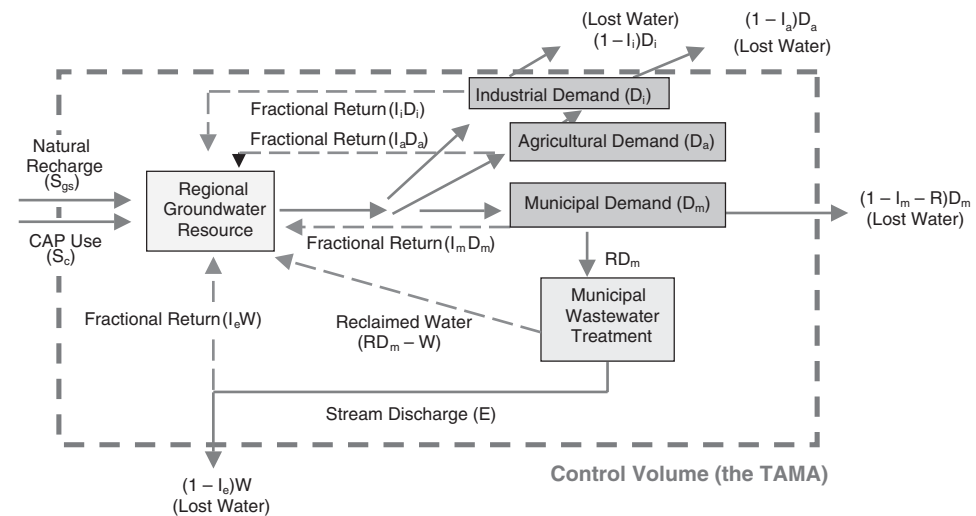


Figure 2.5.6 Water Flow in the Tucson Active Management Area (TAMA). Dotted boundary represents the TAMA control volume used for water balances and sustainability calculations. S_{gs} is the natural rate of groundwater replenishment; S_c is the volume of CAP water supplied to the TAMA; R is the fraction of municipal water demand (D_m) that is recovered, treated and reused or discharged as effluent; D_m , D_i , and D_a are annual municipal, industrial, and agricultural demands; I_m , I_i , and I_a are the fractions of municipal, industrial, and agricultural demands that reenter the ground water as infiltrate; W is the annual volume of wastewater effluent discharged to the Santa Cruz River; and I_e is the fraction of effluent that infiltrates to groundwater in the Santa Cruz River channel (from Arnold and Arnold, 2009).

($\leq 328.8 \times 10^6 \text{ m}^3/\text{yr}$); R is the fraction of municipal water demand (D_m) that is recovered, treated, and reused or discharged as effluent (0.44); D_m , D_i , and D_a are annual municipal, industrial, and agricultural demands; I_m , I_i , and I_a are the fractions of municipal, industrial, and agricultural demands that reenter the groundwater as infiltrate (0.04, 0.12, 0.20); W is the annual volume of wastewater effluent discharged to the Santa Cruz River; and I_e is the fraction of effluent that infiltrates to ground water in the Santa Cruz River channel (0.90).

Equation (2.5.2) can be used to recalculate the maximum sustainable rate of water use in the TAMA using steady conditions for a zero net annual accumulation of groundwater, $G = 0$. Referring to the control volume (Figure 2.5.6), the steady condition is achieved when

$$S_{gs} + S_c = (1 - I_i)D_i + (1 - I_a)D_a + (1 - I_m - R)D_m + (1 - I_e)W \quad (2.5.3)$$

Total water demand is the sum, $D_i + D_a + D_m$, so that under steady (sustainable) conditions,

$$D_i + D_a + D_m = S_{gs} + S_c + I_i D_i + I_i D_a + (I_m + R)D_m + (I_e - 1)W \quad (2.5.4)$$

To maximize the rate of water use, the TAMA must use its entire CAP entitlement ($S_c = S_{c, \max}$) and recycle all municipal wastewater effluent ($W = 0$).

Then

$$(1 - I_m - R)D_m = S_{gs} + S_{c, \max} - (1 - I_i)D_i - (1 - I_a)D_a \quad (2.5.5)$$

or

$$D_m = \frac{S_{gs} + S_{c, \max}}{1 - I_m - R} - \frac{(1 - I_i)D_i}{1 - I_m - R} - \frac{(1 - I_a)D_a}{1 - I_m - R} \quad (2.5.6)$$

in which $R = 0.44$ and $S_{c, \max} = 328.8 \times 10^6 \text{ m}^3 \cdot \text{yr}^{-1}$, etc.

2.6 EXAMPLES OF WATER RESOURCES UNSUSTAINABILITY

2.6.1 Aral Sea

The Aral Sea is located in Central Asia between Uzbekistan and Kazakstan (both countries were part of the former Soviet Union) as shown in Figure 2.6.1. The Amu-Darya and the Syr-Darya (*dar'ya* means river in Turkic) flow into the Aral Sea with no outlet from the sea. Over a 30-year-plus time period, water has been diverted from the Amu-Darya and the Syr-Darya to irrigate millions of acres of land for cotton and rice production, which has resulted in a loss of more than 60 percent of the sea's water. The sea has shrunk from over 65,000 km² to less than half that size, exposing large areas of the lake bed. From 1973 to 1987, the Aral Sea dropped from fourth to sixth among the world's largest inland seas. The satellite photos in Figure 2.6.2 show the Aral Sea in 1985 and 2003, and Figure 2.6.3 illustrates the decrease in size of the Aral Sea from 1957 to 2000.

The lake's salt concentration increased from 10 percent to more than 23 percent, contributing to the devastation of a once-thriving fishing industry. The local climate reportedly has shifted, with hotter, drier summers and colder, longer winters. With the decline in sea level, salty soil has remained on the exposed lake bed. Dust storms have blown up to 75,000 tons of this exposed soil has annually, dispersing its salt particles and pesticide residues. This air pollution has caused widespread nutritional and respiratory ailments, and crop yields have been diminished by the added salinity, even in some of the same fields irrigated with the diverted water. Additional literature on this subject includes Ellis and Turnley (1990), Ferguson (2003), and Perera (1988, 1993).

The major consequences of the continuous desiccation of the Aral Sea since 1960 are summarized as follows:

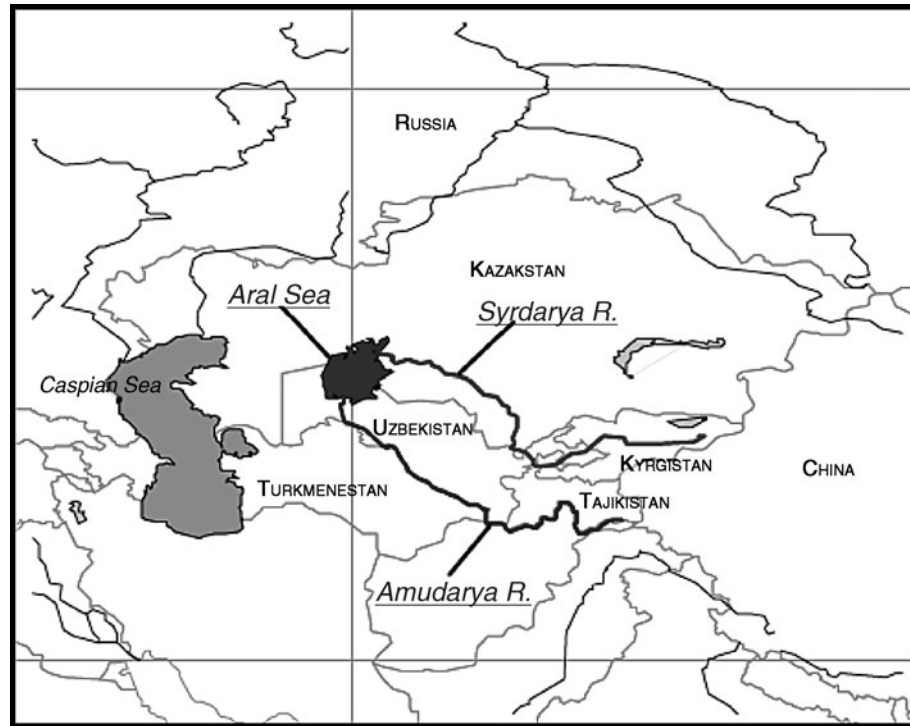


Figure 2.6.1 The Aral Sea Basin (from McKinney, 1996).

- Climatic consequences such as mesoclimatic changes, increase of salt and dust storms, shortening of vegetation period;
- Ecological/economic consequences including degeneration of the delta ecosystems, total collapse of the fishing industry, and decrease of productivity of agricultural fields; and
- Health consequences such as increase in serious diseases, birth defects, and high infant mortality.

People of the region did not make the decision to use the rivers of the Aral Sea basin, but they have certainly suffered the consequences. As stated at the Conference of the Central Asian region ministers, States of Central Asia: Environment Assessment, Aarhus, Denmark, 1998:

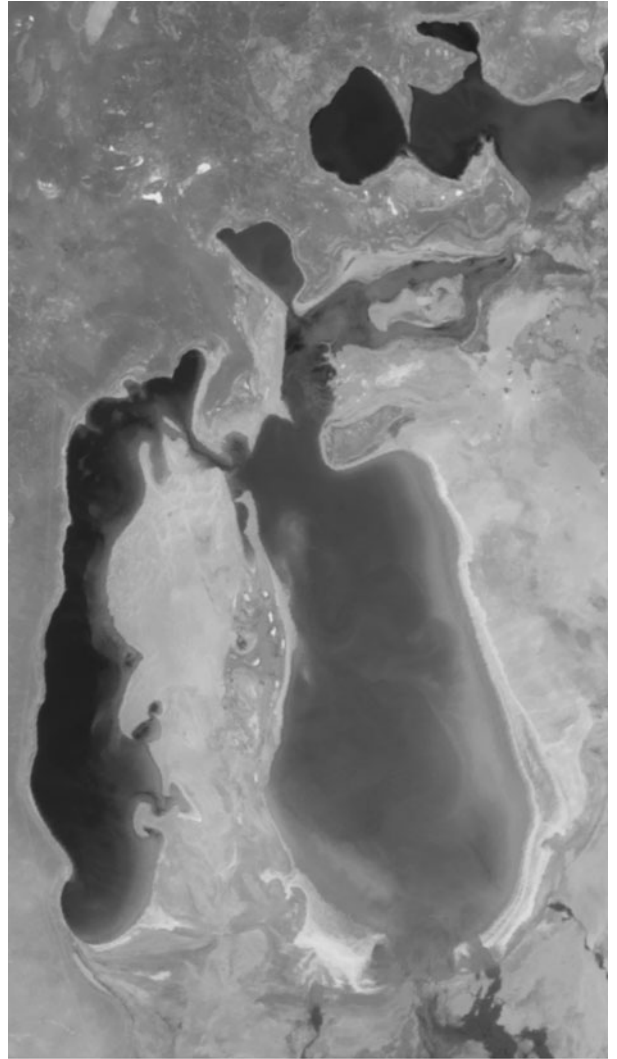
“The Aral crisis is the brightest example of the ecological problem with serious social and economic consequences, directly or indirectly connected with all the states of Central Asia. Critical situation caused by the Aral Sea drying off was the result of agrarian economy tendency on the basis of irrigated agriculture development and volume growth of irrevocable water consumption for irrigation.”

2.6.2 Mexico City

Now let’s look at present day Mexico City, a very large urban center, as another example of water resources unsustainability. Mexico City is the cultural, economic, and industrial center for Mexico. This city is located in the southern part of the Basin of Mexico, which is an extensive, high mountain valley at approximately 2200 m above sea level and surrounded by mountains of volcanic origin with peak altitudes of over 5000 m above sea level.



(a)



(b)

Figure 2.6.2 Comparison of Aral Sea (a) 1989 and (b) 2003 (NASA).

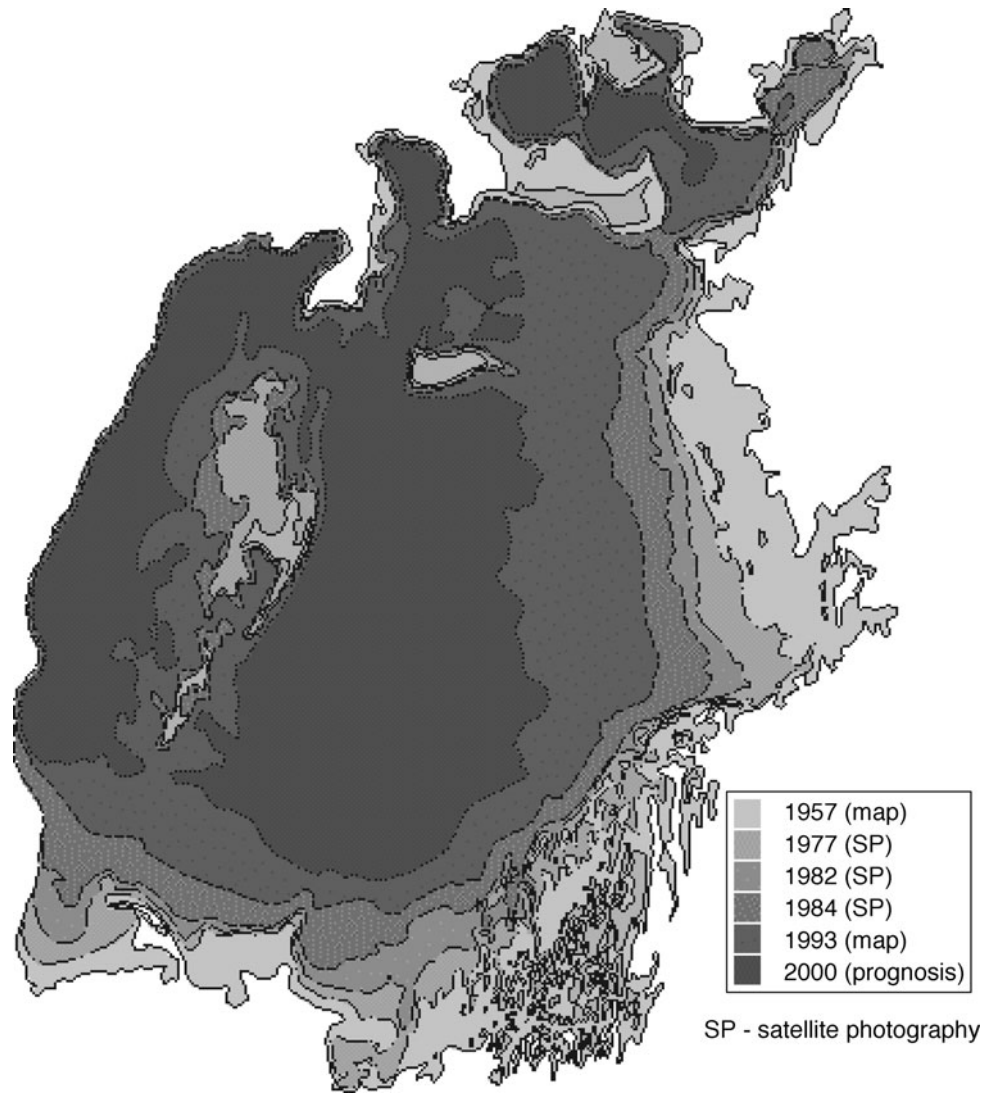


Figure 2.6.3 Aral Sea from 1957 to 2000 from the report “Environment State of the Aral” developed by the International Fund for the Aral Sea (IFAS) and the UN Environment Programme (UNEP) under financial support of the Norway Trust Fund at the World Bank. Coordination from the side of IFAS was held by the Executive Committee of IFAS, and from the side of UNEP–UNEP/GRID-Arendal (<http://enrin.grida.no/aral/aralsea/english/arsea/arsea.htm#2>).

Beginning in the 14th century, the Aztecs made use of a system of aqueducts to convey spring water from the higher elevations in the southern portion of the Basin of Mexico to their city, Tenochtitlan. This ancient city was built on land reclaimed from the saline Lake Texcoco. The Spaniards defeated the Aztecs in 1520, after which they rebuilt the aqueducts and continued to use the spring water until the mid-1850s. Potable groundwater, under artesian conditions, was discovered in 1846. Over the next century, the increased groundwater extraction and the artificial diversions to drain the valley resulted in the drying up of many of the springs, the draining of lakes, loss of pressure in the aquifer with declining groundwater levels, and the consequent subsidence.

Because Mexico City is located on the valley floor, it has always been subject to flooding. Subsidence has worsened this problem by lowering the land surface of Mexico City below the level

of Lake Texcoco, resulting in increased flooding. Drainage systems had to be dug deeper and Lake Texcoco had to be excavated. By 1950, dikes had to be built to confine stormwater flow, and pumping was required to lift drainage water under the city to the level of the drainage canals. By 1953, severe subsidence resulted in the closing of many wells that had to be replaced with new wells.

The Mexico City Metropolitan Area (MCMA) has become a magnet of growth, being the cultural, economic, and industrial center for Mexico, with an estimated population approaching 22 million people. A continual migration of people from rural areas to the city has occurred, with many of the people settling illegally in the urban fringe with the hope of eventually being provided public services. Providing water supply and wastewater services for Mexico City is a formidable challenge. Imagine that the city has the largest population in the world living in an enclosed basin with no natural outflow to the sea. The water supply situation has reached a crisis level, with the continued urban growth and poor system of financing by the government. The consequences include an inability to expand the water supply network to areas that are underserved or not served at all, repair leaks, and provide wastewater treatment. Mexico City cannot meet the water demands of its population.

A case study by Dr. Blanca Jimenez (2008) focuses on water and wastewater management in Mexico City, Mexico, a mega-city experiencing many challenges of urban water management. Mexico City is located in the Mexico Valley, which is a basin of 9600 km² located 2240 m above sea level. The present-day water usage is 85.7 m³/s, of which 48 percent is supplied by the water distribution network, 19 percent is directly pumped from the local aquifer by farmers and industry, and 9 percent is treated wastewater that is reused. Figure 2.6.4 shows the water sources for Mexico City. The first use water (78 m³/s) comes from different sources: 57 m³/s from 1965 wells in the local aquifer located mainly south and west of the city; 1 m³/s from local rivers located in the southern part of the city; 5 m³/s from an aquifer located in the Lerma region 100 km away and 300 m above Mexico City; and 15 m³/s from the Cutzamala River located 130 km away and 1100 m below the city.

The water use varies by the social class of the population as presented in Table 2.6.1. Approximately 40 percent of the 62 m³/s of water distributed to the population is lost due to leakage so that the per capita water use is only 153 L/capita/day instead of 255 L/capita/day.

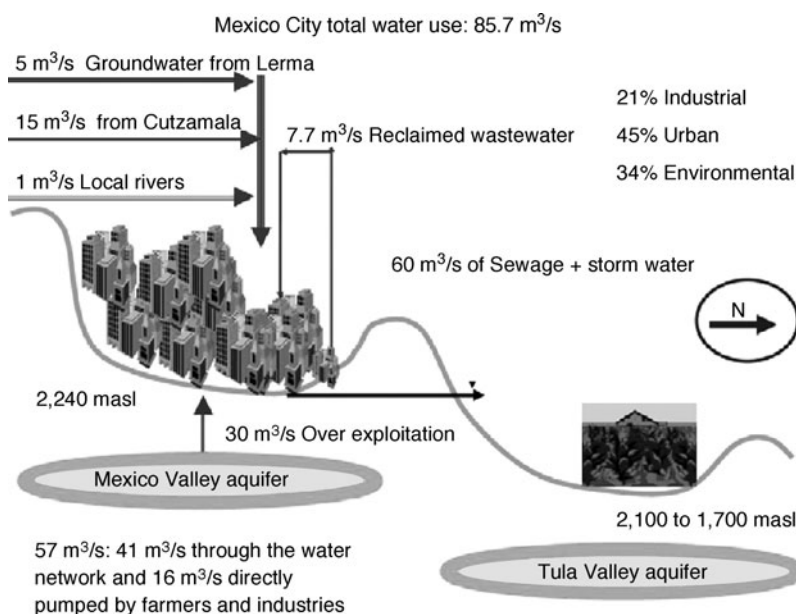


Figure 2.6.4 Water sources for Mexico City (from Jimenez, 2008).

Table 2.6.1 Water Use by Social Class in Mexico City

Social class	Water supply (L/capita/day)	% of the population	Total volume of water demanded (m ³ /s)
Low	128	76.5	9.0
Medium	169	18.0	15.7
Medium	399	3.6	1.3
High	567	1.9	1.0
Total			27.0

Source: DGCOH, 1998, as presented in Jimenez (2008).

The wastewater produced (approximately 67.7 m³/s on a year-round basis), includes pluvial excess water (collected for only six months) and sewage. Total capacity of public wastewater treatment plants is 15 m³/s, but only 11 percent (7.7 m³/s) of the total produced is treated. All of the treated wastewater is reused to fill recreation lakes and canals (54 percent), irrigation (31 percent), industrial cooling (8 percent), diverse commercial uses (5 percent), and recharge (2 percent) (DGCOH, 1998). The system built to drain the excess pluvial water and sewage out of the Mexico Valley is shown in Figure 2.6.5. Three tunnels, the Western Interceptor, the Gran Canal, and the Central Canal were built in 1896, 1989,

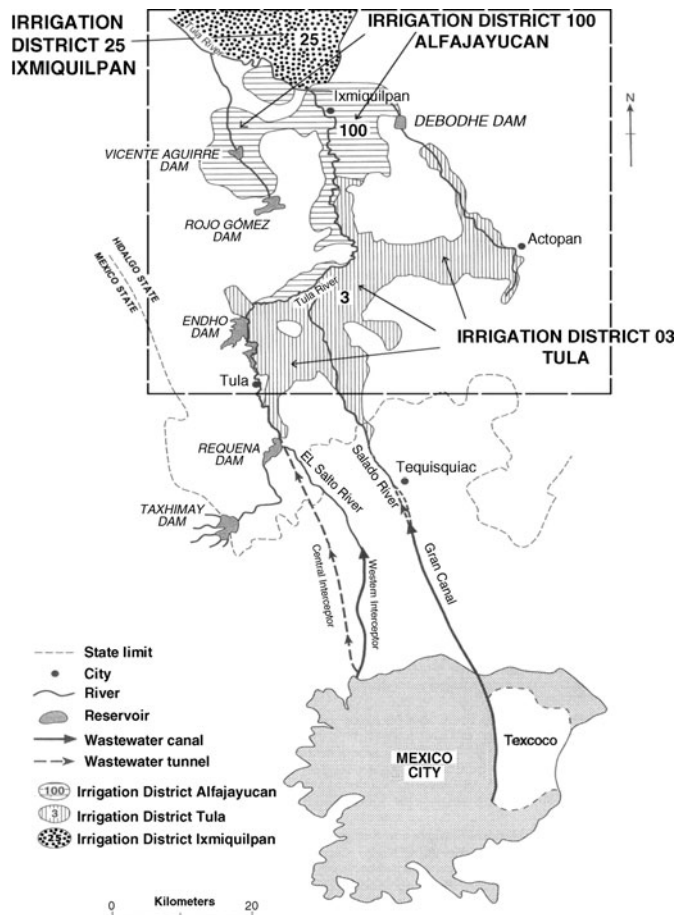


Figure 2.6.5 Mexico City’s wastewater disposal drainage system and main components of the irrigation system in the Tula Valley (from Jimenez, 2008).

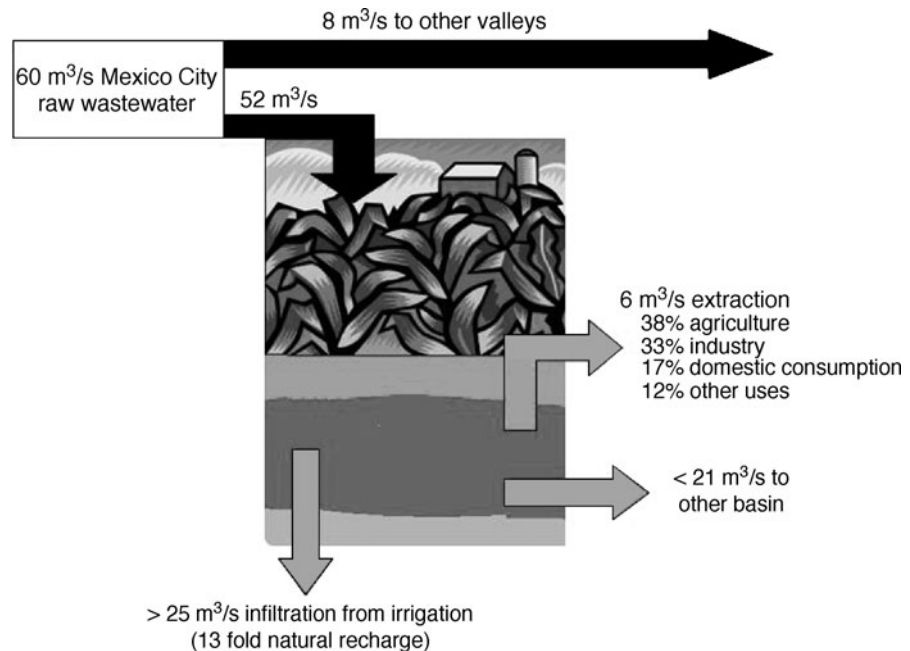


Figure 2.6.6 Water balance of Tula Valley (from Jimenez, 2008).

and 1975, respectively, to transport wastewater to the Tula Valley. The Western Interceptor and the Central Canal are part of the Deep Drainage (see Figure 2.6.5). Average annual volume of water disposed is approximately $60 \text{ m}^3/\text{s}$ (80 percent sewage and 20 percent stormwater); the actual wastewater flow varies from $52 \text{ m}^3/\text{s}$ to greater than $300 \text{ m}^3/\text{s}$.

The Tula Valley shown in Figure 2.6.5 is located 100 km north of Mexico City at an altitude varying from 2100 m in the southern part to 1700 m in the northern part. Because of the wastewater transported for agricultural purposes, the local economy of Tula Valley was improved because of the increased agricultural production. However, serious health problems were created because of the use of untreated wastewater for irrigation. Figure 2.6.6 shows the water balance of $52 \text{ m}^3/\text{s}$ to the Tula Valley and $8 \text{ m}^3/\text{s}$ to other valleys. The wastewater in Tula Valley is transported in hundreds of unlined channels, stored in dams, and applied to the soils using high irrigation rates to wash out salts. As illustrated in Figure 2.6.6, the aquifer has a high recharge rate of greater than $25 \text{ m}^3/\text{s}$ of infiltration from irrigation, which is 13 times the natural recharge (Jimenez and Chavez, 2004). The Tula River flow, which is partially fed from the aquifer, increased significantly as the aquifer level rose.

Mexico City is unique in having the following situations:

- Water transfers from other basins causing problems in the basins from which water was transferred.
- Over-exploitation of groundwater caused huge soil subsidence, resulting in loss of sewage and drainage capacity, leaks in water distribution and wastewater collection networks, deterioration of groundwater quality, and other problems such as serious structural problems with buildings and the releveling of metro rails.
- Very large leakage from the water distribution system (37–40 percent of water conveyed is lost to leakage, $23 \text{ m}^3/\text{s}$ loss).
- Of the wastewater produced ($67.7 \text{ m}^3/\text{s}$), only 11 percent ($7.7 \text{ m}^3/\text{s}$) is treated. Untreated wastewater is transferred to the Tula Valley 100 km north of Mexico City for irrigation purposes (agricultural use), resulting in serious health problems.

- Because of the large recharge of untreated wastewater (13 times the natural recharge) in the Tula Valley, the water table has risen and the Tula River flow has increased significantly. Water quality of the recharged wastewater is reasonably safe; however, chlorination is not the best option for disinfection.
- Wastewater recharge formed a new water course and completely modified the ecology of the Tula Valley from a semi-desert area to having springs and wetlands.

Options for integrated water management would include development of a new metropolitan water authority with the following activities: control soil subsidence, protect groundwater quality, reduce large leakage in the water distribution system, implement aggressive and innovative waste water reuse programs, perform innovative and comprehensive educational program, improve economic tools, harvest rainwater, and implement professional public participation programs.

PROBLEMS

- 2.2.1 Describe how all the goals of the Millennium Development Goals (MDGs) can be related directly or indirectly to water.
- 2.2.2 Write a description of the U.S. Geological Survey's NAWQA program.
- 2.2.3 Develop a write-up describing the World Water Assessment Program.
- 2.2.4 Download the most recent U.S. Drought Monitor and compare the condition to Figure 2.2.5.
- 2.2.5 Download the U.S.G.S. Circular 86 and write a summary of the water-related effects of urbanization on Long Island, New York.
- 2.2.6 Search the latest IPCC Reports and write a summary of the water-related climate change effects in the United States.
- 2.2.7 Search the latest IPCC Reports and write a summary of the water-related climate change effects in Europe.
- 2.2.8 Search the latest IPCC Reports and write a summary of the water-related climate change effects in Africa.
- 2.2.9 What are the definitions of meteorological droughts, agricultural droughts, and hydrological droughts?
- 2.2.10 What is your water footprint? Refer to www.waterfootprint.org.
- 2.3.1 Using the data in Tables 2.4.1 and 2.4.2 develop a curve of the cumulative recharge and the cumulative discharge from the Edwards Aquifer as a function of time for the period 1980–2001. Discuss the results.
- 2.4.1 Describe the water-related organizations in your community and how they interrelate for overall urban water management including water supply management and water excess management.
- 2.4.2 Write an essay on how the conjunctive management of surface and groundwater help to obtain water resources sustainability.
- 2.5.1 Develop a water balance equation for the urban area in which you live.
- 2.5.2 Use the data in Table 2.5.1 for the TAMA to determine the groundwater overdraft needed if the municipal sector demand increased to 210×10^6 m³/year and the CAP water was no longer available.
- 2.5.3 Using the data for TAMA in Table 2.5.1, if the agricultural sector demand were decreased to 60×10^6 m³/year what effect would this have on the groundwater overdraft?
- 2.5.4 Assume a worst case scenario for the TAMA in which no water is available from the CAP, agricultural demand is reduced to 0, and net annual accumulation of groundwater is not 0. Derive an expression for the municipal demand.

REFERENCES

- Allan, J. A., Fortunately there are substitutes for water otherwise our hydro-political futures would be impossible. Priorities for water resources allocation and management, ODA, London, pp. 13–26, 1993.
- Allan, J. A., “Overall Perspectives on Countries and Regions,” in *Water in Arab World: Perspective and Prognoses*, edited by P. Rogers and P. Lydon, Harvard University Press, Cambridge, MA, pp. 65–100, 1994.
- Alley, W. M., T. E. Reilly, and O. L. Franke, *Sustainability of Ground-Water Resources*, U.S. Geological Survey Circular 1186, U.S. Geological Survey, Denver, CO, 1999.
- Arnold, R. G., and K. P. Arnold, “Integrated Urban Water Management in the Tucson, Arizona Metropolitan Area,” *Integrated Urban Water Management: Arid and Semi-Arid (ASA) Regions*, edited by L. W. Mays UNESCO-IHP, Paris, France, 2009.
- Brundtland Commission, *Our Common Future*, World Commission on Environment and Development (WCED), 1987.
- DGCOH (General Department of Construction and Hydraulic Operation), *The Water Situation in the Federal District*, Gobierno del DF. (in Spanish), 1998.
- Ellis, W. S., and D. C. Turnley, “A Soviet Sea Lies Dying,” *National Geographic*, vol. 177, no. 2, February, pp. 73–93, 1990.
- Espeland, W. N., *The Struggle for Water: Politics, Rationality, and Identity in the American Southwest*, the University of Chicago Press, Chicago, IL, 1998.

- Ferguson, R. W., *The Devil and the Disappearing Sea: Murder & Mayhem Amid the Aral Sea Disaster*, Raincoast Books, Vancouver, 2003.
- FLOW (Friends of the Lower Olentangy Watershed), "The Lower Olentangy Watershed Action Plan in 2003—Strategies for Protecting and Improving Water Quality and Recreational Use of the Olentangy River and Tributary Streams in Delaware and Franklin Counties," Columbus, OH. <http://www.olentangywatershed.org/LowerOlentangyActionPlan04.pdf>, 2003.
- Galloway, D., D. Jones, and S. Ingebritsen, (editors), *Land Subsidence in the United States*, U.S. Geological Survey Circular 1182, <http://water.usgs.gov/pubs/circ/circ1182>. Denver, CO, 1999.
- Gleick, P. H. et al., *The World's Water 2004–2005, The Biennial Report on Freshwater Resources*, Island Press, 2004.
- Gleick, P. H., P. Loh, S. Gomez, and J. Morrison, *California Water 2020: A Sustainable Vision*, Pacific Institute for Studies in Development, Environment and Security, Oakland, California, 1995.
- Grigg, N. S., *Urban Water Infrastructure – Planning, Management, and Operations*, Wiley-Interscience, New York, 1986.
- Hamlet, A. F. and D. P. Lettenmaier, "Effects of Climate Change on Hydrology and Water Resources Objectives in the Columbia River Basin," *Journal of the American Water Resources Association*, vol. 35, pp. 1597–1624, 1999.
- Heath, R. C., *Basic Ground-Water Hydrology*, U.S. Geological Survey Water-Supply Paper 2220, 1998.
- Hoekstra, A. Y. and A. K. Chapagain, Water Footprints of Nations: Water Use by People as a Function of their Consumption Pattern, *Water Resources Management*, 21, pp. 35–48, 2007.
- Hoekstra, A. Y. and P. Q. Hung, *Virtual Water Trade: A Quantification of Virtual Water Flows between Nations in Relation to International Crop Trade*, Value of Water Research Report Series, No. 11, UNESCO-IHE, Delft, The Netherlands, 2002. <http://www.waterfootprint.org/Reports/Report11.pdf>.
- Hoyois, P. and D. Guha-Sapir, *Three Decades of Floods in Europe: A Preliminary Analysis of EMDAT data*, Centre for Research on the Epidemiology of Disasters, Catholique University of Louvain, Working Paper No. 197, April 2003.
- International Panel on Climate Change (IPCC), *Climate Change 2007: Synthesis Report*, 2007.
- Jimenez, B., "Water and Wastewater Management in Mexico City, Case Study," in *Integrated Urban Water Management: Arid and Semi-arid (ASA) Regions*, edited by L. W. Mays, UNESCO-IHP, Paris, France, 2008.
- Jimenez, B. and A. Chávez, "Quality Assessment of an Aquifer Recharged with Wastewater for its Potential Use as Drinking Source: 'El Mezquital Valley' case," *Water Science and Technology*, vol. 50, no. 2, pp. 269–273, 2004.
- Kahan, J. P., M. Wu, S. Hajiamiri, and D. Knopman, *From Flood Control to Integrated Water Resource Management: Lessons for the Gulf Coast from Flooding in Other Places in the Last Sixty Years*, Gulf States Policy Institute, Rand Corporation, Santa Monica, CA, 2006.
- Kuniansky, E. L., L. Fahlquist, and A. F. Ardis, "Travel Times along Selected Flow Paths of the Edwards Aquifer, Central Texas," in *U.S. Geological Survey Karst Interest Group Proceedings*, edited by E. L. Kuniansky, U. S. Geological Survey Water-Resources Investigations Report 01-4011, 2001.
- Leeds, R., L. C. Brown, and N. L. Watermeier, *Nonpoint Source Pollution: Water Primer. AEX-465-93. Ohio State University Extension Fact Sheet*. Food, Agricultural and Biological Engineering, The State University of Ohio, Columbus, OH, 1993. <http://ohioline.osu.edu/aex-fact/0465.html>.
- Marsalek J. et al. *Urban Water Cycle: Processes and Interactions*, IHP-VI Technical Publications in Hydrology, no. 78, UNESCO, Paris, 2006.
- Marshall, J., "Megacity, mega mess . . .," *Nature*, vol. 437, pp. 312–314, September 15, 2005.
- Mays, L. W., (editor), *Water Resources Sustainability*, McGraw-Hill, New York, 2007.
- McCann, B., "Resource Risks of Climate Change," in *Water 21*, IWA Publishing, London, October, pp. 16–18, 2006.
- McKinney, D., "Sustainable Water Management in the Aral Sea Basin," in *Water Resources Update*, Universities Council on Water Resources, no. 102, Winter, 1996.
- Miles, E. L., A. K. Snover, A. F., Hamlet, B. Callahan, and D. Fluharty, "Pacific Northwest Regional Assessment: Impacts of the Climate Variability and Climate Change on the Water Resources of the Columbia River Basin," *Journal of the American Water Resources Association*, vol. 36, no. 2, pp. 399–420, April 2000.
- Mortada, H., "Confronting the Challenges of Urban Water Management in Arid Regions: Geographic, Technological, Sociocultural, and Psychological Issues," *Journal of Architectural and Planning Research*, vol. 22, no. 1, Spring, 2005.
- Perera, J., "Where Glasnost Meets the Greens," *New Scientist*, vol. 120, no. 1633, October 8, p. 25–26 1988.
- Perera, J., "A Sea Turns to Dust," *New Scientist*, vol. 140, no. 1896, pp. 24–27, 1993.
- Puente, C., *Method of Estimating Natural Recharge to the Edwards Aquifer in the San Antonio Area, Texas*, U.S. Geological Survey Water- Investigations Report 78–10, 1978.
- Slattery, R. N. and D. E. Thomas, *Recharge to and Discharge from the Edwards Aquifer in the San Antonio Area*, 2001, <http://tx.usgs.gov/reports/dist/dist-2002-01>, San Antonio, TX, October 2002.
- Squillace, P. J. and C. V. Price, *Urban-Land-Use Study Plan for the National Water Quality Assessment Program*, U.S. Geological Survey Open-File Report 96–217, 1996.
- United Nations Children's Fund, *The State of the World's Children 2005: Childhood under Threat*, UNICEF, New York, 2004.
- United Nations, *Report of the World Summit on Sustainable Development, Johannesburg*, South Africa, 26 August – 4 September 2002, United Nations Publications, 2002.
- Water Science and Technology Board, *Colorado River Basin Water Management: Evaluating and Adjusting to Hydroclimatic Variability*, Committee on the Scientific Bases of Colorado River Basin Water Management, Division on Earth and Life Studies, National Research Council of the National Academies, The National Academies Press, Washington, D. C., 2007.
- World Water Assessment Program, *Water, a Shared Responsibility: The UN World Water Development Report 2*, UNESCO and Berghahn Books, 2006.

This page intentionally left blank

Chapter 3

Hydraulic Processes: Flow and Hydrostatic Forces

3.1 PRINCIPLES

The purpose of this chapter is to present some of the fundamental principles of fluid mechanics including fluid properties. Much greater detail can be found in fluid mechanics texts such as the excellent books by Crowe et al. (2009), Finnemore and Fraizini (2002), Fox et al. (2009), and Munson et al. (2002).

3.1.1 Properties Involving Mass or Weight of Water

Mass density, often called *density*, is the mass per unit volume, with units of kilograms (kg) per cubic meter (m^3) or $N \cdot s^2/m^4$ in SI units. The Greek symbol ρ (rho) is used to denote density. The mass density of water at $4^\circ C$ is $1000 \text{ kg}/m^3$ or $1.94 \text{ slugs}/ft^3$. For most applications in hydrologic and hydraulic processes, the density is assumed to be constant so that water is assumed incompressible. Incompressibility does not always mean constant density because salt in water changes the density of water without changing its volume.

Specific weight is the gravitational force (weight) per unit volume of water, denoted by the Greek symbol γ (gamma). The specific weight of water at $4^\circ C$ is $9810 \text{ N}/m^3$ or $62.4 \text{ lb}/ft^3$. The relationship between density and specific weight is

$$\rho = \frac{\gamma}{g} \quad (3.1.1)$$

Specific gravity of a fluid refers to the ratio of the specific weight of a given liquid to the specific weight of water. Tables 3.1.1 and 3.1.2 list the various physical properties of water in English units and SI units, respectively. The relationship between temperature scales is $^\circ C = \frac{5}{9}(^\circ F - 32)$ or $^\circ F = \frac{9}{5}^\circ C + 32$.

3.1.2 Viscosity

In the flow of water shear force exists, producing fluid friction. *Viscosity* is the measure of its resistance to shear or angular deformation. For a velocity gradient, dv/dy , the shear stress τ (tau) between any two thin sheets of fluid is

$$\tau = \mu \frac{dv}{dy} \quad (3.1.2)$$

Table 3.1.1 Physical Properties of Water in English Units

Temp. (°F)	Specific weight, γ (lb/ft ³)	Density, ρ (slugs/ft ³)	Viscosity, $10^{-5}\mu$ (lb·sec/ft ²)	Kinematic viscosity, $10^{-5}\nu$ (ft ² /sec)	Surface tension, 100σ (lb/ft)	Vapor-pressure head, p_v/γ (ft)	Bulk modulus of elasticity, $10^3\beta$ (lb/in ²)
32	62.42	1.940	3.746	1.931	0.518	0.20	293
40	62.43	1.940	3.229	1.664	0.514	0.28	294
50	62.41	1.940	2.735	1.410	0.509	0.41	305
60	62.37	1.938	2.359	1.217	0.504	0.59	311
70	62.30	1.936	2.050	1.059	0.500	0.84	320
80	62.22	1.934	1.799	0.930	0.492	1.17	322
90	62.11	1.931	1.595	0.826	0.486	1.61	323
100	62.00	1.927	1.424	0.739	0.480	2.19	327
110	61.86	1.923	1.284	0.667	0.473	2.95	331
120	61.71	1.918	1.168	0.609	0.465	3.91	333
130	61.55	1.913	1.069	0.558	0.460	5.13	334
140	61.38	1.908	0.981	0.514	0.454	6.67	330
150	61.20	1.902	0.905	0.476	0.447	8.58	328
160	61.00	1.896	0.838	0.442	0.441	10.95	326
170	60.80	1.890	0.780	0.413	0.433	13.83	322
180	60.58	1.883	0.726	0.385	0.426	17.33	313
190	60.36	1.876	0.678	0.362	0.419	21.55	313
200	60.12	1.868	0.637	0.341	0.412	26.59	308
212	59.83	1.860	0.593	0.319	0.404	33.90	300

Table 3.1.2 Physical Properties of Water in SI Units

Temp. (°C)	Specific weight, γ (N/m ³)	Density, ρ (kg/m ³)	Viscosity, $10^{-3}\mu$ (N·s/m ²)	Kinematic viscosity, $10^{-6}\nu$ (m ² /s)	Surface tension, 100σ (N/m)	Vapor-pressure head, p_v/γ (m)	Bulk modulus of elasticity, $10^7\beta$ (N/m ²)
0	9805	999.9	1.792	1.792	7.62	0.06	204
5	9806	1000.0	1.519	1.519	7.54	0.09	206
10	9803	999.7	1.308	1.308	7.48	0.12	211
15	9798	999.1	1.140	1.141	7.41	0.17	214
20	9789	998.2	1.005	1.007	7.36	0.25	220
25	9779	997.1	0.894	0.897	7.26	0.33	222
30	9767	995.7	0.801	0.804	7.18	0.44	223
35	9752	994.1	0.723	0.727	7.10	0.58	224
40	9737	992.2	0.656	0.661	7.01	0.76	227
45	9720	990.2	0.599	0.605	6.92	0.98	229
50	9697	988.1	0.549	0.556	6.82	1.26	230
55	9679	985.7	0.506	0.513	6.74	1.61	231
60	9658	983.2	0.469	0.477	6.68	2.03	228
65	9635	980.6	0.436	0.444	6.58	2.56	226
70	9600	977.8	0.406	0.415	6.50	3.20	225
75	9589	974.9	0.380	0.390	6.40	3.96	223
80	9557	971.8	0.357	0.367	6.30	4.86	221
85	9529	968.6	0.336	0.347	6.20	5.93	217
90	9499	965.3	0.317	0.328	6.12	7.18	216
95	9469	961.9	0.299	0.311	6.02	8.62	211
100	9438	958.4	0.284	0.296	5.94	10.33	207

where μ (mu) is the dynamic viscosity and v is the velocity. The velocity gradient is the time rate of strain. Thus the definition of dynamic viscosity is the ratio of shear stress to the velocity gradient,

$$\mu = \frac{\tau}{dv/dy} \quad (3.1.3)$$

Kinematic viscosity is the ratio of the dynamic viscosity to the density in which the gradient force dimension cancels out in μ/ρ . The Greek symbol ν (nu) is used to identify the kinematic viscosity

$$\nu = \mu/\rho \quad (3.1.4)$$

Kinematic viscosity has been defined because many equations include μ/ρ . Refer to Tables 3.1.1 and 3.1.2 for values of viscosity as a function of temperature.

The shear stress in fluids is involved with the cohesion forces between molecules. Stress applied to fluids causes motion, whereas solids can resist shear stress in a static condition. Considering flow of water in a pipe, the water near the center of the pipe has a greater velocity than the water near the wall. Shear force is increased or decreased in direct proportion to increases or decreases in relative velocity.

Shear stress has units of N/m^2 . Dynamic viscosity has units of

$$\mu = \frac{\tau}{\frac{dv}{dy}} \equiv \frac{\text{N/m}^2}{(\text{m/s})/\text{m}} = \frac{\text{N} \cdot \text{s}}{\text{m}^2}$$

Kinematic viscosity has units of

$$\nu = \frac{\mu}{\rho} \equiv \frac{\text{N} \cdot \text{s}/\text{m}^2}{\text{N} \cdot \text{s}/\text{m}^4} = \frac{\text{m}^2}{\text{s}}$$

The SI unit for dynamic viscosity is centipoise (cP), in which $1 \text{ cP} = 1 \text{ N} \cdot \text{s}/\text{m}^2 \times 10^{-3}$. The SI unit for kinematic viscosity is centistoke (cst), in which $1 \text{ cst} = 1 \text{ m}^2/\text{s} \times 10^{-6}$.

Ideal fluids are defined as the ones in which viscosity is zero, i.e., there is no friction. Such fluids do not exist in reality but the concept is useful in many types of fluid analysis. *Real fluids* do consider viscosity effects so that shear force exists whenever motion takes place, thus producing fluid friction.

3.1.3 Elasticity

Elasticity (or *compressibility*) is important when we talk about water hammer in the hydraulics of pipe flow. Elasticity of water is related to the amount of deformation (expansion or contraction) induced by a pressure change. Elasticity is characterized by the *bulk modulus of elasticity*, E , which is defined as the ratio of relative change in volume, dV/V , due to a differential change in pressure, dp , so that

$$E = -\frac{dp}{dV/V} \quad (3.1.5)$$

Also $-d\rho/\rho = dV/V$, so that

$$E = \frac{dp}{d\rho/\rho} \quad (3.1.6)$$

Refer to Tables 3.1.1 and 3.1.2 for values of the bulk modulus of elasticity as a function of temperature.

3.1.4 Pressure and Pressure Variation

Pressure, p , is the force F acting over an area A , denoted as

$$p = \lim_{\Delta A \rightarrow 0} \frac{\Delta F}{\Delta A} = \frac{dF}{dA} \tag{3.1.7}$$

Pressure at a point is equal in all directions. The pressure at a depth y (neglecting pressure on the surface of water) is

$$p = \gamma y \tag{3.1.8}$$

Units of pressure are N/m^2 (Pascal), lb/in^2 (psi), lb/ft^2 , feet of water, and inches of mercury.

Gauge pressure uses atmospheric pressure as the datum. Absolute pressure is the pressure above absolute zero. Vacuum refers to pressure less than atmospheric pressure. At absolute zero, pressure is a perfect vacuum. Figure 3.1.1 illustrates the relationship among various pressures.

The pressure force F exerted by water on a plane area A is the product of the area and the pressure at its centroid, expressed as

$$F = pA = \gamma y_c A \tag{3.1.9}$$

where y_c is the vertical depth of the water over the centroid.

For static water, the only variation in pressure is with the elevation in the fluid, i.e.,

$$\frac{dp}{dz} = -\gamma \tag{3.1.10}$$

where z refers to elevation. Equation (3.1.10) is the basic equation for hydraulic pressure variation with elevation. For water on a horizontal plane, the pressure everywhere on this plane is constant. The greatest possible change in hydrostatic pressure occurs along a vertical path through water.

Considering the specific weight to be constant, equation (3.1.10) can be integrated to obtain

$$p = -\gamma z + \text{constant} \tag{3.1.11}$$

or

$$\left(\frac{p}{\gamma} + z\right) = \text{constant} \tag{3.1.12}$$

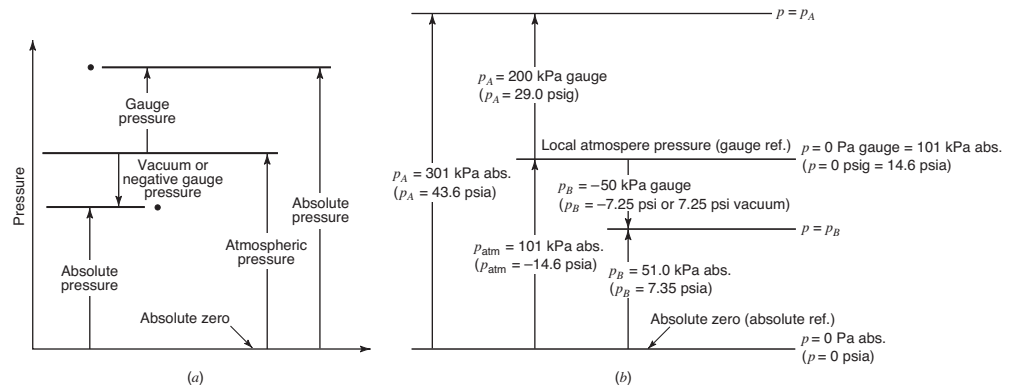


Figure 3.1.1 (a) Relationship between various pressures (from Chaudhry (1996)); (b) Example of pressure relation (from Roberson & Crowe (1993)).

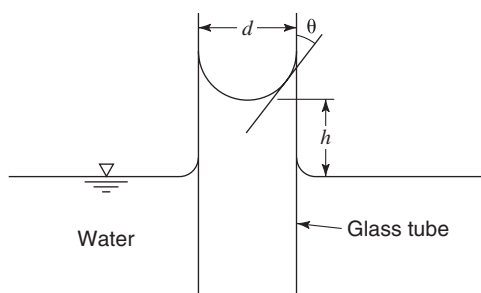


Figure 3.1.2 Capillary action. The effect of surface tension is illustrated for the capillary rise in a small glass tube. θ is the angle of the tangent to the meniscus where it contacts the wall of the tube. Surface tension force acts around the circumference of the tube.

The term $(p/\gamma + z)$ is called the *piezometric head*, which is then constant through any incompressible static fluid. The pressure and elevation at two different points in a static incompressible fluid are then

$$\frac{p_1}{\gamma} + z_1 = \frac{p_2}{\gamma} + z_2 \quad (3.1.13)$$

3.1.5 Surface Tension

Molecules of water below the surface act on each other by forces that are equal in all directions. Molecules near the surface have a greater attraction for each other. Molecules on the surface are not able to bond in all directions and consequently form stronger bonds with adjacent molecules. The water surface acts like a stretched membrane seeking a minimum possible area by exerting a tension on the adjacent portion of the surface or an object in contact with the water surface. This *surface tension* acts in the plane of the surface as illustrated in Figure 3.1.2 for capillary action. Refer to Tables 3.1.1 and 3.1.2 for values of surface tension as a function of temperature.

3.1.6 Flow Visualization

There are two viewpoints on the motion of fluids, the *Eulerian* viewpoint and the *Lagrangian* viewpoint. The Lagrangian viewpoint focuses on the motion of individual fluid particles and follows these particles for all time. It is more common, however, in hydrologic and hydraulic processes to consider that fluids form a continuum wherein the motion of particles is not traced. This Eulerian viewpoint then focuses on a particular point or control volume in space and considers the motion of fluid that passes through as a function of time.

Streamlines are lines drawn through a fluid field so that the velocity vectors of the fluid at all points on the streamlines are tangent to the streamline at any instant in time. The tangent of the curve at any point along the streamline is the direction of the velocity vector at that point in the flow field. Examples of streamlines are shown in Figure 3.1.3. In the Eulerian viewpoint, the total velocity is expressed as a function of position along a streamline, x , and time, t .

$$\mathbf{V} = \mathbf{V}(x, t) \quad (3.1.14)$$

A *uniform flow* is defined as one in which the velocity does not change from point to point along any of the streamlines in the flow field. Thus the streamlines are straight and parallel, so that

$$\frac{\partial \mathbf{V}}{\partial x} = 0 \quad (\text{uniform flow}) \quad (3.1.15)$$

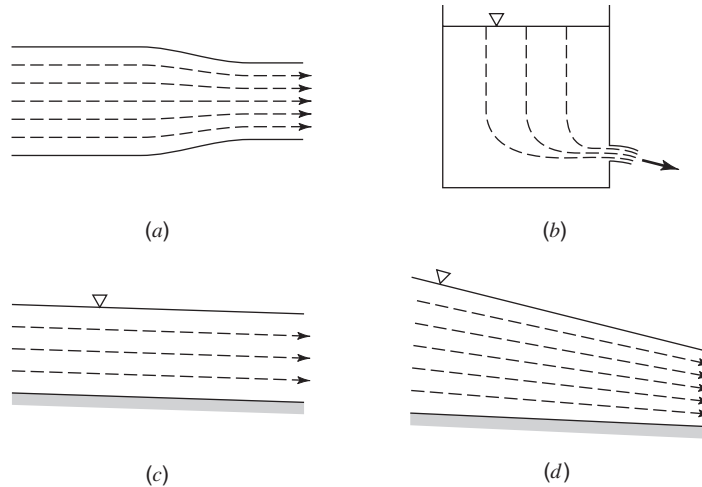


Figure 3.1.3 Streamlines. (a) Flow in a conduit; (b) Flow from a slot; (c) Open-channel flow (uniform); (d) Open-channel flow (nonuniform).

When streamlines are not straight there is a directional change in velocity. If they are not parallel, there is a change in speed along the streamlines. Under such circumstances the flow is *nonuniform flow* and

$$\frac{\partial \mathbf{V}}{\partial x} \neq 0 \text{ (nonuniform flow)} \tag{3.1.16}$$

So this flow pattern has streamlines that are curved in space (converging or diverging) as shown in Figure 3.1.3(d) for nonuniform open-channel flow.

The variation in velocity with respect to time at a given point in a flow field is also used to classify flow. *Steady flow* occurs when the velocity at a point in the flow field does not vary in magnitude or direction with respect to time:

$$\frac{\partial \mathbf{V}}{\partial t} = 0 \text{ (steady flow)} \tag{3.1.17}$$

Unsteady flow occurs when the velocity does vary in magnitude or direction at a point in the flow field with respect to time.

3.1.7 Laminar and Turbulent Flow

Turbulent flow is caused by eddies of varying size within the flow that create a mixing action. The fluid particles follow irregular and erratic paths and no two particles have similar motion. Turbulent flow then is irregular with no definite flow patterns. Flow in rivers is a good example of turbulent flow. The index used to relate to turbulence is the *Reynolds number*

$$R_e = \frac{VD\rho}{\mu} = \frac{VD}{\nu} \tag{3.1.18}$$

where D is a characteristic length such as the diameter of a pipe. For pipe flow, the flow is generally turbulent for $R_e > 2000$.

Laminar flow does not have the eddies that cause the intense mixing and therefore the flow is very smooth. The fluid particles move in definite paths and the fluid appears to move by the sliding of laminations of infinitesimal thickness relative to the adjacent layers. The viscous shear of the

fluid particles produces the resistance to flow. The resistance to flow varies with the first power of the velocity. For pipe flow, the flow is generally laminar for $R_e < 2000$.

Flow can be *one-, two-, or three-dimensional flow*, for which one, two, or three coordinate directions, respectively, are required to describe the velocity and property changes in a flow field.

3.1.8 Discharge

Discharge, or *flow rate*, is the volume rate of flow that passes a given section in a flow stream. The flow velocity v varies across a flow field, as for the example of pipe flow in Figure 3.1.4. The rate of flow through a differential area dA is $v dA$ so that the total volume can be expressed by integrating over the entire flow section as

$$Q = \int_A v dA \quad (3.1.19)$$

Using the mean velocity V , the discharge is defined as

$$Q = AV \quad (3.1.20)$$

By defining an area vector as one that has the magnitude of the area and is oriented normal to the area, then $V \cos \theta dA = \mathbf{V} \cdot d\mathbf{A}$. The discharge is then

$$Q = \int_A \mathbf{V} \cdot d\mathbf{A} \quad (3.1.21)$$

and for a constant (mean) velocity over the cross-sectional area of flow the discharge is

$$Q = \mathbf{V} \cdot \mathbf{A} \quad (3.1.22)$$

The *mass rate of flow* past a flow section is

$$\dot{m} = \int_A \rho v dA \quad (3.1.23a)$$

$$= \rho \int_A v dA \quad (3.1.23b)$$

$$= \rho Q \quad (3.1.23c)$$

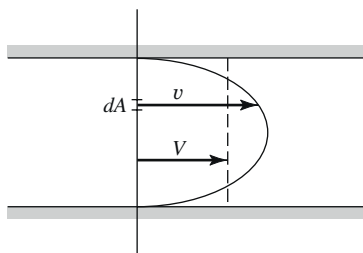


Figure 3.1.4 Velocity distribution in a pipe flow.

3.2 CONTROL VOLUME APPROACH FOR HYDROSYSTEMS

Hydrosystem processes transform the space and time distribution of water in hydrologic systems throughout the hydrologic cycle, in natural and human-made hydraulic systems, and in water resources systems that include both hydrologic and hydraulic systems. The commonality of all hydrosystems is the physical laws that define the flow of fluid in these systems. A consistent mechanism for developing these physical laws is called the *control volume approach*.

The simplified concept of a system is very important in the control volume approach because of the extreme complexity of hydrosystems. Typically a system defined from the fluids viewpoint is defined as a given quantity of mass. A *system* is also a set of connected parts that form a whole. For the present discussion the fluids viewpoint will be used, in which the system has a *system boundary* or *control surface* (CS) as shown in Figure 3.2.1. A control surface is the surface that surrounds the control volume. The control surface can coincide with physical boundaries such as the wall of a pipe or the boundary of a watershed. Part of the control surface may be a hypothetical surface through which fluid flows.

Two properties, *extensive properties* and *intensive properties*, are used in the control volume approach to apply physical properties for discrete masses to a fluid flowing continuously through a control volume. Extensive properties are related to the total mass of the system (control volume), whereas intensive properties are independent of the amount of fluid. The extensive properties are mass m , momentum mV , and energy E . Corresponding intensive properties are mass per unit mass, momentum per unit mass, which is velocity v , and energy per unit mass e . In other words, for an extensive property B , the corresponding intensive property β is defined as the quantity of B per unit mass, $\beta = dB/dm$. Both the extensive and intensive properties can be scalar or vector quantities.

The relationship between intensive and extensive properties for a given system is defined by the following integral over the system:

$$B = \int_{\text{system}} \beta dm = \int \beta \rho d\forall \tag{3.2.1}$$

where dm and $d\forall$ are the differential mass and differential volume, respectively, and ρ is the fluid density.

The volume rate of flow past a given area A is expressed as

$$Q = \mathbf{V} \cdot \mathbf{A} \tag{3.2.2}$$

where \mathbf{V} is the velocity, directed normal to the area and points outward from the control volume, and \mathbf{A} is the area vector.

For the control volume in Figure 3.2.1 the net flowrate \dot{Q} is

$$\begin{aligned} \dot{Q} &= Q_{\text{out}} - Q_{\text{in}} \\ &= \mathbf{V}_2 \cdot \mathbf{A}_2 - \mathbf{V}_1 \cdot \mathbf{A}_1 \\ &= \sum_{\text{CS}} \mathbf{V} \cdot \mathbf{A} \end{aligned} \tag{3.2.3}$$

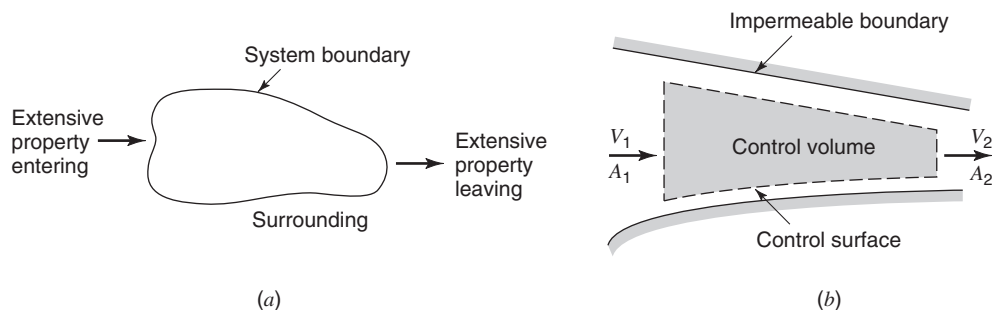


Figure 3.2.1 Control volume approach. (a) System and surrounding; (b) Control volume as a system.

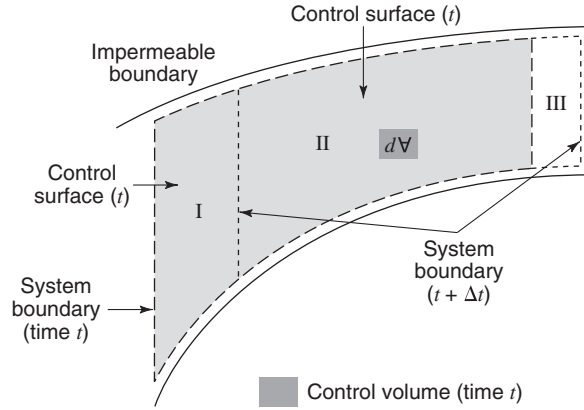


Figure 3.2.2 Control volume at times t and $t + \Delta t$.

In other words, the dot product $\mathbf{V} \cdot \mathbf{A}$ for all flows in and out of a control volume is the net rate of outflow.

The mass rate of flow out of the control volume is

$$\frac{dm}{dt} = \dot{m} = \sum_{CS} \rho \mathbf{V} \cdot \mathbf{A} \quad (3.2.4)$$

The rate of flow of extensive property B is the product of the mass rate and the intensive property:

$$\frac{dB}{dt} = \dot{B} = \sum_{CS} \beta \rho \mathbf{V} \cdot \mathbf{A} \quad (3.2.5)$$

If the velocity varies across the flow section, then it must be integrated across the section, so that the above equation for the rate of flow of extensive property \dot{B} from the control volume becomes

$$\dot{B} = \int_{CS} \beta \rho \mathbf{V} \cdot d\mathbf{A} \quad (3.2.6)$$

Considering the system in Figure 3.2.2, the control volume is defined by the control surface at time t (I + II) with extensive property B_t . At time $t + \Delta t$ the control volume, defined by the control surface, (II + III) has moved and has extensive property $B_{t+\Delta t}$. The rate of change of extensive property B is

$$\frac{dB}{dt} = \lim_{\Delta t \rightarrow 0} \left[\frac{B_{t+\Delta t} - B_t}{\Delta t} \right] \quad (3.2.7)$$

The mass of the system at time $t + \Delta t$, $m_{\text{sys},t+\Delta t}$, is

$$m_{\text{sys},t+\Delta t} = m_{t+\Delta t} + \Delta m_{\text{out}} - \Delta m_{\text{in}} \quad (3.2.8)$$

where $m_{t+\Delta t}$ = mass of fluid within the control volume at time $t + \Delta t$

Δm_{out} = mass of fluid that has moved out of the control volume in time Δt

Δm_{in} = mass of fluid that has moved into the control volume in time Δt

The extensive property of the system at time $t + \Delta t$ is

$$B_{\text{sys}} = B_{CV,t+\Delta t} + \Delta B_{\text{out}} - \Delta B_{\text{in}} \quad (3.2.9)$$

where $B_{CV,t+\Delta t}$ = amount of extensive property in the control volume at time $t + \Delta t$

ΔB_{out} = amount of extensive property of the system that has moved out of the control volume in time Δt

ΔB_{in} = amount of extensive property of the system that has moved into the control volume in time Δt

The time rate of change of extensive property of the system is

$$\frac{dB_{\text{sys}}}{dt} = \lim_{\Delta t \rightarrow 0} \left[\frac{(B_{\text{CV},t+\Delta t} + \Delta B_{\text{out}} - \Delta B_{\text{in}}) - B_{\text{CV},t}}{\Delta t} \right] \quad (3.2.10)$$

The expression can be rearranged to yield

$$\begin{aligned} \frac{dB_{\text{sys}}}{dt} &= \lim_{\Delta t \rightarrow 0} \left[\frac{B_{\text{CV},t+\Delta t} - B_{\text{CV},t}}{\Delta t} \right] + \lim_{\Delta t \rightarrow 0} \left[\frac{\Delta B_{\text{out}} - \Delta B_{\text{in}}}{\Delta t} \right] \\ &= \left\{ \begin{array}{l} \text{Rate of change with} \\ \text{respect to time of} \\ \text{extensive property} \\ \text{in the control volume} \end{array} \right\} + \left\{ \begin{array}{l} \text{Net flow of} \\ \text{extensive property} \\ \text{from the control} \\ \text{volume} \end{array} \right\} \\ &= \frac{dB_{\text{CV}}}{dt} + \frac{dB}{dt} \end{aligned} \quad (3.2.11)$$

The derivative $\frac{dB_{\text{CV}}}{dt} = \frac{d}{dt} \int_{\text{CV}} \beta \rho \, d\forall$ and $\frac{dB}{dt}$ is defined by equation (3.2.5), so that the *control volume equation for one-dimensional flow* becomes

$$\frac{dB_{\text{sys}}}{dt} = \frac{d}{dt} \int_{\text{CV}} \beta \rho \, d\forall + \sum_{\text{CS}} \beta \rho \, \mathbf{V} \cdot \mathbf{A} \quad (3.2.12)$$

The above equation for the general control volume equation was derived for one-dimensional flow so that the rate of flow of B at each section is $\beta \rho \mathbf{V} \cdot \mathbf{A}$. A more general form for rate of flow of an extensive property considers the velocity as variable across a section. Using equation (3.2.6), then, the *general control volume equation* is expressed as

$$\frac{dB_{\text{sys}}}{dt} = \frac{d}{dt} \int_{\text{CV}} \beta \rho \, d\forall + \int_{\text{CS}} \beta \rho \, \mathbf{V} \cdot d\mathbf{A} \quad (3.2.13)$$

This general control volume equation (also referred to as the *Reynolds transport theorem*) states that the total rate of change of extensive property of a flow is equal to the rate of change of extensive property stored in the control volume, $\frac{d}{dt} \int_{\text{CV}} \beta \rho \, d\forall$, plus the net rate of outflow of extensive property through the control surface, $\int_{\text{CS}} \beta \rho \, \mathbf{V} \cdot d\mathbf{A}$.

Throughout this book the general control volume equation (approach) is applied to develop continuity, energy, and momentum equations for hydrosystem (hydrologic and hydraulic) processes.

3.3 CONTINUITY

In order to write the continuity equation, the extensive property is mass ($B = m$) and the intensive property $\beta = dB/dm = 1$. By the law of conservation of mass, the mass of a system is constant, therefore $dB/dt = dm/dt = 0$. The general form of the continuity equation is then

$$0 = \frac{d}{dt} \int_{\text{CV}} \rho \, d\forall + \int_{\text{CS}} \rho \, \mathbf{V} \cdot d\mathbf{A} \quad (3.3.1)$$

which is the *integral equation of continuity for an unsteady, variable-density flow*. Equation (3.3.1) can be rewritten as

$$\int_{CS} \rho \mathbf{V} \cdot d\mathbf{A} = \frac{d}{dt} \int_{CV} \rho d\forall \quad (3.3.2)$$

which states that the net rate of outflow of mass from the control volume is equal to the rate of decrease of mass within the control volume.

For flow with constant density, equation (3.3.2) can be expressed as

$$\int_{CS} \mathbf{V} \cdot d\mathbf{A} = \frac{d}{dt} \int_{CV} d\forall \quad (3.3.3)$$

The continuity equation for flow with a uniform velocity across the flow section and constant density is expressed as

$$\sum_{CS} \mathbf{V} \cdot \mathbf{A} = \frac{d}{dt} \int_{CV} d\forall \quad (3.3.4)$$

For a *constant-density, steady one-dimensional flow*, such as water flowing in a conduit, the velocity is the mean velocity, then

$$\sum_{CS} \mathbf{V} \cdot \mathbf{A} = 0 \quad (3.3.5)$$

For pipe conduit flow we consider a control volume between two locations of the pipe, at sections 1 and 2, then the continuity equation is

$$-V_1A_1 + V_2A_2 = 0 \quad (3.3.6a)$$

or

$$V_1A_1 = V_2A_2 \quad (3.3.6b)$$

or

$$Q_1 = Q_2 \quad (3.3.6c)$$

For a *constant-density unsteady flow*, consider the integral $\int_{CV} d\forall$ as the volume of fluid stored in a control volume denoted by S , so that

$$\frac{d}{dt} \int_{CV} d\forall = \frac{dS}{dt} \quad (3.3.7)$$

The net outflow is defined as

$$\begin{aligned} \int_{CS} \mathbf{V} \cdot d\mathbf{A} &= \int_{\text{outlet}} \mathbf{V} \cdot d\mathbf{A} + \int_{\text{inlet}} \mathbf{V} \cdot d\mathbf{A} \\ &= Q(t) - I(t) \end{aligned} \quad (3.3.8)$$

Then the integral equation of continuity is determined by substituting equations (3.3.7) and (3.3.8) into equation (3.3.2) to obtain

$$Q(t) - I(t) = -\frac{dS}{dt} \quad (3.3.9)$$

which is more commonly expressed as

$$\frac{dS}{dt} = I(t) - Q(t) \quad (3.3.10)$$

This continuity expression is used extensively in describing hydrologic processes.

EXAMPLE 3.3.1

A river section is defined by two bridges. At a particular time the flow at the upstream bridge is $100 \text{ m}^3/\text{s}$, and at the same time the flow at the downstream bridge is $75 \text{ m}^3/\text{s}$. At this particular time, what is the rate at which water is being stored in the river section, assuming no losses?

SOLUTION

Using the continuity equation (3.3.10) yields

$$\begin{aligned} \frac{dS}{dt} &= Q_{\text{up}}(t) - Q_{\text{down}}(t) \\ &= 100 \text{ m}^3/\text{s} - 75 \text{ m}^3/\text{s} \\ &= 25 \text{ m}^3/\text{s} \end{aligned}$$

EXAMPLE 3.3.2

A reservoir has the following monthly inflows and outflows in relative units:

Month	<i>J</i>	<i>F</i>	<i>M</i>	<i>A</i>
Inflows	10	5	0	5
Outflows	5	5	10	0

If the reservoir contains 30 units of water in storage at the beginning of the year, how many units of water in storage are there at the end of April?

SOLUTION

The continuity equation (3.3.10) is used to perform a routing of flows into and out of the reservoir. Because the inflow and outflows are for discrete time intervals, the continuity equation (3.3.10) can be reformulated as

$$dS = I(t)dt - Q(t)dt$$

and integrated over time intervals $j = 1, 2, \dots, J$ of each length Δt :

$$\int_{S_{j-1}}^{S_j} dS = \int_{(j-1)\Delta t}^{j\Delta t} I(t)dt - \int_{(j-1)\Delta t}^{j\Delta t} Q(t)dt$$

or

$$\begin{aligned} S_j - S_{j-1} &= I_j - Q_j \text{ for } j = 1, 2, \dots \\ \Delta S_j &= I_j - Q_j \end{aligned}$$

where I_j and Q_j are the volumes of inflow and outflow for the j th time interval. The cumulative storage is $S_{j+1} = S_j + \Delta S_j$. For the first interval of time,

$$\Delta S_1 = I_1 - Q_1 = 10 - 5 = 5$$

Then $S_2 = S_1 + \Delta S_1 = 30 + 5 = 35$. The remaining computations are:

Time	I_j	Q_j	ΔS_j	S_j
1	10	5	5	30
2	5	5	0	35
3	0	10	-10	25
4	5	0	5	30

3.4 ENERGY

This section uses the first law of thermodynamics along with the control volume approach to develop the energy equation for fluid flow in hydrologic and hydraulic processes. An energy balance for

hydrologic and hydraulic processes considers an accounting of all inputs and outputs of energy to and from a system. By the *first law of thermodynamics*, the rate of change of energy, E , with time is the rate at which heat is transferred into the fluid, dH/dt , minus the rate at which the fluid does work on the surroundings, dW/dt , expressed as

$$\frac{dE}{dt} = \frac{dH}{dt} - \frac{dW}{dt} \quad (3.4.1)$$

The total energy of a fluid system is the sum of the internal energy E_u , the kinetic energy E_k , and the potential energy E_p ; thus

$$E = E_u + E_k + E_p \quad (3.4.2)$$

The extensive property is the amount of energy in the system, $B = E$:

$$B = E_u + E_k + E_p \quad (3.4.3)$$

and the intensive property is

$$\beta = \frac{dB}{dm} = e = e_u + e_k + e_p \quad (3.4.4)$$

where e represents the energy per unit mass. Also, the rate of change of extensive property with respect to time is

$$\frac{dB}{dt} = \frac{dE}{dt} = \frac{dH}{dt} - \frac{dW}{dt} \quad (3.4.5)$$

The *energy balance equation* is now derived by substituting β (equation (3.4.4)) and dB/dt (equation (3.4.5)) into the general control volume equation (3.2.12),

$$\frac{dE}{dt} = \frac{dH}{dt} - \frac{dW}{dt} = \frac{d}{dt} \int_{CV} e \rho d\forall + \sum_{CS} e \rho \mathbf{V} \cdot \mathbf{A} \quad (3.4.6)$$

Next we can replace e by equation (3.3.4):

$$\frac{dH}{dt} - \frac{dW}{dt} = \frac{d}{dt} \int_{CV} (e_u + e_k + e_p) \rho d\forall + \sum_{CS} (e_u + e_k + e_p) \rho \mathbf{V} \cdot \mathbf{A} \quad (3.4.7)$$

The kinetic energy per unit mass e_k is the total kinetic energy of mass with velocity V divided by the mass m :

$$e_k = \frac{mV^2/2}{m} = \frac{V^2}{2} \quad (3.4.8)$$

The potential energy per unit mass e_p is the weight of the fluid $\gamma \forall$ times the centroid elevation z of the mass divided by the mass:

$$e_p = \frac{\gamma \forall z}{m} = \frac{\gamma \forall z}{\rho \forall} = gz \quad (3.4.9)$$

because $\gamma/\rho = g$.

Now the *general energy equation for unsteady variable density flow* can be written as

$$\frac{dH}{dt} - \frac{dW}{dt} = \frac{d}{dt} \int_{CV} \left(e_u + \frac{1}{2} V^2 + gz \right) \rho d\forall + \sum_{CS} \left(e_u + \frac{1}{2} V^2 + gz \right) \rho \mathbf{V} \cdot \mathbf{A} \quad (3.4.10)$$

For steady flow, equation (3.4.10) reduces to

$$\frac{dH}{dt} - \frac{dW}{dt} = \sum_{CS} \left(e_u + \frac{1}{2} V^2 + gz \right) \rho \mathbf{V} \cdot \mathbf{A} \quad (3.4.11)$$

The work done by a system on its surroundings can be divided into *shaft work*, W_s , and *flow work*, W_f . Flow work is the result of pressure force as the system moves through space and shaft work is any other work besides the flow work. In the control volume in Figure 3.2.2 the force on the upstream end of the fluid is $p_1 A_1$ and the distance traveled over time Δt is $l_1 = V_1 \Delta t$. Work done on the surrounding fluid as a result of this force is then the product of the force $p_1 A_1$ in the direction of motion and the distance traveled, $V_1 \Delta t$. The work force on the upstream end is then

$$W_{f_1} = -V_1 p_1 A_1 \Delta t \quad (3.4.12a)$$

and on the downstream end is

$$W_{f_2} = V_2 p_2 A_2 \Delta t \quad (3.4.12b)$$

At the upstream end, a negative sign must be used because the pressure force on the surrounding fluid acts in the opposite direction to the motion of the system boundary. The rate of work at the upstream and downstream ends are, respectively,

$$\frac{dW_{f_1}}{dt} = -V_1 p_1 A_1 \quad (3.4.13)$$

and

$$\frac{dW_{f_2}}{dt} = V_2 p_2 A_2 \quad (3.4.14)$$

The rate of flow work can then be expressed in general terms as

$$\frac{dW_f}{dt} = p \mathbf{V} \cdot \mathbf{A} \quad (3.4.15)$$

or for all streams passing through the control volume as

$$\frac{dW_f}{dt} = \sum_{CS} p \mathbf{V} \cdot \mathbf{A} = \sum_{CS} \frac{p}{\rho} \rho \mathbf{V} \cdot \mathbf{A} \quad (3.4.16)$$

The net rate of work on the system can now be expressed as

$$\frac{dW}{dt} = \frac{dW_s}{dt} + \sum_{CS} \frac{p}{\rho} \rho \mathbf{V} \cdot \mathbf{A} \quad (3.4.17)$$

Using equation (3.4.17), the *general energy equation* (3.4.10) for *unsteady variable density flow* can be expressed as

$$\frac{dH}{dt} - \frac{dW_s}{dt} - \sum_{CS} \frac{p}{\rho} \rho \mathbf{V} \cdot \mathbf{A} = \frac{d}{dt} \int_{CV} \left(e_u + \frac{1}{2} V^2 + gz \right) \rho d\forall + \sum_{CS} \left(e_u + \frac{1}{2} V^2 + gz \right) \rho \mathbf{V} \cdot \mathbf{A} \quad (3.4.18)$$

which can be written as

$$\frac{dH}{dt} - \frac{dW_s}{dt} = \frac{d}{dt} \int_{CV} \left(e_u + \frac{1}{2} V^2 + gz \right) \rho d\forall + \sum_{CS} \left(\frac{p}{\rho} + e_u + \frac{1}{2} V^2 + gz \right) \rho \mathbf{V} \cdot \mathbf{A} \quad (3.4.19)$$

For steady flow, equation (3.4.19) reduces to

$$\frac{dH}{dt} - \frac{dW_s}{dt} = \sum_{CS} \left(\frac{p}{\rho} + e_u + \frac{1}{2} V^2 + gz \right) \rho \mathbf{V} \cdot \mathbf{A} \quad (3.4.20)$$

EXAMPLE 3.4.1

Determine an expression based upon the energy concept that relates the pressures at the upstream and downstream ends of a nozzle assuming steady flow, neglecting change in internal energy, and assuming $dH/dt = 0$ and $dW_s/dt = 0$.

SOLUTION

Using the energy equation (3.4.20) for steady flow yields

$$\frac{dH}{dt} - \frac{dW_s}{dt} = \sum_{CS} \left(\frac{p}{\rho} + e_u + \frac{1}{2} V^2 + gz \right) \rho \mathbf{V} \cdot \mathbf{A}$$

Neglecting dH/dt and dW_s/dt the above energy equation can be expressed as

$$\int_{A_2} \left(\frac{p_2}{\rho} + e_{u_2} + \frac{1}{2} V_2^2 + gz_2 \right) \rho V_2 dA_2 - \int_{A_1} \left(\frac{p_1}{\rho} + e_{u_1} + \frac{1}{2} V_1^2 + gz_1 \right) \rho V_1 dA_1 = 0$$

which can be modified to

$$\int_{A_2} \left(\frac{p_2}{\rho} + e_{u_2} + gz_2 \right) \rho V_2 dA_2 + \int_{A_2} \frac{\rho V_2^3}{2} dA_2 - \int_{A_1} \left(\frac{p_1}{\rho} + e_{u_1} + gz_1 \right) \rho V_1 dA_1 - \int_{A_1} \frac{\rho V_1^3}{2} dA_1 = 0$$

For hydrostatic conditions, $\left(\frac{p}{\rho} + e_u + gz \right)$ is constant across the system, which allows these terms to be taken outside the integral:

$$\left(\frac{p_2}{\rho} + e_{u_2} + gz_2 \right) \int_{A_2} \rho V_2 dA_2 + \int_{A_2} \frac{\rho V_2^3}{2} dA_2 - \left(\frac{p_1}{\rho} + e_{u_1} + gz_1 \right) \int_{A_1} \rho V_1 dA_1 - \int_{A_1} \frac{\rho V_1^3}{2} dA_1 = 0$$

The term $\int \rho V dA$ is the mass rate of flow, \dot{m} , and the term $\int \frac{\rho V^3}{2} dA = \dot{m} \frac{V^2}{2}$, so

$$\left(\frac{p_2}{\rho} + e_{u_2} + gz_2 \right) \dot{m} + \dot{m} \frac{V_2^2}{2} - \left(\frac{p_1}{\rho} + e_{u_1} + gz_1 \right) \dot{m} - \dot{m} \frac{V_1^2}{2} = 0$$

Dividing through by $\dot{m}g$ and rearranging yields

$$\frac{p_1}{\rho g} + \frac{e_{u_1}}{g} + z_1 + \frac{V_1^2}{2g} = \frac{p_2}{\rho g} + \frac{e_{u_2}}{g} + z_2 + \frac{V_2^2}{2g}$$

$\gamma = \rho g$ and rearranging yields

$$\frac{p_1}{\gamma} + \frac{V_1^2}{2g} + z_1 = \frac{p_2}{\gamma} + \frac{V_2^2}{2g} + z_2 + \frac{e_{u_2} - e_{u_1}}{g}$$

Neglecting changes in internal energy, $(e_{u_2} - e_{u_1})/g = 0$

$$\frac{p_1}{\gamma} + \frac{V_1^2}{2g} + z_1 = \frac{p_2}{\gamma} + \frac{V_2^2}{2g} + z_2$$

Assuming the control volume is horizontal, $z_1 = z_2$, then

$$\frac{p_1}{\gamma} + \frac{V_1^2}{2g} = \frac{p_2}{\gamma} + \frac{V_2^2}{2g}$$

This energy equation relates the pressures assuming steady flow, $z_1 = z_2$, neglecting change of internal energy in the fluid and assuming $dH/dt = 0$ and $dW_s/dt = 0$.

EXAMPLE 3.4.2

For a nozzle, determine the pressure change through the nozzle between the upstream and downstream end of the nozzle. Assume steady flow, neglect changes in internal energy of the fluid, assume $dH/dt = 0$ and $dW_s/dt = 0$, and say that the nozzle is horizontal. Assume the temperature is 20°C . The velocities at the entrance and exit are $V_2 = 2.55$ m/s and $V_1 = 1.13$ m/s, respectively.

SOLUTION

Using the energy equation derived in example 3.4.1 yields

$$\begin{aligned}\frac{p_1}{\gamma} + \frac{V_1^2}{2g} &= \frac{p_2}{\gamma} + \frac{V_2^2}{2g} \\ p_1 - p_2 &= (V_2^2 - V_1^2) \frac{\gamma}{2g} \\ &= [(2.55)^2 - (1.13)^2] \times \frac{9.79 \text{ kN/m}^3}{2 \times 9.81 \text{ m/s}^2} \\ &= (5.226 \text{ m}^2/\text{s}^2)(0.499 \text{ kN s}^2/\text{m}^4) \\ &= 2.608 \text{ kN/m}^2 = 2.608 \text{ kPa} = 2608 \text{ Pa}\end{aligned}$$

The pressure change is a pressure decrease of 2608 Pa.

3.5 MOMENTUM

In order to derive the general momentum equation for fluid flow in a hydrologic or hydraulic system, we use the control volume approach along with Newton's second law. *Newton's second law* states that the summation of all external forces on a system is equal to the rate of change of momentum of the system

$$\sum \mathbf{F} = \frac{d(\text{momentum})}{dt} \quad (3.5.1)$$

To apply the control volume approach the extensive property is momentum, $B = mv$, and the intensive property is the momentum per unit mass, $\beta = d(mv)/dt$, so

$$\sum \mathbf{F} = \frac{d(mv)}{dt} \quad (3.5.2)$$

A lowercase \mathbf{v} is used to denote that this velocity is referenced to the inertial reference frame and to distinguish it from \mathbf{V} .

Using the general control volume equation (3.2.13),

$$\frac{dB_{\text{sys}}}{dt} = \frac{d}{dt} \int_{\text{CV}} \beta \rho d\forall + \int_{\text{CS}} \beta \rho \mathbf{V} \cdot d\mathbf{A} \quad (3.2.13)$$

and from equation (3.5.2) then

$$\sum \mathbf{F} = \frac{d}{dt} \int_{\text{CV}} \mathbf{v} \rho d\forall + \int_{\text{CS}} \mathbf{v} \rho \mathbf{V} \cdot d\mathbf{A} \quad (3.5.3)$$

which is the *integral momentum equation for fluid flow*. For steady flow, equation (3.5.3) reduces to

$$\sum \mathbf{F} = \int_{\text{CS}} \mathbf{v} \rho \mathbf{V} \cdot d\mathbf{A} \quad (3.5.4)$$

When a uniform velocity occurs in the stream crossing the control surface, the integral momentum equation is

$$\sum \mathbf{F} = \frac{d}{dt} \int_{CV} \mathbf{v} \rho d\forall + \sum_{CS} \mathbf{v} \rho \mathbf{V} \cdot \mathbf{A} \quad (3.5.5)$$

The momentum can be written for the coordinate directions x , y , and z in the Cartesian coordinate system as

$$\sum F_x = \frac{d}{dt} \int_{CV} v_x \rho d\forall + \sum_{CS} v_x (\rho \mathbf{V} \cdot \mathbf{A}) \quad (3.5.6)$$

$$\sum F_y = \frac{d}{dt} \int_{CV} v_y \rho d\forall + \sum_{CS} v_y (\rho \mathbf{V} \cdot \mathbf{A}) \quad (3.5.7)$$

$$\sum F_z = \frac{d}{dt} \int_{CV} v_z \rho d\forall + \sum_{CS} v_z (\rho \mathbf{V} \cdot \mathbf{A}) \quad (3.5.8)$$

For a steady flow the time derivative in equation (3.5.6) drops out, yielding

$$\sum \mathbf{F} = \sum_{CS} \mathbf{v} \rho \mathbf{V} \cdot \mathbf{A} \quad (3.5.9)$$

For a steady flow in which the cross-sectional area of flow does not change along the length of the flow, $\sum_{CS} \mathbf{v} \rho \mathbf{V} \cdot \mathbf{A} = 0$ (referred to as uniform flow), equation (3.5.9) reduces to

$$\sum \mathbf{F} = 0 \quad (3.5.10)$$

3.6 PRESSURE AND PRESSURE FORCES IN STATIC FLUIDS

In section 3.1.4, pressure, absolute pressure, gauge pressure, piezometric head, and pressure force were defined. This section extends that conversation to hydrostatic forces on submerged surfaces and buoyancy.

3.6.1 Hydrostatic Forces

Hydraulic engineers have many engineering applications in which they have to compute the force being exerted on submerged surfaces. The hydrostatic force on any submerged plane surface is equal to the product of the surface area and the pressure acting at the centroid of the plane surface. Consider the force on the plane surface shown in Figure 3.6.1. This plane surface can be divided into an infinite number of differential horizontal planes with width dy and area dA . The distance to the incremental area from the axis O–O is y . The pressure on dA is $p = \gamma y \sin \theta$ so that the force dF is $dF = p dA = \gamma y \sin \theta dA$. The force on the entire submerged plane is obtained by integrating the differential force on the differential area:

$$F = \int_A \gamma y \sin \theta dA \quad (3.6.1a)$$

$$= \gamma \sin \theta \int_A y dA \quad (3.6.1b)$$

$$= \gamma \sin \theta y_c A \quad (3.6.1c)$$

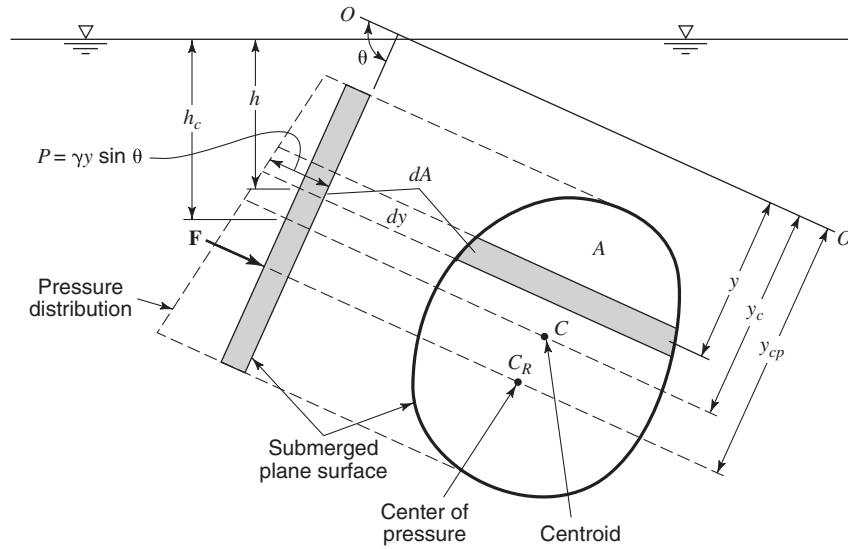


Figure 3.6.1 Hydrostatic pressure on a plane surface.

where γ and $\sin \theta$ are constants. The integral $\int_A y dA$ is by definition the first moment of the area and $\int_A y (dA/A) = y_c$ is the distance from the O–O axis to the centroid (center of gravity) of the submerged plane. The vertical distance to the centroid can be defined as $h_c = y_c \sin \theta$, so that the force on the submerged plane is

$$F = \gamma h_c A \quad (3.6.2)$$

Engineers are normally interested in the forces that are in excess of the ambient atmospheric pressures. Keep in mind that atmospheric pressure, for most applications, acts on both sides of the submerged surface so that gauge pressure is of importance.

Even though pressure forces acting on a submerged surface are distributed throughout the surface, engineers are interested in the location of the *center of pressure*, which is the point on the submerged surface where the resultant force acts. The moment equation is

$$y_{cp} F = \int y dF \quad (3.6.3)$$

where $dF = p dA$, so

$$y_{cp} F = \int_A y p dA \quad (3.6.4)$$

and $p = \gamma y \sin \theta$, so

$$y_{cp} F = \int_A \gamma y^2 \sin \theta dA = \gamma \sin \theta \int_A y^2 dA \quad (3.6.5)$$

The integral $\int_A y^2 dA = I_o$ is the *moment of inertia (moment of the area)*, with respect to an axis formed by the intersection of the plane containing the surface and the free surface. This can also be expressed with respect to the horizontal centroidal axis of the area by the *parallel axis theorem* as

$$I_o = \bar{I} + y_c^2 A \quad (3.6.6)$$

Equation (3.6.5) can now be expressed as

$$y_{cp}F = \gamma \sin \theta I_o = \gamma \sin \theta (\bar{I} + y_c^2 A) \quad (3.6.7)$$

Substituting equation (3.6.1c) and solving for y_{cp} yields

$$y_{cp} = y_c + \frac{\bar{I}}{y_c A} \quad (3.6.8)$$

The vertical distance to the center of pressure h_{cp} is then

$$h_{cp} = y_{cp} \sin \theta \quad (3.6.9)$$

EXAMPLE 3.6.1

Derive the expression for the depth to the center of pressure y_{cp} for a rectangular area ($b \times h$) vertically submerged with the long side (h) at the liquid surface.

SOLUTION

Using equation (3.6.8),

$$y_{cp} = y_c + \frac{\bar{I}}{y_c A}$$

where $y_c = h/2$, $\bar{I} = bh^3/12$, and $A = bh$, we get

$$y_{cp} = \frac{h}{2} + \frac{bh^3/12}{\left(\frac{h}{2}\right)(bh)} = \frac{h}{2} + \frac{h}{6} = \frac{4}{6}h = \frac{2}{3}h$$

EXAMPLE 3.6.2

Determine the hydrostatic force and the location of the center of pressure on the 25 m long dam shown in Figure 3.6.2. The face of the dam is at an angle of 60° . Assume 20°C .

SOLUTION

The diagram in Figure 3.6.2 shows the pressure distribution. Using equation (3.6.2), $h_c = 2.5$ m and $A = (25 \text{ m} \times 5)/\sin 60^\circ$, so the hydrostatic force is

$$\begin{aligned} F &= \gamma h_c A = \left(9.79 \frac{\text{kN}}{\text{m}^3}\right)(2.5 \text{ m})\left(25 \text{ m} \times \frac{5}{\sin 60^\circ} \text{ m}\right) \\ &= 3.532 \text{ kN} \end{aligned}$$

The center of pressure is at $2/3$ of the total water depth, $(2/3) \times 5 = 3.33$ m.

EXAMPLE 3.6.3

Consider a vertical rectangular gate ($b = 4$ m and $h = 2$ m) that is vertically submerged in water so that the top of the gate is 4 m below the surface of the water (as shown in Figure 3.6.3). Determine the total resultant force on the gate and the location of the center of pressure.

SOLUTION

Use the free-body diagram in Figure 3.6.3. The total resultant force is computed using equation (3.6.2), $F = \gamma h_c A$, where $h_c = 4 + (2/2) = 5$ m:

$$F = (9.79 \text{ kN/m}^3)(5 \text{ m})(4 \times 2 \text{ m}^2) = 396.1 \text{ kN}$$

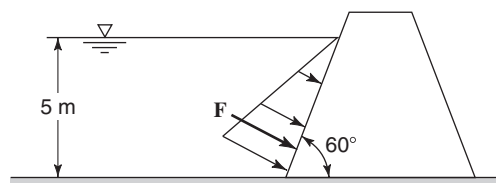


Figure 3.6.2 Hydrostatic force on dam for example 3.6.2.

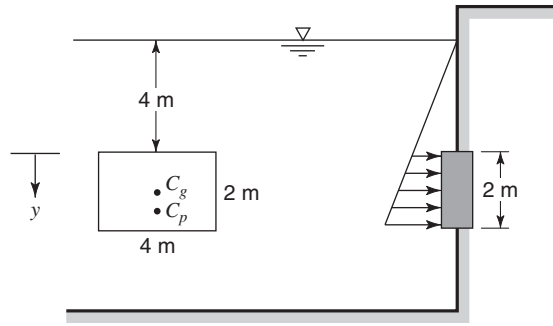


Figure 3.6.3 Vertical rectangular gate for example 3.6.3.

The location of the center of pressure is computed using equation (3.6.8):

$$y_{cp} = y_c + \frac{\bar{I}}{y_c A} = 5 + \frac{\frac{4 \times 2^3}{12}}{5 \times (4 \times 2)}$$

$$= 5.067 \text{ m}$$

Alternatively, this problem can be solved by the simple integration $F = \int_0^2 \gamma h dA$, where $dA = 4 dy$:

$$F = \int_0^2 \gamma h dA = \int_0^2 (9.79)(4 + y)(4 dy)$$

$$= 39.16 \left[4y + \frac{y^2}{2} \right]_0^2 = 39.16 \left[4 \times 2 + \frac{2^2}{2} \right]$$

$$= 391.6 \text{ kN}$$

EXAMPLE 3.6.4

Consider an inclined rectangular gate with water on one side as shown in Figure 3.6.4. Determine the total resultant force acting on the gate and the location of the center of pressure.

SOLUTION

To determine the total resultant force, $F = \gamma h_c A$, where $h_c = 5 + 1/2(4 \cos 60^\circ)$, so that

$$F = (62.4) \left[5 + \frac{1}{2}(4 \cos 60^\circ) \right] (4 \times 6) = 8,986 \text{ lb}$$

The location of the center of pressure is

$$y_{cp} = y_c + \frac{\bar{I}}{y_c A}$$

where $y_c = \frac{5}{\cos 60^\circ} + \frac{4}{2} = 12 \text{ ft}$, $\bar{I} = bh^3/12 = 6 \times 4^3/12 = 32 \text{ ft}^4$ and $A = 6 \times 4 = 24 \text{ ft}^2$:

$$y_{cp} = 12 + \frac{32}{12 \times 24} = 12.11 \text{ ft}$$

Using equation (3.6.9), $h_{cp} = y_{cp} \sin \theta = 12.11(\sin 30^\circ) = 6.06 \text{ ft}$

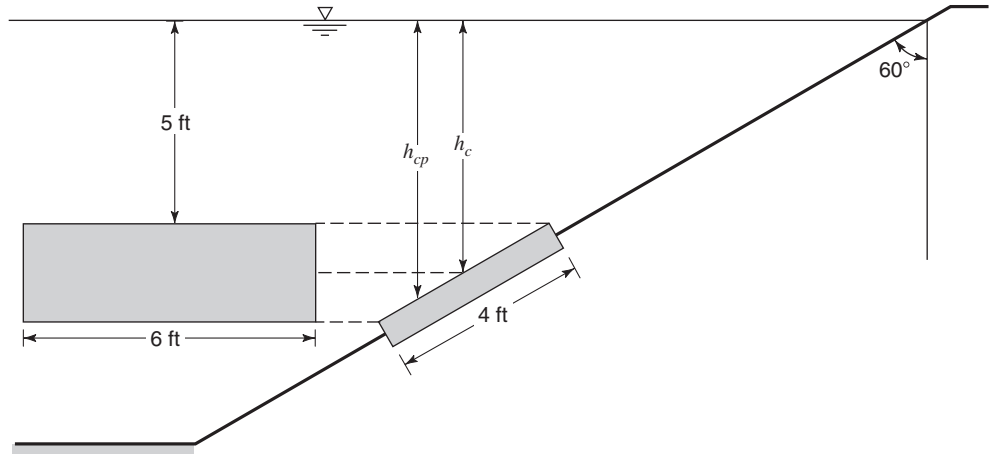


Figure 3.6.4 Inclined rectangular gate for example 3.6.4.

3.6.2 Buoyancy

The submerged body in Figure 3.6.5 is acted upon by gravity and the pressure of the surrounding fluid. On the upper surface of the submerged body, the vertical force is F_y and is equal to the weight of the volume ABCD above the surface. The vertical component of force F'_y on the bottom is the weight of the volume of fluid ABCED. The difference between the two volumes ABCD and ABCED is the volume of the submerged body. Applying the momentum principle, from equation (3.5.7) we get

$$\sum F_y = 0 \tag{3.6.10}$$

The buoyant force F_b is the weight of the volume of fluid DCE and is equal to the weight of the volume of fluid displaced, so that

or
$$F_b - F'_y + F_y = 0 \tag{3.6.11a}$$

$$F_b = F'_y - F_y \tag{3.6.11b}$$

Archimedes' principle (about 250 B.C.) states that the weight of a submerged body is reduced by an amount equal to the weight of liquid displaced by the body. This principle may be viewed as the difference of vertical pressure forces on the two surfaces DC and DEC. Floating bodies are partially submerged due to the balance of the body weight and buoyancy force.

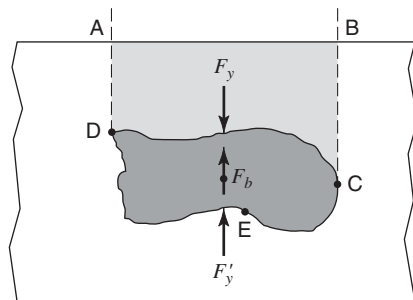


Figure 3.6.5 Forces on a submerged body. Buoyant force, F_b , passes through the centroid of the displaced volume and acts through a point called the center of buoyancy.

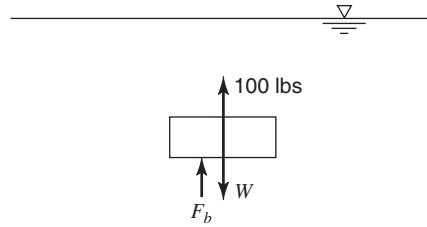


Figure 3.6.6 Free-body diagram for example 3.6.6.

EXAMPLE 3.6.5

A metal block weighs 400 N in air, but when completely submerged in water it weighs 250 N. What is the volume of the metal block?

SOLUTION

Essentially the buoyant force F_b is equal to the weight of water displaced by the metal block, i.e.,

$$F_b = 400 \text{ N} - 250 \text{ N} = 150 \text{ N}$$

The weight $W = (9.79)(1000)\nabla$, where ∇ is the volume.

$$150 = (9.79)(1000)\nabla$$

$$\nabla = 0.0153 \text{ m}^3$$

EXAMPLE 3.6.6

An object is 1 ft thick by 1 ft wide by 2 ft long. It weighs 100 lb at a depth of 10 ft. What is the weight of the object in air and what is its specific gravity?

SOLUTION

Use the free-body diagram in Figure 3.6.6. The summation of forces acting on the object in the vertical direction is

$$\sum F_y = 100 + F_b - W = 0$$

where F_b is the buoyant force and W is the weight of the object.

$$F_b = \left(62.4 \frac{\text{lb}}{\text{ft}^3}\right)(1 \text{ ft})(1 \text{ ft})(2 \text{ ft})$$

$$= 124.8 \text{ lb}$$

$$100 + 124.8 - W = 0$$

$$W = 224.8 \text{ lb}$$

The specific gravity is $224.8/124.8 = 1.8$.

3.7 VELOCITY DISTRIBUTION

We discussed in section 3.1.8 that the actual velocity varies throughout a flow section (see Figure 3.1.4 for pipe flow as an illustration). Figure 3.7.1 illustrates velocity profiles in various open-channel flow sections. As a result of these nonuniform velocity distributions in pipe flow and open-channel flow, the velocity head is generally greater than the value computed according to $V^2/2g$ where V is the mean velocity. When using the energy principle, the true velocity head is expressed as $\alpha V^2/2g$, where α is a *kinetic energy correction factor*. Chow (1959) also referred to α as an energy coefficient or *Coriolis coefficient*.

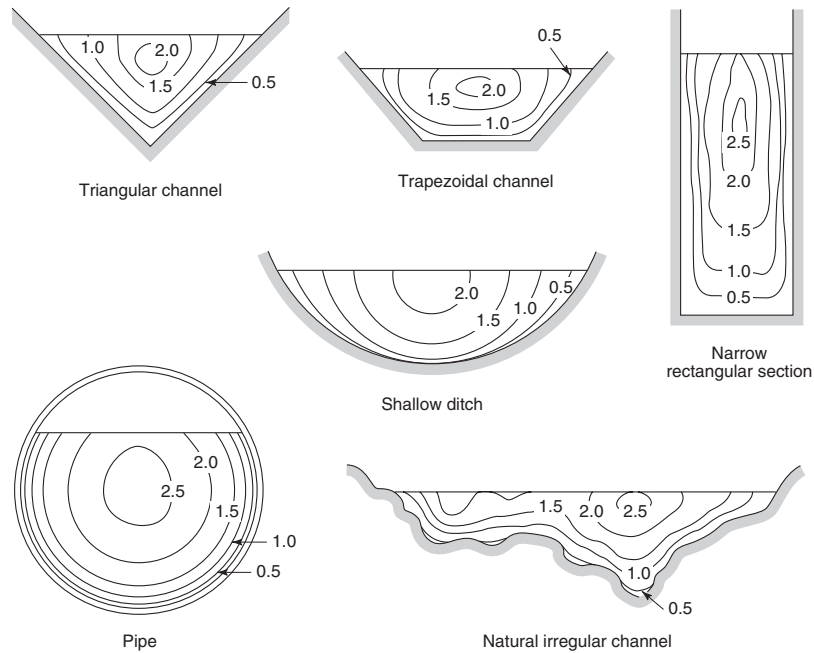


Figure 3.7.1 Typical curves of equal velocity in various channel sections (from Chow (1959)).

Consider the velocity distribution shown in Figure 3.1.4. The mass of fluid flowing through an area dA per unit time is $(\gamma/g)v dA$, where v is the velocity through area dA . The flow of kinetic energy per unit time through this area is $(\gamma/g)v dA(v^2/2) = (\gamma/2g)v^3 dA$. For a known velocity distribution, the total kinetic energy flowing through the section per unit time is

$$\text{Total kinetic energy (per unit time)} = \frac{\gamma}{2g} \int_A v^3 dA \quad (3.7.1)$$

Using the mean flow velocity V and the coefficient α , the total energy per unit weight is $\alpha V^2/2g$; because the flow across the entire section is γAV . The total kinetic energy transmitted is

$$\begin{aligned} \text{Total kinetic energy (per unit time)} &= (\gamma AV) \left(\alpha \frac{V^2}{2g} \right) \\ &= \gamma \alpha A \frac{V^3}{2g} \end{aligned} \quad (3.7.2)$$

From equations (3.7.1) and (3.7.2) we get

$$\frac{\gamma}{2g} \int_A v^3 dA = \gamma \alpha A \frac{V^3}{2g} \quad (3.7.3)$$

and we then solve for the kinetic energy correction factor:

$$\alpha = \frac{1}{AV^3} \int_A v^3 dA \quad (3.7.4)$$

The value of α for flow in circular pipes flowing full with a parabolic velocity distribution is equal to 2 for laminar flow and normally ranges from 1.03 to 1.06 for turbulent flow. Because α is not known precisely, it is not commonly used in pipe flow calculations, and the kinetic energy of fluid per unit weight is $V^2/2g$. The values of α for open-channel flow varies by the type of channel flow. For example, in regular channels, flumes, and spillways, α ranges between 1.10 and 1.20, and for river valleys and areas α ranges between 1.5 and 2.0 with an average of 1.75 (see Chow (1959)).

The nonuniform distribution of velocity also affects the computation of momentum in open-channel flow. The corrected momentum of water passing through a channel section per unit time is

$$\begin{aligned} \text{Total momentum} &= \beta_m \frac{\gamma}{g} QV \\ \text{(per unit time)} & \\ &= \beta_m \frac{\gamma}{g} AV^2 \end{aligned} \tag{3.7.5}$$

where β_m is the *momentum correction factor*, also called the *momentum coefficient* or *Boussinesq coefficient* by Chow (1959). The momentum of water passing through an elemental area dA per unit time is the product of the mass per unit time $(\gamma/g)v dA$ and the velocity v , which is $(\gamma/g)v^2 dA$. The total momentum of fluid per unit time is

$$\begin{aligned} \text{Total momentum} &= \frac{\gamma}{g} \int_A v^2 dA \\ \text{(per unit time)} & \end{aligned} \tag{3.7.6}$$

From equations (3.7.5) and (3.7.6), we get

$$\beta_m \frac{\gamma}{g} AV^2 = \frac{\gamma}{g} \int_A v^2 dA \tag{3.7.7}$$

Solving for the momentum correction factor β_m yields

$$\beta_m = \frac{1}{AV^2} \int_A v^2 dA \tag{3.7.8}$$

According to Chow (1959), the value of β_m for fairly straight prismatic channels varies between 1.01 to 1.12 and for river valleys β_m varies between 1.17 and 1.33.

PROBLEMS

- 3.1.1 If 10 m^3 of a liquid weighs 60 kN, calculate its specific weight, density, and specific gravity.
- 3.1.2 The specific gravity of a certain oil is 0.7. Calculate its specific weight and density in SI and English units.
- 3.1.3 What is the unit of force in SI units? What is it identical to?
- 3.1.4 What is the unit of mass in English units? What is it identical to?
- 3.1.5 A rocket weighing 9810 N on earth is landed on the moon where the acceleration due to gravity is approximately one-sixth that at the earth's surface. What are the mass of the rocket on the earth and the moon, and the weight of the rocket on the moon?
- 3.1.6 The summer temperature in Arizona often exceeds 110°F . What is the Celsius equivalent temperature?
- 3.1.7 What will be the percentage change in the density of water if the temperature changes from 20°C to (a) 50°C and (b) 80°C ?
- 3.1.8 The specific gravity and kinematic viscosity of a certain liquid are 1.5 and $4 \times 10^{-4} \text{ m}^2/\text{s}$, respectively. What is its dynamic viscosity?
- 3.1.9 If the dynamic viscosity of a liquid is $2.09 \times 10^{-5} \text{ lb} \cdot \text{s}/\text{ft}^2$, what is its dynamic viscosity in $\text{N} \cdot \text{s}/\text{m}^2$ and centipoises?
- 3.1.10 If the kinematic viscosity of an oil is 800 centistokes, what is its kinematic viscosity in m^2/s and ft^2/s ?

- 3.1.11 Derive the conversion of stokes to ft^2/s .
- 3.1.12 A liquid has a density of 700 kg/m^3 and a dynamic viscosity of $0.0042 \text{ kg/m} \cdot \text{s}$. What is its kinematic viscosity in m^2/s , ft^2/s , centistokes, and stokes?
- 3.1.13 What is the change in volume of 10 ft^3 of water at 50°F when it is subjected to a pressure increase of 200 psi?
- 3.1.14 What is the bulk modulus of elasticity of a liquid if its volume is reduced by 0.05% by the application of a pressure of 160 psi?
- 3.1.15 Determine the bulk modulus of elasticity of a liquid by using the following data: The volume is $3000 \text{ cm}^3 (= 3 \text{ L})$ at 2 MPa, and the volume is 2750 cm^3 at 3 MPa.
- 3.1.16 The density of sea water is 1025 kg/m^3 at the ocean surface. The bulk modulus of elasticity of sea water is $234 \times 10^7 \text{ Pa}$. What is the pressure at this depth, if the change in density between the surface and that depth is 1.5%?
- 3.1.17 Suppose it is desired to reduce a given volume of water by 1% by increasing the pressures at two different temperatures, 50°F and 100°F . Compare the changes in the pressures applied at these temperatures. Calculate the percentage of the pressure change at 100°F with reference to that at 50°F .
- 3.1.18 A fluid pressure is 10 kPa above standard atmospheric pressure (101.3 kPa). Express the pressure as gauge and absolute.
- 3.1.19 If the pressure 15 ft below the free surface of a liquid is 30 psi, calculate its specific weight and specific gravity.
- 3.1.20 If the absolute pressure at a bottom of an open tank filled with oil (specific gravity = 0.8) is 200 kPa, what is the depth of oil in the tank?
- 3.1.21 A fluid pressure is 5 psi below the standard atmospheric pressure (14.7 psi). Express the pressure as vacuum and absolute.
- 3.1.22 Express the standard atmospheric pressure (14.7 psi) as feet of water and inches of mercury.
- 3.1.23 A Bourdon gauge reads a vacuum of 10 in of mercury (specific gravity = 13.6) when the atmospheric pressure is 14.3 psi. Calculate the corresponding absolute pressure.
- 3.1.24 What is the height of the column of a water barometer for an atmospheric pressure of 100 kPa, if the water is at 10°C , 50°C , and 100°C ?
- 3.1.25 Compare the pressure forces exerted on the face of two dams that hold a fresh water of 1000 kg/m^3 density and a salty water of 1030 kg/m^3 . Assume the faces of both dams are vertical.
- 3.1.26 Determine the equation for calculating the capillary rise h in the tube shown in Figure 3.1.2 in terms of θ , σ , γ , and τ .
- 3.1.27 Derive the relation between the gauge pressure p inside a spherical droplet of a liquid and the surface tension.
- 3.1.28 Derive the relation between the gauge pressure p inside the spherical bubble and the surface tension.
- 3.1.29 Calculate the pressure inside the spherical droplet of water having a diameter of 0.5 mm at 25°C if the pressure outside the droplet is standard atmospheric pressure (101.3 kPa).
- 3.1.30 What is the capillary rise of water in a glass tube having a diameter of 0.02 in at 70°F (take $\theta = 0$)?
- 3.1.31 Calculate the capillary depression of mercury in a glass tube having a diameter of 0.03 in at 68°F (take $\theta = 140$). The surface tension of mercury is 0.03562 lb/ft, and its specific gravity is 13.57. Take $\gamma_w = 62.3 \text{ lb/ft}^3$ at 68°F .
- 3.1.32 Calculate the force necessary to lift a thin wire ring of 10-mm diameter from a water surface at 10°C .
- 3.1.33 Heavy fuel oil flows in a pipe that has a 6-in diameter with a velocity of 7 ft/s. The kinematic viscosity is $0.00444 \text{ ft}^2/\text{s}$. What is the Reynolds number?
- 3.1.34 The discharge of water in a 20-cm diameter pipe is $0.02 \text{ m}^3/\text{s}$. Calculate the velocity, Reynolds number, and mass rate of flow. Assume the temperature is 15°C .
- 3.1.35 Water flows in a rectangular channel having a slope of 25°C at a mean velocity of 3 ft/s. The depth of flow that is measured along a vertical line is 2 ft. Calculate the discharge if the width of the channel is 1 ft.
- 3.1.36 Water flows in a 10-cm diameter pipe at 500 kg/min. Calculate the discharge and mean velocity if the temperature is 20°C .
- 3.1.37 Water flows into a weigh tank for 30 min. Calculate the increase in the weight of the tank, if the discharge is $1.5 \text{ ft}^3/\text{s}$. The temperature is 50°F .
- 3.1.38 The hypothetical velocity distribution in a horizontal, rectangular, open channel is $v = 0.3y$ (m/s), where v is the velocity at a distance y (m) above the bottom of the channel. If the vertical depth of flow is 2 m and the width of the channel is 4 m, what are the maximum velocity, the discharge, and the mean velocity?
- 3.1.39 Assume water flows full in a 10-mm piezometer pipe at a temperature of 20°C . What is the approximate maximum discharge for which a laminar flow may be expected?
- 3.3.1 It is required to reduce a pipe of diameter 8 in to a minimum-diameter pipe that allows the downstream velocity not to exceed twice the upstream velocity. Determine the diameter of the pipe. Assume smooth transition.
- 3.4.1 Water flows through a pipe of diameter 3 in. If it is desired to use another pipe for the same flow rate such that the velocity head in the second pipe is four times the velocity head in the first pipe, determine the diameter of the pipe.
- 3.5.1 If the pipeline in problem 3.3.1 is horizontal, what is the proportion of the potential energy head at the upstream cross-section that is changed to kinetic energy head at the downstream cross-section? Determine the answer in terms of the discharge.
- 3.6.1 Derive an expression for the depth to the center of pressure for a triangle of height h and base b that is vertically submerged in water with the vertex at the water surface.

3.6.2 Derive an expression for the depth to the center of pressure for a triangle of height h and base b that is vertically submerged in water with the vertex a distance x below the water surface.

3.6.3 Determine the magnitude and the location of the hydrostatic force on the 2-m by 4-m vertical rectangular gate shown in Figure 3.6.3. The top of the gate is 6 m below the water surface.

3.6.4 Suppose a vertical flat plate supports water on one side and oil of specific gravity 0.86 on the other side, as shown in Figure P3.6.4. How deep should the oil be so that there is no net horizontal force on the plate? Calculate the moments of the pressure forces about the base of the plate. Are the magnitudes of the moments equal? Why?

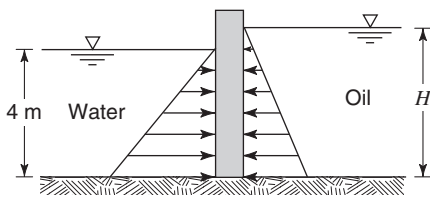


Figure P3.6.4 Vertical flat plate for problem 3.6.4.

3.6.5 Suppose a steel material of specific gravity of 7.8 is attached to a wood of specific gravity 0.8 as shown in Figure P3.6.5. If it is required that the material does not sink or rise when left in static water, what should be the proportion of the volume of the steel to that of the wood in Figure P3.6.5?

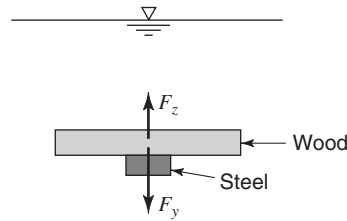


Figure P3.6.5 Problem 3.6.5 system.

3.6.6 Rework example 3.6.4 if the top of the inclined rectangular gate is 3 ft below the water surface.

3.7.1 Figure P3.7.1 shows a compound open channel cross-section. Determine the energy correction factor α . Assume uniform velocities within the subsections.

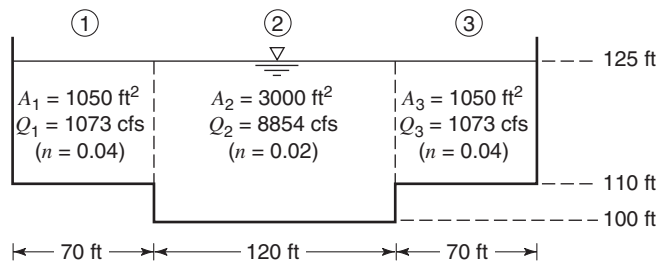


Figure P3.7.1 Compound open-channel cross-section for problem 3.7.1.

3.7.2 Determine the momentum correction factor β for problem 3.7.1.

REFERENCES

Chaudhry, H., "Principles of Flow of Water," Chapter 2 in *Water Resources Handbook*, edited by L. W. Mays, McGraw-Hill, New York, 1996.
 Chow, V. T., *Open-Channel Hydraulics*, McGraw-Hill, New York, 1959.
 Crowe, C. T., D. F. Elger, B. C. Williams, and J. A. Roberson, *Engineering Fluid Mechanics*, 9th edition, John Wiley & Sons, Inc., New York, 2009.
 Finnemore, E. J., and J. B. Franzini, *Fluid Mechanics*, 10th edition, McGraw-Hill, New York, 2002.

Fox, R. W., P. J. Pritchard, and A. T. McDonald, *Introduction to Fluid Mechanics*, 7th edition, John Wiley & Sons, Inc., New York, 2009.
 Munson, B. R., D. F. Young, and T. H. Okiish, *Fundamentals of Fluid Mechanics*, 4th edition, John Wiley and Sons, Inc., New York, 2002.
 Roberson, J. A., and C. T. Crowe, *Engineering Fluid Mechanics*, Houghton Mifflin, Boston, 1993.

Chapter 4

Hydraulic Processes: Pressurized Pipe Flow

4.1 CLASSIFICATION OF FLOW

Hydraulics is typically defined as the study of liquid (water) flow in pipes and open channels, referred to as pipe flow and open-channel flow, respectively. Pipe flow and open-channel flow are similar in many ways but have one major difference. *Open-channel flow* occurs when there is a free surface, whereas pipe flow does not have a free surface. *Pipe flow* here refers to pressurized flow in pipes as long as there is not a free surface. Open-channel flow can occur in pipes. Analogies can be made between pipe flow and groundwater flow in confined aquifers. Also, groundwater flow in unconfined (water table) conditions is analogous to open-channel flow. The major difference is the geometry of the flow paths in groundwater flow as compared to pipe or open-channel flow. Because of the many varied-flow paths that occur in groundwater flow, the macroscopic average of the liquid (water) and medium properties is used. The control volumes for these three types of flow are illustrated in Figure 4.1.1.

Both pipe flow and open-channel flow are expressed in terms of the discharge Q , cross-sectional averaged velocity V , and cross-sectional area of flow A . They are related mathematically as

$$Q = AV \quad (4.1.1)$$

and

$$A = \int_0^y B dy \quad (4.1.2)$$

where y is the depth of flow and B is the channel width, so that

$$Q = \int_A v dA \quad (4.1.3)$$

where v is the local point velocity along the direction normal to A .

For groundwater flow, the discharge is expressed as

$$Q = Aq \quad (4.1.4)$$

where A is the total cross-sectional area including the space occupied by the porous medium and q is the *Darcy flux* or volumetric flow rate per unit area of porous medium Q/A , also sometimes called the *specific discharge* or *Darcy velocity*. This velocity assumes that flow occurs through the entire cross-section of the porous medium without regard to solids and pores. *Darcy's law* states that flow

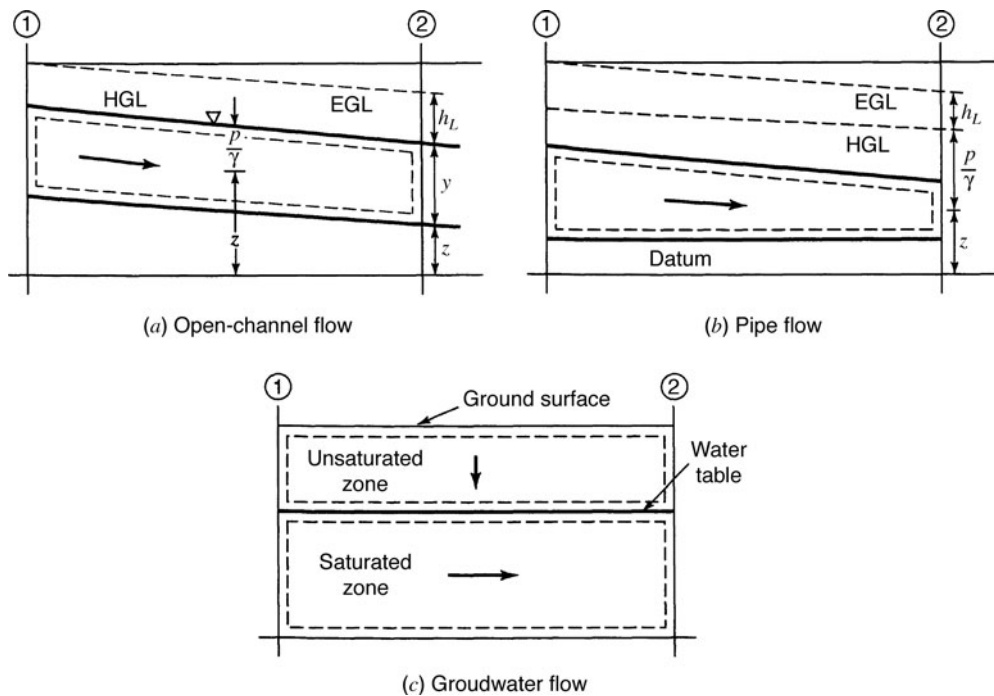


Figure 4.1.1 Control volumes for open-channel flow, pipe flow, and groundwater flow.

through a porous medium is proportional to the headloss and inversely proportional to the length of the flow path, $Q \sim dh/dL$. Darcy’s flux is expressed as

$$q = -K \frac{dh}{dL} \tag{4.1.5}$$

and

$$Q = -KA \frac{dh}{dL} \tag{4.1.6}$$

where K is the saturated hydraulic conductivity (L/T) or units of velocity.

The criterion to differentiate viscosity effects, i.e., turbulent or laminar flow, is the *Reynolds number*, R_e :

$$R_e = \frac{VD}{\nu} = \frac{V4R}{\nu} \tag{4.1.7}$$

where D is a characteristic length such as pipe diameter, R is the *hydraulic radius* defined as the cross-sectional area of flow A divided by the wetted perimeter, P , of A , and ν is the kinematic viscosity of the fluid. For full pipe flow, $R = A/P = \pi D^2/4/\pi D = D/4$. The critical number is around 2000 for pressurized pipe flow and 500 for open-channel flow. Below this critical value is laminar flow and above this number is turbulent flow. For groundwater flow the Reynolds number can be expressed with the velocity being the Darcy flux, q , and the effective grain size (d_{10}) is used for D . The *effective grain size* (d_{10}) is used to indicate that 10% (by weight) of a sample has a diameter smaller than d_{10} . Darcy’s law is typically valid for Reynolds number $R_e < 1$ and does not depart seriously until $R_e = 10$, which can be thought of as the upper limit for Darcy’s law.

The criterion to differentiate gravity effects, i.e., subcritical or supercritical flow, is the *Froude number*:

$$F_r = \frac{V}{\sqrt{gD_h}} \tag{4.1.8}$$

Table 4.1.1 Flow Classification

Classification criteria	Flow classification	Book section defined
Time	Steady flow	3.1.6
	Unsteady flow	3.1.6
Space	Uniform flow	3.1.6
	Nonuniform flow	3.1.6
	Gradually varied	5.3
	Rapidly varied	5.3
Viscosity (Reynolds number)	Laminar	3.1.7
	Turbulent	3.1.7
Gravity (Froude number)	Subcritical	5.2
	Critical	5.2
	Supercritical	5.2

where D_h is the *hydraulic depth* defined as the cross-sectional area of flow divided by the top width of flow. The critical value of the Froude number is 1, $F_r = 1$ for critical flow, i.e., when $F_r < 1$ the flow is subcritical and when $F_r > 1$ the flow is supercritical. Table 4.1.1 lists the flow classification for the criteria of time, space, viscosity, and gravity.

EXAMPLE 4.1.1

Water flows in a trapezoidal channel having a bottom width of 15 ft and side slopes of 1 vertical to 1.5 horizontal at a rate of 200 cfs. Is the flow a subcritical or a supercritical flow if the depth of the flow is 2 ft?

SOLUTION

To find out whether the flow is subcritical or supercritical, the Froude number should be calculated by equation (4.1.8):

$$F_r = \frac{V}{\sqrt{gD_h}}$$

The top width of the channel T is

$$T = 15 + 2 \times (2 \times 1.5) = 21$$

To determine the mean velocity, cross-sectional area must be computed:

$$A = 2 \times (15 + 21)/2 = 36 \text{ ft}^2$$

and from equation (4.1.1)

$$V = Q/A$$

$$V = 200/36 = 5.56 \text{ ft/s}$$

the hydraulic depth is

$$D_h = A/T = 36/21 = 1.71 \text{ ft}$$

Then

$$F_r = \frac{5.56 \text{ ft/s}}{\sqrt{32.2 \text{ ft/s}^2 \times 1.71 \text{ ft}}} = 0.75$$

F_r is < 1 , so the flow is subcritical flow.

4.2 PRESSURIZED (PIPE) FLOW

4.2.1 Energy Equation

In section 3.4, the general energy equation for steady fluid flow was derived as equation (3.4.20). Using equation (3.4.20) and considering pipe flow between sections 1 and 2 (Figure 4.1.1*b*), the energy equation for pipe flow is expressed as

$$\frac{dH}{dt} - \frac{dW_s}{dt} = \int_{A_2} \left(\frac{p_2}{\rho} + e_{u_2} + \frac{1}{2} V_2^2 + gz_2 \right) \rho V_2 dA_2 - \int_{A_1} \left(\frac{p_1}{\rho} + e_{u_1} + \frac{1}{2} V_1^2 + gz_1 \right) \rho V_1 dA_1 \quad (4.2.1)$$

which can be modified to

$$\frac{dH}{dt} - \frac{dW_s}{dt} = \int_{A_2} \left(\frac{p_2}{\rho} + e_{u_2} + gz_2 \right) \rho V_2 dA_2 + \int_{A_2} \frac{\rho V_2^3}{2} dA_2 - \int_{A_1} \left(\frac{p_1}{\rho} + e_{u_1} + gz_1 \right) \rho V_1 dA_1 - \int_{A_1} \frac{\rho V_1^3}{2} dA_1 \quad (4.2.2)$$

Flow is uniform at sections 1 and 2 and therefore hydrostatic conditions prevail across the section. For hydrostatic conditions, $p/\rho + e_u + gz$ is constant across the system. This allows the term $(p/\rho + e_u + gz)$ to be taken outside the integral, so that (4.2.2) can be expressed as

$$\frac{dH}{dt} - \frac{dW_s}{dt} = \left(\frac{p_2}{\rho} + e_{u_2} + gz_2 \right) \int_{A_2} \rho V_2 dA_2 + \int_{A_2} \frac{\rho V_2^3}{2} dA_2 - \left(\frac{p_1}{\rho} + e_{u_1} + gz_1 \right) \int_{A_1} \rho V_1 dA_1 - \int_{A_1} \frac{\rho V_1^3}{2} dA_1 \quad (4.2.3)$$

The term $\int \rho V dA = \dot{m}$ is the mass rate of flow and $\int_A (\rho V^3/2) dA = (\rho V^3/2)A = \dot{m}(\rho V^3/2)$.

Substituting these definitions, equation (4.2.3) now becomes

$$\frac{dH}{dt} - \frac{dW_s}{dt} = \left(\frac{p_2}{\rho} + e_{u_2} + gz_2 \right) \dot{m} + \dot{m} \frac{V_2^2}{2} - \left(\frac{p_1}{\rho} + e_{u_1} + gz_1 \right) \dot{m} - \dot{m} \frac{V_1^2}{2} \quad (4.2.4)$$

Dividing through by \dot{m} and rearranging then yields

$$\frac{1}{\dot{m}} \left(\frac{dH}{dt} - \frac{dW_s}{dt} \right) + \frac{p_1}{\rho} + e_{u_1} + gz_1 + \frac{V_1^2}{2} = \frac{p_2}{\rho} + e_{u_2} + gz_2 + \frac{V_2^2}{2} \quad (4.2.5)$$

The shaft work term (dW_s/dt) can be the result of a turbine (W_T) or a pump (W_P) in the system, so that the shaft work term can be expressed as

$$\frac{dW_s}{dt} = \frac{dW_T}{dt} - \frac{dW_P}{dt} \quad (4.2.6)$$

The minus sign occurs because a pump does work on the fluid and conversely a turbine does shaft work on the surroundings. The term dW/dt has the units of power, which is work per unit time. Substituting equation (4.2.6) into (4.2.5) and dividing through by g results in

$$\left(\frac{1}{\dot{m}g} \right) \frac{dW_P}{dt} + \frac{p_1}{g} + z_1 + \frac{V_1^2}{2g} = \left(\frac{1}{\dot{m}g} \right) \frac{dW_T}{dt} + \frac{p_2}{g} + z_2 + \frac{V_2^2}{2g} + \left[\frac{e_{u_2} - e_{u_1}}{g} - \frac{1}{\dot{m}g} \frac{dH}{dt} \right] \quad (4.2.7)$$

Each term in the above equation has the dimension of length. The following are defined:

$$\text{Head supplied by pumps: } h_p = \left(\frac{1}{\dot{m}g} \right) \frac{dW_p}{dt} \quad (4.2.8)$$

$$\text{Head supplied by turbines: } h_T = \left(\frac{1}{\dot{m}g} \right) \frac{dW_T}{dt} \quad (4.2.9)$$

$$\text{Headloss (loss of mechanical energy due to viscous stress): } h_L = \left[\left(\frac{e_{u_2} - e_{u_1}}{g} \right) - \left(\frac{1}{\dot{m}g} \right) \frac{dH}{dt} \right] \quad (4.2.10)$$

The term $((e_{u_2} - e_{u_1})/g)$ represents finite increases in internal energy of the flow system because some of the mechanical energy is converted to thermal energy through viscous action between fluid particles. The term $-(1/\dot{m}g)dH/dt$ represents heat generated through energy dissipation that escapes the flow system.

Using h_p , h_T , and h_L , the energy equation (4.2.7) is now expressed as

$$\frac{p_1}{\gamma} + z_1 + \frac{V_1^2}{2g} + h_p = \frac{p_2}{\gamma} + z_2 + \frac{V_2^2}{2g} + h_T + h_L \quad (4.2.11)$$

This energy equation is expressed with the velocity representing the mean velocity; p/γ is referred to as the *pressure head* and $V^2/2g$ is referred as the *velocity head*.

Because the velocity is not actually uniform over a cross-section, an *energy correction factor* is typically introduced, which is defined as (see section 3.7)

$$\alpha = \frac{\int v^3 dA}{V^3 A} \quad (4.2.12)$$

where v is the velocity at any point in the section. Using α_1 and α_2 for sections 1 and 2, the energy equation can be expressed as

$$\frac{p_1}{\gamma} + z_1 + \alpha_1 \frac{V_1^2}{2g} + h_p = \frac{p_2}{\gamma} + z_2 + \alpha_2 \frac{V_2^2}{2g} + h_T + h_L \quad (4.2.13)$$

Because α has a value very near 1 for pipe flow, it is typically omitted.

EXAMPLE 4.2.1

The flow of water in a horizontal pipe of constant cross-section has a pressure gauge at location 1 with a pressure of 100 psig and a pressure gauge at location 2 with a pressure of 75 psig. What is the headloss between the two pressure gauges?

SOLUTION

For the energy equation (4.2.11), $h_p = 0$, $h_T = 0$, $z_1 = z_2$, and because the pipe size is constant $V_1^2/2g = V_2^2/2g$; then (4.2.11) reduces to

$$h_L = \frac{p_1 - p_2}{\gamma} = \frac{(100 \text{ lb/in}^2 - 75 \text{ lb/in}^2) \times 144 \text{ in}^2/\text{ft}^2}{62.4 \text{ lb/ft}^3} = \frac{25 \times 144}{62.4}$$

$$h_L = 57.7 \text{ ft}$$

EXAMPLE 4.2.2

For the simple pipe system shown in Figure 4.2.1, the pressures are $p_1 = 14 \text{ kPa}$, $p_2 = 12.5 \text{ kPa}$, and $p_3 = 10 \text{ kPa}$. Determine the headloss between 1 and 2 and the headloss between 1 and 3. The discharge is 7 L/s .

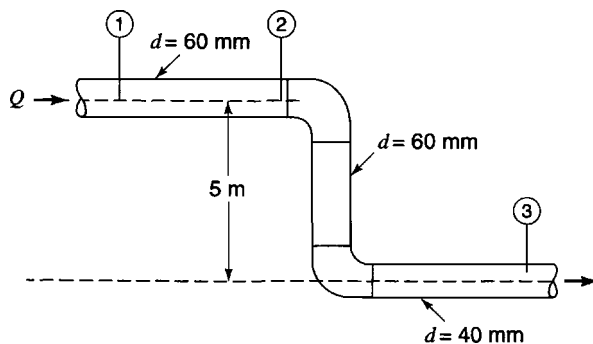


Figure 4.2.1 Pipe system for example 4.2.2.

SOLUTION

The energy equation between 1 and 2 is

$$\frac{p_1}{\gamma} + \frac{V_1^2}{2g} + z_1 = \frac{p_2}{\gamma} + \frac{V_2^2}{2g} + z_2 + h_{L_{1-2}}$$

where $\frac{V_1^2}{2g} = \frac{V_2^2}{2g}$ and $z_1 = z_2$, so

$$\frac{p_1}{\gamma} = \frac{p_2}{\gamma} + h_{L_{1-2}} \text{ and } h_{L_{1-2}} = \frac{p_1 - p_2}{\gamma} = \frac{14 - 12.5}{9.79} = 0.153 \text{ m}$$

The energy equation between 1 and 3 is

$$\frac{p_1}{\gamma} + \frac{V_1^2}{2g} + z_1 = \frac{p_3}{\gamma} + \frac{V_3^2}{2g} + z_3 + h_{L_{1-3}}$$

$$V_1 = Q/A_1 = \frac{(7/1000)}{\left[\frac{\pi(60/1000)^2}{4}\right]} = \frac{0.007}{0.0028} = 2.477 \text{ m/s}$$

$$V_3 = Q/A_3 = \frac{(7/1000)}{\left[\frac{\pi(40/1000)^2}{4}\right]} = \frac{0.007}{0.0013} = 5.385 \text{ m/s}$$

Now using the above energy equation, we get

$$\frac{14}{9.79} + \frac{(2.477)^2}{2 \times 9.81} + 5 = \frac{10}{9.79} + \frac{(5.385)^2}{2 \times 9.81} + 0 + h_{L_{1-3}}$$

$$1.43 + 0.313 + 5 = 1.022 + 1.478 + 0 + h_{L_{1-3}}$$

$$h_{L_{1-3}} = 4.24 \text{ m}$$

EXAMPLE 4.2.3

A *Venturi meter* is a device, as shown in Figure 4.2.2, that is inserted into a pipeline to measure the incompressible flow rate. These meters consist of a convergent section that reduces the diameter to between one-half and one-fourth the pipe diameter, followed by a divergent section. Pressure differences between the position just before the Venturi and at the throat are measured by a differential manometer. Using the energy equation, develop an equation for the discharge in terms of the pressure difference $p_1 - p_2$. Use a coefficient of discharge that takes into account frictional effects.

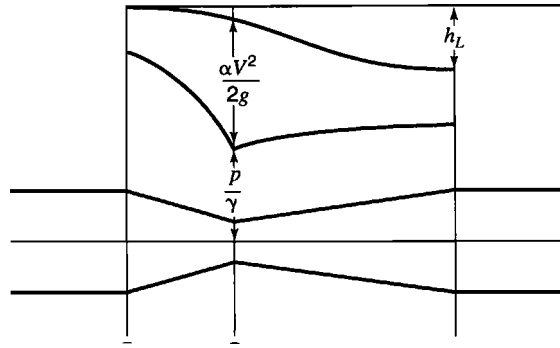


Figure 4.2.2 Venturi tube.

SOLUTION

Write the energy equation between 1 and 2:

$$\frac{p_1}{\gamma} + \frac{V_1^2}{2g} + z_1 = \frac{p_2}{\gamma} + \frac{V_2^2}{2g} + z_2 + h_L$$

For $z_1 = z_2$ and assuming $h_L = 0$, the energy equation reduces to

$$\begin{aligned} \frac{p_1}{\gamma} + \frac{V_1^2}{2g} &= \frac{p_2}{\gamma} + \frac{V_2^2}{2g} \\ V_1^2 - V_2^2 &= 2g \left(\frac{p_2 - p_1}{\gamma} \right) \end{aligned}$$

From continuity, $A_1 V_1 = A_2 V_2$, so $V_1 = V_2 (A_2/A_1)$. Substituting V_1 into the above energy equation yields

$$\begin{aligned} \left[V_2 \frac{A_2}{A_1} \right]^2 - V_2^2 &= 2g \left(\frac{p_2 - p_1}{\gamma} \right) \\ \left[\left(\frac{A_2}{A_1} \right)^2 - 1 \right] V_2^2 &= 2g \left(\frac{p_2 - p_1}{\gamma} \right) \end{aligned}$$

Multiplying through by (-1) and solving for V_2 , we get

$$V_2 = \sqrt{\frac{1}{1 - (A_2/A_1)^2}} \sqrt{2g \left(\frac{p_1 - p_2}{\gamma} \right)}$$

which neglects friction effects. A coefficient of discharge C_d is used in the continuity equation to account for friction effect, so

$$Q = C_d A_2 V_2 = C_d A_2 \left[\frac{1}{1 - (A_2/A_1)^2} \right]^{1/2} \left[2g \left(\frac{p_1 - p_2}{\gamma} \right) \right]^{1/2} = C_d \frac{A_2}{\sqrt{1 - (A_2/A_1)^2}} \sqrt{2g \frac{p_1 - p_2}{\gamma}}$$

The value of C_d must be determined experimentally.

4.2.2 Hydraulic and Energy Grade Lines

The terms in equation (4.2.13) have dimensions of length and units of feet or meters. The concept of the *hydraulic grade line (HGL)* and the *energy grade line (EGL)* can be used to give a physical

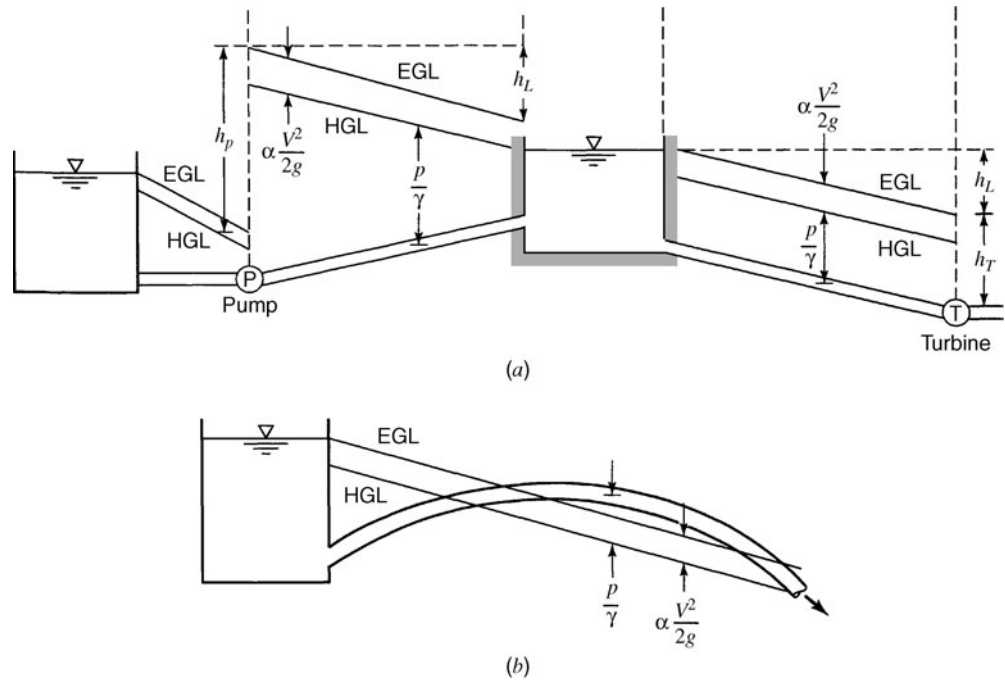


Figure 4.2.3 Energy and hydraulic grade lines. (a) EGL and HGL for system with pump and turbine; (b) System with subatmospheric pressure (pipe is above the HGL).

relationship to these terms. The HGL is essentially the line p/γ above the center line of a pipe, which is the distance water would rise in a piezometer tube attached to the pipe. The EGL is a distance of $\alpha V^2/2g$ above the HGL. Figure 4.2.3 illustrates the HGL and EGL.

4.3 HEADLOSSES

The energy equation (4.2.13) for pipe flow was derived in the previous section. This equation has a headloss term h_L that was defined as the loss of mechanical energy due to viscous stress. The objective of this section is to discuss the headlosses that occur in pressurized pipe flow.

4.3.1 Shear-Stress Distribution of Flow in Pipes

Consider steady flow (laminar or turbulent) in a pipe (a cylindrical element of fluid) of uniform cross-section as shown in Figure 4.3.1. For a uniform flow, the general form of the integral momentum equation in the x -direction is expressed by

$$\sum F_x = \frac{d}{dt} \int_{CV} v_x \rho d\forall + \sum_{CS} v_x (\rho \mathbf{V} \cdot \mathbf{A}) \quad (3.5.6)$$

where $\frac{d}{dt} \int_{CV} v_x \rho d\forall = 0$ because the flow is steady and $\sum_{CS} v_x (\rho \mathbf{V} \cdot \mathbf{A}) = 0$ because there is no flow of extensive property through the control surface so that

$$\sum F_x = 0 \quad (4.3.1)$$

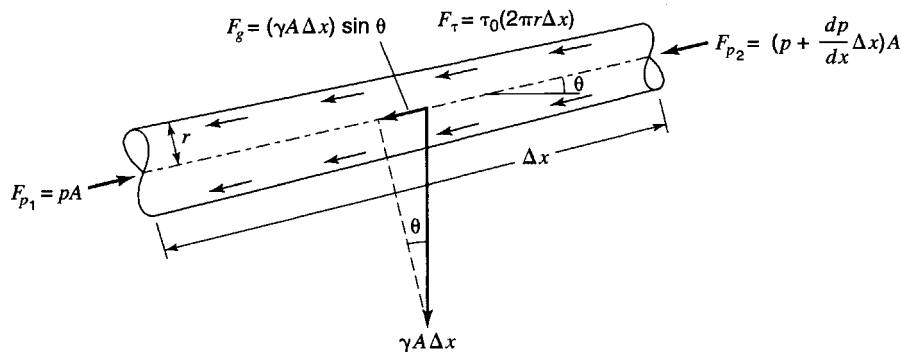


Figure 4.3.1 Cylindrical element of water.

The forces are: (1) the *pressure forces*, $F_{p_1} = pA$ and $F_{p_2} = (p + dp/dx \Delta x)A$; (2) the *gravity force* due to the weight of the water, $F_g = (\gamma A \Delta x) \sin \theta$; and (3) the *shearing force* $F_\tau = \tau(2\pi r \Delta x)$ where τ is the shear stress. The sum of forces is

$$F_{p_1} - F_{p_2} - F_g - F_\tau = 0 \quad (4.3.2)$$

or

$$pA - \left(p + \frac{dp}{dx} \Delta x\right)A - (\gamma A \Delta x) \sin \theta - \tau(2\pi r \Delta x) = 0 \quad (4.3.3)$$

Equation (4.3.3) reduces to

$$-\frac{dp}{dx} \Delta x A - (\gamma A \Delta x) \sin \theta - \tau(2\pi r \Delta x) = 0 \quad (4.3.4)$$

Solving for the shear stress by using $dz = \sin \theta dx$ gives

$$\tau = \frac{r}{2} \left[-\frac{d}{dx} (p + \gamma z) \right] \quad (4.3.5)$$

Equation (4.3.5) indicates that τ is zero at the center of the pipe where $r = 0$ and increases linearly to a maximum at the pipe wall (see Figure 4.3.2). Keep in mind that $p + \gamma z$ is constant across the section because the streamlines are straight and parallel in a uniform flow, so that there is no acceleration of fluid normal to the streamline. In other words, hydrostatic conditions prevail across the flow section, resulting in $p + \gamma z$ being constant across the flow section. The gradient $d(p + \gamma z)/dx$ is therefore negative and constant across the flow section for uniform flow.

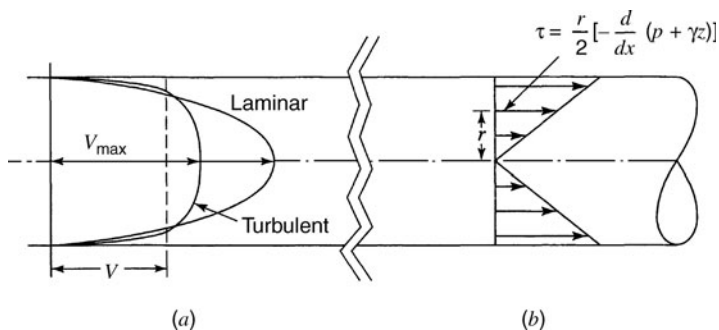


Figure 4.3.2 Distribution of velocity and shear stress for pipe flow. (a) Velocity distribution; (b) Shear stress.

4.3.2 Velocity Distribution of Flow in Pipes

Laminar Flow

In Chapter 3 the following shear stress equation (3.1.2) was introduced:

$$\tau = \mu \frac{dv}{dy} \quad (3.1.2)$$

where μ is the dynamic viscosity and dv/dy is the velocity gradient. For our purposes here, the gradient is actually $dv/dy = -dv/dr$, so that using equation (4.3.5) we get

$$\tau = \mu \frac{dv}{dr} = \frac{r}{2} \left[-\frac{d}{dx}(p + \gamma z) \right] \quad (4.3.6)$$

Integrating this equation by the separation of variables and boundary condition ($r = r_0, v = 0$) yields

$$v = \frac{r_0^2 - r^2}{4\mu} \left[-\frac{d}{dx}(p + \gamma z) \right] \quad (4.3.7)$$

This equation indicates that the velocity distribution for laminar pipe flow is parabolic across the section and has the maximum velocity at the pipe center (refer to Figure 4.3.2). By integrating the velocity across the section using $Q = \int v dA$ and using the energy equation, the headloss for laminar flow is

$$h_{L_f} = \frac{32\mu LV}{\gamma D^2} \quad (4.3.8)$$

where D is the diameter of the pipe.

Turbulent Flow—Smooth Pipes

For a smooth pipe, the following velocity distribution equations are based upon experiment (Roberson and Crowe, 1990):

$$\frac{u}{u_*} = \frac{u_* y}{\nu} \text{ for } 0 < \frac{u_* y}{\nu} < 5 \quad (4.3.9)$$

and

$$\frac{u}{u_*} = 5.75 \log \frac{u_* y}{\nu} + 5.5 \text{ for } 20 < \frac{u_* y}{\nu} < 10^5 \quad (4.3.10)$$

where u is the velocity, y is the distance from the pipe wall, ν is the kinematic viscosity, u_* is the shear velocity ($\sqrt{\tau_0/\rho}$), and τ_0 is the shear stress at the pipe wall.

The velocity distribution for turbulent flow can also be approximated using power law formulas of the form $u/u_{\max} = (y/r_0)^m$, where u_{\max} is the velocity at the center of the pipe, r_0 is the pipe radius, and m is an exponent that increases with Reynolds number (see Roberson and Crowe (1990) for values of m).

Turbulent Flow—Rough Pipes

Experimental results on flow in rough pipes indicate the following form of equation for velocity distribution of turbulent flow in rough pipes:

$$\frac{u}{u_*} = 5.75 \log \frac{y}{k} + B \quad (4.3.11)$$

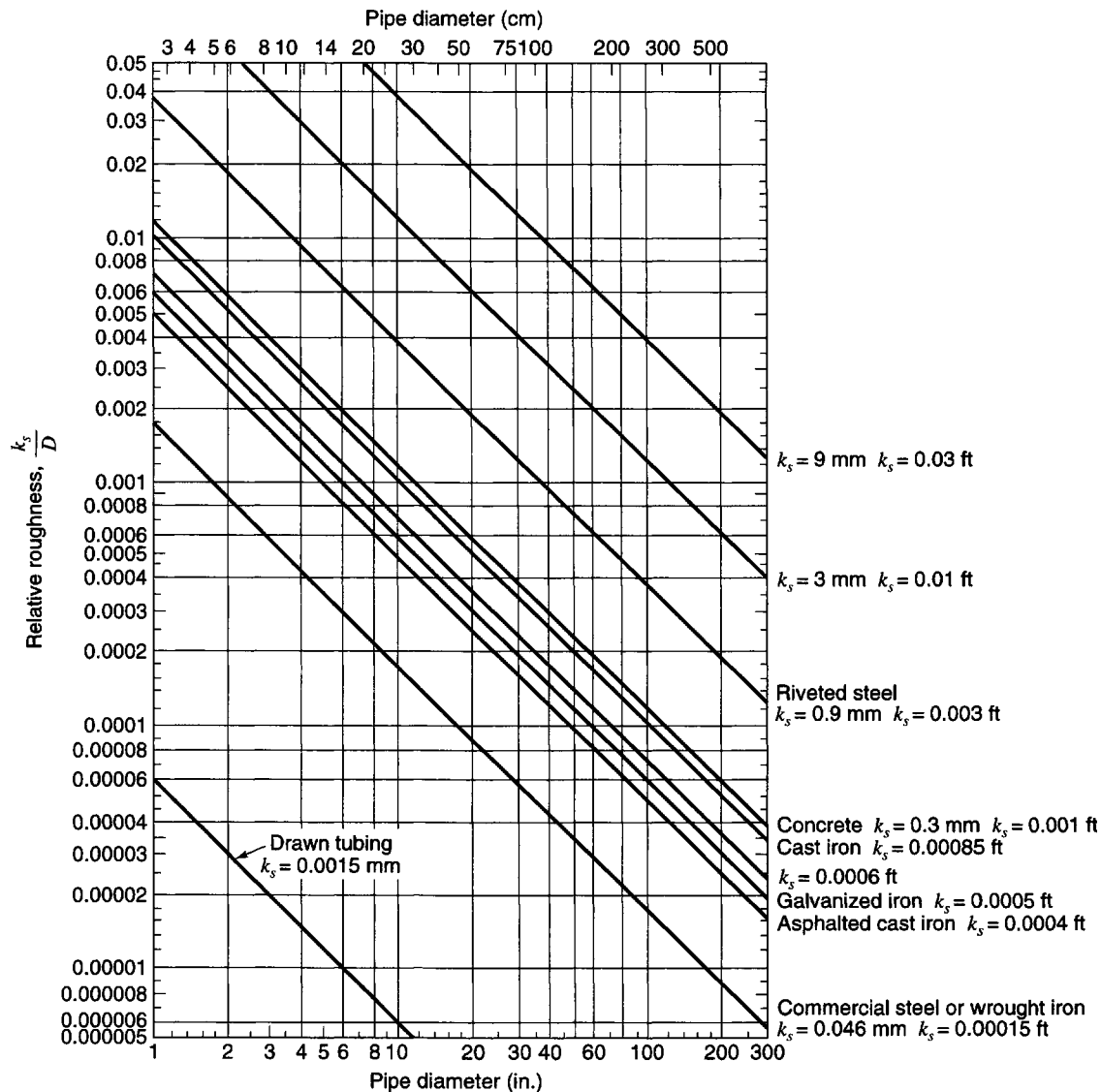


Figure 4.3.3 Relative roughness for various kinds of pipe (from Moody (1944)).

where y is the distance from the wall, k is a measure of the height of the roughness elements, and B is a function of the roughness characteristics. Nikuradse (1933) determined the value of $B = 8.5$, y was measured from the geometric mean of the wall surface, and $k_s = k$ was the sand grain size, so that

$$\frac{u}{u_*} = 5.75 \log \frac{y}{k_s} + 8.5 \quad (4.3.12)$$

Nikuradse's work revealed that (1) for low Reynolds numbers and small sand grains the flow resistance is basically the same as for smooth pipes (roughness elements became submerged in the viscous sublayer) and (2) for high Reynolds numbers the resistance coefficient is a function of only the relative roughness k_s/D , where D is the diameter (the viscous sublayer is very thin so that the roughness elements project into the flow, causing flow resistance from drag of the individual roughness elements). Figure 4.3.3 presents values of relative roughness for different kinds of pipe as a function of pipe diameter.

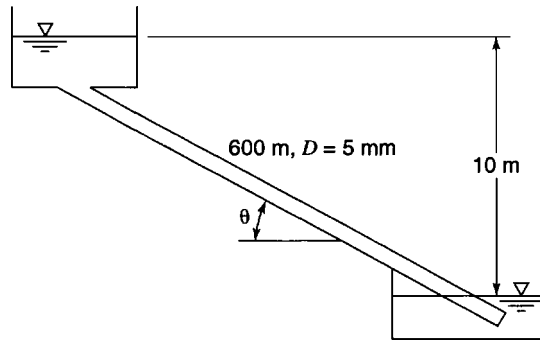


Figure 4.3.4 Pipe system for example 4.3.1.

EXAMPLE 4.3.1

For the system shown in Figure 4.3.4 determine the headloss per unit length of pipe and the discharge, assuming laminar flow ($\mu = 1.002 \times 10^{-3} \text{ N}\cdot\text{s}/\text{m}^2$).

SOLUTION

The headloss equation (4.3.8) for laminar pipe flow is used to determine the velocity of flow in the pipe, where $h_L = 10 \text{ m}$, $D = 5 \text{ mm}$, $\gamma = 9.79 \text{ kN}/\text{m}^3$, $\mu = 1.002 \times 10^{-3} \text{ N}\cdot\text{s}/\text{m}^2$:

$$V = \frac{\gamma h_L D^2}{32\mu L} = \frac{(9.79 \text{ kN}/\text{m}^3 \times 1000)(10\text{m})(5/1000\text{m})^2}{32(1.002 \times 10^{-3} \text{ N}\cdot\text{s}/\text{m}^2)(600\text{m})} = 0.125 \text{ m/s}$$

Check the Reynolds number:

$$R_e = \frac{VD}{\nu} = \frac{VD\rho}{\mu} = \frac{0.125 \times (5/1000) \times 1000}{1.002 \times 10^{-3}} = 6.24 \times 10^2 = 624$$

Flow is laminar. The flowrate is then

$$\begin{aligned} Q &= AV = \left[\frac{\pi(5/1000)^2}{4} \right] \times 0.125 \text{ m/s} = 2.45 \times 10^{-6} \text{ m}^3/\text{s} \\ &= 2.45 \times 10^{-6}(1000)(60) \\ &= 0.147 \text{ L}/\text{min} \end{aligned}$$

The headloss per unit length of pipe is $(10 \text{ m}/600 \text{ m}) = 0.0167 \text{ m}/\text{m}$.

4.3.3 Headlosses from Pipe Friction

Various equations have been proposed to determine the headlosses due to friction, including the Darcy–Weisbach, Chezy, Manning, Hazen–Williams, and Scobey formulas. These equations relate the friction losses to physical characteristics of the pipe and various flow parameters. The Darcy–Weisbach equation is scientifically based and applies to both laminar and turbulent flows. The *Darcy–Weisbach equation* is

$$h_{L_f} = f \frac{L V^2}{D 2g} \tag{4.3.13}$$

where h_{L_f} is the headloss due to pipe friction, f is the dimensionless friction factor, L is the length of the conduit, D is the inside diameter of the pipe, V is the mean flow velocity, and g is the acceleration due to gravity.

The friction factor is a function of the Reynolds number (R_e) and the relative roughness k_s/D , where k_s is the average nonuniform roughness of the pipe. For laminar flow ($R_e < 2000$) the friction factor is

$$f = \frac{64}{R_e} \tag{4.3.14}$$

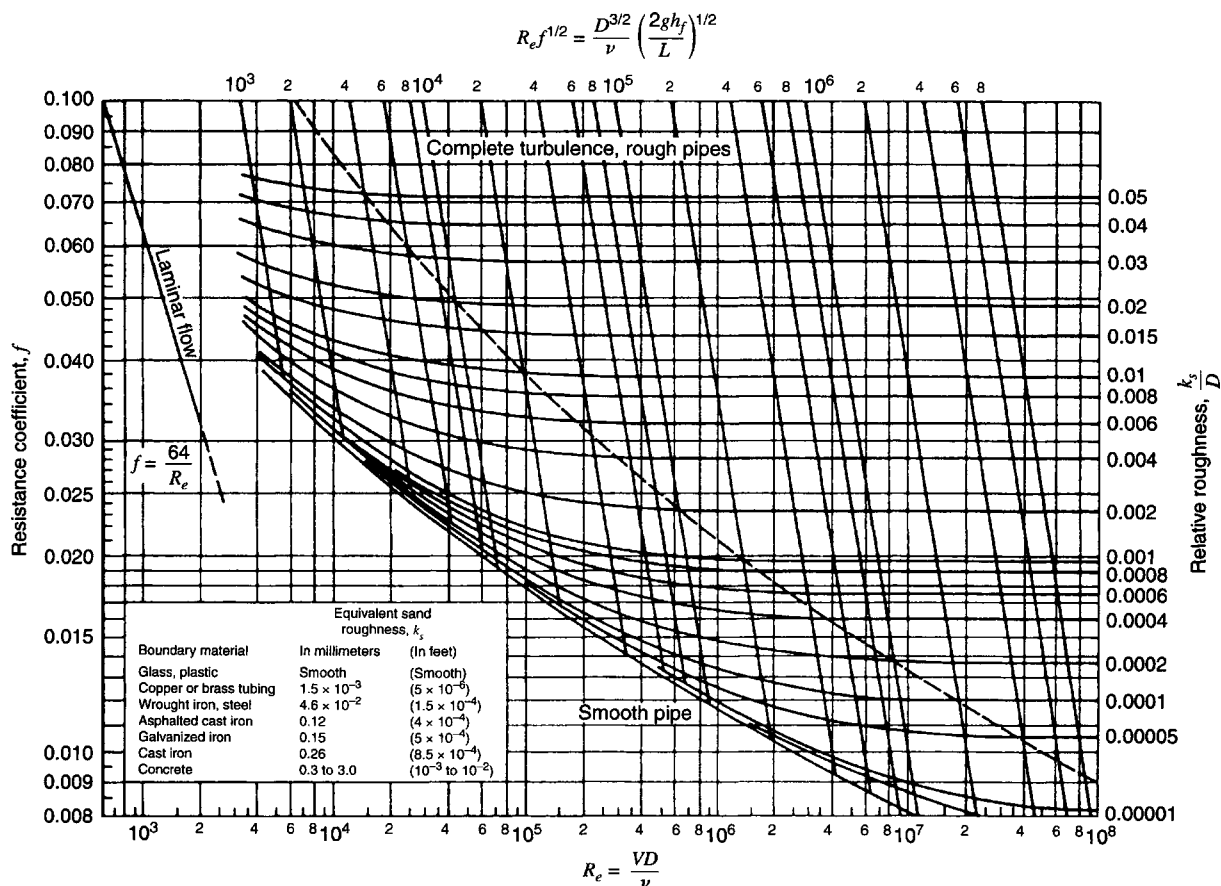


Figure 4.3.5 Resistance coefficient f versus R_e (from Moody (1944)).

where

$$R_e = \frac{VD}{\nu} \quad (4.3.15)$$

and ν is the kinematic viscosity. For turbulent flow in

$$\text{Smooth pipe } \frac{1}{\sqrt{f}} = 2 \log_{10} (R_e \sqrt{f}) - 0.8 \text{ for } R_e > 3000 \quad (4.3.16)$$

$$\text{Rough pipe } \frac{1}{\sqrt{f}} = 2 \log_{10} \frac{D}{(k_s)} + 1.14 = 1.14 - 2 \log_{10} \left(\frac{k_s}{D} \right) \quad (4.3.17)$$

where D is the pipe diameter. Equations (4.3.16) and (4.3.17) were proposed by von Karman and Prandtl based upon experiments by Nikuradse (1932).

Colebrook and White (1939) proposed the following semi-empirical formula:

$$\frac{1}{\sqrt{f}} = -2.0 \log_{10} \left(\frac{k_s/D}{3.7} + \frac{2.51}{R_e \sqrt{f}} \right) \quad (4.3.18)$$

The above equation is asymptotic to both the smooth and rough pipe equations (4.3.16) and (4.3.17) and is valid for the entire nonlaminar range of the Moody diagram.

Moody (1944) developed the *Moody diagram*, shown in Figure 4.3.5, using experimental data on commercial pipes, the Colebrook–White equation, and the Prandtl–Karman experimental data.

Knowing the pipe roughness (relative roughness) and the Reynolds number, the friction factor can be obtained from the Moody diagram. The use of Manning's equation and the Hazen-Williams equation is discussed in Chapter 12.

EXAMPLE 4.3.2

Water flows in a 1000-m long pipeline of diameter 200 mm at a velocity of 5 m/s. The pipeline is a new cast iron pipe with $k_s = 0.00026$ m. Determine the headloss in the pipeline. Use $\nu = 1.007 \times 10^{-6}$ m²/s.

SOLUTION

The headloss is computed using the Darcy-Weisbach equation (4.3.13):

$$h_{L_f} = f \frac{L V^2}{D 2g}$$

To determine the friction factor from the Moody diagram the Reynolds number must be computed:

$$Re = \frac{VD}{\nu} = \frac{5 \times (200/1000)}{1.007 \times 10^{-6}} = 9.93 \times 10^5$$

The relative roughness is $\frac{k_s}{D} = \frac{0.00026}{0.200} = 0.0013$. From Figure 4.3.5, $f = 0.021$, so

$$h_{L_f} = 0.021 \frac{1000}{(200/1000)} \frac{(5)^2}{2(9.81)} = 133.8 \text{ m.}$$

EXAMPLE 4.3.3

A 10-cm diameter, 2000-m long pipeline connects two reservoirs open to the atmosphere. What is the discharge in the pipeline if the water surface elevation difference of the reservoirs is 50 m? Assume a smooth pipe and $\nu = 1.02 \times 10^{-6}$ m²/s.

SOLUTION

The energy equation between the reservoir surfaces is used to determine the headloss due to friction, which is then used to determine the velocity of flow in the pipeline:

$$\frac{p_1}{\gamma} + \frac{V_1^2}{2g} + z_1 = \frac{p_2}{\gamma} + \frac{V_2^2}{2g} + z_2 + h_{L_f}$$

$$0 + 0 + z_1 = 0 + 0 + z_2 + h_{L_f}$$

$$h_{L_f} = z_1 - z_2 = 50 \text{ m}$$

$$h_{L_f} = f \frac{L V^2}{D 2g}$$

$$f \left(\frac{2000}{10/100} \right) \frac{V^2}{2 \times 9.81} = 50$$

$$f V^2 = 0.0491 \text{ (or } V = 0.2215/\sqrt{f}\text{)}$$

This must be solved for V using a trial-and-error procedure by assuming f , computing V , then computing the Reynolds number. Assume $f = 0.02$, $V = 0.2215/\sqrt{0.02} = 1.566$ m/s:

$$Re = \frac{VD}{\nu} = \frac{1.566(10/100)}{1.02 \times 10^{-6}} = 1.54 \times 10^5$$

From Figure 4.3.5, $f = 0.016$, $V = 0.2215/\sqrt{0.016} = 1.751$ m/s, so

$$Re = \frac{VD}{\nu} = \frac{1.751(10/100)}{1.02 \times 10^{-6}} = 1.72 \times 10^5$$

From Figure 4.3.5, $f = 0.016$, which is close enough. The discharge is

$$Q = AV = \frac{\pi(10/100)^2}{4} (1.751) = 0.0137 \text{ m}^3/\text{s.}$$

EXAMPLE 4.3.4

Compute the friction factor for flow having a Reynolds number of 1.37×10^4 and relative roughness $k_s/D = 0.000375$ using the Colebrook–White formula.

SOLUTION

Use equation (4.3.18) $\frac{1}{\sqrt{f}} = -2.0 \log_{10} \left(\frac{0.000375}{3.7} + \frac{2.51}{1.37 \times 10^4 \sqrt{f}} \right)$ and solve using trial and error $f = 0.0291$. Referring to the Moody diagram (Figure 4.3.5), we would read approximately 0.028 or 0.029.

4.3.4 Form (Minor) Losses

Headlosses are also caused by inlets, outlets, bends, and other appurtenances such as fittings, valves, expansions, and contractions. These losses, referred to as *minor losses*, *form losses*, or *secondary losses*, are caused by flow separation and the generation of turbulence. Headlosses produced, in general, can be expressed by

$$h_{L_m} = K \frac{V^2}{2g} \quad (4.3.19)$$

where K is the loss coefficient (see Table 4.3.1) and V is the mean velocity. Table 4.3.2 lists loss coefficients for various transitions and fittings. Table 12.2.5 lists recommended energy loss coefficients for valves and Figure 12.2.12 shows diagrams of various types of valves.

For sudden expansions or enlargements, the headlosses can be expressed as

$$h_{L_m} = \frac{(V_1 - V_2)^2}{2g} \quad (4.3.20)$$

For *gradual enlargements*, such as *conical diffusers*, the headloss is expressed as

$$h_{L_m} = K' \frac{(V_1 - V_2)^2}{2g} \quad (4.3.21)$$

The loss of head due to a *sudden contraction* may be expressed as

$$h_{L_m} = K_c \frac{V_2^2}{2g} \quad (4.3.22)$$

where the values of K_c are a function of the diameter ratios D_2/D_1 .

Entrance losses are computed using

$$h_{L_m} = K_e \frac{V^2}{2g} \quad (4.3.23)$$

where values of K_e are found in Table 4.3.1.

Exit (or discharge) losses (Table 4.3.1) from the end of a pipe into a reservoir that has a negligible velocity are expressed as

$$h_{L_m} = \frac{V^2}{2g} \quad (4.3.24)$$

EXAMPLE 4.3.5

Water flows from reservoir 1 to reservoir 2 through a 12-in diameter, 600-ft long pipeline as shown in Figure 4.3.6. The reservoir 1 surface elevation is 1000 ft and reservoir 2 surface elevation is 950 ft. Consider the minor losses due to the sharp-edged entrance, the butterfly valve ($\theta = 20^\circ$), the two bends (90° elbow), and the sharp-edged exit. The pipe is galvanized iron with $k_s = 0.0005$ ft. Determine the discharge from reservoir 1 to reservoir 2. For 120°F , $\nu = 0.609 \times 10^{-5}$ ft²/s.

SOLUTION

The energy equation between 1 and 2 is

$$\frac{p_1}{\gamma} + \frac{V_1^2}{2g} + z_1 = \frac{p_2}{\gamma} + \frac{V_2^2}{2g} + z_2 + h_{L_f} + \sum h_{L_m}$$

Table 4.3.1 Minor Loss Coefficients for Pipe Flow

Type of minor loss	K Loss in terms of $V^2/2g$
Pipe fittings:	
90° elbow, regular	0.21–0.30
90° elbow, long radius	0.14–0.23
45° elbow, regular	0.2
Return bend, regular	0.4
Return bend, long radius	0.3
AWWA tee, flow through side outlet	0.5–1.80
AWWA tee, flow through run	0.1–0.6
AWWA tee, flow split side inlet to run	0.5–1.8
Valves:	
Butterfly valve ($\theta = 90^\circ$ for closed valve)*	
$\theta = 0^\circ$	0.3–1.3
$\theta = 10^\circ$	0.46–0.52
$\theta = 20^\circ$	1.38–1.54
$\theta = 30^\circ$	3.6–3.9
$\theta = 40^\circ$	10–11
$\theta = 50^\circ$	31–33
$\theta = 60^\circ$	90–120
Check valves (swing check) fully open	0.6–2.5
Gate valves (4 to 12 in) fully open	0.07–0.14
1/4 closed	0.47–0.55
1/2 closed	2.2–2.6
3/4 closed	12–16
Sluice gates:	
As submerged port in 12-in wall	0.8
As contraction in conduit	0.5
Width equal to conduit width and without top submergence	0.2
Entrance and exit losses:	
Entrance, bellmouthed	0.04
Entrance, slightly taunted	0.23
Entrance, square edged	0.5
Entrance, projecting	1.0
Exit, bellmouthed	$0.1 \left(\frac{V_1^2}{2g} - \frac{V_2^2}{2g} \right)$
Exit, submerged pipe to still water	1.0

*Loss coefficients for partially open conditions may vary widely. Individual manufacturers should be consulted for specific conditions.

Source: Adapted from Velon and Johnson (1993).

For the reservoir surface $p_1/\gamma = 0$ and $V^2/2g = 0$, so

$$0 + 0 + 1000 = 0 + 0 + 950 + h_{L_f} + \sum h_{L_m}$$

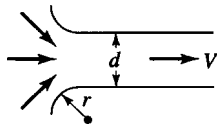
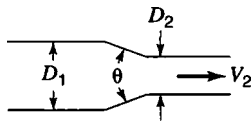
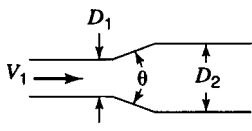
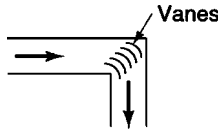
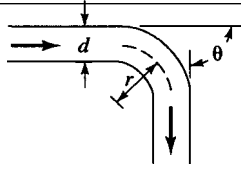
$$50 = h_{L_f} + \sum h_{L_m}$$

where

$$h_{L_f} = \frac{fLV^2}{D2g} = f \frac{600}{(12/12)2 \times 32.2} V^2 = 9.32fV^2$$

The minor losses are

Table 4.3.2 Loss Coefficients for Various Transitions and Fittings

Description	Sketch	Additional data	K	Source	
Pipe entrance $h_{l_m} = K_e V^2/2g$		r/d	K_e	(a)	
		0.0	0.50		
		0.1	0.12		
		>0.2	0.03		
Contraction $h_{l_m} = K_C V_2^2/2g$		D_2/D_1	K_C $\theta = 60^\circ$	K_C $\theta = 180^\circ$	(a)
		0.0	0.08	0.50	
		0.20	0.08	0.49	
		0.40	0.07	0.42	
		0.60	0.06	0.32	
		0.80	0.05	0.18	
		0.90	0.04	0.10	
Expansion $h_{l_m} = K_E V_1^2/2g$		D_1/D_2	K_E $\theta = 10^\circ$	K_E $\theta = 180^\circ$	(a)
		0.0		1.00	
		0.20	0.13	0.92	
		0.40	0.11	0.72	
		0.60	0.06	0.42	
		0.80	0.03	0.16	
90° miter bend		Without vanes	$K_b = 1.1$	(b)	
		With vanes	$K_b = 0.2$	(b)	
Smooth bend		r/d	K_b $\theta = 45^\circ$	K_b $\theta = 90^\circ$	(c) and (d)
		1	0.10	0.35	
		2	0.09	0.19	
		4	0.10	0.16	
		6	0.12	0.21	
Threaded pipe fittings	Globe valve—wide open		$K_v = 10.0$	(b)	
	Angle valve—wide open		$K_v = 5.0$		
	Gate valve—wide open		$K_v = 0.2$		
	Gate valve—half open		$K_v = 5.6$		
	Return bend		$K_b = 2.2$		
	Tee		$K_t = 1.8$		
	90° elbow		$K_b = 0.9$		
45° elbow		$K_b = 0.4$			

(a) ASHRAE (1977)

(b) Streeter (1961)

(c) Beij (1938)

(d) Idel'chik (1966)

Source: After Roberson et al. (1988).

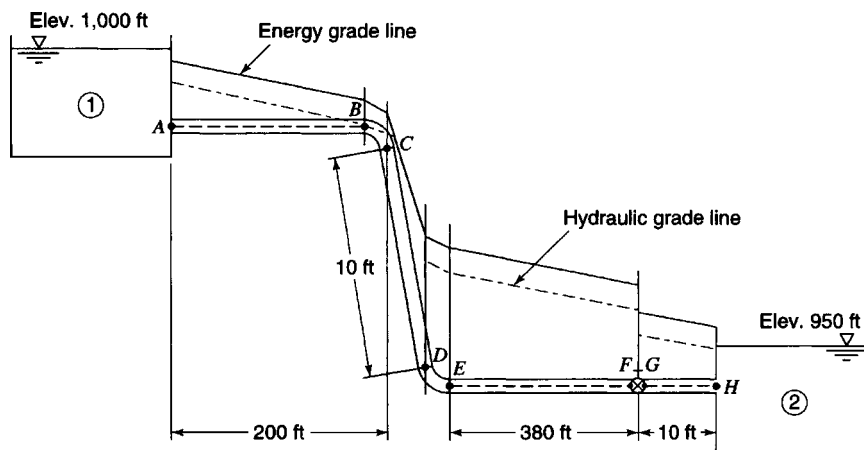


Figure 4.3.6 Pipe system for example 4.3.5.

$$\begin{aligned} \sum h_{L_m} &= h_{L_{\text{entrance}}} + h_{L_{\text{elbow}}} + h_{L_{\text{elbow}}} + h_{L_{\text{globevalve}}} + h_{L_{\text{exit}}} \\ &= K_e \frac{V^2}{2g} + 2K_{\text{elbow}} \frac{V^2}{2g} + K_{\text{valve}} \frac{V^2}{2g} + \frac{V^2}{2g} \\ &= (K_e + 2K_{\text{elbow}} + K_{\text{valve}} + 1) \frac{V^2}{2g} \end{aligned}$$

where $K_e = 0.5$, $K_{\text{elbow}} = 0.25$, and $K_{\text{valve}} = 1.5$. The energy equation is now expressed as

$$50 = (0.5 + 2 \times 0.25 + 1.5 + 1.0) \frac{V^2}{2g} + 9.32f V^2$$

$$50 = 3.5 \frac{V^2}{2g} + 9.32f V^2$$

$$50 = (0.054 + 9.32f) V^2$$

$$V = \sqrt{50 / (0.054 + 9.32f)}$$

Assuming fully turbulent flow and using $k_s/D = 0.0005/1 = 0.0005$, we get $f = 0.0165$ from Figure 4.3.5, then

$$V = \sqrt{50 / (0.054 + 9.32 \times 0.0165)}$$

$$V = 15.51 \text{ ft/s}$$

Compute $R_e = \frac{VD}{\nu} = \frac{15.51 \times 1}{0.609 \times 10^{-5}} = 2.55 \times 10^6$. Referring to Figure 4.3.5 (Moody diagram), we see

that the value of f is OK. Now use the continuity equation to determine Q :

$$Q = AV = [\pi(12/12)^2/4](15.51 \text{ ft/s}) = 12.18 \text{ ft}^3/\text{s}$$

4.4 FORCES IN PIPE FLOW

Change in direction or magnitude of flow velocity of a fluid causes changes in the momentum of the fluid (see Figure 4.4.1). The forces that are required to produce the change in momentum come from the pressure variation within the fluid and from forces transmitted to the fluid from the pipe

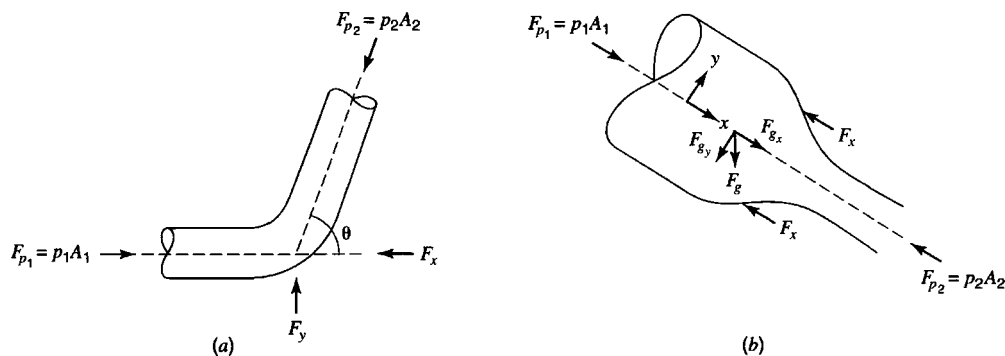


Figure 4.4.1 Forces in pipe flow, (a) Pipe bend; (b) Contraction.

walls. Applying the momentum principle (equation 3.5.6) to the control volumes in Figure 4.4.1, we get

$$\sum F_x = \frac{d}{dt} \int_{CV} v_x \rho d\forall + \sum_{CS} v_x \rho \mathbf{V} \cdot \mathbf{A} \quad (3.5.6)$$

where

$$\frac{d}{dt} \int_{CV} v_x \rho d\forall = 0$$

because flow is steady and

$$\sum_{CS} v_x \rho \mathbf{V} \cdot \mathbf{A} = \rho V_{x_2} Q - \rho V_{x_1} Q \quad (4.4.1)$$

The momentum entering from the upstream is $-\rho V_{x_1} Q$ and the momentum leaving the control volume is $\rho V_{x_2} Q$. The summation of forces in the x direction for the contraction in Figure 4.4.1b is

$$\sum F_x = p_1 A_1 - p_2 A_2 - F_x + F_{g_x} \quad (4.4.2)$$

where F_{g_x} is the weight of the fluid in the x -direction in the contraction. The momentum principle for the x -direction can be stated using equation (3.5.6) as

$$\sum F_x = \rho V_{x_2} Q - \rho V_{x_1} Q = \rho Q (V_{x_2} - V_{x_1}) \quad (4.4.3)$$

Similar equations can be developed for other directions:

$$\sum F_y = \rho Q (V_{y_2} - V_{y_1}) \quad (4.4.4)$$

EXAMPLE 4.4.1

The nozzle has the dimensions shown in Figure 4.4.2. What is the force exerted on the flange bolts for a flow rate of $0.08 \text{ m}^3/\text{s}$? The upstream pipe pressure is 75 kPa .

SOLUTION

Using equation (4.4.3) yields

$$\begin{aligned} \sum F_x &= \rho Q (V_{x_2} - V_{x_1}) \\ F_1 - F_2 - F_{\text{bolt}} &= \rho Q (V_{x_2} - V_{x_1}) \end{aligned}$$

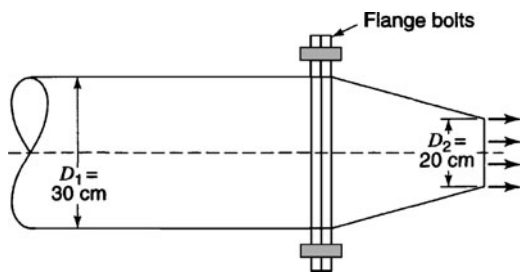


Figure 4.4.2 Nozzle for example 4.4.1.

where $F_1 = p_1A_1$ and $F_2 = p_2A_2 = 0$ (because this end of the nozzle is open to the atmosphere and $p_2 = 0$):

$$p_1A_1 - F_{\text{bolt}} = \rho Q(V_{x_2} - V_{x_1})$$

$$(75,000 \text{ N/m}^2) \left(\frac{\pi(30/100)^2 \text{ m}^2}{4} \right) - F_{\text{bolt}} = (1000 \text{ kg/m}^3)(0.08 \text{ m}^3/\text{s})(2.55 \text{ m/s} - 1.13 \text{ m/s})$$

where $1 \text{ Pa} = 1 \text{ N/m}^2$ and $1 \text{ kg/m}^3 = 1 \text{ N}\cdot\text{s}^2/\text{m}^4$, so

$$5298.8 \text{ N} - F_{\text{bolt}} = 113.6 \text{ N}$$

$$F_{\text{bolt}} = 5185 \text{ N (or 1166 lb)}$$

EXAMPLE 4.4.2

Water flows through a horizontal 45° reducing bend shown in Figure 4.4.3, with a 36-in diameter upstream and a 24-in diameter downstream, at the rate of 20 cfs under a pressure of 15 psi at the upstream end of the bend. Neglecting the headloss in the bend, calculate the force exerted by the water on the bend.

SOLUTION

The free-body diagram shown in Figure 4.4.3 is used. To solve this problem, equations (4.4.3) and (4.4.4) will be used:

$$\sum F_x = \rho Q(V_{x_2} - V_{x_1}) \tag{4.4.3}$$

$$\sum F_y = \rho Q(V_{y_2} - V_{y_1}) \tag{4.4.4}$$

The first objective is to determine the velocities in order to apply the energy equation to determine p_2 :

$$V_{x_1} = V_1 = Q/A_1 = 20/\pi(3)^2/4 = 2.83 \text{ ft/s}$$

$$V_{y_1} = 0$$

$$V_2 = Q/A = 20/\pi(2)^2/4 = 6.37 \text{ ft/s}$$

$$V_{x_2} = V_{y_2} = V_2 \cos 45^\circ = 6.37(0.707) = 4.50 \text{ ft/s}$$

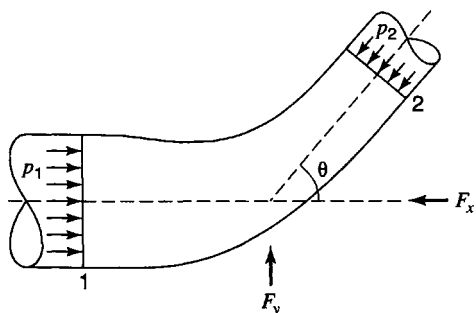


Figure 4.4.3 Reducing bend for example 4.4.2.

Next the energy equation is applied horizontally, $z_1 = z_2 = 0$ and $h_L = 0$:

$$\frac{p_1}{\gamma} + \frac{V_1^2}{2g} = \frac{p_2}{\gamma} + \frac{V_2^2}{2g}$$

$$\frac{15 \text{ lb/in}^2 \times 144 \text{ in}^2/\text{ft}^2}{62.4 \text{ lb/ft}^3} + \frac{(2.83 \text{ ft/s})^2}{2(32.2)\text{ft/s}^2} = \frac{p_2}{\gamma} + \frac{(6.37 \text{ ft/s})^2}{2(32.2)\text{ft/s}^2}$$

$$34.615 + 0.124 = \frac{p_2}{\gamma} + 0.630$$

$$\frac{p_2}{\gamma} = 34.11 \text{ ft}$$

$$p_2 = 34.11 \times \frac{62.4}{144} = 14.78 \text{ lb/in}^2$$

Using equation (4.4.3) yields

$$\sum F_x = p_1 A_1 - p_2 A_2 \cos 45^\circ - F_x = \rho Q (V_{x_2} - V_{x_1})$$

$$F_x = p_1 A_1 - p_2 A_2 \cos 45^\circ - \rho Q (V_{x_2} - V_{x_1})$$

$$F_x = (15 \text{ lb/in}^2)(144 \text{ in}^2/\text{ft}^2) \left(\pi \frac{3^2}{4} \text{ft}^2 \right) - (14.78 \text{ lb/in}^2)(144 \text{ in}^2/\text{ft}^2) \left(\pi \frac{2^2}{4} \text{ft}^2 \right)$$

$$- \left[1.94 \frac{\text{slugs}}{\text{ft}^3} \right] (20 \text{ ft}^3) (4.50 \text{ ft/s} - 2.83 \text{ ft/s})$$

$$F_x = 15,268 - 6686 - 65$$

$$= 8517 \text{ lb}$$

Using equation (4.4.4), we get

$$\sum F_y = F_{y_1} - F_{y_2} + F_y = \rho Q (V_{y_2} - V_{y_1})$$

where $F_{y_1} = 0$ because there is no pressure component in the y direction at 1.

$$-p_2 A_2 \sin 45^\circ + F_y = \rho Q (V_{y_2} - V_{y_1})$$

$$F_y = p_2 A_2 \sin 45^\circ + \rho Q (V_{y_2} - V_{y_1})$$

$$F_y = (14.78)(144) \left(\pi \frac{2^2}{4} \right) (0.707) + (1.94)(20)(4.50 - 0)$$

$$F_y = 4727 + 174$$

$$F_y = 4901 \text{ lb}$$

The resultant force is $F = \sqrt{(8517)^2 + (4901)^2} = 9826 \text{ lb}$ at an angle of $\theta = \tan^{-1}(4901/8517) = 30^\circ$.

4.5 PIPE FLOW IN SIMPLE NETWORKS

4.5.1 Series Pipe Systems

Consider the simple series pipe system in Figure 4.5.1a. Through continuity the discharge is equal in each pipe:

$$Q = Q_1 = Q_2 = Q_3 \quad (4.5.1)$$

and through energy the total headloss is the sum of headlosses in each pipe:

$$h_L = h_{L_1} + h_{L_2} + h_{L_3} \quad (4.5.2)$$

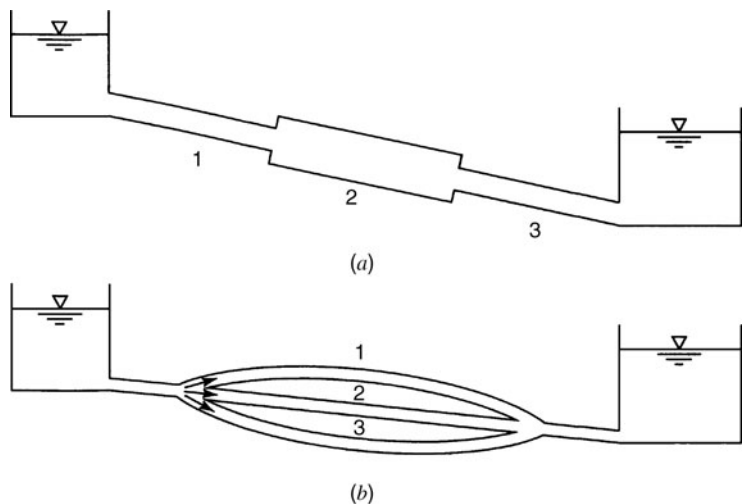


Figure 4.5.1 Pipes in (a) series and (b) parallel.

EXAMPLE 4.5.1

Water flows at a rate of $0.030 \text{ m}^3/\text{s}$ from reservoir 1 to reservoir 2 through three pipes connected in series ($f = 0.025$) as shown in Figure 4.5.2. Neglecting minor losses, determine the difference in water surface elevation.

SOLUTION

Write the energy equation from 1 to 2:

$$z_1 = z_2 + h_{L_f} \quad (\text{or } h_{L_f} = z_1 - z_2)$$

$$h_{L_f} = h_{L_A} + h_{L_B} + h_{L_C} = z_1 - z_2$$

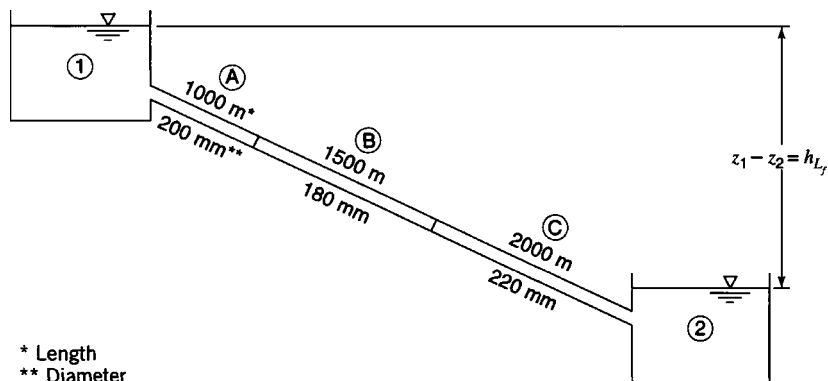
Using the Darcy–Weisbach equation (4.3.13)

$$h_{L_f} = f \frac{L V^2}{D 2g}$$

the energy equation is

$$z_1 - z_2 = 0.025 \frac{1000}{[200/1000]} \frac{V_A^2}{2(9.81)} + 0.025 \frac{1500}{[180/1000]} \frac{V_B^2}{2(9.81)} + 0.025 \frac{2000}{[220/1000]} \frac{V_C^2}{2(9.81)}$$

$$z_1 - z_2 = 6.37V_A^2 + 10.62V_B^2 + 11.58V_C^2$$



* Length
** Diameter

Figure 4.5.2 Pipe system for example 4.5.1.

Use continuity to determine the velocities:

$$V_A = Q/A_A = 0.03 / \frac{\pi(200/1000)^2}{4} = 0.955 \text{ m/s}$$

$$V_A = Q/A_B = 0.03 / \frac{\pi(180/1000)^2}{4} = 1.180 \text{ m/s}$$

$$V_C = Q/A_C = 0.03 / \frac{\pi(220/1000)^2}{4} = 0.790 \text{ m/s}$$

$$\begin{aligned} z_1 - z_2 &= 6.37(0.955)^2 + 10.62(1.180)^2 + 11.58(0.790)^2 \\ &= 5.81 + 14.79 + 7.22 \\ &= 27.82 \text{ m} \end{aligned}$$

4.5.2 Parallel Pipe Systems

Consider the simple parallel pipe system in Figure 4.5.1*b*. Through continuity the total flow is the sum of flow in each of the pipes:

$$Q = Q_1 + Q_2 + Q_3 \quad (4.5.3)$$

Through energy, the flow distribution in the parallel pipes is such that the headloss in each pipe is equal:

$$h_L = h_{L_1} = h_{L_2} = h_{L_3} \quad (4.5.4)$$

EXAMPLE 4.5.2

The three-pipe system shown in Figure 4.5.3 has the following characteristics:

Pipe	D (in)	L (ft)	f
A	8	1500	0.020
B	6	2000	0.025
C	10	3000	0.030

Find the flowrate of water in each pipe and the pressure at point 3. Neglect minor losses.

SOLUTION

Write the energy equation from 1 to 2:

$$\frac{p_1}{\gamma} + \frac{V_1^2}{2g} + z_1 = \frac{p_2}{\gamma} + \frac{V_2^2}{2g} + z_2 + h_{L_f}$$

$$0 + 0 + 200 = 0 + \frac{V_2^2}{2g} + 80 + h_L$$

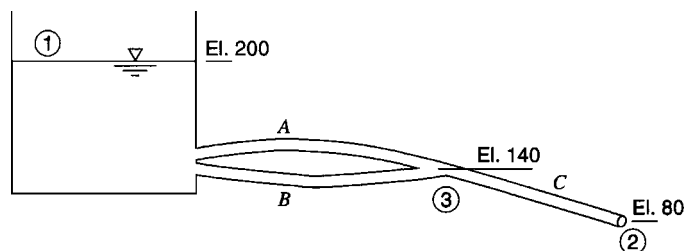


Figure 4.5.3 Pipe system for example 4.5.2.

where V_2 is V_C ; $h_{L_f} = h_{L_A} + h_{L_C}$, and using the Darcy–Weisbach equation (4.3.13), we get

$$120 = \frac{V_C^2}{2g} + f_A \frac{L_A V_A^2}{D_A 2g} + f_C \frac{L_C V_C^2}{D_C 2g}$$

Because pipes A and B are parallel, the headloss in A is equal to the headloss in B, so the headloss for B can also be used in the above energy equation instead of for A. This energy equation has two unknowns, V_A and V_C , so that continuity can be used as a second equation:

$$Q_A + Q_B = Q_C$$

$$A_A V_A + A_B V_B = A_C V_C$$

which introduces a third unknown V_A . Because $h_{L_A} = h_{L_B}$, the third equation is

$$f_A \frac{L_A V_A^2}{D_A 2g} = f_B \frac{L_B V_B^2}{D_B 2g}$$

$$0.020 \left(\frac{1500}{8/12} \right) \frac{V_A^2}{2(32.2)} = 0.025 \left(\frac{2000}{6/12} \right) \frac{V_B^2}{2(32.2)}$$

$$0.699V_A^2 = 1.553V_B^2$$

$$V_A^2 = 2.221V_B^2$$

$$V_B = 0.671V_A$$

So now we have three equations and three unknowns. Using the continuity equation, we get

$$\left[\pi \frac{(8/12)^2}{4} \right] V_A + \left[\pi \frac{(6/12)^2}{4} \right] V_B = \left[\pi \frac{(10/12)^2}{4} \right] V_C$$

$$8^2 V_A + 6^2 V_B = 10^2 V_C$$

substituting

$$V_B = 0.671V_A$$

$$64V_A + 36(0.671)V_A = 100V_C$$

$$88.16V_A = 100V_C$$

$$V_A = 1.134V_C$$

Substitute $V_A = 1.134V_C$ into the energy equation

$$120 = \frac{V_C^2}{2g} + 0.020 \left(\frac{1500}{8/12} \right) \frac{(1.134V_C)^2}{2g} + 0.030 \left(\frac{3000}{10/12} \right) \frac{V_C^2}{2g}$$

and solve for V_C :

$$120 = (1 + 57.82 + 108) \frac{V_C^2}{2g} = 166.82 \frac{V_C^2}{2(32.2)}$$

$$V_C = 6.805 \text{ ft/s}$$

The flow rate is then

$$Q = A_C V_C = \left[\pi \frac{(10/12)^2}{4} \right] \times 6.805 = 3.712 \text{ ft}^3/\text{s}$$

The pressure at 3 can be computed using the energy equation from 1 to 3 or from 3 to 2. Using

$$\frac{p_3}{\gamma} + \frac{V_3^2}{2g} + z_3 = \frac{p_2}{\gamma} + \frac{V_2^2}{2g} + z_2 + h_{L_{3-2}}$$

Because $V_3 = V_2$, the velocity head terms cancel out:

$$\begin{aligned} \frac{p_3}{\gamma} + 140 &= 0 + 80 + h_{L_{3-2}} \\ \frac{p_3}{\gamma} &= -60 + f_C \frac{L_C V_C^2}{D_C 2g} \\ &= -60 + 0.030 \frac{3000}{10/12} \frac{6.805^2}{2(32.2)} \\ &= -60 + 77.66 \\ &= 17.66 \end{aligned}$$

and

$$\begin{aligned} p_3 &= (62.4)(17.66) = 1102 \text{ lb/ft}^2 \\ &= 7.65 \text{ lb/in}^2 \end{aligned}$$

EXAMPLE 4.5.3

The pipe system shown in Figure 4.5.4 connects two reservoirs that have an elevation difference of 20 m. This pipe system consists of 200 m of 50-cm concrete pipe (pipe A), that branches into 400 m of 20-cm pipe (pipe B) and 400 m of 40-cm pipe (pipe C) in parallel. Pipes B and C join into a single 50-cm pipe that is 500 m long (pipe D). For $f = 0.030$ in all the pipes, what is the flow rate in each pipe of the system?

SOLUTION

The objective is to compute the velocity in each pipe. We know that $V_A = V_D$ because they are the same diameter pipe, $h_{L_B} = h_{L_C}$ because pipes B and C are in parallel, and $Q_A = Q_D = Q_B + Q_C$. Express $h_{L_B} = h_{L_C}$ in terms of the velocities

$$f_B \frac{L_B}{D_B} \frac{V_B^2}{2g} = f_C \frac{L_C}{D_C} \frac{V_C^2}{2g}$$

Since $f_B = f_C$ and $L_B = L_C$,

$$\frac{V_B^2}{D_B} = \frac{V_C^2}{D_C}$$

$$\frac{V_B^2}{20/100} = \frac{V_C^2}{40/100} \text{ or } V_B^2 = \frac{1}{2} V_C^2 \text{ or } V_B = \frac{V_C}{\sqrt{2}} \text{ or } V_C = \sqrt{2} V_B$$

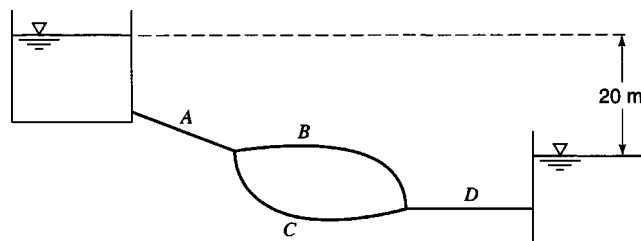


Figure 4.5.4 Pipe system for example 4.5.3.

Using $Q_A = Q_B + Q_C$, we get

$$\left[\frac{\pi(50/100)^2}{4} \right] V_A = \left[\frac{\pi(20/100)^2}{4} \right] V_B + \left[\frac{\pi(40/100)^2}{4} \right] V_C$$

$$50^2 V_A = 20^2 V_B + 40^2 V_C$$

Substituting $V_C = \sqrt{2} V_B$ yields

$$2500V_A = 400V_B + 1600(\sqrt{2} V_B)$$

$$V_A = 1.065V_B \text{ or } V_B = 0.939 V_A$$

Next convert the parallel pipes to a single equivalent $D_A = D_D = 50\text{-cm}$ diameter pipe, with a length of L_E :

$$f \frac{L_B}{D_B} \frac{V_B^2}{2g} = f \frac{L_E}{D_A} \frac{V_A^2}{2g}$$

$$\frac{L_B}{D_B} V_B^2 = \frac{L_E}{D_A} V_A^2$$

$$\frac{400}{(20/100)} V_B^2 = \frac{L_E}{(50/100)} V_A^2$$

$$1000V_B^2 = L_E V_A^2$$

Substitute $V_B = 0.939 V_A$:

$$1000(0.939V_A)^2 = L_E V_A^2$$

$$L_E = 882 \text{ m}$$

Write the energy equation from reservoir surface to reservoir surface $\sum h = 20 \text{ m}$

$$20 = \frac{f(L_A + L_E + L_D)}{(50/100)} \frac{V_A^2}{2g}$$

$$20 = \frac{0.030(200 + 882 + 500)}{(50/100)} \frac{V_A^2}{2(9.81)}$$

$$V_A = 2.033 \text{ m/s}, Q_A = \frac{\pi(50/100)^2}{4} (2.033) = 0.399 \text{ m}^3/\text{s}$$

Also, $V_A = V_D$, so $Q_D = Q_A$:

$$V_B = 0.939(2.033) = 1.909 \text{ m/s}, Q_B = \frac{\pi(20/100)^2}{4} (1.909) = 0.060 \text{ m}^3/\text{s}$$

$$Q_C = Q_A - Q_B = 0.399 - 0.060 = 0.339 \text{ m}^3/\text{s}.$$

4.5.3 Branching Pipe Flow

Consider the branching pipe system shown in Figure 4.5.5. The following energy equations can be written (neglecting the velocity heads):

$$z_A = z_D + \frac{p_D}{\gamma} + h_{L_{AD}} \tag{4.5.5}$$

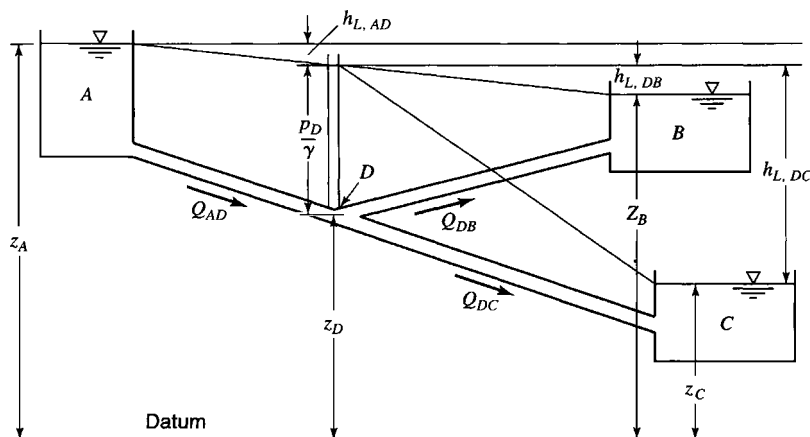


Figure 4.5.5 Branching pipe system.

$$z_B = z_D + \frac{p_D}{\gamma} - h_{L,DB} \quad (4.5.6)$$

$$z_C = z_D + \frac{p_D}{\gamma} - h_{L,DC} \quad (4.5.7)$$

where the headlosses are defined using the Darcy–Weisbach equation (4.3.13)

$$h_{L,AD} = f_{AD} \frac{L_{AD}}{D_{AD}} \frac{V_{AD}^2}{2g} \quad (4.5.8)$$

$$h_{L,DB} = f_{DB} \frac{L_{DB}}{D_{DB}} \frac{V_{DB}^2}{2g} \quad (4.5.9)$$

$$h_{L,DC} = f_{DC} \frac{L_{DC}}{D_{DC}} \frac{V_{DC}^2}{2g} \quad (4.5.10)$$

The continuity equation is

$$Q_{AD} = Q_{DB} + Q_{DC} \quad (4.5.11)$$

or

$$A_{AD}V_{AD} = A_{DB}V_{DB} + A_{DC}V_{DC} \quad (4.5.12)$$

By substituting the headloss expressions (equations (4.5.8)–(4.5.10)) respectively into equations (4.5.5)–(4.5.7), the three energy equations have four unknowns, p_D/γ , V_{AD} , V_{DB} , and V_{DC} . The continuity equation (4.5.12) provides the fourth equation to solve for the four unknowns.

PROBLEMS

4.1.1 Water flows in a pipe of 3/8-in diameter at a temperature of 70°F. The pressures at 1 and 2 (see Figure P4.1.1) are found to be 15 psi and 20 psi, respectively. Determine the direction of flow. What is the minimum discharge above which the flow will not be laminar?

4.1.2 An experiment was done to determine the hydraulic conductivity K of an aquifer. A dye was injected into the aquifer at point 1 (see Figure P4.1.2) and was 36 hours later observed at point 2. The piezometric head difference between points 1 and 2 was

observed to be 0.5 m. Determine the hydraulic conductivity of the aquifer. Take the porosity of the aquifer as 0.24.

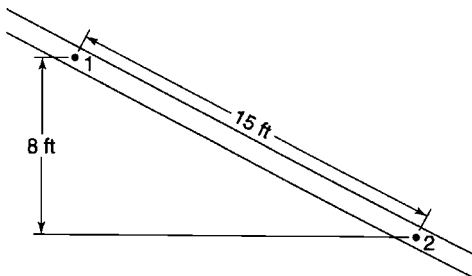


Figure P4.1.1

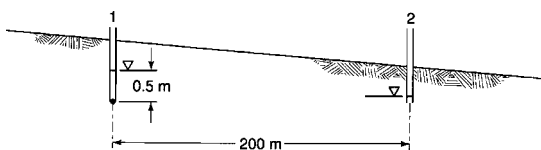


Figure P4.1.2

4.1.3 The piezometric heads at points 1 and 2 in Figure P4.1.3 are found to be 75 ft and 72.5 ft. If the hydraulic conductivity of the aquifer is 50 ft/day, what is the Darcy flux? Determine the discharge by taking the average thickness of the aquifer as 100 ft.

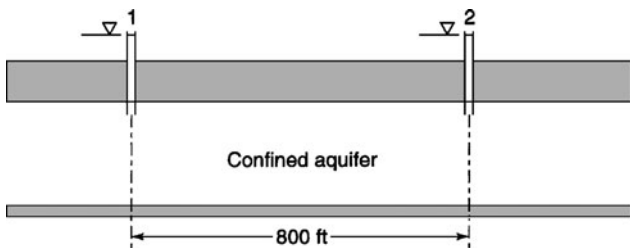


Figure P4.1.3

4.2.1 A Venturi meter with a throat diameter of 150 mm is connected to a pipe of diameter 250 mm to measure the discharge in the pipe. The pressures just upstream of the connection and at the throat were found to be 140 kPa and 80 kPa, respectively. Determine the flow rate in the pipe. Take the coefficient of discharge for the Venturi meter as 0.98.

4.2.2 The pressure difference between the upstream end section and the throat section of a Venturi meter connected to a pipe flow is found to be 12 psi. The diameters of the pipe and the throat of the Venturi meter are 1-7/8 in and 1-1/8 in, respectively. The actual flow in the pipe is 0.353 ft³/s. Calibrate the Venturi meter for Reynolds numbers at the throat greater than 2×10^6 .

4.2.3 Draw (to scale) the hydraulic grade line (HGL) and the energy grade line (EGL) of the system in Figure 4.3.6 (example 4.3.5). Take the length of each pipe as given and neglect the height of the elbows.

4.2.4 Suppose the water fountain in Fountain Hills, Arizona (see Figure P4.2.4), rises vertically to 150 ft above the lake (when operated). Neglecting wind effects and minor losses, determine the velocity at which the water is ejected.

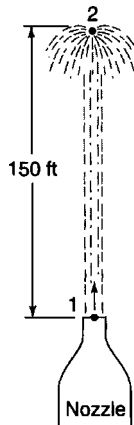


Figure P4.2.4

4.3.1 Develop the expression for the headloss in a pipe for steady, laminar flow of an incompressible fluid (equation (4.3.8)).

4.3.2 Suppose a globe valve ($K = 10$) is present in a pipeline of diameter 300 mm that has a friction factor f of 0.020. What is the equivalent length of this pipe that would cause equal headloss as the globe valve for the same discharge? Repeat this problem for a pipe of 150-mm diameter that has the same friction factor.

4.3.3 Two materials (wrought iron, $k_s = 0.046$ mm, and galvanized iron, $k_s = 0.15$ mm) are being considered for a new pipeline. The expected discharge is 0.15 m³/s. Both the headloss and cost are sought for. Wrought iron pipe costs 5 cents more than the galvanized iron pipe for every meter length of the pipe. Determine the tradeoff between the cost and the energy head for pipe diameters of 200 mm and 150 mm. Take the temperature as 15°C.

4.3.4 For the pipe system shown in Figure P4.3.4 determine the proportion of each pipe so that the pipe friction loss in each pipe is the same. Assume the same friction factor in all pipes.

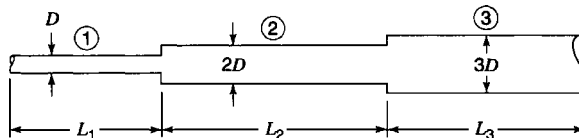


Figure P4.3.4

4.3.5 For the pipe system in problem 4.3.4, compare the expansion losses. Suppose the diameter of the third pipe was twice that of the second. What can you infer by comparing the headlosses at the expansion?

4.4.1 A plate is held against a horizontal water jet in the horizontal plane as shown in Figure P4.4.1. The jet has a diameter of 30 mm and an unknown velocity. A force of 200 N is required to hold the plate in the position. Determine the velocity of flow of the jet just before it hits the plate. What is the discharge?

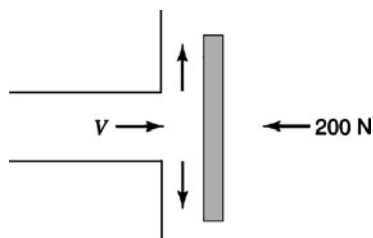


Figure P4.4.1

4.4.2 Suppose the nozzle in example 4.4.1 is connected to the pipe by flange bolts of 1-cm diameter. If the allowable tensile stress in the bolts is 330 N/cm², how many bolts are required for a safe connection?

4.4.3 Suppose the horizontal reducing bend in example 4.4.2 has an unknown bend angle (45° in example 4.4.2). What should be this bend angle so that the horizontal component force F_x is three times the vertical component force, F_y , in magnitude?

4.5.1 If the headloss in example 4.5.1 were 15 m, what would be the discharge? Also, determine the velocity in each pipe.

4.5.2 The rate of flow in the pipe system in Figure P4.5.2 is 0.05 m³/s. The pressure at point 1 is measured to be 260 kPa. All the pipes are galvanized iron with roughness value of 0.15 mm. Determine the pressure at point 2. Take the loss coefficient for the sudden contraction as 0.05 and $\nu = 1.141 \times 10^{-6}$ m²/s.

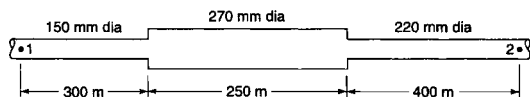


Figure P4.5.2

4.5.3 The pressure difference between points 1 and 2 in the series pipe system in Figure P4.5.3 is 15 psi. All the pipes are galvanized iron with roughness value of 0.0005 ft. The loss coefficient at the sudden contraction is 0.05. Determine the flow rate in the system. The prevailing temperature is 70°F.

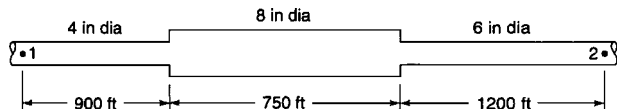


Figure P4.5.3

4.5.4 The pressure at point 1 in the parallel pipe system shown in Figure P4.5.4 is 750 kPa. If the flow rate through the system is 0.50 m³/s, what is the pressure at point 2? Neglect minor losses. All the pipes are steel with roughness value of 0.046 mm. Also, determine the fraction of the flow in each of the parallel pipes and check your solution. Take $\nu = 1.141 \times 10^{-6}$ m²/s.

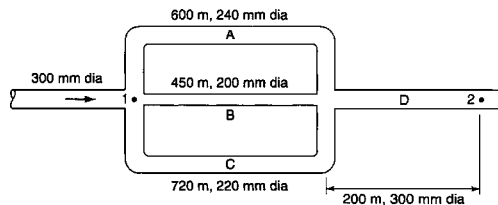


Figure P4.5.4

4.5.5 In problem 4.5.4 above, how far will the water flow before all its energy head is exhausted? Assume pipe D continues horizontally downstream without any other structure.

4.5.6 If the pressure difference between points 1 and 2 in Figure P4.5.6 is 30 psi, what will be the flow rate? The pipes are galvanized iron with $k_s = 0.0005$ ft. Take $\nu = 1.06 \times 10^{-5}$ ft²/s and neglect minor losses.

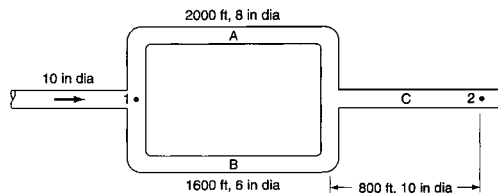


Figure P4.5.6

4.5.7 For the branching pipe system given in Figure P4.5.7, determine the flow to and the elevation of the third reservoir. Neglect minor losses and the velocity heads. The pipes are galvanized iron with $k_s = 0.0005$ ft and $\nu = 1.06 \times 10^{-5}$ ft²/s.

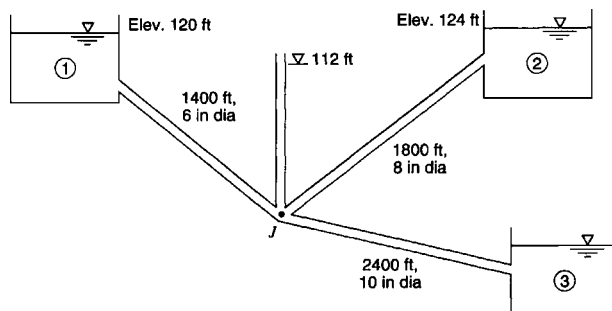


Figure P4.5.7

REFERENCES

- ASHRAE, *ASHRAE Handbook, 1977 Fundamentals*, Am. Soc. of Heating, Refrigerating and Air Conditioning Engineers, New York, 1977.
- Beij, K. H., "Pressure Losses for Fluid Flow in 90° Pipe Bends," *J. Res. Nat. Bur. Std.*, 21, 1938.
- Colebrook, C. F., and C. M. White, "Turbulent Flow in Pipes with Particular Reference to the Transition Region Between Smooth and Rough Pipe Laws," *Institute of Civil Engineers*, London, vol. 11, p. 133, 1939.
- Idel'chik, I. E., *Handbook of Hydraulic Resistance Coefficients of Local Resistance and of Friction*, Trans. A. Barouch, Israel Program for Scientific Translation, 1966.
- Moody, L. R., "Friction Factors for Pipe Flow," *Trans., Amer. Soc. Mech. Engrs.*, 66, Nov., 1944.
- Nikuradse, J., "Gesetzmäßigkeiten der turbulenten Stromung in glatten Rohren," *VDI Forschungsheft* 356, 1932.
- Nikuradse, J., "Stromungsgesetze in rauhen Rohren," *VDI-Forschungsh.*, 361, 1933. Also translated in *NACA Tech. Memo* 1292.
- Roberson, J. A., and C. T. Crowe, *Engineering Fluid Mechanics*, Houghton Mifflin, Boston, 1990.
- Roberson, J. A., J. J. Cassidy, and M. H. Chaudhry, *Hydraulic Engineering*, Houghton Mifflin, Boston, 1988.
- Streeter, V. L. (editor) *Handbook of Fluid Dynamics*, McGraw-Hill, New York, 1961.
- Velon, J. P., and T. J. Johnson, "Water Distribution and Treatment," *Davis' Handbook of Applied Hydraulics*, 4th edition, edited by V. I. Zippano and H. Hasen, McGraw-Hill, New York, 1993.

Chapter 5

Hydraulic Processes: Open-Channel Flow

Open-channel flow refers to that flow whose top surface is exposed to atmospheric pressure. The topic of open-channel flow is covered in detail in textbooks such as Chow (1959), Henderson (1966), French (1985), Townson (1991), Chaudhry (1993), Jain (2001), and Sturm (2001).

5.1 STEADY UNIFORM FLOW

This section describes the continuity, energy, and momentum equations for steady uniform flow in open channels. Consider the control volume shown in Figure 5.1.1 in which the channel cross-section slope and boundary roughness are constant along the length of the control volume. For *uniform flow* the velocity is uniform throughout the control volume, so that $V_1 = V_2$ for the control volume in Figure 5.1.1. Hence for a uniform flow, $Q_1 = Q_2$, $A_1 = A_2$, $V_1 = V_2$, and $y_1 = y_2$. The depth of flow in uniform open-channel flow is also referred to as the *normal depth*. Figure 5.1.2 shows an open-channel flow, in an aqueduct of the Central Arizona Project.

5.1.1 Energy

The energy equation for open-channel flow can be derived in a similar manner as the energy equation for pipe flow (equation 4.2.13) using the control volume approach. In section 3.4, the general energy equation for steady fluid flow was derived as equation (3.4.20). Considering open-channel flow in the control volume in Figure 5.1.1, the energy equation can be expressed as

$$\begin{aligned} \frac{dH}{dt} = & \int_{A_2} \left(\frac{p_2}{\rho} + e_{u_2} + \frac{1}{2} V_2^2 + gz_2 \right) \rho V_2 dA_2 \\ & - \int_{A_1} \left(\frac{p_1}{\rho} + e_{u_1} + \frac{1}{2} V_1^2 + gz_1 \right) \rho V_1 dA_1 \end{aligned} \quad (5.1.1)$$

Assume the energy correction factor (section 3.7) is $\alpha = 1.0$. Refer to equation (3.6.4) for the definition of α . The shaft work term is $dW_s/dt = 0$ because no pump or turbine exists. Because hydrostatic conditions prevail, the terms $(p/\rho + e_u + gz)$ can be taken outside the integral in equation (5.1.1):

$$\frac{dH}{dt} = \left(\frac{p_2}{\rho} + e_{u_2} + gz_2 \right) \int_{A_2} \rho V_2 dA_2 + \int_{A_2} \frac{\rho V_2^2 dA_2}{2} - \left(\frac{p_1}{\rho} + e_{u_1} + gz_1 \right) \int_{A_1} \rho V_1 dA_1 + \int_{A_1} \frac{\rho V_1^2 dA_1}{2} \quad (5.1.2)$$

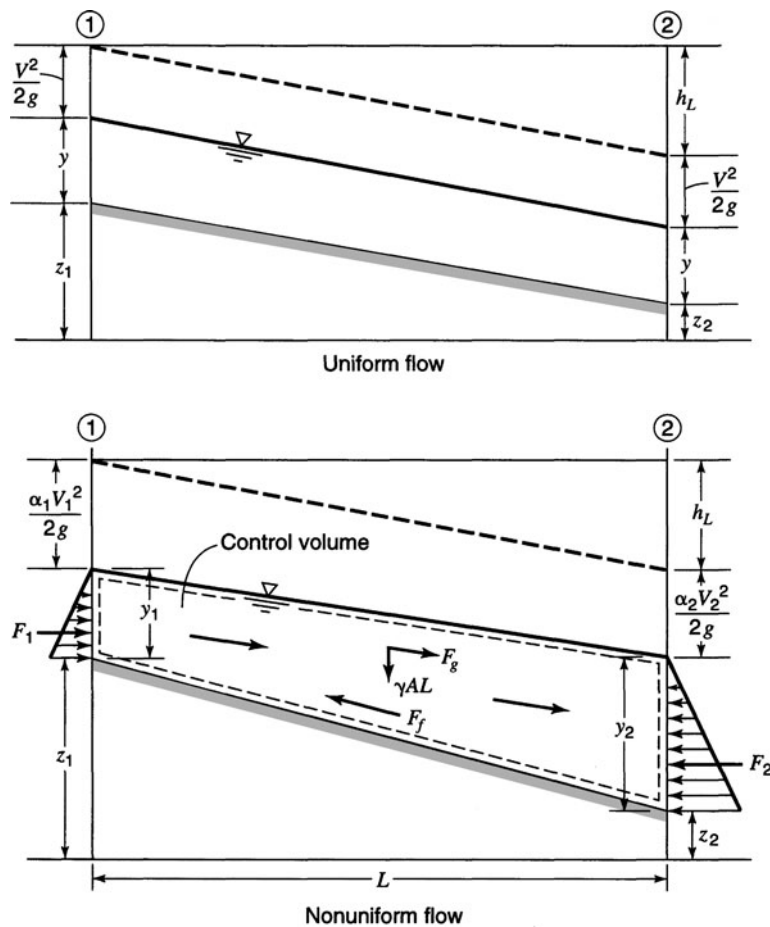


Figure 5.1.1 Open-channel flow: uniform and nonuniform flow.

The terms $\int \rho V dA = \dot{m}$ are the mass rate of flow at sections 1 and 2 and the terms $\int_A (\rho V^3/2) dA = (\rho V^3/2)A = \dot{m} \frac{V^2}{2}$, so that equation (5.1.2) becomes

$$\frac{dH}{dt} = \left(\frac{p_2}{\rho} + e_{u_2} + gz_2 \right) \dot{m} + \dot{m} \frac{V_2^2}{2} - \left(\frac{p_1}{\rho} + e_{u_1} + gz_1 \right) \dot{m} - \dot{m} \frac{V_1^2}{2} \tag{5.1.3}$$

Dividing through by $\dot{m}g$ and rearranging yields

$$\frac{p_1}{\gamma} + z_1 + \frac{V_1^2}{2g} = \frac{p_2}{\gamma} + z_2 + \frac{V_2^2}{2g} + \left[\frac{e_{u_2} - e_{u_1}}{g} - \frac{1}{\dot{m}g} \frac{dH}{dt} \right] \tag{5.1.4}$$

Similar to equation (4.2.10), the terms in square brackets represent the headloss h_L due to viscous stress (friction). This energy loss due to friction effects per unit weight of fluid is denoted as h_L .

The energy equation for one-dimensional flow in an open-channel is

$$\frac{p_1}{\gamma} + z_1 + \alpha_1 \frac{V_1^2}{2g} = \frac{p_2}{\gamma} + z_2 + \alpha_2 \frac{V_2^2}{2g} + h_L \tag{5.1.5}$$



Figure 5.1.2 Hayden-Rhodes Aqueduct, Central Arizona Project. (Courtesy of the U.S. Bureau of Reclamation (1985), photograph by Joe Madrigal Jr.)

where we have put back in the energy correction factor (see section 3.7). Pressure is hydrostatically distributed, and thus $p/\gamma + z$ is constant at each section in the control volume, so that $p_1/\gamma = y_1$ and $p_2/\gamma = y_2$. The energy equation for *nonuniform open-channel flow* is expressed as

$$y_1 + z_1 + \alpha_1 \frac{V_1^2}{2g} = y_2 + z_2 + \alpha_2 \frac{V_2^2}{2g} + h_L \quad (5.1.6)$$

For *uniform flow*, $V_1 = V_2$ and $y_1 = y_2$, so

$$h_L = z_1 - z_2 \quad (5.1.7)$$

By dividing both sides by L , the length of the control volume (channel), the following headloss per unit length of channel, S_f , is obtained as

$$S_f = \frac{h_L}{L} = \frac{z_1 - z_2}{L} \quad (5.1.8)$$

so that the friction slope equals the channel bottom slope. The channel bottom slope $S_0 = \tan \theta$, where θ is the angle of inclination. If θ is small ($< 10^\circ$), then $\tan \theta \approx \sin \theta = (z_1 - z_2)/L$.

5.1.2 Momentum

The forces acting upon the fluid control volume in Figure 5.1.1 are friction, gravity, and hydrostatic pressure. The friction force, F_f , is the product of the wall shear stress τ_0 and the area over which it acts, PL , where P is the wetted perimeter of the cross-section, thus

$$F_f = -\tau_0 PL \quad (5.1.9)$$

where the negative sign indicates that the friction force acts opposite to the direction of flow. The gravity force F_g relates to the weight of the fluid γAL , where γ is the specific weight of the fluid (weight per unit volume). The gravity force on the fluid is the component of the weight acting in the direction of flow, that is,

$$F_g = \gamma AL \sin \theta \quad (5.1.10)$$

The hydrostatic forces are denoted as F_1 and F_2 , and are identical for uniform flow so that $F_1 - F_2 = 0$.

For a steady uniform flow, the general form of the integral momentum equation (3.5.6) in the x direction is

$$\sum F = \sum_{cs} v_x(\rho \mathbf{V} \cdot \mathbf{A}) \quad (5.1.11)$$

or

$$F_1 + F_g + F_f - F_2 = 0 \quad (5.1.12)$$

where $\sum_{cs} v_x(\rho \mathbf{V} \cdot \mathbf{A}) = 0$. Because $F_1 = F_2$, then by equation (5.1.12) $F_g + F_f = 0$, or

$$\gamma AL \sin \theta - \tau_0 PL = 0 \quad (5.1.13)$$

For θ small, $S_0 \approx \sin \theta$ so

$$\gamma ALS_0 = \tau_0 PL \quad (5.1.14)$$

which states that for steady uniform flow the friction and gravity forces are in balance and $S_0 = S_f$. Solving equation (5.1.14) for the wall shear stress (for steady uniform flow) yields

$$\tau_0 = \frac{\gamma ALS_0}{PL} \quad (5.1.15)$$

or

$$\tau_0 = \gamma RS_0 = \gamma RS_f \quad (5.1.16)$$

where $R = A/P$ is the hydraulic radius. Equation (5.1.16) expresses the effects of friction through the wall shear stress τ_0 as represented from a momentum viewpoint and through the rate of energy dissipation S_f represented from an energy viewpoint. Consequently, equation (5.1.16) expresses a linkage between the momentum and energy principles.

The shear stress τ_0 for fully turbulent flow can be expressed as a function of density, velocity, and resistance coefficient C_f as

$$\tau_0 = C_f \rho \left(\frac{V^2}{2} \right) \quad (5.1.17)$$

Equating (5.1.16) and (5.1.17) yields

$$C_f \rho \frac{V^2}{2} = \gamma R S_0 \quad (5.1.18)$$

and solving for the velocity gives

$$V = \sqrt{\frac{2g}{C_f}} \sqrt{R S_0} \quad (5.1.19)$$

Defining $C = \sqrt{2g/C_f}$, then equation (5.1.19) can be simplified to the well-known *Chezy equation*

$$V = C \sqrt{R S_0} \quad (5.1.20)$$

where C is referred to as the *Chezy coefficient*.

Robert Manning (1891, 1895) derived the following empirical relation for C based upon experiments:

$$C = \frac{1}{n} R^{1/6} \quad (5.1.21)$$

where n is the Manning roughness coefficient. Values of n are listed in Table 5.1.1. Values of n for natural channels have been also published by the U.S. Geological Survey (Barnes, 1962). Substituting C from equation (5.1.21) into equation (5.1.20) results in the *Manning equation*

$$V = \frac{1}{n} R^{2/3} S_0^{1/2} \quad (5.1.22)$$

which is valid for SI units and $S_0 = S_f$.

Table 5.1.1 Values of the Roughness Coefficient n
(*Boldface figures are values generally recommended in design*)

Type of channel and description	Minimum	Normal	Maximum
A. Closed conduits flowing partly full			
A-1. Metal			
<i>a.</i> Brass, smooth	0.009	0.010	0.013
<i>b.</i> Steel			
1. Lockbar and welded	0.010	0.012	0.014
2. Riveted and spiral	0.013	0.016	0.017
<i>c.</i> Cast iron			
1. Coated	0.010	0.013	0.014
2. Uncoated	0.011	0.014	0.016
<i>d.</i> Wrought iron			
1. Black	0.012	0.014	0.015
2. Galvanized	0.013	0.016	0.017
<i>e.</i> Corrugated metal			
1. Subdrain	0.017	0.019	0.021
2. Storm drain	0.021	0.024	0.030
A -2. Nonmetal			
<i>a.</i> Lucite	0.008	0.009	0.010
<i>b.</i> Glass	0.009	0.010	0.013
<i>c.</i> Cement			
1. Neat, surface	0.010	0.011	0.013
2. Mortar	0.011	0.013	0.015

(Continued)

Table 5.1.1 (Continued)

Type of channel and description	Minimum	Normal	Maximum
<i>d.</i> Concrete			
1. Culvert, straight and free of debris	0.010	0.011	0.013
2. Culvert with bends, connections, and some debris	0.011	0.013	0.014
3. Finished	0.011	0.012	0.014
4. Sewer with manholes, inlet, etc., straight	0.013	0.015	0.017
5. Unfinished, steel form	0.012	0.013	0.014
6. Unfinished, smooth wood form	0.012	0.014	0.016
7. Unfinished, rough wood form	0.015	0.017	0.020
<i>e.</i> Wood			
1. Stave	0.010	0.012	0.014
2. Laminated, treated	0.015	0.017	0.020
<i>f.</i> Clay			
1. Common drainage tile	0.011	0.013	0.017
2. Vitrified sewer	0.011	0.014	0.017
3. Vitrified sewer with manholes, inlet, etc.	0.013	0.015	0.017
4. Vitrified subdrain with open joint	0.014	0.016	0.018
<i>g.</i> Brickwork			
1. Glazed	0.011	0.013	0.015
2. Lined with cement mortar	0.012	0.015	0.017
<i>h.</i> Sanitary sewers coated with sewage slimes, with bends and connections	0.012	0.013	0.016
<i>i.</i> Paved invert, sewer, smooth bottom	0.016	0.019	0.020
<i>j.</i> Rubble masonry, cemented	0.018	0.025	0.030
B. Lined or built-up channels			
B-1. Metal			
<i>a.</i> Smooth steel surface			
1. Unpainted	0.011	0.012	0.014
2. Painted	0.012	0.013	0.017
<i>b.</i> Corrugated	0.021	0.025	0.030
B-2. Nonmetal			
<i>a.</i> Cement			
1. Neat, surface	0.010	0.011	0.013
2. Mortar	0.011	0.013	0.015
<i>b.</i> Wood			
1. Planed, untreated	0.010	0.012	0.014
2. Planed, creosoted	0.011	0.012	0.015
3. Unplaned	0.011	0.013	0.015
4. Plank with battens	0.012	0.015	0.018
5. Lined with roofing paper	0.010	0.014	0.017
<i>c.</i> Concrete			
1. Trowel finish	0.011	0.013	0.015
2. Float finish	0.013	0.015	0.016
3. Finished, with gravel on bottom	0.015	0.017	0.020
4. Unfinished	0.014	0.017	0.020
5. Gunite, good section	0.016	0.019	0.023
6. Gunite, wavy section	0.018	0.022	0.025
7. On good excavated rock	0.017	0.020	—
8. On irregular excavated rock	0.022	0.027	—
<i>d.</i> Concrete bottom float finished with sides of			
1. Dressed stone in mortar	0.015	0.017	0.020
2. Random stone in mortar	0.017	0.020	0.024

Table 5.1.1 (Continued)

Type of channel and description	Minimum	Normal	Maximum	
3. Cement rubble masonry, plastered		0.016	0.020	0.024
4. Cement rubble masonry		0.020	0.025	0.030
5. Dry rubble or riprap		0.020	0.030	0.035
<i>e.</i> Gravel bottom with sides of				
1. Formed concrete		0.017	0.020	0.025
2. Random stone in mortar		0.020	0.023	0.026
3. Dry rubble or riprap		0.023	0.033	0.036
<i>f.</i> Brick				
1. Glazed		0.011	0.013	0.015
2. In cement mortar		0.012	0.015	0.018
<i>g.</i> Masonry				
1. Cemented rubble		0.017	0.025	0.030
2. Dry rubble		0.023	0.032	0.035
<i>h.</i> Dressed ashlar		0.013	0.015	0.017
<i>i.</i> Asphalt				
1. Smooth		0.013	0.013	—
2. Rough		0.016	0.016	—
<i>j.</i> Vegetal lining		0.030	—	0.500
C. Excavated or dredged				
<i>a.</i> Earth, straight and uniform				
1. Clean, recently completed		0.016	0.018	0.020
2. Clean, after weathering		0.018	0.022	0.025
3. Gravel, uniform section, clean		0.022	0.025	0.030
4. With short grass, few weeds		0.022	0.027	0.033
<i>b.</i> Earth, winding and sluggish				
1. No vegetation		0.023	0.025	0.030
2. Grass, some weeds		0.025	0.030	0.033
3. Dense weeds or aquatic plants in deep channels		0.030	0.035	0.040
4. Earth bottom and rubble sides		0.028	0.030	0.035
5. Stony bottom and weedy banks		0.025	0.035	0.040
6. Cobble bottom and clean sides		0.030	0.040	0.050
<i>c.</i> Dragline-excavated or dredged				
1. No vegetation		0.025	0.028	0.033
2. Light brush on banks		0.035	0.050	0.060
<i>d.</i> Rock cuts				
1. Smooth and uniform		0.025	0.035	0.040
2. Jagged and irregular		0.035	0.040	0.050
<i>c.</i> Channels not maintained, weeds and brush uncut				
1. Dense weeds, high as flow depth		0.050	0.080	0.120
2. Clean bottom, brush on sides		0.040	0.050	0.080
3. Same, highest stage of flow		0.045	0.070	0.110
4. Dense brush, high stage		0.080	0.100	0.140
D. Natural streams				
D-1. Minor streams (top width at flood stage <100 ft)				
<i>a.</i> Streams on plain				
1. Clean, straight, full stage, no rifts or deep pools		0.025	0.030	0.033
2. Same as above, but more stones and weeds		0.030	0.035	0.040
3. Clean, winding, some pools and shoals		0.033	0.040	0.045
4. Same as above, but some weeds and stones		0.035	0.045	0.050
5. Same as above, lower stages, more ineffective slopes and sections		0.040	0.048	0.055

(Continued)

Table 5.1.1 (Continued)

Type of channel and description	Minimum	Normal	Maximum
6. Same as 4, but more stones	0.045	0.050	0.060
7. Sluggish reaches, weedy, deep pools	0.050	0.070	0.080
8. Very weedy reaches, deep pools, or floodways with heavy stand of timber and underbrush	0.075	0.100	0.150
<i>b.</i> Mountain streams, no vegetation in channel, banks usually steep, trees and brush along banks submerged at high stages			
1. Bottom: gravels, cobbles, and few boulders	0.030	0.040	0.050
2. Bottom: cobbles with large boulders	0.040	0.050	0.070
D-2. Flood plains			
<i>a.</i> Pasture, no brush			
1. Short grass	0.025	0.030	0.035
2. High grass	0.030	0.035	0.050
<i>b.</i> Cultivated areas			
1. No crop	0.020	0.030	0.040
2. Mature row crops	0.025	0.035	0.045
3. Mature field crops	0.030	0.040	0.050
<i>c.</i> Brush			
1. Scattered brush, heavy weeds	0.035	0.050	0.070
2. Light brush and trees, in winter	0.035	0.050	0.060
3. Light brush and trees, in summer	0.040	0.060	0.080
4. Medium to dense brush, in winter	0.045	0.070	0.110
5. Medium to dense brush, in summer	0.070	0.100	0.160
<i>d.</i> Trees			
1. Dense willows, summer, straight	0.110	0.150	0.200
2. Cleared land with tree stumps, no sprouts	0.030	0.040	0.050
3. Same as above, but with heavy growth of sprouts	0.050	0.060	0.080
4. Heavy stand of timber, a few down trees, little undergrowth, flood stage below branches	0.080	0.100	0.120
5. Same as above, but with flood stage reaching branches	0.100	0.120	0.100
D-3. Major streams (top width at flood stage > 100 ft). The <i>n</i> value is less than that for minor streams of similar description, because banks offer less effective resistance.			
<i>a.</i> Regular section with no boulders or brush	0.025	—	0.060
<i>b.</i> Irregular and rough section	0.035	—	0.100

Source: Chow (1959).

Manning’s equation in SI units can also be expressed as

$$Q = \frac{1}{n} AR^{2/3} S_0^{1/2} \tag{5.1.23}$$

For *V* in ft/sec and *R* in feet (U.S. customary units), equation (5.1.22) can be rewritten as

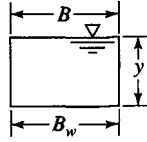
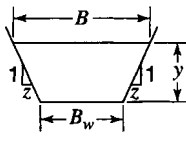
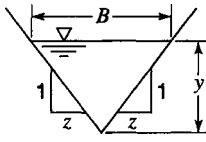
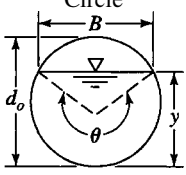
$$V = \frac{1.49}{n} R^{2/3} S_0^{1/2} \tag{5.1.24}$$

and equation (5.1.23) can be written as

$$Q = \frac{1.49}{n} AR^{2/3} S_0^{1/2} \tag{5.1.25}$$

where *A* is in ft² and *S*₀ = *S*_{*f*}. Table 5.1.2 lists the geometric function for channel elements.

Table 5.1.2 Geometric Functions for Channel Elements

Section:	Rectangle	Trapezoid	Triangle	Circle
				
Area A	$B_w y$	$(B_w + zy)y$	zy^2	$\frac{1}{8}(\theta - \sin \theta)d_o^2$
Wetted perimeter P	$B_w + 2y$	$B_w + 2y\sqrt{1 + z^2}$	$2y\sqrt{1 + z^2}$	$\frac{1}{2}\theta d_o$
Hydraulic radius R	$\frac{B_w y}{B_w + 2y}$	$\frac{(B_w + zy)y}{B_w + 2y\sqrt{1 + z^2}}$	$\frac{zy}{2\sqrt{1 + z^2}}$	$\frac{1}{4}\left(1 - \frac{\sin \theta}{\theta}\right)d_o$ $\left[\sin\left(\frac{\theta}{2}\right)\right]d_o$
Top width B	B_w	$B_w + 2zy$	$2zy$	or $\frac{2\sqrt{y(d_o - y)}}{4(2 \sin \theta + 3\theta - 5\theta \cos \theta)}$
$\frac{2dR}{3Rdy} + \frac{1}{A} \frac{dA}{dy}$	$\frac{5B_w + 6y}{3y(B_w + 2y)}$	$\frac{(B_w + 2zy)(5B_w + 6y\sqrt{1 + z^2}) + 4zy^2\sqrt{1 + z^2}}{3y(B_w + zy)(B_w + 2y\sqrt{1 + z^2})}$	$\frac{8}{3y}$	$\frac{3d_o\theta(\theta - \sin \theta) \sin(\theta/2)}{4(2 \sin \theta + 3\theta - 5\theta \cos \theta)}$ where $\theta = 2 \cos^{-1}\left(1 - \frac{2y}{d_o}\right)$

Source: Chow (1959) (with additions).

To determine the normal depth (for uniform flow), equation (5.1.23) or (5.1.25) can be solved with a specified discharge. Because the original shear stress τ_0 in equation (5.1.17) is for fully turbulent flow, Manning's equation is valid only for fully turbulent flow. Henderson (1966) presented the following criterion for fully turbulent flow in an open channel:

$$n^6 \sqrt{RS_f} \geq 1.9 \times 10^{-13} \quad (R \text{ in feet}) \quad (5.1.26a)$$

$$n^6 \sqrt{RS_f} \geq 1.1 \times 10^{-13} \quad (R \text{ in meters}) \quad (5.1.26b)$$

EXAMPLE 5.1.1

An 8-ft wide rectangular channel with a bed slope of 0.0004 ft/ft has a depth of flow of 2 ft. Assuming steady uniform flow, determine the discharge in the channel. The Manning roughness coefficient is $n = 0.015$.

SOLUTION

From equation (5.1.25), the discharge is

$$\begin{aligned} Q &= \frac{1.49}{n} AR^{2/3} S_0^{1/2} \\ &= \frac{1.49}{0.015} (8)(2) \left[\frac{(8)(2)}{8 + 2(2)} \right]^{2/3} (0.0004)^{1/2} \\ &= 38.5 \text{ ft}^3/\text{s} \end{aligned}$$

EXAMPLE 5.1.2 Solve example 5.1.1 using SI units.

SOLUTION The channel width is 2.438 m, with a depth of flow of 0.610 m. Using equation (5.1.23), the discharge is

$$\begin{aligned}
 Q &= \frac{1}{n} AR^{2/3} S_0^{1/2} \\
 &= \frac{1}{0.015} (2.438)(0.610) \left[\frac{(2.438)(0.610)}{2.438 + 2(0.610)} \right]^{2/3} (0.0004)^{1/2} \\
 &= 1.09 \text{ m}^3/\text{s}
 \end{aligned}$$

EXAMPLE 5.1.3 Determine the normal depth (for uniform flow) if the channel described in example 5.1.1 has a flow rate of 100 cfs.

SOLUTION This problem is solved using Newton’s method with Q_j defined by equation (5.1.25):

$$\begin{aligned}
 Q_j &= \frac{1.49}{n} S_0^{1/2} \frac{(B_w y_j)^{5/3}}{(B_w + 2y_j)^{2/3}} \\
 Q_j &= \frac{1.49}{0.015} (0.0004)^{1/2} \frac{(8y_j)^{5/3}}{(8 + 2y_j)^{2/3}} = 1.987 \frac{(8y_j)^{5/3}}{(8 + 2y_j)^{2/3}}
 \end{aligned}$$

Using a numerical method such as Newton’s method (see Appendix A), the normal depth is 3.98 ft.

5.1.3 Best Hydraulic Sections for Uniform Flow in Nonerodible Channels

The conveyance of a channel section increases with an increase in the hydraulic radius or with a decrease in the wetted perimeter. Consequently, the channel section with the smallest wetted perimeter for a given channel section area will have maximum conveyance, referred to as the *best hydraulic section* or the cross-section of greatest hydraulic efficiency. Table 5.1.3 presents the geometric elements of the best hydraulic sections for six cross-section shapes. These sections may not always be practical because of difficulties in construction and use of material. The concept of

Table 5.1.3 Best Hydraulic Sections

Cross-section	Area A	Wetted perimeter P	Hydraulic radius R	Top width T	Hydraulic depth D
Trapezoid, half of a hexagon	$\sqrt{3}y^2$	$2\sqrt{3}y$	$\frac{1}{2}y$	$\frac{4}{3}\sqrt{3}y$	$\frac{3}{4}y$
Rectangle, half of a square	$2y^2$	$4y$	$\frac{1}{2}y$	$2y$	y
Triangle, half of a square	y^2	$2\sqrt{2}y$	$\frac{1}{4}\sqrt{2}y$	$2y$	$\frac{1}{2}y$
Semicircle	$\frac{\pi}{2}y^2$	πy	$\frac{1}{2}y$	$2y$	$\frac{\pi}{4}y$
Parabola, $T = 2\sqrt{2}y$	$\frac{4}{3}\sqrt{2}y^2$	$\frac{8}{3}\sqrt{2}y$	$\frac{1}{2}y$	$2\sqrt{2}y$	$\frac{2}{3}y$
Hydrostatic catenary	$1.39586y^2$	$2.9836y$	$0.46784y$	$1.917532y$	$0.72795y$

Source: Chow (1959).

best hydraulic section is only for nonerodible channels. Even though the best hydraulic section gives the minimum area for a given discharge, it may not necessarily have the minimum excavation.

EXAMPLE 5.1.4

Determine the cross-section of greatest hydraulic efficiency for a trapezoidal channel if the design discharge is $10.0 \text{ m}^3/\text{sec}$, the channel slope is 0.00052 , and Manning's $n = 0.025$.

SOLUTION

From Table 5.1.3, the hydraulic radius should be $R = y/2$, so that the width B and area A are

$$B = \frac{2\sqrt{3}y}{3} = 1.155y \quad (\text{because } B = \frac{1}{3}P \text{ for half of a hexagon})$$

$$A = \sqrt{3}y^2 = 1.732y^2$$

Manning's equation (5.1.23) is used to determine the depth:

$$Q = \frac{1}{n}AR^{2/3}S_0^{1/2} = \frac{1}{0.025}(1.732y^2)\left(\frac{y}{2}\right)^{2/3}(0.00052)^{1/2} = 10$$

so

$$\frac{10 \times 0.025 \times 2^{2/3}}{1.732(0.00052)^{1/2}} = y^{8/3}$$

Thus, $y = 2.38 \text{ m}$, so that $B = 2.75 \text{ m}$ and $A = 9.81 \text{ m}^2$.

5.1.4 Slope-Area Method

The slope-area method can be used to estimate the flood discharge through a channel or river reach of length Δx with known cross-sectional areas of flow at the upstream, A_u , and downstream, A_d , ends of the reach. The use of high-water marks from a flood and a survey of the cross sections allow computation of the cross-sectional areas of flow. Manning's equation (5.1.25) can be expressed as

$$Q = K\sqrt{S_o} \quad (5.1.27)$$

where K is the conveyance factor expressed as $K = \frac{1.49}{n}AR^{2/3}$. Conveyance is a measure of the carrying capacity of a channel since it is directly proportional to the discharge Q . The average conveyance factor is the geometric mean of the conveyance factors at the upstream, K_u , and the downstream, K_d , ends of the channel reach, i.e.,

$$\bar{K} = \sqrt{K_u K_d} \quad (5.1.28)$$

The discharge is then expressed as

$$Q = \bar{K}\sqrt{S} \quad (5.1.29)$$

where S is the water slope given as $S = \frac{(z_u - z_d)}{\Delta x}$, z_u and z_d are the water surface elevations at the upstream and downstream ends of the reach, respectively.

Alternatively the friction slope, S_f could be used in equation (5.1.29), $Q = \bar{K}\sqrt{S_f}$, where (Chow, 1959)

$$S_f = \left[(z_u - z_d) - k \left(\alpha_u \frac{V_u^2}{2g} - \alpha_d \frac{V_d^2}{2g} \right) \right] / \Delta x \quad (5.1.30)$$

The difference in water surface elevations is referred to as the fall. The k is a factor to account for a contraction and expansion of a reach. For a contracting reach $V_u < V_d$ so $k = 1.0$ and for an expanding reach ($V_u > V_d$) so $k = 0.5$. The first approximation would compute the discharge using $Q = \bar{K} \sqrt{S_f}$ with the friction slope computed ignoring the velocity heads. Using the first approximation of Q , the upstream and downstream velocity heads are computed for the next approximation of the friction slope, which is used to compute the second approximation of the discharge. The procedure continues computing the new friction slope using the last discharge approximation to compute the new discharge. This process continues until the discharges approximations do not change significantly.

5.2 SPECIFIC ENERGY, MOMENTUM, AND SPECIFIC FORCE

5.2.1 Specific Energy

The *total head* or *energy head*, H , at any location in an open-channel flow can be expressed as

$$H = y + z + \frac{V^2}{2g} \tag{5.1.6}$$

which assumes that the velocity distribution is uniform (i.e., $\alpha = 1$) and the pressure distribution is hydrostatic (i.e., $p = \gamma y$). Using the channel bottom as the datum (i.e., $z = 0$) then define the total head above the channel bottom as the *specific energy*

$$E = y + \frac{V^2}{2g} \tag{5.2.1}$$

Using continuity ($V = Q/A$), the specific energy can be expressed in terms of the discharge as

$$E = y + \frac{Q^2}{2gA^2} \tag{5.2.2}$$

Specific energy curves, such as are shown in Figure 5.2.1 and 5.2.2, can be derived using equation (5.2.2).

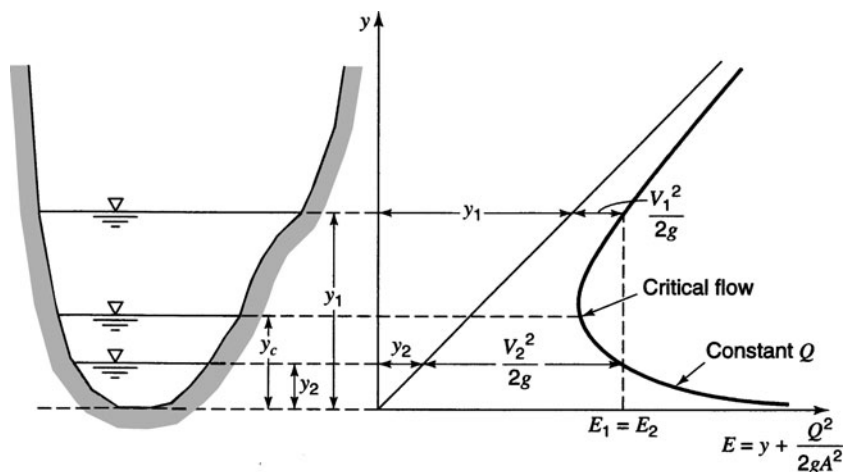


Figure 5.2.1 Specific energy.

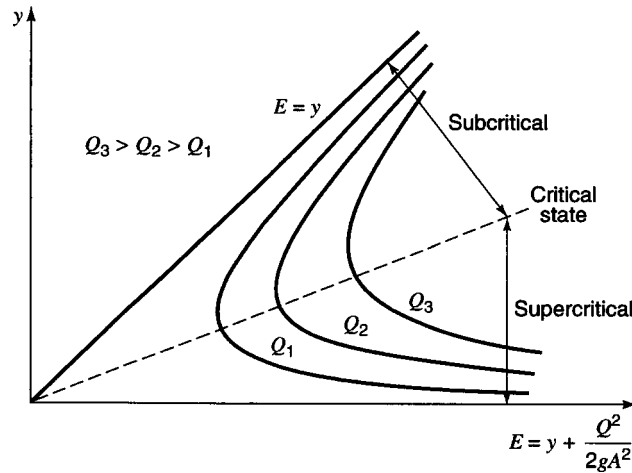


Figure 5.2.2 Specific energy showing subcritical and supercritical flow ranges.

Critical flow occurs when the specific energy is minimum for a given discharge (i.e., $dE/dy = 0$), so that

$$\frac{dE}{dy} = 1 - \frac{Q^2}{gA^3} \frac{dA}{dy} = 0 \quad (5.2.3)$$

Referring to Figure 5.2.1, the top-width is defined as $T = dA/dy$ so equation (5.2.3) can be expressed as

$$1 - \frac{TQ^2}{gA^3} = 0 \quad (5.2.4)$$

or

$$\frac{TQ^2}{gA^3} = 1 \quad (5.2.5)$$

To denote critical conditions use T_c , A_c , V_c , and y_c , so

$$\frac{T_c Q^2}{gA_c^3} = 1 \quad (5.2.6)$$

or

$$\frac{V_c^2}{g} = \frac{A_c}{T_c} \quad (5.2.7)$$

Equation (5.2.6) or (5.2.7) can be used to determine the critical depth and/or the critical velocity.

Rearranging equation (5.2.7) yields

$$\frac{V_c^2}{g(A_c/T_c)} = 1 \quad (5.2.8)$$

The *hydraulic depth* is defined as $D = A/T$ so equation (5.2.7) becomes

$$\frac{V_c^2}{gD_c} = 1 \quad (5.2.9)$$

or

$$\frac{V_c}{\sqrt{gD_c}} = 1 \quad (5.2.10)$$

This is basically the *Froude number*, F_r , which is 1 at critical flow:

$$F_r = \frac{V}{\sqrt{gD}} \begin{cases} < 1 \text{ subcritical flow} \\ = 1 \text{ critical flow} \\ > 1 \text{ supercritical flow} \end{cases} \quad (5.2.11)$$

Figure 5.2.2 illustrates the range of subcritical flow and the range of supercritical flow along with the location of the critical states. Note the relationship of the specific energy curves and the fact that $Q_3 > Q_2 > Q_1$. Figure 5.2.1 illustrates the alternate depths y_1 and y_2 for which $E_1 = E_2$ or

$$y_1 + \frac{V_1^2}{2g} = y_2 + \frac{V_2^2}{2g} \quad (5.2.12)$$

For a rectangular channel $D_c = A_c/T_c = y_c$, so equation (5.2.10) for critical flow becomes

$$\frac{V_c}{\sqrt{gy_c}} = 1 \quad (5.2.13)$$

If we let q be the flow rate per unit width of channel for a rectangular channel, i.e., $q = Q/B$ where $T = B$, the width of the channel (or $q = Q/T$), then equation (5.2.6) can be rearranged, $T_c Q^2 / (g T_c^3 y_c^3) = q^2 / (g y_c) = 1$, and solved for y_c to yield

$$y_c = \left(\frac{q^2}{g} \right)^{1/3} \quad (5.2.14)$$

EXAMPLE 5.2.1

Compute the critical depth for the channel in example 5.1.1 using a discharge of 100 cfs.

SOLUTION

Using equation (5.2.13), $V_c = \sqrt{gy_c} = Q/A = 100/8y_c$, so

$$y_c^{3/2} = \frac{100}{8\sqrt{g}} \text{ or } y_c = \left(\frac{100}{8\sqrt{g}} \right)^{2/3} = 1.69 \text{ ft}$$

Alternatively, using equation (5.2.14) yields

$$y_c = \left(\frac{(100/8)^2}{g} \right)^{1/3} = 1.69 \text{ ft}$$

EXAMPLE 5.2.2

For a rectangular channel of 20 ft width, construct a family of specific energy curves for $Q = 0, 50, 100$, and 300 cfs. Draw the locus of the critical depth points on these curves. For each flow rate, what is the minimum specific energy found from these curves?

SOLUTION

The specific energy is computed using equation (5.2.1):

$$E = y + \frac{V^2}{2g} = y + \frac{1}{2g} \left(\frac{Q}{A} \right)^2 = y + \frac{1}{2g} \frac{Q^2}{(20y)^2} = y + \frac{Q^2}{25,760y^2}$$

Computing critical depths for the flow rates using equation (5.2.14) with $q = Q/B$ yields

$$Q = 0: \quad y_c = \sqrt[3]{\frac{Q^2}{B^2g}} = 0$$

$$Q = 50 \text{ cfs:} \quad y_c = \sqrt[3]{\frac{Q^2}{B^2g}} = \sqrt[3]{\frac{50^2}{20^2(32.2)}} = 0.58 \text{ ft}$$

$$Q = 100 \text{ cfs:} \quad y_c = \sqrt[3]{\frac{Q^2}{B^2g}} = \sqrt[3]{\frac{100^2}{20^2(32.2)}} = 0.92 \text{ ft}$$

$$Q = 300 \text{ cfs:} \quad y_c = \sqrt[3]{\frac{Q^2}{B^2g}} = \sqrt[3]{\frac{300^2}{20^2(32.2)}} = 1.9 \text{ ft}$$

Computed specific energies are listed in Table 5.2.1.

The specific energy curves are shown in Figure 5.2.3. The minimum specific energies are:

$$Q = 50 \text{ cfs:} \quad E_{\min} = 0.868$$

$$Q = 100 \text{ cfs:} \quad E_{\min} = 1.379$$

$$Q = 300 \text{ cfs:} \quad E_{\min} = 2.868$$

Table 5.2.1 Computed Specific Energy Values for Example 5.2.2

Depth, y (ft)	Specific energy, E (ft-lb/lb)			
	$Q = 0$	$Q = 50$	$Q = 100$	$Q = 300$
0.5	0.50	0.89	2.05	14.86
0.6	0.60	0.87	1.68	10.57
0.8	0.80	0.95	1.41	6.41
1.0	1.00	1.10	1.39	4.59
1.2	1.20	1.27	1.47	3.69
1.4	1.40	1.45	1.60	3.23
1.6	1.60	1.64	1.75	3.00
1.8	1.80	1.83	1.92	2.91
2.0	2.00	2.02	2.10	2.90
2.2	2.20	2.22	2.28	2.94
2.4	2.40	2.42	2.47	3.02
2.6	2.60	2.61	2.66	3.13
2.8	2.80	2.81	2.85	3.26
3.0	3.00	3.01	3.04	3.40
3.5	3.50	3.51	3.53	3.79
4.0	4.00	4.01	4.02	4.22
4.5	4.50	4.50	4.52	4.68
5.0	5.00	5.00	5.02	5.14

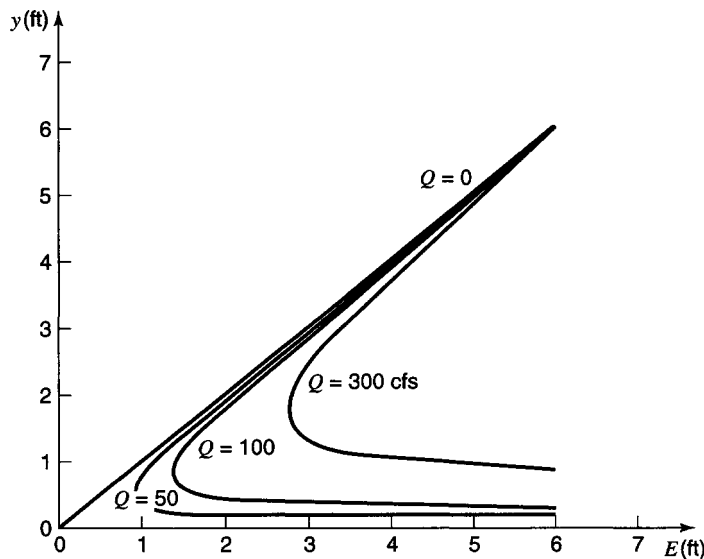


Figure 5.2.3 Specific energy curves for example 5.2.2.

EXAMPLE 5.2.3

A rectangular channel 2 m wide has a flow of 2.4 m³/s at a depth of 1.0 m. Determine whether critical depth occurs at (a) a section where a hump of Δz = 20 cm high is installed across the channel bed, (b) a side wall constriction (with no humps) reducing the channel width to 1.7 m, and (c) both the hump and side wall constrictions combined. Neglect headlosses of the hump and constriction caused by friction, expansion, and contraction.

SOLUTION

(a) The computation is focused on determining the critical elevation change in the channel bottom (hump) Δz_{crit} that causes a critical depth at the hump. The energy equation is $E = E_{min} + \Delta z_{crit}$ or $\Delta z_{crit} = E - E_{min}$, where E is the specific energy of the channel flow and E_{min} is the minimum specific energy, which is at critical depth by definition. If $\Delta z_{crit} \leq \Delta z$, then critical depth will occur. Using equation (5.2.2) yields

$$E = y + \frac{Q^2}{2gA^2} = y + \frac{q^2}{2gy^2}$$

which can be solved for q :

$$q = \sqrt{2g(y^2E - y^3)}$$

Differentiating this equation with respect to y because maximum q and minimum E are equivalent (see Figure 5.2.4) yields

$$\frac{dq}{dy} = \frac{d}{dy} \left[\sqrt{2g(y^2E - y^3)} \right] = 0$$

$$y_c = \frac{2}{3}E_{min} \quad \text{or} \quad E_{min} = \frac{3}{2}y_c$$

To compute specific energy, use

$$E = y + \frac{q^2}{2gy^2} = 1.0 + \frac{(2.4/2.0)^2}{2(9.81)(1)^2} = 1.073 \text{ m}$$

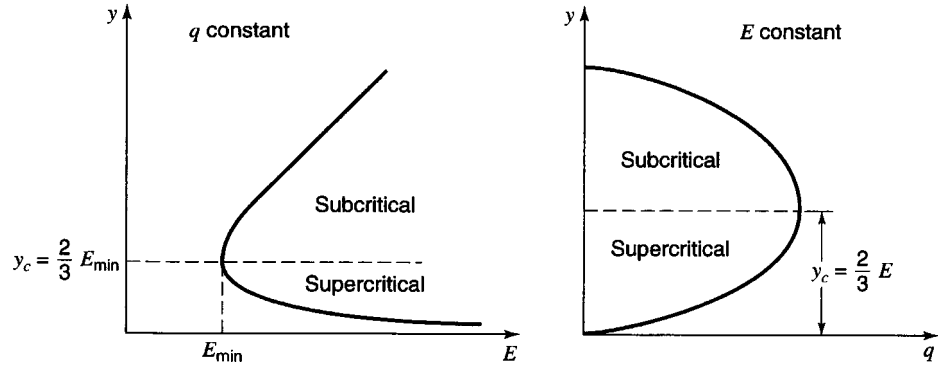


Figure 5.2.4 Specific energy curve and y versus q for constant E .

Next compute E_{\min} using $E_{\min} = 3/2y_c$, where $y_c = (q^2/g)^{1/3}$ (equation (5.2.14)):

$$y_c = \left[\frac{(2.4/2.0)^2}{9.81} \right]^{1/3} = 0.528 \text{ m}$$

So $E_{\min} = 3/2(0.528 \text{ m}) = 0.792 \text{ m}$. Then $\Delta z_{\text{crit}} = E - E_{\min} = 1.073 - 0.792 = 0.281 \text{ m}$. In this case $\Delta z = 20 \text{ cm} = 20/100 \text{ m} = 0.2 \text{ m} < \Delta z_{\text{crit}} = 0.281 \text{ m}$. Therefore, y_c does not occur at the hump.

(b) The critical depth at the side wall constriction is

$$y_c = \left[\frac{(2.4/1.7)^2}{9.81} \right]^{1/3} = 0.588 \text{ m}$$

Thus $E_{\min} = (3/2)y_c = (3/2)(0.588) = 0.882 \text{ m}$. E is computed above as $E = 1.073 \text{ m}$. Because $E_{\min} = 0.882 \text{ m} < E = 1.073 \text{ m}$, critical depth does not occur at the constriction. Remember that energy losses are negligible so that the specific energy in the constriction and upstream of the constriction must be equal. For critical flow to occur, the constriction width can be computed as follows: $E_{\min} = E = 1.073 \text{ m} = (3/2)y_c$, so that $y_c = 0.715 \text{ m}$. Then using equation (5.2.14), $0.715 = [(2.4/B_c)^2/9.81]^{1/3}$ and $B_c = 1.267 \text{ m}$.

(c) With both the hump and the side wall constriction, y_c is 0.588 m , so $E_{\min} = 0.882 \text{ m}$. Then $\Delta z_{\text{crit}} = E - E_{\min} = 1.073 - 0.882 = 0.191 \text{ m}$.

Because $\Delta z = 20/100 \text{ m} = 0.20 \text{ m} > \Delta z_{\text{crit}} = 0.191 \text{ m}$, critical depth will occur at the hump with a constriction.

5.2.2 Momentum

Applying the momentum principle (equation 3.5.6) to a short horizontal reach of channel with steady flow (Figure 5.2.5), we get

$$\sum F_x = \frac{d}{dt} \int_{cv} v_x \rho \, dV + \sum_{cs} v_x \rho \, \mathbf{V} \cdot \mathbf{A} \quad (2.5.6)$$

where

$$\frac{d}{dt} \int_{cv} v_x \rho \, dV = 0 \quad (5.2.15)$$

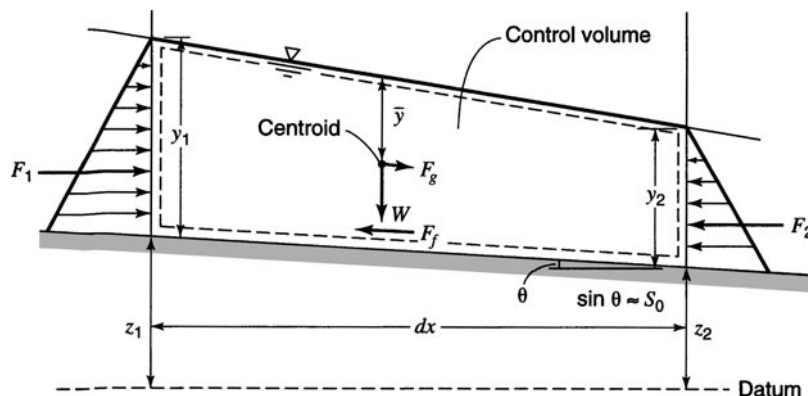


Figure 5.2.5 Application of momentum principle.

The momentum entering from the upstream is $-\rho\beta_1 V_1 Q$ and the momentum leaving the control volume is $\rho\beta_2 V_2 Q$, where β is called the *momentum correction factor* that accounts for the nonuniformity of velocity (equation 3.7.8), so that

$$\sum v_x \rho V \cdot A = -\rho\beta_1 V_1 Q + \rho\beta_2 V_2 Q \tag{5.2.16}$$

The forces are

$$\sum F_x = F_1 - F_2 + F_g - F'_f \tag{5.2.17}$$

The hydrostatic forces are

$$F_1 = \gamma A \bar{y}_1 \tag{5.2.18}$$

and

$$F_2 = \gamma A \bar{y}_2 \tag{5.2.19}$$

where \bar{y}_1 and \bar{y}_2 are the distances to the centroid. The gravity force F_g due to the weight W of the water is $W \sin \theta = \rho g A dx \sin \theta$, where $W = \rho g A dx$. Because the channel slope is small, $S_0 \approx \sin \theta$, and the force due to gravity is

$$F_g = \rho g \bar{A} dx S_0 \tag{5.2.20}$$

where $\bar{A} = (A_1 + A_2)/2$ is the average cross-sectional area of flow. The external force due to friction created by shear between the channel bottom and sides of the control volume is $-\tau_0 P dx$ where τ_0 is the bed shear stress and P is the wetted perimeter. From equation (5.1.6), $\tau_0 = \gamma R S_f = \rho g (A/P) S_f$. So the friction force is then

$$F'_f = -\rho g A S_f dx \tag{5.2.21}$$

For our purposes here we will continue to use F_g and F'_f .

Substituting equations (5.2.15) through (5.2.21) into (3.5.6) gives

$$\gamma A_1 \bar{y}_1 - \gamma A_2 \bar{y}_2 + W \sin \theta - F'_f = -\rho\beta_1 V_1 Q + \rho\beta_2 V_2 Q \tag{5.2.22}$$

which is the *momentum equation for steady state open-channel flow*.

It should be emphasized that in the energy equation the F_f (loss due to friction) is a measure of the internal energy dissipated in the entire mass of water in the control volume, whereas F'_f in the

momentum equation measures the losses due to external forces exerted on the water by the wetted perimeter of the control volume. Ignoring the small difference between the energy coefficient α and the momentum coefficient β in gradually varied flow, the internal energy losses are practically identical with the losses due to external forces (Chow, 1959). For uniform flow, $F_g = F'_f$.

Application of the energy and momentum principles in open-channel flow can be confusing at first. It is important to understand the basic differences, even though the two principles may produce identical or very similar results. Keep in mind that *energy is a scalar quantity* and *momentum is a vector quantity* and that *energy considers internal losses* in the energy equation and *momentum considers external resistance* in the momentum equation. The energy principle is simpler and clearer than the momentum principle; however, the momentum principle has certain advantages in application to problems involving high internal-energy changes, such as the hydraulic jump (Chow, 1959), which is discussed in section 5.5 on rapidly varied flow.

5.2.3 Specific Force

For a short horizontal reach (control volume) with $\theta = 0$ and the gravity force $F_g = W \sin \theta = 0$, the external force of friction F'_f , can be neglected so $F'_f = 0$ and $F_g = 0$. Also assuming $\beta_1 = \beta_2$, the momentum equation (5.2.22) reduces to

$$\gamma A_1 \bar{y}_1 - \gamma A_2 \bar{y}_2 = -\rho V_1 Q + \rho V_2 Q \quad (5.2.23)$$

Substituting $V_1 = Q/A_1$ and $V_2 = Q/A_2$, dividing through by γ and substituting $1/g = \rho/\gamma$, and then rearranging yields

$$\frac{Q^2}{gA_1} + A_1 \bar{y}_1 = \frac{Q^2}{gA_2} + A_2 \bar{y}_2 \quad (5.2.24)$$

The *specific force* F (Figure 5.2.6) is defined as

$$F = \frac{Q^2}{gA} + A\bar{y} \quad (5.2.25)$$

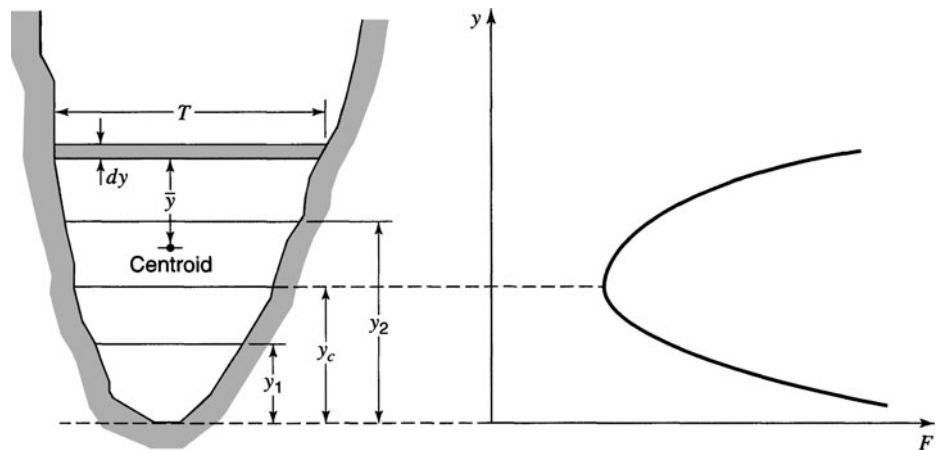


Figure 5.2.6 Specific force curves.

which has units of ft^3 or m^3 . The minimum value of the specific force with respect to the depth is determined using

$$\frac{dF}{dy} = \frac{d\left(\frac{Q^2}{gA}\right)}{dy} + \frac{d(A\bar{y})}{dy} = 0 \tag{5.2.26}$$

which results in

$$\frac{dF}{dy} = -\frac{TQ^2}{gA^2} + A = 0 \tag{5.2.27}$$

Refer to Chow (1959) or Chaudhry (1993) for the proof and further explanation of $d(A\bar{y})/dy = A$. Equation (5.2.27) reduces to $-V^2/g + A/T = 0$ where the hydraulic depth $D = A/T$, so

$$\frac{V^2}{g} = D \quad \text{or} \quad \frac{V^2}{gD} = 1 \tag{5.2.28}$$

which we have already shown is the criterion for critical flow (equation (5.2.9) or (5.2.10)). Therefore, at critical flow the specific force is a minimum for a given discharge.

Summarizing, critical flow is characterized by the following conditions:

- Specific energy is minimum for a given discharge.
- Specific force is minimum for a given discharge.
- Velocity head is equal to half the hydraulic depth.
- Froude number is equal to unity.

Two additional conditions that are not proven here are (Chow, 1959):

- The discharge is maximum for a given specific energy.
- The velocity of flow in a channel of small slope with uniform velocity distribution is equal to the celerity of small gravity waves in shallow water caused by local disturbances.

When flow is at or near the critical state, minor changes in specific energy near critical flow cause major changes in depth (see Figures 5.2.1 or 5.2.2), causing the flow to be unstable. Figure 5.2.7 illustrates examples of locations of critical flow.

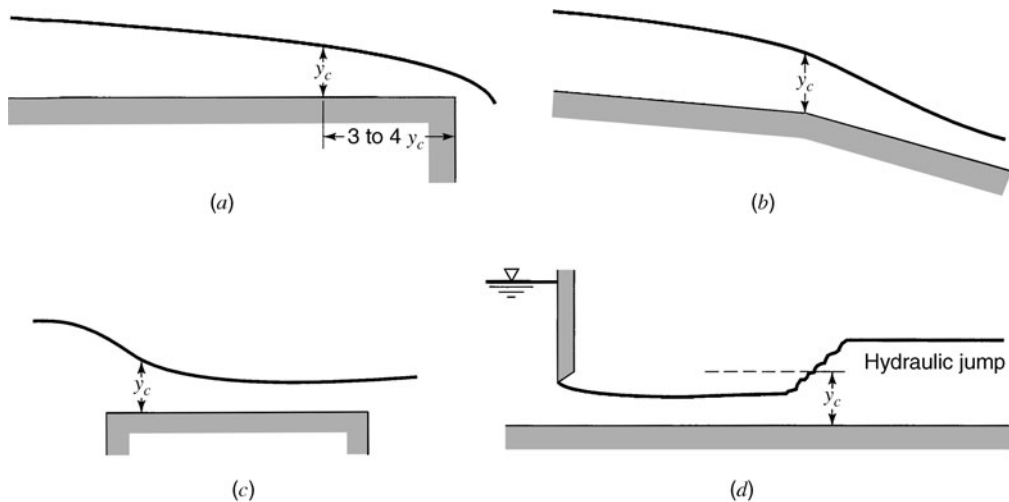


Figure 5.2.7 Example locations of critical flow. (a) Critical depth near free overfall; (b) Change in grade of channel bottom; (c) Flow over a broad-crested weir; (d) Flow through hydraulic jump.

EXAMPLE 5.2.4

Compute the specific force curves for the channel and flow rates used in example 5.2.2.

SOLUTION

The specific force values are computed using equation (5.2.25) with the values presented in Table 5.2.2. The curves are plotted in Figure 5.2.8.

Table 5.2.2 Computed Specific Force Curve Values for Example 5.2.4

Depth, y (ft)	Specific force, F (ft^3)			
	$Q = 0$	$Q = 50$	$Q = 100$	$Q = 300$
0.1	0.10	38.92	155.38	1397.62
0.2	0.40	19.81	78.04	699.16
0.4	1.60	11.30	40.42	350.98
0.6	3.60	10.07	29.48	236.52
0.8	6.40	11.25	25.81	181.09
1.0	10.00	13.88	25.53	149.75
1.2	14.40	17.63	27.34	130.86
1.4	19.60	22.37	30.69	119.42
1.6	25.60	28.03	35.30	112.94
1.8	32.40	34.56	41.03	110.04
2.0	40.00	41.94	47.76	109.88
2.2	48.40	50.16	55.46	111.92
2.4	57.60	59.22	64.07	115.83
2.6	67.60	69.09	73.57	121.35
2.8	78.40	79.79	83.95	128.31
3.0	90.00	91.29	95.18	136.58
3.5	122.50	123.61	126.94	162.43
4.0	160.00	160.97	163.88	194.94
4.5	202.50	203.36	205.95	233.56
5.0	250.00	250.78	253.11	277.95

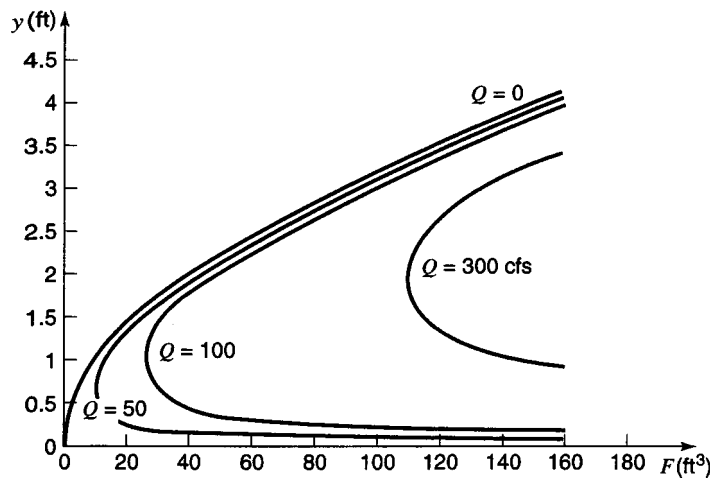


Figure 5.2.8 Specific force curves.

5.3 STEADY, GRADUALLY VARIED FLOW

5.3.1 Gradually Varied Flow Equations

Several types of open-channel flow problems can be solved in hydraulic engineering practice using the concepts of nonuniform flow. The first to be discussed are *gradually varied flow problems* in which the change in the water surface profile is small enough that it is possible to integrate the relevant differential equation from one section to an adjacent section for the change in depth or change in water surface elevation. Consider the energy equation (5.1.6) previously derived for nonuniform flow (Figure 5.1.1) using the control volume approach (with $\alpha_1 = \alpha_2 = 1$):

$$y_1 + z_1 + \frac{V_1^2}{2g} = y_2 + z_2 + \frac{V_2^2}{2g} + h_L \quad (5.1.6)$$

Because $h_L = S_f L = S_f \Delta x$ letting $\Delta y = y_2 - y_1$ and $\Delta z = z_1 - z_2 = S_0 \Delta x$, then equation (5.1.6) can be expressed as

$$S_0 \Delta x + \frac{V_1^2}{2g} = \Delta y + \frac{V_2^2}{2g} + S_f \Delta x \quad (5.3.1)$$

Rearranging yields

$$\Delta y = S_0 \Delta x - S_f \Delta x - \left(\frac{V_2^2}{2g} - \frac{V_1^2}{2g} \right) \quad (5.3.2)$$

and then dividing through by Δx results in

$$\frac{\Delta y}{\Delta x} = S_0 - S_f - \left(\frac{V_2^2}{2g} - \frac{V_1^2}{2g} \right) \frac{1}{\Delta x} \quad (5.3.3)$$

Taking the limit as $\Delta x \rightarrow 0$, we get

$$\lim_{\Delta x \rightarrow 0} \left(\frac{\Delta y}{\Delta x} \right) = \frac{dy}{dx} \quad (5.3.4)$$

and

$$\lim_{\Delta x \rightarrow 0} \left(\frac{V_2^2}{2g} - \frac{V_1^2}{2g} \right) \left(\frac{1}{\Delta x} \right) = \frac{d}{dx} \left(\frac{V^2}{2g} \right) \quad (5.3.5)$$

Substituting these into equation (5.3.3) and rearranging yields

$$\frac{dy}{dx} + \frac{d}{dx} \left(\frac{V^2}{2g} \right) = S_0 - S_f \quad (5.3.6)$$

The second term $\frac{d}{dx} \left(\frac{V^2}{2g} \right)$ can be expressed as $\left[\frac{d \left(\frac{V^2}{2g} \right)}{dy} \right] \frac{dy}{dx}$, so that equation (5.3.6) can be simplified to

$$\frac{dy}{dx} \left[1 + \frac{d \left(\frac{V^2}{2g} \right)}{dy} \right] = S_0 - S_f \quad (5.3.7)$$

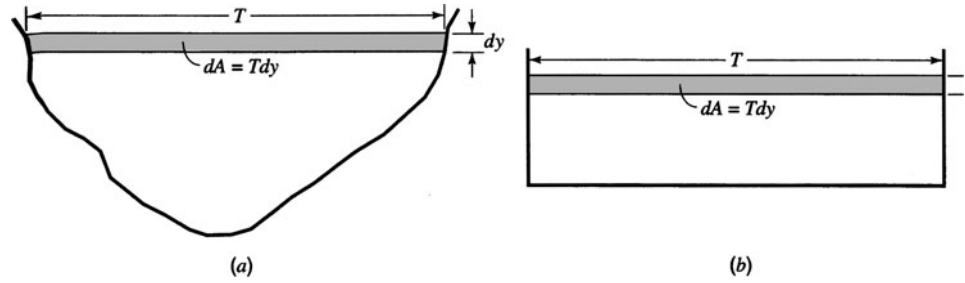


Figure 5.3.1 Definition of top width ($T = dA/dy$). (a) Natural channel; (b) Rectangular channel.

or

$$\frac{dy}{dx} = \frac{S_0 - S_f}{\left[1 + \frac{d\left(\frac{V^2}{2g}\right)}{dy} \right]} \quad (5.3.8)$$

Equations (5.3.7) and (5.3.8) are two expressions of *the differential equation for gradually varied flow*. Equation (5.3.8) can also be expressed in terms of the Froude number. First observe that

$$\frac{d}{dy} \left(\frac{V^2}{2g} \right) = \frac{d}{dy} \left(\frac{Q^2}{2gA^2} \right) = - \left(\frac{Q^2}{gA^3} \right) \frac{dA}{dy} \quad (5.3.9)$$

By definition, the incremental increase in cross-sectional area of flow dA , due to an incremental increase in the depth dy , is $dA = Tdy$, where T is the top width of flow (see Figure 5.3.1). Also $A/T = D$, which is the hydraulic depth. Equation (5.3.9) can now be expressed as

$$\frac{d}{dy} \left(\frac{V^2}{2g} \right) = - \left(\frac{Q^2}{gA^3} \right) \frac{Tdy}{dy} = - \frac{Q^2}{gA^2} \left(\frac{T}{A} \right) = - \frac{Q^2}{gA^2 D} \quad (5.3.10a)$$

$$= - F_r^2 \quad (5.3.10b)$$

where $F_r = \frac{V}{\sqrt{gD}} = \frac{Q}{A\sqrt{gD}}$. Substituting equation (5.3.10b) into (5.3.8) and simplifying, we find that the gradually varied flow equation in terms of the Froude number is

$$\frac{dy}{dx} = \frac{S_0 - S_f}{1 - F_r^2} \quad (5.3.11)$$

EXAMPLE 5.3.1

Consider a vertical sluice gate in a wide rectangular channel ($R = A/P = By/(B + 2Y) \approx y$ because $B \gg 2y$). The flow downstream of a sluice gate is basically a jet that possesses a vena contracta (see Figure 5.3.2). The distance from the sluice gate to the vena contracta as a rule is approximated as the same as the sluice gate opening (Chow, 1959). The coefficients of contraction for vertical sluice gates are approximately 0.6, ranging from 0.598 to 0.611 (Henderson, 1966). The objective of this problem is to determine the distance from the vena contracta to a point b downstream where the depth of flow is known to be 0.5 m deep. The depth of flow at the vena contracta is 0.457 m for a flow rate of 4.646 m³/s per meter of width. The channel bed slope is 0.0003 and Manning's roughness factor is $n = 0.020$.

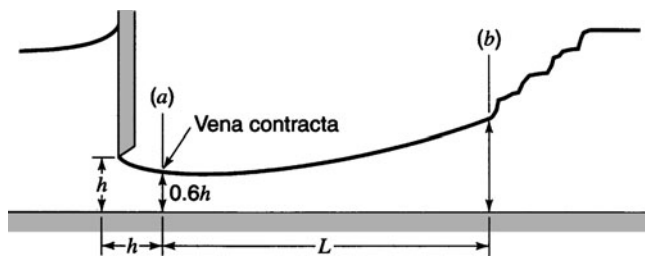


Figure 5.3.2 Flow downstream of a sluice gate in a wide rectangular channel.

SOLUTION

To compute the distance, Δx from y_a to y_b , the gradually varied flow equation (5.3.1) can be used,

$$S_0 \Delta x + \frac{V_1^2}{2g} = \Delta y + \frac{V_2^2}{2g} + S_f \Delta x$$

where $\Delta y = y_2 - y_1$. Solving for Δx , we get

$$(S_0 - S_f) \Delta x = \Delta y + \left(\frac{V_2^2}{2g} - \frac{V_1^2}{2g} \right)$$

$$\Delta x = \frac{\Delta y + \left(\frac{V_2^2}{2g} - \frac{V_1^2}{2g} \right)}{S_0 - S_f}$$

The friction slope is computed using Manning’s equation (5.1.22) with average values of the hydraulic radius

$$V_{ave} = \frac{1}{n} R_{ave}^{2/3} S_f^{1/2}$$

so

$$S_f = \left[\frac{n V_{ave}}{R_{ave}^{2/3}} \right]^2$$

Let us use the following values for this example:

Location	y (m)	$R = y$ (m)	V (m/s)	$V^2/2g$ (m)
<i>a</i>	0.457	0.457	10.17	5.27
<i>b</i>	0.500	0.500	9.292	4.40

Now we get

$$V_{ave} = \frac{10.17 + 9.292}{2} = 9.73 \text{ m/s}$$

$$R_{ave} = \frac{0.457 + 0.500}{2} = 0.479 \text{ m}$$

$$S_f = \left[\frac{0.020(9.73)}{0.479^{2/3}} \right]^2 = 0.101 \text{ m/m}$$

The distance from a to b , Δx , is

$$\Delta x = \frac{(0.500 - 0.457) + (4.40 - 5.27)}{0.0003 - 0.101} = \frac{-0.827}{-0.101} = 8.21 \text{ m}$$

The distance from the sluice gate to b is $\left(\frac{0.457}{0.6}\right) + 8.21 = 8.97 \text{ m}$.

5.3.2 Water Surface Profile Classification

Channel bed slopes may be classified as mild (M), steep (S), critical (C), horizontal (H) ($S_0 = 0$), and adverse (A) ($S_0 < 0$). To define the various types of slopes for the mild, steep, and critical slopes, the normal depth y_n and critical depth y_c are used:

$$\text{Mild: } y_n > y_c \text{ or } \frac{y_n}{y_c} > 1 \quad (5.3.12a)$$

$$\text{Steep: } y_n < y_c \text{ or } \frac{y_n}{y_c} < 1 \quad (5.3.12b)$$

$$\text{Critical: } y_n = y_c \text{ or } \frac{y_n}{y_c} = 1 \quad (5.3.12c)$$

The horizontal and adverse slopes are special cases because the normal depth does not exist for them. Table 5.3.1 lists the types and characteristics of the various types of profiles and Figure 5.3.3 shows the classification of gradually varied flow profiles.

Table 5.3.1 Types of Flow Profiles in Prismatic Channels

Channel slope	Designation			Relation of y to y_n and y_c			General type of curve	Type of flow
	Zone 1	Zone 2	Zone 3	Zone 1	Zone 2	Zone 3		
Horizontal $S_0 = 0$	None			$y > y_n$	$> y_c$		None	None
		$H2$		$y_n > y_c$	$> y_c$		Drawdown	Subcritical
			$H3$	$y_n > y_c$	$> y_c$	$y_c > y$	Backwater	Supercritical
Mild $0 < S_0 < S_c$	$M1$			$y > y_n$	$> y_c$		Backwater	Subcritical
		$M2$		$y_n > y_c$	$> y_c$		Drawdown	Subcritical
			$M3$	$y_n > y_c$	$> y_c$	$y_c > y$	Backwater	Supercritical
Critical $S_0 = S_c > 0$	$C1$			$y > y_c$	$= y_n$		Backwater	Subcritical
		$C2$		$y_n = y_c$	$= y = y_c$		Parallel to channel bottom	Uniform-critical
			$C3$	$y_c = y_n$	$= y_n > y$		Backwater	Supercritical
Steep $S_0 > S_c > 0$	$S1$			$y > y_c$	$> y_n$		Backwater	Subcritical
		$S2$		$y_c > y_n$	$> y_n$		Drawdown	Supercritical
			$S3$	$y_c > y_n$	$> y_n$	$y_n > y$	Backwater	Supercritical
Adverse $S_0 < 0$	None			$y > (y_n)^*$	$> y_c$		None	None
		$A2$		$(y_n)^*$	$> y_c$		Drawdown	Subcritical
			$A3$	$(y_n)^*$	$> y_c$	$y_c > y$	Backwater	Supercritical

* y_n in parentheses is assumed a positive value.

Source: Chow (1959).

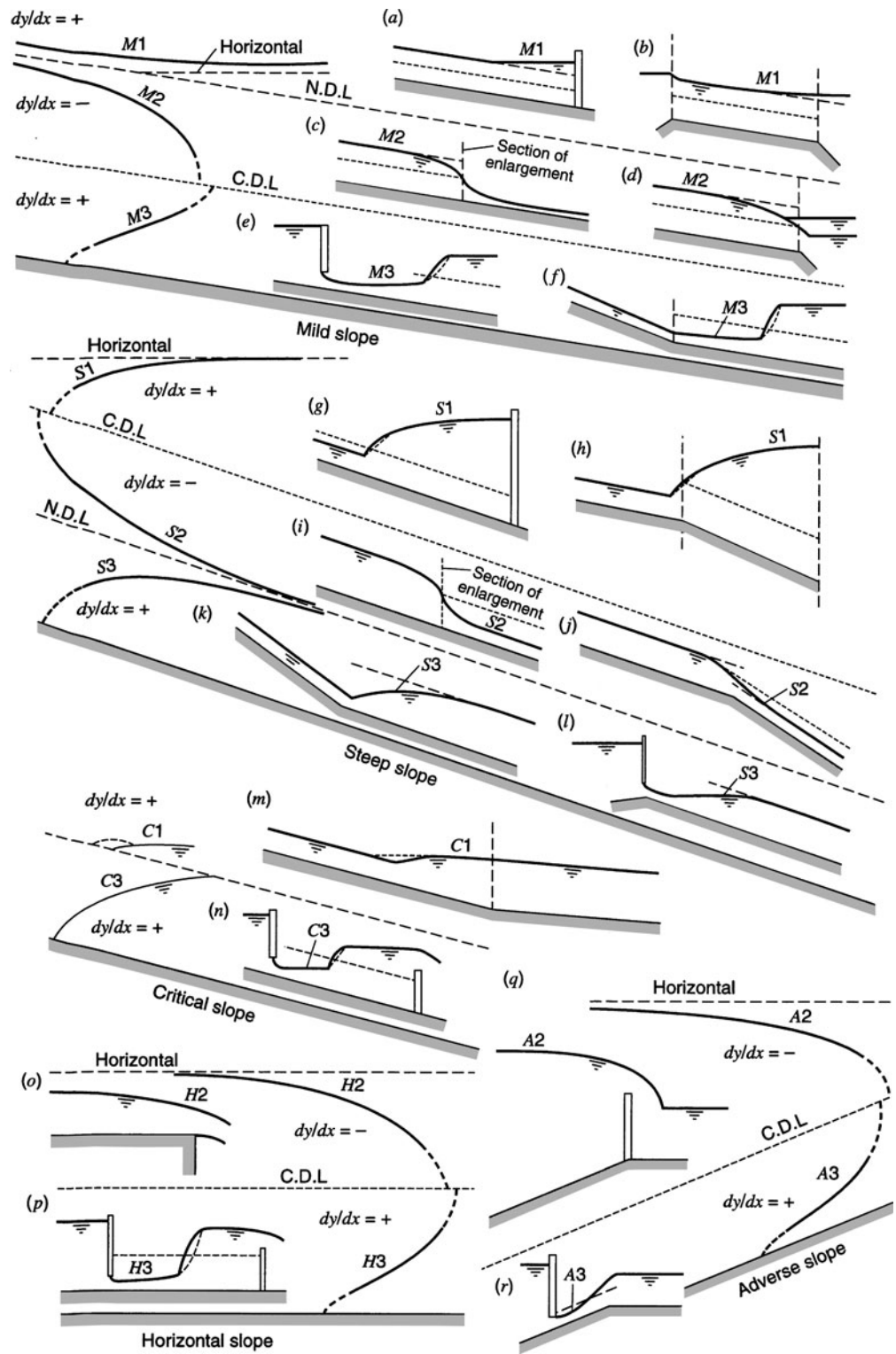


Figure 5.3.3 Flow profiles (from Chow (1959)).

The three zones for mild slopes are defined as

$$\text{Zone 1: } y > y_n > y_c$$

$$\text{Zone 2: } y_n > y > y_c$$

$$\text{Zone 3: } y_n > y_c > y$$

The energy grade line, water surface, and channel bottom are all parallel for uniform flow, i.e., $S_f = S_0$ = slope of water surface when $y = y_n$. From Manning's equation for a given discharge, $S_f < S_0$ if $y > y_n$.

Now consider the qualitative characteristics using the three zones.

Zone 1 (M1 profile): $y > y_n$; then $S_f < S_0$ or $S_0 - S_f = +$
 $F_r < 1$ since $y > y_c$, so $1 - F_r^2 = +$
 by equation (5.3.11), $\frac{dy}{dx} = \frac{S_0 - S_f}{1 - F_r^2} = \frac{+}{+} = +$
 then y increases with x so that $y \rightarrow y_n$

Zone 2 (M2 profile): $y < y_n$; then $S_f > S_0$ or $S_0 - S_f = -$
 $F_r < 1$ since $y > y_c$, so $1 - F_r^2 = +$
 by equation (5.3.11), $\frac{dy}{dx} = \frac{S_0 - S_f}{1 - F_r^2} = \frac{-}{+} = -$
 then y decreases with x so that $y \rightarrow y_c$

Zone 3 (M3 profile): $y < y_n$; then $S_f > S_0$ or $S_0 - S_f = -$
 $F_r > 1$ since $y < y_c$ so $1 - F_r^2 = -$
 by equation (5.3.11), $\frac{dy}{dx} = \frac{S_0 - S_f}{1 - F_r^2} = \frac{-}{-} = +$
 then y increases with x so that $y \rightarrow y_c$

This analysis can be made of the other profiles. The results are summarized in Table 5.3.1.

EXAMPLE 5.3.2

For the rectangular channel described in examples 5.1.1, 5.1.3, and 5.2.1, classify the type of slope. Determine the types of profiles that exist for depths of 5.0 ft, 2.0 ft, and 1.0 ft with a discharge of 100 ft³/s.

SOLUTION

In example 5.1.3, the normal depth is computed as $y_n = 3.97$ ft, and in example 5.2.1, the critical depth is computed as $y_c = 1.69$ ft. Because $y_n > y_c$, this is a mild channel bed slope.

For a flow depth of 5.0 ft, $5.0 > y_n > y_c$, so that an M1 profile with a backwater curve exists (refer to Table 5.3.1 and Figure 5.3.3). The flow is subcritical.

For a flow depth of 2.0 ft, $y_n > 2.0 > y_c$, so that an M2 profile with a drawdown curve exists. The flow is subcritical.

For a flow depth of 1.0 ft, $y_n > y_c > 1.0$, so that an M3 profile with a backwater curve exists. The flow is supercritical.

Prismatic Channels with Changes in Slope

Consider a channel that changes slope from a mild slope to a steep slope. The critical depth is the same for each slope; however, the normal depth changes, for the upstream mild slope, $y_{n1} > y_c$, and for the downstream steep slope, $y_{n2} < y_c$. The only control is the critical depth at the break in slopes where flow transitions from a subcritical flow to a supercritical flow. The flow profiles are an M2

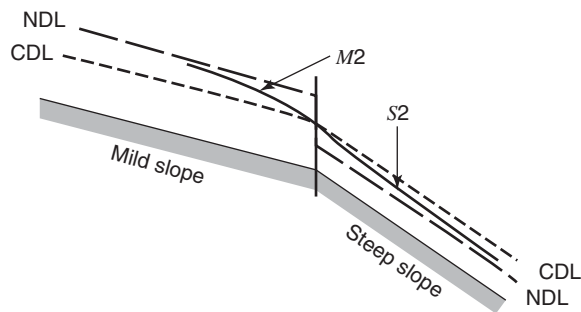


Figure 5.3.4 Water surface profile for prismatic channel with slope change from mild to steep.

profile for the upstream reach and an S2 profile for the downstream reach as shown in Figure 5.3.4. The specific energy for the reaches, E_{n1} and E_{n2} , and the specific energy for critical conditions can be computed. A channel that changes slope from a steep slope to a mild slope is more complicated in that a hydraulic jump forms. This jump could form on the upper steep slope or on the lower mild slope.

5.3.3 Direct Step Method

In example 5.3.1 we computed the location where a specified depth occurred, using the energy equation. This procedure can be extended to compute reach lengths for specified depths at each end of a reach. Computations are performed step by step from one end of the channel reach by reach to the other end. This procedure is called the direct step method and is applicable only to prismatic channels.

The gradually varied flow equation can be expressed in terms of the specific energy. Equation (5.3.1) can be rearranged to

$$S_o \Delta x - \bar{S}_f \Delta x = \left(y_2 + \alpha_2 \frac{V_2^2}{2g} \right) - \left(y_1 + \alpha_1 \frac{V_1^2}{2g} \right) = E_2 - E_1 \tag{5.2.12}$$

where \bar{S}_f is the average friction slope for the channel reach. Solving for Δx ,

$$\Delta x = \frac{E_2 - E_1}{S_o - \bar{S}_f} \tag{5.3.13}$$

The direct step method is based on this equation. Manning’s equation is used to compute the friction slope at the upstream and downstream ends of each reach for the specified depths using

$$S_f = \frac{n^2 v^2}{2.22R^{2/3}} \tag{5.3.14}$$

The average friction slope, $\bar{S}_f = \frac{1}{2} (S_{f1} + S_{f2})$, is used in equation (5.3.13). The computation procedure must be performed from downstream to upstream if the flow is subcritical and from upstream to downstream if the flow is supercritical.

EXAMPLE 5.3.3

A trapezoidal channel has the flowing characteristics: slope = 0.0016; bottom width = 20 ft; and side slopes = 1 vertical to 2 horizontal ($z = 2$). Water at a downstream location is an embankment where the water depth is 5.0 ft just upstream of the embankment and the discharge is 400 cfs. Determine the distance upstream to where the flow depth is 4.60 ft. (Adapted from Chow, 1959.) (Assume $\alpha = 1.10$.)

SOLUTION

The critical depth is $y_c = 2.22$ ft and the normal depth is $y_n = 3.36$ ft, so the flow is subcritical. Because the depth of 5.0 ft is greater than the normal depth of 3.36 ft, this is an M1 profile. Then the depth will decrease proceeding in the upstream direction because $dy/dx = +$ in the downstream direction. In other words, going upstream the depth will approach normal depth. So we will consider the first reach, going upstream to a depth of 5.0 to 4.8 ft and the second reach upstream is from a depth of 4.8 to 4.6 ft depth.

First reach; At $y = 5.0$ ft then $A = 150$ ft², $R = 3.54$ ft, $V = 2.67$ ft/sec, $S_f = 0.000037$, and $E = 5 + (1.1)(2.67)^2/[2(32.2)] = 5.123$ ft, and at $y = 4.80$ ft then $A = 142.1$ ft², $R = 3.43$ ft, $V = 2.82$ ft/sec, $S_f = 0.00043$, and $E = 4.936$ ft. Using equation 5.3.14,

$$\text{where } \bar{S}_f = \frac{1}{2}(0.000037 + 0.00043) = 0.00040,$$

$$\text{then } \Delta x = \frac{E_2 - E_1}{S_o - \bar{S}_f} = \frac{5.123 - 4.938}{0.0016 - 0.00040} = 156 \text{ ft.}$$

Second reach: At $y = 4.60$ ft, $A = 134.3$ ft², $R = 3.31$ ft, $V = 2.98$ ft/sec, $S_f = 0.00051$, and $E = 4.752$ ft. $\bar{S}_f = \frac{1}{2}(0.00043 + 0.00051) = 0.00047$, and $\Delta x = 163$ ft.

So the distance upstream to a depth of 4.60 ft is $156 + 163 = 319$ ft. The procedure can be continued upstream to where the normal depth occurs.

5.4 GRADUALLY VARIED FLOW FOR NATURAL CHANNELS**5.4.1 Development of Equations**

As an alternate to the procedure presented above, the gradually varied flow equation can be expressed in terms of the water surface elevation for application to natural channels by considering $w = z + y$ where w is the water surface elevation above a datum such as mean sea level. The total energy H at a section is

$$H = z + y + \alpha \frac{V^2}{2g} = w + \alpha \frac{V^2}{2g} \quad (5.4.1)$$

including the energy correction factor α . The change in total energy head with respect to location along a channel is

$$\frac{dH}{dx} = \frac{dw}{dx} + \frac{d}{dx} \left(\alpha \frac{V^2}{2g} \right) \quad (5.4.2)$$

The total energy loss is due to friction losses (S_f) and contraction-expansion losses (S_e):

$$\frac{dH}{dx} = -S_f - S_e \quad (5.4.3)$$

S_e is the slope term for the contraction-expansion loss. Substituting (5.4.3) into (5.4.2) results in

$$-S_f - S_e = \frac{dw}{dx} + \frac{d}{dx} \left(\alpha \frac{V^2}{2g} \right) \quad (5.4.4)$$

The friction slope S_f can be expressed using Manning's equation (5.1.23) or (5.1.25):

$$Q = KS_f^{1/2} \quad (5.4.5)$$

where K is defined as the *conveyance* in SI units

$$K = \frac{1}{n} AR^{2/3} \quad (5.4.6a)$$

or in U.S. customary units as

$$K = \frac{1.486}{n} AR^{2/3} \quad (5.4.6b)$$

for equations (5.1.23) or (5.1.25), respectively. The friction slope (from equation 5.4.5) is then

$$S_f = \frac{Q^2}{K^2} = \frac{Q^2}{2} \left[\frac{1}{K_1^2} + \frac{1}{K_2^2} \right] \quad (5.4.7)$$

with the conveyance effect $\frac{1}{K^2} = \frac{1}{2} \left[\frac{1}{K_1^2} + \frac{1}{K_2^2} \right]$, where K_1 and K_2 are the conveyances, respectively, at the upstream and the downstream ends of the reach. Alternatively, the friction slope can be determined using an average conveyance, i.e., $\bar{K} = (K_1 + K_2)/2$ and $Q = \bar{K}S_f^{1/2}$; then

$$S_f = \frac{Q^2}{\bar{K}^2} \quad (5.4.8)$$

The *contraction-expansion loss term* S_e can be expressed for a *contraction loss* as

$$S_e = \frac{C_e}{dx} \left[\alpha_2 \frac{V_2^2}{2g} - \alpha_1 \frac{V_1^2}{2g} \right] \quad \text{for} \quad d \left(\alpha \frac{V^2}{2g} \right) = \left(\alpha_2 \frac{V_2^2}{2g} - \alpha_1 \frac{V_1^2}{2g} \right) > 0 \quad (5.4.9)$$

and for an *expansion loss* as

$$S_e = \frac{C_e}{dx} \left[\alpha_2 \frac{V_2^2}{2g} - \alpha_1 \frac{V_1^2}{2g} \right] \quad \text{for} \quad d \left(\alpha \frac{V^2}{2g} \right) < 0 \quad (5.4.10)$$

The *gradually varied flow equation for a natural channel* is defined by substituting equation (5.4.7) into equation (5.4.4):

$$- \frac{Q^2}{2} \left[\frac{1}{K_1^2} + \frac{1}{K_2^2} \right] - S_e = \frac{dw}{dx} + \frac{d}{dx} \left(\alpha \frac{V^2}{2g} \right) \quad (5.4.11a)$$

or

$$- \frac{Q^2}{2} \left[\frac{1}{K_1^2} + \frac{1}{K_2^2} \right] - S_e = \frac{w_2 - w_1}{\Delta x} + \frac{1}{\Delta x} \left[\alpha_2 \frac{V_2^2}{2g} - \alpha_1 \frac{V_1^2}{2g} \right] \quad (5.4.11b)$$

Rearranging yields

$$w_1 + \alpha_1 \frac{V_1^2}{2g} = w_2 + \alpha_2 \frac{V_2^2}{2g} + \frac{Q^2}{2} \left[\frac{1}{K_1^2} + \frac{1}{K_2^2} \right] \Delta x + S_e \Delta x \quad (5.4.12)$$

EXAMPLE 5.4.1

Derive an expression for the change in water depth as a function of distance along a prismatic channel (i.e., constant alignment and slope) for a gradually varied flow.

SOLUTION

We start with equation (5.3.11):

$$\frac{dy}{dx} = \frac{S_o - S_f}{1 - F_r^2}$$

with

$$F_r^2 = \left(V / \sqrt{gD} \right)^2 = \left(Q / A \sqrt{gD} \right)^2 = \left(Q / A \sqrt{gA/T} \right)^2 = \frac{Q^2 T}{gA^3}.$$

Then

$$\frac{dy}{dx} = \frac{S_0 - S_f}{\left(1 - \frac{Q^2 T}{gA^3} \right)}$$

To determine a gradually varied flow profile, this equation is integrated.

EXAMPLE 5.4.2

For a river section with a subcritical discharge of 6500 ft³/s, the water surface elevation at the downstream section is 5710.5 ft with a velocity head of 3.72 ft. The next section is 500 ft upstream with a velocity head of 1.95 ft. The conveyances for the downstream and upstream sections are 76,140 and 104,300, respectively. Using expansion and contraction coefficients of 0.3 and 0.1, respectively, determine the water surface elevation at the upstream section.

SOLUTION

Using equation (5.4.12), the objective is to solve for the upstream water surface elevation w_1 :

$$\begin{aligned} w_1 &= w_2 + \alpha_2 \frac{V_2^2}{2g} - \alpha_1 \frac{V_1^2}{2g} + \frac{Q^2}{2} \left[\frac{1}{K_1^2} + \frac{1}{K_2^2} \right] \Delta x + S_e \Delta x \\ &= w_2 + \Delta \left(\alpha \frac{V^2}{2g} \right) + \frac{Q^2}{2} \left[\frac{1}{K_1^2} + \frac{1}{K_2^2} \right] \Delta x + S_e \Delta x \end{aligned}$$

The friction slope term is

$$\frac{Q^2}{2} \left[\frac{1}{K_1^2} + \frac{1}{K_2^2} \right] \Delta x = \frac{6500^2}{2} \left[\frac{1}{76,140^2} + \frac{1}{104,300^2} \right] 500 = 2.79 \text{ ft}$$

$$\Delta \left(\alpha \frac{V^2}{2g} \right) = 3.72 - 1.95 = +1.77 \text{ ft}$$

Because $\Delta \left[\alpha (V^2/2g) \right] > 0$, a contraction exists for flow from cross-section 1 to cross-section 2. Then

$$S_e \Delta x = C_c \left[\alpha_2 \frac{V_2^2}{2g} - \alpha_1 \frac{V_1^2}{2g} \right] = 0.1(1.77) = 0.177$$

The water surface elevation at the upstream cross-section is then

$$w_1 = 5710.5 + 1.77 + 2.79 + 0.177 = 5715.2 \text{ ft}$$

5.4.2 Energy Correction Factor

In section 3.7, the formula for the kinetic energy correction factor is derived as

$$\alpha = \frac{1}{AV^3} \int_A v^3 dA \quad (3.7.4)$$

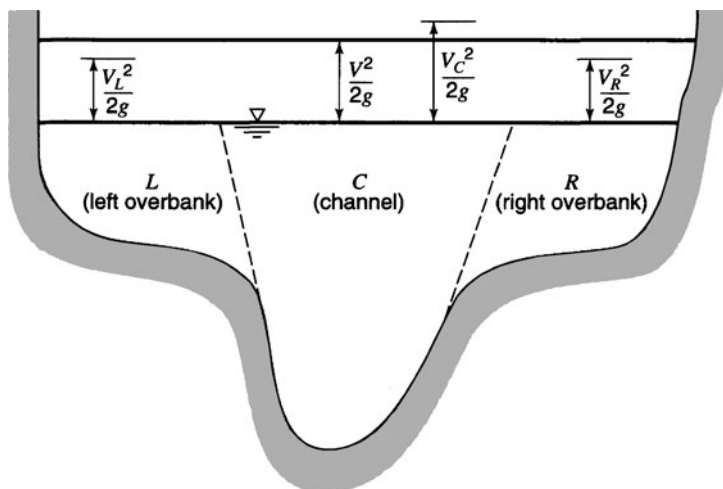


Figure 5.4.1 Compound channel section.

which can be approximated as

$$\alpha = \frac{\sum v^3 \Delta A}{V^3 A} \tag{5.4.13}$$

where V is the mean velocity.

Consider a compound channel section as shown in Figure 5.4.1 that has three flow sections. The objective is to derive an expression for the energy coefficient in terms of the conveyance for a compound channel, so that the velocity head for the entire channel is $\alpha(V^2/2g)$ where V is the mean velocity in the compound channel. Equation (5.4.13) can be expressed as

$$\alpha \approx \frac{\sum_{i=1}^N V_i^3 A_i}{V^3 \sum_{i=1}^N A_i} \tag{5.4.14}$$

where N is the number of sections (subareas) of the channel (e.g., in Figure 5.4.1, $N = 3$), V is the mean velocity in each section (subarea), and A_i is the cross-sectional area of flow in each section (subarea).

The mean velocity can be expressed as

$$V = \frac{\sum_{i=1}^N V_i A_i}{\sum_{i=1}^N A_i} \tag{5.4.15}$$

Substituting $V_i = Q_i/A_i$ and equation (5.4.15) for V into (5.4.14) and simplifying yields

$$\alpha = \frac{\sum_{i=1}^N \left(\frac{Q_i}{A_i}\right)^3 A_i}{\left[\frac{\sum_{i=1}^N \left(\frac{Q_i}{A_i}\right) A_i}{\sum_{i=1}^N A_i}\right]^3} = \frac{\sum_{i=1}^N \left(\frac{Q_i^3}{A_i^2}\right) \left(\sum_{i=1}^N A_i\right)^2}{\left(\sum_{i=1}^N Q_i\right)^3} \tag{5.4.16}$$

Now using equation (5.4.5) for each section, we get

$$Q_i = K_i S_{f_i}^{1/2} \quad (5.4.17)$$

and solving for $S_{f_i}^{1/2}$ yields

$$S_{f_i}^{1/2} = \frac{Q_i}{K_i} \quad (5.4.18)$$

Assuming that the friction slope is the same for all sections, $S_{f_i} = S_f (i = 1, \dots, N)$, then according to equation (5.4.18)

$$\frac{Q_1}{K_1} = \frac{Q_2}{K_2} = \frac{Q_3}{K_3} = \dots = \frac{Q_N}{K_N} \quad (5.4.19)$$

This leads to

$$Q_1 = K_1 \frac{Q_N}{K_N} \quad Q_2 = K_2 \frac{Q_N}{K_N} \quad \dots \quad Q_N = K_N \frac{Q_N}{K_N} \quad (5.4.20)$$

and the total discharge is

$$Q = \sum Q_i = \frac{Q_N}{K_N} \sum K_i \quad (5.4.21)$$

Substituting the above expression for $\sum Q_i$ and

$$Q_i = K_i \frac{Q_N}{K_N} \quad (5.4.22)$$

into equation (5.4.16) and simplifying, we get

$$\alpha = \frac{\sum_{i=1}^N \left(\frac{K_i^3}{A_i^2} \right) \left(\sum_{i=1}^N A_i \right)^2}{\left(\sum_{i=1}^N K_i \right)^3} \quad (5.4.23)$$

or

$$\alpha = \frac{\sum_{i=1}^N \left(\frac{K_i^3}{A_i^2} \right) (A_i)^2}{(K_i)^3} \quad (5.4.24)$$

where A_i and K_i are the totals.

The friction slope for the reach is

$$S_{f_i} = \left(\frac{\sum Q_i}{\sum K_i} \right)^2 = \frac{Q^2}{(\sum K_i)^2} \quad (5.4.25)$$

by eliminating Q_N/K_N from equations (5.4.19) through (5.4.21).

EXAMPLE 5.4.3

For the compound cross-section at river mile 1.0 shown in Figure 5.4.2, determine the energy correction factor α . The discharge is $Q = 11,000$ cfs and the water surface elevation is 125 ft.

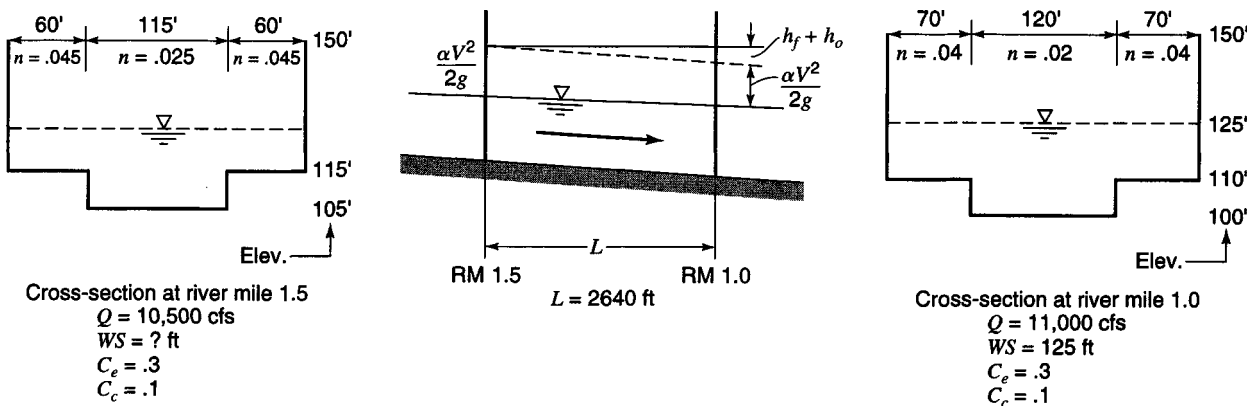


Figure 5.4.2 Cross-section and reach length data for example 5.4.3 (from Hoggan (1997)).

SOLUTION

Step 1 Compute the cross-sectional areas of flow for the left overbank (L), channel (C), and right overbank (R):

$$A_L = 1050 \text{ ft}^2, A_C = 3000 \text{ ft}^2, A_R = 1050 \text{ ft}^2$$

Step 2 Compute the hydraulic radius for L, C, and R:

$$R_L = 1050/85 = 12.35 \text{ ft}; R_C = 3000/140 = 21.40 \text{ ft}; R_R = 1050/85 = 12.35 \text{ ft}$$

Step 3 Compute the conveyance factor for L, C, and R:

$$K_L = \frac{1.486A_LR_L^{2/3}}{n} = \frac{1.486(1050)(12.35)^{2/3}}{0.04} = 208,700$$

$$K_C = \frac{1.486(3000)(21.4)^{2/3}}{0.02} = 1,716,300$$

$$K_R = 208,700 (K_R = K_L)$$

Step 4 Compute totals A_t and K_t :

$$K_t = K_L + K_C + K_R = 2,133,700$$

$$A_t = A_L + A_C + A_R = 5100 \text{ ft}^2$$

Step 5 Compute K^3/A^2 and $\sum K^3/A^2$:

$$K_L^3/A_L^2 = 8.25 \times 10^9$$

$$K_C^3/A_C^2 = 561.8 \times 10^9$$

$$K_R^3/A_R^2 = 8.25 \times 10^9$$

$$\sum K^3/A^2 = 578.3 \times 10^9$$

Step 6 Use equation (5.4.24) to compute α :

$$\alpha = \frac{\sum_{i=1}^N \left(\frac{K_i^3}{A_i^2}\right) (A_t)^2}{(K_t)^3} = \frac{(578.3 \times 10^9)(5100)^2}{(2,133,700)^3} = 1.55$$

EXAMPLE 5.4.4

For the data in Figure 5.4.2, start with the known water surface elevation at river mile 1.0 and determine the water surface at river mile 1.5 (adapted from Hoggan, 1997).

SOLUTION

Computations are presented in Table 5.4.1.

Table 5.4.1 Standard Step Backwater Computation

(1)	(2)	(3)	(4)	(5)	(6)	(7)	(8)	(9)	(10)	(11)	(12)	(13)	(14)	(15)	(16)
River mile	Water surface elevation W_k	Area A (ft ²)	Hydraulic radius R (ft)	Manning roughness n	Conveyance K	Average conveyance \bar{K}	Average friction slope \bar{S}_f	Friction loss h_L (ft)	K^3/A^2 (10 ⁹)	Energy correction factor α	Velocity V (ft/sec)	$\alpha \frac{V^2}{2g}$ (ft/sec)	$\Delta \left(\frac{V^2}{2g} \right)$ (ft/sec)	h_o^{**} (ft)	W_k^{***} (ft)
1.0	125.0	1050	12.35	0.040	208,700				8.25						
		3000	21.43	0.020	1,716,300				561.80						
		<u>1050</u>	12.35	0.040	<u>208,700</u>				<u>8.25</u>						
		5100			2,133,700				578.30	1.55	2.16	0.11			
1.5	126.1	666.0	9.37	0.045	97,650				2.10						
		2426.5	17.97	0.025	989,400				164.50						
		<u>666.0</u>	9.37	0.045	<u>97,650</u>				<u>2.10</u>						
		3758.5			1,184,700	1,659,200	0.000042	0.111	168.70	1.43	2.79	0.17	-0.06	0.02	125.07
1.5	125.0	600	8.57	0.045	83,000				1.59						
		2300	17.04	0.025	905,300				140.22						
		<u>600</u>	8.57	0.045	<u>83,000</u>				<u>1.59</u>						
		3500			1,071,300	1,602,350	0.000043	0.113	143.30	1.43	3.00	0.20	-0.09	0.03	125.05

$$\alpha = \frac{(A_i)^2 \sum K_i^3 / A_i^2}{(K_i)^3}$$

** $h_o = C_e |\Delta(\alpha V^2/2g)|$ for $\Delta(\alpha V^2/2g) < 0$ (loss due to channel expansion); $h_o = C_c |\Delta(\alpha V^2/2g)|$ for $\Delta(\alpha V^2/2g) > 0$ (loss due to channel contraction).

*** $W_2 = W_1 + \Delta(\alpha V^2/2g) + h_L + h_o = 125.0 + (-0.06) + 0.111 + 0.02 = 125.066 \approx 125.07$.

Source: Hoggan (1997).

5.4.3 Application for Water Surface Profile

The change in head with respect to distance x along the channel has been expressed in equation (5.4.2) as

$$\frac{dH}{dx} = \frac{dw}{dx} + \frac{d}{dx} \left(\alpha \frac{V^2}{2g} \right) \tag{5.4.2}$$

The total energy loss term is $dH/dx = -S_f - S_e$, where S_f is the friction slope defined by equation (5.4.7) or equation (5.4.8) and S_e is the slope of the contraction or expansion loss. The differentials dw and $d[\alpha(V^2/2g)]$ are defined over the channel reach as $dw = w_k - w_{k+1}$ and $d[\alpha(V^2/2g)] = \alpha_{k+1} \frac{V_{k+1}^2}{2g} - \alpha_k \frac{V_k^2}{2g}$, where we define $k + 1$ at the downstream and k at the upstream. River cross-sections are normally defined from downstream to upstream for gradually varied flow. Equation (5.4.2) is now expressed as

$$w_k + \alpha_k \frac{V_k^2}{2g} = w_{k+1} + \alpha_{k+1} \frac{V_{k+1}^2}{2g} + S_f dx + S_e dx \tag{5.4.26}$$

The *standard step procedure* for water surface computations is described in the following steps:

- a. Start at a point in the channel where the water surface is known or can be approximated. This is the *downstream boundary condition* for subcritical flow and the *upstream boundary condition*

for supercritical flow. Computation proceeds upstream for subcritical flow and downstream for supercritical flow. Why?

- b. Choose a water surface elevation w_k at the upstream end of the reach for subcritical flow or w_{k+1} at the downstream end of the reach for supercritical flow. This water surface elevation will be slightly lower or higher depending upon the type of profile (see Chow (1959); Henderson (1966); French (1985); or Chaudhry (1993)).
- c. Next compute the conveyance, corresponding friction slope, and expansion and contraction loss terms in equation (5.4.26) using the assumed water surface elevation.
- d. Solve equation (5.4.26) for w_{k+1} (supercritical flow) or w_k (subcritical flow).
- e. Compare the calculated water surface elevation w with the assumed water surface elevation w' . If the calculated and assumed elevations do not agree within an acceptable tolerance (e.g., 0.01 ft), then set $w'_{k+1} = w_{k+1}$ (for supercritical flow) and $w'_k = w_k$ (for subcritical flow) and return to step (c).

Computer models for determining water surface profiles using the standard step procedure include the HEC-2 model and the newer HEC-RAS model. HEC-RAS River Analysis System (developed by the U.S. Army Corps of Engineers (USACE) Hydrologic Engineering Center) computes water surface profiles for one-dimensional steady, gradually varied flow in rivers of any cross-section (HEC, 1997a–c). HEC-RAS can simulate flow through a single channel, a dendritic system of channels, or a full network of open channels (sometimes called a fully looped system).

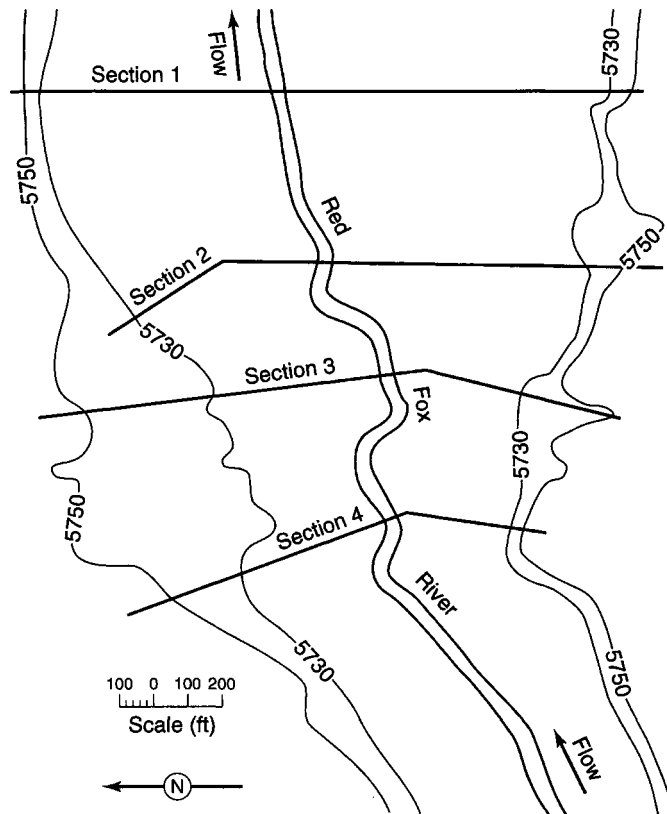


Figure 5.4.3 Map of the Red Fox River indicating cross-sections for water surface profile analysis (from U.S. Bureau of Reclamation (1957)).

HEC-RAS can model sub- or supercritical flow, or a mixture of each within the same analysis. A graphical user interface provides input data entry, data modifications, and plots of stream cross-sections, profiles, and other data. Program options include inserting trapezoidal excavations on cross-sections, and analyzing the potential for bridge scour. The water surface profile through structures such as bridges, culverts, weirs, and gates can be computed. The World Wide Web address to obtain the HEC-RAS model is www.hec.usace.army.mil.

EXAMPLE 5.4.5

A plan view of the Red Fox River in California is shown in Figure 5.4.3, along with the location of four cross-sections. Perform the standard step calculations to determine the water surface elevation at cross-section 3 for a discharge of $6500 \text{ ft}^3/\text{s}$. Figures 5.4.4*a*, *b*, and *c* are plots of cross-sections at 1, 2, and 3, respectively. Figures 5.4.5*a*, *b*, and *c* are the area and hydraulic radius curves for cross-sections 1, 2, and 3, respectively. Use expansion and contraction coefficients of 0.3 and 0.1, respectively. Manning's roughness factors are presented in Figure 5.4.4. The downstream starting water surface elevation at cross-section 1 is 5710.5 ft above mean sea level. This example was originally adapted by the U.S. Army Corps of Engineers from material developed by the U.S. Bureau of Reclamation (1957). Distance between cross-sections 1 and 2 is 500 ft, between cross-sections 2 and 3 is 400 ft, and between cross-sections 3 and 4 is 400 ft.

SOLUTION

The computations for this example are illustrated in Table 5.4.2.

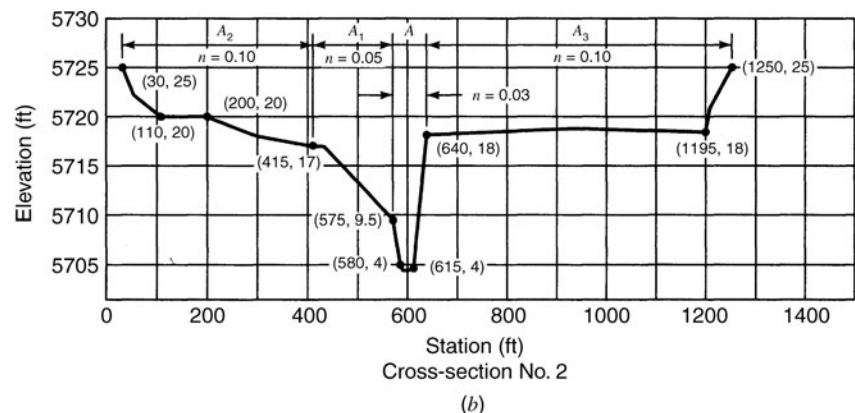
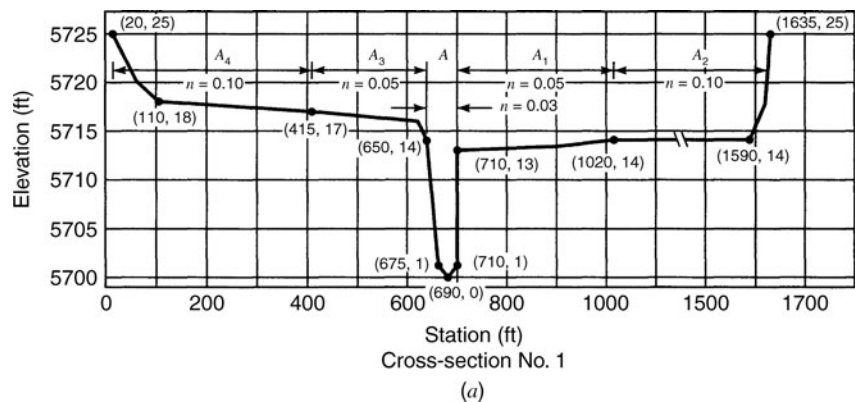


Figure 5.4.4 Cross-sections of the Red Fox River (from U.S. Bureau of Reclamation (1957)).

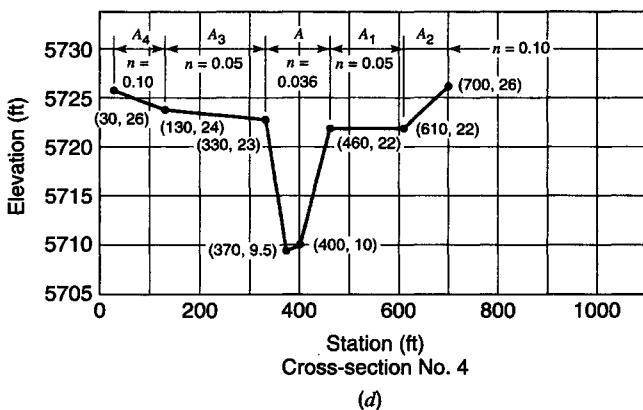
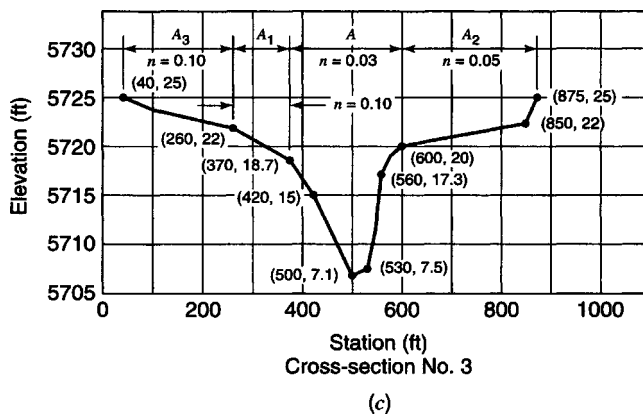


Figure 5.4.4 (Continued)

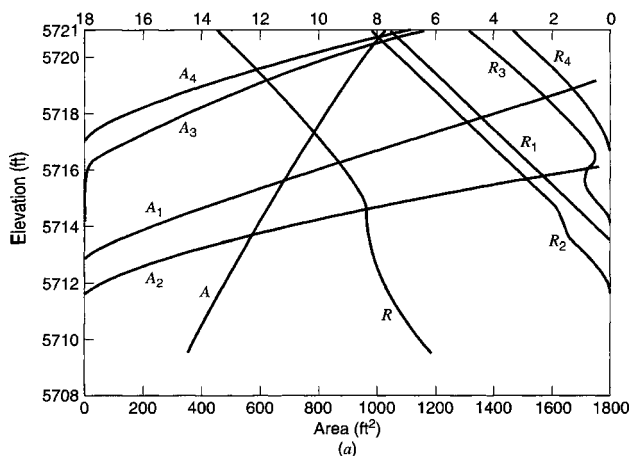


Figure 5.4.5 Area elevation and hydraulic radius—elevation curves for cross-sections 1 to 4. (a) Cross-section 1; (b) Cross-section 2; (c) Cross-section 3; (d) Cross-section 4 (from U.S. Bureau of Reclamation (1957)).

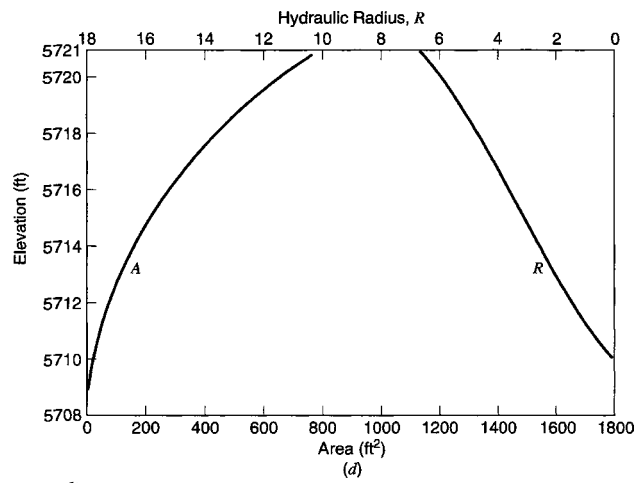
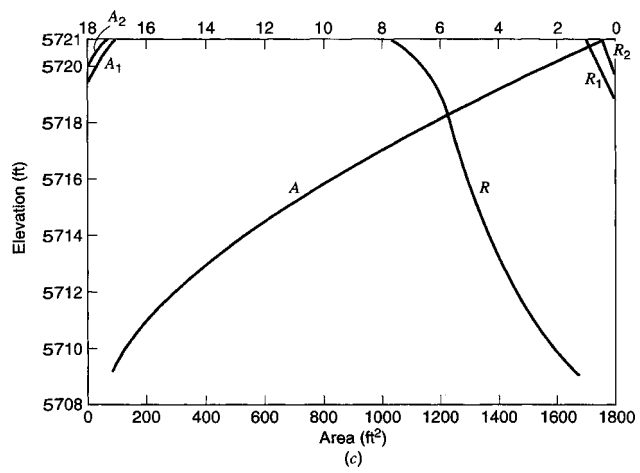
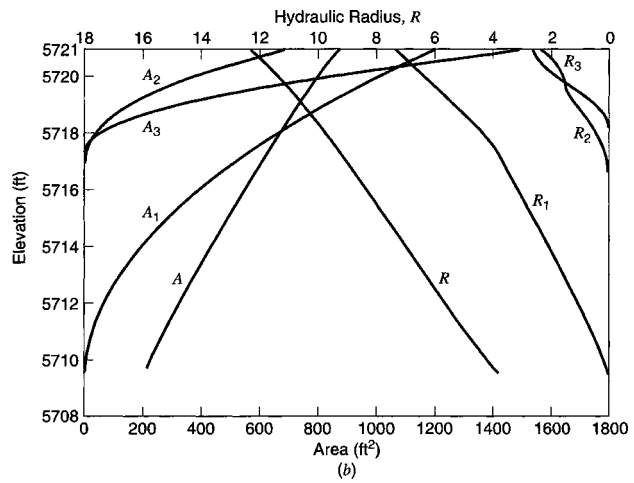


Figure 5.4.5 (Continued)

Table 5.4.2 Standard Step Backwater Computation for Red Fox River

(1)	(2)	(3)	(4)	(5)	(6)	(7)	(8)	(9)	(10)	(11)	(12)	(13)	(14)	(15)	(16)
Cross-section	Water surface elevation	Area	Hydraulic radius	Manning roughness	Conveyance	Average conveyance	Average friction slope	Friction loss	$\frac{K^3}{A^2}$	Energy correction factor	Velocity	$\alpha \frac{V^2}{2g}$	$\Delta\left(\alpha \frac{V^2}{2g}\right)$	h_o	W_k
	W_{k+1}	A (ft ²)	R (ft)	n	K	\bar{K}	$S_f(10^{-3})$ (ft/ft)	h_L (ft)	(10^6)	α	V (ft/sec)	(ft)	(ft)	(ft)	(ft)
1	5710.5*	420	7.0	0.03	76,100					1.0	15.5	3.72			
2	5714.7	470	7.6	0.03	90,100				3311.1						
		260	2.5	0.05	14,200				42.0						
		730			104,300	90,200	5.19	2.60	3353.5	1.58	8.90	1.95	+1.77	0.18	5715.07**
	5715.0														
		500	7.85	0.03	97,800				3741.8						
		300	2.7	0.05	17,300				57.5						
		800			115,100	95,600	4.62	2.31	3799.3	1.59	8.13	1.63	+2.09	0.21	5715.1
3	5718.0	1145	5.85	0.03	184,100	149,600	1.89	0.76		1.0	5.68	0.50	+1.13	0.11	5717.1
	5717.1	970	5.6	0.03	151,500	133,300	2.38	0.95		1.0	6.70	0.70	+ .93	0.09	5717.1

*Known starting water surface elevation.

** $W_{k+1} = 5710.7 + 1.77 + 2.60 + 0.18 = 5715.07 = 5715.1$; $\alpha = (A_i)^2 \sum K^3/A_i^2 / (K_i)^3$; $h_o = C_c |(\alpha V^2/2g)|$ for $\Delta(\alpha V^2/2g) < 0$ (loss due to channel expansion); $h_o = C_c |\Delta(\alpha V^2/2g)|$ for $\Delta(\alpha V^2/2g) > 0$ (loss due to channel contraction); $W_{k+1} = W_k + \Delta(\alpha V^2/2g) + h_L + h_o$.

Source: Hoggan (1997).

5.5 RAPIDLY VARIED FLOW

Rapidly varied flow occurs when a water flow depth changes abruptly over a very short distance. The following are characteristic features of rapidly varied flow (Chow, 1959):

- Curvature of the flow is pronounced, so that pressure distribution cannot be assumed to be hydrostatic.
- The rapid variation occurs over a relatively short distance so that boundary friction is comparatively small and usually insignificant.
- Rapid changes of water area occur in rapidly varied flow, causing the velocity distribution coefficients α and β to be much greater than 1.0.

Examples of rapidly varied flow are hydraulic jumps, transitions in channels, flow over spillways, flow in channels of nonlinear alignment, and flow through nonprismatic channel sections such as flow in channel junctions, flow through trash racks, and flow between bridge piers.

The discussion presented in this chapter is limited to the hydraulic jump. The *hydraulic jump* occurs when a rapid change in flow depth occurs from a small depth to a large depth such that there is an abrupt rise in water surface. A hydraulic jump occurs wherever supercritical flow changes to subcritical flow. Hydraulic jumps can occur in canals downstream of regulating sluices, at the foot of spillways, or where a steep channel slope suddenly becomes flat.

Figure 5.5.1 illustrates a hydraulic jump along with the specific energy and specific force curves. The depths of flow upstream and downstream of the jump are called *sequent depths* or *conjugate depths*. Because hydraulic jumps are typically short in length, the losses due to shear along the wetted perimeter are small compared to the pressure forces. Neglecting these forces and assuming a horizontal channel ($F_g = 0$), the momentum principle can be applied as in section 5.2.3 to derive

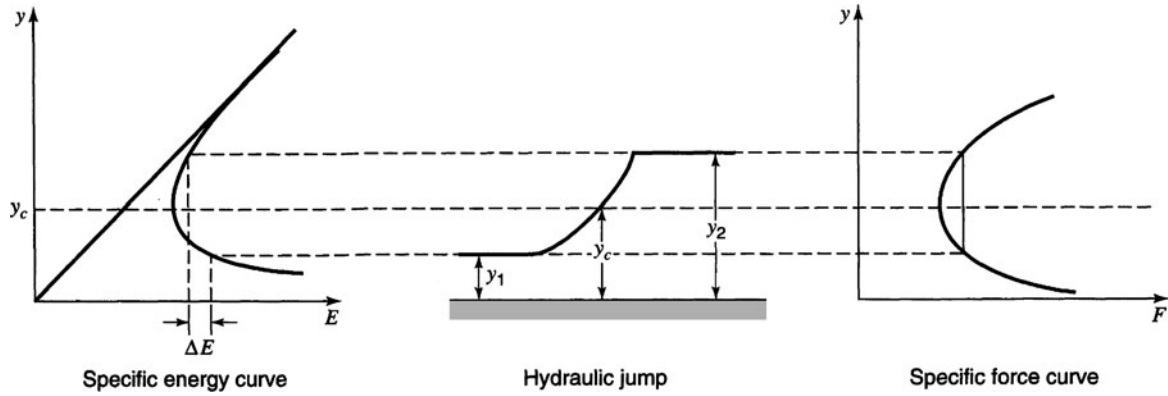


Figure 5.5.1 Hydraulic jump.

equation (5.2.24):

$$\frac{Q^2}{gA_1} + A_1\bar{y}_1 = \frac{Q^2}{gA_2} + A_2\bar{y}_2 \quad (5.2.24)$$

Consider a rectangular channel of width $B > 0$, so $Q = A_1V_1 = A_2V_2$, $A_1 = By_1$, $A_2 = By_2$, $\bar{y}_1 = y_1/2$, and $\bar{y}_2 = y_2/2$:

$$\frac{Q^2}{gBy_1} + By_1\left(\frac{y_1}{2}\right) = \frac{Q^2}{gBy_2} + By_2\left(\frac{y_2}{2}\right) \quad (5.5.1)$$

Simplifying yields

$$\frac{Q^2}{g} \left(\frac{1}{y_1} - \frac{1}{y_2} \right) = \frac{1}{2} B^2 (y_2^2 - y_1^2)$$

$$\frac{Q^2}{g} (y_2 - y_1) = \frac{1}{2} B^2 y_1 y_2 (y_2^2 - y_1^2)$$

$$\frac{B^2 y_1^2 V_1^2}{g} (y_2 - y_1) = \frac{1}{2} B^2 y_1 y_2 (y_2 + y_1)(y_2 - y_1)$$

$$\frac{y_1 V_1^2}{g} = \frac{1}{2} y_2 (y_2 + y_1)$$

Dividing by y_1^2 , we get

$$\frac{2V_1^2}{gy_1} = \frac{y_2}{y_1} \left(\frac{y_2}{y_1} + 1 \right) \quad (5.5.2)$$

The Froude number for a rectangular channel is $F_{r1} = V_1/\sqrt{gD_1} = V_1/\sqrt{gy_1}$; therefore equation (5.5.2) reduces to

$$\left(\frac{y_2}{y_1} \right)^2 + \frac{y_2}{y_1} - 2F_{r1}^2 = 0 \quad (5.5.3)$$

or

$$\frac{y_2}{y_1} = \frac{1}{2} \left(-1 + \sqrt{1 + 8F_{r1}^2} \right) \quad (5.5.4)$$

using the quadratic formula and discarding the negative roots.

Alternatively, $Q = By_2V_2$ and $F_{r_2} = V_2/\sqrt{gy_2}$ could have been used to derive

$$\frac{y_1}{y_2} = \frac{1}{2} \left(-1 + \sqrt{1 + 8F_{r_2}^2} \right) \quad (5.5.5)$$

Equations (5.5.4) and (5.5.5) can be used to find the sequent depths of a hydraulic jump. The use of hydraulic jumps as energy dissipaters is further discussed in Chapters 15 and 17.

EXAMPLE 5.5.1

Consider the 8-ft wide rectangular channel used in examples 5.1.1, 5.1.3, and 5.3.1 with a discharge of 100 cfs. If a weir were placed in the channel and the depth upstream of the weir were 5 ft, would a hydraulic jump form upstream of the weir?

SOLUTION

For the discharge of 100 cfs, the normal depth is $y_n = 3.97$ ft from example 5.1.3, and the critical depth is $y_c = 1.69$. Because $y_c < y_n < 5$ ft, a hydraulic jump would not form. As a result of $y_n > y_c$, a mild slope exists. For a jump to form, $y_n < y_c$, which is a steep slope.

EXAMPLE 5.5.2

For example 5.3.1, determine whether a hydraulic jump will occur.

SOLUTION

The normal depth and critical depth must be computed and compared. Using equation (5.2.14) with $q = 4.646$ m³/s per meter of width, we get

$$y_c = \left(\frac{q^2}{g} \right)^{1/3} = \left(\frac{4.646^2}{9.81} \right)^{1/3} = 1.30 \text{ m.}$$

The depths of flow at $y_a = 0.457$ m and at $y_b = 0.5$ m, so this flow is supercritical flow.

Next, the normal depth is computed using Manning's equation (5.1.23):

$$Q = \frac{1}{n} AR^{2/3} S_0^{1/2}$$

or

$$q = \frac{1}{n} (y_n)(y_n)^{2/3} S_0^{1/2} = \frac{1}{n} y_n^{5/3} S_0^{1/2}$$

$$4.646 = \frac{1}{0.020} y_n^{5/3} (0.0003)^{1/2}$$

Thus $y_n = (5.365)^{3/5} = 2.74$ m. Under these conditions $y_n > y_c > 0.5$ m, an M3 water surface profile exists and a hydraulic jump occurs. If normal depth occurs downstream of the jump, what is the depth before the jump? Using equation (5.5.5) with $y_2 = 2.74$ m, we find that y_1 is 0.5 m.

EXAMPLE 5.5.3

A rectangular channel is 10.0 ft wide and carries a flow of 400 cfs at a normal depth of 3.00. Manning's $n = 0.017$. An obstruction causes the depth just upstream of the obstruction to be 8.00 ft deep. Will a jump form upstream from the obstruction? If so, how far upstream? What type of curve will be present?

SOLUTION

First a determination must be made whether a jump will form by comparing the normal depth and critical depth. Using equation (5.2.14), we find

$$y_c = \left(\frac{q^2}{g} \right)^{1/3} = \left(\frac{40^2}{32.2} \right)^{1/3} = 3.68 \text{ ft}$$

and $y_c > y_n = 3.0$ ft, therefore the channel is steep. Because $y_n < y_c < 8$ ft, a subcritical flow exists on a steep channel, a hydraulic jump forms upstream of the obstruction. If the depth before the jump is considered to be normal depth, $y_n = y_1 = 3$, then the conjugate depth y_2 can be computed using equation (5.5.4), where the Froude number is

$$F_{r1}^2 = \left(\frac{V_1}{\sqrt{gy_1}} \right)^2 = \frac{V_1^2}{gy_1} = \frac{q^2}{gy_1^3}$$

so

$$\begin{aligned} y_2 &= \frac{y_1}{2} \left(-1 + \sqrt{1 + \frac{8q^2}{gy_1^3}} \right) \\ &= \frac{3}{2} \left(-1 + \sqrt{1 + \frac{8(40)^2}{g(3)^3}} \right) \\ &= 4.45 \text{ ft} \end{aligned}$$

Next the distance Δx from the depth of 4.45 ft to the depth of 8 ft is determined using equation (5.3.1):

$$S_0 \Delta x + \frac{V_2^2}{2g} = \Delta y + \frac{V_3^2}{2g} + S_f \Delta x$$

which can be rearranged to yield

$$\begin{aligned} (S_0 - S_f) \Delta x &= y_3 + \frac{V_3^2}{2g} - y_2 - \frac{V_2^2}{2g} \\ &= E_3 - E_2 \end{aligned}$$

so

$$\Delta x = \frac{E_3 - E_2}{S_0 - S_f} = \frac{\Delta E}{S_0 - S_f}$$

To solve for Δx , first compute E_2 and E_3 :

Depth (ft)	A (ft ²)	R (ft)	V (ft/s)	$V^2/2g$ (ft)	E (ft)	R_{ave} (ft)	V_{ave} (ft/s)
8	80	3.08	5.00	0.388	8.388		
4.45	44.5	2.35	8.99	1.25	5.70	2.72	7.00

Now compute S_f from Manning's equation using equation (5.1.24) with V_{ave} and R_{ave} , and rearrange to yield

$$S_f = \frac{n^2 V_{\text{ave}}^2}{2.22 R_{\text{ave}}^{4/3}} = \frac{0.017^2 \times 7^2}{2.22 \times 2.72^{4/3}} = 0.00168$$

Compute S_0 using Manning's equation with the normal depth:

$$Q = \frac{1.49}{n} AR^{2/3} S_0^{1/2}$$

$$400 = \frac{1.49}{0.017} \times 3 \times 10 \times \left(\frac{30}{16} \right)^{2/3} \sqrt{S_0}$$

Thus, $S_0 = 0.0100$. Now, using $\Delta x = \frac{\Delta E}{S_0 - S_f} = \frac{8.388 - 5.71}{0.0100 - 0.00168} = 322$ ft, the distance from the conjugate depth of the jump $y_2 = 4.45$ ft downstream to the depth y_3 of 8 ft (location of the obstruction) is 322 ft. In other words, the hydraulic jump occurs approximately 322 ft upstream of the obstruction. The type of water surface profile after the jump is an S1 profile.

EXAMPLE 5.5.4

A hydraulic jump occurs in a rectangular channel 3.0 m wide. The water depth before the jump is 0.6 m, and after the jump is 1.6 m. Compute (a) the flow rate in the channel, (b) the critical depth, and (c) the head loss in the jump.

SOLUTION

(a) To compute the flow rate knowing $y_1 = 0.6$ m and $y_2 = 1.6$ m, equation (5.5.4) can be used:

$$y_2 = \frac{y_1}{2} \left[-1 + \sqrt{1 + \frac{8q^2}{gy_1^3}} \right]$$

in which $F_{r1} = q / \sqrt{gy_1^3}$ has been substituted:

$$1.6 = \frac{0.6}{2} \left[-1 + \sqrt{1 + \frac{8q^2}{9.81(0.6)^3}} \right]$$

$$6.33 = \sqrt{1 + 3.775q^2}$$

$$40.07 = 3.775q^2$$

$$q = 3.26 \text{ m}^3/\text{s per meter width of channel}$$

and

$$Q = 3q = 9.78 \text{ m}^3/\text{s}.$$

(b) Critical depth is computed using equation (5.2.14):

$$y_c = \left(\frac{q^2}{g} \right)^{1/3} = \left(\frac{3.26^2}{9.81} \right)^{1/3} = 1.03 \text{ m}$$

(c) The headloss in the jump is the change in specific energy before and after the jump

$$h_L = \Delta E = E_1 - E_2$$

so

$$h_L = y_1 + \frac{V_1^2}{2g} - y_2 - \frac{V_2^2}{2g}$$

so

$$V_1 = Q/A_1 = 9.78/(3 \times 0.6) = 5.43 \text{ m/s}$$

$$V_2 = Q/A_2 = 9.78/(3 \times 1.6) = 2.04 \text{ m/s}$$

$$h_L = 0.6 + \frac{5.43^2}{2(9.81)} - 1.6 - \frac{2.04^2}{2(9.81)}$$

$$= 0.6 + 1.5 - 1.6 - 0.21$$

$$h_L = 0.29 \text{ m}.$$

EXAMPLE 5.5.5

Derive an equation to approximate the headloss (energy loss) of a hydraulic jump in a horizontal rectangular channel in terms of the depths before and after the jump, y_1 and y_2 , respectively.

SOLUTION

The energy loss can be approximated by

$$\begin{aligned} h_L &= E_1 - E_2 \\ &= \left(y_1 + \frac{V_1^2}{2g} \right) - \left(y_2 + \frac{V_2^2}{2g} \right) \end{aligned}$$

The velocities can be expressed as $V_1 = Q/A_1 = q/y_1$ and $V_2 = q/y_2$, so

$$\begin{aligned} h_L &= y_1 + \frac{1}{2g} \frac{q^2}{y_1^2} - y_2 - \frac{1}{2g} \frac{q^2}{y_2^2} \\ &= \frac{q^2}{2g} \left(\frac{1}{y_1^2} - \frac{1}{y_2^2} \right) + (y_1 - y_2) \end{aligned}$$

The balance between hydrostatic forces and the momentum flux per unit width of the channel can be expressed using equation (5.2.23):

$$\sum F = F_1 - F_2 = \rho q(V_2 - V_1) = \gamma A_1 \bar{y}_1 - \gamma A_2 \bar{y}_2 = \rho q V_2 - \rho q V_1$$

where $A = (1)(y_1)$ and $\bar{y}_1 = y_1/2$, so

$$\frac{\gamma}{2} y_1^2 - \frac{\gamma}{2} y_2^2 = \rho q \left(\frac{q}{y_2} - \frac{q}{y_1} \right)$$

Solving, we get

$$\frac{q^2}{g} = y_1 y_2 \left(\frac{y_1 + y_2}{2} \right)$$

Substituting this equation into the above equation for the headloss and simplifying gives

$$\Delta E = \frac{(y_2 - y_1)^3}{4y_1 y_2}$$

Prismatic Channels with Change in Slope

Consider the channel that changes slope from a steep slope to a mild slope shown in Figure 5.5.2. In this case $y_{n2} > y_{n1}$. The conjugate depth of y_{n1} is y' computed using equation (5.5.4). If $y' < y_{n2}$, the hydraulic jump occurs upstream of the slope break with control at A, and if $y' > y_{n2}$, the jump occurs downstream of the break in slope with control at B. If $(E_{n1} - \Delta E_{j1}) > E_{n2}$, then a hydraulic jump occurs on the downstream mild slope. If $E_{n2} > (E_{n1} - \Delta E_{j1})$, then the hydraulic jump occurs on the upstream steep slope. ΔE_{j1} is the energy loss in the jump in reach 1. Another way to look at this is if $E_{y'} > E_{n2}$ control is at B because the energy loss ΔE_{j1} in the hydraulic jump in reach 1 is not large enough to decrease the energy from E_{n1} to E_{n2} .

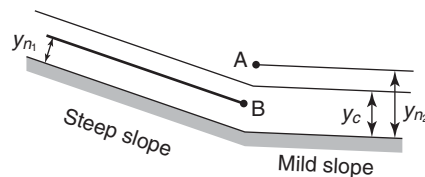


Figure 5.5.2 Rapidly varied flow caused by slope change from steep to mild.

5.6 DISCHARGE MEASUREMENT

5.6.1 Weir

A *weir* is a device (or overflow structure) that is placed normal to the direction of flow. The weir essentially backs up water so that in flowing over the weir, the water goes through critical depth. Weirs have been used for the measurement of water flow in open channels for many years. Weirs can generally be classified as *sharp-crested weirs* and *broad-crested weirs*. Weirs are discussed in detail in Bos et al. (1984), Brater et al. (1996), and Replogle et al. (1999).

A *sharp-crested weir* is basically a thin plate mounted perpendicular to the flow with the top of the plate having a beveled, sharp edge, which makes the nappe spring clear from the plate (see Figure 5.6.1). The rate of flow is determined by measuring the head, typically in a stilling well (see Figure 5.6.2) at a distance upstream from the crest. The head H is measured using a gauge.

Suppressed Rectangular Weir

These sharp-crested weirs are as wide as the channel, and the width of the nappe is the same length as the crest. Referring to Figure 5.6.1, consider an elemental area $dA = Bdh$ and assume the velocity is $\sqrt{2gh}$; then the elemental flow is

$$dQ = Bdh\sqrt{2gh} = B\sqrt{2g}h^{3/2}dh \tag{5.6.1}$$

The discharge is expressed by integrating equation (5.6.1) over the area above the top of the weir crest:

$$Q = \int_0^H dQ = \sqrt{2g} B \int_0^H h^{3/2} dh = \frac{2}{3} \sqrt{2g} BH^{3/2} \tag{5.6.2}$$

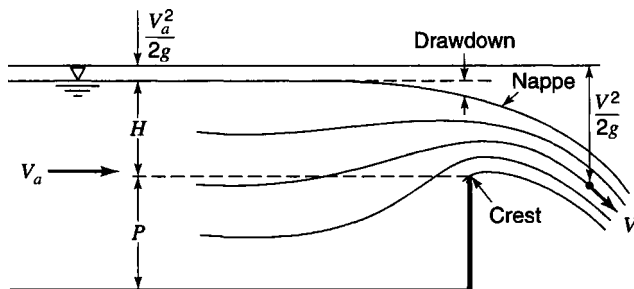


Figure 5.6.1 Flow over sharp-crested weir.

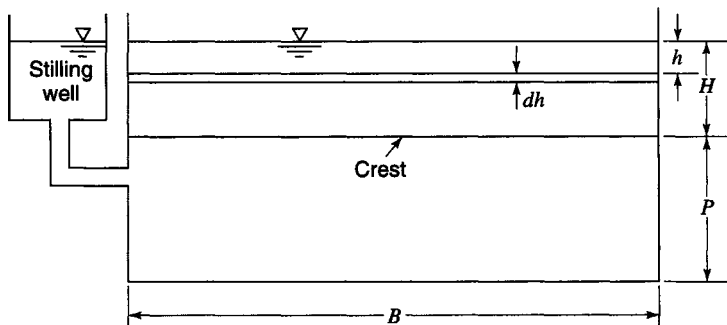


Figure 5.6.2 Rectangular sharp-crested weir without end contraction.

Friction effects have been neglected in derivation of equation (5.6.2). The drawdown effect shown in Figure 5.6.1 and the crest contraction indicate that the streamlines are not parallel or normal to the area in the plane. To account for these effects a coefficient of discharge C_d is used, so that

$$Q = C_d \frac{2}{3} \sqrt{2g} BH^{3/2} \quad (5.6.3)$$

where C_d is approximately 0.62. This is the basic equation for a suppressed rectangular weir, which can be expressed more generally as

$$Q = C_w BH^{3/2} \quad (5.6.4)$$

where C_w is the weir coefficient, $C_w = C_d \frac{2}{3} \sqrt{2g}$. For U.S. customary units, $C_w \approx 3.33$, and for SI units $C_w \approx 1.84$.

If the velocity of approach V_a where H is measured is appreciable, then the integration limits are

$$Q = \sqrt{2g} B \int_{\frac{V_a^2}{2g}}^{H + \frac{V_a^2}{2g}} h^{1/2} dh = C_w B \left[\left(H + \frac{V_a^2}{2g} \right)^{3/2} - \left(\frac{V_a^2}{2g} \right)^{3/2} \right] \quad (5.6.5a)$$

When $\left(\frac{V_a^2}{2g} \right)^{3/2} \approx 0$, equation (5.6.5a) can be simplified to

$$Q = C_w B \left(H + \frac{V_a^2}{2g} \right)^{3/2} \quad (5.6.5b)$$

Contracted Rectangular Weirs

A *contracted rectangular weir* is another sharp-crested weir with a crest that is shorter than the width of the channel and one or two beveled end sections so that water contracts both horizontally and vertically. This forces the nappe width to be less than B . The effective crest length is

$$B' = B - 0.1 nH \quad (5.6.6)$$

where $n = 1$ if the weir is placed against one side wall of the channel so that the contraction on one side is suppressed and $n = 2$ if the weir is positioned so that it is not placed against a side wall.

Triangular Weir

Triangular or V-notch weirs are sharp-crested weirs that are used for relatively small flows, but have the advantage that they can also function for reasonably large flows as well. Referring to Figure 5.6.3,

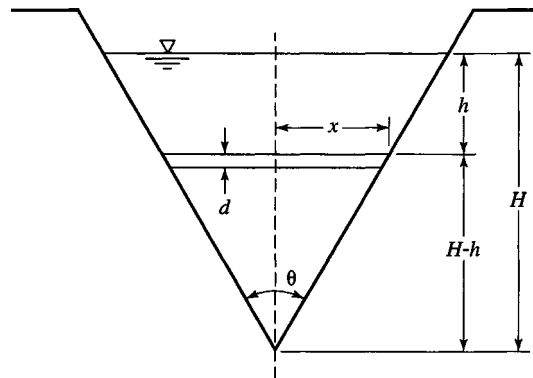


Figure 5.6.3 Triangular sharp-crested weir.

the rate of discharge through an elemental area, dA , is

$$dQ = C_d \sqrt{2gh} dA \tag{5.6.7}$$

where $dA = 2x dh$, and, $x = (H - h) \tan \frac{\theta}{2}$ so $dA = 2(H - h) \tan \left(\frac{\theta}{2}\right) dh$. Then

$$dQ = C_d \sqrt{2gh} \left[2(H - h) \tan \left(\frac{\theta}{2}\right) dh \right] \tag{5.6.8}$$

and

$$\begin{aligned} Q &= C_d 2 \sqrt{2g} \tan \left(\frac{\theta}{2}\right) \int_0^H (H - h) h^{1/2} dh \\ &= C_d \left(\frac{8}{15}\right) \sqrt{2g} \tan \left(\frac{\theta}{2}\right) H^{5/2} \\ &= C_w H^{5/2} \end{aligned} \tag{5.6.9}$$

The value of C_w for a value of $\theta = 90^\circ$ (the most common) is $C_w = 2.50$ for U.S. customary units and $C_w = 1.38$ for SI units.

Broad-Crested Weir

Broad-crested weirs (refer to Figure 5.6.4) are essentially critical-depth weirs in that if the weirs are high enough, critical depth occurs on the crest of the weir. For critical flow conditions

$y_c = (q^2/g)^{1/3}$ and $E = \frac{3}{2} y_c$ for rectangular channels:

$$Q = B \cdot q = B \sqrt{g y_c^3} = B \sqrt{g \left(\frac{2}{3} E\right)^3} = B \left(\frac{2}{3}\right)^{3/2} \sqrt{g} E^{3/2}$$

or, assuming the approach velocity is negligible:

$$\begin{aligned} Q &= B \left(\frac{2}{3}\right)^{3/2} \sqrt{g} H^{3/2} \\ Q &= C_w B H^{3/2} \end{aligned} \tag{5.6.10}$$

Figure 5.6.5 illustrates a broad-crested weir installation in a concrete-lined canal.

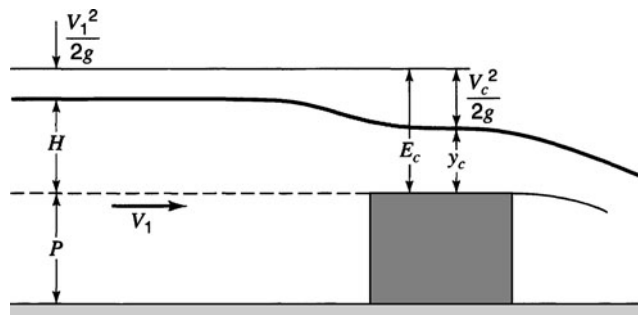


Figure 5.6.4 Broad-crested weir.

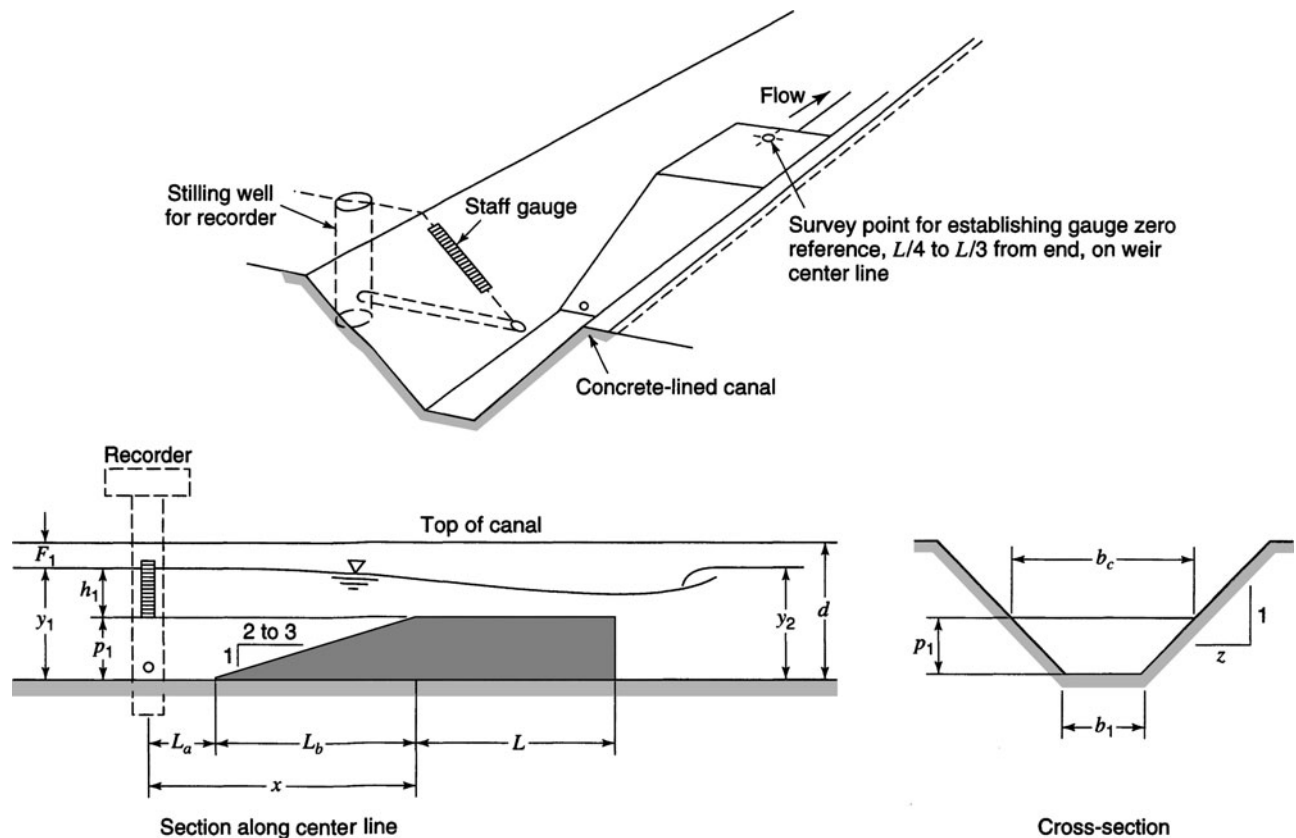


Figure 5.6.5 Broad-crested weir in concrete-lined canal (from Bos et al. (1984)).

EXAMPLE 5.6.1

A rectangular, sharp-crested suppressed weir 3 m long is 1.0 m high. Determine the discharge when the head is 150 mm.

SOLUTION

Using equation (5.6.4), $Q = 1.84 BH^{1.5}$, the discharge is

$$Q = 1.84(3) \left(\frac{150}{1000} \right)^{1.5} = 0.321 \text{ m}^3/\text{s}$$

5.6.2 Flumes

Bos et al. (1984) provide an excellent discussion of flumes. A weir is a control section that is formed by raising the channel bottom, whereas a *flume* is formed by narrowing a channel. When a control section is formed by raising both the channel bottom and narrowing it, the structure is usually called a *flume*. Figure 5.6.6 shows a distinction between weirs and flumes.

Weirs can result in relatively large headlosses and, if the water has suspended sediment, can cause deposition upstream of the weir, resulting in a gradual change of the weir coefficient. These disadvantages can be overcome in many situations by the use of flumes.

Figure 5.6.7 illustrates the general layout of a flow measuring structure. Most flow measurement and flow regulating structures consist of (a) a *converging transition*, where subcritical flow is accelerated and guided into the throat without flow separation; (b) a *throat* where the water

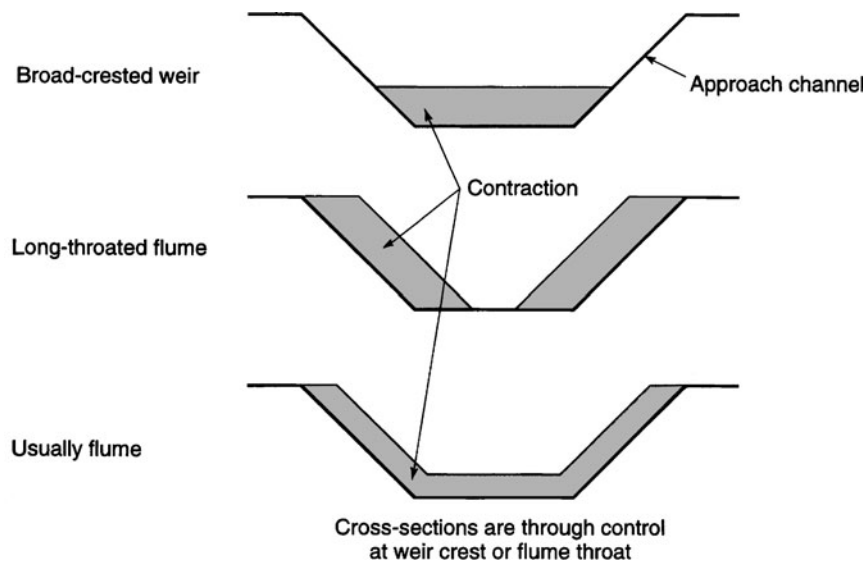


Figure 5.6.6 Distinction between a weir and a flume (from Bos et al. (1984)).

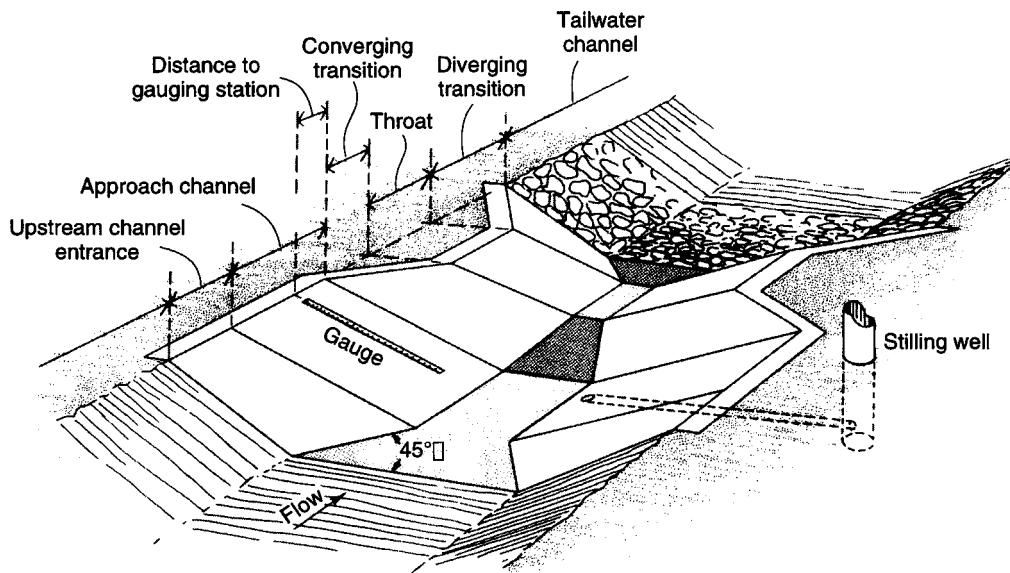
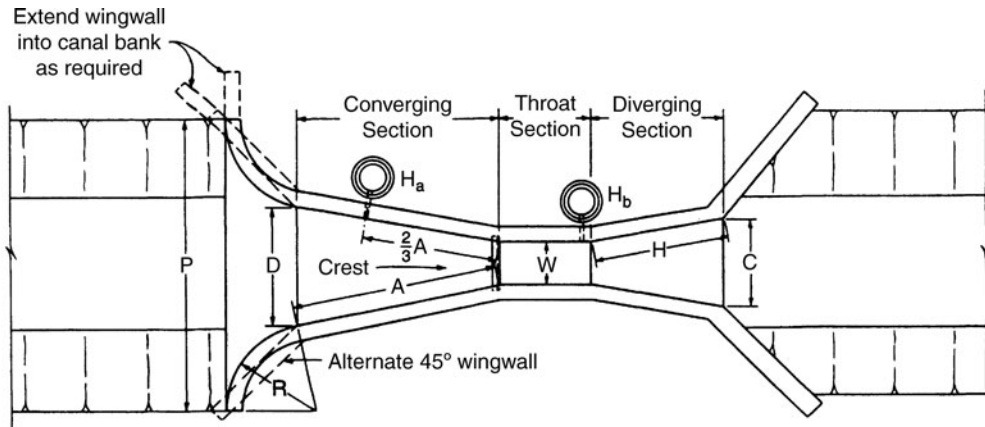


Figure 5.6.7 General layout of a flow-measuring structure (from Bos et al. (1984)).

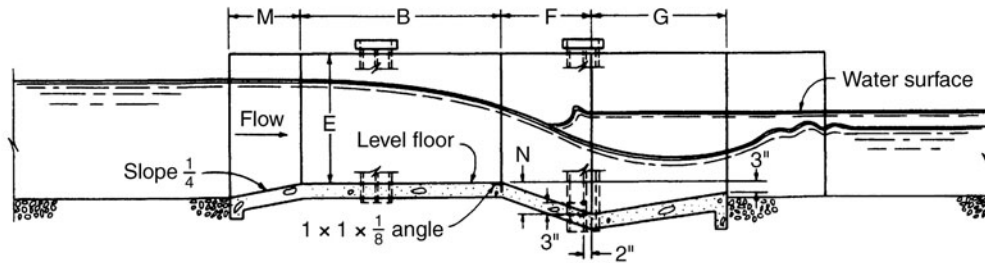
accelerates to supercritical flow so that the discharge is controlled; and (c) a *diverging transition* where flow velocity is gradually reduced to subcritical flow and the potential energy is recovered.

One of the more widely used flumes is the *Parshall flume* (U.S. Bureau of Reclamation, 1981), which is a Venturi-type flume illustrated in Figure 5.6.8. The discharge equation for these flumes with widths of 1 ft (0.31 m) to 8 ft (2.4 m) is

$$Q = 4WH_a^{1.522}W^{0.026} \tag{5.6.11}$$



PLAN



PROFILE

W	A		$\frac{2}{3}A$		B		C		D		E		F		G		M		N		P		R		FREE-FLOW CAPACITY		
	FT.	IN.	FT.	IN.	FT.	IN.	FT.	IN.	FT.	IN.	FT.	IN.	FT.	IN.	FT.	IN.	FT.	IN.	FT.	IN.	FT.	IN.	FT.	IN.	CFS	CFS	
0	6	2	$\frac{7}{16}$	1	$4\frac{5}{16}$	2	0	1	$3\frac{1}{2}$	1	$3\frac{5}{8}$	2	0	1	0	2	0	1	0	0	$4\frac{1}{2}$	2	$11\frac{1}{2}$	1	4	.05	3.9
	9	2	$10\frac{5}{8}$	1	$11\frac{1}{8}$	2	10	1	3	1	$10\frac{5}{8}$	2	6	1	0	1	6	1	0		$4\frac{1}{2}$	3	$6\frac{1}{2}$	1	4	.09	8.9
1	0	4	6	3	0	4	$4\frac{7}{8}$	2	0	2	$9\frac{1}{4}$	3	0	2	0	3	0	1	3		9	4	$10\frac{3}{4}$	1	8	.11	16.1
1	6	4	9	3	2	4	$7\frac{7}{8}$	2	6	3	$4\frac{3}{8}$	3	0	2	0	3	0	1	3		9	5	6	1	8	.15	24.6
2	0	5	0	3	4	4	$10\frac{7}{8}$	3	0	3	$11\frac{1}{2}$	3	0	2	0	3	0	1	3		9	6	1	1	8	.42	33.1
3	0	5	6	3	8	5	$4\frac{3}{4}$	4	0	5	$1\frac{7}{8}$	3	0	2	0	3	0	1	3		9	7	$3\frac{1}{2}$	1	8	.61	50.4
4	0	6	0	4	0	5	$10\frac{5}{8}$	5	0	6	$4\frac{1}{4}$	3	0	2	0	3	0	1	6		9	8	$10\frac{3}{4}$	2	0	1.3	67.9
5	0	6	6	4	4	6	$4\frac{1}{2}$	6	0	7	$6\frac{5}{8}$	3	0	2	0	3	0	1	6		9	10	$1\frac{1}{4}$	2	0	1.6	85.6
6	0	7	0	4	8	6	$10\frac{3}{8}$	7	0	8	9	3	0	2	0	3	0	1	6		9	11	$3\frac{1}{2}$	2	0	2.6	103.5
7	0	7	6	5	0	7	$4\frac{1}{4}$	8	0	9	$11\frac{3}{8}$	3	0	2	0	3	0	1	6		9	12	6	2	0	3.0	121.4
8	0	8	0	5	4	7	$10\frac{1}{8}$	9	0	11	$1\frac{3}{4}$	3	0	2	0	3	0	1	6		9	13	$8\frac{1}{4}$	2	0	3.5	139.5

Figure 5.6.8 Standard Parshall flume dimensions. 103-D-1225 (from U.S. Bureau of Reclamation (1978)).

where Q is the discharge in ft^3/s , W is the width of the flume throat, and H_a is the upstream head in ft. For smaller flumes, e.g., 6-inch flumes,

$$Q = 2.06H_a^{1.58} \tag{5.6.12}$$

and for 9-inch flumes

$$Q = 3.07H_a^{1.53} \tag{5.6.13}$$

EXAMPLE 5.6.2

Water flows through a Parshall flume with a throat width of 4.0 ft at a depth of 2.0 ft. What is the flow rate?

SOLUTION

Using equation (5.6.11).

$$Q = 4.0(4.0)(2.0)^{(1.522)(4.0)^{0.026}} = 47.8 \text{ ft}^3/\text{s}$$

Figure 5.6.9 illustrates a flow-measuring structure for unlined (earthen) channels that are longer, and consequently more expensive, than structures for concrete-lined channels. For concrete-lined channels, the approach channel and sides of the control section are already available.

5.6.3 Stream Flow Measurement: Velocity-Area-Integration Method

As for weirs and flumes, stream flow is not directly measured. Instead, water level is measured and stream flow is determined from a *rating curve*, which is the relationship between water surface elevation and discharge.

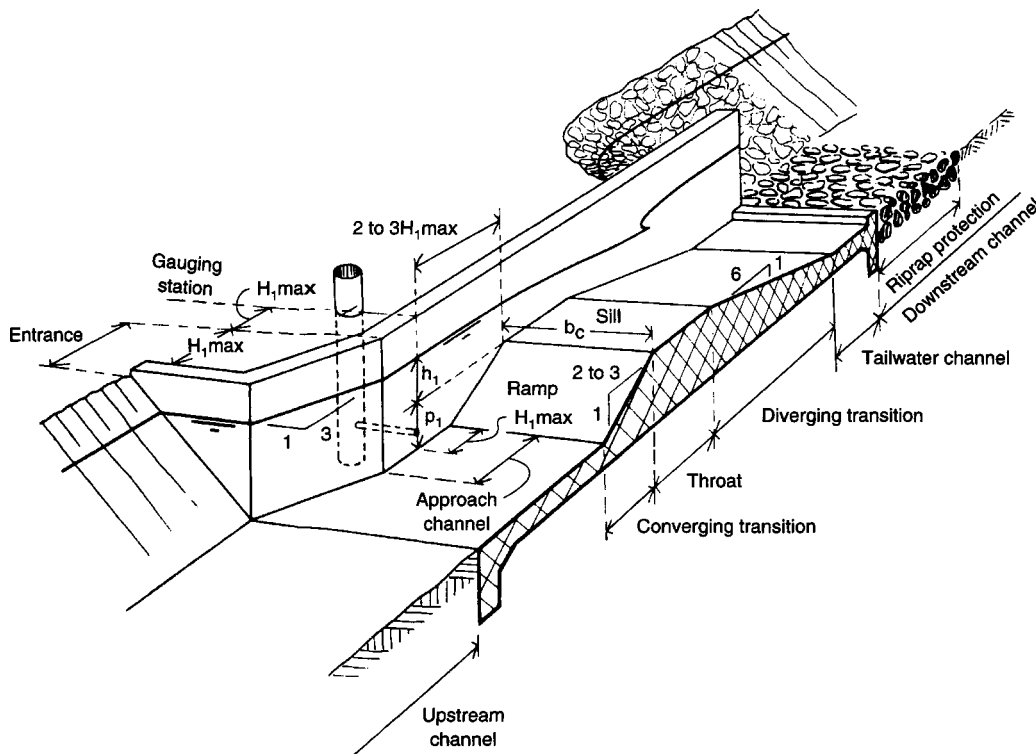


Figure 5.6.9 Flow-measuring structure for earthen channel with rectangular control section (from Bos et al. (1984)).

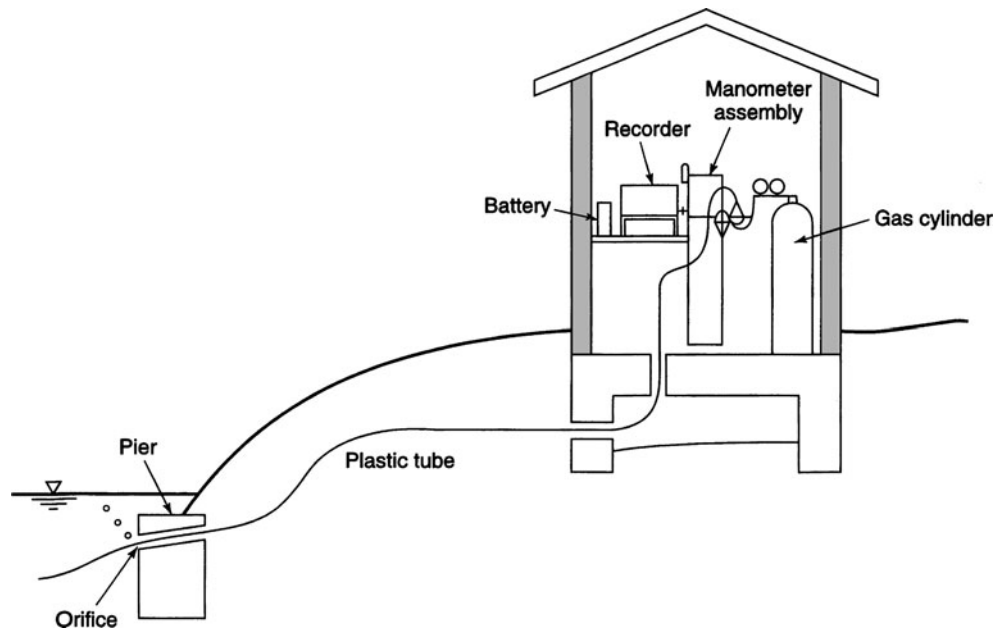


Figure 5.6.10 Water level measurement using a bubble gauge recorder. The water level is measured as the back pressure on the bubbling stream of gas by using a mercury manometer (from Rantz et al. (1982)).

Water surface level (elevation) can be measured manually or automatically. *Crest stage gauges* are used to measure flood crests. They consist of a wooden staff gauge placed inside a pipe with small holes for water entry. Cork in the pipe floats as the water rises and adheres to the staff (scale) at the highest water level. *Bubble gauges* (shown in Figure 5.6.10) sense the water surface level by bubbling a continuous stream of gas (usually carbon dioxide) into the water. The pressure required to continuously force the gas stream out beneath the water surface is a measure of the depth of water over the nozzle of the bubble stream. The pressure is measured with a manometer assembly to provide a continuous record of water level in the stream (gauge height).

Rating curves are developed using a set of measurements of discharge and gauge height in the stream. The discharge is $Q = AV$ where V is the mean velocity normal to the cross-sectional area of flow A , which is a function of the gauge height. So in order to measure discharge the velocity and the gauge height must be determined. In a stream or river, the velocity varies with depth, as discussed in Chapter 3 (Figure 3.7.1). Therefore, the velocity must be recorded at various locations and depths across the stream.

Referring to Figure 5.6.11, the total discharge is computed by summing the incremental discharge calculated from each measurement i , $i = 1, 2, \dots, n$, of velocity V_i , and depth y_i . These

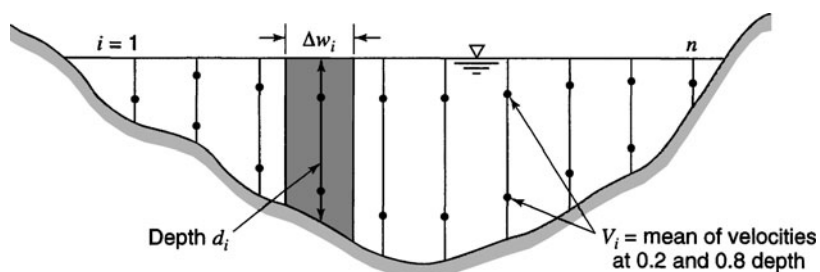


Figure 5.6.11 Computation of discharge from stream gauging data.

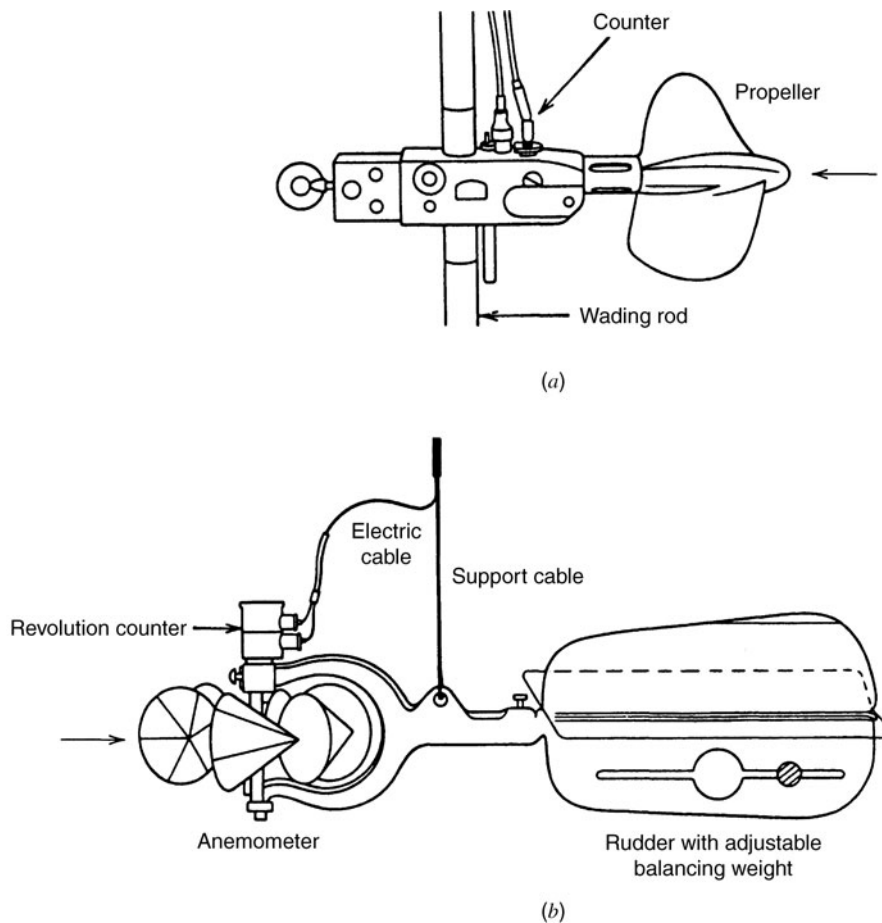


Figure 5.6.12 (a) Propeller- and (b) Price-type current meters (from James (1988)).

measurements represent average values over the width Δw_i of the stream. The total discharge is computed using

$$Q = \sum_{i=1}^n V_i y_i \Delta w_i \tag{5.6.14}$$

Both theory and experimental evidence indicate that the mean velocity in a vertical section can be closely approximated by the average of the velocities at 0.2 depth and 0.8 depth below the water surface, as shown in Figure 5.6.11. If the stream is shallow, it may be possible to take a single measurement of velocity at a 0.6 depth.

To measure the velocity in a stream, a *current meter*, which is an impellor device, can be used. The speed at which the impellor rotates is proportional to the flow velocity. Figure 5.6.12a shows a propeller type current meter on a wading rod and Figure 5.6.12b shows a Price current meter, which is the most commonly used velocity meter in the United States. Refer to Wahl et al. (1995) for detailed descriptions on the stream-gauging program of the U.S. Geological Survey.

PROBLEMS

5.1.1 Compute the hydraulic radius and hydraulic depth for a trapezoidal flood control channel with a bottom width of 20 ft, side slopes 2:1 (h:v), and a top width of 40 ft.

5.1.2 Compute the hydraulic radius and hydraulic depth for a trapezoidal flood control channel with a bottom width of 4 m, side slopes 2:1 (h:v), and a top width of 8 ft.

5.1.3 Compute the hydraulic radius and hydraulic depth for a 36-inch diameter culvert with a depth of flow of 24 in.

5.1.4 Compute the hydraulic radius and hydraulic depth for a 1.5-m diameter culvert with a depth of flow of 1.24 m.

5.1.5 A 2-m wide rectangular channel with a bed slope of 0.0005 has a depth of flow of 1.5 m. Manning's roughness coefficient is 0.015. Determine the steady uniform discharge in the channel.

5.1.6 Determine the uniform flow depth in a rectangular channel 2.5 m wide with a discharge of $3 \text{ m}^3/\text{s}$. The slope is 0.0004 and Manning's roughness factor is 0.015.

5.1.7 Determine the uniform flow depth in a trapezoidal channel with a bottom width of 8 ft and side slopes of 1 vertical to 2 horizontal. The discharge is $100 \text{ ft}^3/\text{s}$. Manning's roughness factor is 0.015 and the channel bottom slope is 0.0004.

5.1.8 Determine the uniform flow depth in a trapezoidal channel with a bottom width of 2.5 m and side slopes of 1 vertical to 2 horizontal with a discharge of $3 \text{ m}^3/\text{s}$. The slope is 0.0004 and Manning's roughness factor is 0.015.

5.1.9 Determine the cross-section of the greatest hydraulic efficiency for a trapezoidal channel with side slope of 1 vertical to 2 horizontal if the design discharge is $10 \text{ m}^3/\text{s}$. The channel slope is 0.001 and Manning's roughness factor is 0.020.

5.1.10 For a trapezoidal-shaped channel ($n = 0.014$ and slope S_0 of 0.0002 with a 20-ft bottom width and side slopes of 1 vertical to 1.5 horizontal), determine the normal depth for a discharge of 1000 cfs.

5.1.11 Show that the best hydraulic trapezoidal section is one-half of a hexagon.

5.1.12 A trapezoidal channel has a bottom width of 10 ft and side slopes of 2:1 (h:v). The channel has a slope of 0.0001 and a Manning's roughness of 0.018. If the uniform flow depth is 4 ft, what is the discharge in the channel?

5.1.13 Compute the normal depth of flow in a 36-in diameter culvert with a slope of 0.0016 and Manning's n of 0.015 for a discharge of 20 cfs.

5.1.14 A 6-ft diameter concrete-lined sewer has a bottom slope of 1.5 ft/mi. Find the depth of flow for a discharge of 20 cfs.

5.1.15 Compute the uniform flow depth in a trapezoidal channel with a bottom width of 20 ft, slope of 0.0016, Manning's n of 0.025, and side slopes of 2:1 (h:v) for a discharge of 500 cfs. What is the velocity of flow?

5.1.16 Design a trapezoidal concrete-lined channel ($n = 0.015$) to convey 100 cfs on a slope of 0.001. Assume the use of a best hydraulic section for the design.

5.1.17 Design a trapezoidal concrete-lined channel ($n = 0.015$) to convey $20 \text{ m}^3/\text{s}$ on a slope of 0.0001. Assume the use of a best hydraulic section for the design.

5.1.18 Phillips and Ingersoll (1998) presented equations for determining the Manning's roughness factor for gravel-bed

streams using the relative roughness defined as (R/d_{50}) where R is the hydraulic radius and d_{50} is the median grain size. The equation was verified for Arizona (for the range in d_{50} 0.28 to 0.36 ft) is $n = (0.0926R^{1/6})/[1.46 + 2.23\log(R/d_{50})]$. Use this equation to develop a graph illustrating the relation of n , R , and d_{50} .

5.1.19 Using the slope-area method, compute the flood discharge through a river reach of 800 ft having known values of water areas, conveyances, and energy coefficients of the upstream and downstream end sections. The fall of the water surface is 1.0 ft.

$$A_u = 11,070 \text{ ft}^2$$

$$A_d = 10,990 \text{ ft}^2$$

$$K_u = 3.034 \times 10^6$$

$$K_d = 3.103 \times 10^6$$

$$\alpha_u = 1.134$$

$$\alpha_d = 1.177$$

5.2.1 Solve example 5.2.2 for discharges of 0, 25, 75, 125, and 200 ft^3/s .

5.2.2 Rework example 5.2.3 for a 30-cm high hump and a side wall constriction that reduces the channel width to 1.6 m.

5.2.3 Compute the critical depth for the channel in problem 5.1.5.

5.2.4 Compute the critical depth for the channel in problem 5.1.6.

5.2.5 Rework example 5.2.4 with discharges of 0, 25, 75, 125, and 200 cfs.

5.2.6 Compute the critical depth in a 36-in diameter culvert with a slope of 0.0016 for a discharge of 20 cfs.

5.2.7 Compute the critical flow depth in a trapezoidal channel with a bottom width of 20 ft a slope of 0.0016, Manning's n of 0.025, and side slopes of 2:1 (h:v) for a discharge of 500 cfs.

5.2.8 A trapezoidal channel has a bottom width of 10 ft and side slopes of 2:1 (h:v). Manning's roughness factor is 0.018. For a uniform flow depth of 2.9 ft, what is the normal slope (corresponding to uniform flow depth) and the critical slope of the channel for a discharge of 200 cfs?

5.3.1 Resolve example 5.3.1 for a channel bed slope of 0.003.

5.3.2 A 2.45-m wide rectangular channel has a bed slope of 0.0004 and Manning's roughness factor of 0.015. For a discharge of $2.83 \text{ m}^3/\text{sec}$, determine the type of water surface profile for depths of 1.52 m, 0.61 m, and 0.30 m.

5.3.3 Rework problem 5.3.2 with a bed slope of 0.004.

5.3.4 If the channel of problem 5.1.10 is preceded by a steep slope and followed by a mild slope and a sluice gate as shown in Figure P5.3.4, sketch a possible water surface profile with the elevations to a scale of 1 in to 10 ft. Consider a discharge of 1500 cfs. For this discharge, the normal depth for a slope of 0.0003 is 8.18 ft and for a slope of 0.0002 is 9.13 ft.

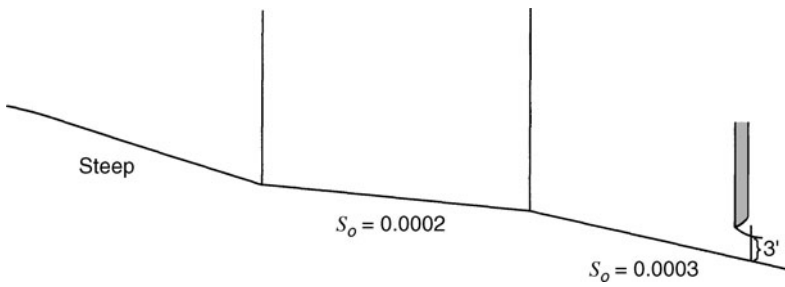


Figure P5.3.4

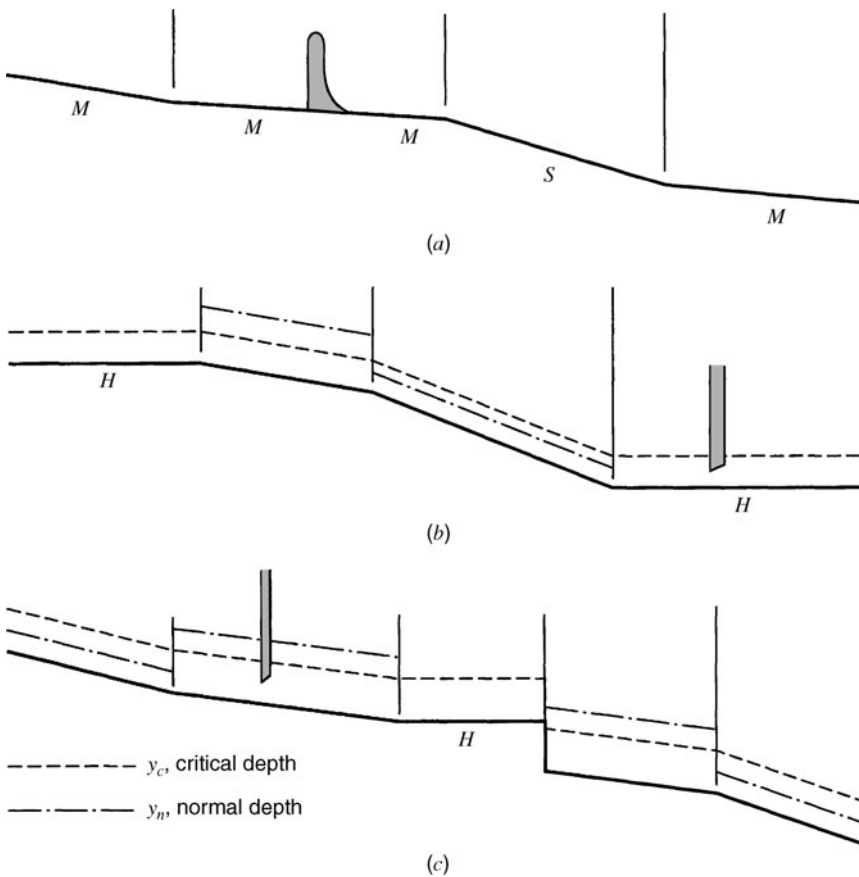


Figure P5.3.5

5.3.5 Sketch possible water surface profiles for the channel in Figure P5.3.5. First locate and mark the control points, then sketch the profiles, marking each profile with the appropriate designation. Show any hydraulic jumps that occur.

5.3.6 Show that for depths less than the normal depth ($y < y_n$) that $S_f > S_o$ and that for $y > y_n$ then $S_f < S_o$.

5.3.7 Show that $dy/dx = +$ for the S1 profile; $dy/dx = -$ for the S2 profile; and that $dy/dx = +$ for the S3 profile.

5.3.8 Using the gradually varied flow equation $dy/dx = (S_o - S_f)/(1 - F_r^2)$ define dy/dx for critical flow and for uniform flow.

5.3.9 A trapezoidal channel with a bottom width of 20 ft, a slope of 0.0016, Manning's n of 0.025, and side slopes of 2:1 (h:v) has a discharge of 500 cfs. An obstruction in this channel causes a backwater profile with a depth of 6.5 ft just upstream of the obstruction. What would be the depth of flow 200 ft

and 400 ft upstream of the obstruction? How far upstream does the normal depth occur? Assume an energy coefficient of 1.1.

5.3.10 Consider a concrete ($n = 0.013$) wide rectangular channel that discharges $2.0 \text{ m}^3/\text{s}$ per unit width of flow. The channel bottom slope is 0.0001. There is a step rise of 0.2 m. Determine the flow depth downstream of the step assuming no transition losses. Does the water rise or fall at the step?

5.3.11 Consider a 5-m wide rectangular channel with a discharge of $12.5 \text{ m}^3/\text{s}$. The depth of flow upstream of the step is 2.5 m. There is a step rise of 0.25 m in the bottom of the channel. Determine the flow depth downstream of the step assuming no transition losses. Does the water rise or fall at the step?

5.3.12 Consider the trapezoidal channel with a bottom width of 20 ft, a slope of 0.0016, Manning's n of 0.025, and side slopes of 2:1 (h:v) having a discharge of 500 cfs. Now a step rise of 1.0 ft is placed in the channel bottom. Determine the flow depth downstream of the bottom step assuming no transition losses. Does the water surface rise or fall at the step?

5.3.13 A 5-m wide rectangular channel with two reaches, each with a different slope, conveys $50 \text{ m}^3/\text{s}$ of water. The channel slope for the first reach is 0.001 and then a sudden change to a slope of 0.010. The Manning's n for the channel is 0.015. Perform the necessary computations to sketch the water surface profile and define the type of profiles.

5.3.14 Consider a concrete ($n = 0.013$) wide rectangular channel ($R = y$) that discharges $2.0 \text{ m}^3/\text{sec}$ per unit width of flow. The slope of the channel is 0.001. A low dam causes a backwater depth of 2.0 m immediately behind (upstream of) the dam. Compute the distance upstream of the dam to where the normal depth occurs.

5.3.15 Consider a concrete ($n = 0.013$) wide rectangular channel ($R = y$) that discharges $2.0 \text{ m}^3/\text{sec}$ per unit width of flow. The slope of the channel is 0.0001. A low dam causes a backwater depth of 2.0 m immediately behind (upstream of) the dam. Compute the distance upstream of the dam to where the normal depth occurs.

5.3.16 Consider a concrete trapezoidal channel with a 4-m bottom width, side slopes of 2:1 (h:v), and a bottom slope of 0.005. Determine the depth 150 m upstream from a section that has a measured depth of 2.0 m.

5.3.17 A wide rectangular channel changes in slope from 0.002 to 0.025. Sketch the water surface profile for a discharge of $1.7 \text{ m}^3/\text{s}/\text{m}$ and Manning's $n = 0.025$.

5.3.18 A 5-m wide rectangular channel with two reaches, each with a different slope, conveys $40 \text{ m}^3/\text{s}$ of water. The channel slope for the first reach is 0.0005 and then a sudden change to a slope of 0.015 so that critical flow occurs at the transition. Determine the depths of flow at locations 10 m, 20 m and 30 m upstream of the critical depth. The Manning's n for the channel is 0.015.

5.3.19 A 500-ft, 6-ft diameter reinforced concrete pipe culvert ($n = 0.012$) is used to convey stormwater from a detention reservoir to a downstream flood control channel. The slope of the

culvert is 0.02. The outlet of the culvert is placed at an elevation so that it will not be submerged. For a discharge of 230 cfs, compute the water surface profile. Develop a spreadsheet to perform the computations.

5.3.20 A 500-ft, 6-ft diameter reinforced concrete pipe culvert ($n = 0.012$) is used to convey stormwater from a detention reservoir to a downstream flood control channel. The slope of the culvert is 0.001. The outlet of the culvert is placed at an elevation so that it will not be submerged, and the flow falls freely into the flood control channel. For a discharge of 75 cfs, compute the water surface profile. Develop a spreadsheet to perform the computations.

5.4.1 Rework example 5.4.2 using equation (5.4.8), $S_f = Q^2/\bar{K}^2$.

5.4.2 Resolve example 5.4.3 with a discharge of 10,000 cfs and a downstream water surface elevation of 123.5 ft.

5.4.3 Rework example 5.4.4 using a discharge at river mile 1.0 of 8000 cfs and a discharge of 7500 cfs at river mile 1.5. The water surface elevation at river mile 1.0 is 123.5 ft. All other data are the same.

5.4.4 Consider a starting (assumed) water surface elevation of 5719.5 ft at cross-section 1 for example 5.4.5 and determine the water surface elevation at cross-section number 4.

5.4.5 Consider a starting (assumed) water surface elevation of 5717.6 ft at cross-section 1 for example 5.4.5 and determine the computed water surface elevation at cross-section 4.

5.4.6 Perform the backwater computations at mile 2.0 for the situation in example 5.4.4. The Manning's n values at mile 2 are 0.02 for the main channel and 0.04 for the overbanks. Use an assumed trial water surface elevation of 125.5 ft. Cross-sections at miles 2.0 and 1.5 are the same.

5.4.7 For most natural channels and many designed channels, the roughness varies along the wetted perimeter of the channel. In order to perform normal flow computations for these composite channels it is necessary to compute the composite (equivalent or effective) roughness factor. For the composite channel in Figure 5.4.2, compute the effective roughness factor (n_e) at river mile 1.0 for a water surface elevation of 125 ft using the following equations:

$$n_e = \left\{ \left[\sum_{i=1}^N P_i n_i^{3/2} \right] / P \right\}^{2/3}$$

and

$$n_e = \left\{ \left[\sum_{i=1}^N P_i n_i^2 \right] / P \right\}^{1/2}$$

where P_i and n_i are, respectively, the wetted perimeter and Manning's n for each subsection of the channel; $P = \sum_{i=1}^N P_i$ is the wetted perimeter of the complete channel section, and N is the number of subsections of the channel.

5.4.8 Use the U.S. Army Corps of Engineers HEC-RAS computer code to solve Example 5.4.4.

5.4.9 Use the U.S. Army Corps of Engineers HEC-RAS computer code to solve example 5.4.5.

5.5.1 Consider a 2.45-m wide rectangular channel with a bed slope of 0.0004 and a Manning’s roughness factor of 0.015. A weir is placed in the channel and the depth upstream of the weir is 1.52 m for a discharge of 5.66 m³/s. Determine whether a hydraulic jump forms upstream of the weir.

5.5.2 A hydraulic jump occurs in a rectangular channel 4.0 m wide. The water depth before the jump is 0.4 m and after the jump is 1.7 m. Compute the flow rate in the channel, the critical depth, and the headloss in the jump.

5.5.3 Rework example 5.5.3 with a flow rate of 450 cfs at a normal depth of 3.2 ft. All other data remain the same.

5.5.4 Rework example 5.5.4 if the depth before the jump is 0.8 m and all other data remain the same.

5.5.5 A rectangular channel is 3.0 m wide ($n = 0.018$) with a discharge of 14 m³/s at a normal depth of 1.0 m. An obstruction causes the depth just upstream of the obstruction to be 2.7 m deep. Will a jump form upstream of the obstruction? If the jump does form, how far upstream is it located?

5.5.6 Rework example 5.5.4 if the depth after the jump is 1.8 m and all other data remain the same.

5.5.7 A 10-ft wide rectangular channel ($n = 0.015$) has a discharge of 251.5 cfs at a uniform flow (normal) depth of 2.5 ft. A sluice gate at the downstream end of the channel controls the flow depth just upstream of the gate to a depth z . Determine the depth z so that a hydraulic jump is formed just upstream of the gate. What is the channel bottom slope? What is the headloss (energy loss) in the hydraulic jump?

5.5.8 A 3-m wide rectangular channel ($n = 0.02$) has a discharge of 10 m³/s at a uniform flow (normal) depth of 0.8 m. A sluice gate at the downstream end of the channel controls the flow depth just upstream of the gate to a depth z . Determine the depth z so that a hydraulic depth is formed just upstream of the gate. What is the channel bottom slope? What is the headloss (energy loss) in the hydraulic jump?

5.5.9 A 5-m wide rectangular channel with two reaches, each with a different slope, conveys 40 m³/s of water. The channel slope for the first reach is 0.015 and then a sudden change to a slope of 0.0005. The Manning’s n for the channel is 0.015. Does a hydraulic jump occur in the channel? If there is a hydraulic jump, where does it occur: on the first reach or the second reach?

5.5.10 A 5-m wide rectangular channel with two reaches, each with a different slope, conveys 80 m³/s of water. The channel slope for the first reach is 0.01 and then a sudden change to a slope of 0.001. The Manning’s n for the channel is 0.015. Does a hydraulic jump occur in the channel? If there is a hydraulic jump, where does it occur: on the first reach or the second reach?

5.5.11 A hydraulic jump is formed in a 10-ft wide channel just downstream of a sluice gate for a discharge of 450 cfs. If the depths of flow are 30 ft and 2 ft just upstream and downstream of the gate, respectively, determine the depth of flow downstream of the jump. What is the energy loss in the jump? What is the thrust [$F_{\text{gate}} = \gamma(\Delta F)$] on the gate? Illustrate the thrust on the specific force and specific energy diagrams for this problem.

5.5.12 Consider a 40-ft wide horizontal rectangular channel with a discharge of 400 cfs. Determine the initial and sequent depths of a hydraulic jump, if the energy loss is 5 ft.

5.6.1 A rectangular, sharp-crested weir with end contraction is 1.6 m long. How high should it be placed in a channel to maintain an upstream depth of 2.5 m for 0.5 m³/s flow rate?

5.6.2 For a sharp-crested suppressed weir ($C_w = 3.33$) of length $B = 8.0$ ft, $P = 2.0$ ft, and $H = 1.0$ ft, determine the discharge over the weir. Neglect the velocity of approach head.

5.6.3 Rework problem 5.6.2 incorporating the velocity of approach head (equation (5.6.5a)).

5.6.4 Rework example 5.6.2 using equation (5.6.5b).

5.6.5 A rectangular sharp-crested weir with end contractions is 1.5 m long. How high should the weir crest be placed in a channel to maintain an upstream depth of 2.5 m for 0.5 m³/s flow rate?

5.6.6 Determine the head on a 60° V-notch weir for a discharge of 150 l/s. Take $C_d = 0.58$.

5.6.7 The head on a 90° V-notch weir is 1.5 ft. Determine the discharge.

5.6.8 Determine the weir coefficient of a 90° V-notch weir for a head of 180 mm for a flow rate of 20 l/s.

5.6.9 Determine the required head for a flow of 3.0 m³/s over a broad-crested weir 1.5 m high and 3 m long with a well-rounded upstream corner ($C_w = 1.67$).

5.6.10 Water flows through a Parshall flume with a throat width of 4.0 ft at a depth of 7.5 ft. Determine the flow rate.

5.6.11 Water flows through a Parshall flume with a throat width of 5.0 ft at a depth of 3.4 ft. Determine the flow rate.

5.6.12 The following information was obtained from a discharge measurement on a stream. Determine the discharge.

Distance from bank (ft)	Depth (ft)	Mean velocity (ft)
0	0.0	0.00
12	0.1	0.37
32	4.4	0.87
52	4.6	1.09
72	5.7	1.34
92	4.3	0.71
100	0.0	0.00

REFERENCES

- Barnes, H. H., Jr., *Roughness Characteristics of Natural Channels*, U.S. Geological Survey, Water Supply Paper 1849, U.S. Government Printing Office, Washington, DC, 1962.
- Bos, M. G., J. A. Replogle, and A. J. Clemmens, *Flow Measuring Flumes for Open Channel System*, John Wiley & Sons, New York, 1984.
- Brater, E. F., H. W. King, J. E. Lindell, and C. Y. Wei, *Handbook of Hydraulics*, 7th edition, McGraw-Hill, New York, 1996.
- Chaudhry, M. H., *Open-Channel Flow*, Prentice Hall, Englewood Cliffs, NJ, 1993.
- Chow, V. T., *Open-Channel Hydraulics*, McGraw-Hill, New York, 1959.
- French, R. H., *Open-Channel Hydraulics*, McGraw-Hill, New York, 1985.
- Henderson, F. M., *Open-Channel Flow*, Macmillan, New York, 1966.
- Hoggan, D. H., *Computer-Assisted Floodplain Hydrology and Hydraulics*, 2nd edition, McGraw-Hill, New York, 1997.
- Hydrologic Engineering Center (HEC), *HEC-RAS River System Analysis System, User's Manual, Version 2.2*, U. S. Army Corps of Engineers Water Resources Support Center, Davis, CA, 1997a.
- Hydrologic Engineering Center (HEC), *HEC-RAS River Analysis System, Hydraulic Reference Manual, Version 2.0*, U.S. Army Corps of Engineers Water Resources Support Center, Davis, CA, 1997b.
- Hydrologic Engineering Center (HEC), *HEC-RAS River Analysis System, Applications Guide, Version 2.0*, U. S. Army Corps of Engineers Water Resources Support Center, Davis, CA, 1997c.
- Jain, S. C., *Open-Channel Flow*, John Wiley & Sons, Inc., New York, 2001.
- James, L. G., *Principles of Farm Irrigation System Design*, John Wiley and Sons, Inc., New York, 1988.
- Manning, R., "On the Flow of Water in Open Channels and Pipes," *Transactions Institute of Civil Engineers of Ireland*, vol. 20, pp. 161–209, Dublin, 1891; Supplement, vol. 24, pp. 179–207, 1895.
- Phillips, J. V., and T. L. Ingersoll, "Verification of Roughness Coefficients for Selected Natural and Constructed Stream Channels in Arizona," U.S. Geological Survey Prof. Paper 1584, 1998.
- Rantz, S. E. et al., *Measurement and Computation of Stream Flow*, vol. 1, *Measurement of Stage and Discharge*, Water Supply Paper 2175, U.S. Geological Survey, 1982.
- Replogle, J. A., A. J. Clemmens, and C. A. Pugh, "Hydraulic Design of Flow Measuring Structures," in *Hydraulic Design Handbook*, edited by L. W. Mays, McGraw-Hill, New York, 1999.
- Sturm, T., *Open Channel Hydraulics*, McGraw-Hill, New York, 2001.
- Townson, J. M., *Free-Surface Hydraulics*, Unwin Hyman, London, 1991.
- U.S. Bureau of Reclamation, *Guide for Computing Water Surface Profiles*, 1957.
- U.S. Bureau of Reclamation, *Design of Small Canal Structures*, U.S. Government Printing Office, Denver, CO, 1978.
- U.S. Bureau of Reclamation, *Water Measurement Manual*, U.S. Government Printing Office, Denver, CO, 1981.
- Wahl, K. L., W. O. Thomas, Jr., and R. M. Hirsch, "Stream-Gauging Program of the U.S. Geological Survey," *Circular 11123*, U.S. Geological Survey, Reston, VA, 1995.

This page intentionally left blank

Hydraulic Processes: Groundwater Flow

Groundwater hydrology is the science that considers the occurrence, distribution, and movement of water below the surface of the earth (Todd and Mays, 2005). It is concerned with both the quantity and quality aspects of this water (Charbeneau, 2000). This chapter only considers the quantity aspects, in particular the hydraulic flow processes, emphasizing *aquifer hydraulics* (also see Batu, 1998; Charbeneau, 2000; and Delleur, 1999).

6.1 GROUNDWATER CONCEPTS

Groundwater flows through *porous media*, *fractured media*, and *large passages (karst)*. Porous media consist of solid material and *voids* or *pore space*. Porous media contain relatively small openings in the solid and are permeable media allowing the flow of water. The porous media that we typically are interested in for groundwater flow include natural soils, unconsolidated sediments, and sedimentary rocks. The size range of particles in a soil is referred to as the *soil texture*. Grain size determines the particle size classification. The fraction of clay, silt, and sand in a soil texture is described by the *soil texture triangle*, shown in Figure 6.1.1. Each point on the triangle corresponds to different percentages by mass (weight) of clay, sand, and silt.

The subsurface occurrence of groundwater, as shown in Figure 6.1.2, can be divided into the *vadose zone (zone operation)* and the *zone of saturation*. The vadose zone, also called the *unsaturated* or *partially saturated zone*, is the subsurface media above the water table. The term vadose is derived from the Latin *vadosus*, meaning shallow. Flow in the unsaturated, or vadose, zone is discussed further in Section 7.4. This chapter is focused on saturated flow, which is referred to as *groundwater flow*.

Groundwater originates through infiltration, influent streams, seepage from reservoirs, artificial recharge, condensation, seepage from oceans, water trapped in the sedimentary rock (*connate water*), and *juvenile* water (volcanic, magmatic, and cosmic). Any significant quantity of subsurface water is stored in subsurface formations defined as *aquifers*. An aquifer may be defined as a formation that contains sufficient saturated permeable material to yield significant quantities of water to wells (Lohman et al., 1972). Aquifers are usually of large areal extent and are essentially underground storage reservoirs. They may be overlain or underlain by a *confining bed*, which is a relatively impermeable material adjacent to the aquifer.

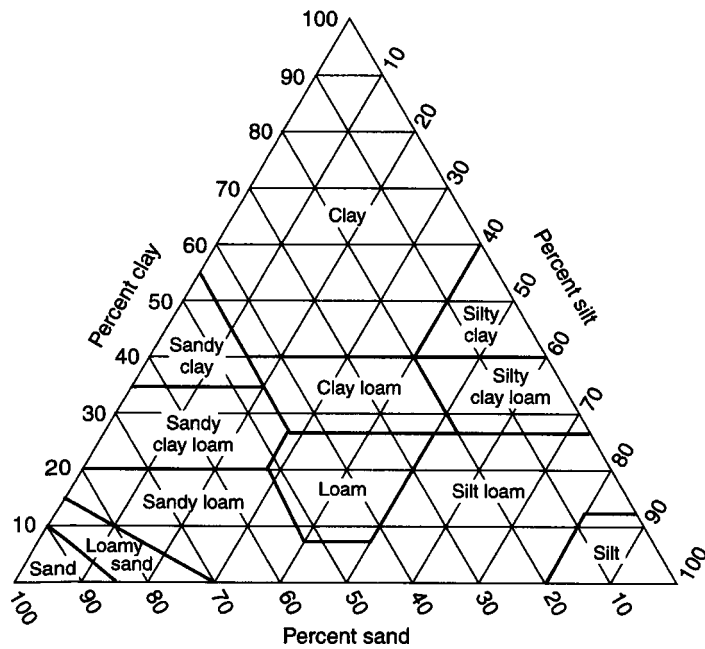


Figure 6.1.1 Triangle of soil textures for describing various combinations of sand, silt, and clay (from U.S. Soil Conservation Service (1951)).

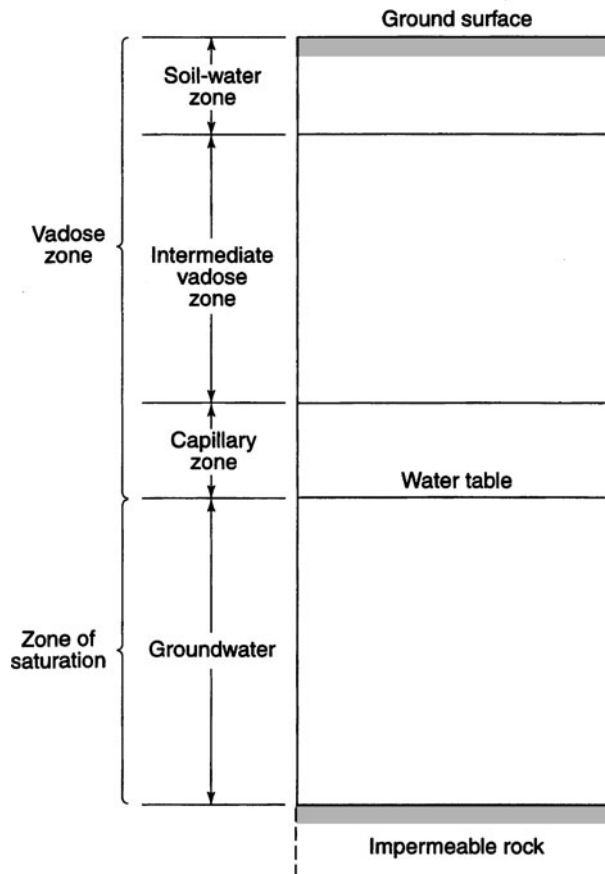


Figure 6.1.2 Divisions of subsurface water (Todd and Mays, 2005).

The following are different types of confining beds (Todd and Mays, 2005):

- *Aquiclude*—A saturated but relatively impermeable material that does not yield appreciable quantities of water to wells; clay is an example.
- *Aquifuge*—A relatively impermeable formation neither containing nor transmitting water; solid granite belongs in this category.
- *Aquitard*—A saturated but poorly permeable stratum that impedes groundwater movement and does not yield water freely to wells, but that may transmit appreciable water to or from adjacent aquifers and, where sufficiently thick, may constitute an important groundwater storage zone; sandy clay is an example.

Table 6.1.1 lists the various aquifer types and their characteristics.

Table 6.1.1 Summary of the Characteristics of Principal Aquifer Types

Aquifer type	Lithology	Groundwater flow regime	Aquifer properties				Residence times
			Porosity (percent)	Permeability (m/day)	Specific yield (percent)	Natural Flow rates (m/day)	
Shallow alluvium	Gravel	Intergranular	25–35	100–1000	12–25	2–10	Could be very short; a few months to years, depending on volume
	Sand	Intergranular	30–42	1–50	10–25	0.05–1	
	Silt	Intergranular	40–45	0.0005–0.1	5–10	0.001–0.1	
Deep sedimentary formations	Sand and silts	Intergranular	30–40	0.1–5	2–10	0.001–0.01	Many thousands of years
Sandstone	Cemented quartz grains	Intergranular and fissure	10–30	0.1–10	8–20	0.001–0.1	Tens to hundreds of years
Limestone	Cemented carbonate	Mainly fissure	5–30	0.1–5.0	5–15	0.001–1	Tens to hundreds of years
Karstic limestone	Cemented carbonate	Fissures and channels	5–25	100–10,000	5–15	10–2000	A few hours to days
Volcanic rock							
Basalt	Fine-grained crystalline	Fissure	2–15	0.1–1000	1–5	1–500	Very wide range; can be very short
Tuff	Cemented grains	Intergranular and fissure	15–30	0.1–5	10–20	0.001–1	Wide range
Igneous and metamorphic rocks (granites and gneisses):							
Fresh	Crystalline	Fissure	0.1–2	$10^{-7} - 5 \times 10^{-5}$		$10^{-6} - 10^{-2}$	Thousands of years, but can be rapid where fractured
Weathered	Disaggregated crystalline	Intergranular and fissure	10–20	0.1–2	1–5	0.001–0.1	Tens to hundreds of years

Source: P. J. Chilton cited in M. Meybeck, D. V. Chapman, and R. Helmer, *Global Freshwater Quality: A First Assessment*, Global Environmental Monitoring System (GEMS), World Health Organization and United Nations Environment Programme, Basil Blackwell, Oxford, 1990, as presented by Gleick (1993).

Aquifers are classified as *unconfined* or *confined* depending upon the presence or absence of a water table (Figure 6.1.3). An *unconfined aquifer* is one in which a water table serves as the upper surface of the *zone of saturation*, also known as a *free*, *phreatic*, or *non-artesian aquifer*. Changes in the water table (rising or falling) correspond to changes in the volume of water in storage within an aquifer. A *confined aquifer* is one in which the groundwater is confined under pressure greater than atmospheric by overlying, relatively impermeable strata. Confined aquifers are also known as *artesian* or *pressure aquifers*. Water enters such aquifers in an area where the confining bed rises to the surface or ends underground, and such an area is known as a *recharge area*. Changes of the water levels in wells penetrating confined aquifers result primarily from changes in pressure rather than changes in storage volumes.

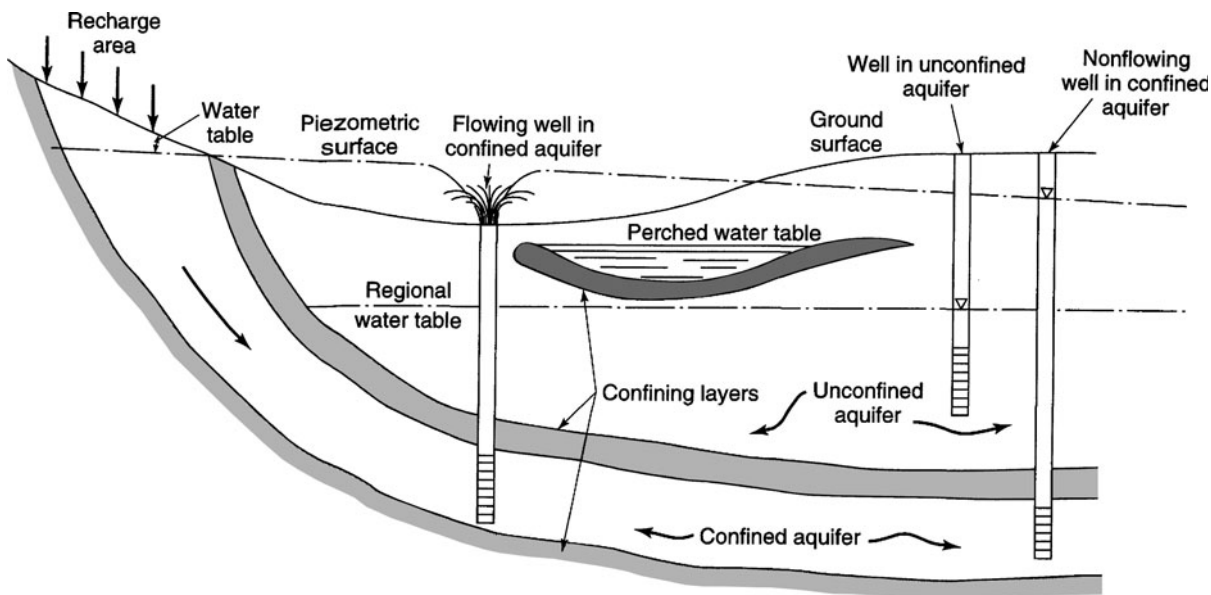


Figure 6.1.3 Types of aquifers (from U.S. Bureau of Reclamation (1981)).

Aquifer Properties

Aquifers perform two important functions—a *storage function* and a *conduit function*. In other words, aquifers store water and also function as a pipeline. When water is drained from a saturated material under the influence of gravity, only a portion of the total saturated volume in the pores is released. Part of the water is retained in interstices due to the losses of the molecular attraction, adhesion, and cohesion. The *specific yield* S_y , which is the storage term for unconfined aquifers, is the volume of water drained from a saturated sample of unit volume (1 ft^3 or 1 m^3) with a unit decrease in the water table. *Specific retention* S_r is the quantity of water that is retained in the unit volume after gravity drainage. The sum of the specific yield and the specific retention for saturated aquifers is the porosity, $\alpha = S_y + S_r$. Porosity is the pore volume divided by the total volume, expressed as a percent. Porosity represents the potential storage of an aquifer but does not indicate the amount of water a porous material will yield. Figure 6.1.4 illustrates the various types of porosities.

The *storativity* (or *storage coefficient*) of an aquifer is the volume of water the aquifer releases from or takes into storage per unit surface area of the aquifer per unit decline or rise of head. This is illustrated in Figure 6.1.5, considering a vertical column of unit area extending through a confined aquifer and an unconfined aquifer. In both cases, the storage coefficient S equals the volume of water (ft^3 or m^3) released from the aquifer when the piezometric surface or water table declines one unit of distance (1 ft or 1 m). The storativity then has dimensions of ft^3/ft^3 or m^3/m^3 . In the case of unconfined aquifers, the storativity corresponds to the specific yield. Confined aquifers have storativities in the range of $10^{-5} \leq S \leq 10^{-3}$. These small values indicate that large pressure changes are required to produce substantial water yields. Storativity can be determined in the field by pump tests. The *specific storage* S_s of a saturated aquifer is the volume of water that a unit volume of aquifer releases from storage under a unit decline in hydraulic head, i.e., $S = S_s b$ where b is the thickness of a confined aquifer.

Hydraulic conductivity (also referred to as *coefficient of permeability*) is the property related to the conduit function of an aquifer. It is the measure of ease of moving groundwater through aquifers, with dimensions of (L/T) . The hydraulic conductivity K is the rate of flow of water through a cross-section of unit area of the aquifer under a unit hydraulic gradient. The *hydraulic gradient* is the

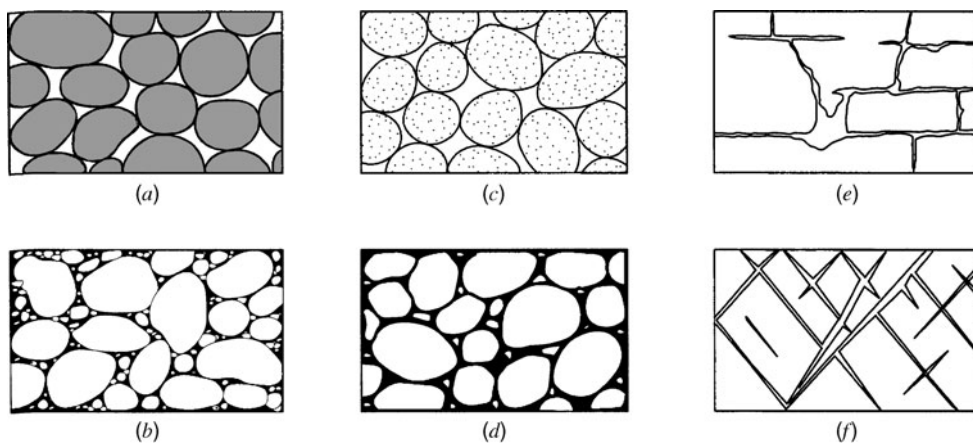


Figure 6.1.4 The various types of porosity: (a) Well-sorted sedimentary deposit possessing high porosity; (b) Poorly sorted sedimentary deposit of low porosity; (c) Similar to a but consisting of pebbles that are themselves porous, so the porosity of the deposit is very high; (d) Also similar to a, but the porosity has been diminished by the deposition of mineral matter in the interstices; (e) Rocks rendered porous by solution; and (f) Rocks rendered porous by fracturing (from Meinzer (1923)).

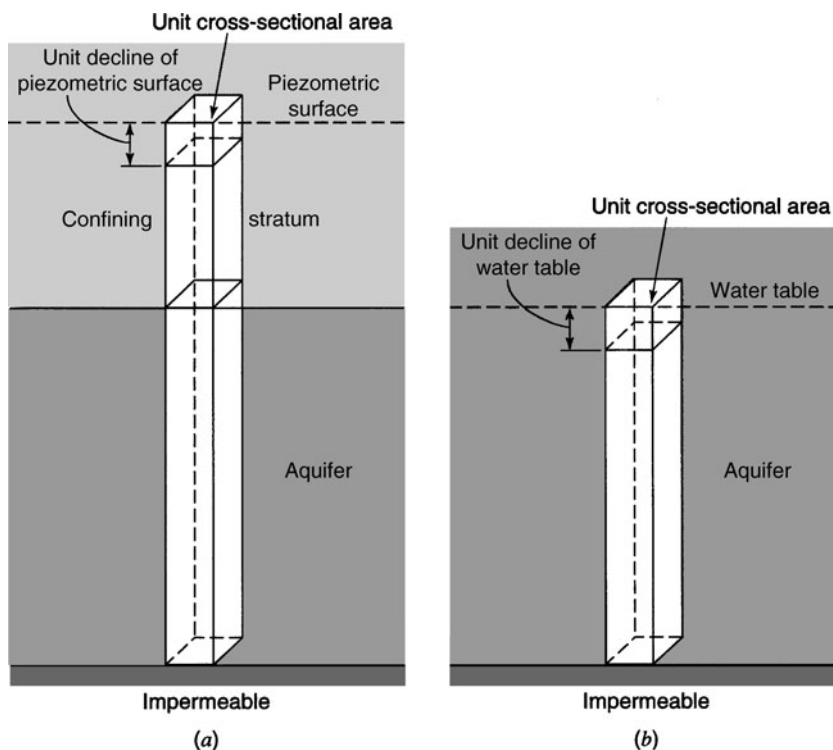
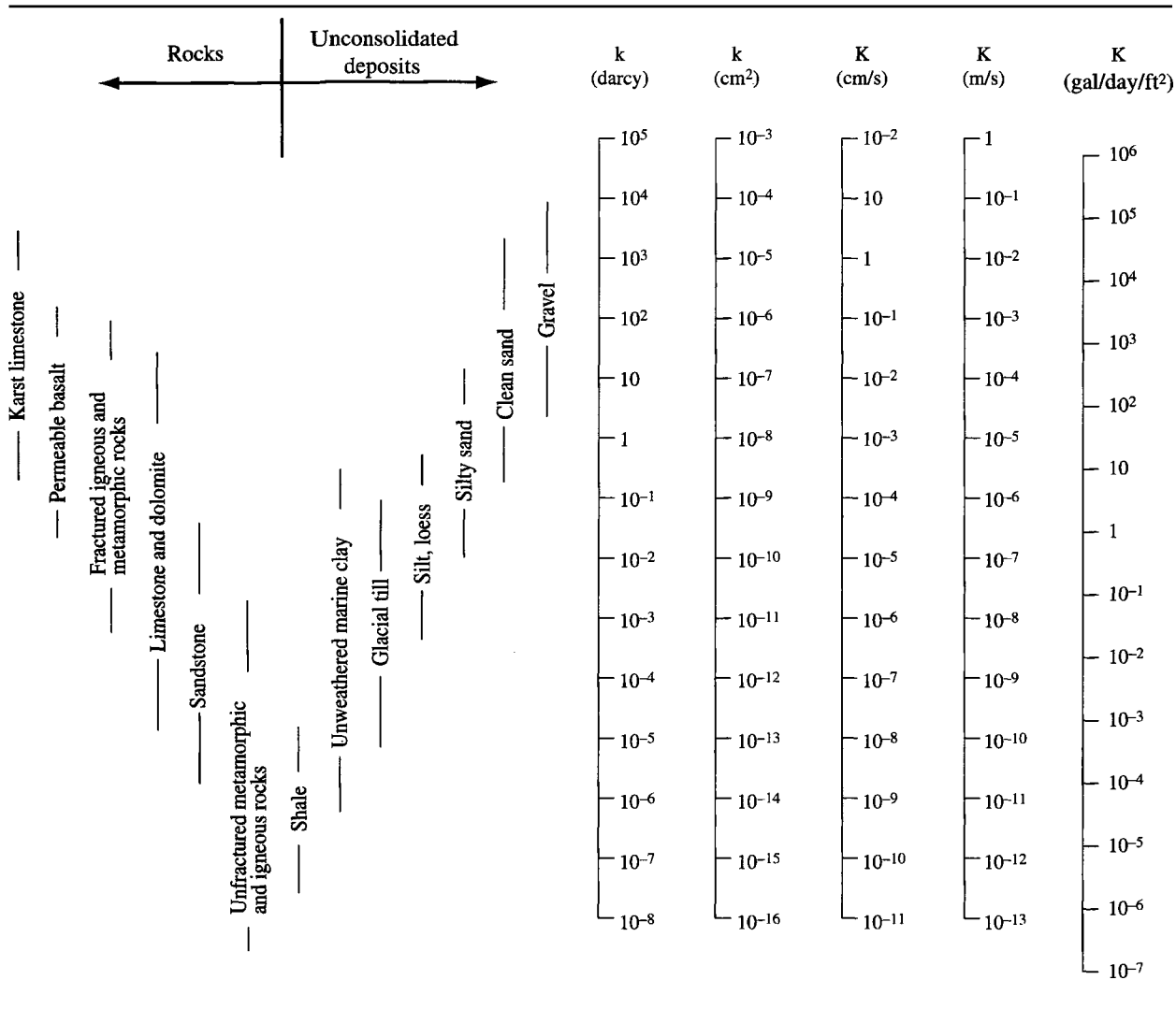


Figure 6.1.5 Illustrative sketches for defining storage coefficient of (a) confined and (b) unconfined aquifers (from Todd and Mays (2005)).

headloss divided by the distance between the two points. The hydraulic conductivity is commonly expressed in gallons per day/ft² or in ft/day in U.S. customary units or cm/d or m/d in SI units. Table 6.1.2 presents a range of hydraulic conductivity. Table 6.1.3 lists, in both the SI and the FPS systems, the dimensions and common units for some of the basic groundwater parameters. The

Table 6.1.2 Range of Values of Hydraulic Conductivity and Permeability



Source: Freeze and Cherry (1979).

Table 6.1.3 Dimensions and Common Units for Basic Groundwater Parameters

Parameter	Symbol	Systeme International*		Foot-Pound-Second System**	
		SI		FPS	
		Dimension	Units	Dimension	Units
Hydraulic head	<i>h</i>	[L]	m	[L]	ft
Elevation head	<i>z</i>	[L]	m	[L]	ft
Fluid pressure	<i>p</i>	[M/LT ²]	N/m ² or Pa	[F/LT ²]	lb/ft ²
Mass density	ρ	[M/L ³]	kg/m ³	—	—
Weight density	γ	—	—	[F/L ³]	lb/ft ³
Specific discharge	<i>v</i>	[L/T]	m/s	[L/T]	ft/s
Hydraulic conductivity	<i>K</i>	[L/T]	m/s	[L/T]	ft/s

*Basic dimensions are length *L*, mass *M*, and time *T*.

**Basic dimensions are length *L*, force *F*, and time *T*.

hydraulic conductivity is a function of both the porous medium and the fluid properties. Table 6.1.1 summarizes the characteristics of principal aquifer types.

A *specific* or *intrinsic* permeability, which is a function of the medium alone and not the fluid properties, is $k = Cd^2$, where C is a constant of proportionality and d is the grain size diameter. This k has simply been referred to as permeability (Freeze and Cherry, 1979). Table 6.1.2 also presents ranges of k values, which have dimensions of $[L^2]$. The *darcy* is also a unit of permeability, where 1 darcy is the permeability that leads to a specific discharge of 1 cm/s for a fluid with a viscosity of 1 cP (1 centipoise, $\text{cP} = \text{N} = \text{s/m}^2 \times 10^{-3}$) under a hydraulic gradient of 1 cm/cm. One darcy is approximately equal to 10^{-8} cm^2 (Freeze and Cherry, 1979). Refer to Table 6.1.2 for the range of values of k .

Closely related to the hydraulic conductivity is the *transmissivity* (or *transmissibility*), which indicates the capacity of an aquifer to transmit water through its entire thickness. The transmissivity, T , is the flow rate (ft^2/s or m^2/s) through a vertical strip of the aquifer 1 unit wide (1 ft or 1 m) and extending through the saturated thickness under a unit hydraulic gradient. The transmissivity is equal to the hydraulic conductivity multiplied by the saturated thickness of the aquifer: $T = Kb$, in which b is the saturated thickness of the aquifer.

Heterogeneity and Anisotropy of Hydraulic Conductivity

In geologic formations the hydraulic conductivity usually varies through space, referred to as *heterogeneity*. A geologic formation is *homogeneous* if the hydraulic conductivity is independent of position in the formation, i.e., $K(x,y,z) = \text{constant}$. A geologic formation is *heterogeneous* if the hydraulic conductivity is dependent on position in the formation, $K(x,y,z) \neq \text{constant}$.

Hydraulic conductivity may also show variations with the direction of measurement at a given point in the formation. A geologic formation is *isotropic* at a point if the hydraulic conductivity is independent of the direction of measurement at the point, $K_x = K_y = K_z$. A geologic formation is *anisotropic* at a point if the hydraulic conductivity varies with the direction of measurement at that point, $K_x \neq K_y \neq K_z$.

Groundwater Basins

Aquifers exist in both *consolidated* (mainly bedrock) and *unconsolidated* (mainly surface deposits) *materials*. Figure 6.1.6 illustrates the distribution of major aquifers of different types. *Groundwater basins* are a group of interrelated bodies of groundwater linked together in a larger flow system (Marsh, 1987). These basins are typically complex, three-dimensional systems. The spatial configurations of groundwater basins are determined by regional geology.

Groundwater Movement

Groundwater in its natural state is invariably moving, and this movement is governed by hydraulic principles. The flow through an aquifer is expressed by *Darcy's law*, which is the foundation of groundwater hydraulics. This law states that the flow rate through porous media is proportional to the headloss and inversely proportional to the length of the flow path, expressed mathematically as

$$Q = -KA \frac{dh}{dL} \quad (6.1.1)$$

Figure 6.1.7 illustrates Darcy's law where $h = dh$ and $L = dL$ so that $Q = KA h/L$.

The Reynolds number for flow in porous media is

$$R_e = \frac{\rho V D}{\mu} \quad (6.1.2)$$

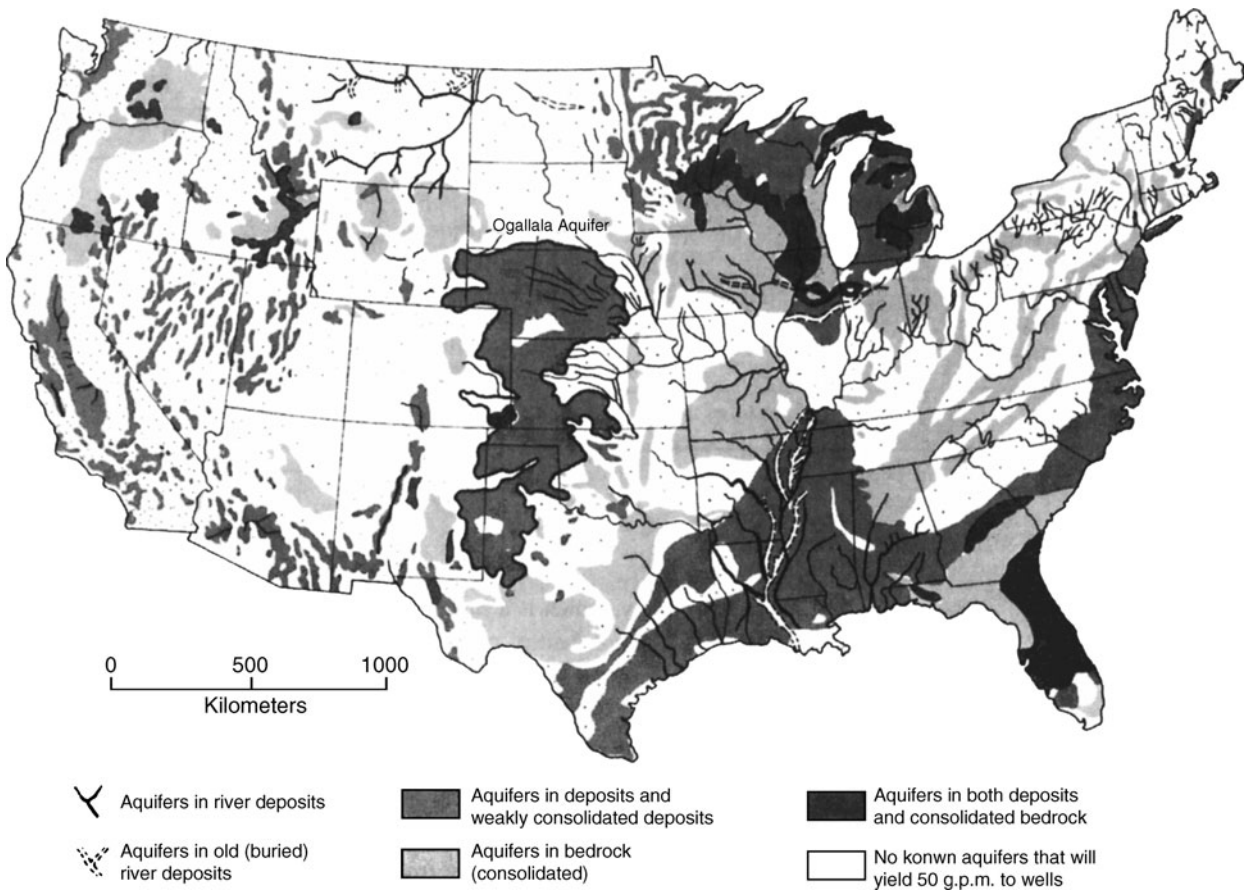


Figure 6.1.6 Distribution of major aquifers of different types (river deposits, other deposits, and consolidated bedrock) in the coterminous United States. A major aquifer is defined as one composed of material capable of yielding 50 gallons per minute or more to an individual well and having water quality generally not containing more than 2000 parts per million of dissolved solids (from Marsh (1987)).

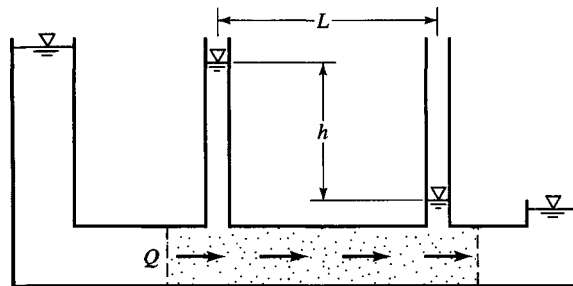


Figure 6.1.7 Illustration of Darcy's law (from U.S. Bureau of Reclamation (1981)).

where ρ is fluid density, V is the apparent velocity, D is the average grain diameter (an approximation to average pore diameter), and μ is viscosity of the fluid. The upper limit of validity for Darcy's law is for R_e , ranging between 1 and 10, and there is really no lower limit. In almost all natural groundwater motion $R_e < 1$; therefore, Darcy's law is applicable to natural groundwater problems. In summary, this law is valid when the flow is laminar or without turbulence.

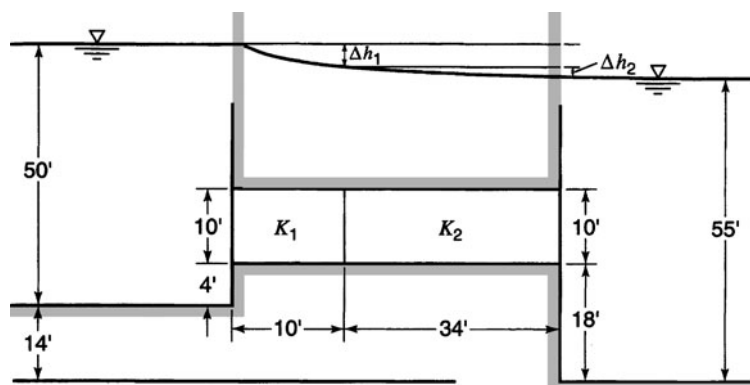


Figure 6.1.8 Two reservoirs connected by conduit of two porous medium for example 6.1.1.

EXAMPLE 6.1.1

Two very large reservoirs are connected by a conduit of two types of porous medium as shown in Figure 6.1.8. Compute the magnitude of flow per unit width between the two reservoirs if $K_1 = 1 \text{ gpd/ft}^2$ and $K_2 = 2 \text{ gpd/ft}^2$.

SOLUTION

Darcy's law for sections 1 and 2 where $Q_1 = Q_2$ is

$$K_1 A_1 \frac{dh_1}{dL_1} = K_2 A_2 \frac{dh_2}{dL_2}$$

Because $A_1 = A_2$,

$$\frac{\Delta h_1}{\Delta L_1} = 2 \frac{\Delta h_2}{\Delta L_2}$$

and

$$\Delta h_1 + \Delta h_2 = 9$$

The two equations above have two unknowns, Δh_1 and Δh_2 , so they can be solved to obtain $\Delta h_2 = 5.67 \text{ ft}$ and $\Delta h_1 = 3.33 \text{ ft}$. The flow rate is computed using Darcy's equation,

$$Q_1 = 1.10 \cdot \frac{3.33}{10} = 3.33 \text{ gpd}$$

6.2 SATURATED FLOW

6.2.1 Governing Equations

The control volume for a saturated flow is shown in Figure 6.2.1. The sides have lengths dx , dy , and dz in the coordinate directions. The total volume of the control volume is $dx dy dz$, the volume of water in control volume is $\theta dx dy dz$, where θ is the moisture content. With the control volume approach, the extensive property B is the mass of the groundwater, the intensive property is $\beta = dB/dm = 1$, and $d\beta/dt = 0$ because no phase change occurs. The general control volume equation for continuity, equation (3.3.1), is applicable:

$$0 = \frac{d}{dt} \int_{CV} \rho dV + \int_{CS} \rho \mathbf{V} \cdot d\mathbf{A} \quad (3.3.1)$$

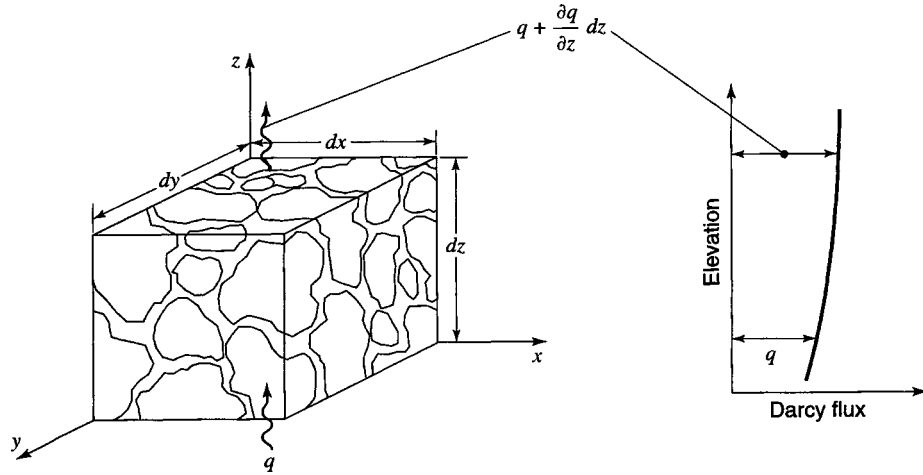


Figure 6.2.1 Control volume for development of the continuity equation in porous medium (from Chow et al. (1988)).

The time rate of change of mass stored in the control volume is defined as the time rate of change of fluid mass in storage, expressed as

$$\frac{d}{dt} \int_{CV} \rho \, dV = \rho S_s \frac{\partial h}{\partial t} (dxdydz) + \rho W (dxdydz) \quad (6.2.1)$$

where S_s is the specific storage and W is the flow out of the control volume, $W = Q/(dxdydz)$. The term $\rho S_s (\partial h / \partial t) (dxdydz)$ includes two parts: (1) the mass rate of water produced by an expansion of the water under change in density and (2) the mass rate of water produced by the compaction of the porous medium due to change in porosity (see Freeze and Cherry (1979) for more details).

The inflow of water through the control surface at the bottom of the control volume is $q dxdy$, and the outflow at the top is $[q + (\partial q / \partial z) dz] dxdy$, so that the net outflow in the vertical direction z is

$$\int_{CS(z)} \rho \mathbf{V} \cdot d\mathbf{A} = \rho \left(q + \frac{\partial q}{\partial z} dz \right) dxdy - \rho q dxdy = \rho dxdydz \frac{\partial q}{\partial z} \quad (6.2.2)$$

where q in $\partial q / \partial z$ is q_z , i.e., in the z direction.

Considering all three directions, we get

$$\int_{CS} \rho \mathbf{V} \cdot d\mathbf{A} = \rho dxdydz \frac{\partial q}{\partial x} + \rho dxdydz \frac{\partial q}{\partial y} + \rho dxdydz \frac{\partial q}{\partial z} \quad (6.2.3)$$

Substituting (6.2.1) and (6.2.3) into (3.3.1) results in

$$0 = \rho S_s \frac{\partial h}{\partial t} dxdydz + \rho W (dxdydz) + \rho dxdydz \frac{\partial q}{\partial x} + \rho dxdydz \frac{\partial q}{\partial y} + \rho dxdydz \frac{\partial q}{\partial z} \quad (6.2.4)$$

Dividing through by $\rho dxdydz$ gives

$$S_s \frac{\partial h}{\partial t} + \frac{\partial q}{\partial x} + \frac{\partial q}{\partial y} + \frac{\partial q}{\partial z} + W = 0 \quad (6.2.5)$$

Using Darcy's law, the Darcy flux in each direction is

$$q_x = -K_x \frac{\partial h}{\partial x} \quad (6.2.6a)$$

$$q_y = -K_y \frac{\partial h}{\partial y} \quad (6.2.6b)$$

$$q_z = -K_z \frac{\partial h}{\partial z} \quad (6.2.6c)$$

Substituting these definitions of q_x , q_y , and q_z into (6.2.5) and rearranging results in

$$\frac{\partial}{\partial x} \left(K_x \frac{\partial h}{\partial x} \right) + \frac{\partial}{\partial y} \left(K_y \frac{\partial h}{\partial y} \right) + \frac{\partial}{\partial z} \left(K_z \frac{\partial h}{\partial z} \right) = S_s \frac{\partial h}{\partial t} + W \quad (6.2.7)$$

This is the equation for *three-dimensional transient flow through a saturated anisotropic porous medium*. For a *homogeneous, isotropic medium* ($K_x = K_y = K_z$), equation (6.2.7) becomes

$$\frac{\partial^2 h}{\partial x^2} + \frac{\partial^2 h}{\partial y^2} + \frac{\partial^2 h}{\partial z^2} = \frac{S_s}{K} \frac{\partial h}{\partial t} + \frac{W}{K} \quad (6.2.8)$$

For a *homogeneous, isotropic medium and steady-state flow*, equation (6.2.8) becomes

$$\frac{\partial^2 h}{\partial x^2} + \frac{\partial^2 h}{\partial y^2} + \frac{\partial^2 h}{\partial z^2} = \frac{W}{K} \quad (6.2.9)$$

For a horizontal confined aquifer of thickness b , $S = S_s b$ and transmissivity $T = Kb$, the two-dimensional form of (6.2.8) with $W = 0$ becomes

$$\frac{\partial^2 h}{\partial x^2} + \frac{\partial^2 h}{\partial y^2} = \frac{S}{T} \frac{\partial h}{\partial t} \quad (6.2.10)$$

The governing equation for radial flow can also be derived using the control volume approach. Alternatively, equation (6.2.10) can be converted into radial coordinates by the relation $r = \sqrt{x^2 + y^2}$. This is known as the *diffusion equation*, expressed as

$$\frac{1}{r} \frac{\partial}{\partial r} \left(r \frac{\partial h}{\partial r} \right) = \frac{\partial^2 h}{\partial r^2} + \frac{1}{r} \frac{\partial h}{\partial r} = \frac{S}{T} \frac{\partial h}{\partial t} \quad (6.2.11)$$

where r is the radial distance from a pumped well and t is the time since the beginning of pumping. For steady-state conditions, $\partial h / \partial t = 0$, so equation (6.2.11) reduces to

$$\frac{1}{r} \frac{\partial}{\partial r} \left(r \frac{\partial h}{\partial r} \right) = 0 \quad (6.2.12)$$

6.2.2 Flow Nets

Flow nets provide a graphical means to illustrate two-dimensional groundwater flow problems. For steady-state conditions, the two-dimensional flow equation (6.2.10) for a homogeneous, isotropic medium becomes

$$\frac{\partial^2 h}{\partial x^2} + \frac{\partial^2 h}{\partial y^2} = 0 \tag{6.2.13}$$

This is the classic partial differential equation form known as the *Laplace equation*. Equation (6.2.13) is linear in terms of the piezometric head h , and its solution depends entirely on the values of h on the boundaries of a flow field in the x - y plane. In other words, h at any point in a flow field can be determined uniquely in terms of h on the boundaries. Laplace’s equation arises in other areas such as hydrodynamics and heat flow.

Velocity of flow is normal to lines of constant piezometric heads. This can be seen through examination of Darcy’s equations $v_x = K_x(\partial h/\partial x)$ and $v_y = -K_y(\partial h/\partial y)$ and continuity equation $(\partial v_x/\partial x) + (\partial v_y/\partial y) = 0$. Figure 6.2.2 is a hypothetical flow net. The velocity vector \mathbf{V} has components v_x and v_y with the resultant velocity vector in the direction of decreasing head h . The *streamlines* are a set of lines that are drawn tangent to the velocity vector and normal to the line of constant piezometric head. The family of streamlines is called the *stream function*, ψ . In steady flow, the streamlines define the paths of flowing particles of fluid. Because the streamlines are normal to the line of constant head, the velocities v_x and v_y can be expressed as

$$v_x = \frac{\partial \psi}{\partial x} \tag{6.2.14}$$

$$v_y = \frac{\partial \psi}{\partial y} \tag{6.2.15}$$

which can be substituted into the differential form of the two-dimensional equation of continuity:

$$\frac{\partial v_x}{\partial x} + \frac{\partial v_y}{\partial y} = 0 \tag{6.2.16}$$

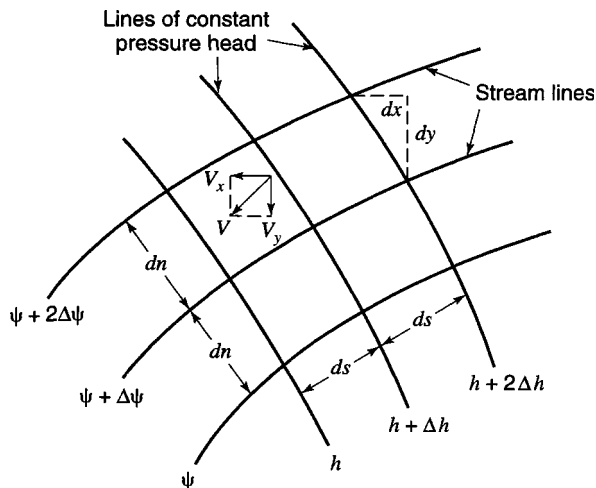


Figure 6.2.2 Hypothetical flow net.

resulting in

$$\frac{\partial^2 \Psi}{\partial x^2} + \frac{\partial^2 \Psi}{\partial y^2} = 0 \quad (6.2.17)$$

which is also the *Laplace equation* (see equation (6.2.13)).

Because the streamlines are everywhere tangent to velocity vectors, no flow exists across them. The rate of flow is constant between any two streamlines. The flow lines in Figure 6.2.2 have been constructed so that $ds = dh$. The discharge through a cross-sectional area of unit depth perpendicular to the flow net is

$$dq = K \frac{dh}{ds} dh \quad (6.2.18)$$

and since $ds = dh$ then

$$dq = Kdh \quad (6.2.19)$$

and with m sections

$$q = mKdh \quad (6.2.20)$$

If the total head drop across the region of flow is H and there are n divisions of head in the flow net ($H = ndh$), then

$$q = \frac{mKH}{n} \quad (6.2.21)$$

This equation is applicable only to simple flow systems with one recharge boundary and one discharge boundary.

The rate of flow between streamlines can also be expressed as

$$dq = v_x dx - v_y dy \quad (6.2.22)$$

Substituting (6.2.14) and (6.2.15) for v_x and v_y , we get

$$\frac{\partial \Psi}{\partial x} dx + \frac{\partial \Psi}{\partial y} dy = dq \quad (6.2.23)$$

which implies that

$$dq = d\Psi \quad (6.2.31)$$

The value of the stream function is numerically equal to the unit discharge. Also, the increment in unit discharge between two streamlines is equal to the change in the value of the stream function between two streamlines.

Figure 6.2.3 illustrates the development of the flow distribution through the use of *equipotential lines* and *flow lines*. Flow lines represent the paths followed by molecules of water as they move through an aquifer in the direction of decreasing head. Equipotential lines intersect the flow lines at right angles, representing the piezometric-surface or water-table contours. The two families of lines or curves together are referred to as a *flow net*.

Figure 6.2.3 illustrates two example applications showing the flow lines and equipotential lines that form the orthogonal network of cells making up the flow net. Theoretically, the flow through any one cell equals the flow through any other cell. This figure shows contrasting flow nets for channel seepage through layered anisotropic media.

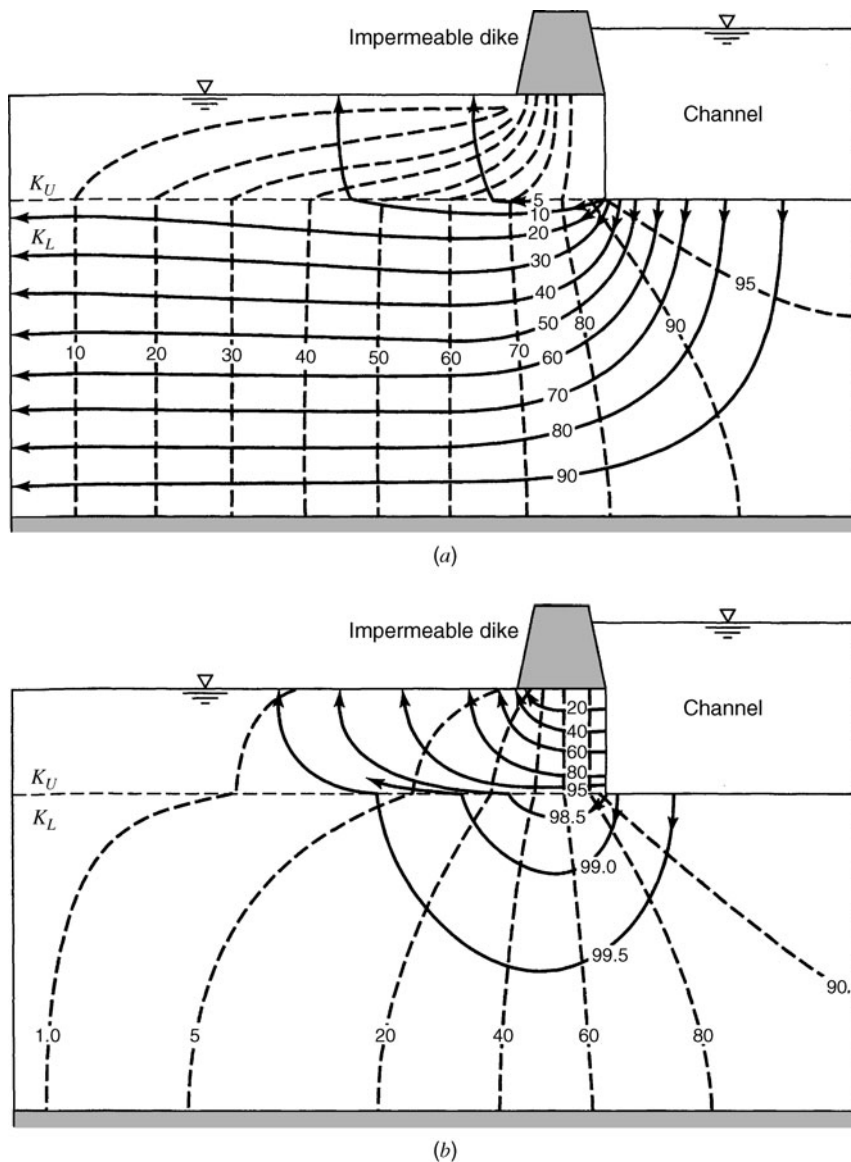


Figure 6.2.3 Flow nets for seepage from one side of a channel through two different anisotropic two-layer systems. (a) $K_U/K_L = 1/50$; (b) $K_U/K_L = 50$. The anisotropy ratio for all layers is $K_x/K_z = 10$ (after Todd and Bear (1961)).

6.3 STEADY-STATE ONE-DIMENSIONAL FLOW

Confined Aquifer

Consider steady-state groundwater flow in a confined aquifer of uniform thickness, as shown in Figure 6.3.1. For one-dimensional steady-state flow, $\partial^2 h / \partial y^2 = 0$ and $\partial h / \partial t = 0$, so equation

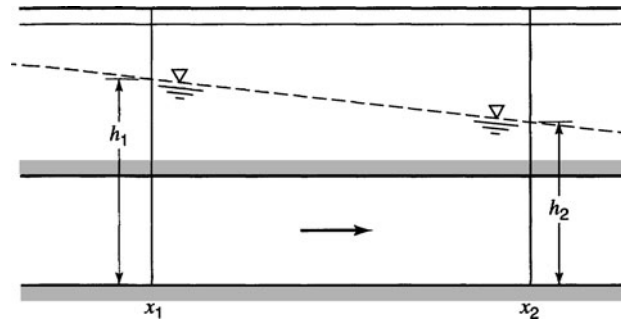


Figure 6.3.1 Flow in a one-dimensional confined aquifer.

(6.2.10) for $W = 0$ reduces to

$$\frac{\partial^2 h}{\partial x^2} = 0 \quad (6.3.1)$$

which has the solution

$$h = C_1 x + C_2 \quad (6.3.2)$$

where h is the head above a given datum and C_1 and C_2 are constants of integration. For $h = h_1$ at $x = 0$, $h = h_2$ at $x = L$, and $\partial h / \partial x = -(q/K)$ from Darcy's law (equation (6.2.6a)), then

$$h = q/K_x + \text{constant} \quad (6.3.3)$$

In other words, the head decreases linearly with flow in the x direction, as shown in Figure 6.3.1.

Unconfined Aquifer

For one-dimensional steady-state flow in an unconfined aquifer (Figure 6.3.2), a direct solution of equation (6.2.10) is not possible (see Todd and Mays, 2005). To obtain a solution, use Darcy's law, $q = -K(\partial h / \partial x)$, and by continuity define the discharge at any vertical section as

$$\sum_{CS} \rho \mathbf{V} \cdot d\mathbf{A} = Q = -Kh \frac{\partial h}{\partial x} \quad (6.3.4)$$

Equation (6.3.4) can be integrated over the distance from x_1 to x_2 where h_1 and h_2 are the respective heads; then

$$Q \int_{x_1}^{x_2} dx = K \int_{h_1}^{h_2} h dh \quad (6.3.5)$$

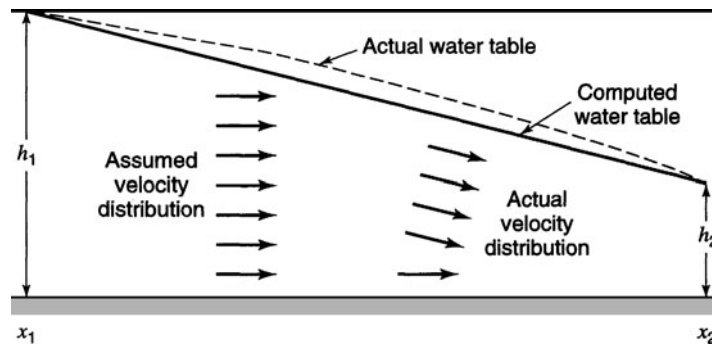


Figure 6.3.2 Flow in a one-dimensional unconfined aquifer.

which becomes

$$Q = K \frac{h_1^2 - h_2^2}{2(x_2 - x_1)} \tag{6.3.6}$$

Equation (6.3.6) indicates a parabolic surface of the saturated portion of the aquifer between x_1 and x_2 .

The assumptions in this derivation are (1) the velocity of flow is proportional to the tangent of the hydraulic gradient and (2) the flow is horizontal and uniform everywhere in a vertical section. The assumption of one-dimensional flow is valid, as velocities are small and dh/dx is small. Using the boundary conditions that $x_1 = 0$ and $h_1 = h_0$ and letting $x = X$ and $h = h_2$, then equation (6.3.6) reduces to the well-known *Dupuit equation*

$$Q = \frac{K}{2X} (h_0^2 - h^2) \tag{6.3.7}$$

Refer to Figure 6.3.3 for an example explanation.

EXAMPLE 6.3.1

A stratum of clean sand and gravel between two channels (see Figure 6.3.3) has a hydraulic conductivity $K = 10^{-1}$ cm/sec and is supplied with water from a ditch ($h_0 = 20$ ft deep) that penetrates to the bottom of the stratum. If the water surface in the second channel is 2 ft above the bottom of the stratum and its distance to the ditch is $x = 30$ ft, which is also the thickness of the stratum, what is the unit flow rate into the gallery?

SOLUTION

The flow is described using the Dupuit equation (6.3.7) for unit flow, where

$$K = 10^{-1} \text{ cm/sec} (60 \text{ sec/min})(1 \text{ in}/2.54 \text{ cm})(1 \text{ ft}/12 \text{ in})(7.48 \text{ gal}/1 \text{ ft}^3) = 1.54 \text{ gpm}/\text{ft}^2 = 2.22 \times 10^3 \text{ gpd}/\text{ft}^2$$

and

$$Q = \frac{1.5}{2(30)} (20^2 - 2^2) = 10.16 \text{ gpm}/\text{ft} = 1.46 \times 10^4 \text{ gpd}/\text{ft}$$

or in SI units with $K = 10^{-1}$ cm/s = 10^{-3} m/s and $h_0 = 20$ ft = 6.10 m, $h = 0.61$ m, and $x = 9.14$ m:

$$Q = \frac{1.0^{-3} (6.10^2 - 0.61^2)}{2(9.14)} = 2.02 \times 10^{-3} \text{ m}^3/\text{s}$$

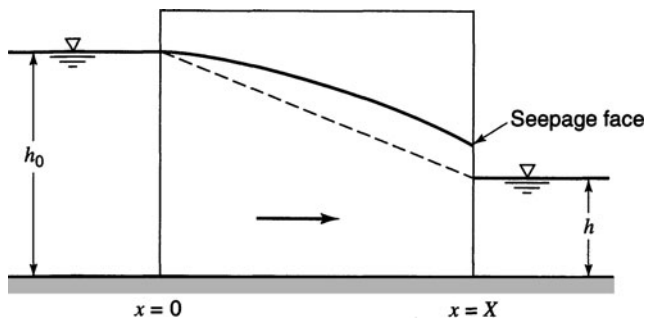


Figure 6.3.3 Steady flow in a one-dimensional unconfined aquifer between two bodies of water with vertical boundaries (application of Dupuit equation (6.3.7)).

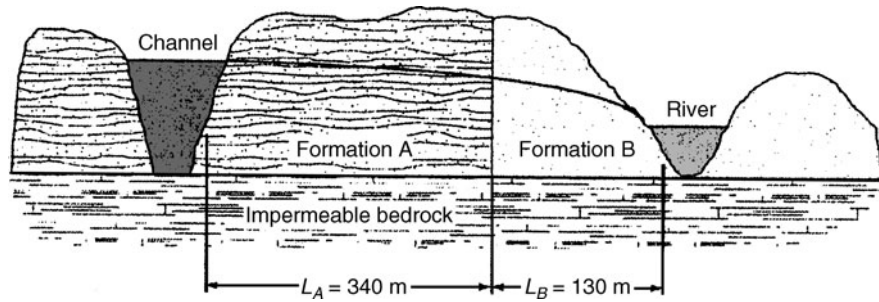


Figure 6.3.4 A channel and river for example 6.3.2.

EXAMPLE 6.3.2

For the channel and river shown in Figure 6.3.4, determine the volume of water that flows from the channel into the river. The water surface elevations in the channel and river with respect to the underlying bedrock are 13 and 10.5 m, respectively. The hydraulic conductivity of formation A is 5.6 m/day and that of formation B is 12.3 m/day.

SOLUTION

To account for multiple formations, first derive an expression by modifying the Dupuit equation (6.3.7). In developing the expression to account for multiple formations, subscript s denotes the separation, or divide, between the two formations so that h_s denotes the water table elevation at the separation. Under steady-state conditions, apply the Dupuit equation between the channel and the separation point, and between the separation point and the river in order to yield the same flow rate:

$$Q = \frac{K_A}{2L_A} (h_C^2 - h_s^2) = \frac{K_B}{2L_B} (h_s^2 - h_R^2)$$

Solving for h_s^2 gives

$$h_s^2 = \frac{\frac{K_A}{2L_A} h_C^2 + \frac{K_B}{2L_B} h_R^2}{\left(\frac{K_A}{2L_A} + \frac{K_B}{2L_B}\right)}$$

and substituting this expression for h_s^2 into the equation for the flow rate gives

$$Q = \frac{h_C^2 - h_R^2}{2 \left[\frac{L_A}{K_A} + \frac{L_B}{K_B} \right]}$$

Now substitute

$h_C = 13$ m, $h_R = 10.5$ m, $K_A = 5.6$ m/day, $K_B = 12.3$ m/day, $L_A = 340$ m, and $L_B = 130$ m:

$$Q = \frac{(13 \text{ m})^2 - (10.5 \text{ m})^2}{2 \left[\frac{340 \text{ m}}{5.6 \text{ m/day}} + \frac{130 \text{ m}}{12.3 \text{ m/day}} \right]} = 0.4121 \text{ m}^2/\text{day}$$

6.4 STEADY-STATE WELL HYDRAULICS

6.4.1 Flow to Wells

At initiation of discharge (pumpage) from a well, theoretically the water level or head in the well is lowered relative to the undisturbed condition of the piezometric surface or water table outside the well. In the aquifer surrounding the well, the water flows radially to the lower level in the well. For

artesian conditions, the actual flow distribution of the flow conforms relatively close to the theoretical shortly after pumping starts. However, in non-artesian (free aquifer) conditions the actual distribution of flow may not conform to the theoretical as illustrated by the successive stages of development of flow distribution in Figure 6.4.1.

The flow net in Figure 6.4.2 illustrates the distribution of flow in an artesian aquifer for a fully penetrating well and a 100-percent open hole. *Drawdown* is the distance the water level is lowered. When the drawdown falls below the bottom of the upper confining bed, a mixed condition of artesian and non-artesian flow occurs. The flow net in Figure 6.4.3 illustrates the distribution of flow in an artesian aquifer for a well that penetrates through the upper confining bed but not into the artesian aquifer. A strong vertical component of flow is established out to a distance approximately equal to the thickness of the aquifer. *Drawdown curves (cones)* show the variation of drawdown with distance from the well.

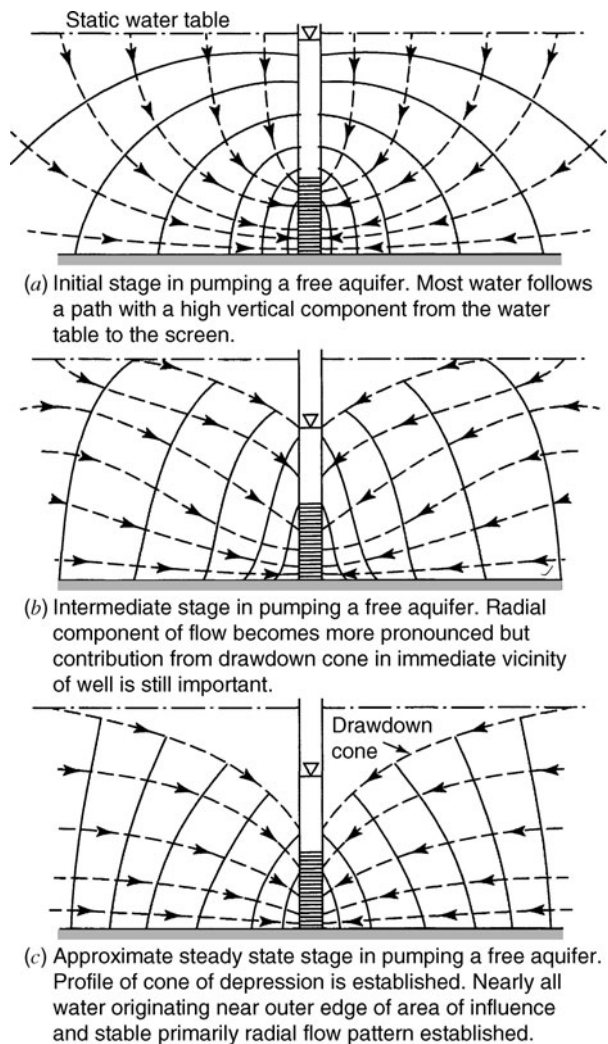


Figure 6.4.1 Development of flow distribution about a discharging well in a free aquifer—a fully penetrating and 33-percent open hole (from U.S. Bureau of Reclamation (1981)).

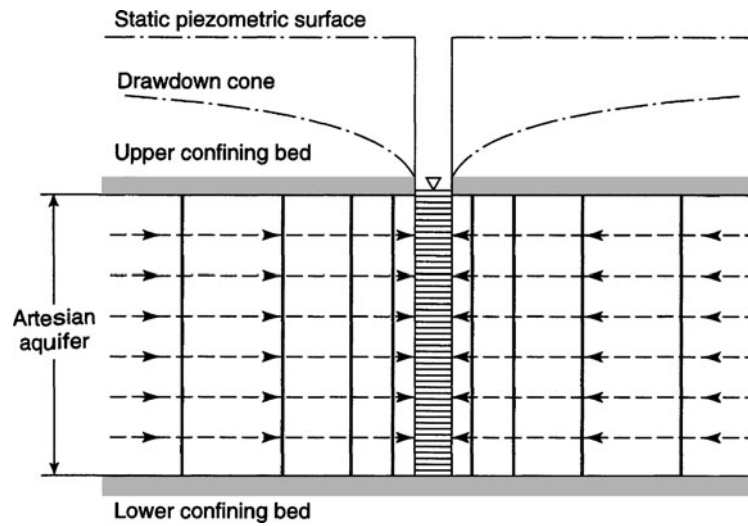


Figure 6.4.2 Distribution of flow to a discharging well in an artesian aquifer—a fully penetrating and 100-percent open hole (from U.S. Bureau of Reclamation (1981)).

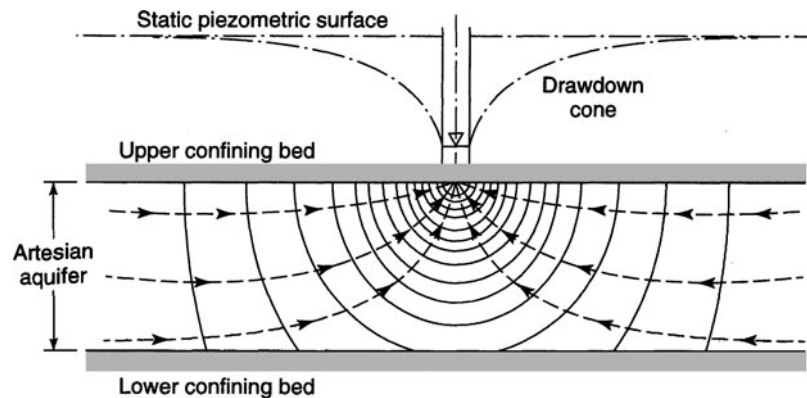


Figure 6.4.3 Distribution of flow to a discharging well—just penetrating to the top of an artesian aquifer (from U.S. Bureau of Reclamation (1981)).

6.4.2 Confined Aquifers

When pumping from a well, water is removed from the aquifer surrounding the well and the piezometric surface is lowered. *Drawdown* is the distance the piezometric surface is lowered (Figure 6.4.4). A radial flow equation can be derived to relate well discharge to drawdown. Consider the confined aquifer with steady-state radial flow to the fully penetrating well that is being pumped, as shown in Figure 6.4.5. For a homogenous, isotropic aquifer, the well discharge at any radial distance r from the pumped well is

$$\sum_{CS} \rho \mathbf{V} \cdot d\mathbf{A} = Q = 2\pi Kr b \frac{dh}{dr} \quad (6.4.1)$$

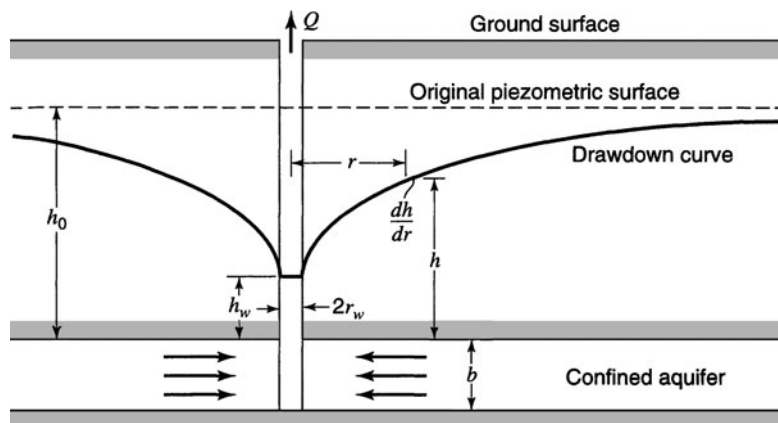


Figure 6.4.4 Well hydraulics for a confined aquifer.

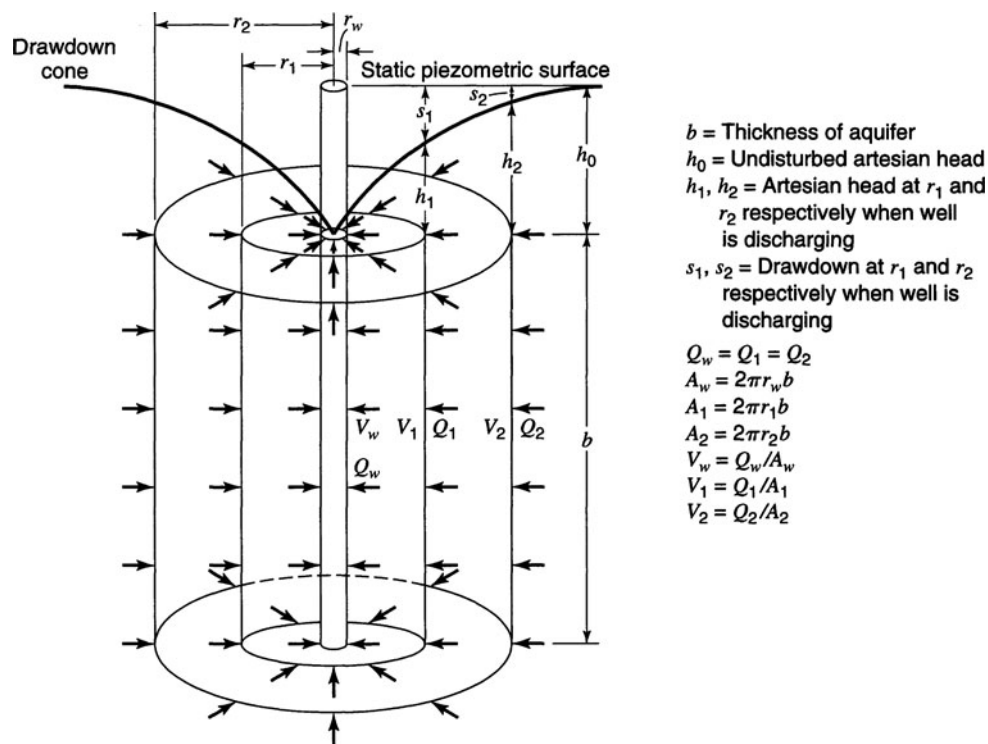


Figure 6.4.5 Flow distribution to a discharging well in an artesian aquifer—a fully penetrating and 100-percent open hole (from U.S. Bureau of Reclamation (1981)).

For boundary conditions of $h = h_1$ at $r = r_1$ and $h = h_2$ at $r = r_2$, then equation (6.4.1) can be integrated:

$$\int_{h_1}^{h_2} dh = \frac{Q}{2\pi Kb} \int_{r_1}^{r_2} \frac{dr}{r} \tag{6.4.2}$$

$$h_2 - h_1 = \frac{Q}{2\pi Kb} \ln \frac{r_2}{r_1}$$

Solving equation (6.4.2) for Q gives

$$Q = 2\pi K b \left[\frac{h_2 - h_1}{\ln(r_2/r_1)} \right] \quad (6.4.3)$$

For the more general case of a well penetrating an extensive confined aquifer, there is no limit for r . Referring to Figure 6.4.4, equation (6.4.3) becomes

$$Q = 2\pi K b \left[\frac{h - h_1}{\ln(r/r_1)} \right] \quad (6.4.4)$$

which shows that the head varies linearly with the logarithm of distance regardless of the rate of discharge.

Equation (6.4.4) is known as the *equilibrium* or *Thiem equation* and enables the aquifer permeability to be determined from a pumped well. Two points define the logarithmic drawdown curve, so drawdown can be measured at two observation wells at different distances from a well that is being pumped at a constant rate. The hydraulic conductivity can be computed using

$$K = \frac{Q \ln(r_2/r_1)}{2\pi b (h_2 - h_1)} \quad (6.4.5)$$

where r_1 and r_2 are the distances and h_1 and h_2 are the heads in the respective observation wells.

EXAMPLE 6.4.1

A well fully penetrates a 25-m thick confined aquifer. After a long period of pumping at a constant rate of $0.05 \text{ m}^3/\text{s}$, the drawdowns at distances of 50 m and 150 m from the well were observed to be 3 m and 1.2 m, respectively. Determine the hydraulic conductivity and the transmissivity. What type of unconsolidated deposit would you expect this to be?

SOLUTION

Use equation (6.4.5) to determine the hydraulic conductivity with $Q = 0.05 \text{ m}^3/\text{s}$, $r_1 = 50 \text{ m}$, $r_2 = 150 \text{ m}$, $s_1 = h_0 - h_1$ and $s_2 = h_0 - h_2$, so $s_1 - s_2 = h_2 - h_1 = 3 - 1.2 = 1.8 \text{ m}$:

$$K = \frac{Q \ln(r_2/r_1)}{2\pi b (s_1 - s_2)} = \frac{0.05 \ln(150/50)}{2\pi (25)(3 - 1.2)} = 1.94 \times 10^{-4} \text{ m/s}$$

Then the transmissivity is $T = Kb = (1.94 \times 10^{-4})(25) = 4.85 \times 10^{-3} \text{ m}^2/\text{s}$. From Table 6.1.1 for $K = 1.94 \times 10^{-4} \text{ m/s}$, this is probably a clean sand or silty sand.

EXAMPLE 6.4.2

A 2-ft diameter well penetrates vertically through a confined aquifer 50 ft thick. When the well is pumped at 500 gpm, the drawdown in a well 50 ft away is 10 ft and in another well 100 ft away is 3 ft. What is the approximate head in the pumped well for steady-state conditions, and what is the approximate drawdown in the well? Also compute the transmissivity. Take the initial piezometric level as 100 ft above the datum.

SOLUTION

First determine the hydraulic conductivity using equation (6.4.5):

$$K = \frac{Q \ln(r_2/r_1)}{2\pi b (h_2 - h_1)} = \frac{500 \ln(100/50)}{2\pi (50)(97 - 90)} = 0.158 \text{ gpm/ft}^2$$

Then compute the transmissivity:

$$T = Kb = 0.158 \times 50 = 7.90 \text{ gpm/ft}$$

Now compute the approximate head, h_w , in the pumped well:

$$h_2 - h_w = \frac{Q \ln(r_2/r_1)}{2\pi K b}$$

$$h_w = h_2 - \frac{Q \ln(r_2/r_w)}{2\pi K b}$$

$$h_w = 97 - \frac{500 \ln(100/1)}{2\pi(7.90)} = 97 - 46.4 = 50.6 \text{ ft}$$

Drawdown is then $s_w = 100 - 50.6 \text{ ft} = 49.6 \text{ ft}$.

6.4.3 Unconfined Aquifers

Now consider steady radial flow to a well completely penetrating an unconfined aquifer as shown in Figure 6.4.6. A concentric boundary of constant head surrounds the well. The well discharge is given by

$$\sum_{CS} \rho \mathbf{V} \cdot d\mathbf{A} = Q = 2\pi K h r \frac{dh}{dr} \tag{6.4.6}$$

Integrating equations (6.4.6) with the boundary conditions $h = h_1$ at $r = r_1$ and $h = h_2$ at $r = r_2$ yields

$$\int_{h_1}^{h_2} h \, dh = \frac{Q}{2\pi K} \int_{r_1}^{r_2} \frac{dr}{r} \tag{6.4.7}$$

$$Q = \pi K \left[\frac{h_2^2 - h_1^2}{\ln(r_2/r_1)} \right] \tag{6.4.8}$$

There are large vertical flow components near the well so that this equation fails to describe accurately the drawdown curve near the well, but can be defined for any two distances r_1 and r_2 away from the pumped well.

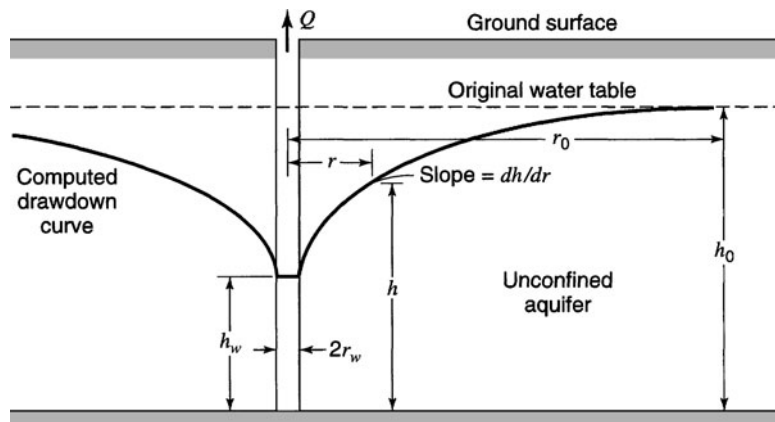


Figure 6.4.6 Well hydraulics for an unconfined aquifer.

EXAMPLE 6.4.3

A well penetrates an unconfined aquifer. Prior to pumping, the water level (head) is $h_0 = 25$ m. After a long period of pumping at a constant rate of $0.05 \text{ m}^3/\text{s}$, the drawdowns at distances of 50 m and 150 m from the well were observed to be 3 m and 1.2 m, respectively. Determine the hydraulic conductivity. What type of deposit would the aquifer material probably be?

SOLUTION

Use equation (6.4.8) and solve for K :

$$K = \frac{Q \ln(r_2/r_1)}{\pi(h_2^2 - h_1^2)}$$

and solve for K with $Q = 0.05 \text{ m}^3/\text{s}$, $r_1 = 50$ m, $r_2 = 150$ m, $h_1 = 25 - 3 = 22$ m, and $h_2 = 25 - 1.2 = 23.8$ m:

$$K = \frac{0.05 \ln(150/50)}{\pi(23.8^2 - 22^2)} = \frac{1.7494 \times 10^{-2}}{(566.4 - 484)} = 2.12 \times 10^{-4} \text{ m/s}$$

The deposit is probably a silty sand or a clean sand.

EXAMPLE 6.4.4

A well 12-in in diameter penetrates 108 ft below the static water table. After a long period of pumping at a rate of 350 gpm, the drawdowns in wells 57 ft and 148 ft from the pumped well were found to be 12 ft and 7.4 ft respectively. What is the transmissivity of the aquifer? What is the approximate drawdown in the pumped well?

SOLUTION

Use equation (6.4.8) for steady-state radial flow to a well in an unconfined aquifer, where $h_1 = 108 - 12 = 96$ ft; $h_2 = 108 - 7.4 = 100.6$ ft; $r_2 = 148$ ft; and $r_1 = 57$ ft. Determine the hydraulic conductivity using equation (6.4.8):

$$K = \frac{Q \ln(r_2/r_1)}{\pi(h_2^2 - h_1^2)} = \frac{350 \cdot \ln(148/57)}{\pi[100.6^2 - 96^2]} = 0.118 \text{ gpm/ft}^2$$

$$T = Kb = 0.118 \times 108 = 12.74 \text{ gpm/ft}$$

Solve for the approximate head and approximate drawdown at the well:

$$h_w = \sqrt{100.6^2 - \frac{350 \cdot \ln(148/0.5)}{\pi \cdot (0.118)}} = 68.90 \text{ ft}$$

$$s_w = 108 - 68.90 = 39.10 \text{ ft.}$$

6.5 TRANSIENT WELL HYDRAULICS—CONFINED CONDITIONS**6.5.1 Nonequilibrium Well Pumping Equation**

Consider the confined aquifer with transient flow conditions due to a constant pumping rate $Q(L^3/T)$ at the well shown in Figure 6.4.4. The initial condition is a constant head throughout the aquifer, $h(r, 0) = h_0$ for all r where h_0 is the constant initial head at $t = 0$. The boundary condition assumes (1) no drawdown in hydraulic head at the infinite boundary, $h(\infty, t) = h_0$ for all t with a constant pumping rate and (2) Darcy's law applies:

$$\lim_{r \rightarrow 0} \left(r \frac{\partial h}{\partial r} \right) = \frac{Q}{2\pi T} \text{ for } t > 0 \quad (6.5.1)$$

The governing differential equation is (6.2.11):

$$\frac{\partial^2 h}{\partial r^2} + \frac{1}{r} \frac{\partial h}{\partial r} = \frac{S}{T} \frac{\partial h}{\partial t} \tag{6.2.11}$$

The confined aquifer is nonleaky, homogeneous, isotropic, infinite in areal extent, and the same thickness throughout. The wells fully penetrate the aquifer and are pumped at a constant rate Q . During pumping of such a well, water is withdrawn from storage within the aquifer, causing the cone of depression to progress outward from the well. There is no stabilization of water levels, resulting in a continual decline of head, provided there is no recharge and the aquifer is effectively infinite in areal extent. The rate of decline of the head, however, continuously decreases as the cone of depression spreads. Water is released from storage by compaction of the aquifer and by the expansion of the water. Theis (1935) presented an analytical solution of equation (6.2.11) to solve for the *drawdown* s given as

$$s = h_0 - h = \frac{Q}{4\pi T} \int_u^\infty \left(\frac{e^{-u}}{u} \right) du \tag{6.5.2}$$

where h_0 is the piezometric surface before pumping started, Q is the constant pumping rate (L^3/T), T is the transmissivity (L^2/T), and

$$u = \frac{r^2 S}{4Tt} \tag{6.5.3}$$

in which r is in L and t is time in T .

The exponential integral can be expanded into a series expansion as

$$W(u) = \int \left(\frac{e^{-u}}{u} \right) du = -0.5772 - \ln u + u - \frac{u^2}{2 \cdot 2!} + \frac{u^3}{3 \cdot 3!} + \dots \tag{6.5.4}$$

where $W(u)$ is called the dimensionless *well function* for nonleaky, isotropic, artesian aquifers fully penetrated by wells having constant discharge conditions. Values of this well function are listed in Table 6.5.1. The well function is also expressed in the form of a type curve, as shown in Figure 6.5.1. Both u and $W(u)$ are dimensionless.

Table 6.5.1 Values of $W(u)$ for Various Values of u

u	1.0	2.0	3.0	4.0	5.0	6.0	7.0	8.0	9.0
$\times 1$	0.219	0.049	0.013	0.0038	0.0011	0.00036	0.00012	0.000038	0.000012
$\times 10^{-1}$	1.82	1.22	0.91	0.70	0.56	0.45	0.37	0.31	0.26
$\times 10^{-2}$	4.04	3.35	2.96	2.68	2.47	2.30	2.15	2.03	1.92
$\times 10^{-3}$	6.33	5.64	5.23	4.95	4.73	4.54	4.39	4.26	4.14
$\times 10^{-4}$	8.63	7.94	7.53	7.25	7.02	6.84	6.69	6.55	6.44
$\times 10^{-5}$	10.94	10.24	9.84	9.55	9.33	9.14	8.99	8.86	8.74
$\times 10^{-6}$	13.24	12.55	12.14	11.85	11.63	11.45	11.29	11.16	11.04
$\times 10^{-7}$	15.54	14.85	14.44	14.15	13.93	13.75	13.60	13.46	13.34
$\times 10^{-8}$	17.84	17.15	16.74	16.46	16.23	16.05	15.90	15.76	15.65
$\times 10^{-9}$	20.15	19.45	19.05	18.76	18.54	18.35	18.20	18.07	17.95
$\times 10^{-10}$	22.45	21.76	21.35	21.06	20.84	20.66	20.50	20.37	20.25
$\times 10^{-11}$	24.75	24.06	23.65	23.36	23.14	22.96	22.81	22.67	22.55
$\times 10^{-12}$	27.05	26.36	25.96	25.67	25.44	25.26	25.11	24.97	24.86
$\times 10^{-13}$	29.36	28.66	28.26	27.97	27.75	27.56	27.41	27.28	27.16
$\times 10^{-14}$	31.66	30.97	30.56	30.27	30.05	29.87	29.71	29.58	29.46
$\times 10^{-15}$	33.96	33.27	32.86	32.58	32.35	32.17	32.02	31.88	31.76

Source: Wenzel (1942).

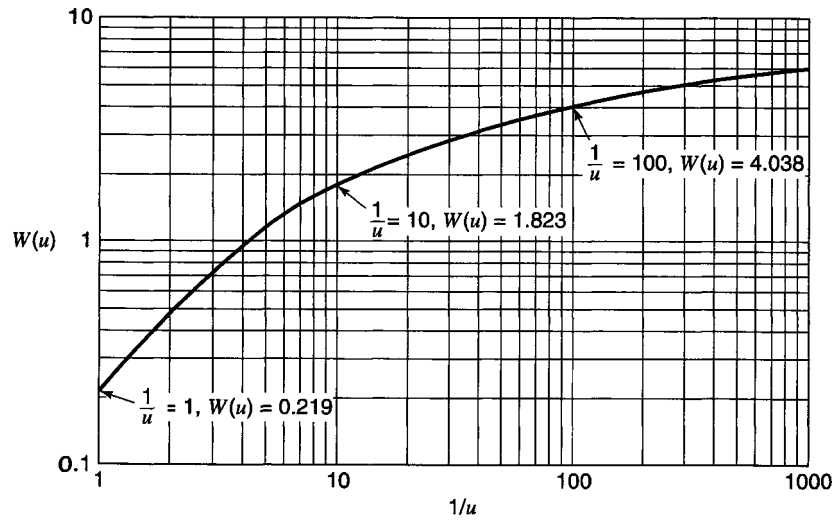


Figure 6.5.1 Type curve for use in solving the Theis's nonequilibrium equation graphically with values of $W(u)$ (well function of u) corresponding to values of $1/u$. The curve is plotted on a logarithmic scale.

The drawdown is then expressed as

$$s = \frac{Q}{4\pi T} W(u) \quad (6.5.5)$$

where Q is m^3/day and T is m^2/day for s in m ; or Q is gal/day and T is gpd/ft for s in ft ; or Q is ft^3/day and T is ft^2/day for s in ft . This equation is commonly referred to as the *nonequilibrium well pumping equation* or *Theis's equation*.

Equations (6.5.3) and (6.5.5) can be expressed in U.S. customary units (gallon-day-foot system) where s is in ft , Q is in gpm , T is in gpd/ft , r is in ft , and t is in days:

$$s = \frac{114.6Q}{T} W(u) \quad (6.5.6)$$

and

$$u = \frac{1.87r^2S}{Tt} \quad (6.5.7)$$

or, for t in minutes,

$$u = \frac{2693r^2S}{Tt} \quad (6.5.8)$$

EXAMPLE 6.5.1

Given that $T = 10,000$ gpd/ft , $S = 10^{-4}$, $t = 2693$ min , $Q = 1000$ gpm , and $r = 1000$ ft , compute the drawdown.

SOLUTION

Step 1. Compute u : (for r in ft , T in gpd/ft , t in minutes)

$$u = \frac{2693r^2S}{Tt} = \frac{2693 \times 10^6 \times 10^{-4}}{10^4 \times 2693} = 10^{-2}$$

Step 2. Find $W(u)$ from Table 6.5.1: $W(u) = 4.04$

Step 3. Compute drawdown: (for Q in gal/min and T in gpd/ft)

$$s = \frac{114.6 Q}{T} W(u) = \frac{114.6 \times 10^3 \times 4.04}{10^4} = 46.30 \text{ ft}$$

6.5.2 Graphical Solution

Theis (1935) developed a graphical procedure for determining T and S , using time-drawdown data by expressing equation (6.5.6) as

$$\log s = \log\left(\frac{114.6Q}{T}\right) + \log W(u) \tag{6.5.9}$$

and equation (6.5.8) as

$$\log t = \log\left(\frac{2693r^2S}{T}\right) + \log \frac{1}{u} \tag{6.5.10}$$

Because $(114.6Q/T)$ and $(2693r^2S/T)$ are constants for a given distance r from the pumped well, the relation between $\log(s)$ and $\log(t)$ must be similar to the relation between $\log W(u)$ and $\log 1/u$. Therefore, if s is plotted against t and $W(u)$ against $1/u$ on the same double-logarithmic paper, the resulting curves are of the same shape, but horizontally and vertically offset by the constants $(114.6Q/T)$ and $(2693r^2S/T)$. Plot each curve on a separate sheet, then match them by placing one graph on top of the other and moving it horizontally and vertically (keeping the coordinate axis parallel) until the curves are matched. This is further illustrated in Figure 6.5.2.

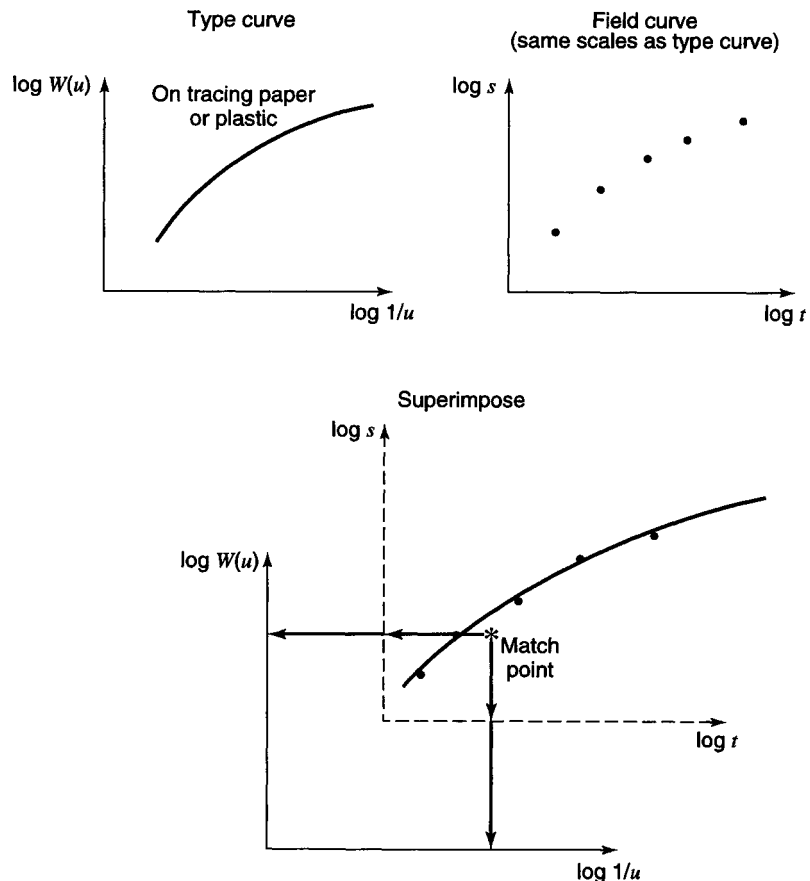


Figure 6.5.2 Graphical procedure to determine T and S from pump test data.

This graphical procedure is used to determine T and S from a field pumping test and requires measurements of a drawdown in at least one observation well. The observation of water levels should be made at proper intervals of time after the instant that pumping starts. Measurements from more than one observation well can also be used.

EXAMPLE 6.5.2

Pump test data (s vs. t) for an observation well are been plotted on log-log paper. The discharge was 150 gpm, and the observation well is 300 ft from the pumped well. The match points for the fitted data are at $W(u) = 1.0$ and $u = 1.0$, $t = 5.5$ min and $s = 0.112$ ft. Compute T and S .

SOLUTION

$$T = \frac{114.6Q}{s} W(u) = \frac{114.6(150)(1)}{0.112} = 153,482 \text{ gpd/ft}$$

and

$$S = \frac{Ttu}{2693r^2} = \frac{(153,482)(5.5)(1)}{2693(300)^2} = 0.00348$$

EXAMPLE 6.5.3

Drawdown was measured during a pumping test at frequent intervals in an observation well 200 ft from a well that was pumped at a constant rate of 500 gpm. The data for this pump test are listed below. These measurements show that the water level is still dropping after 4000 min of pumping; therefore, analysis of the test data requires use of the Theis's nonequilibrium procedure. Determine T and S for this aquifer.

Pump test data	
Time (min)	Drawdown (ft)
1	0.05
2	0.22
3	0.40
4	0.56
5	0.70
7	0.94
10	1.2
20	1.8
40	2.5
100	3.4
300	4.5
1000	5.6
4000	7.0

SOLUTION

Step 1. Plot the time-drawdown data on log-log graph paper. The drawdown is plotted on the vertical axis and the time since pumping started on the horizontal axis.

Step 2. Superimpose this plot on the type curve sheet so that the plotted points match the type curve. The axes of both graphs must be kept parallel.

Step 3. Select a match point, which can be any point in the overlap area of the curve sheets. It is usually found most convenient to select a match point where the coordinates on the type curve are known in advance (e.g., $W(u) = 1$ and $1/u = 1$ or $W(u) = 1$ and $1/u = 10$, etc.). Then determine the value of s and t for this match point: $W(u) = 1$, $s = 1$, $1/u = 1$, and $t = 2$.

Step 4. Determine T :

$$T = \frac{114.6Q}{s} W(u) = \frac{114.6 \times 500}{1} \times 1 = 57,300 \text{ gpd/ft}$$

Step 5. Determine S :

$$S = \frac{Tt}{\frac{1}{u} \times 2693r^2} = \frac{57,300 \times 2}{1 \times 2693 \times 200^2} = 1.06 \times 10^{-3}$$

The above procedure can also be used to determine the drawdown in observation wells at rates of pumping different from those used in the pump test. The Theis nonequilibrium analysis can also be used to determine distance-drawdown information, once the T and S are known for a given time after pumping started. Equations (6.5.6) and (6.5.8) can be expressed as

$$\log s = \log\left(\frac{114.6Q}{T}\right) + \log W(u) \quad (6.5.9)$$

and

$$\log(r^2) = \log\left(\frac{Tt}{2693S}\right) - \log\frac{1}{u} \quad (6.5.11)$$

If the values of Q , T , and S are known (determined from a pump test), then the distance-drawdown curve can be determined for any time t . The terms $(114.6Q/T)$ and $(Tt/2693S)$ are known, and for an assumed match point ($W(u)$ and $1/u$), s and r^2 can be determined.

EXAMPLE 6.5.4

For a pumping rate of 100 gpm in a confined aquifer with $T = 10^4$ gpd/ft and $S = 10^{-4}$, determine the distance-drawdown (r^2 , s) curve after 269.3 min.

SOLUTION

Step 1. Assume $W(u)$ and $1/u$ to compute match points (e.g., $W(u) = 1$ and $1/u = 1$).

Step 2. Compute s :

$$s = \frac{114.6Q}{T} W(u) = \frac{114.6(100)}{10^4} (1) = 1.146 \text{ ft}$$

Compute r^2 :

$$r^2 = \frac{Ttu}{2693S} = \frac{10^4(269.3)(1)}{2693S(10^{-4})} = 10^7 \text{ ft}^2$$

Step 3. Use the computed match points to align the graph of s on the vertical scale and r^2 on the horizontal scale to the type curve. In other words, match points (r^2 , s) with $(1/u, W(u))$ by superimposing the graph sheet onto the type curve. Keep all axes parallel. Once the points are matched, trace the type curve on the (r^2 , s) graph sheet to form the distance-drawdown curve for t minutes after pumping started.

6.5.3 Cooper–Jacob Method of Solution

Time-Drawdown Analysis

Theis's method for nonequilibrium analysis was simplified by Cooper and Jacob (1946) for the conditions of small values of r and large values of t . From equation (6.5.3), it can be observed that, for small values of r or large values of t , u is small, so that the higher-order terms in equation (6.5.4)

become negligible. Then the well function can be expressed as

$$W(u) = -0.5772 - \ln u \quad (6.5.12)$$

which has an error < 3% for $u < 0.1$. The drawdown for this approximation is expressed in U.S. customary units (gallon-day-foot) as

$$s = \frac{114.6 Q}{T} [-0.5772 - \ln u] \quad (6.5.13)$$

and in SI units as

$$s = \frac{Q}{4\pi T} [-0.5772 - \ln u] \quad (6.5.14)$$

Substituting equation (6.5.13) in equation (6.5.8) yields

$$s = \frac{114.6 Q}{T} \left[-0.5772 - \ln \frac{2693r^2 S}{Tt} \right] \quad (6.5.15)$$

This shows that the drawdown is a function of $\log t$ so that the equation plots as a straight line on semilog paper.

Consider the change in drawdown Δs a distance r from the pumped well over the time interval t_1 and t_2 , which are one log cycle apart. The drawdowns at t_1 and t_2 are, respectively, s_1 and s_2 . The change in drawdown Δs is then expressed as

$$\begin{aligned} \Delta s &= s_2 - s_1 = \frac{264 Q}{T} \left[\log \left(\frac{Tt_2}{2693r^2 S} \right) - \log \left(\frac{Tt_1}{2693r^2 S} \right) \right] \\ &= \frac{264 Q}{T} \log \left(\frac{t_2}{t_1} \right) \end{aligned} \quad (6.5.16)$$

If t_2 and t_1 are chosen one log cycle apart, $\log(t_2/t_1) = 1$, the above equation simplifies to

$$\Delta s = \frac{264 Q}{T} \quad (6.5.17)$$

in which Q is in gpm and T is in gpd/ft.

Next consider that at time t_0 , when pumping begins, the drawdown is 0 in the observation well r ft from the pumped well, so that equation (6.5.15) is expressed as

$$0 = \frac{114.6 Q}{T} \left[-0.5772 + 2.3 \log \frac{Tt}{2693r^2 S} \right] \quad (6.5.18)$$

This equation then reduces to

$$S = \frac{Tt_0}{4790 r^2} \quad (6.5.19)$$

The time t_0 is the time intercept on the zero-drawdown axis, keeping in mind that Jacob's method is a straight-line approximation on semilog paper. Refer to Figure 6.5.3.

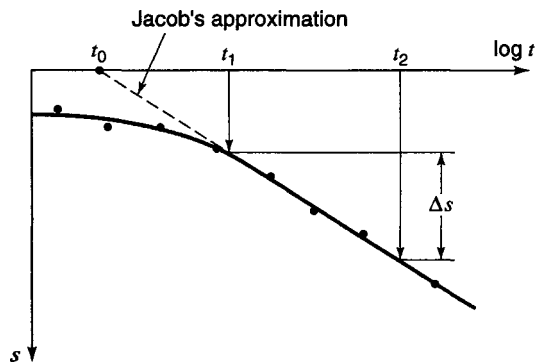


Figure 6.5.3 Illustration of Jacob's method showing the straight-line approximation on semilog paper.

EXAMPLE 6.5.5

For the time-drawdown data listed below, calculate T and S using Jacob's approximation. After computing T and S , check to see that the basic assumption of this approximation is satisfied. For the values of T and S that you computed, after how many minutes of pumping would Jacob's approximation be valid? The discharge is $Q = 1500$ gpm and the radius $r = 300$ ft.

Time after pumping started (min)	Drawdown (ft)
1	0.45
2	0.74
3	0.91
4	1.04
6	1.21
8	1.32
10	1.45
30	2.02
40	2.17
50	2.30
60	2.34
80	2.50
100	2.67
200	2.96
400	3.25
600	3.41
800	3.50
1000	3.60
1440	3.81

SOLUTION

- Step 1. Plot the field data on semilog paper (s vs. $\log t$) as shown in Figure 6.5.4.
- Step 2. Fit a straight line to the data (Figure 6.5.4).
- Step 3. Find t_0 from the plot ($t_0 = 0.45$ min for $s = 0$).
- Step 4. Find Δs for values of t_1 and t_2 one log cycle apart ($t_1 = 10$ min and $t_2 = 100$ min): $\Delta s = s_2 - s_1 = 2.67 - 1.45 = 1.08$ ft.
- Step 5. Compute T (from equation (6.5.17)):

$$T = \frac{264 Q}{\Delta s} = \frac{264(1500)}{1.08} = 366,700 \text{ gpd/ft}$$

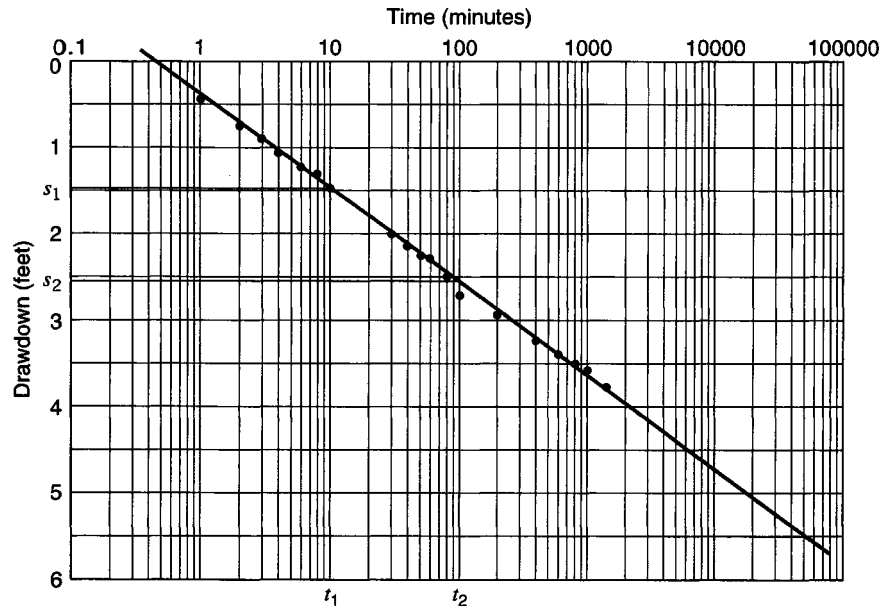


Figure 6.5.4 Time-drawdown for example 6.5.5.

Step 6. Compute S :

$$S = \frac{Tt_0}{4790 r^2} = \frac{366,700(0.45)}{4790(300^2)} = 3.83 \times 10^{-4}$$

Step 7. Check to see if basic assumption is satisfied:

$$u = \frac{2693(300)^2(3.83 \times 10^{-4})}{366,700(1440)} = 0.00017 < 0.01 \quad \text{OK}$$

Jacob's approximation for this problem is valid for

$$t \geq \frac{2693r^2S}{Tu} = \frac{2693(300)^2(3.83 \times 10^{-4})}{366,700(0.01)} \quad \text{where } u = 0.01$$

$$t \geq 25.3 \text{ min}$$

Distance–Drawdown Analysis

A similar analysis using Jacob's approximation can be used to approximate T and S using distance-drawdown field data. The drawdown must be measured simultaneously in three or more observation wells, each at a different distance from the pumped well. The drawdowns in the observation wells plot as a straight line on semilog paper (s vs. $\log r$). By considering the distance r_0 from the pumped well, where the drawdown is 0, then equation (6.5.15) can be expressed as

$$0 = \frac{114.6 Q}{T} \left[-0.5772 - \ln \frac{2693r_0^2 S}{Tt} \right] \quad (6.5.20)$$

which can be simplified to

$$S = Tt/4790r_0^2 \quad (6.5.21)$$

where r_0 is the intercept at $s = 0$ of the extended straight line fitted to the field distance-drawdown data.

Following the same procedure as for the time-drawdown analysis, consider the change in drawdown $\Delta s = s_2 - s_1$ at a time t over the distance r_2 to r_1 , where r_2 and r_1 are chosen to be one log cycle apart on the plot. The drawdowns at r_1 and r_2 are, respectively, s_1 and s_2 . The change in drawdown Δs is then expressed as

$$\Delta s = s_2 - s_1 = \frac{264 Q}{T} \left[\log \frac{2693 r_2^2 S}{Tt} - \log \frac{2693 r_1^2 S}{Tt} \right] = \frac{528 Q}{T} \log \left(\frac{r_2}{r_1} \right) \quad (6.5.22)$$

Because r_2 and r_1 are chosen one log cycle apart, ($\log r_2/r_1 = 1$), the above equation simplifies to

$$\Delta s = \frac{528 Q}{T} \quad (6.5.23)$$

EXAMPLE 6.5.6

A well is pumped at 200 gpm for a period of 500 min. Three observation wells 1, 2, and 3 (50, 30, and 100 ft from the pumped well, respectively) have drawdowns of 10.6, 13.2, and 7.9 ft, respectively. Determine T and S . (From Gehm and Bregman, 1976.)

SOLUTION

- Step 1. Plot the field data on semilog paper (s vs. $\log r$) as shown in Figure 6.5.5.
- Step 2. Fit a straight line to the data (Figure 6.5.5).
- Step 3. Find r_0 from the plot ($r_0 = 500$ ft).
- Step 4. Find Δs for values of r_1 and r_2 that are selected one log-cycle apart: $\Delta s = s_2 - s_1 = 10.6$ ft.
- Step 5. Compute T (from equation (6.5.23)):

$$T = \frac{528 Q}{\Delta s} = \frac{528(200)}{10.6} = 9960 \text{ gpd/ft}$$

Step 6. Compute S :

$$S = \frac{Tt}{4790r_0^2} = \frac{9960(500)}{4790(500^2)} = 4.16 \times 10^{-3}$$

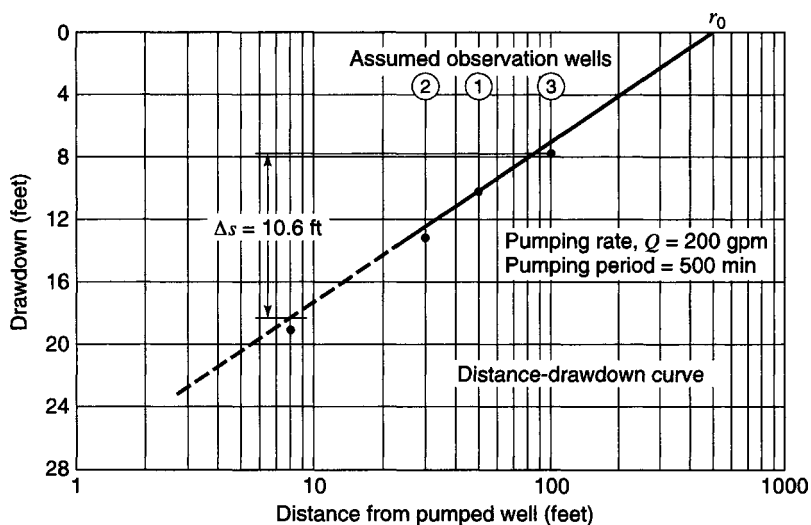


Figure 6.5.5 Trace of the cone of depression plotted on semilog coordinates becomes a straight line. Drawdown in each well was measured at 500 min after starting the pumping test.

6.6 TRANSIENT WELL HYDRAULICS—UNCONFINED CONDITIONS

Unconfined (water table) conditions differ significantly from those of the confined aquifer. For unconfined conditions, the pumped water is derived from storage by gravity drainage of the interstices above the cone of depression, by compaction of the aquifer and expansion of the water as pressure is reduced from pumping. For confined conditions, the nonequilibrium solution is based on the assumptions that the coefficient of storage is constant and water is released from storage instantaneously with a decline in head. The effects of gravity drainage are not considered in the nonequilibrium solution. Gravity drainage is not immediate and, for unsteady flow of water toward a well for unconfined conditions, is characterized by slow drainage of interstices.

There are three distinct segments of the time-drawdown curve for water table conditions, as shown in Figure 6.6.1. The first segment occurs for a short time after pumping begins: the drawdown reacts in the same manner as an artesian aquifer. In other words, the gravity drainage is not immediate, and the water is released instantaneously from storage. It is possible under some conditions to determine the coefficient of transmissivity by applying the nonequilibrium solution to the early time-drawdown data. The coefficient of storage computed using the early time-drawdown is in the artesian range and cannot be used to predict long-term drawdowns. The second segment represents an intermediate stage when the expansion of the cone of depression decreases because of the gravity drainage. The slope of the time-drawdown curve decreases, reflecting recharge. Pump test data deviate significantly from the nonequilibrium theory during the second segment. During the third segment (Figure 6.6.1), the time-drawdown curves conform closely to the nonequilibrium type curves, as shown in Figure 6.6.2. This segment may start from several minutes to several days after pumping starts, depending upon the aquifer condition. The coefficient of transmissivity of an aquifer can be determined by applying the nonequilibrium solution to the third segment of time-drawdown data. The coefficient of storage computed from these data will be in the unconfined range, which can be used to predict long-term effects.

Prickett (1965) and Neuman (1975) developed type curve solutions for water table conditions. The following equation for drawdown in an unconfined aquifer with fully penetrating wells and a constant discharge condition Q was presented by Neuman (1975):

$$s = \frac{Q}{4\pi T} W(u_a, u_y, \eta) \quad (6.6.1)$$

where

$$u_a = \frac{r^2 S}{Tt} \quad (\text{applicable for small values of } t) \quad (6.6.2)$$

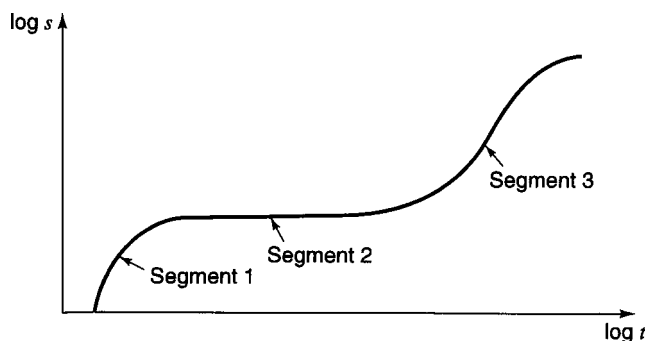


Figure 6.6.1 Three segments of time-drawdown curve for water table conditions.

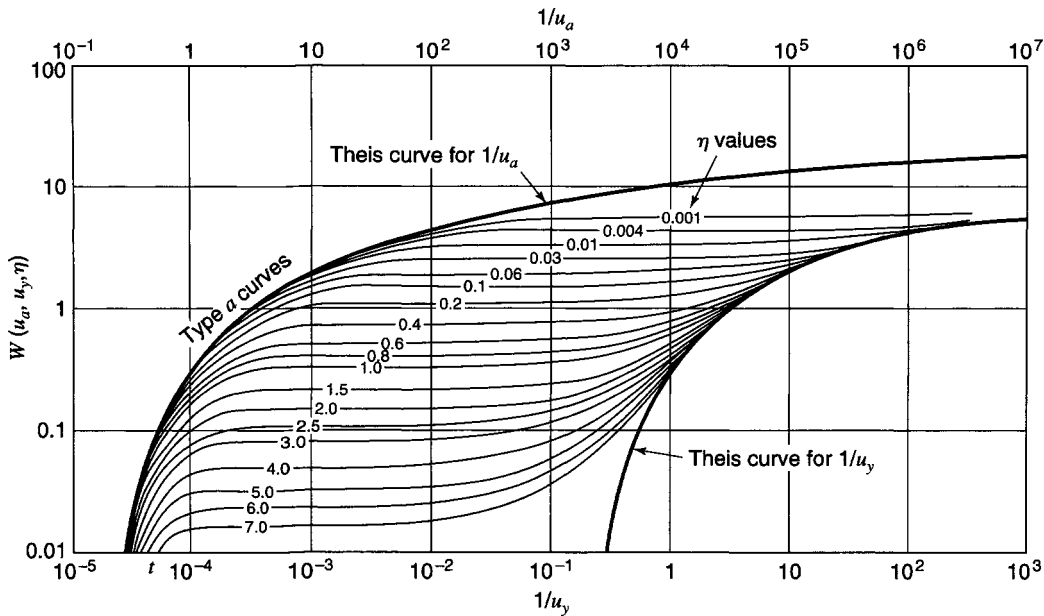


Figure 6.6.2 Theoretical curves of $W(u_a, u_y, \eta)$ versus $1/u_a$ and $1/u_y$ for an unconfined aquifer (after Neuman (1975)).

$$u_y = \frac{r^2 S_y}{Tt} \quad (\text{applicable for large values of } t) \quad (6.6.3)$$

where $\eta = r^2 K_z / b^2 K_r$.

$W(u_a, u_y, \eta)$ is referred to as the *unconfined well function*, and K_r and K_z are the horizontal and vertical hydraulic conductivities, respectively, for an anisotropic aquifer. Neuman (1975) tabulated the well function, as plotted in Figure 6.6.2. For an isotropic aquifer, $K_r = K_z$ and $\eta = r^2 / b^2$. The u_a applies only to early-time response when the rate of drawdown is controlled by the elastic storage properties of the aquifer. The u_y applies to the late-time response when the rate of drawdown is controlled by the specific yield.

Distance-drawdown data for water table conditions can be used to compute T and S_y only after the effects of delayed gravity drainage have dissipated in observation wells. After the effects of delayed gravity drainage cease to influence the drawdown in observation wells, the time-drawdown field data conforms closely to the nonequilibrium solution, as illustrated above. This length of time was discussed in the previous section.

During the time when delayed gravity drainage is affecting the drawdown in observation wells, the cone of depression is distorted; therefore, the distance-drawdown data for this time cannot be analyzed. However, once the effects of delayed gravity drainage are negligible, then the distance-drawdown data can be analyzed using the nonequilibrium solution technique.

6.7 TRANSIENT WELL HYDRAULICS—LEAKY AQUIFER CONDITIONS

In leaky aquifer systems, water enters the aquifer from adjacent lower-permeability units. These conditions provide an additional source of water and reduce the drawdown predicted by the Theis solution. *Leaky-confined conditions* refer to wells penetrating a confined aquifer overlain by an aquitard, which in turn is overlain by a source bed having a water table. There is vertical leakage through the aquitard (confining layer). The aquifer is assumed to be homogeneous, isotropic, infinite

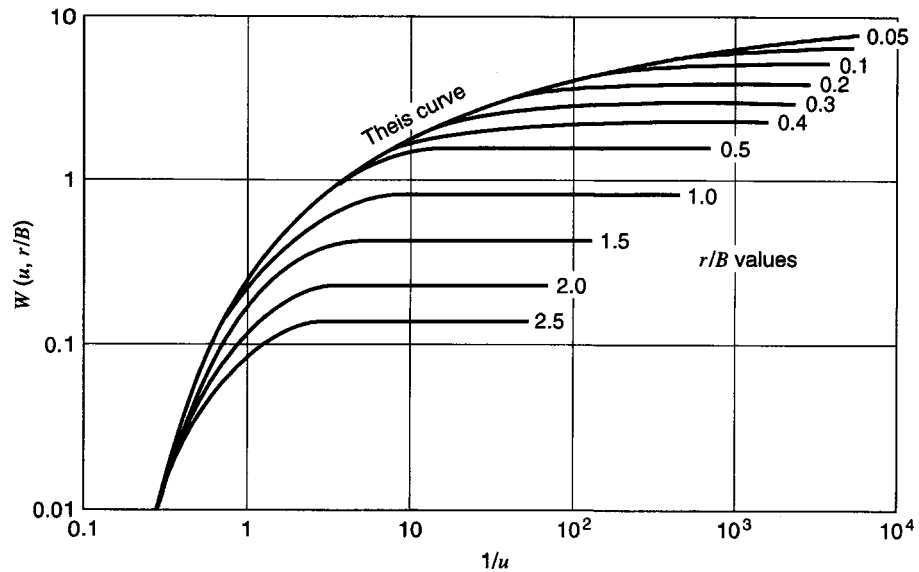


Figure 6.7.1 Theoretical curves of $W(u, r/B)$ versus $1/u$ for a leaky aquifer (after Walton (1960)).

in areal extent, and of constant thickness. Wells fully penetrate the aquifer to which there is radial flow. The confining layer is assumed to be incompressible, neglecting any storage in the layer. Discharge from a well is supplied from both storage within the aquifer and the vertical leakage. The rate of the vertical leakage is proportional to the difference in head between the water table for the source bed and the piezometric surface of the aquifer.

Hantush and Jacob (1955) developed a solution that describes the drawdown in a radially symmetric leaky confined aquifer separated from an overlying aquifer by a confining bed of lower permeability. Leakage into the pumped aquifer is a function of the vertical hydraulic conductivity of the aquitard, K' , the aquitard thickness, b' , and the difference in hydraulic head between the overlying aquifer and the aquifer being pumped. The drawdown is expressed as

$$s(r, t) = \frac{Q}{4\pi T} W[u, (r/B)] \quad (6.7.1)$$

where the *leaky well function*, $W[u, (r/B)]$, is defined as a function of two dimensionless parameters

$$u = \frac{r^2 S}{4Tt} \quad (6.7.2)$$

and

$$r/B = r \sqrt{\frac{K'}{Kbb'}} \quad (6.7.3)$$

The well function is plotted in Figure 6.7.1. The key simplification is that the hydraulic head in the upper aquifer remains constant and that water is not released from storage in the aquitard.

6.8 BOUNDARY EFFECTS: IMAGE WELL THEORY

The *nonequilibrium Theis solution* for unsteady radial flow to a well is based on the assumption that the aquifer is infinite in areal extent; however, often aquifers are delimited by one or more boundaries, causing the time-drawdown data to deviate under the influence of these boundaries. The boundaries may be walls of impervious soil or rock, which are referred to as *barrier boundaries*,

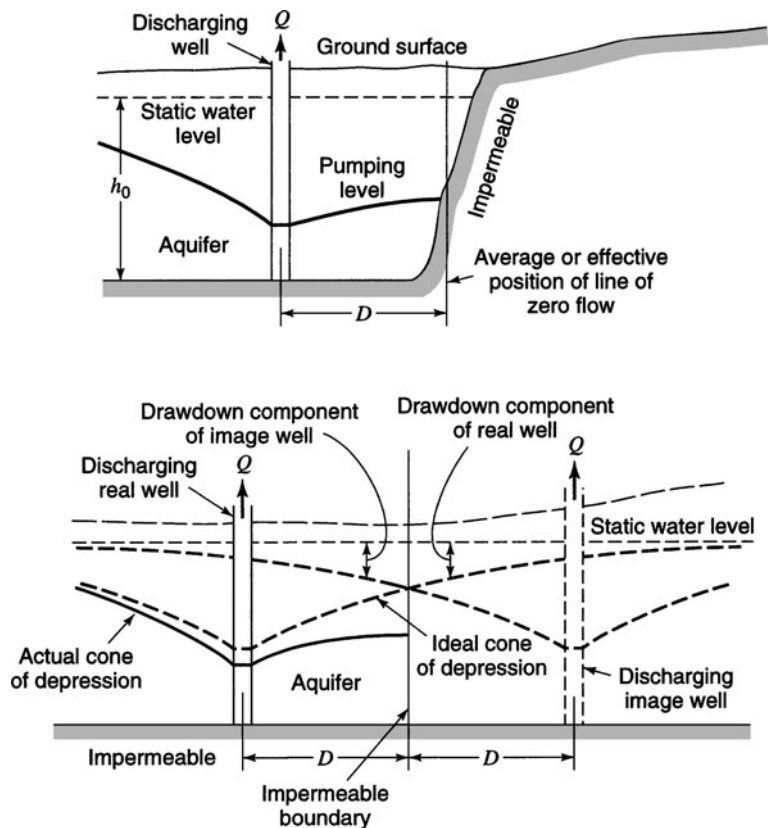


Figure 6.8.1 Relationship of an impermeable boundary and an image well (from U.S. Bureau of Reclamation (1981)).

or recharges of water from rivers, streams, or lakes, which are referred to as *recharge boundaries*. The effects of barrier and recharge boundaries on groundwater movement and storage can be described by image well theory.

Walton (1970) has stated the *image well theory* as “the effect of a barrier boundary on the drawdown in a well, as a result of pumping from another well, is the same as though the aquifer were infinite and a like discharging well were located across the real boundary on a perpendicular thereto and at the same distance from the boundary as the real pumping well. For a recharge boundary the principle is the same except that the image well is assumed to be discharging the aquifer instead of pumping from it.” These concepts give rise to the use of imaginary wells, referred to as *image wells*, that are introduced to simulate a groundwater system reflecting the effects of known physical boundaries on the system. Essentially, then, through the use of image wells, an aquifer of finite extent can be transformed to one of infinite extent. Once this is done, the unsteady radial flow equations can be applied to the transformed system. The concept of image wells is further illustrated in Figure 6.8.1 for a barrier boundary and Figure 6.8.2 for a recharge boundary.

6.8.1 Barrier Boundary

In the case of a *barrier boundary*, water cannot flow across the boundary, so that no water is being contributed to the pumped well from the impervious formation. The cone of depression that would exist for a pumped well in an aquifer of infinite areal extent is shown in Figure 6.8.1. Because of the barrier boundary, the cone of depression shown is no longer valid since there can be no flow across

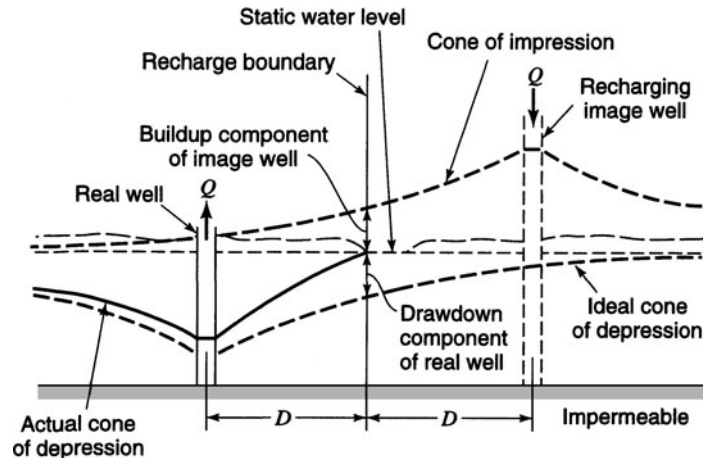
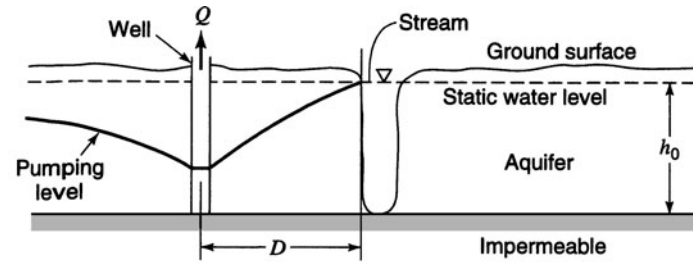


Figure 6.8.2 Relationship of a recharge boundary and an image well (from U.S. Bureau of Reclamation (1981)).

the boundary. Placing an image well, discharging in nature, across the barrier boundary creates the effect of no flow across the boundary. The image well must be placed perpendicular to the barrier boundary and at the same distance from the boundary as the real well. The resulting *real cone of depression* is the summation of the components of both the real and image well depression cones, as shown in Figure 6.8.1. Water levels in wells will decline at an initial rate due only to the influence of the pumped well. As pumping continues, the barrier boundary effects will begin as simulated by the image well affecting the real well. When the effects of the barrier boundary are realized, the time rate of drawdown will increase (Figure 6.8.3). When this occurs, the total rate of withdrawal from the aquifer is equal to that of the pumped well plus that of the discharging image well, causing the cone of depression of the real well to be deflected downward.

The total drawdown in the real well can be expressed as

$$s_B = s_p + s_i \quad (6.8.1)$$

in which s_B is the total drawdown, s_p is the drawdown in an observation well due to pumping of the production well, and s_i is the drawdown due to the discharging image well (barrier boundary).

The total drawdown can be expressed as

$$s_B = \frac{Q}{4\pi T} W(u_p) + \frac{Q}{4\pi T} W(u_i) \quad (6.8.2)$$

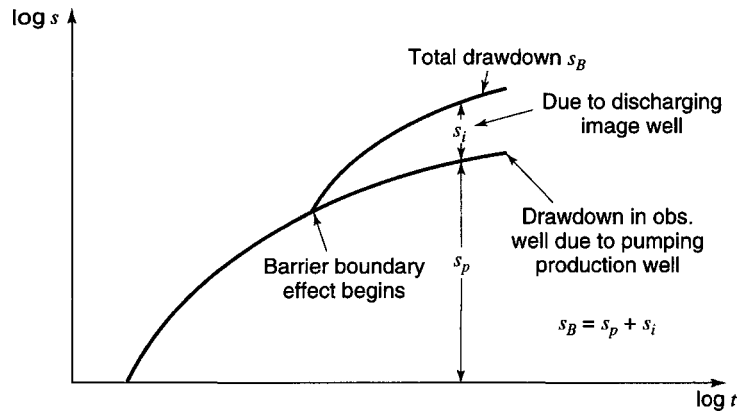


Figure 6.8.3 Barrier boundary effects on time-drawdown curve.

where Q is the constant pumping rate (L^3/T), T is the transmissivity (L^2/T), $W(u_p)$, and $W(u_i)$ are dimensionless, and u_p and u_i are

$$u_p = \frac{r_p^2 S}{4Tt_p} \tag{6.8.3}$$

$$u_i = \frac{r_i^2 S}{4Tt_i} \tag{6.8.4}$$

in which r_i and r_p are in L and t is time in T .

The drawdown equation (6.8.1) can also be expressed in U.S. customary units (gal-day-foot) system where S is in ft, Q is in gpm, T is in gpd/ft, r is in ft, and t is in days:

$$s_B = \frac{114.6Q}{T} W(u_p) + \frac{114.6Q}{T} W(u_i) = \frac{114.6Q}{T} [W(u_p) + W(u_i)] \tag{6.8.5}$$

where

$$u_p = \frac{1.87r_p^2 S}{Tt_p} \tag{6.8.6}$$

$$u_i = \frac{1.87r_i^2 S}{Tt_i} \tag{6.8.7}$$

Now suppose that we choose drawdowns at times t_p and t_i such that $s_p = s_i$, then $W(u_p) = W(u_i)$ and $u_p = u_i$, so that

$$\frac{r_i^2 S}{Tt_i} = \frac{r_p^2 S}{Tt_p} \tag{6.8.8}$$

which reduces to

$$\frac{r_i^2}{t_i} = \frac{r_p^2}{t_p} \tag{6.8.9}$$

Equation (6.8.9) defines the *law of times* (Ingersoll et al., 1948), which states that for a given aquifer, the times of occurrence of equal drawdown vary directly as the squares of distances from an observation well to a production well of equal discharge.

The law of times can be used to determine the distance from an image well to an observation well, using

$$r_i = r_p \sqrt{\frac{t_i}{t_p}} \tag{6.8.10}$$

in which r_i is the distance from the image well to the observation well in feet, r_p is the distance from the pumped well to the observation well in feet, t_p is the time after pumping started and before the barrier boundary is effective, and t_i is the time after pumping started and after the barrier boundary becomes effective, where $s_p = s_i$.

EXAMPLE 6.8.1

A well is pumping near a barrier boundary (see Figure 6.8.4) at a rate of $0.03 \text{ m}^3/\text{s}$ from a confined aquifer 20 m thick. The hydraulic conductivity of the aquifer is 27.65 m/day, and its storativity is 3×10^{-5} . Determine the drawdown in the observation well after 10 hours of continuous pumping. What is the fraction of the drawdown attributable to the barrier boundary?

SOLUTION

The following information is given in the above problem statement: $Q = 0.03 \text{ m}^3/\text{s}$, $b = 20 \text{ m}$, $K = 27.65 \text{ m/day} = 3.2 \times 10^{-4} \text{ m/s}$, $S = 3 \times 10^{-5}$, $t = 10 \text{ hr} = 36,000 \text{ s}$. An image well is placed across the boundary at the same distance from the boundary as the pumped well (as shown in Figure 6.8.4b). The drawdown in the observation well is due to the real well and the imaginary well (which accounts for the barrier boundary). Hence, using equation (6.8.5)

$$s = \frac{Q}{4\pi T} W(u_p) + \frac{Q}{4\pi T} W(u_i)$$

$$u_p = \frac{r_p^2 S}{4Tt} = \frac{(240)^2 (3 \times 10^{-5})}{4(20)(3.2 \times 10^{-4})(36,000)} = 1.88 \times 10^{-3}$$

Next, compute the distance from the observation well to the image well: $r_i^2 = 600^2 + 240^2 - 2(600)(300) \cos 30^\circ = 168,185 \text{ m}^2$ so $r_i = 410 \text{ m}$. Using r_i , compute

$$u_i = \frac{168,185 (3 \times 10^{-5})}{4(20)(3.2 \times 10^{-4})(36,000)} = 5.47 \times 10^{-3}$$

The well functions are now computed using equation (6.5.4) or obtained from Table 6.5.1 as $W(u_p) = 5.72$ for $u_p = 1.88 \times 10^{-1}$ and $W(u_i) = 4.64$ for $u_i = 5.47 \times 10^{-3}$.

The drawdown at the observation well is computed as

$$s = \frac{0.03}{4\pi(20)(3.2 \times 10^{-4})} = (5.72 + 4.64) = 3.86 \text{ m.}$$

The drawdown attributable to the barrier boundary is computed as

$$s_i = \frac{Q}{4\pi T} W(u_i) = \frac{0.03}{4\pi(20)(3.2 \times 10^{-4})} (4.64) = 1.73 \text{ m}$$

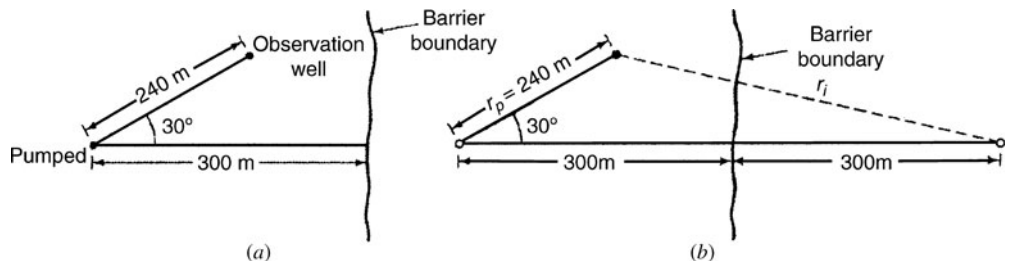


Figure 6.8.4 Example 6.8.1 system. (a) Well locations; (b) Image well location.

and the fraction of the drawdown attributable to the impermeable boundary is

$$\frac{s_i}{s} = \frac{1.73}{3.86} = 0.45 \text{ (45\%)}$$

6.8.2 Recharge Boundary

The effect of recharge boundaries can also be simulated using the concepts of image well theory. For an aquifer bounded on one side by a recharge boundary, the cone of depression cannot extend beyond the stream, as shown in Figure 6.8.2. This results in no drawdown along the line of recharge. By placing an image well, recharging in nature, directly opposite and at the same distance from the stream as the real pumped well and also pumping at the same rate, the finite system can be simulated. The resulting cone of depression is the summation of the real well cone of depression without the recharge and the image well cone of depression, as shown in Figure 6.8.2.

The water level in the wells will draw down initially only under the influence of the pumped well. After a time the effects of the recharge boundary will cause the time rate of drawdown to decrease and eventually reach equilibrium conditions. This occurs when recharge equals the pumping rate, as illustrated in Figure 6.8.5.

The drawdown for equilibrium conditions can be expressed as

$$s_r = s_p - s_i \tag{6.8.11}$$

in which s_r is the drawdown in an observation well near a recharge boundary, s_p is the drawdown due to the pumped well, and s_i is the buildup due to the image well (recharge boundary). The drawdown equation can be written as

$$s_r = \frac{Q}{4\pi T} [W(u_p) - W(u_i)] \tag{6.8.12}$$

or in the gallon-day-foot system as

$$s_r = \frac{114.6Q}{T} [W(u_p) - W(u_i)] \tag{6.8.13}$$

For large values of time t , the well functions can be expressed as

$$W(u_p) = -0.5772 - \ln u_p \tag{6.8.14}$$

$$W(u_i) = -0.5772 - \ln u_i \tag{6.8.15}$$

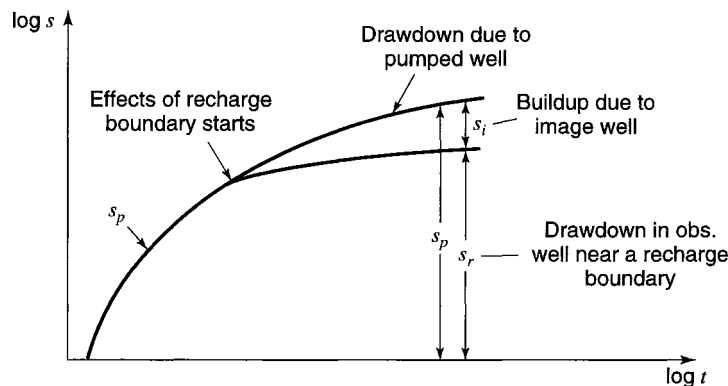


Figure 6.8.5 Recharge boundary effects on time-drawdown curve.

This allows equation (6.8.12) to be simplified to

$$s_r = \frac{Q}{4\pi T} [-\ln u_p + \ln u_i] \quad (6.8.16)$$

and equation (6.8.13) to

$$s_r = \frac{114.6Q}{T} [-\ln u_p + \ln u_i] \quad (6.8.17)$$

Now using the gallon-day-foot system with time in minutes, we get

$$u_p = \frac{2693r_p^2 S}{Tt} \quad (6.8.18)$$

and

$$u_i = \frac{2693r_i^2 S}{Tt} \quad (6.8.19)$$

The drawdown in the observation well from equation (6.8.17) is expressed as

$$s_r = \frac{114.6Q}{T} \left[-\ln \left(\frac{2693r_p^2 S}{Tt} \right) + \ln \left(\frac{2693r_i^2 S}{Tt} \right) \right] \quad (6.8.20)$$

which simplifies to

$$s_r = \frac{528}{T} Q \log \left(\frac{r_i}{r_p} \right) \quad (6.8.21)$$

Rorabaugh (1956) expressed this equation in terms of the distances between the pumped well and the line of recharges as

$$s_r = \frac{528Q \log \sqrt{(4a^2 + r_p^2 - 4ar_p \cos B_r)}/r_p}{T} \quad (6.8.22)$$

where a is the distance from the pumped well to the recharge boundary in feet, and B_r is the angle between a line connecting the pumped and image wells and a line connecting the pumped and observation wells. Refer to Figure 6.8.6 for an explanation of terms.

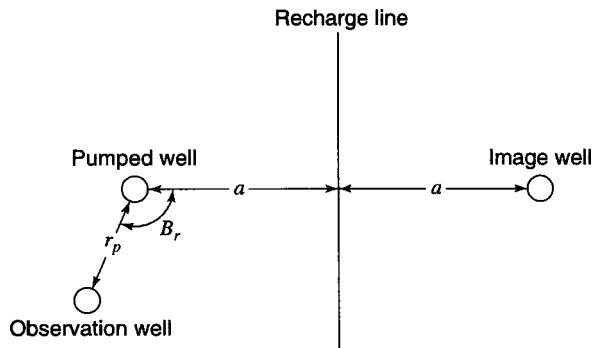


Figure 6.8.6 Definition of terms for equation (6.8.22).

6.8.3 Multiple Boundary Systems

Image well theory can also be applied to aquifer systems with multiple boundaries by considering successive reflections on the barrier and recharge boundaries. This is accomplished through a number of image wells. Placing a primary image well across each boundary balances the effect of the pumped well at each boundary. If a pair of converging boundaries is required, each primary image well then produces an unbalanced effect at the opposite boundary. This unbalanced effect is corrected by placing secondary image wells until the effects of the real and image wells are balanced at both boundaries. These concepts are illustrated in Figure 6.8.7.

A primary image well placed across a barrier boundary is discharging in character. A primary image well placed across a recharge boundary is recharging in character. A secondary image well placed across a barrier boundary has the same character as its parent image well. A secondary image

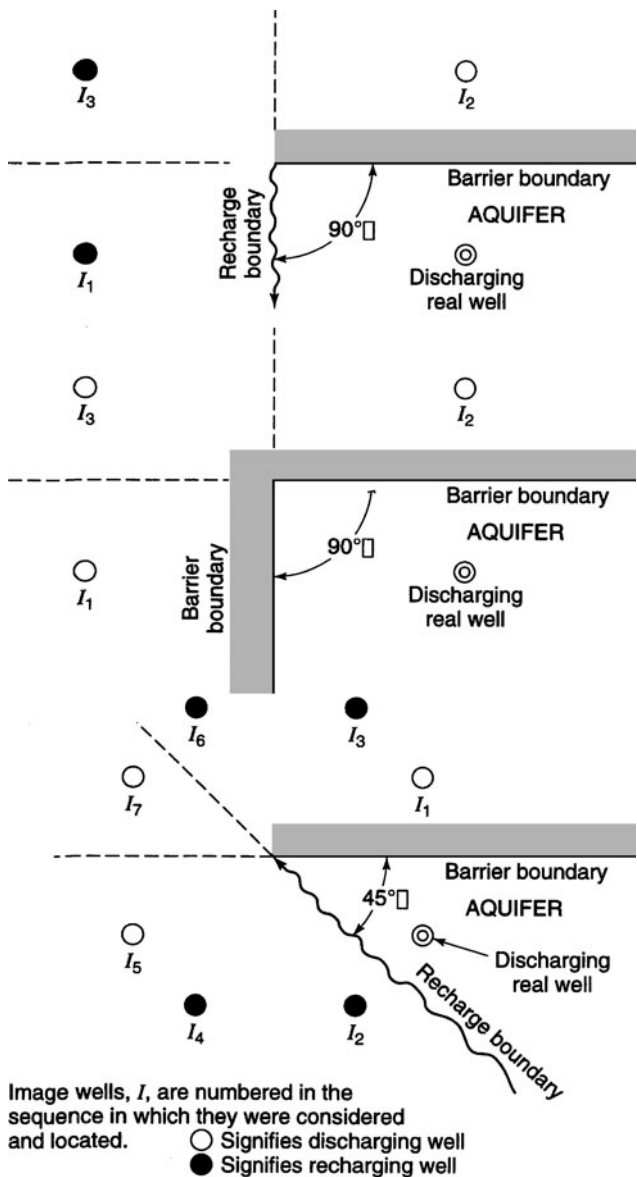


Figure 6.8.7 Plans of image-well systems for several wedge-shaped aquifers (from Ferris et al. (1946)).

well placed across a recharge boundary has the opposite character to its parent image well. Figure 6.8.7 shows image well systems for wedge-shaped aquifers. For parallel boundary systems, it is only necessary to add pairs of image wells until the next pair has negligible influence on the sum of all image well effects out to the point.

6.9 SIMULATION OF GROUNDWATER SYSTEMS

6.9.1 Governing Equations

Darcy's law relates the Darcy flux v with dimension L/T to the rate of headloss per unit length of porous medium $\partial h/\partial l$. The negative sign indicates that the total head is decreasing in the direction of flow because of friction. This law applies to a cross-section of porous medium that is large compared to the cross-section of individual pores and grains of the medium. At this scale, Darcy's law describes a steady uniform flow of constant velocity, in which the net force on any fluid element is zero. For unconfined saturated flow, the two forces are gravity and friction. Darcy's law can also be expressed in terms of the transmissivity for confined conditions as

$$v = -\frac{T}{b} \frac{\partial h}{\partial l} \quad (6.9.1)$$

or for unconfined conditions as

$$v = -\frac{T}{h} \frac{\partial h}{\partial l} \quad (6.9.2)$$

Considering two-dimensional (horizontal) flow, a general flow equation can be derived by considering flow through a rectangular element (control volume) shown in Figure 6.9.1. The flow components ($q = Av$) for the four sides of the element are expressed using Darcy's law where $A = \Delta x \cdot h$ for unconfined conditions and $A = \Delta x \cdot b$ for confined conditions, so that

$$q_1 = -T_{x_{i-1,j}} \Delta y_j \left(\frac{\partial h}{\partial x} \right)_1 \quad (6.9.3a)$$

$$q_2 = -T_{x_{i,j}} \Delta y_j \left(\frac{\partial h}{\partial x} \right)_2 \quad (6.9.3b)$$

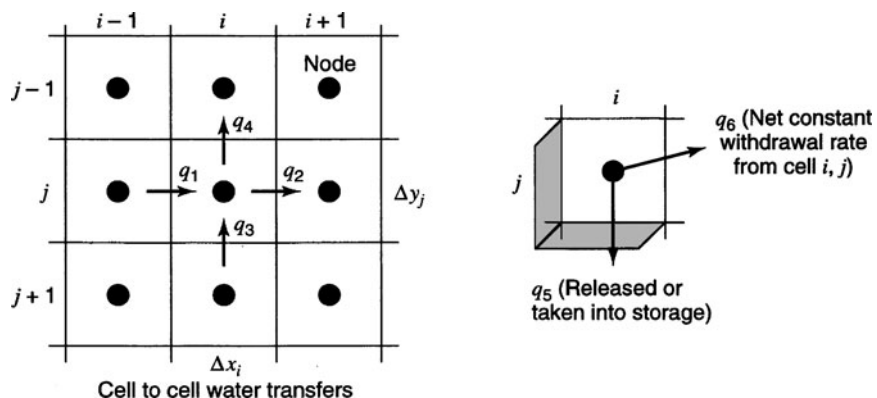


Figure 6.9.1 Finite difference grid.

$$q_3 = -T_{y_{i,j+1}}\Delta x_i \left(\frac{\partial h}{\partial y} \right)_3 \quad (6.9.3c)$$

$$q_4 = -T_{y_{i,j}}\Delta x_i \left(\frac{\partial h}{\partial y} \right)_4 \quad (6.9.3d)$$

where $T_{x_{i,j}}$ is the transmissivity in the x flow direction from element (i, j) to element $(i+1, j)$. The terms $(\partial h/\partial x)_1, (\partial h/\partial x)_2, \dots$ define the hydraulic gradients at the element sides 1, 2, \dots

The rate at which water is stored or released in the element over time is

$$q_5 = S_{i,j}\Delta x_i\Delta y_i \frac{\partial h}{\partial t} \quad (6.9.4)$$

in which $S_{i,j}$ is the storage coefficient for element (i, j) . In addition, the flow rate q_6 for constant net withdrawal or recharge from the element over time interval Δt is considered:

$$q_6 = q_{i,j,t} \quad (6.9.5)$$

in which $q_{i,j,t}$ has a positive value for pumping whereas it has a negative value for recharge.

By continuity, the flow into and out of a grid or cell is

$$q_1 - q_2 + q_3 - q_4 = q_5 + q_6 \quad (6.9.6)$$

Substituting in equations (6.9.3) and (6.9.5) gives

$$-T_{x_{i-1,j}}\Delta y_j \left(\frac{\partial h}{\partial x} \right)_1 + T_{x_{i,j}}\Delta y_i \left(\frac{\partial h}{\partial x} \right)_2 - T_{y_{i,j+1}}\Delta x_i \left(\frac{\partial h}{\partial y} \right)_3 + T_{y_{i,j}}\Delta x_i \left(\frac{\partial h}{\partial y} \right)_4 = S_{i,j}\Delta x_i\Delta y_i \frac{\partial h}{\partial t} + q_{i,j,t} \quad (6.9.7)$$

Dividing equation (6.9.7) by $\Delta x\Delta y$ and simplifying for constant transmissivities in the x and y directions yields

$$-T_x \left[\frac{\left(\frac{\partial h}{\partial x} \right)_1 - \left(\frac{\partial h}{\partial x} \right)_2}{\Delta x_i} \right] - T_y \left[\frac{\left(\frac{\partial h}{\partial y} \right)_3 - \left(\frac{\partial h}{\partial y} \right)_4}{\Delta y_j} \right] = S_{i,j} \frac{\partial h}{\partial t} + \frac{q_{i,j,t}}{\Delta x_i\Delta y_i} \quad (6.9.8)$$

For Δx and Δy infinitesimally small, the terms in brackets become second derivatives of h : then equation (6.9.8) reduces to

$$T_x \frac{\partial^2 h}{\partial x^2} + T_y \frac{\partial^2 h}{\partial y^2} = S \frac{\partial h}{\partial t} + W \quad (6.9.9)$$

which is the general partial differential equation for unsteady flow in the horizontal direction in which $W = q_{i,j,t}/\Delta x_i\Delta y_j$ is a sink term with dimensions L/T .

In the more general unsteady, two-dimensional heterogeneous anisotropic case, equation (6.9.9) is expressed as

$$\frac{\partial}{\partial x} \left(T_x \frac{\partial h}{\partial x} \right) + \frac{\partial}{\partial y} \left(T_y \frac{\partial h}{\partial y} \right) = S \frac{\partial h}{\partial t} + W \quad (6.9.10a)$$

or more simply

$$\frac{\partial}{\partial x_i} \left(T_{i,j} \frac{\partial h}{\partial x_j} \right) = S \frac{\partial h}{\partial t} + W \quad i, j = 1, 2 \quad (6.9.10b)$$

6.9.2 Finite Difference Equations

The partial derivative expressions for Darcy's law, equations (6.9.3 a–d), can be expressed in finite difference form for time t in equation (6.9.7) using

$$\left(\frac{\partial h}{\partial x}\right)_1 = \left(\frac{h_{i-1,j,t} - h_{i,j,t}}{\Delta x_i}\right) \quad (6.9.11a)$$

$$\left(\frac{\partial h}{\partial x}\right)_2 = \left(\frac{h_{i,j,t} - h_{i+1,j,t}}{\Delta x_i}\right) \quad (6.9.11b)$$

$$\left(\frac{\partial h}{\partial y}\right)_3 = \left(\frac{h_{i,j+1,t} - h_{i,j,t}}{\Delta y_j}\right) \quad (6.9.11c)$$

$$\left(\frac{\partial h}{\partial y}\right)_4 = \left(\frac{h_{i,j,t} - h_{i,j-1,t}}{\Delta y_j}\right) \quad (6.9.11d)$$

and the time derivative in equation (6.9.7) is

$$\frac{\partial h}{\partial t} = \left(\frac{h_{i,j,t} - h_{i,j,t-1}}{\Delta t}\right) \quad (6.9.12)$$

Substituting equation (6.9.11) and (6.9.12) into equation (6.9.7) yields

$$\begin{aligned} & -T_{x_{i-1,j}}\Delta y_j \left(\frac{h_{i-1,j,t} - h_{i,j,t}}{\Delta x_i}\right) + T_{x_{i,j}}\Delta y_j \left(\frac{h_{i,j,t} - h_{i+1,j,t}}{\Delta x_i}\right) \\ & -T_{y_{i,j+1}}\Delta x_i \left(\frac{h_{i,j+1,t} - h_{i,j,t}}{\Delta y_j}\right) + T_{y_{i,j}}\Delta x_j \left(\frac{h_{i,j,t} - h_{i,j-1,t}}{\Delta y_j}\right) \\ & -S_{i,j}\Delta x_i\Delta y_j \left(\frac{h_{i,j,t} - h_{i,j,t-1}}{\Delta t}\right) - q_{i,j,t} = 0 \end{aligned} \quad (6.9.13)$$

which can be further simplified to

$$A_{i,j}h_{i,j,t} + B_{i,j}h_{i-1,j,t} + C_{i,j}h_{i+1,j,t} + D_{i,j}h_{i,j+1,t} + E_{i,j}h_{i,j-1,t} + F_{i,j,t} = 0 \quad (6.9.14)$$

where

$$A_{i,j} = \left[T_{x_{i-1,j}}\frac{\Delta y_j}{\Delta x_i} + T_{x_{i,j}}\frac{\Delta y_j}{\Delta x_i} + T_{y_{i,j+1}}\frac{\Delta x_i}{\Delta y_j} + T_{y_{i,j}}\frac{\Delta x_i}{\Delta y_j} - S_{i,j}\frac{\Delta x_i\Delta y_j}{\Delta t}\right] \quad (6.9.15a)$$

$$B_{i,j} = -T_{x_{i-1,j}}\frac{\Delta y_j}{\Delta x_i} \quad (6.9.15b)$$

$$C_{i,j} = -T_{y_{i,j}}\frac{\Delta y_j}{\Delta x_i} \quad (6.9.15c)$$

$$D_{i,j} = -T_{y_{i,j+1}}\frac{\Delta x_j}{\Delta y_j} \quad (6.9.15d)$$

$$E_{i,j} = -T_{y_{i,j}}\frac{\Delta x_i}{\Delta y_j} \quad (6.9.15e)$$

$$F_{i,j,t} = -S_{i,j}\frac{\Delta x_j\Delta y_j}{\Delta t} \left(\frac{h_{i,j,t} - h_{i,j,t-1}}{\Delta t}\right) - q_{i,j,t} \quad (6.9.15f)$$

The coefficients $A_{i,j}$, $B_{i,j}$, $C_{i,j}$, $D_{i,j}$, $E_{i,j}$, and $F_{i,j,t}$ are linear functions of the thickness of cell (i,j) and the thickness of one of the adjacent cells. For artesian conditions, this thickness is a known constant, so if cell (i,j) and its neighbors are artesian, equation (6.9.14) is linear for all t . For unconfined (water table) conditions, the thickness of cell (i,j) is $h_{i,j,t} - BOT_{i,j}$, where $BOT_{i,j}$ is the average elevation of the bottom of the aquifer for cell (i,j) . Then for unconfined conditions, equation (6.9.14) involves products of heads and is nonlinear in terms of the heads.

An *iterative alternating direction implicit (IADI) procedure* can be used to solve the set of equations. The IADI procedure involves reducing a large set of equations to several smaller sets of equations. One such smaller set of equations is generated by writing equation (6.9.14) for each cell or element in a column but assuming that the heads for the nodes on the adjacent columns are known. The unknowns in this set of equations are the heads for the nodes along the column. The head for the nodes along adjoining columns are not considered unknowns. This set of equations is solved by Gauss elimination and the process is repeated until each column is treated. The next step is to develop a set of equations along each row, assuming the heads for the nodes along adjoining rows are known. The set of equations for each row is solved and the process is repeated for each row in the finite difference grid.

Once the sets of equations for the columns and the sets of equations for the row have been solved, one “iteration” has been completed. The iteration process is repeated until the procedure converges. Once convergence is accomplished, the terms $h_{i,j}$ represent the heads at the end of the time step. These heads are used as the beginning heads for the following time step. For a more detailed discussion of IADI procedure, see Peaceman and Rachford (1955), Prickett and Lonquist (1971), Trescott et al., (1976), or Wang and Anderson (1982).

An example of the application of a two-dimensional finite-difference groundwater model is the Edwards (Balcones Fault Zone) aquifer. This aquifer has been modeled using the GWSIM groundwater simulation model developed by the Texas Water Development Board (1974). GWSIM is a finite-difference simulation model that uses the IADI method, similar to the model by Prickett and Lonquist (1971). The finite-difference grid for the Edwards Aquifer is shown in Figure 6.9.2, which has 856 active cells to describe the aquifer. Wanakule (1989) has modeled only a small portion of the Edwards aquifer, called the Barton Springs-Edwards aquifer, Austin, Texas. This application used a finite difference grid system (Figure 6.9.3) containing 330 cells whose dimensions varied from $0.379 \times 0.283 \text{ mi}^2$ to $0.95 \times 1.51 \text{ mi}^2$. Figure 6.9.4 illustrates the 1981 water level contours.

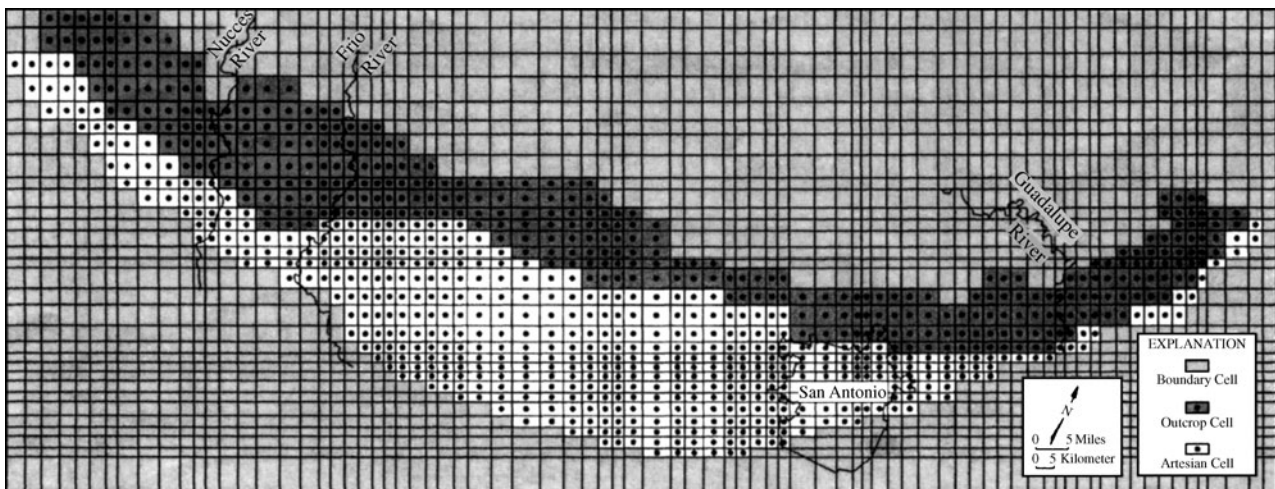


Figure 6.9.2 Cell map used for the digital computer model of the Edwards (Balcones Fault Zone) Aquifer (after Klemt et al. (1979)).

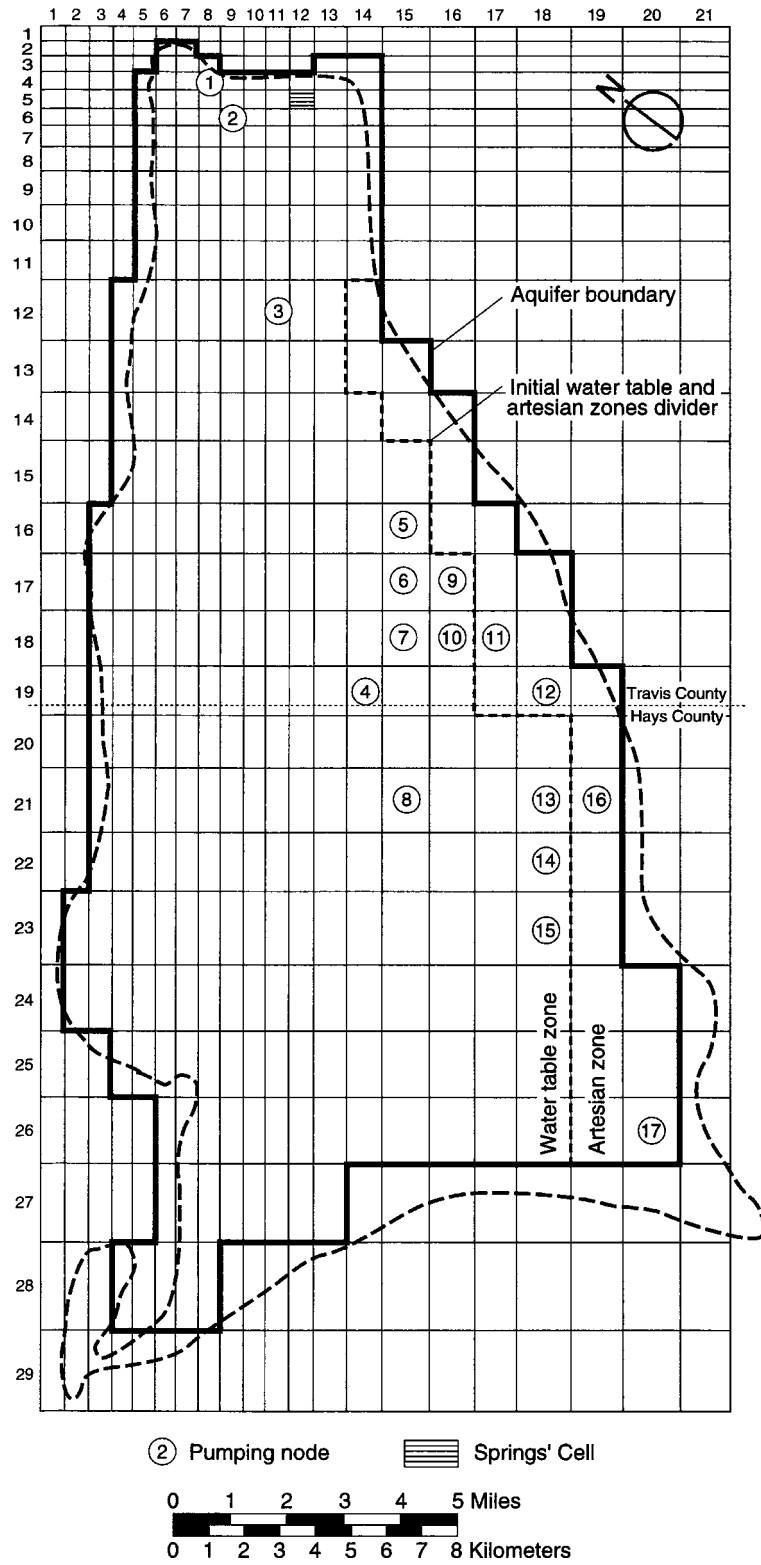
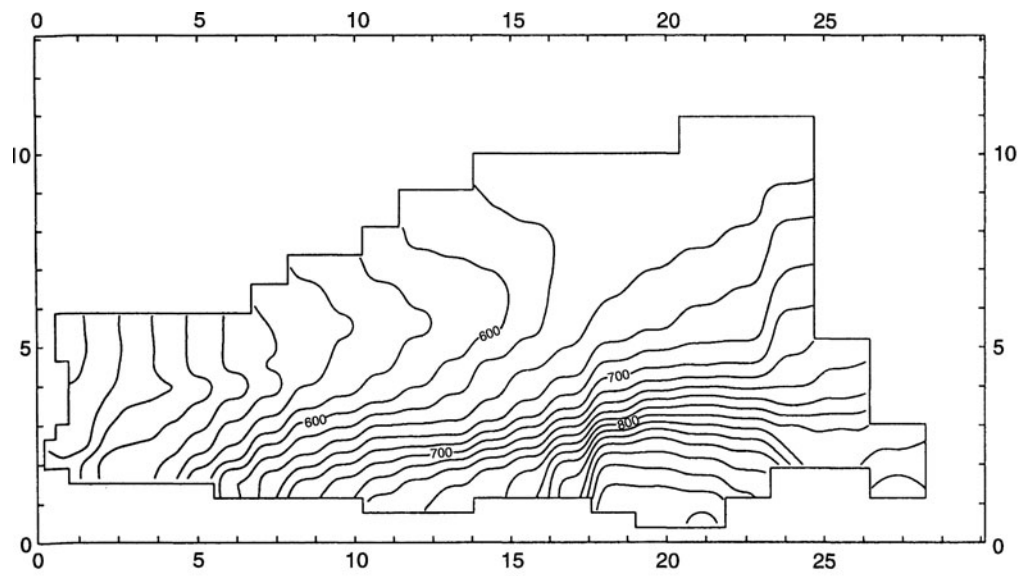
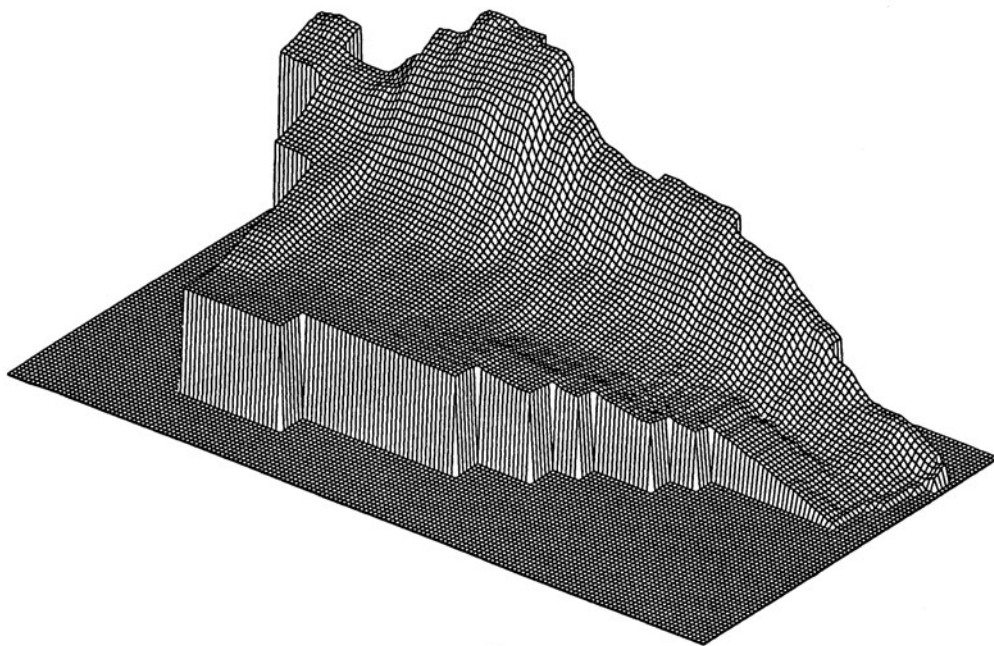


Figure 6.9.3 Pumping locations used in Barton Springs-Edwards Aquifer model (after Wanakule (1989)).



(a)



(b)

Figure 6.9.4 Water levels for Barton Springs-Edwards aquifer. (a) 1981 water-level contours at 20 ft intervals; (b) Perspective block diagram of 1981 water levels viewed from the east side of the aquifer (after Wanakule (1985)).

6.9.3 MODFLOW

One of the most widely used groundwater simulation models is the MODFLOW-2005 Model developed by the U.S. Geological Survey (Harbaugh, 2006). The World Wide Web (WWW) address from which this model can be downloaded is <http://water.usgs.gov/gwsoftware/modflow2005/modflow2005.html>. MODFLOW-2005 is a finite difference model that can be used to solve

groundwater flow problems in one, two, or three dimensions. The computer program is divided into a main program and a series of independent subroutines called *modules*. These modules are grouped into *packages*, each of which is a group of modules that deals with a single aspect of the simulation. A Basic Package handles tasks that are required for each simulation: the Well Package, which simulates the effects of injection and production wells; the River Package, which simulates the effect of rivers; and the Recharge Package, which simulates the effect of recharge. Others include the Evapotranspiration Package, the Drain Package, the General-Head Boundary Package, and the Solution Procedure Package. Individual packages may or may not be required, depending on the problem being simulated.

PROBLEMS

6.1.1 An experiment was conducted to determine the hydraulic conductivity of an artesian aquifer. The piezometric heads at two points 150 m apart were found to be 55 m and 48.5 m above a datum. A tracer injected into the first piezometer was observed after 32 hours in the second well. A test on porosity of a sample of the aquifer shows that $\alpha = 24\%$. What is the hydraulic conductivity of the aquifer? Suggest what the aquifer material may be and verify that your solution holds true. Take the subsurface temperature as 15°C .

6.1.2 Develop an inventory of wells in the county where you live using the USGS data sources for your state. Select a well that has a time history of water levels and print the hydrograph.

6.1.3 Perform a search of USGS publications for the topic "hydrologic budget and water budget." To perform the search go to <http://usgs-georef.cos.com>. How many publications are listed?

6.1.4 Determine the water level rise in an unconfined aquifer produced by a seasonal precipitation of four inches. The aquifer's porosity is 20 percent and its specific retention is 9 percent.

6.1.5 The leakage from the artificially constructed Tempe Town Lake in Tempe, Arizona can be as low as 0.5 ft/day or as high as 3 ft/day. The lake covers 222 surface acres. If the specific yield of

the subsurface formation is 20 percent, estimate the average regional groundwater level rise assuming that the aerial extent of the effect of leakage is (a) 222 acres, (b) 1 square mile, (c) 5 square miles, and 25 square miles.

6.1.6 The coefficient of storage of a confined aquifer is found to be 6.8×10^{-4} as a result of a pumping test. The thickness of the aquifer is 50 m, and the porosity of the aquifer is 0.25. Determine the fractions of the expansibility of water and compressibility of the aquifer skeleton in making up the storage coefficient of the aquifer.

6.1.7 The specific storage of a 45-m thick confined aquifer is $3.0 \times 10^{-5} \text{ m}^{-1}$. How much water would the aquifer produce if the piezometric surface is lowered by 10 m over an area of 1 km^2 ?

6.2.1 Show that the steady state groundwater flow equation can be expressed in polar coordinate systems as $h = C_1 \ln r + C_2$, where C_1 and C_2 are constants.

6.2.2 Water flows through three confined aquifers in series as shown in Figure P6.2.2. For piezometric heads in the observation wells of 66.4 m and 60.6 m, determine the flow rate per unit width of the aquifer and the headlosses in each component of the aquifers between the observation wells. If the headlosses in each aquifer

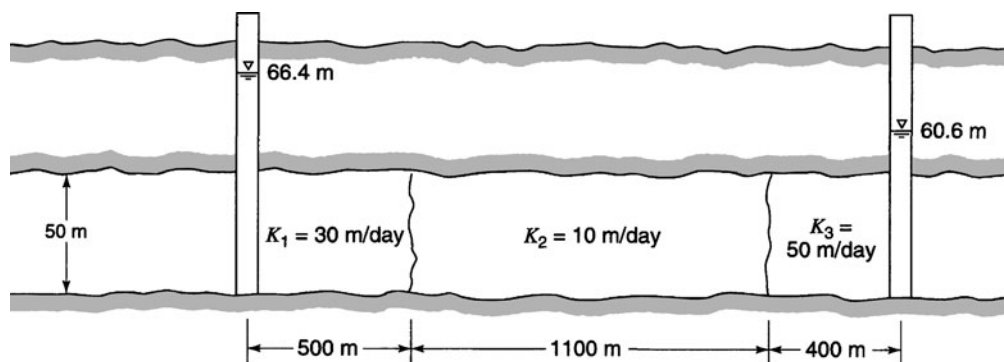


Figure P6.2.2

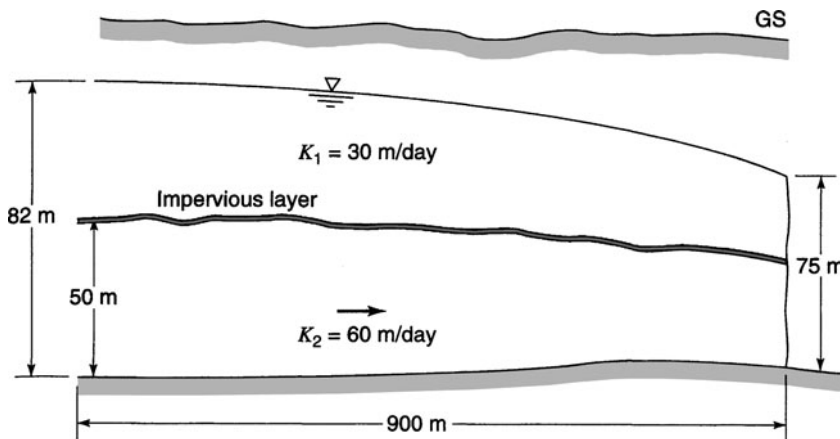


Figure P6.2.3

between the wells were to be equal, what would be the length of each aquifer?

6.2.3 Suppose an unconfined aquifer lies over a confined aquifer as shown in Figure P6.2.3. Determine the flow out of both aquifers.

6.3.1 Rework example 6.3.1 with $h_0 = 10$ ft.

6.3.2 Consider two strata of the same soil material that lie between two channels. The first stratum is confined, and the second one is unconfined, and the water surface elevations in the channels are 24 m and 16 m above the bottom of the unconfined aquifer. What should be the thickness of the confined aquifer for which

- (1) the discharge through both strata are equal?
- (2) the discharge through the confined aquifer is half of that through the unconfined aquifer?

6.3.3 Three monitoring wells are used (as shown in Figure P6.3.3) to determine the direction of groundwater flow in a confined aquifer. The piezometric heads in the wells are found to be 52 m in well 1, 49 m in well 2, and 56 m in well 3. Determine the direction of flow.

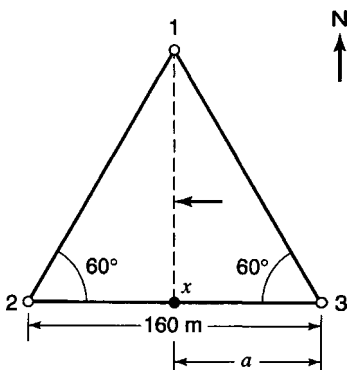


Figure P6.3.3

6.3.4 An earthen dam is 200 m across (i.e., the distance from the upstream face to the downstream face) and underlain by an impermeable bedrock. The average hydraulic conductivity of the material of which the dam is constructed is 0.065 m/day. If the water surface elevations in the reservoir and the tailwater are 25 m and 4.5 m, respectively, estimate the magnitude of leakage from the reservoir to the tailwater per 100-m width of the dam.

6.3.5 For the channel and river shown in Figure 6.3.4, determine the volume of water that flows from the channel into the river. The water surface elevations in the channel and river with respect to the underlying bedrock are 15 m and 11.5 m, respectively. The hydraulic conductivity of formation A is 5.6 m/day and that of formation B is 12.3 m/day.

6.3.6 For the channel and river shown in Figure 6.3.4, determine the volume of water that flows from the channel into the river. The water surface elevations in the channel and river with respect to the underlying bedrock are 15 m and 11.5 m, respectively. The hydraulic conductivity of formation A is 6.6 m/day and that of formation B is 10.3 m/day.

6.4.1 Rework example 6.4.1 with a constant pumping rate of 0.07 m³/s and the same drawdowns.

6.4.2 Rework example 6.4.2 with a pumping rate of 400 gpm and the same drawdowns.

6.4.3 Rework example 6.4.3 with a constant pumping rate of 0.075 m³/s and the same drawdowns.

6.4.4 Rework example 6.4.4 with the same pumping rate but drawdowns of 10 ft and 5 ft in the observation wells.

6.4.5 A 50-cm diameter well fully penetrates vertically through a confined aquifer 12 m thick. When the well is pumped at 0.035 m³/s, the heads in the pumped well and the two other observation wells were found to be as shown in Figure P6.4.5. Does this test suggest that the aquifer material is fairly homogeneous in the directions of the observation wells?

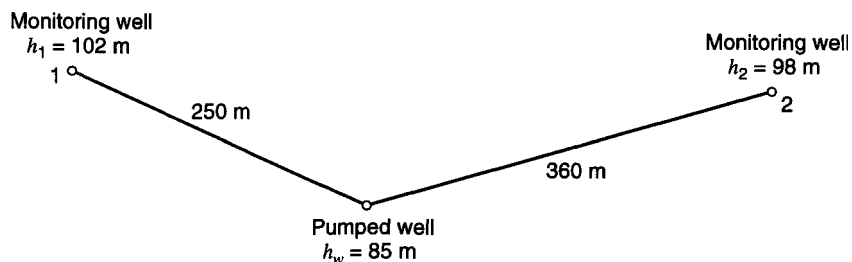


Figure P6.4.5

6.4.6 Three pumping wells along a straight line are spaced 200 m apart. What should be the steady state pumping rate from each well so that the drawdown in each well will not exceed 2 m: The transmissivity of the confined aquifer that all the wells penetrate fully is 2400 m²/day and all the wells are 40 cm in diameter. Take the thickness of the aquifer $b = 40$ m and the radius of influence of each well to be 800 m.

6.4.7 Reposition the wells in problem 6.4.6 such that they form an equilateral triangle (same spacings). For the same restrictions on the drawdown, will the discharge decrease or increase? If so, by what percent? If not, what difference do you perceive between the two problems?

6.4.8 It is required to dewater a construction site 80 m by 80 m. The bottom of the construction will be 1.5 m below the initial water surface elevation of 90 m. Four pumps are to be used in 0.5-m diameter wells at the four corners of the site. Determine the required steady-state pumping rate. The aquifer has $T = 1600$ m²/day and each well has a radius of influence of 600 m.

6.4.9 A 0.75-m radius well fully penetrates a 24-m thick unconfined aquifer and is pumped at a rate of 10 l/s (or 864 m³/day). The drawdown in an observation well 30 m from the pumped well is 1.6 m after a long period of pumping. The drawdown in another observation well 60 m from the pumped well is 1.1 m after the long period of pumping. Determine the (a) hydraulic conductivity of the aquifer, (b) the expected drawdown in the pumped well, and (c) the radius of influence of the pumped well.

6.5.1 Work example 6.5.1 with $T = 8500$ gpd/ft².

6.5.2 A 0.4-m diameter well is pumped continuously at a rate of 5.6 l/s from an aquifer of transmissivity 108 m²/day and storativity 2×10^{-5} . How long will it take before the drawdown in the well reaches 2 m?

6.5.3 In problem 6.5.2, how long will it take before a drawdown at a distance of 400 m from the well becomes 2 m?

6.5.4 In problem 6.5.2, determine the drawdown at a distance 200 m from the well after (a) 1 hr, (b) 1 day, and (c) 1 year of pumping.

6.5.5 A pumping test was performed to determine the transmissivity and the storativity of a confined aquifer. The drawdown versus time data in an observation well 100 m away from the pumping well are given in the following table. The discharge from the pumped well was at a constant rate of 3.6 m³/min throughout the test. Determine the aquifer properties.

Time (min)	Drawdown (m)
0.5	0.12
1	0.18
2	0.25
3	0.28
4	0.31
5	0.33
8	0.38
10	0.41
20	0.47
30	0.51
50	0.56
100	0.62
200	0.69
500	0.79
1000	0.89

6.5.6 The following data were obtained in an observation well 80 m away from the pumped well. The discharge from the pumped well was at 2.5 m³/min. Using Jacob's approximation, determine the aquifer properties. Assume a confined aquifer. Also verify your solution and determine the time after which Jacob's approximation will be valid.

Time (min)	Drawdown (m)
0.5	0.16
1	0.18
2	0.24
3	0.27
4	0.47
5	0.50
7	0.57
10	0.68
20	0.84
30	0.96
50	1.06
100	1.29
200	1.46
500	1.68
1000	1.86

6.5.7 A fully penetrating production well located in a confined aquifer is pumped at a constant rate of 64 l/s. Aquifer characteristics include a transmissibility of 1240 m²/day and coefficient of storage of 4×10^{-4} . Determine the drawdown at a distance of 200 m from the pumped well after 30 days of pumping. Compare results using the Theis and the Cooper–Jacobs procedures.

6.6.1 A fully penetrating well in an unconfined aquifer with a saturated thickness of 25 ft is pumped at a rate of 144.4 ft³/min. Time-drawdown data were collected from an observation well 73 feet from the pumped well and matched to type curves (such as Figure 6.6.2). The matching of early drawdown versus time best fit the type a curve for $\eta = 0.06$, with the selected match point: ($t = 0.17$ min, $s = 0.57$ ft) and ($1/u_a = 1.0$ and $W(u_a, \eta) = 1.0$). Determine the transmissivity and specific yield.

6.6.2 For the situation in problem 6.6.1, the time-drawdown data are now matched for the later in time drawdown data (segment 3) for the $\eta = 0.06$. The late-time match resulted in the match point ($t = 13$ min, $s = 0.57$ ft) and ($1/u_y = 0.1$ and $W(u_y, \eta) = 1.0$). Determine the transmissivity and the storativity. How does the transmissivity differ from that computed in problem 6.6.1?

6.6.3 Determine the vertical hydraulic conductivity of the aquifer described in problems 6.6.1 and 6.6.2.

6.8.1 Draw the generalized flow net showing the flow lines and potential lines in the vicinity of a discharging well near a recharge boundary.

6.8.2 Draw the generalized flow net showing the flow lines and potential lines in the vicinity of a discharging well near a barrier boundary.

6.8.3 A well is pumping near a barrier boundary at a rate of 0.03 m³/s from a confined aquifer 20 m thick (see Figure 6.8.3). The hydraulic conductivity of the aquifer is 3.2×10^{-4} m/s, and its storativity is 3×10^{-5} . Determine the drawdown in the observation well after 30 hours of continuous pumping. What is the fraction of the drawdown attributable to the barrier boundary?

6.8.4 A 0.5-m diameter well is pumping near a river at an unknown rate from a confined aquifer (see Figure 6.8.4). The aquifer properties are $T = 5.0 \times 10^{-3}$ m²/s and $S = 4.0 \times 10^{-4}$. After 8 hours of pumping, the drawdown in the observation well was

0.8 m. Determine the rate of pumping and the drawdown in the pumped well. How great was the effect of the river on the drawdown in the observation well and in the pumped well?

6.8.5 A production well fully penetrating a nonleaky isotropic artesian aquifer delimited by two barrier boundaries perpendicular to each other was continuously pumped at a constant rate of 1485 gpd for a period of 4 hours. The drawdowns in the table below were observed at a distance of 300 ft in a fully penetrating observation well. Compute the coefficients of transmissivity and storage of the aquifer and the distances to each image well from the observation well.

Time (min)	Drawdown (ft)
2	0.80
3	0.92
4	1.06
5	1.17
6	1.23
7	1.32
8	1.37
9	1.43
10	1.48
20	1.88
30	2.11
40	2.34
50	2.52
60	2.70
70	2.83
80	3.00
90	3.17
100	3.30
200	4.21
300	4.43

6.9.1 Search the Internet to find the various ASTM standards that apply to groundwater modeling.

6.9.2 Develop a two- to three-page description of the MODFLOW model.

REFERENCES

Batu, V., *Aquifer Hydraulics*, Wiley Interscience, New York, 1998.

Charbeneau, R. J., *Groundwater Hydraulics and Pollutant Transport*, Prentice-Hall, Upper Saddle River, NJ, 2000.

Chow, V. T., D. R. Maidment, and L. W. Mays, *Applied Hydrology*, McGraw-Hill, New York, 1988.

Cooper, H. H., Jr., and C. E. Jacob, "A Generalized Graphical Method for Evaluating Formation Constants and Summarizing Well Field History," *Trans. Amer. Geophys. Union*, vol. 27, pp. 526–534, 1946.

Delleur, J. W. (editor-in chief), *The Handbook of Groundwater Engineering*, CRC Press, Boca Raton, FL, 1999.

Ferris, J. G., D. B. Knowles, R. H. Brown, and R. W. Stallman, "Theory of Aquifer Tests," U.S. Geological Survey Water-Supply Paper 1536-E, 1946.

Freeze, R. A., and J. A. Cherry, *Groundwater*, Prentice-Hall, Englewood Cliffs, NJ, 1979.

Gehm, H. W., and J. I. Bregman, editors, *Handbook of Water Resources and Pollution Control*, Van Nostrand Reinhold Company, New York, 1976.

Gleick, P. H., *Water in Crisis*, Oxford University Press, Oxford, 1993.

Hantush, M. S., "Hydraulics of Wells," in *Advances in Hydroscience*, Academic Press, New York, 1964.

- Hantush, M. S., and C. E. Jacob, "Non-Steady Radial Flow in an Infinite Leaky Aquifer," *Trans. Am. Geophys. Union*, vol. 36, no. 1, 1955.
- Harbaugh, A. W., "MODFLOW-2005. The U.S. Geological Survey Modular Ground-Water Model—the Ground-Water Flow Process," *U.S. Geological Survey Techniques and Methods, Book 6 Modeling Techniques, Section A Groundwater*, U.S. Geological Survey, 2006.
- Ingersoll, L. R., O. J. Zobel, and A. C. Ingersoll, *Heat Conduction with Engineering and Geological Applications*, McGraw-Hill, New York, 1948.
- Klemt, W. B., T. R. Knowles, G. R. Elder, and T. Sich, "Groundwater Resources and Model Applications for the Edwards (Balcones Fault Zone) Aquifer in the San Antonio Region, Texas," Report 239, Texas Department of Water Resources, Austin, TX, Oct. 1979.
- Lohman, S. W., et al. "Definition of Selected Groundwater Terms-Revision and Conceptual Refinements," U.S. Geological Survey Water Supply Paper No. 1988 1972.
- Marsh, W. M., *Earthscope: A Physical Geography*, John Wiley & Sons, New York, 1987.
- Meinzer, O. E., "The Occurrence of Groundwater in the United States," U.S. Geological Survey Water Supply Paper 489, 1923.
- Neuman, S. P., "Analysis of Pumping Test Data from Anisotropic Unconfined Aquifers Considering Delayed Gravity Response," *Water Resources Research*, vol. 11, pp. 329–342, 1975.
- Peaceman, D. W., and H. H. Rachford, Jr., "The Numerical Solutions of Parabolic and Elliptic Differential Equations," *Journal Soc. Industrial and Applied Mathematics*, vol. 3, pp. 28–41, 1955.
- Prickett, T. A., "Type-Curve Solution to Aquifer Table Tests under Water-Table Conditions," *Groundwater*, vol. 3, no. 3, 1965.
- Prickett, T. A., and C. G. Lonquist, "Selected Digital Computer Techniques for Groundwater Resources Evaluation," *Bulletin No. 55*, Illinois State Water Survey, Urbana, IL, 1971.
- Rorabaugh, M. I., "Ground-Water Resources of the Northeastern Part of the Louisville Area, Kentucky," U.S. Geological Survey Water Supply Paper 1360-B, 1956.
- Texas Water Development Board, "GWS1M—Groundwater Simulation Program, Program Document and User's Manual," UMS7405, Austin, TX, 1974.
- Theis, C. V., "The Relation Between the Lowering of Piezometric Surface and the Rate and Duration of Discharge of a Well Using Groundwater Storage," *Transactions American Geophysical Union*, vol. 2, pp. 519–524, 1935.
- Todd, D. K., and J. Bear, "Seepage Through Layered Anisotropic Porous Media," *Journal of the Hydraulics Division, ASCE*, vol. 87, no. HY 3, pp. 31–57, 1961.
- Todd, D. K. and L. W. Mays, *Groundwater Hydrology*, 3rd edition, John Wiley & Sons, New York, 2005.
- Trescott, P. C., G. F. Pinder, and S. P. Larson, "Finite-Difference Model for Aquifer Simulation in Two Dimensions with Results of Numerical Experiments," in *U.S. Geological Survey Techniques of Water Resources Investigations*, Book 7, C1, U.S. Geological Survey, Reston, VA, 1976.
- U.S. Bureau of Reclamation, *Groundwater Manual*, U.S. Government Printing Office, Denver, CO, 1981.
- U.S. Soil Conservation Service, *Soil Survey Manual*, Handbook no. 18, U.S. Department of Agriculture, 1951.
- Walton, W. C., *Groundwater Resource Evaluation*, McGraw-Hill, New York, 1970.
- Walton, W. E., "Leaky Artesian Conditions in Illinois," Illinois State Water Survey, Dept. of Invest. Urbana, IL 39, 1960.
- Wanakule, N., "Optimal Groundwater Management Models for the Barton Springs-Edwards Aquifer," Edwards Aquifer Research and Data Center, San Marcos, TX, 1989.
- Wang, H. F., and M. P. Anderson, *Introduction to Groundwater Modeling: Finite Difference and Finite Element Models*, W. H. Freeman, San Francisco, CA, 1982.
- Wenzel, L. K., "Methods for Determining Permeability of Water-Bearing Materials with Special Reference to Discharging Well Methods," U.S. Geological Survey Water-Supply Paper 887, pp. 192, 1942.

This page intentionally left blank

Chapter 7

Hydrologic Processes

7.1 INTRODUCTION TO HYDROLOGY

7.1.1 What is Hydrology?

The U.S. National Research Council (1991) presented the following definition of hydrology:

Hydrology is the science that treats the waters of the Earth, their occurrence, circulation, and distribution, their chemical and physical properties, and their reaction with the environment, including the relation to living things. The domain of hydrology embraces the full life history of water on Earth.

For purposes of this book we are interested in the engineering aspects of hydrology, or what we might call *engineering hydrology*. From this point of view we are mainly concerned with quantifying amounts of water at various locations (spatially) as a function of time (temporally) for surface water applications. In other words, we are concerned with solving engineering problems using hydrologic principles. This chapter is not concerned with the chemical properties of water and their relation to living things.

Books on hydrology include: Bedient and Huber (1992); Bras (1990); Chow (1964); Chow, Maidment, and Mays (1988); Gupta (1989); Maidment (1993); McCuen (1998); Ponce (1989); Singh (1992); Viessman and Lewis (1996); and Wanielista, Kersten, and Eaglin (1997).

7.1.2 The Hydrologic Cycle

The central focus of hydrology is the *hydrologic cycle*, consisting of the continuous processes shown in Figure 7.1.1. Water *evaporates* from the oceans and land surfaces to become water vapor that is carried over the earth by atmospheric circulation. The *water vapor* condenses and *precipitates* on the land and oceans. The precipitated water may be *intercepted* by vegetation, become overland flow over the ground surface, *infiltrate* into the ground, flow through the soil as *subsurface flow*, and discharge as *surface runoff*. Evaporation from the land surface comprises evaporation directly from soil and vegetation surfaces, and *transpiration* through plant leaves. Collectively these processes are called *evapotranspiration*. Infiltrated water may percolate deeper to recharge groundwater and later become *springflow* or *seepage* into streams also to become streamflow.

The hydrologic cycle can be viewed on a global scale as shown in Figure 7.1.2. As discussed by the U.S. National Research Council (1991): “As a global average, only about 57 percent of the precipitation that falls on the land (P_l) returns directly to the atmosphere (E_l) without reaching the ocean. The remainder is runoff (R), which find its way to the sea primarily by rivers but also through subsurface (groundwater) movement and by the calving of icebergs from glaciers and ice shelves

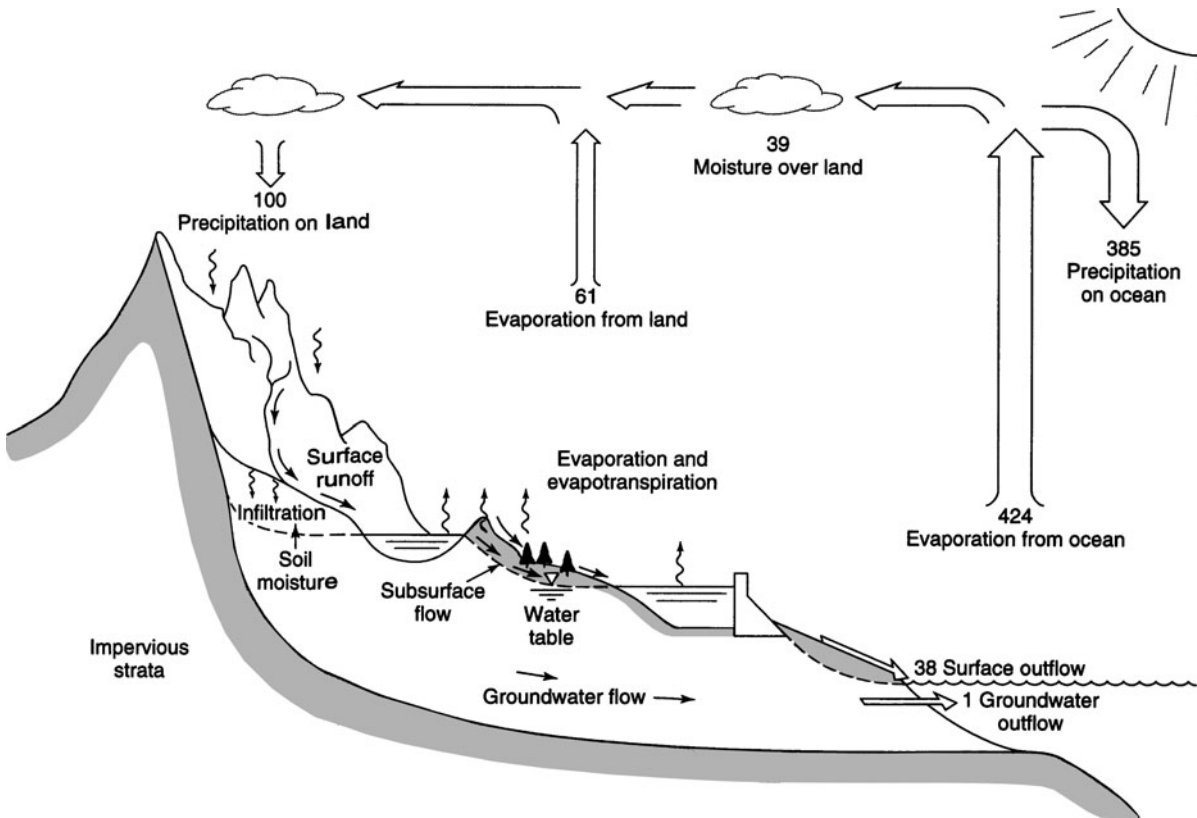


Figure 7.1.1 Hydrologic cycle with global annual average water balance given in units relative to a value of 100 for the rate of precipitation on land (from Chow et al. (1988)).

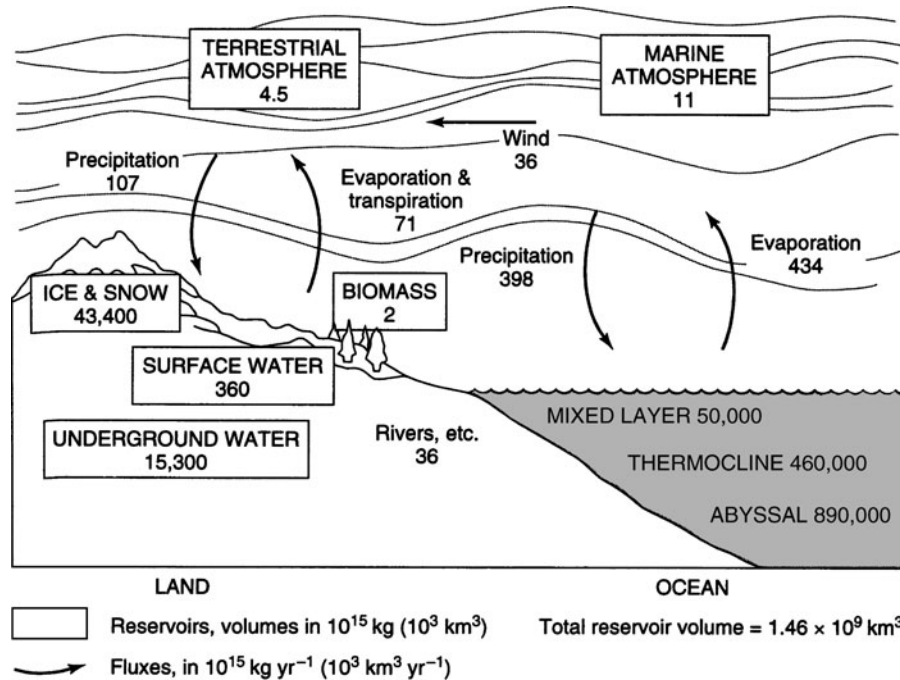


Figure 7.1.2 The hydrologic cycle at global scale (from U.S. National Research Council (1991)).

(W). In this gravitationally powered runoff process, the water may spend time in one or more natural storage reservoirs such as snow, glaciers, ice sheets, lakes, streams, soils and sediments, vegetation, and rock. Evaporation from these reservoirs short-circuits the global hydrologic cycle into subcycles with a broad spectrum of scale. The runoff is perhaps the best-known element of the global hydrologic cycle, but even this is subject to significant uncertainty.”

7.1.3 Hydrologic Systems

Chow, Maidment, and Mays (1988) defined a *hydrologic system* as a structure or volume in space, surrounded by a boundary, that accepts water and other inputs, operates on them internally, and produces them as outputs. The structure (for surface or subsurface flow) or volume in space (for atmospheric moisture flow) is the totality of the flow paths through which the water may pass as throughput from the point it enters the system to the point it leaves. The boundary is a continuous surface defined in three dimensions enclosing the volume or structure. A *working medium* enters the system as input, interacts with the structure and other media, and leaves as output. Physical, chemical, and biological processes operate on the working media within the system; the most common working media involved in hydrologic analysis are water, air, and heat energy.

The *global hydrologic cycle* can be represented as a system containing three subsystems: the atmospheric water system, the surface water system, and the subsurface water system, as shown in Figure 7.1.3. Another example is the storm-rainfall-runoff process on a watershed, which can be represented as a hydrologic system. The input is rainfall distributed in time and space over the watershed, and the output is streamflow at the watershed outlet. The boundary is defined by the watershed divide and extends vertically upward and downward to horizontal planes.

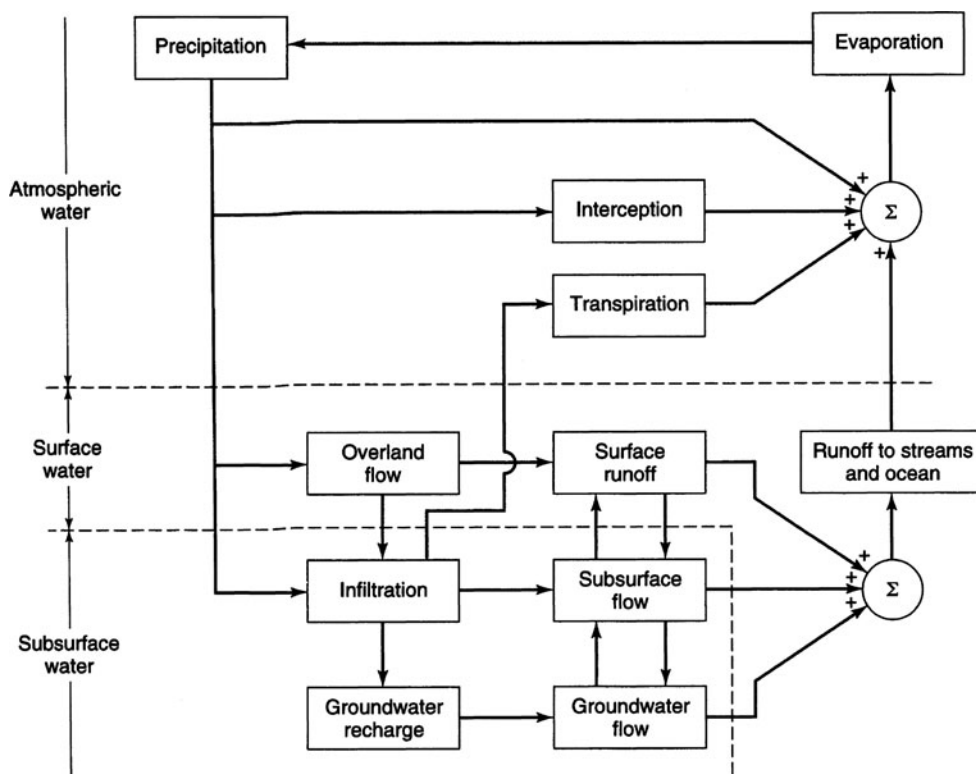


Figure 7.1.3 Block-diagram representation of the global hydrologic system (from Chow et al. (1988)).

Drainage basins, catchments, and watersheds are three synonymous terms that refer to the topographic area that collects and discharges surface streamflow through one outlet or mouth. Catchments are typically referred to as small drainage basins, but no specific area limits have been established. Figure 7.1.4 illustrates the drainage basin divide, watershed divide, or catchment divide, which is the line dividing land whose drainage flows toward the given stream from land whose drainage flows away from that stream. Think of drainage basin sizes ranging from the Mississippi

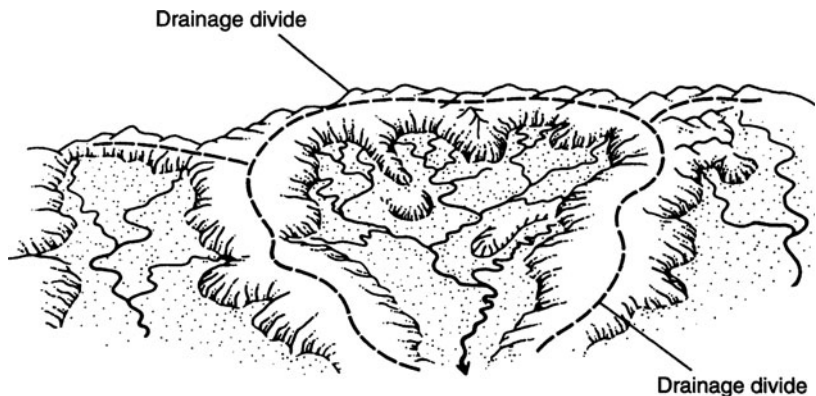


Figure 7.1.4 Schematic diagram of a drainage basin. The high terrain on the perimeter is the drainage divide (from Marsh (1987)).

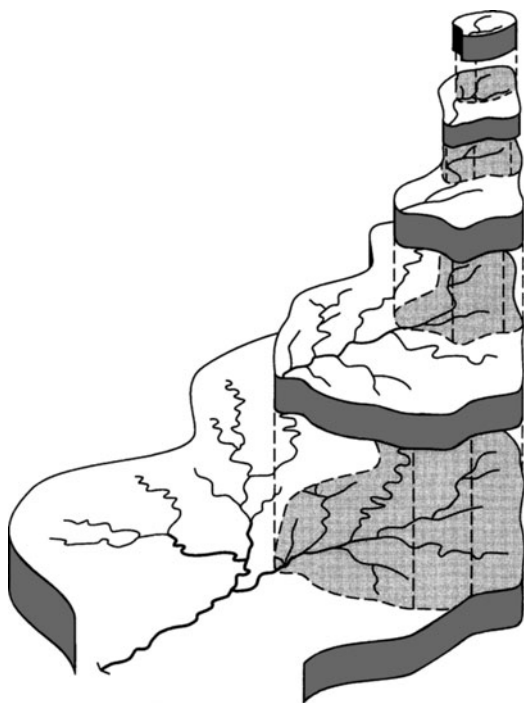


Figure 7.1.5 Illustration of the nested hierarchy of lower-order basins within a large drainage basin (from Marsh (1987)).

River drainage basin to small urban drainage basins in your local community or some small valley in the countryside near you.

As shown in Figure 7.1.5, drainage basins can be pictured in a pyramidal fashion as the runoffs from smaller basins (subsystems) combine to form larger basins (subsystem in system), and the runoffs from these basins in turn combine to form even larger basins, and so on. Marsh (1987) refers to this mode of organization as a *hierarchy* or *nested hierarchy*, as each set of smaller basins is set inside the next layer. A similar concept is that streams that drain small basins combine to form larger streams, and so on.

Figures 7.1.6–7.1.10 illustrate the hierarchy of the Friends Creek watershed located in the Lake Decatur watershed (drainage area upstream of Decatur, Illinois, on the Sangamon River with a drainage area of 925 mi^2 or 2396 km^2). Obviously, the Friends Creek watershed can be subdivided into much smaller watersheds. Figure 7.1.8 illustrates the Illinois River basin ($29,000 \text{ mi}^2$) with the Sangamon River. Figure 7.1.9 illustrates the upper Mississippi River basin (excluding the Missouri River) with the Illinois River. Figure 7.1.10 illustrates the entire Mississippi River basin (1.15 million mi^2). This is the largest river basin in the United States, draining about 40 percent of the country. The main stem of the river is about 2400 miles long.

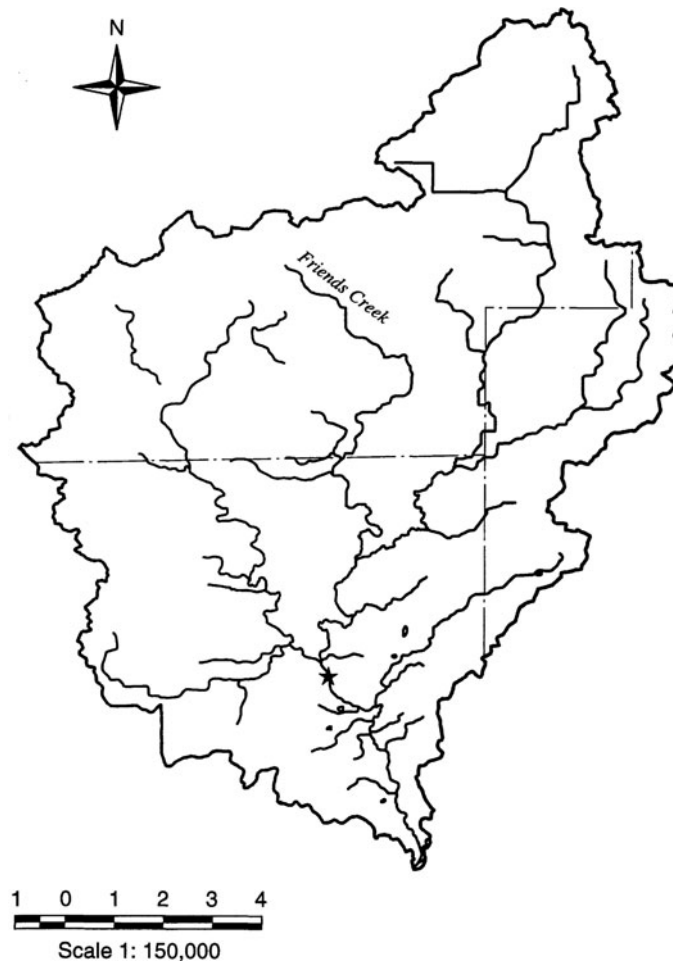


Figure 7.1.6 Friends Creek watershed, subwatershed of the Lake Decatur watershed. (Courtesy of the Illinois State Water Survey, compiled by Erin Hessler Bauer.)

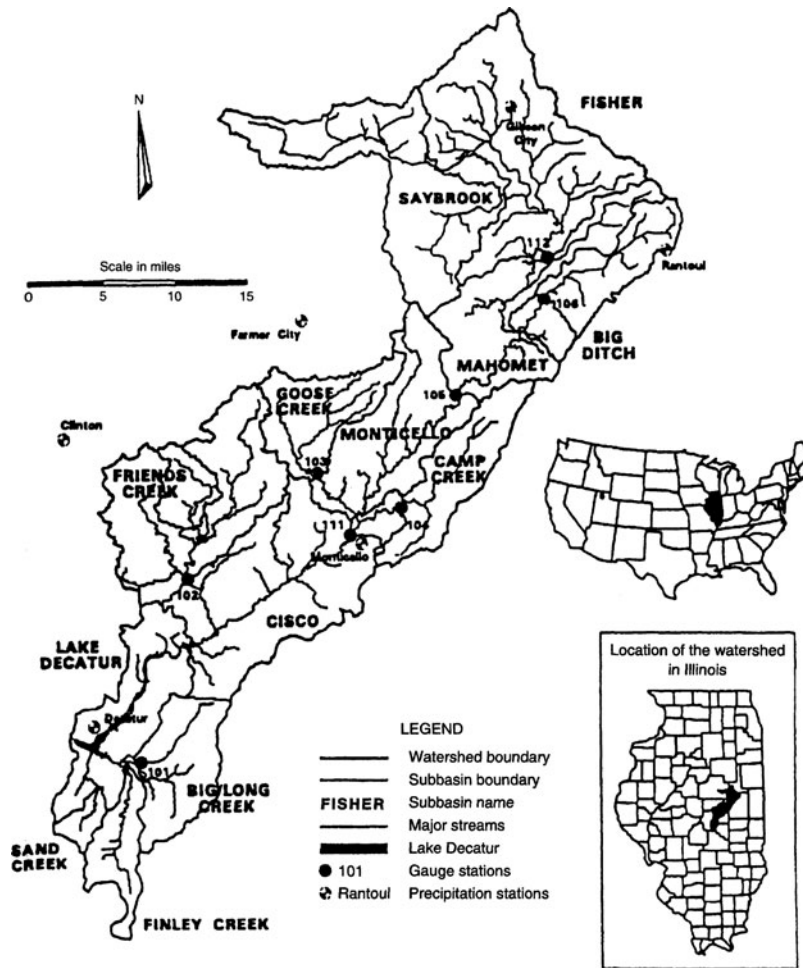


Figure 7.1.7 Lake Decatur watershed in the upper Sangamon River Basin (upstream of Decatur, Illinois). The location of Friends Creek watershed (Figure 7.1.6) is shown (from Demissee and Keefer (1998)).

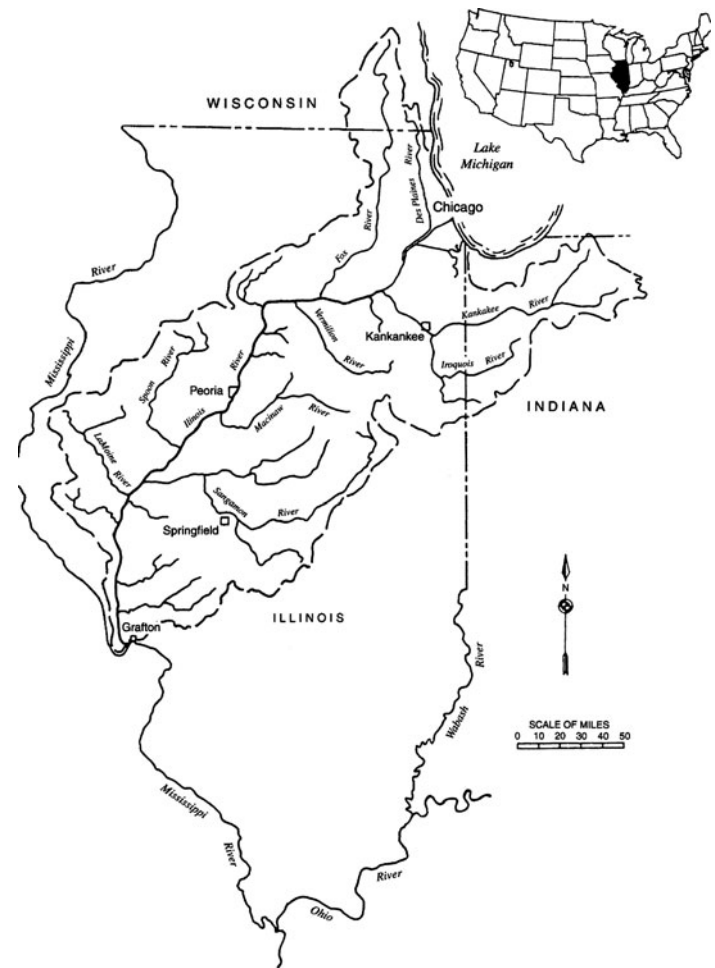


Figure 7.1.8 The Illinois River Basin showing the Sangamon River (from Bhowmik (1998)).

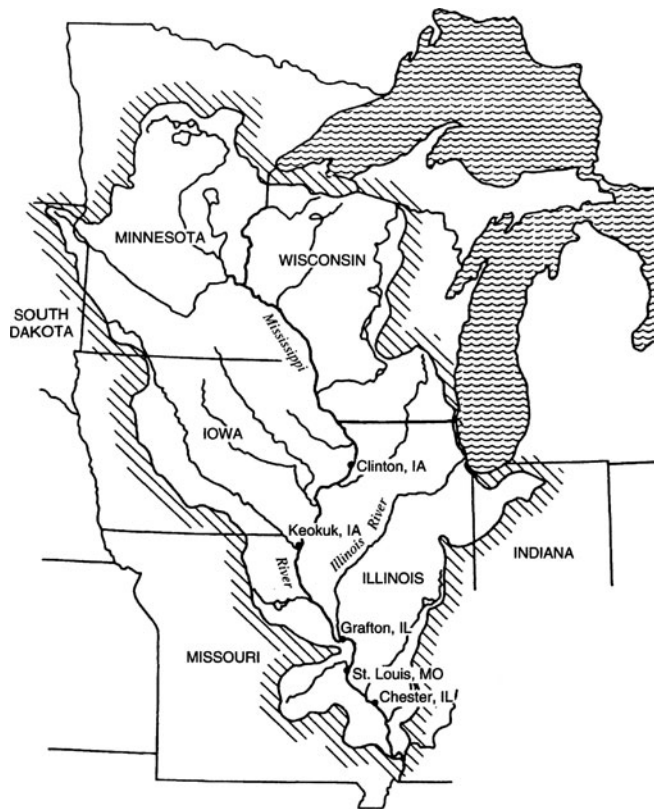


Figure 7.1.9 The Upper Mississippi River excluding the Missouri River. The location of the Illinois River (Figure 7.1.8) is shown (from Bhowmik (1998)).



Figure 7.1.10 The Mississippi River Basin in the United States (from Bhowmik (1998)).

7.1.4 Atmospheric and Ocean Circulation

Atmospheric circulation on Earth is a very complex process that is influenced by many factors. Major influences are differences in heating between low and high altitudes, the earth’s rotation, and heat and pressure differences associated with land and water. The general circulation of the atmosphere is due to latitudinal differences in solar heating of the earth’s surface and inclination of its axis, distribution of land and water, mechanics of the atmospheric fluid flow, and the Coriolis effect. In general, the atmospheric circulation is thermal in origin and is related to the earth’s rotation and global pressure distribution. If the earth were a nonrotating sphere, atmospheric circulation would appear as in Figure 7.1.11. Air would rise near the equator and travel in the upper atmosphere toward the poles, then cool, descend into the lower atmosphere, and return toward the equator. This is called *Hadley circulation*.

The rotation of the earth from west to east changes the circulation pattern. As a ring of air about the earth’s axis moves toward the poles, its radius decreases. In order to maintain angular momentum, the velocity of air increases with respect to the land surface, thus producing a westerly air flow. The converse is true for a ring of air moving toward the equator—it forms an easterly air flow. The effect producing these changes in wind direction and velocity is known as the *Coriolis force*.

The idealized pattern of atmospheric circulation has three cells in each hemisphere, as shown in Figure 7.1.12. In the *tropical cell*, heated air ascends at the equator, proceeds toward the poles at upper levels, loses heat, and descends toward the ground at latitude 30°. Near the ground it branches, one branch moving toward the equator and the other toward the pole. In the *polar cell*, air rises at 60° latitude and flows toward the poles at upper levels, then cools and flows back to 60° near the earth’s surface. The *middle cell* is driven frictionally by the other two; its surface flows toward the pole, producing prevailing westerly air flow in the midlatitudes.

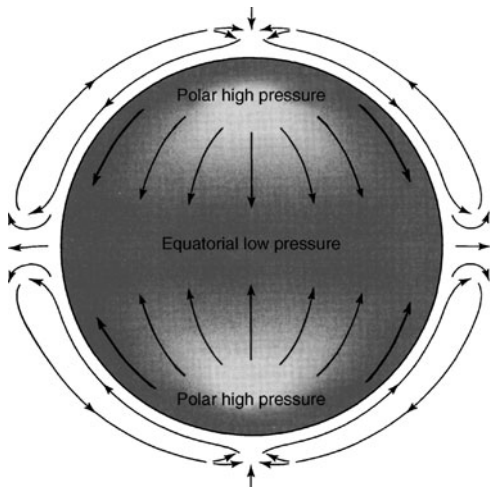


Figure 7.1.11 Atmospheric circulation pattern that would develop on a nonrotating planet. The equatorial belt would heat intensively and would produce low pressure, which would in turn set into motion a gigantic convection system. Each side of the system would span one hemisphere (from Marsh (1987)).

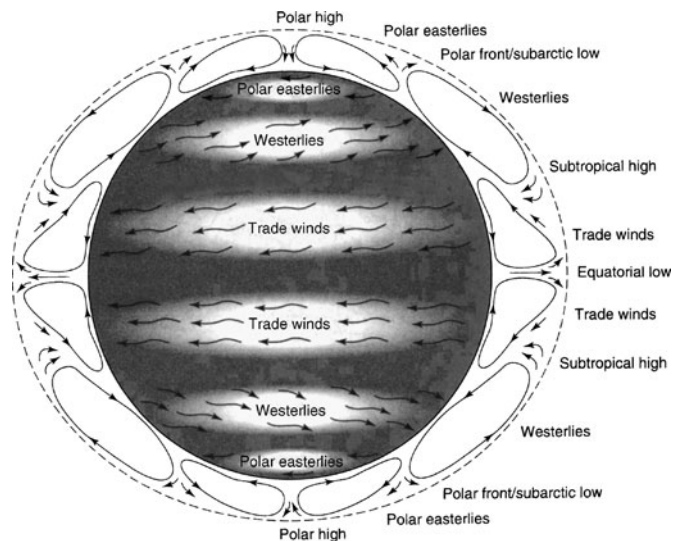


Figure 7.1.12 Idealized circulation of the atmosphere at the earth’s surface, showing the principal areas of pressure and belts of winds (from Marsh (1987)).

The uneven distribution of ocean and land on the earth's surface, coupled with their different thermal properties, creates additional spatial variation in atmospheric circulation. The annual shifting of the thermal equator due to the earth's revolution around the sun causes a corresponding oscillation of the three-cell circulation pattern. With a larger oscillation, exchanges of air between adjacent cells can be more frequent and complete, possibly resulting in many flood years. Also, monsoons may advance deeper into such countries as India and Australia. With a smaller oscillation, intense high pressure may build up around 30° latitude, thus creating extended dry periods. Since the atmospheric circulation is very complicated, only the general pattern can be identified.

The atmosphere is divided vertically into various zones. The atmospheric circulation described above occurs in the *troposphere*, which ranges in height from about 8 km at the poles to 16 km at the equator. The temperature in the troposphere decreases with altitude at a rate varying with the moisture content of the atmosphere. For dry air, the rate of decrease is called the *dry adiabatic lapse rate* and is approximately $9.8^\circ\text{C}/\text{km}$. The *saturated adiabatic lapse rate* is less, about $6.5^\circ\text{C}/\text{km}$, because some of the vapor in the air condenses as it rises and cools, releasing heat into the surrounding air. These are average figures for lapse rates that can vary considerably with altitude. The *tropopause* separates the troposphere from the *stratosphere* above. Near the tropopause, sharp changes in temperature and pressure produce strong narrow air currents known as *jet streams*, with velocities ranging from 15 to 50 m/s (30 to 100 m/h). They flow for thousands of kilometers and have an important influence on air-mass movement.

The oceans exert an important control on global climate. Because water bodies have a high volumetric heat capacity, the oceans are able to retain great quantities of heat. Through wave and current circulation, the oceans redistribute heat to considerable depths and even large areas of the oceans. Redistribution is east-west or west-east and is also across the midlatitudes from the tropics to the subarctic, enhancing the overall poleward heat transfer in the atmosphere. Waves are predominately generated by wind. Ocean circulation is illustrated in Figure 7.1.13.

Oceans have a significant effect on the atmosphere; however, an exact understanding of the relationships and mechanisms involved is not known. The correlation between ocean temperatures and weather trends and midlatitude events has not been solved. One trend is the growth and decline of a warm body of water in the equatorial zone of the eastern Pacific Ocean, referred to as

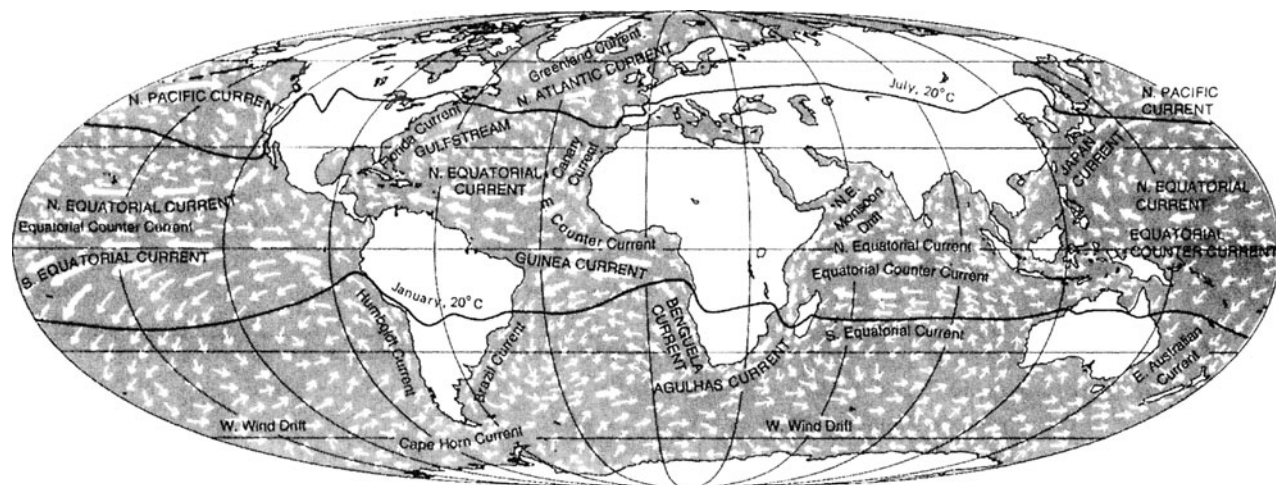


Figure 7.1.13 The actual circulation of the oceans. Major currents are shown with heavy arrows (from Marsh (1987)).

El Niño (meaning “The Infant” in Spanish, alluding to the Christ Child, because the effect typically begins around Christmas). The warm body of water develops and expands every five years or so off the coast of Peru, initiated by changes in atmospheric pressure resulting in a decline of the easterly trade winds. This reduction in wind reduces resistance, causing the eastwardly equatorial countercurrent to rise. As El Niño builds up, the warm body of water flows out into the Pacific and along the tropical west coast of the Americas, displacing the colder water of the California and Humboldt currents. One of the interesting effects of this weather variation is the South Oscillation, which changes precipitation patterns—resulting in drier conditions in areas of normally little precipitation.

7.1.5 Hydrologic Budget

A *hydrologic budget*, *water budget*, or *water balance* is a measurement of continuity of the flow of water, which holds true for any time interval and applies to any size area ranging from local-scale areas to regional-scale areas or from any drainage area to the earth as a whole. The hydrologists usually must consider an open system, for which the quantification of the hydrologic cycle for that system becomes a mass balance equation in which the change of storage of water (dS/dt) with respect to time within that system is equal to the inputs (I) to the system minus the outputs (O) from the system.

Considering the open system in Figure 7.1.14, the water balance equation can be expressed for the surface water system and the groundwater system in units of volume per unit time separately or, for a given time period and area, in depth.

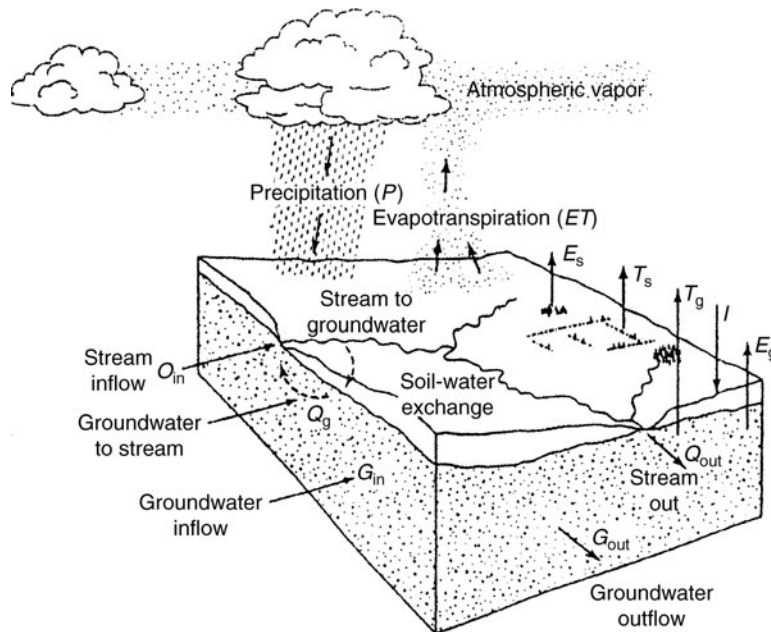


Figure 7.1.14 Components of hydrologic cycle in an open system: the major inflows and outflows of water from a parcel of land (from Marsh and Dozier (1986)) (Courtesy John Wiley & Sons, Inc.)

Surface Water System Hydrologic Budget

$$P + Q_{\text{in}} - Q_{\text{out}} + Q_g - E_s - T_s - I = \Delta S_s \quad (7.1.1)$$

where P is the precipitation, Q_{in} is the surface water flow into the system, Q_{out} is the surface water flow out of the system, Q_g is the groundwater flow into the stream, E_s is the surface evaporation, T_s is the transpiration, I is the infiltration, and ΔS_s is the change in water storage of the surface water system.

Groundwater System Hydrologic Budget

$$I + G_{\text{in}} - G_{\text{out}} - Q_g - E_g - T_g = \Delta S_g \quad (7.1.2)$$

where G_{in} is the groundwater flow into the system, G_{out} is the groundwater flow out of the system, and ΔS_g is the change in groundwater storage. The evaporation, E_g , and the transpiration, T_g , can be significant if the water table is near the ground surface.

System Hydrologic Budget

The system hydrologic budget is developed by adding the above two budgets together:

$$P - (Q_{\text{out}} - Q_{\text{in}}) - (E_s + E_g) - (T_s + T_g) - (G_{\text{out}} - G_{\text{in}}) = \Delta(S_s + S_g) \quad (7.1.3)$$

Using net mass exchanges, the above system hydrologic budget can be expressed as

$$P - Q - G - E - T = \Delta S \quad (7.1.4)$$

EXAMPLE 7.1.1

During January 1996, the water-budget terms for Lake Annie in Florida included precipitation (P) of 1.9 in, evaporation (E) of 1.5 in, surface water inflow (Q_{in}) of 0 in, surface outflow (Q_{out}) of 17.4 in, and change in lake volume (ΔS) of 0 in. Determine the net groundwater flow for January 1996 (the groundwater inflow minus the groundwater outflow).

SOLUTION

The water budget equation to define the net groundwater flow for the lake is

$$G = \Delta S - P + E - Q_{\text{in}} + Q_{\text{out}} = 0 - 1.9 + 1.5 - 0 + 17.4 = 17 \text{ in for January 1996}$$

7.2 PRECIPITATION (RAINFALL)**7.2.1 Precipitation Formation and Types**

Even though precipitation includes rainfall, snowfall, hail, and sleet, our concern in this book will relate almost entirely to rainfall. The formation of water droplets in clouds is illustrated in Figure 7.2.1. *Condensation* takes place in the atmosphere on *condensation nuclei*, which are very small particles ($10^{-3} - 10 \mu\text{m}$) in the atmosphere that are composed of dust or salt. These particles are called *aerosols*. During the initial occurrence of condensation, the droplets or ice particles are very small and are kept aloft by motion of the air molecules. Once droplets are formed they also act as condensation nuclei. These droplets tend to repel one another, but in the presence of an electric field in the atmosphere they attract one another and are heavy enough

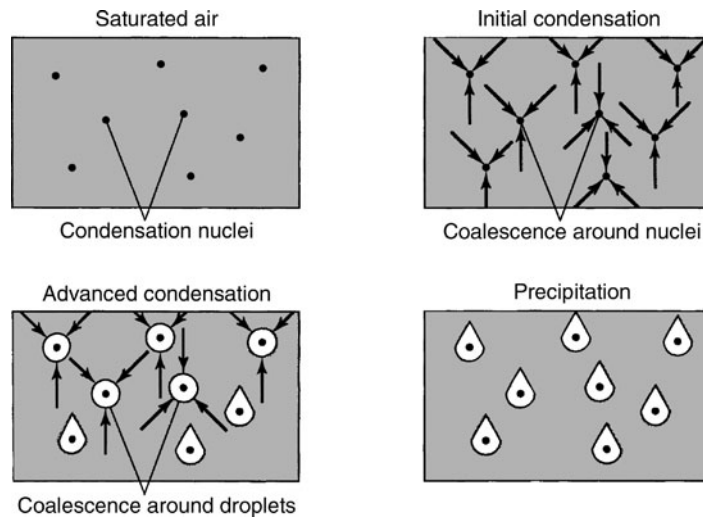


Figure 7.2.1 Precipitation formation. Water droplets in clouds are formed by nucleation of vapor on aerosols, then go through many condensation-evaporation cycles as they circulate in the cloud, until they aggregate into large enough drops to fall through the cloud base (from Marsh (1987)).

(~0.1 mm) to fall through the atmosphere. Some of the droplets evaporate in the atmosphere, some of the droplets decrease in size by evaporation, and some of the droplets increase in size by impact and aggregation.

Basically, the formation of precipitation requires lifting of an air mass in the atmosphere; it then cools and some of its moisture condenses. There are three main mechanisms of air mass lifting: *frontal lifting*, *orographic lifting*, and *convective lifting*. Frontal lifting (Figure 7.2.2) occurs when warm air is lifted over cooler air by frontal passage, orographic lifting (Figure 7.2.3) occurs when an air mass rises over a mountain range, and convective lifting (Figure 7.2.4) occurs when air is drawn upward by convective action such as a thunderstorm cell.

7.2.2 Rainfall Variability

In order to determine the runoff from a watershed and the resulting stream flow, precipitation is one of the primary inputs. Rainfall varies in space and time as a result of the general pattern of atmospheric circulation and local factors. Figure 7.2.5 shows the mean annual precipitation in the United States, and Figure 7.2.6 shows the normal monthly distribution of precipitation in the United States. Figure 7.2.7 shows the mean annual precipitation of the world.

Rainstorms can vary significantly in space and time. *Rainfall hyetographs* are plots of rainfall depth or intensity as a function of time. Figure 7.2.8a shows examples of two rainfall hyetographs. Cumulative rainfall hyetographs (rainfall mass curve) can be developed as shown in Figure 7.2.8b.

Isohyets (contours of constant rainfall) can be drawn to develop isohyetal maps of rainfall depth. *Isohyetal maps* are an interpolation of rainfall data recorded at gauged points. An example is shown in Figure 7.2.9 for the Upper Mississippi River Basin storm of January through July 1993. On a much smaller scale, shown in Figure 7.2.10, is the isohyetal map of the May 24–25, 1981 storm in Austin, Texas.

Figure 7.2.11 illustrates the three methods for determining areal average rainfall using rainfall gauge data. These are the *arithmetic-mean method*, the *Thiessen method*, and the *isohyetal method*.

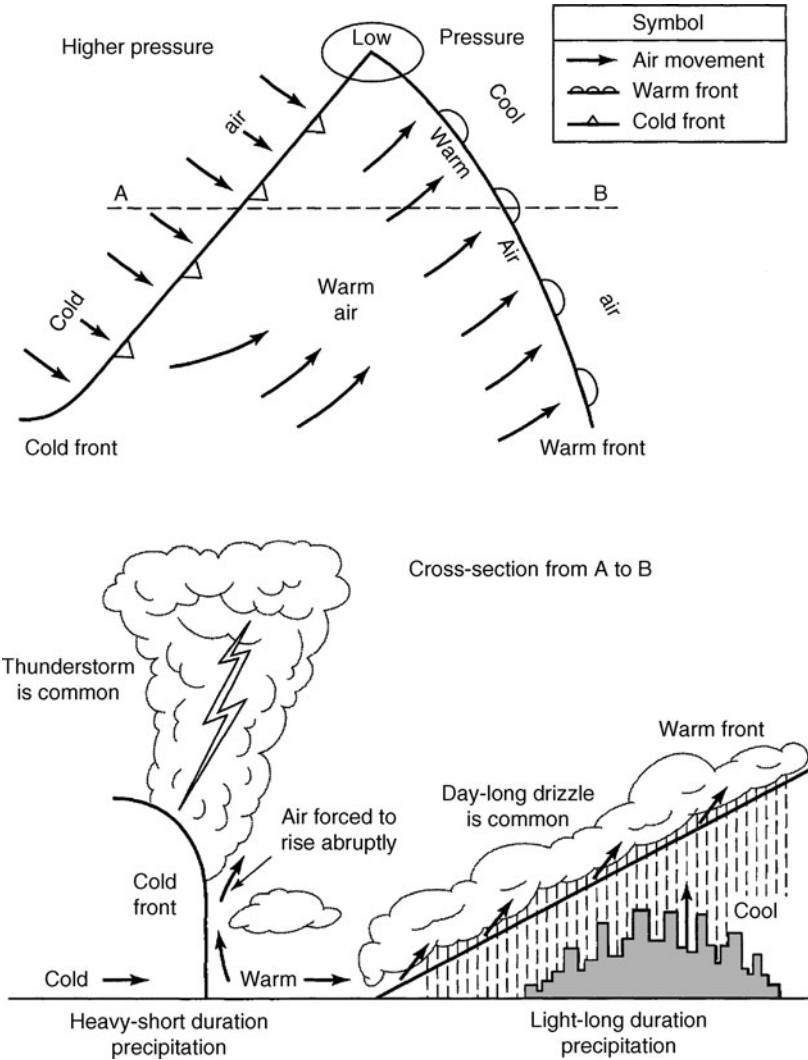


Figure 7.2.2 Cyclonic storms in midlatitude (from Masch (1984)).

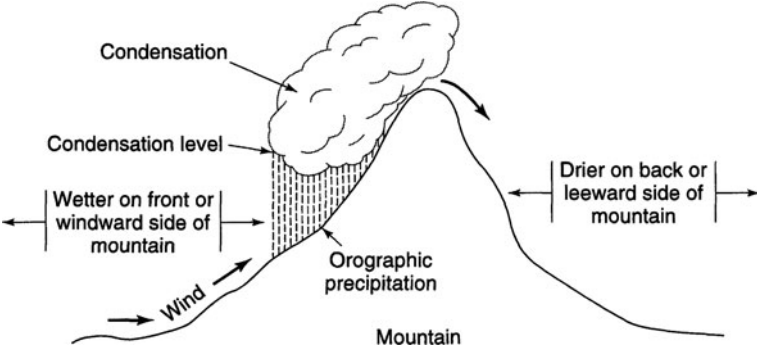


Figure 7.2.3 Orographic storm (from Masch (1984)).

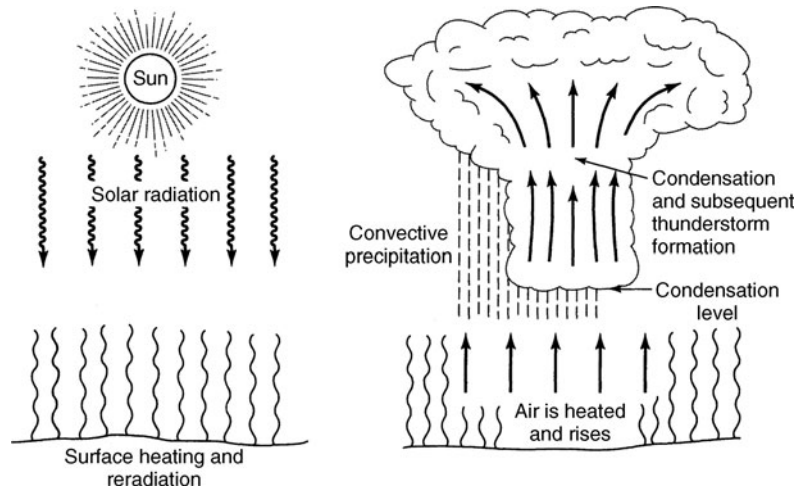


Figure 7.2.4 Convective storm (from Masch (1984)).

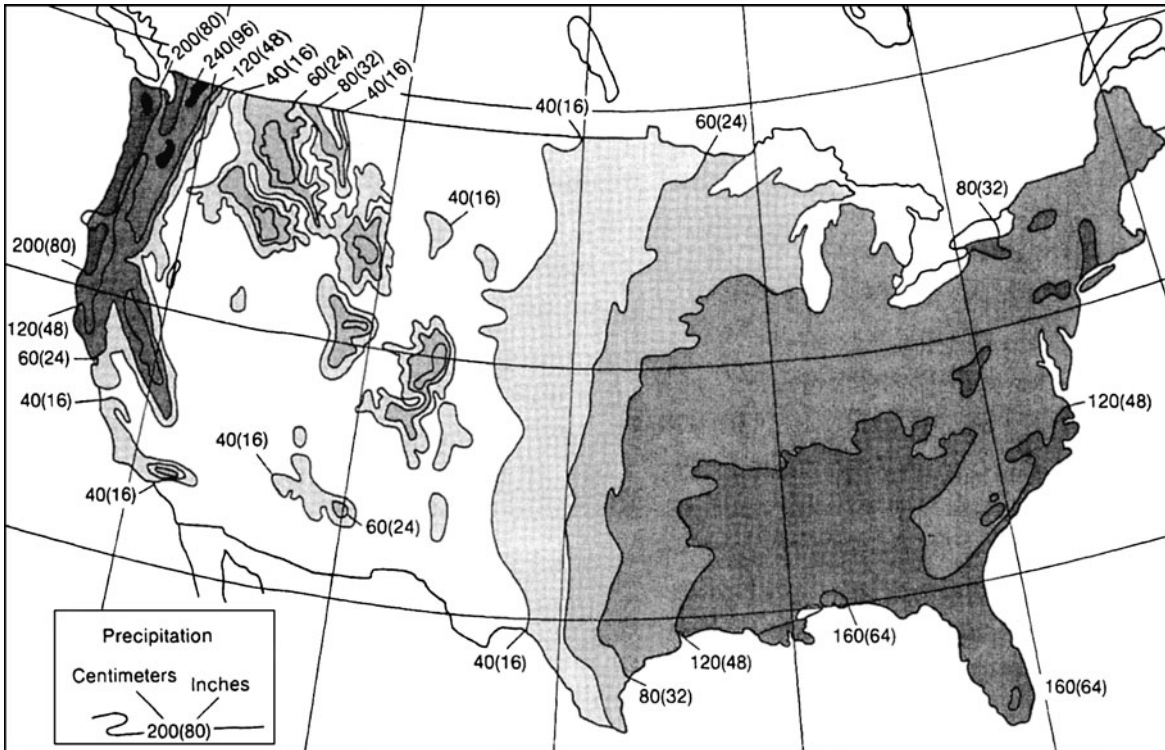


Figure 7.2.5 Mean annual precipitation for the United States in centimeters and inches (from Marsh (1987)).

7.2.3 Disposal of Rainfall on a Watershed

A *watershed* is the area of land draining into a stream at a particular location. The various surface water processes in the hydrologic cycle occur on a watershed. Figure 7.2.12 is a schematic illustration of the disposal of rainfall during a storm on a watershed. This figure

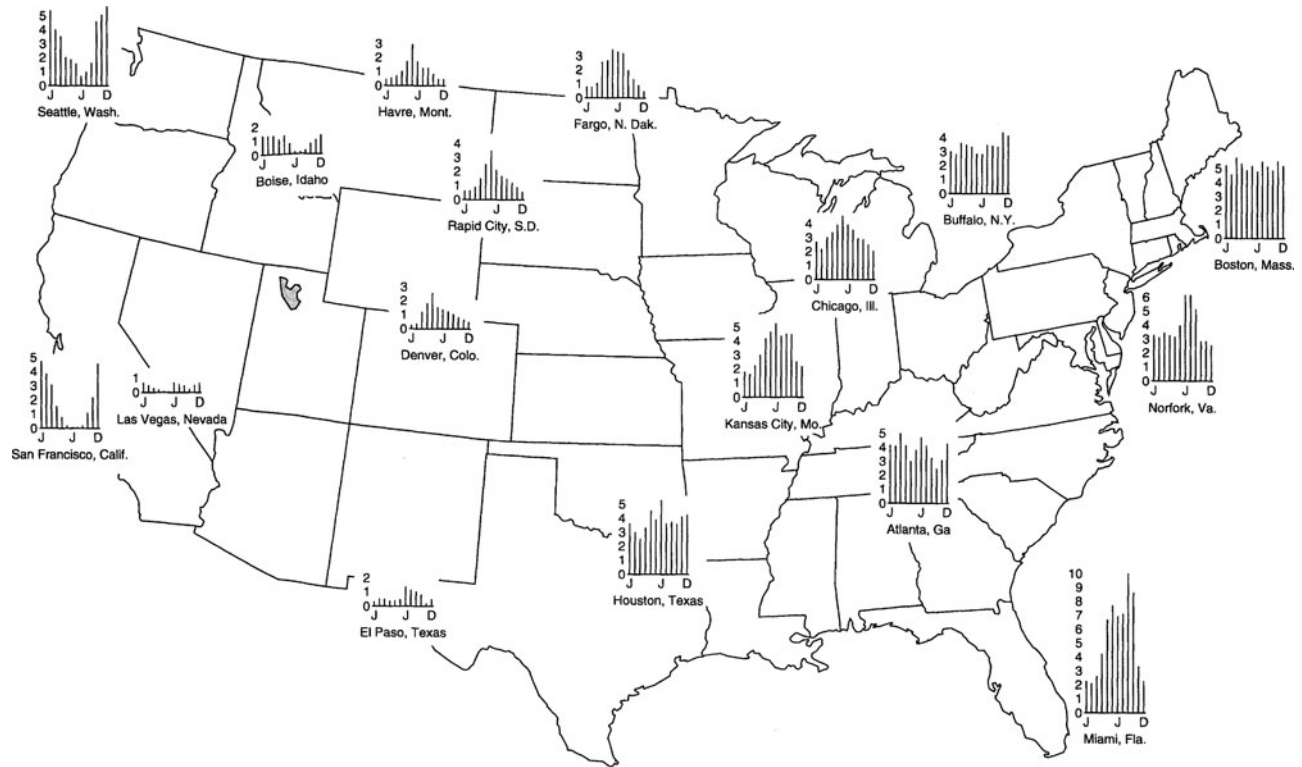


Figure 7.2.6 Normal monthly distribution of precipitation in the United States in inches (1 in = 254 mm) (from U.S. Environmental Data Services (1968)).

illustrates the rate (as a function of time) at which water flows or is added to storage for each of the processes. At the beginning of a storm, a large proportion of rainfall contributes to *surface storage*, and as water infiltrates, the *soil moisture storage* begins. Both *retention storage* and *detention storage* prevail. Retention storage is held for a long period of time and is depleted by evaporation, whereas detention storage is over a short time and is depleted by flow from the storage location.

7.2.4 Design Storms

The determination of flow rates in streams is one of the central tasks of surface water hydrology. For most engineering applications, these flow rates are determined for specified events that are typically extreme events. A major assumption in these analyses is that a certain return period storm results in the same return period flow rates from a watershed. The return period of an event, whether the event is a storm or a flow rate, is the expected value or the average value measured over a very large number of occurrences. In other words, the return period refers to the time interval for which an event will occur once on the average over a very large number of occurrences.

Hershfield (1961), in a publication often referred to as TP-40, presented isohyetal maps of design rainfall depths for the United States for durations from 30 minutes to 24 hours and return periods from 1 to 100 years. The values of rainfall in these isohyetal maps are point precipitation values, which is precipitation occurring at a single point in space (as opposed to areal

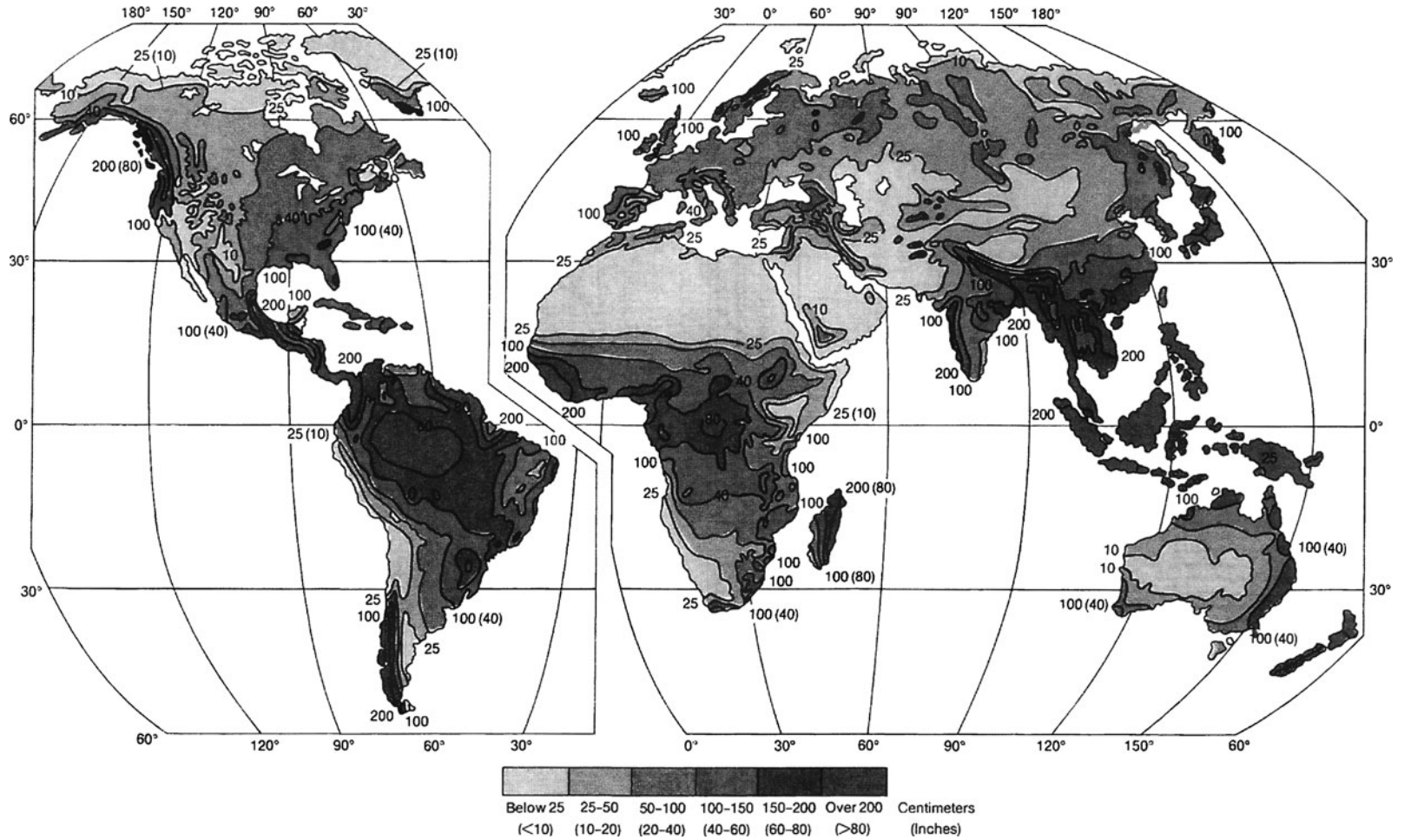


Figure 7.2.7 Average annual precipitation for the world's land areas, except Antarctica (from Marsh (1987)).

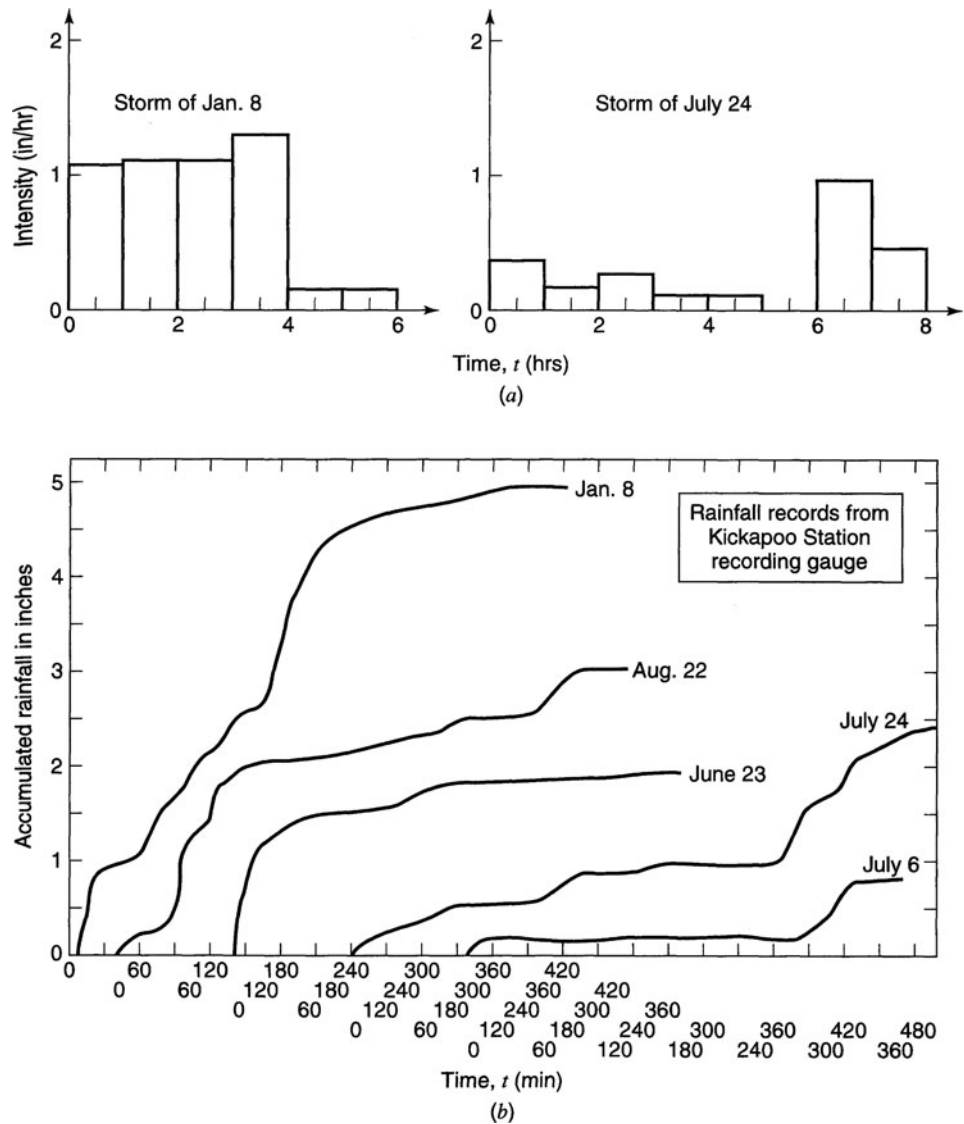
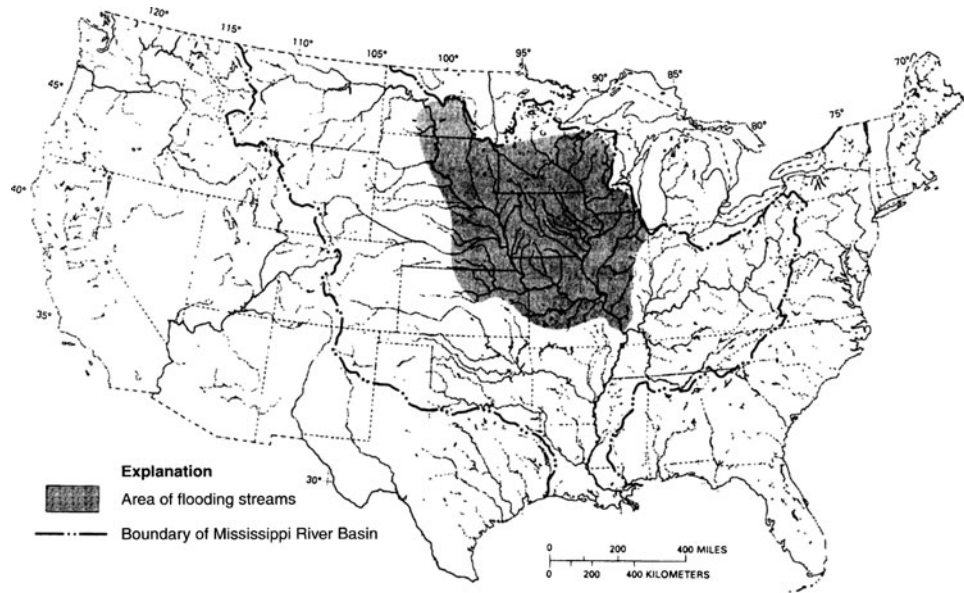


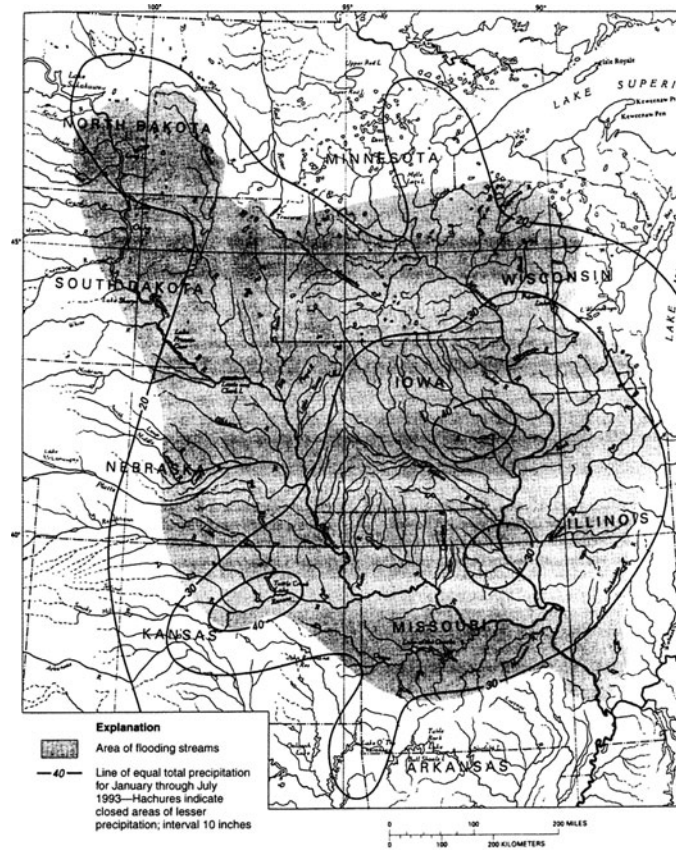
Figure 7.2.8 (a) Rainfall hyetographs for Kickapoo Station; (b) Mass rainfall curves (from Masch (1984)).

precipitation, which is over a larger area). Figure 7.2.13 is the isohyetal map for 100-year 24-hour rainfall. A later publication, U.S. Weather Bureau (1964), included maps for durations for 2 to 10 days, in what is referred to as TP-49. Miller et al. (1973) presented isohyetal maps for 6- and 24-hour durations for the 11 mountainous states in the western United States, which superseded the corresponding maps in TP-40.

Frederick et al. (1977), in a publication commonly referred to as HYDRO-35, presented isohyetal maps for events having durations from 5 to 60 minutes. The maps of precipitation depths for 5-, 15-, and 60-minute durations and return periods of 2 and 100 years for the 37 eastern states are presented in Figures 7.2.14 *a-f*. Depths for a return period are obtained by interpolation from the 5-, 15-, and



(a)



(b)

Figure 7.2.9 (a) Mississippi River Basin and general area of flooding streams, June through August 1993 (from Parrett et al. (1993)). (b) Areal distribution of total precipitation in the area of flooding in the upper Mississippi River Basin, January through May 1993 (from Parrett et al. (1993)).

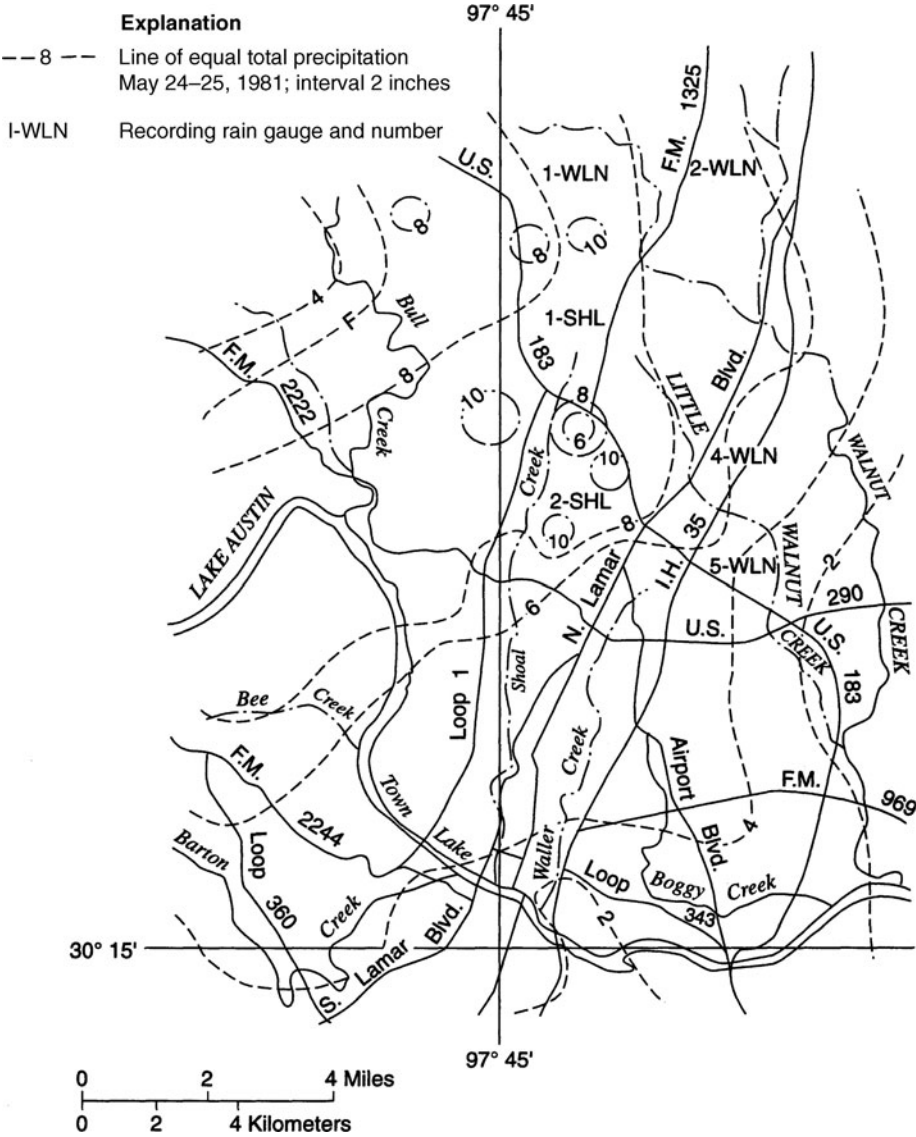


Figure 7.2.10 Isohyetal map of total precipitation (in) on May 24–25, 1981, based on USGS measurements, the City of Austin network, and unofficial precipitation reports (from Moore et al. (1982)).

60-minute data for the same return period:

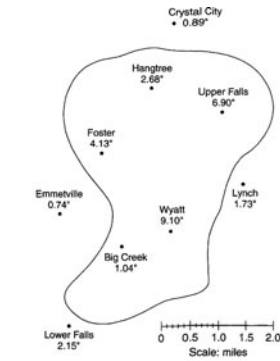
$$P_{10min} = 0.41 P_{5min} + 0.59 P_{15min} \tag{7.2.1a}$$

$$P_{30min} = 0.51 P_{15min} + 0.49 P_{60min} \tag{7.2.1b}$$

To consider return periods other than 2 or 100 years, the following interpolation equation is used:

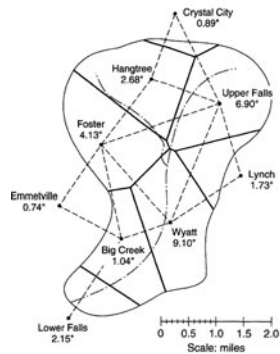
$$P_{T\text{ yr}} = aP_{2\text{ yr}} + bP_{100\text{ yr}} \tag{7.2.2}$$

where the coefficients *a* and *b* are found in Table 7.2.1.



$$\text{Average rainfall} = \frac{0.89 + 2.68 + 6.90 + 4.13 + 1.73 + 0.74 + 1.04 + 9.10 + 2.15}{9} = 3.26 \text{ in}$$

(a)



(1) Station	(2) Recorded Rainfall Depth P (in)	(3) Area A Represented by Station (mi^2)	(4) Rainfall Volume ($\text{mi}^2\text{-in}$)
Crystal City	0.89	0.21	0.187
Hangtree	2.68	2.82	7.558
Upper Falls	6.90	3.00	20.700
Foster	4.13	2.64	10.903
Lynch	1.73	1.00	1.730
Emmetville	0.74	0	0
Wyatt	9.10	2.94	26.754
Big Creek	1.04	2.07	2.153
Lower Falls	2.15	0.82	1.763
		Totals	71.748

$$\text{Average rainfall} = \frac{71.748}{15.50} = 4.63 \text{ in}$$

(b)



Rainfall Depth on Isohyet (in.)	Average Rainfall Depth (in.)	Area Between Isohyets (mi^2)	Rainfall Volume ($\text{mi}^2\text{-in}$)
9.1	8.55	0.407	3.480
8.0	7.0	1.412	9.884
6.0	5.5	$0.841 + 1.375 = 2.216$	1.219
5.0	4.5	$0.592 + 1.697 = 2.289$	10.300
4.0	3.5	3.122	10.927
3.0	2.5	$2.599 + 0.431 = 3.030$	7.575
2.0	1.5	2.281	3.422
1.0	1.0	0.05	0.050
6.9	6.45	0.693	4.470
6.0		Totals	51.327

$$\text{Average rainfall} = \frac{51.327}{15.50} = 3.31 \text{ in.}$$

(c)

Figure 7.2.11 (a) Computation of areal average rainfall by the arithmetic-mean method for a 24-hr storm. This is the simplest method of determining areal average rainfall. It involves averaging the rainfall depths recorded at a number of gauges. This method is satisfactory if the gauges are uniformly distributed over the area and the individual gauge measurements do not vary greatly about the mean (after Roberson et al. (1998)); (b) Computation of areal average rainfall by the Thiessen method for 24-hr storm. This method assumes that at any point in the watershed the rainfall is the same as that at the nearest gauge, so the depth recorded at a given gauge is applied out to a distance halfway to the next station in any direction. The relative weights for each gauge are determined from the corresponding areas of application in a *Thiessen polygon* network, the boundaries of the polygons being formed by the perpendicular bisectors of the lines joining adjacent gauges for J gauges; the area within the watershed assigned to each is A_j and P_j is the rainfall recorded at the j th gauge. The areal average precipitation for the watershed is computed by dividing the total rainfall volume by the total watershed area, as shown in the table (after Roberson et al. (1998)). (c) Computation of areal average rainfall by the isohyetal method for 24-hr storm. This method connects isohyets, using observed depths at rain gauges and interpolation between adjacent gauges. Where there is a dense network of rain gauges, isohyetal maps can be constructed using computer programs for automated contouring. Once the isohyetal map is constructed, the area A_j between each pair of isohyets within the watershed, is measured and multiplied by the average P_j of the rainfall depths of the two boundary isohyets to compute the areal average precipitation (after Roberson et al. (1998)).

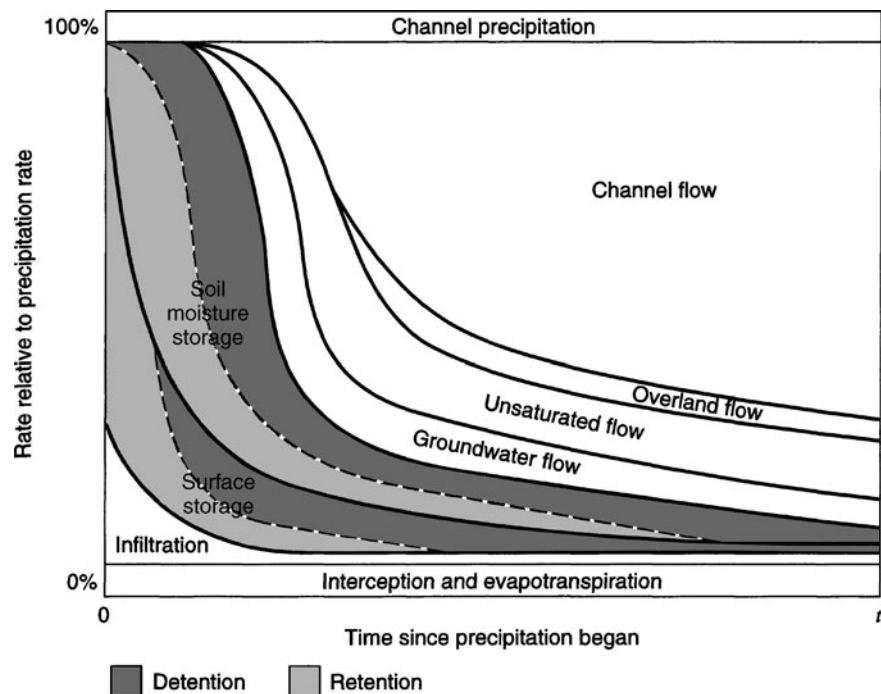


Figure 7.2.12 Schematic illustration of the disposal of precipitation during a storm on a watershed (from Chow et al. (1988)).

NOAA-Atlas 14

The new NOAA Atlas 14, Precipitation – Frequency Atlas of the United States, replaces the use of the old NOAA Atlas in the semi-arid region of the southwestern U.S., and replaces the use of the Hydro-35 and TP 40 in the Ohio River Valley including several surrounding states. The National Weather Service (NWS) Hydrometeorological Design Studies Center (HDSC) has issued the web page (<http://hdsc.nws.noaa.gov/hdsc/pfds/index.html>), which lists publications that should be used for each state in the U.S. and the time periods for which each should be used (5 min–60 min, 1 hr–24 hr, and 2-day–10-day periods). The two areas of the U.S. that are most impacted by the new NOAA Atlas 14 are the semi-arid southwest and the Ohio River Valley.

Semi-arid Southwest: NOAA-Atlas 2 is no longer valid for the semi-arid southwest, which includes: Arizona, Nevada, New Mexico, Utah, and Southeast California. For these states, NOAA-Atlas 2 (Volumes 4, 6, 7, 8, and part of 11) has been replaced by NOAA Atlas 14, Volume 1 which is available online: <http://www.nws.noaa.gov/oh/hdsc/currentpf.htm>

Ohio River Valley: Hydro-35 and Tech Paper No. 40 are no longer valid for most states in the Ohio River Valley and surrounding states, which includes: Delaware, Illinois, Indiana, Kentucky, Maryland, New Jersey, North Carolina, Ohio, Pennsylvania, South Carolina, Tennessee, Virginia, West Virginia, and Washington, DC. For these states, Hydro-35 and Tech Paper-40 have been replaced by NOAA Atlas 14, Volume 2, which is available online: <http://www.nws.noaa.gov/oh/hdsc/currentpf.htm>

Example point precipitation frequency estimates for two locations are presented in Figure 7.2.15. These are Chicago, Illinois and Phoenix, Arizona.

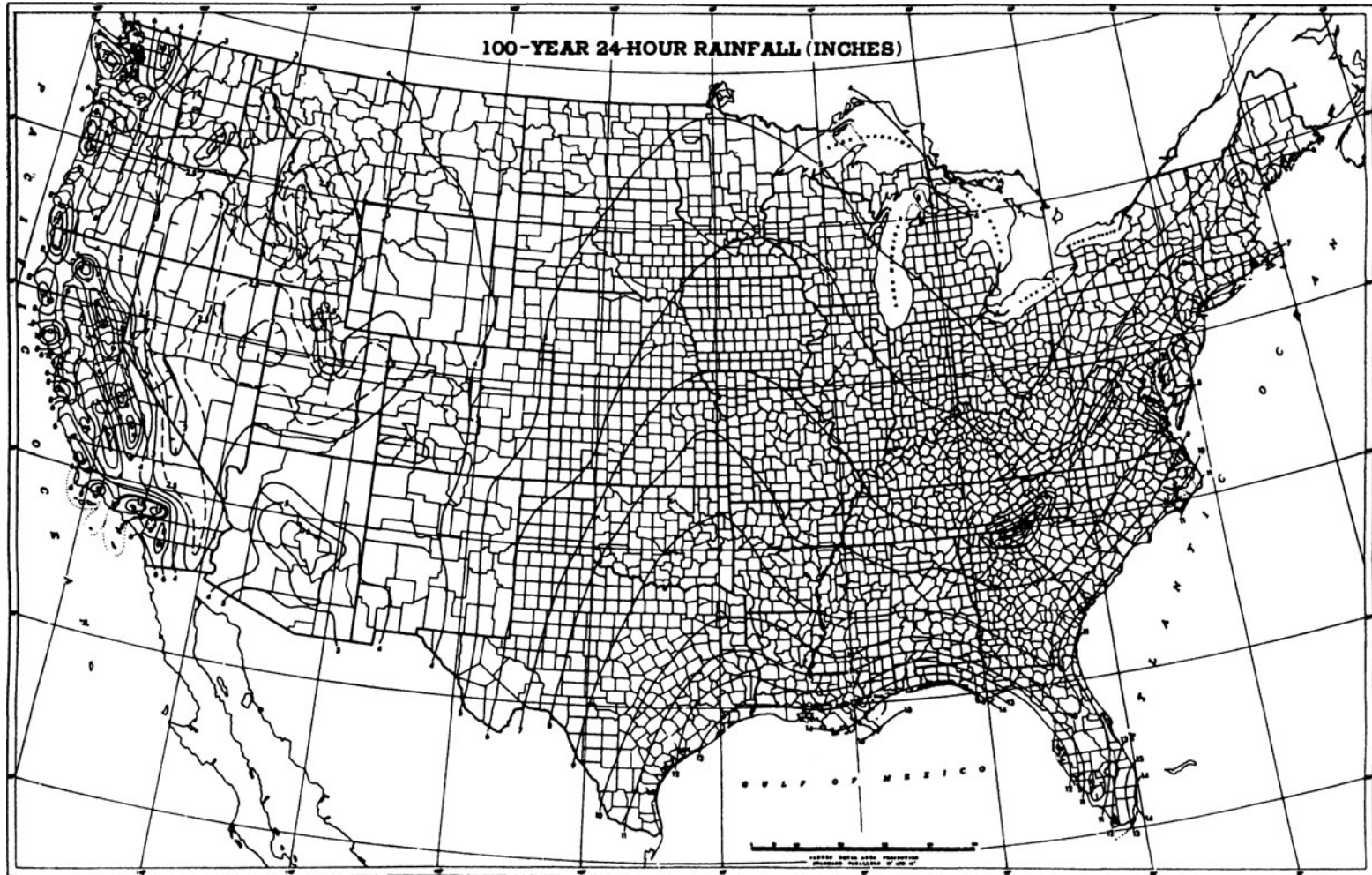
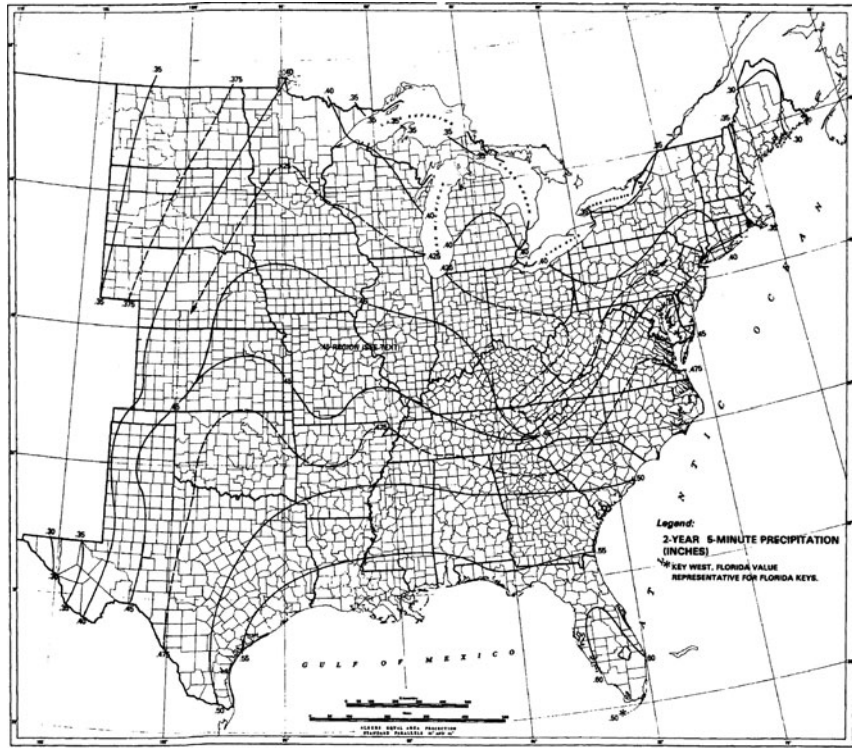
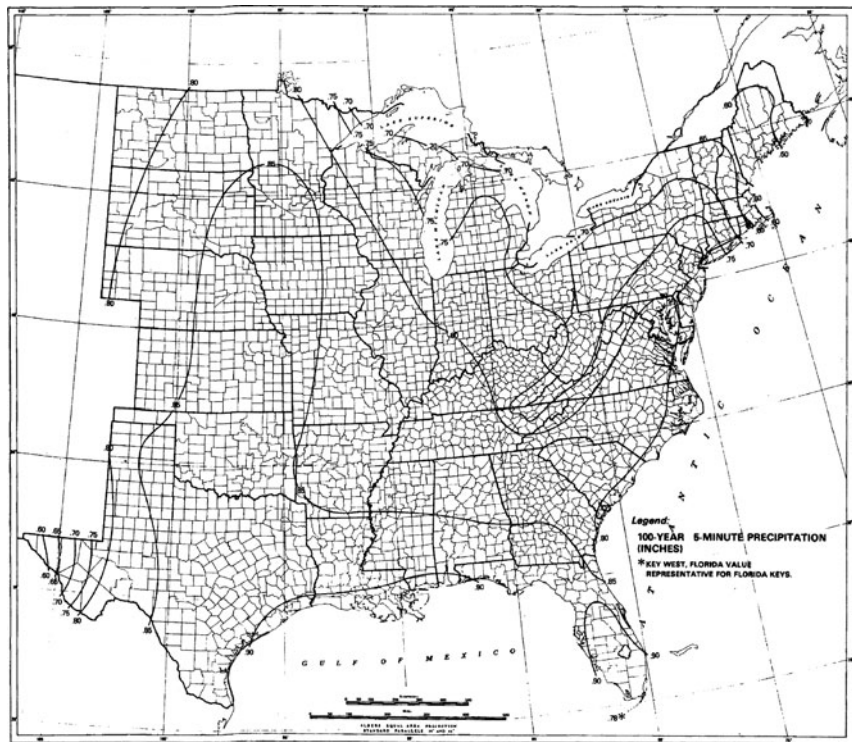


Figure 7.2.13 The 100-year 24-hr rainfall (in) the United States (from Hershfield (1961)).

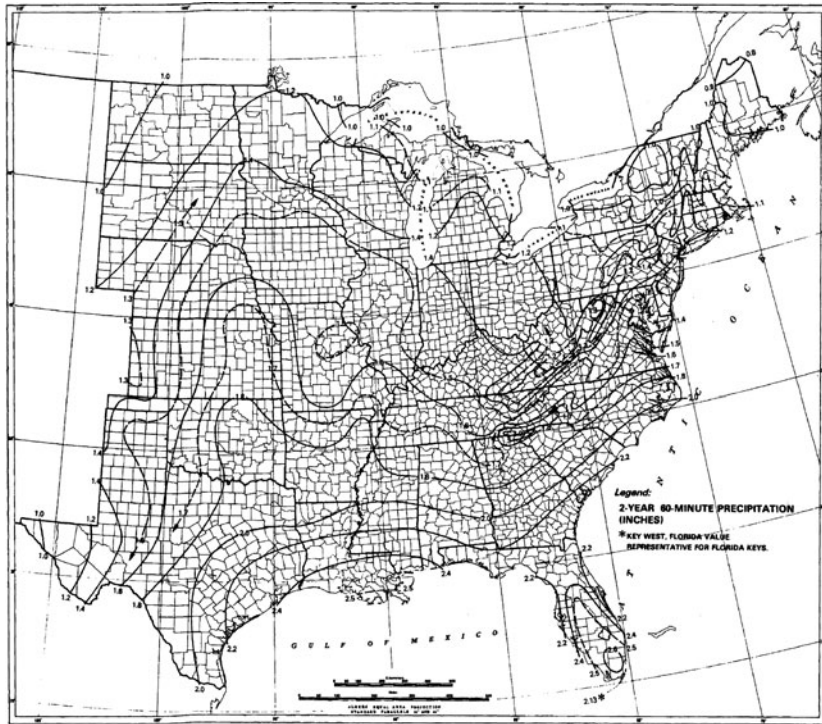


(a)

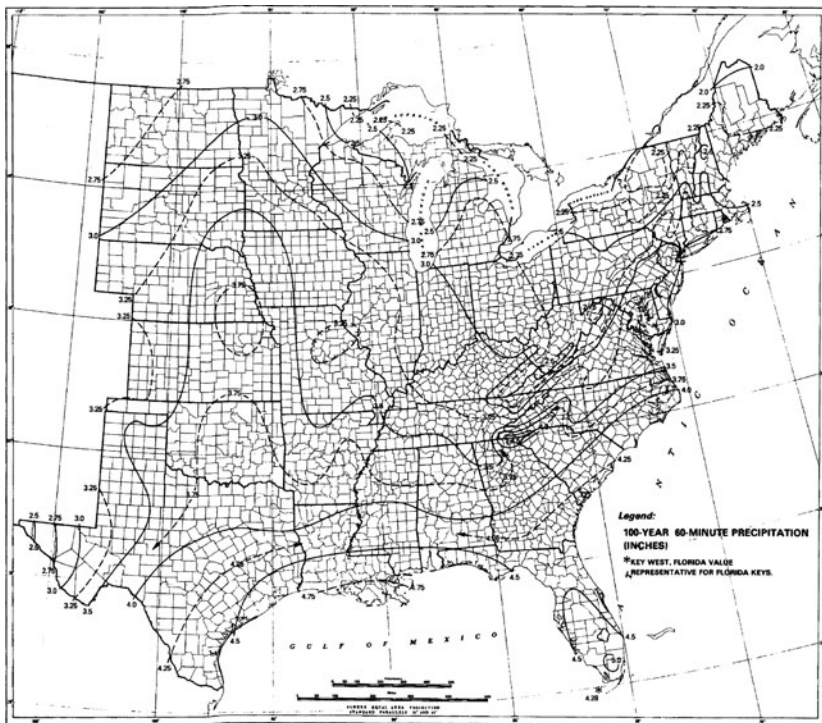


(b)

Figure 7.2.14 (a) 2-year 5-min precipitation (in) (from Frederick, Meyers, and Auciello (1977)). (b) 100-year 5-min precipitation (in) (from Frederick, Meyers, and Auciello (1977)). (c) 2-year 15-min precipitation (in) (from Frederick, Meyers, and Auciello (1977)). (d) 100-year 15-min precipitation (in) (from Frederick, Meyers, and Auciello (1977)). (e) 2-year 60-min precipitation (in) (from Frederick, Meyers, and Auciello (1977)). (f) 100-year 60-min precipitation (in) (from Frederick, Meyers, and Auciello (1977)).



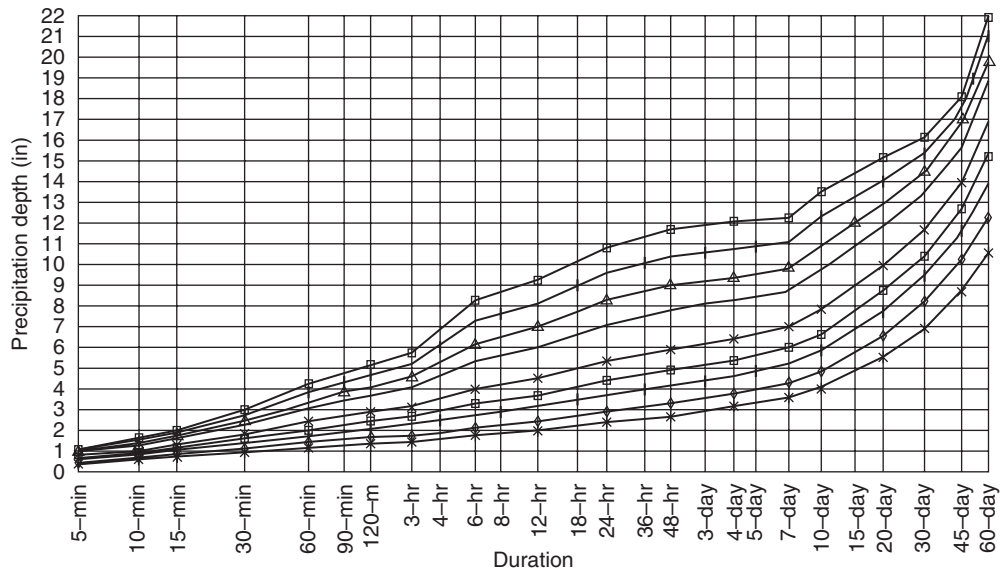
(e)



(f)

Figure 7.2.14 (Continued)

Partial duration based Point Precipitation Frequency Estimates - Version: 3
41.820 N 87.67 W 593 ft



Mon Feb 02 21:45:19 2009

Average recurrence interval (years)	
1	*
2	+
5	+
10	+
25	*
100	—
200	△
500	+
1000	—

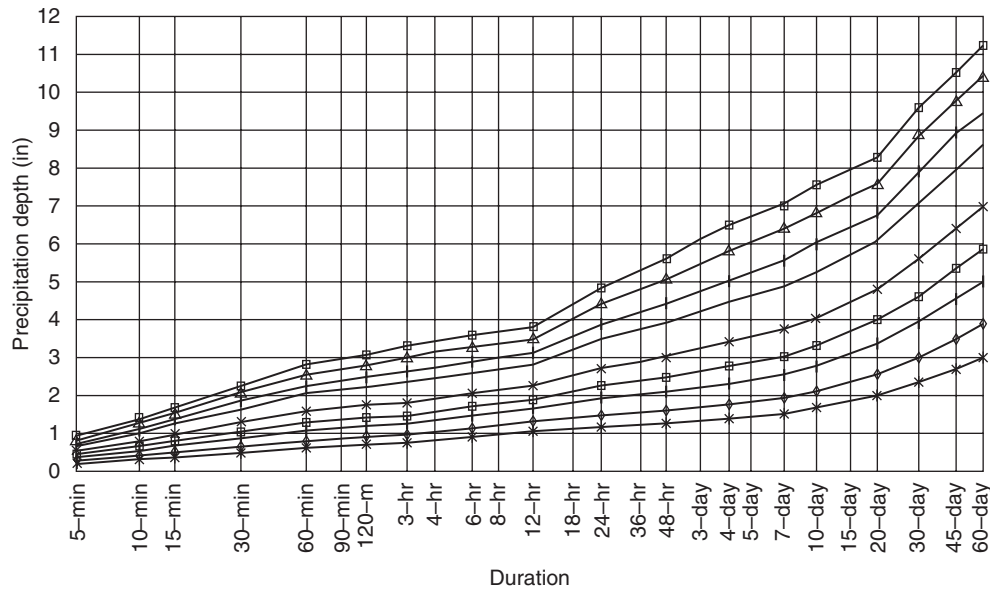
Precipitation Frequency Estimates (in)

ARI (years)	5 min	10 min	15 min	30 min	60 min	120 min	3 hr	6 hr	12 hr	24 hr	48 hr	4 day	7 day	10 day	20 day	30 day	45 day	60 day
1	0.38	0.60	0.73	0.97	1.18	1.38	1.48	1.77	2.04	2.39	2.74	3.15	3.66	4.13	5.55	6.96	8.73	10.4
2	0.46	0.71	0.88	1.17	1.44	1.68	1.81	2.16	2.48	2.91	3.32	3.77	4.36	4.89	6.56	8.20	10.24	12.2
5	0.55	0.85	1.05	1.43	1.80	2.12	2.30	2.78	3.17	3.72	4.21	4.67	5.28	5.88	7.73	9.49	11.65	13.9
10	0.62	0.96	1.18	1.63	2.08	2.47	2.68	3.30	3.75	4.39	4.93	5.40	6.02	6.69	8.64	10.46	12.69	15.2
25	0.71	1.09	1.34	1.90	2.46	2.94	3.21	4.05	4.58	5.37	5.99	6.46	7.06	7.84	9.88	11.70	13.95	16.7
50	0.78	1.19	1.47	2.10	2.77	3.33	3.64	4.70	5.28	6.20	6.88	7.33	7.90	8.79	10.85	12.62	14.87	17.9
100	0.85	1.28	1.60	2.31	3.08	3.73	4.09	5.40	6.05	7.10	7.83	8.27	8.78	9.78	11.82	13.49	15.71	18.9
200	0.93	1.39	1.72	2.52	3.41	4.15	4.57	6.17	6.89	8.10	8.88	9.27	9.70	10.84	12.80	14.34	16.50	19.9
500	1.03	1.52	1.90	2.81	3.88	4.75	5.24	7.31	8.13	9.58	10.41	10.77	11.06	12.33	14.12	15.42	17.47	21.1
1000	1.11	1.62	2.02	3.04	4.26	5.22	5.78	8.29	9.18	10.83	11.71	12.05	12.26	13.56	15.15	16.20	18.15	21.9

(a) Chicago, Illinois 41.820 N 87.67 W 593 feet

Figure 7.2.15 Point Precipitation Frequency Estimates from NOAA Atlas 14, (a) Chicago, Illinois (from Bonnin et al. (2004)); (b) Phoenix, Arizona (from Bonnin et al. (2004)).

Partial duration based Point Precipitation Frequency Estimates - Version: 4
33.482 N 112.05 W 1158 ft



Mon Feb 02 22:31:58 2009

Average recurrence interval (years)	
1	—
2	—
5	—
10	—
25	—
100	—
200	—
500	—
1000	—

Precipitation Frequency Estimates (in)

ARI (years)	5 min	10 min	15 min	30 min	60 min	120 min	3 hr	6 hr	12 hr	24 hr	48 hr	4 day	7 day	10 day	20 day	30 day	45 day	60 day
1	0.19	0.29	0.36	0.48	0.59	0.68	0.72	0.88	0.99	1.14	1.23	1.36	1.50	1.63	1.98	2.31	2.67	2.95
2	0.25	0.38	0.47	0.63	0.78	0.88	0.93	1.11	1.26	1.45	1.57	1.74	1.91	2.08	2.54	2.97	3.44	3.80
5	0.34	0.51	0.64	0.86	1.06	1.18	1.22	1.43	1.60	1.88	2.06	2.29	2.52	2.74	3.35	3.91	4.53	4.99
10	0.41	0.62	0.77	1.03	1.27	1.41	1.46	1.68	1.86	2.22	2.45	2.74	3.01	3.27	3.96	4.62	5.33	5.85
25	0.50	0.76	0.94	1.26	1.56	1.72	1.78	2.03	2.22	2.69	3.00	3.37	3.71	4.01	4.79	5.57	6.38	6.97
50	0.57	0.86	1.07	1.44	1.78	1.96	2.04	2.30	2.50	3.06	3.44	3.88	4.26	4.61	5.42	6.30	7.16	7.79
100	0.64	0.97	1.21	1.62	2.01	2.20	2.32	2.58	2.78	3.45	3.89	4.42	4.85	5.24	6.05	7.05	7.95	8.62
200	0.71	1.08	1.34	1.81	2.24	2.45	2.60	2.87	3.07	3.85	4.37	5.00	5.48	5.90	6.70	7.81	8.74	9.42
500	0.81	1.23	1.53	2.06	2.54	2.78	2.99	3.26	3.46	4.40	5.04	5.81	6.36	6.82	7.57	8.82	9.76	10.4
1000	0.88	1.34	1.67	2.24	2.78	3.04	3.31	3.57	3.75	4.84	5.57	6.47	7.07	7.57	8.23	9.60	10.53	11.2

(b) Arizona 33.482 N 112.05 W 1158 feet

Figure 7.2.15 (Continued)

Table 7.2.1 Coefficients for Interpolating Design Precipitation Depths Using Equation (7.2.2)

Return period T years	a	b
5	0.674	0.278
10	0.496	0.449
25	0.293	0.669
50	0.146	0.835

Source: Frederick, Meyers, and Auciello (1997).

EXAMPLE 7.2.1

Determine the 2-, 10-, 25-, and 100-year rainfall depths for a 15-min duration storm at a location where $P_{2,15} = 0.9$ in and $P_{100,15} = 1.75$ in.

SOLUTION

$P_{10,15}$ and $P_{25,15}$ are determined using equation (7.2.2). From Table 7.2.1, $a = 0.496$ and $b = 0.449$ for 10 years and $a = 0.293$ and $b = 0.669$ for 25 years:

$$P_{10\text{yr}} = aP_{2\text{yr}} + bP_{100\text{yr}}$$

$$P_{10,15} = 0.496 \times 0.9 + 0.449 \times 1.75 = 0.446 + 0.786 = 1.23 \text{ in}$$

$$P_{25,15} = 0.293 P_{2,15} + 0.669 P_{100,15} = 0.293 \times 0.9 + 0.669 \times 1.75 = 1.43 \text{ in}$$

IDF Relationships

In hydrologic design projects, particularly urban drainage design, the use of *intensity-duration-frequency* relationships is recommended. *Intensity* refers to rainfall intensity (depth per unit time), and in some cases depths are used instead of intensity. *Duration* refers to rainfall duration, and *frequency* refers to *return periods*, which is the expected value of the *recurrence interval* (time between occurrences). See Chapter 10 for more details. The intensity-duration-frequency (IDF) relationships are also referred to as *IDF curves*. IDF relationships have also been expressed in equation form, such as

$$i = \frac{c}{T_d^e + f} \tag{7.2.3}$$

where i is the design rainfall intensity in inches per hour, T_d is the duration in minutes, and c , e , and f are coefficients that vary for location and return period. Other forms of these IDF equations include the return period, such as

$$i = \frac{cT^m}{T_d + f} \tag{7.2.4}$$

and

$$i = \frac{cT^m}{T_d^e + f} \tag{7.2.5}$$

where T is the return period. In Chapter 15, these IDF equations are used in urban drainage design. Chow et al. (1988) describe in detail how to derive the coefficients for these relationships using rainfall data.

Synthetic Storm Hyetograph

In many types of hydrologic analysis, such as *rainfall-runoff analysis*, to determine the runoff (discharge) from a watershed the time sequence of rainfall is needed. In such cases it is standard practice to use a *synthetic storm hyetograph*. The United States Department of Agriculture Soil Conservation Service (1973, 1986) developed synthetic storm hyetographs for 6- and 24-hr storms in

Table 7.2.2 SCS Rainfall Distributions

24-hour storm						6-hour storm		
Hour t	$t/24$	P_t/P_{24}				Hour t	$t/6$	P_t/P_6
		Type I	Type IA	Type II	Type III			
0	0	0	0	0	0	0	0	0
2.0	0.083	0.035	0.050	0.022	0.020	0.60	0.10	0.04
4.0	0.167	0.076	0.116	0.048	0.043	1.20	0.20	0.10
6.0	0.250	0.125	0.206	0.080	0.072	1.50	0.25	0.14
7.0	0.292	0.156	0.268	0.098	0.089	1.80	0.30	0.19
8.0	0.333	0.194	0.425	0.120	0.115	2.10	0.35	0.31
8.5	0.354	0.219	0.480	0.133	0.130	2.28	0.38	0.44
9.0	0.375	0.254	0.520	0.147	0.148	2.40	0.40	0.53
9.5	0.396	0.303	0.550	0.163	0.167	2.52	0.42	0.60
9.75	0.406	0.362	0.564	0.172	0.178	2.64	0.44	0.63
10.0	0.417	0.515	0.577	0.181	0.189	2.76	0.46	0.66
10.5	0.438	0.583	0.601	0.204	0.216	3.00	0.50	0.70
11.0	0.459	0.624	0.624	0.235	0.250	3.30	0.55	0.75
11.5	0.479	0.654	0.645	0.283	0.298	3.60	0.60	0.79
11.75	0.489	0.669	0.655	0.357	0.339	3.90	0.65	0.83
12.0	0.500	0.682	0.664	0.663	0.500	4.20	0.70	0.86
12.5	0.521	0.706	0.683	0.735	0.702	4.50	0.75	0.89
13.0	0.542	0.727	0.701	0.772	0.751	4.80	0.80	0.91
13.5	0.563	0.748	0.719	0.799	0.785	5.40	0.90	0.96
14.0	0.583	0.767	0.736	0.820	0.811	6.00	1.0	1.00
16.0	0.667	0.830	0.800	0.880	0.886			
20.0	0.833	0.926	0.906	0.952	0.957			
24.0	1.000	1.000	1.000	1.000	1.000			

Source: U.S. Department of Agriculture Soil Conservation Service (1973, 1986).

the United States. These are presented in Table 7.2.2 and Figure 7.2.16 as cumulative hyetographs. Four 24-hr duration storms, Type I, IA, II, and III, were developed for different geographic locations in the U.S., as shown in Figure 7.2.17. Types I and IA are for the Pacific maritime climate, which has wet winters and dry summers. Type III is for the Gulf of Mexico and Atlantic coastal areas, which have tropical storms resulting in large 24-hour rainfall amounts. Type II is for the remainder of the United States.

In the midwestern part of the United States the Huff (1967) temporal distribution of storms is widely used for heavy storms on areas ranging up to 400 mi². Time distribution patterns were developed for four probability groups, from the most severe (first quartile) to the least severe (fourth quartile). Figure 7.2.18a shows the probability distribution of first-quartile storms. These curves are smooth, reflecting average rainfall distribution with time; they do not exhibit the burst characteristics of observed storms. Figure 7.2.18b shows selected histograms of first-quartile storms for 10-, 50-, and 90-percent cumulative probabilities of occurrence, each illustrating the percentage of total storm rainfall for 10 percent increments of the storm duration. The 50 percent histogram represents a cumulative rainfall pattern that should be exceeded in about half of the storms. The 90 percent histogram can be interpreted as a storm distribution that is equaled or exceeded in 10 percent or less of the storms.

EXAMPLE 7.2.2

Using equation (7.2.3), compute the design rainfall intensities for a 10-year return period, 10-, 20-, and 60-min duration storms for $c = 62.5$, $e = 0.89$, and $f = 9.10$.

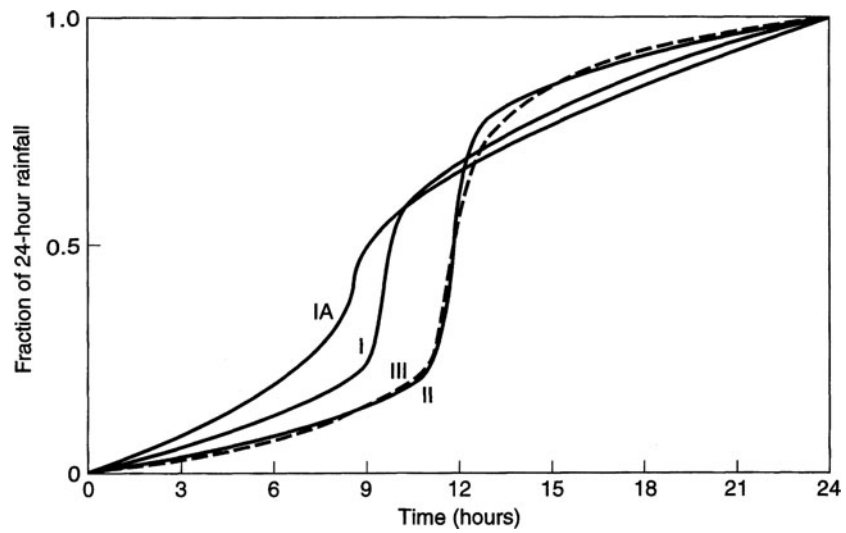


Figure 7.2.16 Soil Conservation Service 24-hour rainfall hyetographs (from U.S. Department of Agriculture Soil Conservation Service (1986)).

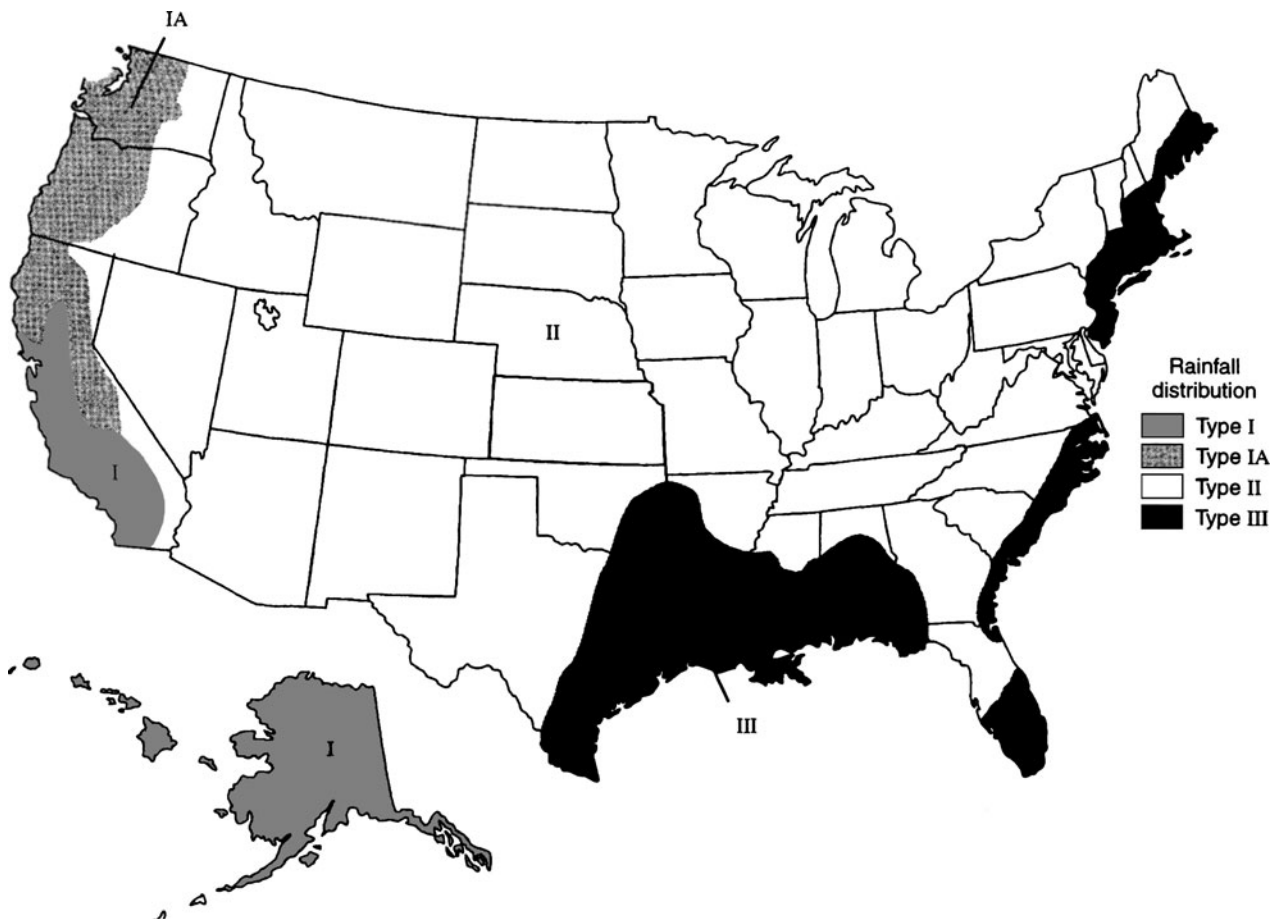


Figure 7.2.17 Location within the United States for application of the SCS 24-hour rainfall hyetographs (from U.S. Department of Agriculture Soil Conservation Service (1986)).

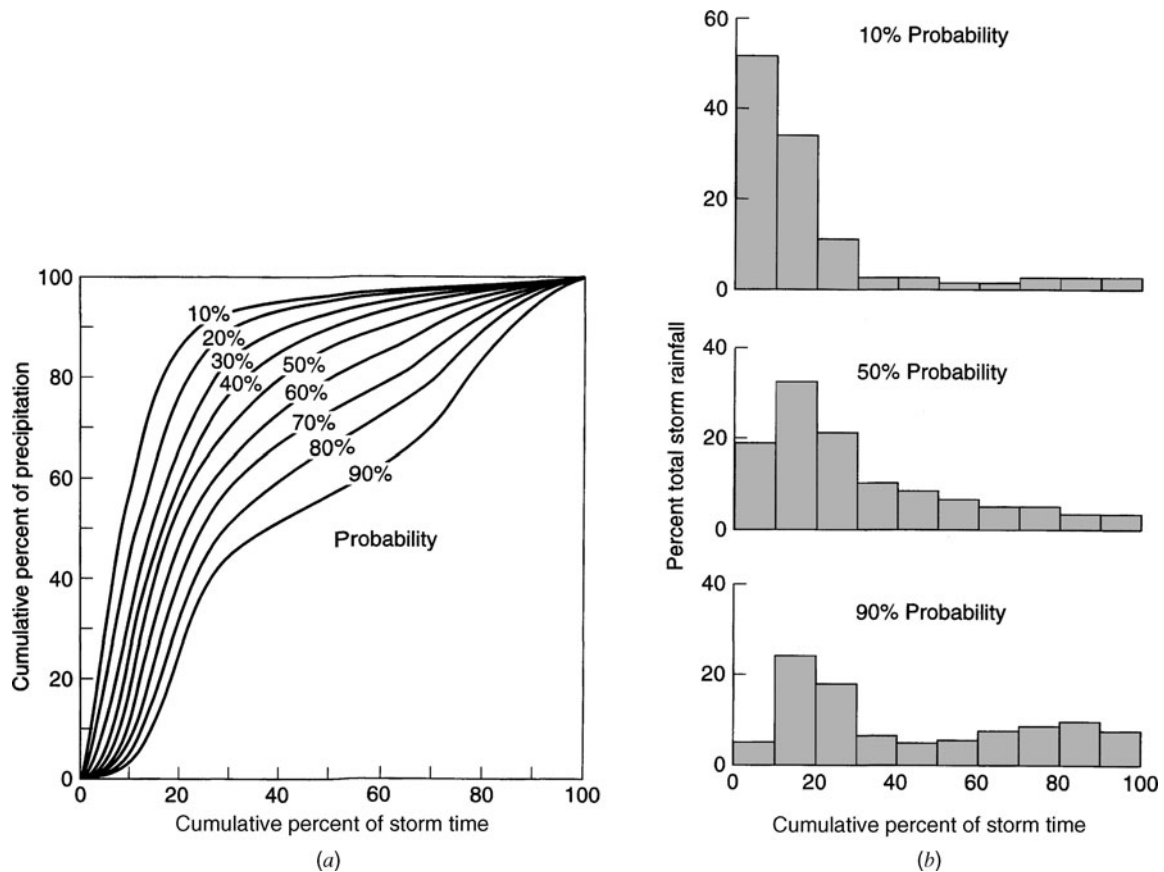


Figure 7.2.18 (a) Time distribution of first-quartile storms. The probability shown is the chance that the observed storm pattern will lie to the left of the curve; (b) Selected histograms for first-quartile storms (from Huff (1967)).

SOLUTION

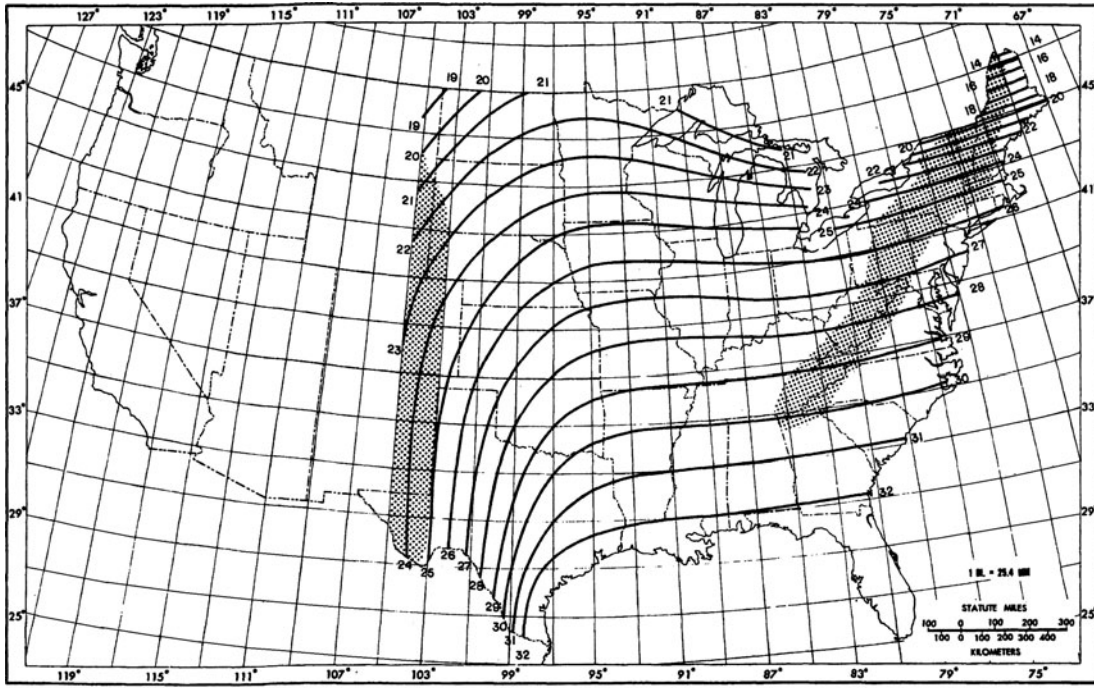
The rainfall intensity duration frequency relationship is then

$$i = \frac{62.5}{T_d^{0.89} + 9.10}$$

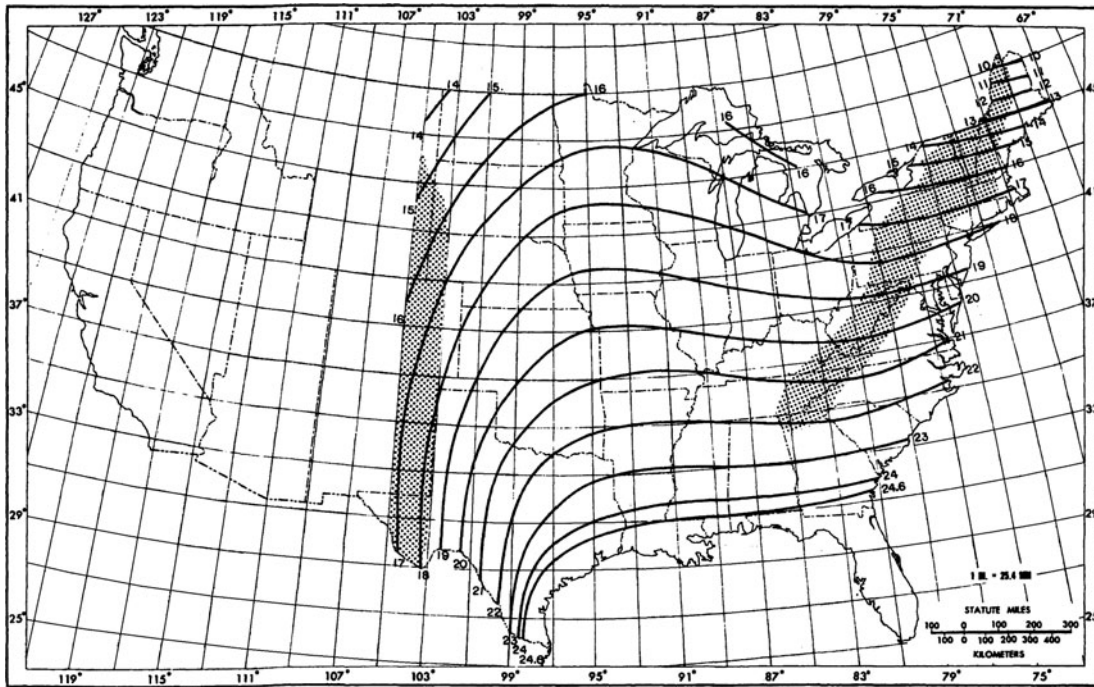
For $T_d = 10$ min, $i = \frac{62.5}{10^{0.89} + 9.10} = 3.71$ in/hr. For $T_d = 20$ min, $i = 2.66$ in/hr, and for $T_d = 60$ min, $i = 1.32$ in/hr.

7.2.5 Estimated Limiting Storms

Estimated limiting values (ELVs) are used for the design of water control structures such as the spillways on large dams. Of particular interest are the *probable maximum precipitation* (PMP) and the *probable maximum storm* (PMS). These are used to derive a *probable maximum flood* (PMF). PMP is a depth of precipitation that is the estimated limiting value of precipitation, defined as the estimated greatest depth of precipitation for a given duration that is physically possible and reasonably characteristic over a particular geographical region at a certain time of year (Chow et al., 1988). Schreiner and Riedel (1978) presented generalized PMP charts for the United States east of the 105th meridian HMR 51. The all-seasons (any time of the year) estimates of PMP are presented in maps as a function of storm area (ranging from 10 to 20,000 mi²) and storm durations ranging from 6 to 72 hours, as shown in Figure 7.2.19. For regions west of the 105th meridian, the diagram in Figure 7.2.20 shows the appropriate U.S. National Weather Service

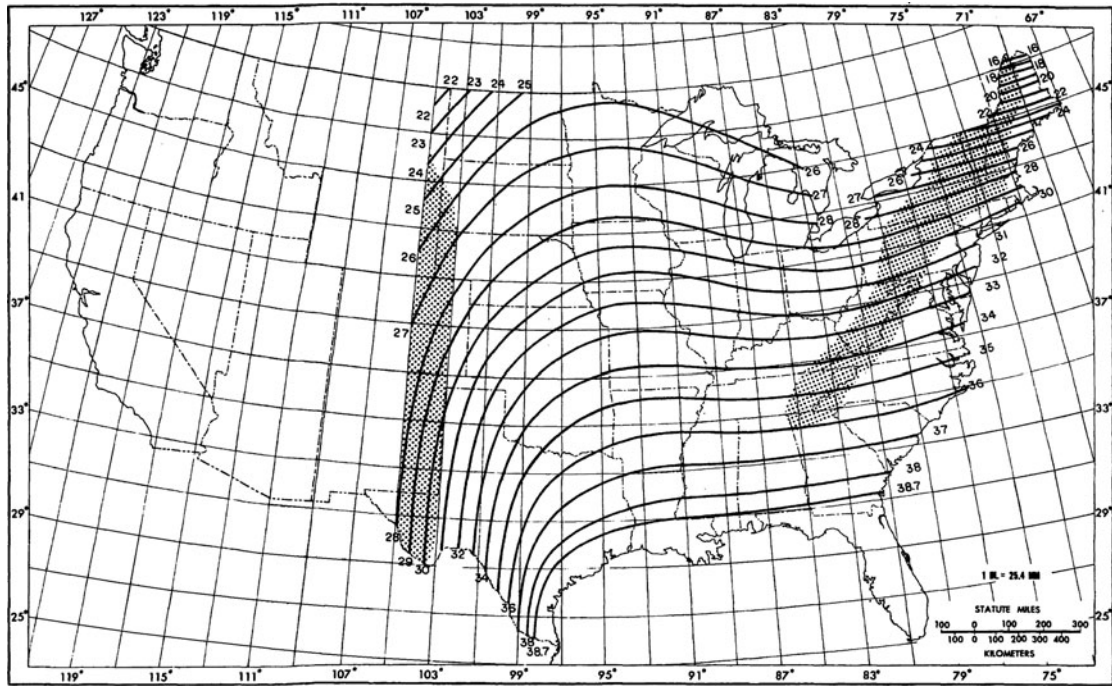


(a)

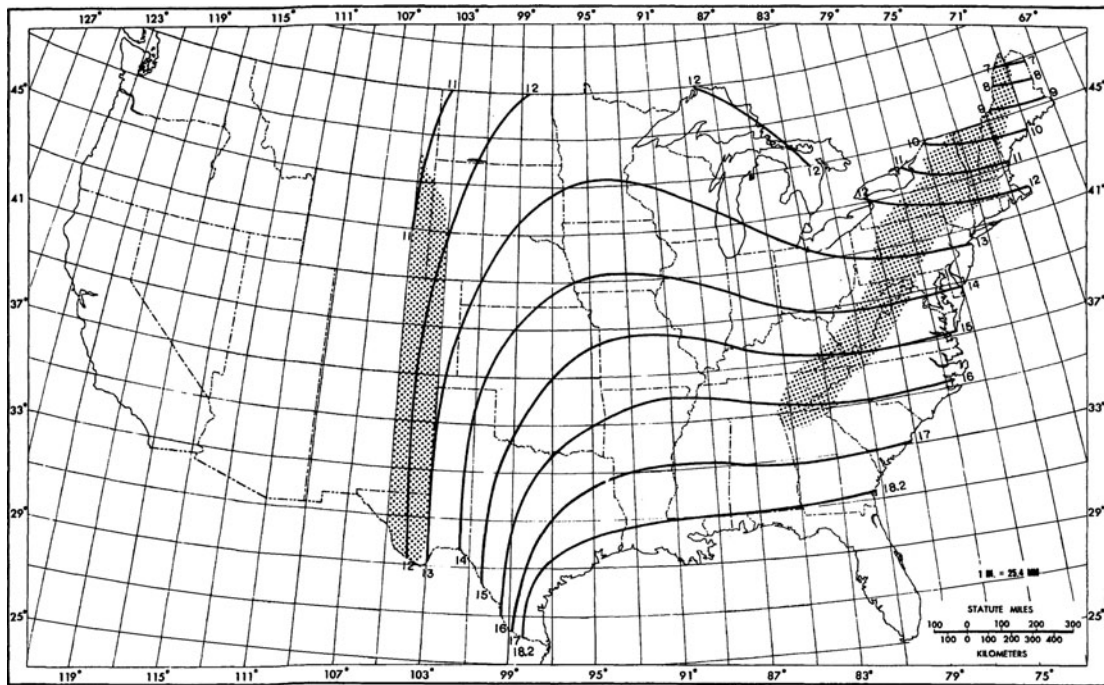


(b)

Figure 7.2.19 (a) Example of all-season PMP (in) for 6 hr, 10 mi² (from Schreiner and Riedel, 1978); (b) Example of all-season PMP (in) for 6 hr, 200 mi² (from Schreiner and Riedel, 1978).



(c)



(d)

Figure 7.2.19 (Continued) (c) Example of all-season PMP (in) for 12 hr, 10 mi² (from Schreiner and Riedel, 1978); (d) Example of all-season PMP (in) for 6 hr, 1000 mi² (from Schreiner and Riedel, 1978).

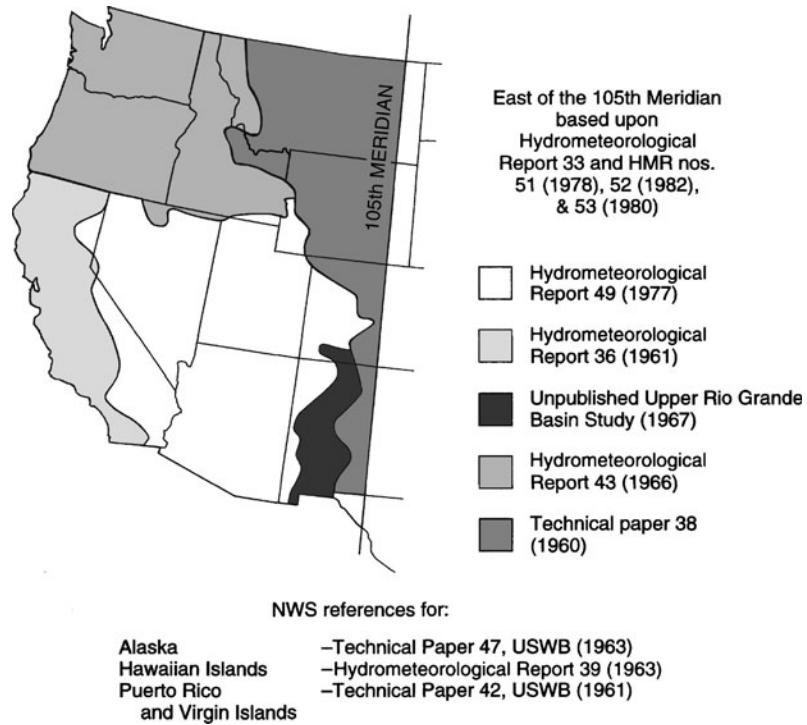


Figure 7.2.20 Sources of information for probable maximum precipitation computation in the United States (from U.S. National Academy of Sciences (1983)).

publication. Hansen et al. (1982), in what is called HMR 52, present the procedure to determine the PMS for areas east of the 105th meridian.

7.3 EVAPORATION

Evaporation is the process of water changing from its liquid phase to the vapor phase. This process may occur from water bodies, from saturated soils, or from unsaturated surfaces. The evaporation process is illustrated in Figure 7.3.1. Above the water surface a number of things are happening. First

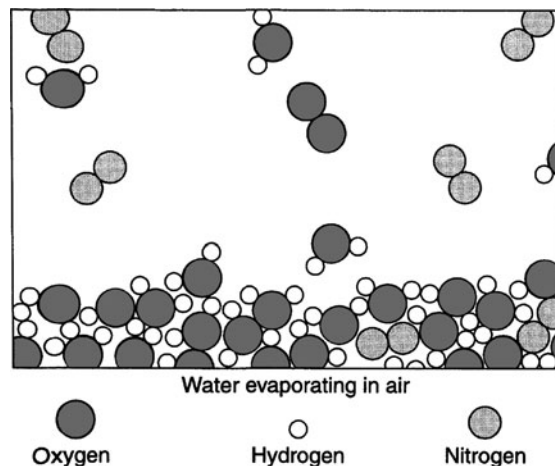


Figure 7.3.1 Evaporation (magnified one billion times) (from Feynman et al. (1963)).

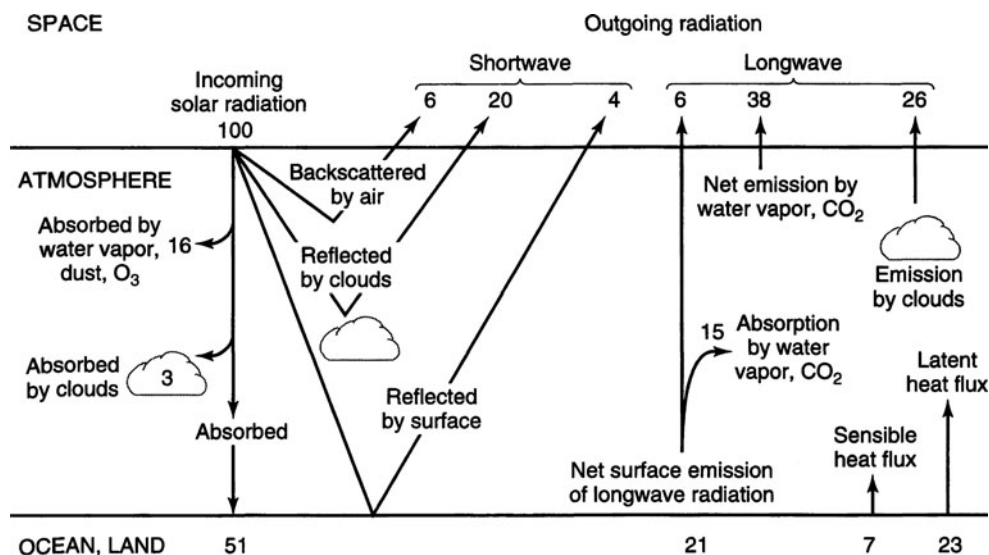


Figure 7.3.2 Radiation and heat balance in the atmosphere and at the earth's surface (from U.S. National Academy of Sciences (1975)).

of all, there are water molecules in the form of *water vapor*, which are always found above liquid water. In addition, there are some other molecules: (a) two oxygen atoms stuck together by themselves, forming an *oxygen molecule*, and (b) two nitrogen atoms stuck together, forming a nitrogen molecule. Above the water surface is the air, a gas, consisting almost entirely of nitrogen, oxygen, some water vapor, and lesser amounts of carbon dioxide, argon, and other substances. The molecules in the water are always moving around. From time to time, one on the surface gets knocked away. In other words, molecule by molecule, the water disappears or evaporates.

The computation of evaporation in hydrologic analysis and design is important in water supply design, particularly reservoir design and operation. The supply of energy to provide *latent heat of vaporization* and the *ability to transport water vapor away* from the evaporative surface are the two major factors that influence evaporation. *Latent heat* is the heat that is given up or absorbed when a phase (solid, liquid, or gaseous state) changes. *Latent heat of vaporization* (l_v) refers to the heat given up during vaporization of liquid water to water vapor, and is given as $l_v = 2.501 \times 10^6 - 2370T$, where T is the temperature in °C and l_v is in joules (J) per kilogram.

Three methods are used to determine evaporation: *the energy balance method*, *the aerodynamic method*, and *the combined aerodynamic and energy balance method*. The energy balance method considers the heat energy balance of a hydrologic system, and the aerodynamic method considers the ability to transport away from an open surface. Figure 7.3.2 illustrates the radiation and heat balance in the atmosphere and at the earth's surface along with relative values for the various components.

7.3.1 Energy Balance Method

Consider the evaporation pan shown in Figure 7.3.3 with the defined control volume. This control volume contains water in both the liquid phase and the vapor phase, with densities of ρ_w and ρ_a , respectively. The continuity equation must be written for both phases. For the liquid phase, the extensive property $B = m$ (mass of liquid water), the intensive property $\beta = 1$, and $dB/dt = \dot{m}_v$, which is the mass flow rate of evaporation. Continuity for the liquid phase is then

$$-\dot{m}_v = \frac{d}{dt} \int_{CV} \rho_w dV + \sum_{CS} \rho_w \mathbf{V} \cdot \mathbf{A} \quad (7.3.1)$$

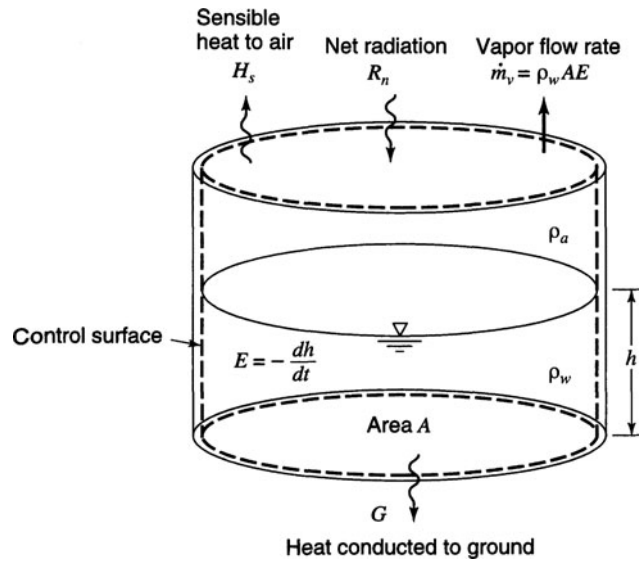


Figure 7.3.3 Control volume defined for continuity and energy equation development for an evaporation pan (from Chow et al. (1988)).

Because the pan has impermeable sides, there is no flow of liquid water across the control surface, so

$$\sum_{CS} \rho_w \mathbf{V} \cdot \mathbf{A} = 0.$$

The rate of change of storage is

$$\frac{d}{dt} \int_{CV} \rho_w d\forall = \rho_w A \frac{dh}{dt} \tag{7.3.2}$$

where A is the cross-sectional area of the pan and h is the depth of water. Substituting equation (7.3.2) into (7.3.1) gives

$$-\dot{m}_v = \rho_w A \frac{dh}{dt} \tag{7.3.3a}$$

or

$$\dot{m}_v = \rho_w AE \tag{7.3.3b}$$

where $E = -dh/dt$ is the evaporation rate.

Considering the vapor phase, the extensive property is $B = m_v$ (mass of water vapor), the intensive property is $\beta = q_v$ (specific humidity), and $dB/dt = \dot{m}_v$. Continuity for the vapor phase is

$$\dot{m}_v = \frac{d}{dt} \int_{CV} q_v \rho_a d\forall + \sum_{CS} q_v \rho_a \mathbf{V} \cdot \mathbf{A} \tag{7.3.4}$$

Considering steady flow over the pan, the time derivative of water vapor in the control volume is zero, $\frac{d}{dt} \int_{CV} q_v \rho_a d\forall = 0$, and \dot{m}_v from equation (7.3.3) is substituted into equation (7.3.4) to obtain

$$\rho_w AE \sum_{CS} q_v \rho_a \mathbf{V} \cdot \mathbf{A} \tag{7.3.5}$$

which is the continuity equation for the pan. Equation (7.3.5) can be rearranged to yield

$$E = \left(\frac{1}{\rho_w A} \right) \sum_{CS} q_v \rho_a \mathbf{V} \cdot \mathbf{A} \quad (7.3.6)$$

Next, consider the heat energy equation (3.4.19):

$$\frac{dH}{dt} - \frac{dW_s}{dt} = \frac{d}{dt} \int_{CV} \left(e_u + \frac{1}{2} V^2 + gz \right) \rho_w d\forall + \sum_{CS} \left(\frac{p}{\rho_w} + e_u + \frac{1}{2} V^2 + gz \right) \rho_w \mathbf{V} \cdot \mathbf{A} \quad (3.4.19)$$

using ρ_w to represent density of water; dH/dt is the rate of heat input from an external source, $dW_s/dt = 0$ because there is no work done by the system; e_u is the specific internal heat energy of the water; $V = 0$ for the water in the pan; and the rate of change of the water surface elevation is small ($dz/dt = 0$). Then the above equation is reduced to

$$\frac{dH}{dt} = \frac{d}{dt} \int_{CV} e_u \rho_w d\forall \quad (7.3.7)$$

The rate of heat input from external sources can be expressed as

$$\frac{dH}{dt} = R_n - H_s - G \quad (7.3.8)$$

where R_n is the *net radiation flux* (watts per meter squared), H_s is the *sensible heat* to the air stream supplied by the water, and G is the *ground heat flux* to the ground surface. Net radiation flux is the net input of radiation at the surface at any instant. The net radiation flux at the earth's surface is the major energy input for evaporation of water, defined as the difference between the radiation absorbed, $R_i(1 - \alpha)$ (where R_i is the *incident radiation* and α is the fraction of radiation reflected, called the *albedo*), and that emitted, R_e :

$$R_n = R_i(1 - \alpha) - R_e \quad (7.3.9)$$

The amount of radiation emitted is defined by the *Stefan-Boltzmann law*

$$R_e = e\sigma T_p^4 \quad (7.3.10)$$

where e is the *emissivity* of the surface, σ is the *Stefan-Boltzmann constant* ($5.67 \times 10^{-8} \text{W/m}^2 \cdot \text{K}^4$), and T_p is the absolute temperature of the surface in degrees Kelvin.

Assuming that the temperature of the water in the control volume is constant in time, the only change in the heat stored within the control volume is the change in the internal energy of the water evaporated $l_v \dot{m}_v$, where l_v is the latent heat of vaporization, so that

$$\frac{d}{dt} \int_{CV} e_u \rho_w d\forall = l_v \dot{m}_v \quad (7.3.11)$$

Substituting equations (7.3.8) and (7.3.11) into (7.3.7) results in

$$R_n - H_s - G = l_v \dot{m}_v \quad (7.3.12)$$

From equation (7.3.3b), $\dot{m}_v = \rho_w A E$. Substituting in (7.3.12) with $A = 1 \text{ m}^2$ and solving for E (to denote energy balance) gives the *energy balance equation for evaporation*,

$$E = \frac{1}{l_v \rho_w} (R_n - H_s - G) \quad (7.3.13)$$

Assuming the sensible heat flux H_s and the ground heat flux G are both zero, then an evaporation rate E_r , which is the rate at which all incoming net radiation is absorbed by evaporation, can be

calculated as

$$E_r = \frac{R_n}{l_v \rho_w} \tag{7.3.14}$$

EXAMPLE 7.3.1

For a particular location the average net radiation is 185 W/m², air temperature is 28.5°C, relative humidity is 55 percent, and wind speed is 2.7 m/s at a height of 2 m. Determine the open water evaporation rate in mm/d using the energy method.

SOLUTION

Latent heat of vaporization in joules (J) per kg varies with T (°C), or $l_v = 2.501 \times 10^6 - 2370T$, so $l_v = 2501 - 2.37 \times 28.5 = 2433$ kJ/kg, $\rho_w = 996.3$ kg/m³. The evaporation rate by the energy balance method is determined using equation (7.3.14) with $R_n = 185$ W/m²:

$$E_r = R_n / (l_v \rho_w) = 185 / (2433 \times 10^3 \times 996.3) = 7.63 \times 10^{-8} \text{ m/s} = 6.6 \text{ mm/d.}$$

7.3.2 Aerodynamic Method

As mentioned previously, the aerodynamic method considers the ability to transport water vapor away from the water surface; that is, generated by the humidity gradient in the air near the surface and the wind speed across the surface. These processes can be analyzed by coupling the equation for mass and momentum transport in the air. Considering the control volume in Figure 7.3.4, the vapor flux \dot{m}_v , passing upward by convection can be defined along with the momentum flux (as a function of the humidity gradient and the wind velocity gradient, respectively) (see Chow et al., 1988). The ratio of the vapor flux and the momentum flux can be used to define the *Thornthwaite–Holzman equation* for vapor transport (Thornthwaite and Holzman, 1939). Chow et al. (1988) present details of this derivation. The final form of the evaporation equation for the aerodynamic method expresses the evaporation rate E_a as a function of the difference of the vapor pressure at the surface e_{as} , which is the *saturation vapor pressure* at ambient air temperature (when the rate of evaporation and condensation are equal), and the vapor pressure at a height z_2 above the water surface, which is taken as the ambient vapor pressure in air e_a .

$$E_a = B(e_{as} - e_a) \tag{7.3.15}$$

where E_a has units of mm/day and B is the vapor transfer coefficient with units of mm/day · Pa, given as

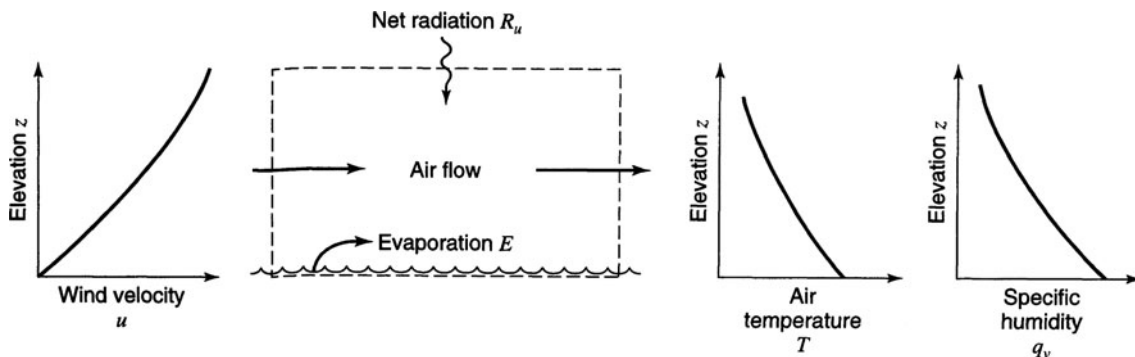


Figure 7.3.4 Evaporation from an open water surface (from Chow et al. (1988)).

$$B = \frac{0.102u_2}{[\ln(z_2/z_0)]^2} \quad (7.3.16)$$

where u_2 is the wind velocity (m/s) measured at height z_2 (cm) and z_0 is the roughness height (0.01–0.06 cm) of the water surface. The vapor pressures have units of Pa (N/m²). The saturation vapor pressure is approximated as

$$e_{as} = 611 \exp\left(\frac{17.27T}{237.3 + T}\right) \quad (7.3.17)$$

and the vapor pressure is

$$e_a = R_h e_{as} \quad (7.3.18)$$

where T is the air temperature in °C and R_h is the relative humidity ($R = e_a/e_{as}$) and ($0 \leq R_h \leq 1$).

EXAMPLE 7.3.2

Solve example 7.3.1 using the aerodynamic method, by using a roughness height $z_0 = 0.03$ cm.

SOLUTION

From equation (7.3.17), the saturated vapor pressure is

$$\begin{aligned} e_{as} &= 611 \exp[17.27T/(237.3 + T)] = 611 \exp[17.27 \times 28.5/(237.3 + 28.5)] \\ &= 3893 \text{ Pa} \end{aligned}$$

The ambient vapor pressure e_a is determined from equation (7.3.18); for a relative humidity $R_h = 0.55$, $e_a = e_{as} R_h = 3893 \times 0.55 = 2141$ Pa. The vapor transfer coefficient B is given by equation (7.3.16) in which $u_2 = 2.7$ m/s, $z_2 = 2$ m, and $z_0 = 0.03$ cm for an open water surface, so that $B = 0.102u_2/[\ln(z_2/z_0)]^2 = 0.102 \times 2.7/[\ln(200/0.03)]^2 = 0.0036$ mm/d · Pa; then the evaporation rate by the aerodynamic method is given by equation (7.3.15):

$$E_a = B(e_{as} - e_a) = 0.0036(3893 - 2141) = 6.31 \text{ mm/d.}$$

7.3.3 Combined Method

When the energy supply is not limiting, the aerodynamic method can be used, and when the vapor transport is not limiting, the energy balance method can be used. However, both of these factors are not normally limiting, so a combination of these methods is usually required. The combined method equation is

$$E = \left(\frac{\Delta}{\Delta + \gamma}\right)E_r + \left(\frac{\gamma}{\Delta + \gamma}\right)E_a \quad (7.3.19)$$

in which $(\)E_r$ is the vapor transport term and $(\)E_a$ is the aerodynamic term. γ is the *psychrometric constant* (approximately 66.8 Pa/°C) and Δ is the *gradient of the saturated vapor pressure curve* $\Delta = de_{as}/dT$ at air temperature T_α given as

$$\Delta = \frac{4098e_{as}}{(237.3 + T_\alpha)} \quad (7.3.20)$$

in which e_{as} is the *saturated vapor pressure* (the maximum moisture content the air can hold for a given temperature).

The combination method is best for application to small areas with detailed climatological data including net radiation, air temperature, humidity, wind speed, and air pressure. For very large areas, energy (vapor transport) largely governs evaporation. Priestley and Taylor (1972) discovered that the aerodynamic term in equation (7.3.19) is approximately 30 percent of the energy term, so that

equation (7.3.19) can be simplified to

$$E = 1.3 \left(\frac{\Delta}{\Delta + \gamma} \right) E_r \tag{7.3.21}$$

which is known as the *Priestley–Taylor evaporation equation*.

EXAMPLE 7.3.3 Solve example 7.3.1 using the combined method.

SOLUTION

The gradient of the saturated vapor pressure curve is, from equation (7.3.20),

$$\Delta = 4098 e_{as} / (237.3 + T)^2 = 4098 \times 3893 / (237.3 + 28.5)^2 = 225.8 \text{ Pa/}^\circ\text{C}$$

The psychrometric constant γ is approximately 66.8 Pa/°C; then E_r and E_a may be combined according to equation (7.3.19) to give

$$\begin{aligned} E &= \Delta / (\Delta + \gamma) E_r + \gamma / (\Delta + \gamma) E_a \\ &= (225.8 / (225.8 + 66.8)) 6.6 + (66.8 / (225.8 + 66.8)) 6.31 = 0.772(6.6) + 0.228(6.31) \\ &= 5.10 + 1.44 = 6.54 \text{ mm/d} \end{aligned}$$

EXAMPLE 7.3.4 Solve example 7.3.1 using the Priestley–Taylor method.

SOLUTION

The evaporation is computed using equation (7.3.21):

$$\begin{aligned} E &= 1.3 \left(\frac{\Delta}{\Delta + \gamma} \right) E_r = 1.3 \left(\frac{225.8}{225.8 + 66.8} \right) 6.6 \\ &= 6.62 \text{ mm/d} \end{aligned}$$

7.4 INFILTRATION

The process of water penetrating into the soil is *infiltration*. The rate of infiltration is influenced by the condition of the soil surface, vegetative cover, and soil properties including porosity, hydraulic conductivity, and moisture content. In order to discuss infiltration, we must first consider the division of subsurface water (see Figure 6.1.2) and the various subsurface flow processes shown in Figure 7.4.1. These processes are infiltration of water to become *soil moisture*, *subsurface flow* (unsaturated flow) through the soil, and *groundwater flow* (saturated flow). *Unsaturated flow* refers to flow through a porous medium when some of the voids are occupied by air. *Saturated flow* occurs when the voids are filled with water. The *water table* is the interface between the saturated and unsaturated flow, where atmospheric pressure prevails. Saturated flow occurs below the water table and unsaturated flow occurs above the water table.

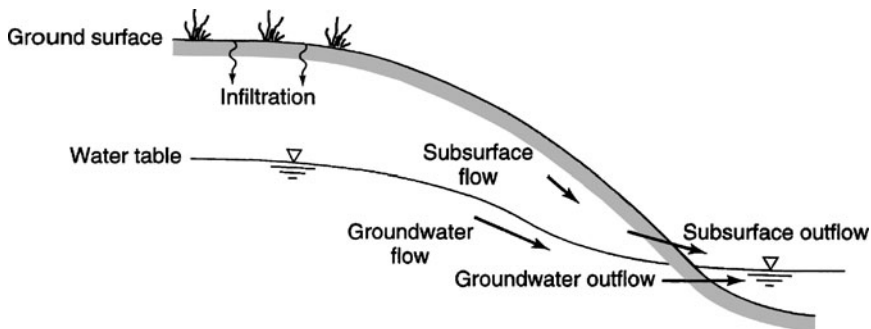


Figure 7.4.1 Subsurface water zones and processes (from Chow et al. (1988)).

7.4.1 Unsaturated Flow

The cross-section through an unsaturated porous medium (Figure 7.4.2a) is now used to define *porosity*, η :

$$\eta = \frac{\text{volume of voids}}{\text{total volume}} \quad (7.4.1)$$

in which η is $0.25 < \eta < 0.40$, and the *soil moisture content*, θ ,

$$\theta = \frac{\text{volume of water}}{\text{total volume}} \quad (7.4.2)$$

in which θ is $0 \leq \theta \leq \eta$. For saturated conditions, $\theta = \eta$.

Consider the control volume in Figure 7.4.2b for an unsaturated soil with sides of lengths dx , dy , and dz , with a volume of $dx dy dz$. The volume of water contained in the control volume is $\theta dx dy dz$. Flow through the control volume is defined by the *Darcy flux*, $q = Q/A$, which is the volumetric flow rate per unit of soil area. For this derivation, the horizontal fluxes are ignored and only the vertical (z) direction is considered, with z positive upward.

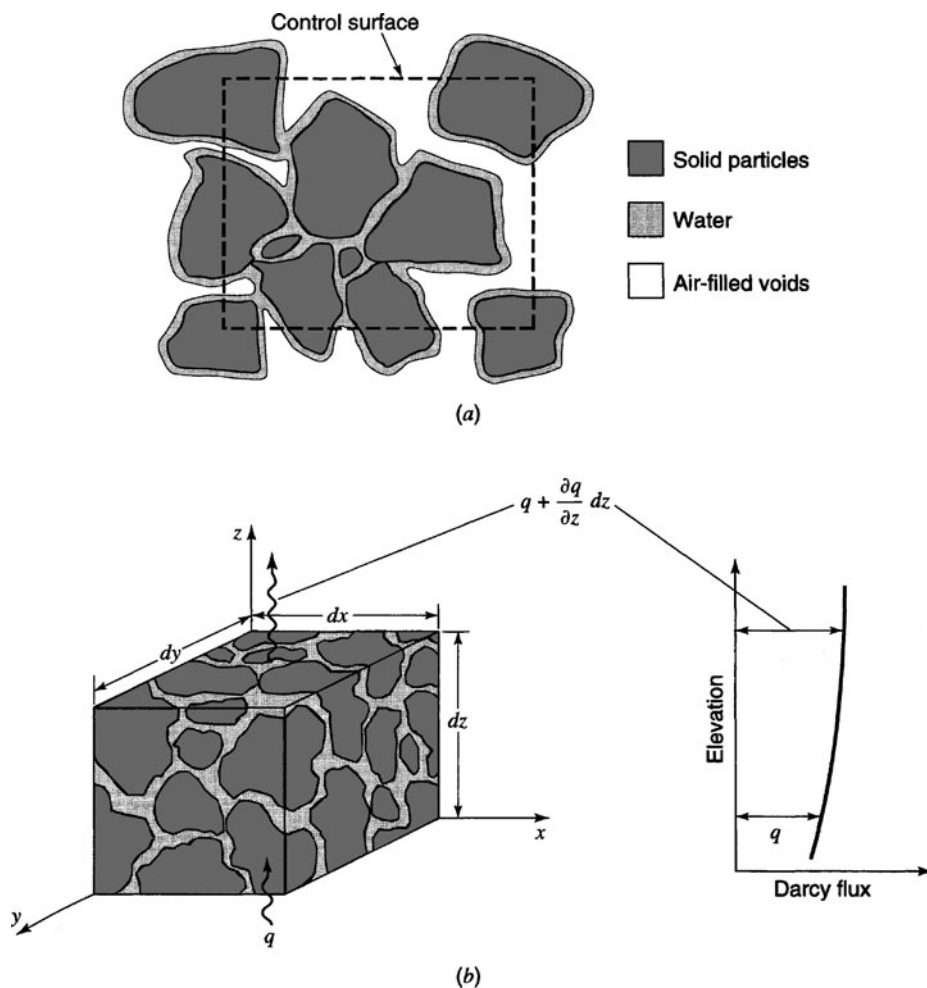


Figure 7.4.2 (a) Cross-section through an unsaturated porous medium; (b) Control volume for development of the continuity equation in an unsaturated porous medium (from Chow et al. (1988)).

With the control volume approach, the extensive property B is the mass of soil water, so the intensive property $\beta = dB/dm = 1$ and $dB/dt = 0$, because no phase changes are occurring in water. The general control volume equation for continuity, equation (3.3.1), is applicable:

$$0 = \frac{d}{dt} \int_{CV} \rho dV + \int_{CS} \rho \mathbf{V} \cdot d\mathbf{A} \tag{7.4.3}$$

The time rate of change of mass stored in the control volume is

$$\frac{d}{dt} \int_{CV} \rho dV = \frac{d}{dt} (\rho \theta dx dy dz) = \rho dx dy dz \frac{\partial \theta}{\partial t} \tag{7.4.4}$$

where the density is assumed constant. The net outflow of water is the difference between the volumetric inflow at the bottom ($q dx dy$) and the volumetric outflow at the top [$q + (\partial q / \partial z) dz$] $dx dy$, so

$$\int_{CV} \rho \mathbf{V} \cdot d\mathbf{A} = \rho \left(q + \frac{\partial q}{\partial z} dz \right) dx dy - \rho q dx dy = \rho dx dy dz \frac{\partial q}{\partial z} \tag{7.4.5}$$

Substituting equations (7.4.4) and (7.4.5) into (7.4.3) and dividing by $\rho dx dy dz$ results in the following continuity equation for one-dimensional unsteady unsaturated flow in a porous medium:

$$\frac{\partial \theta}{\partial t} + \frac{\partial q}{\partial z} = 0 \tag{7.4.6}$$

Darcy's law relates the Darcy flux q to the rate of headloss per unit length of medium. For flow in the vertical direction the headloss per unit length is the change in total head ∂h over a distance, ∂z , i.e., $-\partial h / \partial z$, where the negative sign indicates that total head decreases (as a result of friction) in the direction of flow. Darcy's law can now be expressed as

$$q = -K \frac{\partial h}{\partial z} \tag{7.4.7}$$

where K is the hydraulic conductivity. This law applies to areas that are large compared with the cross-section of individual pores and grains of the medium. Darcy's law describes a steady uniform flow of constant velocity with a net force of zero in a fluid element. In unconfined saturated flow, the forces are gravity and friction. For unsaturated flow the forces are gravity, friction, and the suction force that binds water to soil particles through surface tension.

In unsaturated flow the void spaces are only partially filled with water, so that water is attracted to the particle surfaces through electrostatic forces between the water molecule polar bonds and the particle surfaces. This in turn draws water up around the particle surfaces, leaving air in the center of the voids. The energy due to the soil suction forces is referred to as the suction head ψ in unsaturated flow, which varies with moisture content. Total head is then the sum of the suction and gravity heads:

$$h = \psi + z \tag{7.4.8}$$

Note that the velocities are so small that there is no term for velocity head in this expression for total head.

Darcy's law can now be expressed as

$$q = -K \frac{\partial (\psi + z)}{\partial z} \tag{7.4.9}$$

Darcy's law was originally conceived for saturated flow and was extended by Richards (1931) to unsaturated flow with the provision that the hydraulic conductivity is a function of the suction head, i.e., $K = K(\psi)$. Also, the hydraulic conductivity can be related more easily to the degree of saturation, so that $K = K(\theta)$. Because the soil suction head varies with moisture content and moisture content varies with elevation, the *suction gradient* can be expanded by using the chain rule to obtain

$$\frac{\partial \psi}{\partial z} = \frac{d\psi}{d\theta} \frac{\partial \theta}{\partial z} \quad (7.4.10)$$

in which $\partial\theta/\partial z$ is the *wetness gradient*, and the reciprocal of $d\psi/d\theta$, i.e., $d\theta/d\psi$, is the *specific water capacity*. Now equation (7.4.9) can be modified to

$$q = -K \left(\frac{\partial \psi}{\partial z} + \frac{\partial z}{\partial z} \right) = -K \left(\frac{\partial \psi}{\partial \theta} \frac{\partial \theta}{\partial z} + 1 \right) = - \left(K \frac{d\psi}{d\theta} \frac{\partial \theta}{\partial z} + K \right) \quad (7.4.11)$$

The *soil water diffusivity* $D(L^2/T)$ is defined as

$$D = K \frac{d\psi}{d\theta} \quad (7.4.12)$$

so substituting this expression for D into equation (7.4.11) results in

$$q = - \left(D \frac{\partial \theta}{\partial z} + K \right) \quad (7.4.13)$$

Using the continuity equation (7.4.6) for one-dimensional, unsteady, unsaturated flow in a porous medium yields

$$\frac{\partial \theta}{\partial t} = - \frac{\partial q}{\partial z} = \frac{\partial}{\partial z} \left(D \frac{\partial \theta}{\partial z} + K \right) \quad (7.4.14)$$

which is a one-dimensional form of *Richards' equation*. This equation is the governing equation for unsteady unsaturated flow in a porous medium (Richards, 1931). For a homogeneous soil, $\partial K/\partial z = 0$, so that $\partial\theta/\partial t = \partial(D\partial\theta/\partial z)/\partial z$.

EXAMPLE 7.4.1

Determine the flux for a soil in which the hydraulic conductivity is expressed as a function of the suction head as $K = 250(-\psi)^{-2.11}$ in cm/d at depth $z_1 = 80$ cm, $h_1 = -145$ cm, and $\psi_1 = -65$ cm at depth $z_2 = 100$ cm, $h_2 = -160$ cm, and $\psi_2 = -60$ cm.

SOLUTION

The flux is determined using equation (7.4.7). First the hydraulic conductivity is computed using an average value of $\psi = [-65 + (-60)]/2 = -62.5$ cm. Then $K = 250(-\psi)^{-2.11} = 250(62.5)^{-2.11} = 0.041$ cm/d. The flux is then

$$q = -K \left(\frac{h_1 - h_2}{z_1 - z_2} \right) = -0.041 \left[\frac{-145 - (-160)}{-80 - (-100)} \right] = -0.03 \text{ cm/d}$$

The flux is negative because the moisture is flowing downward in the soil.

EXAMPLE 7.4.2

Determine the soil water diffusivity for a soil in which $\theta = 0.1$ and $K = 3 \times 10^{-11}$ mm/s from a relationship of $\psi(\theta)$ at $\theta = 0.1$, $\Delta\psi = 10^7$ mm, and $\Delta\theta = 0.35$.

SOLUTION

Using equation (7.4.12), the soil water diffusivity is $D = Kd\psi/d\theta = (3 \times 10^{-11} \text{ mm/s})(10^7 \text{ mm}/0.35) = 8.57 \times 10^{-4} \text{ mm/s}$.

7.4.2 Green-Ampt Method

Figure 7.4.3 illustrates the distribution of soil moisture within a soil profile during downward movement. These moisture zones are the *saturated zone*, the *transmission zone*, a *wetting zone*, and a *wetting front*. This profile changes as a function of time as shown in Figure 7.4.4.

The *infiltration rate* f is the rate at which water enters the soil surface, expressed in in/hr or cm/hr. The *potential infiltrate rate* is the rate when water is ponded on the soil surface, so if no ponding occurs the actual rate is less than the potential rate. Most infiltration equations describe a potential infiltration rate. *Cumulative infiltration* F is the accumulated depth of water infiltrated, defined mathematically as

$$F(t) = \int_0^t f(\tau) d\tau \tag{7.4.15}$$

and the infiltration rate is the time derivative of the cumulative infiltration given as

$$f(t) = \frac{dF(t)}{dt} \tag{7.4.16}$$

Figure 7.4.5 illustrates a rainfall hyetograph with the infiltration rate and cumulative infiltration curves. (See Section 8.2 for further details on the rainfall hyetograph.)

Green and Ampt (1911) proposed the simplified picture of infiltration shown in Figure 7.4.6. The *wetting front* is a sharp boundary dividing soil with moisture content θ_i below from saturated soil

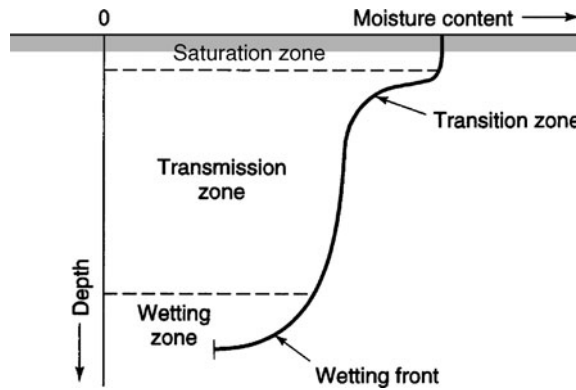


Figure 7.4.3 Moisture zones during infiltration (from Chow et al. (1988)).

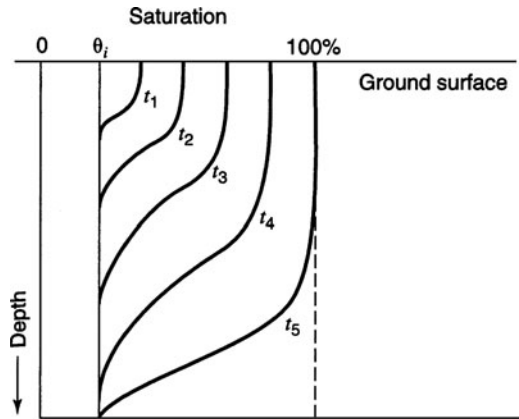


Figure 7.4.4 Moisture profile as a function of time for water added to the soil surface.

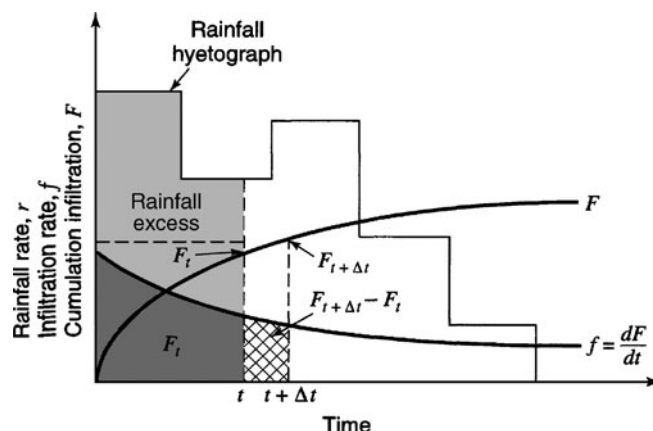


Figure 7.4.5 Rainfall infiltration rate and cumulative infiltration. The rainfall hyetograph illustrates the rainfall pattern as a function of time. The cumulative infiltration at time t is F_t or $F(t)$ and at time $t + \Delta t$ is $F_{t+\Delta t}$ or $F(t + \Delta t)$ and are computed using equation (7.4.15). The increase in cumulative infiltration from time t to $t + \Delta t$ is $F_{t+\Delta t} - F_t$ or $F(t + \Delta t) - F(t)$, as shown in the figure. Rainfall excess is defined in Chapter 8 as that rainfall that is neither retained on the land surface nor infiltrated into the soil.

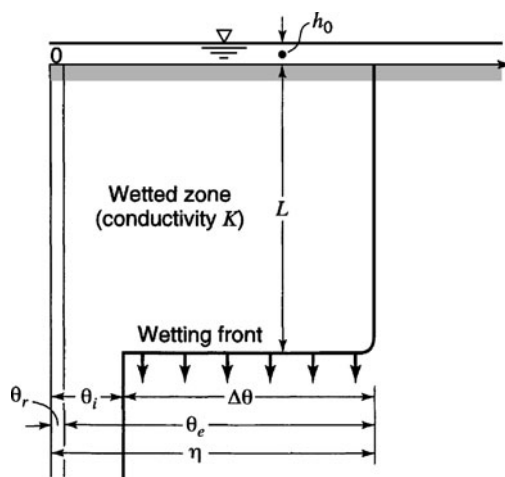


Figure 7.4.6 Variables in the Green–Ampt infiltration model. The vertical axis is the distance from the soil surface; the horizontal axis is the moisture content of the soil (from Chow et al. (1988)).

with moisture content η above. The wetting front has penetrated to a depth L in time t since infiltration began. Water is ponded to a small depth h_0 on the soil surface.

Consider a vertical column of soil of unit horizontal cross-sectional area (Figure 7.4.7) with the control volume defined around the wet soil between the surface and depth L . For a soil initially of moisture content θ_i throughout its entire depth, the *moisture content* will increase from θ_i to η (the porosity) as the wetting front passes. The moisture content θ is the ratio of the volume of water to the total volume within the control surface. $L(\eta - \theta_i)$ is then the increase in the water stored within the control volume as a result of infiltration, through a unit cross-section. By definition this quantity is equal to F , the cumulative depth of water infiltrated into the soil, so that

$$F(t) = L(\eta - \theta_i) = L\Delta\theta \quad (7.4.17)$$

where $\Delta\theta = (\eta - \theta_i)$.

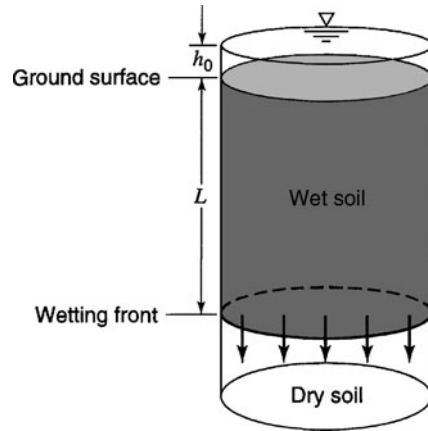


Figure 7.4.7 Infiltration into a column of soil of unit cross-sectional area for the Green–Ampt model (from Chow et al. (1988)).

Darcy’s law may be expressed (using equation (7.4.7)) as

$$q = K \frac{\partial h}{\partial z} = -K \frac{\Delta h}{\Delta z} \tag{7.4.18}$$

The Darcy flux q is constant throughout the depth and is equal to $-f$, because q is positive upward while f is positive downward. If points 1 and 2 are located at the ground surface and just on the dry side of the wetting front, respectively, then equation (7.4.18) can be approximated by

$$f = K \left[\frac{h_1 - h_2}{z_1 - z_2} \right] \tag{7.4.19}$$

The head h_1 at the surface is equal to the ponded depth h_0 . The head h_2 , in the dry soil below the wetting front, equals $-\psi - L$. Darcy’s law for this system is written as

$$f = K \left[\frac{h_0 - (-\psi - L)}{L} \right] \tag{7.4.20a}$$

and if the ponded depth h_0 is negligible compared to ψ and L ,

$$f \approx K \left[\frac{\psi + L}{L} \right] \tag{7.4.20b}$$

This assumption ($h_0 = 0$) is usually appropriate for surface water hydrology problems because it is assumed that ponded water becomes surface runoff.

From equation (7.4.17), the wetting front depth is $L = F/\Delta\theta$, and assuming $h_0 = 0$, substitution into equation (7.4.20) gives

$$f = K \left[\frac{\psi\Delta\theta + F}{F} \right] \tag{7.4.21}$$

Since $f = dF/dt$, equation (7.4.21) can be expressed as a differential equation in the one unknown F as

$$\frac{dF}{dt} = K \left[\frac{\psi\Delta\theta + F}{F} \right]$$

To solve for F , cross-multiply to obtain

$$\left[\frac{F}{F + \psi\Delta\theta} \right] dF = K dt$$

Then divide the left-hand side into two parts

$$\left[\frac{F + \psi\Delta\theta}{F + \psi\Delta\theta} - \frac{\psi\Delta\theta}{F + \psi\Delta\theta} \right] dF = Kdt$$

and integrate

$$\int_0^{F(t)} \left[1 - \frac{\psi\Delta\theta}{F + \psi\Delta\theta} \right] dF = \int_0^t Kdt$$

to obtain

$$F(t) - \psi\Delta\theta \{ \ln[F(t) + \psi\Delta\theta] - \ln(\psi\Delta\theta) \} = Kt \quad (7.4.22a)$$

or

$$F(t) - \psi\Delta\theta \ln \left(1 + \frac{F(t)}{\psi\Delta\theta} \right) = Kt \quad (7.4.22b)$$

Equation (7.4.22) is the *Green–Ampt equation* for cumulative infiltration. Once F is computed using equation (7.4.22), the infiltration rate f can be obtained from equation (7.4.21) or

$$F(t) = K \left[\frac{\psi\Delta\theta}{F(t)} + 1 \right] \quad (7.4.23)$$

When the ponded depth h_0 is not negligible, the value of $\psi + h_0$ is substituted for ψ in equations (7.4.22) and (7.4.23).

Equation (7.4.22) is a nonlinear equation in F that can be solved by the method of successive substitution by rearranging (7.4.22)

$$F(t) = Kt + \psi\Delta\theta \ln \left(1 + \frac{F(t)}{\psi\Delta\theta} \right) \quad (7.4.24)$$

Given K , t , ψ , and $\Delta\theta$, a trial value F is substituted on the right-hand side (a good trial value is $F = Kt$), and a new value of F calculated on the left-hand side, which is substituted as a trial value on the right-hand side, and so on until the calculated values of F converge to a constant. The final value of cumulative infiltration F is substituted into (7.4.23) to determine the corresponding infiltration rate f .

Equation (7.4.22) can also be solved by Newton's method, which is more complicated than the method of successive substitution but converges in fewer iterations. Newton's iteration method is explained in Appendix A. Referring to equation (7.4.24), application of the Green–Ampt model requires estimates of the hydraulic conductivity K , the wetting front soil suction head ψ (see Table 7.4.1), and $\Delta\theta$.

The *residual moisture content* of the soil, denoted by θ_r , is the moisture content after it has been thoroughly drained. The *effective saturation* is the ratio of the available moisture ($\theta - \theta_r$) to the maximum possible available moisture content ($\eta - \theta_r$), given as

$$s_e = \frac{\theta - \theta_r}{\eta - \theta_r} \quad (7.4.25)$$

where $\eta - \theta_r$ is called the *effective porosity* θ_e .

The effective saturation has the range $0 \leq s_e \leq 1.0$, provided $\theta_r \leq \theta \leq \eta$. For the initial condition, when $\theta = \theta_i$, cross-multiplying equation (7.4.25) gives $\theta_i - \theta_r = s_e\theta_e$, and the change in the moisture content when the wetting front passes is

$$\begin{aligned} \Delta\theta &= \eta - \theta_i = \eta - (s_e\theta_e + \theta_r) \\ \Delta\theta &= (1 - s_e)\theta_e \end{aligned} \quad (7.4.26)$$

Table 7.4.1 Green–Ampt Infiltration Parameters for Various Soil Classes*

Soil class	Porosity η	Effective porosity θ_e	Wetting front soil suction head ψ (cm)	Hydraulic conductivity K (cm/h)
Sand	0.437 (0.374–0.500)	0.417 (0.354–0.480)	4.95 (0.97–25.36)	11.78
Loamy sand	0.437 (0.363–0.506)	0.401 (0.329–0.473)	6.13 (1.35–27.94)	2.99
Sandy loam	0.453 (0.351–0.555)	0.412 (0.283–0.541)	11.01 (2.67–45.47)	1.09
Loam	0.463 (0.375–0.551)	0.434 (0.334–0.534)	8.89 (1.33–59.38)	0.34
Silt loam	0.501 (0.420–0.582)	0.486 (0.394–0.578)	16.68 (2.92–95.39)	0.65
Sandy clay loam	0.398 (0.332–0.464)	0.330 (0.235–0.425)	21.85 (4.42–108.0)	0.15
Clay loam	0.464 (0.409–0.519)	0.309 (0.279–0.501)	20.88 (4.79–91.10)	0.10
Silty clay loam	0.471 (0.418–0.524)	0.432 (0.347–0.517)	27.30 (5.67–131.50)	0.10
Sandy clay	0.430 (0.370–0.490)	0.321 (0.207–0.435)	23.90 (4.08–140.2)	0.06
Silty clay	0.479 (0.425–0.533)	0.423 (0.334–0.512)	29.22 (6.13–139.4)	0.05
Clay	0.475 (0.427–0.523)	0.385 (0.269–0.501)	31.63 (6.39–156.5)	0.03

* The numbers in parentheses below each parameter are one standard deviation around the parameter value given.

Source: Rawls, Brakensiek, and Miller (1983).

A logarithmic relationship between the effective saturation s_e and the soil suction head ψ can be expressed by the *Brooks–Corey equation* (Brooks and Corey, 1964):

$$s_e = \left[\frac{\psi_b}{\psi} \right]^\lambda \quad (7.4.27)$$

in which ψ_b and λ are constants obtained by draining a soil in stages, measuring the values of s_e and ψ at each stage, and fitting equation (7.4.27) to the resulting data.

Brakensiek et al. (1981) presented a method for determining the Green–Ampt parameters using the Brooks–Corey equation. Rawls et al. (1983) used this method to analyze approximately 5000 soil horizons across the United States and determined average values of the Green–Ampt parameters η , θ_e , ψ , and K for different soil classes, as listed in Table 7.4.1. As the soil becomes finer, moving from sand to clay, the wetting front soil suction head increases while the hydraulic conductivity decreases. Table 7.4.1 also lists typical ranges for η , θ_e , and ψ . The ranges are not large for η and θ_e , but ψ can vary over a wide range for a given soil. K varies along with ψ , so the values given in Table 7.4.1 for both ψ and K should be considered typical values that may show a considerable degree of variability in application (American Society of Agricultural Engineers, 1983; Devanrs and Gifford, 1986).

Table 7.4.2 Infiltration Computations Using the Green–Ampt Method

Time t (hr)	0.0	0.1	0.2	0.3	0.4	0.5	1.0	1.5	2.0	2.5	3.0	3.5	4.0	4.5	5.0	5.5	6.0
Infiltration rate f (cm/hr)	∞	1.78	1.20	0.97	0.84	0.75	0.54	0.44	0.39	0.35	0.32	0.30	0.28	0.27	0.26	0.25	0.24
Infiltration depth F (cm)	0.00	0.29	0.43	0.54	0.63	0.71	1.02	1.26	1.47	1.65	1.82	1.97	2.12	2.26	2.39	2.51	2.64

EXAMPLE 7.4.3

Use the Green–Ampt method to evaluate the infiltration rate and cumulative infiltration depth for a silty clay soil at 0.1-hr increments up to 6 hr from the beginning of infiltration. Assume an initial effective saturation of 20 percent and continuous ponding.

SOLUTION

From Table 7.4.1, for a silty clay soil, $\theta_e = 0.423$, $\psi = 29.22$ cm, and $K = 0.05$ cm/hr. The initial effective saturation is $s_e = 0.2$, so $\Delta\theta = (1 - s_e)\theta_e = (1 - 0.20)0.423 = 0.338$, and $\psi\Delta\theta = 29.22 \times 0.338 = 9.89$ cm. Assuming continuous ponding, the cumulative infiltration F is found by successive substitution in equation (7.4.24):

$$F = Kt + \psi\Delta\theta \ln[1 + F/(\psi\Delta\theta)] = 0.05t + 9.89 \ln[1 + F/9.89]$$

For example, at time $t = 0.1$ hr, the cumulative infiltration converges to a final value $F = 0.29$ cm. The infiltration rate f is then computed using equation (7.4.23):

$$f = K(1 + \psi\Delta\theta/F) = 0.05(1 + 9.89/F)$$

As an example, at time $t = 0.1$ hr, $f = 0.05(1 + 9.89/0.29) = 1.78$ cm/hr. The infiltration rate and the cumulative infiltration are computed in the same manner between 0 and 6 hr at 0.1-hr intervals; the results are listed in Table 7.4.2.

EXAMPLE 7.4.4

Ponding time t_p is the elapsed time between the time rainfall begins and the time water begins to pond on the soil surface. Develop an equation for ponding time under a constant rainfall intensity i , using the Green–Ampt infiltration equation (see Figure 7.4.8).

SOLUTION

The infiltration rate f and the cumulative infiltration F are related in equation (7.4.22). The cumulative infiltration at ponding time t_p is $F_p = it_p$, in which i is the constant rainfall intensity (see Figure 7.4.8). Substituting $F_p = it_p$ and the infiltration rate $f = i$ into equation (7.4.23) yields

$$i = K \left(\frac{\psi\Delta\theta}{it_p} + 1 \right)$$

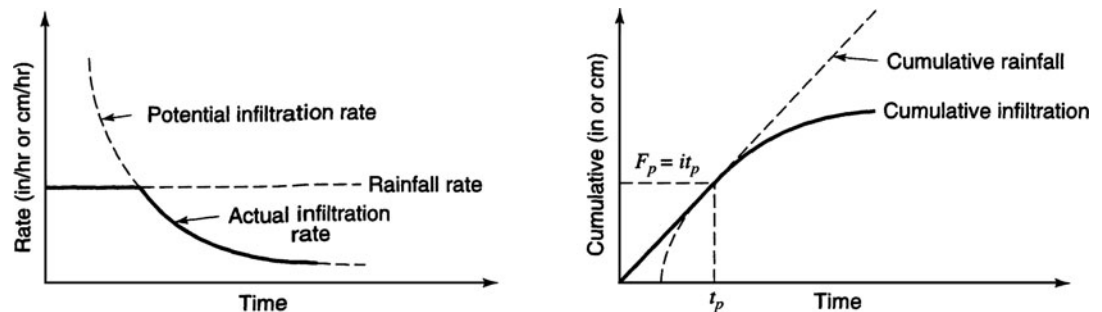


Figure 7.4.8 Ponding time. This figure illustrates the concept of ponding time for a constant intensity rainfall. Ponding time is the elapsed time between the time rainfall begins and the time water begins to pond on the soil surface.

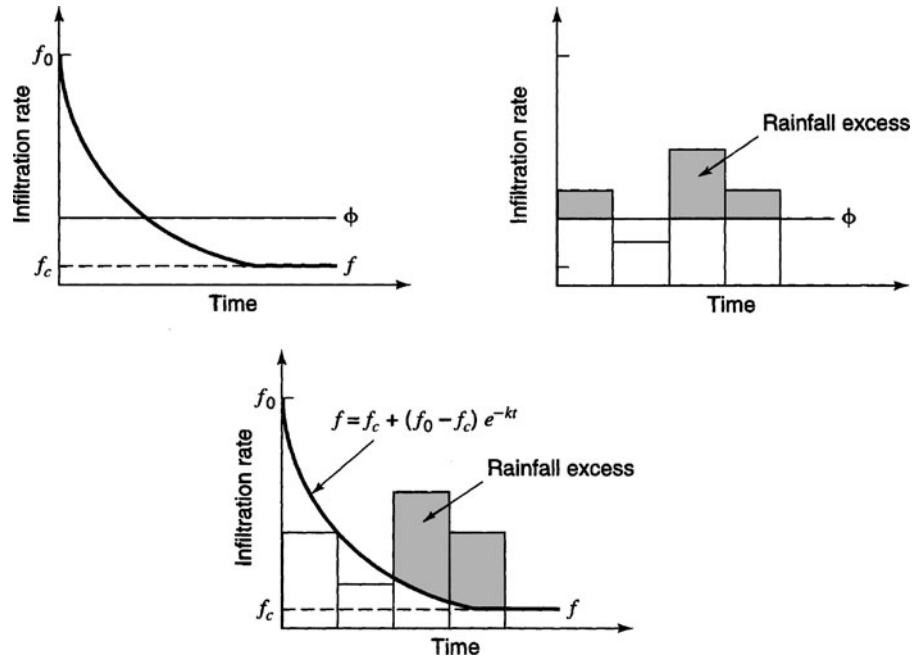


Figure 7.4.9 Φ -index and Horton’s equation.

and solving, we get

$$t_p = \frac{K\psi\Delta\theta}{i(i - K)}$$

which is the ponding time for a constant rainfall intensity.

7.4.3 Other Infiltration Methods

The simplest accounting of abstraction is the Φ -index (refer to Figure 7.4.9 and Section 8.2), which is a constant rate of abstraction (in/h or cm/h). Other cumulative infiltration and infiltration rate equations include Horton’s and the SCS method. Horton’s equation (Horton, 1933) is an empirical relation that assumes infiltration begins at some rate f_0 and exponentially decreases until it reaches a constant rate f_c (refer to Figure 7.4.9). The infiltration capacity is expressed as

$$f_t = f_c + (f_0 - f_c)e^{-kt} \tag{7.4.28}$$

and the cumulative infiltration capacity is expressed as

$$F_t = f_c t + \frac{(f_0 - f_c)}{k} (1 - e^{-kt}) \tag{7.4.29}$$

where k is a decay constant. Many other empirical infiltration equations have been developed that can be found in the various hydrology texts.

Richard’s equation can be solved (Philip, 1957, 1969) under less restrictive conditions by assuming that K and D (equation 7.4.14) can vary with moisture content. Philip used the Boltzmann transformation $B(\theta) = zt^{-1/2}$ to convert Richard’s equation (7.4.14) into an ordinary differential equation in B and solved to obtain an intimate series for cumulative infiltration F_t , approximated as

$$F_t = St^{1/2} + Kt \tag{7.4.30}$$

in which S is the sorptivity, a parameter that is a function of the soil suction potential, and K is the hydraulic conductivity. Differentiating $f(t) = df/dt$, the infiltration rate is defined as

$$f(t) = \frac{1}{2}St^{-1/2} + K \tag{7.4.31}$$

As $t \rightarrow \infty$, $f(t) \rightarrow K$. The two terms S and K represent the effects of soil suction head and gravity head.

There are many other infiltration methods, including the SCS method described in Sections 8.6–8.8. In summary, the Green–Ampt and the SCS are both used in the U.S. Army Corps of Engineers HEC-1 and HEC-HMS models, and both are used widely in the United States.

PROBLEMS

7.2.1 Determine the 25-year return period rainfall depth for a 30-min duration in Chicago, Illinois.

7.2.2 Determine the 2-, 10-, 25-, and 100-year precipitation depths for a 15-min duration storm in Memphis, Tennessee.

7.2.3 Determine the 2- and 25-year intensity-duration-frequency curves for Memphis, Tennessee.

7.2.4 Determine the 10- and 50-year intensity-duration-frequency curves for Chicago, Illinois.

7.2.5 Determine the 2-, 5-, 10-, 25-, 50-, and 100-year depths for a 1-hr duration storm in Phoenix, Arizona. Repeat for a 6-hr duration storm.

7.2.6 Develop the Type I, IA, II, and III 24-hour storms for a 24-hour rainfall of 20 in. Plot and compare these storms.

7.2.7 Develop the SCS 6-hr storm for a 6-hr rainfall of 12 in.

7.2.8 Determine the design rainfall intensities (mm/hr) for a 25-year return period, 60-min duration storm using equation (7.2.5) with $c = 12.1$, $m = 0.25$, $e = 0.75$, and $f = 0.125$.

7.2.9 What is the all-season 6-hr PMP (in) for 200 mi² near Chicago, Illinois?

7.2.10 Tabulated are the data derived from a drainage basin of 21,100 hectares, given the areas covered with each of the rainfall isohyetal lines.

Interval of isohyets (cm)	0-2	2-4	4-6	6-8	8-10	10-42	12-44
Enclosed area (hectares × 1000)	5.3	4.4	3.2	2.6	2.3	1.9	1.4

- (a) Determine the average depth of precipitation for the storm within the basin by the isohyetal method.
- (b) Develop the depth-area relationship based on the data.

7.2.11 For a particular 24-hr storm event on a river basin, an isohyetal map was developed. The corresponding isohyets and area relationship is given in the table below. Based on the given information, (a) develop the depth-area relationship in tabular form for the basin and (b) assuming the maximum point rainfall

is 145 mm, estimate the parameters in the following dimensionless depth-area equation that best fit the existing data, $\frac{\bar{P}_A}{P_{\max}} = \exp(-k \times A^n)$, where \bar{P}_A = equivalent uniform rainfall depth for an area of A ; P_{\max} = maximum point rainfall depth; and k and n = parameters.

Isohyet (mm)	130	120	110	100	90
Incremental area between isohyets (km ²)	143	245	258	290	484

7.2.12 Based on the 100-year rainfall records at the Hong Kong Observatory, the rainfall intensities with an annual exceedance probability of 0.1 (i.e., 10-yr return period) of different durations are given in the table below.

Duration, t_d (min)	15	30	60	120
Intensity, i (mm/h)	161	132	103	74

- (a) Determine the least-squares estimates of coefficients a and c in the following rainfall intensity-duration equation and the associated R^2 value, $i = \frac{a}{(t_d + 4.5)^c}$, in which i = rainfall intensity (in mm/h) and t_d = storm duration in (minutes).
- (b) Estimate the total rainfall depth (in cm) for a 10-year, 4-hr storm event.

7.2.13 Based on the 100-year rainfall records at the Hong Kong Observatory, the rainfall intensities with an annual exceedance probability of 0.1 (i.e., 10-year return period) of different durations are given in the table below.

Return period, T (year)	5	10	50	100	200
Duration, t_d (hr)	6	8	12	18	24
Depth, d (mm/h)	192	255	392	500	622

Consider the following empirical model to be used to fit the above rainfall intensity-duration-frequency (IDF) data,

$$d(T, t_d) = \frac{aT^m}{(t_d + b)^c}, \text{ in which } d = \text{rainfall depth (in mm) corres-}$$

ponding to a storm event of return period T -year and duration t_d -hr.

- (a) Describe a least-squares-based procedure to optimally estimate the coefficients a , b , c , and m in the above rainfall IDF model.
- (b) Assuming $b = 4.0$, determine the least-squares estimates of coefficients a , c , and m in the above rainfall intensity-duration equation and the associated R^2 value.
- (c) Estimate the average rainfall intensity (in mm/hr) for the 25-year, 4-hr storm event.

7.2.14 Consider a rainfall event having 5-min cumulative rainfall record given below:

Time (min)	0	5	10	15	20	25	30
Cumulative rainfall (mm)	0	7	14	23	34	45	58
Time (min)	35	40	45	50	55	60	65
Cumulative rainfall (mm)	70	81	91	100	110	119	125
Time (min)	70	75	80	85	90		
Cumulative rainfall (mm)	131	136	140	140	140		

- (a) What is the duration of the entire rainfall event and the corresponding total rainfall amount?
- (b) Find the rainfall depth hyetograph (in tabular form) with 10-min time interval for the storm event.
- (c) Find the maximum 10-min and 20-min average rainfall intensities (in mm/hr) for the storm event.

7.2.15 Based on available rainfall records at a location, the rainfall intensity with an annual exceedance probability of 0.1 (i.e., 10-year return period) of different durations are given in the table below.

Duration, t_d (min)	15	30	60	120
Intensity, i (mm/h)	160	132	105	75

- (a) Determine the least-squares estimates of coefficients a and c in the following rainfall intensity-duration equation and calculate the corresponding R^2 value, $i = \frac{a}{(t_d + 4.5)^c}$ in which i = rainfall intensity (in mm/h) and t_d = storm duration (in minutes).
- (b) Estimate the total rainfall depth (in mm) for a 10-year, 90-min storm event.

7.2.16 Based on the available rainfall records at the Hong Kong Observatory, the rainfall intensities corresponding to different durations with an annual exceedance probability of 0.1 (i.e. 10-year return period) are given in the table below.

Duration, t_d (min)	15	30	60	120
Intensity, i (mm/h)	161	132	103	74

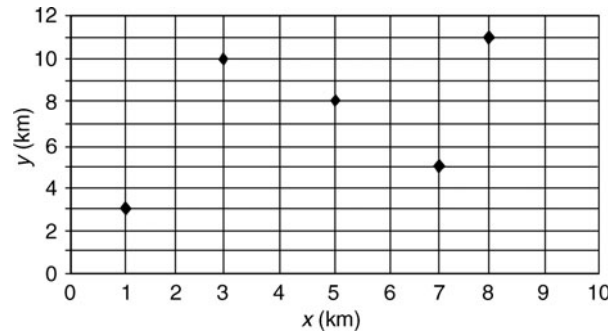
- (a) Determine the least-squares estimates of coefficients a and c in the following rainfall intensity-duration equation, $i = \frac{a}{(t_d + 45)^c}$ in which i = rainfall intensity (in mm/h) and t_d = storm duration (in minutes).

- (b) Estimate the total rainfall depth (in cm) for a 10-year, 4-hr storm event.

7.2.17 An experimental rectangular plot of 10 km \times 12 km has five rain gauge stations as shown in the figure. The storm rainfall and coordinates of the stations are given in the table.

Station	(x , y)	Mean annual rainfall (cm)	Storm rainfall (cm)
A	(1, 3)	128	12.0
B	(8, 11)	114	11.4
C	(3, 10)	136	13.2
D	(5, 8)	144	14.6
E	(7, 5)	109	?

- (a) Estimate the missing rainfall amount at station E.
- (b) Based on the position of the five rain gauges, construct the Thiessen polygon for them.



7.3.1 Solve example 7.3.1 for an average net radiation of 92.5 W/m². Compare the resulting evaporation rate with that in example 7.3.1.

7.3.2 Solve example 7.3.2 for a roughness height $z_0 = 0.04$ cm. Compare the resulting evaporation rate with that in example 7.3.2.

7.3.3 Solve example 7.3.3 for an average net radiation of 92.5 W/m². Compare the resulting evaporation rate with that in example 7.3.3.

7.3.4 Solve example 7.3.4 for an average net radiation of 92.5 W/m². Compare the resulting evaporation rate with that in example 7.3.4.

7.3.5 At a certain location during the winter, the average air temperature is 10°C and the net radiation is 40 W/m² and during the summer the net radiation is 200 W/m² and the temperature is 25°C Compute the evaporation rates using the Priestley–Taylor method.

7.3.6 The average weather conditions are net radiation = 40 W/m²; air temperature = 28.5°C; relative humidity = 55 percent; and wind speed = 2.7 m/s at a height of 2 m. Calculate the open water evaporation rate in millimeters per day using the energy method, the aerodynamic method, the combination method, and

the Priestley–Taylor method. Assume standard atmospheric pressure is 101 kPa and z_o is 0.03 cm.

7.3.7 A 600-hectare farm land receives annual rainfall of 2500 mm. There is a river flowing through the farm land with inflow rate of $5 \text{ m}^3/\text{s}$ and outflow rate of $4 \text{ m}^3/\text{s}$. The annual water storage in the farm land increases by $2.5 \times 10^6 \text{ m}^3$. Based on the hydrologic budget equation, determine the annual evaporation amount (in mm). [Note: 1 hectare = $10,000 \text{ m}^2$]

7.4.1 Determine the infiltration rate and cumulative infiltration curves (0 to 5 h) at 1-hr increments for a clay loam soil. Assume an initial effective saturation of 40 percent and continuous ponding.

7.4.2 Rework problem 7.4.1 using an initial effective saturation of 20 percent.

7.4.3 Rework example 7.4.3 for a sandy loam soil.

7.4.4 Compute the ponding time and cumulative infiltration at ponding for a sandy clay loam soil with a 30-percent initial effective saturation, subject to a rainfall intensity of 2 cm/h.

7.4.5 Rework problem 7.4.4 for a silty clay soil.

7.4.6 Determine the cumulative infiltration and the infiltration rate on a sandy clay loam after 1 hr of rainfall at 2 cm/hr if the initial effective saturation is 25 percent. Assume the ponding depth is negligible in the calculations.

7.4.7 Rework problem 7.4.6 assuming that any ponded water remains stationary over the soil so that the ponded depth must be accounted for in the calculations.

7.4.8 Derive the equation for cumulative infiltration using Horton’s equation.

7.4.9 Use the Green–Ampt method to compute the infiltration rate and cumulative infiltration for a silty clay soil ($\eta = 0.479$, $\psi = 29.22 \text{ cm}$, $K = 0.05 \text{ cm/hr}$) at 0.25-hr increments up to 4 hr from the beginning of infiltration. Assume an initial effective saturation of 30 percent and continuous ponding.

7.4.10 The parameters for Horton’s equation are $f_0 = 3.0 \text{ in/h}$, $f_c = 0.5 \text{ in/h}$, and $K = 4.0 \text{ h}^{-1}$. Determine the infiltration rate and cumulative infiltration at 0.25-hr increments up to 4 hr from the beginning of infiltration. Assume continuous ponding.

7.4.11 Derive an equation for ponding time using Horton’s equation.

7.4.12 Compute the ponding time and cumulative infiltration at ponding for a sandy clay loam soil of 25 percent initial effective saturation for a rainfall intensity of (a) 2 cm/h, (b) 3 cm/h, and (c) 5 cm/h.

7.4.13 Rework problem 7.4.12 considering a silt loam soil.

7.4.14 Consider a soil with porosity $\eta = 0.43$ and suction $\psi = 11.0 \text{ cm}$. Before the rainfall event, the initial moisture content $\theta_i = 0.3$. It is known that after one hour of rainfall, the total infiltrated water is 2.0 cm.

- (a) Determine the hydraulic conductivity in the Green–Ampt infiltration model.
- (b) Estimate the potential total infiltration amount 1.5 hr after the beginning of the storm.

- (c) Determine the instantaneous potential infiltration rate at $t = 1.5 \text{ hr}$.

7.4.15 The following experimental data are obtained from an infiltration study. The objective of the study is to establish a plausible relationship between infiltration rate (f_i) and time (t).

Time, t (mm)	3	15	30	60	90
Infiltration rate, f_i (cm/hr)	8.5	7.8	7.0	6.1	5.6

From the scatter plot of infiltration rate and time, the following relationship between f_i and t is plausible, $f_i = 5.0 + (f_o - 5.0)\exp(-k \times t)$, where f_o is the initial infiltration rate (in cm/hr) and k is the decay constant (in min^{-1}).

- (a) Determine the values of the two constants, i. e., f_o and k , by the least-squares method.
- (b) Based on the result in part (a), estimate the infiltration rate at time $t = 150 \text{ min}$.

7.4.16

- (a) For a sandy loam soil, using Green–Ampt equation to calculate the infiltration rate (cm/h) and cumulative infiltration depth (cm) after 1, 60, and 150 min if the effective saturation is 40 percent. Assume a continuously ponded condition.
- (b) Take the infiltration rates computed in Part (a) at 1 min and 150 min as the initial and ultimate infiltration rates in Horton’s equation, respectively. Determine the decay constant, k .
- (c) Use the decay constant, k , found in Part (b) to compute the cumulative infiltration at $t = 60 \text{ min}$ by Horton’s equation.

7.4.17 Assume that ponded surface occurs at the beginning of a storm event.

- (a) Calculate the potential infiltration rates (cm/hr) and potential cumulative infiltration depth (cm) by the Green–Ampt model for loamy sand at times 30 and 60 min. The initial effective saturation is 0.2.
- (b) Based on the infiltration rates or cumulative infiltration depth computed in Part (a), determine the two parameters S and K in the following Philip two-term infiltration model.

$$F(t) = S t^{1/2} + K t; \quad f(t) = 0.5 S t^{0.5} + K$$

- (c) Based on the S and K computed in Part (b), determine the effective rainfall hyetograph for the following total hyetograph of a storm event.

Time (min)	0-30	30-60	60-90	90-120
Intensity (cm/hr)	8.0	15.0	5.0	3.0

- (d) Find the value of the Φ -index and the corresponding effective rainfall hyetograph having the total effective rainfall depth obtained in Part (c).

7.4.18 Consider the sandy loam soil with effective porosity $\theta_e = 0.43$, suction $\psi = 11.0$ cm, and hydraulic conductivity $K = 1.1$ cm/h. Before the rainfall event, the initial effective saturation is $S_e = 0.3$. It is known that, after 1 hr of rainfall, the total infiltrated water is 2.0 cm.

- (a) Estimate the potential total infiltration amount 1.5 hr after the beginning of the storm event by the Green–Ampt equation.
- (b) Also, determine the instantaneous potential infiltration rate at $t = 1.5$ hr.

7.4.19 Considering a plot of land with sandy loam soil, use the Green–Ampt equation to calculate the infiltration rate (cm/h) and cumulative infiltration depth (cm) at $t = 30$ min under the initial degree of saturation of 40 percent and continuously ponding condition. The relevant parameters are: suction head = 6.0 cm; porosity = 0.45; and hydraulic conductivity = 3.00 cm/h.

7.4.20 Suppose that the infiltration of water into a certain type of soil can be described by Horton’s equation with the following parameters: initial infiltration rate = 50 mm/h; ultimate infiltration rate = 10 mm/h; and decay constant = 4 h^{-1} . A rain storm event has occurred and its pattern is given below.

Time (min)	0	15	30	45	60	75	90
Cumu. rain (mm)	0	15	25	30	32	33	33

- (a) Determine the effective rainfall intensity hyetograph (in mm/h) from the storm event.
- (b) What is the percentage of total rainfall infiltrated into the ground?
- (c) What assumption(s) do you use in the Part (a) calculation? Justify them.

7.4.21 Consider a 2-hr storm event with a total rainfall amount of 80 mm. The measured direct runoff volume produced by the storm is 40 mm.

- (a) Determine the decay constant k in Horton’s infiltration model knowing that the initial and ultimate infiltration rates are 30 mm/hr and 2 mm/hr, respectively.
- (b) Use the Horton equation developed in Part (a) to determine the effective rainfall intensity hyetograph for the following storm event.

Time (min)	0-10	10-20	20-30
Incremental rainfall depth (mm)	5	20	10

7.4.22 An infiltration study is to be conducted. A quick site investigation indicates that the soil has an effective porosity $\theta_e = 0.40$ and the initial effective saturation $S_e = 0.3$. Also, from the double-ring infiltrometer test, we learn that the cumulative infiltration amounts at $t = 1$ hr and $t = 2$ hr are 1 cm and 1.6 cm, respectively.

- (a) It is decided that the Green–Ampt equation is to be used. Determine the parameters suction (ψ) and hydraulic conductivity (K) from the test data. (You can use an iterative procedure or apply simple approximation using $\ln(1+x) = 2x/(2+x)$ for a direct solution.)
- (b) Also, determine the cumulative infiltration and the corresponding instantaneous potential infiltration rate at $t = 3$ hr. (You can use the Newton method to obtain the solution with accuracy within 0.1 mm or the most accurate direct solution approach.)

7.4.23 You are working on a proposal to do some rainfall runoff modeling for a small city nearby. One of the things the city does not have is a hydrology manual. You must decide upon an infiltration methodology for the analysis. You are going to consider methods such as the Φ -index method, empirical methods (such as Horton’s and Holtan’s), the SCS method, and the Green–Ampt method. Would you choose the Green–Ampt method over the others? Why?

REFERENCES

American Society of Agricultural Engineers, “Advances in Infiltration,” in *Proc. National Conf. on Advances in Infiltration*, Chicago, IL, ASAE Publication 11–83, St. Joseph, MI 1983.

Bedient, P. B., and W. C. Huber, *Hydrology and Floodplain Analysis*, second edition, Addison-Wesley, Reading, MA, 1992.

Bhowmik, N., “River Basin Management: An Integrated Approach” *Water International*, International Water Resources Association, vol. 23, no. 2, pp. 84–90, June 1998.

Bonnin, G. M., D. Martin, B. Lin, T. Parzybok, M. Yekta, and D. Riley, “Precipitation-Frequency Atlas of the United States,” NOAA Atlas 14, vol. 2, version 3, NOAA, National Weather Service, Silver Spring, MD, 2004.

Bonnin, G. M., D. Martin, B. Lin, T. Parzybok, M. Yekta, and D. Riley, “Precipitation-Frequency Atlas of the United States,” NOAA Atlas 14, vol. 1, version 4, NOAA, National Weather Service, Silver Spring, MD, 2006.

Brakensiek, D. L., R. L. Engleman, and W. J. Rawls, “Variation within Texture Classes of Soil Water Parameters,” *Trans. Am. Soc. Agric. Eng.*, vol. 24, no. 2, pp. 335–339, 1981.

Bras, R. L., *Hydrology: An Introduction to Hydrologic Science*, Addison-Wesley, Reading, MA, 1990.

Brooks, R. H., and A. T. Corey, “Hydraulic Properties of Porous Media,” *Hydrology Papers*, no. 3, Colorado State University, Fort Collins, CO, 1964.

Chow, V. T., *Handbook of Applied Hydrology*, McGraw Hill, New York 1964.

Chow, V. T., D. R. Maidment, and L. W. Mays, *Applied Hydrology*, McGraw-Hill, New York, 1988.

Demissee, M., and L. Keefer, “Watershed Approach for the Protection of Drinking Water Supplies in Central Illinois,” *Water International*, IWRA, vol. 23, no. 4, pp. 272–277, 1998.

Devanrs, M., and G. F. Gifford, “Applicability of the Green and Ampt Infiltration Equation to Rangelands,” *Water Resource Bulletin*, vol. 22, no. 1, pp. 19–27, 1986.

Feynman, R. P., R. B. Leighton, and M. Sands, *The Feynman Lecture Notes on Physics*, vol. I, Addison-Wesley, Reading, MA, 1963.

- Frederick, R. H., V. A. Meyers, and E. P. Auciello, "Five to 60-Minute Precipitation Frequency for the Eastern and Central United States," NOAA Technical Memo NWS HYDRO-35, National Weather Service, Silver Spring, MD, June 1977.
- Green, W. H., and G. A. Ampt, "Studies on Soil Physics. Part I: The Flow of Air and Water Through Soils," *J. Agric. Sci.*, vol. 4, no. 1, pp. 1–24, 1911.
- Gupta, R. S., *Hydrology and Hydraulic Systems*, Prentice-Hall, Englewood Cliffs, NJ, 1989.
- Hansen, E. M., L. C. Schreiner, and J. F. Miller, "Application of Probable Maximum Precipitation Estimates—United States East of 105th Meridian," NOAA Hydrometeorological Report 52, U.S. National Weather Service, Washington, DC, 1982.
- Hershfield, D. M., "Rainfall Frequency Atlas of the United States for Durations from 30 Minutes to 24 Hours and Return Periods from 1 to 100 Years," Tech. Paper 40, U.S. Department of Commerce, Weather Bureau, Washington, DC, 1961.
- Horton, R. E., "The Role of Infiltration in the Hydrologic Cycle," *Trans. Am. Geophysical Union*, vol. 14, pp. 446–460, 1933.
- Huff, F. A., "Time Distribution of Rainfall in Heavy Storms," *Water Resources Research*, vol. 3, no. 4, pp. 1007–1019, 1967.
- Maidment, D. R. (editor-in-chief), *Handbook of Hydrology*, McGraw-Hill, New York, 1993.
- Marsh, W. M., *Earthscape: A Physical Geography*, John Wiley & Sons, New York, 1987.
- Marsh, W. M., and J. Dozier, *Landscape: An Introduction to Physical Geography*, John Wiley & Sons, New York, 1986.
- Masch, F. D., *Hydrology*, Hydraulic Engineering Circular No. 19, FHWA-10-84-15. Federal Highway Administration, U.S. Department of the Interior, McLean, VA, 1984.
- McCuen, R. H., *Hydrologic Analysis and Design*, 2nd edition Prentice-Hall, Englewood Cliffs, NJ, 1998.
- Miller J. F., R. H. Frederick, and R. J. Tracey, *Precipitation Frequency Atlas of the Conterminous Western United States (by States)*, NOAA Atlas 2, 11 vols., National Weather Service, Silver Spring, MD, 1973.
- Moore, W. L., E. Cook, R. S. Gooch, and C. F. Nordin, Jr., "The Austin, Texas, Flood of May, 24-25, 1981," National Research Council, Committee on Natural Disasters, Commission on Engineering and Technical Systems National Academy Press, Washington, DC, 1982.
- Parrett, C., N. B. Melcher, and R. W. James, Jr., "Flood Discharges in the Upper Mississippi River Basin," in *Floods in the Upper Mississippi River Basin*, U.S. Geological Survey Circular, 1120-A U.S. Government Printing Office, Washington, DC, 1993.
- Philip, J. R., "Theory of Infiltration: 1. The Infiltration Equation and Its Solution," *Soil Science* 83, pp. 345–357, 1957.
- Philip, J. R., "The Theory of Infiltration," in *Advances in Hydro Sciences*, edited by V. T. Chow, vol. 5, pp. 215–296, 1969.
- Ponce, V. M., *Engineering Hydrology: Principles and Practices*, Prentice-Hall, Englewood Cliffs, NJ, 1989.
- Priestley, C. H. B., and R. J. Taylor, "On the Assessment of Surface Heat Flux and Evaporation Using Large-Scale Parameter," *Monthly Weather Review*, vol. 100, pp. 81–92, 1972.
- Rawls, W. J., D. L. Brakensiek, and N. Miller, "Green-Ampt Infiltration Parameters from Soils Data," *J. Hydraulic Div., ASCE*, vol. 109, no. 1, pp. 62–70, 1983.
- Richards, L. A., "Capillary Conduction of Liquids Through Porous Mediums," *Physics*, vol. 1, pp. 318–333, 1931.
- Roberson, J. A., J. J. Cassidy, and M. H. Chaudhry, *Hydraulic Engineering*, 2nd edition, John Wiley & Sons, New York, 1998.
- Schreiner, L. C., and J. T. Riedel, Probable Maximum Precipitation Estimates, United States East of the 105th Meridian, NOAA Hydrometeorological Report no. 51, National Weather Service, Washington, DC, June 1978.
- Singh, V. P., *Elementary Hydrology*, Prentice-Hall, Englewood Cliffs, NJ, 1992.
- Thornthwaite, C. W., and B. Holzman, "The Determination of Evaporation from Land and Water Surface," *Monthly Weather Review*, vol. 67, pp. 4–11, 1939.
- U.S. Army Corps of Engineers, Hydrologic Engineering Center, HEC-1, *Flood Hydrograph Package*, User's Manual, Davis, CA, 1990.
- U.S. Department of Agriculture Soil Conservation Service, *A Method for Estimating Volume and Rate of Runoff in Small Watersheds*, Tech. Paper 149, Washington, DC, 1973.
- U.S. Department of Agriculture Soil Conservation Service, *Urban Hydrology for Small Watersheds*, Tech. Release no. 55, Washington, DC, 1986.
- U.S. Department of Commerce, *Probable Maximum Precipitation Estimates, Colorado River and Great Basin Drainages*, Hydrometeorological Report no 49, NOAA, National Weather Service, Silver Spring, MD, 1977.
- U.S. Environmental Data Services, *Climate Atlas of the US.*, U.S. Environment Printing Office, Washington, DC, pp. 43–44, 1968.
- U.S. National Academy of Sciences, *Understanding Climate Change*, National Academy Press, Washington, DC, 1975.
- U.S. National Academy of Sciences, *Safety of Existing Dams; Evaluation and Improvement*, National Academy Press, Washington, DC, 1983.
- U.S. National Research Council, *Global Change in the Geosphere-Biosphere*, National Academy Press, Washington, DC, 1986.
- U.S. National Research Council, Committee on Opportunities in the Hydrologic Science, Water Science and Technology Board, *Opportunities in the Hydrologic Sciences*, National Academy Press, Washington, DC, 1991.
- U.S. Weather Bureau, *Two- to Ten-Day Precipitation for Return Periods of 2 to 100 Years in the Contiguous United States*, Tech. Paper 49, Washington, DC, 1964.
- Viessman, W. Jr., and G. L. Lewis, *Introduction to Hydrology*, 4th edition, Harper and Row, New York, 1996.
- Wanielista, M., R. Kersten, and R. Eaglin, *Hydrology: Water Quantity and Quality Control*, John Wiley & Sons, New York, 1997.

This page intentionally left blank

Chapter 8

Surface Runoff

8.1 DRAINAGE BASINS AND STORM HYDROGRAPHS

8.1.1 Drainage Basins and Runoff

As defined in Chapter 7, *drainage basins*, *catchments*, and *watersheds* are three synonymous terms that refer to the topographic area that collects and discharges surface streamflow through one outlet or mouth. The study of topographic maps from various physiographic regions reveals that there are several different types of drainage patterns (Figure 8.1.1). *Dendritic patterns* occur where rock and weathered mantle offer uniform resistance to erosion. Tributaries branch and erode headward in a random fashion, which results in slopes with no predominant direction or orientation. *Rectangular*

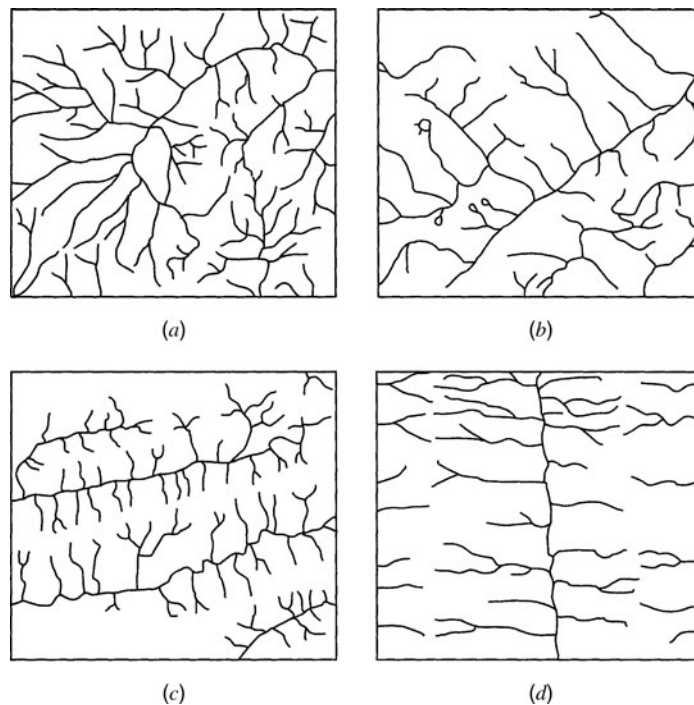


Figure 8.1.1 Common drainage patterns: (a) Dendritic; (b) Rectangular; (c) Trellis on folded terrain; (d) Trellis on mature, dissected coastal plain (from Hewlett and Nutter (1969)).

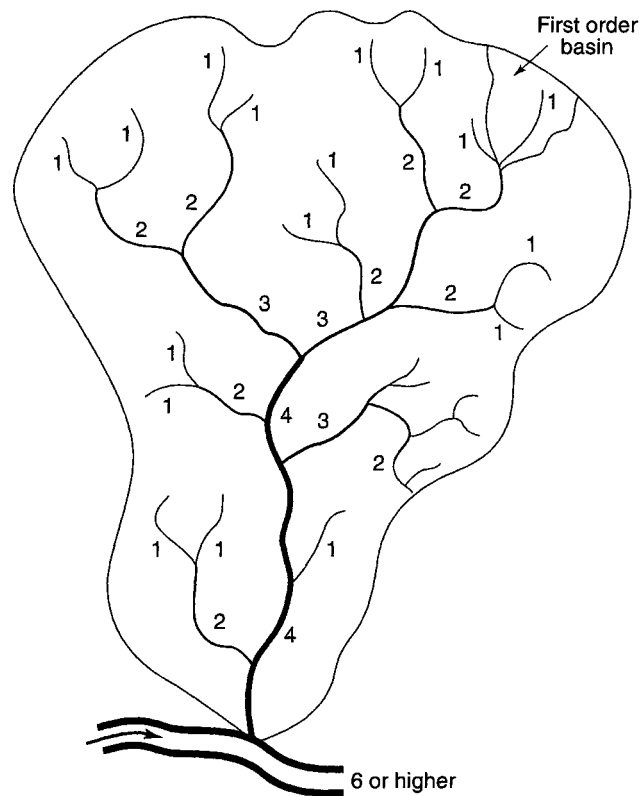


Figure 8.1.2 Stream orders (from Hewlett and Nutter (1969)).

patterns occur in faulted areas where streams follow a more easily eroded fractured rock in fault lines. *Trellis patterns* occur where rocks being dissected are of unequal resistance so that the extension and daunting of tributaries is most rapid on least resistant areas.

Streams can also be classified within a basin by systematically ordering the network of branches. Horton (1945) originated the quantitative study of stream networks by developing an ordering system and laws relating to the number and length of streams of different order (see Chow, et al. 1988). Strahler (1964) slightly modified Horton's stream ordering to that shown in Figure 8.1.2. Essentially, each non-branching channel segment is a *first-order stream*. Streams, which receive only first-order segments, are *second order*, and so on. When a channel of lower order joins a channel of higher order, the channel downstream retains the higher of the two orders. The order of a drainage basin is the order of the stream draining its outlet.

Streams can also be classified by the period of time during which flow occurs. *Perennial streams* have a continuous flow regime typical of a well-defined channel in a humid climate. *Intermittent streams generally* have flow occurring only during the wet season (50 percent of the time or less). *Ephemeral streams generally* have flow occurring during and for short periods after storms. These streams are typical of climates without very well-defined streams.

The *stream flow hydrograph* or *discharge hydrograph* is the relationship of flow rate (discharge) and time at a particular location on a stream (see Figure 8.1.3a). The *hydrograph* is "an integral expression of the physiographic and climatic characteristics that govern the relation between rainfall and runoff of a particular drainage basin" (Chow, 1964). Figures 8.1.3b and c illustrate the rising and falling of the water table in response to rainfall. Figures 8.1.3d and e illustrate that the flowing stream channel network expands and contracts in response to rainfall.

The spatial and temporal variations of rainfall and the concurrent variation of the abstraction processes define the runoff characteristics from a given storm. When the local abstractions have been

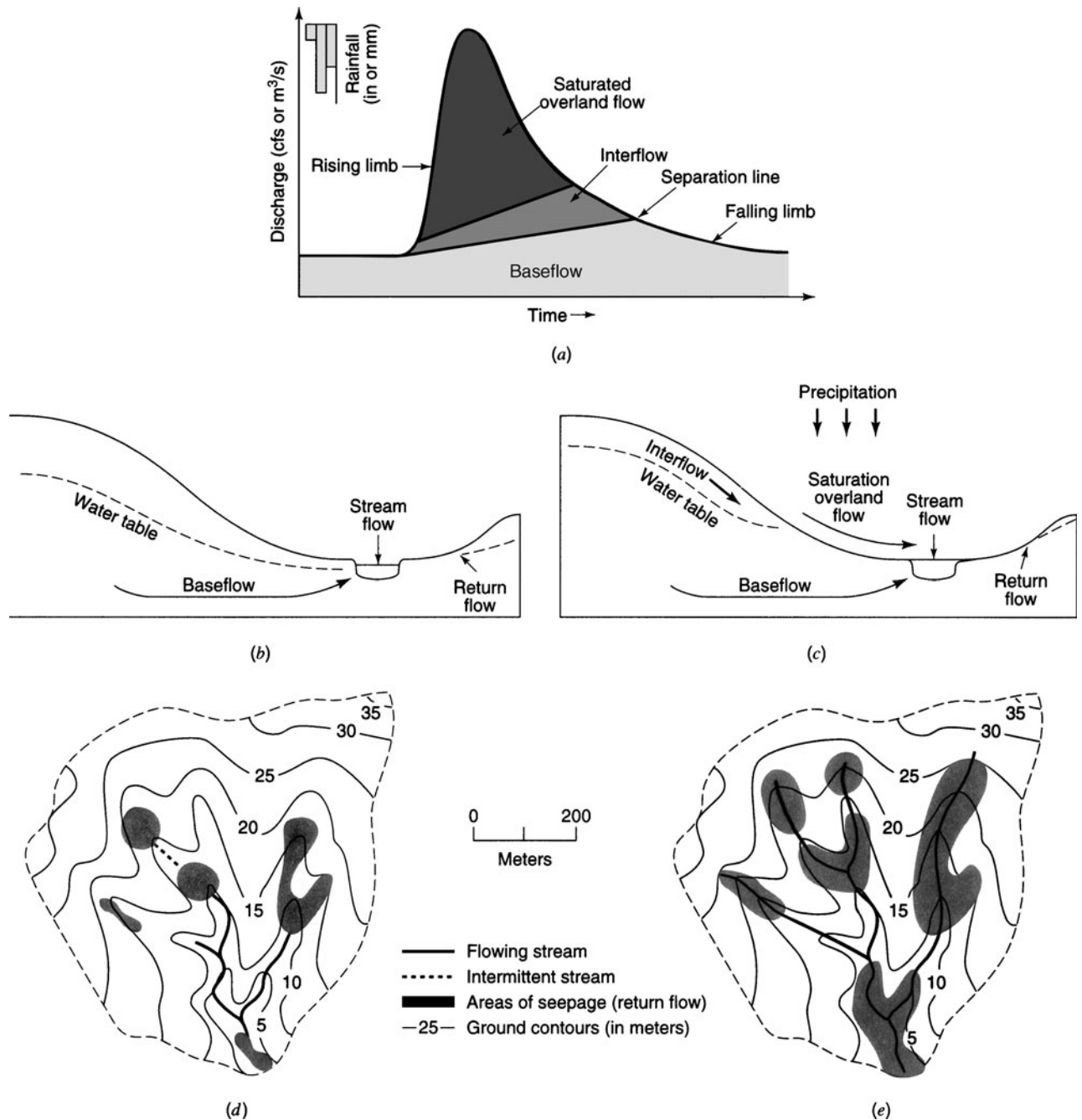


Figure 8.1.3 (a) Separatism of sources of streamflow on an idealized hydrograph; (b) Sources of streamflow on a hillslope profile during a dry period; (c) During a rainfall event; (d) Stream network during dry period; (e) Stream network extended during and after rainfall (from Mosley and McKerchar (1993)).

accomplished for a small area of a watershed, water begins to flow overland as *overland flow* and eventually into a drainage channel (in a gully or stream valley). When this occurs, the hydraulics of the natural drainage channels have a large influence on the runoff characteristics from the watershed. Some of the factors that determine the hydraulic character of the natural drainage system include:

(a) drainage area, (b) slope, (c) hydraulic roughness, (d) natural and channel storage, (e) stream length, (f) channel density, (g) antecedent moisture condition, and (h) other factors such as vegetation, channel modifications, etc. The individual effects of each of these factors are difficult, and in many cases impossible, to quantify. Figure 8.1.4 illustrates the effects of some of the drainage

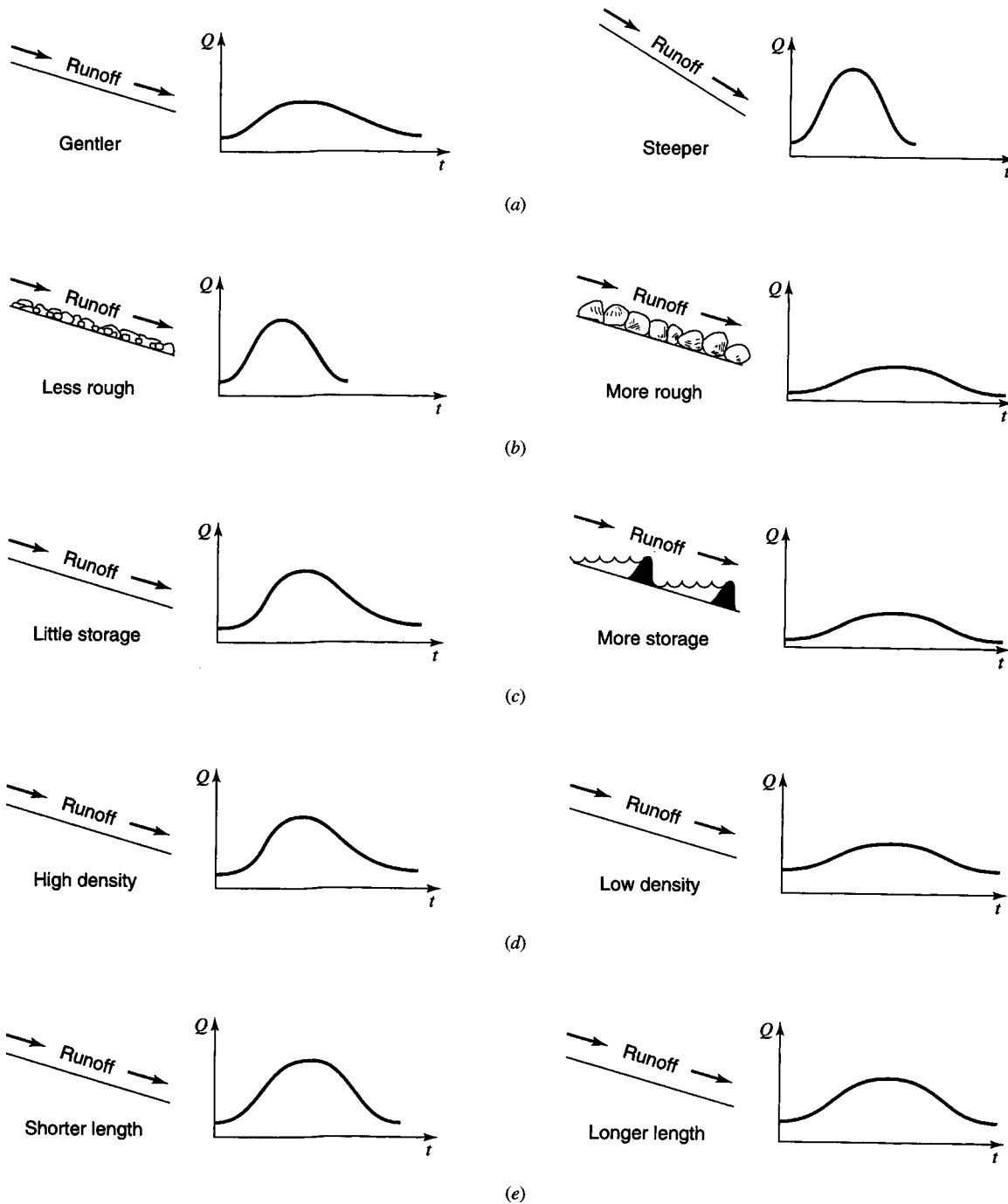


Figure 8.1.4 Effects of basin characteristics on the flood hydrograph. (a) Relationship of slope to peak discharge. (b) Relationship of hydraulic roughness to runoff. (c) Relationship of storage to runoff. (d) Relationship of drainage density to runoff. (e) Relationship of channel length to runoff (from Masch (1984)).

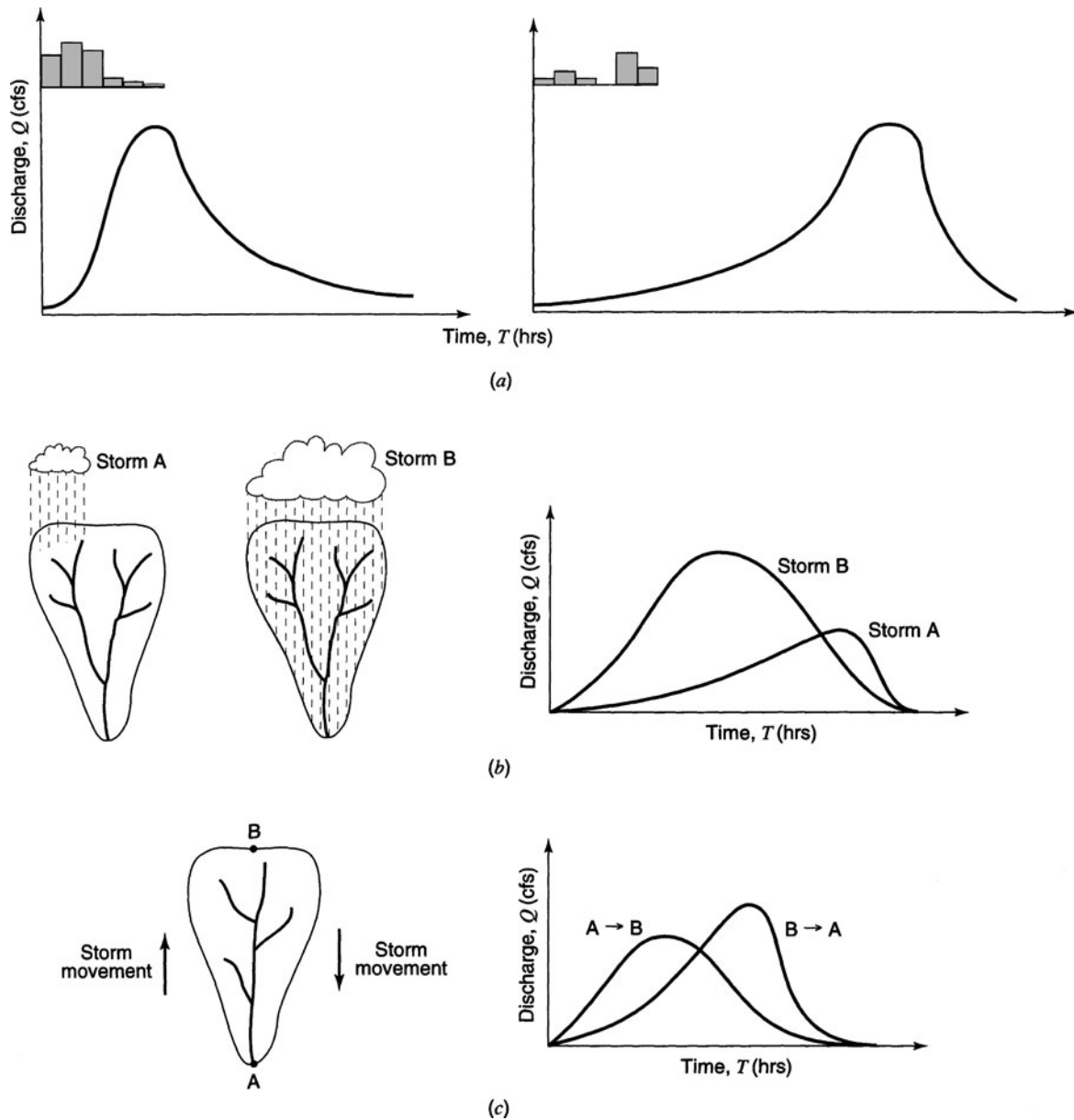


Figure 8.1.5 Effects of storm shape, size, and movement on surface runoff. (a) Effect of time variation of rainfall intensity on the surface runoff. (b) Effect of storm size on surface runoff. (c) Effect of storm movement on surface runoff (from Masch (1984)).

basin characteristics on the surface runoff (discharge hydrographs) and Figure 8.1.5 illustrates the effects of storm shape, size, and movement on surface runoff.

8.2 HYDROLOGIC LOSSES, RAINFALL EXCESS, AND HYDROGRAPH COMPONENTS

Rainfall excess, or *effective rainfall*, is that rainfall that is neither retained on the land surface nor infiltrated into the soil. After flowing across the watershed surface, rainfall excess becomes direct runoff at the watershed outlet. The graph of rainfall excess versus time is the rainfall excess hyetograph. As shown in Figure 8.2.1, the difference between the observed total rainfall hyetograph

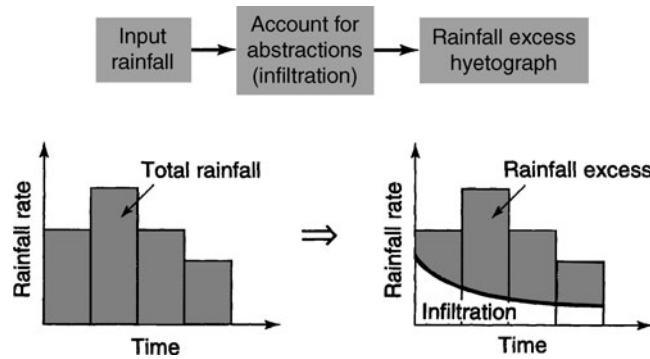


Figure 8.2.1 Concept of rainfall excess. The difference between the total rainfall hyetograph on the left and the total rainfall excess hyetograph on the right is the abstraction (infiltration).

and the rainfall excess hyetograph is the *abstractions*, or *losses*. Losses are primarily water absorbed by infiltration with some allowance for interception and surface storage. The relationships of rainfall, infiltration rate, and cumulative infiltration are shown in Figure 8.2.2. Figure 8.2.2 illustrates the relationships for rainfall and runoff data of an actual storm that can be obtained from data recorded by the U.S. Geological Survey. Using the rainfall data, rainfall hyetographs can be computed.

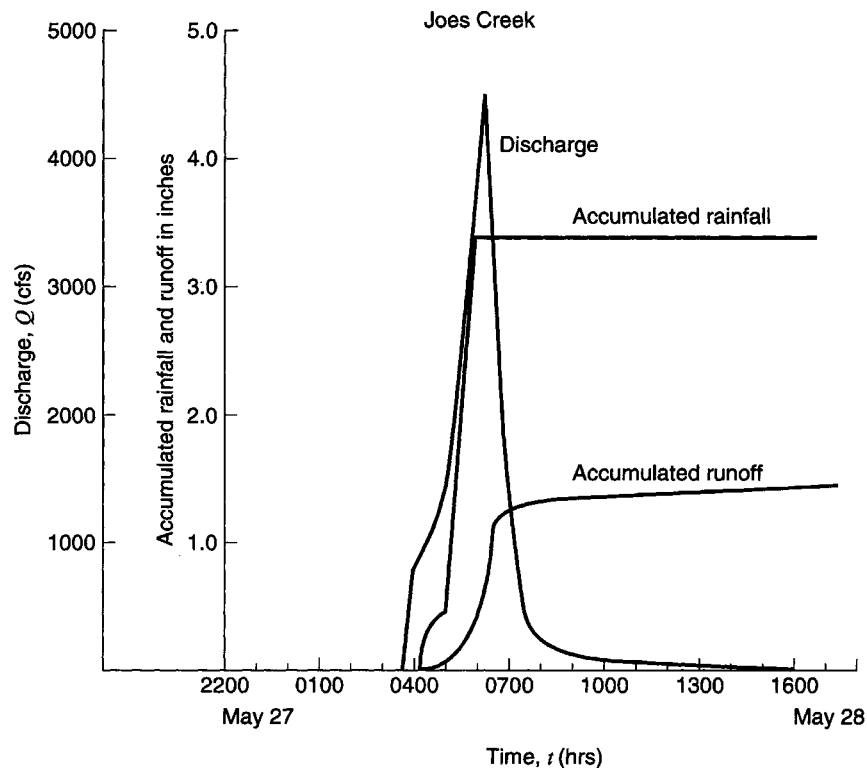


Figure 8.2.2 Precipitation and runoff data for Joes Creek, storm of May 27–28, 1978 (from Masch (1984)).

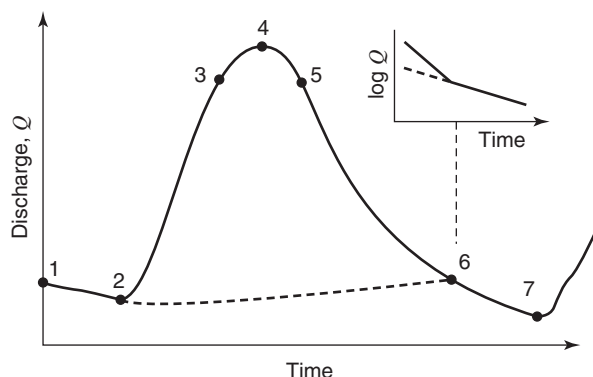


Figure 8.2.3 Components of a streamflow hydrograph: (1-2) baseflow recession; (2-3) rising limb; (3-5) crest segment; (4) peak; (5-6) falling limb; and (6-7) baseflow recession.

8.2.1 Hydrograph Components

There are several sources that make up a hydrograph (total runoff hydrograph) including direct surface runoff, interflow, baseflow (groundwater), and channel precipitation. Figure 8.1.3a illustrates the direct runoff (saturated overland flow), interflow, and baseflow. For hydrologic purposes, the total runoff consists of only two parts, direct runoff and baseflow. Baseflow is the result of water entering the stream from the groundwater that discharges from the aquifer. Figure 8.2.3 defines the components of the hydrograph, showing the baseflow recession (1-2) and (6-7), the rising limb (2-3), the crest segment (3-5), and the falling limb (5-6).

The process of defining the baseflow is referred to as baseflow separation. A number of baseflow separation methods have been suggested. Baseflow recession curves (Figure 8.2.3) can be described in the form of an exponential decay

$$Q(t_2) = Q(t_1)e^{-k(t_2 - t_1)}, \quad t_2 > t_1 \quad (8.2.1)$$

where k is the exponential decay constant having dimensions of $(\text{time})^{-1}$. With a known streamflow runoff hydrograph, the decay constant can be determined by plotting the curve of $\log Q$ versus time as shown in Figure 8.2.3 or by using a least-squares procedure. Baseflow recession curves for particular streams can be superimposed to develop a normal depletion curve or master baseflow recession curve.

8.2.2 Φ -Index Method

The Φ -index is a constant rate of abstractions (in/hr or cm/hr) that can be used to approximate infiltration. Using an observed rainfall pattern and the resulting known volume of direct runoff, the Φ -index can be determined. Using the known rainfall pattern, Φ is determined by choosing a time interval Δt , identifying the number of rainfall intervals N of rainfall that contribute to the direct runoff volume, and then subtracting $\Phi \cdot \Delta t$ from the observed rainfall in each time interval. The values of Φ and N will need to be adjusted so that the volume of direct runoff (r_d) and excess rainfall are equal

$$r_d = \sum_{n=1}^N (R_n - \Phi \cdot \Delta t) \quad (8.2.2)$$

where R_n is the observed rainfall (in or cm) in time interval n .

EXAMPLE 8.2.1

Consider the following storm event given below for a small catchment of 120 hectares. For a baseflow of $0.05 \text{ m}^3/\text{s}$, (a) compute the volume of direct runoff (in mm), (b) assuming the initial losses (abstractions) are 5 mm, determine the value of Φ -index (in mm/hr), and (c) the corresponding effective rainfall intensity hyetograph (in mm/hr).

Time (min)	0	5	10	15	20	25	30
Cumulative rainfall Depth (mm)	0	5	20	35	45		
Discharge (m^3/s)	0.05	0.05	0.25	0.65	0.35	0.15	0.05

SOLUTION

The following table shows the analysis to obtain the incremental rainfalls and rainfall intensities. There are three remaining pulses of rainfall after eliminating the first 5 mm as initial abstractions. For each of the first two rainfall increments after the initial losses are accounted for, the incremental rainfall volume is $\Phi \cdot \Delta t = \Phi(5 \text{ min})(1 \text{ hr}/60 \text{ min}) = 15 \text{ mm}$, so solving $\Phi = 180 \text{ mm/hr}$. For the third interval, $\Phi \cdot \Delta t = \Phi(5 \text{ min})(1 \text{ hr}/60 \text{ min}) = 10$, so the rainfall intensity is 120 mm/hr .

Time (min)	Discharge (m^3/sec)	Direct runoff (m^3/sec)	Cumulative rainfall (mm)	Incremental rainfall (mm)	Rainfall intensity (mm/hr)
0	0.05	0	0		
5	0.05	0	5 (initial loss)	0	
10	0.25	0.20	20	15	180
15	0.65	0.60	35	15	180
20	0.35	0.30	45	10	120
25	0.15	0.10			
30	0.05	0			

- (a) The direct runoff volume = $(0.2 + 0.6 + 0.3 + 0.1) \text{ m}^3/\text{sec} (5 \text{ min.}) (60 \text{ sec}/\text{min}) = 360 \text{ m}^3$, which converts to $r_d = 360 \text{ m}^3 / (120 \text{ hectares} \times 10,000 \text{ m}^2/\text{hectare}) = 0.3 \text{ mm}$.
- (b) There are three pulses of rainfall after eliminating the first 5 mm as initial abstractions. Considering the two largest rainfall pulses, the rainfall volume above the 120 mm/hr level is 10 mm , and

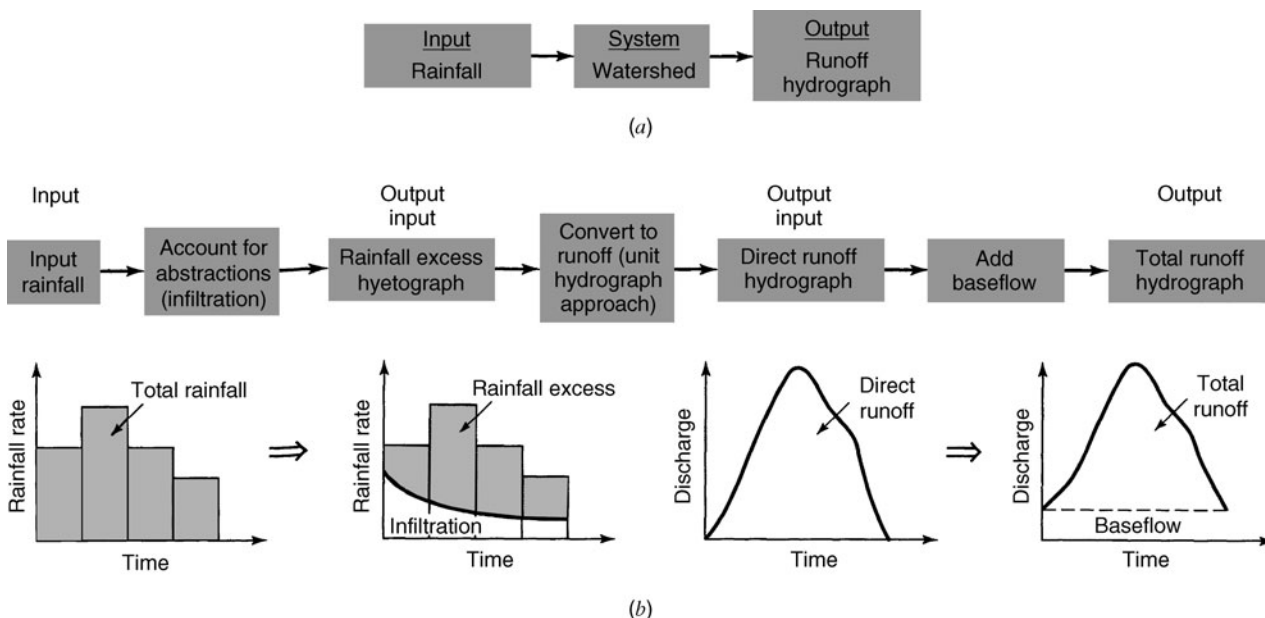


Figure 8.2.4 Storm runoff hydrographs. (a) Rainfall-runoff modeling; (b) Steps to define storm runoff.

because the direct rainfall volume is only 0.3 mm, then Φ is above the 120 mm/hr level. The direct runoff is 0.3 mm, so applying equation (8.2.2) to the two largest pulses, $r_d = 0.3 \text{ mm} = 2[(15 \text{ mm} - \Phi(5 \text{ min})(1 \text{ hr}/60 \text{ min})]$. Solving, $\Phi = 178.2 \text{ mm/hr}$.

- (c) The excess rainfall hyetograph has an intensity of $180 \text{ mm/hr} - 178.2 \text{ mm/hr} = 1.8 \text{ mm/hr}$ for the two rainfall pulses.

8.2.3 Rainfall-Runoff Analysis

The objective of many hydrologic design and analysis problems is to determine the surface runoff from a watershed due to a particular storm. This process is commonly referred to as *rainfall-runoff analysis*. The processes (steps) are illustrated in Figure 8.2.4 to determine the *storm runoff hydrographs* (or streamflow or discharge hydrograph) using the unit hydrograph approach.

8.3 RAINFALL-RUNOFF ANALYSIS USING UNIT HYDROGRAPH APPROACH

The objective of *rainfall-runoff analysis* is to develop the runoff hydrograph as illustrated in Figure 8.2.4a, where the system is a watershed or river catchment, the input is the rainfall hyetograph, and the output is the runoff or discharge hydrograph. Figure 8.2.4b defines the processes (steps) to determine the runoff hydrograph from the rainfall input using the *unit hydrograph approach*.

A *unit hydrograph* is the direct runoff hydrograph resulting from 1 in (or 1 cm in SI units) of excess rainfall generated uniformly over a drainage area at a constant rate for an effective duration. The unit hydrograph is a simple linear model that can be used to derive the hydrograph resulting from any amount of excess rainfall. The following basic assumptions are inherent in the unit hydrograph approach:

1. The excess rainfall has a constant intensity within the effective duration.
2. The excess rainfall is uniformly distributed throughout the entire drainage area.
3. The base time of the direct runoff hydrograph (i.e., the duration of direct runoff) resulting from an excess rainfall of given duration is constant.
4. The ordinates of all direct runoff hydrographs of a common base time are directly proportional to the total amount of direct runoff represented by each hydrograph.
5. For a given watershed, the hydrograph resulting from a given excess rainfall reflects the unchanging characteristics of the watershed.

The following *discrete convolution equation* is used to compute direct runoff hydrograph ordinates Q_n , given the rainfall excess values P_m and given the unit hydrograph ordinates U_{n-m+1} (Chow et al., 1988):

$$Q_n = \sum_{m=1}^{n \leq M} P_m U_{n-m+1} \quad \text{for } n = 1, 2, \dots, N \quad (8.3.1)$$

where n represents the direct runoff hydrograph time interval and m represents the precipitation time interval ($m = 1, \dots, n$).

The reverse process, called *deconvolution*, is used to derive a unit hydrograph given data on P_m and Q_n . Suppose that there are M pulses of excess rainfall and N pulses of direct runoff in the storm considered; then N equations can be written for Q_n , $n = 1, 2, \dots, N$, in terms of $N - M + 1$ unknown values of the unit hydrograph, as shown in Table 8.3.1. Figure 8.3.1 diagrammatically illustrates the calculation and the runoff contribution by each rainfall input pulse.

Once the unit hydrograph has been determined, it may be applied to find the direct runoff and streamflow hydrographs for given storm inputs. When a rainfall hyetograph is selected, the abstractions are subtracted to define the excess rainfall hyetograph. The time interval used in

Table 8.3.1 The Set of Equations for Discrete Time Convolution

Q_1	$= P_1 U_1$
Q_2	$= P_2 U_1 + P_1 U_2$
Q_3	$= P_3 U_1 + P_2 U_2 + P_1 U_3$
...	
Q_M	$= P_M U_1 + P_{M-1} U_2 + \dots + P_1 U_M$
Q_{M+1}	$= 0 + P_M U_2 + \dots + P_2 U_M + P_1 U_{M+1}$
...	
Q_{N-1}	$= 0 + 0 + \dots + 0 + 0 + \dots + P_M U_{N-M} + P_{M-1} U_{N-M+1}$
Q_N	$= 0 + 0 + \dots + 0 + 0 + \dots + 0 + P_M U_{N-M+1}$

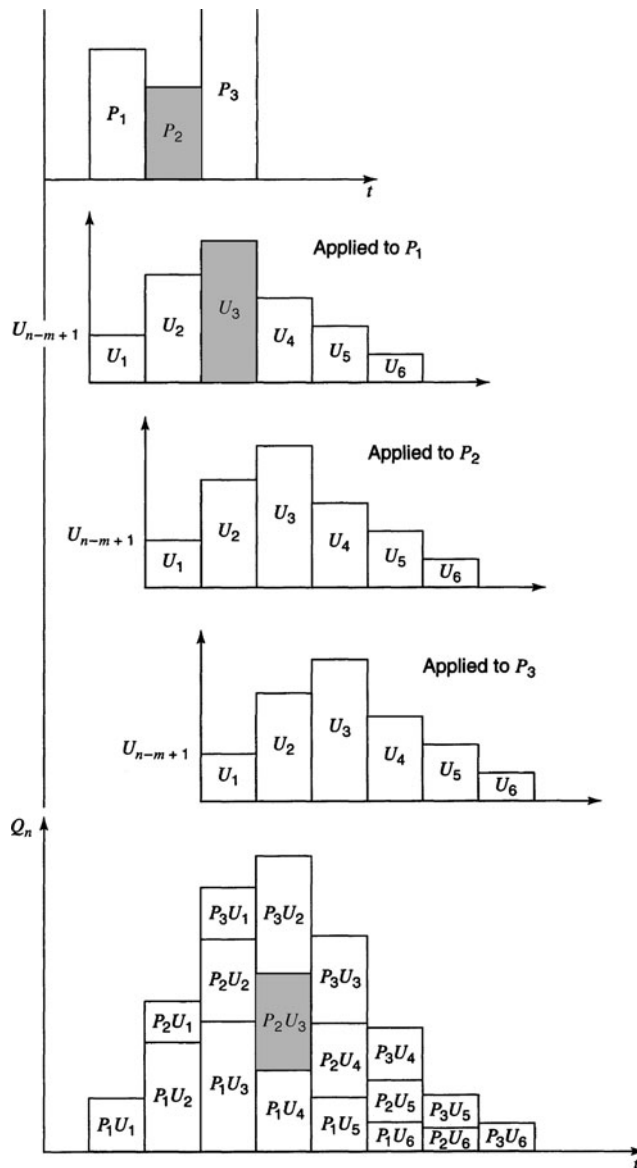


Figure 8.3.1 Application of unit hydrograph to rainfall input.

defining the excess rainfall hyetograph ordinates must be the same as that for which the unit hydrograph is specified.

EXAMPLE 8.3.1

The 1-hr unit hydrograph for a watershed is given below. Determine the runoff from this watershed for the storm pattern given. The abstractions have a constant rate of 0.3 in/h.

Time (h)	1	2	3	4	5	6
Precipitation (in)	0.5	1.0	1.5	0.5		
Unit hydrograph (cfs)	10	100	200	150	100	50

SOLUTION

The calculations are shown in Table 8.3.2. The 1-hr unit hydrograph ordinates are listed in column 2 of the table; there are $L = 6$ unit hydrograph ordinates, where $L = N - M + 1$. The number of excess rainfall intervals is $M = 4$. The excess precipitation 1-hr pulses are $P_1 = 0.2$ in, $P_2 = 0.7$ in, $P_3 = 1.2$ in, and $P_4 = 0.2$ in, as shown at the top of the table. For the first time interval $n = 1$, the discharge is computed using equation (8.3.1):

$$Q_1 = P_1 U_1 = 0.2 \times 10 = 2 \text{ cfs}$$

For the second time interval, $n = 2$,

$$Q_2 = P_1 U_2 + P_2 U_1 = 0.2 \times 100 + 0.7 \times 10 = 27 \text{ cfs}$$

and similarly for the remaining direct runoff hydrograph ordinates. The number of direct runoff ordinates is $N = L + M - 1 = 6 + 4 - 1 = 9$; i.e., there are nine nonzero ordinates, as shown in Table 8.3.2. Column 3 of Table 8.3.2 contains the direct runoff corresponding to the first rainfall pulse, $P_1 = 0.2$ in, and column 4 contains the direct runoff from the second rainfall pulse, $P_2 = 0.7$ in, etc. The direct runoff hydrograph, shown in column 7 of the table, is obtained, from the principle of superposition, by adding the values in columns 3–6.

Table 8.3.2 Calculation of the Direct Runoff Hydrograph

(1)	(2)	(3)	(4)	(5)	(6)	(7)
		Total precipitation (in)				
		0.5	1	1.5	0.5	
		Excess precipitation (in)				
Time (hr)	Unit hydrograph (cfs/in)	0.2	0.7	1.2	0.2	Direct runoff (cfs)
0	0	0	0			0
1	10	2	0	0		2
2	100	20	7	0	0	27
3	200	40	70	12	0	122
4	150	30	140	120	2	292
5	100	20	105	240	20	385
6	50	10	70	180	40	300
7	0	0	35	120	30	185
8			0	60	20	80
9				0	10	10
10					0	0

EXAMPLE 8.3.2

Determine the 1-hr unit hydrograph for a watershed using the precipitation pattern and runoff hydrograph below. The abstractions have a constant rate of 0.3 in/hr, and the baseflow of the stream is 0 cfs.

Time (h)	1	2	3	4	5	6	7	8	9	10
Precipitation (in)	0.5	1.0	1.5	0.5						
Runoff (cfs)	2	27	122	292	385	300	185	80	10	0

SOLUTION

Using the deconvolution process, we get $Q_1 = P_1 U_1$

so that for $P_1 = 0.5 - 0.3 = 0.2$ in and $Q_1 = 2$ cfs,

$$U_1 = Q_1 / P_1 = 2 / 0.2 = 10 \text{ cfs.}$$

$Q_2 = P_1 U_2 + P_2 U_1$, so that

$$U_2 = (Q_2 - P_2 U_1) / P_1$$

where

$$P_2 = 1.0 - 0.3 = 0.7 \text{ in and } Q_2 = 27 \text{ cfs.}$$

$$U_2 = (27 - 0.7(10)) / 0.2 = 100 \text{ cfs and}$$

$$Q_3 = P_1 U_3 + P_2 U_2 + P_3 U_1$$

then

$$U_3 = (Q_3 - P_2 U_2 - P_3 U_1) / P_1, \text{ so that}$$

$$U_3 = (122 - 0.7(100) - 1.2(10)) / 0.2 = 200 \text{ cfs.}$$

The rest of the unit hydrograph ordinates can be calculated in a similar manner.

8.4 SYNTHETIC UNIT HYDROGRAPHS

8.4.1 Snyder's Synthetic Unit Hydrograph

When observed rainfall-runoff data are not available for unit hydrograph determination, a *synthetic unit hydrograph* can be developed. A unit hydrograph developed from rainfall and streamflow data in a watershed applies only to that watershed and to the point on the storm where the streamflow data were measured. Synthetic unit hydrograph procedures are used to develop unit hydrographs for other locations on the stream in the same watershed or other watersheds that are of similar character.

One of the most commonly used synthetic unit hydrograph procedures is Snyder's synthetic unit hydrograph. This method relates the time from the centroid of the rainfall to the peak of the unit hydrograph to geometrical characteristics of the watershed. To determine the regional parameters C_t and C_p , one can use values of these parameters determined from similar watersheds. C_t can be determined from the relationship for the *basin lag*:

$$t_p = C_1 C_t (L \cdot L_c)^{0.3} \tag{8.4.1}$$

where C_1 , L , and L_c are defined in Table 8.4.1. Solving equation (8.4.1) for C_t gives

$$C_t = \frac{t_p}{C_1 (L \cdot L_c)^{0.3}} \tag{8.4.2}$$

To compute C_t for a gauged basin, L and L_c are determined for the gauged watershed and t_p from the derived unit hydrograph for the gauged basin.

To compute the other required parameter C_p , the expression for peak discharge of the standard unit hydrograph can be used:

$$Q_p = \frac{C_2 C_p A}{t_p} \quad (8.4.3)$$

or for a unit discharge (discharge per unit area)

$$q_p = \frac{C_2 C_p}{t_p} \quad (8.4.4)$$

Solving equation (8.4.4) for C_p gives

$$C_p = \frac{q_p t_p}{C_2} \quad (8.4.5)$$

This relationship can be used to solve for C_p for the ungauged watershed, knowing the terms in the right-hand side. Table 8.4.1 defines the steps for this procedure.

Section 8.8 discusses the SCS-unit hydrograph procedure.

EXAMPLE 8.4.1

A watershed has a drainage area of 5.42 mi^2 ; the length of the main stream is 4.45 mi , and the main channel length from the watershed outlet to the point opposite the center of gravity of the watershed is 2.0 mi . Using $C_t = 2.0$ and $C_p = 0.625$, determine the standard synthetic unit hydrograph for this basin. What is the standard duration? Use Snyder's method to determine the 30-min unit hydrograph parameter.

SOLUTION

For the standard unit hydrograph, equation (8.4.1) gives

$$t_p = C_1 C_t (L L_c)^{0.3} = 1 \times 2 \times (4.45 \times 2)^{0.3} = 3.85 \text{ hr}$$

The standard rainfall duration $t_r = 3.85/5.5 = 0.7 \text{ hr}$. For a 30-min unit hydrograph, $t_R = 30 \text{ min} = 0.5 \text{ hr}$. The basin lag $t_{pR} = t_p - (t_r - t_R)/4 = 3.85 - (0.7 - 0.5)/4 = 3.80 \text{ hr}$. The peak flow for the required unit hydrograph is $q_{pR} = q_p t_p / t_{pR}$, and substituting equation (8.4.4) in the previous equation, $q_{pR} = q_p t_p / t_{pR} = (C_2 C_p / t_p) t_p / t_{pR} = C_2 C_p / t_{pR}$, so that $q_{pR} = 640 \times 0.625 / 3.80 = 105.26 \text{ cfs (in} \cdot \text{mi}^2)$, and the peak discharge is $Q_{pR} = q_{pR} A = 105.26 \times 5.42 = 570 \text{ cfs/in}$.

The widths of the unit hydrograph are computed next. At 75 percent of the peak discharge, $W_{75} = C_{W_{75}} q_{pR}^{-1.08} = 440 \times 105.26^{-1.08} = 2.88 \text{ hr}$. At 50 percent of the peak discharge, $W_{50} = C_{W_{50}} q_{pR}^{-1.08} = 770 \times 105.26^{-1.08} = 5.04 \text{ hr}$.

The base time t_b may be computed assuming a triangular shape. This, however, does not guarantee that the volume under the unit hydrograph corresponds to 1 in (or 1 cm, for SI units) of excess rainfall. To overcome this, the value of t_b may be exactly computed taking into account the values of W_{50} and W_{75} by solving the equation in step 5 of Table 8.4.1 for t_b :

$$t_b = 2581 A / Q_{pR} - 1.5 W_{50} - W_{75}$$

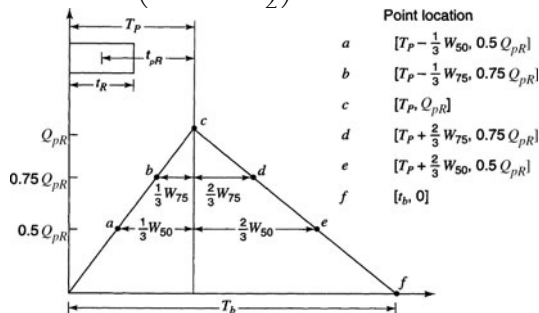
so that, with $A = 5.42 \text{ mi}^2$, $W_{50} = 5.04 \text{ hr}$, $W_{75} = 2.88 \text{ hr}$, and $Q_{pR} = 570 \text{ cfs/in}$, $T_b = 2581(5.42)/570 - 1.5 \times 5.04 - 2.88 = 14.1 \text{ hr}$.

8.4.2 Clark Unit Hydrograph

The Clark unit hydrograph procedure (Clark, 1945) is based upon using a time-area relationship of the watershed that defines the cumulative area of the watershed contributing runoff to the watershed outlet as a function of time. Ordinates of the time-area relationship are converted to a volume of runoff per second for an excess (1 cm or 1 in) and interpolated to the given time interval to define a

Table 8.4.1 Steps to Compute Snyder's Synthetic Unit Hydrograph

- Step 0 Measured information from topography map of watershed
- L = main channel length in mi (km)
 - L_c = length of the main stream channel from outflow point of watershed to a point opposite the centroid of the watershed in mi (km)
 - A = watershed area in mi^2 (km^2)
- Regional parameters C_t and C_p determined from similar watersheds.
- Step 1 Determine time to peak (t_p) and duration (t_r) of the standard unit hydrograph:
- $$t_p = C_1 C_t (L \cdot L_c)^{0.3} \quad (\text{hours})$$
- $$t_r = t_p / 5.5 \quad (\text{hours})$$
- where $C_1 = 1.0$ (0.75 for SI units)
- Step 2 Determine the time to peak t_{pR} for the desired duration t_R :
- $$t_{pR} = t_p + 0.25(t_R - t_r) \quad (\text{hours})$$
- Step 3 Determine the peak discharge, Q_{pR} , in cfs/in ($(\text{m}^3/\text{s})/\text{cm}$ in SI units)
- $$Q_{pR} = \frac{C_2 C_p A}{t_{pR}}$$
- where $C_2 = 640$ (2.75 for SI units)
- Step 4 Determine the width of the unit hydrograph at $0.5Q_{pR}$ and $0.75Q_{pR}$. W_{50} is the width at 50% of the peak given as
- $$W_{50} = \frac{C_{50}}{(Q_{pR}/A)^{1.08}}$$
- where $C_{50} = 770$ (2.14 for SI units). W_{75} is the width at 75% of the peak given as
- $$W_{75} = \frac{C_{75}}{(Q_{pR}/A)^{1.08}}$$
- where $C_{75} = 440$ (1.22 for SI units)
- Step 5 Determine the base, T_b , such that the unit hydrograph represents 1 in (1 cm in SI units) of direct runoff volume;
- $$1 \text{ in} = \left[\left(\frac{W_{50} + T_b}{2} \right) (0.5Q_{pR}) + \left(\frac{W_{75} + W_{50}}{2} \right) (0.25Q_{pR}) + \frac{1}{2} W_{75} (0.25Q_{pR}) \right] \left(\text{hr} \times \frac{\text{ft}^3}{\text{sec}} \right)$$
- $$\left(\frac{1}{A(\text{mi})^2} \times \frac{1 \text{ mi}^2}{(5,280)^2 \text{ ft}^2} \times \frac{12 \text{ in}}{\text{ft}} \times \frac{3,600 \text{ sec}}{\text{hr}} \right)$$
- Solving for T_b , we get
- $$T_b = 2,581 \frac{A}{Q_{pR}} - 1.5W_{50} - W_{75}$$
- for A in mi^2 , Q_{pR} in cfs, W_{50} and W_{75} in hours.
- Step 6 Define known points of the unit hydrograph. ($T_p = t_{pR} + \frac{t_R}{2}$)



translation hydrograph. The assumption is a pure translation of the rainfall excess without storage effects of the watershed to define a translation hydrograph. This translation hydrograph is routed through a linear reservoir ($S = RQ$) in order to simulate the effects of storage of the watershed, where R is the storage coefficient. The resulting routed hydrograph for the instantaneous excess is averaged to produce the unit hydrograph for the excess (1 cm or 1 inch) occurring in the given time interval.

Synthetic time-area relationships can be expressed in the following form such as that used by the U.S. Army Corps of Engineers (1990)

$$A/A_c = 1.414(t/T_c)^{1.5} \quad \text{for } 0 \leq t/T_c \leq 0.5 \quad (8.4.6a)$$

and

$$A/A_c = 1 - 1.414(1 - t/T_c)^{1.5} \quad \text{for } 0.5 \leq t/T_c \leq 1.0 \quad (8.4.6b)$$

where A is the contributing area at time t , A_c is the total watershed area, and T_c is the time of concentration of the watershed area. Some investigators such as Ford et al. (1980) indicate that a detailed time-area curve usually is not necessary for accurate synthetic unit hydrograph estimation. A comparison of the HEC (Hydrologic Engineering Center) default relation found in HEC-1 and HEC-HMS to that used in Phoenix, Arizona is given in Table 8.4.2.

The average instantaneous flow over time interval t to $t + \Delta t$, defining the translation hydrograph is denoted as $I_{ave,t}$. To compute $I_{ave,t}$, assuming a pure translation over a Δt hr time period, the flowing equations are used. For 1 cm (0.01 m), the $I_{ave,t}$ in m^3/s is expressed as

$$I_{ave,t} = (0.01 \text{ m})(\Delta A \text{ km}^2)(10^6 \text{ m}^2/\text{km}^2)(1/\Delta t \text{ hr})(1 \text{ hr}/3600 \text{ sec}) \quad (8.4.7)$$

where ΔA is the incremental area in km^2 between runoff isochrones (lines of equal runoff at a certain time) and Δt is the time increment in hours. For 1 in in the $I_{ave,t}$ in ft^3/s is expressed as

$$I_{ave,t} = (1 \text{ in})(1 \text{ ft}/12 \text{ in})(\Delta A \text{ mi}^2)(5280 \text{ ft}^2/\text{mi}^2)(1/\Delta t \text{ hr})(1 \text{ hr}/3600 \text{ sec}) \quad (8.4.8)$$

Storage effects in the watershed are incorporated by routing the translation hydrograph through a linear reservoir using the continuity equation

$$I_{ave,t} - 0.5(Q_t + Q_{t+\Delta t}) = (S_t + S_{t+\Delta t})/\Delta t \quad (8.4.9)$$

Table 8.4.2 Synthetic Dimensionless Time-Area Relations

Time as a percent of T_c	Contributing area, as a percent of total area		
	Urban* watersheds	Natural* watersheds	HEC default
0	0	0	0.0
10	5	3	4.5
20	16	5	12.6
30	30	8	23.2
40	65	12	35.8
50	77	20	50.0
60	84	43	64.2
70	90	75	76.8
80	94	90	87.4
90	97	96	95.5
100	100	100	100

*Flood Control District of Maricopa County, Phoenix, AZ (1995)

$I_{ave,t}$ is the average instantaneous inflow over time interval t to $t + \Delta t$, defining the translation hydrograph, Q is the outflow from the linear reservoir, and S is the storage in the linear reservoir. In the linear reservoir assumption, storage S_t is assumed to be linearly proportional to Q_t

$$S_t = RQ_t \tag{8.4.10}$$

in which R is the proportionality constant (watershed storage coefficient) with units of time. Combining equations (8.4.9) and (8.4.10) the routing equation is

$$Q_{t+\Delta t} = CI_{ave,t} + (1 - C)Q_t \tag{8.4.11}$$

where $I_{ave,t}$ is the average translated runoff (inflow rate to the linear reservoir) during time increment, and

$$C = 2 \Delta t / (2R + \Delta t) \tag{8.4.12}$$

The discharge, Q_t , from the linear reservoir now includes the effects of the storage of the watershed. This hydrograph is an instantaneous (duration = 0 hr) unit hydrograph, which is converted to the desired unit hydrograph of duration τ by averaging the ordinates over the time interval

$$U_\tau(t) = 0.5[Q_t + Q_{t-\tau}] \tag{8.4.13}$$

The above equations are the basis for the Clark unit hydrograph procedure.

EXAMPLE 8.4.2

A small watershed has an area of 10 km² and a time of concentration of 1.5 hr. The watershed storage coefficient is 0.75 hr. The time-area relationship is the HEC default values in Table 8.4.2. Compute the 1-hr unit hydrograph for this small watershed. Use a time interval of 0.5-hr for the computations.

SOLUTION

First the incremental areas of the watershed are determined using the HEC time-area relationship in Table 8.4.2. The translation hydrograph is then computed by applying equation (8.4.7) to each ΔA . Next the translation hydrograph is routed through a linear reservoir using the given watershed storage coefficient. Compute the routing coefficient $C = 2(0.5) / [2(0.75) + 0.5] = 0.5$, so the linear reservoir routing equation is $Q_{t+\Delta t} = 0.5I_{ave,t} + (1 - 0.5)Q_t = 0.5I_{ave,t} + 0.5Q_t$. The unit hydrograph ordinates are computed using equation (8.4.13) with $\tau = 1$ hr. For example, the unit hydrograph ordinate for time 0.5 hr is $(0 + 7.56) / 2 = 3.78$ m³/s, for time 1.0 hr is $(0 + 16.4) / 2 = 8.20$ m³/s and for 1.5 hr is $(7.56 + 15.8) / 2 = 11.7$ m³/s.

t (hr)	t/T_c	A/A_c	A (km ²)	ΔA (km ²)	$I_{ave,t}$ (m ³ /s)	$Q_{t+\Delta t}$ (m ³ /s)	$U_\tau(t)$ (m ³ /s)
0.0							0.0
0.5	0.333	0.272	2.72	2.72	15.1	7.56	3.78
1.0	0.667	0.728	7.28	4.56	25.3	16.4	8.20
1.5	1.0	1.0	10.0	2.72	15.1	15.8	11.7
2.0					0.0	7.89	12.2
2.5						3.94	9.86
3.0						1.97	4.93
3.5						0.986	2.46
4.0						0.493	1.23
4.5						0.247	0.616
5.0						0.123	0.308

The use of the model HEC-HMS (HEC-1) requires the time of concentration, T_c , and the storage coefficient R . Various locations have developed relationships for these parameters to make the methods more accurate and easier to use. Straub et al. (2000) developed the following equations for small rural watersheds (0.02-2.3 mi²) in Illinois

$$T_c = 1.54L^{0.875} S_o^{-0.181} \quad (8.4.14)$$

and

$$R = 16.4L^{0.342} S_o^{-0.790} \quad (8.4.15)$$

where L is the stream length measured along the main channel from the watershed outlet to the watershed divide in miles, and S_o is the main-channel slope determined from elevations at points that represent 10 and 85 percent of the distance along the channel from the watershed outlet to the watershed divide in ft/mi.

Others have used time of concentration equations that have included additional parameters. For example Phoenix, Arizona (Flood Control District of Maricopa County) uses the following time of concentration equations developed by Papadakis and Kazan (1987) for urban areas

$$T_c = 11.4L^{0.50} K_b^{0.52} S_o^{-0.31} i^{-0.38} \quad (8.4.16)$$

where T_c is the time of concentration in hours, L is the length of the longest flow path in miles, K_b is a watershed resistance coefficient ($K_b = -0.00625 \log A + 0.04$) for commercial and residential areas, A is the watershed area in acres, S is the slope of the flow path in ft/mi, and i is the rainfall intensity in in/hr. The storage coefficient is

$$R = 0.37T_c^{1.11} A^{-0.57} L^{0.80} \quad (8.4.17)$$

where A is the watershed area in mi².

8.5 S-HYDROGRAPHS

In order to change a unit hydrograph from one duration to another, the *S-hydrograph method*, which is based on the principle of superposition, can be used. An S-hydrograph results theoretically from a continuous rainfall excess at a constant rate for an indefinite period. This curve (see Figure 8.5.1) has an S-shape with the ordinates approaching the rate of rainfall excess at the time of equilibrium.

Basically the S-curve (hydrograph) is the summation of an infinite number of t_R duration unit hydrographs, each lagged from the preceding one by the duration of the rainfall excess, as illustrated in Figure 8.5.2.

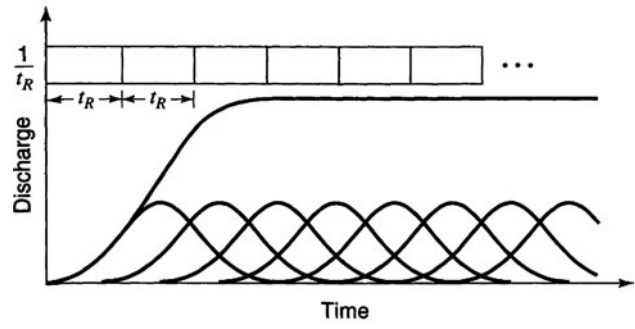
A unit hydrograph for a new duration t'_R is obtained by: (1) lagging the S-hydrograph (derived with the t_R duration unit hydrographs) by the new (desired) duration t'_R , (2) *subtracting* the two S-hydrographs from one another, and (3) *multiplying* the resulting hydrograph ordinates by the ratio t_R/t'_R . Theoretically the S-hydrograph is a smooth curve because the input rainfall excess is assumed to be a constant, continuous rate. However, the numerical processes of the procedures may result in an undulatory form that may require smoothing or adjustment of the S-hydrograph.

EXAMPLE 8.5.1

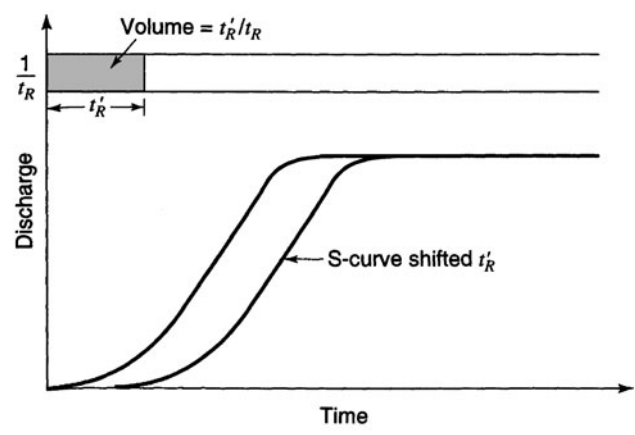
Using the 2-hr unit hydrograph in Table 8.5.1, construct a 4-hr unit hydrograph (adapted from Sanders (1980)).

SOLUTION

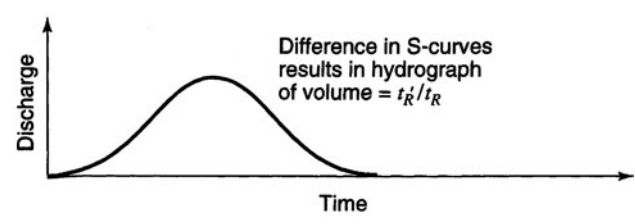
See the computations in Table 8.5.1.



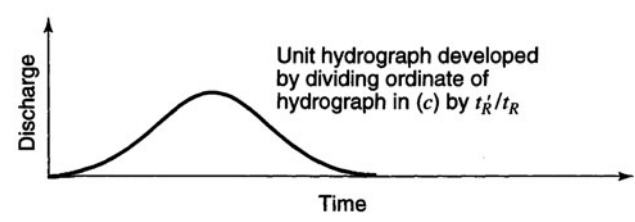
(a)



(b)



(c)



(d)

Figure 8.5.1 Development of a unit hydrograph for duration t'_R from a unit hydrograph for duration t_R .

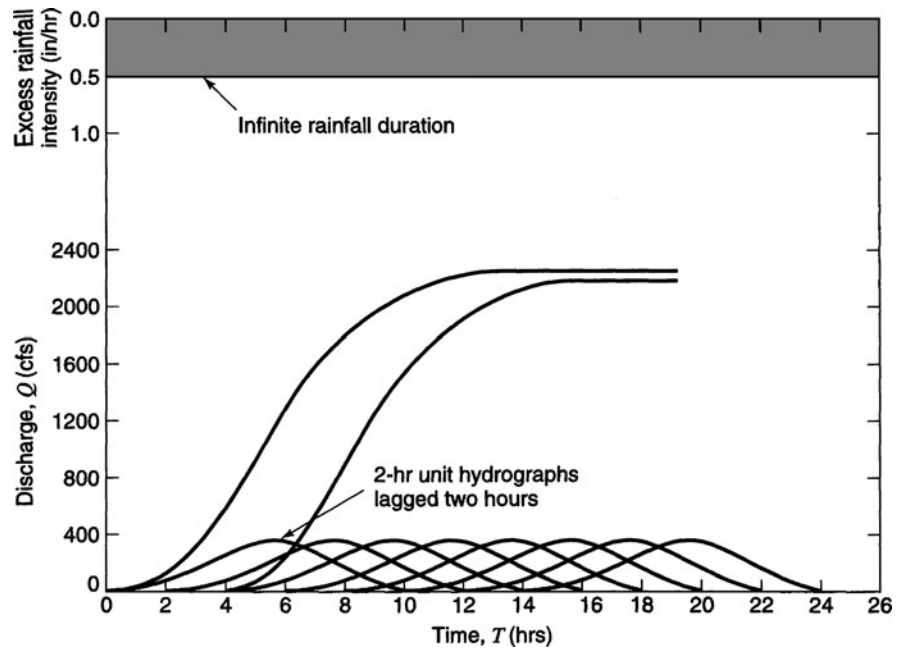


Figure 8.5.2 Graphical illustration of the S-curve construction (from Masch (1984)).

Table 8.5.1 S-Curve Determined from a 2-hr Unit Hydrograph to Estimate a 4-hr Unit Hydrograph

Time (hr)	2-hr unit hydrograph (cfs/in)	Lagged 2-hr unit hydrograph (cfs/in)	S-curve	Lagged S-curve	4-hr hydrograph	4-hr-unit hydrograph (cfs/in)
0	0		0	—	0	0
2	69	0	69	—	69	34
4	143	69	212	0	212	106
6	328	143	540	69	471	235
8	389	328	929	212	717	358
10	352	389	1281	540	741	375
12	266	352	1547	929	618	309
14	192	266	1739	1281	458	229
16	123	192	1862	1547	315	158
18	84	123	1946	1739	207	103
20	49	84	1995	1862	133	66
22	20	49	2015	1946	69	34
24	0	20	*2015	1995	20	10
26	0	0	*2015	2015	0	0

*Adjusted values

Source: Sanders (1980).

8.6 NRCS (SCS) RAINFALL-RUNOFF RELATION

The U.S. Department of Agriculture Soil Conservation Service (SCS) (1972), now the National Resources Conservation Service (NRCS), developed a rainfall-runoff relation for watershed. For the storm as a whole, the depth of excess precipitation or direct runoff P_e is always less than or equal to

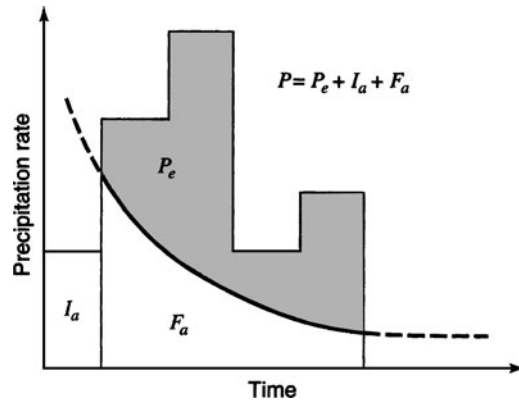


Figure 8.6.1 Variables in the SCS method of rainfall abstractions: I_a = initial abstraction, P_e = rainfall excess, F_a = continuing abstraction, and P = total rainfall.

the depth of precipitation P ; likewise, after runoff begins, the additional depth of water retained in the watershed F_a is less than or equal to some *potential maximum retention* S (see Figure 8.6.1). There is some amount of rainfall I_a (initial abstraction before ponding) for which no runoff will occur, so the potential runoff is $P - I_a$. The SCS method assumes that the ratios of the two actual to the two potential quantities are equal, that is,

$$\frac{F_a}{S} = \frac{P_e}{P - I_a} = \frac{\text{Actual}}{\text{Potential}} \tag{8.6.1}$$

From continuity,

$$P = P_e + I_a + F_a \tag{8.6.2}$$

so that combining equations (8.6.1) and (8.6.2) and solving for P_e gives

$$P_e = \frac{(P - I_a)^2}{P - I_a + S} \tag{8.6.3}$$

which is the basic equation for computing the depth of excess rainfall or direct runoff from a storm by the SCS method.

From the study of many small experimental watersheds, an empirical relation was developed for I_a :

$$I_a = 0.2S \tag{8.6.4}$$

so that equation (8.6.3) is now expressed as

$$P_e = \frac{(P - 0.2S)^2}{P + 0.8S} \tag{8.6.5}$$

Empirical studies by the SCS indicate that the potential maximum retention can be estimated as

$$S = \frac{1000}{CN} - 10 \tag{8.6.6}$$

where CN is a runoff curve number that is a function of land use, antecedent soil moisture, and other factors affecting runoff and retention in a watershed. The curve number is a dimensionless number defined such that $0 \leq CN \leq 100$. For impervious and water surfaces $CN = 100$; for natural surfaces $CN < 100$.

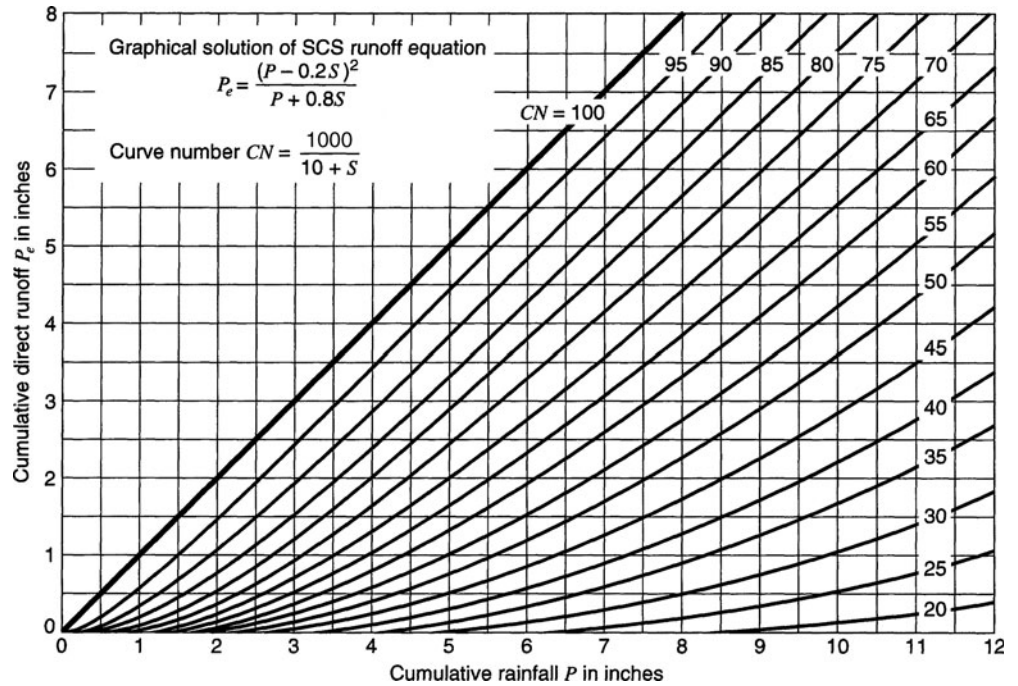


Figure 8.6.2 Solution of the SCS runoff equations (from U.S. Department of Agriculture Soil Conservation Service (1972)).

The SCS rainfall-runoff relation (equation (8.6.5)) can be expressed in graphical form using the curve numbers as illustrated in Figure 8.6.2. Equation (8.6.5) or Figure 8.6.2 can be used to estimate the volume of runoff when the precipitation volume P and the curve number CN are known.

8.7 CURVE NUMBER ESTIMATION AND ABSTRACTIONS

8.7.1 Antecedent Moisture Conditions

The curve numbers shown in Figure 8.6.2 apply for normal *antecedent moisture conditions* (AMC II). Antecedent moisture conditions are grouped into three categories:

AMC I—Low moisture

AMC II—Average moisture condition, normally used for annual flood estimates

AMC III—High moisture, heavy rainfall over the preceding few days

For dry conditions (AMC I) or wet conditions (AMC III), equivalent curve numbers can be computed using

$$CN(I) = \frac{4.2CN(II)}{10 - 0.058CN(II)} \quad (8.7.1)$$

and

$$CN(III) = \frac{23CN(II)}{10 + 0.13CN(II)} \quad (8.7.2)$$

The range of antecedent moisture conditions for each class is shown in Table 8.7.1. Table 8.7.2 lists the adjustment of curve numbers to conditions I and III for known II conditions.

Table 8.7.1 Classification of Antecedent Moisture Classes (AMC) for the SCS Method of Rainfall Abstractions

AMC group	Total 5-day antecedent rainfall (in)	
	Dormant season	Growing season
I	Less than 0.5	Less than 1.4
II	0.5 to 1.1	1.4 to 2.1
III	Over 1.1	over 2.1

Source: U.S. Department of Agriculture Soil Conservation Service (1972).

Table 8.7.2 Adjustment of Curve Numbers for Dry (Condition I) and Wet (Condition III) Antecedent Moisture Conditions

CN for condition II	Corresponding CN for condition	
	I	III
100	100	100
95	87	99
90	78	98
85	70	97
80	63	94
75	57	91
70	51	87
65	45	83
60	40	79
55	35	75
50	31	70
45	27	65
40	23	60
35	19	55
30	15	50
25	12	45
20	9	39
15	7	33
10	4	26
5	2	17
0	0	0

Source: U.S. Department of Agriculture Soil Conservation Service (1972).

8.7.2 Soil Group Classification

Curve numbers have been tabulated by the Soil Conservation Service on the basis of soil type and land use in Table 8.7.3. The four soil groups in Table 8.7.3 are described as:

Group A: Deep sand, deep loess, aggregated silts

Group B: Shallow loess, sandy loam

Group C: Clay loams, shallow sandy loam, soils low in organic content, and soils usually high in clay

Group D: Soils that swell significantly when wet, heavy plastic clays, and certain saline soils

The values of *CN* for various land uses on these soil types are given in Table 8.7.3. For a watershed made up of several soil types and land uses, a composite *CN* can be calculated.

Minimum infiltration rates for the various soil groups are:

Group	Minimum infiltration rate (in/hr)
A	0.30 – 0.45
B	0.15 – 0.30
C	0 – 0.05

Table 8.7.3 Runoff Curve Numbers (Average Watershed Condition, $I_a = 0.2S$)

Land use description	Curve numbers for hydrologic soil group			
	A	B	C	D
Fully developed urban areas ^a (vegetation established)				
Lawns, open spaces, parks, golf courses, cemeteries, etc.				
Good condition; grass cover on 75% or more of the area	39	61	74	80
Fair condition; grass cover on 50% to 75% of the area	49	69	79	84
Poor condition; grass cover on 50% or less of the area	68	79	86	89
Paved parking lots, roofs, driveways, etc.	98	98	98	98
Streets and roads				
Paved with curbs and storm sewers	98	98	98	98
Gravel	76	85	89	91
Dirt	72	82	87	89
Paved with open ditches	83	89	92	93
	Average % impervious ^b			
Commercial and business areas	85	89	92	94
Industrial districts	72	81	88	91
Row houses, town houses, and residential with lot sizes 1/8 acre or less	65	77	85	90
Residential: average lot size				
1/4 acre	38	61	75	83
1/3 acre	30	57	72	81
1/2 acre	25	54	70	80
1 acre	20	51	68	79
2 acre	12	46	65	77
Developing urban areas ^c (no vegetation established)				
Newly graded area	77	86	91	94
Cover				
Land use	Treatment of practice	Hydrologic condition ^d		
Cultivated agricultural land				
Fallow	Straight row		77	86
	Conservation tillage	Poor	76	85
	Conservation tillage	Good	74	83
Row crops	Straight row	Poor	72	81
	Straight row	Good	67	78
	Conservation tillage	Poor	71	80

(Continued)

Table 8.7.3 (Continued)

Cover		Hydrologic condition ^d	Curve numbers for hydrologic soil group			
Land use	Treatment of practice		A	B	C	D
Small grain	Conservation tillage	Good	64	75	82	85
	Contoured	Poor	70	79	84	88
	Contoured	Good	65	75	82	86
	Contoured and conservation tillage	Poor	69	78	83	87
		Good	64	74	81	85
	Contoured and terraces	Poor	66	74	80	82
	Contoured and terraces	Good	62	71	78	81
	Contoured and terraces and conservation tillage	Poor	65	73	79	81
		Good	61	70	77	80
	Straight row	Poor	65	76	84	88
	Straight row	Good	63	75	83	87
	Conservation tillage	Poor	64	75	83	86
	Conservation tillage	Good	60	72	80	84
	Contoured	Poor	63	74	82	85
	Contoured	Good	61	73	81	84
	Contoured and conservation tillage	Poor	62	73	81	84
		Good	60	72	80	83
	Contoured and terraces	Poor	61	72	79	82
Contoured and terraces	Good	59	70	78	81	
Contoured and terraces and conservation tillage	Poor	60	71	78	81	
	Good	58	69	77	80	
Close-seeded legumes or rotation meadow	Straight row	Poor	66	77	85	89
	Straight row	Good	58	72	81	85
	Contoured	Poor	64	75	83	85
	Contoured	Good	55	69	78	83
	Contoured and terraces	Poor	63	73	80	83
	Contoured and terraces	Good	51	67	76	80
Noncultivated agricultural land, pasture or range	No mechanical treatment	Poor	68	79	86	89
	No mechanical treatment	Fair	49	69	79	84
	No mechanical treatment	Good	39	61	74	80
	Contoured	Poor	47	67	81	88
	Contoured	Fair	25	59	75	83
	Contoured	Good	6	35	70	79
	Meadow	—	30	58	71	78
Forested—grass or orchards—evergreen or deciduous	Brush	Poor	55	73	82	86
		Fair	44	65	76	82
		Good	32	58	72	79
		Poor	48	67	77	83
Woods		Good	20	48	65	73
		Poor	45	66	77	83
		Fair	36	60	73	79
		Good	25	55	70	77
Farmsteads	—	59	74	82	86	
Forest-range Herbaceous		Poor		79	86	92
		Fair		71	80	89
		Good		61	74	84

Table 8.7.3 (Continued)

Land use	Cover Treatment of practice	Hydrologic condition ^d	Curve numbers for hydrologic soil group			
			A	B	C	D
Oak–aspen		Poor	65	74		
		Fair	47	57		
		Good	30	41		
Juniper–grass		Poor	72	83		
		Fair	58	73		
		Good	41	61		
Sage–grass		Poor	67	80		
		Fair	50	63		
		Good	35	48		

^aFor land uses with impervious areas, curve numbers are computed assuming that 100% of runoff from impervious areas is directly connected to the drainage system. Pervious areas (lawn) are considered to be equivalent to lawns in good condition and the impervious areas have a *CN* of 98.

^bIncludes paved streets.

^cUse for the design of temporary measures during grading and construction. Impervious area percent for urban areas under development vary considerably. The user will determine the percent impervious. Then using the newly graded area *CN* and Figure 8.7.1*a* or *b*, the composite *CN* can be computed for any degree of development.

^dFor conservation tillage in poor hydrologic condition, 5 percent to 20 percent of the surface is covered with residue (less than 750-lb/acre row crops or 300-lb/acre small grain).

For conservation tillage in good hydrologic condition, more than 20 percent of the surface is covered with residue (greater than 750-lb/acre row crops or 300-lb/acre small grain).

^eClose-drilled or broadcast.

For noncultivated agricultural land:

Poor hydrologic condition has less than 25 percent ground cover density.

Fair hydrologic condition has between 25 percent and 50 percent ground cover density.

Good hydrologic condition has more than 50 percent ground cover density.

For forest–range:

Poor hydrologic condition has less than 30 percent ground cover density.

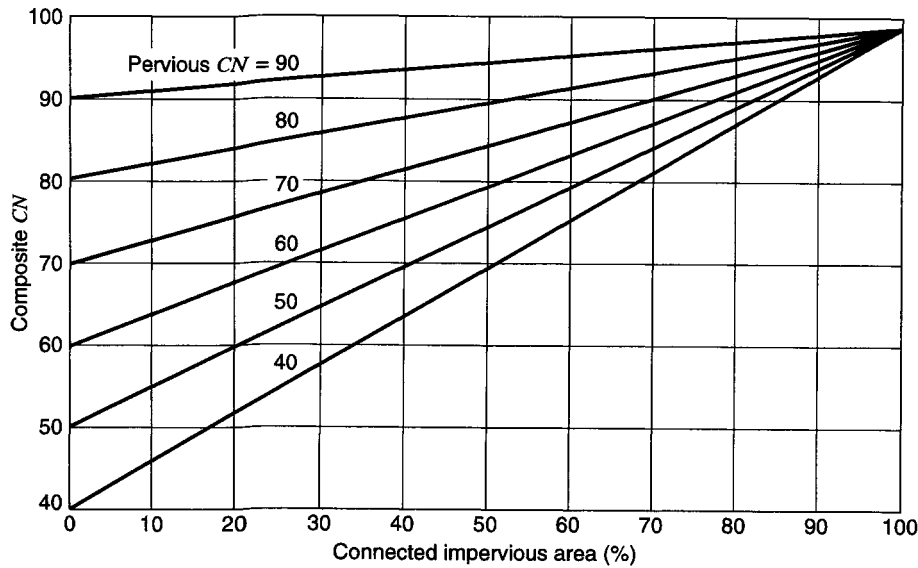
Fair hydrologic condition has between 30 percent and 70 percent ground cover density.

Good hydrologic condition has more than 70 percent ground cover density.

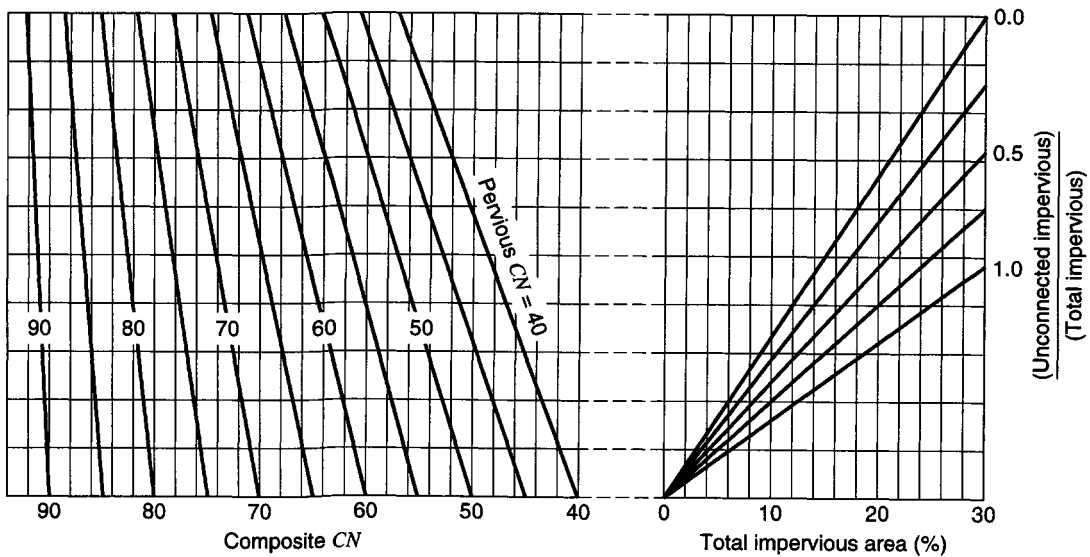
Source: U.S. Department of Agriculture Soil Conservation Service (1986).

8.7.3 Curve Numbers

Table 8.7.3 gives the curve numbers for average watershed conditions, $I_a = 0.2S$, and antecedent moisture condition II. For watersheds consisting of several subcatchments with different *CNs*, the area-averaged composite *CN* can be computed for the entire watershed. This analysis assumes that the impervious areas are directly connected to the watershed drainage system (Figure 8.7.1*a*). If the percent imperviousness is different from the value listed in Table 8.7.3 or if the impervious areas are not directly connected, then Figures 8.7.1*a* or *b*, respectively, can be used. The pervious *CN* used in these figures is equivalent to the open-space *CN* in Table 8.7.3. If the total impervious area is less than 30 percent, Figure 8.7.1*b* is used to obtain a composite *CN*. For natural desert landscaping and newly graded areas, Table 8.7.3 gives only the *CNs* for pervious areas.



(a)



(b)

Figure 8.7.1 Relationships for determining composite *CN*. (a) Connected impervious area; (b) Unconnected impervious area (from U.S. Department of Agriculture Soil Conservation Service (1986)).

EXAMPLE 8.7.1

Determine the weighted curve numbers for a watershed with 40 percent residential (1/4-acre lots), 25 percent open space, good condition, 20 percent commercial and business (85 percent impervious), and 15 percent industrial (72 percent impervious), with corresponding soil groups of C, D, C, and D.

SOLUTION

The corresponding curve numbers are obtained from Table 8.7.3:

Land use (%)	Soil group	Curve number
40	C	83
25	D	80
20	C	94
15	D	93

The weighted curve number is

$$\begin{aligned}
 CN &= 0.40(83) + 0.25(80) + 0.20(94) + 0.15(93) \\
 &= 33.2 + 20 + 18.8 + 13.95 \\
 &= 85.95(\text{use } 86)
 \end{aligned}$$

EXAMPLE 8.7.2

The watershed in example 8.7.1 experienced a rainfall of 6 in. What is the runoff volume?

SOLUTION

Using equation (8.6.5), P_e = runoff volume is

$$P_e = \frac{(P - 0.2S)^2}{P + 0.8S}$$

where S is computed with the weighted curve number of 86 from example 8.7.1:

$$S = \frac{1000}{86} - 10 = 1.63$$

So

$$\begin{aligned}
 P_e &= \frac{[6 - 0.2(1.63)]^2}{6 + 0.8(1.63)} = \frac{32.19}{7.3} \\
 &= 4.41 \text{ in of runoff}
 \end{aligned}$$

EXAMPLE 8.7.3

For the watershed in examples 8.7.1 and 8.7.2, the 6-in rainfall pattern was 2 in the first hour, 3 in the second hour, and 1 in the third hour. Determine the cumulative rainfall and cumulative rainfall excess as functions of time.

SOLUTION

The initial abstractions are computed as $I_a = 0.2S$ with $S = 1.63$ from example 8.7.2, so $I_a = 0.2(1.63) = 0.33$ in. The remaining losses for time period (the first hour) are computed using the following equation, derived by combining equations (8.6.1) and (8.6.2):

$$\begin{aligned}
 F_{a,t} &= \frac{S(P_t - I_a)}{P_t - I_a + S} = \frac{1.63(P_t - 0.33)}{P_t - 0.33 + 1.63} = \frac{1.63(P_t - 0.33)}{P_t + 1.3} \\
 F_{a,1} &= \frac{1.63(2 - 0.33)}{2 + 1.3} = 0.82 \text{ in}
 \end{aligned}$$

The total loss for the first hour is $0.33 + 0.82 = 1.15$ in, and the excess is

$$P_{e1} = P_1 - I_a - F_{a,1} = 2 - 0.33 - 0.82 = 0.85 \text{ in}$$

For the second hour, $P_t = 2 + 3 = 5$ in, so

$$F_{a,2} = \frac{1.63(5 - 0.33)}{5 + 1.3} = 1.21 \text{ in}$$

and the cumulative rainfall excess is $P_e = 5 - 0.33 - 1.21 = 3.46$ in.

For the third hour, $P_3 = 2 + 3 + 1 = 6$ in, so

$$F_{a,3} = \frac{1.63(6 - 0.33)}{6 + 1.3} = 1.27 \text{ in}$$

and $P_e = 6 - 0.33 - 1.27 = 4.40$ in (which compares well with the results of example 8.7.2).

The results are summarized below, along with the rainfall excess hyetograph.

Time (h)	Cumulative rainfall P_t (in)	Cumulative abstractions		Cumulative rainfall excess P_e (in)	Rainfall excess hyetograph (in)
		I_a (in)	$F_{a,t}$ (in)		
1	2	0.33	0.82	0.85	0.85
2	5	0.33	1.21	3.46	2.61
3	6	0.33	1.27	4.40	0.94

8.8 NRCS (SCS) UNIT HYDROGRAPH PROCEDURE

The SCS dimensionless unit hydrograph and mass curve are shown in Figure 8.8.1 and tabulated in Table 8.8.1. The SCS dimensionless equivalent triangular unit hydrograph is also shown in Figure 8.8.1. The following section discusses how to develop a unit hydrograph from these dimensionless unit hydrographs.

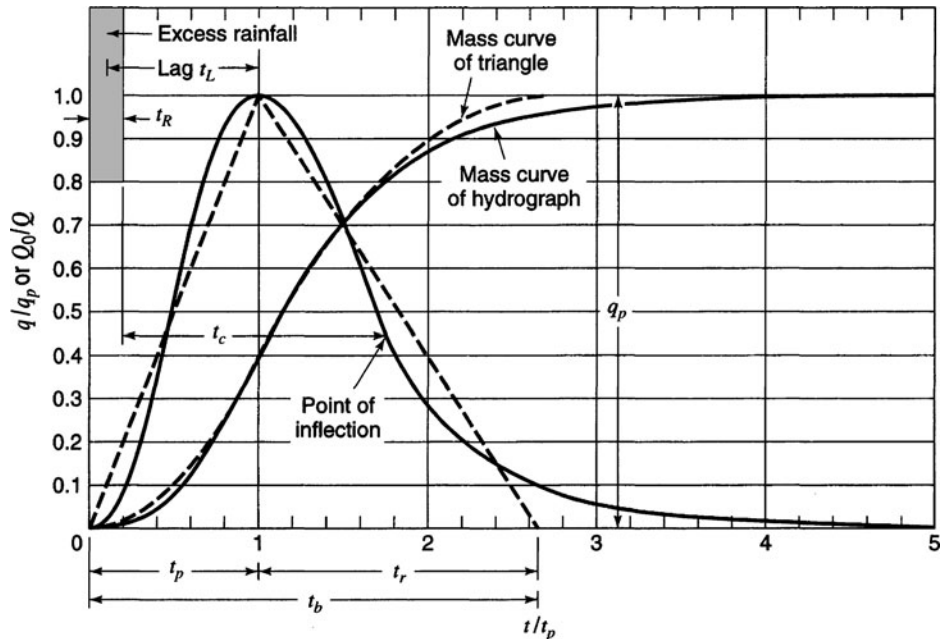


Figure 8.8.1 Dimensionless curvilinear unit hydrograph and equivalent triangular hydrograph (from U.S. Department of Agriculture Soil Conservation Service (1986)).

Table 8.8.1 Ratios for Dimensionless Unit Hydrograph and Mass Curve

Time ratios t/t_p	Discharge ratios q/q_p	Mass curve ratios Q_a/Q
0	0.000	0.000
0.1	0.030	0.001
0.2	0.100	0.006
0.3	0.190	0.012
0.4	0.310	0.035
0.5	0.470	0.065
0.6	0.660	0.107
0.7	0.820	0.163
0.8	0.930	0.228
0.9	0.990	0.300
1.0	1.000	0.375
1.1	0.990	0.450
1.2	0.930	0.522
1.3	0.860	0.589
1.4	0.780	0.650
1.5	0.680	0.700
1.6	0.560	0.751
1.7	0.460	0.790
1.8	0.390	0.822
1.9	0.330	0.849
2.0	0.280	0.871
2.2	0.207	0.908
2.4	0.147	0.934
2.6	0.107	0.953
2.8	0.077	0.967
3.0	0.055	0.977
3.2	0.040	0.984
3.4	0.029	0.989
3.6	0.021	0.993
3.8	0.015	0.995
4.0	0.011	0.997
4.5	0.005	0.999
5.0	0.000	1.000

Source: U.S. Department of Agriculture Soil Conservation Service (1972).

8.8.1 Time of Concentration

The *time of concentration* for a watershed is the time for a particle of water to travel from the hydrologically most distant point in the watershed to a point of interest, such as the outlet of the watershed. SCS has recommended two methods for time of concentration, the *lag method* and the *upland*, or *velocity method*.

The lag method relates the *time lag* (t_L), defined as the time in hours from the center of mass of the rainfall excess to the peak discharge, to the slope (Y) in percent, the hydraulic length (L) in feet, and the potential maximum retention (S), expressed as

$$t_L = \frac{L^{0.8}(S+1)^{0.7}}{1900Y^{0.5}} \quad (8.8.1)$$

The SCS uses the following relationship between the time of concentration (t_c) and the lag (t_L):

$$t_c = \frac{5}{3} t_L \tag{8.8.2}$$

or

$$t_c = \frac{L^{0.8}(S+1)^{0.7}}{1140V^{0.5}} \tag{8.8.3}$$

where t_c is in hours. Refer to Figure 8.8.1 to see the SCS definition of t_c and t_L .

The velocity (upland) method is based upon defining the time of concentration as the ratio of the hydraulic flow length (L) to the velocity (V):

$$t_c = \frac{L}{3600V} \tag{8.8.4}$$

where t_c is in hours, L is in feet, and V is in ft/s. The velocity can be estimated knowing the land use and the slope in Figure 8.8.2. Alternatively, we can think of the concentration as being the sum of

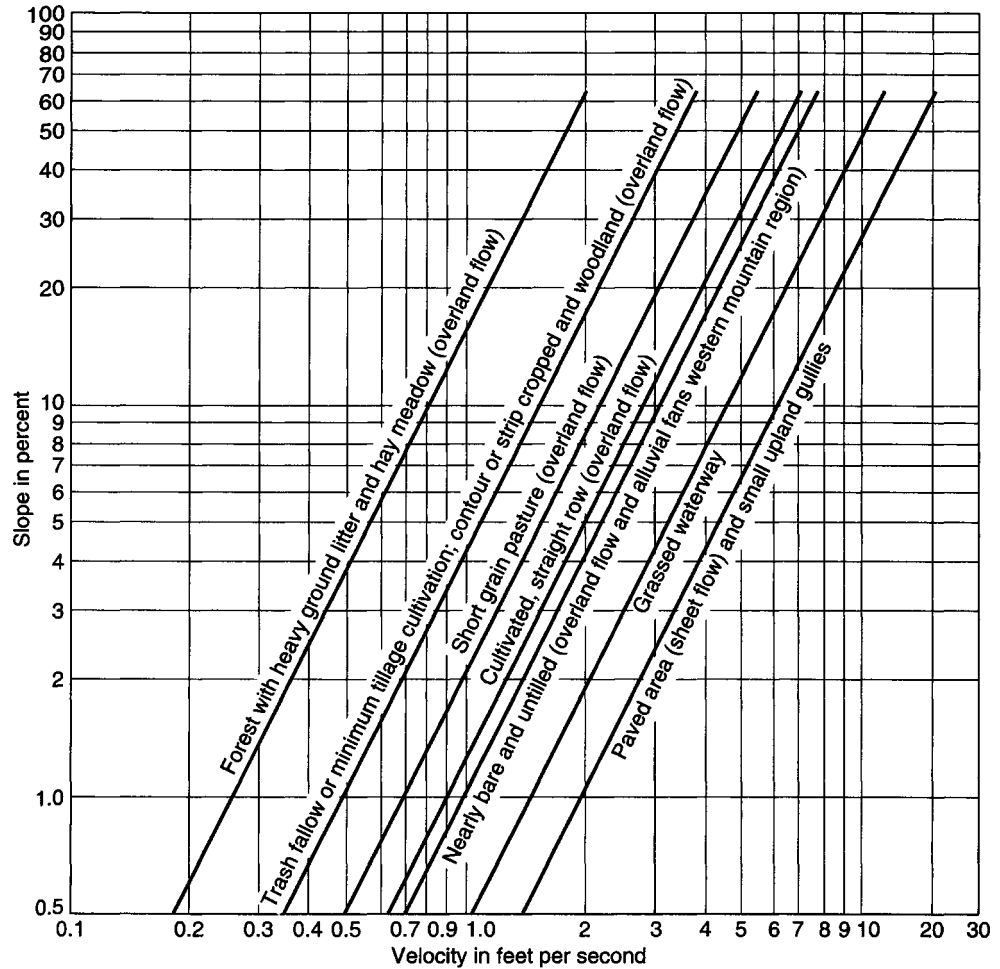


Figure 8.8.2 Velocities for velocity upland method of estimating t_c (from U.S. Department of Agriculture Soil Conservation Service (1986)).

travel times for different segments

$$t_c = \frac{1}{3600} \sum_{i=1}^k \frac{L_i}{V_i} \quad (8.8.5)$$

for k segments, each with different land uses.

8.8.2 Time to Peak

Time to peak (t_p) is the time from the beginning of rainfall to the time of the peak discharge (Figure 8.8.1)

$$t_p = \frac{t_R}{2} + t_L \quad (8.8.6)$$

where t_p is in hours, t_R is the duration of the rainfall excess in hours, and t_L is the lag time in hours. The SCS recommends that t_R be 0.133 of the time of concentration of the watershed, t_c :

$$t_R = 0.133t_c \quad (8.8.7)$$

and because $t_L = 0.6t_c$ by equation (8.8.2), then by equation (8.8.6) we get

$$\begin{aligned} t_p &= \frac{0.133t_c}{2} + 0.6t_c \\ t_p &= 0.67t_c \end{aligned} \quad (8.8.8)$$

8.8.3 Peak Discharge

The area of the unit hydrograph equals the volume of direct runoff Q , which was estimated by equation (8.6.5). With the equivalent triangular dimensionless unit hydrograph of the curvilinear dimensionless unit hydrograph in Figure 8.8.1, the time base of the dimensionless triangular unit hydrograph is 8/3 of the time to peak t_p , as compared to $5t_p$ for the curvilinear. The areas under the rising limb of the two dimensionless unit hydrographs are the same (37 percent).

Based upon geometry (Figure 8.8.1), we see that

$$Q = \frac{1}{2} q_p (t_p + t_r) \quad (8.8.9)$$

for the direct runoff Q , which is 1 in where t_r is the recession time of the dimensionless triangular unit hydrograph and q_p is the peak discharge. Solving equation (8.8.9) for q_p gives

$$q_p = \frac{Q}{t_p} \left[\frac{2}{1 + t_r/t_p} \right] \quad (8.8.10)$$

Letting $K = \left[\frac{2}{1 + t_r/t_p} \right]$, then

$$q_p = \frac{KQ}{t_p} \quad (8.8.11)$$

where Q is the volume, equals to 1 in for a unit hydrograph.

The above equation can be modified to express q_p in ft^3/sec , t_p in hours, and Q in inches:

$$q_p = 645.33K \frac{AQ}{t_p} \quad (8.8.12)$$

The factor 645.33 is the rate necessary to discharge 1 in of runoff from 1 mi² in 1 hr. Using $t_r = 1.67t_p$ gives $K = [2/(1 + 1.67)] = 0.75$; then equation (8.8.12) becomes

$$q_p = \frac{484AQ}{t_p} \quad (8.8.13)$$

For SI units,

$$q_p = \frac{2.08AQ}{t_p} \quad (8.8.14)$$

where A is in square kilometers.

The steps in developing a unit hydrograph are:

Step 1 Compute the time of concentration using the lag method (equation (8.8.3)) or the velocity method (equation (8.8.4) or (8.8.5)).

Step 2 Compute the time to peak $t_p = 0.67t_c$ (equation (8.8.8)) and then the peak discharge q_p using equation (8.8.13) or (8.8.14).

Step 3 Compute time base t_b and the recession time t_r :

Triangular hydrograph: $t_b = 2.67t_p$

Curvilinear hydrograph: $t_b = 5t_p$

$t_r = t_b - t_p$

Step 4 Compute the duration $t_R = 0.133 t_c$ and the lag $t_L = 0.6 t_c$ by using equations (8.8.7) and (8.8.2), respectively.

Step 5 Compute the unit hydrograph ordinates and plot. For the triangular only t_p , q_p , and t_r are needed. For the curvilinear, use the dimensionless ratios in Table 8.8.1.

EXAMPLE 8.8.1

For the watershed in example 8.7.1, determine the triangular SCS unit hydrograph. The average slope of the watershed is 3 percent and the area is 3.0 mi². The hydraulic length is 1.2 mi.

SOLUTION

Step 1 The time of concentration is computed using equation (8.8.1), with $S = 1.63$ from example 8.7.2:

$$t_L = \frac{(6336)^{0.8}(1.63 + 1)^{0.7}}{1900\sqrt{3}} = 0.66 \text{ hr}$$

and $t_c = \frac{5}{3}t_L = 1.1 \text{ hr}$

Step 2 The time to peak $t_p = 0.67t_c = 0.67(1.1) = 0.74 \text{ hr}$.

Step 3 The time base is $t_b = 2.67t_p = 1.97 \text{ hr}$.

Step 4 The duration is $t_R = 0.133t_c = 0.133(1.1) = 0.15 \text{ hr}$, and t_L is 0.66 hr.

Step 5 The peak is (for $Q = 1 \text{ in}$)

$$q_p = \frac{484AQ}{t_p} = \frac{484(3)(1)}{0.74} = 1962 \text{ cfs.}$$

In summary, the triangular unit hydrograph has a peak of 1962 cfs at the time to peak of 0.74 hr with a time base of 1.97 hr. This is a 0.15-hr duration unit hydrograph.

8.9 KINEMATIC-WAVE OVERLAND FLOW RUNOFF MODEL

Hortonian overland flow occurs when the rainfall rate exceeds the infiltration capacity and sufficient water ponds on the surface to overcome surface tension effects and fill small depressions. Overland flow is surface runoff that occurs in the form of sheet flow on the land surface without concentrating

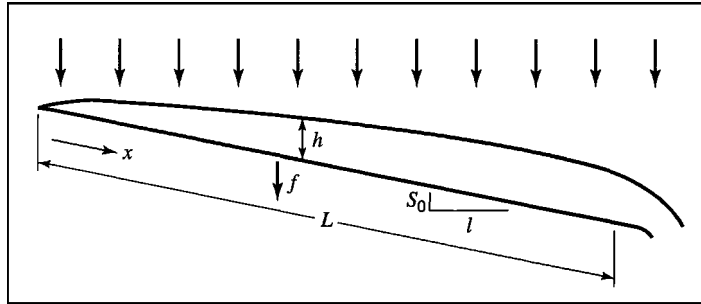


Figure 8.9.1 Definition sketch of overland flow on a plane as a one-dimensional flow (from Woolhiser et al. (1990)).

in clearly defined channels (Ponce, 1989). For the purposes of rainfall-runoff analysis, this flow can be viewed as a one-dimensional flow process (Figure 8.9.1) in which the flux is proportional to some power of the storage per unit area, expressed as (Woolhiser et al., 1990):

$$Q = \alpha h^m \quad (8.9.1)$$

where Q is the discharge per unit width, h is the storage of water per unit area (or depth if the surface is a plane), and α and m are parameters related to slope, surface roughness, and whether the flow is laminar or turbulent.

The mathematical description of overland flow can be accomplished through the continuity equation in one-dimensional form and a simplified form of the momentum equation. This model is referred to as the *kinematic wave model*. *Kinematics* refers to the study of motion exclusive of the influence of mass and force. A *wave* is a variation in flow, such as a change in flow rate or water surface elevation. *Wave celerity* is the velocity with which this variation travels. *Kinematic waves* govern flow when inertial and pressure forces are negligible.

The *kinematic wave equations* (also see Chapter 9) for a one-dimensional flow are expressed as follows:

Continuity:

$$\frac{\partial A}{\partial t} + \frac{\partial Q}{\partial x} = q(x, t) \quad (8.9.2)$$

Momentum:

$$S_0 - S_f = 0 \quad (8.9.3)$$

where A is the cross-sectional area of flow, Q is the discharge, t is time, x is the spatial coordinate, $q(x, t)$ is the lateral inflow rate, S_0 is the overland flow slope, and S_f is the friction slope.

Equation (8.9.3) indicates that the gravity and friction forces are balanced, so that flow does not accelerate appreciably. The inertial (local and convective acceleration) term and pressure term are neglected in the kinematic wave model (refer to Section 9.4). Eliminating these terms eliminates the mechanism to describe backwater effects and flood wave peak attenuation.

Considering that h is the storage per unit area or depth, then $A = h$, so that equation (8.9.2) becomes

$$\frac{\partial h}{\partial t} + \frac{\partial Q}{\partial x} = q(x, t) \quad (8.9.4)$$

Substituting equation (8.9.1) into (8.9.4) gives

$$\frac{\partial h}{\partial t} + \frac{\partial(\alpha h^m)}{\partial x} = q(x, t) \quad (8.9.5)$$

The one-dimensional overland flow on a plane surface (illustrated in Figure 8.9.1) is not the type of flow found in most watershed situations (Woolhiser et al., 1990). The kinematic assumption does not require sheet flow as shown; it requires only that the discharge be some unique function of the amount of water stored per unit of area.

Woolhiser and Liggett (1967) and Morris and Woolhiser (1980) showed that the kinematic-wave formulation is an excellent approximation for most overland flow conditions. Keep in mind that these equations are a simplification of the Saint-Venant equations (see Chapter 9).

The kinematic-wave equation (8.9.5) for overland flow can be solved numerically using a four-point implicit method where the finite-difference approximations for the spatial and temporal derivatives are, respectively,

$$\frac{\partial h}{\partial x} = \theta \frac{h_{i+1}^{j+1} - h_i^{j+1}}{\Delta x} + (1 - \theta) \frac{h_{i+1}^j - h_i^j}{\Delta x} \quad (8.9.6)$$

and

$$\frac{\partial h}{\partial t} = \frac{1}{2} \left[\frac{h_i^{j+1} - h_i^j}{\Delta t} + \frac{h_{i+1}^{j+1} - h_{i+1}^j}{\Delta t} \right]$$

or

$$\frac{\partial h}{\partial t} = \frac{h_i^{j+1} + h_{i+1}^{j+1} - h_i^j - h_{i+1}^j}{2\Delta t} \quad (8.9.7)$$

and

$$q = \frac{1}{2} (\bar{q}_{i+1} + \bar{q}_i) \quad (8.9.8)$$

where θ is a weighting parameter for spatial derivative, $\theta = \Delta' t / \Delta t$ (see Figure 8.9.2). The derivative $\partial h / \partial t$ is the average of the temporal derivatives at locations i and $i + 1$ or for the midway locations between i and $i + 1$, and \bar{q}_i and \bar{q}_{i+1} are the average lateral inflows at i and $i + 1$, respectively. Notation for the finite-difference grid is shown in Figure 8.9.2. Substituting these finite difference expressions (8.9.6), (8.9.7), and (8.9.8) into (8.9.5) and simplifying results in the following finite-difference equation:

$$\begin{aligned} & h_{i+1}^{j+1} - h_{i+1}^j + h_i^{j+1} - h_i^j \\ & + \frac{2\Delta t}{\Delta x} \left\{ \theta \left[\alpha_{i+1}^{j+1} (h_{i+1}^{j+1})^m - \alpha_i^{j+1} (h_i^{j+1})^m \right] + (1 - \theta) \left[\alpha_{i+1}^j (h_{i+1}^j)^m - \alpha_i^j (h_i^j)^m \right] \right\} \\ & - \Delta t (\bar{q}_{i+1} + \bar{q}_i) = 0 \end{aligned} \quad (8.9.9)$$

The only unknown in the above equation is h_{i+1}^{j+1} , which must be solved by using Newton's method (see Appendix A). Using Manning's equation to express equation (8.9.1), $Q = \alpha h^m$, we

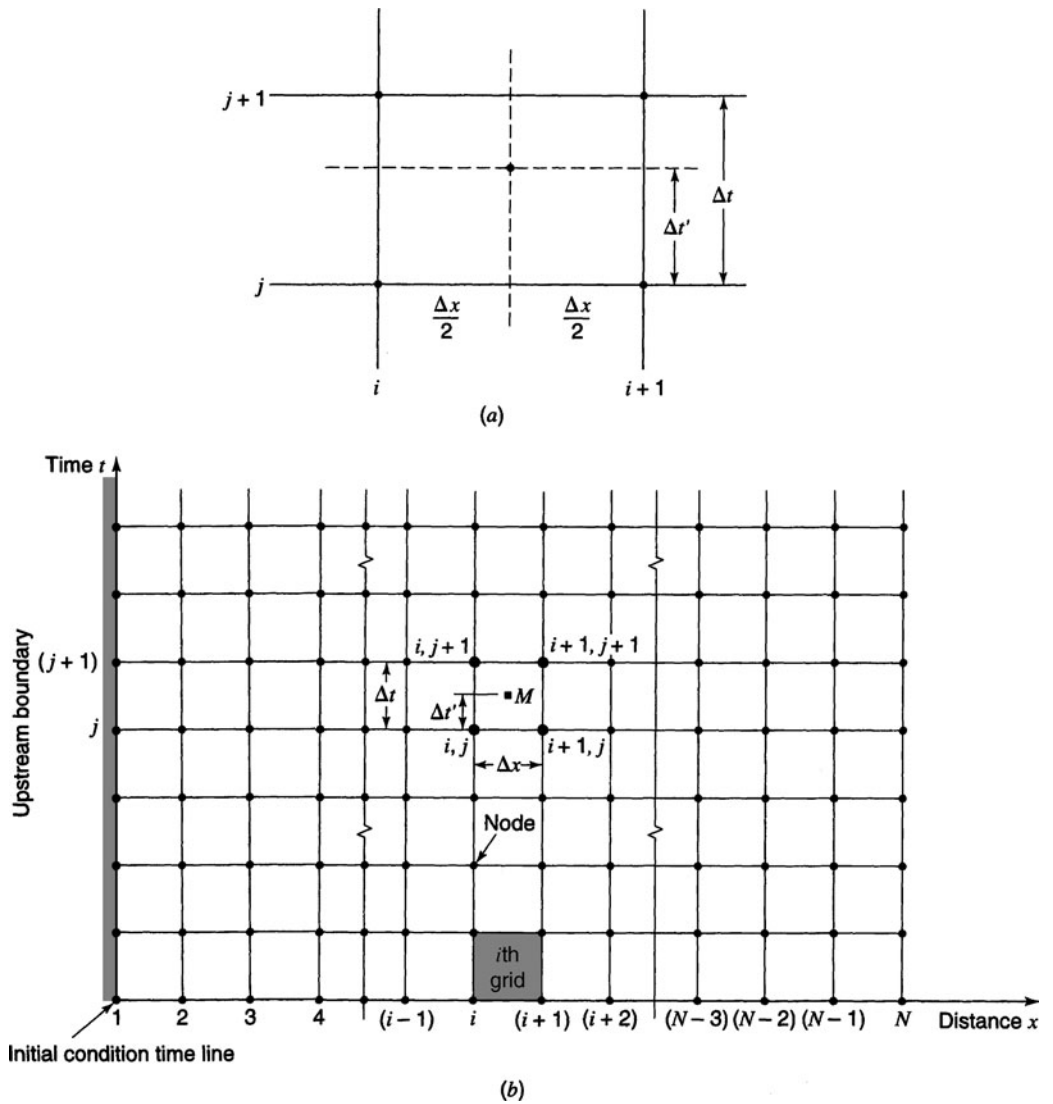


Figure 8.9.2 The $x-t$ solution plane: The finite-difference forms of the Saint-Venant equations are solved at a discrete number of points (values of the independent variables x and t) arranged to the time axis represent locations along the plane, and those parallel to the distance axis represent times. (a) Four points of finite-difference grid; (b) Finite difference grid.

find

$$Q = \left[\frac{1.49S_0^{1/2}}{n} \right] h^{5/3} \tag{8.9.10}$$

where

$$\alpha = \frac{1.49S_0^{1/2}}{n}, m = 5/3 \tag{8.9.11}$$

Table 8.9.1 Recommended Manning's Roughness Coefficients for Overland Flow

Cover or treatment	Residue rate, Tons/Acre	Value recommended	Range
Concrete or asphalt		0.011	0.010–0.013
Bare sand		0.01	0.010–0.016
Graveled surface		0.02	0.012–0.03
Bare clay loam (eroded)		0.02	0.012–0.033
Fallow, no residue		0.05	0.006–0.16
Chisel plow	<1/4	0.07	0.006–0.17
	<1/4–1	0.18	0.07–0.34
	1–3	0.30	0.19–0.47
	>3	0.40	0.34–0.46
Disk/harrow	<1/4	0.08	0.008–0.41
	1/4–1	0.16	0.10–0.25
	1–3	0.25	0.14–0.53
	>3	0.30	—
No till	<1/4	0.04	0.03–0.07
	1/4–1	0.07	0.01–0.13
	1–3	0.30	0.16–0.47
Moldboard plow (fall)		0.06	0.02–0.10
Colter		0.10	0.05–0.13
Range (natural)		0.13	0.01–0.32
Range (clipped)		0.10	0.02–0.24
Grass (bluegrass sod)		0.45	0.39–0.63
Short grass prairie		0.15	0.10–0.20
Dense grass ¹		0.24	0.17–0.30
Bermuda grass ¹		0.41	0.30–0.48

¹Weeping lovegrass, bluegrass, buffalo grass, blue gamma grass, native grass mix (OK), alfalfa, lespedeza (from Palmer, 1946).

Sources: Woolhiser (1975), Engman (1986), Woolhiser et al. (1990).

where n is Manning's roughness coefficient and S_0 is the slope of the overland flow plane. Recommended values of Manning's roughness coefficients for overland flow are given in Table 8.9.1. The *time to equilibrium* of a plane of length L and slope S_0 can be derived using Manning's equation as

$$t_c = \frac{nL}{1.49S_0^{1/2}h^{2/3}} \quad (8.9.12)$$

The U.S. Department of Agriculture Agricultural Research Service (Woolhiser et al., 1990) has developed a KINematic runoff and EROSION model referred to as KINEROS. This model is event-oriented, i.e., it is a physically based model describing the processes of interception, infiltration, surface runoff, and erosion from small agricultural and urban watersheds. The model is distributed because flows are modeled for both the watershed and the channel elements, as illustrated in Figures 8.9.3 and 8.9.4. The model is *event-oriented* because it does not have components describing evapotranspiration and soil water movement between storms. In other words, there is no hydrologic balance between storms.

Figures 8.9.3 and 8.9.4 illustrate that the approach to describing a watershed is to divide it into a branching system of channels with plane elements contributing lateral flow to channels. The

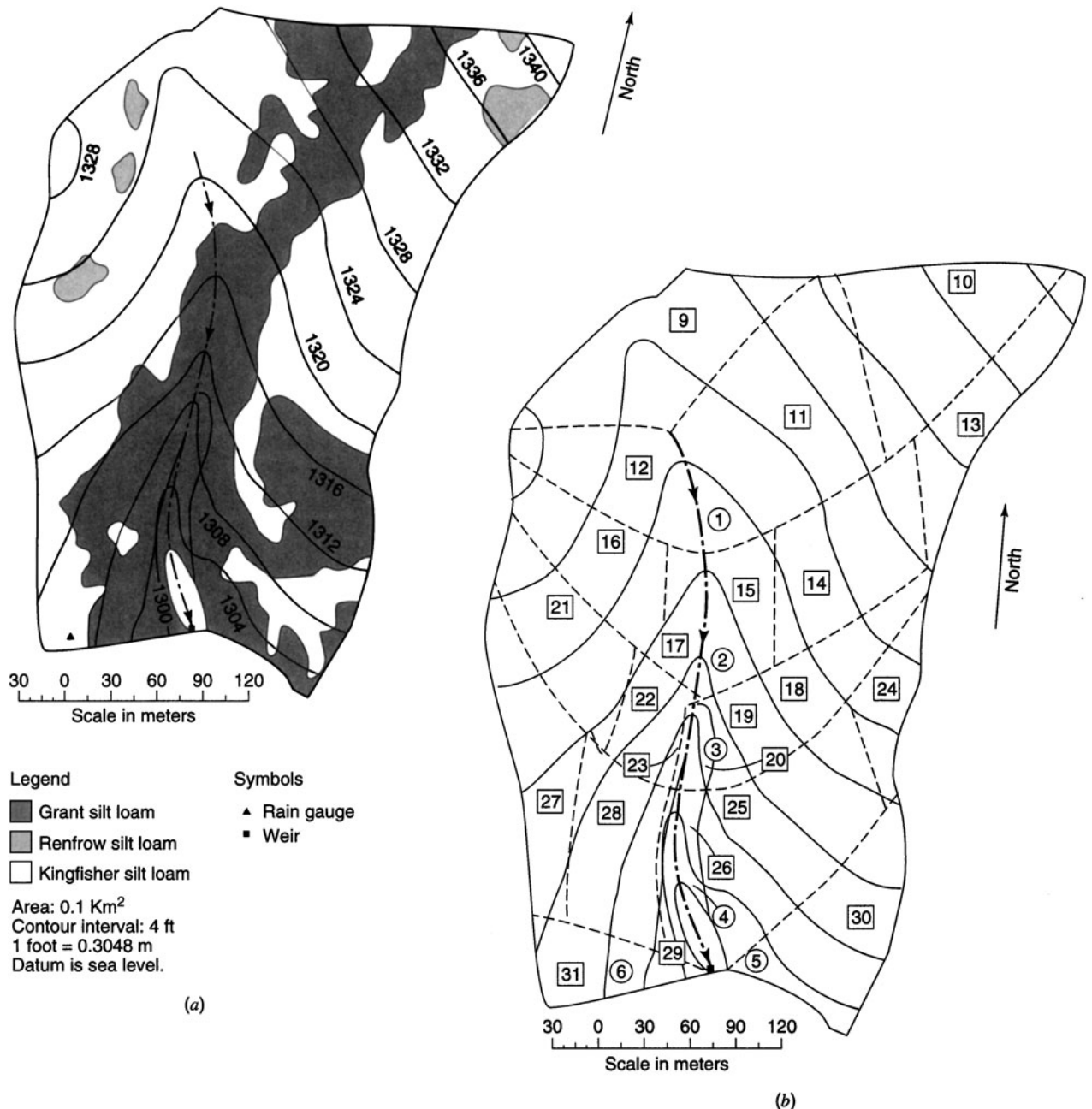


Figure 8.9.3 R-5 catchment, Chickasha, OK. (a) Contour map; (b) Division into plane and channel elements (from Woolhiser et al. (1990)).

KINEROS model takes into account interception, infiltration, overland flow routing, channel routing, reservoir routing, erosion, and sediment transport. Overland flow routing has been described in this section. Channel routing is performed using the kinematic-wave approximation described in Chapter 9. The reservoir routing in KINEROS is basically a level-pool routing procedure, as described in Chapter 9.

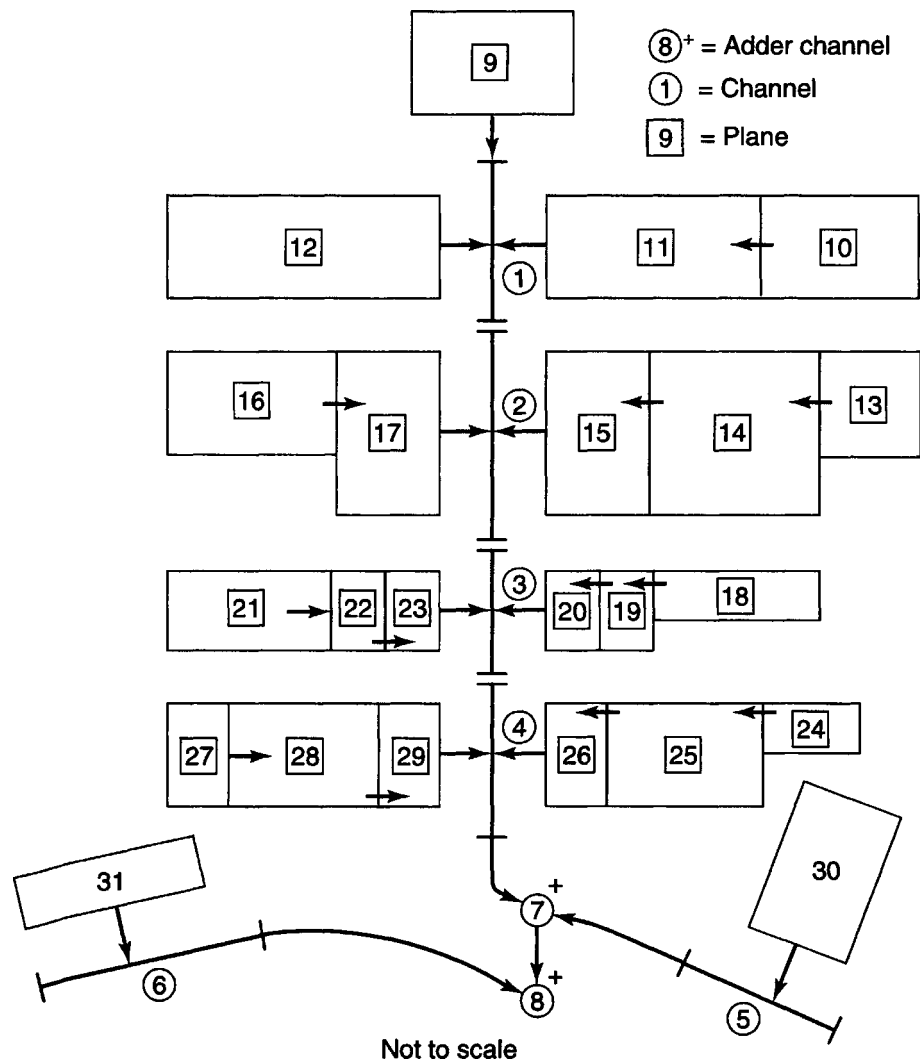


Figure 8.9.4 Schematic of R-5 plane and channel configuration (from Woolhiser et al. (1990)).

8.10 COMPUTER MODELS FOR RAINFALL-RUNOFF ANALYSIS

Computer models for runoff analysis can be classified as event-based models or continuous simulation models. *Event-based models* are used to simulate the discrete rainfall-runoff events using, for example, the unit hydrograph approach. These models emphasize infiltration and surface-runoff components with the objective of determining direct runoff, and are applicable to excess-water flow calculations in cases where direct runoff is the major contributor to streamflow. The HEC-HMS (HEC-1) and the TR-20 and TR-55 models are single-event models. The KINEROS model (Woolhiser et al., 1990) described in the previous section is an overland flow model based on the kinematic-wave routing. This model is a *distributed event-based model*. Other examples include the kinematic-wave model for overland flow routing in the HEC-HMS (HEC-1) model.

Continuous-simulation models account for the overall moisture balance of the basin, including moisture accounting between storm events. These models explicitly account for all runoff components including surface flow and indirect runoff such as interflow and baseflow, and are well suited for *long-term runoff forecasting*.

PROBLEMS

8.1.1 Suppose that the runoff peak discharge (Q_p) from an urban watershed is related to rainfall intensity (I) and drainage area (A) in the following form, $Q_p = a \times I^b \times A^b$, in which a and b are unknown parameters to be determined from the data given in the following table.

Q_p (ft ³ /sec)	23	45	68	62
I (in/hr)	3.2	4.6	6.1	7.4
A (acres)	12	21	24	16

- (a) Use the least-squares method to determine the values of unknown parameters a and b .
- (b) Assess how good the resulting equation is.
- (c) Estimate the expected peak discharge for watershed with an area of 20 acres resulting from a 4-in/hr rain.

8.1.2 The following data were obtained to study the relationship between peak discharge (Q_p) of a watershed with drainage area (A) and average rainfall intensity (I).

Peak discharge (Q_p in ft ³ /sec)	23	45	44	64	68
Rainfall intensity (I in in/hr)	3.2	4.2	5.1	3.8	6.1
Drainage area (A in acres)	12	21	18	32	24

Suppose that the relationship between Q_p , I , and A can be expressed as $Q_p = I^a \times A^b$ in which a and b are constants.

- (a) Determine the values of the two constants, i.e., a and b , by the least-squares method.
- (b) How good is the least-squares fit?
- (c) Based on the result in part (a), estimate the peak discharge per unit area for a watershed with basin area of 15 acres under a storm with rainfall depth of 15 in in 3 hr.

8.1.3 The following table contains measurements of peak discharge, average rainfall intensity, and drainage area.

Data	Peak discharge Q (m ³ /s)	Rainfall intensity I (mm/hr)	Drainage area A (km ²)
1	0.651	81.3	0.0486
2	1.246	129.5	0.0728
3	1.812	96.5	0.1295
4	1.926	154.9	0.0971

- (a) Determine the coefficients a and b in the equation $Q = a \times (I \times A)^b$ using the least-squares method.
- (b) Determine the corresponding coefficient of determination and standard error of estimate for part (a).
- (c) Physically, when a storm with constant rainfall intensity I continues indefinitely, the term $I \times A$ represents the steady-state peak discharge. Under the steady-state condition, let $b = 1$ in the above equation. Determine the least-squares estimate for the constant a and the corresponding coefficient of determination.

How do you interpret the meaning of constant a ? Does your estimated value of a make sense from the physical viewpoint? Please explain.

8.1.4 For a particular watershed, the observed runoff volume and the corresponding peak discharges, Q_p , are shown below.

Q_p (m ³ /s)	0.42	0.12	0.58	0.28	0.66
Runoff (cm)	1.28	0.40	2.29	1.42	3.19

- (a) Determine the coefficients (a and b) in the equation $QP = a \times RO^b$ using the least-squares method where Q_p = peak discharge, RO = runoff volume, and a , b = coefficients.
- (b) Estimate the peak discharge for the runoff volume of 4 cm.

8.2.1 Consider a 10-km² catchment receiving rainfall with intensity that varies from 0 to 30 mm/hr in a linear fashion for the first 6 hr. Then, rainfall intensity stays constant at 30 mm/hr over the next 6 hr before it stops. During the rainfall period of 12 hr, the rate of surface runoff from the catchment increases linearly from 0 at $t = 0$ hr to 30 mm/hr at $t = 12$ hr.

- (a) Assume that hydrologic losses, such as infiltration, evaporation, etc. are negligible in the catchment. Determine the time when the surface runoff ends, if surface runoff decreases linearly to zero from 30 mm/hr at $t = 12$ hr.
- (b) At what time does the total storage in the catchment reach its maximum and what is the corresponding storage (in km³)?
- (c) Identify the times at which the rate of increase and decrease in storage are the largest.

8.2.2 The following table contains the records of rainfall and surface runoff data from a catchment with the drainage area of 2.25 km². Column (2) is the rainfall hyetograph for the averaged intensity whereas column (3) is the runoff hydrograph for instantaneous flow rate.

Time	Avg. intensity (mm/h)	Instantaneous discharge (m ³ /s)
1:00		0
1:10	60	12
1:20	150	24
1:30	30	48
1:40	18	30
1:50	60	18
2:00	72	24
2:10	24	30
2:20	12	18
2:30		12
2:40		6
2:50		0

- (a) Determine the rolling-time and clock-time maximum rainfall depth (in mm) for durations of 30 min and 50 min.
- (b) Determine the time and the corresponding volume (in m³) when the maximum storage occurs. Assume that the initial storage volume is zero.
- (c) Determine the percentage of rainfall volume that becomes the surface runoff.

8.2.3 Based on the table given below showing the hydrograph ordinates at 24-hour intervals, use graph paper to (a) identify the time instant at which the direct runoff ends and (b) determine the recession constant, *k*, in the following equation:

$$Q(t_2) = Q(t_1) \times e^{-k(t_2 - t_1)}$$

in which $t_2 > t_1$ are two time points on the baseflow recession of a hydrograph.

Time (day)	Flow (m ³ /s)	Time (day)	Flow (m ³ /s)
1	6	8	91
2	970	9	79
3	707	10	68
4	400	11	58
5	254	12	50
6	162	13	43
7	121	14	37

8.2.4 The following table contains the records of rainfall and surface runoff data of a particular storm event for a watershed with the drainage area of 8.4 km².

- (a) Determine the maximum rainfall intensity for durations of 30 min, 60 min, and 120 min.
- (b) Determine the percentage of total rainfall that is lost from appearing as the surface runoff.
- (c) Determine the time period that the storage volume of the water is increasing in the watershed.

Time of day	Cumulative rainfall (mm)	Instantaneous runoff (m ³ /s)
4:00	0	0.0
4:30	30	0.3
5:00	80	4.2
5:30	90	11.3
6:00	95	13.0
6:30	127	34.0
7:00	130	45.3
7:30	132	21.2
8:00		9.3
8:30		4.8
9:00		2.5
9:30		1.4
10:00		0.8
10:30		0.0

8.2.5 The following table contains the records of rainfall and surface runoff data of a storm event for a watershed having the drainage area of 8.0 km².

- (a) Determine the maximum rainfall intensity for durations of 15 min, 30 min, and 60 min.
- (b) Determine the percentage of total rainfall that is lost from appearing as the surface runoff.
- (c) Determine the time period that the storage volume of the water is increasing in the watershed and the maximum storage volume (in cm).
- (d) Determine the Φ index and the corresponding rainfall excess hyetograph.

Time	Cumul. rainfall (mm)	Instant. flow rate (m ³ /s)
4:00	0	0
4:15	15	1
4:30	40	4
4:45	45	11
5:00	48	13
5:15	64	35
5:30	65	45
5:45	66	21
6:00	66	10
6:15	66	5
6:30		3
6:45		1
7:00		0

8.2.6 Consider a watershed with drainage area of 1 km². For a given storm event, the recorded average rainfall intensity and total instantaneous discharge at the outlet of the watershed are listed in the following table. Assume that the baseflow is 1 m³/s and rainfall amount in the first 30 min is the initial loss.

- (a) Determine the total amount of rainfall.
- (b) Determine the volume of direct runoff.
- (c) Determine the average infiltration rate, i.e., ϕ index
- (d) Determine the rainfall excess intensity hyetograph corresponding to the ϕ index obtained in (c). Also, what is the duration of rainfall excess hyetograph?

Time (min)	Intensity (mm/h)	Discharge (m ³ /s)
0	10	1
30	20	1
60	38	4
90	26	8
120	10	6
150	20	4
180	24	3
210		1

8.2.7 On a particular day in 1990, there was a rainstorm event that produced the following rainfall and runoff on a 36-km² drainage basin.

Time (min)	0	15	30	45	60	75	90	105	120
Cumulative rainfall (mm)	0	10	50	75	90	100			
Instantaneous runoff (m ³ /s)	10	30	160	360	405	305	125	35	10

For the above rainstorm event, assume that the baseflow is 10 m³/s.

- (a) Find the volume of direct runoff (in mm).
- (b) Assuming the initial loss is 10 mm, determine the value of ϕ index (in mm/hr) and the corresponding effective rainfall intensity hyetograph (in mm/hr).

8.3.1 Determine the 4-hr unit hydrograph using the following data for a watershed having a drainage area of 200 km², assuming a constant rainfall abstraction rate and a constant baseflow of 20 m³/s.

Four-hour period	1	2	3	4	5	6	7	8	9	10	11
Rainfall (cm)	1.0	2.5	4.0	2.0							
Storm flow (m ³ /s)	20	30	60	95	130	170	195	175	70	25	20

8.3.2 Using the unit hydrograph developed in problem 8.3.1, determine the direct runoff from the 200 km² watershed using the following rainfall excess pattern.

Four-hour period		1	2	3	4
Rainfall excess (cm)		2.0	3.0	0.0	1.5

8.3.3 The ordinates at 1-hr intervals of a 1-hr unit hydrograph are 100, 300, 500, 700, 400, 200, and 100 cfs. Determine the direct runoff hydrograph from a 3-hr storm in which 1 in of excess rainfall occurred in the first hour, 2 in the second hour, and 0.5 in the third hour. What is the area of the watershed in mi²?

8.3.4 You are responsible for developing the runoff hydrograph for a watershed that fortunately has gauged information at a very nearby location on the stream. You have obtained information on an actual rainfall-runoff event for this watershed. This information includes the actual rainfall hyetograph and the resulting runoff hydrograph. You have been asked to develop the runoff hydrograph for a design rainfall event. The peak discharge from this new developed storm hydrograph will be used to design a hydraulic structure. You will assume a constant baseflow and a constant rainfall abstraction. Explain the hydrologic analysis procedure that you will use to solve this problem.

8.3.5 Consider a drainage basin with an area of 226.8 km². From a storm event, the observed cumulative rainfall depth and the corresponding runoff hydrograph are given in the following table. Assume that the baseflow is 10 m³/s.

Time (hr)	0	3	6	9	12	15	18	21	24	27	30	33	36
Cumulative rainfall (cm)	0.0	0.5	1.5	2.5	4.5	6.5	8.0	9.5					
Discharge (m ³ /s)	10	10	30	50	130	175	260	240	220	145	70	40	10

- (a) Determine the value of the ϕ index and the corresponding effective rainfall hyetograph.
- (b) Set up the system of equations, $Pu = Q$, and solve for the unit hydrograph.

8.3.6 Suppose the 4-hr unit hydrograph for a watershed is

Time (hr)	0	2	4	6	8	10	12
UH (m ³ /s/cm)	0	20	50	75	90	40	0

- (a) Determine the 2-hr unit hydrograph.
- (b) Suppose that a 10-year design storm has a total effective rainfall of 50 mm and the corresponding hyetograph has a rainfall of 30 mm in the first 2 hr period, no rain in the second period, and 20 mm in the third period. Assuming the baseflow is 10 m³/s, calculate the total runoff hydrograph from this 10-year design storm.

8.3.7 Consider a drainage basin with an area of 151.2 km². From a storm event, the observed cumulative rainfall depth and the corresponding runoff hydrograph are given in the following table. Assume that the baseflow is 10 m³/s.

Time (hr)	0	2	4	6	10	12	14	16	18	20	22	24	26
Cumulative rainfall (cm)	0.0	0.5	1.5	2.5	4.5	6.5	8.0	9.5					
Instantaneous discharge (m ³ /s)	10	10	30	50	130	175	260	240	220	145	70	40	10

- (a) Determine the value of the ϕ index and the corresponding effective rainfall hyetograph.
- (b) Set up the system of equations, $Pu = Q$, for deriving the 6-hr unit hydrograph and define the elements in P , u , and Q . Solve for the unit hydrograph.

8.3.8 Suppose the 30-min unit hydrograph for a watershed is

Time (hr)	0	3	6	9	12	15	18	21
UH (m ³ /s/cm)	0	15	45	65	50	25	10	0

- (a) Determine the 1-hr unit hydrograph.
- (b) A storm has a total depth of 4 cm with an effective rainfall hyetograph of 2 cm in the first 2 hr, 1 cm in the second 2 hr. Assuming the baseflow is 10 m³/s, calculate the total runoff hydrograph from the storm.

8.3.9 The following table lists a 15-min unit hydrograph.

Time (min)	0	5	10	15	20	25	30	35	40	45
15 min UH (m ³ /s/cm)	0.0	1.5	3.5	6.0	5.5	5.0	3.0	2.0	0.5	0.0

- (a) Determine the corresponding area of the drainage basin.
- (b) Determine the 10-min unit hydrograph.
- (c) Determine the total runoff hydrograph resulting from the following effective rainfall, assuming the base flow is 2 m³/s.

Time (min)	0	10	20	30
Cumul. rainfall excess (mm)	0	10	30	35

8.3.10 Consider there are two rain gauges (A and B) in a watershed with an area of 21.6 km². The cumulative rainfall depths over time for a particular storm event at both rain gauge stations are given in the table below. The storm also produces a runoff hydrograph at the outlet of the watershed, shown in the last row of the table. Assume that the baseflow is 10 m³/s. It is known, by the Thiessen polygon, that the contributing areas for the rain gauges are identical.

Time (hr)	0	1	2	3	4	5	6	7	8	9	10
Cumul. Rainfall at Station A (mm)	0	25	80	105	100	140	180	230	230		
Cumul. rainfall at Station B (mm)	0	15	40	85	130	180	210	230	230		
Instantaneous discharge (m ³ /s)	10	10	30	60	30	40	80	40	30	10	10

- (a) Determine the basin-wide representative rainfall hyetograph (in mm/hr) for the storm event. Furthermore, determine the value of ϕ index (in mm/hr) and the corresponding effective rainfall hyetograph (in mm/hr).
- (b) Set up the system of equations $Pu = Q$.
- (c) Solve part (b) by the least-squares method for the unit hydrograph. What is the duration of the unit hydrograph obtained?

8.3.11 Consider a drainage basin with an area of 167.95 km². From a storm event, the observed cumulative rainfall depth and the corresponding runoff hydrograph are given in the following table. Assume that the baseflow is 10 m³/s.

Time (hr)	0	2	4	6	8	10	12	14	16	18	20	22	24
Cumulative rainfall (cm)	0.0	0.5	1.5	2.5	4.5	6.5	8.0	9.5					
Instantaneous discharge (m ³ /s)	10	10	30	50	130	175	260	240	220	145	70	40	10

- (a) Determine the value of the ϕ index and the corresponding effective rainfall hyetograph.
- (b) Set up the system of equations, $Pu = Q$, for deriving the 4-hr unit hydrograph and define the elements in P , u , and Q .
- (c) Solve for the unit hydrograph ordinates.

8.3.12 Consider a drainage basin with an area of 216 km². From a storm event, the observed cumulative rainfall depth and the corresponding runoff hydrograph are given in the following table. Assume that the baseflow is 20 m³/s.

Time (hr)	0	6	12	18	24	30
Cumulative rainfall (cm)	0.0	1.5	4.5	9.5		
Discharge (m ³ /s)	20	50	160	340	180	20

- (a) Determine the value of the ϕ index and the corresponding effective rainfall hyetograph.
- (b) Determine the 6-hr unit hydrograph by the least-squares method.

8.3.13 On a particular date, the measured rainfall and runoff from a drainage basin of 54 ha (54×10^4 m²) are listed in the table below.

- (a) Assuming that the base flow is 2 m³/s, determine the effective rainfall hyetograph by the ϕ index method.
- (b) Based on the effective rainfall hyetograph and direct runoff hydrograph obtained in Part (a), use the least-squares method to determine the 15-min unit hydrograph.

Time (min)	0	15	30	45	60	75
Cumul. rain (mm)	0	5	20	40	50	
Instant. flow (m ³ /s)	2	6	10	7	3	2

8.3.14 You have been given information on an actual rainfall-runoff event and asked to develop the runoff hydrograph for another storm hydrograph for the watershed. The following is known:

Time (hr)	Rainfall (in)	Discharge (cfs)
0		10
1	1.1	20
2	2.1	130
3	0	410
4	1.1	570
5		510
6		460
7		260
8		110
9		60
10		10

A constant base flow of 10 cfs and a uniform rainfall loss of 0.1 in/hr are applicable. Determine the size of the drainage basin. Then determine the direct runoff hydrograph for a 2.0-in excess precipitation for the first hour, no rainfall for the second hour, followed by a 2.0-in excess precipitation for the third hour.

8.4.1 A watershed has a drainage area of 14 km²; the length of the main stream is 7.16 km, and the main channel length from the watershed outlet to the point opposite the center of gravity of the watershed is 3.22 km. Use $C_t = 2.0$ and $C_p = 0.625$ to determine the standard synthetic unit hydrograph for the watershed. What is the standard duration? Use Snyder's method to determine the 30-min unit hydrograph for the watershed.

8.4.2 Watershed A has a 2-hr unit hydrograph with $Q_{pR} = 276$ m³/s, $I_{pR} = 6$ hr, $W_{50} = 4.0$ hr, and $W_{75} = 2$ hr. The watershed area = 259 km², $L_c = 16.1$ km, and $L = 38.6$ km. Watershed B is assumed to be hydrologically similar with an area of 181 km², $L = 25.1$ km, and $L_c = 15.1$ km. Determine the 1-hr synthetic unit hydrograph for watershed B. Determine the direct runoff hydrograph for a 2-hr storm that has 1.5 cm of excess rainfall the first hour and 2.5 cm of excess rainfall the second hour.

8.4.3 A watershed has an area of 39.3 mi² and a main channel length of 18.1 mi, and the main channel length from the watershed outlet to the point opposite the centroid of the watershed is 6.0 mi. The regional parameters are $C_t = 2.0$ and $C_p = 0.6$. Compute the T_p , Q_p , W_{50} , W_{75} , and T_B for Snyder's standard synthetic unit hydrograph and the same information for a 3-hr Snyder's synthetic unit hydrograph. Also, what is the duration of the standard synthetic unit hydrograph?

8.4.4 Compute the 3-hr Snyder's synthetic unit hydrograph for the watershed in problem 8.4.3.

8.4.5 You are performing a hydrologic study (rainfall-runoff analysis) for a watershed Z. Unfortunately, there is no gauged data or other hydrologic studies so you do not have a unit hydrograph. However, you do have data for another nearby watershed, known as watershed X, which has gauged information (including the discharge hydrograph for a known rainfall event). What procedure would you use to develop a design runoff hydrograph for a design storm for watershed Z? What are you assuming about the watersheds in this procedure?

8.4.6 You have determined the following from the basin map of a given watershed: $L = 100$ km, $L_c = 50$ km, and drainage area = 2000 km². From the unit hydrograph developed for the watershed, the following were determined: $t_R = 6$ hr, $t_{pR} = 15$ hr, and the peak discharge = 80 km³/s/cm. Determine the regional parameters used in the Snyder's synthetic unit hydrograph procedure.

8.4.7 Derive a 3-hr unit hydrograph by the Snyder method for a watershed of 54 km² area. It has a main stream that is 10-km long. The distance measured from the watershed outlet to a point on the stream nearest to the centroid of the watershed is 3.75 km. Take $C_t = 2.0$ and $C_p = 0.65$. Sketch the 3-hr unit hydrograph for the watershed.

8.4.8 Derive a 2-hr unit hydrograph by the Snyder method for a watershed of 50 km² area. It has a main stream that is 8 km long. The distance measured from the watershed outlet to a point on the stream nearest to the centroid of the watershed is 4 km. Take $C_t = 2.0$ and $C_p = 0.65$. Graph the 2-hr unit hydrograph for the watershed.

8.4.9 Use the Clark unit hydrograph procedure to compute the 1-hr unit hydrograph for a watershed that has an area of 5.0 km² and a time of concentration of 5.5 hr. The Clark storage coefficient is estimated to be 2.5 hr. Use a 1-hr time interval for the computations. Use the HEC U.S. Army Corps of Engineer synthetic time-area relationship.

8.4.10 Compute the Clark unit hydrograph parameters (T_c and R) for a 2.17-mi² (1389 acre) urban watershed in Phoenix, Arizona that has a flow path of 1.85 mi, a slope of 30.5 ft/mi, and an imperviousness of 21 percent. A rainfall intensity of 2.56 in/hr is to be used. The time of concentration for the watershed is computed using $T_c = 11.4L^{0.50} K_b^{0.52} S^{-0.31} i^{-0.38}$, where T_c is the time of concentration in hours, L is the length of the longest flow path in miles, K_b is a watershed resistance coefficient ($K_b = -0.00625 \log A + 0.04$) for commercial and residential areas, A is the watershed area in acres, S is the slope of the flow path

in ft/mi, and i is the rainfall intensity in in/hr. The storage coefficient is $R = 0.37T_c^{1.11} A^{-0.57} L^{0.80}$, where A is the area in mi².

8.4.11 Compute the 15-min Clark unit hydrograph for the Phoenix watershed in problem 8.4.10.

8.4.12 For the situation in problem 8.4.10, compute the time of concentration. However, now the rainfall intensity is not given, instead use the rainfall intensity duration frequency relation in Figure 7.2.15, with a 25-year return period.

8.4.13 Develop the 15-min Clark unit hydrograph for a 2.17-mi² (1389 acre) rural watershed that has a flow path of 1.85 mi, a slope of 30.5 ft/mi, and an imperviousness of 21 percent. A rainfall intensity of 2.56 in/hr is to be used. The time of concentration for the watershed is computed using $T_c = 11.4L^{0.50} K_b^{0.52} S^{-0.31} i^{-0.38}$, where T_c is the time of concentration in hours, L is the length of the longest flow path in miles, K_b is a watershed resistance coefficient ($K_b = -0.01375 \log A + 0.08$), A is the watershed area in acres, and S is the slope of the flow path in ft/mi, and i is the rainfall intensity in in/hr.

8.5.1 Using the 4-hr unit hydrograph developed in problem 8.3.1, use the S-curve method to develop the 8-hr unit hydrograph for this 200 km² watershed.

8.5.2 Using the one-hour unit hydrograph given in problem 8.3.3, develop the 3-hr unit hydrograph using the S-curve method.

8.5.3 Suppose the 4-hr unit hydrograph for a watershed is

Time (hr)	0	2	4	6	8	10	12	14
UH (m ³ /s/10 mm)	0	15	45	65	50	25	10	0

- (a) Determine the 2-hr unit hydrograph.
- (b) From the frequency analysis, the 10-year 4-hr storm has a total depth of 3 cm with an effective rainfall intensity of 1 cm/hr in the first 2 hr and 0.5 cm/hr in the second 2 hr. Assuming the baseflow is 10 m³/s, calculate the total runoff hydrograph from the 10-year 4-hr storm.

8.5.4 Suppose the 4-hr unit hydrograph for the watershed is

Time (hr)	0	2	4	6	8	10	12	14	16
UH (m ³ /s/cm)	0	19	38	32	22	13	6	2	0

- (a) What is the area of the watershed?
- (b) Determine the 2-hr unit hydrograph.
- (c) Suppose that a 25-year design storm has a total effective rainfall of 7 cm and the corresponding hyetograph has 5 cm in the first 2 hr and 2 cm in the second 2 hr. Assuming the baseflow is 10 m³/s, calculate the total runoff hydrograph from this 25-year design storm.

8.5.5 Suppose the 6-hr unit hydrograph for the watershed is

Time (hr)	0	3	6	9	12	15	18	21
UH (m ³ /s/cm)	0	15	45	65	50	25	10	0

- (a) What is the area of the watershed?
- (b) Determine the 3-hr unit hydrograph.
- (c) Suppose that a 10-year design storm has a total effective rainfall of 6 cm and the corresponding hyetograph has 4 cm in the first 3 hr and 2 cm in the second 3 hr. Assuming the baseflow is 10 m³/s, calculate the total runoff hydrograph from this 10-year design storm.

8.5.6 Suppose the 6-hr unit hydrograph for a watershed is

Time (hr)	0	3	6	9	12	15	18
UH (m ³ /s/cm)	0	60	90	50	30	10	0

- (a) Determine the 3-hr unit hydrograph.
- (b) Suppose that a 50-year design storm has a total effective rainfall of 9 cm and the corresponding hyetograph has 2 cm in the first 3 hr, 5 cm in the second 3 hr, and 2 cm in the third 3 hr. Assuming the baseflow is 20 m³/s, determine the total runoff hydrograph from this 50-year design storm.

8.5.7 Suppose the 6-hr unit hydrograph for a watershed is

Time (hr)	0	3	6	9	12	15	18	21
UH (m ³ /s/cm)	0	15	45	65	50	25	10	0

- (a) Determine the 2-hr unit hydrograph.
- (b) Assuming the baseflow is 10 m³/s, calculate the total runoff hydrograph from an effective rainfall hyetograph of 2 cm in the first 2 hr and 1 cm in the second 2 hr.

8.7.1 Determine the weighted curve numbers for a watershed with 60 percent residential (1/4-acre lots), 20 percent open space, good condition, and 20 percent commercial and business (85 percent impervious) with corresponding soil groups of C, D, and C.

8.7.2 Rework example 8.7.1 with corresponding soil groups of B, C, D, and B.

8.7.3 The watershed in problem 8.7.1 experienced a rainfall of 5 in; what is the runoff volume per unit area?

8.7.4 Rework example 8.7.2 with a 7-in rainfall.

8.7.5 Calculate the cumulative abstractions and the excess rainfall hyetograph for the situation in problems 8.7.1 and 8.7.3. The rainfall pattern is 1.5 in during the first hour, 2.5 in during the second hour, and 1.0 in during the third hour.

8.7.6 Calculate the cumulative abstraction and the excess rainfall hyetograph for the situation in problems 8.7.2 and 8.7.4. The rainfall pattern is 2.0 in during the first hour, 3.0 in during the second hour, and 2.0 in during the third hour.

8.7.7 Consider an urban drainage basin having 60 percent soil group B and 40 percent soil group C. The land use pattern is 1/2 commercial area and 1/2 industrial district. Determine the rainfall excess intensity hyetograph under the dry antecedent moisture condition (AMC I) from the recorded storm given in problem 8.2.6.

8.7.8 Consider a drainage basin having 60 percent soil group B and 40 percent soil group C. Five years ago, the watershed land use

pattern was 1/2 wooded area with good cover and 1/2 pasture with good condition. Now, the land use has been changed to 1/3 wooded area, 1/3 pasture land, and 1/3 residential area (1/4-acre lot). Estimate the volume of increased runoff due to the land use change over the past 5-year period for a storm with 6 in of rainfall under the dry antecedent moisture condition (AMC I).

8.7.9 Refer to problem 8.7.8 for the present watershed land use pattern. Determine the effective rainfall hyetograph for the following storm event using the SCS method under the dry antecedent moisture condition (AMC I). Next determine the value of the ϕ index corresponding to the effective rainfall hyetograph.

Time (h)	0–0.5	0.5–1.0	1.0–1.5	1.5–2.0
Rainfall intensity (in/h)	6.0	3.0	2.0	1.0

8.7.10 Consider a drainage basin having 60 percent soil group A and 40 percent soil group B. Five years ago, the land use pattern in the basin was 1/2 wooded area with poor cover and 1/2 cultivated land with good conservation treatment. Now, the land use has been changed to 1/3 wooded area, 1/3 cultivated land, and 1/3 commercial and business area. Estimate the increased runoff volume during the dormant season due to the land use change over the past 5-year period for a storm of 350 mm in total depth. This storm depth corresponds to a duration of 6-hr and 100-year return period. The total 5-day antecedent rainfall amount is 30 mm. Note: 1 inch = 25.4 mm.

8.7.11 Consider a drainage basin of 500-ha having hydrologic soil group D. In 1970, the watershed land use pattern was 50% wooded area with good cover, 25% range land with good condition, and 25% residential area (1/4-acre lot). Ten years later, the land use has been changed to 30% wooded area, 20% pasture land, 40% residential area (1/4-acre lot), and 10% commercial and business area.

- (a) Compute the weighted curve numbers in 1970 and 1980.
- (b) Using the SCS method, estimate the percentage of change (increase or decrease) in runoff volume with respect to year 1970 due to the land use change over the 10-year period for a 2-hr, 50-mm rainfall event under the wet antecedent moisture condition.
- (c) Suppose that the 2-hr, 50-mm rainfall event has the following hyetograph. Determine the rainfall excess intensity hyetograph (in mm/hr) and the corresponding incremental infiltration (in mm) over the storm duration under 1980 conditions.

Time (hr)	0–0.5	0.5–1.0	1.0–1.5	1.5–2.0
Rainfall intensity (mm/hr)	4.0	50.0	30.0	16.0

8.7.12 Consider a drainage basin of 36 km² having hydrologic soil group B. In 1970, the watershed land use pattern was 60 percent wooded area with good cover, 25 percent range land with good condition, and 15 percent residential area (1/4-acre lot). Twenty years later (i.e., in 1990), the land use has been changed to 30 percent wooded area with good cover, 20 percent pasture land with good condition, 40 percent residential area (1/4-acre lot), and 10 percent commercial and business area.

On a particular day in 1990, there was a rainstorm event that produced rainfall and runoff recorded in the following table.

Time (min)	0	15	30	45	60	75	90	105	120
Cumulative rainfall (mm)	0	10	50	75	90	100			
Instantaneous runoff (m ³ /s)	10	30	160	360	405	305	125	35	10

- (a) Using the SCS method, estimate the percentage of change (increase or decrease) in runoff volume in 1990 with respect to that of 1970 for the above rainstorm event under the normal antecedent moisture condition.
- (b) Under the wet antecedent moisture condition, determine the rainfall excess intensity hyetograph (in mm/hr) and the corresponding incremental infiltration (in mm) over the storm duration for the above rainstorm event under the 1990 conditions.
- (c) For a baseflow of 10 m³/s, determine the volume of direct runoff.
- (d) Assuming an initial loss of 10 mm, determine the Φ index (in mm/hr) and the corresponding excess rainfall hyetograph.

8.7.13 Consider a drainage basin with an area of 200 km². From a storm event, the observed cumulative rainfall depth and the corresponding runoff hydrograph are given in the following table. Assume that the baseflow is 20 m³/s.

Time (hr)	0	4	8	12	16	20
Cum. rainfall (cm)	0.0	1.6	5.5	7.5	7.5	7.5
Discharge (m ³ /s)	20	40	130	300	155	20

- (a) Determine the effective rainfall hyetograph by the SCS method with a curve number $CN = 85$.
- (b) Determine the 4-hr unit hydrograph by the least-squares method.

8.7.14 During a rain storm event, rain gauge at location X broke down and rainfall record was not available. Fortunately, three rain gauges nearby did not have a technical problem and their rainfall readings, along with other information, are provided in the table below.

Rain gauge	A	B	C	X
Event depth (mm)	40	60	50	Missing
Distance to gauge X (km)	10	8	12	0
Elevation (m)	20	50	40	60
Mean annual rainfall (mm)	1500	2000	1800	2200
Polygon area (km ²)	10	30	20	40

The four rain gauges are located either within or in the neighborhood of a watershed having a drainage area of 100 km². According to the Thiessen polygon method, the contributing area of each rain gauge is shown in the above table.

For this particular storm event, the duration of the storm is 3 hr and the percentage of rainfall depth in the first hour is 50 percent, in the second hour 30 percent, and in the third hour 20 percent. The

watershed largely consists of woods and meadow of good hydrologic condition with soil group B. Among the two land cover types, woods occupy 60 percent of the total area while the meadow makes up the remaining 40 percent.

For this watershed, the 1-hr unit hydrograph resulting from 1 cm of effective rainfall has been derived and is given below:

Time (hr)	0	1	2	3	4	5
Flow rate (m ³ /s/cm)	0	10	30	20	10	0

- (a) Select a method to estimate missing rainfall depth at station X by an appropriate method. Explain the reasons why the method is selected.
- (b) Determine the basin-wide equivalent uniform rainfall depth and the corresponding hyetograph for this particular storm.
- (c) According to part (b), determine the total effective rainfall depth and the corresponding rainfall excess hyetograph for the storm. It is known that a storm occurred 2 days before this particular storm and, therefore, the ground is quite wet.
- (d) What is the magnitude of peak runoff discharge produced by this particular storm? It is reasonable to assume that the baseflow is 5 m³/s.

8.7.15 Consider a drainage basin having 60 percent soil group A and 40 percent soil group B. Five years ago, the land use pattern in the basin was 1/2 wooded area with poor cover and 1/2 cultivated land with good conservation treatment. Now the land use has been changed to 1/3 wooded area, 1/3 cultivated land, and 1/3 commercial and business area.

- (a) Estimate the increased runoff volume during the dormant season due to the land use change over the past 5-year period for a storm of 35 cm total depth under the dry antecedent moisture condition (AMC I). This storm depth corresponds to a duration of 6-hr and 100-year return period. The total 5-day antecedent rainfall amount is 30 mm. (Note: 1 in = 25.4 mm.)
- (b) Under the present watershed land use pattern, find the effective rainfall hyetograph (in cm/hr) for the following storm event using SCS method under the dry antecedent moisture condition (AMC I).

Time (hr)	0–0.5	0.5–1.0	1.0–1.5	1.5–2.0
Avg. rainfall intensity (cm/hr)	16.0	9.0	5.0	3.0

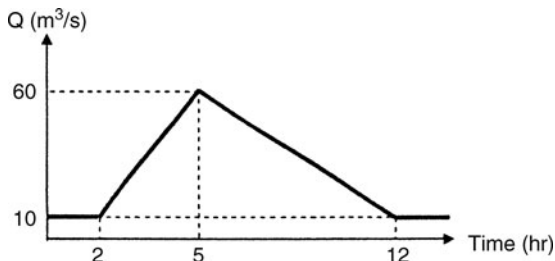
8.7.16 Consider a drainage basin having 60 percent soil group B and 40 percent soil group C. Five years ago, the watershed land use pattern was 1/2 wooded area with good cover and 1/2 pasture with good condition. Today, the wooded area and pasture each have been reduced down to 1/3 and the remaining 1/3 of the drainage basin has become a residential area (1/4-acre lot). Consider the rainstorm event having the observed rainfall mass data given below.

Time (min)	0	30	60	90	120
Cumulative Rainfall (mm)	0	152	228	278	304

- (a) Estimate the increased total runoff volume due to the land use change over the past 5-year period for the above rainstorm event under the dry antecedent moisture condition (AMC I).
- (b) Referring to the present watershed land use condition, find the effective rainfall hyetograph (in mm/hr) for the rainstorm event given the above using the SCS method under the dry antecedent moisture condition (AMC I).

8.7.17 Consider a drainage basin of 1,200 hectares having 60 percent soil group B and 40 percent soil group C. Five years ago, the watershed land use pattern was 1/2 wooded area with good cover and 1/2 pasture with good condition. Now the land use has been changed to 1/3 wooded area, 1/3 pasture land, and 1/3 residential area (1/4-acre lot). For a storm event, the cumulative rainfall and the corresponding runoff hydrograph are shown in the following table and figure, respectively. (Note: 1 hectare = 10,000 m²; 1 in = 25.4 mm).

Time (hr)	0	1	2	3	4
Cumulative rainfall (mm)	0	60	120	160	180



- (a) Estimate the increased total runoff volume by the SCS method due to the land use change over the past 5-year period for this storm under the wet antecedent moisture condition.
- (b) Find the effective rainfall intensity hyetograph for the storm event using the SCS method under the wet antecedent moisture condition and current land use condition.

- (c) Find the value of the ϕ index corresponding to the above direct runoff hydrograph assuming the baseflow is 10 m³/s.

8.7.18 Consider a drainage basin having soil group D. The land use pattern in the basin is 1/3 wooded area with good cover, 1/3 cultivated land with conservation treatment, and 1/3 commercial and business area. For the rainstorm event given below, use the SCS method under the dry antecedent moisture condition (AMC I).

- (a) Estimate the total volume of effective rainfall (in cm).
- (b) Find the effective rainfall hyetograph (in cm/hr) for the following storm event.

Time (hr)	0–0.5	0.5–1.0	1.0–1.5	1.5–2.0
Avg. rainfall intensity (cm/hr)	16.0	9.0	5.0	3.0

8.8.1 Develop the SCS triangular unit hydrograph for a 400-acre watershed that has been commercially developed. The flow length is 1,500 ft, the slope is 3 percent, and the soil group is group B.

8.8.2 Prior to development of the 400-acre watershed in problem 8.8.1, the land use was contoured pasture land with fair condition. Compute the SCS triangular unit hydrograph and compare with the one for commercially developed conditions.

8.8.3 Using the watershed defined in problems 8.8.1 and 8.8.2, determine the SCS triangular unit hydrograph assuming residential lot size. Compare with the results in problem 8.8.2.

8.8.4 A 20.7-km² watershed has a time of concentration of 1.0 hr. Calculate the 10-min unit hydrograph for the watershed using the SCS triangular unit hydrograph method. Determine the direct runoff hydrograph for a 30-min storm having 1.5 cm of excess rainfall in the first 10 min, 0.5 cm in the second 10 min, and 1.0 cm in the third 10 min.

8.9.1 Develop a flowchart of the kinematic overland flow runoff model described in Section 8.9.

8.9.2 Develop the appropriate equations to solve equation (8.9.9) by Newton’s method.

8.9.3 Derive equation (8.9.12).

REFERENCES

Chow, V. T. (editor), *Handbook of Applied Hydrology*, McGraw-Hill, New York, 1964.

Chow, V. T., D. R. Maidment, and L. W. Mays, *Applied Hydrology*, McGraw-Hill, New York, 1988.

Clark, C. O., “Storage and the Unit Hydrograph,” *Trans. American Society of Civil Engineers*, Vol. 110, pp. 1419–1488, 1945.

Engman, E. T., “Roughness Coefficients for Routing Surface Runoff”, *Journal of Irrigation and Drainage Engineering*; American Society of Civil Engineers, 112(1), pp. 39–53, 1986.

Flood Control District of Maricopa County, *Drainage Design Manual for Maricopa County, Arizona*, Phoenix, AZ, 1995.

Ford, D., E. C. Morris, and A. D. Feldman, “Corps of Engineers’ Experience with Automatic Calibration Precipitation-Runoff Model,” in *Water and Related Land Resource Systems* edited by Y. Haimes and J. Kindler, p. 467–476, Pergamon Press, New York, 1980.

Hewlett, J. D., and W. L. Nutter, *An Outline of Forest Hydrology*, University of Georgia Press, Athens, GA, 1969.

Horton, R. E., “Erosional Development of Streams and Their Drainage Basins; Hydrological Approach to Quantitative Morphology,” *Bull. Geol. Soc. Am.*, vol. 56, pp. 275–370, 1945.

Masch, F. D., *Hydrology*, Hydraulic Engineering Circular No. 19, FHWA-10-84-15, Federal Highway Administration, U.S. Department of the Interior, McLean, VA, 1984.

Morris, E. M., and D. A. Woolhiser, “Unsteady One-Dimensional Flow over a Plane: Partial Equilibrium and Recession Hydrographs,” *Water Resources Research*, vol. 16, no. 2, pp. 355–360, 1980.

- Mosley, M. P., and A. I. McKerchar, "Streamflow," in *Handbook of Hydrology* (edited by D. R. Maidment), McGraw-Hill, New York, 1993.
- Palmer, V. J., "Retardance Coefficients for Low Flow in Channels Lined with Vegetation," *Transactions of the American Geophysical Union*, 27(11), pp. 187–197, 1946.
- Papadakis, C. N., and M. N. Kazan, "Time of Concentration in Small, Rural Watersheds," *Proceedings of the Engineering Hydrology Symposium*, ASCE, Williamsburg, Virginia, pp. 633–638, 1987.
- Ponce, V. M., *Engineering Hydrology: Principles and Practices*, Prentice-Hall, Englewood Cliffs, NJ, 1989.
- Sanders, T. G. (editor), *Hydrology for Transportation Engineers*, U.S. Dept. of Transportation, Federal Highway Administration, 1980.
- Strahler, A. N., "Quantitative Geomorphology of Drainage Basins and Channel Networks," section 4-II in *Handbook of Applied Hydrology* (edited by V. T. Chow), McGraw-Hill, New York, 1964.
- Straub, T. D., C. S. Melching, and K. E. Kocher, *Equations for Estimating Clark Unit-Hydrograph Parameters for Small Rural Watersheds in Illinois*, U.S. Geological Survey Water-Resources Investigations Report 00-4184, Urbana, IL, 2000.
- U.S. Army Corps of Engineers, Hydrologic Engineering Center, HEC-1 Flood Hydrograph Package, User's Manual, Davis, CA, 1990.
- U.S. Department of Agriculture Soil Conservation Service, National Engineering Handbook, Section 4, *Hydrology*, available from U.S. Government Printing Office, Washington, DC, 1972.
- U.S. Department of Agriculture Soil Conservation Service, "Urban Hydrology for Small Watersheds," Tech. Release No., 55, Washington, DC, June, 1986.
- Woolhiser, D. A., and J. A. Liggett, "Unsteady, One-Dimensional Flow over a Plane—the Rising Hydrograph," *Water Resources Research*, vol. 3(3), pp. 753–771, 1967.
- Woolhiser, D. A., R. E. Smith, and D. C. Goodrich, *KINEROS, A. Kinematic Runoff and Erosion Model: Documentation and User Manual*, U. S. Department of Agricultural Research Service, ARS-77, Tucson, AZ, 1990.

This page intentionally left blank

Reservoir and Stream Flow Routing

9.1 ROUTING

Figure 9.1.1 illustrates how stream flow increases as the *variable source area* extends into the drainage basin. The variable source area is the area of the watershed that is actually contributing flow to the stream at any point. The variable source area expands during rainfall and contracts thereafter.

Flow routing is the procedure to determine the time and magnitude of flow (i.e., the flow hydrograph) at a point on a watercourse from known or assumed hydrographs at one or more points upstream. If the flow is a flood, the procedure is specifically known as flood routing. Routing by lumped system methods is called *hydrologic (lumped) routing*, and routing by distributed systems methods is called *hydraulic (distributed) routing*.

For hydrologic routing, input $I(t)$, output $Q(t)$, and storage $S(t)$ as functions of time are related by the continuity equation (3.3.10)

$$\frac{dS}{dt} = I(t) - Q(t) \quad (9.1.1)$$

Even if an inflow hydrograph $I(t)$ is known, equation (9.1.1) cannot be solved directly to obtain the outflow hydrograph $Q(t)$, because, both Q and S are unknown. A second relationship, or storage function, is required to relate S , I , and Q ; coupling the storage function with the continuity equations provides a solvable combination of two equations and two unknowns.

The specific form of the storage function depends on the nature of the system being analyzed. In reservoir routing by the level pool method (Section 9.2), storage is a nonlinear function of Q , $S = f(Q)$, and the function $f(Q)$ is determined by relating reservoir storage and outflow to reservoir water level. In the Muskingum method (Section 9.3) for flow routing in channels, storage is linearly related to I and Q .

The effect of storage is to redistribute the hydrograph by shifting the centroid of the inflow hydrograph to the position of the outflow hydrograph in a *time of redistribution*. In very long channels, the entire flood wave also travels a considerable distance, and the centroid of its hydrograph may then be shifted by a time period longer than the time of redistribution. This additional time may be considered the *time of translation*. The total time of flood movement between the centroids of the inflow and outflow hydrographs is equal to the sum of the time of redistribution and the time of translation. The process of redistribution modifies the shape of the hydrograph, while translation changes its position.

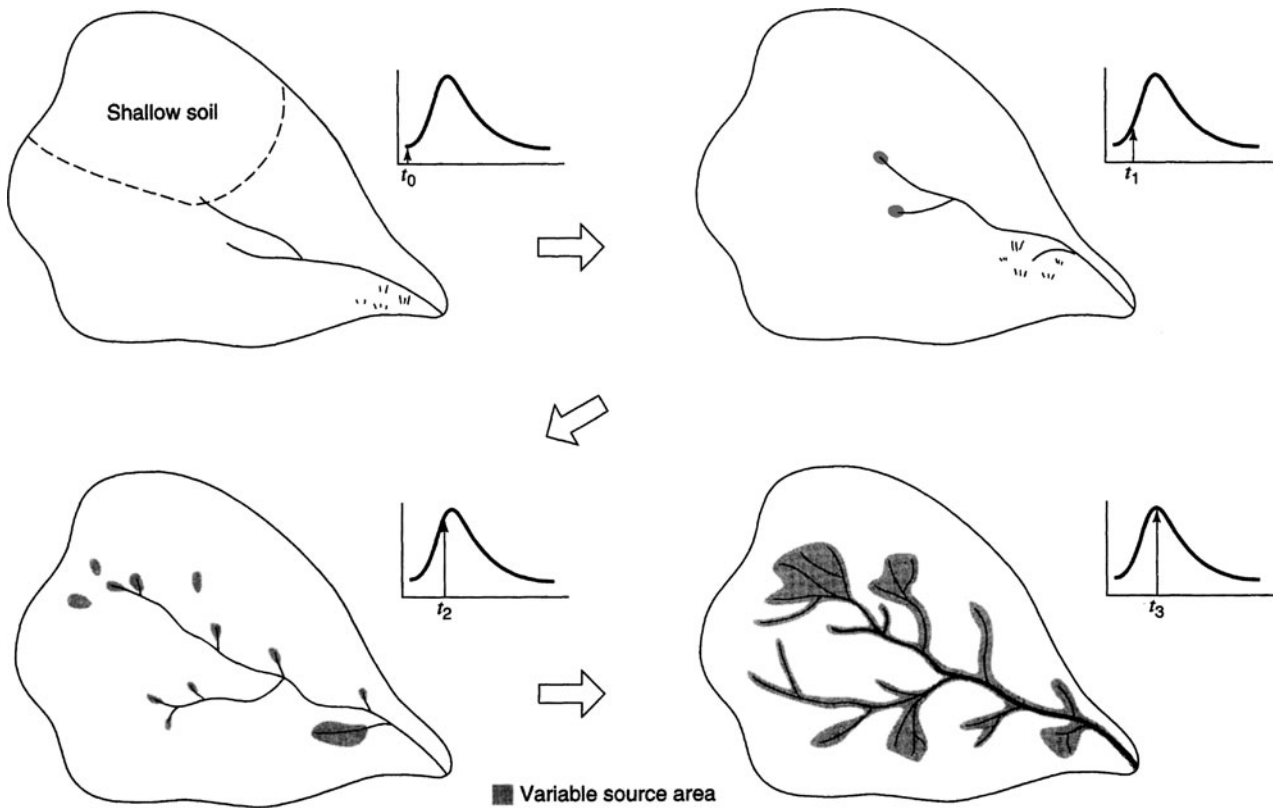


Figure 9.1.1 The small arrows in the hydrographs show how streamflow increases as the variable source extends into swamps, shallow soils, and ephemeral channels. The process reverses as streamflow declines (from Hewlett (1982)).

9.2 HYDROLOGIC RESERVOIR ROUTING

Level pool routing is a procedure for calculating the outflow hydrograph from a reservoir assuming a horizontal water surface, given its inflow hydrograph and storage-outflow characteristics. Equation (9.1.1) can be expressed in the infinite-difference form to express the change in storage over a time interval (see Figure 9.2.1) as

$$S_{j+1} - S_j = \frac{I_j + I_{j+1}}{2} \Delta t - \frac{Q_j + Q_{j+1}}{2} \Delta t \tag{9.2.1}$$

The inflow values at the beginning and end of the j th time interval are I_j and I_{j+1} , respectively, and the corresponding values of the outflow are Q_j and Q_{j+1} . The values of I_j and I_{j+1} are prespecified. The values of Q_j and S_j are known at the j th time interval from calculations for the previous time interval. Hence, equation (9.2.1) contains two unknowns, Q_{j+1} and S_{j+1} , which are isolated by multiplying (9.2.1) through by $2/\Delta t$, and rearranging the result to produce:

$$\left[\frac{2S_{j+1}}{\Delta t} + Q_{j+1} \right] = (I_j + I_{j+1}) + \left[\frac{2S_j}{\Delta t} - Q_j \right] \tag{9.2.2}$$

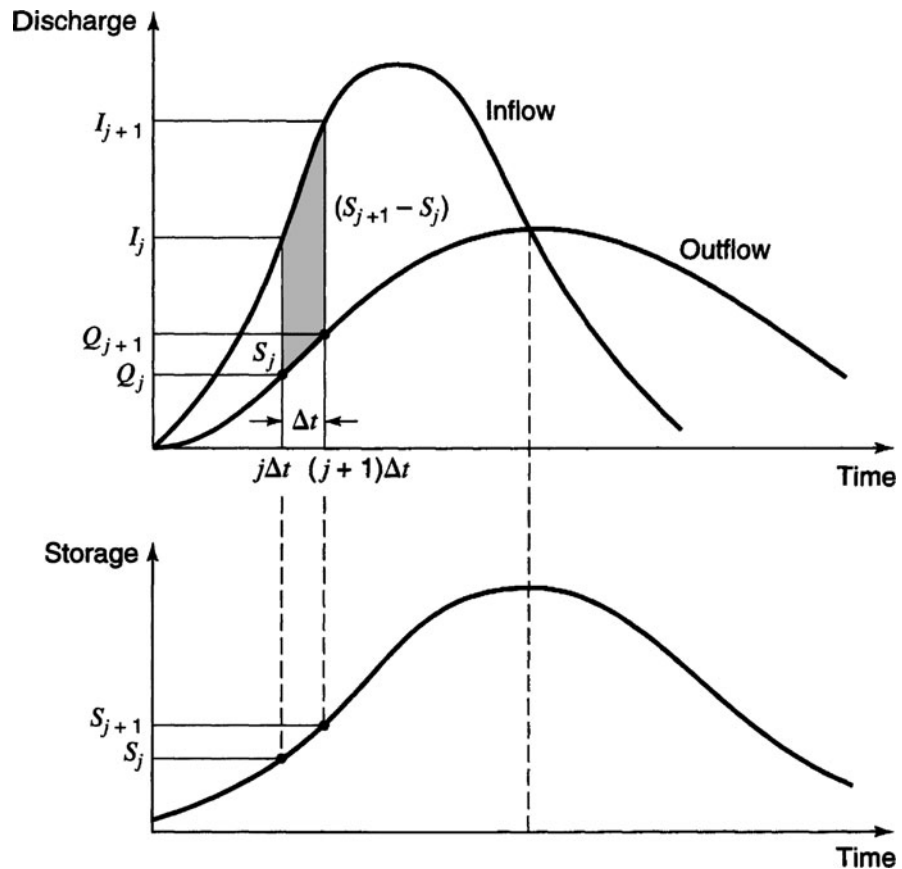


Figure 9.2.1 Change of storage during a routing period Δt .

In order to calculate the outflow Q_{j+1} , a storage-outflow function relating $2S/\Delta t + Q$ and Q is needed. The method for developing this function using elevation-storage and elevation-outflow relationships is shown in Figure 9.2.2. The relationship between water surface elevation and reservoir storage can be derived by planimetry of topographic maps or from field surveys. The elevation-discharge relation is derived from hydraulic equations relating head and discharge for various types of spillways and outlet works. (See Chapter 17.) The value of Δt is taken as the time interval of the inflow hydrograph. For a given value of water surface elevation, the values of storage S and discharge Q are determined (parts (a) and (b) of Figure 9.2.2), and then the value of $2S/\Delta t + Q$ is calculated and plotted on the horizontal axis of a graph with the value of the outflow Q on the vertical axis (part (c) of Figure 9.2.2).

In routing the flow through time interval j , all terms on the right side of equation (9.2.2) are known, and so the value of $2S_{j+1}/\Delta t + Q_{j+1}$ can be computed. The corresponding value of Q_{j+1} can be determined from the storage-outflow function $2S/\Delta t + Q$ versus Q , either graphically or by linear interpolation of tabular values. To set up the data required for the next time interval, the value of $(2S_{j+1}/\Delta t - Q_{j+1})$ is calculated using

$$\left[\frac{2S_{j+1}}{\Delta t} - Q_{j+1} \right] = \left[\frac{2S_{j+1}}{\Delta t} + Q_{j+1} \right] - 2Q_{j+1} \quad (9.2.3)$$

The computation is then repeated for subsequent routing periods.

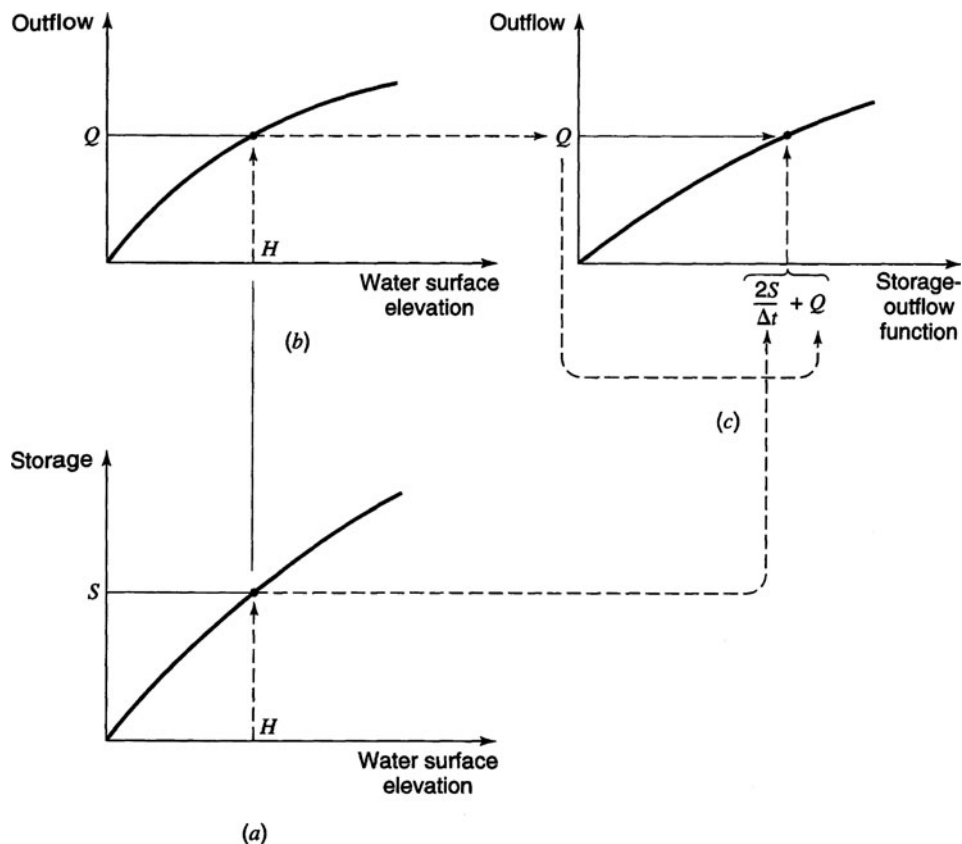


Figure 9.2.2 Development of the storage-outflow function for level pool routing on the basis of storage-elevation-outflow curves (from Chow et al. (1988)).

EXAMPLE 9.2.1

Consider a 2-acre stormwater detention basin with vertical walls. The triangular inflow hydrograph increases linearly from zero to a peak of 60 cfs at 60 min and then decreases linearly to a zero discharge at 180 min. Route the inflow hydrograph through the detention basin using the head-discharge relationship for the 5-ft diameter pipe spillway in columns (1) and (2) of Table 9.2.1. The pipe is located at the bottom of the basin. Assuming the basin is initially empty, use the level pool routing procedure with a 10-min time interval to determine the maximum depth in the detention basin.

SOLUTION

The inflow hydrograph and the head-discharge (columns (1) and (2)) and discharge-storage (columns (2) and (3)) relationships are used to determine the routing relationship in Table 9.2.1. A routing interval of 10 min is used to determine the routing relationship $2S/\Delta t + Q$ vs. Q , which is columns (2) and (4) in Table 9.2.1. The routing computations are presented in Table 9.2.2. These computations are carried out using equation (9.2.3). For the first time interval, $S_1 = Q_1 = 0$ because the reservoir is empty at $t = 0$; then $(2S_1/\Delta t - Q_1) = 0$. The value of the storage-outflow function at the end of the time interval is

$$\left[\frac{2S_2}{\Delta t} + Q_2 \right] = (I_1 + I_2) + \left[\frac{2S_1}{\Delta t} - Q_1 \right] = (0 + 10) + 0 = 10$$

The value of Q_2 is determined using linear interpolation, so that

$$Q_2 = 0 + \frac{(3 - 0)}{(148.2 - 0)}(10 - 0) = 0.2 \text{ cfs}$$

Table 9.2.1 Elevation-Discharge-Storage Data for Example 9.2.1

1 Head H (ft)	2 Discharge Q (cfs)	3 Storage S (ft ³)	4 $\frac{2S}{\Delta t} + Q$ (cfs)
0.0	0	0	0.00
0.5	3	43,500	148.20
1.0	8	87,120	298.40
1.5	17	130,680	452.60
2.0	30	174,240	610.80
2.5	43	217,800	769.00
3.0	60	261,360	931.20
3.5	78	304,920	1094.40
4.0	97	348,480	1258.60
4.5	117	392,040	1423.80
5.0	137	435,600	1589.00

Table 9.2.2 Routing of Flow Through Detention Reservoir by the Level Pool Method (Example 9.2.1)

Time t (min)	Inflow I_j (cfs)	$I_j + I_{j+1}$ (cfs)	$\frac{2S_j}{\Delta t} - Q_j$ (cfs)	$\frac{2S_{j+1}}{\Delta t} + Q_{j+1}$ (cfs)	Outflow (cfs)
0.00	0.00				0.00
10.00	10.00	10.00	0.00	10.00	0.20
20.00	20.00	30.00	9.60	39.60	0.80
30.00	30.00	50.00	37.99	87.99	1.78
40.00	40.00	70.00	84.43	154.43	3.21
50.00	50.00	90.00	148.01	238.01	5.99
60.00	60.00	110.00	226.04	336.04	10.20
70.00	55.00	115.00	315.64	430.64	15.72
80.00	50.00	105.00	399.21	504.21	21.24
90.00	45.00	95.00	461.72	556.72	25.56
100.00	40.00	85.00	505.61	590.61	28.34
110.00	35.00	75.00	533.93	608.93	29.85
120.00	30.00	65.00	549.24	614.24	30.28
130.00	25.00	55.00	553.67	608.67	29.83
140.00	20.00	45.00	549.02	594.02	28.62
150.00	15.00	35.00	536.78	571.78	26.79
160.00	10.00	25.00	518.19	543.19	24.44
170.00	5.00	15.00	494.30	509.30	21.66
180.00	0.00	5.00	465.98	470.98	18.51
190.00	0.00	0.00	433.96	433.96	15.91
200.00	0.00	0.00	402.14	402.14	14.05
210.00	0.00	0.00	374.03	374.03	12.41
220.00	0.00	0.00	349.20	349.20	10.97
230.00	0.00	0.00	327.27	327.27	9.69
240.00	0.00	0.00	307.90	307.90	8.55

With $Q_1 = 0.2$, then $2S_2/\Delta t - Q_2$ for the next iteration is

$$\left[\frac{2S_2}{\Delta t} - Q_2 \right] = \left[\frac{2S_2}{\Delta t} + Q_2 \right] - 2Q_2 = 10 - 2(0.2) = 9.6 \text{ cfs}$$

The computation now proceeds to the next time interval. Refer to Table 9.2.2 for the remaining computations.

9.3 HYDROLOGIC RIVER ROUTING

The *Muskingum method* is a commonly used hydrologic routing method that is based upon a variable discharge-storage relationship. This method models the storage volume of flooding in a river channel by a combination of wedge and prism storage (Figure 9.3.1). During the advance of a flood wave, inflow exceeds outflow, producing a wedge of storage. During the recession, outflow exceeds inflow, resulting in a negative wedge. In addition, there is a prism of storage that is formed by a volume of constant cross-section along the length of prismatic channel.

Assuming that the cross-sectional area of the flood flow is directly proportional to the discharge at the section, the *volume of prism storage* is equal to KQ , where K is a proportionality coefficient (approximate as the travel time through the reach), and the *volume of wedge storage* is equal to $KX(I - Q)$, where X is a weighting factor having the range $0 \leq X \leq 0.5$. The total storage is defined as the sum of two components,

$$S = KQ + KX(I - Q) \tag{9.3.1}$$

which can be rearranged to give the storage function for the Muskingum method

$$S = K[XI + (I - X)Q] \tag{9.3.2}$$

and represents a linear model for routing flow in streams.

The value of X depends on the shape of the modeled wedge storage. The value of X ranges from 0 for reservoir-type storage to 0.5 for a full wedge. When $X = 0$, there is no wedge and hence no backwater; this is the case for a level-pool reservoir. In natural streams, X is between 0 and 0.3, with a mean value near 0.2. Great accuracy in determining X may not be necessary because the results of the method are relatively insensitive to the value of this parameter. The parameter K is the time of travel of the flood wave through the channel reach. For hydrologic routing, the values of K and X are assumed to be specified and constant throughout the range of flow.

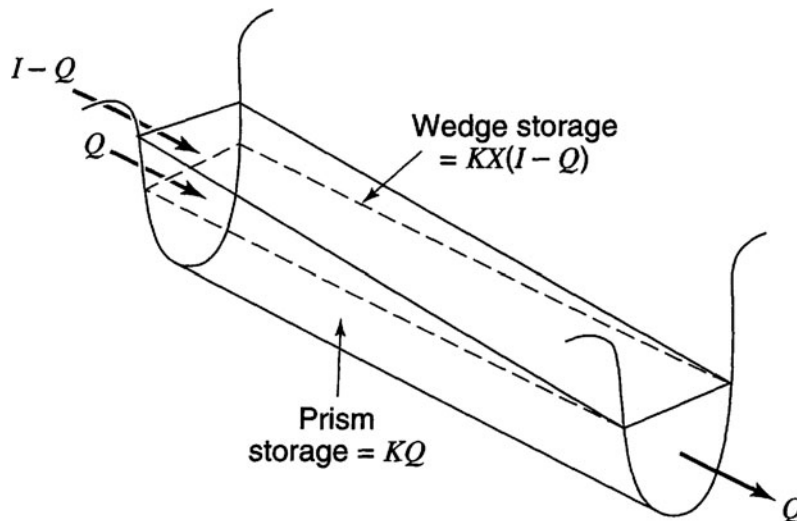


Figure 9.3.1 Prism and wedge storages in a channel reach.

The values of storage at time j and $j + 1$ can be written, respectively, as

$$S_j = K[XI_j + (1 - X)Q_j] \quad (9.3.3)$$

$$S_{j+1} = K[XI_{j+1} + (1 - X)Q_{j+1}] \quad (9.3.4)$$

Using equations (9.3.3) and (9.3.4), the change in storage over time interval Δt is

$$S_{j+1} - S_j = K\{[XI_{j+1} + (1 - X)Q_{j+1}] - [XI_j + (1 - X)Q_j]\} \quad (9.3.5)$$

The change in storage can also be expressed using equation (9.2.1). Combining equations (9.3.5) and (9.2.1) and simplifying gives

$$Q_{j+1} = C_1I_{j+1} + C_2I_j + C_3Q_j \quad (9.3.6)$$

which is the routing equation for the Muskingum method, where

$$C_1 = \frac{\Delta t - 2KX}{2K(1 - X) + \Delta t} \quad (9.3.7)$$

$$C_2 = \frac{\Delta t + 2KX}{2K(1 - X) + \Delta t} \quad (9.3.8)$$

$$C_3 = \frac{2K(1 - X) - \Delta t}{2K(1 - X) + \Delta t} \quad (9.3.9)$$

Note that $C_1 + C_2 + C_3 = 1$.

The routing procedure can be repeated for several sub-reaches (N_{steps}) so that the total travel time through the reach is K . To insure that the method is computationally stable and accurate, the U.S. Army Corps of Engineers (1990) uses the following criterion to determine the number of routing reaches:

$$\frac{1}{2(1 - X)} \leq \frac{K}{N_{\text{steps}}\Delta t} \leq \frac{1}{2X} \quad (9.3.10)$$

If observed inflow and outflow hydrographs are available for a river reach, the values of K and X can be determined. Assuming various values of X and using known values of the inflow and outflow, successive values of the numerator and denominator of the following expression for K , derived from equations (9.3.5) and (9.2.1), can be computed using

$$K = \frac{0.5\Delta t[(I_{j+1} + I_j) - (Q_{j+1} + Q_j)]}{X(I_{j+1} - I_j) + (1 - X)(Q_{j+1} - Q_j)} \quad (9.3.11)$$

The computed values of the numerator (storage) and denominator (weighted discharges) are plotted for each time interval, with the numerator on the vertical axis and the denominator on the horizontal axis. This usually produces a graph in the form of a loop, as shown in Figure 9.3.2. The value of X that produces a loop closest to a single line is taken to be the correct value for the reach, and K , according to equation (9.3.11), is equal to the slope of the line. Since K is the time required for the incremental flood wave to traverse the reach, its value may also be estimated as the observed time of travel of peak flow through the reach.

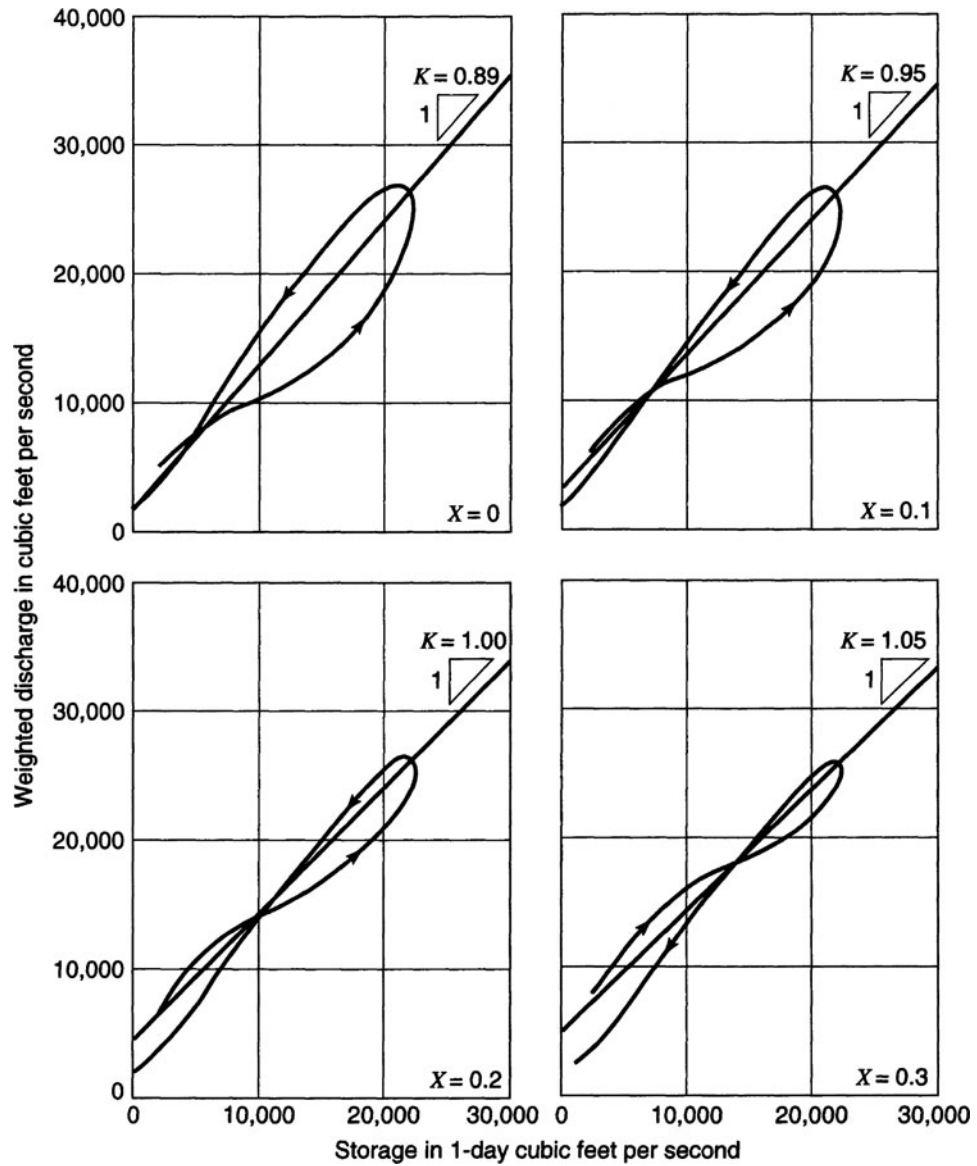


Figure 9.3.2 Typical valley storage curves (after Cudworth (1989)).

EXAMPLE 9.3.1

The objective of this example is to determine K and X for the Muskingum routing method using the February 26 to March 4, 1929 data on the Tuscarawas River from Dover to Newcomerstown. This example is taken from the U.S. Army Corps of Engineers (1960) as used in Cudworth (1989). Columns (2) and (3) in Table 9.3.1 are the inflow and outflow hydrographs for the reach. The numerator and denominator of equation (9.3.11) were computed (for each time period) using four values of $X = 0, 0.1, 0.2,$ and 0.3 . The accumulated numerators are in column (9) and the accumulated denominators (weighted discharges) are in columns (11), (13), (15), and (17). In Figure 9.3.2, the accumulated numerator (storages) from column (9) are plotted against the corresponding accumulated denominator (weighted discharges) for each of the four X values. According to Figure 9.3.2, the best fit (linear relationship) appears to be for $X = 0.2$, which has a resulting $K = 1.0$. To perform a routing, K should equal Δt , so that if $\Delta t = 0.5$ day, as in this case, the reach should be subdivided into two equal reaches ($N_{\text{steps}} = 2$) and the value of K should be 0.5 day for each reach.

Table 9.3.1 Determination of Coefficients K and X for the Muskingum Routing Method. Tuscarawas River, Muskingum Basin, Ohio Reach from Dover to Newcomerstown, February 26 to March 4, 1929

(1) Date $\Delta t = 0.5$ day	(2) In-flow ¹ , ft ³ /s	(3) Out-flow ² , ft ³ /s	(4) $I_2 + I_1$, ft ³ /s	(5) $O_2 + O_1$, ft ³ /s	(6) $I_2 - I_1$, ft ³ /s	(7) $O_2 - O_1$, ft ³ /s	(8) ³ N	(9) ΣN	Values of D and ΣD for assumed values of X							
									$X = 0$		$X = 0.1$		$X = 0.2$		$X = 0.3$	
									⁴ D (10)	ΣD (11)	D (12)	ΣD (13)	D (14)	ΣD (15)	D (16)	ΣD (17)
2-26-29 a.m.	2200	2000	16,700	9000	12,300	5000	1900		5000		5700		6500		7200	
p.m.	14,500	7000	42,900	18,700	13,900	4700	6100	1900	4700	5000	5600	5700	6500	6500	7500	7200
2-27-29 a.m.	28,400	11,700	60,200	28,200	3400	4800	8000	8000	4800	9700	4600	11,300	4500	13,000	4300	14,700
p.m.	31,800	16,500	61,500	40,500	-2100	7500	5200	16,000	7500	14,500	6700	15,900	5600	17,500	4600	19,000
2-28-29 a.m.	29,700	24,000	55,000	53,100	-4400	5100	500	21,200	5100	22,000	4100	22,600	3200	23,100	2300	23,600
p.m.	25,300	29,100	45,700	57,500	-4900	-700	-2900	21,700	-700	27,100	-1100	26,700	-1500	26,300	-2000	25,900
3-01-29 a.m.	20,400	28,400	36,700	52,200	-4100	-4600	-3900	18,800	-4600	26,400	-4600	25,600	-4500	24,800	-4400	23,900
p.m.	16,300	23,800	28,900	43,200	-3700	-4400	-3600	14,900	-4400	21,800	-4300	21,000	-4300	20,300	-4200	19,500
3-02-29 a.m.	12,600	19,400	21,900	34,700	-3300	-4100	-3200	11,300	-4100	17,400	-4000	16,700	-3900	16,000	-3900	15,300
p.m.	9300	15,300	16,000	26,500	-2600	-4100	-2500	8100	-4100	13,300	-4000	12,700	-3800	12,100	-3600	11,400
3-03-29 a.m.	6700	11,200	11,700	19,400	-1700	-3000	-1900	5500	-3000	9200	-2800	8700	-2800	8300	-2600	7800
p.m.	5000	8200	9100	14,600	-900	-1800	-1400	3600	-1800	6200	-1700	5900	-1600	5500	-1600	5200
3-04-29 a.m.	4100	6400	7700	11,600	-500	-1200	-1000	2200	-1200	4400	-1200	4200	-1100	3900	-900	3600
p.m.	3600	5200	6000	9800	-1200	-600	-1000	1200	-600	3200	-600	3000	-700	2800	-800	2700
3-05-29 a.m.	2400	4600	—	—	—	—	—	200	—	2600	—	2400	—	2100	—	1900

¹Inflow to reach was adjusted to equal volume of outflow.

²Outflow is the hydrograph at Newcomerstown.

³Numerator, N , is $\Delta t/2$, column (4) - column (5).

⁴Denominator, D , is column (7) + X [column (6) - column (7)].

Note: From plottings of column (9) versus columns (11), (13), (15), and (17), the plot giving the best fit is considered to define K and X .

$$K = \frac{\text{Numerator, } N}{\text{Denominator, } D} = \frac{0.5\Delta t[(I_2 + I_1) - (O_2 + O_1)]}{X(I_2 - I_1) + (1 - X)(O_2 - O_1)}$$

Source: Cudworth (1989).

EXAMPLE 9.3.2

Route the inflow hydrograph below using the Muskingum method; $\Delta t = 1$ hr, $X = 0.2$, $K = 0.7$ hr.

Time (hr)	0	1	2	3	4	5	6	7
Inflow (cfs)	0	800	2000	4200	5200	4400	3200	2500
Time (hr)	8	9	10	11	12	13		
Inflow (cfs)	2000	1500	1000	700	400	0		

$$C_1 = \frac{1.0 - 2(0.7)(0.2)}{2(0.7)(1 - 0.2) + 1.0} = 0.3396$$

$$C_2 = \frac{1.0 + 2(0.7)(0.2)}{2(0.7)(1 - 0.2) + 1.0} = 0.6038$$

$$C_3 = \frac{2(0.7)(1 - 0.2) - 1.0}{2(0.7)(1 - 0.2) + 1.0} = 0.0566$$

(Adapted from Masch (1984).)

Check to see if $C_1 + C_2 + C_3 = 1$:

$$0.3396 + 0.6038 + 0.0566 = 1$$

Using equation (9.3.6) with $I_1 = 0$ cfs, $I_2 = 800$ cfs, and $Q_1 = 0$ cfs, compute Q_2 at $t = 1$ hr:

$$\begin{aligned} Q_2 &= C_1 I_2 + C_2 I_1 + C_3 Q_1 \\ &= (0.3396)(800) + 0.6038(0) + 0.0566(0) \\ &= 272 \text{ cfs (} 7.7 \text{ m}^3\text{/s)} \end{aligned}$$

Next compute Q_3 at $t = 2$ hr :

$$\begin{aligned} Q_3 &= C_1 I_3 + C_2 I_2 + C_3 Q_2 \\ &= (0.3396)(2000) + 0.6038(800) + 0.0566(272) \\ &= 1,178 \text{ cfs (} 33 \text{ m}^3\text{/s)} \end{aligned}$$

The remaining computations result in

Time (hr)	0	1	2	3	4	5	6	7
Q (cfs)	0	272	1178	2701	4455	4886	4020	3009
Time (hr)	8	9	10	11	12	13	14	15
Q (cfs)	2359	1851	1350	918	610	276	16	1

9.4 HYDRAULIC (DISTRIBUTED) ROUTING

Distributed routing or *hydraulic routing*, also referred to as *unsteady flow routing*, is based upon the one-dimensional unsteady flow equations referred to as the *Saint-Venant equations*. The hydrologic river routing and the hydrologic reservoir routing procedures presented previously are lumped procedures and compute flow rate as a function of time alone at a downstream location. Hydraulic (distributed) flow routings allow computation of the flow rate and water surface elevation (or depth) as a function of both space (location) and time. The Saint-Venant equations are presented in Table 9.4.1 in both the *velocity-depth (nonconservation) form* and the *discharge-area (conservation) form*.

The momentum equation contains terms for the physical processes that govern the flow momentum. These terms are: the *local acceleration term*, which describes the change in momentum due to the change in velocity over time, the *convective acceleration term*, which describes the change in momentum due to change in velocity along the channel, the *pressure force term*,

Table 9.4.1 Summary of the Saint-Venant Equations*

<i>Continuity equation</i>				
Conservation form	$\frac{\partial Q}{\partial x} + \frac{\partial A}{\partial t} = 0$			
Nonconservation form	$V \frac{\partial y}{\partial x} + \frac{\partial V}{\partial x} + \frac{\partial y}{\partial t} = 0$			
<i>Momentum equation</i>				
Conservation form				
$\frac{1}{A} \frac{\partial Q}{\partial t} + \frac{1}{A} \frac{\partial}{\partial x} \left(\frac{Q^2}{A} \right) + g \frac{\partial y}{\partial x} - g(S_0 - S_f) = 0$				
Local acceleration term	Convective acceleration term	Pressure force term	Gravity force term	Friction force term
Nonconservation form (unit with element)				
$\frac{\partial V}{\partial t} + V \frac{\partial V}{\partial x} + g \frac{\partial y}{\partial x} - g(S_0 - S_f) = 0$				
			_____	Kinematic wave
			_____	Diffusion wave
_____			_____	Dynamic wave

*Neglecting lateral inflow, wind shear, and eddy losses, and assuming $\beta = 1$.

x = longitudinal distance along the channel or river, t = time, A = cross-sectional area of flow, h = water surface elevation, S_f = friction slope, S_0 = channel bottom slope, g = acceleration due to gravity, V = velocity of flow, and y = depth of flow.

proportional to the change in the water depth along the channel, the gravity force term, proportional to the bed slope S_0 , and the friction force term, proportional to the friction slope S_f . The local and convective acceleration terms represent the effect of inertial forces on the flow.

Alternative distributed flow routing models are produced by using the full continuity equation while eliminating some terms of the momentum equation (refer to Table 9.4.1). The simplest distributed model is the *kinematic wave model*, which neglects the local acceleration, convective acceleration, and pressure terms in the momentum equation; that is, it assumes that $S_0 = S_f$ and the friction and gravity forces balance each other. The *diffusion wave model* neglects the local and convective acceleration terms but incorporates the pressure term. The *dynamic wave model* considers all the acceleration and pressure terms in the momentum equation.

The momentum equation can also be written in forms that take into account whether the flow is steady or unsteady, and uniform or nonuniform, as illustrated in Table 9.4.1. In the continuity equation, $\partial A / \partial t = 0$ for a steady flow, and the lateral inflow q is zero for a uniform flow.

9.4.1 Unsteady Flow Equations: Continuity Equation

The *continuity equation* for an unsteady variable-density flow through a control volume can be written as in equation (3.3.1):

$$0 = \frac{d}{dt} \int_{CV} \rho dV + \int_{CS} \rho \mathbf{V} \cdot d\mathbf{A} \tag{9.4.1}$$

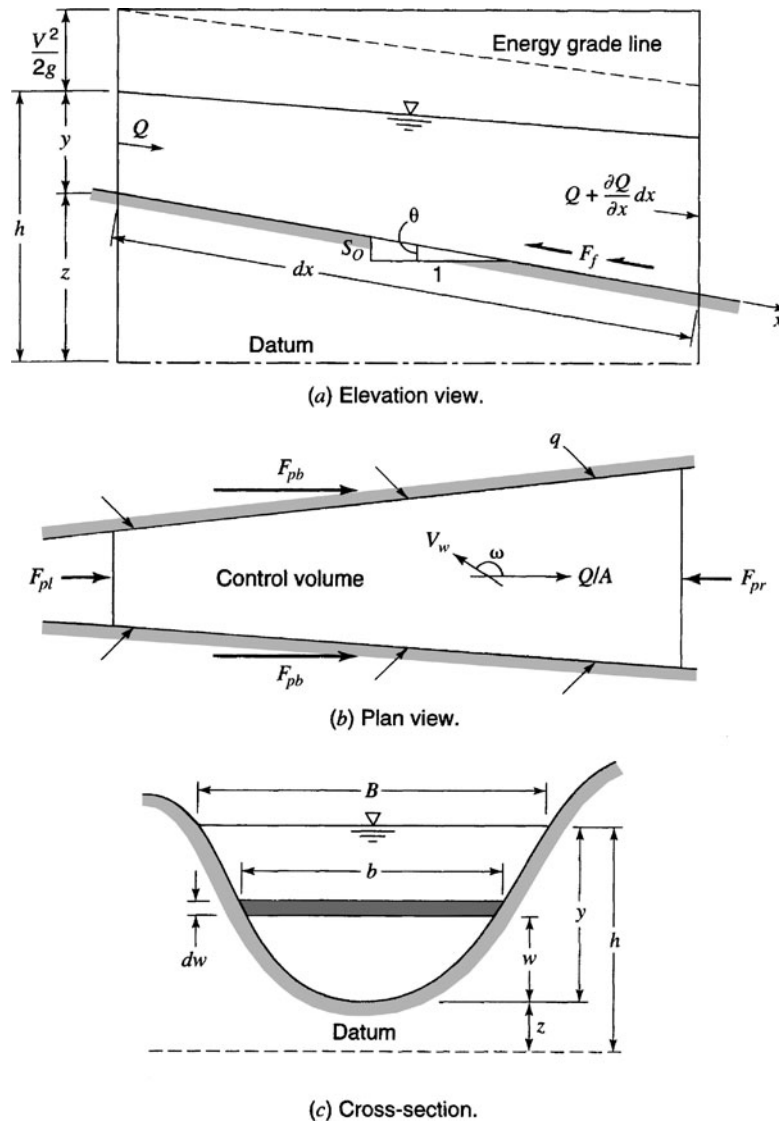


Figure 9.4.1 An elemental reach of channel for derivation of Saint-Venant equations.

Consider an elemental control volume of length dx in a channel. Figure 9.4.1 shows three views of the control volume: (a) an elevation view from the side, (b) a plan view from above, and (c) a channel cross-section. The inflow to the control volume is the sum of the flow Q entering the control volume at the upstream end of the channel and the lateral inflow q entering the control volume as a distributed flow along the side of the channel. The dimensions of q are those of flow per unit length of channel, so the rate of lateral inflow is qdx and the mass inflow rate is

$$\int_{\text{inlet}} \rho \mathbf{V} \cdot d\mathbf{A} = -\rho(Q + qdx) \quad (9.4.2)$$

This is negative because inflows are considered negative in the control volume approach (Reynolds transport theorem). The mass outflow from the control volume is

$$\int_{\text{outlet}} \rho \mathbf{V} \cdot d\mathbf{A} = \rho \left(Q + \frac{\partial Q}{\partial x} dx \right) \quad (9.4.3)$$

where $\partial Q/\partial x$ is the rate of change of channel flow with distance. The volume of the channel element is $A dx$, where A is the average cross-sectional area, so the rate of change of mass stored within the control volume is

$$\frac{d}{dt} \int_{CV} \rho d\forall = \frac{\partial(\rho A dx)}{\partial t} \quad (9.4.4)$$

where the partial derivative is used because the control volume is defined to be fixed in size (though the water level may vary within it). The net outflow of mass from the control volume is found by substituting equations (9.4.2)–(9.4.4) into (9.4.1):

$$\frac{\partial(\rho A dx)}{\partial t} - \rho(Q + q dx) + \rho \left(Q + \frac{\partial Q}{\partial x} dx \right) = 0 \quad (9.4.5)$$

Assuming the fluid density ρ is constant, equation (9.4.5) is simplified by dividing through by ρdx and rearranging to produce the *conservation form* of the continuity equation,

$$\frac{\partial Q}{\partial x} + \frac{\partial A}{\partial t} - q = 0 \quad (9.4.6)$$

which is applicable at a channel cross-section. This equation is valid for a *prismatic* or a *non-prismatic* channel; a prismatic channel is one in which the cross-sectional shape does not vary along the channel and the bed slope is constant.

For some methods of solving the Saint-Venant equations, the *nonconservation form* of the continuity equation is used, in which the average flow velocity V is a dependent variable, instead of Q . This form of the continuity equation can be derived for a unit width of flow within the channel, neglecting lateral inflow, as follows. For a unit width of flow, $A = y \times 1 = y$ and $Q = VA = Vy$. Substituting into equation (9.4.6) yields

$$\frac{\partial(Vy)}{\partial x} + \frac{\partial y}{\partial t} = 0 \quad (9.4.7)$$

or

$$V \frac{\partial y}{\partial x} + y \frac{\partial V}{\partial x} + \frac{\partial y}{\partial t} = 0 \quad (9.4.8)$$

9.4.2 Momentum Equation

Newton's second law is written in the form of Reynolds transport theorem as in equation (3.5.5):

$$\sum \mathbf{F} = \frac{d}{dt} \int_{CV} \mathbf{v} \rho d\forall + \sum_{CS} \mathbf{v} \rho \mathbf{V} \cdot d\mathbf{A} \quad (9.4.9)$$

This states that the sum of the forces applied is equal to the rate of change of momentum stored within the control volume plus the net outflow of momentum across the control surface. This equation, in the form $\sum F = 0$, was applied to steady uniform flow in an open channel in Chapter 5. Here, unsteady nonuniform flow is considered.

Forces. There are five forces acting on the control volume:

$$\sum F = F_g + F_f + F_e + F_p \quad (9.4.10)$$

where F_g is the *gravity force* along the channel due to the weight of the water in the control volume, F_f is the *friction force* along the bottom and sides of the control volume, F_e is the *contraction/*

expansion force produced by abrupt changes in the channel cross-section, and F_p is the *unbalanced pressure force* (see Figure 9.4.1). Each of these four forces is evaluated in the following paragraphs.

Gravity. The volume of fluid in the control volume is $A dx$ and its weight is $\rho g A dx$. For a small angle of channel inclination θ , $S_0 \approx \sin \theta$ and the gravity force is given by

$$F_g = \rho g A dx \sin \theta \approx \rho g A S_0 dx \quad (9.4.11)$$

where the channel bottom slope S_0 equals $-\partial z / \partial x$.

Friction. Frictional forces created by the shear stress along the bottom and sides of the control volume are given by $-\tau_0 P dx$, where $\tau_0 = \gamma R S_f = \rho g (A/P) S_f$ is the bed shear stress and P is the wetted perimeter. Hence the friction force is written as

$$F_f = -\rho g A S_f dx \quad (9.4.12)$$

where the friction slope S_f is derived from resistance equations such as Manning's equation.

Contraction/expansion. Abrupt contractions or expansions of the channel cause energy losses through eddy motion. Such losses are similar to minor losses in a pipe system. The magnitude of eddy losses is related to the change in velocity head $V^2/2g = (Q/A)^2/2g$ through the length of channel causing the losses. The drag forces creating these eddy losses are given by

$$F_e = -\rho g A S_e dx \quad (9.4.13)$$

where S_e is the eddy loss slope

$$S_e = \frac{K_e}{2g} \frac{\partial(Q/A)^2}{\partial x} \quad (9.4.14)$$

in which K_e is the nondimensional expansion or contraction coefficient, negative for channel expansion (where $\partial(Q/A)^2/\partial x$ is negative) and positive for channel contractions.

Pressure. Referring to Figure 9.4.1, the unbalanced pressure force is the resultant of the hydrostatic force on the each side of the control volume. Chow et al. (1988) provide a detailed derivation of the pressure force F_p as simply

$$F_p = \rho g A \frac{\partial y}{\partial x} dx \quad (9.4.15)$$

The sum of the forces in equation (9.4.10) can be expressed, after substituting equations (9.4.11), (9.4.12), (9.4.13), and (9.4.15), as

$$\sum F = \rho A S_0 dx - \rho g A S_f dx - \rho g A S_e dx - \rho g A \frac{\partial y}{\partial x} dx \quad (9.4.16)$$

Momentum. The two momentum terms on the right-hand side of equation (9.4.9) represent the rate of change of storage of momentum in the control volume, and the net outflow of momentum across the control surface, respectively.

Net momentum outflow. The mass inflow rate to the control volume (equation (9.4.2)) is $-\rho(Q + q dx)$, representing both stream inflow and lateral inflow. The corresponding momentum is computed by multiplying the two mass inflow rates by their respective velocity and a *momentum correction factor* β :

$$\int_{\text{inlet}} \mathbf{V} \rho \mathbf{V} d\mathbf{A} = -\rho(\beta V Q + \beta v_x q dx) \quad (9.4.17)$$

where $-\rho\beta V Q$ is the momentum entering from the upstream end of the channel, and $-\rho\beta v_x q dx$ is the momentum entering the main channel with the lateral inflow, which has a velocity v_x in the x

direction. The term β is known as the *momentum coefficient* or *Boussinesq coefficient*; it accounts for the nonuniform distribution of velocity at a channel cross-section in computing the momentum. The value of β is given by

$$\beta = \frac{1}{V^2 A} \int v^2 dA \quad (9.4.18)$$

where v is the velocity through a small element of area dA in the channel cross-section. The value of β ranges from 1.01 for straight prismatic channels to 1.33 for river valleys with floodplains (Chow, 1959; Henderson, 1966).

The momentum leaving the control volume is

$$\int_{\text{outlet}} \mathbf{V} \rho \mathbf{V} d\mathbf{A} = \rho \left[\beta V Q + \frac{\partial(\beta V Q)}{\partial x} dx \right] \quad (9.4.19)$$

The net outflow of momentum across the control surface is the sum of equations (9.4.17) and (9.4.19):

$$\int_{\text{CS}} \mathbf{V} \rho \mathbf{V} d\mathbf{A} = -\rho(\beta V Q + \beta v_x q dx) + \rho \left[\beta V Q + \frac{\partial(\beta V Q)}{\partial x} dx \right] = -\rho \left[\beta v_x q - \frac{\partial(\beta V Q)}{\partial x} \right] dx \quad (9.4.20)$$

Momentum storage. The time rate of change of momentum stored in the control volume is found by using the fact that the volume of the elemental channel is $A dx$, so its momentum is $\rho A dx V$, or $\rho Q dx$, and then

$$\frac{d}{dt} \int_{\text{CV}} \mathbf{V} \rho d\forall = \rho \frac{\partial Q}{\partial x} dx \quad (9.4.21)$$

After substituting the force terms from equation (9.4.16) and the momentum terms from equations (9.4.20) and (9.4.21) into the momentum equation (9.4.9), it reads

$$\rho g A S_0 dx - \rho g A S_f dx - \rho g A S_e dx - \rho g A \frac{\partial y}{\partial x} dx = -\rho \left[\beta v_x q - \frac{\partial(\beta V Q)}{\partial x} \right] dx + \rho \frac{\partial Q}{\partial t} dx \quad (9.4.22)$$

Dividing through by ρdx , replacing V with Q/A , and rearranging produces the conservation form of the momentum equation:

$$\frac{\partial Q}{\partial t} + \frac{\partial(\beta Q^2/A)}{\partial x} + gA \left(\frac{\partial y}{\partial x} - S_0 + S_f + S_e \right) - \beta q v_x = 0 \quad (9.4.23)$$

The depth y in equation (9.4.23) can be replaced by the water surface elevation h , using

$$h = y + z \quad (9.4.24)$$

where z is the elevation of the channel bottom above a datum such as mean sea level. The derivative of equation (9.4.24) with respect to the longitudinal distance x along the channel is

$$\frac{\partial h}{\partial x} = \frac{\partial y}{\partial x} + \frac{\partial z}{\partial x} \quad (9.4.25)$$

but $\partial z/\partial x = -S_0$, so

$$\frac{\partial h}{\partial x} = \frac{\partial y}{\partial x} - S_0 \quad (9.4.26)$$

The momentum equation can now be expressed in terms of h by using equation (9.4.26) in (9.4.23):

$$\frac{\partial Q}{\partial t} + \frac{\partial(\beta Q^2/A)}{\partial x} + gA \left(\frac{\partial h}{\partial x} + S_f + S_e \right) - \beta q v_x = 0 \quad (9.4.27)$$

The Saint-Venant equations, (9.4.6) for continuity and (9.4.27) for momentum, are the governing equations for one-dimensional, unsteady flow in an open channel. The use of the terms S_f and S_e in equation (9.4.27), which represent the rate of energy loss as the flow passes through the channel, illustrates the close relationship between energy and momentum considerations in describing the flow. Strelkoff (1969) showed that the momentum equation for the Saint-Venant equations can also be derived from energy principles, rather than by using Newton's second law as presented here.

The nonconservation form of the momentum equation can be derived in a similar manner to the nonconservation form of the continuity equation. Neglecting eddy losses, wind shear effect, and lateral inflow, the nonconservation form of the momentum equation for a unit width in the flow is

$$\frac{\partial V}{\partial t} + V \frac{\partial V}{\partial x} + g \left(\frac{\partial y}{\partial x} - S_0 + S_f \right) = 0 \quad (9.4.28)$$

9.5 KINEMATIC WAVE MODEL FOR CHANNELS

In Section 8.9, a kinematic wave overland flow runoff model was presented. This is an implicit nonlinear kinematic model that is used in the KINEROS model. This section presents a general discussion of the kinematic wave followed by a brief description of the very simplest linear models, such as those found in the U.S. Army Corps of Engineers HEC-HMS and HEC-1, and the more complicated models such as the KINEROS model (Woolhiser et al., 1990).

Kinematic waves govern flow when inertial and pressure forces are not important. Dynamic waves govern flow when these forces are important, as in the movement of a large flood wave in a wide river. In a kinematic wave, the gravity and friction forces are balanced, so the flow does not accelerate appreciably.

For a kinematic wave, the energy grade line is parallel to the channel bottom and the flow is steady and uniform ($S_0 = S_f$) within the differential length, while for a dynamic wave the energy grade line and water surface elevation are not parallel to the bed, even within a differential element.

9.5.1 Kinematic Wave Equations

A *wave* is a variation in a flow, such as a change in flow rate or water surface elevation, and the *wave celerity* is the velocity with which this variation travels along the channel. The celerity depends on the type of wave being considered and may be quite different from the water velocity. For a kinematic wave, the acceleration and pressure terms in the momentum equation are negligible, so the wave motion is described principally by the equation of continuity. The name kinematic is thus applicable, as *kinematics* refers to the study of motion exclusive of the influence of mass and force; in *dynamics* these quantities are included.

The kinematic wave model is defined by the following equations.

Continuity:

$$\frac{\partial Q}{\partial x} + \frac{\partial A}{\partial t} = q(x, t) \quad (9.5.1)$$

Momentum:

$$S_0 = S_f \quad (9.5.2)$$

where $q(x, t)$ is the net lateral inflow per unit length of channel.

The momentum equation can also be expressed in the form

$$A = \alpha Q^\beta \quad (9.5.3)$$

For example, Manning's equation written with $S_0 = S_f$ and $R = A/P$ is

$$Q = \frac{1.49 S_0^{1/2}}{nP^{2/3}} A^{5/3} \quad (9.5.4)$$

which can be solved for A as

$$A = \left(\frac{nP^{2/3}}{1.49\sqrt{S_0}} \right)^{3/5} Q^{3/5} \quad (9.5.5)$$

so $\alpha = [nP^{2/3}/(1.49\sqrt{S_0})]^{0.6}$ and $\beta = 0.6$ in this case.

Equation (9.5.1) contains two dependent variables, A and Q , but A can be eliminated by differentiating equation (9.5.3):

$$\frac{\partial A}{\partial t} = \alpha\beta Q^{\beta-1} \left(\frac{\partial Q}{\partial t} \right) \quad (9.5.6)$$

and substituting for $\partial A/\partial t$ in equation (9.5.1) to give

$$\frac{\partial Q}{\partial x} + \alpha\beta Q^{\beta-1} \left(\frac{\partial Q}{\partial t} \right) = q \quad (9.5.7)$$

Alternatively, the momentum equation could be expressed as

$$Q = aA^B \quad (9.5.8)$$

where a and B are defined using Manning's equation. Using

$$\frac{\partial Q}{\partial x} = \frac{dQ}{dA} \frac{\partial A}{\partial x} \quad (9.5.9)$$

the governing equation is

$$\frac{\partial A}{\partial t} + \frac{dQ}{dA} \frac{\partial A}{\partial x} = q \quad (9.5.10)$$

where dQ/dA is determined by differentiating equation (9.5.8):

$$\frac{dQ}{dA} = aBA^{B-1} \quad (9.5.11)$$

and substituting in equation (9.5.10):

$$\frac{\partial A}{\partial t} + aBA^{B-1} \frac{\partial A}{\partial x} = q \quad (9.5.12)$$

The kinematic wave equation (9.5.7) has Q as the dependent variable and the kinematic wave equation (9.5.12) has A as the dependent variable. First consider equation (9.5.7), by taking the logarithm of (9.5.3):

$$\ln A = \ln \alpha + \beta \ln Q \quad (9.5.13)$$

and differentiating

$$\frac{dQ}{Q} = \frac{1}{\beta} \left(\frac{dA}{A} \right) \quad (9.5.14)$$

This defines the relationship between relative errors dA/A and dQ/Q . For Manning’s equation $\beta < 1$, so that the discharge estimation error would be magnified by the ratio $1/\beta$ if A were the dependent variable instead of Q .

Next consider equation (9.5.12); by taking the logarithm of (9.5.8):

$$\begin{aligned} \ln Q &= \ln a + B \ln A \\ \frac{dA}{A} &= \frac{1}{B} \left(\frac{dQ}{Q} \right) \end{aligned} \tag{9.5.15}$$

or

$$\frac{dQ}{Q} = B \left(\frac{dA}{A} \right) \tag{9.5.16}$$

In this case $\beta > 1$, so that the discharge estimation error would be decreased by B if A were the dependent variable instead of Q . In summary, if we use equation (9.5.3) as the form of the momentum equation, then Q is the dependent variable with equation (9.5.7) being the governing equation; if we use equation (9.5.8) as the form of the momentum equation, then A is the dependent variable with equation (9.5.12) being the governing equation.

9.5.2 U.S. Army Corps of Engineers Kinematic Wave Model for Overland Flow and Channel Routing

The HEC-1 (HEC-HMS) computer program actually has two forms of the kinematic wave. The first is based upon equation (9.5.12) where an explicit finite difference form is used (refer to Figures 9.5.1 and 8.9.2):

$$\frac{\partial A}{\partial t} = \frac{A_{i+1}^{j+1} - A_{i+1}^j}{\Delta t} \tag{9.5.17}$$

$$\frac{\partial A}{\partial x} = \frac{A_{i+1}^j - A_i^j}{\Delta x} \tag{9.5.18}$$

and

$$A = \frac{A_{i+1}^j + A_i^j}{2} \tag{9.5.19}$$

$$q = \frac{q_{i+1}^{j+1} + q_{i+1}^j}{2} \tag{9.5.20}$$

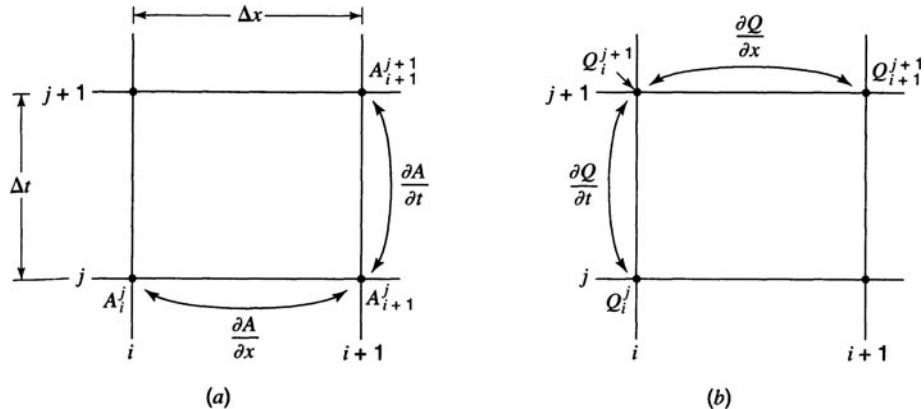


Figure 9.5.1 Finite difference forms. (a) HEC-1 “standard form;” (b) HEC-1 “conservation form.”

Substituting these finite-difference approximations into equation (9.5.12) gives

$$\frac{1}{\Delta t}(A_{i+1}^{j+1} - A_{i+1}^j) + aB \left[\frac{A_{i+1}^j + A_i^j}{2} \right]^{B-1} \left[\frac{A_{i+1}^j - A_i^j}{\Delta x} \right] = \frac{q_{i+1}^{j+1} + q_{i+1}^j}{2} \quad (9.5.21)$$

The only unknown in equation (9.5.21) is A_{i+1}^{j+1} , so

$$A_{i+1}^{j+1} = A_{i+1}^j - aB \left(\frac{\Delta t}{\Delta x} \right) \left[\frac{A_{i+1}^j + A_i^j}{2} \right]^{B-1} (A_{i+1}^j - A_i^j) + (q_{i+1}^{j+1} + q_{i+1}^j) \frac{\Delta t}{2} \quad (9.5.22)$$

After computing A_{i+1}^{j+1} at each grid along a time line going from upstream to downstream (see Figure 8.9.2), compute the flow using equation (9.5.8):

$$Q_{i+1}^{j+1} = a(A_{i+1}^{j+1})^B \quad (9.5.23)$$

The HEC-1 model uses the above kinematic wave model as long as a stability factor $R < 1$ (Alley and Smith, 1987), defined by

$$R = \frac{a}{q\Delta x} \left[(q\Delta t + A_i^j)^B - (A_i^j)^B \right] \text{ for } q > 0 \quad (9.5.24a)$$

$$R = aB(A_i^j)^{B-1} \frac{\Delta t}{\Delta x} \text{ for } q = 0 \quad (9.5.24b)$$

Otherwise the form of equation (9.5.1) is used, where (see Figure 9.5.1)

$$\frac{\partial Q}{\partial x} = \frac{Q_{i+1}^{j+1} - Q_i^{j+1}}{\Delta x} \quad (9.5.25)$$

$$\frac{\partial A}{\partial t} = \frac{A_i^{j+1} - A_i^j}{\Delta t} \quad (9.5.26)$$

so

$$\frac{Q_{i+1}^{j+1} - Q_i^{j+1}}{\Delta x} + \frac{A_i^{j+1} - A_i^j}{\Delta x} = q \quad (9.5.27)$$

Solving for the only unknown Q_{i+1}^{j+1} yields

$$Q_{i+1}^{j+1} = Q_i^{j+1} + q\Delta x - \frac{\Delta x}{\Delta t} (A_i^{j+1} - A_i^j) \quad (9.5.28)$$

Then solve for A_{i+1}^{j+1} using equation (9.5.23):

$$A_{i+1}^{j+1} = \left(\frac{1}{a} Q_{i+1}^{j+1} \right)^{1/B} \quad (9.5.29)$$

The *initial condition* (values of A and Q at time 0 along the grid, referring to Figure 8.9.2) are computed assuming uniform flow or nonuniform flow for an initial discharge. The *upstream boundary* is the inflow hydrograph from which Q is obtained.

The kinematic wave schemes used in the HEC-1 (HEC-HMS) model are very simplified. Chow, et al. (1988) presented both linear and nonlinear kinematic wave schemes based upon the equation (9.5.7) formulation. An example of a more desirable kinematic wave formulation is that by Woolhiser et al. (1990) presented in the next subsection.

9.5.3 KINEROS Channel Flow Routing Model

The KINEROS channel routing model uses the equation (9.5.10) form of the kinematic wave equation (Woolhiser et al., 1990):

$$\frac{\partial A}{\partial t} + \frac{dQ}{dA} \frac{\partial A}{\partial x} = q(x, t) \quad (9.5.10)$$

where $q(x, t)$ is the net lateral inflow per unit length of channel. The derivatives are approximated using an implicit scheme in which the spatial and temporal derivatives are, respectively,

$$\frac{\partial A}{\partial x} = \theta \frac{A_{i+1}^{j+1} - A_i^{j+1}}{\Delta x} + (1 - \theta) \frac{A_{i+1}^j - A_i^j}{\Delta x} \quad (9.5.30)$$

$$\frac{dQ}{dA} \frac{\partial A}{\partial x} = \theta \left(\frac{dQ}{dA} \right)^{j+1} \left(\frac{A_{i+1}^{j+1} - A_i^{j+1}}{\Delta x} \right) + (1 - \theta) \left(\frac{dQ}{dA} \right)^{j+1} \left(\frac{A_{i+1}^j - A_i^j}{\Delta x} \right) \quad (9.5.31)$$

and

$$\frac{\partial A}{\partial t} = \frac{1}{2} \left[\frac{A_{i+1}^{j+1} - A_i^j}{\Delta t} + \frac{A_{i+1}^{j+1} - A_{i+1}^j}{\Delta t} \right] \quad (9.5.32)$$

or

$$\frac{\partial A}{\partial t} = \frac{A_i^{j+1} + A_{i+1}^{j+1} - A_i^j - A_{i+1}^j}{2\Delta t} \quad (9.5.33)$$

Substituting equations (9.5.31) and (9.5.33) into (9.5.10), we have

$$\begin{aligned} & \frac{A_{i+1}^{j+1} - A_{i+1}^j + A_i^{j+1} - A_i^j}{2\Delta t} + \left\{ \theta \left[\left(\frac{dQ}{dA} \right)^{j+1} \left(\frac{A_{i+1}^{j+1} - A_i^{j+1}}{\Delta x} \right) \right] + (1 - \theta) \left[\left(\frac{dQ}{dA} \right)^{j+1} \left(\frac{A_{i+1}^j - A_i^j}{\Delta x} \right) \right] \right\} \\ & = \frac{1}{2} (q_{i+1}^{j+1} + q_i^{j+1} + q_{i+1}^j + q_i^j) \end{aligned} \quad (9.5.34)$$

The only unknown in this equation is A_{i+1}^{j+1} , which must be solved for numerically by use of an iterative scheme such as the Newton-Raphson method (see Appendix A).

Woolhiser et al. (1990) use the following relationship between channel discharge and cross-sectional area, which embodies the kinematic wave assumption:

$$Q = \alpha R^{m-1} A \quad (9.5.35)$$

where R is the hydraulic radius and $\alpha = 1.49S^{1/2}/n$ and $m = 5/3$ for Manning's equation.

9.5.4 Kinematic Wave Celerity

Kinematic waves result from changes in Q . An increment in flow dQ can be written as

$$dQ = \frac{\partial Q}{\partial x} dx + \frac{\partial Q}{\partial t} dt \quad (9.5.36)$$

Dividing through by dx and rearranging produces:

$$\frac{\partial Q}{\partial x} + \frac{dt}{dx} \frac{\partial Q}{\partial t} = \frac{dQ}{dx} \quad (9.5.37)$$

Equations (9.5.7) and (9.5.37) are identical if

$$\frac{dQ}{dx} = q \quad (9.5.38)$$

and

$$\frac{dx}{dt} = \frac{1}{\alpha\beta Q^{\beta-1}} \quad (9.5.39)$$

Differentiating equation (9.5.3) and rearranging gives

$$\frac{dQ}{dA} = \frac{1}{\alpha\beta Q^{\beta-1}} \quad (9.5.40)$$

and by comparing equations (9.5.39) and (9.5.40), it can be seen that

$$\frac{dx}{dt} = \frac{dQ}{dA} \quad (9.5.41)$$

or

$$c_k = \frac{dx}{dt} = \frac{dQ}{dA} \quad (9.5.42)$$

where c_k is the kinematic wave celerity. This implies that an observer moving at a velocity $dx/dt = c_k$ with the flow would see the flow rate increasing at a rate of $dQ/dx = q$. If $q = 0$, the observer would see a constant discharge. Equations (9.5.38) and (9.5.42) are the *characteristic equations* for a kinematic wave, two ordinary differential equations that are mathematically equivalent to the governing continuity and momentum equations.

The kinematic wave celerity can also be expressed in terms of the depth y as

$$c_k = \frac{1}{B} \frac{dQ}{dy} \quad (9.5.43)$$

where $dA = Bdy$.

Both kinematic and dynamic wave motion are present in natural flood waves. In many cases the channel slope dominates in the momentum equation; therefore, most of a flood wave moves as a kinematic wave. Lighthill and Whitham (1955) proved that the velocity of the main part of a natural flood wave approximates that of a kinematic wave. If the other momentum terms ($\partial V/\partial t$, $V(\partial V/\partial x)$ and $(1/g)\partial y/\partial x$) are not negligible, then a dynamic wave front exists that can propagate both upstream and downstream from the main body of the flood wave.

9.6 MUSKINGUM–CUNGE MODEL

Cunge (1969) proposed a variation of the kinematic wave method based upon the Muskingum method (see Chapter 8). With the grid shown in Figure 9.6.1, the unknown discharge Q_{i+1}^{j+1} can be expressed using the Muskingum equation ($Q_{j+1} = C_1 I_{j+1} + C_2 I_j + C_3 Q_j$):

$$Q_{i+1}^{j+1} = C_1 Q_i^{j+1} + C_2 Q_i^j + C_3 Q_{i+1}^j \quad (9.6.1)$$

where $Q_{i+1}^{j+1} = Q_{j+1}$; $Q_i^{j+1} = I_{j+1}$; $Q_i^j = I_j$; and $Q_{i+1}^j = Q_j$. The Muskingum coefficients are

$$C_1 = \frac{\Delta t - 2KX}{2K(1-X) + \Delta t} \quad (9.6.2)$$

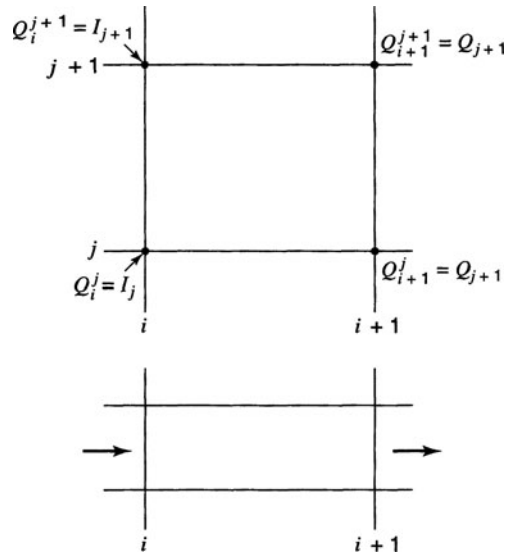


Figure 9.6.1 Finite-difference grid for the Muskingum–Cunge method.

$$C_2 = \frac{\Delta t + 2KX}{2K(1 - X) + \Delta t} \tag{9.6.3}$$

$$C_3 = \frac{2K(1 - X) - \Delta t}{2K(1 - X) + \Delta t} \tag{9.6.4}$$

Cunge (1969) showed that when K and Δt are considered constant, equation (9.6.1) is an approximate solution of the kinematic wave. He further demonstrated that equation (9.6.1) can be considered an approximation of a modified diffusion equation if

$$K = \frac{\Delta x}{c_k} = \frac{\Delta x}{dQ/dA} \tag{9.6.5}$$

and

$$X = \frac{1}{2} \left(1 - \frac{Q}{Bc_k S_0 \Delta x} \right) \tag{9.6.6}$$

where c_k is the celerity corresponding to Q and B , and B is the width of the water surface. The value of $\Delta x/(dQ/dA)$ in equation (9.6.5) represents the time propagation of a given discharge along a channel reach of length Δx . Numerical stability requires $0 \leq X \leq 1/2$. The solution procedure is basically the same as the kinematic wave.

9.7 IMPLICIT DYNAMIC WAVE MODEL

The conservation form of the Saint-Venant equations is used because this form provides the versatility required to simulate a wide range of flows from gradual long-duration flood waves in rivers to abrupt waves similar to those caused by a dam failure. The equations are developed from equations (9.4.6) and (9.4.25) as follows.

Weighted four-point finite-difference approximations given by equations (9.7.1)–(9.7.3) are used for dynamic routing with the Saint-Venant equations. The spatial derivatives $\partial Q/\partial x$ and $\partial h/\partial x$ are

estimated between adjacent time lines:

$$\frac{\partial Q}{\partial x} = \theta \frac{Q_{i+1}^{j+1} - Q_i^{j+1}}{\Delta x_i} + (1 - \theta) \frac{Q_{i+1}^j - Q_i^j}{\Delta x_i} \quad (9.7.1)$$

$$\frac{\partial h}{\partial x} = \theta \frac{h_{i+1}^{j+1} - h_i^{j+1}}{\Delta x_i} + (1 - \theta) \frac{h_{i+1}^j - h_i^j}{\Delta x_i} \quad (9.7.2)$$

and the time derivatives are:

$$\frac{\partial(A + A_0)}{\partial t} = \frac{(A + A_0)_i^{j+1} + (A + A_0)_{i+1}^{j+1} - (A + A_0)_i^j - (A + A_0)_{i+1}^j}{2\Delta t_j} \quad (9.7.3)$$

$$\frac{\partial Q}{\partial t} = \frac{Q_i^{j+1} + Q_{i+1}^{j+1} - Q_i^j - Q_{i+1}^j}{2\Delta t_j} \quad (9.7.4)$$

The nonderivative terms, such as q and A , are estimated between adjacent time lines, using:

$$q = \theta \frac{q_i^{j+1} + q_{i+1}^{j+1}}{2} + (1 - \theta) \frac{q_i^j + q_{i+1}^j}{2} = \theta \bar{q}_i^{j+1} + (1 - \theta) \bar{q}_i^j \quad (9.7.5)$$

$$A = \theta \left[\frac{A_i^{j+1} + A_{i+1}^{j+1}}{2} \right] + (1 - \theta) \left[\frac{A_i^j + A_{i+1}^j}{2} \right] = \theta \bar{A}_i^{j+1} + (1 - \theta) \bar{A}_i^j \quad (9.7.6)$$

where \bar{q}_i and \bar{A}_i indicate the lateral flow and cross-sectional area averaged over the reach Δx_i .

The finite-difference form of the continuity equation is produced by substituting equations (9.7.1), (9.7.3), and (9.7.5) into (9.4.6):

$$\begin{aligned} & \theta \left(\frac{Q_{i+1}^{j+1} - Q_i^{j+1}}{\Delta x_i} - \bar{q}_i^{j+1} \right) + (1 - \theta) \left(\frac{Q_{i+1}^j - Q_i^j}{\Delta x_i} - \bar{q}_i^j \right) \\ & + \frac{(A + A_0)_i^{j+1} + (A + A_0)_{i+1}^{j+1} - (A + A_0)_i^j - (A + A_0)_{i+1}^j}{2\Delta t_j} = 0 \end{aligned} \quad (9.7.7)$$

Similarly, the momentum equation (9.4.27) is written in finite-difference form as:

$$\begin{aligned} & \frac{Q_{i+1}^{j+1} + Q_{i+1}^{j+1} - Q_i^j - Q_{i+1}^j}{2\Delta t_j} \\ & + \theta \left[\frac{(\beta Q^2/A)_{i+1}^{j+1} - (\beta Q^2/A)_{i+1}^{j+1}}{\Delta x_i} + g\bar{A}_i^{j+1} \left(\frac{h_{i+1}^{j+1} - h_i^{j+1}}{\Delta x_i} + (\bar{S}_f)_{i+1}^{j+1} + (\bar{S}_e)_{i+1}^{j+1} \right) - (\beta q v_x)_{i+1}^{j+1} \right] \\ & + (1 - \theta) \left[\frac{(\beta Q^2/A)_{i+1}^j - (\beta Q^2/A)_{i+1}^j}{\Delta x_i} + g\bar{A}_i^j \left(\frac{h_{i+1}^j - h_i^j}{\Delta x_i} + (\bar{S}_f)_i^j + (\bar{S}_e)_i^j \right) - (\beta q v_x)_i^j \right] = 0 \end{aligned} \quad (9.7.8)$$

The four-point finite-difference form of the continuity equation can be further modified by multiplying equation (9.7.7) by Δx_i to obtain

$$\begin{aligned} & \theta \left(Q_{i+1}^{j+1} - Q_i^{j+1} - \bar{q}_i^{j+1} \Delta x_i \right) + (1 - \theta) \left(Q_{i+1}^j - Q_i^j - \bar{q}_i^j \Delta x_i \right) \\ & + \frac{\Delta x_i}{2\Delta t_j} \left[(A + A_0)_i^{j+1} + (A + A_0)_{i+1}^{j+1} - (A + A_0)_i^j - (A + A_0)_{i+1}^j \right] = 0 \end{aligned} \quad (9.7.9)$$

Similarly, the momentum equation can be modified by multiplying by Δx_i to obtain

$$\begin{aligned} & \frac{\Delta x_i}{2\Delta t_j} \left(Q_i^{j+1} + Q_{i+1}^{j+1} - Q_i^j - Q_{i+1}^j \right) \\ & + \theta \left\{ \left(\frac{\beta Q^2}{A} \right)_{i+1}^{j+1} - \left(\frac{\beta Q^2}{A} \right)_i^{j+1} + g\bar{A}_i^{j+1} \left[h_{i+1}^{j+1} - h_i^{j+1} + (\bar{S}_f)_i^{j+1} + (\bar{S}_e)_i^{j+1} \Delta x_i \right] - (\overline{\beta q v_x})_i^{j+1} \Delta x_i \right\} \\ & + (1 - \theta) \left\{ \left(\frac{\beta Q^2}{A} \right)_{i+1}^j - \left(\frac{\beta Q^2}{A} \right)_i^j + g\bar{A}_i^j \left[h_{i+1}^j - h_i^j + (\bar{S}_f)_i^j \Delta x_i + (\bar{S}_e)_i^j \Delta x_i \right] - (\overline{\beta q v_x})_i^j \Delta x_i \right\} = 0 \end{aligned} \quad (9.7.10)$$

where the average values (marked with an overbar) over a reach are defined as

$$\bar{\beta}_i = \frac{\beta_i + \beta_{i+1}}{2} \quad (9.7.11)$$

$$\bar{A}_i = \frac{A_i + A_{i+1}}{2} \quad (9.7.12)$$

$$\bar{B}_i = \frac{B_i + B_{i+1}}{2} \quad (9.7.13)$$

$$\bar{Q}_i = \frac{Q_i + Q_{i+1}}{2} \quad (9.7.14)$$

Also,

$$\bar{R}_i = \bar{A}_i / \bar{B}_i \quad (9.7.15)$$

for use in Manning's equation. Manning's equation may be solved for S_f and written in the form shown below, where the $|Q|Q$ has magnitude Q^2 and sign positive or negative depending on whether the flow is downstream or upstream, respectively:

$$(\bar{S}_f)_i = \frac{\bar{n}_i^2 |\bar{Q}_i| \bar{Q}_i}{2.208 \bar{A}_i^2 \bar{R}_i^{4/3}} \quad (9.7.16)$$

The minor headlosses arising from contraction and expansion of the channel are proportional to the difference between the squares of the downstream and upstream velocities, with a contraction/expansion loss coefficient K_e :

$$(\bar{S}_e)_i = \frac{(K_e)_i}{2g\Delta x_i} \left[\left(\frac{Q}{A} \right)_{i+1}^2 - \left(\frac{Q}{A} \right)_i^2 \right] \quad (9.7.17)$$

The terms having superscript j in equations (9.7.9) and (9.7.10) are known either from initial conditions or from a solution of the Saint-Venant equations for a previous time line. The terms g , Δx_i , β_i , K_e , C_w , and V_w are known and must be specified independently of the solution. The unknown terms are Q_i^{j+1} , Q_{i+1}^{j+1} , h_{i+1}^{j+1} , A_i^{j+1} , A_{i+1}^{j+1} , B_i^{j+1} , and B_{i+1}^{j+1} . However, all the terms can be expressed as functions of the unknowns Q_i^{j+1} , Q_{i+1}^{j+1} , h_i^{j+1} , and h_{i+1}^{j+1} , so there are actually four unknowns. The unknowns are raised to powers other than unity, so equations (9.7.9) and (9.7.10) are nonlinear equations.

The continuity and momentum equations are considered at each of the $N-1$ rectangular grids shown in Figure 9.7.1 between the upstream boundary at $i = 1$ and the downstream boundary at

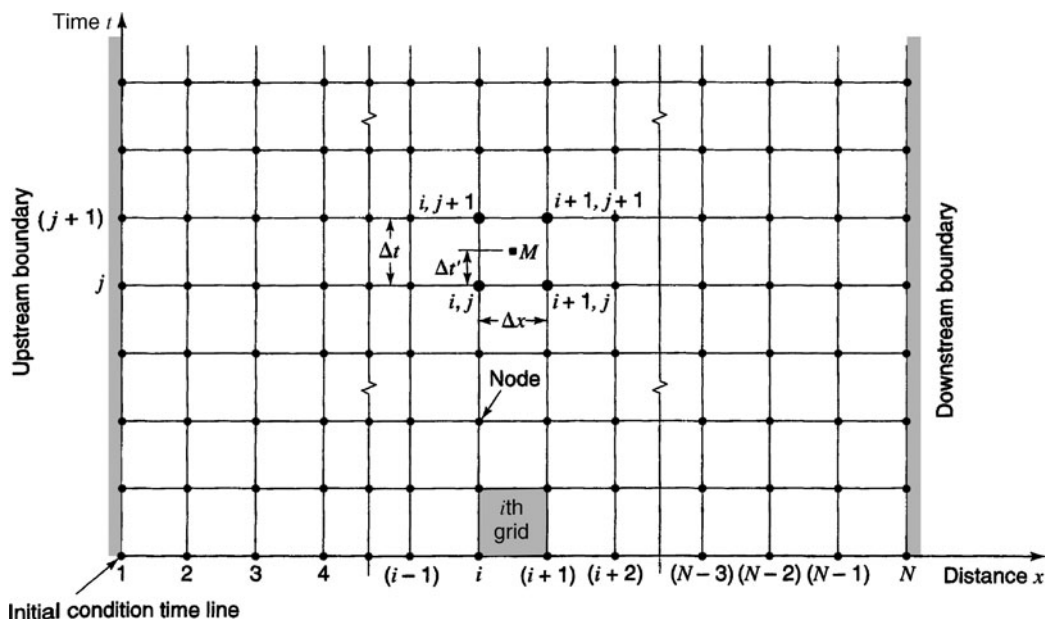


Figure 9.7.1 The $x-t$ solution plane. The finite-difference forms of the Saint–Venant equations are solved at a discrete number of points (values of the independent variables x and t) arranged to form the rectangular grid shown. Lines parallel to the time axis represent locations along the channel, and those parallel to the distance axis represent times (from Fread (1974)).

$i = N$. This yields $2N-2$ equations. There are two unknowns at each of the N grid points (Q and h), so there are $2N$ unknowns in all. The two additional equations required to complete the solution are supplied by the upstream and downstream boundary conditions. The upstream boundary condition is usually specified as a known inflow hydrograph, while the downstream boundary condition can be specified as a known stage hydrograph, a known discharge hydrograph, or a known relationship between stage and discharge, such as a rating curve. The U.S. National Weather Service FLDWAV model (hsp.nws.noaa.gov/oh/hrl/rvmech) uses the above to describe the implicit dynamic wave model formulation.

PROBLEMS

9.1.1 Consider a river segment with the surface area of 5 km^2 . For a given flood event, the measured time variation of inflow rate (called inflow hydrograph) at the upstream section of the river segment and the outflow hydrograph at the downstream section are shown in Figure P9.1.1. Assume that the initial storage of water in the river segment is 10 mm in depth.

- (a) Determine the time at which the change in storage of the river segment is increasing, decreasing, and at its maximum.
- (b) Calculate the storage change (in mm) in the river segment during the time periods of $[0, 4 \text{ hr}]$, and $[6, 8 \text{ hr}]$.
- (c) Determine the amount of water (in mm) that is ‘lost’ or ‘gained’ in the river segment over the time period of 12 hours.
- (d) What is the storage volume (in mm) at the end of the twelfth hour?

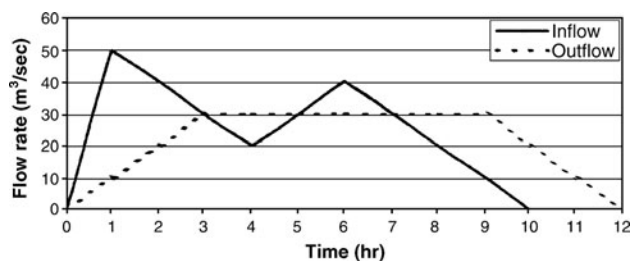


Figure P9.1.1

9.1.2 Consider a river segment with the surface area of 5 km^2 . For a given flood event, the measured time variation of inflow rate (called inflow hydrograph, in m^3/sec) at the upstream section of the river segment and the outflow hydrograph at the downstream section are shown in Figure P9.1.1. Assume that the initial storage of water in the river segment is 10 mm in depth.

- (a) Determine the time at which the change in storage of the river segment is increasing or decreasing, at its maximum.
- (b) Calculate the storage change (in mm) in the river segment during the time periods of [0, 4 hr], and [6, 8 hr].
- (c) Determine the amount of water (in mm) that is “lost” or “gained” in the river segment over the time period of 12 hr.
- (d) What is the storage volume (in mm) at the end of the 12th hour?

9.1.3 There are two reservoirs, A and B, connected in series. Reservoir A is located upstream and releases its water to reservoir B. The surface area of reservoir A is half of the surface area of B. In the past one year, the two reservoirs received the same amount of rainfall of 100 cm and evaporated 30 cm of water. However, during the same period, reservoir A experienced a change in storage of 20 cm whereas storage in reservoir B remained constant. Please clearly state any assumption used in the calculation.

- (a) Determine the outflow volume from reservoir A to B during the past year.
- (b) Determine the outflow volume from reservoir B during the past year.
- (c) How big is the flow rate from reservoir B as compared with that of reservoir A?

9.2.1 The storage-outflow characteristics for a reservoir are given below. Determine the storage-outflow function $2S/\Delta t + Q$ versus Q for each of the tabulated values using $\Delta t = 1.0$ hr. Plot a graph of the storage-outflow function.

Storage (10^6 m ³)	70	80	85	100	115
Outflow (m ³ /s)	0	50	150	350	700

9.2.2 Route the inflow hydrograph given below through the reservoir with the storage-outflow characteristics given in problem 9.2.1 using the level pool method. Assume the reservoir has an initial storage of 70×10^6 m³.

Time (h)	0	1	2	3	4	5	6	7	8
Inflow (m ³ /s)	0	40	60	150	200	300	250	200	180
Time (h)	9	10	11	12	13	14	15	16	
Inflow (m ³ /s)	220	320	400	280	190	150	50	0	

9.2.3 Rework problem 9.2.2 assuming the reservoir storage is initially 80×10^6 m³.

9.2.4 Write a computer program to solve problems 9.2.2 and 9.2.3.

9.2.5 Rework example 9.2.2 using a 1.5-acre detention basin.

9.2.6 Rework example 9.2.2 using a triangular inflow hydrograph that increases linearly from zero to a peak of 90 cfs at 120 min and then decreases linearly to a zero discharge at 240 min. Use a 30-min routing interval.

9.2.7 Consider a reservoir with surface area of 1 km². Initially, the reservoir has a storage volume of 500,000 m³ with no flow coming

out of it. Suppose it receives, from the beginning, a uniform inflow of 40 cm/h continuously for 5 hr. During the time instant when the reservoir receives the inflow, it starts to release water simultaneously. After 10 hr, the reservoir is empty and outflow becomes zero thereafter. It is also known that the outflow discharge reaches its peak value at the same time instant when the inflow stops. For simplicity, assume that the variation in outflow is linear during its rise as well as during its recession.

- (a) Determine the peak outflow discharge in m³/s.
- (b) Determine the time when the total storage volume (in m³) in the reservoir is maximum and its corresponding total storage volume.
- (c) What is the total storage volume (in m³) in the reservoir at the end of the eighth hour?

9.2.8 A rectangular reservoir equipped with an outflow-control weir has the following characteristics: $S = 5 \times h$ and $Q = 2 \times h$, in which S is the storage (m³/s-day), Q is the outflow discharge (in m³/s), and h is the water elevation (in m). With an initial water elevation being 0.25 m, route the following inflow hydrograph to determine:

- (a) the percentage of reduction in peak discharge by the reservoir; and
- (b) the peak water surface elevation.

Time	6:00 am	9:00 am	12:00 nn	3:00 pm	6:00 pm
Inflow (m ³ /S)	30	120	450	300	30

9.2.9 A rectangular detention basin is equipped with an outlet. The basin storage-elevation relationship and outflow-elevation relationship can be described by the following simple equations:

Storage-elevation relation: $S = 10 \times h$;
 Outflow-elevation relation: $Q = 2 \times h^2$

in which S is the storage (in m³/s-hr), Q is the outflow discharge (in m³/s), and h is the water elevation (in m). With an initial water elevation being 0.25 m, route the following inflow hydrograph to determine:

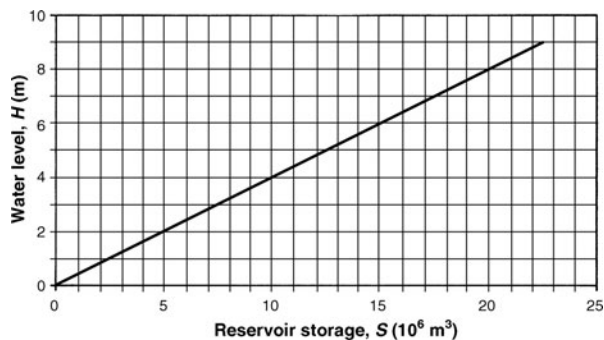
- (a) the percentage of reduction in peak discharge by the reservoir; and
- (b) the peak water surface elevation.

Time	1:00 pm	2:00 pm	3:00 pm	4:00 pm	5:00 pm	6:00 pm
Inflow (m ³ /s)	5	20	75	50	15	5

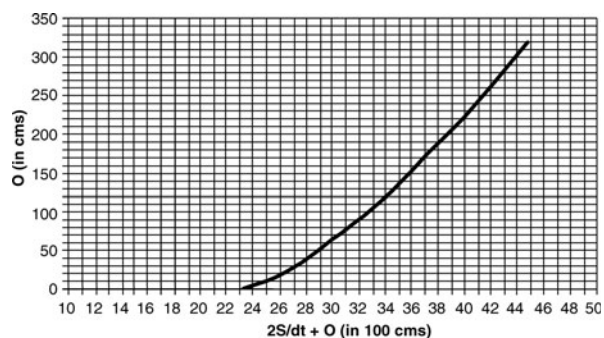
9.2.10 To investigate the effectiveness of a flood control reservoir, a 100-year design flood hydrograph is used as an input in the routing exercise. The reservoir has a surface area of 250 hectares and its only outlet is an uncontrolled spillway located 5 m above the datum. The design flood hydrograph is given in the following table and other physical characteristics of the reservoir are provided in the Figures P9.2.10a and b. Assuming that the initial reservoir level is 4 m above the datum, determine

the effectiveness of the reservoir in terms of the reduction in inflow peak discharge.

Time (hr)	0	3	6	9	12	15	18	21
Inflow (m ³ /s)	50	200	400	600	300	200	100	50



(a)



(b)

Figure P9.2.10 (a) Reservoir water level storage curve; (b) Reservoir routing curve.

9.2.11 To investigate the effectiveness of a flood control reservoir, a 100-year design flood hydrograph is used as input in the routing exercise. The reservoir has only one flow outlet located on the spillway crest with the elevation of 104 m. The reservoir has the elevation-storage-discharge relationship shown in Table 9.2.11(a). Given the design flood hydrograph as shown in Table 9.2.11(b) and assuming that the initial reservoir elevation level is at 103 m, determine the effectiveness of the reservoir in terms of the reduction in inflow peak discharge. (Note: 1 hectare = 0.01 km²)

Table 9.2.11(a) Reservoir Elevation-Storage-Outflow Relation

Elevation (m)	100	101	102	103	104	105	106	107
Storage (×10 ⁵ m ³)	50	60	70	80	92	105	120	140
Outflow (m ³ /s)	0	0	0	0	8	17	27	40

Table 9.2.11(b) Inflow Hydrograph

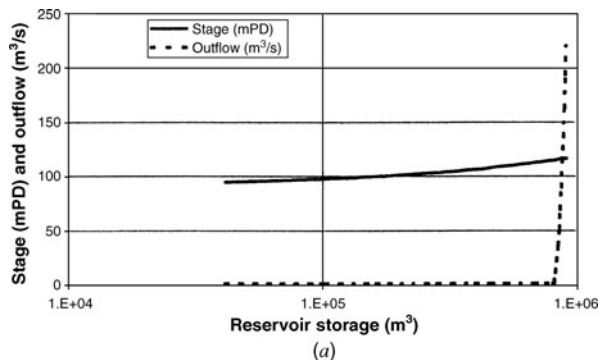
Time (hr)	0	12	24	36	48	60	72	84
Inflow (m ³ /s)	10	20	30	40	30	25	15	10

9.2.12 The Kowloon Bywash Reservoir (KBR) is located on the upstream of the Lai Chi Kok area. It is a small reservoir equipped with a tunnel with a maximum capacity of 2 m³/s delivering reservoir water to the downstream Tai Po Road water treatment plant. There is an uncontrolled spillway with the crest elevation at 115 m. The stage-volume-outflow relationships of KBR are shown in the attached table and Figure P9.2.12a. Further, the reservoir routing curve, i.e., $2S/\Delta t + O$ vs. O , for $\Delta t = 1$ hr is shown in the Figure P9.2.12b.

Elevation (mPD)	Outflow (m ³ /s)	Storage (m ³)	$2S/\Delta t + O$ (m ³ /s)
109.73	2.00	531,000	297.0
112.78	2.00	679,182	379.3
115.06	2.00	801,442	447.2
115.22	4.02	809,759	453.9
115.37	12.11	818,107	466.6
115.52	22.21	826,488	481.4
115.67	36.36	834,901	500.2
115.83	51.50	843,347	520.0
115.98	69.72	851,824	543.0
116.13	89.93	860,333	567.9
116.28	114.20	868,874	596.9
116.44	136.43	877,447	623.9
116.59	162.72	886,051	655.0
116.74	193.03	894,688	690.1
116.89	228.40	903,355	730.3

Consider the inflow hydrograph given in the table below. Determine the peak outflow discharge from the KBR and the corresponding water surface elevation and the storage volume. Assume that the initial storage in the reservoir is 500,000 m³.

Time (hr)	1	2	3	4	5	6	7
Inflow (m ³ /s)	10	80	200	150	100	60	20



(a)

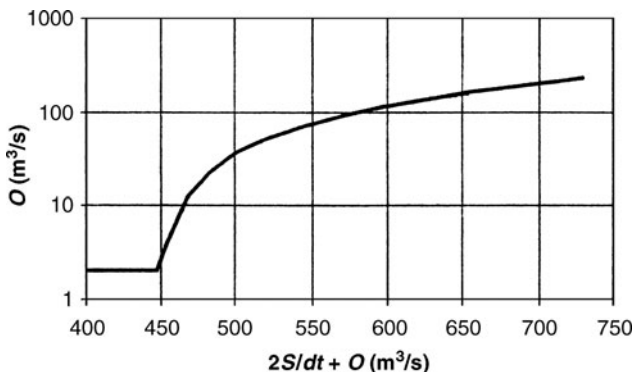


Figure P9.2.12 (a) Stage-Storage-Outflow relationship; (b) Reservoir routing curve

- 9.3.1 Rework example 9.3.4 using $\Delta t = 2$ hr.
- 9.3.2 Rework example 9.3.4 assuming $X = 0.3$.
- 9.3.3 Rework example 9.3.4 assuming $K = 1.4$ hr.
- 9.3.4 Calculate the Muskingum routing K and number of routing steps for a 1.25-mi long channel. The average cross-section dimensions for the channel are a base width of 25 ft and an average depth of 2.0 ft. Assume the channel is rectangular and has a Manning's n of 0.04 and a slope of 0.009 ft/ft.
- 9.3.5 Route the following upstream inflow hydrograph through a downstream flood control channel reach using the Muskingum method. The channel reach has a $K = 2.5$ hr and $X = 0.2$. Use a routing interval of 1 hr.

Time (h)	1	2	3	4	5	6	7
Inflow (cfs)	90	140	208	320	440	550	640
Time (h)	8	9	10	11	12	13	14
Inflow (cfs)	680	690	630	570	470	390	360
Time (h)	15	16	17	18	19	20	
Inflow (cfs)	330	250	180	130	100	90	

- 9.3.6 Use the U.S. Army Corps of Engineers HEC-HMS computer program to solve Problem 9.3.5.
- 9.3.7 A city engineer has called you wanting some information about how you would model a catchment called the Castro Valley catchment. In particular, he wants to know about how you would model the channel modifications. The 2.65-mi-long natural channel through subcatchment 1 has an approximate width of 25 ft and a Manning's n of 0.04. The slope is 0.0005 ft/ft. He thinks that a 25-ft wide trapezoidal concrete-lined channel (Manning's $n = 0.015$) would be sufficient to construct through subcatchment 1. So now you have to put together some information. Obviously you are going to have to tell him something about the channel routing procedure and the coefficients needed. He is particular and wants to know the procedure you will go through to determine these, including the number of routing steps. The natural and the concrete channels can be considered as wide-rectangular channels for your

calculations so that the hydraulic radius can be approximated as the channel depth. At this time you don't know any peak discharges because you have not done any hydrologic calculations but yet you still need to approximate the X and K for the C_1 , C_2 , and C_3 and the number of steps for the routing method. You have decided that the approximate value of X for natural conditions is about 0.2 and for the modified conditions is about 0.3. What is the value of K and the number of routing steps needed?

9.3.8 Given the following flood hydrograph entering the upstream end of a river reach, apply the Muskingum routing procedure (with $K = 2.0$ and $X = 0.1$) to determine the peak discharge at the downstream end of the river reach and the time of its occurrence. Assume that the initial flow rate at the downstream end is $10 \text{ m}^3/\text{s}$.

Time (hr)	0	3	6	9	12	15	18	21
Inflow (m^3/s)	10	70	160	210	140	80	30	10

9.3.9 Given the following flood hydrograph entering the upstream end of a river reach, apply the Muskingum routing procedure (with $K = 6.0$ and $X = 0.2$) to determine the peak discharge at the downstream end of the river reach and the time of its occurrence. Assume that the initial flow rate at the downstream end is $20 \text{ m}^3/\text{s}$.

Time (hr)	0	3	6	9	12	15	18	21
Inflow (m^3/s)	20	260	380	580	320	180	80	20

9.3.10 Given the following flood hydrograph entering the upstream end of a river reach, apply the Muskingum routing procedure (with $K = 5.0$ hr and $X = 0.2$) to determine the peak discharge at the downstream end of the river reach and the time of its occurrence. Assume that the initial flow rate at the downstream end is $10 \text{ m}^3/\text{s}$.

Time (hr)	0	2	4	6	8	10	12
Inflow (m^3/s)	10	150	400	350	200	80	10

- 9.3.11 The table given below lists the inflow hydrograph.

Time (hr)	1	2	3	4	5	6
Instantaneous discharge (m^3/s)	5	40	100	75	30	10

 - (a) Determine the percentage of attenuation in peak discharge as the hydrograph travels a distance of 10 km downstream using the Muskingum method with $X = 0.1$ and $K = 2.0$ hr. Assume that the initial outflow rate is $5 \text{ m}^3/\text{s}$.
 - (b) Also, it is known that the channel bank-full capacity 10 km downstream is $50 \text{ m}^3/\text{s}$, determine the overflow volume (in m^3) of outflow hydrograph exceeding $50 \text{ m}^3/\text{s}$.

9.3.12 From a storm event, the flood hydrographs at the upstream end and downstream end of a river reach were observed and are tabulated below.

Time (hr)	Inflow (m ³ /s)	Outflow (m ³ /s)
09:00	15	15
12:00	35	30
15:00	63	42
18:00	54	56
21:00	42	45
24:00	36	40

- (a) Determine the Muskingum parameters K and X by an appropriate method of your choice.
- (b) Determine the peak discharge for the following inflow hydrograph as it travels down the river.

Time (hr)	0	3	6	9	12	15	18	21	24	27
Inflow (m ³ /s)	10	40	80	100	60	50	40	30	20	10

9.3.13 The following table contains observed inflow and outflow hydrographs for a section of river.

Time (hr)	0	1	2	3	4	5	6
Inflow (m ³ /s)	200	400	700	550	400	300	200
Outflow (m ³ /s)	200	215	290	410	440	420	380

- (a) Determine the parameters K and X in the Muskingum model by the least-squares method.
- (b) Based on the K and X obtained in part (a), determine the outflow peak discharge for the following inflow hydrograph. What is the percentage of attenuation (reduction) in peak discharge?

Time (hr)	0	0.5	1.0	1.5	2.0	2.5	3.0
Inflow (m ³ /s)	100	400	300	200	100	100	100

9.3.14 From a storm event, the flood hydrographs at the upstream end and downstream end of a river reach are tabulated below.

Time (hr)	Inflow (m ³ /s)	Outflow (m ³ /s)
09:00	15	15
12:00	35	30
15:00	63	42
18:00	54	56
21:00	42	45

- (a) Determine the Muskingum parameters K and X by the least-squares method of your choice.
- (b) Based on the estimated values of K and X from part (a), determine the outflow peak discharge at the downstream end of the river reach for the following inflow hydrograph.

Time (hr)	0	2	4	6	8
Flow rate (m ³ /s)	20	70	50	40	30

9.3.15 Given the following flood hydrograph entering the upstream end of a river reach, apply the Muskingum routing procedure (with $K = 4.0$ hr and $X = 0.2$) to determine:

- (a) the peak discharge at the downstream end of the river reach;
- (b) the time of its occurrence; and
- (c) the percentage of peak flow attenuation.

Assume that the initial flow rate at the downstream end is 10 m³/s.

Time (hr)	0	2	4	6	8	10	12
Inflow (m ³ /s)	10	250	570	320	180	70	10

9.3.16 Consider the following flood hydrograph entering the upstream end of a river reach. Apply the Muskingum routing procedure (with $K = 6.0$ and $X = 0.2$) to:

- (a) determine the peak discharge at the downstream end of the river reach; and
- (b) find the time to peak at the downstream section.

Assume that the initial flow rate at the downstream end is 50 m³/s.

Time (hr)	0	3	6	9	12	15	18	21
Inflow (m ³ /s)	50	150	300	500	300	150	100	50

9.3.17 The Castro Valley watershed has a total watershed area of 5.51 mi² and is divided into four subcatchments as shown in Figure P9.3.17. The following table provides existing characteristics of the subcatchments.

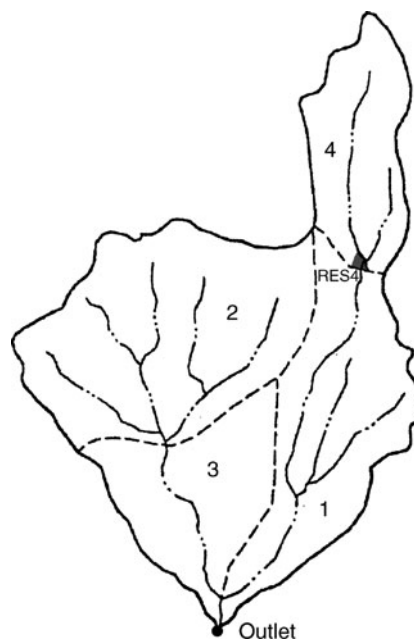


Figure P9.3.17 Castro Valley watershed

Subcatchment number	Area (mi ²)	Watershed length (L) (mi)	Length to centroid (L _{CA}) (mi)	SCS curve number
1	1.52	2.65	1.40	70
2	2.17	1.85	0.68	84
3	0.96	1.13	0.60	80
4	0.86	1.49	0.79	70

Parameters for Snyder’s synthetic unit hydrograph for existing conditions are $C_p = 0.25$ and $C_t = 0.38$. The Muskingum $K = 0.3$ hr for area 3 and $K = 0.6$ hr for area 1. The Muskingum X for each stream reach is 0.2. The rainfall to be used is the 100-year return period SCS type I storm pattern with a total rainfall of 10 in. Use the HEC-HMS model to determine the runoff hydrograph at the outlet of the watershed.

9.3.18 For the watershed described in problem 9.3.17, a residential development will be considered for area 4. This development will increase the impervious area so that the SCS curve number will be 85. The unit hydrograph parameters will change to $C_t = 0.19$ and $C_p = 0.5$. The natural channel through area 1 will be modified so that the Muskingum routing parameters will be $K = 0.4$ hr and $X = 0.3$. Use the HEC-HMS model to determine the change in the runoff hydrographs for area 4 and for the entire watershed.

9.3.19 Refer to problems 9.3.17 and 9.3.18. A detention basin is to be constructed at the outlet of area 4 with a low-level outlet and an overflow spillway (ogee type). The low-level outlet is a 5-ft-diameter pipe (orifice coefficient = 0.71) at a center line elevation of 391 ft above mean sea level (MSL). The overflow spillway has a length of 30 ft, crest elevation of 401.8 ft (above MSL), and a weir coefficient of 2.86. The characteristics of the detention basin are given in the following table.

Reservoir capacity (ac-ft)	Elevation (ft above MSL)
0	388.5
6	394.2
12	398.2
18	400.8
23	401.8
30	405.8

Use the HEC-HMS model to determine the runoff hydrograph at the watershed outlet for the developed conditions with the detention basin. Graphically show a comparison of the runoff hydrograph for the undeveloped, developed, and developed conditions with the detention basin.

9.3.20 Use the HEC-HMS model to solve problems 9.3.17, 9.3.18, and 9.3.19 considering the three as plans 1, 2, and 3 and solve through one simulation.

9.5.1 Determine the $\partial Q/\partial x$ on the time line $j + 1$ for the linear kinematic wave model. Consider a 100-ft-wide rectangular channel with a bed slope of 0.015 ft/ft and a Manning’s $n = 0.035$. The distance between cross-sections is 3000 ft and the routing time interval is 10 min. $Q_i^{j+1} = 1000$ cfs, $Q_i^j = 800$ cfs, and $Q_{i+1}^j = 700$ cfs. Use the linear kinematic wave (conservation form) approach to compute $\partial Q/\partial x$ on time line $j + 1$.

9.5.2 Develop a flow chart of the linear kinematic wave (conservation form) method.

9.6.1 Determine the $\partial Q/\partial A$ using Q_i^{j+1} and Q_{i+1}^j for the Muskingum–Cunge model. Consider a 100-ft-wide rectangular channel with a bed slope of 0.015 ft/ft and a Manning’s $n = 0.035$. The distance between cross-sections is 2000 ft and the routing time interval is 10 min. Given are $Q_i^{j+1} = 1000$ cfs, $Q_i^j = 800$ cfs, and $Q_{i+1}^j = 700$ cfs. Next compute K and x and then the routing coefficients.

9.6.2 Develop a flowchart of the Muskingum–Cunge method.

REFERENCES

Alley, W. M., and P. E. Smith, *Distributed Routing Rainfall-Runoff Model, Open File Report 82-344*, U.S. Geological Survey, Reston, VA, 1987.

Chow, V. T., *Open Channel Hydraulics*, McGraw-Hill, New York, 1959.

Chow, V. T., D. R. Maidment, and L. W. Mays, *Applied Hydrology*, McGraw-Hill, New York, 1988.

Cudworth, A. G., Jr., *Flood Hydrology Manual*, U. S. Department of the Interior, Bureau of Reclamation, Denver, CO, 1989.

Cunge, J. A., “On the Subject of a Flood Propagation Method (Muskingum Method),” *Journal of Hydraulics Research*, International Association of Hydraulic Research, vol. 7, no. 2, pp. 205–230, 1969.

Fread, D. L., *Numerical Properties of Implicit Form-Point Finite Difference Equation of Unsteady Flow*, NOAA Technical Memorandum NWS HYDRO 18, National Weather Service, NOAA, U.S. Dept. of Commerce, Silver Spring, MD, 1974.

Henderson, F. M., *Open Channel Flow*, Macmillan, New York, 1966.

Hewlett, J. D., *Principles of Forest Hydrology*, University of Georgia Press, Athens, GA, 1982.

Lighthill, M. J., and G. B. Whitham, “On Kinematic Waves, I: Flood Movement in Long Rivers,” *Proc. Roy. Soc. London A*, vol. 229, no. 1178, pp. 281–316, 1955.

Masch, F. D., *Hydrology*, Hydraulic Engineering Circular No. 19, FHWA-10-84-15, Federal Highway Administration, U.S. Department of the Interior, McLean, VA, 1984.

Strelkoff, T., “The One-Dimensional Equations of Open-Channel Flow,” *Journal of the Hydraulics Division*, American Society of Civil Engineers, vol. 95, no. Hy3, pp. 861–874, 1969.

U.S. Army Corps of Engineers, “Routing of Floods Through River Channels,” *Engineer Manual*, 1110-2-1408, Washington, DC, 1960.

U.S. Army Corps of Engineers, Hydrologic Engineering Center, *HEC-1, Flood Hydrograph Package, User’s Manual*, Davis, CA, 1990.

Woolhiser, D. A., R. E. Smith, and D. C. Goodrich, *KINEROS, A Kinematic Runoff and Erosion Model: Documentation and User Manual*, U. S. Department of Agricultural Research Service, ARS-77, Tucson, AZ, 1990.

Probability, Risk, and Uncertainty Analysis for Hydrologic and Hydraulic Design

10.1 PROBABILITY CONCEPTS

This section very briefly covers probability concepts that are important in the probabilistic, risk, and uncertainty analysis for hydrologic and hydraulic design and analysis. Table 10.1.1 provides definitions of the various probability concepts needed for analysis. Many hydraulic and hydrologic variables must be treated as random variables because of the uncertainties involved in the respective hydraulic and hydrologic processes. As an example, the extremes that occur are random hydrologic events and can therefore be treated as such.

A *random variable* X is a variable described by a *probability distribution*. The distribution specifies the chance that an observation x of the variable will fall in a specified range of X . A set of observations x_1, x_2, \dots, x_n , of the random variable X is called a *sample*. It is assumed that samples are drawn from a population (generally unknown) possessing constant statistical properties, while the properties of a sample may vary from one sample to another. The possible range of variation of all of the samples that could be drawn from the population is called the *sample space*, and an *event* is a subset of the sample space.

A *probability distribution* is a function representing the frequency of occurrence of the value of a random variable. By fitting a distribution to a set of data, a great deal of the probabilistic information in the sample can be compactly summarized in the function and its associated parameters. Fitting distributions can be accomplished by the method of moments or the method of maximum likelihood (see Chow et al., 1988). Between the two methods, the method of moments is more widely used, primarily for its computational simplicity. The method relates the parameters in a probability distribution model to the statistical moments to which the parameter-moment relationships for commonly used distributions in frequency analysis and reliability analysis are immediately available (see Table 10.1.2). In practice, the true mechanism that generates the observed random process is not entirely known. Therefore, to estimate the parameter values in a probability distribution model by the method of moments, sample moments are used.

Table 10.1.1 Various Parameters and Statistics Used to Describe Populations and Samples

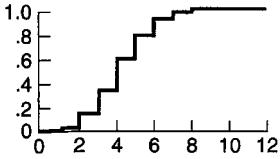
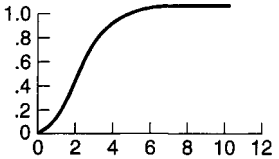
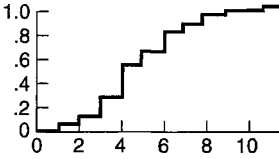
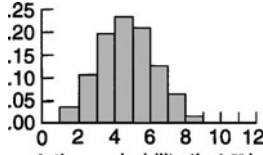
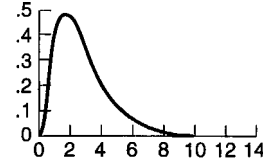
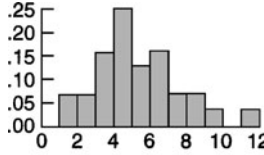
Concept	Population value, Discrete case	Population value, Continuous case	Sample value
Cumulative distribution function (cdf)	 <p>Describes the probability that a random variable is less than or equal to a specified value x</p>	 <p>Describes the probability that a random variable is less than or equal to a specified value x</p>	 <p>Empirical distribution function (edf): describes the observed frequency of a random variable being less than or equal to a specified value x</p>
Probability mass function (pmf) and probability density function (pdf)	 <p>pmf: the probability that X is equal to k</p>	 <p>pdf: first derivative of the cumulative distribution function</p>	 <p>Histogram: observed frequency with which random variable X falls into the assigned ranges</p>
Mean, average, or expected value	$\sqrt{0.368}$	$f(x) \equiv \frac{dF(x)}{dx}$ $\mu \equiv \int_{-\infty}^{\infty} xf(x)dx$	$\bar{X} \equiv \sum_{i=1}^n \frac{X_i}{n}$
Variance	$\sigma^2 \equiv \sum_{i=1}^{\infty} P(X = x_i)(x_i - \mu)^2$	$\sigma^2 \equiv \int_{-\infty}^{\infty} (x - \mu)^2 f(x)dx$	$S^2 \equiv \sum_{i=1}^n \frac{(X_i - \bar{X})^2}{n - 1}$
k th central moment	$M_k \equiv \sum_{i=1}^{\infty} P(X = x_i)(x_i - \mu)^k$	$M_k \equiv \int_{-\infty}^{\infty} (x - \mu)^k f(x)dx$	$\bar{M}_k \equiv \sum_{i=1}^n \frac{(X_i - \bar{X})^k}{n}$
Standard deviation		$\sigma \equiv \sqrt{\sigma^2}$	$S \equiv \sqrt{S^2}$
Coefficient of variation or relative standard deviation (if $\mu \neq 0$)		$CV \equiv \frac{\sigma}{\mu}$	$CV \equiv \frac{S}{\bar{X}}$
Coefficient of skew (a measure of asymmetry)		$\gamma \equiv \frac{M_3}{\sigma^3}$	$G \equiv \frac{\bar{M}_3}{S^3}$
Quantiles	x_p is any value of X that has the properties that		\hat{x}_p is the p th quantile of edf
	$P[X < x_p] \leq p$ $P[X > x_p] \leq 1 - p$		
		$x_{0.5}$	$\hat{X}_{0.5}$
Median (useful for describing central tendency regardless of skewness)	Any value of X that has the property that		The middle observation in a sorted sample, or the average of the two middle observations if the sample size is even.
	$P[X < x_p] \leq 0.5$ $P[X > x_p] \leq 0.5$		

Table 10.1.1 (Continued)

Concept	Population value, Discrete case	Population value, Continuous case	Sample value
Upper quartile, lower quartile, and hinges	Upper quartile = $x_{0.75}$ Lower quartile = $x_{0.25}$		Upper hinge = $\widehat{X}_{0.75}$ This is an approximation to the sample upper quartile; it is defined as the median of all sample values of $X \leq x_{0.50}$. The lower hinge, $\widehat{X}_{0.25}$, is defined analogously.
Interquartile range (useful for describing spread of data regardless of symmetry)	$x_{0.75} - x_{0.25}$ Width of central region of population containing probability of 0.5		$\widehat{X}_{0.75} - \widehat{X}_{0.25}$ Width of central region of data set encompassing approximately half the data

Source: Hirsh, et al (1993).

Table 10.1.2 Probability Distributions Commonly Used

Distribution	Probability density function	Range	Parameter-Moment relations
Normal	$f(x) = \frac{1}{\sqrt{2\pi}\sigma} e^{-(x-\mu)^2/2\sigma^2}$	$-\infty < x < \infty$	
Log-normal	$f(x) = \frac{1}{\sqrt{2\pi x}\sigma_{\ln x}} e^{-(\ln x - \mu_{\ln x})^2/(2\sigma_{\ln x}^2)}$	$x > 0$	$\mu_{\ln x} = \frac{1}{2} \ln \left[\frac{\mu_x^2}{1 + \Omega_x^2} \right]$ $\sigma_{\ln x}^2 = \ln(1 + \Omega_x^2)$ $\Omega_x = \sigma_x/\mu_x$
Exponential	$f(x) = \lambda e^{-\lambda x}$	$x \geq 0$	$\lambda = \frac{1}{\mu_x}$
Gamma	$f(x) = \frac{\lambda^\beta x^{\beta-1} e^{-\lambda x}}{\Gamma(\beta)}$ where $\Gamma =$ gamma function	$x \geq 0$	$\lambda = \frac{\mu_x}{\sigma_x^2}, \beta = \frac{\mu_x^2}{\sigma_x^2} = \frac{1}{C_v^2}$
Extreme Value Type I	$f(x) = \frac{1}{\alpha} e^{-(x-\beta)/\alpha} e^{-e^{-(x-\beta)/\alpha}}$	$-\infty < x < \infty$	$\alpha = \sqrt{6}\sigma_x/\pi$ $\beta = \mu_x - 0.5772\alpha$
Log Pearson Type III	$f(x) = \frac{\lambda^\beta (y - \epsilon)^{\beta-1} e^{-\lambda(y - \epsilon)}}{x\Gamma(\beta)}$ where $y = \log x$	$\log x \geq \epsilon$	$\lambda = \frac{s_y}{\sqrt{\beta}},$ $\beta = \left[\frac{2}{G_s(y)} \right]^2$ $\epsilon = \bar{y} - s_y \sqrt{\beta}$ (assuming $G_s(y)$ is positive)

10.2 COMMONLY USED PROBABILITY DISTRIBUTIONS

Of the distributions presented in Table 10.1.2, only the normal and log-normal distributions are discussed in this subsection. Section 10.4 discusses the Pearson Type III distribution. Section 10.6 discusses the exponential distribution.

10.2.1 Normal Distribution

The normal distribution is a well-known probability distribution, also called the *Gaussian distribution*. Two parameters are involved in a normal distribution: the mean and the variance. A normal random variable having a mean μ and a variance σ^2 is herein denoted as $X \sim N(\mu, \sigma^2)$ with a PDF (probability density function) of

$$f(x) = \frac{1}{\sqrt{2\pi}\sigma} \exp\left[-\frac{1}{2}\left(\frac{x-\mu}{\sigma}\right)^2\right] \quad \text{for } -\infty < x < \infty \quad (10.2.1)$$

A normal distribution is bell-shaped and symmetric with respect to $x = \mu$. Therefore, the skew coefficient for a normal random variable is zero. A random variable Y that is a linear function of a normal random variable X is also normal. That is, if $X \sim N(\mu, \sigma^2)$ and $Y = aX + b$ then $Y \sim N(a\mu + b, a^2\sigma^2)$. An extension of this theorem is that the sum of normal random variables (independent or dependent) is also a normal random variable.

Probability computations for normal random variables are made by first transforming to the standardized variate as

$$Z = (X - \mu)/\sigma \quad (10.2.2)$$

in which Z has a zero mean and unit variance. Since Z is a linear function of the random variable X , Z is also normally distributed. The PDF of Z , called the *standard normal distribution*, can be expressed as

$$\phi(z) = \frac{1}{\sqrt{2\pi}} \exp\left[-\frac{z^2}{2}\right] \quad \text{for } -\infty < z < \infty \quad (10.2.3)$$

A table of the CDF of Z is given in Table 10.2.1. Computations of probability for $X \sim N(\mu, \sigma^2)$ can be performed using

$$P(X \leq x) = P\left[\frac{X - \mu}{\sigma} \leq \frac{x - \mu}{\sigma}\right] = P[Z \leq z] = \Phi(z) \quad (10.2.4)$$

where $\Phi(z)$ is the CDF of the standard normal random variable Z defined as

$$\Phi(z) = \int_{-\infty}^z \phi(z) dz \quad (10.2.5)$$

10.2.2 Log-Normal Distribution

The log-normal distribution is a commonly used continuous distribution in hydrologic event analysis when random variables cannot be negative. A random variable X is said to be log-normally distributed if its logarithmic transform $Y = \ln(X)$ is normally distributed with mean $\mu_{\ln X}$ and variance $\sigma_{\ln X}^2$. The PDF of the log-normal random variable is

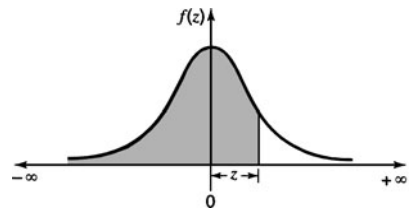
$$f(X) = \frac{1}{\sqrt{2\pi X} \sigma_{\ln X}} \exp\left[-\frac{1}{2}\left(\frac{\ln X - \mu_{\ln X}}{\sigma_{\ln X}}\right)^2\right] \quad \text{for } 0 < X < \infty \quad (10.2.6)$$

Table 10.2.1 Cumulative Probability of the Standard Normal Distribution*

<i>z</i>	.00	.01	.02	.03	.04	.05	.06	.07	.08	.09
0	0.5000	0.5040	0.5080	0.5120	0.5160	0.5199	0.5239	0.5279	0.5319	0.5359
0.1	0.5398	0.5438	0.5478	0.5517	0.5557	0.5596	0.5636	0.5675	0.5714	0.5753
0.2	0.5793	0.5832	0.5871	0.5910	0.5948	0.5987	0.6026	0.6064	0.6103	0.6141
0.3	0.6179	0.6217	0.6255	0.6293	0.6331	0.6368	0.6406	0.6443	0.6480	0.6517
0.4	0.6554	0.6591	0.6628	0.6664	0.6700	0.6736	0.6772	0.6808	0.6844	0.6879
0.5	0.6915	0.6950	0.6985	0.7019	0.7054	0.7088	0.7123	0.7157	0.7190	0.7224
0.6	0.7257	0.7291	0.7324	0.7357	0.7389	0.7422	0.7454	0.7486	0.7517	0.7549
0.7	0.7580	0.7611	0.7642	0.7673	0.7704	0.7734	0.7764	0.7794	0.7823	0.7852
0.8	0.7881	0.7910	0.7939	0.7967	0.7995	0.8023	0.8051	0.8078	0.8106	0.8133
0.9	0.8159	0.8186	0.8212	0.8238	0.8164	0.8289	0.8315	0.8340	0.8365	0.8389
1.0	0.8413	0.8438	0.8461	0.8485	0.8508	0.8531	0.8554	0.8577	0.8599	0.8621
1.1	0.8643	0.8665	0.8686	0.8708	0.8729	0.8749	0.8770	0.8790	0.8810	0.8830
1.2	0.8849	0.8869	0.8888	0.8907	0.8925	0.8944	0.8962	0.8980	0.8997	0.9015
1.3	0.9032	0.9049	0.9066	0.9082	0.9099	0.9115	0.9131	0.9147	0.9162	0.9177
1.4	0.9192	0.9207	0.9222	0.9236	0.9251	0.9265	0.9279	0.9292	0.9306	0.9319
1.5	0.9332	0.9345	0.9357	0.9370	0.9382	0.9394	0.9406	0.9418	0.9429	0.9441
1.6	0.9452	0.9463	0.9474	0.9484	0.9495	0.9505	0.9515	0.9525	0.9535	0.9545
1.7	0.9554	0.9564	0.9573	0.9582	0.9591	0.9599	0.9608	0.9616	0.9625	0.9633
1.8	0.9641	0.9649	0.9656	0.9664	0.9671	0.9678	0.9686	0.9693	0.9699	0.9706
1.9	0.9713	0.9719	0.9726	0.9732	0.9738	0.9744	0.9750	0.9756	0.9761	0.9767
2.0	0.9772	0.9778	0.9783	0.9788	0.9793	0.9798	0.9803	0.9808	0.9812	0.9817
2.1	0.9821	0.9826	0.9830	0.9834	0.9838	0.9842	0.9846	0.9850	0.9854	0.9857
2.2	0.9861	0.9864	0.9868	0.9871	0.9875	0.9878	0.9881	0.9884	0.9887	0.9890
2.3	0.9893	0.9896	0.9898	0.9901	0.9904	0.9906	0.9909	0.9911	0.9913	0.9916
2.4	0.9918	0.9920	0.9922	0.9925	0.9927	0.9929	0.9931	0.9932	0.9934	0.9936
2.5	0.9938	0.9940	0.9941	0.9943	0.9945	0.9946	0.9948	0.9949	0.9951	0.9952
2.6	0.9953	0.9955	0.9956	0.9957	0.9959	0.9960	0.9961	0.9962	0.9963	0.9964
2.7	0.9965	0.9966	0.9967	0.9968	0.9969	0.9970	0.9971	0.9972	0.9973	0.9974
2.8	0.9971	0.9975	0.9976	0.9977	0.9977	0.9978	0.9979	0.9979	0.9980	0.9981
2.9	0.9981	0.9982	0.9982	0.9983	0.9984	0.9984	0.9985	0.9985	0.9986	0.9986
3.0	0.9987	0.9987	0.9987	0.9988	0.9988	0.9989	0.9989	0.9989	0.9990	0.9990
3.1	0.9990	0.9991	0.9991	0.9991	0.9992	0.9992	0.9992	0.9992	0.9993	0.9993
3.2	0.9993	0.9993	0.9994	0.9994	0.9994	0.9994	0.9994	0.9995	0.9995	0.9995
3.3	0.9995	0.9995	0.9995	0.9996	0.9996	0.9996	0.9996	0.9996	0.9996	0.9997
3.4	0.9997	0.9997	0.9997	0.9997	0.9997	0.9997	0.9997	0.9997	0.9997	0.9998

*To employ the table for $z < 0$, use $F_z(z) = 1 - F_z(|z|)$ where $F_z(|z|)$ is the tabulated value.

Source: Grant and Leavenworth (1972).



which can be derived from the normal PDF, that is, equation (10.2.1). Statistical properties of a log-normal random variable of the original scale can be computed from those of the log-transformed variable. To compute the statistical moments of X from those of $\ln X$, the following formulas are useful:

$$\mu_x = \exp(\mu_{\ln X} + \sigma_{\ln X}^2/2) \tag{10.2.7}$$

$$\sigma_X^2 = \mu_X^2 [\exp(\sigma_{\ln X}^2) - 1] \quad (10.2.8)$$

$$\Omega_X^2 = \exp(\sigma_{\ln X}^2) - 1 \quad (10.2.9)$$

$$\lambda_X = \Omega_X^2 + 3\Omega_X \quad (10.2.10)$$

From equation (10.2.10), it is obvious that log-normal distributions are always positively skewed because $\Omega_X > 0$. Conversely, the statistical moments of $\ln X$ can be computed from those of X by

$$\mu_{\ln X} = \frac{1}{2} \ln \left[\frac{\mu_X^2}{1 + \Omega_X^2} \right] \quad (10.2.11)$$

$$\sigma_{\ln X}^2 = \ln(\Omega_X^2 + 1) \quad (10.2.12)$$

Since the sum of normal random variables is normally distributed, the multiplication of log-normal random variables is also log-normally distributed. Several properties of log-normal random variables are useful:

1. If X is a log-normal random variable and $Y = aX^b$, then Y has a log-normal distribution with mean $\mu_{\ln Y} = \ln a + b\mu_{\ln X}$ and variance $\sigma_{\ln Y}^2 = b^2\sigma_{\ln X}^2$.
2. If X and Y are independently log-normally distributed, $W = XY$ has a log-normal distribution with mean $\mu_{\ln W} = \mu_{\ln X} + \mu_{\ln Y}$ and variance $\sigma_{\ln W}^2 = \sigma_{\ln X}^2 + \sigma_{\ln Y}^2$.
3. If X and Y are independent and log-normally distributed, then $R = X/Y$ is log-normal with $\mu_{\ln R} = \mu_{\ln X} - \mu_{\ln Y}$ and variance $\sigma_{\ln R}^2 = \sigma_{\ln X}^2 + \sigma_{\ln Y}^2$.

EXAMPLE 10.2.1

The annual maximum series of flood magnitudes in a river is assumed to follow a log-normal distribution with a mean of 6000 m³/s and a standard deviation of 4000 m³/s. (a) What is the probability in each year that a flood magnitude would exceed 7000 m³/s? (b) Determine the flood magnitude with a return period of 100 years.

SOLUTION

- (a) Let Q be a random variable representing the annual maximum flood magnitude. Since Q is assumed to follow a log-normal distribution, $\ln(Q)$ is normally distributed with mean and variance that can be computed using $\mu_Q = 6000$ and $\Omega_Q = \sigma_Q/\mu_Q = 4000/6000 = 0.667$. By equations (10.2.11) and (10.2.12), respectively, we find

$$\mu_{\ln Q} = \frac{1}{2} \ln \left[\frac{\mu_Q^2}{1 + \Omega_Q^2} \right] = \frac{1}{2} \ln \left[\frac{6000^2}{1 + 0.667^2} \right] = 8.515$$

$$\sigma_{\ln Q}^2 = \ln(\Omega_Q^2 + 1) = \ln(0.667^2 + 1) = 0.368$$

The probability that the flood magnitude exceeds 7000 m³/s is

$$\begin{aligned} P(Q > 7000) &= P(\ln Q > \ln 7000) = 1 - P(\ln Q \leq \ln 7000) \\ &= 1 - P\left\{ \frac{(\ln Q - \mu_{\ln Q})/\sigma_{\ln Q}}{1} \leq \frac{(\ln 7000 - \mu_{\ln Q})/\sigma_{\ln Q}}{1} \right\} \\ &= 1 - P[Z \leq (\ln 7000 - 8.515)/\sqrt{0.368}] \\ &= 1 - P[Z \leq 0.558] \\ &= 1 - F(0.558) = 1 - 0.712 = 0.288 \end{aligned}$$

- (b) A 100-year event in hydrology represents the event that occurs, on the average, once every 100 years. Therefore, the probability in every single year that a 100-year event is equaled or exceeded is 0.01, i.e., $P(Q \geq q_{100}) = 0.01$ in which q_{100} is the magnitude of the 100-year flood. This part of the problem is to determine q_{100} , which is the reverse of part (a).

$$P(Q \leq q_{100}) = 1 - P(Q = q_{100}) = 1 - 0.01 = 0.99$$

$$\text{Since } P(Q \leq q_{100}) = P[\ln Q \leq \ln q_{100}] = P[Z \leq (\ln q_{100} - \mu_{\ln Q})/\sigma_{\ln Q}] = 0.99,$$

$$0.99 = P[Z \leq (\ln q_{100} - 8.515)/\sqrt{0.368}]$$

$$0.99 = \Phi\{(\ln q_{100} - 8.515)/\sqrt{0.368}\}$$

$$0.99 = \Phi(z)$$

From the standard normal probability table (Table 10.2.1), $z = 2.33$ for $\Phi(2.33) = 0.99$. Solving $z = (\ln q_{100} - 8.515)/\sqrt{0.368}$ for q_{100} first yields $\ln q_{100} = 9.928$, then $q_{100} = 20,500 \text{ m}^3/\text{s}$.

10.2.3 Gumbel (Extreme Value Type I) Distribution

Gumbel (extreme value type I) distribution is another probability distribution function useful for hydrologic analysis, particularly rainfall analysis. The probability distribution function is presented in Table 10.1.2 and the CDF is

$$F(x) = \exp\{-\exp[-(x - \beta)/\alpha]\} \quad -\infty < x < \infty \quad (10.2.13)$$

The parameters are estimated as

$$\alpha = 6^{0.5} \sigma_x / \pi \quad (10.2.14)$$

$$\beta = \mu_x - 0.5772\alpha \quad (10.2.15)$$

where β is the mode (point of maximum probability) of the distribution. The inverse of the CDF is

$$x = \beta - \alpha \ln[-\ln F] \quad (10.2.16)$$

EXAMPLE 10.2.2

Using an exceedance series of 30-min duration rainfall values, the mean is 1.09 in and the standard deviation is 0.343 in. Determine the 100-year 30-min duration rainfall value using the Gumbel (extreme value type I) distribution.

SOLUTION

Determine the parameters α and β .

$$\alpha = 6^{0.5} \sigma_x / \pi = 6^{0.5} (0.343) / 3.14 = 0.268$$

$$\beta = \mu_x - 0.5772\alpha = 1.09 - 0.5772(0.268) = 0.935$$

Use the parameters α and β in the CDF with $F(x) = 1 - 0.01$ where 0.01 is the probability in any given year that the 100-year 30-min duration rainfall is equaled or exceeded, i.e., $P(x \geq x_{100}) = 1/100 = 0.01$.

$$F(x) = \exp\{-\exp[-(x - 0.935)/0.268]\} = 1 - 0.01 = 0.99$$

The inverse of the CDF $F(x)$ is $x = \beta - \alpha \ln[-\ln F]$ so that the 100-year 30-min duration rainfall is $x = 0.935 - 0.268 \ln[-\ln 0.99] = 2.167$ in.

10.3 HYDROLOGIC DESIGN FOR WATER EXCESS MANAGEMENT

Hydrologic design is the process of assessing the impact of hydrologic events on a water resource system and choosing values for the key variables of the system so that it will perform adequately (Chow et al., 1988). This section focuses on water excess management; however, many of the concepts are applicable to water supply (use) management.

10.3.1 Hydrologic Design Scale

The *hydrologic design scale* is the range in magnitude of the design variable (such as the design discharge) within which a value must be selected to determine the inflow to the system (see Figure 10.3.1). The most important factors in selecting the design value are cost and safety. The optimal magnitude for design is one that balances the conflicting considerations of cost and safety. The practical upper limit of the hydrologic design scale is not infinite, since the global hydrologic cycle is a closed system; that is, the total quantity of water on earth is essentially constant. Although the true upper limit is unknown, for practical purposes an estimated upper limit may be determined. This *estimated limiting value (ELV)* is defined as the largest magnitude possible for a hydrologic event at a given location, based on the best available hydrologic information.

The concept of an estimated limiting value is implicit in the *probable maximum precipitation (PMP)* and the corresponding *probable maximum flood (PMF)*. The probable maximum precipitation is defined by the World Meteorological Organization (1983) as a “quantity of precipitation that is close to the physical upper limit for a given duration over a particular basin.” However, the return period varies geographically. Some arbitrarily assign a return period, say 10,000 years, to the PMP or PMF, but this has no physical basis.

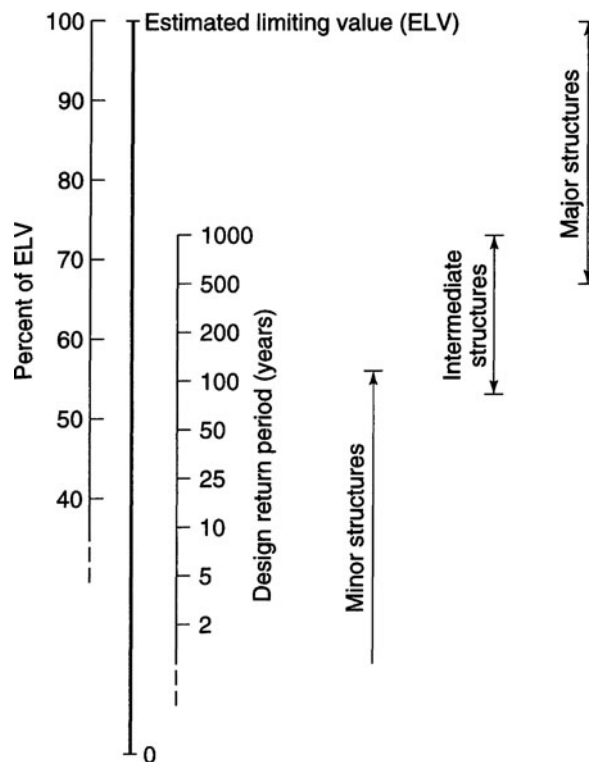


Figure 10.3.1 Hydrologic design scale. Approximate ranges of the design level for different types of structures are shown. Design may be based on a percentage of the ELV or on a design return period. The values for the two scales shown in the diagram are illustrative only and do not correspond directly with one another (from Chow et al. (1988)).

Table 10.3.1 Generalized Design Criteria for Water-Control Structures

Type of structure	Return period (Years)	ELV (%)
Highway culverts		
Low traffic	5–10	—
Intermediate traffic	10–25	—
High traffic	50–100	—
Highway bridges		
Secondary system	10–50	—
Primary system	50–100	—
Farm drainage		
Culverts	5–50	—
Ditches	5–50	—
Urban drainage		
Storm sewers in small cities	2–25	—
Storm sewers in large cities	25–50	—
Airfields		
Low traffic	5–10	—
Intermediate traffic	10–25	—
High traffic	50–100	—
Levees		
On farms	2–50	—
Around cities	50–200	—
Dams with no likelihood of loss of life (low hazard)		
Small dams	50–100	—
Intermediate dams	100 +	—
Large dams	—	50–100
Dams with probable loss of life (significant hazard)		
Small dams	100 +	50
Intermediate dams	—	50–100
Large dams	—	100
Dams with high likelihood of considerable loss of life (high hazard)		
Small dams	—	50–100
Intermediate dams	—	100
Large dams	—	100

Source: Chow et al. (1988).

Generalized design criteria for water-control structures have been developed, as summarized in Table 10.3.1. According to the potential consequence of failure, structures are classified as *major*, *intermediate*, and *minor*; the corresponding approximate ranges on the design scale are shown in Figure 10.3.1. The criteria for dams in Table 10.3.1 pertain to the design of spillway capacities, and are taken from the National Academy of Sciences (1983). The Academy defines a *small dam* as having 50–1000 acre-ft of storage or being 25–40 ft high, an *intermediate dam* as having 1000–50,000 acre-ft of storage or being 40–100 ft high, and a *large dam* as having more than 50,000 acre-ft of storage or being more than 100 ft high. In general, there would be considerable loss of life and extensive damage if a major structure failed. In the case of an intermediate structure, a small loss of life would be possible and the damage would be within the financial capability of the owner. For minor structures, there generally would be no loss of life, and the damage would be of the same magnitude as the cost of replacing or repairing the structure.

10.3.2 Hydrologic Design Level (Return Period)

A *hydrologic design level* on the design scale is the magnitude of the hydrologic event to be considered for the design of a structure or project. As it is not always economical to design structures and projects for the estimated limiting values, the ELV is often modified for specific design purposes. The final design value may be further modified according to engineering judgment and the experience of the designer or planner. Table 10.3.1 presents generalized criteria for water-control structures. A large number of the structures are designed using return periods.

An extreme hydrologic event is defined to have occurred if the magnitude of the event X is greater than or equal to some level x_T , i.e., $X \geq x_T$. The *return period* T of the event $X = x_T$ is the expected value of the *recurrence interval* (time between occurrences). The expected value $E(\cdot)$ is the average value measured over a very large number of occurrences. Consequently, the return period of a hydrologic event of a given magnitude is defined as the *average recurrence interval* between events that equal or exceed a specified magnitude.

10.3.3 Hydrologic Risk

The *probability of occurrence* $P(X \geq x_T)$ of the hydrologic event ($X \geq x_T$) for any observation is the inverse of the return period, i.e.,

$$P(X \geq x_T) = \frac{1}{T} \quad (10.3.1)$$

For a 100-year peak discharge, the probability of occurrence in any given year is $P(X \geq x_{100}) = 1/100 = 0.01$.

The probability of nonexceedance is

$$P(X < x_T) = 1 - \frac{1}{T} \quad (10.3.2)$$

Because each hydrologic event is considered independent, the *probability of nonexceedance* for n years is

$$P(X < x_T \text{ each year for } n \text{ years}) = \left(1 - \frac{1}{T}\right)^n$$

The complement, the *probability of exceedance* at least once in n years, is

$$P(X \geq x_T \text{ at least once in } n \text{ years}) = 1 - \left(1 - \frac{1}{T}\right)^n$$

which is the probability that a T -year return period event will occur at least once in n years. This is also referred to as the *natural, inherent, or hydrologic risk of failure* \bar{R} :

$$\bar{R} = 1 - \left(1 - \frac{1}{T}\right)^n = 1 - [1 - P(X \geq x_T)]^n \quad (10.3.3)$$

where n is referred to as the expected life of the structure. The hydrologic risk relationship is plotted in Figure 10.3.2.

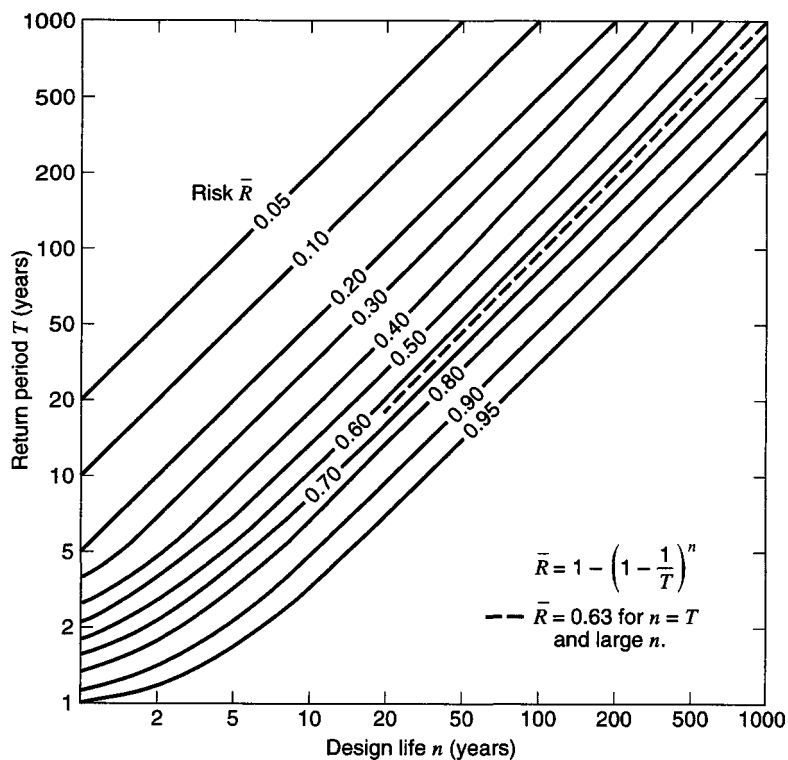


Figure 10.3.2 Risk of at least one exceedance of the design event during the design life (from Chow et al. (1988)).

EXAMPLE 10.3.1

Determine the hydrologic risk of a 100-year flood occurring during the 30-year service life of a project.

SOLUTION

Use equation (10.3.3) to determine the risk:

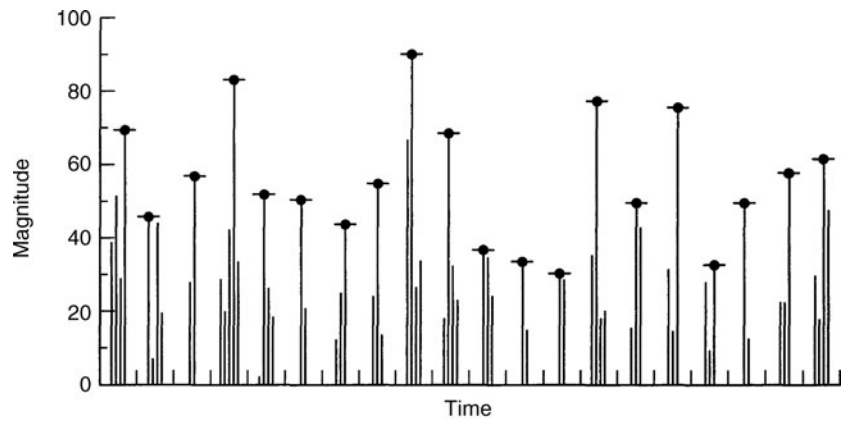
$$\bar{R} = 1 - \left(1 - \frac{1}{T}\right)^n = 1 - \left(1 - \frac{1}{100}\right)^{30} = 0.26$$

10.3.4 Hydrologic Data Series

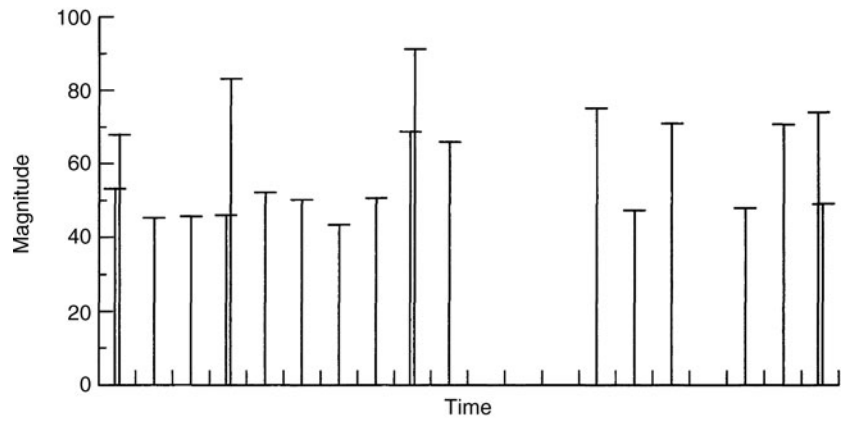
Figure 10.3.3a shows all the data available (that have been collected) for a hydrologic event. This represents a *complete-duration series*. A *partial-duration series* includes data that are selected so that their values are greater than some base value. An *annual-exceedance series* has a base value so that the number of values in the series is equal to the number of years of record. Figure 10.3.3b illustrates the annual exceedance series. An *extreme-value series* consists of the largest or smallest values occurring in each of the equally long time intervals of the record. If the time interval length is one year, the series is an *annual series*. An *annual maximum series* over the largest values in each respective year (Figure 10.3.3c) consists of the largest annual values and an *annual minimum series* consists of the smallest annual values in each of the respective years. Figure 10.3.4 illustrates the annual-exceedance series and the annual maximum series of the hypothetical data in Figure 10.3.3.

The return periods for annual exceedance series T_E are related to the corresponding annual maximum series return period T by (Chow, 1964)

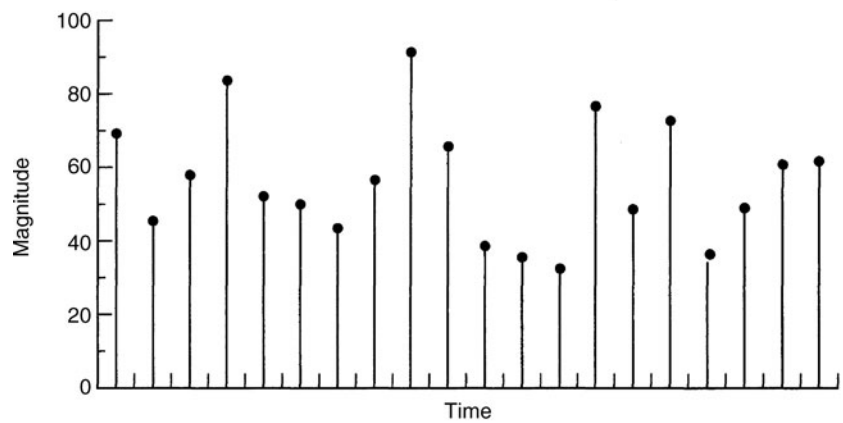
$$T_E = \left[\ln \left(\frac{T}{T-1} \right) \right]^{-1} \quad (10.3.4)$$



(a)



(b)



(c)

Figure 10.3.3 Hydrologic data arranged by time of occurrence. (a) Original data: $N = 20$ years; (b) Annual exceedances; (c) Annual maxima (from Chow (1964)).

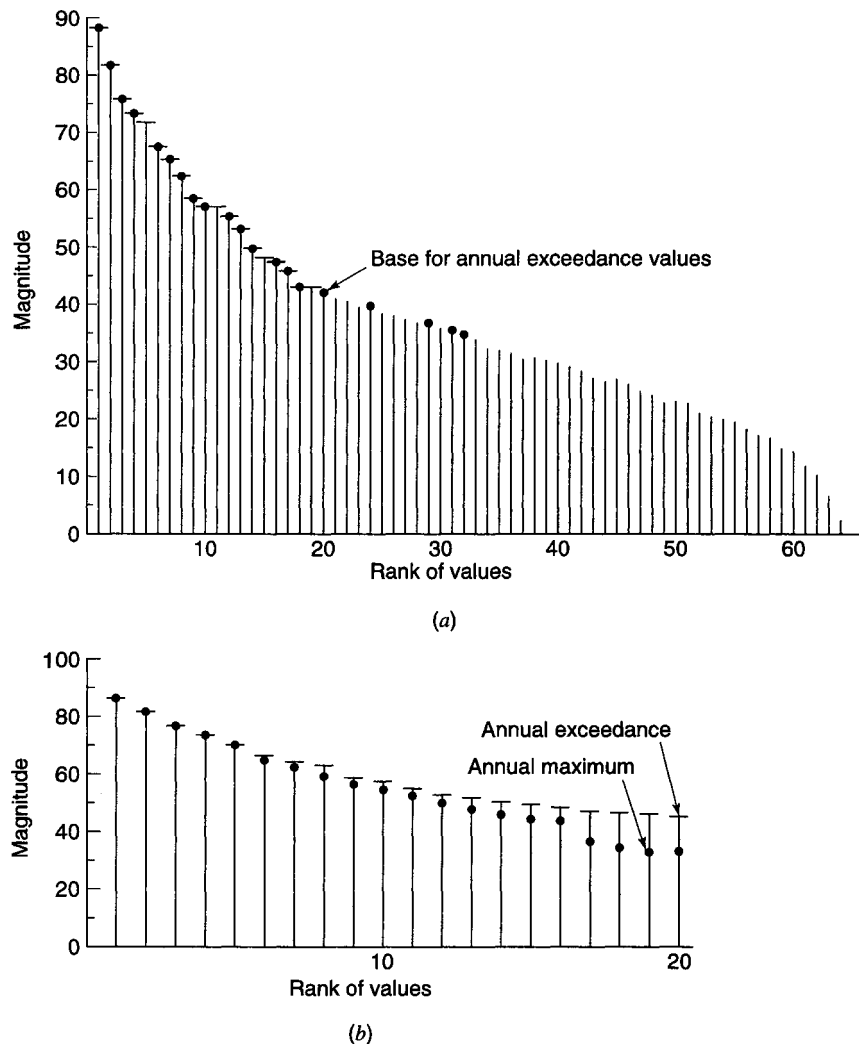


Figure 10.3.4 Hydrologic data arranged in the order of magnitude. (a) Original data; (b) Annual exceedance and maximum values (from Chow (1964)).

10.4 HYDROLOGIC FREQUENCY ANALYSIS

10.4.1 Frequency Factor Equation

One of the primary objectives of the frequency analysis of hydrologic data is to determine the recurrence interval of a hydrologic event of a given magnitude. The *recurrence interval*, which is the same as the return period, may also be defined as the average interval of time within which the magnitude of a hydrologic event will be equaled or exceeded once, on the average. The term “frequency” is often used interchangeably with “recurrence interval”; however, it should not be construed to indicate a regular or stated interval of occurrence or recurrence. *Hydrologic frequency analysis* is the approach of using probability and statistical analysis to estimate future frequencies (probabilities of hydrologic events occurring) based upon information contained in hydrologic records. Through the use of statistical methods, observed data is analyzed so as to provide not only a

more accurate estimate of future frequencies than is indicated by the observed data, but also criteria for determining the reliability of frequency estimates. The emphasis of hydrologic frequency analysis in this section is for the determination of flood frequency curves for streams and rivers.

The results of flood flow frequency analysis can be used for many engineering purposes: (1) for the design of dams, bridges, culverts, water supply systems, and flood control structures; (2) to determine the economic value of flood control projects; (3) to determine the effect of encroachments in the floodplain; (4) to determine a reservoir stage for real estate acquisition and reservoir-use purposes; (5) for the selection of runoff magnitudes for interior drainage, pumping plant, and local protection project design; and (6) for flood-plain zoning, etc.

In the application of statistical methods to hydrologic frequency analysis, theoretical probability distributions are utilized. The hydrologic events that have occurred are assumed to constitute a random sample (observed set of events) and then are used to make inferences about the true population (all possible events) for the theoretical distribution considered. These inferences are subject to considerable uncertainty because a set of observed hydrologic events represents only a sample or small subset of the many sets of physical conditions that could represent the population described by the theoretical probability distribution.

The existing methods of frequency analysis are numerous, with many diverse and confusing viewpoints and theories. Several types of probability distributions have been used in the past for hydrologic frequency determination. The most popular of these for flood flow frequency determination have been the log-normal, Gumbel (extreme value type I), and log-Pearson Type III distribution (see Table 10.2.2). Because of the range of uncertainty and diversity of methods in determining flood flow estimates and the varying results that can be obtained using the various methods, the U.S. Water Resources Council (1981) attempted to promote a uniform or consistent approach to flood-flow frequency studies.

Computation of the magnitudes of extreme events, such as flood flows, requires that the probability distribution function be invertible; that is, given a value for T or $[f(x_T) = T/(T - 1)]$, the corresponding value of x_T can be determined. Some probability distribution functions are not readily invertible, including the normal and Pearson Type III distributions, and an alternative method of calculating the magnitudes of extreme events is required for these distributions.

The magnitude x_T of a hydrologic event may be represented as the mean \bar{x} plus a departure of the variate from the mean. This departure is equal to the product of the standard deviation S_x and a frequency factor K_T . The departure Δx_T and the frequency factor K_T are functions of the return period and the type of probability distribution to be used in the analysis. Chow (1951) proposed the following frequency factor equation:

$$x_T = \bar{x} + K_T S_x \quad (10.4.1)$$

When the variable analyzed is $y = \log x$, then the same method is applied to the statistics for the logarithms of the data, using

$$y_T = \bar{y} + K_T S_y \quad (10.4.2)$$

and the required value of x_T is found by taking the antilog of y_T . For a given distribution, a K - T relationship can be determined between the frequency factor and the corresponding return period.

10.4.2 Application of Log-Pearson III Distribution

For the log-Pearson Type III distribution, the first step is to compute the logarithms of the hydrologic data, $y = \log x$. Usually, logarithms to base 10 are used. The mean \bar{y} , standard deviation S_y , and coefficient of skewness G_s are calculated for the logarithms of the data. Note that while γ is generally used for skew coefficient, G_s is used for a sample space (see Table 10.1.1). The frequency factor depends on the return period T and the coefficient of skewness G_s . When $G_s = 0$, the frequency factor

is equal to the standard normal variable z . When $G_s \neq 0$, K_T is approximated by Kite (1977) as

$$K(T, G_s) = z + (z^2 - 1)k + \frac{1}{3}(z^3 - 6z)k^2 - (z^2 - 1)k^3 + zk^4 + \frac{1}{3}k^5 \tag{10.4.3}$$

where $k = G_s/6$. Table 10.4.1 lists values of the frequency factor for the Pearson Type III (and log-Pearson Type III) distribution for various values of the return period and coefficient of skewness.

The U.S. Water Resources Council (WRC) recommended that the log-Pearson Type III be used as a base method for flood flow frequency studies (U.S. Water Resources Council, 1981). This was an attempt to promote a consistent, uniform approach to flood flow frequency determination for use in all federal planning involving water and related land resources. This choice of the log-Pearson Type III is, however, subjective to some extent, in that no rigorous statistical criteria exist on which a comparison of distributions can be made.

The frequency factor equation for the log-Pearson Type III distribution is written in terms of discharge as

$$\log Q_T = \bar{y} + K(T, G_s) \cdot S_y \tag{10.4.4}$$

where Q_T is the discharge for the T -year return period.

The steps in the procedure to compute the discharge Q_T of return period T are as follows:

Step 1 Transform all discharge values to $\log Q_1, \log Q_2, \dots, \log Q_n$.

Step 2 Determine the mean (\bar{y}), standard deviation (S_y) and skew (G_s) of the log-transformed values.

Step 3 Use Table 10.4.1 to determine the frequency factors for the return periods of interest.

Step 4 Apply the frequency factor equation (10.4.4) and compute $Q_T = \text{antilog}(\log Q_T)$.

Table 10.4.1 K_T Values for Pearson Type III Distribution

Skew coeff.	Recurrence interval (Yr)										
	1.0101	1.0526	1.1111	1.2500	2	5	10	25	50	100	200
	Exceedance probability										
	.99	.95	.90	.80	.50	.20	.10	.04	.02	.01	.005
3.0	-0.667	-0.665	-0.660	-0.636	-0.396	0.420	1.180	2.278	3.152	4.051	4.970
2.9	-0.690	-0.688	-0.681	-0.651	-0.390	0.440	1.195	2.277	3.134	4.013	4.909
2.8	-0.714	-0.711	-0.702	-0.666	-0.384	0.460	1.210	2.275	3.114	3.973	4.847
2.7	-0.740	-0.736	-0.724	-0.681	-0.376	0.479	1.224	2.272	3.093	3.932	4.783
2.6	-0.769	-0.762	-0.747	-0.696	-0.368	0.499	1.238	2.267	3.071	3.889	4.718
2.5	-0.799	-0.790	-0.771	-0.711	-0.360	0.518	1.250	2.262	3.048	3.845	4.652
2.4	-0.832	-0.819	-0.795	-0.725	-0.351	0.537	1.262	2.256	3.023	3.800	4.484
2.3	-0.867	-0.850	-0.819	-0.739	-0.341	0.555	1.274	2.248	2.997	3.753	4.515
2.2	-0.905	-0.882	-0.844	-0.752	-0.330	0.574	1.284	2.240	2.970	3.705	4.444
2.1	-0.946	-0.914	-0.869	-0.765	-0.319	0.592	1.294	2.230	2.942	3.656	4.372
2.0	-0.990	-0.949	-0.895	-0.777	-0.307	0.609	1.302	2.219	2.912	3.605	4.298
1.9	-1.037	-0.984	-0.920	-0.788	-0.294	0.627	1.310	2.207	2.881	3.553	4.223
1.8	-1.087	-1.020	-0.945	-0.799	-0.282	0.643	1.318	2.193	2.848	3.499	4.147
1.7	-1.140	-1.056	-0.970	-0.808	-0.268	0.660	1.324	2.179	2.815	3.444	4.069
1.6	-1.197	-1.093	-0.994	-0.817	-0.254	0.675	1.329	2.136	2.780	3.388	3.990
1.5	-1.256	-1.131	-1.018	-0.825	-0.240	0.690	1.333	2.146	2.743	3.330	3.910
1.4	-1.318	-1.168	-1.041	-0.832	-0.225	0.705	1.337	2.128	2.706	3.271	3.838
1.3	-1.383	-1.260	-1.064	-0.838	-0.210	0.719	1.339	2.108	2.666	3.211	3.745
1.2	-1.449	-1.243	-1.086	-0.844	-0.195	0.732	1.340	2.087	2.626	3.149	3.661

(Continued)

Table 10.4.1 (Continued)

Skew coeff.	Recurrence interval (yr)										
	1.0101	1.0526	1.1111	1.2500	2	5	10	25	50	100	200
	Exceedance probability										
	.99	.95	.90	.80	.50	.20	.10	.04	.02	.01	.005
1.1	-1.518	-1.280	-1.107	-0.848	-0.180	0.745	1.341	2.066	2.585	3.087	3.575
1.0	-1.588	-1.317	-1.128	-0.852	-0.164	0.758	1.340	2.043	2.542	3.022	3.489
0.9	-1.660	-1.353	-1.147	-0.854	-0.148	0.769	1.339	2.018	2.498	2.957	3.401
0.8	-1.733	-1.388	-1.166	-0.856	-0.132	0.780	1.336	1.993	2.453	2.891	3.312
0.7	-1.806	-1.423	-1.183	-0.857	-0.116	0.790	1.333	1.967	2.407	2.824	3.223
0.6	-1.880	-1.458	-1.200	-0.857	-0.099	0.800	1.328	1.939	2.359	2.755	3.132
0.5	-1.955	-1.491	-1.216	-0.856	-0.083	0.808	1.323	1.910	2.311	2.686	3.041
0.4	-2.029	-1.524	-1.231	-0.855	-0.066	0.816	1.317	1.880	2.261	2.615	2.949
0.3	-2.104	-1.555	-1.245	-0.853	-0.050	0.824	1.309	1.849	2.211	2.544	2.856
0.2	-2.178	-1.586	-1.258	-0.850	-0.033	0.830	1.301	1.818	2.159	2.472	2.763
0.1	-2.252	-1.616	-1.270	-0.846	-0.017	0.836	1.292	1.785	2.107	2.400	2.670
0.0	-2.326	-1.645	-1.282	-0.842	0	0.842	1.282	1.751	2.054	2.326	2.576
-0.1	-2.400	-1.673	-1.292	-0.836	0.017	0.846	1.270	1.716	2.000	2.252	2.482
-0.2	-2.472	-1.700	-1.301	-0.830	0.033	0.850	1.258	1.680	1.945	2.178	2.388
-0.3	-2.544	-1.726	-1.309	-0.824	0.050	0.853	1.245	1.643	1.890	2.104	2.294
-0.4	-2.615	-1.750	-1.317	-0.816	0.066	0.855	1.231	1.606	1.834	2.029	2.201
-0.5	-2.686	-1.774	-1.323	-0.808	0.083	0.856	1.216	1.567	1.777	1.955	2.108
-0.6	-2.755	-1.797	-1.328	-0.800	0.099	0.857	1.200	1.528	1.720	1.880	2.016
-0.7	-2.824	-1.819	-1.333	-0.790	0.116	0.857	1.183	1.488	1.663	1.806	1.929
-0.8	-2.891	-1.839	-1.336	-0.780	0.132	0.856	1.166	1.448	1.606	1.733	1.837
-0.9	-2.957	-1.858	-1.339	-0.769	0.148	0.854	1.147	1.407	1.549	1.660	1.749
-1.0	-3.022	-1.877	-1.340	-0.758	0.164	0.852	1.128	1.366	1.492	1.588	1.664
-1.1	-3.087	-1.894	-1.341	-0.745	0.180	0.848	1.107	1.324	1.435	1.518	1.581
-1.2	-3.149	-1.910	-1.340	-0.732	0.195	0.844	1.086	1.282	1.379	1.449	1.501
-1.3	-3.211	-1.925	-1.339	-0.719	0.210	0.838	1.064	1.240	1.324	1.383	1.424
-1.4	-3.271	-1.938	-1.337	-0.705	0.225	0.832	1.041	1.198	1.270	1.318	1.351
-1.5	-3.330	-1.951	-1.333	-0.690	0.240	0.825	1.018	1.157	1.217	1.256	1.282
-1.6	-3.388	-1.962	-1.329	-0.675	0.254	0.817	0.994	1.116	1.166	1.197	1.216
-1.7	-3.444	-1.972	-1.324	-0.660	0.268	0.808	0.970	1.075	1.116	1.140	1.155
-1.8	-3.499	-1.981	-1.318	-0.643	0.282	0.799	0.945	1.035	1.069	1.087	1.097
-1.9	-3.553	-1.989	-1.310	-0.627	0.294	0.788	0.920	0.996	1.023	1.037	1.044
-2.0	-3.605	-1.996	-1.302	-0.609	0.307	0.777	0.895	0.959	0.980	0.990	0.995
-2.1	-3.656	-2.001	-1.294	-0.592	0.319	0.765	0.869	0.923	0.939	0.946	0.949
-2.2	-3.705	-2.006	-1.284	-0.574	0.330	0.752	0.844	0.888	0.900	0.905	0.907
-2.3	-3.753	-2.009	-1.274	-0.555	0.341	0.739	0.819	0.855	0.864	0.867	0.869
-2.4	-3.800	-2.011	-1.262	-0.537	0.351	0.725	0.795	0.823	0.830	0.832	0.833
-2.5	-3.845	-2.012	-1.250	-0.518	0.360	0.711	0.771	0.793	0.798	0.799	0.800
-2.6	-3.889	-2.013	-1.238	-0.499	0.368	0.696	0.747	0.764	0.768	0.769	0.769
-2.7	-3.932	-2.012	-1.224	-0.479	0.376	0.681	0.724	0.738	0.740	0.740	0.741
-2.8	-3.973	-2.010	-1.210	-0.460	0.384	0.666	0.702	0.712	0.714	0.714	0.714
-2.9	-4.013	-2.007	-1.195	-0.440	0.390	0.651	0.681	0.683	0.689	0.690	0.690
-3.0	-4.051	-2.003	-1.180	-0.420	0.396	0.636	0.660	0.666	0.666	0.667	0.667

EXAMPLE 10.4.1

The mean, standard deviation, and skew of the log transformed discharges for the Medina River, Texas, are 3.639, 0.394, and 0.200, respectively, where the discharges are in ft^3/s . Compute the 10-year and 100-year peak discharges.

SOLUTION

Assume that the peak discharges follow a log-Pearson Type III distribution and the procedures recommended by WRC will be used. First, we need to determine the frequency factors for 10-year and 100-year storm events from Table 10.4.1. To determine the frequency factors, we need to know the exceedance probability and the skew coefficient. Since the exceedance probability for a T -year storm event is $1/T$, the exceedance probabilities for 10-year and 100-year storm events are 0.1 and 0.01, respectively. Since the skew coefficient is given as $G_s = 0.200$, the frequency factors for the 10-year and 100-year storm events can be found from Table 10.4.1 as $K_{10} = 1.301$ and $K_{100} = 2.472$. Next, compute the 10-year and 100-year peak discharges:

$$\begin{aligned}\log Q_T &= \bar{y} + K(T, G_s)S_y \\ \log Q_{10} &= 3.639 + 1.301(0.394) \\ Q_{10} &= 14,180 \text{ cfs} \\ \log Q_{100} &= 3.639 + 2.472(0.394) \\ Q_{100} &= 41,020 \text{ cfs}\end{aligned}$$

EXAMPLE 10.4.2

The annual maximum series for the U.S.G.S. gauge on the Wichita River near Cheyenne, Oklahoma, is listed in Table 10.4.2. The objective is to compute the 25-year and 100-year peak discharges using the log-Pearson Type III distribution. Also compute the plotting position using the Weibull plotting position formula, $P(X > x_T) = 1/T = m/(n+1)$, where m is the rank of descending values and n is the number of peaks in the annual maximum series. (Adapted from Cudworth, 1989.)

SOLUTION

Step 1 Transform data using logarithms, computed as given in Table 10.4.2.

Step 2 Determine the mean, standard deviation, and skew of the log-transformed values:

$$\begin{aligned}\bar{y} &= \frac{\sum y}{n} = \frac{156.876}{47} = 3.338 \\ S_y &= \sqrt{\frac{\sum y^2 - \frac{(\sum y)^2}{n}}{n-1}} = \frac{543.222 - \frac{(156.876)^2}{47}}{47-1} = 0.653 \\ G_s &= \frac{n^2(\sum y^3) - 3n(\sum y)(\sum y^2) + 2(\sum y)^3}{n(n-1)(n-2)(S_y^3)} \\ &= \frac{(47)^2(1940.423) - (3)(47)(156.876)(543.222) + (2)(156.876)^3}{(47)(47-1)(47-2)(0.653)^3} \\ &= -0.294 \\ G_s &\approx -0.3\end{aligned}$$

Step 3 Determine frequency factors for the 25-year and the 100-year events using Table 10.4.1:

$$\begin{aligned}K(25, -0.3) &= 1.643 \\ K(100, -0.3) &= 2.104\end{aligned}$$

Table 10.4.2 Annual Peak Discharges for Each Year of Record for the Drainage Area Above Foss Dam

(1)	(2)	(3)	(4)	(5)	(6)	(7)
Year	Annual Peak Discharge, ft ³ /s	Ranked Annual Peak Discharge, ft ³ /s	Weibull Plotting Position	Logarithm of Discharge y	y ²	y ³
1938	14,600	69,800	0.021	4.84386	23.46298	113.65139
1939	3070	40,000	0.042	4.60206	21.17896	97.46683
1940	1080	14,600	0.063	4.16435	17.34181	72.21737
1941	40,000	14,000	0.083	4.14613	17.19039	71.27359
1942	14,000	11,900	0.104	4.07555	16.61011	67.69533
1943	2190	9900	0.125	3.99563	15.96506	63.79047
1944	1240	8900	0.146	3.94939	15.59768	61.60133
1945	9900	8900	0.167	3.94939	15.59768	61.60133
1946	8900	8450	0.189	3.92686	15.42023	60.55308
1947	7100	7310	0.208	3.86392	14.92988	57.68785
1948	8900	7100	0.229	3.85126	14.83220	57.12267
1949	11,900	6420	0.250	3.80754	14.49736	55.19928
1950	8450	5830	0.271	3.76567	14.18027	53.39822
1951	5040	5040	0.292	3.70243	13.70799	50.75287
1952	465	4710	0.313	3.67302	13.49108	49.55299
1953	3550	4650	0.333	3.66839	13.45709	49.36584
1954	69,800	4470	0.354	3.65031	13.32476	48.63952
1955	5830	4210	0.375	3.62428	13.13541	47.60639
1956	3890	3890	0.396	3.58995	12.88774	46.26635
1957	4210	3550	0.417	3.55023	12.60413	44.74757
1958	1750	3070	0.438	3.48714	12.16015	42.40413
1959	6420	2990	0.458	3.47567	12.08028	41.98707
1960	1510	2930	0.479	3.46687	12.01919	41.66896
1961	7310	2280	0.500	3.35793	11.27569	37.86299
1962	2930	2190	0.521	3.34044	11.15854	37.27443
1963	574	1960	0.542	3.29226	10.83898	35.68473
1964	159	1800	0.563	3.25527	10.59678	34.49539
1965	1400	1750	0.583	3.24304	10.51731	34.10805
1966	1800	1510	0.604	3.17898	10.10591	32.12650
1967	2990	1420	0.625	3.15229	9.93693	31.32409
1968	4470	1400	0.646	3.14613	9.89813	31.14082
1969	2280	1360	0.667	3.13354	9.81907	30.76846
1970	734	1240	0.688	3.09342	9.56925	29.60170
1971	4710	1080	0.708	3.03342	9.20164	27.91243
1972	1360	1050	0.729	3.02119	9.12759	27.57618
1973	265	734	0.750	2.86570	8.21224	23.53381
1974	592	592	0.771	2.77232	7.68576	21.30738
1975	1050	574	0.792	2.75891	7.61158	20.99968
1976	1960	560	0.813	2.74819	7.55255	20.75584
1977	4660	465	0.833	2.66745	7.11529	18.97968
1978	297	427	0.854	2.63043	6.91916	18.20037
1979	400	400	0.875	2.60206	6.77072	17.61781
1980	560	297	0.896	2.47276	6.11454	15.11980
1981	38	265	0.917	2.42325	5.87214	14.22967
1982	1420	159	0.938	2.20140	4.84616	10.66834
1983	427	119	0.958	2.07555	4.30791	8.94128
1984	119	38	0.979	1.57978	2.49570	3.94266
			Totals	156.87558	543.2220	1940.4225

Source: Cudworth (1989).

Step 4 Apply frequency factor equations to determine Q_{25} and Q_{100}

$$\begin{aligned}\log Q_{25} &= \bar{y} + K(25, -0.3)S_y \\ &= 3.338 + 1.643(0.653) \\ &= 4.411 \\ Q_{25} &= \text{antilog}(4.411) = 25,765 \text{ cfs} \\ \log Q_{100} &= \bar{y} + K(100, -0.3)S_y \\ &= 3.338 + 2.104(0.653) \\ &= 4.712 \\ Q_{100} &= \text{antilog}(4.712) = 51,525 \text{ cfs}\end{aligned}$$

The annual peak discharges are ranked in descending order in column (3) of Table 10.4.2 and the Weibull plotting positions are listed in column (4) for the corresponding discharge in column (3). As an example, the largest discharge has a plotting position of $m = 1$, so $1/T = 1/(47 + 1) = 0.021$. The second largest, $m = 2$, has a Weibull plotting position of $2/(47 + 1) = 0.042$.

10.4.3 Extreme Value Distribution

For the extreme value type I (Gumbel) distribution, the frequency factor can be derived by substituting the frequency equation (10.4.1), $x_T = \bar{x} + K_T S_x$ into the cumulative distribution function, equation (10.2.13), $F(x_T) = \exp\{-\exp[-(x_T - \beta)/\alpha]\}$ so that

$$F(x) = \exp\{-\exp[-(\bar{x} + K_T S_x - \beta)/\alpha]\} = 1 - 1/T \quad (10.4.5)$$

Substitute the parameters α and β (equations (10.2.14) and (10.2.15)) into equation (10.4.5) and solve for K_T in terms of the return period T ,

$$K_T = - (6^{0.5}/\pi) \{0.5772 + \ln[\ln(T/(T-1))]\} \quad (10.4.6)$$

The return period T can also be expressed in terms of K_T as

$$T = \{1 - \exp[-\exp(-0.5772 - \pi K_T/6^{0.5})]\}^{-1} \quad (10.4.7)$$

EXAMPLE 10.4.3

Following example 10.2.2, the exceedance series of 30-min duration rainfall values has a mean of 1.09 in and standard deviation of 0.343 in. Determine the 100-year 30-min duration rainfall value using the Gumbel (extreme value type I) distribution with the frequency factor method.

SOLUTION

First solve for the frequency factor using equation (10.4.6), $K_T = - (6^{0.5}/\pi) \{0.5772 + \ln[\ln(T/(T-1))]\}$ with $T = 100$, giving $K_T = 3.138$. Using the frequency factor equation (10.4.1),

$$x_T = \bar{x} + K_T S_x = 1.09 + 3.138(0.343) = 2.166 \text{ in}$$

The 100-year 30-min duration rainfall is 2.166 in.

10.5 U.S. WATER RESOURCES COUNCIL GUIDELINES FOR FLOOD FLOW FREQUENCY ANALYSIS

Flood flow frequency analysis is another method of discharge determination using statistical methods when gauged data are available to develop annual maximum series. Section 10.4 introduced hydrologic frequency analysis for flood flow. This section extends the concepts to the so-called *U.S. Water Resources Council (WRC) method*.

10.5.1 Procedure

The skew coefficient is very sensitive to the size of the sample; thus, it is difficult to obtain an accurate estimate from small samples. Because of this, the U.S. Water Resources Council (1981) recommended using a generalized estimate of the skew coefficient when estimating the skew for short records. As the length of record increases, the skew is usually more reliable. The guidelines recommend the use of a *weighted skew* G_w , based upon the equation

$$G_w = WG_s + (1 - W)G_m \tag{10.5.1}$$

where W is a weight, G_s is the skew coefficient computed using the sample data, and G_m is a map skew, values of which for the United States are found in Figure 10.5.1. The generalized skew is derived as a weighted average between skew coefficients computed from sample data (sample skew) and regional or map skew coefficients (referred to as a generalized skew in U.S. Water Resources Council (1981)).

A weighting procedure was derived that is a function of the variance of the sample skew and the variance of the map skew. Such a procedure considers the uncertainty of deriving skew coefficients from both sample data and regional or map values to obtain a generalized skew that minimizes uncertainty based upon information known.

The estimates of the sample skew coefficient and the map skew coefficient in equation (10.5.1) are assumed to be independent with the same mean and respective variances. Assuming independence of G_s and G_m , the variance (mean square error) of the weighted skew, $V(G_w)$, can be expressed as

$$V(G_w) = W^2 \cdot V(G_s) + (1 - W)^2 \cdot V(G_m) \tag{10.5.2}$$

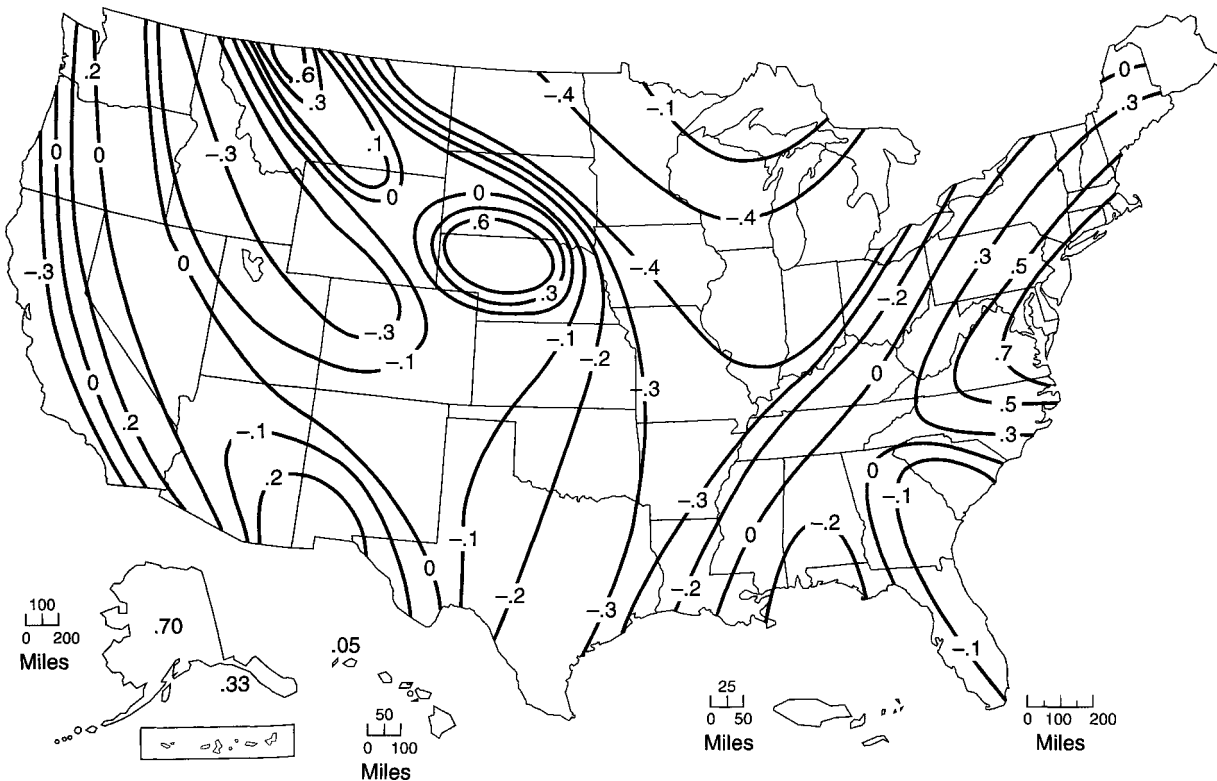


Figure 10.5.1 Generalized skew coefficients of annual maximum streamflow (from U.S. Water Resources Council (1981)).

where $V(G_s)$ is the variance of the sample skew and $V(G_m)$ is the variance of the map skew. The skew weight that minimizes the variance of the weighted skew can be determined by differentiating equation (10.5.2) with respect to W and solving $d[V(G_w)]/dW = 0$ for W to obtain

$$W = \frac{V(G_m)}{V(G_s) + V(G_m)} \quad (10.5.3)$$

Equation (10.5.3) is a convex function and the second derivative of equation (10.5.2) is greater than 0, proving that equation (10.5.3) gives the value of W that minimizes the weighted skew.

Determination of W using equation (10.5.3) requires the values of $V(G_m)$ and $V(G_s)$. $V(G_m)$ can be estimated from the map of the skew coefficients as the squared value of the standard deviation of station values of skew coefficients about the isolines of the skew map. The value of $V(G_m)$, estimated for the skew map in U.S. Water Resources Council (1981), is 0.3025. Alternatively, $V(G_m)$ could be derived from a regression study relating the skew to physiographical and meteorological characteristics of the basins and determining $V(G_m)$ as the square of the standard error of the regression equation (Tung and Mays, 1981).

The weighted skew G_w can be determined by substituting equation (10.5.3) into equation (10.5.1), resulting in

$$G_w = \frac{V(G_m) \cdot G_s + V(G_s) \cdot G_m}{V(G_m) + V(G_s)} \quad (10.5.4)$$

The variance (mean square error) of the station skew for log-Pearson Type II random variables can be obtained from the results of Monte Carlo experiments by Wallis et al. (1974). Their results showed that $V(G_s)$ of the logarithmic station skew is a function of record length and population skew. For use in calculating G_w , this function $V(G_s)$ can be approximated with sufficient accuracy using

$$V(G_s) = 10^{A - B[\log_{10}(n/10)]} \quad (10.5.5)$$

where

$$A = -0.33 + 0.08 |G_s| \quad \text{if } |G_s| \leq 0.90 \quad (10.5.6a)$$

$$A = -0.52 + 0.30 |G_s| \quad \text{if } |G_s| > 0.90 \quad (10.5.6b)$$

$$B = 0.94 - 0.26 |G_s| \quad \text{if } |G_s| \leq 1.50 \quad (10.5.7a)$$

$$B = 0.55 \quad \text{if } |G_s| > 1.50 \quad (10.5.7b)$$

in which $|G_s|$ is the absolute value of the station skew (used as an estimate of population skew) and n is the record length in years. The same steps used in section 10.4 can be used to compute the discharge Q_T of return period T .

10.5.2 Testing for Outliers

The WRC method recommends that outliers be identified and adjusted according to their recommended methods. *Outliers* are data points that depart significantly from the trend of the remaining data. The retention or deletion of these outliers can significantly affect the magnitude of statistical parameters computed from the data, especially for small samples. Procedures for treating outliers require judgment involving both mathematical and hydrologic considerations. According to the U.S. Water Resources Council (1981), if the station skew is greater than +0.4, tests for high outliers are considered first. If the station skew is less than -0.4, tests for low outliers are considered first. Where the station skew is between ± 0.4 , tests for both high and low outliers should be applied before eliminating any outliers from the data set.

Table 10.5.1 Outlier Test K Values: 10 Percent Significance Level K Values

Sample size	K value	Sample size	K value	Sample size	K value	Sample size	K value
10	2.036	45	2.727	80	2.940	115	3.064
11	2.088	46	3.736	81	2.945	116	3.067
12	2.134	47	2.744	82	2.949	117	3.070
13	2.175	48	2.753	83	2.953	118	3.073
14	2.213	49	2.760	84	2.957	119	3.075
15	2.247	50	2.768	85	2.961	120	3.078
16	2.279	51	2.775	86	2.966	121	3.081
17	2.309	52	2.783	87	2.970	122	3.083
18	2.335	53	2.790	88	2.973	123	3.086
19	2.361	54	2.798	89	2.977	124	3.089
20	2.385	55	2.804	90	2.981	125	3.092
21	2.408	56	2.811	91	2.984	126	3.095
22	2.429	57	2.818	92	2.989	127	3.097
23	2.448	58	2.824	93	2.993	128	3.100
24	2.467	59	2.831	94	2.996	129	3.102
25	2.486	60	2.837	95	3.000	130	3.104
26	2.502	61	2.842	96	3.003	131	3.107
27	2.519	62	2.849	97	3.006	132	3.109
28	2.534	63	2.854	98	3.011	133	3.112
29	2.549	64	2.860	99	3.014	134	3.114
30	2.563	65	2.866	100	3.017	135	3.116
31	2.577	66	2.871	101	3.021	136	3.119
32	2.591	67	2.877	102	3.024	137	3.122
33	2.604	68	2.883	103	3.027	138	3.124
34	2.616	69	2.888	104	3.030	139	3.126
35	2.628	70	2.893	105	3.033	140	3.129
36	2.639	71	2.897	106	3.037	141	3.131
37	2.650	72	2.903	107	3.040	142	3.133
38	2.661	73	2.908	108	3.043	143	3.135
39	2.671	74	2.912	109	3.046	144	3.138
40	2.682	75	2.917	110	3.049	145	3.140
41	2.692	76	2.922	111	3.052	146	3.142
42	2.700	77	2.927	112	3.055	147	3.144
43	2.710	78	2.931	113	3.058	148	3.146
44	2.719	79	2.935	114	3.061	149	3.148

This table contains one-sided 10 percent significance level K values for a normal distribution.

Source: U.S. Water Resources Council (1981).

The following frequency equation can be used to detect high outliers:

$$y_H = \bar{y} + K_N S_y \tag{10.5.8}$$

where y_H is the high outlier threshold in log units and K_N is the K value from Table 10.5.1 for sample size N . If the logarithms of peaks in the sample are greater than y_H in the above equation, then they are considered high outliers. Flood peaks considered high outliers should be compared with historic flood data and flood information at nearby sites. According to the U.S. Water Resources Council (1981), if information is available indicating that a high outlier(s) is the maximum in an extended period of time, the outlier(s) is treated as historic flood data. If useful historic information is not available to adjust for high outliers, then the outliers should be retained as part of the systematic record.

The following frequency equation can be used to detect low outliers:

$$y_L = \bar{y} - K_n S_y \quad (10.5.9)$$

where y_L is the low outlier threshold in log units. Flood peaks considered low outliers are deleted from the record and a conditional probability adjustment described in the U.S. Water Resources Council (1981) is applied. Use of the K values in Table 10.5.1 is equivalent to a one-sided test that detects outliers at the 10 percent level of significance. The K values are based on a normal distribution for detection of single outliers.

EXAMPLE 10.5.1

Using the data for example 10.4.2 (annual maximum series for the gauge on the Wichita River near Cheyenne, Oklahoma), compute the 25-year and the 100-year peak discharges using the U.S. Water Resource Council (1981) guidelines. The map skew for this location is -0.015 .

SOLUTION

Steps 1–2 Transform data using logarithms and compute statistics as in example 10.4.2, where $\bar{y} = 3.338$, $S_y = 0.653$, and $G_s = -0.294 \approx -0.3$.

Step 3 Compute the weighted skew coefficient, G_w .

Step 3a Compute A and B using equations (10.5.6a) and (10.5.7a):

$$A = -0.33 + 0.08 | -0.294 | = -0.306$$

$$B = 0.94 - 0.26 | -0.294 | = 0.864$$

Step 3b Compute $V(G_s)$.

$$V(G_s) = 10^{A-B \log(n/10)} = 10^{-0.306 - 0.864 \log(47/10)} = 0.130$$

Step 3c Use equation (10.5.4) to compute the weighted skew coefficient using $V(G_m) = 0.302$ (as estimated in U.S. Water Resources Council (1981)):

$$G_w = \frac{0.302(-0.294) + 0.130(-0.015)}{0.302 + 0.130} = -0.210$$

Step 4 Use Table 10.4.1 to obtain the frequency factors using the weighted skew:

$$K(25, -0.210) = 1.676$$

$$K(100, -0.210) = 2.171$$

Step 5 Apply the frequency factor equation to determine Q_{25} and Q_{100} :

$$\begin{aligned} \log Q_{25} &= \bar{y} + K(25, -0.251)S_y \\ &= 3.338 + 1.676(0.653) = 4.432 \end{aligned}$$

$$Q_{25} = 27,070 \text{ cfs}$$

$$\log Q_{100} = 3.338 + 2.171(0.653) = 4.756$$

$$Q_{100} = 56,975 \text{ cfs}$$

Note that in example 10.4.2 we computed $Q_{25} = 25,765$ cfs and $Q_{100} = 51,525$ cfs when the sample skew was used.

EXAMPLE 10.5.2

Using the data in examples 10.4.2 and 10.5.1, determine whether any outliers exist in the annual maximum series (Table 10.4.2).

SOLUTION

Determine whether the data include any high or low outliers. First, consider high outliers. From Table 10.5.1, $K_n = 2.744$ for $n = 47$, and using equation (10.5.8) to determine the threshold value y_H ,

we find

$$y_H = \bar{y} + K_n S_y = 3.338 + 2.744(0.653) = 5.130$$

so

$$Q_H = 10^{y_H} = (10)^{5.130} = 134,900 \text{ cfs}$$

The largest recorded value of 69,800 cfs for the year 1954 in Table 10.4.2 does not exceed the threshold value of 134,900 cfs.

Next consider low outliers and use equation (10.5.9) to determine the threshold:

$$y_L = \bar{y} + K_N S_y = 3.338 - 2.744(0.653) = 1.546$$

so

$$Q_L = 10^{y_L} = (10)^{1.546} = 35 \text{ cfs}$$

The smallest recorded peak, 38 cfs for 1963, is larger than 35 cfs, so there are no low outliers by this methodology.

10.6 ANALYSIS OF UNCERTAINTIES

In the design and analysis of hydrosystems, many quantities of interest are functionally related to a number of variables, some of which are subject to uncertainty. For example, hydraulic engineers frequently apply weir flow equations such as $Q = CLH^{1.5}$ to estimate spillway capacity in which the coefficient C and head H are subject to uncertainty. As a result, discharge over the spillway is not certain. A rather straightforward and useful technique for the approximation of such uncertainties is the *first-order analysis of uncertainties*, sometimes called the *delta method*.

The use of the first-order analysis of uncertainties is quite popular in many fields of engineering because of its relative ease in application to a wide array of problems. First-order analysis is used to estimate the uncertainty in a deterministic model formulation involving parameters that are uncertain (not known with certainty). More specifically, first-order analysis enables one to estimate the mean and variance of a random variable that is functionally related to several other variables, some of which are random. By using first-order analysis, the combined effect of uncertainty in a model formulation, as well as the use of uncertain parameters, can be assessed.

Consider a random variable y that is a function of k random variables (multivariate case):

$$y = g(x_1, x_2, \dots, x_k) \quad (10.6.1)$$

This can be a deterministic equation such as the weir equation mentioned above, or the rational formula or Manning's equation; or this function can be a complex model that must be solved on a computer. The objective is to treat a deterministic model that has uncertain inputs in order to determine the effect of the uncertain parameters x_1, \dots, x_k on the model output y .

Equation (10.6.1) can be expressed as $y = g(\mathbf{x})$ where $\mathbf{x} = x_1, x_2, \dots, x_k$. Through a Taylor series expansion about k random variables, ignoring the second- and higher-order terms, we get

$$y \approx g(\bar{\mathbf{x}}) + \sum_{i=1}^k \left[\frac{\partial g}{\partial x_i} \right]_{\bar{\mathbf{x}}} (X_i - \bar{x}_i) \quad (10.6.2)$$

The derivation $[\partial g / \partial x_i]_{\bar{\mathbf{x}}}$ are the *sensitivity coefficients* that represent the rate of change of the function value $g(\mathbf{x})$ at $\mathbf{x} = \bar{\mathbf{x}}$.

Assuming that the k random variables are independent, then the variance of y is approximated as

$$\sigma_y^2 = \text{Var}[y] = \sum a_i^2 \sigma_{x_i}^2 \quad (10.6.3)$$

and the coefficient of variation is Ω_y :

$$\Omega_y = \left[\sum_{\tau=1}^k a_i^2 \left(\frac{\bar{x}_i}{\mu_y} \right)^2 \Omega_{x_i}^2 \right]^{1/2} \quad (10.6.4)$$

where $a_i = (\partial g / \partial x)_{\bar{x}}$. Refer to Mays and Tung (1992) for a detailed derivation of equations (10.6.3) and (10.6.4).

EXAMPLE 10.6.1

Apply the first-order analysis to the rational equation $Q = CiA$, in which C is the runoff coefficient, i is the rainfall intensity in in/m, and A is the drainage area in acres, to determine formulas for σ_Q and Ω_Q . Consider C , i , and A to be uncertain.

SOLUTION

The first-order approximation of Q is determined using equation (10.6.2), so that

$$Q \approx \bar{Q} + \left[\frac{\partial Q}{\partial C} \right]_{\bar{C}, \bar{i}, \bar{A}} (C - \bar{C}) + \left[\frac{\partial Q}{\partial i} \right]_{\bar{C}, \bar{i}, \bar{A}} (i - \bar{i}) + \left[\frac{\partial Q}{\partial A} \right]_{\bar{C}, \bar{i}, \bar{A}} (A - \bar{A})$$

For $C = \bar{C}$, $i = \bar{i}$, and $A = \bar{A}$, $\bar{Q} = \bar{C}\bar{i}\bar{A}$. The variance is computed using equation (10.6.3):

$$\begin{aligned} \sigma_Q^2 &= \left[\frac{\partial Q}{\partial C} \right]_{(\bar{C}, \bar{i}, \bar{A})}^2 \sigma_C^2 + \left[\frac{\partial Q}{\partial i} \right]_{(\bar{C}, \bar{i}, \bar{A})}^2 \sigma_i^2 + \left[\frac{\partial Q}{\partial A} \right]_{(\bar{C}, \bar{i}, \bar{A})}^2 \sigma_A^2 \\ \sigma_Q &= \left\{ \left[\frac{\partial Q}{\partial C} \right]_{(\bar{C}, \bar{i}, \bar{A})}^2 \sigma_C^2 + \left[\frac{\partial Q}{\partial i} \right]_{(\bar{C}, \bar{i}, \bar{A})}^2 \sigma_i^2 + \left[\frac{\partial Q}{\partial A} \right]_{(\bar{C}, \bar{i}, \bar{A})}^2 \sigma_A^2 \right\}^{1/2} \end{aligned}$$

The coefficient of variation is computed using equation (10.6.4):

$$\begin{aligned} \Omega_Q^2 &= \left[\frac{\partial Q}{\partial C} \right]^2 \left(\frac{\bar{C}}{\bar{Q}} \right) \Omega_C^2 + \left[\frac{\partial Q}{\partial i} \right]^2 \left(\frac{\bar{i}}{\bar{Q}} \right) \Omega_i^2 + \left[\frac{\partial Q}{\partial A} \right]^2 \left(\frac{\bar{A}}{\bar{Q}} \right) \Omega_A^2 \\ &= (\bar{i}\bar{A})^2 \left(\frac{\bar{C}}{\bar{Q}} \right)^2 \Omega_C^2 + (\bar{C}\bar{A})^2 \left(\frac{\bar{i}}{\bar{Q}} \right)^2 \Omega_i^2 + (\bar{C}\bar{i})^2 \left(\frac{\bar{A}}{\bar{Q}} \right)^2 \Omega_A^2 \\ &= \Omega_C^2 + \Omega_i^2 + \Omega_A^2 \\ \Omega_Q &= [\Omega_C^2 + \Omega_i^2 + \Omega_A^2]^{1/2} \end{aligned}$$

EXAMPLE 10.6.2

Determine the mean, coefficient of variation, and standard deviation of the runoff using the rational equation with the following parameter values:

Parameter	Mean	Coefficient of variation
C	0.8	0.09
i	100 mm/h	0.5
A	0.1 km ²	0.005

$Q = KCiA$, where $K = 0.28$ for SI units for i in mm/hr and A in km².

SOLUTION

Using $\bar{Q} = 0.28 \bar{C} \bar{i} \bar{A}$ from example (10.6.1), we find

$$\bar{Q} = 0.28(0.8)(100)(0.1) = 2.24 \text{ m}^3/\text{s}$$

Using $\Omega_Q = [\Omega_C^2 + \Omega_i^2 + \Omega_A^2]^{1/2}$ from example 10.6.1, we find

$$\Omega_Q = [0.09^2 + 0.5^2 + 0.005^2]^{1/2} = 0.508$$

The standard deviation of Q can be determined using

$$\sigma_Q = \bar{Q} \Omega_Q = 2.24(0.508) = 1.138 \text{ m}^3/\text{s}$$

EXAMPLE 10.6.3

Apply the first-order analysis to Manning’s equation for full pipe flow, given in U.S. customary units as

$$Q = \frac{0.463}{n} S^{1/2} D^{8/3}$$

to determine equations for computing σ_Q and Ω_Q . Consider the diameter D to be deterministic without any uncertainty, and consider n and S to be uncertain.

SOLUTION

Since n and S are uncertain, Manning’s equation can be rewritten as

$$Q = Kn^{-1}S^{1/2}$$

where $K = 0.463D^{8/3}$. The first-order approximation of Q is determined using equation (10.6.2), so that

$$\begin{aligned} Q &\approx \bar{Q} + \left[\frac{\partial Q}{\partial n} \right]_{\bar{n}, \bar{S}} (n - \bar{n}) + \left[\frac{\partial Q}{\partial S} \right]_{\bar{n}, \bar{S}} (S - \bar{S}) \\ &= \bar{Q} + \left[-K\bar{n}^{-2}\bar{S}^{1/2} \right] (n - \bar{n}) + \left[0.5K\bar{n}^{-1}\bar{S}^{-1/2} \right] (S - \bar{S}) \end{aligned}$$

where $\bar{Q} = K\bar{n}^{-1}\bar{S}^{-1/2}$.

Next compute the variance of the pipe capacity using equation (10.6.3):

$$\begin{aligned} \sigma_Q^2 &= \left[\frac{\partial Q}{\partial n} \right]_{(\bar{n}, \bar{S})}^2 \sigma_n^2 + \left[\frac{\partial Q}{\partial S} \right]_{(\bar{n}, \bar{S})}^2 \sigma_S^2 \\ \sigma_Q &= \left\{ \left[\frac{\partial Q}{\partial n} \right]_{(\bar{n}, \bar{S})}^2 \sigma_n^2 + \left[\frac{\partial Q}{\partial S} \right]_{(\bar{n}, \bar{S})}^2 \sigma_S^2 \right\}^{1/2} \end{aligned}$$

Determine the coefficient of variation of Q using equation (10.6.4):

$$\begin{aligned} \Omega_Q^2 &= \sum_{i=1}^2 \left[\frac{\partial Q}{\partial x_i} \right]^2 \left[\frac{\bar{x}_i}{\bar{Q}} \right]^2 \Omega_{x_i}^2 \\ &= \left[\frac{\partial Q}{\partial n} \right]^2 \left[\frac{\bar{n}}{\bar{Q}} \right]^2 \Omega_n^2 + \left[\frac{\partial Q}{\partial S} \right]^2 \left[\frac{\bar{S}}{\bar{Q}} \right]^2 \Omega_S^2 \\ &= \left[\frac{-K\bar{S}^{1/2}}{\bar{n}^2} \right]^2 \left[\frac{\bar{n}}{\bar{Q}} \right]^2 \Omega_n^2 + \left[\frac{0.5K}{\bar{n}\bar{S}^{1/2}} \right]^2 \left[\frac{\bar{S}}{\bar{Q}} \right]^2 \Omega_S^2 \\ &= \left[\frac{-K\bar{S}^{1/2}}{\bar{Q}} \right]^2 \left[\frac{1}{\bar{n}^2} \right] \Omega_n^2 + \left[0.5 \right]^2 \left[\frac{K}{\bar{n}\bar{S}^{1/2}} \right]^2 \left[\frac{\bar{S}}{\bar{Q}} \right]^2 \Omega_S^2 \\ &= \left[\bar{n}^2 \right] \left[\frac{1}{\bar{n}^2} \right] \Omega_n^2 + 0.25 \left[\frac{1}{\bar{S}} \right] [\bar{S}]^2 \Omega_S^2 \\ &= \Omega_n^2 + 0.25 \Omega_S^2 \\ \Omega_Q &= [\Omega_n^2 + 0.25 \Omega_S^2]^{1/2} \end{aligned}$$

EXAMPLE 10.6.4

Determine the mean capacity of a storm sewer pipe, the coefficient of variation of the pipe capacity, and the standard deviation of the pipe capacity using Manning's equation for full pipe flow. Refer to example 10.6.3. The following parameter values are to be considered:

Parameter	Mean	Coefficient of variation
n	0.015	0.01
D	1.5 m	0
S	0.001	0.05

SOLUTION

Manning's equation in SI units for full pipe flow is

$$Q = \frac{0.311}{n} S^{1/2} D^{8/3}$$

so for first-order analysis we have

$$\begin{aligned}\bar{Q} &= \frac{0.311}{\bar{n}} \bar{S}^{1/2} D^{8/3} = \frac{0.311}{0.015} (0.001)^{1/2} (1.5)^{8/3} \\ &= 1.93 \text{ m}^3/\text{s}\end{aligned}$$

Using example 10.6.3, we find

$$\begin{aligned}\Omega_Q &= \left[(0.01)^2 + 0.25(0.05)^2 \right]^{1/2} = 0.027 \\ \sigma_Q &= \bar{Q}\Omega_Q = 1.93(0.027) \\ &= 0.052 \text{ m}^3/\text{s}\end{aligned}$$

10.7 RISK ANALYSIS: COMPOSITE HYDROLOGIC AND HYDRAULIC RISK

The *resistance* or strength of a component is defined as the ability of the component to fulfill its required purpose satisfactorily without a failure when subjected to an external stress. *Stress* is the loading of the component, which may be a mechanical load, an environmental exposure, a flow rate, temperature fluctuation, etc. The stress or loading tends to cause failure of the component. When the strength of the component is less than the stress imposed on it, failure occurs. This type of analysis can be applied to the reliability analysis of components of various hydraulic systems. The *reliability of a hydraulic system* is defined as the probability of the resistance to exceed the loading, i.e., the probability of survival. The terms "stress" and "strength" are more meaningful to structural engineers, whereas the terms "loading" and "resistance" are more descriptive to water resources engineers. The *risk of a hydraulic component, subsystem, or system* is defined as the probability of the loading exceeding the resistance, i.e., the *probability of failure*. The mathematical representation of the reliability R can be expressed as

$$R = P(r > \ell) = P(r - \ell > 0) \quad (10.7.1)$$

where $P()$ refers to probability, r is the resistance, and ℓ is the loading. The relationship between reliability R and risk \bar{R} is

$$R = 1 - \bar{R} \quad (10.7.2)$$

The resistance of a hydraulic system is essentially the flow-carrying capacity of the system, and the loading is essentially the magnitude of flows through or pressure imposed on the system by demands. Since the loading and resistance are random variables due to the various hydraulic and demand uncertainties, a knowledge of the probability distributions of r and ℓ is required to develop

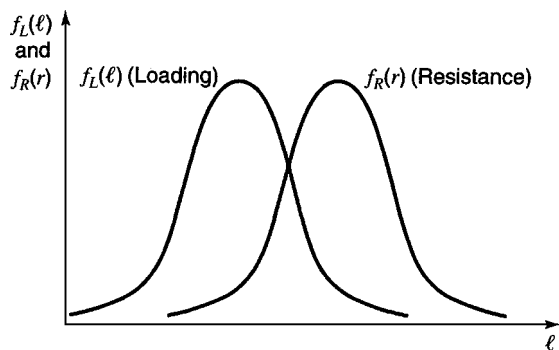


Figure 10.7.1 Load-resistance interference reliability analysis.

reliability models. The computation of risk and reliability can be referred to as *loading-resistance interference*. Probability distributions for loading and resistance are illustrated in Figure 10.7.1. The *reliability* is the probability that the resistance is greater than the loading for all possible values of the loading.

The word “static,” from the reliability computation point of view, represents the worst single stress, or load, applied. Actually, the loading applied to many hydraulic systems is a random variable. Also, the number of times a loading is imposed is random.

10.7.1 Reliability Computation by Direct Integration

Following the reliability definition given in equation (10.7.1), the reliability can be expressed as

$$R = \int_0^\infty f_R(r) \left[\int_0^r f_L(\ell) d\ell \right] dr = \int_0^\infty f_R(r) F_L(r) dr \tag{10.7.3}$$

in which $f_R()$ and $f_L()$ represent the probability density functions of resistance and loading, respectively. The reliability computations require the knowledge of the probability distributions of loading and resistance. A schematic diagram of the reliability computation by equation (10.7.3) is shown in Figure 10.7.2.

To illustrate the computation procedure involved, we consider that the loading ℓ and the resistance r are distributed exponentially, i.e.,

$$f_L(\ell) = \lambda_\ell e^{-\lambda_\ell \ell}, \quad \ell \geq 0 \tag{10.7.4}$$

$$f_R(r) = \lambda_r e^{-\lambda_r r}, \quad r \geq 0 \tag{10.7.5}$$

Then the static reliability can be derived by applying equation (10.7.3) in a straightforward manner as

$$R = \int_0^\infty \lambda_r e^{-\lambda_r r} \left[\int_0^r \lambda_\ell e^{-\lambda_\ell \ell} d\ell \right] dr = \int_0^\infty \lambda_r e^{-\lambda_r r} [1 - e^{-\lambda_\ell r}] dr = \frac{\lambda_\ell}{\lambda_r + \lambda_\ell} \tag{10.7.6}$$

For some special combinations of load and resistance distributions, the static reliability can be derived analytically in the closed form. In cases in which both the loading ℓ and resistance r are log-normally distributed, the reliability can be computed as (Kapur and Lamberson, 1977)

$$R = \int \phi(z) dz = \Phi(z) \tag{10.7.7}$$

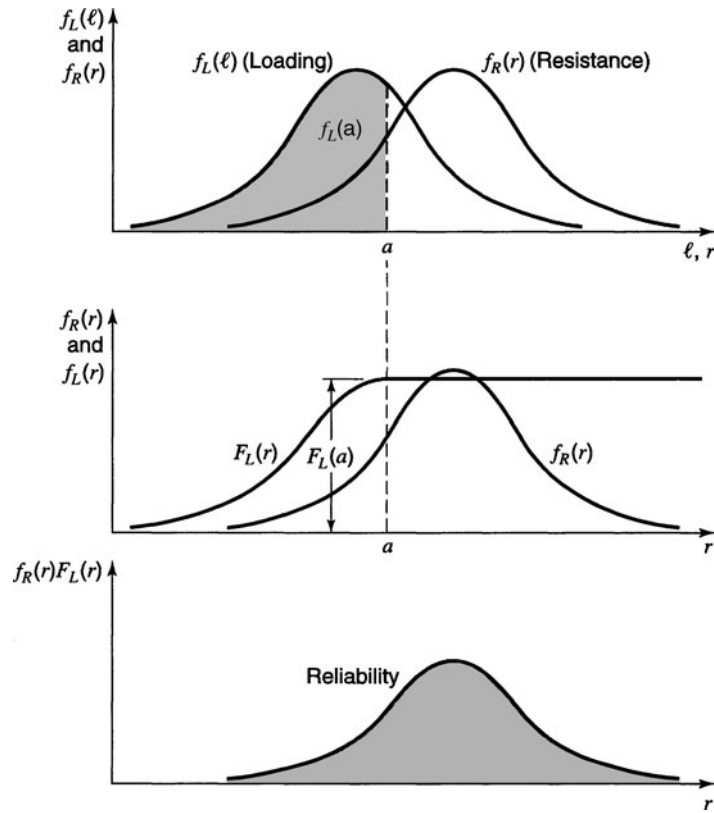


Figure 10.7.2 Graphical illustration of the steps involved in reliability computation, by equation (10.7.3).

where $\phi(z)$ and $\Phi(z)$ are the probability density function and the cumulative distribution function, respectively, for the standard normal variate z given as

$$z = \frac{\mu_{\ln r'} - \mu_{\ln \ell}}{\sqrt{\sigma_{\ln r'}^2 + \sigma_{\ln \ell}^2}} \quad (10.7.8)$$

The values of the cumulative distribution function $\Phi(z)$ for the standard normal variate are given in Table 10.2.1.

In cases in which the loading ℓ is exponentially distributed and the resistance is normally distributed, the reliability can be expressed as (Kapur and Lamberson, 1977)

$$R = 1 - \Phi\left(\frac{\mu_r}{\sigma_r}\right) - \exp\left[-\frac{1}{2}\left(2\mu_r\lambda_\ell - \lambda_\ell^2\sigma_r^2\right)\right] \times \left[1 - \Phi\left(-\frac{\mu_r - \lambda_\ell\sigma_r^2}{\sigma_r}\right)\right] \quad (10.7.9)$$

EXAMPLE 10.7.1

Consider a water distribution system (see Figure 10.7.3) consisting of a storage tank serving as the source and a 2-ft diameter cast-iron pipe 1 mi long, leading to a user. The head elevation at the source is maintained at a constant height of 100 ft above the elevation at the user end. It is also known that, at the user end, the required pressure head is fixed at 20 psi with variable demand on flow rate. Assume that the demand in flow rate is random, having a log-normal distribution with mean 1 cfs and standard deviation 0.3 cfs. Because of the uncertainty in pipe roughness, the supply to the user is not certain. We know that the

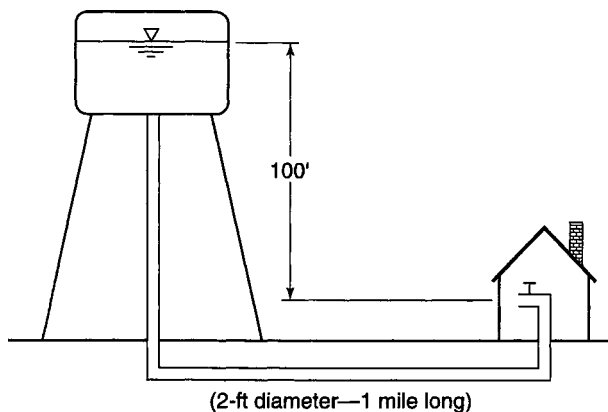


Figure 10.7.3 Example system.

pipe has been installed for about three years. Therefore, our estimation of the pipe roughness in the Hazen–Williams equation is about 130, with some errors of ± 20 . Again, we further assume that the Hazen–Williams C coefficient has a log-normal distribution with a mean of 130 and a standard deviation of 20. It is required to estimate the reliability with which the water demand by the user will be satisfied.

SOLUTION

In this example, the resistance of the system is the water supply from the source, while the loading is the water demand by the user. Both supply and demand are random variables. By the Hazen–Williams equation, the supply is calculated as

$$r = Q_s = \frac{C}{149.2} \left(\frac{\Delta h}{L} \right)^{0.54} D^{2.63}$$

where Δh is the head difference (in feet) between the source and the user, D is the pipe diameter in feet, and L is the pipe length in feet. Because the roughness coefficient C is a random variable, so is the supply. Due to the multiplicative form of the Hazen–Williams equation, the logarithmic transformation leads to a linear relation among variables, i.e.,

$$\begin{aligned} \ln Y &= \ln C - \ln(149.2) + 0.54 \ln \left[\frac{100 - \frac{(20)(144)}{62.4}}{5280} \right] + 2.63 \ln(2) \\ &= \ln C - 5.659 \end{aligned}$$

Assume that the roughness coefficient C is log-normally distributed; then $\ln C$ is normally distributed, as is the log-transformed water supply (resistance). From the moment relations given in Table 10.1.2 for log-normal distribution, the mean and the standard deviation of $\ln C$ are determined as follows. From Table 10.1.2,

$$\mu_{\ln r} = \mu_{\ln C} = \ln C - \sigma_{\ln r}^2 / 2$$

where $\sigma_{\ln r}^2 = \sqrt{\ln(1 + \Omega_C^2)} = \sqrt{\ln[1 + (20/130)^2]} = 0.153$. Thus, $\mu_{\ln r} = \ln 130 - (0.153^2/2) = 4.856$. From these results, the mean and the standard deviation of $\ln Y$ are -0.803 and 0.153 , respectively.

Because the water demand (loading) has a log-normal distribution, the mean and standard deviation of its log-transformed scale can be calculated in the same manner as for roughness coefficient C . That is,

$$\sigma_{\ln \ell} = \sqrt{\ln[1 + (0.3/1)^2]} = 0.294 \text{ and } \mu_{\ln \ell} = 1 - (0.294^2/2) = -0.043.$$

Knowing the distributions and statistical properties of the load (water demand) and resistance (water supply), both log-normal in this example, we can calculate the reliability of the system by equation (10.7.7) as

$$R = \Phi \left[z = \frac{-0.803 - (-0.043)}{\sqrt{0.153^2 + 0.294^2}} \right] = \Phi(z = -2.293) = 1 - \Phi(2.293) = 0.013$$

This means that the water demanded by the user will be met with a probability of 1.3 percent.

10.7.2 Reliability Computation Using Safety Margin/Safety Factor

Safety Margin

The *safety margin* (SM) is defined as the difference between the project capacity (resistance) and the value calculated for the design loading, $SM = r - \ell$. The reliability is equal to the probability that $r > \ell$, or equivalently,

$$R = p(r - \ell > 0) = P(SM > 0) \quad (10.7.10)$$

If r and ℓ are independent random variables, then the mean value of SM is given by

$$\mu_{SM} = \mu_r - \mu_\ell \quad (10.7.11)$$

and its variance by

$$\sigma_{SM}^2 = \sigma_r^2 + \sigma_\ell^2 \quad (10.7.12)$$

If the safety margin is normally distributed, then

$$z = (SM - \mu_{SM}) / \sigma_{SM} \quad (10.7.13)$$

is a standard normal variate z . By subtracting μ_{SM} from both sides of the inequality in equation (10.7.10) and dividing both sides by σ_{SM} , it can be seen that

$$R = P \left(z > \frac{\mu_{SM}}{\sigma_{SM}} \right) = \Phi \left(\frac{\mu_{SM}}{\sigma_{SM}} \right) \quad (10.7.14)$$

The key assumption of this analysis is that it considers that the safety margin is normally distributed but does not specify the distributions of loading and capacity. Ang (1973) indicated that, provided $R > 0.001$, R is not greatly influenced by the choice of distribution for r and ℓ and the assumption of a normal distribution for SM is satisfactory. For lower risk than this (e.g., $R = 0.00001$), the shape of the tails of the distributions for r and ℓ becomes critical, in which case accurate assessment of the distribution of SM of direct integration procedure should be used to evaluate the risk or probability of failure.

EXAMPLE 10.7.2

Apply the safety margin approach to evaluate the reliability of the simple water distribution system described in Example 10.7.1.

SOLUTION

Calculate the mean and standard deviation of the resistance (i.e., water supply) as

$$\mu_r = \exp \left(\mu_{\ln \ell} + \frac{1}{2} \sigma_{\ln \ell}^2 \right) = \exp \left[-0.803 + \frac{1}{2} (0.153)^2 \right] = 0.453 \text{ cfs}$$

and

$$\sigma_r = \sqrt{\mu_r^2 [\exp(\sigma_{\ln \ell}^2) - 1]} = \sqrt{0.453^2 [\exp(0.153^2) - 1]} = 0.070 \text{ cfs}$$

From the problem statement, the mean and standard deviation of the load (water demand) are $\mu_\ell = 1$ cfs and $\sigma_\ell = 0.3$ cfs, respectively. Therefore, the mean and variance of the safety margin can be calculated as

$$\begin{aligned}\mu_{SM} &= \mu_r - \mu_\ell = 0.453 - 1.0 = -0.547 \text{ cfs} \\ \sigma_{SM}^2 &= \sigma_r^2 + \sigma_\ell^2 = (0.070)^2 + (0.3)^2 = 0.095 (\text{cfs})^2\end{aligned}$$

Now, the reliability of the system can be assessed, by the safety margin approach, as

$$R = \Phi\left[\frac{-0.453}{\sqrt{0.095}}\right] = \Phi[-1.470] = 1 - \Phi[1.470] = 1 - 0.929 = 0.071$$

The reliability computed by the safety margin method is not identical to that of direct integration although the difference is practically negligible. It should, however, be pointed out that the distribution of the safety margin in this example is not exactly normal, as assumed. Thus, the reliability obtained should be regarded as an approximation to the true reliability.

EXAMPLE 10.7.3

Determine the risk (probability) that the surface runoff (loading) exceeds the capacity of the storm sewer pipe for the problems in examples 10.6.2 and 10.6.4. Use the safety margin approach.

SOLUTION

From example 10.6.2, $\bar{Q}_\ell = 2.24$ m³/s and $\sigma_\ell = 1.138$ m³/s. From example 10.6.4, $\bar{Q}_r = 1.93$ m³/s and $\sigma_r = 0.052$ m³/s. Compute μ_{SM} using equation (10.7.11):

$$\mu_{SM} = \mu_r - \mu_\ell = \bar{Q}_r - \bar{Q}_\ell = 1.93 - 2.24 = -0.31 \text{ m}^3/\text{s}$$

Compute σ_{SM} using equation (10.7.12):

$$\sigma_{SM} = [\sigma_r^2 + \sigma_\ell^2]^{1/2} = [(0.052)^2 + (1.138)^2]^{1/2} = 1.139 \text{ m}^3/\text{s}$$

Compute the reliability using equation (10.7.14):

$$R = \Phi\left(\frac{\mu_{SM}}{\sigma_{SM}}\right) = \Phi\left(\frac{-0.310}{1.139}\right) = \Phi(-0.272) = 0.607$$

The risk (the probability of $Q_\ell > Q_r$) is thus

$$\begin{aligned}\bar{R} &= 1 - R = 1 - 0.607 \\ &= 0.393 \text{ or } 39.3\%\end{aligned}$$

Safety Factor

The *safety factor* (SF) is given by the ratio r/ℓ and the reliability can be specified by $P(SF > 1)$. Several safety factor measures and their usefulness in hydraulic engineering are discussed by Mays and Tung (1992) and Yen (1978). By taking logarithms of both sides of this inequality, we find

$$\begin{aligned}R &= P(SF > 1) = P[\ln(SF) > 0] = P[\ln(r/\ell) > 0] \\ &= P\left(z \leq \frac{\mu_{\ln SF}}{\sigma_{\ln SF}}\right) = \Phi\left(\frac{\mu_{\ln SF}}{\sigma_{\ln SF}}\right)\end{aligned}\tag{10.7.15}$$

If the resistance and loading are independent and log-normally distributed, then the risk can be expressed as

$$\bar{R} = \Phi \left\{ \frac{\ln \left[\frac{\mu_r}{\mu_\ell} \sqrt{\frac{1 + \Omega_\ell^2}{1 + \Omega_r^2}} \right]}{\ln [(1 + \Omega_\ell^2)(1 + \Omega_r^2)]^{1/2}} \right\} \quad (10.7.16)$$

EXAMPLE 10.7.4

Determine the risk (probability) that the surface runoff (loading) exceeds the capacity of the storm sewer pipe for the problems in examples 10.6.2 and 10.6.4. Use the safety factor approach.

SOLUTION

$\bar{Q}_\ell = 2.24 \text{ m}^3/\text{s}$, $\Omega_\ell = 0.508$, $\bar{Q}_r = 1.93 \text{ m}^3/\text{s}$, $\Omega_r = 0.027$. Use equation (10.7.16) to compute the risk:

$$\begin{aligned} \bar{R} &= \Phi \left\{ \frac{\ln \left[\frac{\bar{Q}_r}{\bar{Q}_\ell} \sqrt{\frac{1 + \Omega_\ell^2}{1 + \Omega_r^2}} \right]}{\ln \sqrt{(1 + \Omega_\ell^2)(1 + \Omega_r^2)}} \right\} \\ &= \Phi \left\{ \frac{\ln \left[\frac{1.93}{2.24} \sqrt{\frac{1 + 0.508^2}{1 + 0.027^2}} \right]}{\ln \sqrt{(1 + 0.508^2)(1 + 0.027^2)}} \right\} \\ &= \Phi(-0.300) \\ &= 0.382 = 38.2\% \end{aligned}$$

Note that the risk values (magnitudes) calculated for the same problem by the safety margin approach in example 10.7.3 and by the safety factor approach in this example are very close.

10.8 COMPUTER MODELS FOR FLOODFLOW FREQUENCY ANALYSIS

Table 10.8.1 describes the features of the HEC-FFA (U.S. Army Corps of Engineers, 1992) and PEAKFQ (U.S. Geological Survey) models that are used for flood flow frequency analysis, based upon fitting the log-Pearson Type III distribution to observed annual maximum flood series. The

Table 10.8.1 HEC-FFA and PEAKFQ Features

Feature	Analysis Procedure
Parameter estimation	Estimate parameters with method of moments; this assumes sample mean, standard deviation, skew coefficient = parent population mean, standard deviation, and skew coefficient. To account for variability in skew computed from small samples, use weighted sum of station skew and regional skew.

(Continued)

Table 10.8.1 (Continued)

Feature	Analysis Procedure
Outliers	These are observations that “. . . depart significantly from the trend of the remaining data.” Models identify high and low outliers. If information available indicates that a high outlier is maximum in the extended time period, it is treated as historical flow. Otherwise, they are treated as part of a systematic sample. Low outliers are deleted from the sample, and conditional probability adjustment is supplied.
Zero flows	If the annual maximum flow is zero (or below a specified threshold), the observations are deleted from the sample. The model parameters are estimated with the remainder of the sample. The resulting probability estimates are adjusted to account for the conditional probability of exceeding a specified discharge, given that a nonzero flow occurs.
Historical flood information	If information is available indicating that an observation represents the greatest flow in a period longer than that represented by the sample, model parameters are computed with “historically” weighted moments.
Broken record	If observations are missed due to “. . . conditions not related to flood magnitude,” different sample segments are analyzed as a single sample with the size equal to the sum of the sample sizes.
Expected probability adjustment	This adjustment is made to the model results “. . . to incorporate the effects of uncertainty in application of the [frequency] curve.”

Source: Ford and Hamilton (1996).

World Wide Web (www) site for the U.S. Army Corps of Engineers is www.usace.army.mil and for the U.S. Geological Survey is www.usgs.gov.

PROBLEMS

10.2.1 Solve example 10.2.1 to determine the flood magnitude having a return period of 50 years.

10.2.2 The annual maximum series of flood magnitude in a river has a log-normal distribution with a mean of 8000 m³/s and a standard deviation of 3000 m³/s. (a) What is the probability in each year that a flood magnitude would exceed 12,000 m³/s? (b) Determine the flood magnitude for return periods of 25 and 100 years.

10.2.3 Solve problem 10.2.2 for a mean of 5000 m³/s.

10.2.4 Determine the rainfall depths for the 2-, 5-, 10-, and 25-year storms for a 60-min duration storm for a mean depth of 1.5 inches and a standard deviation of 0.5 in. Use the Gumbel (extreme value type I) distribution.

10.2.5 In the Yuen-Long area of Hong Kong, there is an observatory rain gauge from which the annual maximum 3-hr rainfall depth from 1971–1975 is extracted in the table below. Conduct a frequency analysis to determine the average 3-hr rainfall intensity (mm/h) associated with an annual exceedance probability of 1% by (a) using the Gumbel (extreme value type I) distribution; and (b) using the log-normal distribution.

Year	3-hr rainfall (mm)
1971	108.2
1972	93.0
1973	104.8
1974	61.3
1975	70.3

10.2.6 The following table contains annual maximum 15-min rainfall data from a rain gauge. Assume that the data follow the Gumbel (extreme type I) distribution.

- (a) Determine the magnitude of 100-year rainfall intensity (mm/hr).
- (b) Determine the return period corresponding to a rainfall depth of 60 mm.

Year	15-min annual max. depth (mm)
1991	25
1992	37
1993	30
1994	33
1995	45

10.2.7 The following table contains annual maximum 15-min rainfall data from a rain gauge. Assume that the data follow the Gumbel (extreme value type I) distribution.

- (a) Approximate the magnitude of 15-min, 100-year rainfall intensity (mm/hr).
- (b) Determine the return period corresponding to a 15-min rainfall depth of 60 mm.

Year	15-min annual max. depth (mm)
1991	25
1992	37
1993	30
1994	33
1995	45

10.3.1 Determine the hydrologic risk of a 100-year flood occurring during the 20-year service life of a project. What is the chance that the 25-year flood will not occur?

10.3.2 Determine the hydrologic risk of a 25-year flood occurring during the 20-year service life of a project. What is the chance that the 25-year flood will not occur?

10.3.3 Determine the corresponding return periods of an annual exceedance series for corresponding annual maximum series return periods of 2, 5, 10, 25, and 100 years.

10.3.4 Given flood data in a river are shown in the table below.

Year	Date	Peak discharge (m ³ /s)
1963	June 1	95
	August 3	300
1964	June 7	60
1965	August 2	80
1966	May 28	100
	August 15	90
1967	July 11	800
	August 25	700
	September 4	90

- (a) Determine the data set for both annual maximum series and annual exceedance series.
- (b) Determine the magnitude of a 50-year flood.

10.4.1 The mean, standard deviation, and skew coefficient of the log-transformed discharges (in ft³/s) for a river are 4.5, 0.6, and 0.2, respectively. Compute the 10-year and 100-year peak discharges.

10.4.2 Solve example 10.4.1 to compute the 25-year and 200-year peak discharges using the log-Pearson Type III distribution.

10.4.3 Solve example 10.4.2 using the annual peak discharges for 1938–1960 using the log-Pearson Type III distribution.

10.4.4 Solve example 10.4.2 to compute the 10-year and 200-year peak discharges using the log-Pearson Type III distribution.

10.4.5 Determine the rainfall depths for the 2-, 5-, 10-, and 25-year storms for a 60-min duration storm for a mean depth of 1.5 in and a standard deviation of 0.5 in. Use the frequency factor method with the Gumbel (extreme value type I) distribution.

10.4.6 The annual exceedance series of rainfall data (maximum depth in inches) for a 15-min duration is ranked in order of largest to smallest as follows: 1.423 in, 0.940, 0.920, 0.910, 0.890, 0.884, 0.860, 0.810, 0.805, 0.783, 0.770, 0.770, 0.750, 0.750, 0.733, 0.732, 0.710, 0.707, 0.700, 0.700, 0.700, 0.692, 0.688, 0.687, 0.670. Plot the rainfall depth-frequency data with return period on the x-axis and rainfall depth (inches) on the y-axis. Use the extreme value type I distribution to fit a line for the 15-min duration. Also plot this line.

10.4.7 Perform a frequency analysis using the extreme value type I distribution for the 15-min duration rainfall depths given in problem 10.4.6. What are the 2-, 5-, 10-, 25-, and 100-year 15-min duration rainfall depths?

10.4.8 The following table contains annual maximum flow data for 1927–1933.

Year	1927	1928	1929	1930	1931	1932	1933
Flow (100 m ³ /s)	90	116	142	99	63	128	126

Determine the 200-year flow by the frequency-factor method assuming that the flows follow (a) log normal distribution and (b) log-Pearson type III distribution.

10.4.9 A river flowing by a village situated in a low-lying area has 5 years of discharge measurements. The peak discharges in the river exceeding 100 m³/s over the period of record are shown in the table below. Due to frequent flooding of the village, a dike system is to be constructed by the local government for protecting the village. From the viewpoint of safety performance of the system, the local government requires that the failure probability of the dike system over an expected service period of 50 years is 0.30 or less.

- (a) What return period should the dike system be designed for?
- (b) Based on the annual maximum floods, determine the magnitude of design discharge corresponding to the return period obtained in part (a).
- (c) Repeat part (b) using the annual exceedance series of floods applying the frequency factor method with a log-Pearson type III distribution.

Year	2000	2001	2002	2003	2004
Discharge (m ³ /s)	105, 130, 341	101	107, 110	104, 240	111, 124, 105

10.4.10 You are hired as a consultant to help design a coffer dam for protecting the construction of bridge piers in a river. Based on 30 years of flood data in the river, the largest flood is 7800 m³/s and the smallest is 2400 m³/s. The probability plot indicates that the flood magnitude and the corresponding return period, estimated by the Weibull plotting position formula, $Pr[X \geq x_{(m)}] \approx m/(n + 1)$, reveals a linear relation. Assume that the bridge piers have a construction period of 3 years and the required overtopping probability over the construction period must not exceed 10 percent.

- (a) Determine the required design return period for the coffer dam.
- (b) Determine the magnitude of flood to be protected against for the coffer dam.

10.4.11 A river flowing by a village situated in a low-lying area has 4 years of discharge measurements. The peak discharges in the river exceeding 100 m³/s over the record period are shown in the table below. Due to frequent flooding of the village, a dike system is to be constructed by the local government for protecting the village. From the viewpoint of safety and cost the local government decided that the dike system should be designed to have a failure probability of 0.30 or less over an expected service period of 50 years.

- (a) What should be the design return period for the dike system?
- (b) Based on annual maximum floods, determine the magnitude of design discharge corresponding to the return period obtained in part (a).
- (c) Due to relatively short stream flow record, the underlying distribution is uncertain. To have some idea about the effect of using different distributions, you are asked to recalculate design discharge for the dike system based on annual exceedance floods using the frequency factor method and log-Pearson type III distribution.

Year	2000	2001	2002	2003
Discharge (m ³ /s)	105, 130, 340	95 100	100 107, 125	104, 240

10.4.12 The following table contains annual maximum 15-min rainfall data from a rain gauge. Assume that the data follow the Gumbel (Extreme value type I) distribution.

- (a) Determine the magnitude of 100-year rainfall intensity with and without the frequency factor method.
- (b) Determine the return period corresponding to a rainfall depth of 60 mm by both methods in part (a).

Year	1991	1992	1993	1994	1995
Depth (mm)	25	37	30	33	45

10.5.1 Use the annual flood data for the Floyd River, James, Iowa, in the table below to perform a flood frequency analysis using the U.S. Water Resources Council Guidelines. The map skew for this location is -0.4.

Year	Discharge (cfs)	Year	Discharge (cfs)
1935	1460	1955	2260
1936	4050	1956	318
1937	3570	1957	1330
1938	2060	1958	970
1939	1300	1959	1920
1940	1390	1960	15,100
1941	1720	1961	2870
1942	6280	1962	20,600
1943	1360	1963	3810
1944	7440	1964	726
1945	5320	1965	7500
1946	1400	1966	7170
1947	3240	1967	2000
1948	2710	1968	829
1949	4520	1969	17,300
1950	4840	1970	4740
1951	8320	1971	13,400
1952	13,900	1972	2940
1953	71,500	1973	5660
1954	6250		

10.5.2 Solve problem 10.5.1 using only the maximum series for 1935–1950.

10.5.3 Solve problem 10.5.1 using only the maximum series for 1935–1970.

10.5.4 Consider the annual maximum series for the U.S. Geological Survey gauging station on Clear Creek near Pearland, Texas. The statistics of the log-transformed flows are $\bar{y} = 2.98$ cfs, $S_y = 0.27$, $G_s = -1.1$, and $n = 46$. Using the log-Pearson Type III distribution, compare the 100-year discharges with and without the U.S. Water Resources Council (1981) recommendation on skew coefficients. The map skew for this location is -0.3.

10.5.5 In problem 10.5.4, what is the 100-year flood using the normal distribution?

10.5.6 You are performing a flood flow frequency analysis of a stream. Here's the information that you have been able to compute:

- Period of record: 1990–2009
- Mean annual flood = 7000 cfs
- Standard deviation of annual floods = 1000 cfs
- Skew coefficient of annual floods = 1.0
- Mean of logarithms (base 10) of annual floods = 3.52
- Standard deviation of logarithms = 0.50
- Coefficient of skew of logarithms of annual flows = 2.0

Generalized (map) skew coefficient = -0.1

Your first task is to make a comparison of the 100-year floods using both the log-Pearson type III distribution and a separate evaluation using the U.S. Water Resources Council guidelines.

10.5.7 Using the data in Problem 10.5.6, your second task concerns the design of a water control structure that is to be constructed on the stream. This structure will fail if the flow rate exceeds 20,000 cfs. What is the risk of failure for this structure over its expected life of 25 years?

10.6.1 Apply the first-order analysis of uncertainty to the weir flow equation for spillways: $Q = CLH^{1.5}$. Consider C and H to be uncertain.

10.6.2 Solve example 10.6.1 considering only C and i to be uncertain.

10.6.3 Solve example 10.6.2 assuming no uncertainty in A .

10.6.4 Apply first-order analysis to Manning's equation for full pipe flow assuming n , S , and D to be uncertain.

10.7.1 Calculate the risk of failure (walls are overtopped) of an open channel, using the safety margin approach (SM is normally distributed). The capacity is computed using Manning's equation and a first-order analysis is used to determine the coefficient of variation of the capacity. The mean loading is 2500 cfs and the coefficient of variation of loading is 0.20. The slope of the channel is 0.002 with a coefficient of variation of 0.10. Manning's rough-

ness factor is 0.04 and has a coefficient of variation of 0.10. The channel cross-section is rectangular with a width of 50 ft and a wall height of 10 ft.

10.7.2 Solve problem 10.7.1 using the safety factor approach.

10.7.3 Solve problem 10.7.1 assuming the capacity and loading to be log-normally distributed.

10.7.4 Solve example 10.7.1 assuming that the demand in flow rate is log-normal with a mean of 0.5 cfs and a standard deviation of 0.3 cfs. The Hazen-Williams C has a log-normal distribution with a mean of 120 and a standard deviation of 20.

10.7.5 What would be the reliability in example 10.7.1 if the safety margin approach were used, assuming the SM is distributed normally?

10.7.6 Compare the risks of a discharge of 2000 cfs being equaled or exceeded at least once over the next 10 years with and without the U.S. Water Resources Council recommendation on the skew coefficient. Assume $G_w = -0.7$. Use data in problem 10.5.4.

10.8.1 Use the HEC-FFA model to solve problem 10.5.1.

10.8.2 Use the HEC-FFA model to solve example 10.4.2.

REFERENCES

- Ang, A. H. S., "Structural Risk Analysis and Reliability-Based Design," *Journal of the Structural Engineering Division*, American Society of Civil Engineers, vol. 99, no. ST9, pp. 1891-1910, 1973.
- Chow, V. T., "A General Formula for Hydrologic Frequency Analysis," *Trans. Am. Geophysical Union*, vol. 32, no. 2, pp. 231-237, 1951.
- Chow, V. T., "Statistical and Probability Analysis of Hydrologic Data," Sec. 8-1 in *Handbook of Applied Hydrology* (edited by V. T. Chow), McGraw-Hill, New York, 1964.
- Chow, V. T., D. R. Maidment, and L. W. Mays, *Applied Hydrology*, McGraw-Hill, New York, 1988.
- Cudworth, A. D., Jr., *Flood Hydrology Manual*, U.S. Dept. of the Interior, Bureau of Reclamation, U.S. Government Printing Office, Denver, CO, 1989.
- Ford, D., and D. Hamilton, "Computer Models for Water-Excess Management," in *Water Resources Handbook* edited by L. W. Mays, McGraw-Hill, New York, 1996.
- Grant, E. L., and R. S. Leavenworth, *Statistical Quality and Control*, McGraw-Hill, New York, 1972.
- Hirsch, R. M., D. R. Helsel, T. A. Cohn, and E. J. Gilroy, "Statistical Analysis of Hydrologic Data," Chapter 17 in *Handbook of Hydrology* edited by D. R. Maidment, McGraw-Hill, New York, 1993.
- Kapur, K. C., and L. R. Lamberson, *Reliability in Engineering Design*, John Wiley and Sons, New York, 1977.
- Kite, G. W., *Frequency and Risk Analysis in Hydrology*, Water Resources Publications, Fort Collins, CO, 1977.
- Mays, L. W., and Y. K. Tung, *Hydrosystems Engineering and Management*, McGraw-Hill, New York, 1992.
- Mays, L. W. et al. "Methodologies for the Assessment of Aging Water Distribution Systems," Report No. CRWR 227, Center for Research in Water Resources, The University of Texas at Austin, (July) 1989.
- National Academy of Sciences, *Safety of Existing Dams: Evaluation and Improvement*, National Academy Press, Washington, DC, 1983.
- Tung, Y. K., and L. W. Mays, "Reducing Hydrologic Parameter Uncertainty," *Journal of Water Resources Planning and Management Division*, American Society of Civil Engineers, vol. 107, no. WR1, pp. 245-262, 1981.
- U.S. Army Corps of Engineers, "HEC-FFA: Flood Frequency Analysis: User's Manual," Hydrologic Engineering Center, Davis, CA, 1992.
- U.S. Water Resources Council (now called Interagency Advisory Committee on Water Data), *Guidelines for Determining Flood Flow Frequency*, Bulletin 17B, available from Office of Water Data Coordination, U.S. Geological Survey, Reston, VA, 1981.
- Wallis, J. R., N. C. Matalas, and J. R. Slack, "Just a Moment," *Water Resources Research*, vol. 10, no. 2, pp. 211-219, 1974.
- World Meteorological Organization, *Guide to Hydrological Practices*, Vol. II, *Analysis, Forecasting, and Other Applications*, WMO no. 168, 4th edition, Geneva, Switzerland, 1983.
- Yen, B. C., "Safety Factor in Hydrologic and Hydraulic Engineering Design," *Proceedings, International Symposium on Risk Reliability in Water Resources*, University of Waterloo, Waterloo, Ontario, Canada, (June) 1978.

This page intentionally left blank

Chapter 11

Water Withdrawals and Uses

11.1 WATER-USE DATA—CLASSIFICATION OF USES

Care should be taken in using or reading the terms that describe water uses, as these terms are often used inconsistently and misleadingly in the water literature. Gleick (1998) points out that the term “water use” has encompassed many different ideas to mean the withdrawal of water, gross water use, and the consumptive use of water. According to Gleick, *withdrawal* should refer to the act of taking water from a source for storage or use. *Gross water use* is distinguished from water withdrawal by the inclusion of recirculated or reused water. *Water consumption* or *consumptive use* should refer to the use of water in a manner that prevents its immediate reuse, such as through evaporation, plant transpiration, contamination, or incorporation into a finished product. As an example, water for cooling power plants may be withdrawn from a river or lake, used and then returned to the river or lake. According to Gleick, this should not be considered consumptive use. Agricultural water may have both consumptive and nonconsumptive uses, as some water is transpired or incorporated into plant material, with the remainder returning to the groundwater or surface water sources.

The U.S. Geological Survey (USGS) conducts the National Water Use Information (NWUI) program, which established the national system of water-use accounting. Water-use circulars are prepared by the USGS at five-year intervals. *Water use* is defined from a hydrologic perspective as all water flows that are a result of human intervention within the hydrologic cycle. The USGS uses the following seven water-use flows: (1) water withdrawals for offstream purposes, (2) water deliveries at point of use or quantities released after use, (3) consumptive use, (4) conveyance loss, (5) reclaimed waste water, (6) return flow, and (7) instream flow (Solley et al., 1993). A schematic of water-use flows and losses is presented in Figure 1.3.1.

Table 11.1.1 provides the USGS definition of water-use terms. Figure 1.3.2 is a diagram that tracks the sources, uses, and disposition of freshwater using the hydrologic accounting system (see Figure 1.3.1). Table 1.3.1 provides definitions of the major water-use purposes. Water use defined by purpose of actual use is a more restrictive definition of water use.

Table 1.2.3 illustrates the dynamics of water use in the world. For the world as whole, water requirements are growing and will continue to grow in all types of economic activity. This trend continues despite the progressive trends towards stabilization of water needs that have clearly taken shape in a number of countries (Shiklomanov, 1993). Table 1.2.4 compares annual runoff and water consumption by continents and by physiographic and economic regions of the world. This table can be used to compare the amounts of water withdrawal and consumption throughout the world with stream flow resources.

Table 11.1.1 Definitions of Water-Use Terms

Term	Definition
Consumptive use	That part of water withdrawn that is evaporated, transpired, incorporated into products or crops, consumed by humans or livestock, or otherwise removed from the immediate water environment.
Conveyance loss	The quantity of water that is lost in transit from a pipe, canal, conduit, or ditch by leakage or evaporation.
Delivery and release	The amount of water delivered to the point of use and the amount released after use.
Instream use	Water that is used, but not withdrawn, from a surface- or ground-water source for such purposes as hydroelectric-power generation, navigation, water-quality improvement, fish propagation, and recreation.
Offstream use	Water withdrawn or diverted from a surface- or ground-water source for public water supply, industry, irrigation, livestock, thermoelectric-power generation, and other uses.
Public supply	Water withdrawn by public or private water suppliers and delivered to users.
Return flow	The water that reaches a surface- or ground-water source after release from the point of use and thus becomes available for further use.
Reclaimed wastewater	Wastewater-treatment-plant effluent that has been diverted for beneficial use before it reaches a natural waterway or aquifer.
Self-supplied water	Water withdrawn from a surface- or groundwater source by a user rather than being obtained from a public supply.
Withdrawal	Water removed from the ground or diverted from a surface-water source for offstream use.

Source: Adapted from Solley, et al. (1993) as presented in Dziegielewski, et al. (1996).

Trends in freshwater withdrawals and consumption in the United States for 1960–1990 are illustrated in Figure 11.1.1. The per-capita consumption of water in 1990 was less than in 1965, despite an almost 50 percent increase in real per-capita income over that period (Rogers, 1993). Total water demand continued to decrease from the high in 1980, although the 1990 demand was slightly higher than the 1985 demand. Large reductions in water use by agriculture and industry appear to have occurred between 1980 and 1990 (Rogers, 1993). Tables 11.1.2–11.1.5 provide estimates of water use for industrial water use, municipal water use, and residential interior water use, respectively.

Sustainable water use has been defined by Gleick et al. (1995) as “the use of water that supports the ability of human society to endure and flourish into the indefinite future without undermining the integrity of the hydrological cycle or the ecological systems that depend on it.” The following seven sustainability requirements were presented:

1. A basic water requirement will be guaranteed to all humans to maintain human health.
2. A basic water requirement will be guaranteed to restore and maintain the health of ecosystems.
3. Water quality will be maintained to meet certain minimum standards. These standards will vary depending on location and how the water is to be used.
4. Human actions will not impair the long-term renewability of freshwater stocks and flows.
5. Data on water-resources availability, use, and quality will be collected and made accessible to all parties.
6. Institutional mechanisms will be set up to prevent and resolve conflicts over water.
7. Water planning and decision making will be democratic, ensuring representation of all affected parties and fostering direct participation of affected interests.

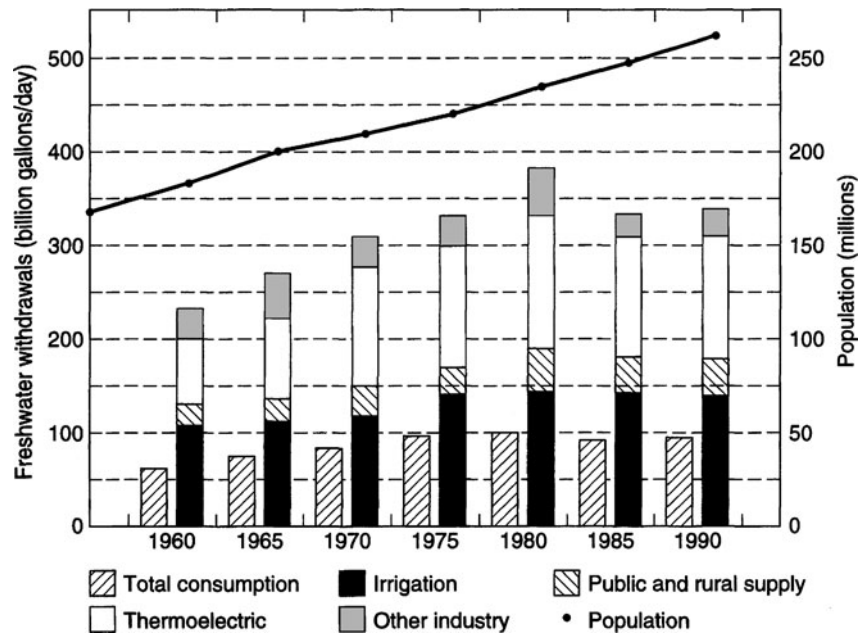


Figure 11.1.1 Trends in U.S. freshwater withdrawals and consumption, 1960–1990 (from Solley, et al. (1993), as presented in Rogers (1993)).

Table 11.1.2 Typical Rates of Water Use for Various Industries

Industry	Range of flow (gal/ton product)
<i>Cannery</i>	
Green beans	12,000–17,000
Peaches and pears	3600–4800
Other fruits and vegetables	960–8400
<i>Chemical</i>	
Ammonia	24,000–72,000
Carbon dioxide	14,400–21,600
Lacrose	144,000–192,000
Sulfur	1920–2400
<i>Food and beverage</i>	
Beer	2400–3840
Bread	480–960
Meat packing	3600–4800 ¹
Milk products	2400–4800
Whisky	14,000–19,200
<i>Pulp and paper</i>	
Pulp	60,000–190,000
Paper	29,000–38,000
<i>Textile</i>	
Bleaching	48,000–72,000 ²
Dyeing	7200–14,400 ²

¹Live weight.

²Cotton.

Source: Metcalf and Eddy, Inc. (1991).

Table 11.1.3 Water Used by Industries in the United States, 1983^a

Industry Group	Gross water used (10 ⁶ m ³ /yr)			Water discharged		
	Total	Intake	Reuse	Total (10 ⁶ m ³ /yr)	Untreated (%)	Treated (%)
All mineral industries	12,600	4540	8080	3930	31.9	68.1
Metal mining	2780	645	2140	504	39.7	60.3
Anthracite mining	20	8	12	28	12	87
Bituminous coal and lignite mining	449	172	278	440	26.2	73.8
Oil and gas extraction	5500	2280	3220	1800	31.0	69.0
Nonmetallic minerals, except fuels	3860	1430	2430	1150	32.6	67.4
All manufacturing industries	128,000	38,500	90,200	33,800	54.9	45.1
Food and kindred products	5330	2560	2880	2090	64.5	35.5
Tobacco products	128	20	108	15	<i>b</i>	<i>b</i>
Textile mill products	1260	503	759	438	52.9	47.1
Lumber and wood products	827	326	501	269	63.2	36.8
Furniture and fixtures	26	13	13	13	88	12
Paper and allied products	28,200	7200	21,000	6700	27.1	72.9
Chemicals and allied products	36,500	12,900	23,600	11,300	67.0	33.0
Petroleum and coal products	23,400	3100	20,300	2650	46.2	53.8
Rubber and miscellaneous plastic products	1240	288	954	237	63.6	36.4
Leather and leather products	25	23	2	22	<i>b</i>	<i>b</i>
Stone, clay, and glass products	1280	586	689	503	74.9	25.1
Primary metal industries	22,300	8950	13,400	8000	58.1	41.9
Fabricated metal products	977	248	730	233	48.4	51.6
Machinery, except electrical	1170	455	706	398	67.9	32.2
Electrical and electronic equipment	1270	281	988	266	60.5	39.5
Transportation equipment	3830	579	3250	528	67.5	32.5
Instruments and related products	424	113	312	105	49.3	50.4
Miscellaneous manufacturing industries	58.4	16	42.1	15	<i>b</i>	<i>b</i>

^aPercentages may not add to 100.0% due to rounding.

^bWithheld to avoid disclosing data for individual companies.

Source: Gleick (1993a).

Table 11.1.4 Water Requirements for Municipal Establishments

Type	Unit	Average Use	Peak Use
Hotels	Liter/day/square meter	10.4	17.6
Motels	Liter/day/square meter	9.1	63.1
Barber shops	Liter/day/barber chair	207	1470
Beauty shops	Liter/day/station	1020	4050
Restaurants	Liter/day/seat	91.6	632
Night clubs	Liter/day/person served	5	5
Hospitals	Liter/day/bed	1310	3450
Nursing homes	Liter/day/bed	503	1600
Medical offices	Liter/day/square meter	25.2	202
Laundry	Liter/day/square meter	10.3	63.9
Laundromats	Liter/day/square meter	88.4	265
Retail space	Liter/day/sales square meter	4.3	11
Elementary schools	Liter/day/student	20.4	186
High schools	Liter/day/student	25.1	458

(Continued)

Table 11.1.4 (Continued)

Type	Unit	Average Use	Peak Use
Bus-rail depot	Liter/day/square meter	136	1020
Car washes	Liter/day/inside square meter	194.7	1280
Churches	Liter/day/member	0.5	17.8
Golf-swim clubs	Liter/day/member	117	84
Bowling alleys	Liter/day/alley	503	503
Residential colleges	Liter/day/student	401	946
New office buildings	Liter/day/square meter	3.8	21.2
Old office buildings	Liter/day/square meter	5.8	14.4
Theaters	Liter/day/seat	12.6	12.6
Service stations	Liter/day/inside square meter	10.2	1280
Apartments	Liter/day/occupied unit	821	1640
Fast food restaurants	Liter/day/establishment	6780	20,300

Source: Gleick (1993b).

Table 11.1.5 Typical Household Water Use in the United States

Use	Unit	Range
Washing machine	Liters per load	130–270
Standard toilet	Liters per flush	10–30
Ultra volume toilet	Liters per flush	6 or less
Silent leak	Liters per day	150 or more
Nonstop running toilet	Liters per minute	20 or less
Dishwasher	Liters per load	50–120
Water-saver dishwasher	Liters per load	40–100
Washing dishes with tap running	Liters per minute	20 or less
Washing dishes in a filled sink	Liters	20–40
Running the garbage disposal	Liters per minute	10–20
Bathroom faucet	Liters per minute	20 or less
Brushing teeth	Liters	8
Shower head	Liters per minute	20–30
Low-flow shower head	Liters per minute	6–11
Filling a bathtub	Liters	100–300
Watering a 750 m ² lawn	Liters per month ^a	7600–16,000
Standard sprinkler	Liters per hour	110–910
One drip-irrigation emitter	Liters per hour	1–10
1/2 in diameter hose	Liters per hour	1100
5/8 in diameter hose	Liters per hour	1900
3/4 in diameter hose	Liters per hour	2300
Slowly dripping faucet	Liters per month	1300–2300
Fast-leaking faucet	Liters per month	7600 or more
Washing a car with running water	Liters in 20 minutes	400–800
Washing a car with pistol-grip faucet	Liters in 20 minutes	60 or more
Uncovered pool (60 m ²)	Liters lost per month ^a	3000–11,000 +
Covered pool	Liters lost per month ^a	300–1200

^aDepending on climate.

Source: Gleick (1993b).

11.2 WATER FOR ENERGY PRODUCTION

Freshwater and energy are two resources that are intricately connected. Energy is used to help clean and transport water and water is used to help produce energy. This section looks at the connection between demand for and use of energy and water. As a comparison, Table 11.2.1 summarizes water use for energy production and Table 11.2.2 summarizes consumptive water use for electricity production.

Table 11.2.1 Consumptive Water Use for Energy Production

Energy Technology	Consumptive use (m ³ /10 ¹² J(th))
Nuclear fuel cycle	
Open pit uranium mining	20
Underground uranium mining	0.2
Uranium milling	8–10
Uranium hexafluoride conversion	4
Uranium enrichment: gasoline diffusion	11–13 ^a
Uranium enrichment: gas centrifuge	2
Fuel fabrication	1
Nuclear fuel reprocessing	50
Coal fuel cycle	
Surface mining: no revegetation	2
Surface mining: revegetation	5
Underground mining	3–20 ^b
Beneficiation	4
Slurry pipeline	40–85
Other plant operations	90 ^d
Oil fuel cycle	
Onshore oil exploration	0.01
Onshore oil extraction and production	3–8
Enhanced oil recovery	120
Water flooding	600
Thermal steam injection	100–180
Forward combustion/air injection	50
Micellar polymer	8900 ^c
Caustic injection	100
Carbon dioxide	640 ^c
Oil refining (traditional)	25–65
Oil refining (reforming and hydrogenation)	60–120
Other plant operations	70 ^d
Nuclear fuel cycle	
Natural gas fuel cycle	
Onshore gas exploration	Negligible
Onshore gas extraction	Negligible
Natural gas processing	6
Gas pipeline operation	3
Other plant operations	100 ^d
Synthetic fuels	
Solvent refined and H-coal	175
Lurgi with subbituminous	175
Lurgi with lignite	225
<i>In situ</i> gasification	90–130
Coal gasification	40–95
Coal liquefaction	35–70

(Continued)

Table 11.2.1 (Continued)

Energy Technology	Consumptive use (m ³ /10 ¹² J(th))
TOSCO II shale oil retorting	100
<i>In situ</i> retorting of oil shale	30–60
Tar sands (Athabasca)	70–180
Other technologies	
Solar active space heat	265
Solar passive space heat	Negligible

^a Excluding water use by additional power plants required for the energy-intensive uranium enrichment process.

^b Top end of range reflects once-through system with no recycle.

^c Median of a wide range.

^d Other plant operations includes plant service, potable water requirements, and boiler makeup water. For coal facilities, this also includes ash handling and flue gas desulfurization process makeup water.

Source: Gleick (1993a).

Table 11.2.2 Consumptive Water Use for Electricity Production

Energy Technology	System efficiency ^a (%)	Consumptive use (m ³ /10 ³ kWh)
Conventional coal combustion		
Once-through cooling	35	1.2
Cooling towers	35	2.6
Fluidized bed coal combustion		
Once-through cooling	36	0.8
Oil and natural gas combustion		
Once-through cooling	36	1.1
Cooling towers	36	2.6
Nuclear generation (LWR)		
Cooling towers	31	3.2
Nuclear generation (HTGR)		
Cooling towers	40	2.2
Geothermal generation (vapor-dominated)		
Cooling towers (Geysers, US)	15	6.8
Once-through cooling (Wairakei, NZ)	7.5	13
Geothermal generation (water-dominated)		
Cooling towers (Heber, US)	10	15
Wood-fired generation		
Cooling towers	32	2.3
Renewable energy systems		
Photovoltaics: residential		Negligible
Photovoltaics: central utility		0.13 ^b
Solar thermal: Luz system		4
Wind generation		Negligible
Ocean thermal		No freshwater
Hydroelectric systems ^c		
United States (average)		17
California (median of range)		5.4
California (average of range)		26

^a Efficiency of conversion of thermal energy to electrical energy.

^b Maximum water use for array washing and portable water needs.

^c Assumes all evaporative losses are attributable to the hydroelectrical facilities. For reservoirs with significant non-hydroelectric uses, such as recreation and flood control.

Source: Gleick (1993a).

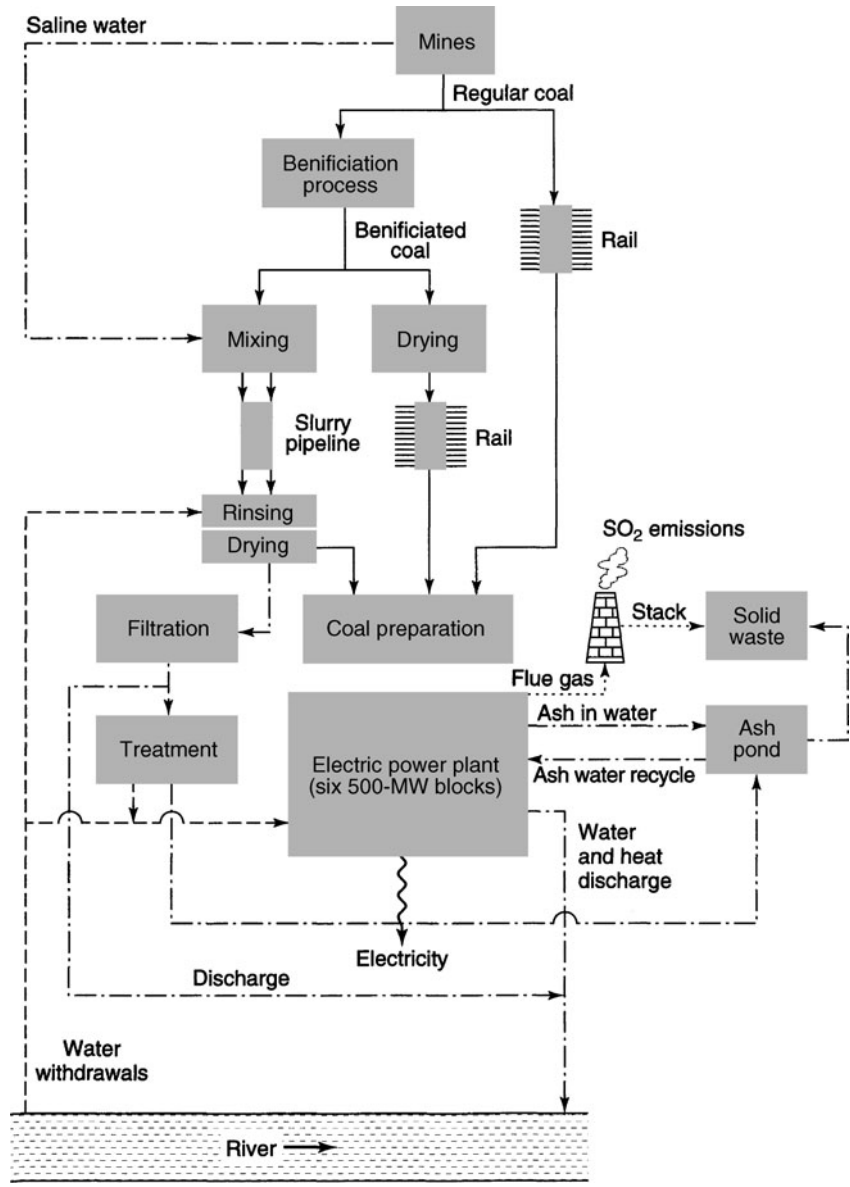


Figure 11.2.1 Flows of processes and materials in the generation of electricity with emphasis on coal handling and combustion, where --- denotes river water, - - - denotes polluted water, ——— denotes coal, and . . . denotes flue gas or solid waste (from Kindler and Russell (1984)).

The largest consumptive use of water for electricity production is, by far, for thermal power production. Thermal power plants (nuclear and fossil steam plant) need boiler makeup water, condenser-cooling water, potable water, and plant service water, with the most important use being for cooling purposes.

Figure 11.2.1 presents an overview of the processes and materials flows with emphasis on activities outside the basic electricity generation processes. Figure 11.2.2 displays in greater detail the processes contained in the box for the electric power plant (in Figure 11.2.1). Figure 11.2.2 identifies the major flows of water, steam, and fuel-related materials. Three basic types of cooling

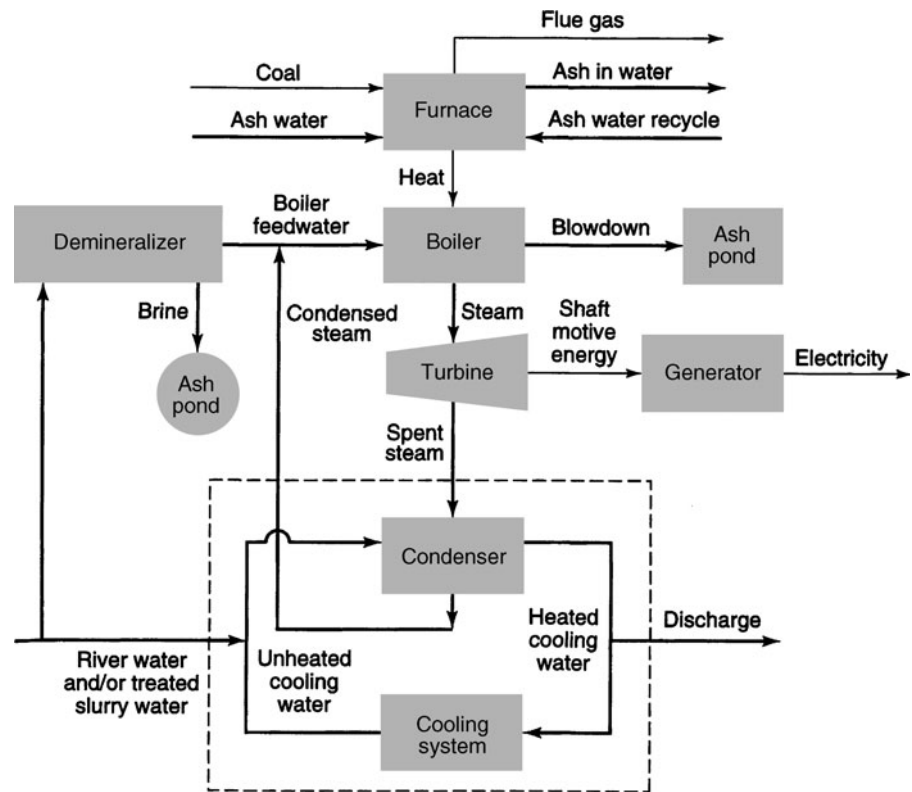


Figure 11.2.2 Basic unit processes for the electric power plant (from Kindler and Russell (1984)).

water systems have been developed for thermal power plants, *once-through cooling*, *pond cooling*, and *evaporative cooling towers*. These are illustrated in Figure 11.2.3.

Once-through cooling (Figure 11.2.3a) withdraws water from the source, passes the water through condensers, and then immediately returns the water to the source at an elevated temperature. The advantages of once-through cooling are that it is the least costly to construct, imposes the smallest capacity penalty (i.e., power loss due to fan and pump requirements and turbine back pressure), requires less water treatment, and evaporates less water than cooling ponds or evaporation cooling towers. The major drawback of once-through cooling is thermal pollution. As a result of the 1972 Federal Water Pollution Control Act Amendments, all new power plants must adapt the “best available control technology” (BACT) for thermal pollution. BACT was subsequently defined by the U.S. Environmental Protection Agency as closed cycle evaporative cooling towers.

Cooling ponds (Figure 11.2.3b) are basically large ponds where warm water is stored or detained to allow cooling before returning to the boilers to once again produce steam. Most evaporatively cooled facilities use cooling towers rather than ponds, because ponds require more land (1 to 5 acres/MW) and conserve more water. If land and water are cheap, or if water storage is desired for other purposes, these cooling ponds may be considered because of the low capital and maintenance costs.

Evaporative-cooling tower systems pass water in a secondary cooling loop through an air stream, where it is cooled and then recycled to the condensers (Figure 11.2.3c).

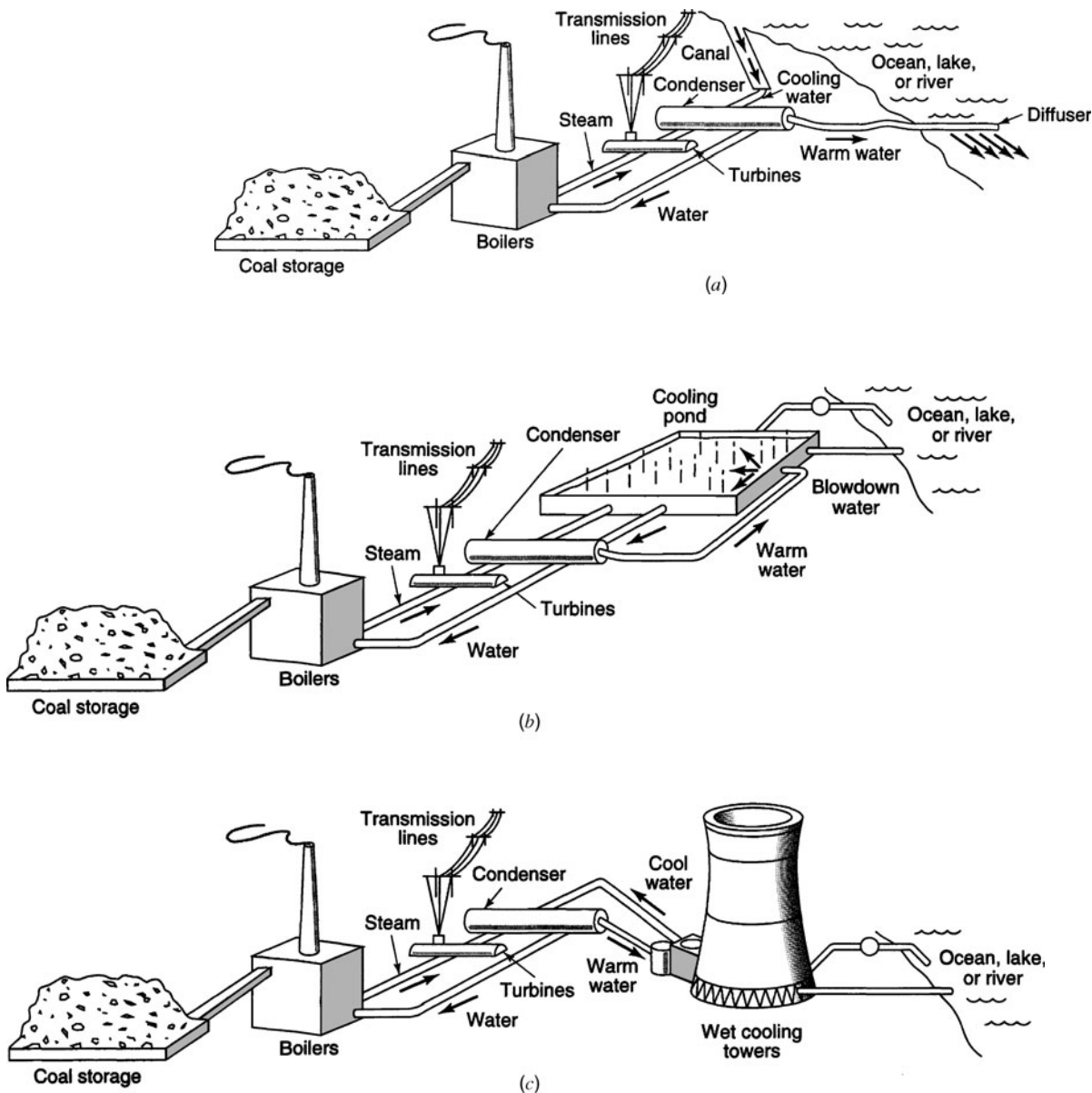


Figure 11.2.3 Three methods of providing cooling water to condenser for a thermal power plant. (a) Once-through cooling; (b) Pond cooling; (c) Wet-tower cooling (from Roberson, et al. (1998)).

Figures 11.2.4–11.2.7 illustrate the basic types of cooling towers. In the *conventional mechanical-draft wet-cooling tower system* in Figure 11.2.4, air is induced by fans. Air can also be induced through the chimney effect by building a 200-ft or taller hyperbolic shell. Figure 11.2.5 shows two types of *mechanical cooling towers* and two types of *natural-draft cooling towers*. Natural-draft cooling towers require more capital cost but less energy cost to operate. Natural-draft towers also require favorable climatic conditions. The actual costs of either type of system depend strongly on climate (Hobbs et al., 1996).

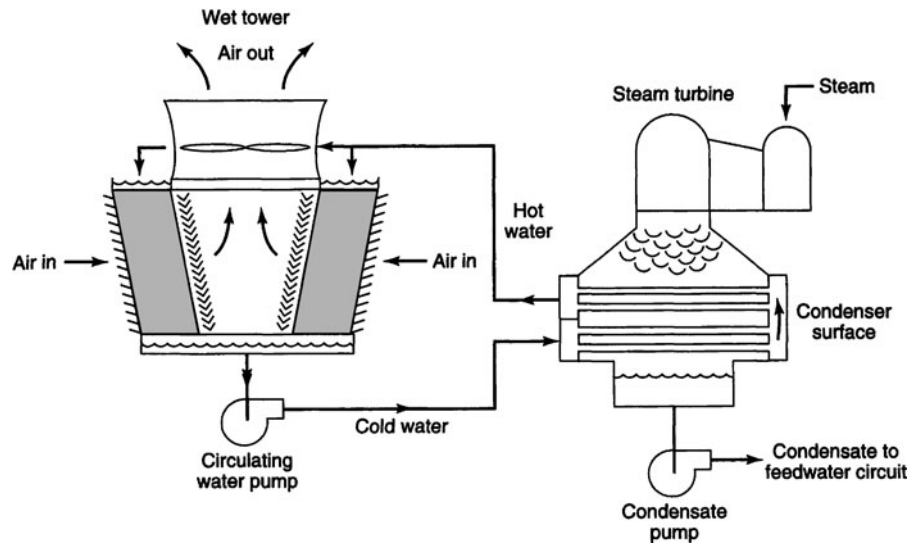


Figure 11.2.4 Conventional mechanical-draft wet-cooling-tower system (from Mitchell (1989)).

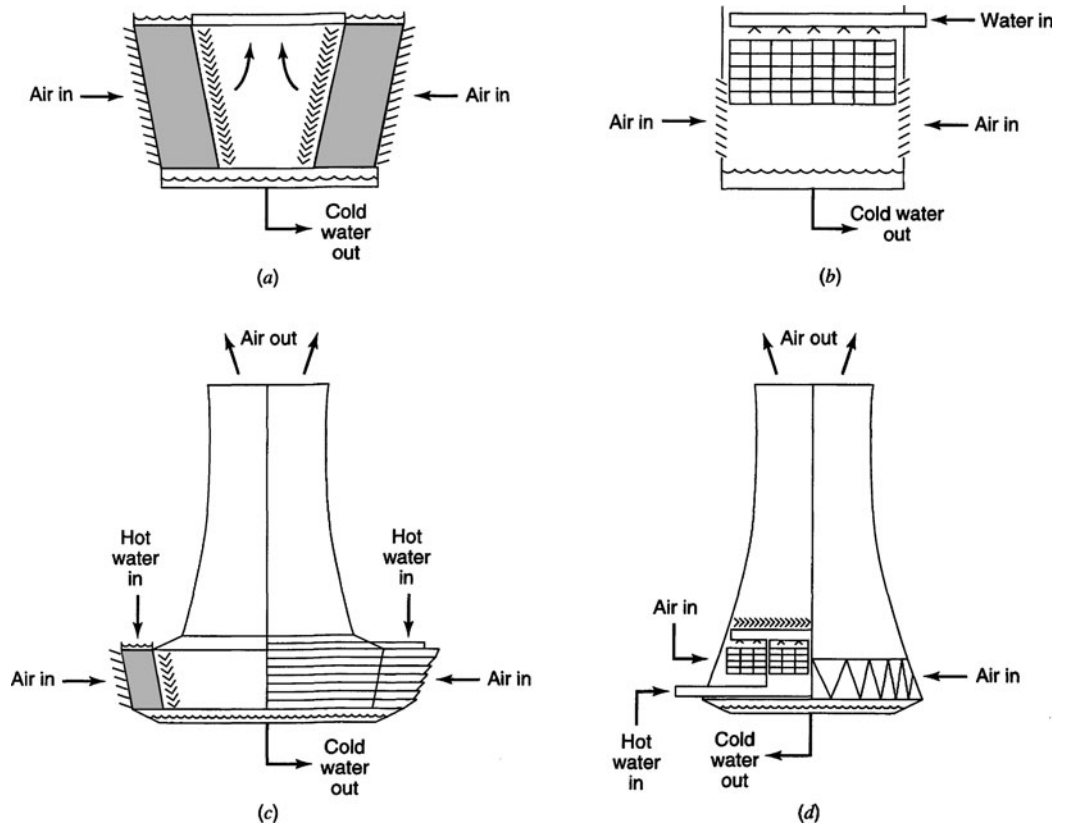


Figure 11.2.5 Different types of wet-cooling towers. (a) Mechanical-draft crossflow; (b) Mechanical-draft counterflow; (c) Natural-draft crossflow; (d) Natural-draft counterflow (from Mitchell (1989)).

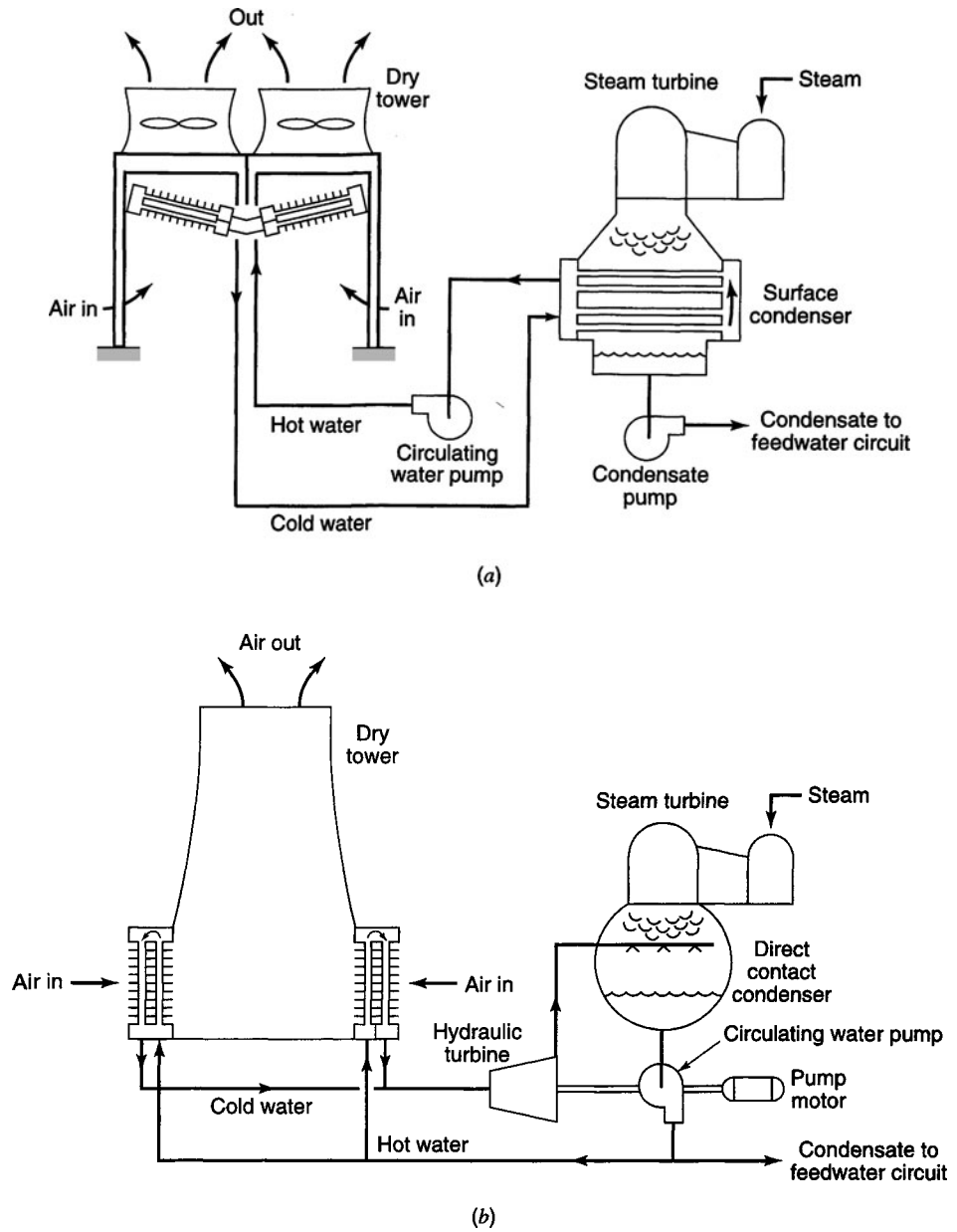


Figure 11.2.6 Indirect dry cooling-tower system. (a) With surface condenser and mechanical-draft tower; (b) With direct-contact condenser and natural-draft tower (from Mitchell (1989)).

Figure 11.2.6 shows two alternative *indirect dry-cooling tower systems*, one using mechanical draft and the other a natural-draft tower. Indirect systems contain a secondary loop that picks up heat at the condensers and rejects it at the towers. Direct dry-cooling systems pass the condensing system from the turbine directly to the heat exchangers.

Figure 11.2.7 shows a *combined wet/dry-cooling tower system* with separate wet and dry towers. The dry section handles the heat load for most of the year and during warm periods, some of the thermal load is directed to the wet tower.

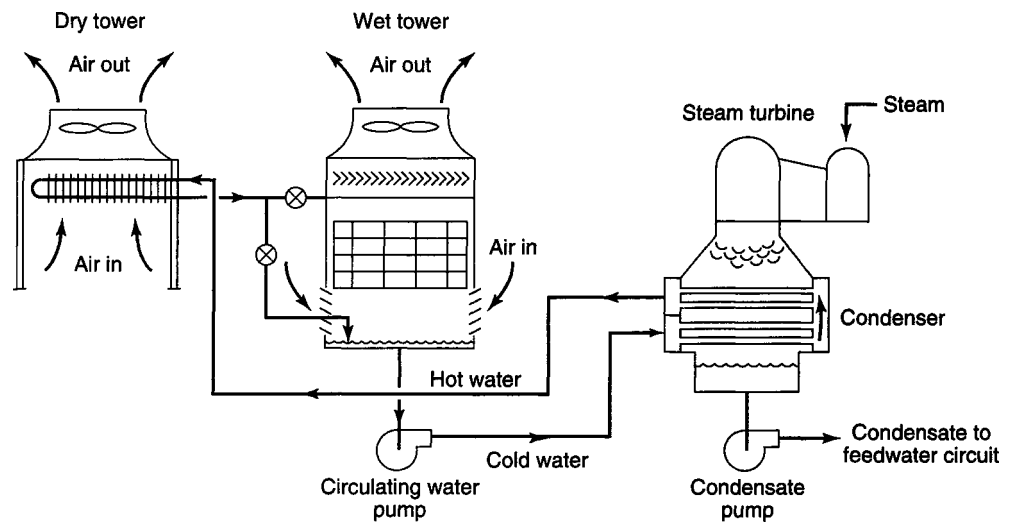


Figure 11.2.7 Series-connected wet/dry cooling-tower system with separate wet and dry towers (from Mitchell (1989)).

11.3 WATER FOR AGRICULTURE

11.3.1 Irrigation Trends and Needs

During the 1970s, irrigation expanded worldwide, followed in the 1980s by a drastically slowed rate of expansion, with a general worldwide emphasis on rehabilitation and management of existing projects during the 1990s (Replogle et al., 1996). Worldwide irrigation development has historically paralleled world population growth. According to Postel (1993), today one-third of the global harvest comes from the 16 percent of the world's croplands that is irrigated (see Table 11.3.1). Many countries—such as China, Egypt, India, Indonesia, Israel, Japan, North Korea and South Korea, Pakistan, and Peru—rely on such land for more than half their domestic food production (Postel, 1993). Gleick (1993c) and the Food and Agriculture Organization (FAO) (1993) provide detailed data and statistics on various aspects throughout the world.

According to the FAO (1993) and the U.S. Department of Agriculture (1992), approximately 47 million acres (19 million hectares) are irrigated in the United States. Throughout the world each year, some areas are withdrawn from irrigation and others are added. In the United States, there has been a decrease of around 9 percent of irrigation area during the last decade. On a worldwide basis, salinity problems have reduced the area irrigated in some areas, while irrigation is constantly added in other areas.

11.3.2 Irrigation Infrastructure

The three basic types of irrigation methods are *surface irrigation*, *sprinkler irrigation*, and *micro-irrigation*. Some methods actually cross these three traditional boundaries and are therefore difficult to categorize. Surface irrigation is the distribution of water across fields by flowing over the field surfaces. Sprinkler and micro-irrigation in contrast use closed pipes (conduits) to distribute water. Micro-irrigation is a general category that includes various types of low-emission rate devices, including drip irrigation, trickle irrigation, subsurface irrigation, bubbler irrigation, and others. Table 11.3.2 illustrates the use of micro-irrigation throughout the world.

Table 11.3.1 Net Irrigated Area, Top 20 Countries and World, 1989

Country	Net irrigated area ^a (thousand hectares)	Share of cropland that is irrigated (%)
China	43,379	47
India	45,039	25
Soviet Union	21,064	9
United States	20,162	11
Pakistan	16,220	78
Indonesia	7550	36
Iran	5750	39
Mexico	5150	21
Thailand	4230	19
Romania	3450	33
Spain	3360	17
Italy	3100	26
Japan	2868	62
Bangladesh	2738	29
Brazil	2700	3
Afghanistan	2660	33
Egypt	2585	100
Iraq	2550	47
Turkey	2220	8
Sudan	1890	15
Other	36,664	7
World	235,299	16

^a Area actually irrigated; does not take into account double cropping.

Source: Postel (1992).

Table 11.3.2 Use of Micro-irrigation, Leading Countries and World, 1991^a

Country	Area under micro-irrigation (hectares)	Share of total irrigated area under micro-irrigation ^b (%)
United States	606,000	3.0
Spain	160,000	4.8
Australia	147,000	7.8
Israel ^c	104,302	48.7
South Africa	102,250	9.0
Egypt	68,450	2.6
Mexico	60,600	1.2
France	50,953	4.8
Thailand	41,150	1.0
Columbia	29,500	5.7
Cyprus	25,000	71.4
Portugal	23,565	3.7
Italy	21,700	0.7
Brazil	20,150	0.7
China	19,000	<0.1
India	17,000	<0.1

(Continued)

Table 11.3.2 (Continued)

Country	Area under micro-irrigation (hectares)	Share of total irrigated area under micro-irrigation ^b (%)
Jordan	12,000	21.1
Taiwan	10,005	2.4
Morocco	9766	0.8
Chile	8830	0.7
Other	39,397	—
World ^d	1,576,618	0.7

^a Micro-irrigation includes primarily drop (surface and subsurface) methods and micro-sprinklers.

^b Irrigated areas are for 1989, the latest available.

^c Israel's drip and total irrigated area are down 18 and 15 percent, respectively, from 1986, reflecting water allocation cutbacks due to drought.

^d 13,280 hectares (11,200 of them in the Soviet Union) were reported in 1981 by countries that did not report at all in 1991; world total does not include this area.

Source: Postel (1992).

11.3.2.1 Water Supply Infrastructure

Water supplies for irrigation depend on: (1) managing precipitation runoff, either diverted from streams or from reservoir storage, (2) existing groundwater sources, or (3) reclaimed water from municipalities, either directly or as recharge to groundwater (Replogle et al., 1996). Most irrigation water supplies require the management of reservoirs and/or groundwater aquifers, while some water supplies are directly from rivers. Figure 11.3.1 illustrates the changes in world-irrigated area per capita from 1960 to 1990.

Figures 11.3.2 and 11.3.3 illustrate the Chief Joseph Dam Project located in the north central part of the state of Washington in the United States. This project extends approximately 140 mi along the Columbia and Okanogan Rivers from the city of Wenatchee to the Canadian border. This is an

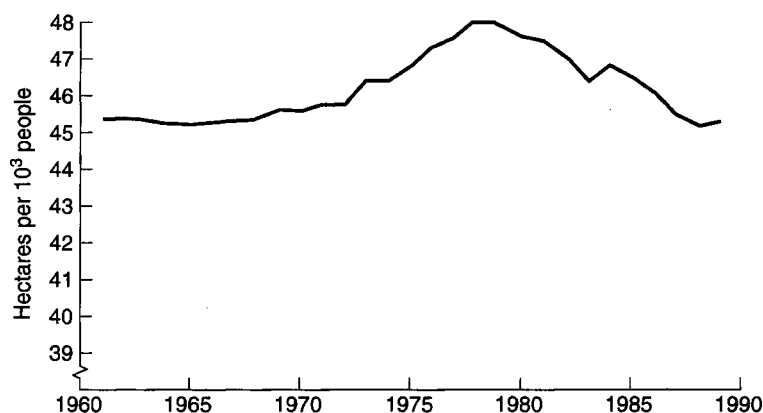


Figure 11.3.1 World irrigated area per capita, 1960–1990. Increases in irrigated area are now failing to keep up with increases in population. After increasing through the 1970s, per-capita irrigated area worldwide is now falling. If this trend continues, feeding the world's growing population will require even greater improvements in yields per hectare or greater food production from nonirrigated lands. Such improvements are likely to be increasingly difficult (from Postel (1992)).

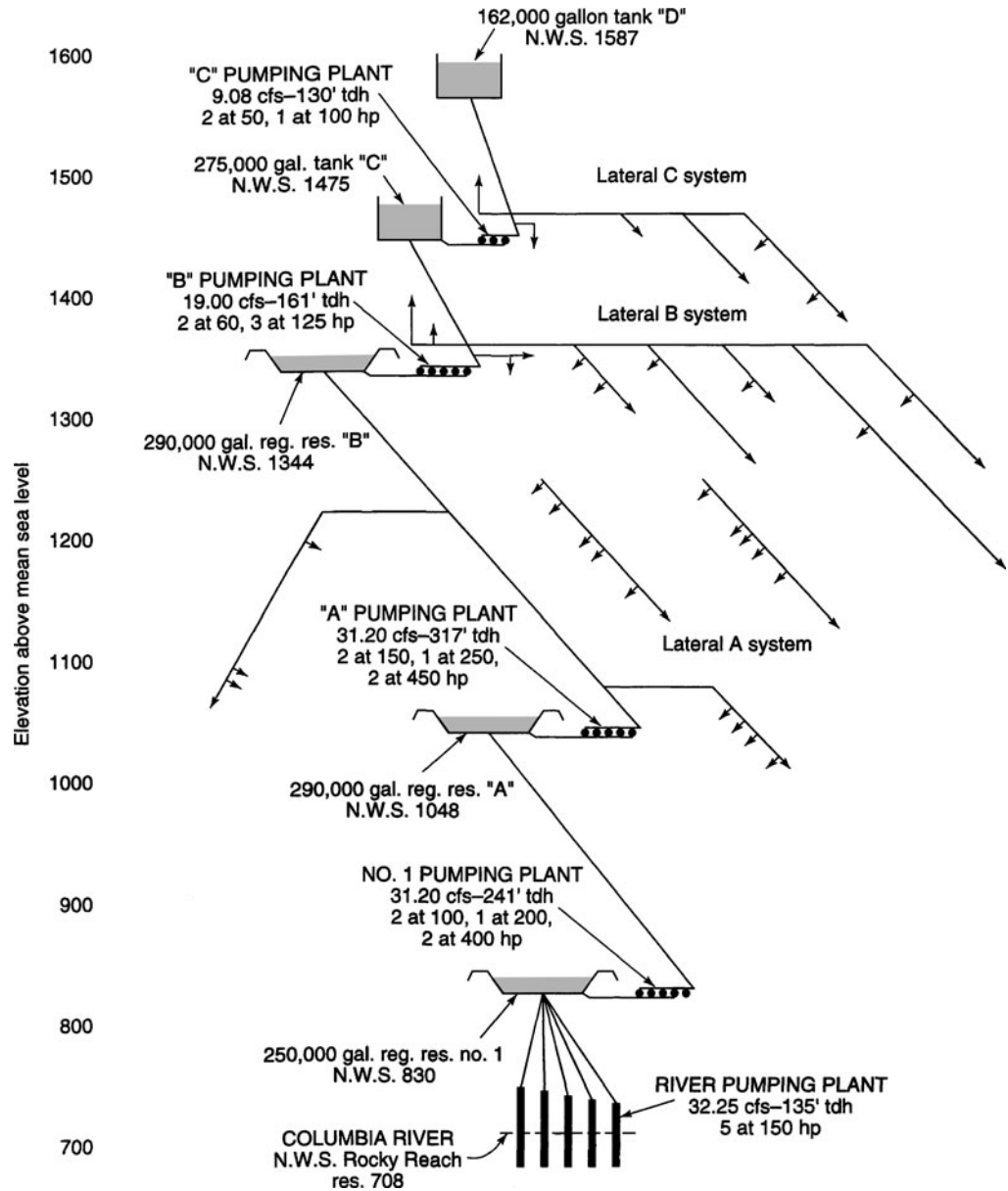


Figure 11.3.2 Brays Landing Unit—Greater Wenatchee Division, Chief Joseph Dam Project, Washington (from Walter (1971)).

all-pressure system, which means that water is pumped from a river or reservoir through pipelines and delivered to the individual farm tracts under sufficient pressure for irrigation to use sprinklers without a booster pump. Figures 11.3.2 and 11.3.3 illustrate the Brays Landing and East Units, respectively, showing the vertical schematic layouts of the units. Each lateral serves a considerable range of elevations. Difference in terrain of these two units dictated a somewhat different system layout. The land for the Brays Landing Unit is located on benches (level areas) so that this system was built using a series of lifts, as compared to the design of the East Unit.

Water supply infrastructure for irrigation systems at the project level requires an institutional framework such as irrigation districts, mutual companies, or commercial companies (Replogle et al.,

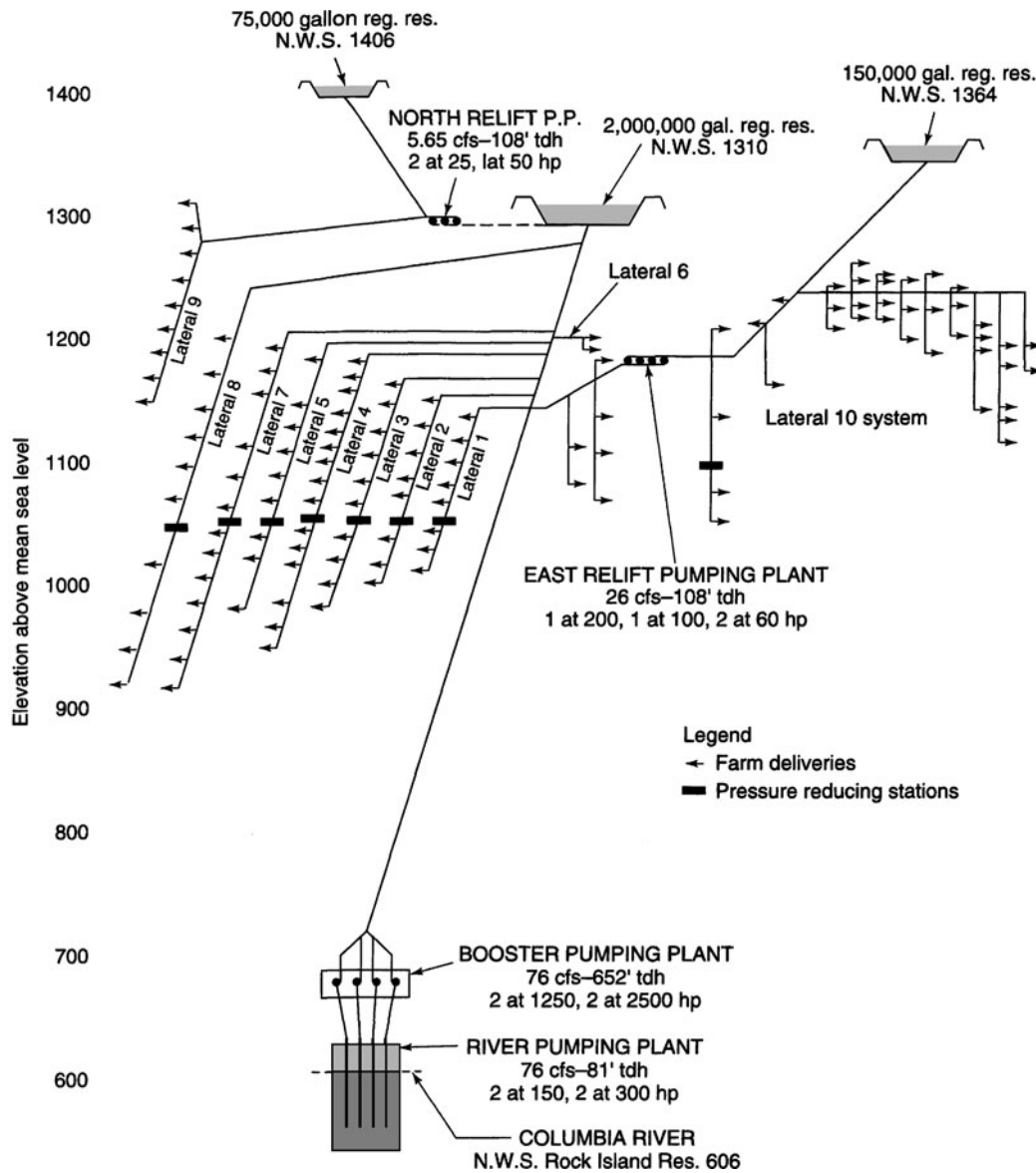


Figure 11.3.3 East Unit—Greater Wenatchee Division, Chief Joseph Dam Project, Washington (from Walter (1971)).

1996). The ASCE Manuals and Reports on Engineering Practice No. 57 (1991) provides information on the management, operation, and maintenance of irrigation and drainage systems, providing additional details on the institutional framework.

On a project level, the infrastructure includes structures such as reservoirs, well fields, river diversion, canals, high-pressure pipelines, low-head pipelines, semi-closed pipelines, and various hydraulic structures such as inlet structures, drop structures, check structures, diversion boxes, and measurement structures.

11.3.2.2 Farm Infrastructure

The three basic types of irrigation methods have been previously defined as surface irrigation, sprinkler irrigation, and micro-irrigation.

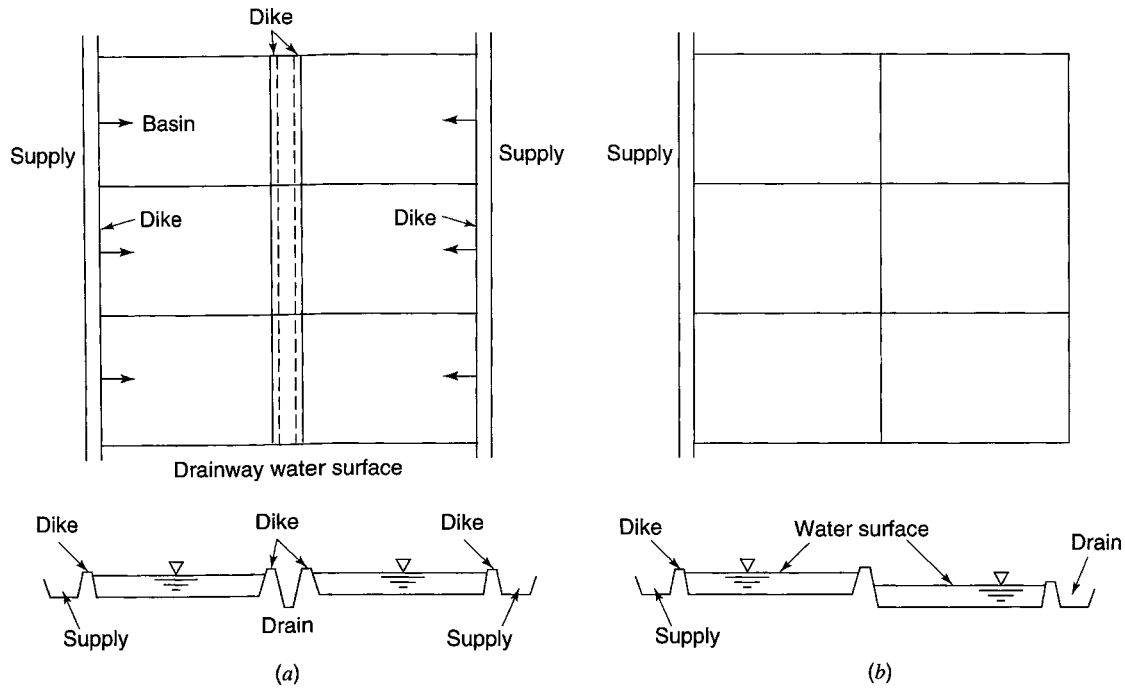


Figure 11.3.4 Basin irrigation system layouts. (a) A drainway midway between supply laterals; (b) A tier arrangement (from James (1988)).

Surface Irrigation

Surface irrigation includes the following types (Replogle et al., 1996):

- (a) *continuous-flood or paddy irrigation*, in which small basins are flooded during essentially the entire growing season;
- (b) *basin irrigation* confines water to a given area by ponding over the area but does not remain ponded for a long time such as one day (Figure 11.3.4);
- (c) *furrow irrigation* uses furrows that are dug between crops planted in rows to control and guide water for either steep land or very level land (Figure 11.3.5);
- (d) *level basin irrigation* has no soil-surface slope in any direction;
- (e) *border-strip irrigation* applies water to one end of a rectangular strip of sloping land so that water advances down slope and either runs off the end or ponds behind a dike;
- (f) *surge-flow irrigation* applies water to the head of a furrow for a time period, then stops until the flow has infiltrated, then a second surge is applied, and so on, until a satisfactory amount of irrigation has been completed; and
- (g) *reuse irrigation* collects irrigation-runoff water (tail water) from a field and uses the water.

Control structures are required in open canals (*ditch delivery systems*) to regulate velocity, head, and the quantity of water released into distribution laterals, basins, borders, and furrows. *Division boxes*, as shown in Figure 11.3.6, direct or divide flow from a supply pipe or channel between two or more distribution laterals. Figure 11.3.6a shows a fixed proportional flow divider-type division box. Some division boxes have movable splitters to change the flow proportions. Figure 11.3.6b shows a division box with a weir-type overflow outlet. Figure 11.3.7 illustrates commonly used drop structures in open-channel delivery systems.

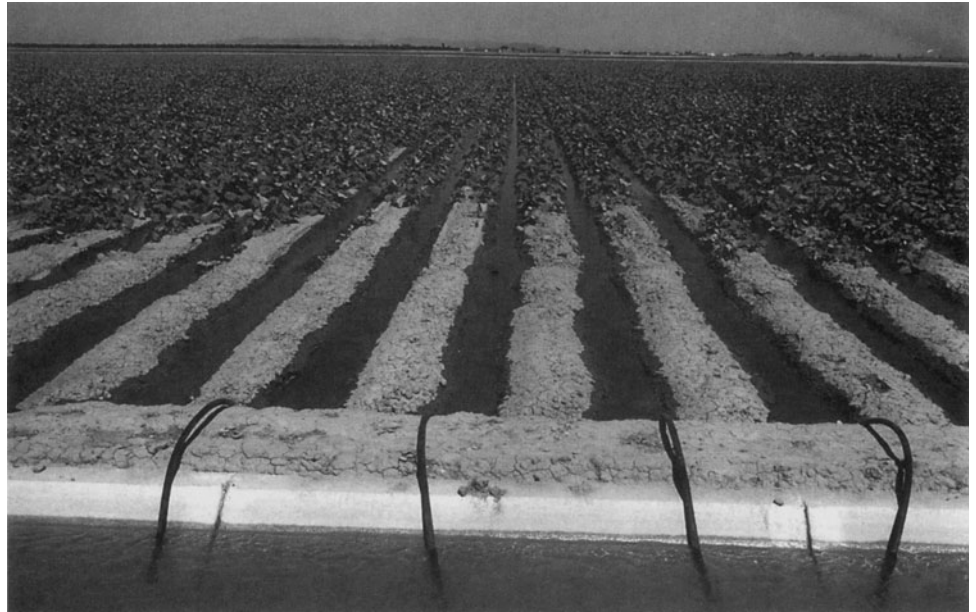


Figure 11.3.5 Furrow irrigation system. (Courtesy of U.S. Bureau of Reclamation.)

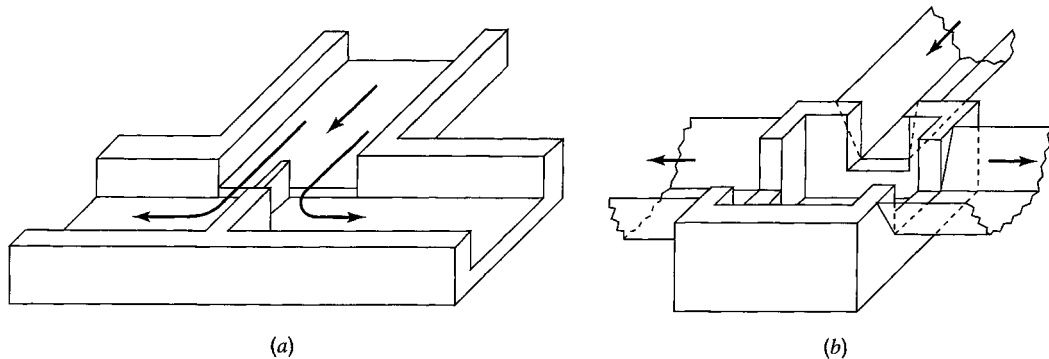


Figure 11.3.6 Division boxes. (a) A fixed proportional flow divider; (b) Weir-type overflow outlets (from James (1988)).

Sprinkler Irrigation

Sprinkler irrigation systems are distinguished by whether or not the structures move in the field during the irrigation event, so there are two basic categories, moving (Figure 11.3.8) and fixed-in-place systems (Figure 11.3.9). Sprinkler irrigation systems include the following types:

- (a) *permanent, solid-set sprinklers* are fixed on risers from buried lines or lines suspended above a crop or over trees (Figure 11.3.9);
- (b) *hand-move sprinklers* are fixed sprinklers that are disassembled, moved, and reassembled between irrigations;
- (c) *continuous-move sprinkler systems* move continuously during irrigation; and
- (d) *center-pivot irrigation systems* (the most common moving irrigation systems) supply water at a central point and a lateral line rotates around this center.

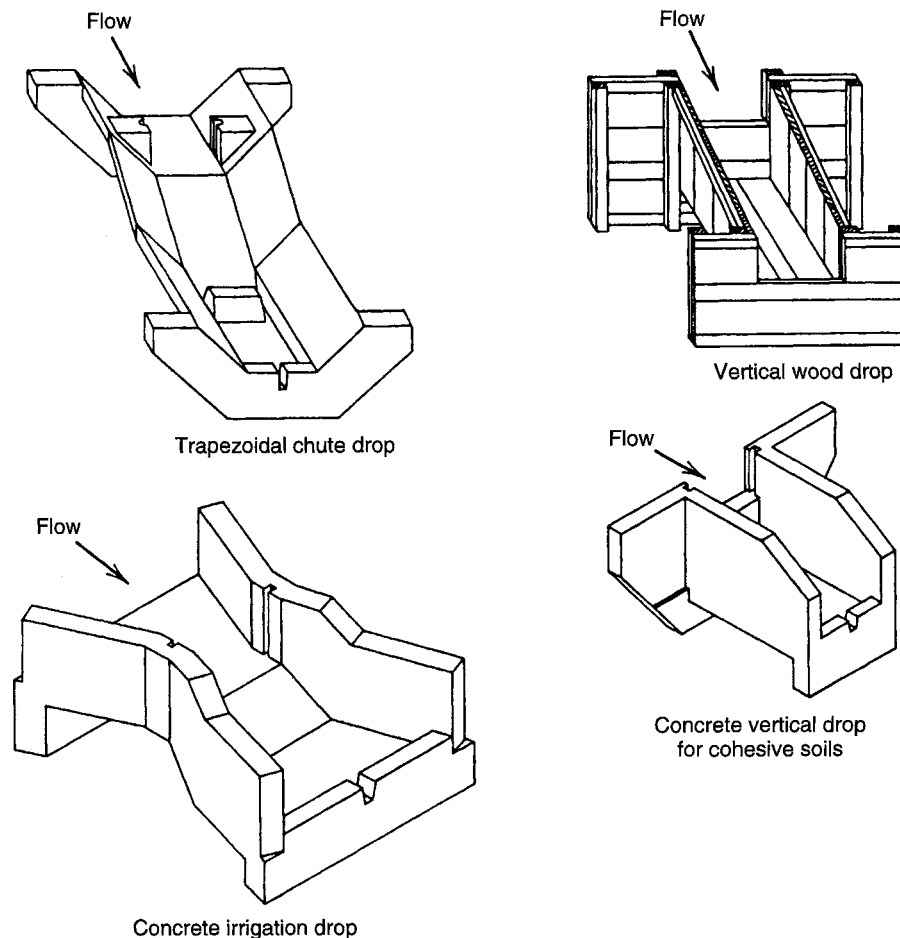


Figure 11.3.7 Some drop structures used in open-channel delivery systems (from James (1988)).

Micro-irrigation

Micro-irrigation is a general category of various types of low-emission-rate devices, including drip irrigation, trickle irrigation, subsurface irrigation, bubbler irrigation, and the moving low-energy precision-application (LEPA) systems (Replogle et al., 1996). Micro-irrigation methods do not wet the entire soil surface or volume, but only that portion that needs to be watered for the particular crop.

Trickle irrigation is the frequent, slow application of water either directly to the land surface or into the root zone of the crop. In other words, trickle irrigation irrigates only the root zone of the crop and maintains the water content of the root zone at near-optimal level. Figure 11.3.10 illustrates the components of a trickle irrigation system.

James (1988) categorizes trickle irrigation as including drip irrigation, subsurface irrigation, bubbler irrigation, and spray irrigation, defined as follows:

- (a) *drip irrigation* applies water as discrete drops on a slow, nearly continuous basis;
- (b) *subsurface irrigation* applies water below the soil surface using point and line source emitters;
- (c) *bubbler irrigation* applies water to the land surface on small streams from tubes that are attached to buried laterals; and
- (d) *spray irrigation* sprays water as a mist over the land surface using small sprinkler-like devices often called *micro sprinklers*.

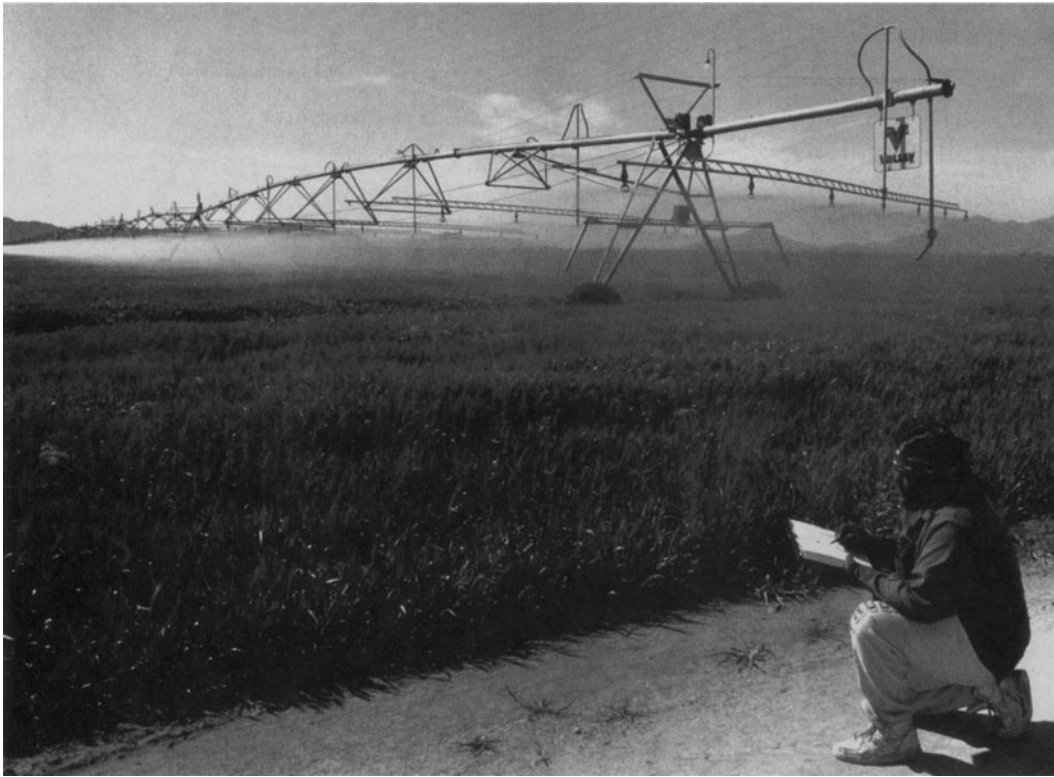


Figure 11.3.8 Moving sprinkler irrigation system (center-pivot irrigation system). (Courtesy of the U.S. Bureau of Reclamation.)

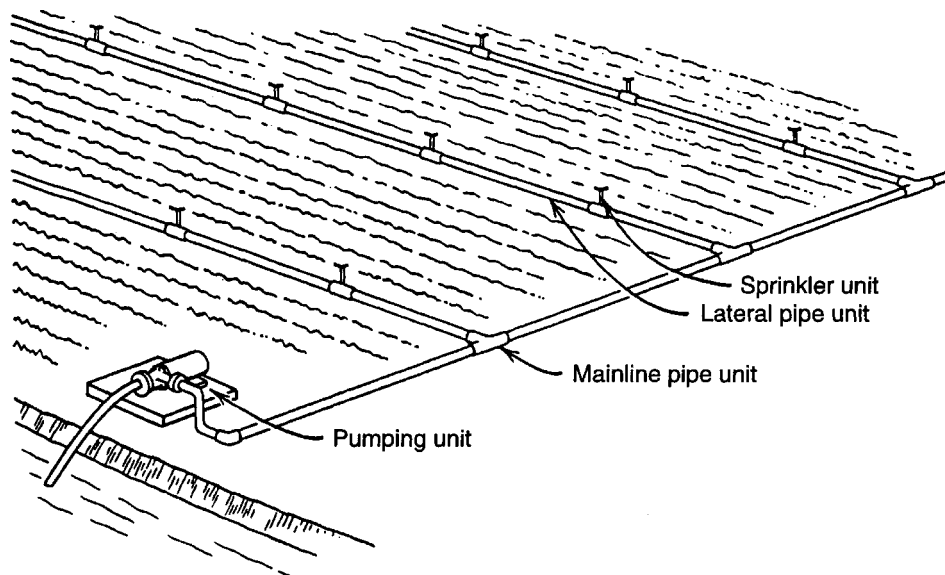


Figure 11.3.9 A typical sprinkler irrigation system consists of four basic units: a pumping unit, mainline pipes, lateral pipes, and one or more sprinklers (from James (1988)).

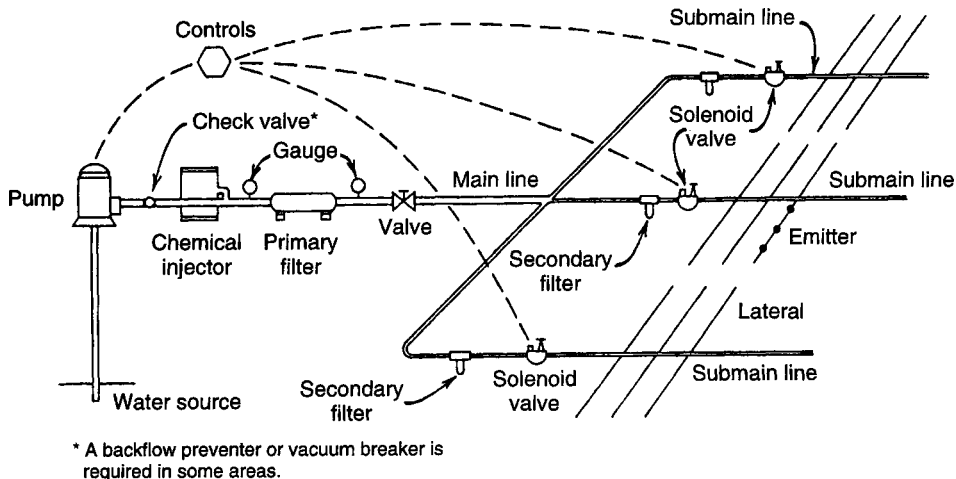


Figure 11.3.10 The components of a trickle irrigation system (from James (1988)).

11.3.3 Irrigation System Selection and Performance

Characteristics of Systems

Table 11.3.3 provides a qualitative overview of the characteristics of several alternative irrigation types. The advantages and disadvantages of each may also depend on site-specific properties and economic considerations.

Selection of Irrigation Systems

Table 11.3.4 provides a list of factors affecting the selection of the appropriate irrigation method. Table 11.3.5 provides a guide for selection of a method of irrigation. This table, however, provides some information on the cost of water provided by the different irrigation methods. Cost is often a limiting factor in any new development. Also, this table does not address water and soil qualities, which are also important factors.

Performance

From a crop-production perspective, the irrigation system performance is often described by the *irrigation efficiency* (Replogle et al., 1996):

$$E_l = \frac{\text{volume of irrigation water beneficially used}}{\text{volume of irrigation water supplied}} \times 100\% \quad (11.3.1)$$

which describes water use in terms of benefit for agricultural production. Beneficial uses include crop evapotranspiration (ET), water needed for removing excess salt from the soil, climate control, soil preparation, and weed control. Some of these uses actually consume water, while others do not.

From a hydrologic balance perspective, the use of water by agriculture can be described by the *consumptive use coefficient* (Replogle et al., 1996):

$$C_{cu} = \frac{\text{volume of water consumptively used}}{\text{volume of irrigation water supplied}} \times 100\% \quad (11.3.2)$$

which includes uses that are not directly beneficial for agricultural production, such as evapotranspiration and sprinkler and reservoir evaporation. These two definitions of water use are not the same, but are related.

Table 11.3.3 Characteristics of Alternative Irrigation Systems

Site and situation factor	Surface systems		Sprinkler system			Drip systems	
	Redesigned surface system	Level basins	Intermittent mechanical move	Continuous mechanical move	Solid set	Emitters and porous tubes	Bubblers and splitters
Average efficiency rating	60–70%	80%	70–80%	80%	70–80%	80–90%	80–90%
Soil	Uniform soils with moderate to low infiltration	Uniform soils with moderate to low infiltration	All	Sandy or high infiltration rate soils	All	All	All, basin required for medium and low-intake soils
Topography	Moderate slopes	Small slopes	Level to rolling	Level to rolling	Level to rolling	All	All
Crops	All	All	Generally shorter crops	All but trees and vineyards	All	High value required	High value required
Water supply	Large streams	Very large streams	Small streams nearly continuous	Small streams nearly continuous	Small streams	Small streams continuous and clean	Small streams continuous
Water quality	All but very high salts	All	Salty water may harm plants	Salty water may harm plants	Salty water may harm plants	All, can potentially use high salt waters	All, can potentially use high salt waters
Labor requirement	High, training required	Low, some training	Moderate, some training	Low, some training	Low to high, little training	Low to high, some training	Low, little training
Energy requirement	Low	Low	Moderate to high	Moderate to high	Moderate	Low to moderate	Low
Management skill	Moderate	Moderate	Moderate	Moderate to high	Moderate	High	High
Machinery operations	Medium to long fields	Short fields	Medium field length, small interference	Circular fields, some interference	Some interference	May have considerable interference	Some interference
Duration of use	Short to long term	Long term	Short to medium term	Short to medium term	Long term	Long term, durability unknown	Long term
Weather	All	All	Poor in windy conditions	Better in windy conditions than other sprinklers	Windy conditions reduce performance; good for cooling	All	All

Source: Wade (1986), as presented in Gleick (1993c).

Different terms are often used for defining the performance of the irrigation system (i.e., separated from crop management). Common terms include *the application efficiency* E_a and *low-quarter distribution uniformity*, DU_{lq} , defined in terms of that 25 percent of the field receiving the least depth of infiltrated water (American Society of Agricultural Engineers, 1993):

$$E_a = \frac{\text{average depth of water stored in the root zone}}{\text{average depth applied}} \quad (11.3.3)$$

$$DU_{lq} = \frac{\text{average low-quarter depth of water infiltrated}}{\text{average depth of water infiltrated}} \quad (11.3.4)$$

Table 11.3.4 Factors Affecting the Selection of an Appropriate Irrigation Method

Irrigation method	Factors affecting selection					
	Land	Soil	Crop	Climate	Pluses	Minuses
Surface	Level or graded to central slope and surface smoothness	Suited for medium to fine textures but not for infiltrability	For most crops, except those sensitive to standing water or poor aeration	For most climates only slightly affected by wind	Low cost, simple low pressure required	Prone to overirrigate and rising water table
Sprinklers	For all lands	For most soils	For most crops, except sensitive to fungus disease and leaf scorch by salts	Affected by wind (drift, evaporation, and poor distribution)	Control of rate and frequency allows irrigation of sloping and sandy soils	Initial costs and water pressure requirements
Drip	For all regular and irregular slopes	For all soils and intake rates	For row crops and orchards, but not close-growing crops	Not affected by wind, adapted to all climates	High-frequency and precise irrigation, can use saline water and rough land, reduced evaporation	Initial and annual costs, requires expert management, prone to clogging, requires filtration
Microsprayer	For all lands	For all intake rates	For row crops and orchards	May be affected by wind	High-frequency and precise irrigation, less prone to clog	High costs and maintenance
Bubbler	Flat lands and gentle slopes	For all intake rates	For tree crops	Not affected by wind	High-frequency irrigation, no clogging, simple	Not a commercial product

Source: Hillel (1987), as presented in Gleick (1993c).

Table 11.3.5 Guide for Selecting a Method of Irrigation

Irrigation method	Topography	Crops	Remarks
Widely spaced borders	Land slopes capable of being graded to less than 1% slope and preferably 0.2%	Alfalfa and other deep rooted close-growing crops and orchards	The most desirable surface method for irrigating close-growing crops where topographical conditions are favorable. Even grade in the direction of irrigation is required on flat land and is desirable but not essential on slopes of more than 0.5%. Grade changes should be slight and reverse grades must be avoided. Cross slope is permissible when confined to differences in elevation between border strips of 6–9 cm.
Closely spaced borders	Land slopes capable of being graded to 4% slope or less and preferably less than 1%	Pastures	Especially adapted to shallow soils underlain by claypan or soils that have a lower water intake rate. Even grade in the direction of irrigation is desirable but not essential. Sharp grade changes and reverse grades should be smoothed out. Cross slope is permissible when confined to differences in elevation between borders of 6–9 cm. Since the border strips may have less width, a greater total cross slope is permissible than for border-irrigated alfalfa.

(Continued)

Table 11.3.5 (Continued)

Irrigation method	Topography	Crops	Remarks
Check back and cross furrows	Land slopes capable of being graded to 0.2% slope or less	Fruit	This method is especially designed to obtain adequate distribution and penetration of moisture in soils with low-water intake rates.
Corrugations	Land slopes capable of being graded to slopes of 0.5–12%	Alfalfa, pasture, and grain	This method is especially adapted to steep land and small irrigation streams. An even grade in the direction of changes and reverse grades should at least be smoothed out. Due to the tendency of corrugations to clog and overflow and cause serious erosion, cross slopes should be avoided as much as possible.
Graded contour furrows	Variable land slopes of 2–25% but preferably less	Row crops and fruit	Especially adapted to row crops on steep land, though hazardous due to possible erosion from heavy rainfall. Unsuitable for rodent-infested fields or soils that crack excessively. Actual grade in the direction of irrigation 0.5–1.5%. No grading required beyond filling gullies and removal of abrupt ridges.
Contour ditches	Irregular slopes up to 12%	Hay, pasture, and grain	Especially adapted to foothill condition. Requires little or no surface grading.
Rectangular checks (levees)	Land slopes capable of being graded so single or multiple tree basins will be leveled within 6 cm	Orchards	Especially adapted to soils that have either a relatively high- or low-water intake rate. May require considerable grading.
Contour levee	Slightly irregular land slopes of less than 1%	Fruits, rice, grain, and forage crops	Reduces the need to grade land. Frequently employed to avoid altogether the necessity of grading. Adapted best to soils that have either a high- or low-intake rate.
Portable pipes	Irregular slopes up to 12%	Hay, pasture, and grain	Especially adapted to foothill conditions. Requires little or no surface grading.
Subirrigation	Smooth-flat	Shallow-rooted crops such as potatoes or grass	Requires a water table, very permeable subsoil conditions, and precise leveling. Very few areas adapted to this method.
Sprinkler	Undulating 1–>35% slope	All crops	High operation and maintenance costs. Good for rough or very sandy lands in areas of high production and good markets. Good method where power costs are low. May be the only practical method in areas of steep or rough topography. Good for high rainfall areas where only a small supplemental water supply is needed.
Contour bench terraces	Sloping land—best for slopes under 3% but useful upto 6%	Any crop but particularly suited to cultivated crops	Considerable loss of productive land due to berms. Requires expensive drop structures for water erosion control.
Subirrigation (installed pipes)	Flat to uniform slopes up to 1% surface should be smooth	Any crop; row crops of high-value crops usually used	Requires installation of perforated plastic pipe in root zone at narrow spacings. Some difficulties in roots plugging the perforations. Also a problem as to correct spacing. Field trials on different soils are needed. This is still in the development stage.
Localized (drip, trickle, etc.)	Any topographic condition suitable for row crop farming	Row crops or fruit	Perforated pipe on the soil surface drips water at base of individual vegetable plants or around fruit trees. Has been successfully used in Israel with saline irrigation water. Still in development stage.

Source: Doneen and Westcot (1984), as presented in Gleick (1993c).

11.3.4 Water Requirements for Irrigation

The *total water requirement* or *diversion requirement* for an irrigation system includes the water needed by the crop in addition to the losses associated with the application and delivery of water. The *crop water requirement* or the *consumptive use* can be determined experimentally by planting a crop in a lysimeter or tank of soil and keeping account of water added and soil moisture changes. The overall consumptive use for large areas can be defined by a moisture accounting or balance, as illustrated in Figure 11.3.11. Table 11.3.6 provides a list of crop water requirements and crop evapotranspiration for various crops.

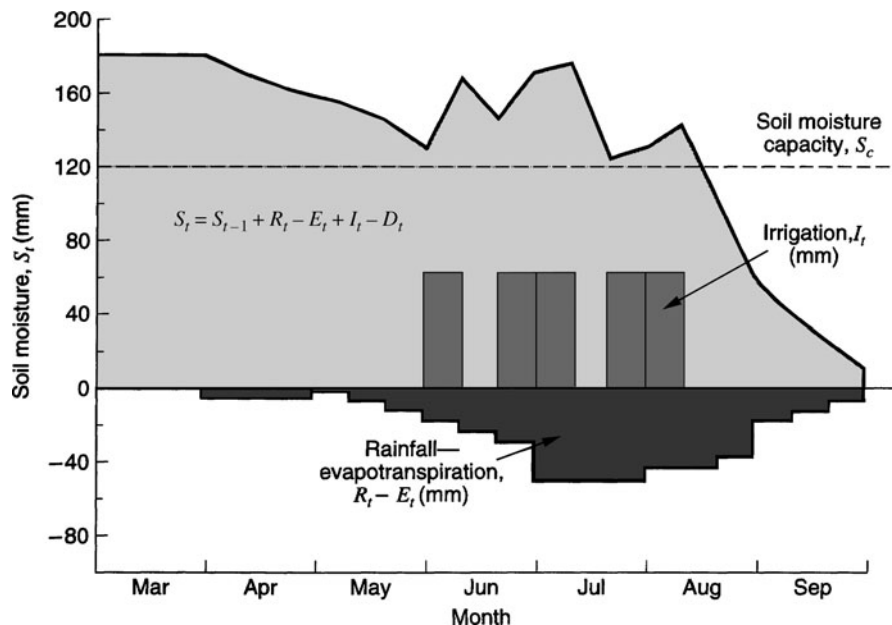


Figure 11.3.11 Soil moisture balance with irrigation (from Gouevsky and Maidment (1984)).

Table 11.3.6 Crop Water Requirements and Crop Evapotranspiration

Crop	Southwest United States Range (mm)	Missouri and Arkansas Basins Range (mm)	FAO Guidelines Range (mm)	United States and Canada ^a Range (mm)
<i>Farm crops</i>				
Alfalfa/forage	1060–1550	591–799	600–1600	594–1890
Barley	378–558	405–555		384–643
Broomcorn	296–351			
Buckwheat		320–396		
Cocoa			800–1200	
Coffee			800–1200	
Corn (maize)	439–607	375–558	400–750	373–617
Cotton	716–1070		550–950	912–1050
Emmer	363–570			
Feterita	296–335			
Flax	375–485	448–564	450–900	381–795
Grains (small)			300–450	
Grass				579–1320
Groundnut			500–700	

(Continued)

Table 11.3.6 (Continued)

Crop	Southwest United States Range (mm)	Missouri and Arkansas Basins Range (mm)	FAO Guidelines Range (mm)	United States and Canada ^a Range (mm)
Kafir	402–469	436–479		
Millet	277–332	247–287		
Milo	293–509	332–518		
Oats	579–637	411–552		
Oil seeds			300–600	
Potatoes	485–622	421–518	350–625	455–617
Rhodes grass	1060–1350			
Rice			500–950	920
Safflower				635–1150
Sisal			550–800	
Sorghum	515–634	323–448	300–650	549–645
Soybeans	506–856		450–825	399–564
Sudan grass	878–963			
Sugar beets	539–829	488–762	450–850	546–1050
Sugar cane	1060–1390		1000–1500	
Sunflowers		366–427		
Tobacco			300–500	
Wheat	445–683	415–549	450–650	414–719
<i>Vegetable crops</i>				
Beans		396–488	250–500	396–417
Beans, snap	253–439			
Beets, table	265–418			
Broccoli				500
Cabbage	287–454			437–622
Carrots	387–488			422
Cauliflower	436–539			472
Corn, sweet				386–498
Cucumbers		528–1140		
Lettuce	219–411			216
Melons	756–1040			
Onions	223–463		350–600	592
Onions, greens				445
Peas	369–475	415–591		340
Spinach	244–326			
Sweet potatoes	539–686		400–675	
Tomatoes	290–433	640–853	300–600	366–681
<i>Fruit</i>				
Apples		640–792		531–1060
Avocados			650–1000	
Bananas			700–1700	
Cantaloupes		457–701		485
Dates			900–1300	
Deciduous trees			700–1050	
Grapefruit			650–1000	1220
Oranges			600–950	933
Plums				1070
Vineyards			450–900	
Walnuts			700–1000	

^aFood and Agriculture Organization (1977), Kammerer (1982), U.S. Department of Agriculture as cited in van der Leeden, Troise and Todd (1990), as presented in Gleick (1993c).

EXAMPLE 11.3.1

Determine the water requirements for irrigation of corn, per acre land per day, during the crop’s active growing season. Assume a consumptive use coefficient (C_{cu} , equation (11.3.2)) of 50 percent. Use the Blaney–Criddle formula for determining the reference crop evapotranspiration ET_0 (mm/day), given as (FAO, 1977)

$$ET_0 = c[p(0.46T + 8)]$$

where T is the mean daily temperature in °C over the month considered, p is the mean daily percentage of total annual daytime hours, given as a function of the month used and the latitude of the location, and c is an adjustment factor that depends on minimum relative humidity, sunshine hours, and daytime wind estimates. Use $T = 33^\circ\text{C}$, $p = 0.33$, $c = 1.0$. Note that the evapotranspiration for a given crop must be corrected from the reference evapotranspiration using the formula $ET_c = K_c ET_0$, where K_c is the crop coefficient. K_c for corn during its active growing season can be taken as 0.8.

SOLUTION

From the given values of T , p , and c , $ET_0 = 1.0\{0.33[0.46(33) + 8]\} = 7.65$ mm/day. For corn, $ET_c = K_c ET_0 = 0.8(7.65) = 6.12$ mm/day. In terms of the volume of water consumptively used per acre, we get volume of water consumptively used = 6.12 mm/day (1 acre) = 6.12 mm/day (10^{-3} m/mm) (3.281 ft/m) (1 acre) = 0.02 ac-ft/day.

Table 11.3.7 Impacts of Irrigation Development

Casual activity	Possible impact	Possible remedies
Surface irrigation	<ol style="list-style-type: none"> 1. Waterlogging 2. Soil salinization 3. Increase of diseases 4. Degradation of water quality 	<ol style="list-style-type: none"> 1. Increased irrigation efficiency 2. Construction of drainage systems 3. Disease control measures 4. Control of irrigation water quality
Sewage irrigation	<ol style="list-style-type: none"> 1. Contamination of food crops 2. Direct contamination of humans 3. Dispersion in air 4. Contamination of grazing animals 	<ol style="list-style-type: none"> 1. Regulatory control 2. Tertiary treatment and sterilization of sewage
Use of fertilizers	<ol style="list-style-type: none"> 1. Pollution of groundwater, especially with nitrates 2. Pollution of surface flow 	<ol style="list-style-type: none"> 1. Controlled use of fertilizers 2. Increased irrigation efficiency
Use of pesticides	<ol style="list-style-type: none"> 1. Pollution of surface flow 2. Destruction of fish 	<ol style="list-style-type: none"> 1. Limited use of pesticides 2. Coordination with schedule of irrigation
Irrigation with high silt load	<ol style="list-style-type: none"> 1. Clogging of canals 2. Raising of level of fields 3. Harmful sediment deposits on fields and crops 	<ol style="list-style-type: none"> 1. Avoiding use of flow with high silt load 2. Soil conservation measures on upstream watershed
High-velocity surface flow	<ol style="list-style-type: none"> 1. Erosion of earth canals 2. Furrow erosion 3. Surface erosion 	<ol style="list-style-type: none"> 1. Proper design of canals 2. Proper design of furrows 3. Land leveling 4. Correctly built and maintained terraces
Intensive sprinkling of sloping land	<ol style="list-style-type: none"> 1. Soil erosion 	<ol style="list-style-type: none"> 1. Correctly designed and operated system

Source: Economic and Social Commission for Asia and the Pacific (1987) and United Nations Environment Programme (1979), as presented in Gleick (1995c).

Table 11.3.8 Selected Environmental Effects of Agriculture on Water Quality

Agricultural practices	Soil	Groundwater	Surface Water
Land development, land consolidation programs	Inadequate management leading to soil degradation	Other water management influencing groundwater table	Soil degradation, siltation, water pollution with soil particles
Irrigation, drainage	Excess salts, waterlogging	Loss of quality (more salts), drinking water supply affected	Soil degradation, siltation, water pollution with soil particles
Tillage	Wind erosion, water erosion		Soil degradation, siltation, water pollution with soil particles
Mechanization: large or heavy equipment	Soil compaction, soil erosion		Soil degradation, siltation, water pollution with soil particles
Nitrogen fertilizer use		Nitrate leaching	
Phosphate fertilizer use	Accumulation of heavy metals (such as cadmium)		Runoff leaching or direct discharge leading to eutrophication
Manure, slurry use	Excess accumulation of phosphates, copper (pig slurry)	Nitrate, phosphate combination (by use of excess slurry)	Runoff leaching or direct discharge leading to eutrophication
Sewage sludge compost	Accumulation of heavy metals contaminants		Runoff leaching or direct discharge leading to eutrophication
Applying pesticides	Accumulation of pesticides and degradation products	Leaching of mobile pesticide residues and degradation products	
Input of feeder additives, medicines	Adverse effects depend on input		
Modern building (e.g., silos) and intensive livestock farming	Excess accumulation of phosphates, copper (pig slurry)	Nitrate, phosphate contamination (by use of excess slurry)	Runoff leaching or direct discharge leading to eutrophication

Source: Organization for Economic Co-operation and Development (1985) and Meyback, Chapman, and Helmer (1989), as presented in Gleick (1993c).

Using equation (11.3.2), we find

$$\begin{aligned} \text{volume of irrigation water required} &= \frac{\text{volume of water consumptively used}}{C_{cu}} = 0.02/0.5 \\ &= 0.04 \text{ ac-ft/day} \end{aligned}$$

11.3.5 Impacts of Irrigation

Table 11.3.7 illustrates some of the impacts of irrigation development, as presented in Gleick (1993c). Table 11.3.8 illustrates some of the environmental effects of agriculture on water quality, as presented in Gleick (1993c).

11.4 WATER SUPPLY/WITHDRAWALS

11.4.1 Withdrawals

Most fresh water is supplied by pumping groundwater and withdrawing water from lakes and rivers. The demand for fresh water supplies increases because of population growth and increasing development. Figure 11.4.1 illustrates water demand that can be supplied at different levels of mobilization of the potentially available water. Table 11.4.1 provides six estimates of the global stocks of fresh and saline water, as presented by Gleick (1993d). Table 11.4.2 presents the total water

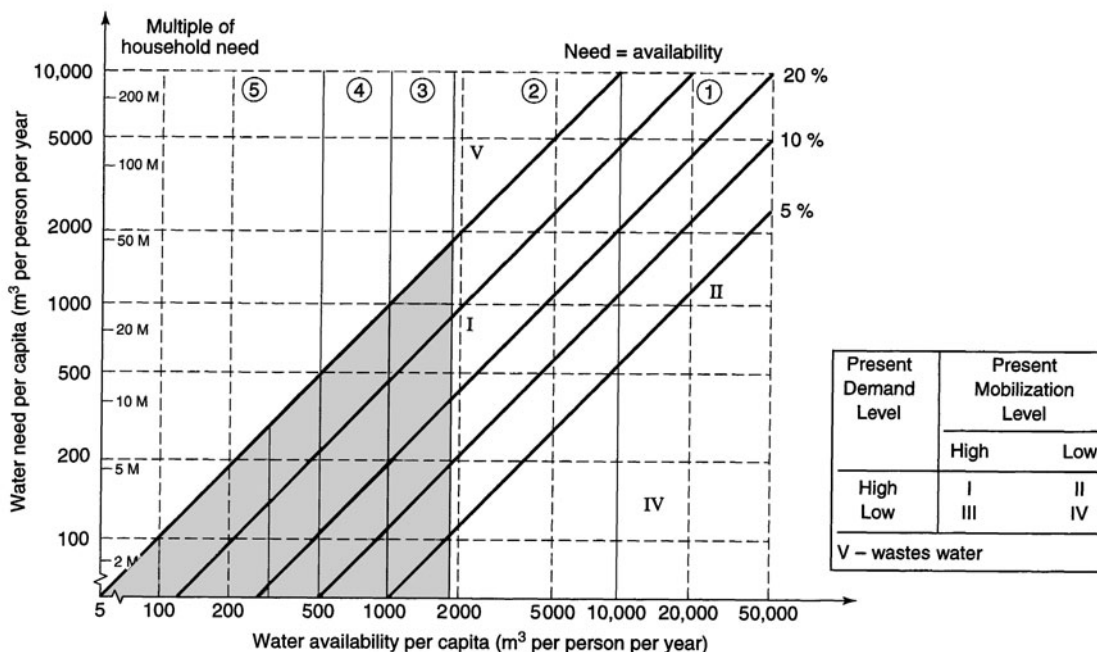
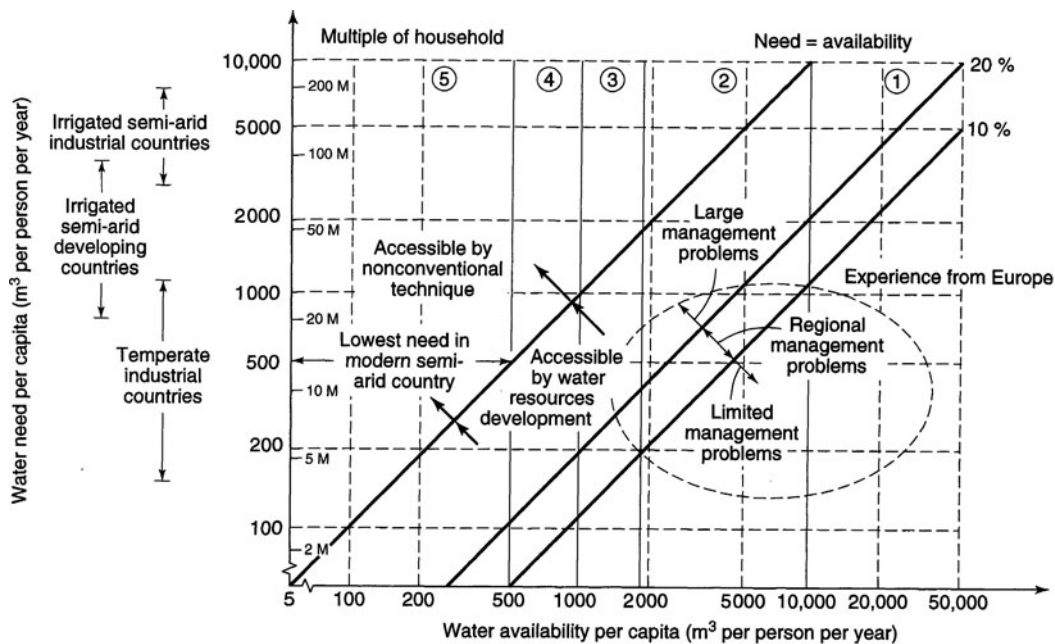


Figure 11.4.1 Logarithmic diagram showing water demand possible to supply at different levels of mobilization of potentially available water. The horizontal axis shows per capita availability (m^3 per person and year). Circled code numbers at the top of the diagrams refer to the water competition levels. The vertical axis shows water demand expressed both as m^3 per person and year and as multiples of a household demand H, assumed to be 1001 per person and day. Crossing lines show different mobilization levels of water availability, achieved through water storage, flow control, and other measures of water resources development. Roman numerals refer to water predicament positions (from Falkenmark, et al. (1989) and Falkenmark and Lindh (1993)).

Table 11.4.1 Global Stocks of Water (10³ km³)

Stock	Nace (1967)	UNESCO (1974)	L'vovich (1979)	Baumgartner and Reichel (1975)	Berner and Berner (1987)	WRI (1988)
Freshwater lakes	125	91	280 ^e	225 ^f	125 ^e	100
Saline lakes and inland seas	104	854	<i>e</i>	<i>f</i>	<i>e</i>	105
Rivers ^a	1.25	2.12	1.2	<i>f</i>	1.7	1.7
Soil moisture	67 ^b	16.5	85	<i>g</i>	65	70
Groundwater	8350 ^c	23,400 ^k	60,000 ^h	8062 ^g	9500 ^c	8200
Ice caps and glaciers	29,200	24,064	24,000	27,820	29,000	27,500
Underground permafrost ice	<i>d</i>	300	<i>d</i>	<i>d</i>	<i>d</i>	<i>d</i>
Swamp water	<i>d</i>	11.47	<i>d</i>	<i>d</i>	<i>d</i>	<i>d</i>
Biota	<i>d</i>	1.12	<i>d</i>	<i>d</i>	0.6	1.1
Total inland water	37,800					
Atmospheric water	13	12.9	14	13	13	13
Ocean water	1,320,000	1,338,000	1,370,323	1,348,000	1,370,000	1,350,000
Total stocks ^j	1,360,000	1,385,985	1,454,193	1,384,120	1,408,700	<i>i</i>

^a Average instantaneous volume.

^b Includes vadose water (subsurface water above the water table level).

^c To depth of 4 km.

^d These values included in other categories or not included.

^e Fresh and saline water.

^f All lake and river water included in the value for freshwater lakes.

^g Soil water included in groundwater value.

^h Refers to volume of water in upper 5 km of earth's crust, excluding chemically bound water.

ⁱ No total given in original source.

^j Total given in original source. May not add up to sum of individual stocks.

^k Of this total, 10,530 are freshwater.

Sources: Baumgartner and Reichel (1975), Berner and Berner (1987), L'vovich (1979), Nace (1967), UNESCO (1974), WRI (1988), and presented in Gleick (1993d).

Table 11.4.2 U.S. Water Withdrawals, by Region, 1960–1990 (km³/yr)

Region	1960	1965	1970	1975	1980	1985	1990
New England	8.9	10.0	13.4	19.4	18.0	22.5	19.2
Mid-Atlantic	37.5	46.5	62.3	71.9	71.9	60.5	65.8
South Atlantic-Gulf	26.1	39.3	48.4	59.5	67.8	60.2	61.1
Great Lakes	40.1	45.7	54.0	49.8	52.6	44.1	44.8
Ohio	33.2	41.5	49.8	49.8	52.6	43.2	42.0
Tennessee	10.4	11.3	10.9	15.2	16.6	12.7	12.7
Upper Mississippi	15.2	22.1	22.1	26.3	31.8	23.4	28.7
Lower Mississippi	7.3	7.2	18.0	22.1	29.1	24.3	26.4
Souris-Red-Rainy	0.2	0.4	0.4	0.5	0.3	0.4	0.4
Missouri	29.9	28.8	33.2	48.4	54.0	47.7	51.9
Arkansas-White-Red	14.4	14.4	16.6	20.8	33.2	21.2	21.7

(Continued)

Table 11.4.2 (Continued)

Region	1960	1965	1970	1975	1980	1985	1990
Texas-Gulf	30.4	22.1	29.1	30.4	23.5	26.0	25.6
Rio Grande	^a	10.1	8.7	7.5	6.5	7.8	8.3
Upper Colorado	19.4	9.3	11.2	5.7	11.8	10.5	9.8
Lower Colorado	^b	9.1	10.0	11.8	12.0	10.2	10.7
Great Basin	9.7	9.5	9.3	9.5	10.4	11.4	10.1
Pacific Northwest	40.1	40.1	41.5	45.7	47.0	49.1	50.2
California	45.7	52.6	66.4	70.6	74.7	69.0	65.1
Alaska	0.3	0.1	0.3	0.3	0.3	0.6	0.9
Hawaii	2.2	2.8	3.7	3.5	3.5	3.0	3.8
Caribbean	1.7	2.4	4.2	5.7	4.6	3.8	4.4
Total ^c	374	429	512	581	625 ^d	552	564

^aIncluded in Texas-Gulf.^bIncluded in Upper Colorado.^cFigures may not add to total due to independent rounding.^dThis total revised in 1988 to 600 km³/yr.

Source: Data from U.S. Geological Survey as presented by Gleick (1993b).

withdrawals by major users in selected OECD (Organization for Economic Cooperation and Development) countries.

Table 11.4.3 provides a summary of groundwater withdrawals in the United States by water resource region and by use sector. All the data are for withdrawals, not consumption. This table

Table 11.4.3 Groundwater Withdrawals in the United States, by Water Resources and Sector, 1990^a

Region	Freshwater Withdrawals (10 ⁶ m ³ /yr)								Total
	Public supply	Domestic	Commercial	Irrigation	Livestock	Industrial	Mining	Thermo-electric	
New England	453	233	113	12	7.5	133	1.8	4.0	958
Mid-Atlantic	1934	547	130	141	98	497	290	6.4	3640
South Atlantic-Gulf	3468	910	166	3178	274	1238	531	57	9820
Great Lakes	636	390	37	182	70	325	30	4.4	1680
Ohio	1069	486	80	39	75	735	1083	90	3660
Tennessee	151	77	77	5.2	44	32	35	0.0	421
Upper Mississippi	1603	513	185	489	300	482	15	29	3620
Lower Mississippi	968	124	28	8607	981	692	11	104	11,500
Souris-Red-Rainy	47	30	0.1	77	22	1.8	0.3	0.0	179
Missouri Basin	844	191	46	9947	334	157	133	69	11,700
Arkansas-White-Red	503	163	37	9118	218	93	68	43	10,200
Texas-Gulf	1451	109	65	5485	75	195	116	64	7560
Rio Grande	511	32	26	2238	28	15	90	22	2960
Upper Colorado	44	14	7.7	44	7.3	4.0	54	0.0	175
Lower Colorado	709	51	32	3095	41	68	192	65	4250
Great Basin	489	18	10	1948	37	106	106	10	2730
Pacific Northwest	1004	293	68	10,873	816	464	6.9	14	13,500
California	4504	290	80	14,644	278	174	21	6.4	20,000
Alaska	47	8.6	12	0.1	0.1	72	5.9	6.5	87
Hawaii	305	12	54	276	4.7	28	1.9	131	813
Caribbean	112	5.1	0.6	75	7.2	15	2.6	3.6	221
Total	20,900	4500	1250	70,500	3720	5460	2790	728	110,000

^aFigures may not add to totals due to independent rounding.

Source: U.S. Geological Survey as presented by Gleick (1993c).

presents only freshwater, as a few regions use modest quantities of saline groundwater, primarily for power plant cooling (Gleick, 1993b).

Table 11.4.4 presents some water supply techniques and compares their costs, stage of development, physical requirements, advantages and disadvantages, reliability, and common application. These water systems include desalination, transport—tankers, transport—icebergs, water reuse, and cloud seeding. The advantages and disadvantages of each method obviously depend on the alternatives available in a region, level of technical knowledge of water managers, location, and climate characteristics, among many other factors. The characteristics in the table are applicable only generally. Figure 11.4.2 shows the Yuma Desalting Plant near Yuma, Arizona.

Table 11.4.4 Characteristics of Unconventional Water-Supply Systems

	Desalination	Transport—tankers	Transport—icebergs	Water reuse	Cloud seeding
Cost of water (\$1,985/m ³)	Brackish \$0.25–1.00 Seawater \$1.30–8.00	\$1.25–7.50	Saudi Arabian project \$0.02–0.85	\$0.07–1.80	\$0.01
Stage of development	Moderate to high	Low to moderate	Very low	Moderate to high	Low to moderate
Special physical requirements	1. Source of clean brackish or seawater 2. Method or place to dispose of a brine solution 3. Major equipment and facility construction	1. Port facilities 2. Storage facilities	1. Large tugboats 2. A need for water adjacent to a coastal area 3. Deep draught channels 4. Storage facilities 5. Equipment to melt ice and collect water	1. Source of wastewater 2. Major equipment and facility construction	1. Suitable clouds 2. Scientific staff 3. Structures and land use to take advantage of increased rainfall
Advantages	1. Proven systems available 2. Wide range of suppliers 3. Provides independence from external sources of supply	1. Low level of technology required 2. Can be implemented quickly for emergency use		1. Proven techniques available 2. Wide range of suppliers 3. Nonpotable applications 4. Can reduce problems associated with present methods of wastewater disposal	1. Only moderate to small capital investment needed
Disadvantages	1. Requires skilled techniques for operation and repair 2. Generally requires use of foreign exchange to purchase equipment 3. Energy-intensive process	1. Deep channels and facilities needed for large vessels 2. Must depend on sources outside country. The potential for a supply interruption because of storms, conflicts, boycotts, or strikes is relatively high 3. Can only meet low-volume demand	1. Essentially untried method 2. Not suitable for small-scale experimentation	1. Requires some operation and maintenance 2. Improper operation could create the potential for adverse public health effects 3. May not be aesthetically or culturally acceptable	1. Still in the limited development stage with many uncertainties 2. Cannot control the results
Certainty of operation	High	High	Low	High	Low to moderate
Typical applications for water	Potable Industrial	Potable Agriculture Industrial	Potable Agriculture Industrial	Agriculture Industrial	Potable Agricultural Industrial

Source: Gleick (1993b), modified and updated from United Nations (1985).

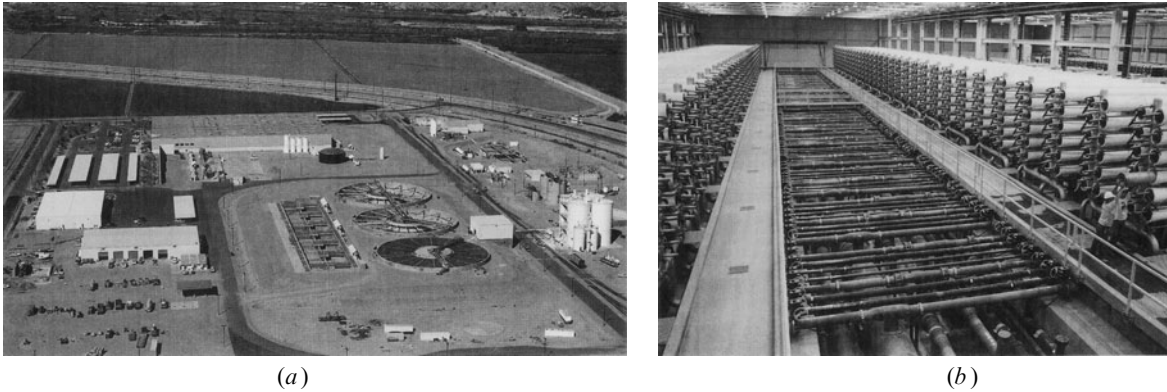


Figure 11.4.2 (a) Yuma Desalting Plant in the Colorado River near Yuma, Arizona. This is a reverse osmosis desalting plant that was constructed to reduce salinity levels of water delivered to Mexico in the Colorado River; (Courtesy of U.S. Bureau of Reclamation.) (b) Yuma Desalting Plant process area, which is located in the large building shown in Figure 11.4.2a. Operators are shown loading the membrane elements into the reverse osmosis vessels. (Courtesy of U.S. Bureau of Reclamation.)

11.4.2 Examples of Regional Water Supply Systems

Central Arizona Project

An example of a regional water supply system is the Central Arizona Project (CAP), shown on the map in Figure 11.4.3. CAP is a 336-mi long system of aqueducts, tunnels, pumping plants, and pipelines. Constructed by the U.S. Bureau of Reclamation, the CAP delivers Colorado River water from Lake Havasu on Arizona's western border to Maricopa, Pinal, and Pima Counties in Central and Southern Arizona. Operated and maintained by the Central Arizona Water Conservation District (CAWCD), the CAP delivers water to users in the three-county service area. The CAP can deliver an average of 1.5 maf of water each year to cities, industries, Indian communities, and farmers. During shortages, cities, industries, and Indian communities have priority for the water. Once these uses are met, non-Indian agricultural users will receive water.

Figure 11.4.4 shows the Havasu, the project's largest pumping plant, which lifts the water intake from Lake Havasu to the Buckskin Mountains Tunnel's inlet 824 ft above the lake's surface. The water then flows 7 mi through the tunnel to the first section of canal.

The first 17 mi of the Hayden–Rhodes Aqueduct play a specific role in the project's operation. This oversized section of canal between Havasu and Bouse Hills pumping plants acts as an in-line storage reservoir. Because the Havasu plant will use about half the energy needed for project pumping, it will be operated primarily when energy costs are lowest to reduce pumping costs. The water will then be pumped through the rest of the system as demand requires. Figure 11.4.5 shows the CAP through a residential area in Scottsdale, Arizona. A part of this overall project is the recharge of water in facilities as shown in Figure 11.4.7. Figure 11.4.6 shows the control room at CAP headquarters in Phoenix, Arizona. The CAP SCADA (Supervisory Control and Data Acquisition) is used for real-time monitoring and control of the CAP.

Southeast Anatolian Project (GAP)

The Southeast Anatolian Project (GAP) is a regional development scheme in the southeastern region of Turkey that involves the construction of 22 dams, 19 hydroelectric generation stations, and the irrigation of 1.7 million hectares of land. This project, shown in Figure 11.4.8a, is known by the Turkish acronym GAP (for Guneýdogu Anadolu Projesi). The Atatürk Dam (shown in Figure 11.4.8b), one of the largest in the world, is the centerpiece of the GAP project. Figure 13.2.2 shows closer views of the hydroelectric generation facility at the Atatürk Dam.



Figure 11.4.3 Central Arizona Project map. Colorado River water is delivered to users by pumping it from Lake Havasu into the conveyance system, then relifting it through a series of pumping plants across the state. From Lake Havasu to the end of the aqueduct, the water is lifted nearly 2,900 feet in elevation by 14 pumping plants. (Courtesy of Central Arizona Project.)

Israel's National Water Carrier System

The main water resources of Israel (Figure 11.4.9) are concentrated in Lake Kinneret (also known as Lake Galilee), the Coastal Aquifer, and the Western Mountain Aquifer (or Limestone Aquifer). About 80 percent of all the water used in Israel is derived from these three sources (Bruins, 1999).

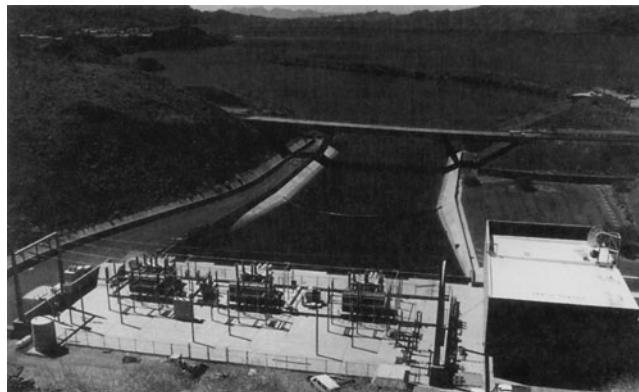


Figure 11.4.4 Havasu intake and pumping plant with Lake Havasu shown in background. (Courtesy of Central Arizona Project.)



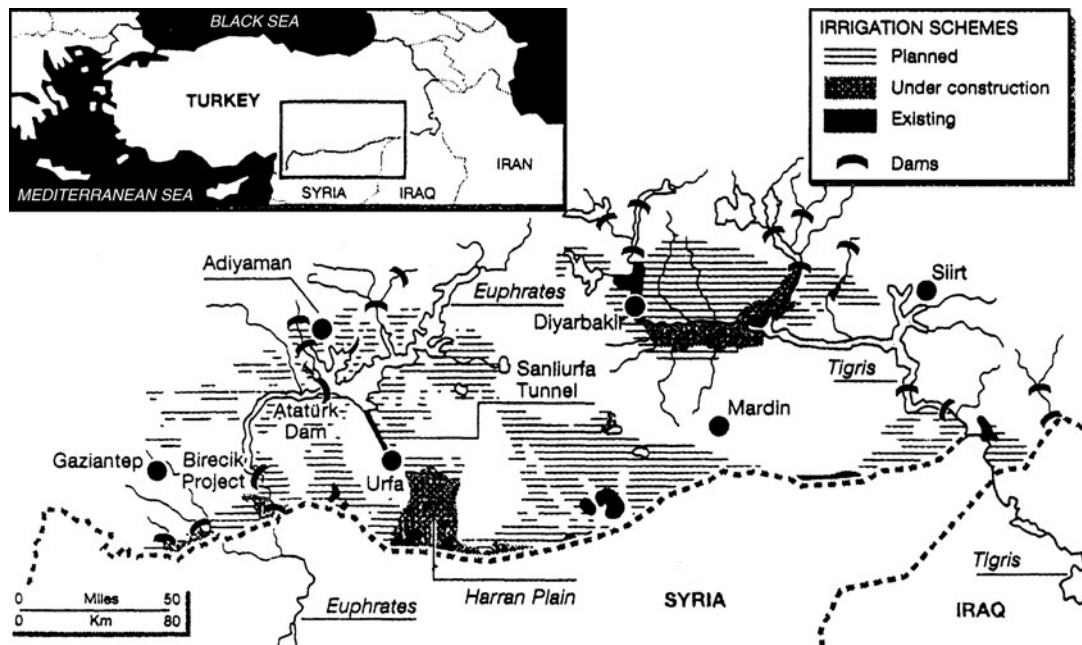
Figure 11.4.5 CAP through a residential area in Scottsdale, Arizona. (Courtesy of Central Arizona Project.)



Figure 11.4.6 CAP control room. The CAP's operating features—pumping plants, check structures and turnouts—are remotely operated from the project's headquarters in north Phoenix by a computer assisted control and communications system. Cables buried along the aqueduct carry operating commands from the Control Center's computer to check structures and turnouts. The commands raise or lower gates in these structures so water can be moved through the system or delivered to users. A microwave system is used for communicating with the pumping plants. Commands are sent from the Control Center through the microwave system to pump units at the plants, starting and stopping them as needed. The communications systems also carry information from the operating features back to operators at the Control Center. The operators, who plan system operations, also monitor the system's performance and adjust it as necessary, correcting problems that may occur. The microwave and cable systems can be used interchangeably to operate the project features. If this remote operations capability is temporarily lost, each individual operating feature can be operated locally. (Courtesy of Central Arizona Project.)



Figure 11.4.7 Avra Valley Recharge Facility near Tucson, Arizona. Recharge facilities consist of five major components: (1) the pipeline that carries the water (or treated effluent) from the source (or wastewater treatment plant); (2) percolation (infiltration) basins where the treated effluent infiltrates into the ground; (3) the soil immediately below the infiltration basins (vadose zone); (4) the aquifer where water is stored for a long duration; and (5) the recovery well where water is pumped from the aquifer for potable or non-potable reuse. (Courtesy of Central Arizona Project, photograph by M. Early.)



(a)



(b)

Figure 11.4.8 (a) Southeast Anatolia Project (GAP) in Turkey; (b) Ataturk Dam. The Ataturk Dam is the largest structure ever built in Turkey for irrigation and hydropower generation. Located on the Euphrates, it is the key structure for the development of the Lower Euphrates Project as well as for the Southeastern Anatolian Project. Also refer to Figures 13.2.2 and 17.2.14. (Courtesy of the Southeast Anatolia Project.)

Lake Kinneret is the principal natural storage reservoir of fresh surface water, having an area of 165 km² and a maximum capacity of almost 4,000 mcm (million cubic meters) of water. Water is supplied to the lake by the Jordan River and its tributaries, and to a lesser extent by wadis and springs. Lake Kinneret remains the main water source of the National Water Carrier.

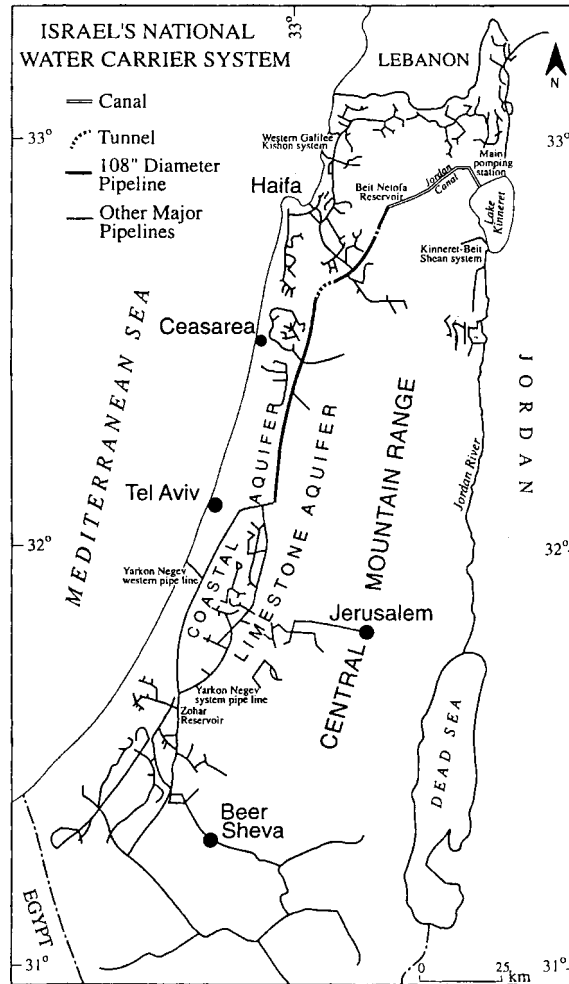


Figure 11.4.9 Israel's National Water Carrier System (from Bruin, 1999)

11.5 WATER DEMAND AND PRICE ELASTICITY

11.5.1 Price Elasticity of Water Demand

From an economic viewpoint, *demand* is a general concept denoting the willingness of consumers or users to purchase goods, services, or inputs to production processes. Demand is often used interchangeably with requirement in discussing water use. A common-sense rule concerning demand is that for a single consumer or group of consumers, the quantity demanded increases as the price (cost) per unit decreases. A *requirement*, however, is a purchase at the same quantity no matter what the price. Water demand is a function of several factors, including price.

The *elasticity of demand* is the responsiveness of consumers' purchases to varying price. The most frequently used elasticity concept is *price elasticity*, which is defined as the percentage change in quantity taken if price is changed 1 percent. Young (1996) states that "the price elasticity of demand for water measures the willingness of consumers to give up water use in the face of rising prices, or conversely, the tendency to use more as price falls."

Table 11.5.1 Summary of Some of the Price Elasticity Values

No.	Researchers	Research area	Estimated price elasticity	Estimated income elasticity	Remarks
1	Howe & Linaweaver (1967)	Eastern U.S.	-0.860		
2	Howe & Linaweaver (1967)	Western U.S.	-0.52		
3	Wong (1972)	Chicago	-0.02	0.20	
4	Wong (1972)	Chicago suburb	-0.28	0.26	
5	Young (1973)	Tucson	-0.60 - -0.65		Exponential and linear models used
6	Gibbs (1978)	Metropolitan Miami	-0.51	0.51	Elasticity measured with the mean marginal price
7	Gibbs (1978)	Metropolitan Miami	-0.62	0.82	Elasticity measured with the average price
8	Agthe & Billings (1980)	Tucson	-0.27 - -0.71		Long-run model
9	Agthe & Billings (1980)	Tucson	-0.18 - -0.36		Short-run model
10	Howe (1982)		-0.06		
11	Howe (1982)	Eastern U.S.	-0.57		
12	Howe (1982)	Western U.S.	-0.43		
13	Hanke & de Maré (1982)	Malmö, Sweden	-0.15		
14	Jones & Morris (1984)	Metropolitan Denver	-0.14 - -0.44	0.40-0.55	Linear and log-log models used
15	Moncur (1989)	Honolulu	-0.27		Short-run model
16	Moncur (1989)	Honolulu	-0.35		Long-run model
17	Jordan (1994)	Spalding County, Georgia	-0.33		A price elasticity of -0.07 was also reported for no rate structure, but increased price level

The price elasticity of water is defined as

$$\eta_p = \frac{\Delta d}{\bar{d}} \div \frac{\Delta P}{\bar{P}} \quad (11.5.1)$$

where η_p is the price elasticity, \bar{d} is the average quantity of water demanded, \bar{P} is the average price, Δd is the change in the demand, and ΔP is the change in the price. For a continuous-demand function, the following more general formula is applicable:

$$\eta_p = \frac{dd}{\bar{d}} \div \frac{dP}{\bar{P}} \quad (11.5.2)$$

Table 11.5.1 summarizes some of the values of price elasticity of water demand reported in the literature. Two different ways have been used to formulate the price elasticity of demand for water, one based upon average price and the other based upon marginal price. Agthe and Billings (1980) state that the elasticity determined based upon average price overestimates the result; therefore, they (like several others) recommend that the marginal price be used.

The use of the price elasticity of water has been applied to some cities, and some important achievements have been made. The following schematic may depict the general trend of this principle, as derived from the conclusion reached by Jordan (1994):

$$\uparrow (\text{price}) \Rightarrow \downarrow (\text{water demand}) \ \& \ \uparrow (\text{revenue}) \quad (11.5.3)$$

An increase by less than 40 percent of the price resulted in a 10 percent decrease in the demand in Honolulu, Hawaii—the announced goal of the restrictions imposed in the drought episodes of 1976 to 1978 and in 1984 (Moncur, 1987). This was achieved using a price elasticity of only -0.265 . In Tucson, Arizona, an inverted rate structure was credited with reducing public demand from about 200 gallons per capita per day (gpcd) to 140–160 gpcd (Maddock and Hines, 1995).

The manner in which water utilities are structured is probably the most important factor, which complicates the study of price elasticity. For instance, some customers who own homes or who pay water bills react more or less to the price change, whereas those who rent apartments or who do not pay water bills are indifferent. Furthermore, the water necessities for residential, commercial, and industrial purposes are not equally important. Because of these factors, different researchers had to study demand elasticity by categorizing water distribution systems for industrial, commercial, and residential uses. The demand patterns under these categories are not uniform.

One of the most comprehensive studies on price elasticity of water demand, done by Schneider and Whitlatch (1991) for six user categories (residential, commercial, industrial, government, school, and total metered), showed different results for these categories. Residential water use is further complicated by different factors: many residents who rent housing do not pay for water and thus are indifferent to demand regulations; the patterns for indoor and outdoor water demand differ quite significantly and hence necessitate different approaches to demand analysis. The climatic conditions of a given area and the time of the year are basic reasons why apparently different elasticity values are reported for the eastern and the western United States and for winter and summer uses.

From the studies enumerated so far, however, a general conclusion can be reached: that demand is elastic to price increase. Almost all research has reinforced this hypothesis. However, differences exist between the elasticity values calculated for different geographic locations. For instance, Howe (1982) obtained values of -0.57 and -0.43 for the eastern and the western United States, respectively. On the other hand, no clear consistency exists in how elasticity is calculated: some use average price, some use marginal price, and some include an intramarginal rate structure.

EXAMPLE 11.5.1

If the price elasticity for water is -0.5 , interpret the meaning of this.

SOLUTION

A 1.0 percent increase in the price of water results in a 0.5 percent decrease in water demand, with all other factors remaining constant. This pertains only to the situation where price-quantities data pairs are close to each other, or where a smooth demand function (section 11.5.2) can be fitted statistically to the known data (see Kindler and Russell, 1984).

11.5.2 Demand Models

A *demand function* (Figure 11.5.1) relates the quantity of a commodity that a consumer is willing to purchase to price, income, and other variables. Demand curves are generally negatively sloped; that is, the lower the price, the greater the quantity demanded. Typically, demand is expressed as a function of different variables. A general form of *demand models* is

$$d = f(x_1, x_2, \dots, x_k) + \epsilon \quad (11.5.4)$$

where f is the function of variables x_1, x_2, \dots, x_k , and ϵ is a random error (random variable) describing the joint effect on q of all the factors not explicitly considered by the variables.

Several explicit, linear, semilogarithmic, and logarithmic models have been developed. Agthe and Billings (1980), for example, gave the following water demand function for Tucson, Arizona:

$$\ln(d) = -7.36 - 0.267 \ln(P) + 1.61 \ln(I) - 0.123 \ln(DIF) + 0.0897 \ln(W) \quad (11.5.5)$$

In the above equation, d is the monthly water consumption of the average household in 100 ft³; P is the marginal price facing the average household in cents per 100 ft³; DIF is the difference between

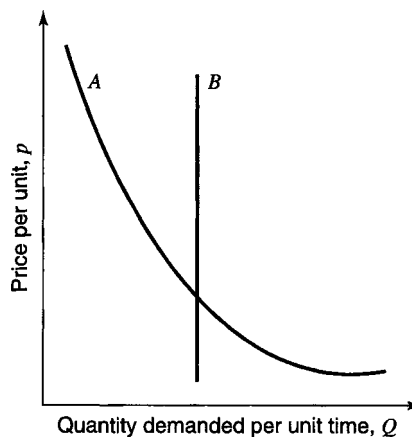


Figure 11.5.1 Demand functions. Curve A is a typical demand curve and curve B is the demand curve for a requirement for which the same quantity is demanded no matter what the price.

the actual water and sewer use bill minus what would have been paid if all water were sold at the marginal rate (\$); I is the personal income per household (\$/month); and W is the evapotranspiration minus rainfall (in inches). The above equation implicitly relates demand to the hydrologic index W . The positive coefficient of W shows that demand increases exponentially with W , which indirectly indicates increases in demand with the dryness of weather conditions.

Equation (11.5.5) may be rearranged as

$$d = 0.00006362P^{-0.267}I^{1.61}(DIF)^{-0.123}W^{0.0897} \tag{11.5.6}$$

or, in more general terms,

$$d = a'P^{b'}I^{c'}(DIF)^{d'}W^{e'} \tag{11.5.7}$$

where a' , b' , c' , d' , and e' are constants. The price elasticity of demand for equation (11.5.6) is -0.267 . Therefore, changing the price while keeping the other variables constant results in different average demand values \bar{d}_P . Again, varying W while keeping the other variables constant gives a general relation of the average demand associated with the return period T .

EXAMPLE 11.5.2

Foster and Beattie (1980) developed a demand function for urban residential water demand for application in the United States:

$$\ln Q = -1.3895 - 0.1278P_{av} + 0.4619 \ln(I) - 0.1699 \ln(F) + 0.4345 \ln(H)$$

where Q is the quantity of water demanded at a meter (1000 ft³ per year); P_{av} is the average water price (dollars per 1000 ft³); I is the median household income (dollars per year); F is the precipitation in inches during the growing season; and H is the average number of residents per meter. Determine the price elasticity of demand calculated at the mean price, \$3.67/1000 gallons.

SOLUTION

The demand function can be expressed as

$$Q = e^{-1.3895 - 0.1278P_{av}} I^{0.4619} F^{-0.1699} H^{0.4345}$$

and the derivative of Q with respect to price is

$$dQ/dP = I^{0.4619} F^{-0.1699} H^{0.4345} e^{-1.3895 - 0.1278P_{av}} (-0.1278) = -0.1278Q$$

Price elasticity of demand is then

$$\epsilon = \frac{P}{Q} \frac{dQ}{dP} = \frac{P}{Q} (-0.1278Q) = -0.1278(3.67) = -0.469$$

The price elasticity of -0.469 indicates that for a 1.0 percent increase in price, a 0.469 percent decrease in quantity demanded would be expected; conversely, a 1.0 percent decrease in price would produce a 0.469 percent increase in quantity demanded.

11.6 DROUGHT MANAGEMENT

11.6.1 Drought Management Options

Droughts are generally associated with sustained periods of significantly lower soil moisture levels and water supply than the normal levels around which the local environment and society have stabilized (Rasmusson et al., 1993). Droughts have been defined from several viewpoints, including: (1) meteorological definition; (2) agricultural definition; (3) hydrologic definition; and (4) economic definition. *Hydrologic drought* typically refers to periods of below-normal streamflow and/or depleted reservoir storage. *Economic drought* concerns the economic areas of human activity affected by drought as a result of physical processes. *Agricultural drought* typically refers to periods where the soil moisture is inadequate to initiate and sustain crop growth. *Meteorological drought* is the time when the actual cumulative moisture supply falls short.

Droughts continue to rate as one of the most severe weather-induced problems around the world. Global attention to natural hazard reduction includes drought as one of the major hazards.

Shortage of water supply during drought periods is such a significant factor for the general welfare that its effect cannot easily be overstated. Domestic water supply shortages during these periods in particular have been crucial in some cases and as a result, various measures have been initiated by different water supply agencies to reduce water demand during such periods. These measures, which may be considered as semi-empirical to empirical, include water metering, leak detection and repair, rate structures, regulations on use, educational programs, drought contingency planning, water recycling and reuse, pressure reduction, and so on. Such efforts are collectively termed *water conservation*, although there has not been a uniform definition among authors.

Experience from past droughts have shown that the action of water managers can greatly influence the magnitude of the monetary and nonmonetary losses from drought. A variety of drought management options have been undertaken in response to anticipated shortages of water, which can be categorized as (Dziegielewski, et al. 1986): (1) demand reduction measures; (2) efficiency improvements in water supply and distribution system; and (3) emergency water supplies. A topology of drought management options is given in Table 11.6.1.

Not only is water conservation necessary during drought periods, but its economic merits are also important to consider. In the United States, federal mandates urge that opportunities for water conservation be included as a part of the economic evaluation of proposed water supply projects (Griffin and Stoll, 1983). Water conservation during drought periods, however, requires important attention because our demand for water may exceed the available resource in the demand environment. Conservation may be achieved through different activities. According to the U.S. Water Resources Council (1979), these activities include but are not limited to:

1. reducing the level and/or altering the time pattern of demand by metering, leak detection and repair, rate structure changes, regulations on use (e.g., plumbing codes), education programs, drought contingency planning;
2. modifying management of existing water development and supplies by recycling, reuse, and pressure reduction; and

Table 11.6.1 A Topology of Drought Management Options

- I. Demand Reduction Measures
 - 1. Public education campaign coupled with appeals for voluntary conservation
 - 2. Free distribution and/or installation of particular water-saving devices:
 - 2.1 Low-flow showerheads
 - 2.2 Shower flow restrictors
 - 2.3 Toilet dams
 - 2.4 Displacement devices
 - 2.5 Pressure-reducing valves
 - 3. Restrictions on nonessential uses:
 - 3.1 Filling of swimming pools
 - 3.2 Car washing
 - 3.3 Lawn sprinkling
 - 3.4 Pavement hosing
 - 3.5 Water-cooled air conditioning without recirculation
 - 3.6 Street flushing
 - 3.7 Public fountains
 - 3.8 Park irrigation
 - 3.9 Irrigation of golf courses
 - 4. Prohibition of selected commercial and institutional uses:
 - 4.1 Car washes
 - 4.2 School showers
 - 5. Drought emergency pricing:
 - 5.1 Drought surcharge on total water bills
 - 5.2 Summer use charge
 - 5.3 Excess use charge
 - 5.4 Drought rate (special design)
 - 6. Rationing programs:
 - 6.1 Per capita allocation of residential use
 - 6.2 Per household allocation of residential use
 - 6.3 Prior use allocation of residential use
 - 6.4 Percent reduction of commercial and institutional use
 - 6.5 Percent reduction of industrial use
 - 6.6 Complete closedown of industries and commercial establishments with heavy uses of water
- II. System Improvements
 - 1. Raw water sources
 - 2. Water treatment plant
 - 3. Distribution system:
 - 3.1 Reduction of system pressure to minimum possible levels
 - 3.2 Implementation of a leak detection and repair program
 - 3.3 Discontinuing hydrant and main flushing
- III. Emergency Water Supplies
 - 1. Inter-district transfers:
 - 1.1 Emergency interconnections
 - 1.2 Importation of water by trucks
 - 1.3 Importation of water by railroad cars
 - 2. Cross-purpose diversions:
 - 2.1 Reduction of reservoir releases for hydropower production
 - 2.2 Reduction of reservoir releases for flood control
 - 2.3 Diversion of water from recreation water bodies
 - 2.4 Relaxation of minimum steamflow requirements

(Continued)

Table 11.6.1 (Continued)

3.	Auxiliary emergency sources:
3.1	Utilization of untapped creeks, ponds, and quarries
3.2	Utilization of dead reservoir storage
3.3	Construction of a temporary pipeline to an abundant source of water (major river)
3.4	Reactivation of abandoned wells
3.5	Drilling of new wells
3.6	Cloud seeding

Source: Dziegielewski et al. (1986).

3. increasing upstream watershed management and conjunctive use of ground and surface water (Griffin and Stoll, 1983).

The effort to conserve water started out with metering. Both domestic and sprinkling demands reduced significantly as a result of the introduction of water meters (Hanke, 1970). Grunewald, et al. (1976) stated: “Traditionally, water utility managers have adjusted water quantity (rather) than prices as changes in demand occurred.”

Increasing the price of domestic water supply has been a focus of many studies. These studies were conducted to analyze the effect of urban water pricing and how it contributes to water conservation during a drought period (Agthe and Billings, 1980; Moncur, 1989). However, variations have been observed in the approaches followed. According to Jordan (1994), *water pricing* is an effective way of conserving water, compared to the other measures mentioned above. An increase in the price of water contributes to water conservation because of the fact that customers have limited money. For every percent increase in the price, there is some decrease in the demand, as explained by the price elasticity (defined in section 1.5.2). A significant number of studies have been undertaken in different regions to determine price elasticity associated with pricing. The following section discusses price elasticity.

Figure 11.6.1 shows three of the municipal pricing options commonly used: (1) the *uniform block rate* (average cost pricing) with a service charge; (2) an *increasing block (tier) rate* with minimum allowance; and (3) an *increasing seasonal block rate* with minimum allowance. The increasing block pricing schemes are increasingly common. They are typically used by water agencies facing water shortages or limited supply capacity. Increasing block rates are used to encourage water conservation and more efficient use of water.

11.6.2 Drought Severity

Every natural phenomenon with which detrimental effects to human beings and their environment are associated need our keen attention on how and when it occurs. Unfortunately, the degree of some such phenomena, including drought, is difficult to determine as accurately as desirable before they occur. A study by the National Research Council (1986) indicated that there is not a firm rationale or explanation of the drought mechanism. It adds that, though empirical relations have been documented so far, why and when these relations trigger the occurrence of significant drought is not understood.

No single definite method is used as a drought severity indicator. Nonetheless, there are some that are being used in different fields. According to Wilhite (1993), the simplest drought index in widespread use is the percent of normal precipitation. This, indeed, is a good approach to infer the status of the available supply. However, it does not imply an obvious forecast to enable a risk-management body to be prepared for a forthcoming drought period.

Several drought-severity indices have been used so far. Some of them are used to assess past drought events' severity, and a few others are used for forecasting. The *Palmer Drought Severity*

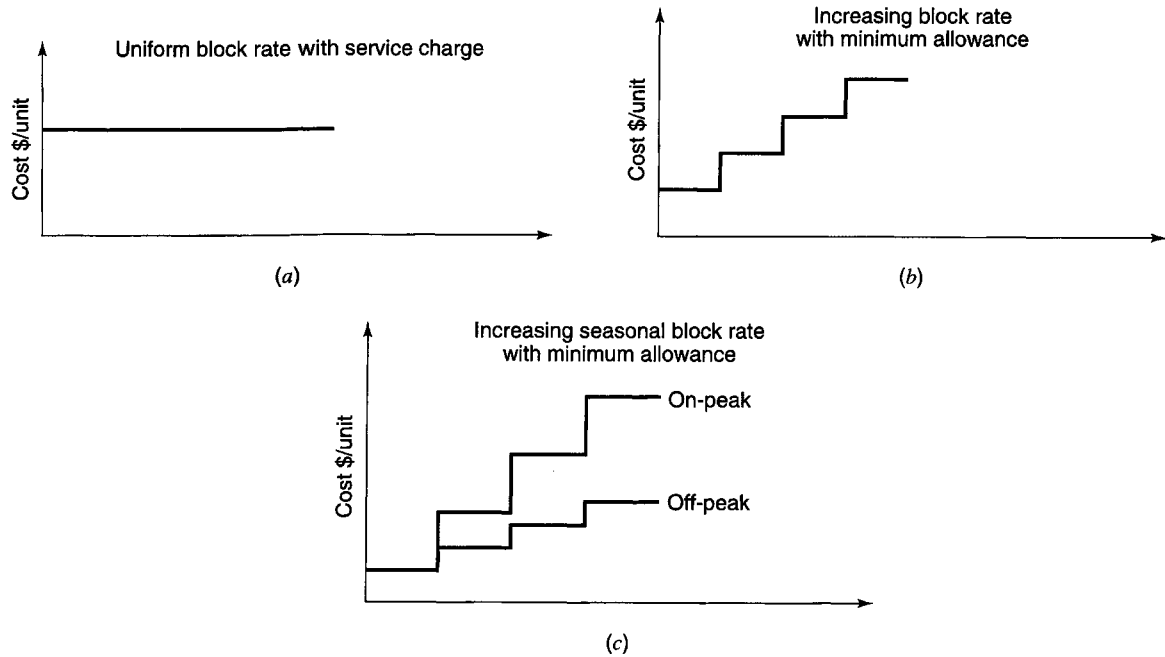


Figure 11.6.1 Common municipal pricing options. (a) Quantity used plus monthly service charge; (b) Quantity used plus monthly service charge for minimum amount; (c) Quantity used plus monthly service charge for minimum amount.

Index (PDSI) is an example of the former category, while the *Surface Water Supply Index (SWSI)* and the *Southern Oscillation Index (SOI)* are examples of the latter.

Palmer (1965) expressed the severity of a drought event by the following equation (Steila, 1972; Puckett, 1981):

$$PDSI_i = 0.897PDSI_{i-1} + \frac{1}{3}Z_i \quad (11.6.1)$$

where $PDSI$ is the Palmer Drought Severity Index and Z is an adjustment to soil moisture for carryover from one month to the next, expressed as

$$Z_i = k_j[PPT_i - (\alpha_j PE_i + \beta_j G_i + \gamma_j R_i - \delta_j L_i)] \quad (11.6.2)$$

in which the subscript j represents one of the calendar months and i is a particular month in a series of months. PPT_i is the precipitation, PE_i is the potential evapotranspiration, G_i is the soil moisture recharge, R_i is the surface runoff (excess precipitation), and L_i is the soil moisture loss for month i . The coefficients α_j , β_j , γ_j , and δ_j are the ratios for long-term averages of actual to potential magnitudes for E , G , R , and L based on a standard 30-year climatic period.

The Surface Water Supply Index (SWSI) gives a forecast of a drought event. It was introduced as a better indicator of water availability in the western United States than the Palmer Drought Index (Garen, 1993). It is a weighted index that generally expresses the potential availability of the forthcoming season's water supply (U.S. Soil Conservation Service, 1988). It is formulated as a re-scaled weighted of nonexceedance probabilities of four hydrologic components: snowpack, precipitation, streamflow, and reservoir storage (Garen, 1993):

$$SWSI = \frac{\alpha p_{\text{snow}} + \beta p_{\text{prec}} + \gamma p_{\text{strm}} + \omega p_{\text{resv}} - 50}{12} \quad (11.6.3)$$

where α , β , γ , and ω are weights for each hydrologic component and add up to unity; P_i is the probability of nonexceedance (in percent) for component i ; and the subscripts *snow*, *prec*, *strm*, and

resv stand for the snowpack, precipitation, streamflow, and reservoir storage hydrologic components, respectively. This index has a numerical value for a given basin that varies between -4.17 to $+4.17$. The following are the ranges for the index for practical purposes: $+2$ or above, $-2 - +2$, $-3 - -2$, $-4 - -3$, and -4 or below. These ranges are associated with the qualitative expressions of abundant water supply, near-normal, moderate drought, severe drought, and extreme drought conditions, respectively.

The *SWSI* has been in use to forecast different basins' monthly surface water supply availabilities (see, for example, the U.S. Soil Conservation Service, 1988). In fact, it gives a forecast of both wet and dry (drought) months.

The Southern Oscillation Index (SOI) is also used to forecast drought based on the Southern Oscillation, a phenomenon that affects large-scale atmospheric and oceanographic features of the tropical Pacific Ocean (Kawamura, et al. 1998). The oscillation is characterized by either sea-surface temperatures or differences in barometric pressures. The SOI's best-known extremes are El Niño events (Kawamura, et al. 1998). Wilhite (1993) reports that several scientists agree that it has been possible to forecast drought for up to six months in Australia by using the SOI.

11.6.3 Economic Aspects of Water Shortage

The general trend of the average demand with the return period may be shown by the demand curve in Figure 11.6.2. Demand increases with the return period of the drought severity because the more severe the drought, the more the customers are prompted to use more water. Different demand curves are illustrated in Figure 11.6.3 for different price levels. As shown in this figure, the higher the price, the lower the demand for given hydrologic conditions.

In equation (11.5.7), the demand d is related to the hydrologic index W , which is related to the return period. The available supply (flow) q is also related to the return period (Hudson and Hazen, 1964). Thus the general relationships between demand and return period and supply and return period shown in Figure 11.6.2 are based on these trends.

Shortage of water supply during drought periods results in different types of losses in the economy, including, but not limited to, agricultural, commercial, and industrial. In agriculture, lack of water supply results in crop failures; in commerce it may result in a recession of business; and in industry it may result in underproduction of commodities. The loss in each production or service sector depends on the purpose of the sector. For instance, the economic impact of drought on agriculture depends on the crop type, etc. (Easterling, 1993). There is no single common way of assessing the economic impact of drought on any one of the sectors. Evaluating and comparing what actually happens during a drought period with what would have happened had there been no drought

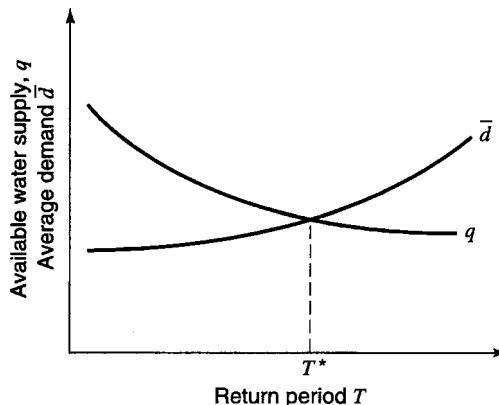


Figure 11.6.2 Water supply availability and average demand as related to the return period T .

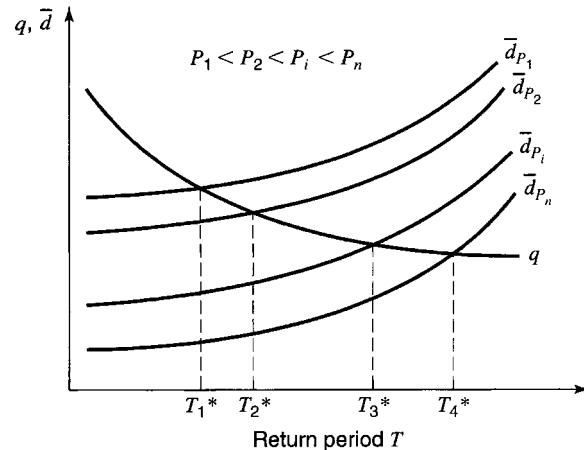


Figure 11.6.3 Water supply and average demands for different price values as related to T .

may be one way of assessing the effects of drought. Dixon, et al. (1996) adopted the concept of *willingness-to-pay* to value changes in well-being. They define willingness-to-pay as the maximum individuals would have been willing to pay to avoid the drought management strategies imposed by water agencies.

On the other hand, since water is supplied during a drought period at a greater price, it can be viewed as a revenue generator. Therefore, when the demand exceeds the available supply, the revenue collected by the water supply agency is less than what could have been collected had there been more supply than that actually available. In other words, if the demand exceeds the supply, the problem is not limited to lack of water; there will also be economic loss, since the customers would pay for more supply if there were enough. Depending on the risk level, it is possible to decide whether supply augmentation is necessary or the pressure for more demand could be tolerated with the available supply.

Some water shortage relief efforts can be undertaken so that emergency water supplies may be made available to users. This can be implemented by well drilling, trucking in potable supplies, or transporting water through small-diameter emergency water lines. In such cases, it may be required that the emergency supply construction costs be paid by the users (Dziegielewski, et al. 1991). The estimation of the expected financial loss can be used to determine and inform the users of its extent and advise them of the necessity, if any, of paying for the emergency supply construction costs.

If the option for emergency supply construction is justified, then the design needs to take into consideration the possibilities of optimization. The construction can be designed such that the financial risk and the cost of construction are optimal. Figure 11.6.4 illustrates this optimization process.

The economic loss (damage) can be calculated as shown below, and the cost of emergency construction must be determined from the physical conditions at the disposal of the water supply agency. The damage that would result if a certain drought event occurred is one of the main decision factors. Since the time of occurrence of the drought event that causes the damage is difficult to determine, only the expected value is assessed by associating its magnitude with its probability of occurrence.

The *expected annual damage cost* D_T for the event $x > x_T$ is (Ejeta and Mays, 1998)

$$D_T = \int_{x_T}^{\infty} D(x)f(x)dx \quad (11.6.4)$$

where $f(x) dx$ is the probability that an event of magnitude x will occur in any given year and $D(x)$ is the damage cost that would result from that event. The event x in this case can be taken as the demand and x_T can be the available supply during a drought event of return period T .

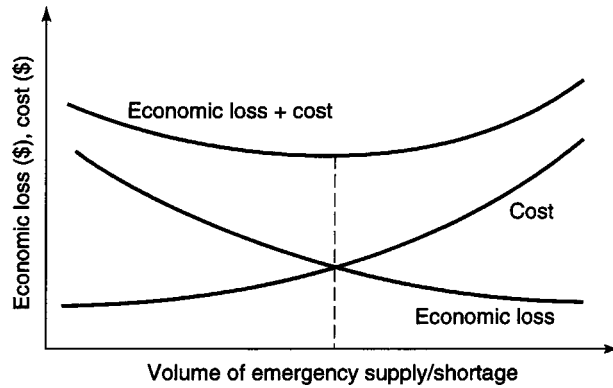


Figure 11.6.4 Optimization for emergency water supply construction.

Breaking down the expected damage cost into intervals, we get

$$\Delta D_i = \int_{x_{i-1}}^{x_i} D(x)f(x)dx \tag{11.6.5}$$

from which the finite-difference approximation is obtained

$$\begin{aligned} \Delta D_i &= \left[\frac{D(x_{i-1}) + D(x_i)}{2} \right] \int_{x_{i-1}}^{x_i} f(x)dx \\ &= \left[\frac{D(x_{i-1}) + D(x_i)}{2} \right] [p(x \geq x_{i-1}) - p(x \geq x_i)] \end{aligned} \tag{11.6.6}$$

Thus the annual damage cost for a return period T is given as

$$D_T = \sum_{i=1}^{\infty} \left[\frac{D(x_{i-1}) + D(x_i)}{2} \right] [p(x \geq x_{i-1}) - p(x \geq x_i)] \tag{11.6.7}$$

To determine the annual expected damage in the above equation, the damage that results from drought events of different severity levels must be quantified.

The magnitude of the drought (in monetary units) may be obtained by estimating the volume of water shortage that would result from that drought. In other words, not having the water results in some financial loss to the water supply customer. The resulting financial loss to the customer from a certain drought event is thus considered as the damage from that drought event.

As shown in Figure 11.6.5, after the critical return period T^* , the divergence between the demand and the supply increases with the return period. Expressing the demand and the supply as a function of return period T of drought events enables one to estimate the annual expected water supply shortage volume, as given by the following:

$$S_V = \int_{T^*}^T [d(T) - q(T)]dt \tag{11.6.8}$$

The *shortage volume* S_V is illustrated by the shaded area in Figure 11.6.5. The shortage volume for a drought event of a higher return period above the critical one results in higher shortage volume and consequently a higher associated damage. The relationship between the shortage volume and the

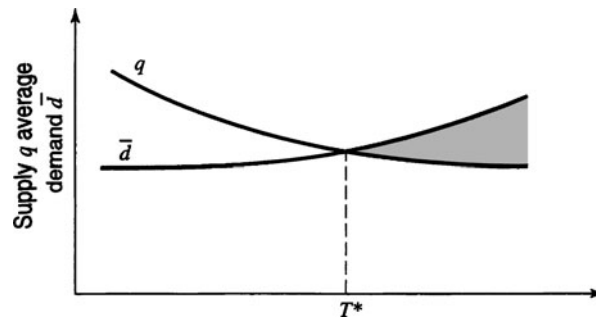


Figure 11.6.5 Demand and supply, showing water shortage volume when demand exceeds supply.

associated damage generally depends on several factors, including water use category—residential, industrial, commercial, agricultural, and so on. To use the procedure presented herein for assessing the damage that results from certain water-shortage volume, the damage given by equation (11.6.8) must be developed for a specific user category.

EXAMPLE 11.6.1

The hypothetical annual average damage cost that would occur if a flood of return period T were to occur is given, in \$1000, as

$$D(T) = T^2 - T = \frac{1}{p^2} - \frac{1}{p}$$

where $p = 1/T$, that is, annual exceedance probability. Determine

- (a) $D(T)$ for $T = 1, 2, 5, 10, 20, 50, 100, 200, 500,$ and 1000 ;
- (b) The damages between the return period intervals given in part (a); and
- (c) The annual expected damage cost for a structure designed for each of the return periods given in (a).

SOLUTION

The solutions to this problem are given in the table below.

Column 3 gives $D(T)$ for $T = 1, 2, 5, 10, 20, 50, 100, 200, 500,$ and 1000 . Column (6) gives the damages between the return periods indicated and column (7) gives the total expected damage cost for a structure designed for these return periods.

T	p	$D(T)$	$p(T_i) - p(T_{i-1})$	$[(D(T_{i-1}) + D(T_i))/2]$	(4) * (5)	Total expected damage
(1)	(2)	(3)	(4)	(5)	(6)	(7)
1	1.000	0				0.000
2	0.500	2	0.500	1	0.5	0.500
5	0.200	20	0.300	11	3.3	3.800
10	0.100	90	0.100	55	5.5	9.300
20	0.050	380	0.050	235	11.75	21.050
40	0.025	1560	0.025	970	24.25	45.300
100	0.010	9900	0.015	5730	85.95	131.250
200	0.005	39,800	0.005	24,850	124.25	255.500
500	0.002	249,500	0.003	144,650	433.95	689.450
1000	0.001	999,000	0.001	624,250	624.25	1313.700

11.7 ANALYSIS OF SURFACE WATER SUPPLY

11.7.1 Surface-Water Reservoir Systems

The primary function of reservoirs is to smooth out the variability of surface-water flow through control and regulation and make water available when and where it is needed. The use of reservoirs for temporary storage would result in an undesirable increase in water loss through seepage and evaporation. However, the benefits that can be derived through regulating the flow for water supplies, hydropower generation, irrigation uses, and other activities can offset such losses. The net benefit associated with any reservoir development project is dependent on the size and operation of the reservoir as well as the various purposes of the project.

Reservoir system operations may be grouped into two general operation purposes: conservation and flood control. Conservation purposes include water supply, low-flow augmentation for water quality, recreation, navigation, irrigation and hydroelectric power, and any other purpose for which water is saved for later release. Flood control is simply the retention or detention of water during flood events for the purpose of reducing downstream flooding. This chapter focuses only on surface-water reservoir systems for conservation. The flood control aspect of reservoir system operation is discussed in section 14.6.

Generally, the total reservoir storage space in a multipurpose reservoir has three major parts (see Figure 11.7.1): (1) the *dead storage zone*, mainly required for sediment collection, recreation, or hydropower generation; (2) the *active storage*, used for conservation purposes, including water supplies, irrigation, navigation, etc.; (3) the *flood control storage* reserved for storage of excessive flood volume to reduce potential downstream flood damage. In general, these storage spaces can be determined separately and combined later to arrive at a total storage volume for the reservoir.

11.7.2 Storage—Firm Yield Analysis for Water Supply

The determination of storage-yield relationships for a reservoir project is one of the basic hydrologic analyses associated with the design of reservoirs. Two basic problems in *storage-yield studies* (U.S. Army Corps of Engineers, 1977) are: (1) determination of storage required to supply a specified yield; and (2) determination of yield for a given amount of storage. The former is usually encountered in the planning and early design phases of a water resources development study, while the latter often occurs in the final design phases or in the reevaluation of an existing project for a more comprehensive analysis. Other objectives of storage-yield analysis include: (1) the determination of complementary or competitive aspects of multiple-project development; (2) determination of complementary or competitive aspects of multiple-purpose development in a single project; and (3) analysis of alternative operation rules for a project or group of projects.

The procedures used to develop a storage-yield relationship include (U.S. Army Corps of Engineers, 1977): (1) simplified analysis; and (2) detailed sequential analysis. The simplified techniques are satisfactory when the study objectives are limited to preliminary or feasibility studies. Detailed methods that include both simulation and optimization analysis are usually required when the study objectives advance to the design phase. The objective of simplified methods is to obtain a reasonably good estimate of the results, which can be further improved by a detailed sequential analysis. Factors affecting the selection of method for analysis are: (1) study requirements; (2) degrees of accuracy required; and (3) the basic data required and available.

Firm yield is defined as the largest quantity of flow or flow rate that is dependable at the given site along the stream at all times. More specifically, Chow, et al. (1988) define the firm yield of a reservoir as the mean annual withdrawal rate that would lower the reservoir to its minimum allowable level just once during the critical drought of record. The most commonly used method to determine the firm yield of an unregulated river is to construct a *flow-duration curve*, which is a graph of the discharge as a function of the percent of time that flow is equaled or exceeded.

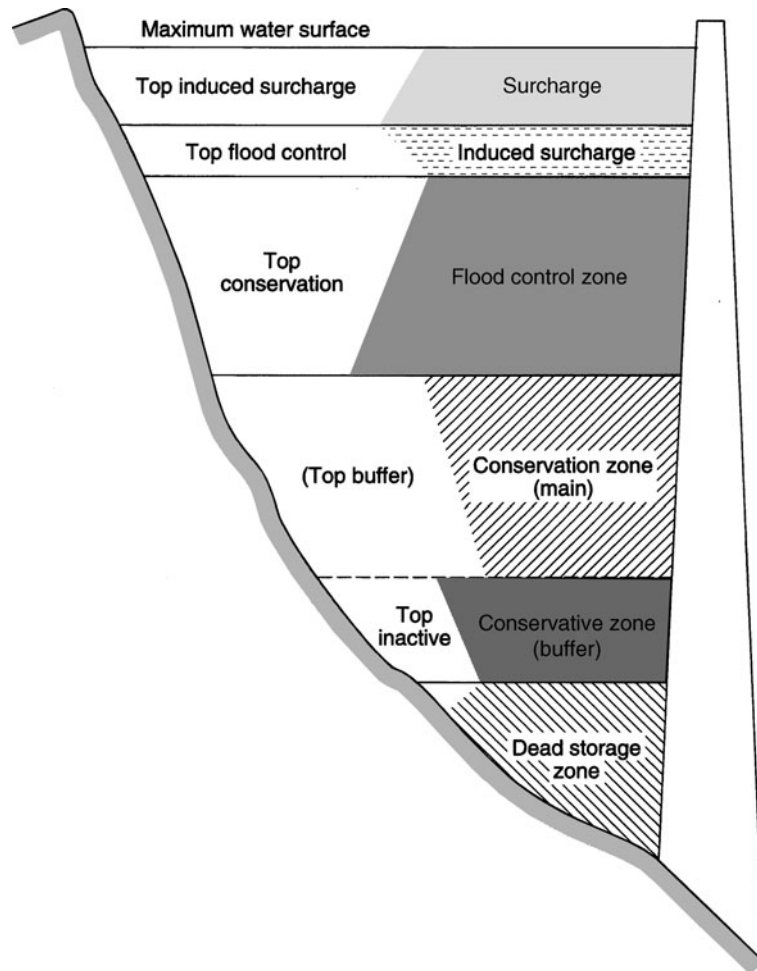


Figure 11.7.1 Reservoir storage allocation zones (from U.S. Army Corps of Engineers (1977)).

The flow-duration curve can be developed for a given location on the stream by arranging the observed flow rates in order of descending magnitude. From this, the percentage of time for each flow magnitude to be equaled can be computed. Then, this percentage of time of exceedance is plotted against the flow magnitude to define the flow-duration relationship. The firm yield is the flow magnitude that is equaled or exceeded 100 percent of the time for a historical sequence of flows. Flow-duration curves are used in determining the water supply potential for the planning and design of water resource projects, in particular hydropower plants.

EXAMPLE 11.7.1

Use the monthly flow data for the Little Weiser River given in Table 11.7.1 to develop the flow-duration curve and determine the firm yield for this site.

SOLUTION

To develop a flow-duration curve, first arrange the flows in descending order with the largest flow ordered as 1 and the smallest as N , where N is the total number of months in the record (Table 11.7.2). The percentage of time flow magnitude equaled or exceeded is computed by $100 m/N$ where m is the rank of flow magnitude shown in column (1). Using columns (2) and (3), one can construct the flow-duration curve as shown in Figure 11.7.2. The firm yield of the river at this particular site is 283 ac-ft per month,

Table 11.7.1 Monthly Water Flows in the Little Weiser River Near Indian Valley, Idaho, 1966–1970

t	Year	Month	Flow (AF)	$\sum QF_t$ (AF)	t	Year	Month	Flow (AF)	$\sum QF_t$ (AF)
1	1965	10	742	742	31		4	6720	129,105
2		11	1060	1802	32		5	13,290	142,395
3		12	1000	2802	33		6	9290	151,685
4	1966	1	1500	3302	34		7	1540	153,225
5		2	1080	4382	35		8	915	154,140
6		3	6460	10,842	36		9	506	154,646
7		4	10,000	20,842	37		10	886	155,532
8		5	13,080	33,922	38		11	3040	158,572
9		6	4910	38,832	39		12	2990	161,562
10		7	981	39,813	40	1969	1	8170	169,732
11		8	283	40,096	41		2	2800	172,532
12		9	322	40,398	42		3	4590	177,122
13		10	404	40,822	43		4	21,960	199,082
14		11	787	41,609	44		5	30,790	229,872
15		12	2100	43,709	45		6	14,320	244,192
16	1967	1	4410	48,119	46		7	2370	246,562
17		2	2750	50,869	47		8	709	247,271
18		3	3370	54,239	48		9	528	247,799
19		4	5170	59,409	49		10	859	248,658
20		5	19,680	79,089	50		11	779	249,437
21		6	19,630	98,719	51		12	1250	250,687
22		7	3590	102,309	52	1970	1	11,750	262,437
23		8	710	103,019	53		2	5410	267,849
24		9	518	103,537	54		3	5560	273,407
25		10	924	104,461	55		4	5610	279,017
26		11	1020	105,481	56		5	24,330	303,347
27		12	874	106,355	57		6	32,870	336,217
28	1968	1	1020	107,375	58		7	7280	343,497
29		2	8640	116,015	59		8	1150	344,647
30		3	6370	122,385	60		9	916	345,563

Table 11.7.2 Ranking of Flows for the Little Weiser River

Rank (m)	Flow (AF)	% time equaled and exceeded	Rank (m)	Flow (AF)	% time equaled and exceeded
1	32,870	1.7	31	2750	51.7
2	30,790	3.3	32	2370	53.3
3	24,330	5.0	33	2100	55.0
4	21,960	6.7	34	1540	56.7
5	19,680	8.3	35	1500	58.3
6	19,630	10.0	36	1250	60.0
7	14,320	11.7	37	1150	61.7
8	13,290	13.3	38	1080	63.3
9	13,080	15.0	39	1060	65.0
10	11,750	16.7	40	1020	66.7
11	10,000	18.3	41	1020	68.3
12	9290	20.0	42	1000	70.0
13	8640	21.7	43	981	71.7
14	8170	23.3	44	924	73.3

(Continued)

Table 11.7.2 (Continued)

Rank (m)	Flow (AF)	% time equaled and exceeded	Rank (m)	Flow (AF)	% time equaled and exceeded
15	7280	25.0	45	916	75.0
16	6720	26.7	46	915	76.7
17	6460	28.3	47	886	78.3
18	6370	30.0	48	874	80.0
19	5610	31.7	49	859	81.7
20	5560	33.3	50	787	83.3
21	5410	35.0	51	779	85.0
22	5170	36.7	52	742	86.7
23	4910	38.3	53	710	88.3
24	4590	40.0	54	709	90.0
25	4410	41.7	55	528	91.7
26	3590	43.3	56	518	93.3
27	3370	45.0	57	506	95.0
28	3040	46.7	58	404	96.7
29	2990	48.3	59	322	98.3
30	2800	50.0	60	283	100.0

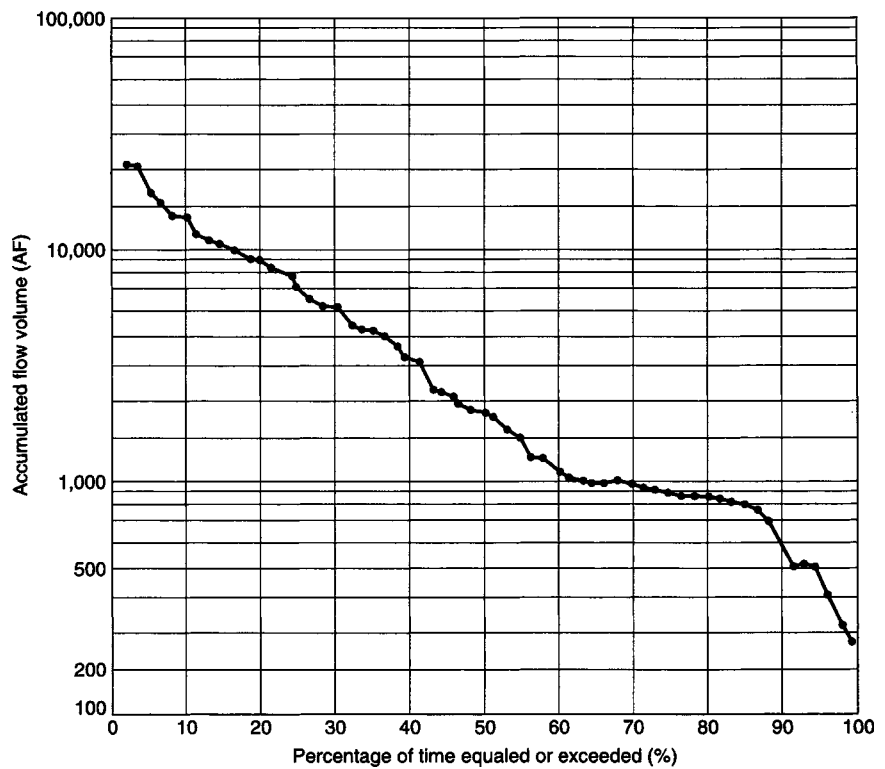


Figure 11.7.2 Flow-duration curve for the Little Weiser River near Indian Valley, Idaho, 1966–1970.

which is equivalent to an average flow rate of 4.76 cfs. In general, a firm yield based upon average daily flows is less than a firm yield based upon average monthly flows: the shorter the time period, the more erratic the flow-duration curve appears.

Mass-Curve Analysis. To increase the firm yield of an unregulated river, surface impoundment facilities are constructed to regulate the river. Two methods, *mass-curve analysis* and *sequent-peak analysis*, can be used to develop storage-yield relationships for specific locations along a river. A *mass curve* is a plot of

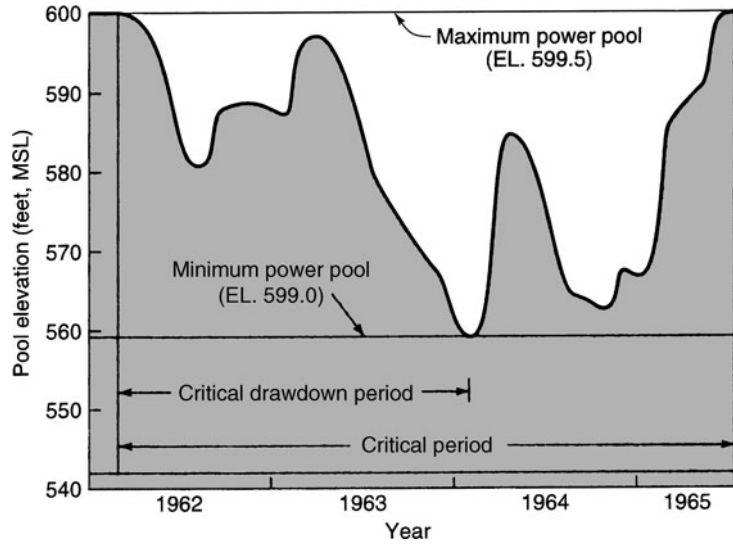


Figure 11.7.3 Critical period and critical drawdown period (from U.S. Army Corps of Engineers (1977)).

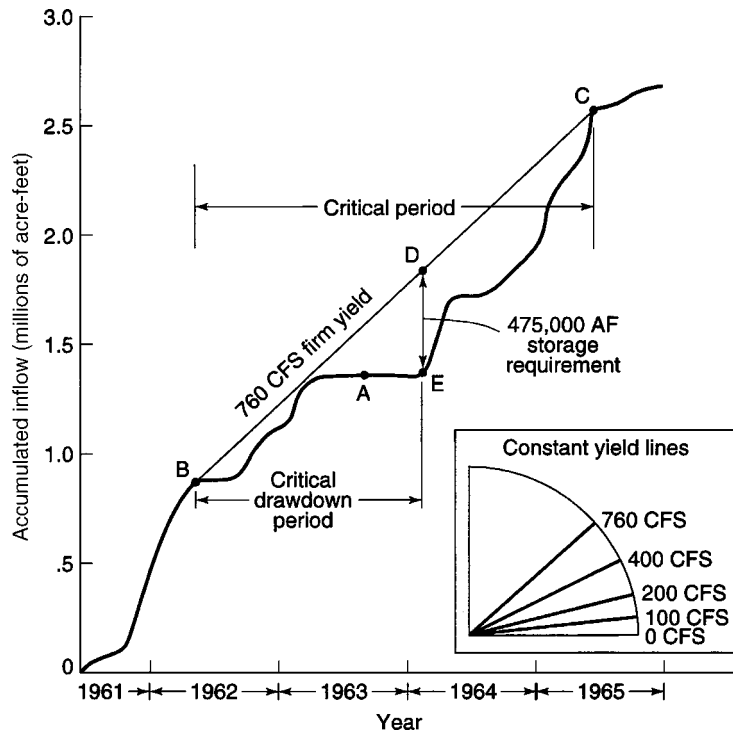


Figure 11.7.4 Mass curve and constant yield lines (from U.S. Army Corps of Engineers (1977)).

the cumulative flow volumes as a function of time. The mass-curve was first developed by Ripple in 1883. The method uses historical or synthetic stream flow sequences over a time interval $[0, T]$. Implicitly, the analysis assumes that the time interval includes the *critical period*, which is the time period over which the flows have reached a minimum, causing the greatest drawdown of a reservoir. Mass-curve analysis can be implemented using graphical procedures to determine the critical period and firm yield.

A critical period (Figure 11.7.3) always begins at the end of a preceding high-flow period that leaves the reservoir full. A critical period ends when the reservoir has refilled after the drought period. The *critical drawdown period* (Figure 11.7.3) begins when the reservoir is full and ends when the reservoir is empty. The mass curve for the critical period is presented in Figure 11.7.4.

The *Ripple method* is applicable when the release is constant. In cases where the releases vary, however, it is easier to compute the difference between the cumulative reservoir inflows and cumulative reservoir releases. The required active storage volume is the maximum difference. Of course, this alternative approach can be applied to a constant release case and can be implemented graphically. The procedures can be applied repeatedly by varying releases to derive the storage-yield curve at a given reservoir site.

The assumption implicitly built into the mass-curve method is that the total release over the time interval of analysis does not exceed the total reservoir inflows. In mass-curve analysis, the critical sequence of flows might occur at the end of the streamflow record. When this occurs, the period of analysis is doubled from $[0, T]$ to $[0, 2T]$ with the inflow sequence repeating itself in the second period, and the analysis proceeds. If the required total release exceeds the total historical inflow over the recorded period, the mass-curve analysis does not yield a finite reservoir capacity.

EXAMPLE 11.7.2

Using the monthly data in Table 11.7.1 for the Little Weiser River, construct the cumulative mass curve over the five-year period and determine the required active storage capacity to produce a firm yield of 2000 ac-ft/month.

SOLUTION

The cumulative monthly flows in column (5) of Table 11.7.1 are obtained by successively adding monthly flow in column (4). Cumulative monthly flow is plotted as a function of time to develop the mass curve shown in Figure 11.7.5.

Points $A_1, A_2, A_3,$ and A_4 define the beginning of low-flow periods and points $B_1, B_2, B_3,$ and B_4 define the end of the low-flow periods. A line representing the constant reservoir release of 2000 ac-ft per month is placed tangent to the beginning of each low-flow period, i.e., $A_1, A_2, A_3,$ and A_4 . Then the locations in each low-flow period with the largest vertical distance between the mass curve at points $B_1, B_2, B_3,$ and B_4 and the tangent lines are identified. The largest of the four vertical distances at B_1 is 7200 ac-ft, which is the required active storage.

EXAMPLE 11.7.3

For the critical period shown by the mass curve in Figure 11.7.4, determine whether the unregulated inflow can be increased to a firm flow of 760 cfs. (Adapted from U.S. Army Corps of Engineers, 1977.)

SOLUTION

The 760-cfs firm yield curve is applied to a positive point of tangency on the mass curve (point B) and is extended to the point where it again intersects the mass curve (point C). Period B–C is a complete storage draft-refill cycle (which corresponds to the critical period on Figure 11.7.3). The length of the vertical coordinate between the 760-cfs yield curve and the mass diagram represents the amount of storage drafted from the reservoir at any point in time, and the point where this ordinate is at its maximum length (point D) represents the total amount of reservoir storage required to maintain a firm flow of 760 cfs during this particular flow period.

Period B–C is the most adverse sequence of flows in the period of record; a volume of 475,000 ac-ft is required to assure a firm yield of 760 cfs at the project.

Sequent-Peak Analysis. The *sequent-peak* method computes the cumulative sum of inflows QF_t minus the reservoir releases R_t , that is, $\sum_t u_t = \sum_t (QF_t - R_t)$, for all time periods t over the time interval of analysis $[0, T]$. To solve this problem graphically, the cumulative sum of u_t is plotted against t . The required storage for the interval is the vertical difference between the first peak and the low point before the sequent peak. The method has the same two assumptions as the mass-curve analysis.

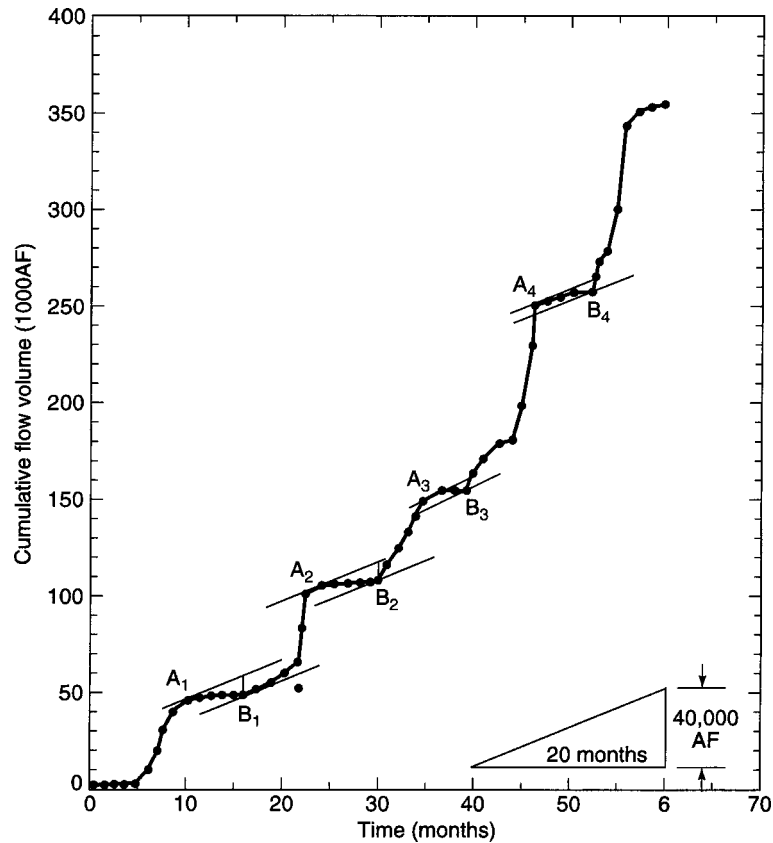


Figure 11.7.5 Cumulative mass curve for Little Weiser River, and application of mass curve analysis to compute firm yield (Example 11.7.2).

Algebraically, the sequent-peak method can be implemented using the following equation recursively:

$$K_t = \begin{cases} R_t - QF_t + K_{t-1} & \text{if positive} \\ 0 & \text{otherwise} \end{cases} \quad (11.7.1)$$

where K_t is the required storage capacity at the beginning of period t . The initial value of K_t at $t = 0$ is set to zero. In general, the method using equation (11.7.1) is applied repeatedly, up to twice the length of the recorded time span, to take into account the possibility that the critical flow sequence occurs at the end of the streamflow record. The maximum value of the calculated K_t , is the required active reservoir storage capacity for the flow sequence and the considered releases.

In reality, the hydrological components, precipitation, evaporation, and seepage, in addition to the streamflow inflows, determine the storage volume in a reservoir.

Precipitation that falls directly on the reservoir surface contributes to the storage volume. Evaporation and seepage result in losses to the available water in active reservoir storage. Depending on the location and the geological conditions of the reservoir site, the total losses from evaporation and seepage are an important influence on the mass balance of the reservoir system. Neglecting such factors would result in serious overestimation of the water availability and, consequently, underestimation of the required reservoir storage capacity to support the desired releases. In arid and semi-arid areas, such as the southwestern United States, the quantity of water loss through evaporation may be large enough to lessen significantly the positive effects of impounding the water.

The amount of water loss through evaporation and seepage is a function of storage, impounding surface area, and geological and meteorological factors. The net inflows to a reservoir must be adjusted and used in the mass-curve and the sequent-peak methods. The adjusted reservoir inflow QF_{ta} in period t can be estimated as

$$QF_{ta} = QF_t + PP_t - EV_t - SP_t \tag{11.7.2}$$

in which PP_t is the precipitation amount on the reservoir surface, EV_t is the evaporation, and SP_t is the seepage loss during period t . The elements on the right-hand side of equation (11.7.2) depend on the storage and reservoir surface area during time period t , which are, in turn, a function of those hydrological components.

Mass-curve analysis and the sequent-peak method are used in the planning stages to determine the capacity of a single-surface reservoir for a specified release pattern. It enables engineers to develop storage-yield curves for the reservoirs under consideration. However, the ability of the two methods to analyze a reservoir system involving several reservoirs is severely restricted. Furthermore, active storage capacity of a reservoir depends on various hydrologic elements whose contributions to the mass balance, in turn, are a function of unknown reservoir storage. Such an implicit relationship cannot be accounted for directly by the mass-curve and sequent-peak analysis.

Optimization models, on the other hand, can explicitly consider such implicit relationships and can be solved directly by appropriate methods. In addition, systems consisting of several multiple-purpose reservoirs can be modeled and their interrelationships accounted for in an optimization model. Refer to Mays and Tung (1992) for further details on this topic.

EXAMPLE 11.7.4

Use the following monthly evaporation loss and precipitation data and use the sequent-peak method to determine the required active storage for producing 2000 ac-ft/month firm yield. Seepage losses are negligible.

Month	10	11	12	1	2	3	4	5	6	7	8	9
$EV(AF)$	270	275	280	350	470	450	400	350	370	330	300	290
$PP(AF)$	3	5	5	10	30	50	100	150	70	10	2	3

SOLUTION

Computations by the sequent-peak method considering other hydrologic components are shown in Table 11.7.3. Columns (2)–(5) contain data for monthly required release, surface inflow, precipitation, and evaporation, respectively. Columns (3)–(5) are used to compute the adjusted inflow according to equation

Table 11.7.3 Computations of Sequent-Peak Method Considering Other Hydrologic Components

t (month) (1)	R_t (AF/mon) (2)	QF_t (AF/mon) (3)	PP_t (AF/mon) (4)	EV_t (AF/mon) (5)	K_{t-1} (AF/mon) (6)	K_t (AF/mon) (7)
1	2000	742	3	270	0	1525
2	2000	1060	5	275	1525	2735
3	2000	1000	5	280	2735	4010
4	2000	1500	10	350	4010	4850
5	2000	1080	30	470	4850	6210
6	2000	6460	50	450	6210	2150
7	2000	10,000	100	400	2150	0
8	2000	13,080	150	350	0	0
9	2000	4910	70	370	0	0
10	2000	981	10	330	0	1339
11	2000	283	2	300	1339	3354

(Continued)

Table 11.7.3 (Continued)

t (month) (1)	R_t (AF/mon) (2)	QF_t (AF/mon) (3)	PP_t (AF/mon) (4)	EV_t (AF/mon) (5)	K_{t-1} (AF/mon) (6)	K_t (AF/mon) (7)
12	2000	322	3	290	3354	5319
13	2000	404	3	270	5319	7182
14	2000	787	5	275	7182	8665
15	2000	2100	5	280	8665	8840
16	2000	4410	10	350	8840	6770
17	2000	2750	30	470	6770	6460
18	2000	3370	50	450	6460	5490
19	2000	5170	100	400	5490	2620
20	2000	19,680	150	350	2620	0
21	2000	19,630	70	370	0	0
22	2000	3590	10	330	0	0
23	2000	710	2	300	0	1588
24	2000	518	3	290	1588	3357
25	2000	924	3	270	3357	4700
26	2000	1020	5	275	4700	5950
27	2000	874	5	280	5950	7351
28	2000	1020	10	350	7351	8671
29	2000	8640	30	470	8671	2471
30	2000	6370	50	450	2471	0
31	2000	6720	100	400	0	0
32	2000	13,290	150	350	0	0
33	2000	9290	70	370	0	0
34	2000	1540	10	330	0	780
35	2000	915	2	300	780	2163
36	2000	506	3	290	2163	3944
37	2000	886	3	270	3944	5325
38	2000	3040	5	275	5325	4555
39	2000	2990	5	280	4555	3840
40	2000	8170	10	350	3840	0
41	2000	2800	30	470	0	0
42	2000	4590	50	450	0	0
43	2000	21960	100	400	0	0
44	2000	30,790	150	350	0	0
45	2000	14,320	70	370	0	0
46	2000	2370	10	330	0	0
47	2000	709	2	300	0	1589
48	2000	528	3	290	1589	3348
49	2000	859	3	270	3348	4756
50	2000	779	5	275	4756	6247
51	2000	1250	5	280	6247	7272
52	2000	11,750	10	350	7272	0
53	2000	5410	30	470	0	0
54	2000	5560	50	450	0	0
55	2000	5610	100	400	0	0
56	2000	24,330	150	350	0	0
57	2000	32,870	70	370	0	0
58	2000	7280	10	330	0	0
59	2000	1150	2	300	0	1148
60	2000	916	3	290	1148	2519

Source: Mays and Tung (1992).

(11.7.2). The adjusted inflow for each month is used in equation (11.7.1) to compute K_t . The active storage required is 8840 ac-ft, as indicated in Table 11.7.3. The presence of evaporation loss results in an increase in required active storage. It should be pointed out that, in this example, the monthly precipitation and evaporation amounts are constants and are assumed independent of storage. In actuality, monthly values for PP_t and EV_t are functions of storage, which is an unknown quantity in the exercise. To account accurately for the values of PP_t and EV_t as storage changes, a trial-and-error procedure is needed to determine the required K_a for a given firm yield.

11.7.3 Reservoir Simulation

11.7.3.1 Operation Rules

Operating rules (policies) are used to specify how water is managed in a reservoir and throughout a reservoir system. These rules are specified to achieve system stream-flow requirements and system demands in a manner that maximizes objectives, which may be expressed in the form of benefits. *System demands* may be expressed as minimum desired and minimum required flows to be met at selected locations in the system. Operation rules may be designed to vary seasonally in response to the seasonal demands for water and the stochastic nature of supplies. Operating rules, often established on a monthly basis, prescribe how water is to be regulated during the subsequent month (or months) based on the current state of the system.

In reservoir operation, the *benefit function* used should indicate that shortages cause severe adverse consequences while surpluses may enhance benefits only moderately. It is common practice to define operating rules in terms of a minimum yield or target value. If water supply to all demand points is rigidly constrained when droughts occur, it may be impossible to satisfy all demands.

Reservoir storage is commonly divided into different zones, as shown in Figure 11.7.1. *Rule curves* indicate the boundary of various zones (see Figure 11.7.6) throughout the year. In developing rule curves for a multipurpose reservoir, consideration must be given to whether or not conflicts in serving various purposes occur. When a number of reservoirs serve the same purpose, system rule curves should be developed.

It is essential that operating rules be formulated with information that will be available at the time when operation decisions are made. If forecasts are used in operation, their degree of reliability should be taken into account in deriving operating rules. Likewise, all physical, legal, and other constraints should be considered in formulating and evaluating operation rules. Further, uncertainties associated with the rule curves and changes in physical and legal conditions should be incorporated in developing the rule curves, if possible.

Rule curves are developed to provide guidance on what operational policy is to be employed at a reservoir or dam site. The *operational decision* is based on the current state of the system and the time of year in order to take into account the seasonal variation of reservoir inflows. A simple rule curve may specify the next period's release based solely on the storage level in the current month. A more complicated rule curve might consider storage at other reservoirs, specifically at downstream control points, and perhaps a forecast of future expected inflows to the reservoir.

Three basic methods have been used in planning, design, and operation of reservoir systems: (a) simplified methods such as nonsequential analysis; (b) simulation; and (c) optimization. Simple methods are generally used for analyzing systems involving one reservoir with one purpose, using data for only a critical flow period. Simulation models can handle much more complex system configurations and can preserve much more fully the stochastic, dynamic characteristics of reservoir systems. The search for an optimal alternative is dependent on the engineer's ability to manipulate design variables and operating policies in an efficient manner. There may be no guarantee that a globally optimal alternative is found. Optimization models may have a greater number of assumptions and approximations than the simulation models; these are generally needed to make the model mathematically tractable; the combined use of simulation and optimization models can overcome this difficulty. Refer to Mays and Tung (1992) and Mays (1997) for more detail.

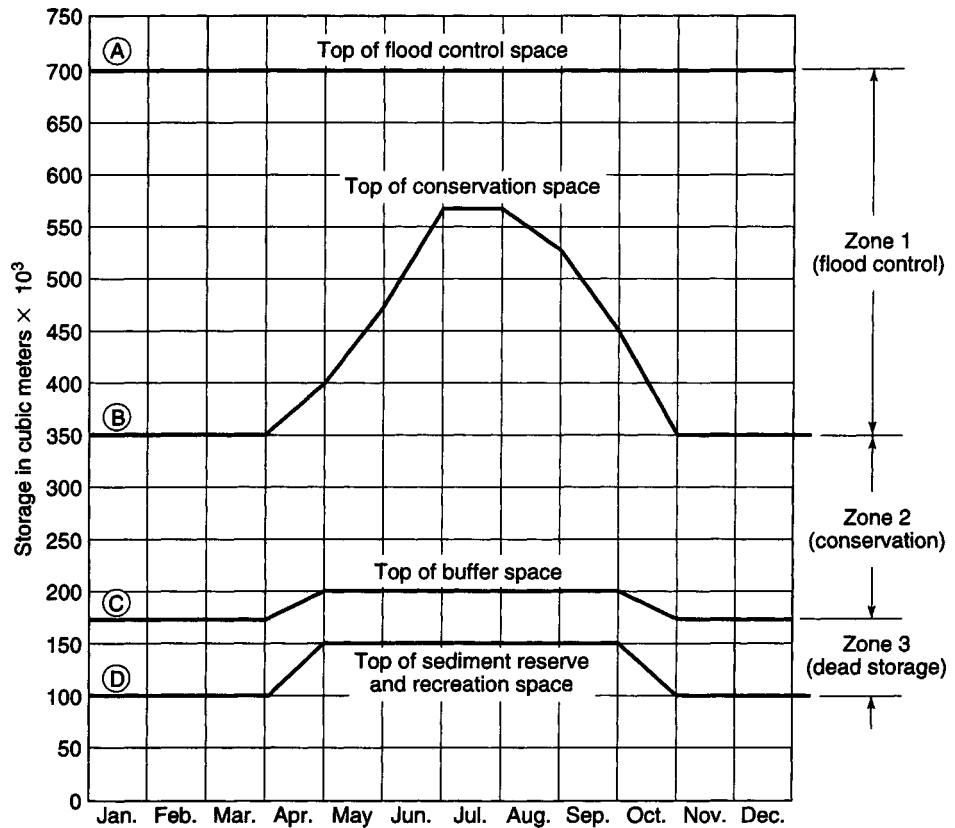


Figure 11.7.6 Example of seasonally varying storage boundaries for multipurpose reservoir (from U.S. Army Corps of Engineers (1977)).

11.7.3.2 Conservation Simulation

Reservoir simulation refers to the mathematical simulation of a river network with reservoir(s). The planning and operation of a reservoir system requires the simulation of these systems to determine whether demands can be met for water supply (municipal, industrial, and/or agricultural users, hydropower, instream flow maintenance for water quality, and flood control). For purposes of discussion here, water uses are considered in two categories: flood control and conservation, where conservation use refers to all nonflood control uses.

The purpose of *reservoir simulation* for a given multiple-purpose, multiple-reservoir system is to determine the reservoir operation (reservoir releases) over a given time period with known streamflows at input points to these reservoirs and other control points throughout the system. The objective is to operate the reservoirs so as best to meet flow demands for water uses. Reservoir simulation can be used to determine whether a reservoir operation policy for a particular system can be used to meet demands. Reservoir simulation can also be used in a trial-and-error fashion to develop reservoir operation strategies (policies), and for determining reservoir storage requirements.

The general procedure for conducting a reservoir system analysis for conservation purposes using simulation involves (U.S. Army Corps of Engineers, 1977):

1. identifying the system;
2. determining the study objectives and specifying the criteria used to measure the objectives;
3. examining the availability of the system data;
4. formulating a model that is mathematically and quantitatively representative of the system's components hydrology, and operating criteria;

5. validating the model;
6. organizing and solving the model; and
7. analyzing and evaluating the results according to how well they achieve the objectives of the study.

PROBLEMS

11.3.1 Rework example 11.3.1 for areas that have T values of 20°C, 25°C, and 30°C and compare the results. Assume that all the other parameters remain the same.

11.3.2 Consider a rice field of 100 hectares located at latitude of 42°N. The growing season for the rice is from January to March. The consumptive use coefficient for the rice is 1.1. The following table contains the climatic data from a nearby weather station.

Month	January	February	March
Mean temp. (°F)	54	60	75
Total rainfall (mm)	90	120	130

- (a) Use the Blaney–Criddle method to estimate the total consumptive use of the rice crop in the field.
- (b) Estimate the volume of irrigated water (in m³) needed for each of the months during the rice-growing season.

11.5.1 Determine the price elasticity of demand for the demand function (equation (11.5.6)) developed by Billings and Agthe (1980).

11.5.2 The linear demand model derived by Hanke and de Maré (1984) for Malmö, Sweden, is

$$Q = 64.7 + 0.00017(\text{Inc}) + 4.76(\text{Ad}) + 3.92(\text{Ch}) - 0.406(R) + 29.03(\text{Age}) - 6.42(P)$$

where

Q = quantity of metered water used per house, per semiannual period (in m³).

Inc = real gross income per house per annum (in Swedish crowns; actual values reported per annum and interpolated values used for mid-year periods).

Ad = number of adults per house, per semiannual period.

Ch = number of children per house, per semiannual period.

R = rainfall per semiannual period (in mm).

Age = age of house, with the exception that it is a dummy variable with a value of 1 for houses built in 1968 and 1969, and a value of 0 for houses built between 1936 and 1946.

P = real price in Swedish crowns per m³ of water, per semiannual period (includes all water and sewer commodity charges that are a function of water use).

Using the average values of $P = 1.7241$ and $Q = 75.2106$ for the Malmö data, determine the elasticity of demand. Explain the meaning of the result.

11.5.3 Determine the elasticities of demand for the water-demand model in problem 11.5.2 using $P = 1.5$ and $Q = 75.2106$; $P = 2.0$ and $Q = 75.2106$; $P = 1.7241$ and $Q = 50$; and $P = 1.7241$ and $Q = 100$.

11.6.1 In example 11.6.1, assume that the capital cost as a function of the return period can be given as

$$\text{Cost} = 10.5 + 0.0166T - 8 * 10^{-6}T^2$$

for $T \leq 1000$. Determine the optimum design return period.

11.7.1 Table 11.7.1 contains monthly runoff volumes for water years 1966 to 1970 for the Little Weiser River near Indian Valley, Idaho. Construct the flow-duration curve using the years 1967 to 1970 and determine the firm-yield for this site.

11.7.2 Using the monthly flow data in Table 11.7.1 for the Little Weiser River, construct the cumulative mass curve over a five-year period and determine the required active storage capacity to produce a firm yield of 2500 ac-ft/month.

11.7.3 Use problem 11.7.2 to determine the active storage capacity required to produce 2,000 ac-ft/month firm yield by computing the cumulative difference between supply and demand.

11.7.4 Consider two reservoirs, A and B, connected in series with reservoir A situated upstream of reservoir B. The surface area of A is half of B. The area of B is 40 km². Both reservoirs A and B are subject to a total rainfall of 50 cm and evaporation of 30 cm on an annual basis. To preserve the ecological environment in the riparian zone along the water course, reservoir A is required to release a constant flow of 0.1 m³/s to reservoir B, whereas reservoir B releases 0.3 m³/s to its downstream channel. At the present time, other than the in-stream flow requirement, there is no man-made structure withdrawing water from reservoir B. A small town of 50,000 is located near reservoir B. The per-capita water consumption is 400 liters per day. The town is contemplating to use reservoir B as a water supply reservoir. (*Note: Clearly state the assumptions you use in the following calculations, 1 liter = 0.001 m³.*)

- (a) Determine the annual water storage change of water (in cm) in each of the two reservoirs if water is to be delivered from reservoir B to satisfy the water consumption stipulated above.
- (b) To maintain the required in-stream flow requirement and per-capita consumption as stipulated above, for how long can this reservoir system supply water to the town?
- (c) If the annual water storage change in reservoir B cannot be negative, how much of the per-capita water consumption has to be adjusted?

11.7.5 From the monthly flow mass curve shown in Figure P11.7.5 for a potential water supply reservoir site, answer the following questions. In the computation, you can assume that each month has 30 days.

- (a) Determine the minimum reservoir storage (in m^3) required for maintaining the demand of $50 m^3/s$.
- (b) Determine the maximum demand (in m^3/s) that can be satisfied without shortage over the 12-month period and identify the corresponding critical period as well as the required storage (in m^3).

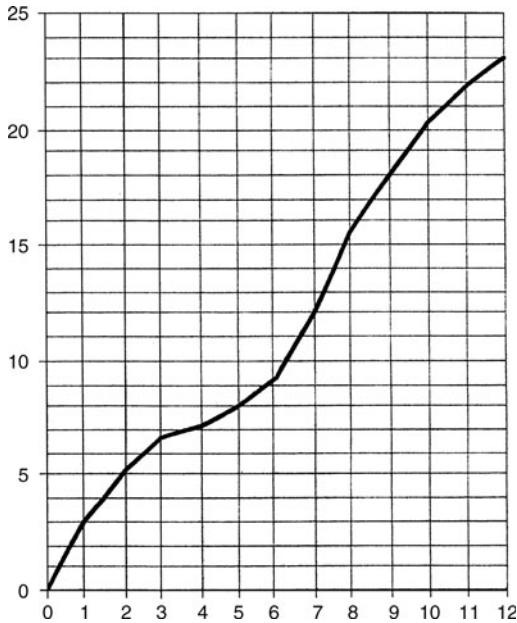


Figure P11.7.5

11.7.6 From the monthly flow mass curve shown in Figure P11.7.5 for a potential water supply reservoir site, answer the

following questions. In the computations you can assume that each month has 30 days.

- (a) What is the average flow rate during the recording period?
- (b) Determine the minimum reservoir storage (in m^3) required for maintaining the demand of average flow rate obtained in part (a).

11.7.7 From the monthly flow mass curve shown in Figure 11.7.7 for a potential water supply reservoir site, answer the following questions. In the computation, you can assume that each month has 30 days.

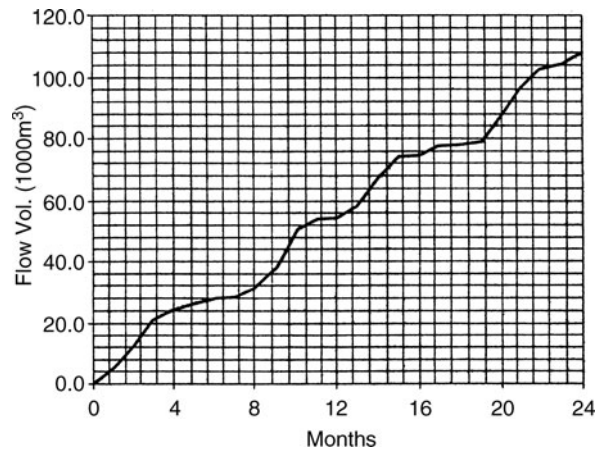


Figure P11.7.7

- (c) What is the average flow rate during the recording period?
- (d) Determine the minimum reservoir storage (in $1000 m^3$) required to ensure the water yield of $4,000 m^3/month$ over the 2-year period.

REFERENCES

Agthe, D. E., and R. B. Billings, "Dynamic Models of Residential Water Demand," *Water Resources Research* vol. 3, pp. 476–480, 1980.

American Society of Agricultural Engineers (ASAE), *Soil and Water Engineering Terminology*, Standard ASAE 5526, St. Joseph, MI, 1993.

American Society of Civil Engineers (ASCE), *Management, Operation, and Maintenance of Irrigation and Drainage Systems*, ASCE Manuals and Reports on Engineering Practice No. 57, ASCE, New York, 1991.

Baumgartner, A., and E. Reichel, *The World Water Balance: Mean Annual Global, Continental and Maritime Precipitation, Evaporation, and Runoff*, Elsevier, Amsterdam, 1975.

Berner, E. K., and R. A. Berner, *The Global Water Cycle: Geochemistry and Environment*, pp. 13–14, reprinted/adapted by permission of Prentice-Hall, Englewood Cliffs, New Jersey, 1987.

Billings, R. B., and D. E. Agthe, "Price Elasticities for Water: A Case of Increasing Block Rates," *Land Economics*, vol. 56, no. 1, pp. 73–84, 1980.

Bruins, H. J., "Drought Management and Water Supply Systems in Israel," *Drought Management Planning in Water Supply Systems* edited by E. Cabrera and J. Garcia-Serra, pp. 299–321, Kluwer Academic Publishers, Dordrecht, 1999.

Chow, V. T., D. R. Maidment, and L. W. Mays, *Applied Hydrology*, McGraw-Hill, New York, 1988.

Dixon, L. S., et al., *Drought Management Policies and Economic Effects in Urban Areas of California, 1987–1992*, RAND, 1996.

Doneen, L. D., and D. W. Westcot, *Irrigation Practice and Water Management*, FAO Irrigation and Drainage Paper No. 1, Rev. 1, Food and Agriculture Organization of the United Nations, Rome, 1984.

Dziegielewski, B., et al., "Drought Management Option," *Drought Management and Its Impact on Public Water Systems*, Report on a Colloquium Sponsored by the Water Science and Technology Board, September 5, 1985, National Academy Press, Washington, DC, 1986.

- Dziegielewski, B., et al., *National Study of Water Management During Drought: A Research Assessment for the U.S. Army Corps of Engineers Water Resources Support Center*, Institute for Water Resources, IWR Report 91-NDS-3, 1991.
- Dziegielewski, B., E. M. Optiz, and D. R. Maidment, "Water Demand Analysis," in *Water Resources Handbook* edited by L. W. Mays, McGraw-Hill, New York, 1996.
- Easterling, W. E., "Assessing the Regional Consequences of Drought: Putting the MINK Methodology to Work on Today's Problems," in *Drought Assessment, Management and Planning: Theory and Case Studies* edited by Donald A. Wilhite, Kluwer Academic Publishers, Boston, MA, 1993.
- Economic and Social Commission for Asia and the Pacific (ESCAP), *Water Resources Development in Asia and the Pacific: Some Issues and Concerns*, United Nations, Water Resources Series No. 62, United Nations Publishers, New York, 1987.
- Ejeta, M. Z., and L. W. Mays, "Urban Water Pricing and Drought Management: A Risk-Based Approach," in *Drought Management Planning in Water Supply Systems* edited by E. Cabrera, Kluwer Academic Publishers, 1998.
- Falkenmark, M., J. Lundquist, and C. Widstrand, "Marco-Scale Water Scarcity Requires Micro-Scale Approaches: Aspects of Vulnerability in Semi-arid Development," *Natural Resources Forum*, vol. 13, no. 4, pp. 258–267, 1989.
- Falkenmark, M., and G. Lindh, "Water and Economic Development," *Water in Crisis* edited by P. H. Gleick, Oxford University Press, Oxford, 1993.
- Food and Agriculture Organization, *Crop Water Requirements*, Irrigation and Drainage Paper No. 24, U.N., Rome, 1977.
- Food and Agriculture Organization, *FAO Production Yearbook 1992*, FAO Statistical Series, vol. 46, no. 112, Rome, 1993.
- Food and Agriculture Organization, *Guidelines for Predicting Crop Water Requirements*, Irrigation and Drainage Paper No. 24 (revised), Food and Agriculture Organization of the United Nations, Rome, 1977.
- Foster, H. S., Jr., and B. R. Beattie, "Price Elasticities for Water: A Case of Increasing Block Rates," *Land Economics*, vol. 56, no. 1, pp. 73–84, 1980.
- Garen, D. C., "Revised Surface-Water Supply Index for Western United States," *Journal of Water Resources Planning and Management*, ASCE, vol. 119, no. 4, 437–454, 1993.
- Gibbs, K., "Price Variables in Residential Water Demand Models," *Water Resources Research*, vol. 14, no. 1, pp. 15–18, 1978.
- Gleick, P. H., "Water and Energy Appendix G," in *Water in Crisis* edited by P. H. Gleick, Oxford University Press, Oxford, 1993a.
- Gleick, P. H., "Water and Human Use Appendix H," in *Water in Crisis* edited by P. H. Gleick, Oxford University Press, Washington, DC, 1993b.
- Gleick, P. H., "Water and Agriculture Appendix E," in *Water in Crisis* edited by P. H. Gleick, Oxford University Press, Washington, DC, 1993c.
- Gleick, P. H., "Global and Regional Fresh Water Resources," in *Water in Crisis* edited by P. H. Gleick, Oxford University Press, Oxford, 1993d.
- Gleick, P. H., *The World Water: The Biennial Report on Freshwater Resources*, Island Press, Washington, DC, 1998.
- Gleick, P. H., P. Loh, S. Gomes, and J. Morrison, *California Water 2020: A Sustainable Vision*, Pacific Institute for Studies in Development, Environment, and Security Oakland, CA, 1995.
- Gouevsky, I. U., and D. R. Maidment, "Agricultural Water Demands," in *Modeling Water Demands* edited by J. Kindler and C. S. Russell, in Academic Press, London, 1984.
- Griffin, R. C., and J. Stoll, "The Enhanced Role of Water Conservation in the Cost-Benefit Analysis of Water Projects," *Water Resources Bulletin*, American Water Resources Association, vol. 19, no. 3, pp. 447–457, 1983.
- Grunewald, O. C., et al. "Rural Residential Water Demand: An Econometric and Simulation Analysis," *Water Resources Bulletin*, American Water Resources Association, vol. 12, no. 5, pp. 951–961, 1976.
- Hanke, S. H., and L. de Maré, "Residential Water Demand: A Pooled Time Series, Cross Section Study of Malmö," *Water Resources Bulletin*, American Water Resources Association, vol. 18, no. 4, pp. 621–625, 1982.
- Hanke, S. H., "Demand for Water Under Dynamic Conditions," *Water Resources Research*, vol. 6, no. 5, pp. 1253–1261, 1970.
- Hillel, D., *The Efficient Use of Water in Irrigation*, World Bank Technical Paper No. 64, The International Bank for Reconstruction and Development (World Bank), Washington, DC, 1987.
- Hobbs, B. F., R. L. Mittelstadt, and J. R. Lund, "Energy and Water," in *Water Resources Handbook* edited by L. W. Mays, McGraw-Hill, New York, 1996.
- Howe, C. W., "The Impact of Price on Residential Water Demand: Some New Insights," *Water Resources Research*, vol. 18, no. 4, pp. 713–716, 1982.
- Howe, C. W., and F. P. Linaweaver, Jr., "The Impact of Price on Residential Water Demand and Its Relation to System Design and Price Structure," *Water Resources Research*, vol. 3, no. 1, pp. 13–32, 1967.
- Hudson, H. E., Jr., and R. Hazen, "Drought and Low Stream Flows," in *Handbook of Applied Hydrology* edited by V. T. Chow, McGraw-Hill, New York, 1964.
- James, L. G., *Principles of Farm Irrigation System Design*, John Wiley & Sons, New York, 1988.
- Jones, C. V., and J. R. Morris, "Instrumental Price Estimates and Residential Water Demand," *Water Resources Research*, vol. 20, no. 2, pp. 197–202, 1984.
- Jordan, J. L., "The Effectiveness of Pricing as a Stand-Alone Water Conservation Program," *Journal of the American Water Resources Association*, vol. 30, no. 5, pp. 871–877, 1994.
- Kammerer, J. C., "Estimated Demand of Water for Different Purposes," in *Water for Human Consumption*, International Water Resources Association, Tycooly International, Dublin, 1982.
- Kawamura, A., et al., "Chaotic Characteristics of the Southern Oscillation Index Time Series," *Journal of Hydrology*, vol. 204, pp. 168–181, 1998.
- Kindler, J., and C. S. Russell, *Modeling Water Demands*, Academic Press, London, 1984.
- L'vovich, M. I., *World Water Resources and Their Future*, Copyright by American Geophysical Union, Washington, DC (English translation of a 1974 USSR publication edited by R. Nace), 1979.
- Maddock, T. S., and W. G. Hines, "Meeting Future Public Water Supply Needs a Southwest Perspective," *Journal of the American Water Resources Association*, vol. 31, no. 2, pp. 317–329, 1995.
- Mays, L. W., *Optimal Control of Hydrosystems*, Marcel Dekker, New York, 1997.
- Mays, L. W., and Y. K. Tung, *Hydrosystems Engineering and Management*, McGraw-Hill, New York, 1992.
- Metcalf and Eddy, Inc., *Wastewater Engineering Treatment, Disposal, and Reuse*, 3rd edition, McGraw-Hill, New York, 1991.
- Mitchell, R. D., *Survey of Water-Conserving Heat Rejection Systems*, Report EPRI GS-6252, Electric Power Research Institute, Palo Alto, CA, 1989.
- Moncur, J. E. T., "Drought Episodes Management: The Role of Price," *Water Resources Bulletin*, American Water Resources Association, vol. 25, no. 3, pp. 499–505, 1989.
- Moncur, J. E. T., "Urban Water Pricing and Drought Management," *Water Resources Research*, vol. 23, no. 3, pp. 393–398, 1987.
- Nace, R. Are We Running Out of Water? U.S. Geological Survey Circular no. 536, Washington, DC, 1967.

- National Research Council, *Drought Management and Its Impact on Public Water Systems*, Colloquium 1, National Academy Press, Washington, DC, 1986.
- Palmer, W. C., *Meteorological Drought*, U.S. Weather Bureau Research Paper No. 45, 1965.
- Postel, S., *Last Oasis: Facing Water Scarcity*, W. W. Norton, New York, 1992.
- Postel, S., "Water and Agriculture," in *Water in Crisis* edited by P. H. Gleick, Oxford University Press, Oxford 1993.
- Puckett, L. J., *Dendroclimatic Estimates of a Drought Index for Northern Virginia*, Geological Survey Water Supply Paper No. 2080, United States Government Printing Office, Washington, DC, 1981.
- Rasmusson, E. M., R. E. Dickinson, J. E. Kutzbach, and M. K. Cleveland, "Climatology," in *Handbook of Hydrology* edited by D. R. Maidment, McGraw-Hill, New York, 1993.
- Replogle, J. A., A. J. Clemmens, and M. E. Jensen, "Irrigation Systems," in *Water Resources Handbook* edited by L. W. Mays, McGraw-Hill, New York, 1996.
- Roberson, J. A., J. J. Cassidy, and M. H. Chaudhry, *Hydraulic Engineering*, 2nd edition, John Wiley & Sons, New York, 1998.
- Rogers, P., *America's Water: Federal Roles and Responsibilities*, MIT Press, Cambridge, MA, 1993.
- Schneider, M. L., and E. E. Whitlatch, "User-Specific Water Demand Elasticities," *Journal of Water Resources Planning and Management*, vol. 117, no. 1, pp. 52–73, 1991.
- Shiklomanov, I. A., "World Fresh Water Resources," in *Water in Crisis* edited by P. H. Gleick, Oxford University Press, Oxford, 1993.
- Solley, W., R. R. Pierce, and H. A. Perlman, *Estimated Use of Water in the United States 1990*, U. S. Geological Survey Circular 1081, U.S. Geological Survey, Washington, DC, 1993.
- Steila, D., *Drought in Arizona: A Drought Identification Methodology and Analysis*, University of Arizona, Tucson, AZ, 1972.
- United Nations, *Use of Nonconventional Water Resources in Developing Countries*, National Resource/Water Series No. 14, New York, 1985.
- United Nations Environment Programme, *Draft Guidelines on the Environment Impacts of Irrigation in Arid and Semi-arid Regions*, Nairobi, Kenya, 1979.
- U.S. Army Corps of Engineers, *Hydrologic Engineering Methods for Water Resources Development: Reservoir System Analysis for Conservation*, vol. 9, Davis, CA, 1977.
- U.S. Department of Agriculture, *Agricultural Statistics—1992*, U.S. Government Printing Office, Washington, DC, 1992.
- U.S. Soil Conservation Service, *Colorado Water Supply Outlook*, United States Department of Agriculture, U.S. Government Documents, 1988.
- U.S. Water Resources Council, "Procedures for Evaluation of National Economic Development (NED) Benefits and Costs in Water Resources Planning (Level C): Final Rule," *Federal Register*, vol. 44, no. 242, pp. 72891–72976, 1979.
- Van der Leeden, F. F. L. Troise, and D. K. Todd, *The Water Encyclopedia*, Lewis Publishers, Chelsea, Michigan, 1990.
- Wade, J. C., "Efficiency and Optimization in Irrigation Analysis," *Energy and Water Management in Western Irrigation Agriculture*, in edited by N. K. Whitlesey, Studies in Water Policy and Management No. 7, West View Press, Boulder, CO, pp. 73–100, 1986.
- Walter, B. H., "Construction and Operation of Pump Irrigation Facilities Along the Columbia and Okanogan Rivers," in *Optimization of Irrigation and Drainage Systems*, Proceedings, ASCE Irrigation and Drainage Specialty Conference, Lincoln, Nebraska, ASCE, New York, 1971.
- Wilhite, D. A., "Planning for Drought: A Methodology," in *Drought Assessment, Management and Planning: Theory and Case Studies* edited by D. A. Wilhite, Kluwer Academic Publishers, Norwell, MA, pp. 87–108, 1993.
- Wong, S. T., "A Model on Municipal Water Demand: A Case Study of Northern Illinois," *Land Economics*, pp. 34–44, 1972.
- World Resources Institutes (WRI), *World Resources 1988–89*, World Resources Institute and the International Institute for Environment and Development in collaboration with the United Nations Environment Programme, Basic Books, New York, 1988.
- Young, R. A., "Price Elasticity of Demand for Municipal Water: A Case Study of Tucson, Arizona," *Water Resources Research*, vol. 9, no. 4, pp. 1068–1072, 1973.
- Young, R. A., "Water Economics," in *Water Resources Handbook* edited by L. W. Mays, McGraw-Hill, New York, 1996.

Chapter 12

Water Distribution

The purpose of this chapter is to provide a detailed introduction to water distribution systems (networks). The distribution systems (networks) considered in this chapter are pressurized conduit systems; we do not consider water distribution systems consisting of canals with open-channel flow. A much more extensive treatment of water distribution systems is provided in Mays (2000) and Jones et. al. (2008).

12.1 INTRODUCTION

12.1.1 Description, Purpose, and Components of Water Distribution Systems

The purpose of a water distribution network is to supply the system's users with the amount of water demanded and to supply this water with adequate pressure under various loading conditions. A *loading condition* is defined as a time pattern of demands. A municipal water supply system may be subject to a number of different loading conditions: fire demands at different nodes; peak daily demands; a series of patterns varying throughout a day; or a critical load when one or more pipes are broken. In order to insure that a design is adequate, a number of loading conditions, including critical conditions, must be considered. The ability to operate under a variety of load patterns is required of a reliable network.

Water distribution systems have three major components: *pumping stations*, *distribution storage*, and *distribution piping*. These components may be farther divided into subcomponents, which in turn can be divided into sub-subcomponents. For example, the pumping station component consists of structural, electrical, piping, and pumping unit subcomponents. The pumping unit can be divided farther into sub-subcomponents: pump, driver, controls, power transmission. The exact definition of components, subcomponents, and sub-subcomponents depends on the level of detail of the required analysis and to a somewhat greater extent on the level of detail of available data. In fact, the concept of component–subcomponent–sub-subcomponent merely defines a hierarchy of building blocks used to construct the water distribution system. Figure 12.1.1 shows the hierarchical relationship of system, components, subcomponents, and sub-subcomponents for a water distribution system.

A water distribution system operates as a system of independent components. The hydraulics of each component is relatively straightforward; however, these components depend directly upon each other and as a result affect one another's performance. The purpose of design and analysis is to determine how the systems perform hydraulically under various demands and operation conditions. Such analyses are used for the following situations:

- Design of a new distribution system
- Modification and expansion of an existing system
- Analysis of system malfunction such as pipe breaks, leakage, valve failure, pump failure

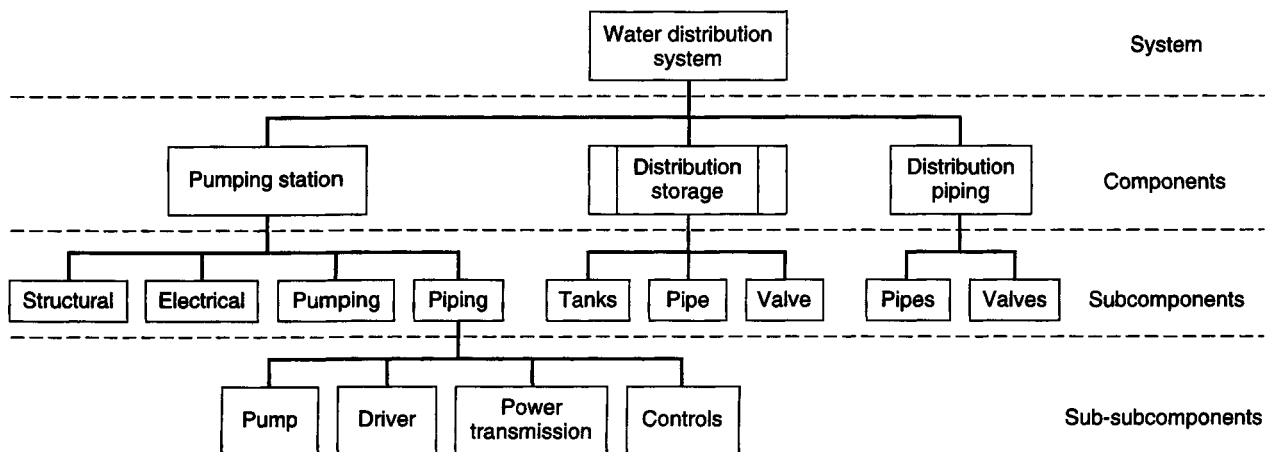


Figure 12.1.1 Hierarchical relationship of system, components, subcomponents, and sub-subcomponents for a water distribution system (from Cullinane (1989)).

- Evaluation of system reliability
- Preparation for maintenance
- System performance and operation optimization

Figure 12.1.2 illustrates a typical municipal water utility showing the water distribution system as a part of this overall water utility. In some locations where excellent quality groundwater is available, water treatment may involve only chlorination.

Pipe sections or links are the most abundant elements in the network. These sections are constant in diameter and may contain fittings and other appurtenances, such as valves, storage facilities, and pumps. Pipes are manufactured in different sizes and are composed of different materials, such as

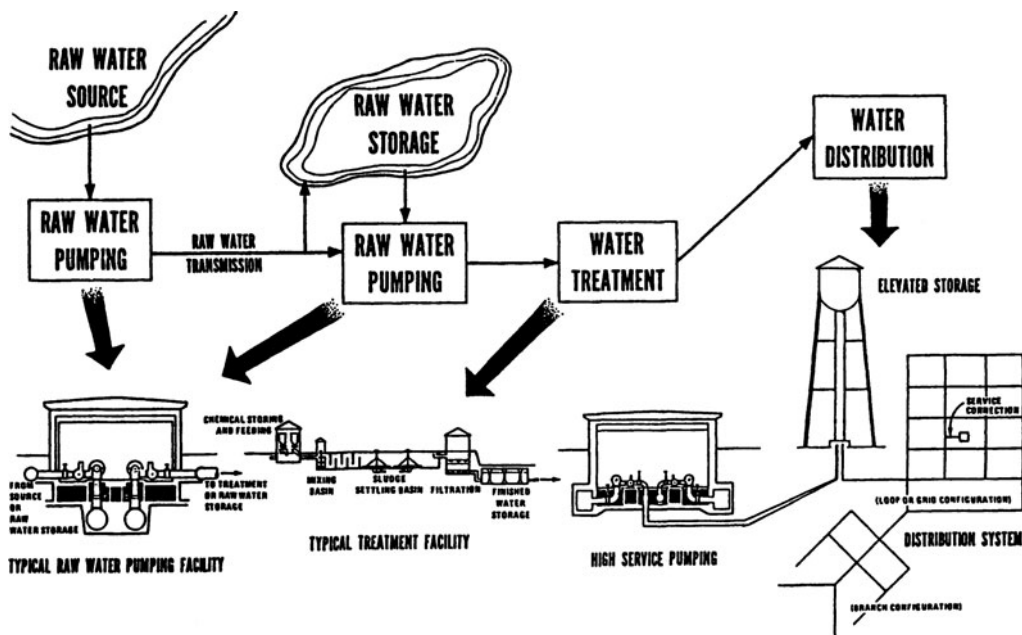


Figure 12.1.2 Functional components of a water utility (from Cullinane (1989)).



Figure 12.1.3 Cement-lined and coated steel pipe (42-in diameter) being transported to trench. (Courtesy of Northwest Pipe Company.)

steel, cast or ductile iron, reinforced or prestressed concrete, asbestos cement, polyvinyl chloride, polyethylene, and fiberglass. The American Water Works Association publishes standards for pipe construction, installation, and performance in the C-series standards (continually updated). Pipes are the largest capital investment in a distribution system. Figure 12.1.3 shows a steel pipeline that is cement coated and lined. Figure 12.1.4 shows steel pipelines being installed that are polyethylene-coated. Various types of joints and couplings to connect pipes are shown in Figure 12.1.5.



Figure 12.1.4 Parallel 60-in and 42-in diameter steel water transmission lines being installed in Aurora, Colorado. Lightweight polyethylene tape coating and O-ring bell and spigot joints helped speed installation. (Courtesy of Northwest Pipe Company.)

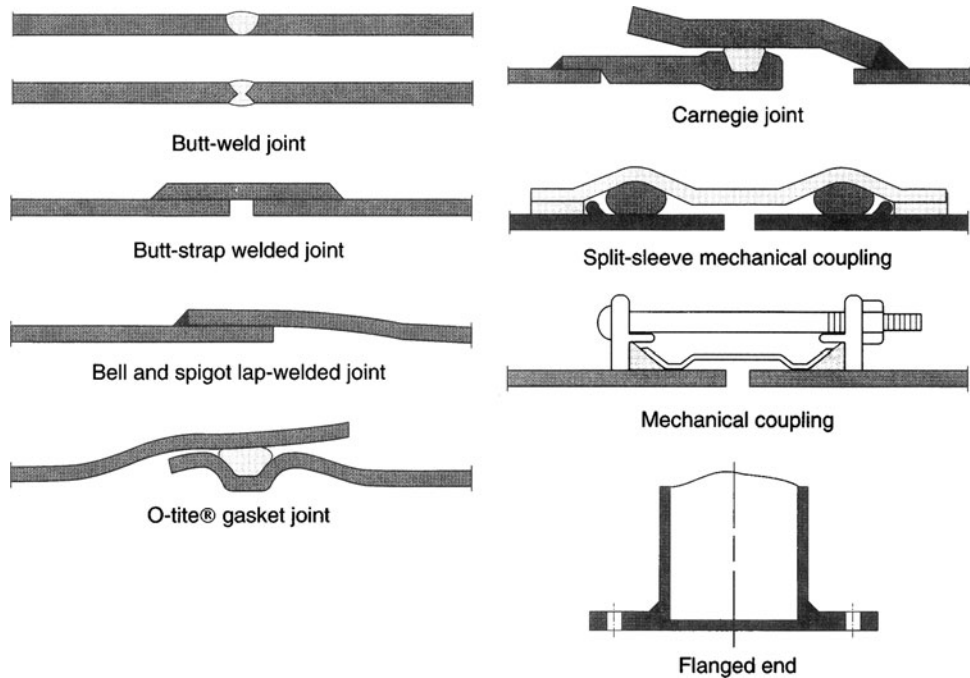


Figure 12.1.5 Variety of joints and couplings used for water pipe systems. Gasketed joints can be used for pressures up to 400 psi, and welded joints are recommended for higher pressure applications. Couplings and flanges are used for valve connections or where the diameter changes. (Courtesy of Northwest Pipe Company.)

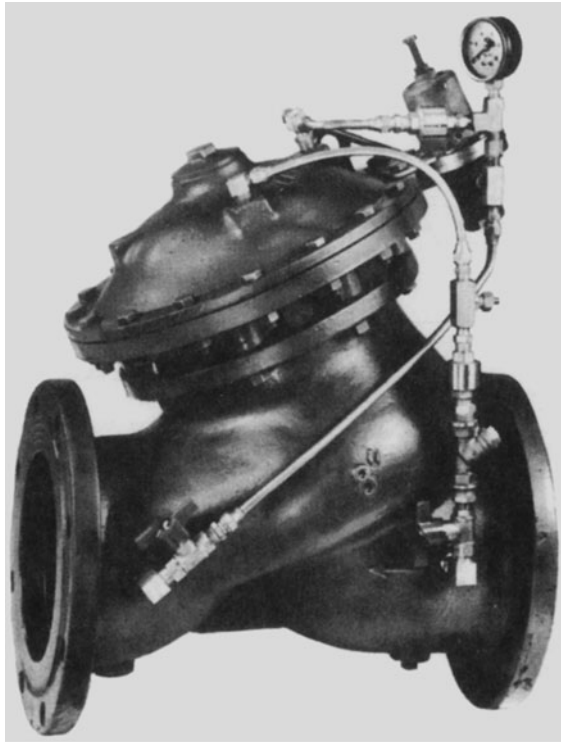
A *node* refers to either end of a pipe. Two categories of nodes are junction nodes and fixed-grade nodes. Nodes where the inflow or the outflow is known are referred to as junction nodes. These nodes have lumped demand, which may vary with time. Nodes to which a reservoir is attached are referred to as fixed-grade nodes. These nodes can take the form of tanks or large constant-pressure mains.

Control valves regulate the flow or pressure in water distribution systems. If conditions exist for flow reversal, the valve will close and no flow will pass. The most common type of control valve is the *pressure-reducing (pressure-regulating) valve (PRV)*, which is placed at pressure zone boundaries to reduce pressure. The PRV maintains a constant pressure at the downstream side of the valve for all flows with a pressure lower than the upstream head. When connecting high-pressure and low-pressure water distribution systems, the PRV permits flow from the high-pressure system if the pressure on the low side is not excessive.

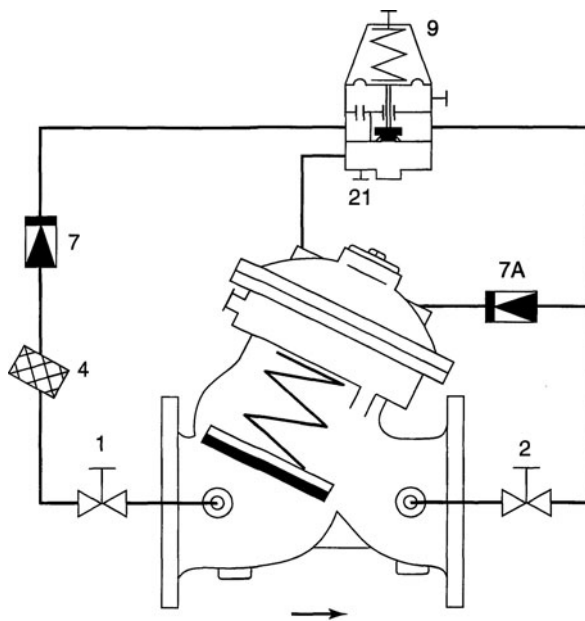
The headloss through the valve varies, depending upon the downstream pressure and not on the flow in the pipe. If the downstream pressure is greater than the PRV setting, then the pressure in chamber A will close the valve. Another type of check valve, a *horizontal swing valve*, operates under similar principle. *Pressure-sustaining valves* operated similarly to PRVs monitoring pressure at the upstream side of the valve. Figure 12.1.6 illustrates a pressure-reducing and check valve. Figure 12.1.6c illustrates the typical application of these valves.

There are many other types of valves, including isolation valves to shut down a segment of a distribution system; direction-control (check) valves to allow the flow of water in only one direction, such as swing check valves, rubber-flapper check valves, slanting check disk check valves, and double-door check valves; and air-release/vacuum-breaker valves to control flow in the main. Figure 12.1.7 show the typical application of a two-way altitude valve.

Distribution-system storage is needed to equalize pump discharge near an efficient operation point in spite of varying demands, to provide supply during outages of individual components, to



(a)



(b)

CONTROLS LIST

- 1. Cock valve
- 2. Cock valve
- 3. Cover plug
- 4. Filter
- 7. Check valve
- 7A. Check valve
- 9. Pressure relief pilot valve
- 21. Needle valve

Figure 12.1.6 Pressure-reducing valve and check valve. (a) Pressure-reducing valve; (b) Control diagram of pressure-reducing valve; (c) Typical application of pressure-reducing and check valve. (Courtesy of Bermad.)

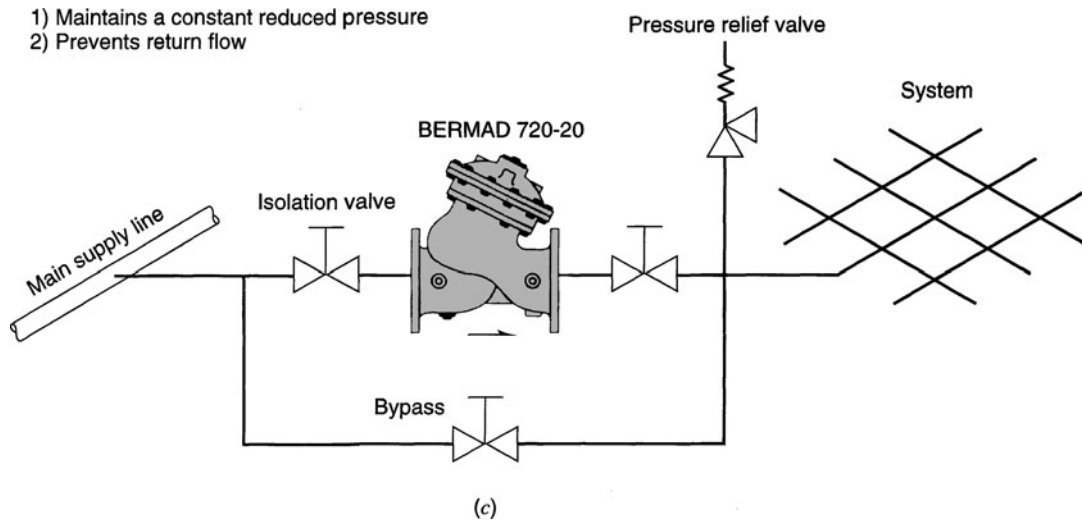


Figure 12.1.6 (Continued)

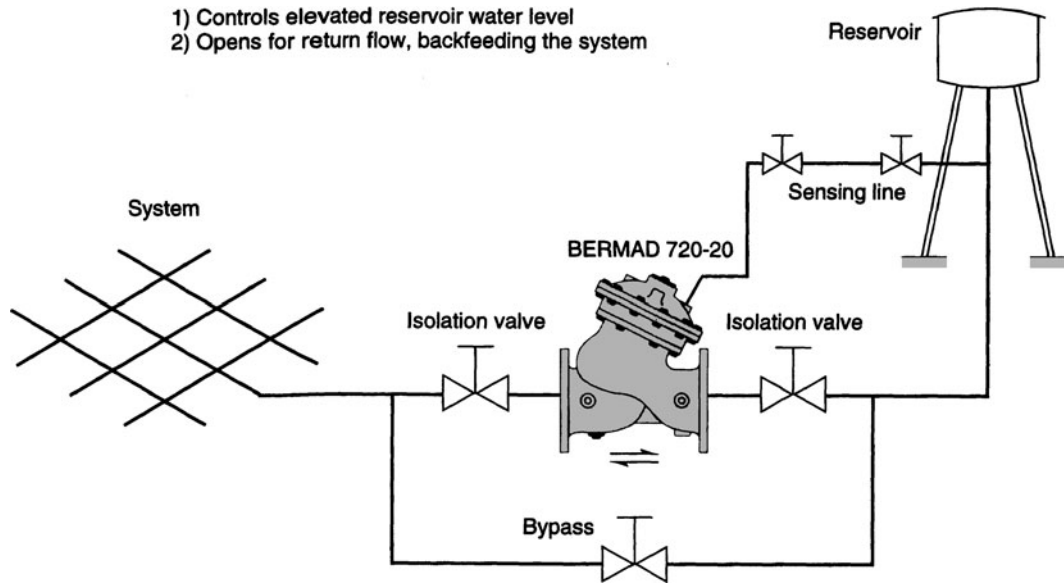


Figure 12.1.7 Two-way altitude valve. Controls water level in reservoirs by sensing built-up reservoir head without using external devices such as floats. Valve opens to fill reservoir and closes at a predetermined reservoir level. Valve reopens to discharge reservoir water back into system when system pressure drops below reservoir static head. (Courtesy of Bermad.)

provide water for fire fighting, and to dampen out hydraulic transients (Walski, 1996). Distribution storage in a water distribution network is closely associated with the water tank. An elevated storage tank installation is illustrated in Figure 12.1.8. Tanks are usually made of steel and can be built at ground level or be elevated at a certain height above the ground. The water tank is used to supply water to meet the requirements during high system demands or during emergency conditions when pumps cannot adequately satisfy the pressure requirements at the demand nodes. If a minimum volume of water is kept in the tank at all times, then unexpected high demands cannot be met during critical conditions. The higher the pump discharge, the lower the pump head becomes. Thus, during a period of peak demands, the amount of available pump head is low.

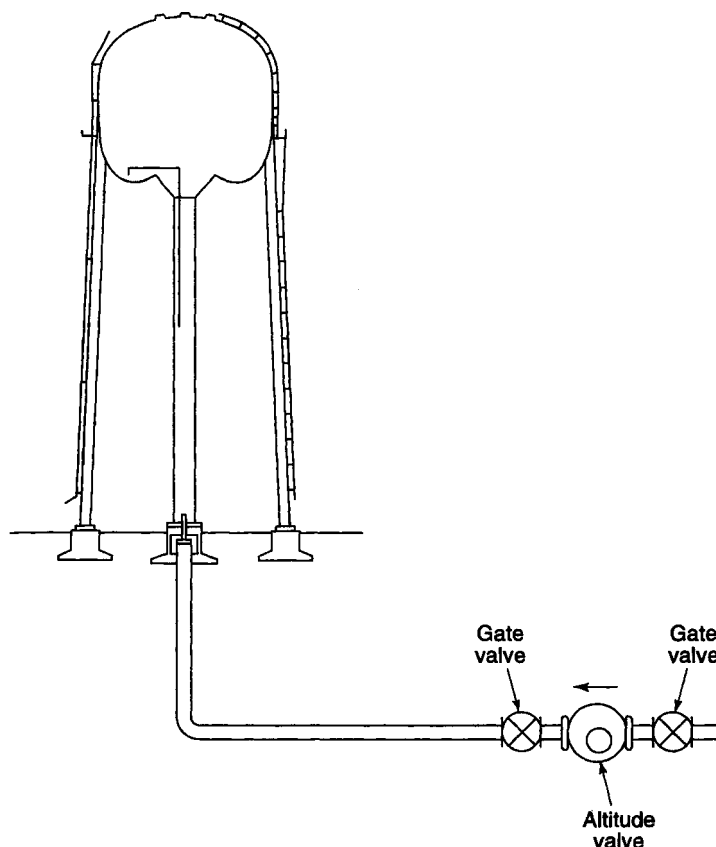


Figure 12.1.8 Typical elevated storage tank installations.

Pumps are used to increase the energy in a water distribution system. A pumping station in Mesa, Arizona, is shown in Figure 12.1.9. There are many different types of pumps (positive-displacement pumps, kinetic pumps, turbine pumps, horizontal centrifugal pumps, vertical pumps, and horizontal pumps). The most commonly used type of pump used in water distribution systems is the *centrifugal pump*. Figure 12.1.10 illustrates a pumping station with centrifugal pumps. *Pumping stations* house the pump, motors, and the auxiliary equipment. Figure 12.1.11 shows a pump at a well site in Mesa, Arizona. Figure 12.1.12 shows the Elmwood pumping station and storage reservoir in Mesa, Arizona.

The *metering* (flow measurement) of water mains involves a wide array of metering devices. These include electromagnetic meters, ultrasonic meters, propeller or turbine meters, displacement meters, multijet meters, proportional meters, and compound meters. *Electromagnetic meters* measure flow by means of a magnetic field generated around an insulated section of pipe. *Ultrasonic meters* utilize sound-generating and sound-receiving sensors (transducers) attached to the sides of the pipe. *Turbine meters* (Figure 12.1.13) have a measuring chamber that is turned by the flow of water. *Multijet meters* have a multiblade rotor mounted on a vertical spindle within a cylindrical measuring chamber. *Proportional meters* utilize restriction in the water line to divert a portion of water into a loop that holds a turbine or displacement meter, with the diverted flow being proportional to the flow in the main line. *Compound meters* connect different sized meters in parallel.

Refer to Mays (1999, 2000), Ysusi (1999, 2000), and Walski (1996) for further descriptions of water distribution system components.

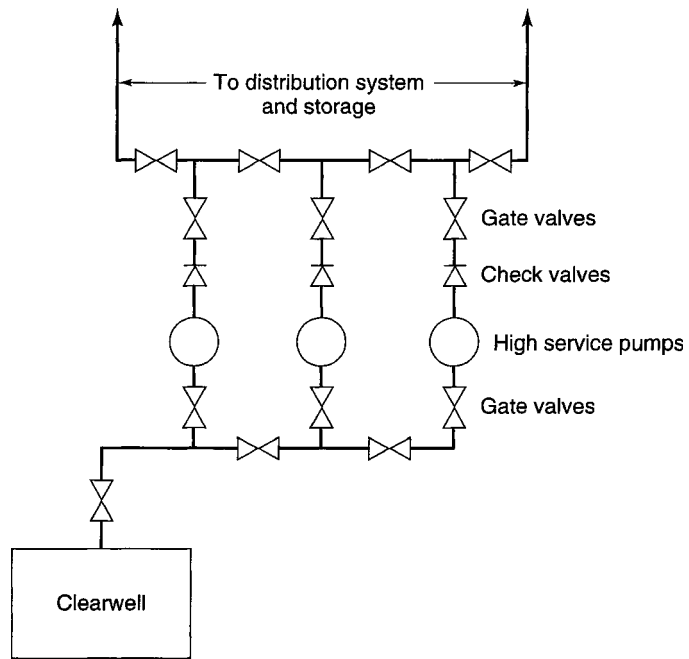


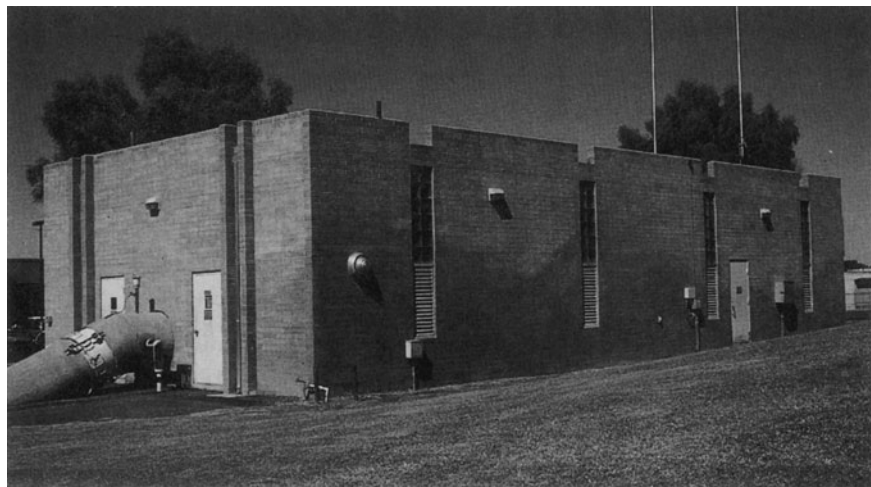
Figure 12.1.9 Schematic of a typical water distribution system pumping station.

12.1.2 Pipe Flow Equations

Typically for water distribution systems, the relationship used to describe flow or velocity in pipes is the *Hazen–Williams equation*:

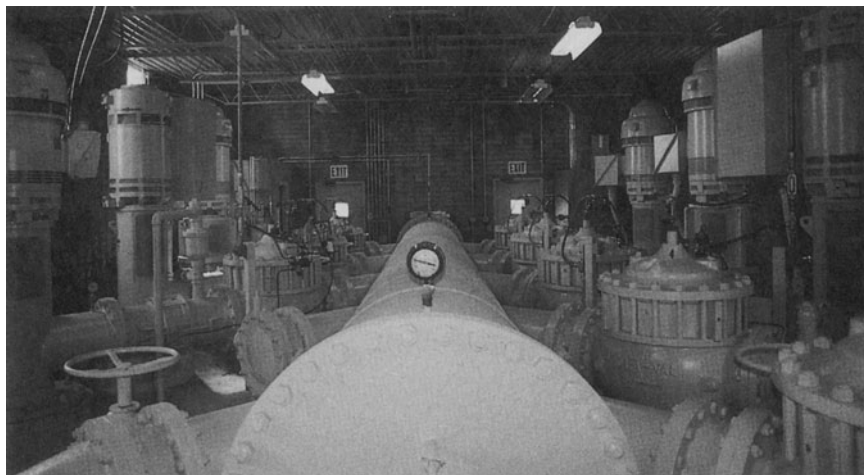
$$V = K_H CR^{0.63} S_f^{0.54} \tag{12.1.1}$$

where $K_H = 1.318$ for U.S. customary units and $K_H = 0.849$ for SI units, V is the average flow velocity in ft/s (m/s), C is the *Hazen–Williams roughness coefficient* as listed in Table 12.1.1 for

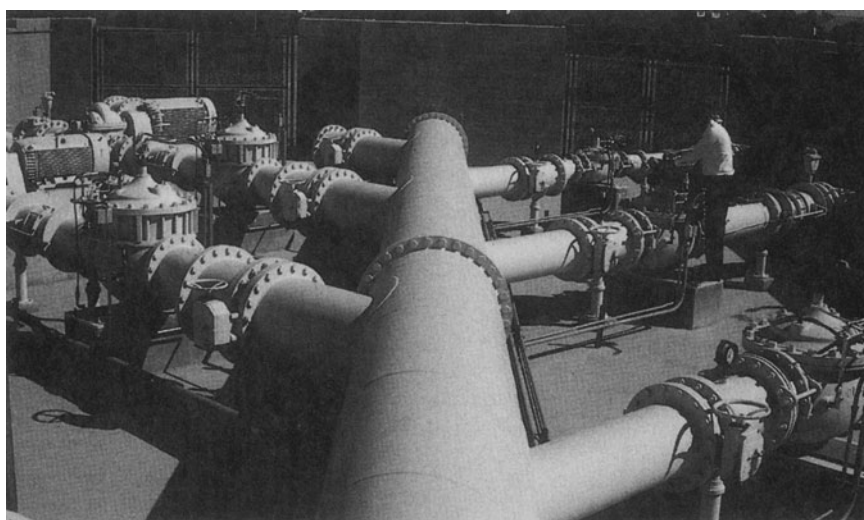


(a)

Figure 12.1.10 Pumping station in Mesa, Arizona. (a) Pump house; (b) Centrifugal pumps; (c) Manifold at pump station. (Courtesy of City of Mesa, Arizona.)



(b)



(c)

Figure 12.1.10 (Continued)

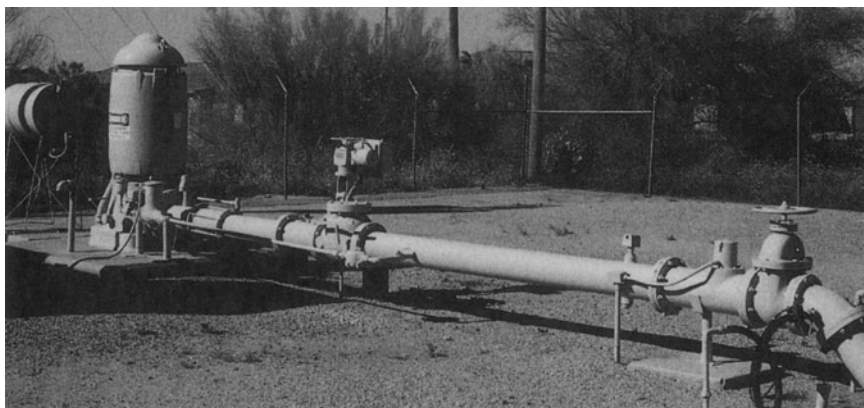


Figure 12.1.11 Pump at a well site in Mesa, Arizona. (Courtesy of City of Mesa, Arizona.)

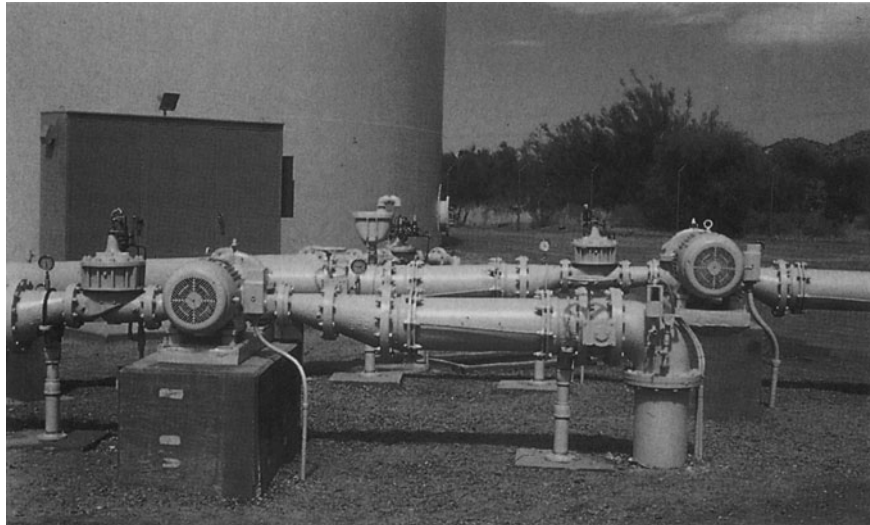


Figure 12.1.12 Elmwood pumping station and reservoir in Mesa, Arizona. (Courtesy of City of Mesa, Arizona.)

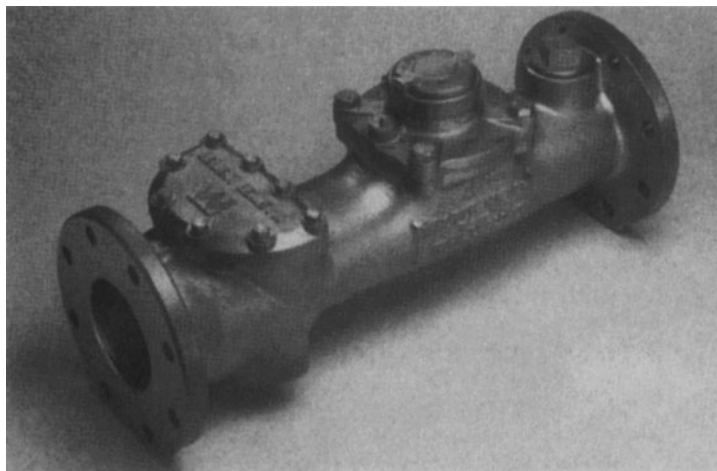


Figure 12.1.13 Turbine meter. (Courtesy of Master Meter.)

pipes of different materials and ages, R is the hydraulic radius in ft (m), and S_f is the friction slope in ft/ft (m/m). The friction headloss as a gradient in terms of feet per 1000 ft (or meters per 1000 m) can be expressed as

$$h_L = A \left(\frac{Q}{C} \right)^{1.85} D^{-4.87} = \left(\frac{BQ}{CD^{2.63}} \right)^{1.85} \quad (12.1.2)$$

where Q is the discharge in gpm for U.S. customary units and m^3/s for SI units, where $A = 10,500$ for U.S. customary units and $A = 10,700$ for SI units, $B = 149$ for U.S. customary units and $B = 151$ for SI units, h_L is ft/1000 ft (m/1000 m), and D is the pipe diameter in in. (m). Later in this chapter the headloss is expressed as a function of discharge:

$$h_L = KQ^n \quad (12.1.3)$$

Table 12.1.1 Typical Coefficients of Pipe Friction for Design^a

Material	Hazen–Williams C	Manning n^b	Moody Diagram ϵ^b	
			mm	in
New pipe or lining				
Smooth glass or plastic ^c	150	0.009	0.919	0.00075
Centrifugally spun cement-mortar lining ^d	145	0.009	0.028	0.0015
Cement-mortar lining troweled in place	140	0.009	0.076	0.003
Commercial steel or wrought iron	140	0.009	0.076	0.003
Galvanized iron	135	0.010	0.13	0.005
Ductile or cast iron, uncoated	130	0.010	0.19	0.0075
Asbestos cement, coated	145	0.009	0.038	0.0015
Asbestos cement, uncoated	140	0.009	0.076	0.003
Centrifugally cast concrete pressure pipe	135	0.010	0.13	0.005
Ten-State Standards (1978)				
Cement mortar or plastic lining	120	0.011	0.41	0.016
Unlined steel or ductile iron	100	0.011	1.5	0.060
Old pipe or lining [in moderate service (20 years or more), nonaggressive water] ^e				
Smooth glass or plastic	135	0.010	0.13	0.005
Centrifugally spun cement-mortar lining ^f	130	0.010	0.19	0.0075
Cement mortar troweled in place	125	0.010	0.28	0.011
Asbestos cement, coated	130	0.010	0.19	0.0075
Asbestos cement, uncoated	125	0.010	0.28	0.011
Ductile iron or carbon steel, uncoated	100	0.013	1.5	0.060
Centrifugally cast concrete pressure pipe	130	0.010	0.19	0.0075
Wood stave	110	0.012	0.89	0.035
Riveted steel	80	0.016	5.6	0.22
Concrete, formed	80	0.016	5.6	0.22
Clay (not pressurized)	100	0.013	1.5	0.060
Wrought iron	100	0.013	1.5	0.060
Galvanized iron	90	0.014	0.30	0.012

^aFor critical problems, consult the other sources.

^bValues are calculated from C coefficients for 300-mm (12-in) pipe, a velocity of 1.1–2.1 m/s (3.7–6.9 ft/s), and a temperature of 20°C (68°F).

^cPVC, polyethylene, polypropylene, polybutylene, reinforced thermosetting resin pipe, and polyvinyl chloride.

^dAverage value for pipes 150 to 900 mm (6 to 36 in) diameter.

^eFor conservative design, reduce old pipe C values (and increase n values) by 0.02%/mm (0.5%/in) for pipe less than 450 mm (18 in).

Note that the Hazen–Williams and Manning equations predict headloss on the unsafe side for small pipes and/or low velocities.

^fConservative values for water pipe 150–500 mm (6–20 in).

Source: Sanks (1998).

where K is referred to as a pipe coefficient and n is an exponential flow coefficient. For the Hazen–Williams equation

$$h_L = KQ^{1.85} \quad (12.1.4)$$

where

$$K = \left[\frac{\phi L}{C^{1.85} D^{4.87}} \right] \quad (12.1.5)$$

where $\phi = 4.73$ for U.S. customary units and $\phi = 10.66$ for SI units. The headloss h_L is in ft (m); L is the pipe length in ft (m), Q is the flow rate in cfs (m³/s), and D is the pipe diameter in ft (m).

Another pipe flow equation for headloss is the *Darcy–Weisbach equation* (4.3.13):

$$h_L = f \frac{L V^2}{D 2g} \quad (12.1.6)$$

where f is the Darcy–Weisbach friction factor. The friction factor is a function of the Reynold's number and the *relative roughness*, which is the absolute roughness of the interior pipe surface divided by the pipe diameter. The friction factor can be determined from a Moody diagram (Figure 4.3.5), or other friction formulas presented in Chapter 4. Equation (12.1.6) can be expressed in terms of the discharge as

$$h_L = KQ^2 \quad (12.1.7)$$

where

$$K = \left[\frac{8fL}{\pi^2 g D^5} \right] \quad (12.1.8)$$

and h_L is the headloss in ft (m), L is the pipe length in ft (m), Q is the flow rate in cfs (m^3/s), D is the pipe diameter in ft (m), and g is the acceleration due to gravity, 32.2 ft/s^2 (9.81 m/s^2).

Another equation that can be used for headloss, which is valid for fully turbulent flow, is Manning's equation (5.1.23 and 5.1.25):

$$h_L = \frac{n^2 V^2 L}{\beta R^{4/3}} = \left[\frac{n^2 L}{\beta R^{4/3} A^2} \right] Q^2 = KQ^2 \quad (12.1.9)$$

where ($\beta = 2.21$ for U.S. customary units and $\beta = 1$ for SI units, h_L is the headloss in ft (m), n is Manning's roughness factor, R is the hydraulic radius in ft (m), L is the pipe length in ft (m), and A is the cross-sectional area of the pipe in ft^2 (m^2). Also,

$$K = \left[\frac{n^2 L}{\phi D^{5.33}} \right] \quad (12.1.10)$$

where $\phi = 0.216$ in U.S. customary units and $\phi = 0.0972$ in SI units.

EXAMPLE 12.1.1

Determine the headloss due to friction in a 1-m diameter, 300-m long pipe using Manning's equation with $n = 0.013$ and the Hazen–Williams equation with $C = 100$. Solve for $Q = 1 \text{ m}^3/\text{s}$ and $Q = 2 \text{ m}^3/\text{s}$.

SOLUTION

Using Manning's equation, we find

$$\begin{aligned} h_L &= \left[\frac{n^2 L}{[AR^{2/3}]^2} \right] Q^2 = \left[\frac{n^2 L}{[(\pi(D^2/4))(D/4)^{2/3}]^2} \right] Q^2 = \left[\frac{n^2 L}{0.0972 D^{16/3}} \right] Q^2 \\ &= \left[\frac{(0.013)^2 (300)}{0.0972 (1)^{16/3}} \right] Q^2 = 0.522 Q^2 \end{aligned}$$

For $Q = 1 \text{ m}^3/\text{s}$, $h_L = 0.522 \text{ m}$. For $Q = 2 \text{ m}^3/\text{s}$, $h_L = 2.09 \text{ m}$.

Using the Hazen–Williams equation yields

$$\begin{aligned} \frac{Q}{A} &= 0.849CR^{0.63} \left(\frac{h_L}{L} \right)^{0.54} \\ h_L &= L \left[\frac{1}{0.849CAR^{0.63}} \right]^{1.85} Q^{1.85} = L \left[\frac{1}{0.849C \left(\frac{\pi D^2}{4} \right) \left(\frac{D}{4} \right)^{0.63}} \right]^{1.85} Q^{1.85} \\ &= \left[\frac{10.66L}{C^{1.85} D^{4.87}} \right] Q^{1.85} = \left[\frac{10.66(300)}{(100)^{1.85} (1)^{4.87}} \right] Q^{1.85} = 0.638 Q^{1.85} \end{aligned}$$

For $Q = 1 \text{ m}^3/\text{s}$, $h_L = 0.638 \text{ m}$. For $Q = 2 \text{ m}^3/\text{s}$, $h_L = 2.3 \text{ m}$.

12.2 SYSTEM COMPONENTS

12.2.1 Pumps

12.2.1.1 Classification

Centrifugal pumps are most commonly used in water distribution applications because of their low cost, simplicity, and reliability in the range of flows and heads encountered (see Walski, 1996, for more details). As a result, the discussion on pumps in this chapter is restricted to centrifugal pumps. A *centrifugal pump* is any pump in which fluid is energized by a rotating impeller, whether the flow is radial, axial, or a combination of both (mixed), using colloquial usage in the United States (Tchobanoglous, 1998). In Europe, centrifugal pumps are strictly defined as radial flow pumps only. Here we use the U.S. usage. Centrifugal pumps are classified into three groups according to the manner in which the fluid moves through the pump (refer to Figure 12.2.1):

- *Radial flow pumps* displace the fluid radially in the pump.
- *Axial flow pumps or propeller pumps* displace the fluid axially in the pump.
- *Mixed-flow pumps* displace the flow both radially and axially in the pump.

The *pump capacity* (Q) is the flow rate or discharge of a pump expressed in SI units in cubic meters per second for large pumps or liters per second and cubic meters per hour for small pumps. Using U.S. customary units, pump capacity is expressed in gallons per minute, million gallons per day, or cubic feet per second. The *head* is the difference in elevation between a free surface of water above (or below) the reference datum, which varies with the type of pump, as shown in Figure 12.2.2.

Multistage pumps are pumps with more than one impeller (stage). The stages are in series so that the discharge of the first stage (first impeller) discharges directly into the suction side of the second stage (second impeller), etc. The impellers are on a single shaft and are enclosed in a single pump housing. Figure 12.2.3a shows a single-stage pump and Figure 12.2.3b shows a multistage pump.

Figures 12.2.4a and b show screw pumps and centrifugal pumps at a water treatment plant. Also refer to Figure 12.1.2. *Screw pumps* are classified as *positive-displacement pumps*. These pumps are used for pumping irrigation water, drainage water, and wastewater. They are based on the Archimedes screw principle in which a revolving shaft fitted with helical blades rotates in an inclined trough pushing water up the trough (as shown in Figure 12.2.4a). Two advantages of the

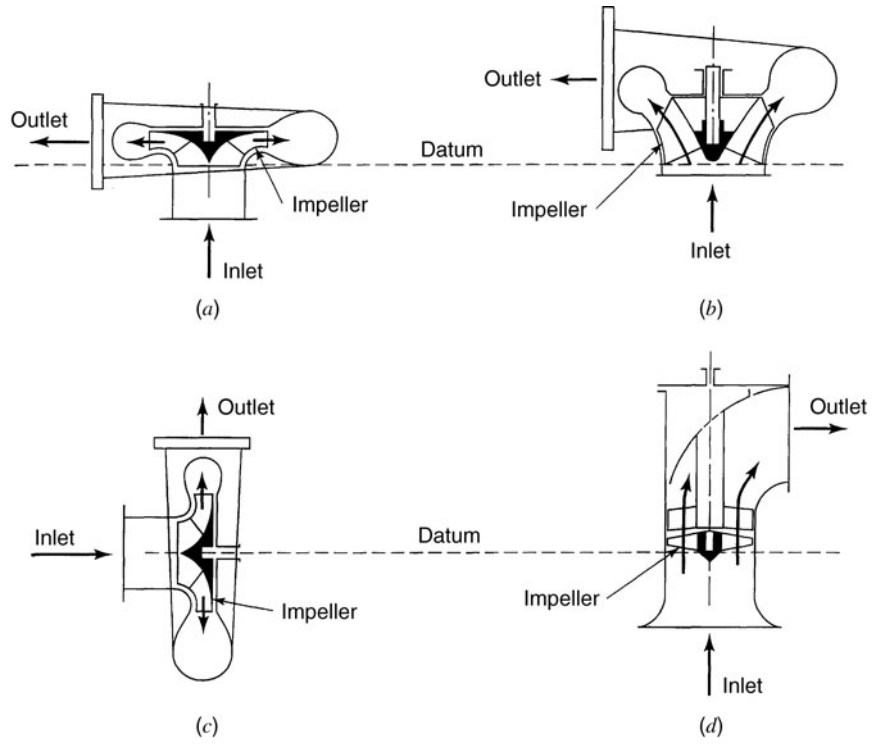


Figure 12.2.1 Typical flow paths in centrifugal pump. (a) Radial flow, vertical; (b) Mixed flow; (c) Radial flow, horizontal; (d) Axial flow (from Tchobanoglous (1998)).

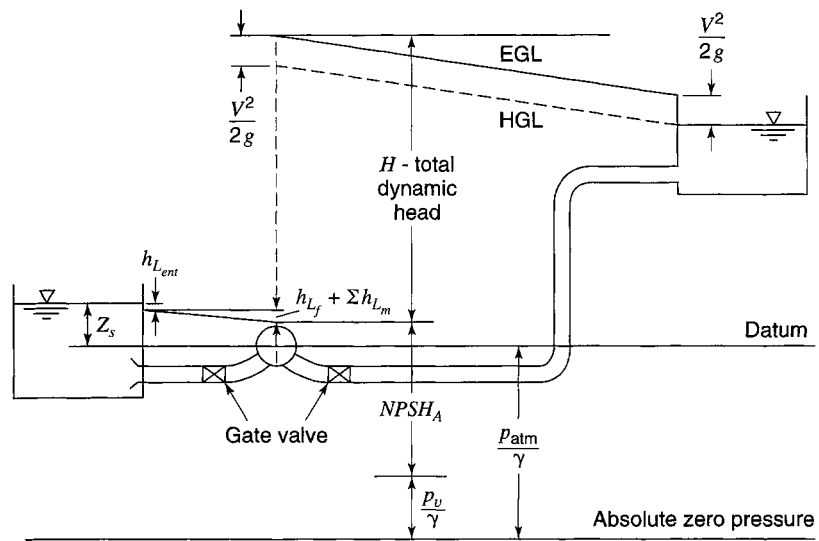


Figure 12.2.2 Illustration of total dynamic head and net positive suction head available for a simple pipe and pump station.

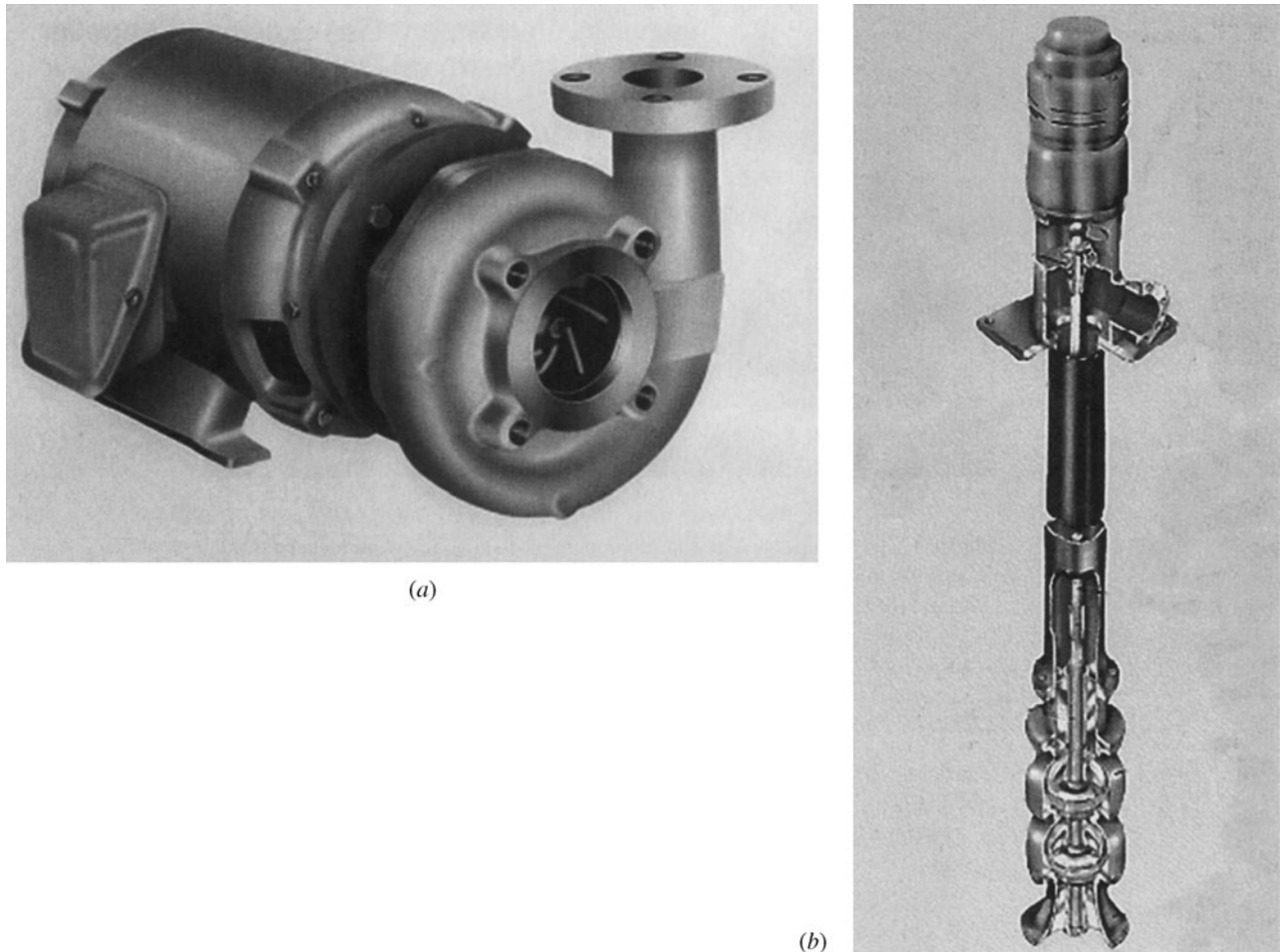


Figure 12.2.3 Single- and multistage pump. (a) Single-stage pump; (b) Multistage pump. (Courtesy of Paco Pumps.)

screw pump over a centrifugal pump are: (1) they can pump large solids without clogging; and (2) they operate at a constant speed over a wide range of flows at relatively good efficiencies.

12.2.1.2 Operating Characteristics

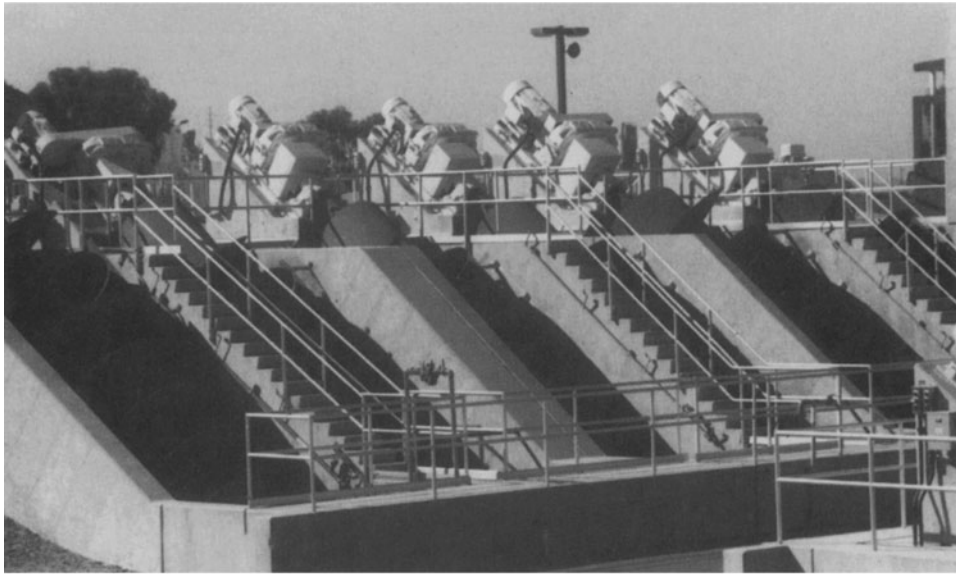
Operating characteristics of pumps are dependent upon their size, speed, and design. In centrifugal pumps, similar flow patterns occur in geometrically similar pumps. Through dimensional analysis the following three independent coefficients can be derived to describe the operation of pumps:

$$\text{Discharge coefficient: } C_Q = \frac{Q}{nD^3} \quad (12.2.1)$$

$$\text{Head coefficient: } C_H = \frac{H}{n^2 D^2} \quad (12.2.2a)$$

$$\text{or } C_H = \frac{gH}{n^2 D^2} \text{ (for dimensional correctness)} \quad (12.2.2b)$$

$$\text{Power coefficient: } C_P = \frac{P}{\rho n^3 D^5} \quad (12.2.3)$$



(a)



(b)

Figure 12.2.4 Pumps used at water treatment plants. (a) Screw pump used in water treatment plant to lift water (raw water) from pretreatment section to balance of treatment plant in Phoenix, Arizona; (b) High-service pumps at a water treatment plant in Phoenix, Arizona. (Photographs by L. W. Mays.)

Even though equation (12.2.2a) is not dimensionally correct, it is commonly used. These equations are the same either in SI or U.S. customary units, but with different values. Q is pump capacity in m^3/sec (ft^3/min), n is the speed in radians per second (revolutions per minute), D is the impeller diameter in meters (ft), H is the head in meters (ft), g is the acceleration due to gravity (9.81 m/s^2) (32.2 ft/s^2), P is the power input in kilowatts (horsepower), and ρ is the density in kilograms per cubic meter (slugs per cubic foot).

The above coefficients can be used to define the *affinity laws* for a pump operating at two different speeds and the same diameter. Consider the ratios $(C_Q)_1 = (C_Q)_2$ for the same diameter and

different speeds n_1 and n_2 , then

$$\frac{Q_1}{Q_2} = \frac{n_1}{n_2} \quad (12.2.4)$$

Similarly for $(C_H)_1 = (C_H)_2$:

$$\frac{H_1}{H_2} = \left(\frac{n_1}{n_2}\right)^2 \quad (12.2.5)$$

and similarly for $(C_P)_1 = (C_P)_2$:

$$\frac{P_1}{P_2} = \left(\frac{n_1}{n_2}\right)^3 \quad (12.2.6)$$

where 1 and 2 represent corresponding points. These relationships (*affinity laws*) are used to determine the effect of changes in speed on the pump capacity, head, and power. These relationships assume that the efficiency remains the same from one point on a pump curve to a homologous point on another pump curve. Affinity laws for discharge (equation 12.2.4) and for head (equation 12.2.5) are accurate; however, the affinity law for power may not be accurate.

EXAMPLE 12.2.1

A pump operating at 1800 rpm delivers 180 gal/min at 80 ft head. If the pump is operated at 2160 rpm, what are the corresponding head and discharge?

SOLUTION

Use the affinity law, equation (12.2.4), to compute the corresponding discharge:

$$\begin{aligned} \frac{Q_{2160}}{Q_{1800}} &= \frac{2160}{1800} \\ Q_{2160} &= 180 \left(\frac{2160}{1800}\right) = 216 \text{ gal/min} \end{aligned}$$

Use the affinity law equation (12.2.5) to compute the corresponding head:

$$\begin{aligned} \frac{H_{2160}}{H_{1800}} &= \left(\frac{2160}{1800}\right)^2 \\ H_{2160} &= 80 \left(\frac{2160}{1800}\right)^2 = 115.2 \text{ ft} \end{aligned}$$

12.2.1.3 Specific Speed

The *specific speed* n_s is a parameter used to select the type of centrifugal pump that is best suited to a particular application. The diameter term in equations (12.2.1) and (12.2.2a) can be eliminated by dividing $C_Q^{1/2}$ by $C_H^{3/4}$, that is

$$n_s = \frac{C_Q^{1/2}}{C_H^{3/4}} = \frac{(Q/nD^3)^{1/2}}{(H/n^2D^2)^{3/4}} = \frac{nQ^{1/2}}{H^{3/4}} \quad (12.2.7)$$

The *total dynamic head* is the total head against which a pump must operate. For a given speed of pump operation, the Q and H must be at the point of maximum efficiency. Equation (12.2.7) is dimensionally incorrect; however, it is the customary definition used in the United States. Using equations (12.2.1) and (12.2.2b) results in a dimensionally correct definition of the specific speed, with a conversion factor of 17,200, resulting in n_s ranging from about 0.03 to about 0.91 in U.S.

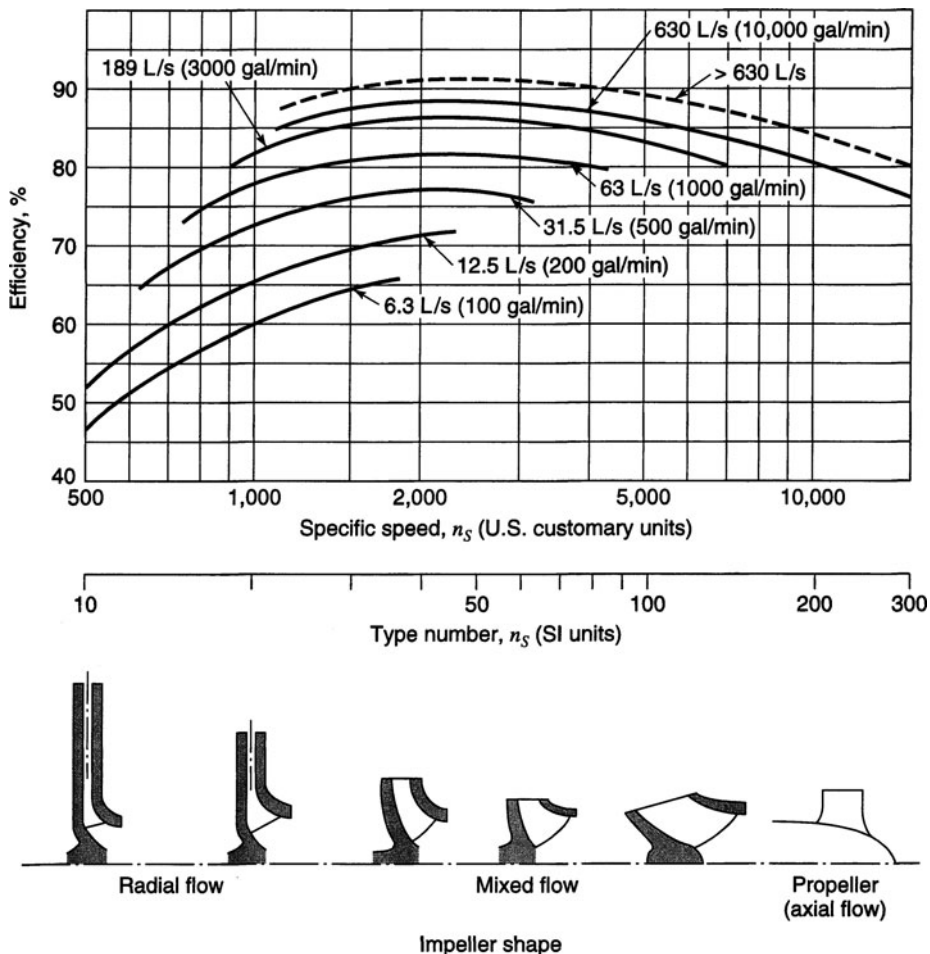


Figure 12.2.5 Pump efficiency as related to specific speed and discharge (from Tchobanoglous (1998)).

customary units. Figure 12.2.5 relates pump efficiency to specific speed and discharge showing the various impeller shapes. In determining the specific speed for multistage pumps, the head is the head per stage. Because $n_s \sim 1/H^{3/4}$, n_s decreases with an increase in H and the efficiency is small for the smaller n_s , one impeller used for large heads results in low efficiency. As a result, multistage pumps can increase efficiency.

EXAMPLE 12.2.2

A flow of $0.02 \text{ m}^3/\text{s}$ must be pumped against a head of 25 m. The pump will be driven by an electric motor with a speed of 1450 rpm. What type of pump should be used and what is the corresponding efficiency?

SOLUTION

Compute the specific speed using equation (12.2.7) and Figure 12.2.5 to select the type of pump:

$$n_s = \frac{nQ^{1/2}}{H^{3/4}} = \frac{1450(0.02)^{1/2}}{(25)^{3/4}} = 18.34$$

From Figure 12.2.5, a radial flow centrifugal pump would be used, with an efficiency of around 68 percent.

EXAMPLE 12.2.3

Solve example 12.2.2 using U.S. customary units.

SOLUTION

Using the flow rate of $0.02 \text{ m}^3/\text{s}$ yields 317 gal/min and the head of 25 m is 82 ft; the specific speed is

$$n_s = \frac{1450(317)^{1/2}}{(82)^{3/4}} = 947$$

From Figure 12.2.5, a radial flow centrifugal pump is selected with an efficiency of around 68 percent.

12.2.1.4 Cavitation and Net Positive Suction Head

The objective of this section is to illustrate how to determine whether or not cavitation will be a problem for a particular pump operation. *Cavitation* occurs in pumps when the absolute pressure at the pump inlet decreases below the vapor pressure of the fluid, at which time vapor bubbles form at the impeller inlet (suction side). As shown in Figure 12.2.6, the bubbles are transported through the impeller, where they reach a higher pressure and abruptly collapse. When the collapse occurs on the surface of the impeller blade, the liquid rapidly moves on to fill the space left by the bubble, impacting very small areas with very large localized pressures that pit and erode the plane surface. Collapse of the vapor bubbles can produce noise and vibration.

In order to determine if cavitation will be a problem, the concept of net positive suction head is used. The *available net positive suction head* ($NPSH_A$) at the eye of an impeller is computed and compared to the *required net positive suction head* ($NPSH_R$) of the pump, which is specified by the manufacturer to minimize cavitation. $NPSH_R$ is the absolute dynamic head in the impeller eye, defined by (refer to Figure 12.2.2)

$$NPSH_A = \frac{p_{\text{atm}}}{\gamma} + Z_s - \frac{p_v}{\gamma} - h_{L_{\text{ent}}} - h_{L_f} - \sum h_{L_m} \quad (12.2.8)$$

where p_{atm}/γ is the atmospheric pressure head in meters (feet), Z_s is the static suction head in meters (feet) at the impeller eye (negative if there is a suction lift), p_v/γ is the vapor pressure head in meters (feet), $h_{L_{\text{ent}}}$ is the entrance headloss in meters (feet), h_{L_f} is the suction pipe friction headloss in meters (feet), and $\sum h_{L_m}$ is the sum of minor losses of valves and fittings in meters (feet). The $NPSH_A$ should always be greater than the $NPSH_R$.

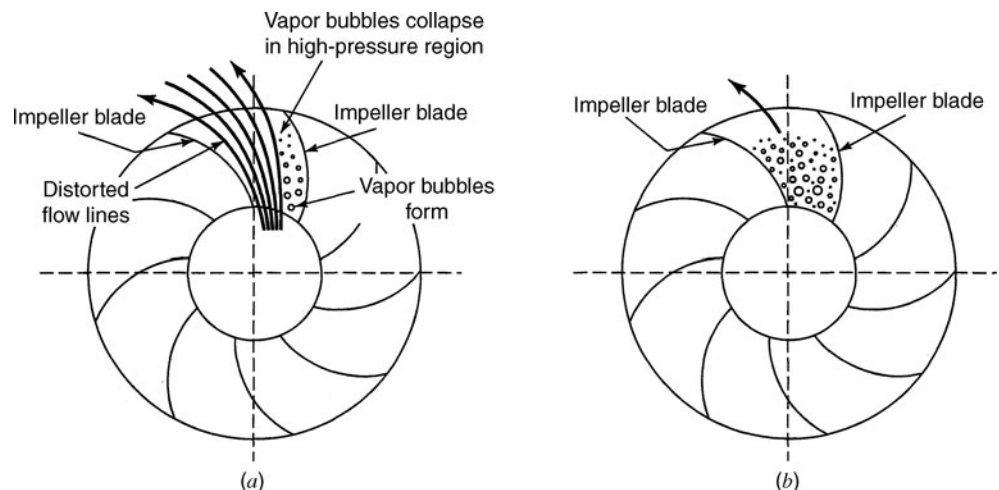


Figure 12.2.6 Formation of vapor bubbles in a pump impeller. (a) Partial cavitation; (b) Full cavitation.

Table 12.2.1 Values of K for Equation (12.2.10)^a

Pump efficiency (%)	K	
	SI units ^b	U.S. customary units ^c
70	1726	9.4
80	1210	6.3
90	796	4.3

^a For double-suction pumps, use the same formula with Q equal to half of the actual value.

^b Use with n , values in cubic meters per second, meters, and revolutions per minute.

^c Use with n , values in gallons per minute, feet, and revolutions per minute.

Source: Tchobanoglous (1998).

A cavitation constant known as *Thoma’s cavitation constant* is defined as the ratio of the *net positive suction head at the point of cavitation inception* ($NPSH_i$) to the total dynamic head H , expressed mathematically as

$$\sigma = \frac{NPSH_i}{H} \tag{12.2.9}$$

When applied to multistage pumps, H is the total dynamic head per stage. The value of $NPSH_R$ cannot be used in the above equation.

Thoma’s cavitation constant can be related approximately to specific speed and pump efficiency (Rutschi, 1960, and Tchobanoglous, 1998) as

$$\sigma = \frac{Kn_S^{4/3}}{10^6} \tag{12.2.10}$$

where values of K are given in Table 12.2.1. Equations (12.2.9) and (12.2.10) should not be used for design decisions; instead, recommended values of $NPSH_R$ from pump manufacturers should be used. Combining equations (12.2.9) and (12.2.10) we can estimate $NPSH_i$ using

$$NPSH_i = \frac{HKn_S^{4/3}}{10^6} \tag{12.2.11}$$

EXAMPLE 12.2.4

Estimate the available net positive suction head ($NPSH_A$) for a new system with the configuration shown in Figure 12.2.2 for a discharge of 0.12 m³/s. The suction piping and the discharge piping are both cement mortar-lined ductile iron pipe with a Hazen–Williams coefficient of 140. The suction piping has an inside diameter (ID) of 300 mm and a length of 5 m. The static suction head is + 3 m. The system has a bell mouth entrance, two 90° bends, and a gate valve on the suction side. The elevation is at 1000 m above mean sea level, the temperature is 20°C, and $p_{atm}/\gamma = 9.19$ m.

SOLUTION

The $NPSH_A$ is computed using equation (12.2.8):

$$NPSH_A = \frac{p_{atm}}{\gamma} + Z_s - \frac{p_v}{\gamma} - h_{L_{ent}} - h_{L_f} - \sum h_{L_m}$$

Referring to Table 3.1.2, $p_v/\gamma = 0.25$ m. The losses due to friction are computed using the Hazen–Williams equation (12.1.1):

$$V = 0.849CR^{0.63}S_f^{0.54}$$

The friction loss in meters per 1000 m of pipe can be expressed more conveniently as (equation 12.1.2)

$$h_{L_f} = 10,700 \left(\frac{Q}{C} \right)^{1.85} D^{-4.87} = \left(\frac{151Q}{CD^{2.63}} \right)^{1.85}$$

where h_{L_f} is meters per 1000 m, Q is m^3/s and D is in meters.

Suction piping losses:

$$\begin{aligned} h_{L_f} &= 10,700 \left(\frac{0.12}{140} \right)^{1.85} (0.300)^{-4.87} \\ &= 7.988 \text{ m per 1000 m of pipe} \\ &= (7.988)(5 \text{ m}/1000 \text{ m}) = 0.0399 \text{ m total loss} \end{aligned}$$

Bend losses (suction piping):

$$\begin{aligned} h_{L_b} &= K \frac{V^2}{2g} \\ V &= \frac{Q}{A} = \frac{0.12}{0.049} = 2.45 \text{ m/s} \\ K &= 0.25 \text{ (Table 12.2.4)} \\ h_{L_b} &= (0.25) \frac{(2.45)^2}{(2)(9.81)} = 0.076 \text{ m} \end{aligned}$$

Gate valve loss (suction piping):

$$\begin{aligned} V &= \frac{Q}{A} = \frac{0.12}{0.071} = 1.69 \text{ m/s} \\ h_{L_G} &= (0.2) \frac{(1.69)^2}{(2)(9.81)} = (0.2)(0.145) = 0.029 \text{ m} \end{aligned}$$

Bell mouth entrance loss:

$$\begin{aligned} K &= 0.05 \text{ (Table 12.2.4)} \\ h_{L_{en1}} &= K \frac{V^2}{2g} = 0.05(0.145) = 0.007 \end{aligned}$$

Total minor losses:

$$\sum h_{L_m} = 0.076 + 0.076 + 0.029 + 0.007 = 0.188 \text{ m}$$

Applying equation (12.2.8) yields

$$NPSH_A = 9.19 + 3 - 0.25 - 0.0399 - 0.188 = +11.71$$

EXAMPLE 12.2.5

Estimate the net positive suction head at the point of cavitation inception ($NPSH_i$) for a system in which the total dynamic head is 40 m. The pump delivers $400 \text{ m}^3/\text{h}$ at a rotational speed of 1200 rpm at around 80 percent efficiency. The pump is to operate at an elevation of 1000 m above sea level and the temperature is 20°C .

SOLUTION

$NPSH_i$ is computed using equation (12.2.11)

$$NPSH_i = \frac{HKn_s^{4/3}}{10^6}$$

Use a K value of 1210 from Table 12.2.1. The specific speed is

$$n_s = \frac{nQ^{1/2}}{H^{3/4}} = \frac{1200 \left(\frac{400}{3600} \right)^{1/2}}{40^{3/4}} = 25.15$$

$$NPSH_i = \frac{40(1210)(25.15)^{4/3}}{10^6} = 3.566$$

EXAMPLE 12.2.6

For the situation in example 12.2.5, the manufacturer's $NPSH_R$ is 3.3. What is the allowable suction head? The entrance loss is 0.001 m, the bend losses add up to 0.15 m, and the sum of headlosses due to friction in the suction piping is 1.5 m.

SOLUTION

To compute the allowable suction head, use equation (12.2.8) and solve for Z_s with $NPSH_R$ replacing $NPSH_A$:

$$NPSH_R = \frac{p_{\text{atm}}}{\gamma} + Z_s - \frac{p_V}{\gamma} - h_{L_{\text{ent}}} - h_{L_f} - \sum h_{L_m}$$

$$p_{\text{atm}}/\gamma = 9.19 \text{ m}, p_V/\gamma = 0.24 \text{ m}.$$

Solving the above equation for Z_s yields

$$Z_s = NPSH_R - \frac{p_{\text{atm}}}{\gamma} + \frac{p_V}{\gamma} + h_{L_{\text{ent}}} + h_{L_f} + \sum h_{L_m}$$

$$Z_s = 3.3 - 9.19 + 0.24 + 0.001 + 1.5 + 0.15$$

$$Z_s = -4 \text{ m}$$

The minus sign means a suction lift. In practice, this lift should be reduced by about 0.6 m. The $NPSH_A$ should always be greater than the $NPSH_R$.

12.2.1.5 Pump Characteristics

A *pump head-characteristic curve* is a graphical representation of the total dynamic head versus the discharge that a pump can supply. These curves, which are determined from pump tests, are supplied by the pump manufacturer. Figure 12.2.7 shows the head-characteristic curve for various impeller diameters along with the efficiency and brake horsepower curves. When two or more pumps are operated, the *pump station losses*, which are the headlosses associated with the piping into and out of the pump, should be subtracted from the manufacturer's pump curve to derive the *modified head-characteristic curve*, as shown in Figure 12.2.8.

Two points of interest on the pump curve are the shutoff head and the normal discharge or rated capacity. The *shutoff head* is the head output by the pump at zero discharge, while the *normal discharge* (or *head*) or *rated capacity* is the discharge (or head) where the pump is operating at its most efficient level. Variable-speed motors can drive pumps at a series of rotative speeds, which would result in a set of pump curves for the single pump, as illustrated in Figure 12.2.9. Typically, to supply a given flow and head, a set of pumps is provided to operate in series or parallel and the number of pumps working depends on the flow requirements. This makes it possible to operate the pumps near their peak efficiency.

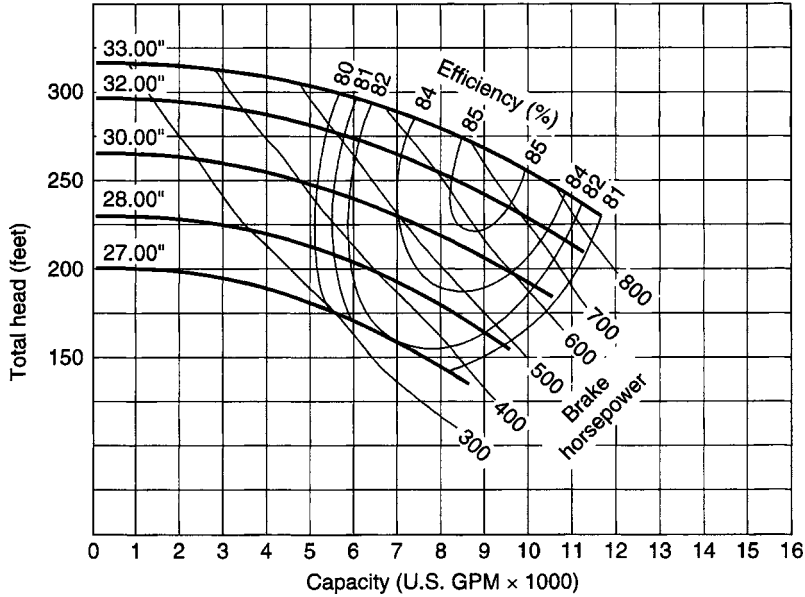


Figure 12.2.7 Manufacturer's pump performance curves.

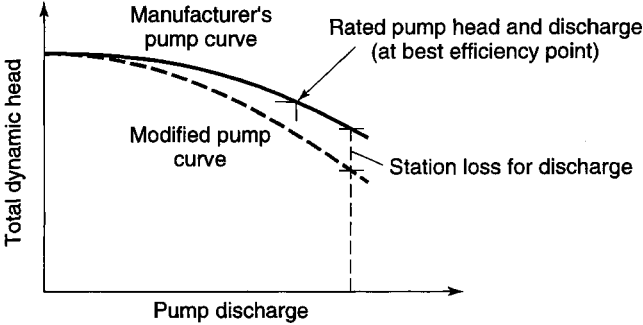


Figure 12.2.8 Modified pump curve.

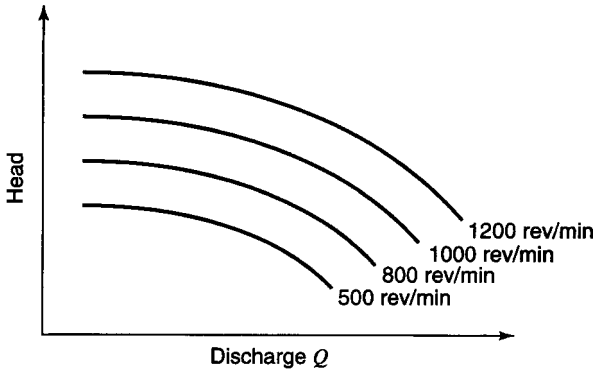


Figure 12.2.9 Pump performance curves for variable-speed pumps.

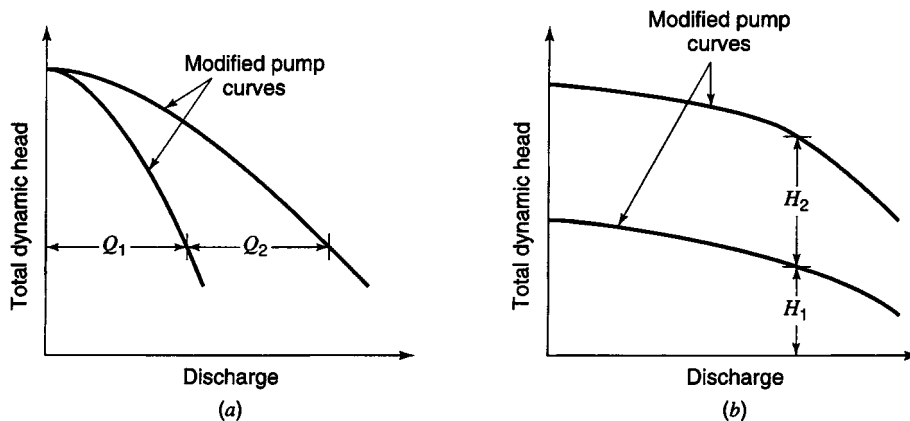


Figure 12.2.10 Pumps operating (a) in parallel and (b) in series.

Multiple-pump operation for one or more pumps in parallel or in series requires the addition of the modified head-characteristic curves. For pumps operating in parallel, the modified head-characteristic curves are added horizontally with the respective heads remaining the same (see Figure 12.2.10a). For pumps operating in series, the modified head-characteristic curves are added vertically, with the respective discharges remaining the same (Figure 12.2.10b).

Pump manufacturers also provide curves relating the *brake horsepower* (required by pump) to the pump discharge (see Figure 12.2.7). The brake horsepower (*bhp*) is calculated using

$$bhp = \frac{\gamma QH}{550e} \tag{12.2.12}$$

where Q is the pump discharge in cfs, H is the total dynamic head in ft, γ is the specific weight of water in lb/ft³, and e is the pump efficiency.

The *power input (bhp)* in SI units is defined as

$$bhp = \frac{\gamma QH}{e} \tag{12.2.13}$$

where bhp is the power in kilowatts, γ is the specific weight in kilonewtons per cubic meter, Q is the flow rate in cubic meter per second, and H is the total dynamic head in meters.

The *pump efficiency* is the power delivered by the pump to the water (water horsepower) divided by the power delivered to the pump by the motor (brake horsepower). *Efficiency curves*, as shown in Figure 12.2.7, define how well the pump is transmitting energy to water. Pumps operate best at their *best efficiency point* (bep) because of minimum radial loads on the impeller and minimum cavitation problems.

Operating ranges of a pump can be developed by (1) establishing a minimum acceptable efficiency and (2) setting upper and lower limits on the allowable impeller diameters. Figure 12.2.11 illustrates the operating range of a pump based on these criteria.

12.2.2 Pipes and Fittings

Water distribution piping can be of several types, including ductile iron pipe (DIP), steel, polyvinyl chloride (PVC) pipe, asbestos cement (AC) pipe (ACP), reinforced concrete pressure pipe (RCPP), and others. The American Water Works Association (AWWA) publishes C-series standards that provide standards for pipe construction, installation, and performance. The following are several factors that must be considered in the selection of both exposed and buried pipe and fittings (Bosserman et al., 1998a):

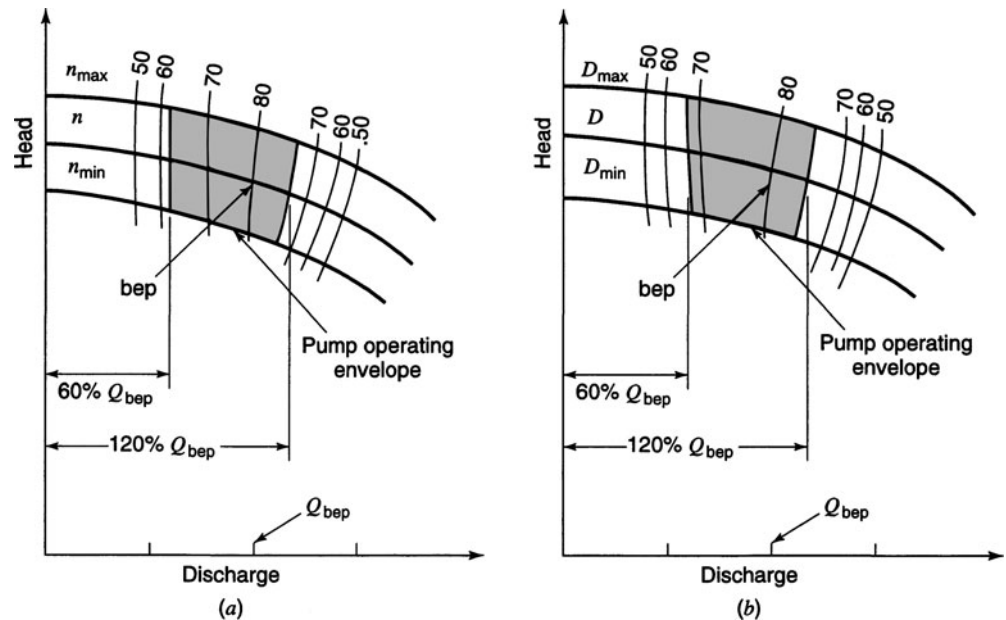


Figure 12.2.11 Pump operating envelopes based on the percentage of capacity at the best efficiency capacity. (a) Rotational speed; (b) Impeller diameter (from Tchobanoglous (1998)).

- Properties of the fluid
 - Corrosive or scale-forming properties
 - Unusual characteristics, e.g., viscosity of sludge
- Service conditions
 - Pressure (including surges and transients)
 - Corrosive atmosphere for exposed piping
 - Soil loads, bearing capacity and settlement, external loads, and corrosion potential for buried piping
- Availability
 - Sizes
 - Thickness
 - Fittings
- Properties of the pipe
 - Strength (static and fatigue, especially for water hammer)
 - Ductility
 - Corrosion resistance
 - Fluid friction resistance of pipe or lining
- Economics
 - Required life
 - Maintenance
 - Cost (FOB plus freight to job site)
 - Repairs
 - Salvage value

Tables 12.2.2 and 12.2.3 present comparisons of pipe for exposed service and buried service, respectively. Bosserman et al. (1998a) present a more detailed discussion of the factors that affect pipe selection. Table 12.2.4 presents energy loss coefficients for flanged pipe fittings.

Table 12.2.2 Comparison of Pipe for Exposed Service

Pipe	Advantages	Disadvantages/Limitations
Ductile iron pipe (DIP)	Yield strength: 290,000 kPa (42,000 lb/in ²) Ultimate strength: 414,000 kPa (60,000 lb/in ²) $E = 166 \times 10^6$ kPa (24×10^6 lb/in ²) Ductile, elongation = 10% Good corrosion resistance Wide variety of available fittings and joints Available sizes: 100–1350 mm (4–54 in) ID Wide range of available thicknesses Good resistance to water hammer	Maximum pressure = 2400 kPa (350 lb/in ²) High cost, especially for long freight hauls No diameters above 1350 mm (54 in) Difficult to weld Class 53 is the thinnest allowed for American flanged pipe (with screwed flanges in the U.S.)
Steel	Yield strengths: 207,000–414,000 kPa (30,000 to 60,000 lb/in ²) Ultimate strengths: 338,000–518,000 kPa (49,000–75,000 lb/in ²) $E = 207 \times 10^6$ kPa (30×10^6 lb/in ²) Ductile, elongation varies from 17 to 35% Pressure rating to 17,000 kPa (2500 lb/in ²) Diameters to 3.66 m (12 ft) Widest variety of available fittings and joints Custom fittings can be mitered and welded Excellent resistance to water hammer Low cost	Corrosion resistance low unless lined

Source: Bosserman et al. (1998a).

12.2.3 Valves

Valves are very important for the proper functioning of water distribution systems. The types of valves include:

- *Isolation valves* (Figure 12.2.12), used to shut down portions of a system, include:
 - Ball
 - Butterfly
 - Cone

Table 12.2.3 Comparison of Pipe for Buried Service

Pipe	Advantages	Disadvantages/Limitations
Ductile iron pipe (DIP)	See Table 12.2.2; high strength for supporting earth loads, long life	See Table 12.2.2; may require wrapping or cathodic protection in corrosive soils
Steel pipe	See Table 12.2.2; high strength for supporting earth loads	See Table 12.2.2; poor corrosion resistance unless both lined and coated or wrapped, may require cathodic protection in corrosive soils
Polyvinyl chloride (PVC) pipe	Tensile strength (hydrostatic design basis = 26,400 kPa (4000 lb/in ²); $E = 2,600,000$ kPa (400,000 lb/in ²); light in weight, very durable, very smooth, liners and wrapping not required, good variety of fittings available or can use ductile or cast-iron fittings with adapters, can be solvent-welded; diameters from 100 to 375 mm (4 to 36 in)	Maximum pressure = 2,400 kPa (350 lb/in ²); little reserve of strength for water hammer if ASTM D 2,241 is followed, AWWA C900 includes allowances for water hammer; limited resistance to cyclic loading, unsuited for outdoor use above ground

(Continued)

Table 12.2.3 (continued)

Pipe	Advantages	Disadvantages/Limitations
Asbestos cement (AC) pipe (ACP)	Yield strength: not applicable; design based on crushing strength, see ASTM C 296 and C 500; $E = 23,500,000$ kPa (3,400,000 lb/in ²); rigid, light weight in long lengths, low cost; diameters from 100 to 1050 mm (4 to 42 in) compatible with cast-iron fittings, pressure ratings from 1600 to 3100 kPa (225 to 450 lb/in ²) for large pipe 450 mm (18 in) or more	Attacked by soft water, acids, sulfates; requires trust blocks at elbows, tees, and dead ends; maximum pressure = 1380 kPa (200 lb/in ²) for pipe up to 400 mm (16 in); health hazards of asbestos in potable water service are controversial, U.S. EPA proposed ban on most asbestos products in 1988, being reconsidered for AC pipe
Reinforced concrete pressure pipe (RCP)	Several types available to suit different conditions; high strength for supporting earth loads, wide variety of sizes and pressure ratings, low cost, sizes from 600 to 3600 mm (24 to 144 in)	Attacked by soft water, acids, sulfides, sulfates, and chlorides, often requires protective coatings; water hammer can crack outer shell, exposing reinforcement to corrosion and destroying its strength with time; maximum pressure = 1380 kPa (200 lb/in ²)

Source: Bosserman et al., (1998b).

Table 12.2.4 Recommended Energy Loss Coefficients, K , for Flanged Pipe Fittings^a

Fitting	K	Fitting	K
Entrance		Forged or cast fittings	
Bell mouth	0.05	Return bent, $r = 1.4 D$	0.40
Rounded	0.25	Tee, line flow	0.30
Sharp edged	0.5	Tee, branch flow	0.75
Projecting	0.8		
Exits		Cross, line flow	0.50
All of the above	1.0	Cross, branch flow	0.75

(Continued)

Table 12.2.4 (continued)

Fitting	K	Fitting	K
Bends, mitered		Wye, 45°	0.50
$\theta = 15^\circ$	0.05	Increases	
$\theta = 22.5^\circ$	0.075		
$\theta = 30^\circ$	0.10	Conical	$h = K \left[1 - \left(\frac{D_1}{D_2} \right)^2 \right] V_2^2 / 2g$
$\theta = 45^\circ$	0.20		
$\theta = 60^\circ$	0.35	Conical (approximate)	$K = 3.5(\tan \theta)^{1.22}$ $h = 0.25(V_1^2 - V_2^2) / 2g$
$\theta = 90^\circ$	0.80		
90° bend $3 \times 30^\circ = 90^\circ$ $4 \times 22.5^\circ = 90^\circ$	0.30	Sudden	$h = \frac{V_1^2 - V_2^2}{2g} = \left[\left(\frac{A_1}{A_2} \right)^2 - 1 \right] \frac{V_2^2}{2g}$
Forged or cast fittings		Reducers	
90° elbow, standard	0.25	Conical	$h = KV_2^2 / 2g$ $K = 0.03 \pm 0.01$
90° elbow long radius	0.18	Sudden	$h = \frac{1}{2} \left[1 - \left(\frac{D_1}{D_2} \right)^2 \right] V_2^2 / 2g$
45° elbow	0.18		

^a $h = KV^2/2g$, where v is the maximum velocity in nonprismatic fittings. Increase K by 5 percent for each 25 mm (1 in) decrement in pipe smaller than 300 mm (12 in). Expect K values to vary from -20 to +30% or more.

Source: Sanks (1998).

- Eccentric plug
- Gate
- Plug
- *Check valves* (Figure 12.2.12) are directional control valves that allow flow of water to only one direction
 - Swing check valves
 - Counterpost-guided (or silent) check valves
 - Double-door (or double-disc or double-leaf) check valves
 - Foot valves
 - Ball lift valves
 - Tilting (or slanting) disc check valves

Control valves are used to regulate flow or pressure by operating partly open, creating high headlosses and pressure differentials. These include *pressure-reducing valves* (PRV) and *pressure-*

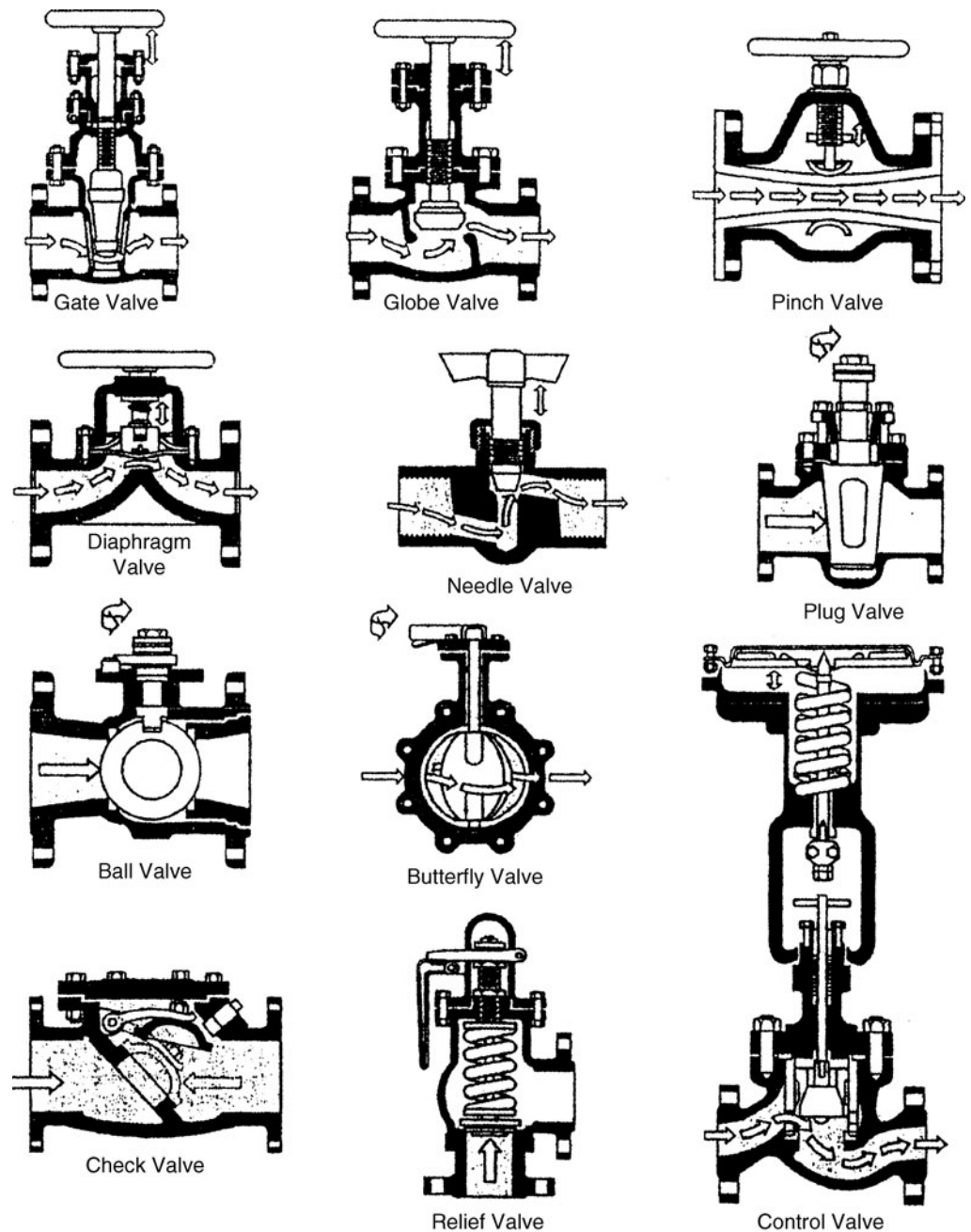


Figure 12.2.12 Types of water utility valves. (Courtesy of the Valve Manufacturers Association of America, Washington, DC.)

sustaining valves (PSV). PRVs are used to monitor (reduce) downstream pressures and PSVs are used to monitor pressures upstream of the valve. *Flow control valves* are used to maintain flow at a preset rate through throttling. Table 12.2.5 lists energy loss coefficients for fully open valves and Table 4.3.1 provides loss coefficients for valves.

Table 12.2.5 Recommended Energy Loss Coefficients, K , for Valves Fully Open^{a,b,c}

Valve type	K
Angle	1.8–2.9
Ball	0.04
Butterfly	
25-lb Class	0.16
75-lb Class	0.27
150-lb Class	0.35
Check valves	
Center-guided globe style	2.6
Double door	
8 in or smaller	2.5
10 to 16 in	1.2
Foot	
Hinged disc	1–1.4
Poppet	5–1.4
Rubber flapper	
$V < 6$ ft/s	2.0
$V > 6$ ft/s	1.1
Slanting disc ^d	0.25–2.0
Swing ^d	0.6–2.2
Cone	0.04
Diaphragm or pinch	0.2–0.75
Gate	
Double disc	0.1–0.2
Resilient seat	0.3
Globe	4.0–6.0
Knife gate	
Metal seat	0.2
Resilient seat	0.3
Plug	
Lubricated	0.5–1.0
Eccentric	
Rectangular (80%) opening	1.0
Full bore opening	0.5

^a $h = KV^2/2g$, where V is the velocity in the approach piping.

^b For 300-mm (12-in) valves and velocities of about 2 m/s (6 ft/s).

Note that K may increase significantly for smaller valves. Consult the manufacturer.

^c Expect K to vary from –20 to + 50% or more.

^d Depending on adjustment of closure mechanism, velocity may have to exceed 4 m/s (12 ft/s) to open the valve fully. Adjustment is crucial to prevent valve slam, so be very conservative in estimating K (which can be several times the tabulated value). Consult the manufacturer.

Source: Sanks (1998).

12.3 SYSTEM CONFIGURATION AND OPERATION

Water distribution systems are made up of networks of discrete components: pipes, fittings, pumps, valves, and storage tanks. The configurations of these systems vary significantly. These systems are typically very large and complex, especially for a large number of consumers spread over a wide

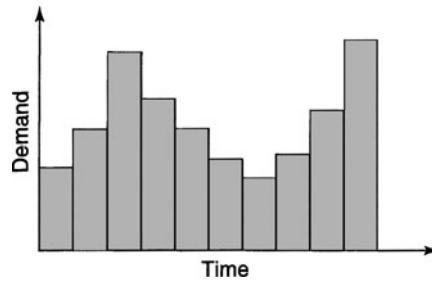


Figure 12.3.1 A demand curve.

service area. Hundreds to thousands of pipes may be required to distribute water to users throughout the system. Storage tanks and pumping stations are required to provide flexibility in demands as a function of time and location. The time variation in demand is illustrated in Figure 12.3.1.

Large systems may include several pressure zones where pumps, valves, and tanks maintain required service pressures. Figures 12.3.2 and 12.3.3 illustrate an example system that includes two pressure zones served from a single treatment plant. In this system the one pressure zone is served by pumps at the treatment plant and an elevated storage tank. The other pressure zone is served by a booster pumping station and an elevated storage tank.

The *piezometric* surface (surface of hydraulic grade line, HGL) is one way to visualize water-distribution-system hydraulics for various water-distribution-system configurations. Figure 12.3.4 illustrates the hydraulic grade line for a simple system under two operating conditions: (1) a low-demand condition and (2) a high-demand condition. During the low-demand conditions, water is pumped from the pumping station to satisfy demand and to fill the elevated tank. During the high-demand condition, the pumping station cannot supply the required demand, so water is supplied to the network by both the pumping station and the elevated storage tank. During low-demand conditions, the HGL is highest at the pumping station and slopes downward to meet the free surface at the elevated storage tank. The HGL slope indicates the energy required to pump water to the elevated storage tanks. During high demand, the HGL drops to a minimum in the highest-demand area.

For more complex systems the piezometric surface, represented by contour plots of the HGL elevation, and contour plots of the pressure can be very helpful in analyzing the configuration and

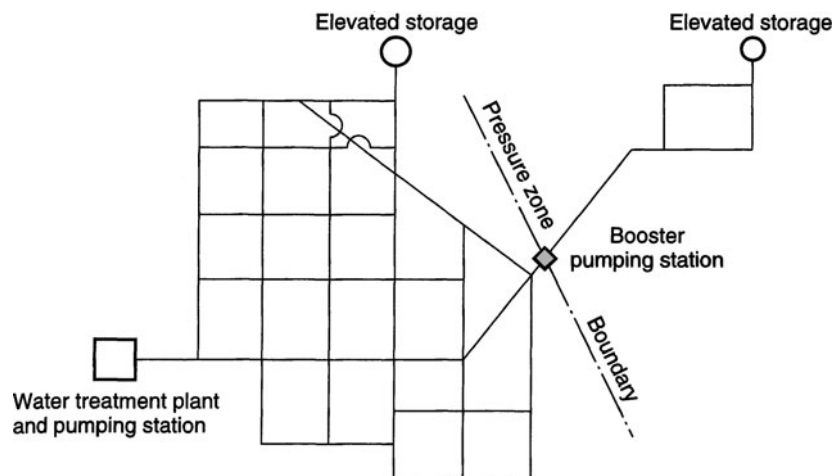


Figure 12.3.2 Schematic of example system (from Velon and Johnson (1993)).

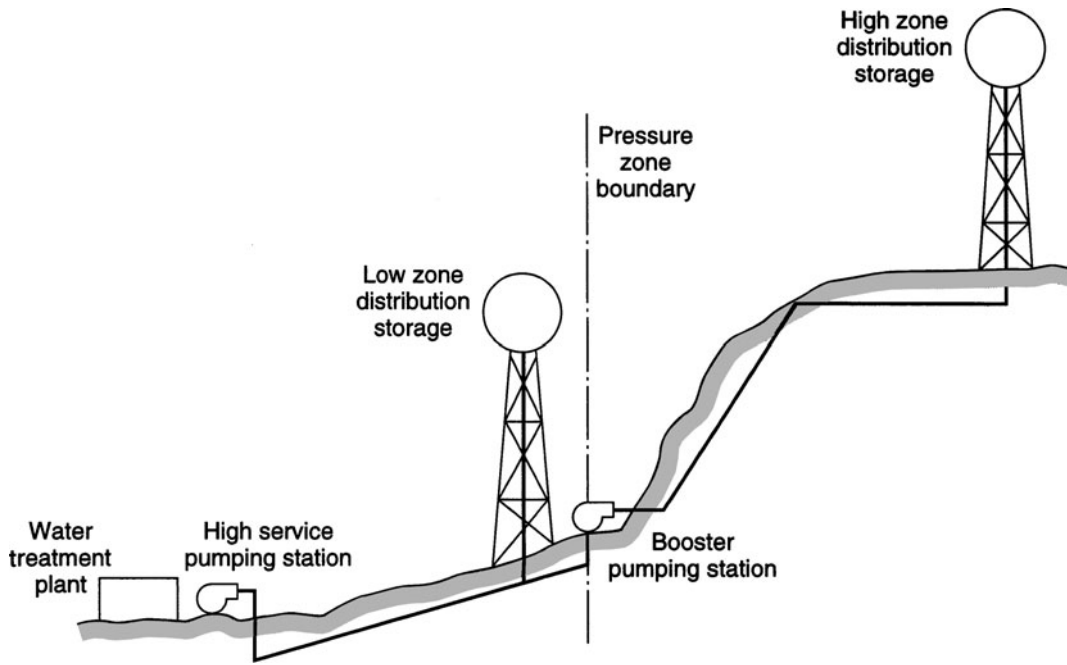


Figure 12.3.3 Typical two-pressure-zone system (from Velon and Johnson (1993)).

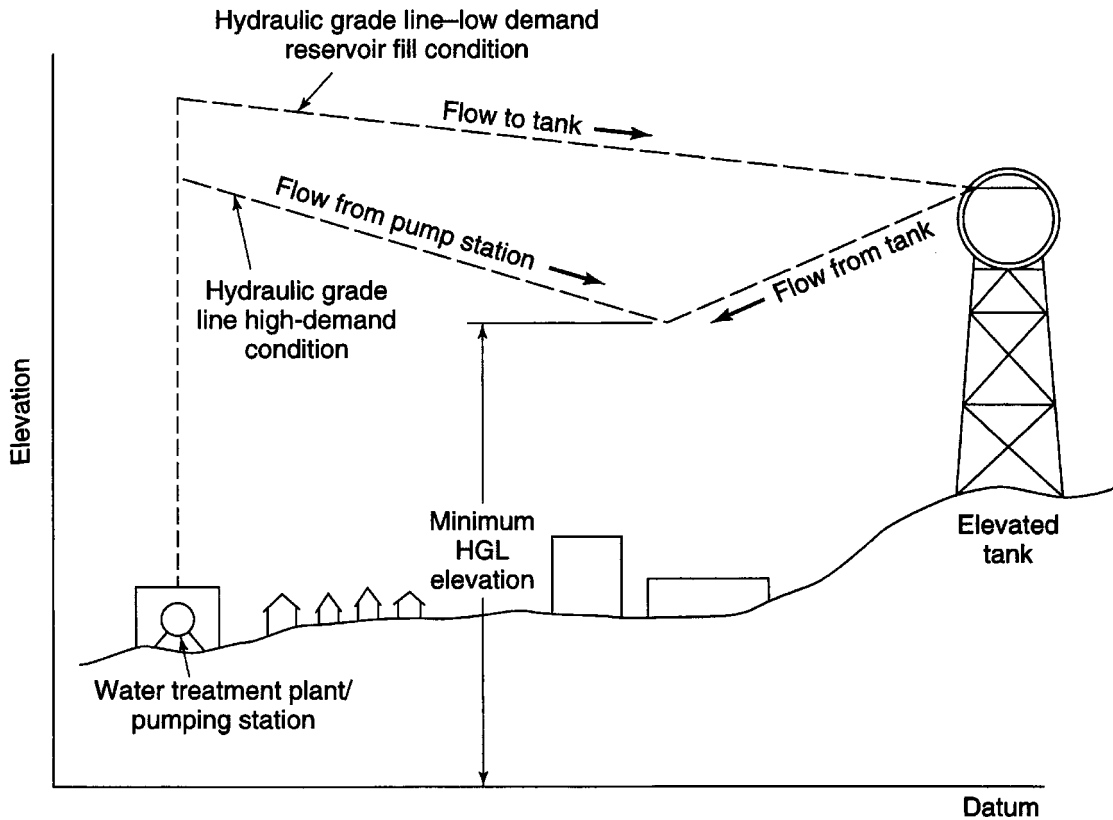


Figure 12.3.4 Hydraulic grade line under two demand conditions (from Velon and Johnson (1993)).

design of a system. Areas of a water distribution system that are subject to low pressures under various demand conditions can be identified. The portions of a water distribution system with high friction losses can be identified from these plots. Also, facilities that limit the ability of a system to meet demand and pressure requirements can be identified. Piezometric surface plots and contour pressure plots are a convenient means for reviewing and analyzing either new or existing water distribution system operations.

12.4 HYDRAULICS OF SIMPLE NETWORKS

12.4.1 Series and Parallel Pipe Flow

Pipe networks can include series pipes (Figure 12.4.1a), parallel pipes (Figure 12.4.1b), and branching pipes (Figure 12.4.1c). These simple networks can be converted to an *equivalent pipe*, which is helpful in simplifying and analyzing these networks. Two pipes are equivalent when, for the same headloss, both deliver the same rate of flow.

Series Pipes

For a system with two or more pipes in series, the total headloss is

$$h_{L_e} = \sum_i h_{L_i} \quad (12.4.1)$$

or

$$K_e Q^n = \sum K_i Q_i^n = K_1 Q_1^n + K_2 Q_2^n \dots \quad (12.4.2)$$

where K_e is the pipe coefficient for the equivalent pipe. When using the Hazen–Williams equation, all $n = 1.85$, and when using the Darcy–Weisbach equation, $n = 2$ for rough pipes and $n = 1.75$ for smooth pipes for fully turbulent flow; therefore K_e simplifies to

$$K_e = K_1 + K_2 + \dots = \sum K_i \quad (12.4.3)$$

Parallel Pipes

The concept of an equivalent pipe can be applied to two or more pipes in parallel. The headloss in each parallel pipe between junctions must be equal:

$$h_L = h_{L_1} = h_{L_2} = h_{L_3} = \dots \quad (12.4.4)$$

The total flow rate is the sum of individual flows in each pipe and is given as

$$Q = Q_1 + Q_2 + \dots = \sum Q_i \quad (12.4.5)$$

Substituting $Q = \left(\frac{h_L}{K_e}\right)^{\frac{1}{n_e}}$, from $h_L = KQ^n$, into equation (12.4.5) yields

$$\left(\frac{h_L}{K_e}\right)^{\frac{1}{n_e}} = \left(\frac{h_L}{K_1}\right)^{\frac{1}{n_1}} + \left(\frac{h_L}{K_2}\right)^{\frac{1}{n_2}} + \dots = \sum \left(\frac{h_L}{K_i}\right)^{\frac{1}{n_i}} \quad (12.4.6)$$

When using the Hazen–Williams equation, all the exponents n_i are equal; when using the Darcy–Weisbach equation, it is customary to assume n_i equal for all pipes (i.e., fully turbulent,

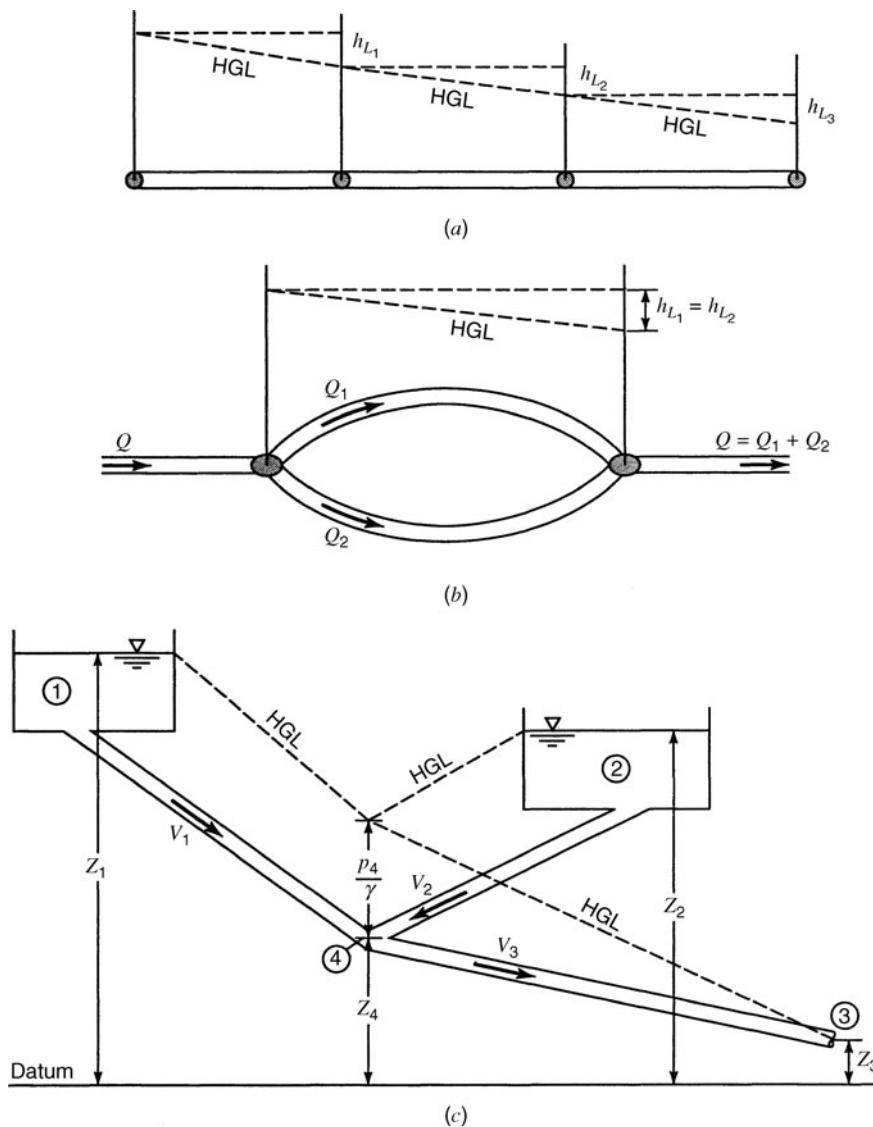


Figure 12.4.1 Simple pipe systems. (a) Series pipe system; (b) Parallel pipe system; (c) Branching pipe system.

$n = 2$) for rough pipes. Then equation (12.4.6) can be reduced to

$$\left(\frac{1}{K_e}\right)^{\frac{1}{n}} = \left(\frac{1}{K_1}\right)^{\frac{1}{n}} + \left(\frac{1}{K_2}\right)^{\frac{1}{n}} + \dots = \sum_i \left(\frac{1}{K_i}\right)^{\frac{1}{n}} \quad (12.4.7)$$

EXAMPLE 12.4.1

The system shown in Figure 12.4.2 consists of two reservoirs, the pump, pipe AB, and parallel pipes BC and BD. Headlosses between the lower reservoir and the pump are to be ignored. The Manning roughness factor for each pipe is $n = 0.01$. For a flow rate of 6 cfs, determine the total head to pump if $\Delta Z = 34$ ft. What is the brake horsepower required for an efficiency of 0.80?

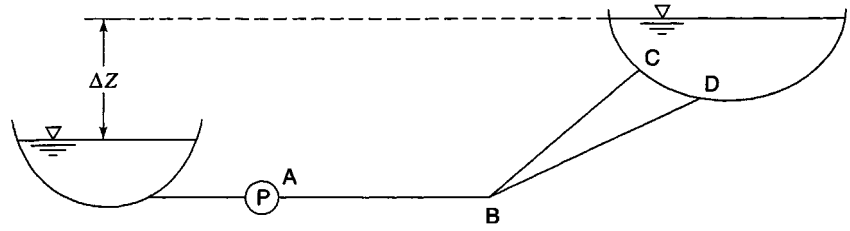


Figure 12.4.2 Example 12.4.1 pipe system.

Pipe	Diameter	Length
AB	18"	7000 ft
BC	9"	3000 ft
BD	12"	4000 ft

SOLUTION

The headloss for Manning's equation can be expressed in terms of the diameter using equation (12.1.10), so that

$$K_{AB} = \frac{(0.01)^2(7000)}{0.216(1.5)^{5.33}} = 0.373$$

Similarly $K_{BC} = 6.436$ and $K_{BD} = 1.852$. The headlosses in pipes BC and BD are equal, so that

$$h_{L_{BC}} = K_{BC}Q_{BC}^2 = h_{L_{BD}} = K_{BD}Q_{BD}^2$$

or

$$Q_{BC} = \sqrt{\frac{K_{BD}}{K_{BC}}} Q_{BD}$$

The total flow in pipes BC and BD ($Q_{BC} + Q_{BD}$) must equal the flow in pipe AB, i.e.,

$$\begin{aligned} Q_{AB} &= Q_{BC} + Q_{BD} = \sqrt{\frac{K_{BD}}{K_{BC}}} Q_{BD} + Q_{BD} \\ &= \left(\sqrt{\frac{K_{BD}}{K_{BC}}} + 1 \right) Q_{BD} = (0.536 + 1) Q_{BD} = 1.536 Q_{BD} \end{aligned}$$

$$Q_{BD} = 0.651 Q_{AB}$$

$$Q_{BC} = 0.349 Q_{AB}$$

The total headloss from the lower reservoir to the upper reservoir is

$$\begin{aligned} h_L &= h_{L_{AB}} + h_{L_{BD}} = h_{L_{AB}} + h_{L_{BC}} = K_{AB}Q_{AB}^2 + K_{BD}Q_{BD}^2 \\ &= K_{AB}Q_{AB}^2 + K_{BD}(0.651Q_{AB})^2 = 0.373Q_{AB}^2 + 1.852(0.651Q_{AB})^2 \\ h_L &= 1.158Q_{AB}^2 \end{aligned}$$

The total head to pump is then

$$H_T = \Delta Z + 1.158Q_{AB}^2$$

(a) For $Q_{AB} = 6$ cfs and $\Delta Z = 34$ ft:

$$H_T = 34 + 1.158(6)^2 = 75.69 \text{ ft.}$$

(b) $bhp = \frac{QH_T\gamma}{550e} = \frac{6 \times 75.69 \times 62.4}{550 \times 0.80} = 64.4 \text{ hp}$

12.4.2 Branching Pipe Flow

The flow distribution in branching systems can be determined by applying the continuity and energy equations. Figure 12.4.1c illustrates a branching system with the hydraulic grade line shown. The energy equation for the pipe from reservoir surface 1 to the junction at 4 is

$$Z_1 = Z_4 + \frac{p_4}{\gamma} + h_{L1} \tag{12.4.8}$$

From reservoir 2 to 4, the energy equation is

$$Z_2 = Z_4 + \frac{p_4}{\gamma} + h_{L2} \tag{12.4.9}$$

and from junction 4 to the outlet at 3, the energy equation is

$$Z_3 = Z_4 + \frac{p_4}{\gamma} + h_{L3} \tag{12.4.10}$$

The continuity equation is

$$Q_1 + Q_2 = Q_3 \tag{12.4.11}$$

Knowing the pipe sizes, lengths, and controlling elevations, we can solve these equations for the pressure head at 4, p_4/γ and the velocities, V_1 , V_2 , and V_3 . Knowing the velocities, the flow in each pipe can be determined.

EXAMPLE 12.4.2

The three reservoirs shown in Figure 12.4.3 are connected by riveted steel pipes. Determine the flow rate in each pipe, assuming fully turbulent flow.

SOLUTION

First, develop an expression for the headloss $h_L = KQ^2$ for riveted steel pipe. The relative roughness values are determined from Figure 4.3.3 and the resulting friction factors are based on fully turbulent flow from

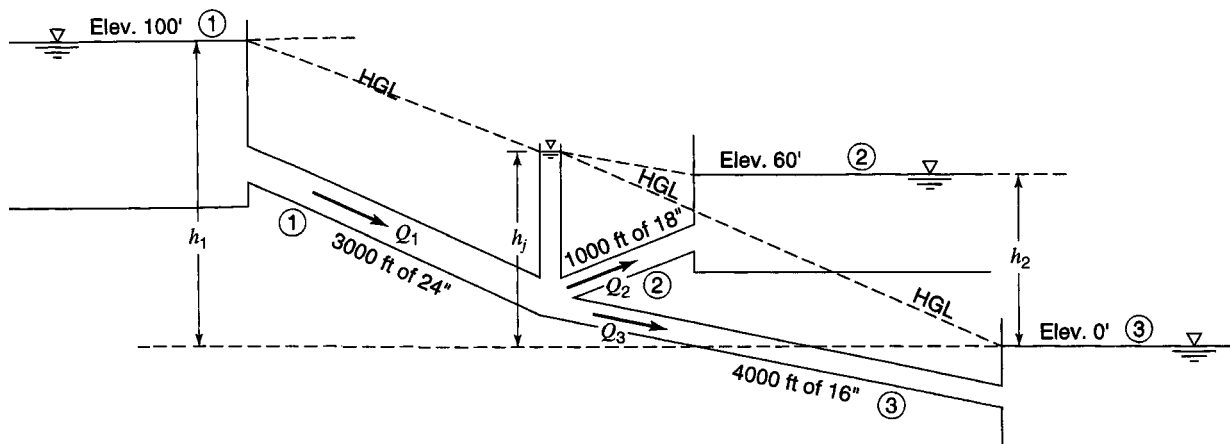


Figure 12.4.3 Example 12.4.2 pipe system.

the Moody diagram (Figure 4.3.5):

$$\text{Pipe 1: } \epsilon/D = 0.0015, f_1 = 0.0215: K_1 = \frac{fL}{39.7D^5} = \frac{0.0215(3000)}{39.7(24/12)^5} = 0.0508$$

$$\text{Pipe 2: } \epsilon/D = 0.0020, f_2 = 0.0234: K_2 = \frac{fL}{39.7D^5} = \frac{0.0234(1000)}{39.7(18/12)^5} = 0.0776$$

$$\text{Pipe 3: } \epsilon/D = 0.0023, f_3 = 0.0242: K_3 = \frac{fL}{39.7D^5} = \frac{0.0242(4000)}{39.7(16/12)^5} = 0.579$$

The expressions for headloss are

$$h_{L_1} = K_1 Q_1^2 = h_1 - h_j$$

$$h_{L_2} = K_2 Q_2^2 = h_j - h_2$$

$$h_{L_3} = K_3 Q_3^2 = h_j - h_3$$

where h_j is the HGL elevation at the pipe junction. The continuity at the pipe junction is $Q_1 - Q_2 - Q_3 = 0$. Substituting values of K_1 , K_2 , and K_3 and h_1 , h_2 , and h_3 into the above headloss equations results in

$$0.0508 Q_1^2 = 100 - h_j$$

$$0.0776 Q_2^2 = h_j - 60$$

$$0.579 Q_3^2 = h_j - 0$$

These three equations and the continuity relationship $Q_1 - Q_2 - Q_3 = 0$ result in four equations with four unknowns Q_1 , Q_2 , Q_3 , and h_j . They can be solved simultaneously to obtain $Q_1 = 23.5$, $Q_2 = 12.4$, $Q_3 = 11.2$ cfs, and $h_j = 72$ ft. The Reynolds number should be checked to assume the f values are correct.

A trial-and-error procedure can be used by finding an expression of the discharge in term of h_j and substituting these into the continuity equation:

$$Q_1 = \sqrt{\frac{h_1 - h_j}{K_1}} = \sqrt{\frac{100 - h_j}{0.0508}}$$

$$Q_2 = \sqrt{\frac{h_j - h_2}{K_2}} = \sqrt{\frac{h_j - 60}{0.0776}}$$

$$Q_3 = \sqrt{\frac{h_j - h_3}{K_3}} = \sqrt{\frac{h_j - 0}{0.579}}$$

Substituting these into the continuity equation at the pipe junction yields

$$\sqrt{\frac{100 - h_j}{0.0508}} - \sqrt{\frac{h_j - 60}{0.0776}} - \sqrt{\frac{h_j - 0}{0.579}} = 0$$

Then solve for $h_j = 72$ ft.

12.5 PUMP SYSTEMS ANALYSIS

12.5.1 System Head Curves

First we consider a pump-force main system. The head developed by the pump must equal the total dynamic head in the system. To determine the operating point, the pump head-characteristic curve

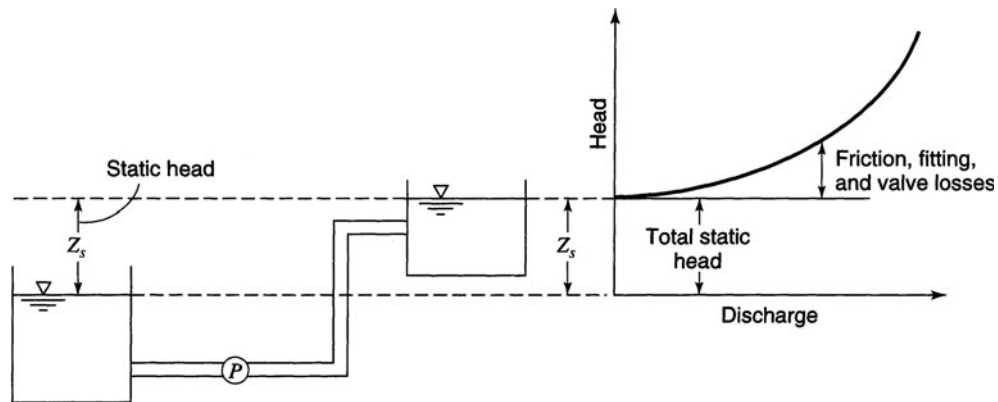


Figure 12.5.1 Typical system-head-capacity curve with positive lift.

(H-Q curve of the pump) and a *system-head-capacity curve* (H-Q curve of the piping system) are required. The *pump operating point* is the single point on these two H-Q curves where they intersect. Figure 12.5.1 illustrates a system-head-capacity curve in which the head is the sum of friction, fitting, and valve losses. These curves are plotted over a range of discharges, starting at zero discharge and varying up to the maximum expected. The system-head-capacity curves are approximate functions of the velocity head $V^2/2g$. These curves are typically approximated as parabolas, keeping in mind that headlosses are a function of 1.85 for the Hazen–Williams equation.

Figure 12.5.2 illustrates a typical system-head-capacity curve with a negative lift. Figure 12.5.3 illustrates a system with two different discharge heads. The combined system-head curve is obtained by adding the flow rates for the two pipes at the same head. Figure 12.5.4 illustrates a system with a varying static lift. Note that there are separate system-head curves, one for the maximum lift and one for the minimum lift. Figure 12.5.5 illustrates a system-head curve for a throttled system in which various valve openings are used to vary the head-discharge relationship.

12.5.2 Pump Operating Point

In order to determine the operating point for a pump or pumps in a piping system, the modified pump head-capacity curve is superimposed on the system-head-capacity curve. Figure 12.5.6 illustrates a single-speed pump head-capacity curve superimposed on a system-head-capacity curve for a piping

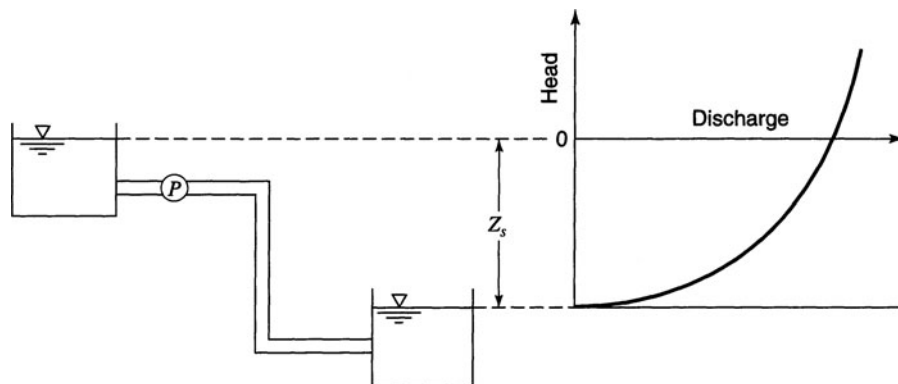


Figure 12.5.2 Typical system-head-capacity curve with negative lift.

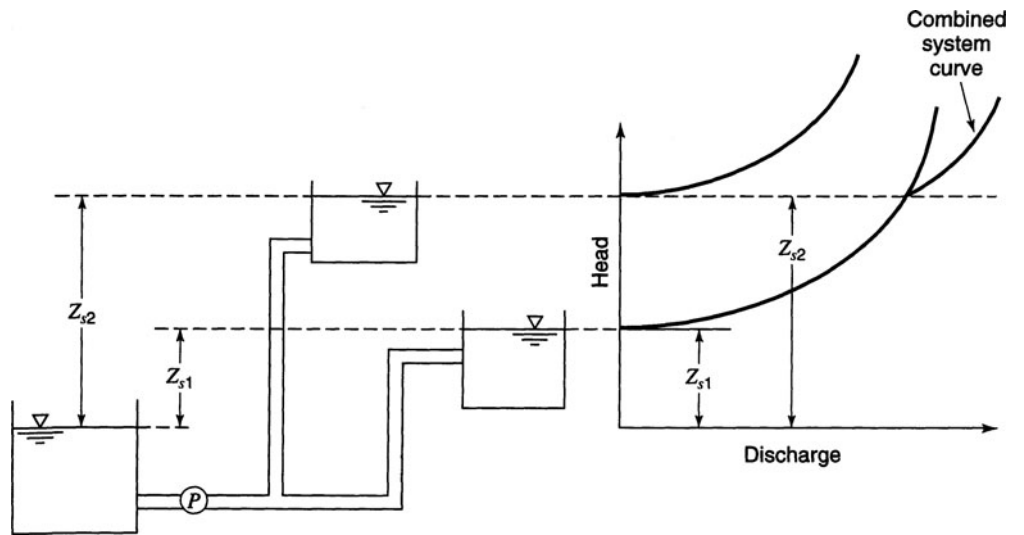


Figure 12.5.3 System with two different discharge heads. The combined system-head curve is obtained by adding the flow rates for the two pipes at the same head.

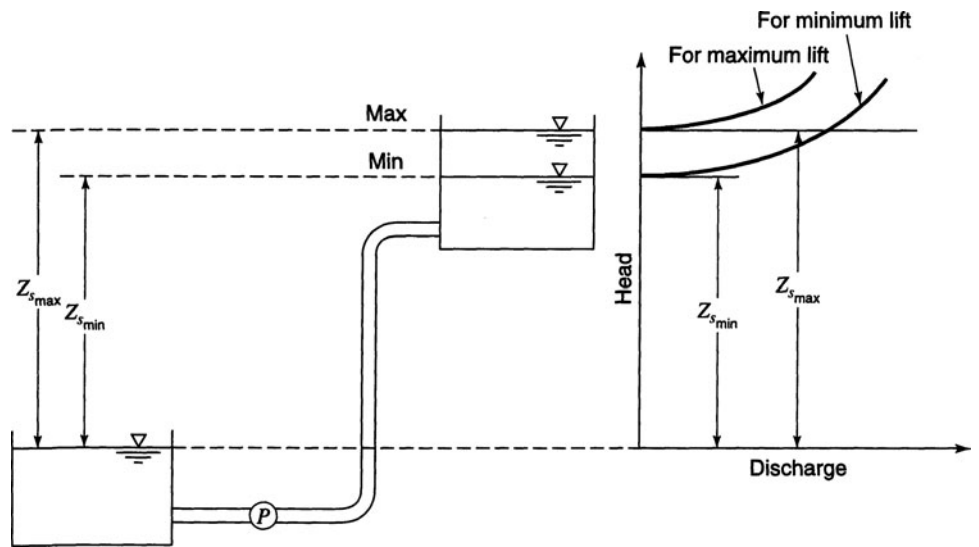


Figure 12.5.4 System with varying static lift.

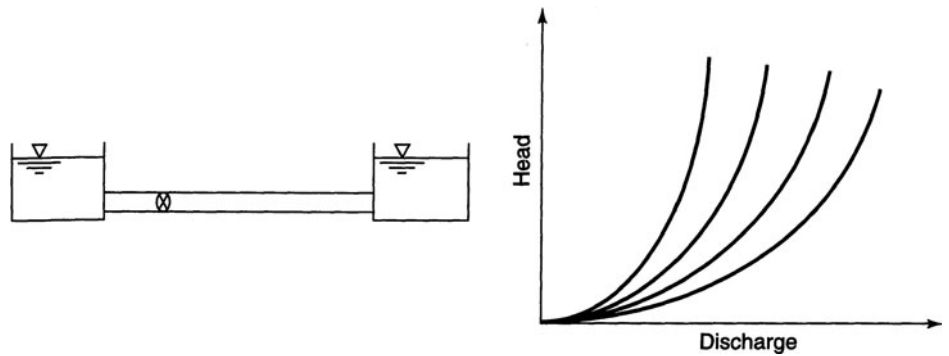


Figure 12.5.5 System throttled by valve operation.

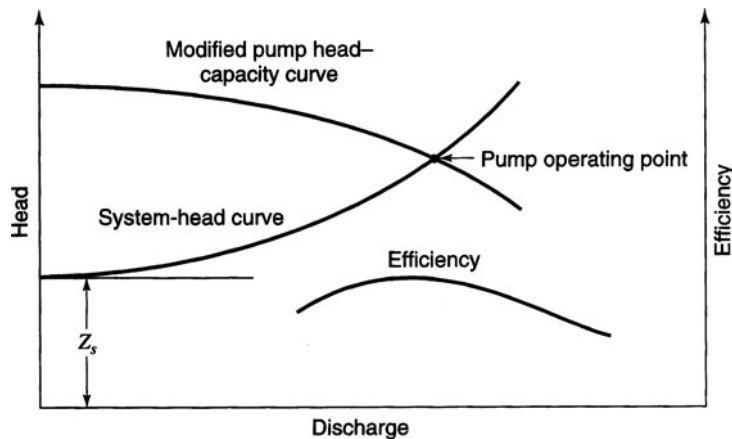


Figure 12.5.6 Determining operating points for a single-speed pump with a fixed static lift Z_s .

system with a fixed static lift Z_s . The point of intersection of the two head-capacity curves is the pump operating point. The pump operating point should be at or near the maximum efficiency of the pump, as shown in Figure 12.5.6.

Figure 12.5.7 illustrates the operating points for two single-speed pumps operating in parallel for a piping system that has a range of static lift. Note that system-head curves are shown for the maximum lift and for the minimum lift. Also shown is the range of operating points (between minimum and maximum static lift) for a single pump.

Figure 12.5.8 shows a system with three single-speed pumps of different sizes operating in parallel. Figure 12.5.9 illustrates the operating points for a variable-speed pump with a system-head curve. The affinity laws (described in section 12.2.1.2) can be used to determine the rotational speed at any desired operating point.

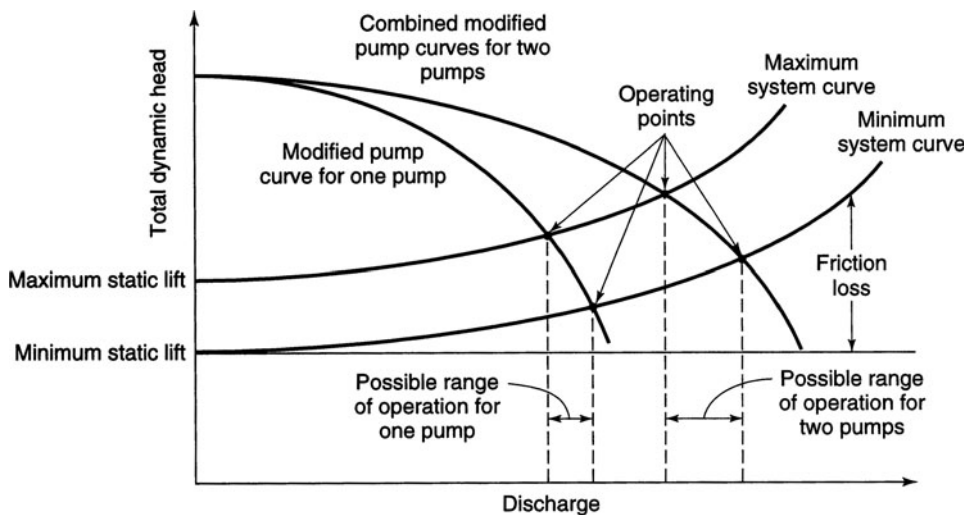


Figure 12.5.7 Determining operating points for two single-speed pumps in parallel and a variable static lift.

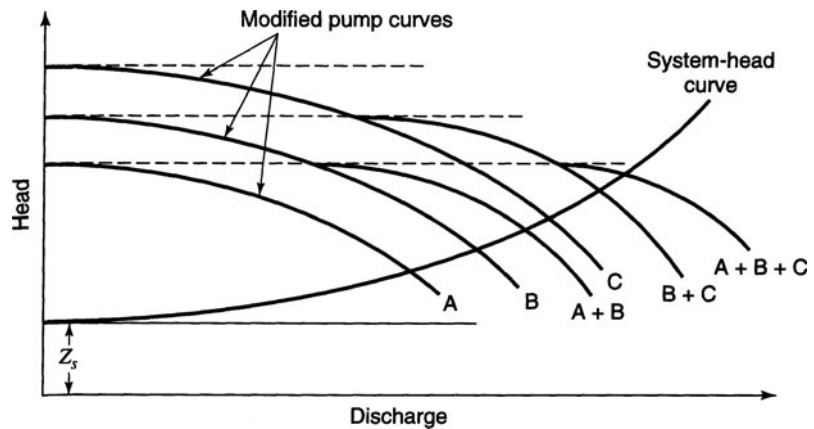


Figure 12.5.8 System with three single-speed pumps of different sizes operating in parallel.

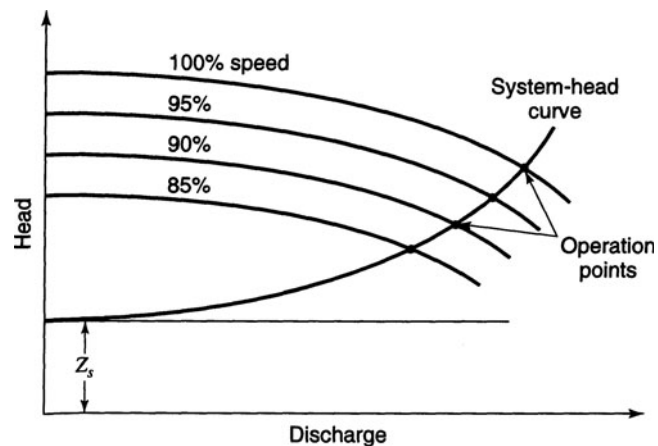


Figure 12.5.9 System with a single pump operated at variable speed.

As pipes age, the system-head curve rises due to changes in frictional resistance, resulting from scaling (deposition) on the pipe walls. Figure 12.5.10 illustrates the changing operating point for the decrease in the Hazen–Williams coefficient that can result from aging. Figure 12.5.11 illustrates the operating point for two pumps operating in series.

12.5.3 System Design for Water Pumping

Water pumping stations can be considered to fall into the following general types of systems (Bosserman et al., 1998b):

- Pumping into an elevated storage tank from a source such as a well
- Pumping raw water from a river or lake
- Pumping (high-service pumping) of finished water at high pressure
- Booster pumping
 - In-line booster pumping into an elevated tank or a reservoir (Figure 12.5.12)
 - Distribution system booster pumping without a storage tank

Pumping stations (except for well pumping stations) require redundant pumps, so that when each pump is taken out of service for maintenance, the other pumps can meet all demands.

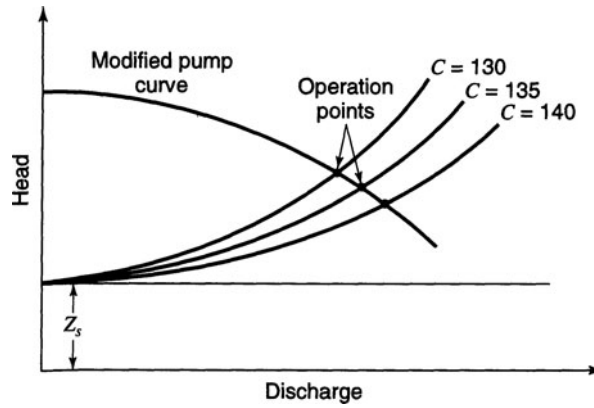


Figure 12.5.10 Change in operating points for decreasing Hazen–Williams coefficient due to pipe aging.

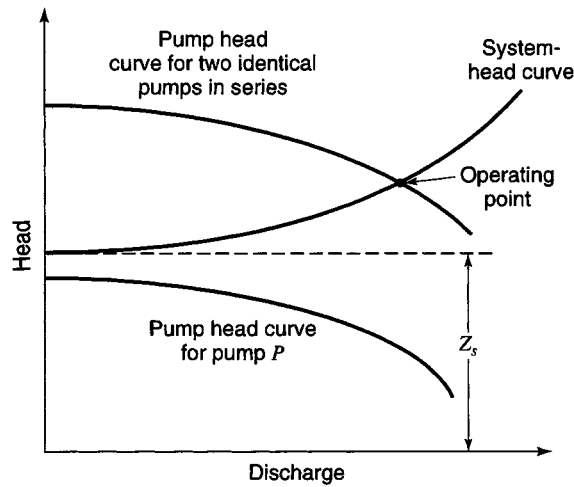


Figure 12.5.11 Operating point for two pumps operating in series.

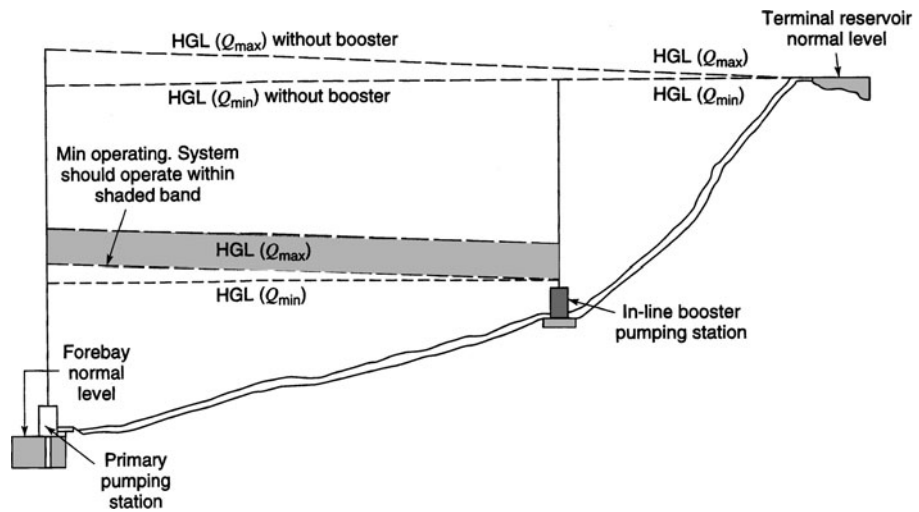


Figure 12.5.12 Transmission main with a primary pumping station and a booster pumping station (from Bosserman et al. (1998b)).

Table 12.5.1 Comparison of Water Pumping Station Types

Advantages	Disadvantages
Vertical wet well pumps	
Wide selection is available: axial flow (single stage), mixed flow (single and multistage), Francis turbine (single and multistage), and radial flow (turbine is single or multistage)	High superstructure to pull pumps or, at greater expense, pumps can be pulled through a hatch in the roof of a low superstructure by a truck crane parked outside, which may be cheaper than inside crane
Small floor area and small superstructure	Requires disconnecting the motor and pulling the pump for inspection or repair
Ground floor pump motors above flooding	Requires more shaft bearings
Pump suction always flooded; no priming	Priming may be required if air in the pump column causes problems
NPSH easily met	If idle pumps collect air in pump column, either (1) an automatic air vent valve at the discharge elbow or (2) priming must be installed
Ideal for deep installation and large variations in water level	
Vertical turbines are especially flexible in meeting head requirements by adding stages	
Wet well–dry well, horizontal pumps below water level (flooded suction)	
Pump types available include split-case centrifugal, end-suction overhung-shaft, and horizontally mounted axial-flow (propeller and mixed-flow) types	Large pump room floor area
Eliminates priming and air problems	Greater excavation
Low headroom requirement	Motors are subject to flooding
Easy maintenance and accessibility	Longer electric conduits
Service can be accomplished without disconnecting motor	Pumping stations are more costly due to additional floor area, access, lighting, ventilation, etc.
	Greater forced ventilation needed to cool motors
Horizontal pumps on floor above suction well	
Easy maintenance and accessibility	Requires priming equipment
Short electric conduits	Dependability (due to priming equipment) is reduced
Motors above floor level	Limits the choice of pumps to those for negative suction
Ventilation minimized	
Reduced excavation and below-ground construction; similar to wet pit	

Source: Klein and Sanks (1998).

Table 12.5.1 compares water pumping station types, describing the advantages and disadvantages of each type. Vertical mixed-flow or radial flow pumps are almost always used for pumping of wells. Table 12.5.2 compares well pumps. Bosserman (1999, 2000) provides additional detail on pump system hydraulic design.

Table 12.5.2 Comparison of Well Pumps

Advantages	Disadvantages
Self-priming centrifugals	
Capacity to 0.25 m ³ /s (4000 gal/min)	Limited to caisson, gallery, or wells with a water table less than 4.6 m (15 ft) below the pump
Vertical turbines (V/T)	
Most common type of well pump	Efficiency as low as 50% depending on the size and application
Motor or engine driven	
Diameter: 50 to > 1200 mm (2 to > 48 in)	
Capacities exceeding 0.6 m ³ /s (10,000 gal/min)	
Use for finished water and booster pumping is increasing	
Can be tailored for specific head by adding bowls	

(Continued)

Table 12.5.2 (continued)

Advantages	Disadvantages
Vertical turbines, lineshaft	
Minimum maintenance	Unsuited to crooked wells
Driver accessible	Somewhat noisy
Excellent for wells less than 90 m (300 ft) deep	Suitability is marginal at depths over 300 m (1000 ft). Even at depths less than 180 m (600 ft), shaft stretch wears impellers and bowls unless the thrust bearing is kept carefully adjusted
Vertical turbines, submersible	
Quiet, so they are suitable near hospitals, schools, and residences	Maintenance requires pulling the entire unit
Only solution for crooked wells	Regular maintenance is required
Practical at depths over 210 m (700 ft)	Seal problems may be severe
Water cooling is very effective	Long electric cables
No long-shaft problems	

Source: Klein and Sanks (1998).

EXAMPLE 12.5.1

Water at 60°F is pumped from reservoir A (surface elevation 20.0 ft) to reservoir B (surface elevation 50.0 ft), as shown in Figure 12.5.13(a). A 12-in diameter suction pipe (from reservoir A to pump) is 100 ft long and the discharge pipe (from pump to reservoir B) is 10.0 in in diameter and 1500 ft long. Assume that the friction factor for each pipe is 0.015. The suction pipe has an entrance loss coefficient of $K_e = 1.0$ and a check valve loss coefficient of $K_V = 2.5$. The discharge pipe has two gate valves $K_{GV} = 0.2$ fully open. The pump has the head-discharge curve and efficiency curves shown in Figure 12.5.13b. The pump is operated at 1800 rpm.

- (a) What is the flow rate?
- (b) Find the power required to drive the pump.

SOLUTION

(a) Begin by developing an expression for the system curve. Write the energy equation from reservoir surface A to reservoir surface B:

$$0 + 0 + 20 + h_p = 0 + 0 + 50 + \sum h_{L_{A-B}}$$

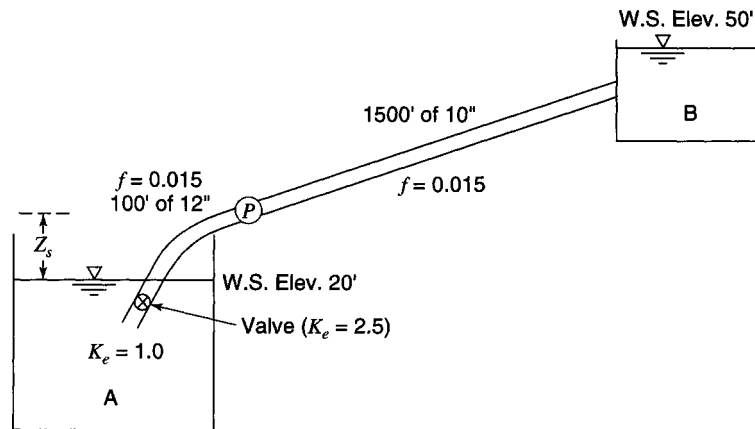
$$h_p = 30 + \frac{V_{12}^2}{2g} \left[K_{entr} + K_V + f_{12} \frac{L_{12}}{D_{12}} \right] + \frac{V_{10}^2}{2g} \left[2K_{GV} + f_{10} \frac{L_{10}}{D_{10}} + K_{exit} \right]$$

$$h_p = 30 + \frac{V_{12}^2}{2g} \left[1.0 + 2.5 + 0.015 \frac{100}{1.0} \right] + \frac{V_{10}^2}{2g} \left[2(0.2) + 0.015 \frac{1500}{10/12} + 1 \right]$$

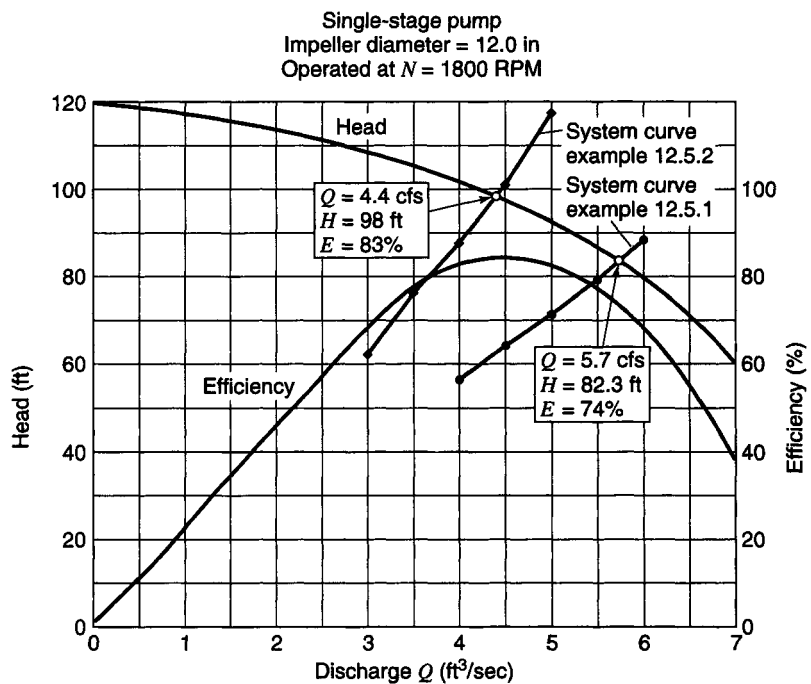
Next, obtain an expression for the system-head curve in terms of Q :

$$h_p = 30 + \frac{Q^2}{2g \left(\pi(1)^2/4 \right)^2} (5) + \frac{Q^2}{2g \left(\pi(10/12)^2/4 \right)^2} (28.4) = 30 + (0.126 + 1.482)Q^2$$

$$h_p = 30 + 1.61 Q^2 \text{ (system-head curve)}$$



(a)



(b)

Figure 12.5.13 (a) Figure for Example 12.5.1. (b) Characteristic curves for Examples 12.5.1 and 12.5.2.

Plot a few points of the system-head curve on the pump-characteristic curve:

Q (cfs)	h_p (ft)
4	55.8
5	70.2
6	88.0
5.5	78.7

From the plot, the operating point is at $Q = 5.7$ cfs at a head of 82.3 ft, and $e = 74\%$.

(b) The power required to drive the pump is computed using equation (12.2.12) with $Q = 5.7$ cfs, $h_p = 82.3$ ft, and $e = 74\%$

$$bhp = \frac{\gamma Q h_p}{550e} = \frac{(62.4 \text{ lb/ft}^3)(5.7 \text{ cfs})(82.3 \text{ ft})}{550(0.74)} = 71.9 \text{ HP}$$

EXAMPLE 12.5.2

The pump whose characteristic curves are shown in Figure 12.5.13b is used to pump water from reservoir A to reservoir B through 1000 ft of 8.00-in diameter pipe whose friction factor is 0.017 (as shown in Figure 12.5.14). Use the entrance loss coefficient of $K_e = 0.5$ and gate valve loss of $K_{GV} = 0.2$. (a) What flow rate does it pump? (b) What input power is required to drive the pump?

SOLUTION

(a) Write the energy equation:

$$\frac{p_A}{\gamma} + Z_A + \frac{V_A^2}{2g} + h_p = \frac{p_B}{\gamma} + Z_B + \frac{V_B^2}{2g} + \sum h_L$$

and solving for h_p :

$$h_p = 30 + \left[0.5 + 2(0.2) + 0.017 \frac{1000}{8/12} + 1.0 \right] \frac{V_{8''}^2}{2g}$$

Since h_p is needed as a function of Q , replace $V_{8''}$ with Q/A :

$$V_{8''} = \frac{Q}{A} = \frac{Q}{\frac{\pi}{4} \left(\frac{8}{12} \right)^2} = 0.349 Q$$

$$h_p = 30 + [1.9 + 25.5] \frac{Q^2}{2g(0.349)^2} = 30 + 3.49 Q^2$$

Calculate h_p required for a few values of Q and plot on the characteristic curve:

Q (cfs)	h_p (ft)
3	61.4
4	85.5
5	117.3
4.5	100.7
4.4	97.6

From the plot, $Q = 4.4$ cfs at a head of 98 ft and $e = 83\%$.

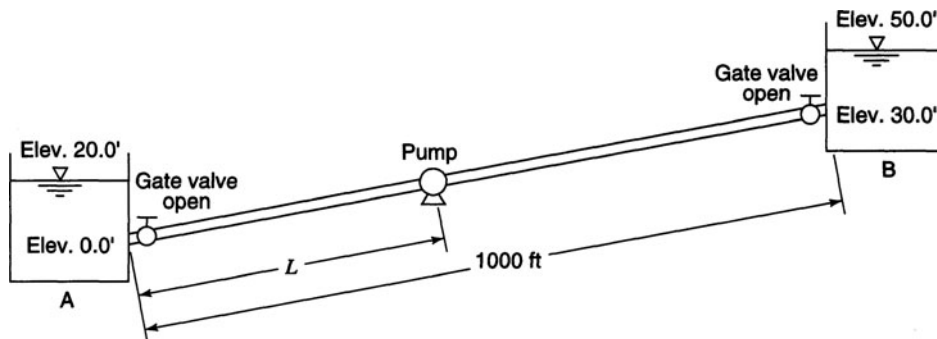


Figure 12.5.14 Example 12.5.2 pipe system.

(b) The power required to drive the pump is

$$bhp = \frac{\gamma Q h_p}{550(0.83)} = \frac{62.4(4.4)(98)}{550(0.83)} = 59 \text{ HP}$$

EXAMPLE 12.5.3

Two reservoirs A, and B, are connected by a long pipe that has characteristics such that the headloss through the pipe is expressible as $h_L = 20(Q/100)^2$, where h_L is in feet and Q is the flow rate in gpm. A single pump with the head-capacity curve for 1800 rpm given below is used to pump the water from A to B. (a) For the single pump, plot a curve showing delivery rate versus difference in elevation, Δz , for ΔZ ranging from -20 to $+80$ ft. (b) Repeat for a rotative speed of 2160 rpm.

Head (ft)	Flow rate (gpm)
100	0
90	110
80	180
60	250
40	300
20	340

SOLUTION

(a) Compute the system-head curve for $\Delta z = -20, 0, 40,$ and 80 ft.

Head (ft)	Flow rate (gpm)	h_L (ft)	System head ($\Delta Z + h_L$)			
			$\Delta Z = -20$	$\Delta Z = 0$	$\Delta Z = 40$	$\Delta Z = 80$
100	0	0	-20	0	40	80
90	110	24.2	4.2	24.2	64.2	104.2
80	180	64.8	44.8	64.8	104.8	144.8
60	250	125	105.0	125.0	165.0	205.0
40	300	180	160.0	180.0	220.0	260.0
20	340	231.2	211.2	231.2	271.2	311.2

Next plot the pump head-characteristic curve and the system-head curve for each ΔZ shown in Figure 12.5.15a. From this figure obtain the ΔZ -discharge relationship:

Δz (ft)	-20	0	40	80
Q_{1800} (gpm)	216	192	150	80

This relationship is plotted in Figure 12.5.15b.

(b) Repeat the above process for a rotative speed of 2160 for the same pump, using the affinity laws, equations (12.2.4) and (12.2.5):

$$Q_{2160} = Q_{1800} \left(\frac{2160}{1800} \right) = 1.2 \times Q_{1800}$$

$$H_{2160} = Q_{1800} \left(\frac{2160}{1800} \right)^2 = 1.44 \times H_{1800}$$

The resulting pump-head characteristic curve is

H_{2160} (ft)	144	129.6	115.2	86.4	57.6	28.8
Q_{2160} (gpm)	0	132	216	300	360	408

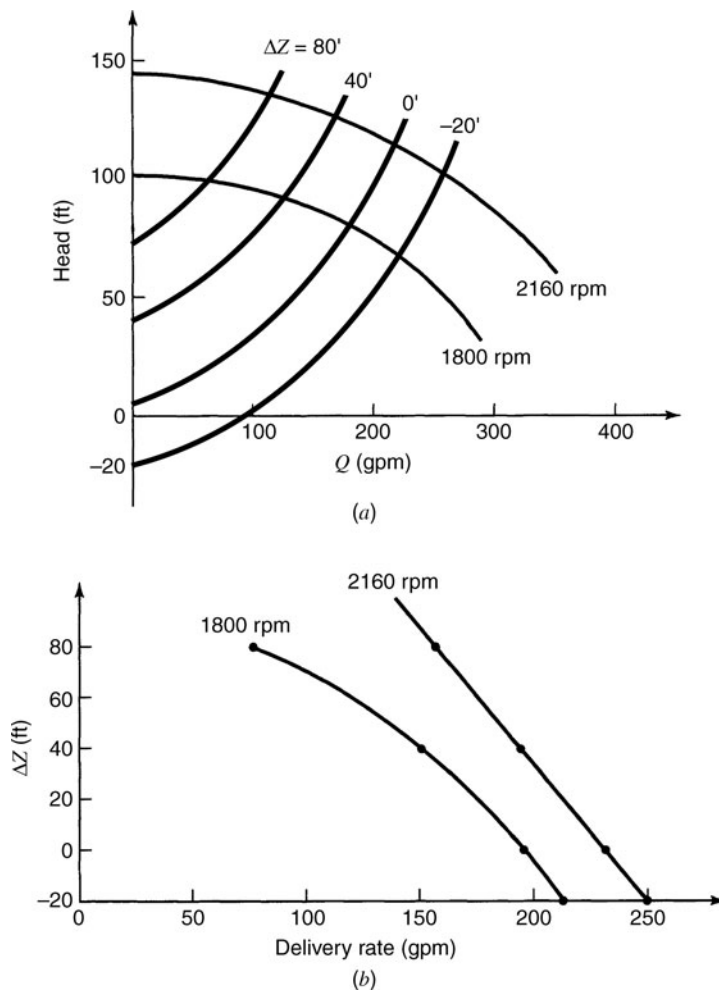


Figure 12.5.15 Example 12.5.3 results. (a) Head-characteristic and system-head curves; (b) Delivery-rate curve.

This is plotted in Figure 12.5.15a. Using this figure, the ΔZ -discharge relationship is

ΔZ (ft)	-20	0	40	80
Q_{2160} (gpm)	250	232	195	158

which is plotted in Figure 12.5.15b.

EXAMPLE 12.5.4

A water supply facility consists of two reservoirs, two pumps, and connecting pipe lines. A schematic of the installation is shown in Figure 12.5.16. Water is supplied to reservoir 2 from reservoir 1.

The elevation of the water surface of reservoir 1 is 100 ft and the elevation of the water surface of reservoir 2 is 250 ft. The suction and discharge lines are all located 10 ft below the water surfaces. The Darcy–Weisbach friction factor is 0.021 for all pipes. The pump characteristics are shown in Figure 12.5.17. Determine:

- (a) When both pumps are operating, what is the total discharge to reservoir 2?
- (b) What is the percentage of total discharge from line A?

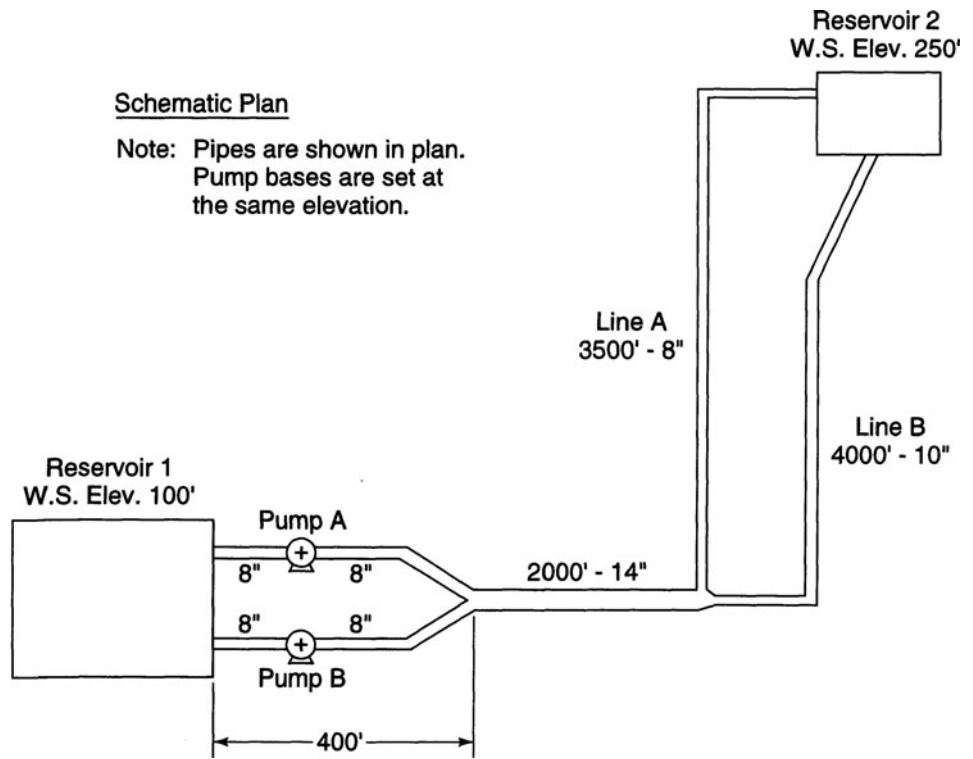


Figure 12.5.16 Example 12.5.4 system.

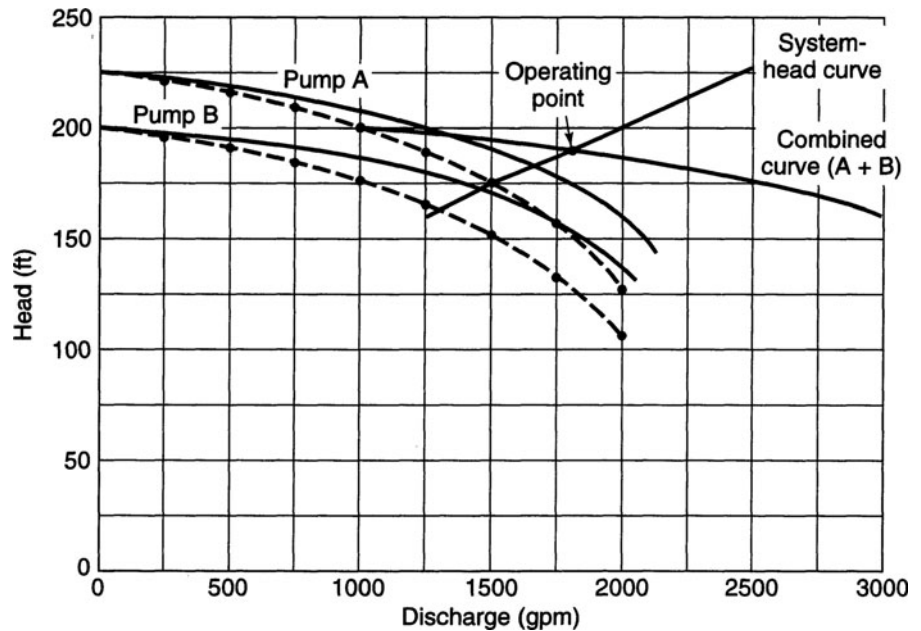


Figure 12.5.17 Pump characteristics for Example 12.5.4.

- (c) What is the discharge delivered through pump A (cfs or gpm)?
 (d) What is the efficiency of pump A if its input horsepower is 80?

SOLUTION

The first objective is to develop an expression for the system head losses. Develop an expression for headloss in terms of the discharges. Pipe 1 is the 400 ft pipe in which pump A is placed. Using the Darcy–Weisbach equation (12.1.6), the headloss due to friction is

$$h_{L_{f_1}} = f \frac{L V^2}{D 2g} = \left[\frac{8fL}{\pi^2 g D^5} \right] Q^2 = K_1 Q^2$$

$$K_1 = \frac{8(0.021)(400)}{\pi^2 g (8/12)^5} = 1.606$$

$$\text{so } h_{L_{f_1}} = 1.606 Q_1^2$$

Pipe 2 is the 400 ft pipe in which pump B is placed. This pipe is the same size as pipe A, so $h_{L_{f_2}} = 1.606 Q_2^2$.

Develop modified pump curves for pumps A and B to account for headlosses in the 400 ft 8 in pipes. (1 gpm = 2.23×10^{-3} ft³/s):

Q_1 (gpm)	Q_1 (cfs)	$h_{L_{f_1}} = 1.606 Q_1^2$
0	0	0
500	1.115	1.997
1000	2.230	7.986
1500	3.345	17.970
2000	4.460	31.946

These values are the same for pump B because its length and diameter are the same as pipe 1. The modified pump characteristic curves are shown in Figure 12.5.17. The combined pump curve for pumps A and B in parallel can now be developed using the modified pump curves, as shown in Figure 12.5.17.

Next determine the system-head curve for the remaining part of the system: $H_T = 250 - 100 + h_{L_f}$. The headloss due to

$$\begin{aligned} h_{L_f} &= h_{L_{f_3}} + h_{f_A} = h_{L_{f_3}} + h_{f_B} \\ &= K_3 Q_3^2 + K_A Q_A^2 = K_3 Q_3^2 + K_B Q_B^2 \end{aligned}$$

Pipe 3 is the 2000 ft, 14-in diameter pipe:

$$K_3 = \frac{8(0.021)(2000)}{\pi^2 g (14/12)^5} = 0.489$$

$$h_{L_{f_3}} = 0.489 Q_3^2$$

For pipe (line) A:

$$K_A = \frac{8(0.021)(3500)}{\pi^2 g (8/12)^5} = 14.050$$

$$h_{L_A} = 14.050 Q_A^2$$

For pipe (line) B:

$$K_B = \frac{8(0.021)(4000)}{\pi^2 g (10/12)^5} = 5.262$$

$$h_{L_B} = 5.262 Q_B^2$$

The total head is then

$$\begin{aligned} H_T &= 150 + h_{L_f} \\ &= 150 + 0.489Q_3^2 + 14.050Q_A^2 \\ H_T &= 150 + 0.489Q_3^2 + 5.262Q_B^2 \end{aligned}$$

Pipes A and B are parallel so that $h_{L/A} = h_{L/B}$:

$$\begin{aligned} 14.050Q_A^2 &= 5.262Q_B^2 \\ Q_A &= 0.612Q_B \\ Q_B &= 1.634Q_A \end{aligned}$$

From continuity,

$$\begin{aligned} Q_3 &= Q_A + Q_B = Q_A + 1.634Q_A \\ Q_3 &= 2.634Q_A \\ Q_A &= 0.380Q_3 \end{aligned}$$

Now H_T can be expressed in terms of one flow Q_3 , which is also the total flow:

$$\begin{aligned} H_T &= 150 + 0.489Q_3^2 + 14.050(0.380Q_3)^2 \\ &= 150 + 0.489Q_3^2 + 2.025Q_3^2 \\ &= 150 + 2.514Q_3^2 \\ &= 150 + 2.514Q^2 \end{aligned}$$

Next plot the system-head curve on the combined pump curve to find the point of operation, as given in Figure 12.5.17.

Q (gpm)	Q (cfs)	H_T (ft)
1500	3.345	178.1
2000	4.460	200.0
2500	5.575	228.1
3000	6.690	262.5

(a) The operating point is a flow of approximately 1850 gpm, so that the total discharge to the reservoir is 1850 gpm.

$$\text{Flow in line A, } Q_A = 0.380 Q_3 = 0.380(1850) = 703 \text{ gpm}$$

$$\text{Flow in line B, } Q_B = 1850 - 703 = 1147 \text{ gpm}$$

(b) The percentage of discharge in line A is 38 percent, or 703 gpm.

(c) From Figure 12.5.17, the discharge delivered through pump A is approximately 1200 gpm and through pump B is approximately 650 gpm.

(d) Efficiency of pump A is computed using

$$e_A = \frac{\gamma H_{\text{pump A}} Q_{\text{pump A}}}{bhp(550)}$$

$$Q_{\text{pump A}} = 1200 \text{ gpm} = 2.676 \text{ ft}^3/\text{s}$$

$$\begin{aligned} H_{\text{pump A}} &= H_T = 150 + 2.514Q^2 + 1.606(Q_{\text{pump A}})^2 \\ &= 150 + 2.514(4.126)^2 + 1.606(2.676)^2 \\ &= 205 \text{ ft} \end{aligned}$$

$$e_A = \frac{62.4(205)(2.676)}{80(550)} = 0.78$$

$$= 78\% \text{ efficiency}$$

12.6 NETWORK SIMULATION

12.6.1 Conservation Laws

The distribution of flows through a network under a certain *loading pattern* (demands as a function of time) must satisfy the conservation of mass and the conservation of energy. Figure 12.6.1 shows a simple example network consisting of 19 pipes. Assuming water is an incompressible fluid, by the conservation of mass, flow at each of the junction nodes must be conserved, that is,

$$\sum Q_{in} - \sum Q_{out} = \sum Q_{ext} \tag{12.6.1}$$

where Q_{in} and Q_{out} are the pipe flows into and out of the node, respectively, and Q_{ext} is the external demand or supply at the node.

For each *primary loop*, which is an independent closed path, the conservation of energy must hold; that is, the sum of energy or headlosses, h_L , minus the energy gains due to pumps, H_{pump} , around the loop must be equal to zero:

$$\sum_{i,j \in I_p} h_{L_{i,j}} - \sum_{k \in J_p} H_{pump,k} = 0 \tag{12.6.2}$$

where $h_{L_{i,j}}$ refers to the headloss in the pipe connecting nodes i and j , I_p is the set of pipes in the loop p , k refers to pumps, J_p is the set of pumps in loop p , and $H_{pump,k}$ is the energy added by pump k contained in the loop and summed over the number of pumps. Equation (12.6.2) must be written for all independent loops.

Energy must be conserved between *fixed-grade nodes* (FGN), which are points of known constant grade (elevation plus pressure head). If there are N_F such nodes, then there are $N_F - 1$ independent equations of the form

$$\Delta E_{FGN} = \sum_{i,j \in I_p} h_{L_{i,j}} - \sum_{k \in J_p} H_{pump,k} \tag{12.6.3}$$

where ΔE_{FGN} is the difference in total grade between the two FGNs. The total number of equations, $N_J + N_L + (N_F - 1)$, also defines the number of pipes in the network, in which N_J is the number of junction nodes and N_L is the total number of independent loops. The headloss due to pipe friction can be defined by equations (12.1.4), (12.1.7), or (12.1.9).

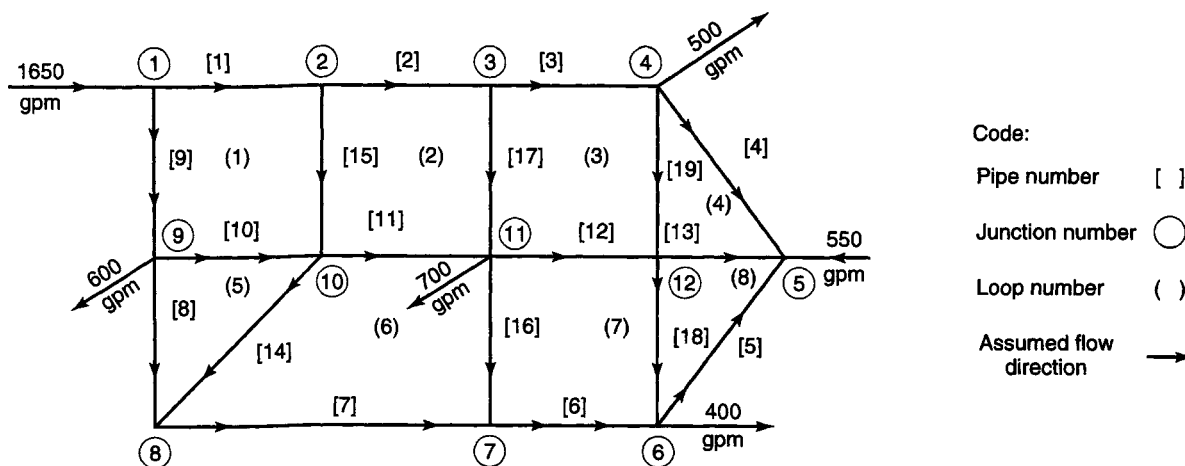


Figure 12.6.1 Example network (from Wood and Charles (1972)).

The change in head that occurs across each component is related to the flow through the component. By substituting the appropriate relationships for each component into the continuity and energy equations, it is possible to set up a system of nonlinear equations with the same number of unknowns. This set of equations can be solved by iterative techniques for the unknowns. Several computer programs have been written to automate these procedures. These models, called *network solvers* or *simulation models*, are now widely accepted and applied. This section presents the equations used to describe the relationships between headloss and flow and then discusses how each component is represented in a network simulation model.

The relationship between the added head H_{pump} and discharge Q is typically a concave curve with H_{pump} increasing as Q decreases, as shown in Figure 12.2.7. For the normal operating range, this curve is usually well approximated by a quadratic or exponential equation, that is:

$$H_{\text{pump}} = A Q^2 + B Q + H_c \quad (12.6.4)$$

or

$$H_{\text{pump}} = H_c - C Q^n \quad (12.6.5)$$

with A , B , and n being coefficients and H_c the *cutoff head* or maximum head. Also associated with a pump is an efficiency curve that defines the relationship of energy consumption and pump output (Figure 12.2.7). Efficiency e is a function of Q and appears as a function of power bhp from equation (12.2.12) as

$$e = \frac{QH_{\text{pump}}\gamma}{550(bhp)} \quad (12.6.6)$$

A pump achieves maximum efficiency at the *design* or *rated discharge*. Depending upon the simulation model a pump may also be described by a curve of constant power, bhp .

As noted in the previous section, the limiting constraints in the design problem are usually the pressure restrictions at the nodes. Since the headlosses in the system increase almost quadratically with the flow rates, as seen in the Hazen–Williams equation, less head is required for patterns with lower total demand and as the demand level increases, the head needed increases but faster than linearly. This relationship is a system curve from which the least-cost operation of pumps can be determined.

12.6.2 Network Equations

The governing conservation equations can be written in terms of the unknown nodal heads or the pipe flows using loop equations, head or nodal equations, or ΔQ equations. The loop or flow equations consist of the junction relationships written with respect to the N_p unknown flow rates. The component equations with pipe flows are substituted for h_L in the energy equations to form an additional $N_L + (N_F - 1)$ equations. This results in N_p equations written with respect to the N_p unknown flow rates.

The head or nodal equations use only flow continuity and consider the nodal heads as unknown rather than the pipe flows. In this case, additional equations are required for each pump and valve, increasing the total number of equations. For a link the difference in head between the connected nodes i and j is equal to h_{Lij} :

$$h_{Lij} = H_i - H_j \quad (12.6.7)$$

This relationship can be substituted into the Hazen–Williams equation, which in turn is rewritten and substituted for Q in the continuity equations.

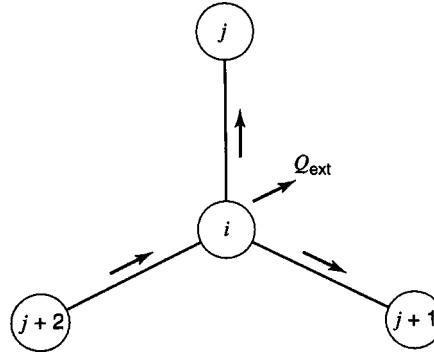


Figure 12.6.2 Node connected with three links.

The following *nodal equation* results for the node shown in Figure 12.6.2 with assumed flow directions defined by the arrows (flow from a junction is assumed negative):

$$-\left(\frac{H_i - H_j}{K_{p,i,j}}\right)^{0.54} - \left(\frac{H_i - H_{j+1}}{K_{p,i,j+1}}\right)^{0.54} + \left(\frac{H_{j+2} - H_i}{K_{p,j+2,i}}\right)^{0.54} - Q_{\text{ext},i} = 0 \quad (12.6.8)$$

where $K_{p,i,j}$ is the coefficient defined in equations (12.1.5), (12.1.8), and (12.1.10) for the pipe connecting nodes i and j . These nodal equations can be written for each junction and component node, resulting in a system of nonlinear equations with the same number of unknowns, which is the total number of nodal heads. Similarly, the equations for the other components can be rewritten with respect to the nodal heads. The nodal equations can be linearized in an iterative solution technique.

The ΔQ equations directly use the *loop equations* and implicitly ensure that the node equations are satisfied. In this formulation, the energy equation for each loop is written in terms of the flows:

$$\sum_{(i,j) \in I_p} K_{p,i,j} (Q_{i,j} + \Delta Q_{i,j})^n = 0 \quad (12.6.9)$$

12.6.3 Network Simulation: Hardy Cross Method

Several iterative solution approaches have been applied to solve the sets of equations described in the previous section, including the *linear theory method*, the *Newton–Raphson method* (Appendix A), and the *Hardy Cross technique*. Due to the nature of the equations, the linear theory method for solving the flow equations and the Newton–Raphson method for solving the node equations are considered most efficient.

The energy equation for each loop in a water distribution system expressed in equation (12.6.9) must be rewritten to take into account the direction of flow as

$$\sum h_{L,i,j} = \sum_{(i,j) \in I_p} K_{p,i,j} (Q_{i,j} + \Delta Q_{i,j}) |(Q_{i,j} + \Delta Q_{i,j})|^{n-1} = 0 \quad (12.6.10)$$

or

$$\sum h_{L,i,j} = \sum_{(i,j) \in I_p} K_{p,i,j} \text{sgn}(Q_{i,j} + \Delta Q_{i,j}) (Q_{i,j} + \Delta Q_{i,j})^n = 0 \quad (12.6.11)$$

This summation can be expanded as follows:

$$\sum K_{p,i,j} Q_{i,j}^n + \sum n K_{p,i,j} (\Delta Q_{i,j}) (Q_{i,j})^{n-1} + \left(\frac{n-1}{2}\right) \sum n K_{p,i,j} (\Delta Q_{i,j})^2 (Q_{i,j})^{n-2} + \dots = 0 \quad (12.6.12)$$

Assuming the $\Delta Q_{i,j}$ are small, the $(\Delta Q_{i,j})^2$ and succeeding terms can be neglected, leaving

$$\sum K_{p,i,j} Q_{i,j}^n + \sum n K_{p,i,j} \Delta Q_{i,j} (Q_{i,j})^{n-1} = 0 \quad (12.6.13)$$

The procedure, presented by Hardy Cross (1936), first assumes a flow distribution in a network. These assumed flows, however, may not satisfy the energy requirement (equation (12.6.10)). Therefore, the same correction $\Delta Q_{i,j}$ is made to all pipes in a particular loop p . To compute ΔQ , use the equation (12.6.13) rearranged as follows:

$$\sum K_{p,i,j} Q_{i,j}^n + \Delta Q_p \sum n K_{p,i,j} (Q_{i,j})^{n-1} = 0 \quad (12.6.14)$$

and solve for ΔQ_p :

$$\Delta Q_p = - \frac{\sum K_{p,i,j} Q_{i,j}^n}{\sum |n K_{p,i,j} Q_{i,j}^{n-1}|} \quad (12.6.15)$$

The numerator is the algebraic sum of the headloss in loop p with regard to the sign of the flow. For example, if positive is taken as clockwise, then pipes with flows in the clockwise direction have a positive headloss term $+K_{p,i,j} Q_{i,j}^n$ and pipes with flow in the counterclockwise direction have a negative headloss term, $-K_{p,i,j} Q_{i,j}^n$. The denominator is the absolute sum because in equation (12.6.15), ΔQ_p was given the same sign in all pipes in the loop.

The correction ΔQ_p for loop p is applied in the same sense to each pipe in the loop. In other words, if clockwise is positive, then ΔQ is added to flows in the clockwise direction and subtracted from flows in the counterclockwise direction. This method basically determines the ΔQ_p for each loop separately. Then the flows for each pipe are corrected using

$$Q_{i,j}(\text{new}) = Q_{i,j}(\text{old}) + \sum_{p \in M_p} \Delta Q_p \quad (12.6.16)$$

where M_p is the set of loops to which pipe i,j belongs. M_p has at most two loops because each pipe can only be common to one or two loops. The new flows are then used to repeat the process until the values of ΔQ_p are within a desired accuracy.

Basically the Hardy Cross method is an adaptation of the Newton iterative method. One equation (loop) is solved at a time before proceeding to the next equation (loop) during each iteration. This requires the assumption that all other ΔQ except ΔQ_p are known, i.e., $\Delta Q_1, \Delta Q_2, \dots, \Delta Q_{p-1}, \Delta Q_{p+1} \dots$ are temporarily known, as described previously.

Dropping subscripts except for p to represent the loop yields

$$\sum h_L = \sum K \text{sgn}(Q + \Delta Q_p) (Q + \Delta Q_p)^n = 0 \quad (12.6.17)$$

Applying Newton's method (Appendix A) to the above equation, we find that the function $f(\Delta Q_p)$ is

$$f(\Delta Q_p) = \sum K \text{sgn}(Q + \Delta Q) (Q + \Delta Q_p)^n - \sum h_L \quad (12.6.18)$$

and the derivative is

$$f'(\Delta Q_p) = n \sum K (Q + \Delta Q_p)^{n-1} \quad (12.6.19)$$

Note that $d[\text{sgn}f(x)f(x)^n]/dx = nf(x)^{n-1}df(x)/dx$.

Applying Newton's method yields the iterative equation

$$x(k+1) = x(k) - \frac{f(x(k))}{f'(x(k))} \quad (12.6.20)$$

for the k th iteration; then

$$\Delta Q_p(k+1) = \Delta Q_p(k) - \frac{f(\Delta Q_p(k))}{f'(\Delta Q_p(k))} \quad (12.6.21)$$

The Hardy Cross method commonly applies one iterative correction to each equation (loop) before proceeding to the next equation (loop). Several variations of this exist in the literature. After applying one iterative correction to all equations (loops), the process is repeated until convergence is achieved. It is also common to adjust the flow rates in all pipes in the loop immediately upon computing each ΔQ . Therefore, each equation $f(\Delta Q_p(k+1)) = 0$ is evaluated with all previous ΔQ , i.e., $\Delta Q_p(k) = 0$, so that equation (12.6.21) reduces to

$$\Delta Q_p(k+1) = - \frac{f(\Delta Q_p(k))}{f'(\Delta Q_p(k))} \quad (12.6.22)$$

Upon substituting equations (12.6.18) and (12.6.19), the new $\Delta Q_p(k+1)$ or ΔQ_p (new) is computed using

$$\Delta Q_p(\text{new}) = - \frac{\sum K \text{sgn}(Q + \Delta Q_p)(Q + \Delta Q_p)^n}{n \sum K(Q + \Delta Q_p)^{n-1}} \quad (12.6.23)$$

Steps of the Hardy Cross method are summarized below (modified from Jeppson, 1976):

1. Determine the values of K using equation (12.1.5), (12.1.8), or (12.1.10).
2. Start with initial guesses of the flow rate in each pipe such that continuity at all junctions are satisfied; assume initial $\Delta Q_p = 0$ for all loops.
3. Compute sum of headlosses around a loop, applying the appropriate sign, $\text{sgn}(Q + \Delta Q_p)$. This sum is the numerator in equation (12.6.23). If the direction of movement around the loop is opposite to the direction of flow, then $\text{sgn}(Q + \Delta Q_p)$ is negative.
4. Compute the denominator of equation (12.6.23) for the same loop.
5. Solve equation (12.6.23) for ΔQ_p (new).
6. Repeat steps 3 through 5 for each loop in the network.
7. Define new flows using equation (12.6.16).
8. Repeat steps 3 through 7 iteratively until all the ΔQ_p computed during an iteration are small enough to be insignificant.

EXAMPLE 12.6.1

Determine the flow rate in each pipe for the simple network in Figure 12.6.3. Assume that fully turbulent flow exists for all pipes and the Darcy–Weisbach friction factor is $f = 0.02$. Use the Hardy Cross method.

SOLUTION

Step 1

$$\text{Using equation (12.1.7), } h_L = KQ^2 = \left[\frac{8fL}{\pi^2 g D^5} \right] Q^2 = \left[\frac{8fL}{313.4 D^5} \right] Q^2$$

$$\text{so } K = \left(\frac{L}{1959 D^5} \right)$$

Determining the K -values yields

$$K_{AB} = \left[\frac{5000}{1959(2)^5} \right] = 0.079$$

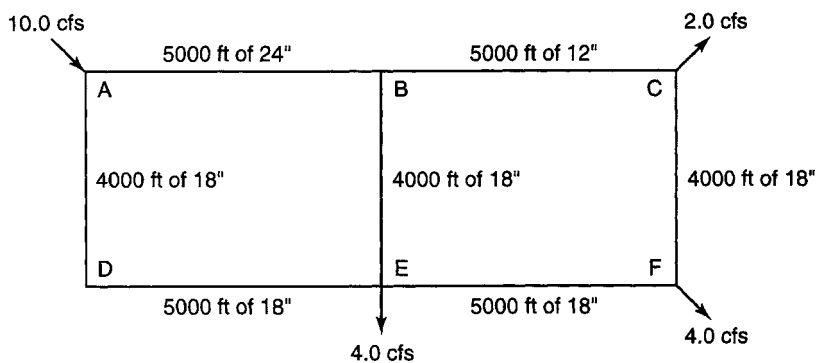


Figure 12.6.3 Pipe network for Example 12.6.1.

$$K_{BC} = 2.520$$

$$K_{AD} = K_{BE} = K_{CF} = 0.265$$

$$K_{DE} = K_{EF} = 0.332$$

Step 2 The initial guesses of flow for each pipe are shown in Figure 12.6.4a.

Steps 3, 4, and 5 Consider loop 1 first and compute ΔQ_1 :

$$\Delta Q_1 = -\frac{1}{2} \frac{[K_{AD}Q_{AD}^2 + K_{DE}Q_{DE}^2 - K_{BE}Q_{BE}^2 - K_{AB}Q_{AB}^2]}{[K_{AD}Q_{AD} + K_{DE}Q_{DE} + K_{BE}Q_{BE} + K_{AB}Q_{AB}]}$$

$$\Delta Q_1 = -\frac{1}{2} \frac{[(0.265)(3.8)^2 + (0.332)(3.8)^2 - (0.265)(4.0)^2 - (0.079)(6.2)^2]}{[(0.265)(3.8) + (0.332)(3.8) + (0.265)(4.0) + (0.079)(6.2)]}$$

$$\Delta Q_1 = -\frac{1.344}{7.637} = -0.176$$

Step 6 Next consider remaining loop, loop 2, to compute ΔQ_2 :

$$\Delta Q_2 = -\frac{1}{2} \frac{[K_{BE}Q_{BE}^2 + K_{EF}Q_{EF}^2 - K_{CF}Q_{CF}^2 - K_{BC}Q_{BC}^2]}{[K_{BE}Q_{BE} + K_{EF}Q_{EF} + K_{CF}Q_{CF} + K_{BC}Q_{BC}]}$$

$$\Delta Q_2 = -\frac{1}{2} \frac{[(0.265)(4.0)^2 + (0.332)(3.8)^2 - (0.265)(0.2)^2 - (2.520)(2.2)^2]}{[(0.265)(4.0) + (0.332)(3.8) + (0.265)(0.2) + (2.520)(2.2)]}$$

$$\Delta Q_2 = -\frac{-3.173}{15.837} = 0.200$$

Step 7 Define new flows for next iteration:

$$Q_{AD} = 3.8 + (-0.176) = 3.624$$

$$Q_{DE} = 3.8 + (-0.176) = 3.624$$

$$Q_{BE} = 4.0 - \Delta Q_1 + \Delta Q_2 = 4.0 - (-0.176) + 0.200 = 4.376$$

$$Q_{AB} = 6.2 - (-0.176) = 6.376$$

$$Q_{BC} = 2.2 - 0.200 = 2.000$$

$$Q_{EF} = 3.8 + 0.200 = 4.000$$

$$Q_{CF} = 0.2 - 0.200 = 0.000$$

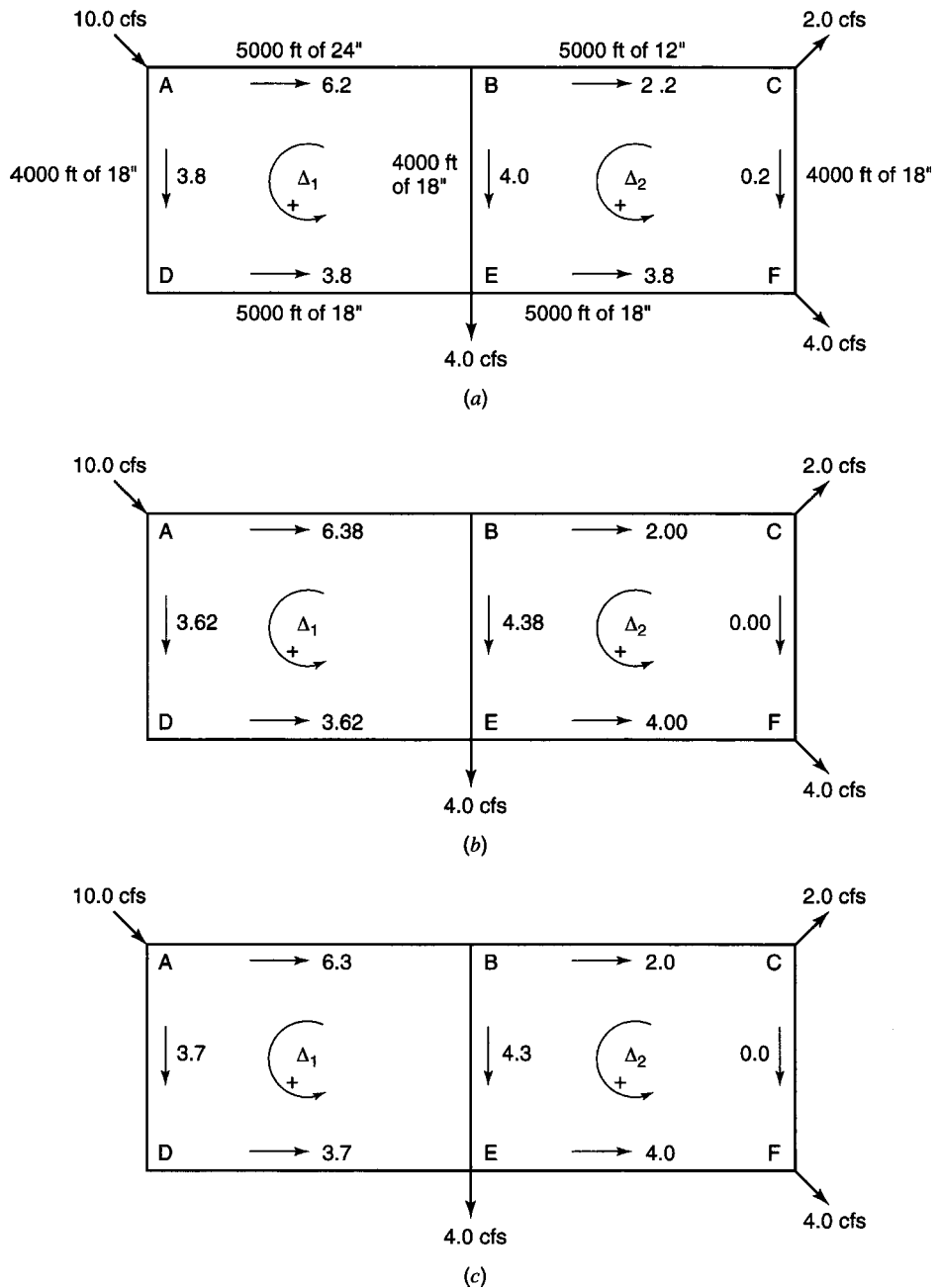


Figure 12.6.4 Solution results for (a) One; (b) Two; and (c) Three iterations for Example 12.6.1.

Steps 3–6 For the next iteration, repeat steps 3–6 with the new flows determined in Step 7 and shown in Figure 12.6.4b:

$$\Delta Q_1 = -\frac{1[-0.446]}{2[3.827]} = 0.058$$

$$\Delta Q_2 = -\frac{1[0.307]}{2[7.528]} = -0.020$$

Step 7 Define new flows for next iteration:

$$\begin{aligned}Q_{AD} &= 3.624 + 0.058 = 3.682 \\Q_{DE} &= 3.624 + 0.058 = 3.682 \\Q_{BE} &= 4.376 - 0.058 + (-0.02) = 4.298 \\Q_{AB} &= 6.376 - 0.058 = 6.318 \\Q_{BC} &= 2.000 - (-0.020) = 2.020 \\Q_{EF} &= 4.000 + (-0.020) = 3.980 \\Q_{CF} &= 0.000 - (-0.020) = 0.020\end{aligned}$$

For the next iteration, repeat steps 3–6 with the new flows determined above and shown in Figure 12.6.3c:

$$\begin{aligned}\Delta Q_1 &= \frac{-[0.045]}{2[3.836]} = -0.006 \text{ cfs} \\ \Delta Q_2 &= \frac{-[-0.128]}{2[7.556]} = 0.008 \text{ cfs}\end{aligned}$$

The above corrections ΔQ_1 and ΔQ_2 are insignificant, so the final flows are those shown in Figure 12.6.4c.

EXAMPLE 12.6.2

For the network in example 12.6.1, determine the headloss from A to F.

SOLUTION

There are several sets of pipes that represent a path from node A to node F. Each of these should result in the same headloss.

$$\begin{aligned}\text{(a)} \\ h_{L_{A-F}} &= \sum h_{L_{f_i}} = h_{L_{AD}} + h_{L_{DE}} + h_{L_{EF}} \\ &= (K_{AD}Q_{AD}^2 + K_{DE}Q_{DE}^2 + K_{EF}Q_{EF}^2) \\ &= [(0.265)(3.682)^2 + (0.332)(3.682)^2 + (0.332)(3.980)^2] \\ h_{L_{A-F}} &= 13.35 \text{ ft}\end{aligned}$$

$$\begin{aligned}\text{(b)} \\ \text{or } h_{L_{A-F}} &= h_{L_{AB}} + h_{L_{BE}} + h_{L_{EF}} \\ &= K_{AB}Q_{AB}^2 + K_{BE}Q_{BE}^2 + K_{EF}Q_{EF}^2 \\ &= [(0.079)(6.318)^2 + (0.265)(4.298)^2 + (0.332)(3.980)^2] \\ h_{L_{A-F}} &= 13.31 \text{ ft}\end{aligned}$$

$$\begin{aligned}\text{(c)} \\ \text{or } h_{L_{A-F}} &= h_{L_{AB}} + h_{L_{BC}} + h_{L_{CF}} = K_{AB}Q_{AB}^2 + K_{BC}Q_{BC}^2 + K_{CF}Q_{CF}^2 \\ &= [(0.079)(6.318)^2 + (2.520)(2.020)^2 + (0.265)(0.020)^2] \\ h_{L_{A-F}} &= 13.44 \text{ ft}\end{aligned}$$

Every path should have the same headloss ($h_{L_{A-F}}$) from A–F; the differences are due to roundoffs.

Pumps and Pseudo Loops

When pumps are included in a closed loop, then the conservation of energy (equation (12.6.2)) can be expressed as

$$\sum KQ^n - \sum h_p = 0 \quad (12.6.24)$$

where h_p is the pump head. Energy must be conserved between two points of known energy, called fixed-grade nodes (FGN). If there are N_f fixed-grade nodes, then $N_f - 1$ independent equations are in the form of

$$\sum KQ^n - \sum h_p = \Delta E_{FGN} \tag{12.6.25}$$

or

$$\sum KQ^n - \sum h_p - \Delta E_{FGN} = 0 \tag{12.6.26}$$

where ΔE_{FGN} is the change in energy between the two fixed-grade nodes.

EXAMPLE 12.6.3

Figure 12.6.5 shows a simple network with two closed loops and a pseudo loop between the two fixed-grade nodes. Write out the equations for the ΔQ corrections for each loop of the system.

SOLUTION

A ΔQ correction is made for the pseudo loop in addition to the two closed loops. Clockwise is the positive direction. The ΔQ for the pseudo loop based on equation (12.6.22) is expressed as

$$\Delta Q_{\text{pseudo loop}} = \frac{[K_4 Q_4^2 - (135 - 6Q_4^2) + K_3 Q_3^2 - K_2 Q_2^2 - K_1 Q_1^2 - E_{FGN,2} + E_{FGN,1}]}{[nK_4 Q_4 + 2(6)Q_4 - nK_3 Q_3 - nK_2 Q_2 - nK_1 Q_1]}$$

The corrections for loops I and II are respectively,

$$\Delta Q_I = \frac{[K_2 Q_2^2 + K_6 Q_6^2 - K_8 Q_8^2 - K_5 Q_5^2]}{[nK_2 Q_2 - nK_6 Q_6 - nK_8 Q_8 - nK_5 Q_5]}$$

and

$$\Delta Q_{II} = \frac{[K_7 Q_7^2 - K_6 Q_6^2 - K_3 Q_3^2]}{[nK_7 Q_7 + nK_6 Q_6 + nK_3 Q_3]}$$

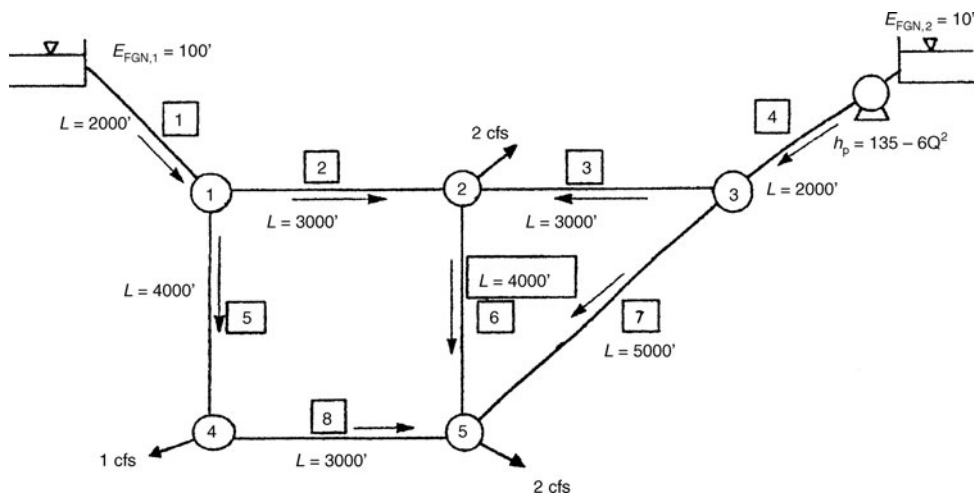


Figure 12.6.5 Example network (all pipes have a diameter of 1 ft and friction factors of 0.032) (Lansley and Mays, 2000).

12.6.4 Network Simulation: Linear Theory Method

The linear theory method was presented by Wood and Charles (1972) for simple networks and later extended to include pumps and other appurtenances (Wood, 1980). Comparing the other approaches, the Newton–Raphson method may converge more quickly than the linear method for small systems, whereas it may converge very slowly for large networks compared to the linear method (Wood and Charles, 1972). The linear theory method, however, has the capability to analyze all components, with more flexibility in the representation of pumps and better convergence properties. The University of Kentucky model, KYPIPE, by Wood (1980) and Wood et al. (1995) is a widely used and accepted program based on the linear theory method.

The linear theory method solves for the discharge Q using the *path (energy) equations*,

$$\Delta E = \sum h_L + \sum h_{Lm} - \sum H_{\text{pump}} \quad (12.6.27)$$

and using equation (12.1.3) for friction losses and equation (12.6.4) or (12.6.5) for the pump curve:

$$\Delta E = \sum (K_p Q^n + K_m Q^2) - \sum (A Q^2 + B Q + H_c) \quad (12.6.28)$$

where $n = 1.85$ for the Hazen–Williams equation, $n = 2$ for the Darcy–Weisbach equation, and $n = 2$ for Manning’s equation (which is valid for fully turbulent flow only).

The pressure head (grade) difference in a pipe section with a pump for $Q = Q_r$ can be expressed as

$$f(Q_r) = K_p Q_r^n + K_m Q_r^2 - (A Q_r^2 + B Q_r + H_c) \quad (12.6.29)$$

where r represents the r th iteration. The gradient $\partial f / \partial Q$ evaluated at Q_r is

$$G_r = \left[\frac{\partial f}{\partial Q_r} \right] = n K_p Q_r^{n-1} + 2 K_m Q_r - (2 A Q_r + B) \quad (12.6.30)$$

The nonlinear energy equations are linearized in terms of the unknown flow rate Q_{r+1} in each pipe using

$$\begin{aligned} f(Q_{r+1}) &= f(Q_r) + \left[\frac{\partial f}{\partial Q} \right]_{Q_r} (Q_{r+1} - Q_r) \\ &= f(Q_r) + G_r (Q_{r+1} - Q_r) \end{aligned} \quad (12.6.31)$$

The *path equations* (either from one fixed grade to another one or around a loop) can be written as

$$\Delta E = \sum f(Q_{r+1}) = \sum f(Q_r) + \sum G_r (Q_{r+1} - Q_r) \quad (12.6.32)$$

where the \sum refers to summing over each pipe and $\Delta E = 0$, so that

$$\sum G_r Q_{r+1} = \sum (G_r Q_r - f(Q_r)) \quad (12.6.33)$$

For a path between two fixed-grade nodes, ΔE is a constant; then by equation (12.6.32) we find

$$\sum G_r Q_{r+1} = \sum (G_r Q_r - f(Q_r)) + \Delta E \quad (12.6.34)$$

Equations (12.6.33) and/or (12.6.34) are used to formulate $N_L + (N_F - 1)$ equations and are combined with the N_j continuity equations (12.6.1) to form a set of $N_p = N_L + (N_F - 1) + N_j$ linear equations (number of pipes) in terms of the unknown flow rate Q_{r+1} in each pipe. Using a set of initial flow rates Q_r in each pipe, the system of linear equations is solved for Q_{r+1} using a matrix procedure. This new set of flow rates Q_{r+1} is used as the known values to obtain a second solution of the linear equations. This procedure continues until the change in flow rates $|Q_{r+1} - Q_r|$ is insignificant and meets some convergence criterion.

EXAMPLE 12.6.4

Develop the system of equations to solve for the pipe flows of the 19-pipe water distribution network shown in Figure 12.6.1 (example adapted from Wood and Charles (1972)). The equations are to be based upon the linear theory method using loop equations.

SOLUTION

Let $Q_1, Q_2 \dots$ represent the flow in pipe 1, pipe 2. . . .

Conservation of flow at each node:

$$\begin{array}{ll} \text{Node 1: } Q_1 + Q_9 = 1,650 & \text{Node 7: } Q_7 + Q_{16} - Q_6 = 0 \\ \text{Node 2: } Q_1 - Q_2 - Q_{15} = 0 & \text{Node 8: } Q_8 + Q_{14} - Q_7 = 0 \\ \text{Node 3: } Q_2 - Q_3 - Q_{17} = 0 & \text{Node 9: } Q_9 - Q_{10} - Q_8 = 600 \\ \text{Node 4: } Q_3 - Q_4 - Q_{19} = 500 & \text{Node 10: } Q_{10} + Q_{15} - Q_{11} - Q_{14} = 0 \\ \text{Node 5: } Q_4 + Q_5 + Q_{13} = -550 & \text{Node 11: } Q_{11} + Q_{17} - Q_{12} - Q_{16} = 700 \\ \text{Node 6: } Q_{18} + Q_6 - Q_5 = 400 & \text{Node 12: } Q_{12} + Q_{19} - Q_{13} - Q_{18} = 0 \end{array}$$

Only 11 of the 12 conservation of flow constraints are needed.

Conservation of energy (loop equations):

$$\begin{array}{l} \text{Loop 1: } K_{p,1}Q_1^n + K_{p,15}Q_{15}^n - K_{p,10}Q_{10}^n - K_{p,9}Q_9^n = 0 \\ \text{Loop 2: } K_{p,2}Q_2^n + K_{p,17}Q_{17}^n - K_{p,11}Q_{11}^n - K_{p,15}Q_{15}^n = 0 \\ \text{Loop 3: } K_{p,3}Q_3^n + K_{p,19}Q_{19}^n - K_{p,12}Q_{12}^n - K_{p,17}Q_{17}^n = 0 \\ \text{Loop 4: } K_{p,4}Q_4^n - K_{p,13}Q_{13}^n - K_{p,19}Q_{19}^n = 0 \\ \text{Loop 5: } K_{p,10}Q_{10}^n + K_{p,14}Q_{14}^n - K_{p,8}Q_8^n = 0 \\ \text{Loop 6: } K_{p,11}Q_{11}^n + K_{p,16}Q_{16}^n - K_{p,7}Q_7^n - K_{p,14}Q_{14}^n = 0 \\ \text{Loop 7: } K_{p,12}Q_{12}^n + K_{p,18}Q_{18}^n - K_{p,6}Q_6^n - K_{p,16}Q_{16}^n = 0 \\ \text{Loop 8: } K_{p,13}Q_{13}^n - K_{p,5}Q_5^n - K_{p,18}Q_{18}^n = 0 \end{array}$$

The above eight conservation of energy equations are linearized using $k = K_p Q^{n-1}$:

$$\begin{array}{l} \text{Loop 1: } k_1Q_1 + k_{15}Q_{15} - k_{10}Q_{10} - k_9Q_9 = 0 \\ \text{Loop 2: } k_2Q_2 + k_{17}Q_{17} - k_{11}Q_{11} - k_{15}Q_{15} = 0 \\ \text{Loop 3: } k_3Q_3 + k_{19}Q_{19} - k_{12}Q_{12} - k_{17}Q_{17} = 0 \\ \text{Loop 4: } k_4Q_4 - k_{13}Q_{13} - k_{19}Q_{19} = 0 \\ \text{Loop 5: } k_{10}Q_{10} + k_{14}Q_{14} - k_8Q_8 = 0 \\ \text{Loop 6: } k_{11}Q_{11} + k_{16}Q_{16} - k_7Q_7 - k_{14}Q_{14} = 0 \\ \text{Loop 7: } k_{12}Q_{12} + k_{18}Q_{18} - k_6Q_6 - k_{16}Q_{16} = 0 \\ \text{Loop 8: } k_{13}Q_{13} - k_5Q_5 - k_{18}Q_{18} = 0 \end{array}$$

This system of 19 equations (11 conservation of flow equations and eight energy equations) can be solved for the 19 unknown discharges.

12.6.5 Extended-Period Simulation

The equations described above are the relationships between flow and head for the main components in the network and can be solved for a single demand pattern operating in a steady state. An *extended-period simulation* (EPS) analyzes a series of demand patterns in sequence. The purpose of an EPS is to determine the variation in tank levels and their effect on the pressures in the system.

The water surface elevation in a tank varies depending upon the pressure distribution at the node at which the tank level is connected to the system.

Unlike a single-period analysis where a tank level is considered fixed, in an EPS the tank levels change with progressive simulations to take into account inflow and outflow. In an extended period simulator, flows are assumed constant throughout a subperiod. Tank levels, which are modeled as FGNs, are adjusted using simple continuity at the end of the subperiod and these new levels are then used as the fixed grades for the next subperiod. The accuracy of the simulation is dependent upon the length of the subperiods and the magnitude of flows to and from the tank.

12.7 MODELING WATER DISTRIBUTION SYSTEMS

12.7.1 Computer Models

Numerous computer models (computer software) have been developed to solve the network simulation equations. The types of models can be classified into four basic types:

- Steady-state hydraulic models
- Extended-period hydraulic simulation models
- Water quality simulation models
- Optimization models

The previous sections in this chapter have explained the mathematics and algorithms for the steady-state and extended-period simulation models. Section 12.7.4 briefly explains the water quality fundamentals in more detail.

Two of the more widely used models in the United States are the EPANET model and the KYP-IPE2 (KYQUAL) model. Each of these models can simulate steady-state conditions, extended period simulation, and water quality.

EPANET (Rossman et al., 1993; Rossman, 1994; and Rossman, 2000) is a model developed by the U.S. Environmental Protection Agency that can be used for steady-state and extended-period hydraulic simulation and for water quality simulation. This model is an explicit time-driven water-quality modeling algorithm for tracking transient concentrations of substances in pipe networks. “Explicit” refers to the fact that the calculation of concentrations at a given time are directly obtained from the previously known concentration front. Substance transport is simulated directly in the modeling process. Substance mass is allocated to discrete volume elements in each pipe during each time step. Reaction occurs in each element and mass is transported between elements. Mass and flow volumes are mixed together at downstream nodes. The algorithm used for the water-quality modeling is referred to as a *discrete volume element method* (DVEM). The algorithm used to solve the hydraulic equations is a gradient algorithm.

KYPIPE2/KYQUAL (Wood et al., 1995) is a model developed at the University of Kentucky. The original model KYPIPE was developed for steady-state and extended-period hydraulic simulation. The KYQUAL model performs the water-quality simulation. The network-simulation algorithm is based upon the linear theory method presented in section 12.6.4.

12.7.2 Calibration

Calibration is the process of adjusting model input data so that simulated hydraulics and water quality results adequately reflect observed field data. Calibration is an extremely important part of the modeling process of distribution systems. The process of calibration can be difficult, time-consuming, and costly. An accurate representation of the system and components is a must adequately to perform the calibration process. Two of the major sources of error in simulation analysis for hydraulics are demands (loading distribution) and pipe-carrying capacity. The importance of each of these error sources will depend on the network application.

To simulate the hydraulics, fire-flow pressure measurements are traditionally used. This involves measuring pressures and flow in isolated pipes or pipe sections. Use the measured values in a simulation model and adjust pipe friction factors followed by a simulation. Continue this process until friction factors are selected that provide simulated pressures and flows that reflect the measured data. Other adjustments that may be necessary are adjusting pressure-regulating valves (PRVs and PSVs), redistributing demands, adjusting pipe diameters, and adjusting pump lifts. Calibration can also be performed by comparing measured water surface elevations in tanks with simulated elevations in tanks. A hydraulic model should first be calibrated with field data before being used in any design or evaluation process.

Water-quality tracers such as fluoride can be used for the calibration process. These tracers are added to the distribution system followed by observation of the concentration in various parts of the system. Adjustments of the model parameters are made followed by simulation, and continued until simulated and observed concentrations match. Refer to Ormsbee and Lingireddy (2000) for a detailed discussion of the calibration of water distribution system models.

12.7.3 Application of Models

The following steps are used in applying simulation models (Clark et al., 1988):

1. *Model selection*—Definition of model requirements and selection of a model (hydraulic and/or water quality) that fits desired requirements.
2. *Network representation*—Representation of the distribution system components in the model.
3. *Calibration*—Adjustment of model parameters so that predicted results adequately reflect observed field data.
4. *Verification*—Independent comparison of model and field results to verify the adequacy of the model representation.
5. *Problem definition*—Definition of the specific design or operational problem to be studied and incorporation of the situation (i.e., demands, system operation) into the model.
6. *Model application*—Use of the model to study the specific problem/situation.
7. *Analysis/display of results*—Following the application of the model, the results should be displayed and analyzed to determine the reasonableness of the results and to translate the results into a solution to the problem.

12.7.4 Water Quality Modeling

This section provides a very brief description of the fundamentals of dynamic water quality simulation for water distribution systems. Models such as EPANET and KYQUAL are designed to track the fate of dissolved substances flowing through a pipe network over time. The interest in water quality modeling in water distribution systems in the United States is a result of the Safe Drinking Water Act of 1974 (SDWA) and its amendment of 1986 (SDWAA). These require the U.S. Environmental Protection Agency to establish *maximum contaminant level* (MCL) goals for each contaminant that may have adverse health effects on humans. As a result of the SDWAA, there has been increased interest in understanding the variation of water quality in municipal water distribution systems. The following discussion is based upon the procedure used in EPANET.

Water quality models use flows determined from the hydraulic simulation for each time step to solve the conservation of mass equation for the substance within each link connecting nodes i and j , given as

$$\frac{\partial C_{ij}}{\partial t} = -\frac{q_{ij}}{A_{ij}} \left(\frac{\partial C_{ij}}{\partial x_{ij}} \right) + \theta(C_{ij}) \quad (12.7.1)$$

where $C_{i,j}$ is the concentration of the substance in link i, j as a function of distance $x_{i,j}$ and time t (i.e., $C_{i,j} = C_{i,j}(x_{i,j}, t)$ (mass/ft³), $q_{i,j}$ is the flow rate in link i, j at time t (ft³/sec), $A_{i,j}$ is the cross-sectional area of link i, j (ft²), and $\theta(C_{i,j})$ is the reaction rate of the substance in link i, j (mass/ft³/day).

Equation (12.7.1) is solved with a known initial condition (at time $t = 0$) and the following boundary condition at the beginning of link i, j (where $x_{i,j} = 0$):

$$C_{i,j}(0, t) = \frac{\sum_k q_{ki} C_{ki}(L_{ki}, t) + M_i}{\sum_k q_{ki} + Q_{si}} \quad (12.7.2)$$

where M_i is the mass of substance introduced by an external source at node i , Q_{si} is the flow rate of the source, and $L_{k,i}$ is the length of link k, i . The summations are over all links k, i that have flow into node i of link i, j . The above boundary condition for link i, j depends on the end node concentration of all links k, i that deliver flow into link i, j . EPANET uses the discrete volume element method (DVEM) to numerically solve equations (12.7.1) and (12.7.2) (Rossman et al., 1993).

The rate of reaction of a constituent can be described through first-order kinetics. Reactions can occur in the bulk flow and with material along the pipe wall. The equation for first-order kinetics for both reactions is expressed as

$$\theta(C) = -k_b C - \left(\frac{k_f}{R_H} \right) (C - C_w) \quad (12.7.3)$$

where k_b is the first-order bulk reaction rate constant (1/sec), k_f is the mass transfer coefficient between the bulk flow and pipe wall (ft/sec), R_H is the hydraulic radius of the pipe (ft), and C_w is the concentration of the substance at the wall (mass/ft³). The term $k_b C$ in equation (12.7.3) is the bulk flow reaction and the term $(k_f/R_H)(C - C_w)$ is the rate at which the substance is transported between the bulk flow and reaction on the pipe wall.

Assuming a first-order reaction rate at the wall and assuming no accumulation occurs, the mass balance for the wall reaction is

$$k_f(C - C_w) = k_w C_w \quad (12.7.4)$$

where k_w is the wall reaction rate (ft/sec). Solving for C_w in equation (12.7.4) and substituting into equation (12.7.3) results in

$$\theta(C) = - \left[k_b + \frac{k_w k_f}{R_H (k_w + k_f)} \right] C \quad (12.7.5)$$

The term in brackets [] is the overall first-order rate constant. The negative sign refers to substance decay (mass transfer from the bulk flow to the pipe wall) and a positive sign in equation (12.7.5) models substance growth (mass transfer from the pipe wall to the bulk flow). Determining the reaction rates k_b , k_w , and k_f is discussed in textbooks on transfer processes such as Edwards et al. (1976). Refer to Clark (2000), Clark et al. (1988), Grayman and Kirmeyer (2000), Grayman et al. (2000), and Rossman (2000) for more detailed discussions on water quality modeling.

12.8 HYDRAULIC TRANSIENTS

12.8.1 Hydraulic Transients in Distribution Systems

Hydraulic transient flow occurs when flow changes suddenly from one steady-state flow to another steady-state flow. *Transient flow* is then the intermediate-stage flow during the transition. This *hydraulic (or fluid) transient* has also been referred to as *water hammer*. The easiest explanation of transient flow or hydraulic transient is to consider the steady-state flow in the pipe, as shown in Figure 12.8.1. If the valve is instantaneously closed, a positive pressure wave is developed upstream

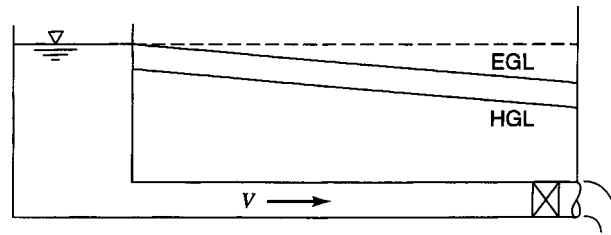


Figure 12.8.1 Steady-state flow in a pipe.

of the valve and travels up the pipe at approximately the speed of sound. This positive pressure can be much larger than the steady-state pressure, and even large enough to cause pipe failure.

Hydraulic transients are important in water distribution systems because they can cause (1) rupture of pipe and pump casings, (2) pipe collapse, (3) vibration, (4) excessive pipe displacement, pipe line fitting and support deformation and/or failure, and (5) vapor cavity formation (cavitation, column separation) (Bosserman and Hunt, 1998). Causes of hydraulic transients in water distribution systems include (1) valve opening and closing (frequently occurs), (2) flow demand changes (rarely occurs), (3) controlled pump shutdown (rarely occurs), (4) pump failure (often occurs), (5) pump start-up (rarely occurs), (6) air-venting from lines (frequently occurs), (7) failure of flow on pressure regulation (rarely occurs), and (8) pipe rupture (rarely occurs) (Bosserman and Hunt, 1998).

This section presents the fundamentals of hydraulic transients and then discusses their control. For a more detailed discussion refer to Martin (1999, 2000).

12.8.2 Fundamentals of Hydraulic Transients

12.8.2.1 Physical Description

In order to describe the variation in pipe pressures during transient flow, consider the initial flow ($t = 0$) in Figure 12.8.2a in which the valve at the downstream end of the pipe is open and flow in the pipe has a velocity of V . For the sake of illustration headlosses are neglected, so that the initial pipe pressure is p_0 throughout the length of the pipe. The valve is instantaneously closed, at which time a pressure wave is developed that moves toward the reservoir at the speed of sound v_c . Referring to Figure 12.8.2b, water between the pressure wave and the valve is at rest, whereas water between the pressure wave and the reservoir has the initial velocity V . The pressure head in the water between the pressure wave and the valve is $\Delta p/\gamma + p_0/\gamma$, where Δp refers to the increased pressure. When the pressure wave reaches the reservoir, the pressure imbalance causes water to flow from the pipe back into the reservoir at velocity V . This causes a new pressure wave that travels to the valve (see Figure 12.8.2c). As the pressure wave travels to the valve, the pressure in the pipe between the reservoir and the pressure wave returns to pressure p_0 and the velocity V is toward the reservoir. When this pressure wave reaches the valve, water in the pipe is flowing toward the reservoir at velocity V .

When the pressure wave reaches the valve, a rarefied pressure wave moves back toward the reservoir, as shown in Figure 12.8.2d. Note that the pressure head in the pipe between the wave and the valve is now less than that in the reservoir. The velocity in the pipe between the pressure wave and the valve is now zero. When the pressure wave reaches the reservoir, the water velocity in the pipe is zero and has a pressure less than in the reservoir at the pipe end. This pressure imbalance causes flow once again in the pipe toward the valve, as shown in Figure 12.8.2e. Now the process repeats and continues to repeat until frictional forces dampen out the pressure wave.

Figure 12.8.3a illustrates the pressure rise at the valve and the velocity at the reservoir for instantaneous closure, neglecting friction. Figure 12.8.3b illustrates the pressure rise at the valve and the velocity at the reservoir for instantaneous closure with friction included.

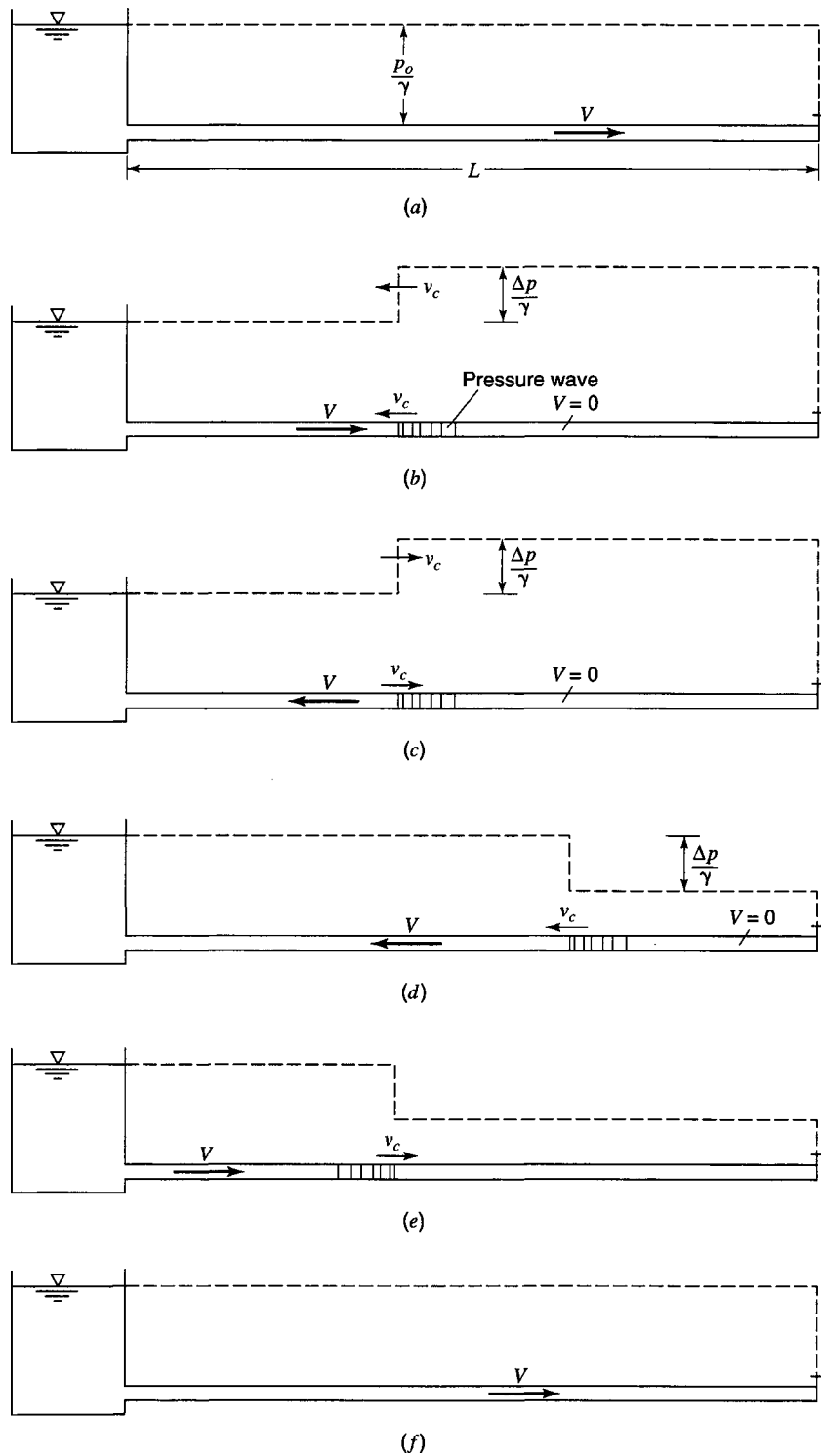


Figure 12.8.2 Water-hammer conditions. (a) Water-hammer process—initial condition; (b) Condition during time $0 < t < L/v_c$; (c) Condition during time $L/v_c < t < 2L/v_c$; (d) Condition during time $2L/v_c < t < 3L/v_c$; (e) Condition during time $3L/v_c < t < 4L/v_c$; (f) Condition at time $t = 4L/v_c$ (from Roberson and Crowe (1990)).

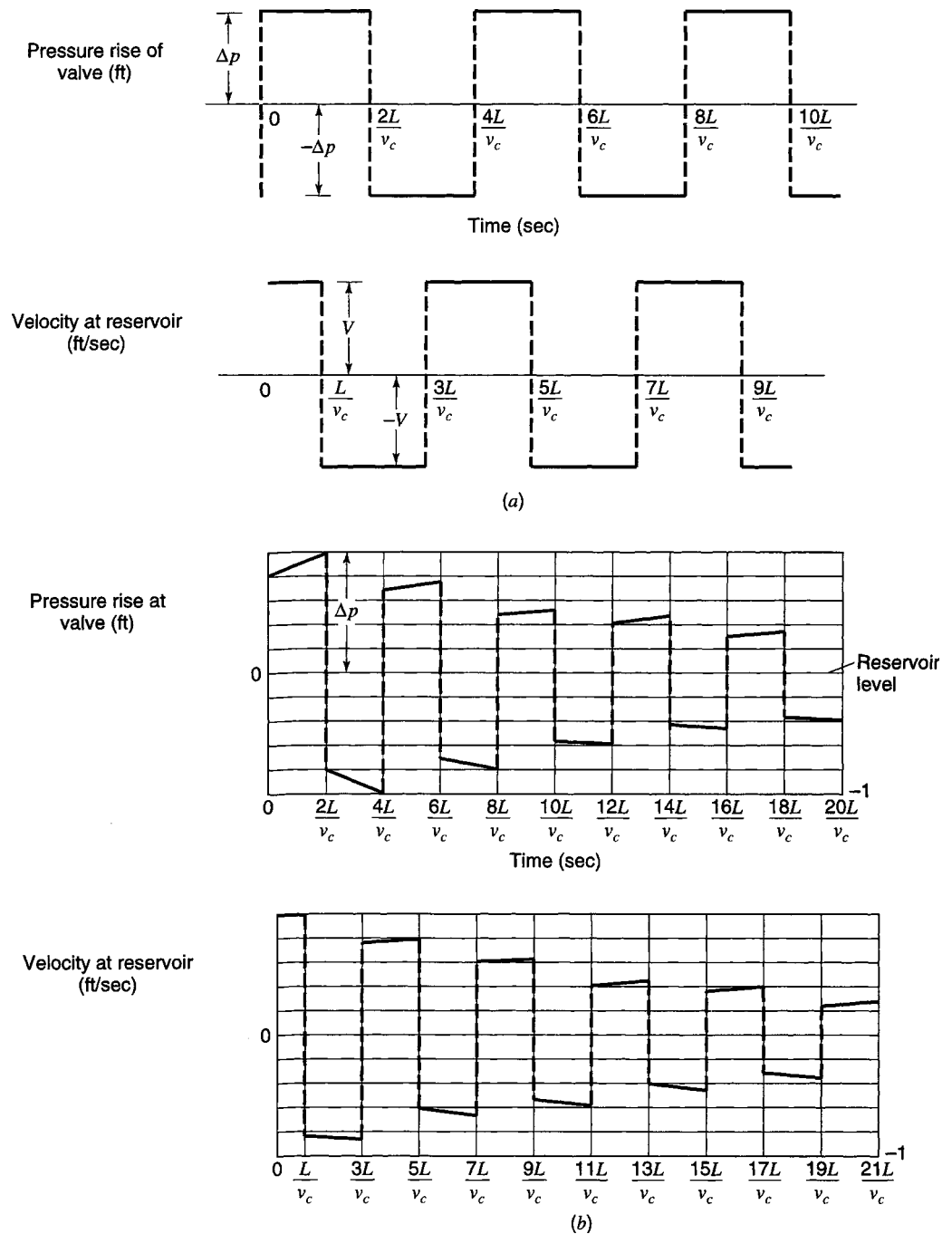


Figure 12.8.3 Pressure and velocity fluctuations for valve closure in a pipe. (a) Simple conduit, instantaneous closure, friction neglected; (b) Simple conduit, instantaneous closure, friction included.

12.8.2.2 Wave Speed and Pressure

For purposes of deriving the wave speed and pressure, assume a rigid pipe (i.e., no expansion or contraction of the pipe). Density, pressure, and velocity of the water are $\rho, p,$ and V on the reservoir side of the pressure wave, and are $\rho + \Delta\rho, p + \Delta p,$ and $V = 0$ on the valve side of the wave. The

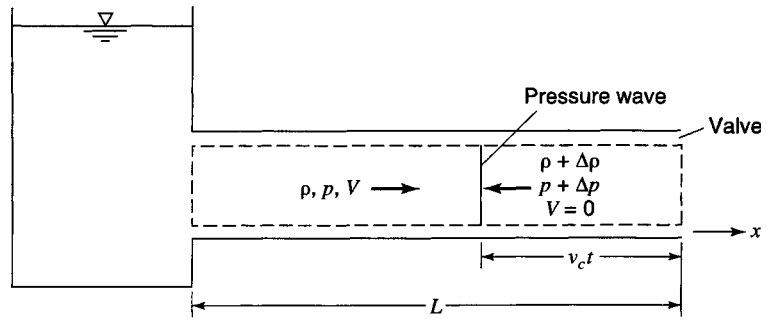


Figure 12.8.4 Control volume for pressure wave.

momentum equation (3.5.6),

$$\sum F_x = \frac{d}{dt} \int_{CV} v_x \rho d\forall + \sum_{CS} v_x (\rho \cdot \mathbf{V} \cdot \mathbf{A}) \quad (3.5.6)$$

is applied to the control volume defined in Figure 12.8.4. The terms in equation (3.5.6) are

$$\sum F_x = pA - (p + \Delta p)A \quad (12.8.1)$$

$$\frac{d}{dt} \int_{CV} v_x \rho d\forall = \frac{d}{dt} [V\rho(L - v_c t)A] = -V\rho v_c A \quad (12.8.2)$$

$$\sum_{CS} v_x (\rho \mathbf{V} \cdot \mathbf{A}) = V\rho(-VA) \quad (12.8.3)$$

Substituting equation (12.8.1) to (12.8.3) into (3.5.6) yields

$$pA - (p + \Delta p)A = -\rho V^2 A - \rho V v_c A \quad (12.8.4)$$

which simplifies to

$$\Delta p = \rho V^2 + \rho V v_c \quad (12.8.5)$$

where ρV^2 is considered negligible as compared to the $\rho V v_c$. Then

$$\Delta p = \rho V v_c \quad (12.8.6)$$

As discussed later, v_c is considerably larger than V , allowing this assumption.

Next we apply the continuity equation (3.3.1) to determine the *pressure wave velocity* v_c . The continuity equation (3.3.1) is

$$0 = \frac{d}{dt} \int_{CV} \rho d\forall + \int_{CS} \rho \mathbf{V} \cdot d\mathbf{A} \quad (3.3.1)$$

where

$$\begin{aligned} \frac{d}{dt} \int_{CV} \rho d\forall &= \frac{d}{dt} [\rho(L - v_c t)A + (\rho + \Delta\rho)v_c t A] \\ &= -\rho v_c A + (\rho + \Delta\rho)v_c A = \Delta\rho v_c A \end{aligned} \quad (12.8.7)$$

and

$$\int_{CS} \rho \mathbf{V} \cdot d\mathbf{A} = \rho(-VA) \quad (12.8.8)$$

Substituting equations (12.8.7) and (12.8.8) into (3.3.1) yields

$$0 = \rho(-VA) + \Delta p v_c A \quad (12.8.9)$$

which reduces to

$$(\Delta p / \rho) = (V / v_c) \quad (12.8.10)$$

The bulk modulus of elasticity E is defined in Chapter 3 as

$$E = \frac{dp}{(d\rho/\rho)} = \frac{\Delta p}{(\Delta\rho/\rho)} \quad (3.1.6)$$

so that

$$\frac{\Delta p}{\rho} = \frac{\Delta p}{E} \quad (12.8.11)$$

Equating (12.8.10) and (12.8.11) and solving for v_c yields

$$v_c = \frac{VE}{\Delta p} \quad (12.8.12)$$

Substituting $\Delta p = \rho V v_c$ (equation (12.8.6)) and solving for the pressure wave speed, we get

$$v_c = \sqrt{\frac{E}{\rho}} \quad (12.8.13)$$

which is for rigid pipes.

For an elastic pipe, however, this velocity of the pressure wave v_c is modified by the stretching of the pipe walls. In reality, pipes are elastic and the stretching results in the modulus of the combination of water and the pipe. A *combined modulus* K can be used to define the pressure wave speed for an elastic pipe as

$$v_c = \sqrt{\frac{K}{\rho}} \quad (12.8.14)$$

To derive K , assume that the longitudinal stress in the pipe can be ignored and let

\mathcal{V} = volume in pipe

$d\mathcal{V}$ = change in volume due to compression of the water

$d\mathcal{V}''$ = change in volume due to stretching of the pipe wall

$d\mathcal{V}$ = total change in volume

E_p = modulus of the pipe wall

The combined modulus is defined as

$$K = - \frac{\mathcal{V}}{(d\mathcal{V}' + d\mathcal{V}'')} dp \quad (12.8.15)$$

which can be rearranged to produce

$$\frac{1}{K} = -\frac{d\forall'}{\forall dp} - \frac{d\forall''}{\forall dp} = \frac{1}{E} - \frac{d\forall''}{\forall dp} \quad (12.8.16)$$

By equation (3.1.5), $E = -(dp)/(d\forall/\forall)$. For a pipe wall $\forall = \pi r^2$ per unit length of pipe, where r is the radius and $d\forall'' = 2\pi r dr$.

The *modulus of elasticity of the pipe* E_p is the incremental stress divided by the increment of unit deformation. Incremental stress is $r dp/t_w$ where t_w is the wall thickness and the increment of unit deformation is dr/r . The pipe modulus of elasticity is then

$$E_p = \frac{r dp/t_w}{dr/r} \quad (12.8.17)$$

and solving for dp yields

$$dp = \frac{E_p t_w dr}{r^2} \quad (12.8.18)$$

The term $-d\forall''/\forall dp$ in equation (12.8.16) can now be expressed as

$$-\frac{d\forall''}{\forall dp} = \frac{2\pi r dr}{\pi r^2 (E_p t_w dr/r^2)} = \frac{D}{E_p t_w} \quad (12.8.19)$$

where D is the inside diameter of the pipe.

The *combined modulus* K can now be written using the above definition:

$$\frac{1}{K} = \frac{1}{E} + \frac{D}{E_p t_w}$$

or

$$K = \frac{E}{1 + (D/t_w)(E/E_p)} \quad (12.8.20)$$

Equation (12.8.14) can now be expressed as

$$v_c = \sqrt{\frac{K}{\rho}} = \sqrt{\frac{E}{\rho} \left(\frac{1}{1 + (D/t_w)(E/E_p)} \right)} \quad (12.8.21)$$

To consider various types of pipe support conditions, the above equation can be modified to include a factor k defined in Table 12.8.1:

$$v_c = \sqrt{\frac{E}{\rho} \left(\frac{1}{1 + (D/t_w)(E/E_p)k} \right)} \quad (12.8.22)$$

The time for a pressure wave to travel from the valve to the reservoir and back to the valve is $2L/v_c$. If the time of closure is less than $2L/v_c$, then the maximum pressure developed at the valve is essentially the same as for instantaneous closure. In other words, the change in pressure is the same for a given change in velocity unless the negative wave from the reservoir mitigates the positive pressure, keeping in mind that it takes $2L/v_c$ time for the negative wave to reach the valve. The *critical time of closure* is then

$$t_c = 2L/v_c \quad (12.8.23)$$

Table 12.8.1 Values of k from Solid Mechanics

Support conditions	k (thick walls)	k (thin walls)
Anchored at upstream end only. Free to move longitudinally	$\frac{2t}{D}(1+\mu) + \left(\frac{D}{D+t}\right) - \left(1 - \frac{\mu}{2}\right)$	$1 - \frac{\mu}{2}$
Anchored against axial (longitudinally) movement so axial stress = 0	$\frac{2t}{D}(1+\mu) + \left(\frac{D}{D+t}\right)(1-\mu^2)$	$1 - \mu^2$
Expansion joints throughout (axial stress = 0)	$\frac{2t}{D}(1+\mu) + \left(\frac{D}{D+t}\right)(1)$	1
Tunnels ($t = \infty$)	$\frac{2t}{D}(1+\mu)$	

^aNote: $D/D+t = 1/(1+t/D)$; μ = Poisson's ratio = 0.25 to 0.30 for many pipe materials.

EXAMPLE 12.8.1

A cast iron pipe with 20-cm diameter and 15-mm wall thickness is carrying water when the outlet is suddenly closed. Use $E_{\text{water}} = 2.17 \times 10^9 \text{ N/m}^2$ and $E_p = 16 \times 10^{11} \text{ N/m}^2$. If the design discharge is 40 l/s, calculate the water hammer pressure rise for:

- rigid pipe walls;
- consider stretching of pipe walls, neglecting the longitudinal stress;
- pipeline that is anchored at upstream end only.

SOLUTION

(a) Rigid pipe walls: The water hammer pressure rise is computed using equation (12.8.6), $\Delta p = \rho V v_c$, assuming a sudden valve closure. The pressure wave speed v_c is computed using equation (12.8.13) for a rigid pipe:

$$v_c = \sqrt{\frac{E}{\rho}} = \sqrt{\frac{2.17 \times 10^9}{1000}} = 1473 \text{ m/s}$$

The velocity of flow in the pipe is computed using continuity: $V = Q/A = (400 \times 10^{-3})/[\pi(0.2)^2/4] = 1.27 \text{ m/s}$. The water hammer pressure rise is then $\Delta p = \rho V v_c = 1000(1.27)(1473) = 1.87 \times 10^6 \text{ N/m}^2$.

(b) Consider stretching of pipe walls, neglecting longitudinal stress: The water hammer pressure is computed using equation (12.8.6), $\Delta p = \rho V v_c$, where the velocity v_c is computed using (12.8.21)

$$v_c = \sqrt{\frac{K}{\rho}} = \sqrt{\frac{E}{\rho} \left(\frac{1}{1 + (D/t_w)(E/E_p)} \right)}$$

where $D = 0.2 \text{ m}$, $t_w = 15 \times 10^{-3} \text{ m}$, and $E_p = 16 \times 10^{11} \text{ N/m}^2$:

$$v_c = \left[\frac{2.17 \times 10^9}{1000} \left(\frac{1}{1 + \left(\frac{0.2}{15 \times 10^{-3}} \right) \left(\frac{2.17 \times 10^9}{16 \times 10^{11}} \right)} \right) \right]^{1/2} = 1460 \text{ m/s}$$

The water hammer pressure increase is $\Delta p = 1000(1460)(1.27) = 1.854 \times 10^6 \text{ N/m}^2$.

(c) Pipeline that is anchored at upstream end only: The modulus is modified by $k = (1 - 0.5\mu)$ from Table 12.8.1, where μ is Poisson's ratio for the pipe. Using equation (12.8.22) yields

$$v_c = \sqrt{\frac{E}{\rho} \left(\frac{1}{1 + (D/t_w)(E/E_p)k} \right)}$$

where $\mu = 0.25$ for steel pipes:

$$v_c = \left[\frac{2.17 \times 10^9}{1000} \left(\frac{1}{1 + \left(\frac{0.2}{15 \times 10^{-3}} \right) \left(\frac{2.17 \times 10^9}{16 \times 10^{11}} \right) (1 - 0.5 \times 0.25)} \right) \right]^{1/2} = 1462 \text{ m/s}$$

$$\Delta p = 1000(1462)(1.27) = 1.857 \times 10^6 \text{ N/m}^2$$

EXAMPLE 12.8.2

A steel pipe 1500 m long (Figure 12.8.5) placed on a uniform slope has a 0.5-m diameter and a 5-cm wall thickness. The pipe carries water from a reservoir and discharges it into the air at an elevation 50 m below the reservoir free surface. A valve installed at the downstream end of the pipe allows a flow rate of $0.8 \text{ m}^3/\text{s}$. If the valve is completely closed in 1.4 s, calculate the maximum water hammer pressure at the valve and at the midlength of the pipe. Neglect longitudinal stresses. Use $E_{\text{water}} = 2.17 \times 10^9 \text{ N/m}^2$ and $E_p = 1.9 \times 10^{11} \text{ N/m}^2$.

SOLUTION

First determine the steady-state pressure. Use the energy equation between 1 and 2:

$$Z_1 = \frac{p_2}{\gamma} + \frac{V^2}{2g} + Z_2 + h_{L_{1-2}}$$

For steel pipe, use $\epsilon = 0.046 \text{ mm}$, so that $\epsilon/D = 0.046/0.5 \times 10^3 = 0.000092$. The velocity of the flow in the pipe is $V = Q/A = 0.8/(0.5^2 \pi/4) = 4.074 \text{ m/s}$. The Reynolds number is

$$R_e = \frac{VD}{\nu} = \frac{4.074(0.5)}{1.14 \times 10^{-6}} = 1.8 \times 10^6$$

Using the Moody diagram (Figure 4.3.5), $f = 0.0129$. The pressure head at 2 is

$$\begin{aligned} \frac{p_2}{\gamma} &= Z_1 - Z_2 - \frac{V^2}{2g} - h_{L_{1-2}} = Z_1 - Z_2 - \left(1 + f \frac{L}{D}\right) \frac{V^2}{2g} \\ &= 50 - 0 - \left(1 + 0.0129 \frac{1500}{0.5}\right) \frac{(4.074)^2}{2(9.8)} = 16.4 \text{ m} \end{aligned}$$

The pressure at 2 is $P_2 = 16.4\gamma = 16.4 \times 9800 = 1.6 \times 10^5 \text{ N/m}^2$ (at valve).

At midlength (3),

$$\frac{p_3}{\gamma} = Z_1 - Z_3 - \frac{V^2}{2g} - h_{L_{1-3}} = 50 - 25 - \left(1 + 0.0129 \frac{750}{0.5}\right) \frac{4.074^2}{2 \times 9.8} = 7.767 \text{ m}$$

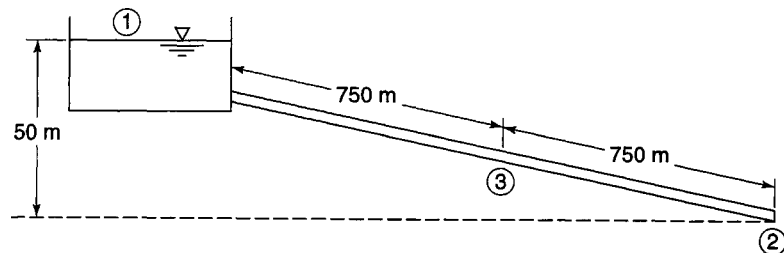


Figure 12.8.5 Example 12.8.2.

The pressure at 3 is $p_3 = 7.6 \times 10^4 \text{ N/m}^2$. Determine wave speed using equation (12.8.21):

$$v_c = \sqrt{\frac{E}{\rho} \left(\frac{1}{1 + (D/t_w)(E/E_p)} \right)}$$

$$\left[\frac{2.17 \times 10^9}{1000} \left(\frac{1}{1 + \left(\frac{0.5}{0.05} \right) \left(\frac{2.17 \times 10^9}{1.9 \times 10^{11}} \right)} \right) \right]^{1/2} = 1395.6 \text{ m/s}$$

To determine maximum pressure, first determine the critical time of closure using equation (12.8.23):

$$t_c = \frac{2L}{v_c} = \frac{2(1500)}{1395.6} = 2.15 \text{ sec}$$

Since time of closure $1.4 \text{ sec} < t_c = 2.15 \text{ sec}$, the valve closure is rapid; hence the maximum increase of pressure generated by water hammer is

$$\Delta p = \rho V v_c = 1000(4.074)(1395.6) = 5.69 \times 10^6 \text{ N/m}^2$$

The maximum pressure at the valve is $p_2 + \Delta p = 1.6 \times 10^5 + 5.69 \times 10^6 = 5.85 \times 10^6 \text{ N/m}^2$.

The maximum pressure at midlength is $p_3 + \Delta p = 7.6 \times 10^4 + 5.69 \times 10^6 = 5.77 \times 10^6 \text{ N/m}^2$.

EXAMPLE 12.8.3

A steel pipeline ($\epsilon = 0.00015 \text{ ft}$) 2 ft in diameter and 2 mi long discharges freely at its lower end under a head of 200 ft. What water-hammer pressure would develop if a valve at the outlet were closed in 4 sec? 60 sec? Wall thickness = 0.2 in for both cases of closure. Compute the stress that would develop in the walls of the pipe near the valve. If the working stress of steel is taken as 16,000 psi, what would be the minimum time of safe closure? Consider $E = 4.32 \times 10^7 \text{ lb/ft}^2$ and $E_p = 4.32 \times 10^9 \text{ lb/ft}^2$.

SOLUTION

We need to compute the stresses developed near the valve. First use the energy equation to determine the velocity of flow in the pipe, neglecting minor losses:

$$200 = \left(1 + f \frac{L}{D} \right) \frac{V^2}{2g}$$

Using $\epsilon = 0.00015$, we find $\epsilon/D = 0.000075$; then for fully turbulent flow, $f = 0.0115$ from the Moody diagram, so that

$$200 = \left(1 + 0.0115 \frac{2 \times 5280}{2} \right) \frac{V^2}{2g}$$

and $V = 14.4 \text{ ft/s}$. Check the Reynolds number: $R_e = 14.4 \times 2/1.217 \times 10^{-5} = 2.37 \times 10^6$. Entering the Moody diagram with $R_e = 2.37 \times 10^6$ and $\epsilon/D = 0.000075$ gives $f = 0.012$ so that

$$200 = \left(1 + 0.012 \frac{2 \times 5280}{2} \right) \frac{V^2}{2g}$$

and $V = 14.1 \text{ ft/s}$. Check the Reynolds number, $R_e = 14.1 \times 2/1.217 \times 10^{-5} = 2.32 \times 10^6$. Entering the Moody diagram with $R_e = 2.32 \times 10^6$ and $\epsilon/D = 0.000075$ gives $f = 0.012$. Therefore $V = 14.1 \text{ ft/s}$ is OK.

Determine the velocity v_c using equation (12.8.21) as

$$\begin{aligned}
 v_c &= \sqrt{\frac{E}{\rho} \left(\frac{1}{1 + (D/t_w)(E/E_p)} \right)} \\
 &= \left[\frac{4.32 \times 10^7}{1.94} \left(\frac{1}{1 + \left(\frac{2}{0.2/12} \right) \left(\frac{4.32 \times 10^7}{4.32 \times 10^9} \right)} \right) \right]^{1/2} \\
 &= \left[\frac{4.32 \times 10^7}{1.94} \left(\frac{1}{2.2} \right) \right]^{1/2} = 3181 \text{ ft/sec} \\
 t_c &= \frac{2L}{v_c} = \frac{2(2 \times 5280)}{3181} = 6.64 \text{ sec}
 \end{aligned}$$

- (a) For $t = 4$ sec, this is a rapid closure; then $\Delta p = \rho V v_c = 1.94 (14.1)(3181) = 87,013 \text{ lb/ft}^2 = 604 \text{ psi}$.
The pressure at the valve is

$$\begin{aligned}
 p_{\text{valve}} &= p_{\text{static}} + \Delta p = \rho g h + \Delta p = 1.94(32.2)(200)/144 + 604 \\
 &= 86.8 + 604 = 690.8 \text{ psi}
 \end{aligned}$$

$$\text{Stress is } \sigma = \frac{p_{\text{valve}}}{t_w} (r) = \frac{690.8}{0.2} (12) = 41,448 \text{ psi.}$$

- (b) A 60-sec closure is in excess of $2L/v_c$. Let $v_c = 2L/t_c$; then

$$\Delta p = \frac{2L\rho V}{t_c} = \frac{2(2 \times 5280)(1.94)(14.1)}{60} = 9628.6 \text{ lb/ft}^2 = 66.9 \text{ psi}$$

$$p_{\text{valve}} = p_{\text{static}} + \Delta p = 86.8 + 66.9 \text{ psi} = 153.7 \text{ psi}$$

$$\text{The stress is then } \sigma = \frac{p_{\text{valve}}}{t_w} r = \frac{153.7}{0.2} (12) = 9222 \text{ psi}$$

- (c) The minimum time of closure for a working stress of 16,000 psi is now computed:

$$\Delta \sigma_a = \sigma_a - \sigma_{\text{static}} = 16,000 - \frac{p_{\text{static}}}{t_w} r = 16,000 - \frac{86.8}{0.2} (12) = 10,792 \text{ psi}$$

$$\Delta \sigma_a = \frac{\Delta p}{t_w} r = \frac{r}{t_w} \left(\frac{2L\rho V}{t_c} \right)$$

Solving for the time of closure gives

$$t_c = \frac{2L\rho V r}{\Delta \sigma_a t_w} = \frac{2(2 \times 5280)(1.94)(14.1)(12/12)}{(10,792)(0.2/12)(144)} = 22.3 \text{ sec}$$

12.8.3 Control of Hydraulic Transients

12.8.3.1 Methods of Control

Various methods are used to control hydraulic transients (Martin, 1999, 2000) including:

- Pump-control valves (Figure 12.8.6)
- Air chambers (Figure 12.8.7)

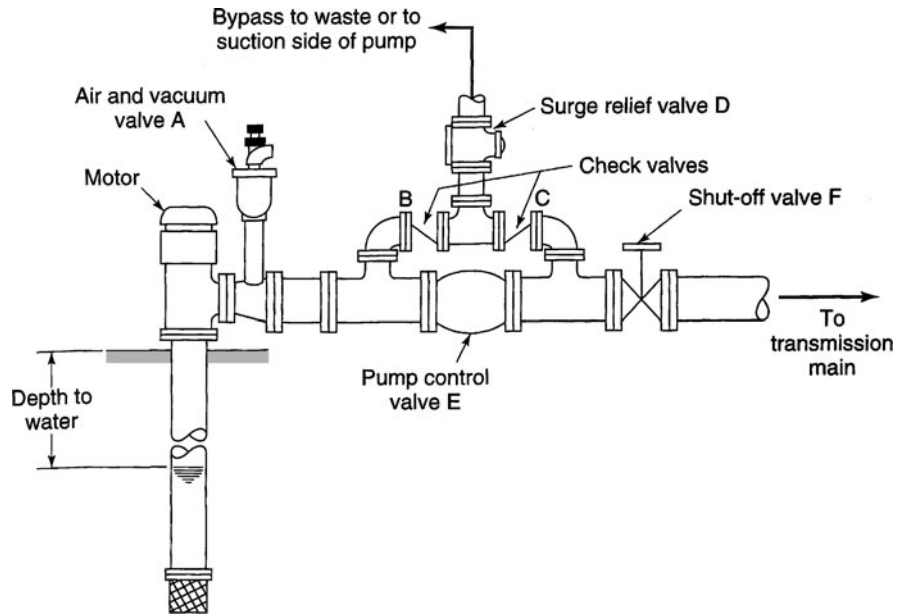


Figure 12.8.6 Upstream and downstream bypass of a pump-control valve (from Bosserman (1998)).

- Surge tanks (Figure 12.8.8)
 - Open-end surge tank or stand pipe
 - One-way surge tank
 - Two-way surge tank
- Valves
 - Air release and vacuum relief valves
 - Swing check valves
 - Cushioned swing check valves
 - Surge relief valves (Figure 12.8.9)
- High-pressure-rated piping, valves, and equipment

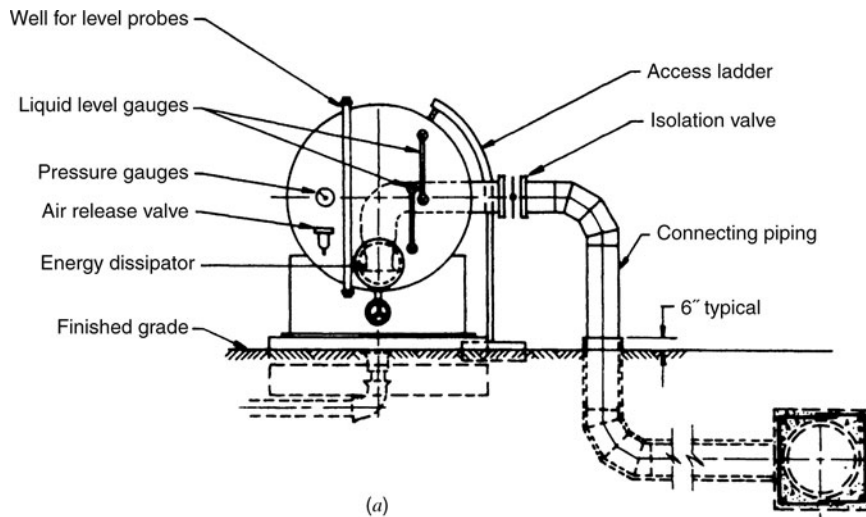


Figure 12.8.7 Horizontal air chamber for clean water service. (a) End elevation; (b) Side elevation (from Bosserman (1998)).

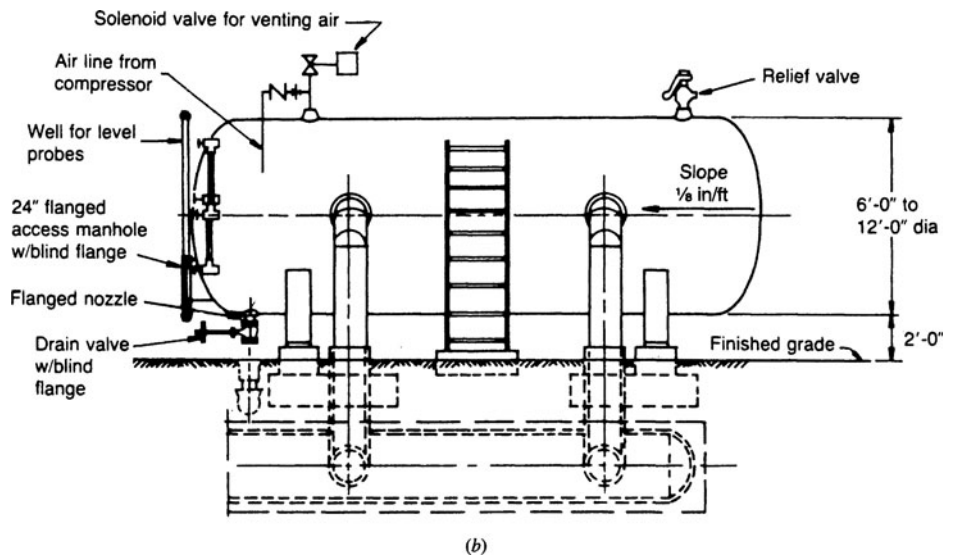


Figure 12.8.7 (Continued)

12.8.3.2 Surge Tank Analysis

This section derives the continuity and energy equations that can be used to analyze simple surge tanks (standpipes), as shown in Figure 12.8.10. The surge tank is upstream of the valve and has the condition prior to valve closure shown in Figure 12.8.10a. When the valve is suddenly closed, water rises in the surge tank (or standpipe). To simplify the analysis the following derivation neglects friction and velocity head in the surge tank and losses at the pipe entrance and surge tank entrance (modified from Roberson et al., 1997).

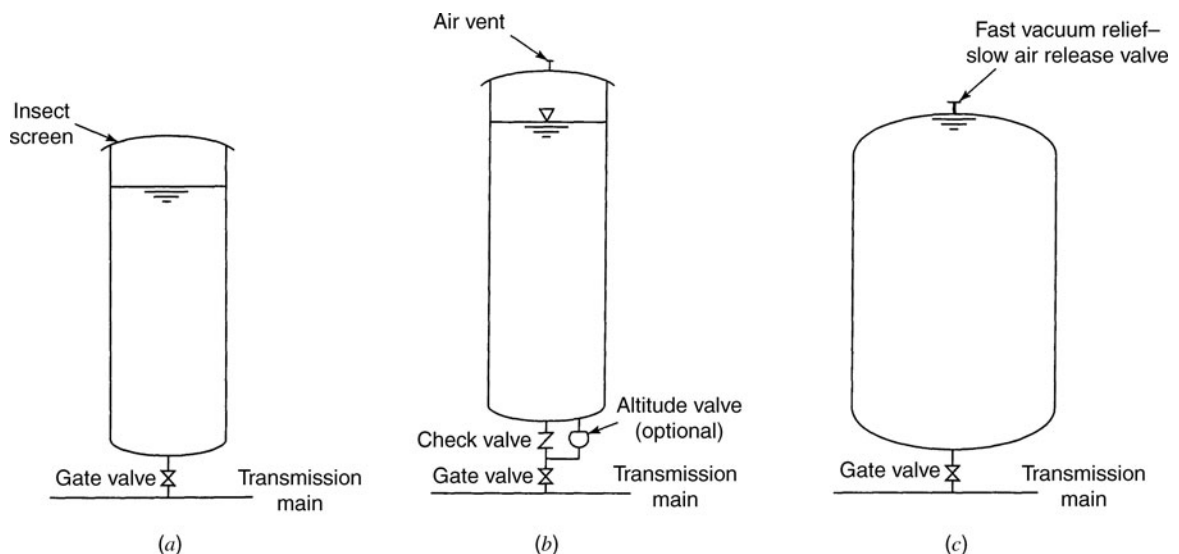


Figure 12.8.8 Surge tank. (a) Open-end surge tank or stand pipe; (b) One-way surge tank; (c) Two-way surge tank (from Bosserman (1998)).

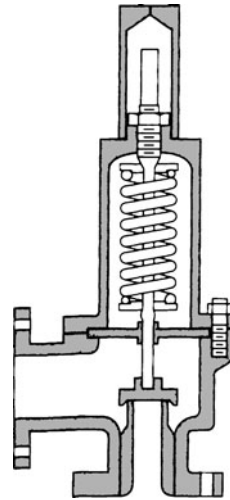


Figure 12.8.9 Pressure-actuated surge relief valve (from Bosserman (1998)).

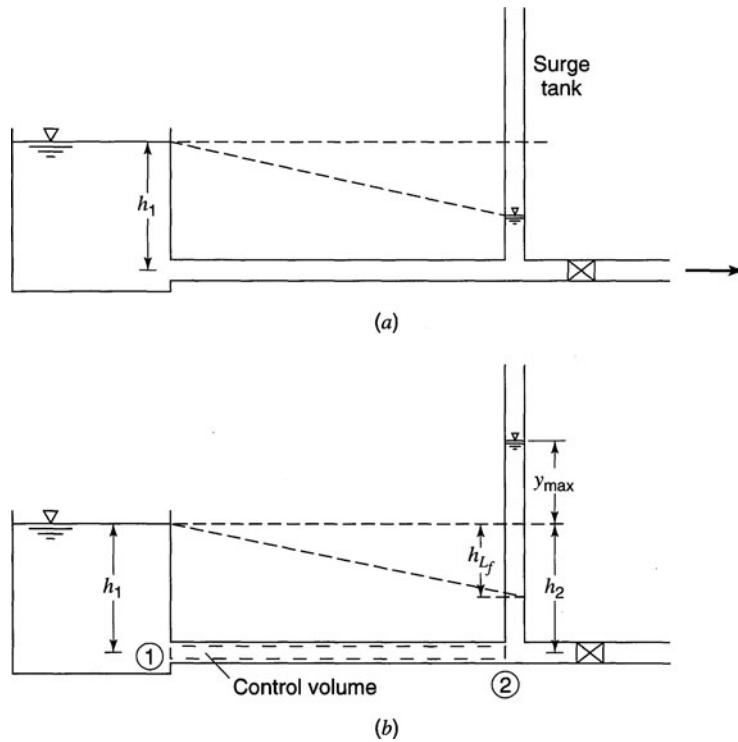


Figure 12.8.10 Surge tank analysis. (a) Conditions for valve open; (b) Condition immediately after valve closure.

Using the integral momentum equation (3.5.5), we find

$$\sum \mathbf{F} = \frac{d}{dt} \int_{CV} \rho \mathbf{v} dV + \sum_{CS} \rho \mathbf{v} \mathbf{V} \cdot \mathbf{A} \quad (3.5.5)$$

The summation of forces acting on a horizontal pipe is

$$\sum \mathbf{F} = F_1 - F_2 - F_f \quad (12.8.24)$$

where F_1 is the pressure force at 1, F_2 is the pressure force acting at 2, and F_f is friction loss. F_1 is expressed as

$$F_1 = \gamma Ah_1 \quad (12.8.25)$$

where A is the cross-sectional area of the pipe between 1 and 2. F_2 is expressed as

$$F_2 = \gamma A(h_1 + y) \quad (12.8.26)$$

F_f can be expressed as

$$F_f = \gamma Ah_L \quad (12.8.27)$$

where h_L is the headloss due to friction. The other terms in equation (3.5.5) are

$$\frac{d}{dt} \int_{CV} \mathbf{v} \rho d\forall = \rho LA \frac{dV}{dt} \quad (12.8.28)$$

and

$$\sum_{CS} \mathbf{v} \rho \mathbf{V} \cdot \mathbf{A} = 0 \quad (12.8.29)$$

Substituting equations (12.8.24) through (12.8.29) into equation (3.5.5) gives

$$\gamma Ah_1 - \gamma A(h_1 + y) - \gamma Ah_L = \rho LA \frac{dV}{dt} + 0 \quad (12.8.30)$$

Simplifying and rearranging equation (12.8.30) produces

$$\frac{\rho}{\gamma} L \frac{dV}{dt} + y + h_L = 0 \quad (12.8.31)$$

where $h_L = f \frac{L V^2}{D 2g}$. A continuity equation can be derived using equation (3.3.1):

$$0 = \frac{d}{dt} \int_{CV} \rho d\forall + \int_{CS} \rho \mathbf{V} \cdot \mathbf{dA} \quad (3.3.1)$$

in which

$$\frac{d}{dt} \int_{CV} \rho d\forall = A_s \frac{dy}{dt} \quad (12.8.32)$$

and

$$\int_{CS} \rho \mathbf{V} \cdot \mathbf{dA} = -AV \quad (12.8.33)$$

where A_s is the cross-sectional area of the surge tank. Substituting equations (12.8.32) and (12.8.33) into (3.3.1) gives

$$A_s \frac{dy}{dt} = AV \quad (12.8.34)$$

EXAMPLE 12.8.4

Derive an expression for the maximum depth in a simple surge tank (standpipe) if friction is neglected.

SOLUTION

By neglecting friction losses ($h_L = 0$), equation (12.8.31) can be simplified to

$$\frac{\rho}{\gamma} L \frac{dV}{dt} + y = 0 \quad (\text{a})$$

$$\frac{dV}{dt} = - \frac{yg}{L} \quad (\text{b})$$

$$\frac{dV}{dt} = \frac{dV}{dy} \frac{dy}{dt} \quad (\text{c})$$

$$\frac{dV}{dy} \frac{dy}{dt} = - \frac{yg}{L} \quad (\text{d})$$

Using the continuity relationship, equation (12.8.34), yields

$$\frac{dy}{dt} = \frac{A}{A_s} V \quad (\text{e})$$

and substituting this expression (e) for dy/dt into (d) gives

$$\frac{dV}{dy} \left(\frac{AV}{A_s} \right) = - \frac{yg}{L} \quad (\text{f})$$

$$\frac{dV}{dy} = - \left(\frac{A_s}{AV} \right) \left(\frac{g}{L} \right) y \quad (\text{g})$$

Integrating yields

$$\int_{V_0}^V V dV = - \int_0^y \left[\left(\frac{A_s}{A} \right) \left(\frac{g}{L} \right) y \right] dy$$

where V_0 is the velocity in the pipe when the valve is open.

$$V^2 = V_0^2 - \left(\frac{A_s}{A} \right) \left(\frac{g}{L} \right) y^2$$

Knowing that $y \rightarrow y_{\max}$ as $V \rightarrow 0$, then when the valve is completely closed $y = y_{\max}$ and $V = 0$; therefore

$$y_{\max} = V_0 \sqrt{\left(\frac{A}{A_s} \right) \left(\frac{L}{g} \right)}$$

EXAMPLE 12.8.5

Derive an expression for the time to reach the maximum surge depth for the simple surge tank (example 12.8.4), if friction is neglected.

SOLUTION

From example 12.8.4, we have

$$V^2 = V_0^2 - \left(\frac{A_s}{A} \right) \left(\frac{g}{L} \right) y^2 \quad (\text{a})$$

$$\frac{dy}{dt} = \frac{A}{A_s} V \quad \text{or} \quad dy = \left(\frac{A}{A_s} \right) V dt \quad (\text{b})$$

Substituting V from equation (a) into (b) and integrating (Morris and Wiggert, 1972) yields

$$\int_0^T dt = \int_0^y \left(\frac{A_s}{A} \right) \left[V_0^2 - \left(\frac{A_s}{A} \right) \left(\frac{L}{g} \right) y^2 \right]^{-1/2} dy \quad (c)$$

$$T = \frac{A_s}{A} \left[\sin^{-1} \frac{y}{V_0 \sqrt{\left(\frac{A}{A_s} \right) \left(\frac{L}{g} \right)}} \right] \sqrt{\left(\frac{A}{A_s} \right) \left(\frac{L}{g} \right)} \quad (d)$$

$$= \sqrt{\left(\frac{A_s}{A} \right) \left(\frac{L}{g} \right)} \sin^{-1} \left(\frac{y}{y_{\max}} \right) \quad (e)$$

For $y = y_{\max}$, $\sin^{-1} \left(\frac{y}{y_{\max}} \right) = \frac{\pi}{2}$, so

$$T_{\max} = \frac{\pi}{2} \sqrt{\left(\frac{A_s}{A} \right) \left(\frac{L}{g} \right)} \quad (f)$$

EXAMPLE 12.8.6

A simple surge tank of 4-ft diameter is placed near the terminus of a 6000-ft long, 24-in steel pipe. This steel pipe has 1-in thick walls with a modulus of elasticity of 30×10^6 psi. The modulus of elasticity of water is 300,000 psi. The pipe flow rate is 20 cfs. What is the maximum surge that will be experienced? How soon after the assumed instantaneous valve closure will this maximum surge be attained? Use a Darcy–Weisbach friction factor of $f = 0.012$. Also neglect the effects of friction.

SOLUTION

Neglecting the effects of friction, use the equation developed in example 12.8.4 to compute the maximum height y_{\max} . First compute the velocity in the 24-in steel pipe:

$$A = \pi \times (2)^2 / 4 = 3.14 \text{ ft}^2$$

$$A_s = \pi \times (4)^2 / 4 = 12.57 \text{ ft}^2$$

$$Q = AV_0 = 20 \text{ ft}^3/\text{s}$$

$$V_0 = \frac{20}{\pi(2)^2/4} = 6.37 \text{ ft/s}$$

$$y_{\max} = V_0 \sqrt{\left(\frac{A}{A_s} \right) \left(\frac{L}{g} \right)} = (6.37) \sqrt{\left(\frac{3.14}{12.57} \right) \left(\frac{6000}{32.2} \right)} = 43.46 \text{ ft}$$

The time to maximum depth in the surge tank is computed using equation (f) in example 12.8.5:

$$T_{\max} = \frac{\pi}{2} \sqrt{\left(\frac{A_s}{A} \right) \left(\frac{L}{g} \right)} = \frac{\pi}{2} \sqrt{\left(\frac{12.57}{3.14} \right) \left(\frac{6000}{32.2} \right)} = 42.9 \text{ sec}$$

PROBLEMS

12.1.1 Solve example 12.1.1 using a 1.5-m diameter pipe.

12.2.1 A pump operating at 1800 rpm delivers 180 gal/min at 80 ft head. If the pump operates at 1500 rpm, what are the corresponding head and discharge?

12.2.2 A flow of $0.03 \text{ m}^3/\text{s}$ must be pumped against a head of 30 m. The pump will be driven by an electric motor with a speed of 1800 rev/min. What type of pump should be used and what is the corresponding efficiency?

12.2.3 Solve problem 12.2.2 using U.S. customary units.

12.2.4 Solve problem 12.2.2 using a speed of 2000 rev/min.

12.2.5 Solve example 12.2.4 using a discharge of $0.18 \text{ m}^3/\text{s}$.

12.2.6 Solve example 12.2.4 with a static suction head of -3 m .

12.2.7 Solve example 12.2.5 using a total dynamic head of 60 m .

12.2.8 Solve example 12.2.5 using a total dynamic head of 20 m .

12.2.9 Solve example 12.2.6 with the manufacturer's $NPSH_R = 5.0$.

12.2.10 Determine the brake horsepower required by a pump for a discharge of $0.2 \text{ m}^3/\text{s}$ and a total dynamic head of 20 m , with an efficiency of 80 percent.

12.2.11 A water system has a pump that delivers $400 \text{ m}^3/\text{h}$ at a rotational speed of 1200 rpm at 80 percent efficiency. The pump operates at an elevation of 1000 m above sea level (use an atmospheric pressure head of 9.19 m) and the temperature is 20°C . The total dynamic head is 40 m and the pump manufacturer's required net positive suction head is $NPSH_R = 5.0$. What is the allowable suction head for the pump? The entrance loss is 0.0001 m , the bend losses add up to 0.15 m , and the sum of head losses due to friction in the suction piping is 1.5 m .

12.2.12 For a system with a dynamic head of 60 m , estimate the net positive suction head at cavitation inception ($NPSH_i$). The pump delivers $400 \text{ m}^3/\text{h}$ at a rotational speed of 1200 rpm at 80 percent efficiency. The pump is to operate at an elevation of 1000 m above sea level and the temperature is 20°C . The atmospheric pressure head is 9.19 m .

12.2.13 A flow of $0.02 \text{ m}^3/\text{s}$ must be pumped against a head of 25 m . The pump will be driven by an electric motor with a speed of 1450 rev/min. What is the specific speed of the pump?

12.4.1 Solve example 12.4.1 for a flow rate of 8 cfs and $\Delta Z = 25 \text{ ft}$.

12.4.2 Solve example 12.4.1 for a flow rate of 4 cfs and $\Delta Z = 40 \text{ ft}$.

12.4.3 Solve example 12.4.2 assuming the elevation of reservoir 1 is 120 ft .

12.4.4 Solve example 12.4.2 assuming the elevation of reservoir 1 is 80 ft .

12.5.1 Solve example 12.5.1 using a 12-in diameter discharge pipe from the pump to reservoir B. All other information is the same.

12.5.2 Solve example 12.5.1 assuming the reservoir elevation is increased to 60 ft .

12.5.3 Solve example 12.5.3 using a pump speed of 1500 rpm.

12.5.4 Solve example 12.5.4 assuming reservoir 2 has an elevation of 200 ft . All other information is the same.

12.5.5 Solve example 12.5.4 assuming line A is 10-in line.

12.6.1 Solve example 12.6.1 using the Hazen–Williams equation with $C = 140$.

12.6.2 Solve example 12.6.1 using Manning's equation with $n = 0.012$.

12.6.3 Solve example 12.6.2 using the Hazen–Williams equation with $C = 140$.

12.6.4 Determine the flows in each pipe of the network in Figure 12.6.3 if the demand at C changes to 4 cfs and the inflow at A changes to 12 cfs.

12.6.5 Determine the flows in each pipe of the network in Figure 12.6.3 if the demands at E and F each change to 3 cfs and the inflow at A changes to 8 cfs.

12.6.6 Determine the flows in each pipe of the network in Figure 12.6.3 if there is a demand of 4.0 cfs at D and the inflow at A changes to 14 cfs.

12.6.7 Solve example 12.6.2 using Manning's equation with $n = 0.012$.

12.6.8 Develop the system of equations to determine the discharge for the network in Figure 12.6.3 for the linear theory method.

12.6.9 Solve for the flows in the network shown in Figure 12.6.5 using the Hardy Cross method.

12.6.10 The demands at nodes 2, 4, and 5 are increased by 0.5 cfs in the network in Figure 12.6.5. Use the Hardy Cross method to solve for the flows in the network.

12.7.1 Use the KYPIPE2 computer program to solve example 12.6.1.

12.7.2 Use the EPANET computer program to solve example 12.6.1.

12.7.3 Use the EPANET model to solve for the flows in the network shown in Figure 12.6.5.

12.7.4 Use the EPANET model to solve for the flows in the network shown in Figure 12.6.5 with the demands for nodes 2, 4, and 5 increased by 0.5 cfs.

12.8.1 Solve example 12.8.1 using a design discharge of 50 l/s.

12.8.2 Solve example 12.8.1 assuming the cast iron pipe has a diameter of 15 cm.

12.8.3 Solve example 12.8.2 assuming the pipe is 2000 m long.

12.8.4 Solve example 12.8.2 assuming the reservoir elevation is 100 m above the downstream end of the pipe.

12.8.5 Solve example 12.8.3 assuming the pipe diameter is 18 in.

12.8.6 Solve example 12.8.3 assuming the pipe diameter is 30 in.

12.8.7 Solve example 12.8.6 assuming the pipe diameter is 30 in.

12.8.8 Solve example 12.8.6 assuming the surge tank has a diameter of 6 ft.

12.8.9 Solve example 12.8.6 assuming the pipe is only 4000 ft long.

12.8.10 A butterfly valve is located at the end of a 2-mi long level pipeline having a diameter of 8 in. The headloss coefficient as a function of disc angle for the valve is shown in Figure P12.8.10. The valve discharges 220 gpm to the atmosphere. With this discharge the gage pressure just upstream of the valve is 80 psi. Compute the headloss coefficient for the valve and the degrees open of the valve (disc angle).

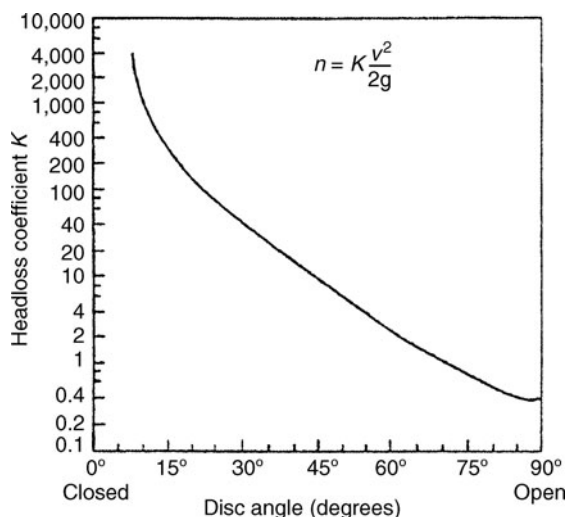


Figure P12.8.10 Headloss coefficient for a butterfly valve (Bosserman and Hunt, 1998).

12.8.11 For the system in problem 12.8.10, the valve has a linear closure from 90 degrees (open) to 0 degrees (closed) in 45 sec. For the disc angle that you computed in problem 12.8.10, is the closure time adequate for the full pressure wave to be realized? What will be the total pressure upstream of the valve?

12.8.12 A butterfly valve is placed on the end of a 3-mi long level pipeline having a diameter of 8 in. The headloss coefficient for the valve is shown in Figure P12.8.10. The valve has a linear closure from 90 degrees (open) to 0 degrees (closed) in 45 sec. The valve discharges 220 gpm into the atmosphere. With this discharge, the gauge pressure just upstream of the valve is 90 psi. For what range of initial valve openings would there be a safe close for this linear closure scheme? Compute v_c , then t_c and use t_c in the $x/90 = t_c/45$

12.8.13 Consider a 30-cm diameter pipe with a 15-mm wall thickness, $E_{\text{water}} = 2.17 \times 10^9 \text{ N/m}^2$. Calculate the water hammer pressure for a discharge of 40 l/s assuming a rigid pipe. The pipe is now considered as having a length of 1000 m. What is the critical time of closure?

REFERENCES

- Bosserman, B. E. II, "Control of Hydraulic Transients," Chapter 7 in *Pumping Station Design* edited by R. L. Sanks, Butterworth-Heinemann, Woburn, MA, 1998.
- Bosserman, B. E. II, "Pump System Hydraulic Design," *Water Distribution System Handbook* edited by L. W. Mays, McGraw-Hill, New York, 2000.
- Bosserman, B. E. II, "Pump System Hydraulic Design," in *Hydraulic Design Handbook* edited by L. W. Mays, McGraw-Hill, New York, 1999.
- Bosserman, B. E. II, and W. A. Hunt, "Fundamentals of Hydraulic Transients," in *Pumping Station Design* edited by R. L. Sanks, Butterworth-Heinemann, Woburn, MA, 1998.
- Bosserman, B. E. II, J. C. Dowell, E. M. Huning, and R. L. Sanks, "Pipes and Fittings," in *Pumping Station Design* edited by R. L. Sanks, Butterworth-Heinemann, Woburn, MA, 1998b.
- Bosserman, B. E. II, R. J. Ringwood, M. D. Schmidt, and M. G. Thalhamer, "System Design for Water Pumping," in *Pumping Station Design* edited by R. L. Sanks, Butterworth-Heinemann, Woburn, MA, 1997.
- Clark, R., "Water Quality Modeling—Case Studies," *Water Distribution Systems Handbook*, in edited by L. W. Mays McGraw-Hill, New York, 2000.
- Clark, R. M., W. M. Grayman, and R. M. Males, "Contaminant Propagation in Distribution Systems," *Journal of Environmental Engineering*, ASCE, vol. 114, no. 4, 1988.
- Cross, H., *Analysis of Flow in Networks of Conduits or Conductors*, University of Illinois Bulletin 286, November 1936.
- Cullinane, M. J., Jr., "Methodologies for the Evaluation of Water Distribution System Reliability/Availability," Ph.D. Dissertation, University of Texas at Austin, 1989.
- Edwards, D. K., V. E. Denny, and A. F. Mills, *Transfer Processes*, McGraw-Hill, New York, May 1976.
- Grayman, W. M., and G. J. Kirmeyer, "Quality of Water in Storage," in *Water Distribution Systems Handbook* edited by L. W. Mays, McGraw-Hill, New York, 2000.
- Grayman, W. M., L. A. Rossman, and E. E. Geldreich, "Water Quality," in *Water Distribution Systems Handbook* edited by L. W. Mays, McGraw-Hill, New York, 2000.
- Jeppson, R. W., *Analysis of Flow in Pipe Networks*, Ann Arbor Science, Ann Arbor, MI, 1976.
- Jones, G. M., R. L. Sanks, G. Tchobanoglous, and B. E. Bosserman II, B.E (editors), *Pumping Station Design*, 3rd edition, 2008.
- Klein, F., and R. L. Sanks, "Preliminary Design Consideration," in Chapter 25 in *Pumping Station Design* edited by R. L. Sanks, Butterworth-Heinemann, Woburn, MA, 1998.
- Lansley, K., and L. W. Mays, "Hydraulics of Distribution Systems," in *Water Distribution Systems Handbook* edited by L. W. Mays, McGraw-Hill, New York, 2000.
- Martin, C. S., "Hydraulic Transient Design for Pipeline Systems," in *Water Distribution Systems Handbook* edited by L. W. Mays, McGraw-Hill, New York, 2000.
- Martin, C. S., "Hydraulic Transient Design for Pipeline Systems," *Hydraulic Design Handbook* edited by L. W. Mays, McGraw-Hill, New York, 1999.
- Mays, L. W., (editor-in-chief), *Hydraulic Design Handbook*, McGraw-Hill, New York, 1999.
- Mays, L. W., (editor-in-chief), *Water Distribution Systems Handbook*, McGraw-Hill, New York, 2000.
- Morris, H. M., and J. M. Wiggert, *Applied Hydraulics in Engineering*, Ronald Press Company, New York, 1972.
- Ormsbee, L. E., and S. Lingireddy, "Calibration of Hydraulic Network Models," in *Water Distribution Systems Handbook* edited by L. W. Mays, McGraw-Hill, New York, 2000.
- Roberson, J. A., J. J. Cassidy, and M. H. Chaudhry, *Hydraulic Engineering*, 2nd edition, John Wiley and Sons, New York, 1997.
- Roberson, J. A., and C. T. Crowe, *Engineering Fluid Mechanics*, Houghton Mifflin Company, Boston, MA, 1990.

Rossman, L. A., "Computer Models/EPANET," in *Water Distribution Systems Handbook* edited by L. W. Mays, McGraw-Hill, New York, 2000.

Rossman, L. A., "EPANET Users Manual," Risk Reduction Engineering Lab, U.S. Environmental Protection Agency, Cincinnati, OH, 1994.

Rossman, L. A., P. F. Boulous, and T. A. Altman, "Discrete Volume Element Method for Network Water Quality Models," *Journal of Water Resources Planning and Management*, ASCE, vol. 119, no. 5, pp. 505–517, 1993.

Rutschi, K., "Die fleiderer–Sauqzahl als gutegrad der Saugfahigkeit von Kreiselpumpen," *Schweizerische Bauzeitung*, no. 12, Zurich, 1960.

Sanks, R. L., "Data for Flow in Pipes, Fittings, and Valves," Appendix B in *Pumping Station Design* edited by R. L. Sanks, Butterworth-Heinemann, Woburn, MA, 1998.

Tchobanoglous, G., "Theory of Centrifugal Pumps," Chapter 10 in *Pumping Station Design* edited by R. L. Sanks, Butterworth-Heinemann, Woburn, MA, 1998.

Ten-State Standards, *Recommended Standards for Sewage Works*, Great Lakes-Upper Mississippi Board of Sanitary Engineers, Health Education Service, Inc., Albany, NY, 1978.

Velon, J. P., and T. J. Johnson, "Water Distribution and Treatment," in *Davis' Handbook of Applied Hydraulics*, 4th edition edited by V. J. Zipparo and H. Hasen, McGraw-Hill, New York, 1993.

Walski, T., "Water Distribution," in *Water Resources Handbook* edited by L. W. Mays, McGraw-Hill, New York, 1996.

Wood, D., "Computer Analysis of Flow in Pipe Networks Including Extended Period Simulation–User's Manual," Office of Engineering, Continuing Education and Extension, University of Kentucky, 1980.

Wood, D., and C. Charles, "Hydraulic Network Analysis Using Linear Theory," *Journal of Hydraulics Division*, ASCE, vol. 98, no. HY7, pp. 1157–1170, 1972.

Wood, D. J., L. E. Ormsbee, S. Reddy, and W. D. Wood, "Users' Manual, KYQUAL, Kentucky Water Quality Analysis Program," Civil Engineering Software Center, Dept. of Civil Engineering, University of Kentucky, Lexington, KY, 1995.

Ysusi, M. A., "System Design: An Overview," in *Water Distribution System Design* edited by L. W. Mays, McGraw-Hill, New York, 2000.

Ysusi, M. A., "Water Distribution System Design," in *Hydraulic Design Handbook* edited by L. W. Mays, McGraw-Hill, New York, 1999.

Chapter 13

Water for Hydroelectric Generation

13.1 ROLE OF HYDROPOWER

Water and energy are two resources that are very necessary for humankind and are intricately connected. This chapter focuses on the need for water in the production of energy, in particular water for hydroelectric generation and for thermal power production. Table 11.2.1 summarizes consumptive water use for energy production. Table 11.2.2 summarizes consumptive water use for electricity production.

Hydroelectric power production is the most obvious use of water for the production of energy. The energy in falling water is used directly to turn turbines that generate electricity. Table 13.1.1 lists the hydroelectric capacity and generation of the various continents.

The demand for electricity, referred to as the *load*, can be expressed in terms of *energy demand* (or use power demand) or *capacity demand* (peak power demand). *The daily load shape* (power demand as a function of time of day) is illustrated in Figure 13.1.1. Load is divided into three segments (Figure 13.1.1): (1) *base load*, which is continuous for 24 hours a day; (2) *peak load*, which is the highest load occurring for a few hours a day; and (3) *intermediate load*, which is the portion between

Table 13.1.1 World Hydroelectric Capacity and Generation, 1990

Continent ^a	Installed hydroelectric capacity (10 ³ MW)	Percent of total	Hydroelectric generation (10 ⁶ MWh per year)	Percent of total
North America	156.8	26	599.6	28
Central and South America	80.3	13	353.4	17
Western Europe	155.0	25	444.7	21
Eastern Europe	15.1	2	26.3	1
Soviet Union	64.4	10	217.3	10
Middle East	3.1	1	12.6	1
Africa	18.9	3	43.2	2
Far East and Oceania	121.3	20	415.8	20
Totals	614.9	100	2112.9	100

^aContinental sums use the country assignments of the original source. Since 1990, substantial changes in Eastern Europe and the Soviet Union have occurred.

Source: Gleick, (1994); U.S. Department of Energy (1992).

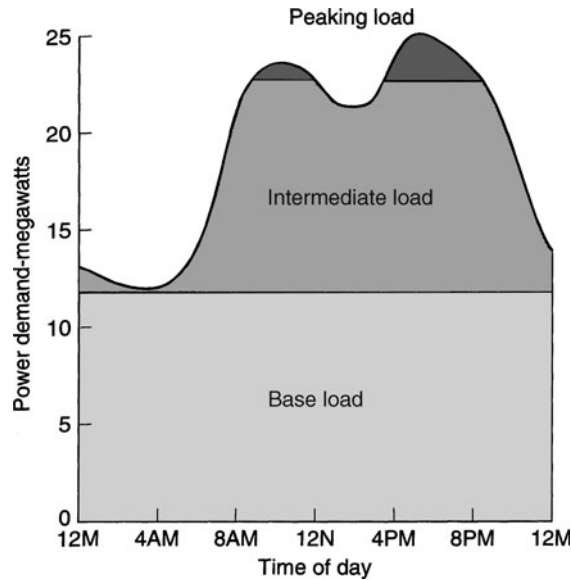


Figure 13.1.1 Daily load shape showing load types (from U.S. Army Corps of Engineers (1985)).

the load and the peak load. The load for the peak day of the year determines the required generating capacity, and the peak weekly or monthly load dictates the amount of energy stored in the form of fuel for thermal power plants or water for hydroelectric plants.

Load curves show the daily or weekly fluctuation in load as a function of time for an electric power system. Figure 13.1.2 shows a weekly load curve of a large electric utility. This figure illustrates how different types of generating units are used to meet daily demands. The value of a unit of energy is a function of the time of day, which explains why hydropower is used whenever possible as a peaking unit to replace high-cost energy.

A *load factor* is the ratio of the average load over a certain period of time to the peak load during that time. Load factors are expressed as daily, weekly, monthly, or yearly. If a load factor is high, the unit cost of energy is comparatively low because the system should be operating near capacity and near best efficiency. For a small load factor, much of the system's generating capacity is idle a large part of the time.

The *plant factor* is the ratio of the average load on a plant for the time period being considered to its aggregate rated capacity (installed capacity). An average annual *plant factor* is the average annual energy (KWh) divided by the installed capacity (KW) times 8760 hours.

The major types of hydroelectric developments are

- Run-of-river developments
- Pondage developments (Figure 13.1.3)
- Storage developments (Figure 13.1.4)
- Reregulating developments
- Pumped storage (Figures 13.1.5 and 13.1.6)

Run-of-river developments have a dam with a short supply pipe (penstock) that directs the water to the turbines. The natural flow of the river is used with very little alteration to the terrain stream channel at the site and there is very little impoundment of the water. Typical run-of-river projects include: (1) navigation projects, (2) irrigation diversion dams, and (3) projects lacking storage as a result of the topography. A *pure run-of-river* project has no usable storage.

Pondage developments are run-of-river projects with a small amount of storage (daily or weekly) that can be used to regulate discharges to follow daily and weekly load patterns. *Pondage* refers to

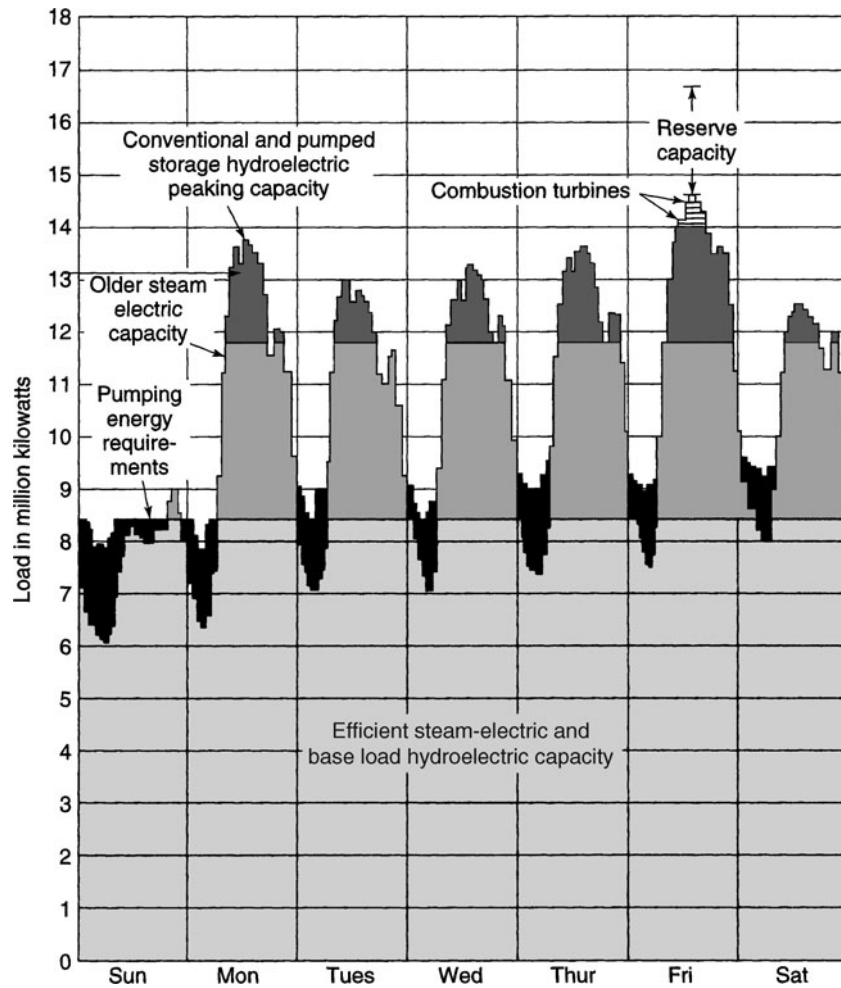


Figure 13.1.2 Weekly load curve of a large electric utility system (from U.S. Army Corps of Engineers (1979)).

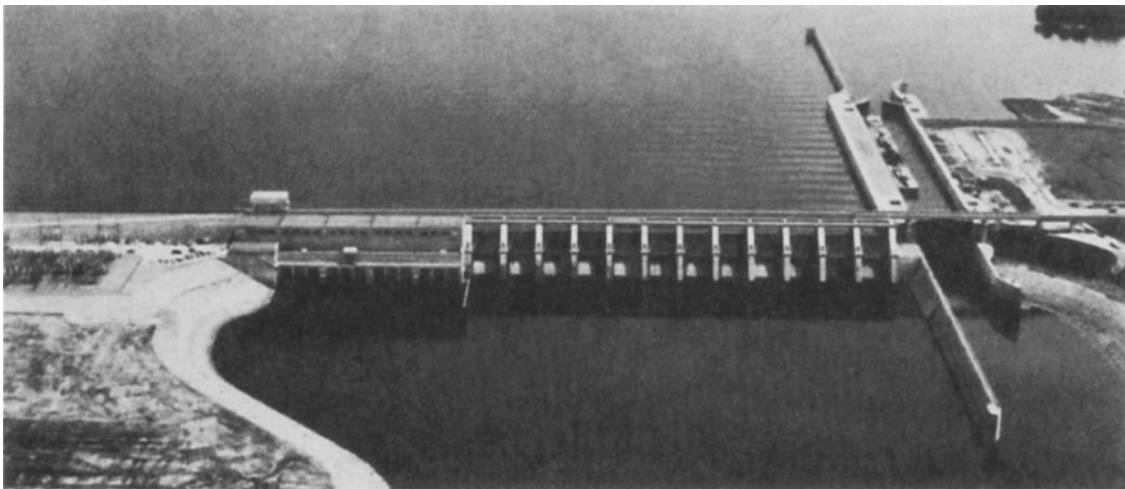


Figure 13.1.3 Barkley Lock and Dam, a run-of-river project with pondage. (Courtesy of U.S. Army Corps of Engineers Nashville District.)



Figure 13.1.4 Hoover Dam and power houses on Colorado River in Arizona. Example of storage project having maximum reservoir storage of $34.852 \times 10^6 \text{ m}^3$. Present rated capacity is 1951 MW with planned rated capacity of 2451 MW. (Courtesy of U.S. Bureau of Reclamation, photograph by A. Pernick, March 31, 1996.)



Figure 13.1.5 New Waddell Dam on the Agua Fria River in Arizona impounds Lake Pleasant. Shown downstream of dam and intake structure is the Waddell Pump/Generating Plant, which lifts Central Arizona Project (CAP) 192 feet from the canal into Lake Pleasant. The Waddell Canal connects the main CAP aqueduct with the dam. (Courtesy of Central Arizona Project.)

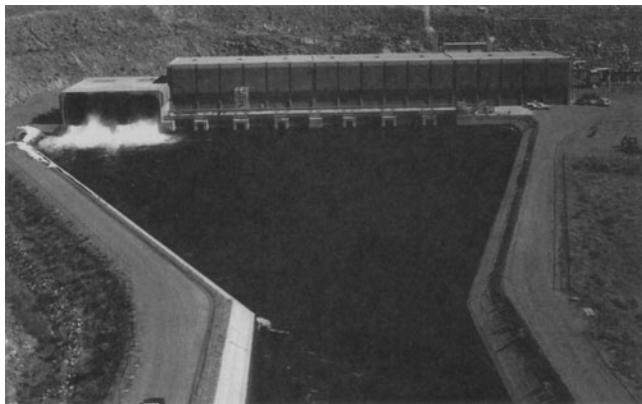


Figure 13.1.6 Waddell Pump/Generating Plant, which has eight units: four adjustable-speed pumps and four two-speed pump generators. Maximum power generation is 44 MW. CAP water is pumped into Lake Pleasant during colder months and released during the summer to generate electricity. (Courtesy of U.S. Bureau of Reclamation, photograph by J. Madrigal, Jr., August 22, 1995.)

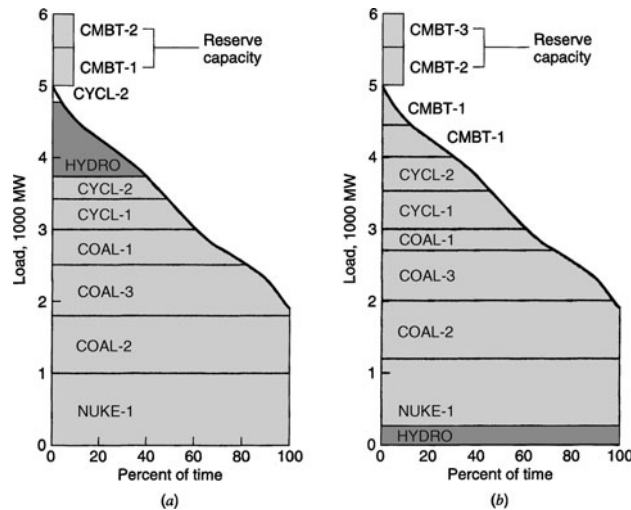


Figure 13.1.7 Duration curve showing operation of system with hydro plant. (a) In peaking mode; (b) In base load (from U.S. Army Corps of Engineers (1985)).

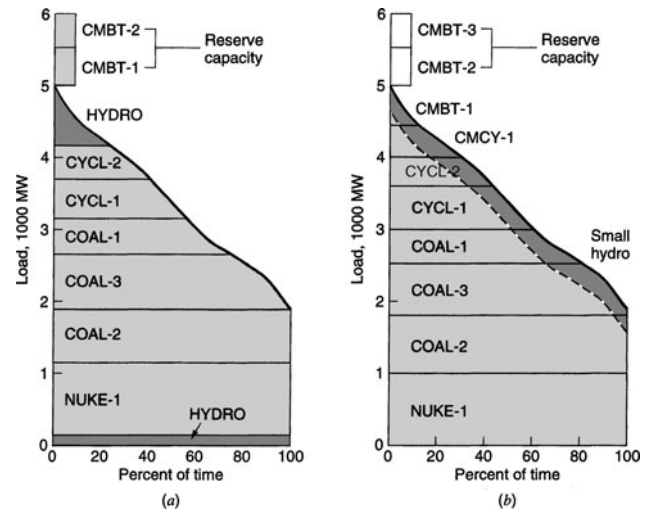


Figure 13.1.8 Duration curve showing operation of system. (a) With hydro plant carrying both base and peaking loads; (b) With pure run-of-river hydropower plant (from U.S. Army Corps of Engineers (1985)).

the short time in ponding of water, as these projects have insufficient storage for seasonal flow regulation.

Storage developments have an extensive impoundment at the power plant or are at the reservoir upstream of the power plant. *Storage* is the long-time impounding of water to allow seasonal regulation capability.

Reregulating developments receive fluctuating discharges from large hydroelectric peaking plants and release the discharges to meet downstream flow criteria. *Reregulating reservoirs* are also called *after-bay reservoirs*.

Pumped-storage developments convert low-volume off-peak energy to high-value on-peak energy. Water is pumped from a lower reservoir to a higher reservoir using inexpensive power during periods of low energy demand. Water is then discharged through the turbine to produce to meet peak demands. Pumped storage projects can also be operated on a seasonal basis as the New Waddell Dam (Figure 13.1.5).

Hydropower can be used in power systems for peaking, for meeting intermediate loads, for base load operation, or for meeting a combination of these loads (U.S. Army Corps of Engineers, 1985). A *load-duration curve* expresses the load as a function of percent of time and is commonly used to describe system operation. Figures 13.1.7a and b show the operation of a system with the hydro-power facility operating in the peaking mode and the base load, respectively. Figure 13.1.8a shows operation of a system with the hydropower facility operating in both the peaking and base modes. Figure 13.1.8b shows the operation of a run-of-river plant.

EXAMPLE 13.1.1

Determine the energy in MWh for the 1000-MW peak capacity hydroelectric plant placed in the base load as shown in Figure 13.1.7b. The plant has an average power output of 250 MW for the week.

SOLUTION

The energy is computed as $\text{Energy} = 250 \text{ MW} \times 168 \text{ hr} = 42,000 \text{ MWh}$.

EXAMPLE 13.1.2

Determine the energy in MWh for the 1000-MW peak capacity hydroelectric plant placed in the peaking mode as shown in Figure 13.1.7a. The plant factor is 25 percent.

SOLUTION

The energy is computed using

$$\begin{aligned} \text{Energy} &= (\text{capacity, MW}) \times (\text{plant factor, \%}) \times 168 \text{ hr}/100 \\ &= 1000 \text{ MW} \times 25\% \times 168 \text{ hr}/100 \\ &= 42,000 \text{ MWh} \end{aligned}$$

Note that this is the same energy as for the hydropower plant placed in the base in Example 13.1.1.

13.2 COMPONENTS OF HYDROELECTRIC PLANTS

13.2.1 Elements to Generate Electricity

Three basic elements are needed for a power generation facility:

- A means to create a head
- Conduit to convey water
- Power plant

Figure 13.2.1 illustrates some of the elements in a hydroelectric plant needed to generate electricity. The dam has the two major functions of creating the head necessary to move the turbines and impounding the storage used to maintain the necessary flow release pattern. The height of the dam establishes the generating head and the available storage for power plant operation. The *reservoir* is the water impoundment behind a dam. *Storage capacity* is the volume of reservoir available to store water. *Intake structures* direct water from the reservoir into the penstock. *Penstocks* convey water from the intake structure to the powerhouse. The *powerhouse* shelters the turbines, generating units, and control and auxiliary equipment. *Turbines* convert the potential energy of water into mechanical energy, which drives the generator. *Draft tubes* convey water from the discharge side of the turbine to the tailrace. The *tailrace* maintains a minimum tailwater elevation below the power plant and keeps the draft tube submerged. Figure 13.2.2 shows the penstocks, powerhouse, and tailrace for the Atatürk Dam in Turkey.

The various energy elements are illustrated in Figure 13.2.3. For a constant discharge, the energy relation between the forebay and any other section is $z_1 + (V_1^2/2g) = z_2 + (V_2^2/2g) + h_c$, where h_c is the loss between the two sections. The various losses are illustrated in Figure 13.2.3. A *forebay* is a regulating reservoir that temporarily stores water to facilitate one or more of the following: (1) low-approach velocity to intake, (2) surge reduction, (3) sediment removal (descending), or (4) storage.

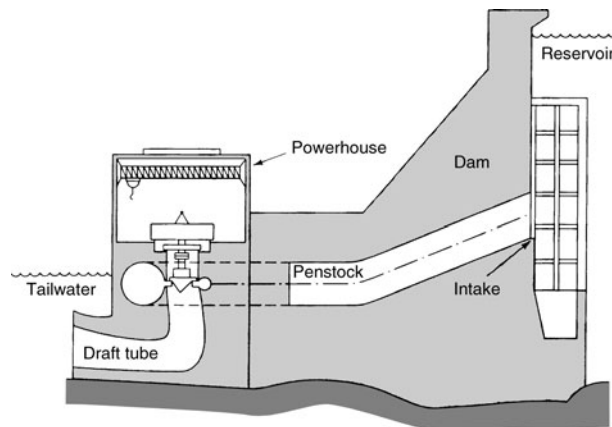


Figure 13.2.1 Components of a hydropower project (from U.S. Army Corps of Engineers (1985)).

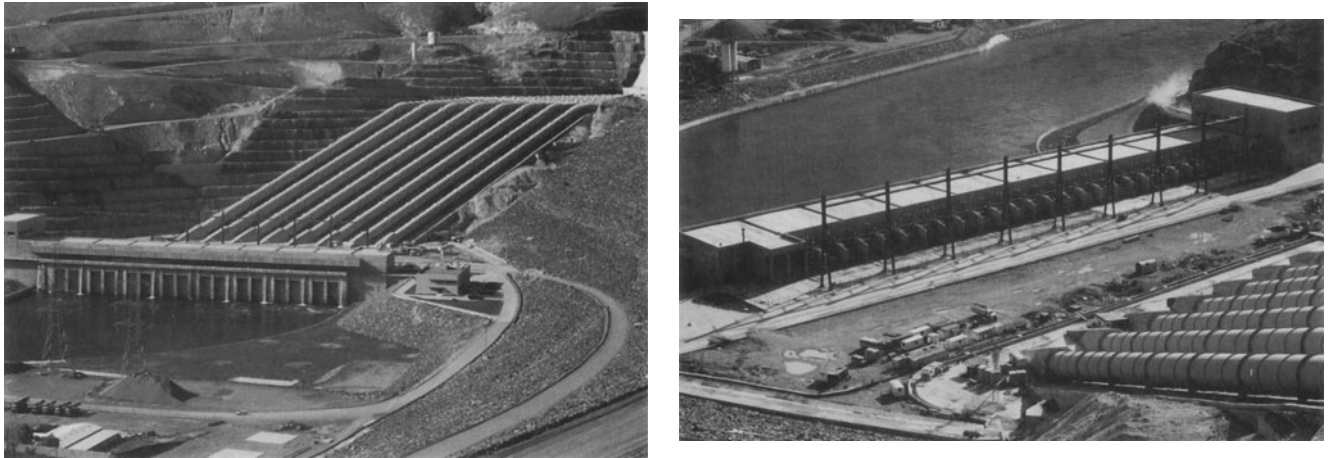


Figure 13.2.2 View of the Atatürk Dam Hydroelectric Facility on the Euphrates River in Turkey. Shown are the powerhouse and tailrace. The rated capacity is 2400 MW. Dam height is 184 m, crest length is 1820 m, dam volume is $84.5 \times 10^6 \text{ m}^3$, and maximum reservoir capacity is $48.7 \times 10^6 \text{ m}^3$. Also refer to Figures 11.4.8 and 17.2.14. (Photographs by L.W. Mays).

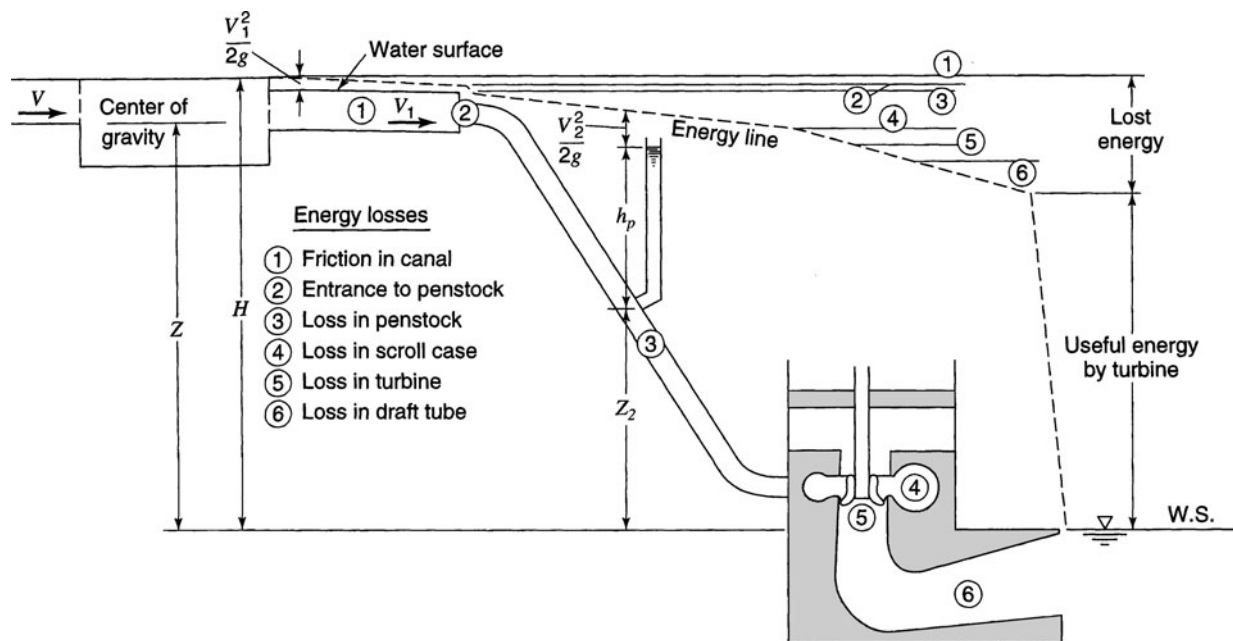


Figure 13.2.3 Energy relations in a typical hydroelectric plant (from Hasen and Antonopoulos (1993)).

They are designed to maintain the approach flow conditions as smoothly as possible (see Coleman, et al. (1999) for more details).

There are two basic types of turbines: (1) *impulse turbines* (commonly called *Pelton turbines*), in which a free jet of water impinges on a revolving element of the machine that is exposed to the atmosphere (Figure 13.2.4) and (2) *reaction turbines*, in which the flow takes place under pressure in a closed chamber (Figures 13.2.5 and 13.2.6). Reaction turbines extract power from both the kinetic energy of the water and the difference in pressure between the front end and the back of each runner

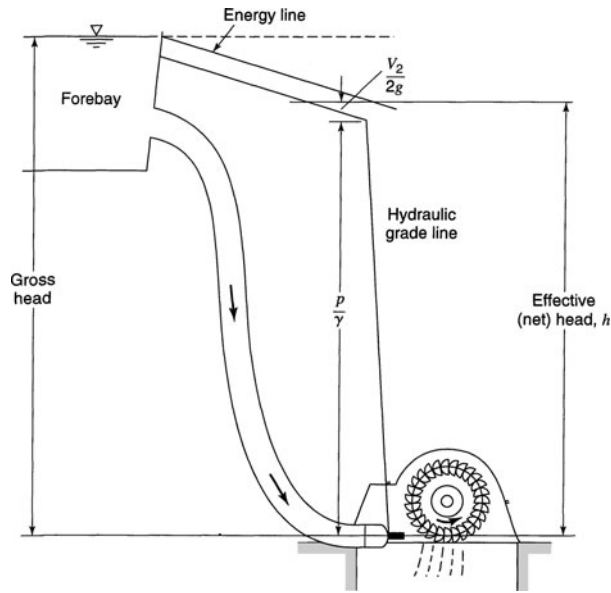


Figure 13.2.4 Definition sketch for impulse-turbine installation (from Linsley et al. (1999)).

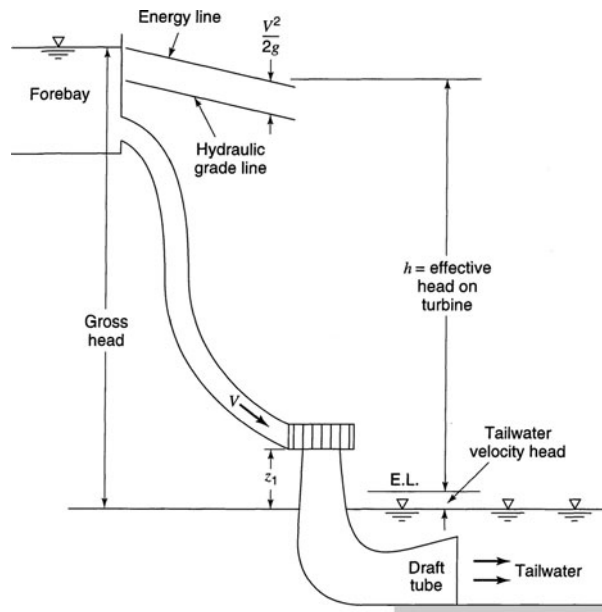


Figure 13.2.5 Definition sketch for a reaction-turbine installation (from Linsley et al. (1999)).

blade. Figure 13.2.7 presents the application ranges for conventional turbines and Figure 13.2.8 presents turbine efficiency curves.

Impulse or Pelton turbines have a runner with numerous spoon-shaped buckets attached to the periphery and are driven by one or more jets of water issuing from fixed or adjustable nozzles, as shown in Figure 13.2.9. Large Pelton turbines can be used at heads above 1000 feet and smaller turbines can be used at heads of less than 100 feet.

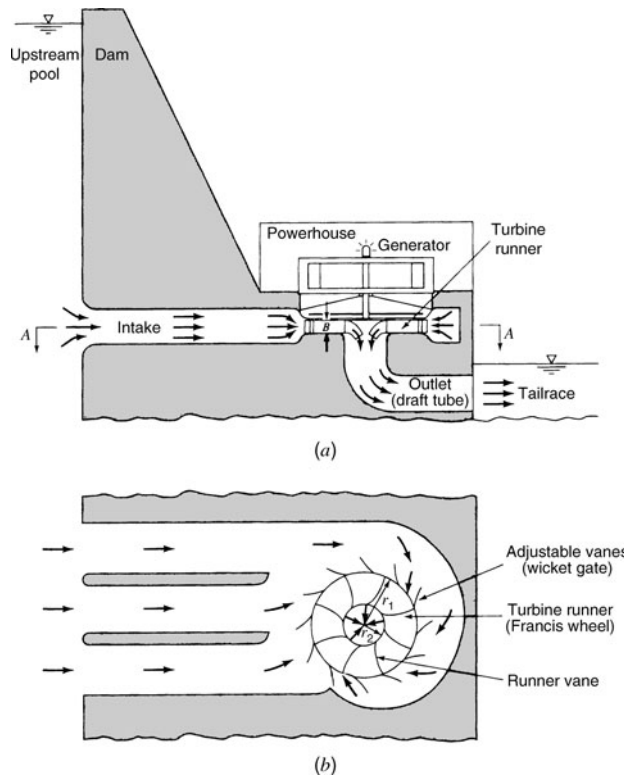


Figure 13.2.6 Schematic view of reaction-turbine installation. (a) Elevation view; (b) Plan view—section A–A (from Roberson et al. (1998)).

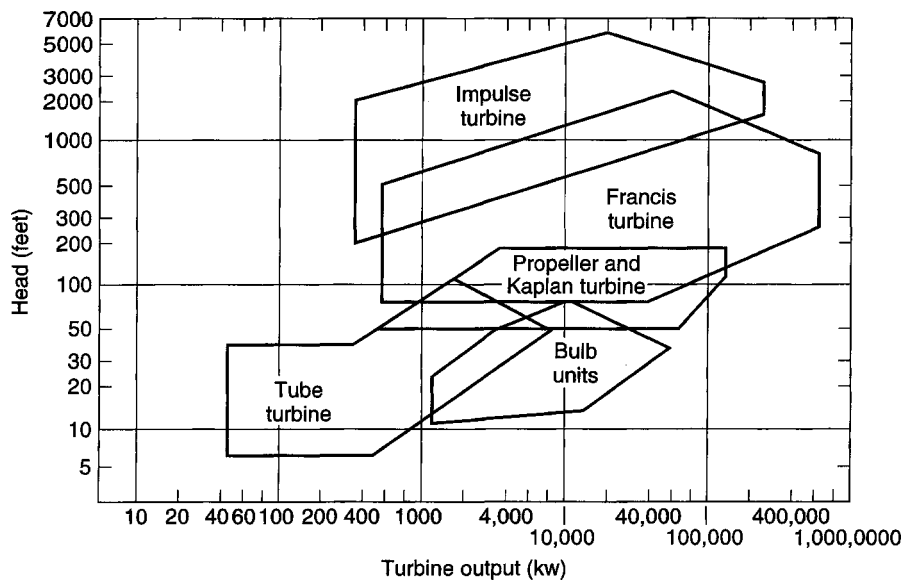


Figure 13.2.7 Application ranges for standard and custom hydraulic turbines (from U.S. Army Corps of Engineers (1985)).

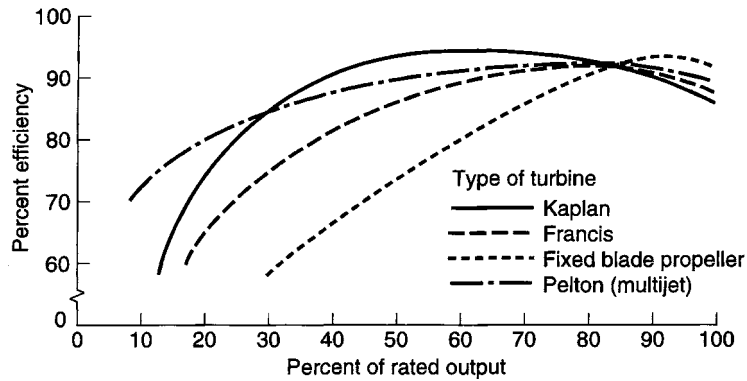


Figure 13.2.8 Turbine efficiency curves (from U.S. Army Corps of Engineers (1985)).

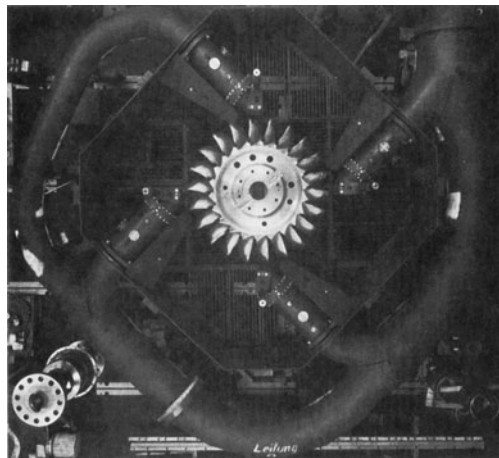


Figure 13.2.9 Pelton turbine and nozzle layout. (Courtesy of Sulzer-Escher Wyss Ltd.)

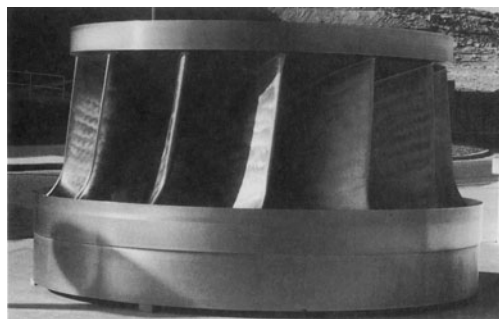


Figure 13.2.10 Francis turbine (turbine runner) used at Glenn Canyon Dam, on the Colorado River near Page, Arizona (Photograph by L.W. Mays).

Reaction turbines include *Francis turbines*, which are constructed so that water enters the runner radially and then flows towards the center and along a turbine shaft axis. These turbines have been typically used for heads ranging from 100 to 1500 feet and are the economical choice for heads ranging from 150 to 1500 feet. Figure 13.2.10 illustrates a Francis turbine.

Fixed-blade propeller turbines are constructed so that water passes through the propeller blades in an axial direction. These turbines are typically used in the 10–200 feet head range and are the

economical choice in the 50–150 foot head range. Kaplan turbines are propeller turbines with adjustable pitch blades that operate in the same general range as propeller turbines.

Tubular turbines have a guide vane assembly that is in line with the turbine and contributes to the tubular shape. These turbines may be vertical, horizontal, or slant-mounted axial flow turbines. Tubular turbines can be the economical choice for heads less than 50 feet. *Bulb turbines* are horizontal axial-flow turbines with a turbine runner connected directly to a generator or through a speed-increasing gearbox. A *rim turbine* is similar to the bulb turbine with the generator mounted on the periphery of the turbine runner blades. Rim turbines are suitable for 10- to 50-foot heads.

13.2.2 Hydraulics of Turbines

This subsection briefly describes the hydraulic action of turbines; see Figure 13.2.11 for impulse turbines and Figure 13.2.12 for reaction turbines. The impulse turbine rotates at a velocity u at the center line of the buckets. When water enters the bucket, it is in position A and the bucket moves to position B, where the water leaves the bucket. The velocity changes from V_1 at the entrance to V_2 at the exit. The velocity v represents the velocity of the water relative to the bucket, so that at entry $V_1 = u + v$. Ignoring fluid friction, the magnitude of the water velocity relative to the bucket remains constant with a change in direction so that it is tangential to the bucket. The force F exerted by the discharge of water Q on the bucket is described by the impulse-momentum, neglecting friction, as

$$F = \rho Q(V_1 - V_2 \cos \alpha) \quad (13.2.1)$$

Equation (13.2.1) can also be expressed in terms of relative velocities as

$$F = \rho Q(v - v \cos \beta) = \rho Q(V_1 - u)(1 - \cos \beta) \quad (13.2.2)$$

where the relative velocity $v = V_1 - u$.

The power transmitted to the buckets is the product of force and velocity

$$P = Fu = \rho Q(V_1 - u)(1 - \cos \beta)u \quad (13.2.3)$$

From equation (13.2.3) it is apparent that no power is developed when $u = 0$ or $u = V_1$. Maximum power with respect to u occurs when

$$dP/du = \rho Q(1 - \cos \beta)(V_1 - u - u) = 0 \quad (13.2.4)$$

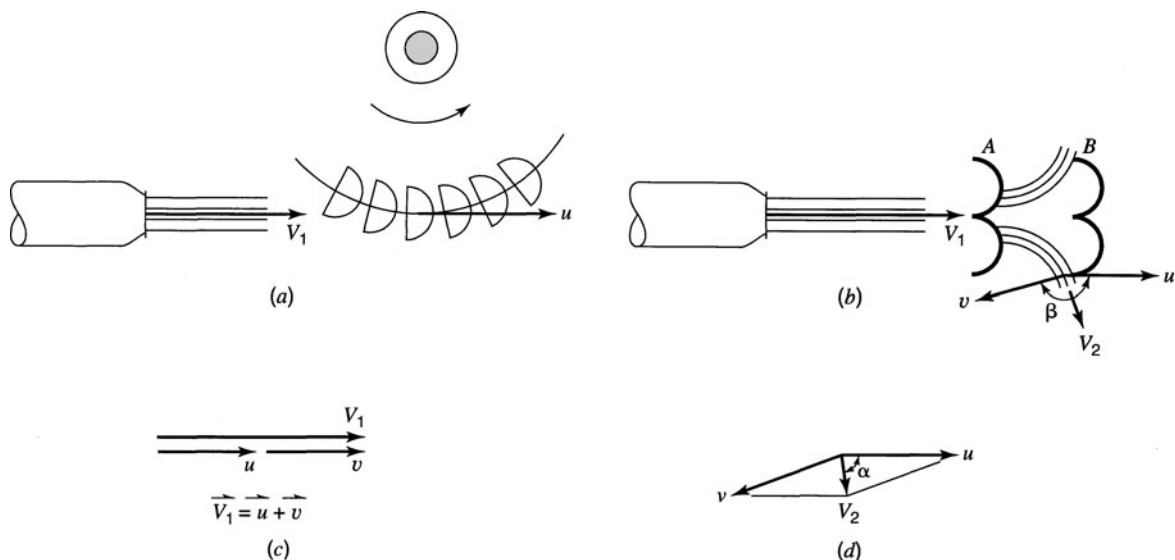


Figure 13.2.11 Hydraulic relationships for an impulse turbine (from Linsley et al. (1999)).

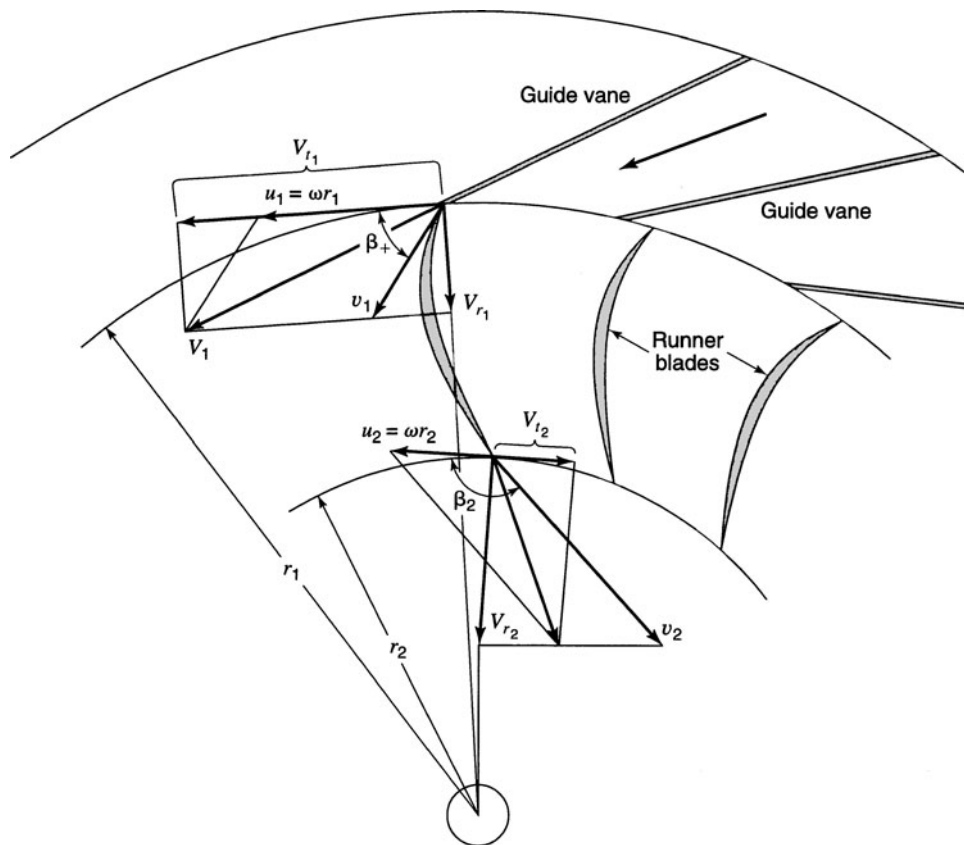


Figure 13.2.12 Vector diagrams for a reaction turbine (from Linsley et al. (1999)).

which can be solved for

$$u = V_1/2 \tag{13.2.5}$$

This argument says that, when friction is negligible, the best hydraulic efficiency occurs when the peripheral speed of the wheel is half of the velocity of the jet of water.

The *brake power* delivered by a turbine to the generator is

$$Bh_p = \frac{\gamma h e}{550} Q \tag{13.2.6}$$

in English units where Bh_p is in horsepower, h is the effective head, and γ , Q , and h are expressed in customary units of lb/ft^3 , ft^3/s , and ft , respectively. In SI units, the brake power is expressed as

$$Bk_w = \gamma Q h e \tag{13.2.7}$$

where Bk_w is brake kilowatts and γ , Q , and h are expressed in kN/m^3 , m^3/s , and m , respectively. Note that $1 \text{ hp} = 550 \text{ ft}\cdot\text{lb}/\text{s} = 0.746 \text{ kW}$.

The flow through the radial-flow runner of a Francis turbine is used to explain the action of reaction turbines. In Figure 13.2.12, the velocity is $u_1 = \omega r_1$ at the entrance edge of the runner blade, where ω is the rotative speed of the runner in radians per second. This entering velocity to the blade is essentially tangential to the exit end of the guide vane. The component of V_1 that is tangent (V_{t1}) to the entrance of the runner blade is

$$V_{t1} = \omega r_1 + V_{r1} \cot \beta_1 \tag{13.2.8}$$

where V_{r1} is the radial component of the velocity. The tangential component of the velocity at the exit is

$$V_{t2} = \omega r_2 + V_{r2} \cot \beta_2 \quad (13.2.9)$$

The torque T exerted on the runner blades is

$$T = \rho Q (V_{t1} r_1 - V_{t2} r_2) \quad (13.2.10)$$

where Q is the total discharge through the turbine. The power transmitted to the turbine from the water is

$$P = T\omega = \rho Q \omega (V_{t1} r_1 - V_{t2} r_2) \quad (13.2.11)$$

The following continuity equation can be used to determine the radial velocity components:

$$Q = 2\pi r_1 Z V_{r1} = 2\pi r_2 Z V_{r2} \quad (13.2.12)$$

where Z is the height of the turbine blades.

As with pumps, the concept of a *turbine-specific speed* is also used. For turbines, we are more interested in the power of the turbine than the discharge. The dimensional form of the specific speed n_s used by the hydraulic turbine industry is

$$n_s = \frac{NP^{1/2}}{H^{5/4}} \quad (13.2.13)$$

where N is the rotational speed in rpm, P is the power in horsepower, and H is the head on the turbine in feet. For a given Q and H , the actual speed is directly proportional to the specific speed.

Cavitation in turbines is very undesirable, since it causes pitting, mechanical vibration, and loss of efficiency. The concept of cavitation is discussed in more detail in Chapter 12. Cavitation can be avoided by designing, installing, and operating turbines so that the local absolute pressure never drops to the vapor pressure of the water. The susceptibility to cavitation in turbines is given by the *cavitation index*, defined as

$$\sigma = \frac{p_0/\gamma - p_v/\gamma - (z_1 - z_0)}{H} \quad (13.2.14)$$

where p_0 = absolute atmospheric pressure, p_v = absolute vapor pressure of the water, z_1 = elevation of the downstream side of the turbine above the water surface in the tailrace, z_0 = elevation of tailrace water surface, and H = net head across the turbine (head change from upstream of turbine to the downstream end of draft tube). As previously described, the tailrace is the channel into which the flow from the draft tube discharges. See Figures 13.2.2, 13.2.5, and 13.2.6.

For a given turbine operating with a given H and speed, if z_1 is increased or p_0 decreased, the pressure acting on the blades of the turbine decreases and eventually reaches a point at which cavitation would occur. Then lower values of σ indicate a greater tendency for cavitation. Cavitation susceptibility also changes with the speed of the impeller because greater speed means greater relative velocities and less pressure on the downstream side of the impeller. Critical σ_c values are obtained from experiments.

13.2.3 Power System Terms and Definitions

Many useful power system terms are defined in this subsection. *Power* is the rate of energy, and the *energy* produced by a power-generating unit is equal to the power multiplied by the time

period of production. The SI unit for power is kilowatt (KW), where one horsepower is 0.7457 KW. The common units for energy are kilowatt-hour (KWh), or the amount of power that can be generated and produced with little or no interruption, and *firm energy* is the corresponding energy. *Firm power* is typically thought of as being available 100 percent of the time. The power generated in excess of firm power is called *secondary* (or *surplus, interruptible power*). Secondary power cannot be relied upon, and therefore the rate of secondary power is generally well below that of firm power. Secondary power is interruptible but is available more than 50 percent of the time. The third type of power, *dump power*, is much less reliable and is available less than 50 percent of the time.

The *capacity* is the maximum amount of power that a generating unit or power plant can deliver at any given time in KW. The *rated capacity* of a generating unit is the capacity that the unit is designed to deliver. The *overflow capacity* is the capacity that a generating unit can deliver for a limited time in excess of normal rated capacity (or *nameplate capacity*).

The *installed capacity* is the nominal capacity of a power plant determined as the sum of the rated (or nameplate) capacities of all units in a power plant. The *dependable* or *firm capacity* is the capacity that a power plant can reliably contribute to meet peak power demands. *Hydraulic capacity* is the maximum discharge that a hydroelectric plant can use for power generation.

EXAMPLE 13.2.1

A reaction turbine is supplied with water through a 150-cm pipe (penstock) ($e = 1.0$ mm) that is 40 m long. The water surface in the reservoir is 20 m above the draft tube inlet, which is 4.5 m above the water level in the tailrace. If the turbine efficiency is 92 percent and the discharge is $12 \text{ m}^3/\text{s}$, what is the power output of the turbine in kilowatts? Use $f = 0.0185$.

SOLUTION

To determine the power, use equation (13.2.7). The velocity through the 40-m penstock is computed using continuity, $V = Q/A = 12/(\pi(1.5)^2/4) = 6.8$ m/s. The headloss due to friction in the pipe is computed using the Darcy–Weisbach equation:

$$h_L = f \frac{L}{D} \frac{V^2}{2g} = 0.0185 \left(\frac{40}{1.5} \right) \left(\frac{(6.8)^2}{2(9.81)} \right) = 1.16 \text{ m}$$

The effective head is

$$h = \frac{p}{\gamma} + z - h_L = 20 + 4.5 - 1.16 = 23.34 \text{ m}$$

Therefore, the power output of the turbine is computed as

$$BK_w = \gamma Q h e = 9.81(12)(23.34)(0.92) = 2,528 \text{ KW}$$

EXAMPLE 13.2.2

A turbine is to be installed at a location where the net available head is 350 ft and the available flow will average 1000 cfs. What type of turbine is recommended? If the turbine has an operating speed of 300 rpm and an efficiency of 0.90, what is the specific speed?

SOLUTION

The brake horsepower delivered by the turbine is computed using equation (13.2.6):

$$Bh_p = P = \frac{\gamma Q h e}{550} = \frac{62.4(1000)(350)(0.9)}{550} = 35,738 \text{ hp} = 26,650 \text{ KW}$$

For a head of 350 ft and 26,650 KW output, according to Figure 13.2.7, this falls into the range of application of the Francis turbine. The specific speed is computed using equation (13.2.13):

$$n_s = \frac{NP^{1/2}}{H^{5/4}} = \frac{300(35,738)^{1/2}}{(350)^{5/4}} = 37.46$$

13.3 DETERMINING ENERGY POTENTIAL

13.3.1 Hydrologic Data

This section briefly discusses the types and sources of hydrologic data needed for hydropower studies. The most important data for a hydropower feasibility study is stream-flow data, which is used to develop estimates of water available for power generation. The most commonly used stream-flow data is mean daily flows, mean weekly flows, and mean monthly flows. This data is used to develop flow-duration curves, which show the percentage of time that flow equals or exceeds various values during the period of record, as shown in Figure 13.3.1. *Flow-duration curves* summarize the stream-flow characteristics and can be constructed from daily, weekly, or monthly stream-flow data. These curves, unfortunately, do not present flow in chronological sequence, do not describe the seasonal distribution of streamflows, and do not take into account variations of head independent of streamflow. Figure 13.3.2 illustrates a monthly flow distribution, which describes the seasonal distribution. Other types of hydrologic data required include tailwater rating curves, reservoir elevation-area-capacity relationships, sediment data, water quality data, downstream flow information, water surface fluctuation data, and evaporation seepage loss analysis.

13.3.2 Water Power Equations

The quantity of water available (discharge Q), the net hydraulic head H across the turbine, and the efficiency of the turbine e_t , define the amount of power that a hydraulic turbine can provide. This relationship is expressed by the *water power equation* as

$$H_p = \frac{QHe_t}{8.815} \quad (13.3.1)$$

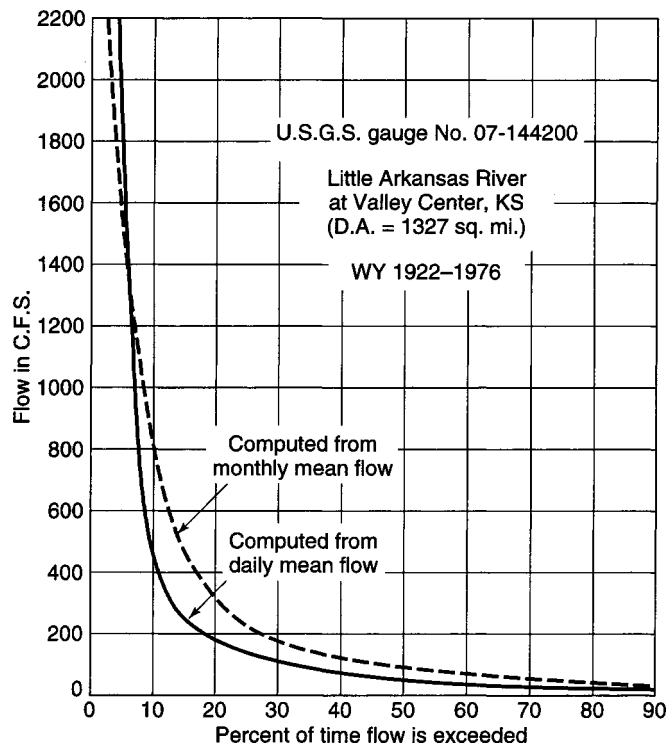


Figure 13.3.1 Flow duration curves (from U.S. Army Corps of Engineers (1979)).

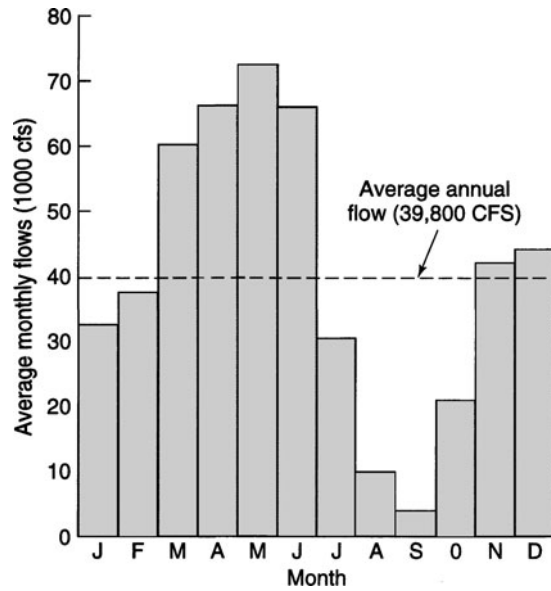


Figure 13.3.2 Monthly flow distribution (from U.S. Army Corps of Engineers (1985)).

where H_p is the theoretical horsepower available, Q is in cfs, and H is in ft. Equation (13.3.1) can also be expressed in terms of kilowatts of electrical output as

$$KW = \frac{QHe}{11.81} \tag{13.3.2}$$

where e is the overall efficiency defined as

$$e = e_g e_t \tag{13.3.3}$$

where e_g is the generator efficiency. For preliminary studies, a turbine and generator efficiency of 80 to 85 percent is typically used (U.S. Army Corps of Engineers, 1985).

To convert the power output (KW) to energy (KWh), equation (13.3.2) must be integrated over time:

$$KWh = \frac{1}{11.81} \int Q(t)H(t)e dt \tag{13.3.4}$$

The discharges in this equation are those available for power generation. The integration process can be performed using either a sequential streamflow routing procedure or flow-duration analysis, in

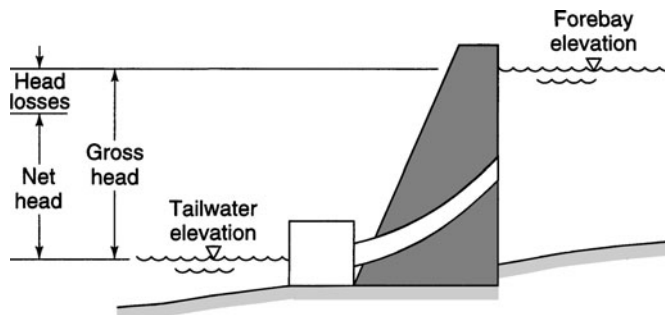


Figure 13.3.3 Gross head versus net head (from U.S. Army Corps of Engineers (1985)).

which the series of expected flows are represented by a flow-duration curve. For either approach, the streamflow used must represent the usable flow available for power generation. The *gross* or *static head* is determined by subtracting the tailwater elevation from the water surface elevation in the forebay (see Figure 13.3.3). The *net head* is the actual head available for power generation and is used in computing the energy. The net head is the gross head minus the head losses due to intake structures, penstocks, and outlet works. The losses within the turbine are accounted for in the turbine efficiency.

EXAMPLE 13.3.1

Determine the average discharge from a reservoir required to generate 4700 MWh of energy at the hydropower plant for a month (30 days). The average head is 95 ft and the overall efficiency is 0.85. What is the storage draft, that is, the volume of water that must be released, assuming this is a critical drawdown period for the reservoir?

SOLUTION

The average discharge is determined using a simplified form of equation (13.3.4),

$$Q = \frac{11.81 \text{ KWh}}{Het} = \frac{11.81(47,000,000 \text{ KWh})}{95(0.85)(720)}$$

$$= 955 \text{ cfs}$$

The storage draft is computed considering that 955 cfs is continuous over the 30-day time period. For 30 days compute the number of acre-ft/cfs, which can be shown to be 59.5 ac-ft/cfs. Therefore,

$$(955 \text{ cfs})(59.5 \text{ acre-ft/cfs}) = 56,800 \text{ ac-ft}$$

EXAMPLE 13.3.2

The release for hydropower production over a 30-day month resulted in a loss of head of 10 ft in the reservoir. The average discharge for the next month is 1824 cfs. What is the loss of energy over the next 30 days due to the drop in head?

SOLUTION

Use the energy equation to determine the energy loss:

$$\text{Energy loss(KWh)} = \frac{QHe}{11.81} t = \frac{1824(0.85)(10)}{11.81} (720) = 945,000 \text{ KWh} = 945 \text{ MWh}$$

13.3.3 Turbine Characteristics and Selection

13.3.3.1 Turbine Characteristics

The efficiency, usable head range, and minimum discharge are turbine characteristics that can have an effect on energy output. For preliminary studies, a fixed efficiency and ignoring the minimum discharge and head range limitation are sufficient; however, for feasibility studies these characteristics must be taken into account as they may have a significant impact on the results.

Design head is the head at which a turbine operates at maximum efficiency. This design head is normally specified at or near the average head, where the project will operate most of the time. However, the design head should be selected so that the desired range of heads is within the permissible operating range of the turbine. The design head for run-of-river projects can be determined from a head-duration curve as the midpoint of the head range where the project is generating power (see Figure 13.3.4). Design head is normally based on an entire year of operation; however, it may be based on the peak months only, where dependable capacity is important. For pondage projects, the design head can be based on a weighted average head, where the weight is a

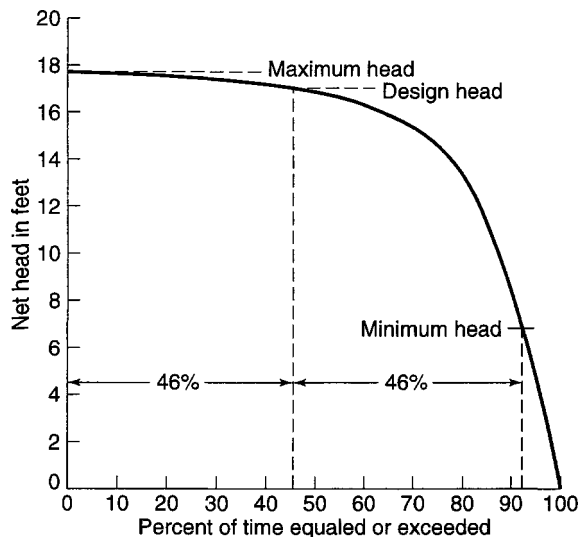


Figure 13.3.4 Head-duration curve for run-of-river project, showing how design head can be determined (from U.S. Army Corps of Engineers (1985)).

function of the generation at each head:

$$\text{Weighted average head} = \frac{\sum(\text{head generation})}{\sum(\text{generation})}$$

Rated head is the head at which rated power is obtained with the wicket gates fully open; thus, rated head is the minimum head at which rated output can be obtained. As shown in Figure 13.3.5, the

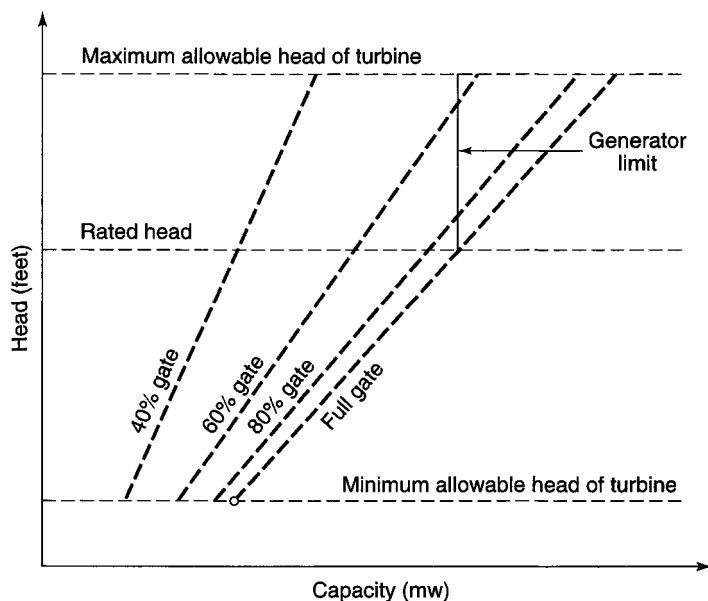


Figure 13.3.5 Turbine performance curve for a specific design (solid line represents maximum output of unit) (from U.S. Army Corps of Engineers (1985)).

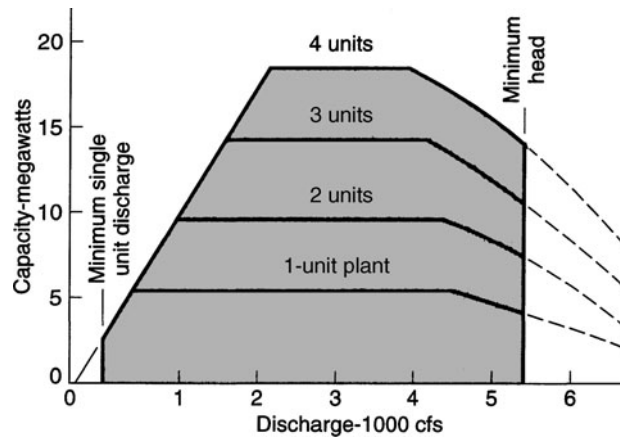


Figure 13.3.6 Capacity versus discharge for run-of-river project for alternative plant sizes (from U.S. Army Corps of Engineers (1985)).

rated head capacity of a generator limits the power output, and as a consequence full-rated capacity can be obtained for all heads above the rated head. Below the rated head, the maximum achievable power output is less than the rated capacity, even with the turbines completely open. Figure 13.3.5 illustrates a turbine performance curve for a specific design. The range of head for the normal operation of some projects is small enough that the rated output is accomplished over the entire operating range, while for other projects, the range of head is such that the operating head falls below the rated head, so that the generator capability decreases. This occurs at storage projects with a large drawdown and at pondage projects with a large installed capacity where the tailwater elevation increases at high plant discharges. This is further illustrated in Figure 13.3.6, showing capacity versus discharge curves for different numbers of 5 MW units at a low head and run-of-river projects. Power output drops off at higher discharges as a result of tailwater encroachment.

Rated discharge is the discharge at rated head with the wicket gates fully open. Because of cavitation and vibration problems, the minimum discharge in turbines is 30 to 50 percent of the rated discharge. Table 13.3.1 lists minimum discharges. For preliminary power studies, minimum discharges normally can be ignored; however, for feasibility and more abnormal studies, the minimum discharge must be taken into account.

The efficiency used in power studies is the combined efficiency of the turbine and the generator. Generator efficiency is usually assumed at 98 percent for large units and 95 to 96 percent for units smaller than 5 MW (U.S. Army Corps of Engineers, 1985). Turbine efficiency, on the other hand,

Table 13.3.1 Discharge and Head Ranges for Different Types of Turbines

Turbine type	Ratio of minimum discharge to rated discharge	Ratio of minimum head to maximum head
Francis	0.40	0.50
Vertical-shaft Kaplan	0.40	0.40
Horizontal-shaft Kaplan	0.35	0.33
Fixed-blade propeller	0.65	0.40
Fixed-gate adjustable blade propeller	0.50	0.40
Fixed geometry units (pumps as turbines)	—	0.80
Pelton (adjustable nozzles)	0.20	0.80

Source: U.S. Army Corps of Engineers (1985).

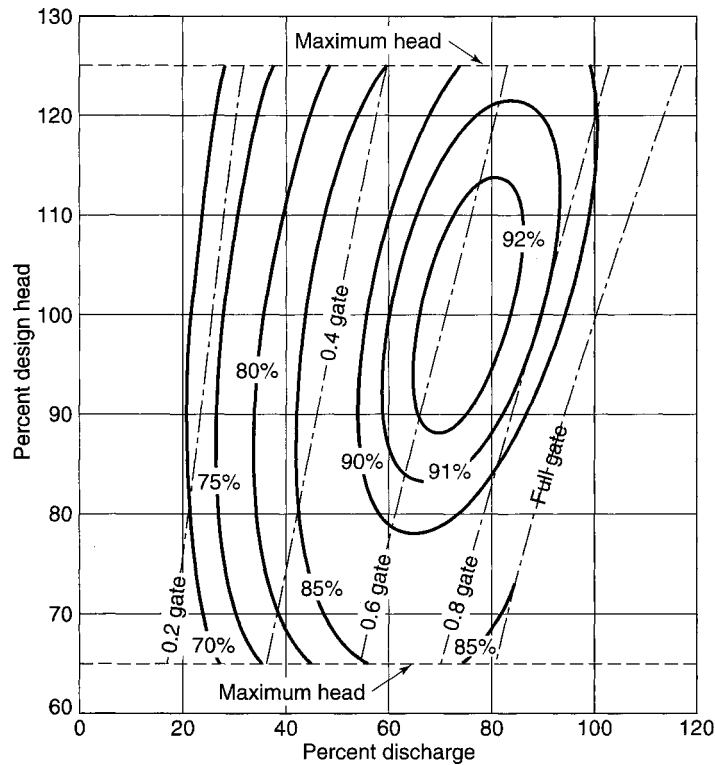


Figure 13.3.7 Typical Francis turbine performance curve (from U.S. Army Corps of Engineers (1985)).

varies with the percent of discharge head, as illustrated in Figure 13.3.7 for a typical Francis-type turbine.

13.3.3.2 Turbine Selection

The selection of a turbine is an iterative process in which preliminary power studies provide approximate plant capacity, expected head range, and an estimated design head. Preliminary turbine designs are selected and used as input for more detailed studies, making it possible to better identify the desired operating characteristics, final turbine design, and plant configuration. Performance data for various types of turbines is required in the turbine selection process. This data can be obtained from manufacturers. For turbine selection, the U.S. Army Corps of Engineers (1985) recommends the following data: (a) expected head range; (b) head-duration data (not required but very useful); (c) design head (optional); (d) total plant capacity (either hydraulic capacity in cfs or generator installed capacity in megawatts); (e) minimum discharge at which generation is desired; (f) alternative combination of size and number of units to be considered (optional); (g) head range at which full-rated capacity should be provided if possible (optional); and (h) tailwater rating curve.

The *generator rated output* is selected to match the turbine output at rated head and discharge. The head at which a turbine is rated can vary with type of operation.

13.3.4 Flow Duration Method

The *flow duration method* is limited to the analysis of small hydro projects, particularly run-of-river projects, and for preliminary analysis only of other projects. The sequential streamflow-routing method (see section 13.3.5) should be used for storage projects.

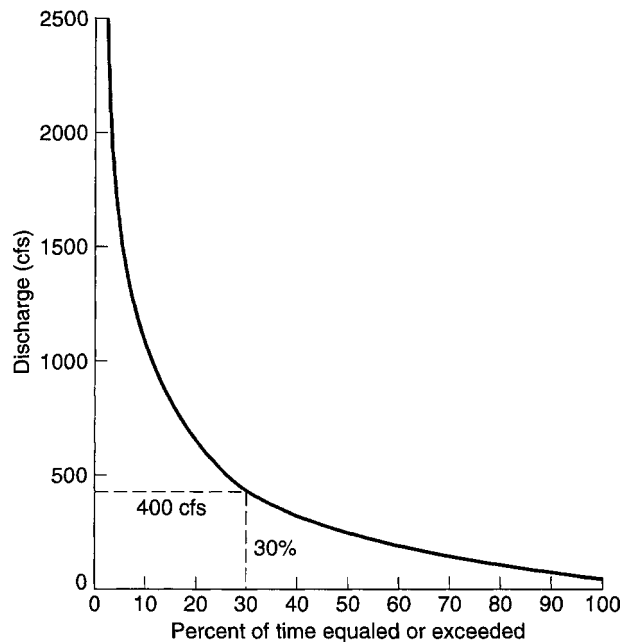


Figure 13.3.8 Flow-duration curve (from U.S. Army Corps of Engineers (1985)).

The flow-duration curve previously described is the basis for this method. Flow-duration curves are typically developed from historical records to represent the percent of time different levels of streamflow are equaled or exceeded. A flow-duration curve can be converted to a *power-duration curve* by using the water power equation. The power-duration curve can then be used to estimate a site's energy potential. These types of *duration curve–energy analyses* are based on flow for an entire year for engineering purposes. For marketing purposes it is necessary to develop duration curves monthly or seasonally. Dependable capacity for small projects is usually based on the average capacity available during peak demand months.

Data requirements. The data required include (U.S. Army Corps of Engineers, 1985) routing interval (daily time interval), streamflow data, minimum length of record (representative period), streamflow losses (both consumptive and nonconsumptive), reservoir characteristics (elevation versus discharge, or assume fixed elevation), tailwater data (tailwater curve or fixed value), installed capacity (specific capacity in all but preliminary studies), turbine characteristics (specific maximum and minimum discharges and maximum and minimum heads), efficiency (fixed efficiency or efficiency versus discharge curve), headlosses (fixed value or headloss versus discharge curve), and nonpower operating criteria (use flow data that incorporate criteria).

The following is a summary of the basic steps for computing average annual energy and dependable capacity using the flow duration method (see U.S. Army Corps of Engineers (1985) for further details).

Step 1—Develop flow-duration curve. Use available streamflow records that have been adjusted to reflect depletion and streamflow regulation. The flow duration curve for example 13.3.1 is shown in Figure 13.3.8.

Step 2—Adjust flow-duration curve. The U.S. Army Corps of Engineers (1983) recommends that if less than 30 years of flow data is available, streamflow records from nearby stations with larger periods should be analyzed to determine if substantially wetter or drier periods than the long-term average occurred. If there were substantially wetter or drier periods, then the flow-duration should be adjusted by correlating with the flow duration determined by the larger records.

Step 3—Determine flow losses. Flow losses such as consumptive losses include reservoir surface evaporation losses and diversion such as for irrigation and water supply. Nonconsumptive losses include irrigation lock requirements, fish-passage facility requirements, leakage through or around dams and embankment structures, leakage around spillway or regulating outlet gate, and leakage through turbine wicket gates.

Step 4—Develop head data. A head versus discharge curve can be developed that reflects the variation of tailwater elevation with discharge (and forebay elevation with discharge if this relation exists). A second approach is to include the head computation directly in the water power equation so that the net head is the forebay elevation minus the tailwater elevation minus the trashrack and penstock head losses.

Step 5—Select plant size. First the plant hydraulic maximum discharge that can be passed through the turbine is selected. For preliminary studies the initial plant size can be based on the average annual flow or a point between 15 and 30 percent exceedance on the flow-duration curve. Next the net head corresponding to the assumed hydraulic capacity is identified. For pure run-of-river plants the head at hydraulic capacity is the rated head. The water power equation is now used with the hydraulic capacity, rated head, and an assumed overall efficiency to compute the plant's installed capacity. Data from Table 13.3.1 can be used to establish the minimum discharge and corresponding head and the minimum head.

Step 6—Define usable flow range and derive head-duration curve. The flow-duration curve is reduced to include only the usable flow range, because the turbine characteristics limit the portion of streamflow that can be used for power generation. Using the flow-duration data and the head versus discharge data, a head-duration curve can be constructed.

Step 7—Derive the power-duration curve. Use 20 to 30 points from the flow-duration curve and determine the power for each using the water power equation. Heads are computed for each point or are taken from the head-discharge curve. Losses are subtracted from the flow in the flow-duration curve. The results are plotted as a usable generation curve with the generation values plotted at the percent exceedance points corresponding to the discharges on the flow-duration curve. The data from the usable generation-duration curve can be used to develop a true duration curve.

Step 8—Compute average annual energy. The power-duration curve, being based on all years of record, is an annual generation curve. The area under this curve represents the *average annual energy*, expressed as

$$\text{Annual energy (KWh)} = \frac{8760}{100} \int_0^{100} P dp \quad (13.3.5)$$

where P is the power in KW and p is the percent of time.

Step 9—Compute dependable capacity. The dependable capacity is the average power obtained from the generation-duration curve. For a run-of-river project, the generation-duration curve is based on streamflows for the peak demand months. The *dependable capacity* is

$$\text{Dependable capacity} = \text{average generation} = \frac{1}{100} \int_0^{100} P dp \quad (13.3.6)$$

For pondage projects a peaking capacity-duration curve is developed to determine dependable capacity. This curve is similar to a capacity-duration curve, which shows the percent of time different levels of peaking capacity are available. The power-duration curve and the capacity-duration for run-of-river projects are identical.

EXAMPLE 13.3.3

The flow-duration curve method is used to compute the average annual energy and dependable capacity for a typical low-head run-of-river project with no pondage. The flow-duration curve is presented in Figure 13.3.1 (adapted from U.S. Army Corps of Engineers (1985)).

SOLUTION

Step 1 The area under the flow-duration curve represents an average annual flow of 390 cfs.

Step 2 No adjustments are made to the flow-duration curve.

Step 3 An average loss of 20 cfs will be used for leakage around gates, and the dam structure and evaporation losses are ignored.

Step 4 The head-discharge curve and the tailwater elevation-discharge curve are shown in Figure 13.3.9. The head curve is based on the tailwater curve with a fixed forebay elevation of 268 ft and an average headloss of 10 ft.

Step 5 To select a plant size, the initial size will be based on the 30-percent exceedance point (400 cfs as shown in Figure 13.3.8). The installed capacity is computed as

$$KW = \frac{QHe}{11.81} = \frac{(400 - 20)(31)(0.85)}{11.81} = 850 \text{ KW}$$

A single turbine with movable blades (horizontal-shaft Kaplan) is to be installed. Using Table 13.3.1, the ratio of minimum to rated discharge is 0.35 and the ratio of minimum to maximum head is 0.33. The minimum discharge is $0.35 \times (400 - 20) = 135$ cfs, which has a corresponding streamflow discharge of $135 + 20 = 155$ cfs. This corresponds to a head of 34 ft (from Figure 13.3.10). This plant is a pure run-of-river plant so that heads greater than 34 ft occur only at streamflows of less than the minimum generation streamflow of 155 cfs. Then the maximum generating head is 34 ft and the minimum head is approximately 33 percent of this, or 11 ft.

Step 6 The usable flow range is a minimum discharge of 155 cfs and a maximum head of 11 ft. (For a pure run-of-river project, the upper flow limit is defined by the minimum generating capacity.) The flow-duration data in Figure 13.3.11 and the head-discharge data in Figure 13.3.10 are used to develop the head-duration curve in Figure 13.3.12. The design head shown is the midpoint of the usable head range.

Step 7 Use points on the flow-duration curve (Figure 13.3.12) and compute the power for each discharge using the water power equation. As an example, for 270 cfs the head is 33.2 ft, which would be obtained from the head-discharge curve; then

$$KW = \frac{QHe}{11.81} = \frac{(270 - 20)(33.2)(0.85)}{11.81} = 597.38$$

After performing similar computations for all the desired points, the usable generation curve (solid line) is constructed as shown in Figure 13.3.13. This figure, however, is not a true power-duration curve because

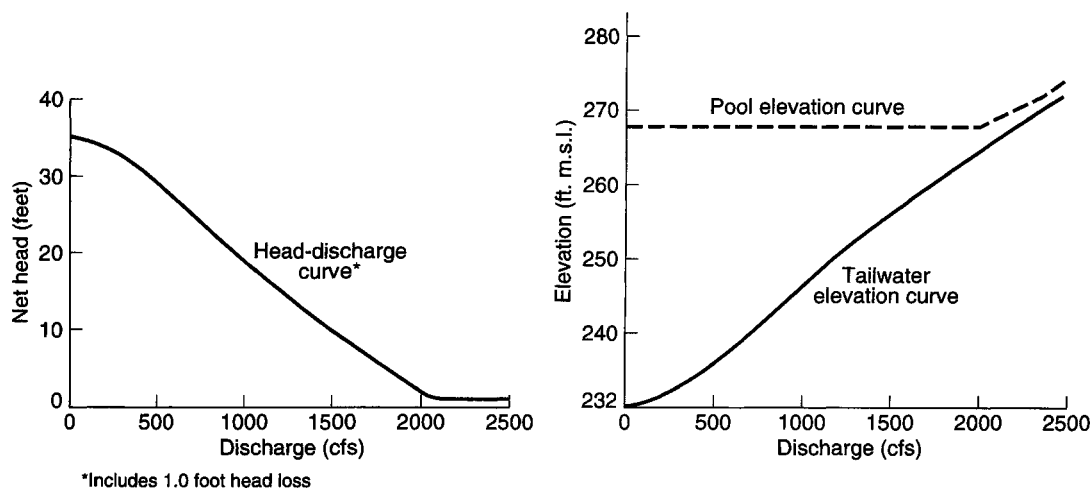
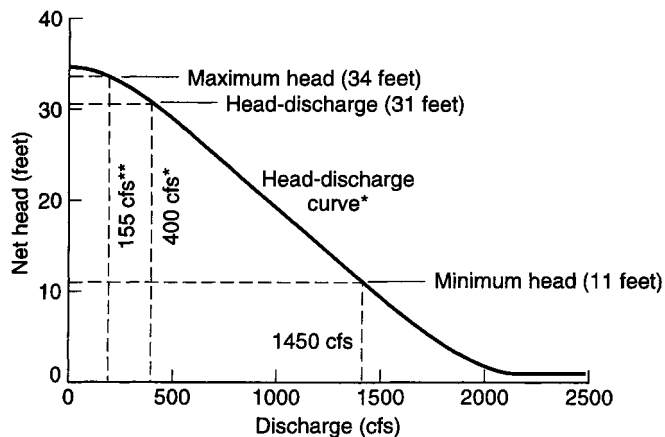


Figure 13.3.9 Tailwater and head-discharge curves (from U.S. Army Corps of Engineers (1985)).



* Includes 1.0 foot head loss
 ** 135 cfs minimum turbine discharge plus 20 cfs flow loss

Figure 13.3.10 Net head-discharge curve showing maximum head, minimum head, and rated head (from U.S. Army Corps of Engineers (1985)).

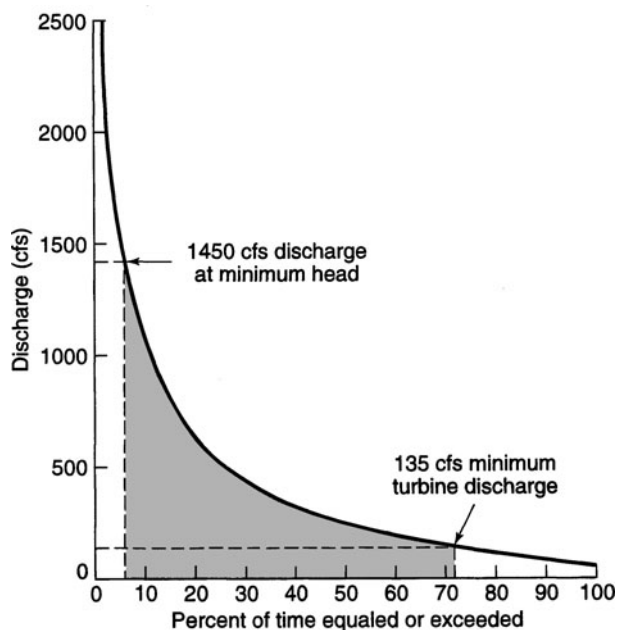


Figure 13.3.11 Total flow-duration curve showing limits imposed by minimum head and maximum discharge (from U.S. Army Corps of Engineers (1985)).

the generation values actually correspond to percent exceedances of flows. At flows greater than the rated discharge (32 percent), there is no reduction in power output due to reduced head and other factors.

Step 8 The power-duration curve (Figure 13.3.14) is integrated to determine the area. With equation (13.3.5), the average annual energy is computed as 3,390,000 KWh.

Step 9 Figure 13.3.15 is constructed for the project using the peak demand month. The dependable capacity, the average power from this curve, is computed from equation (13.3.6) as 538 KW.

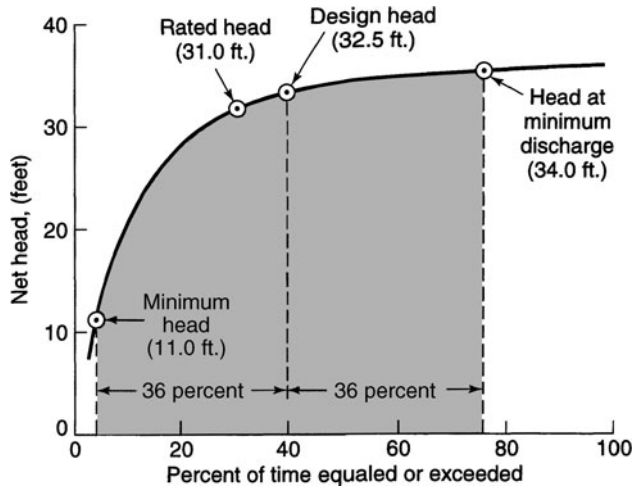


Figure 13.3.12 Head-duration curve showing minimum head, maximum head, design head, and rated head (from U.S. Army Corps of Engineers (1985)).

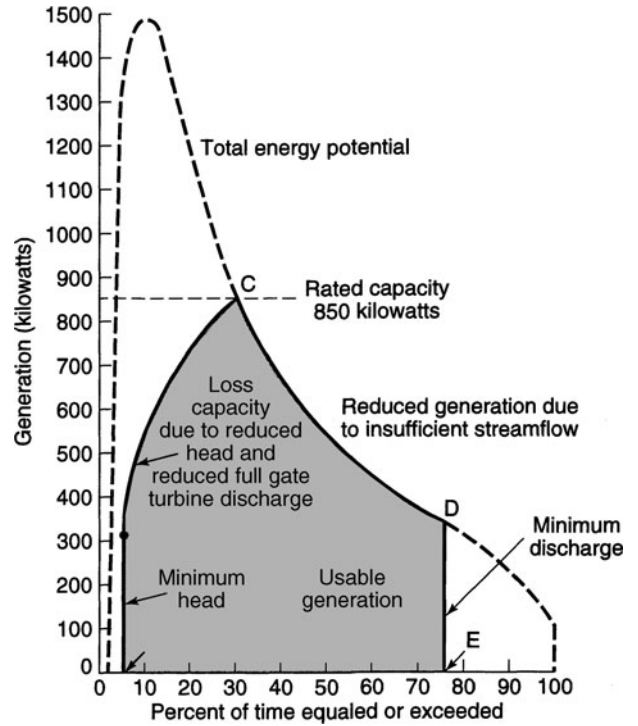


Figure 13.3.13 Usable generation-duration curve (from U.S. Army Corps of Engineers (1985)).

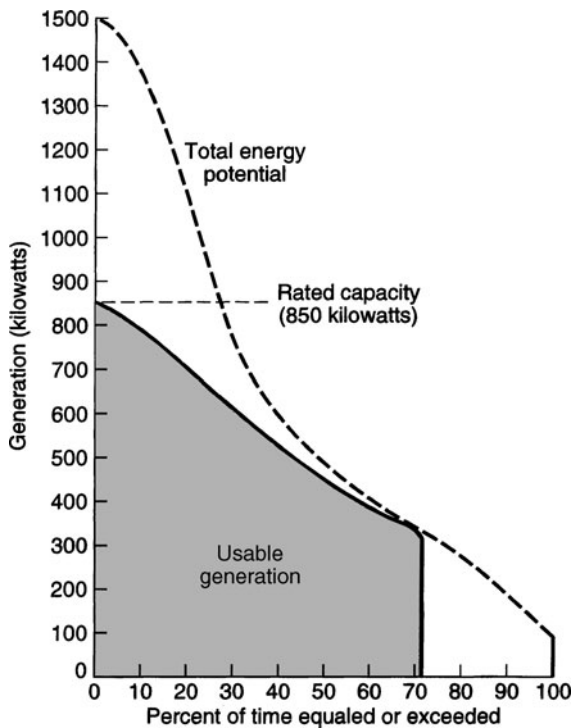


Figure 13.3.14 Usable power-duration curve (from U.S. Army Corps of Engineers (1985)).

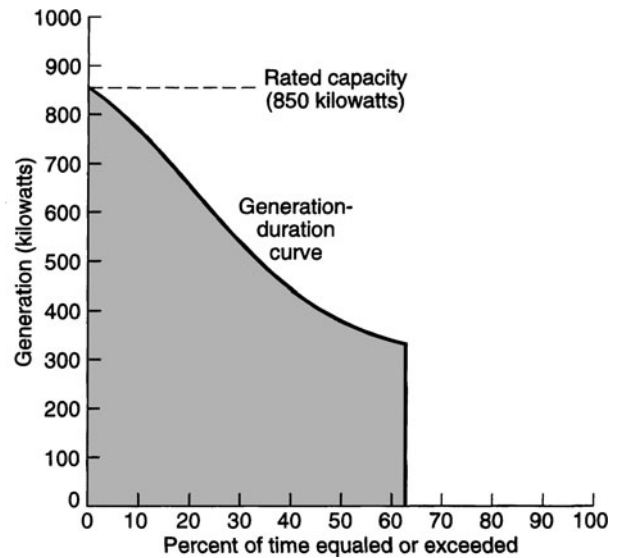


Figure 13.3.15 Generation-duration curve peak demand months (from U.S. Army Corps of Engineers (1985)).

13.3.5 Sequential Streamflow-Routing Method

The *sequential streamflow-routing method* sequentially computes the energy output for each time interval in the period of analysis. A continuity equation is used to route the streamflows through the project, taking into account the variations in reservoir elevation as a result of the reservoir regulation. Use of the sequential routing in the continuity equation allows the simulation of not only the hydropower but also flood control operation and water supply operation.

This method was developed primarily to evaluate storage projects and systems of storage projects. The method is based upon the continuity equation

$$\Delta S = I - O - L \quad (13.3.7)$$

where ΔS is the change in reservoir storage, I is the reservoir inflow, O is the reservoir outflow, and L is the sum of losses due to evaporation, diversions, and so on.

The sequential streamflow-routing method can be applied to basically any type of hydropower analysis. These include run-of-river projects; run-of-river projects with pondage; projects with flood control storage only; projects with conservation storage not regulated for power; projects with storage regulated only for power; and projects with storage regulated for multiple purposes including power, peaking hydro projects, and pumped-storage hydro projects.

The basic types of data needed are the historical streamflows and other information similar to the frequency-duration method. The basic steps for this procedure are as follows (U.S. Army Corps of Engineers, 1985):

- Step 1—Select plant capacity
- Step 2—Compute stream flow available for power generation
- Step 3—Determine average pond elevation
- Step 4—Compute net head
- Step 5—Estimate efficiency
- Step 6—Compute generation
- Step 7—Compute average annual energy

To perform the routing, the continuity equation (13.3.7) is expanded to

$$\Delta S = I - (Q_p + Q_L + Q_s) - (E + W) \quad (13.3.8)$$

where Q_p is the power discharge, Q_L is the leakage and nonconsumptive project water requirements, Q_s is the spill, E is the net evaporation losses (evaporation minus precipitation on the reservoir), and W includes the withdrawals for water supply, irrigation, and so on. The change in storage ΔS for a given time interval can be defined as

$$\Delta S = \frac{(S_{t+\Delta t} - S_t)}{C_s} \quad (13.3.9)$$

where S_t is the beginning-of-period storage, $S_{t+\Delta t}$ is the end-of-period storage, Δt is the routing period, and C_s is a discharge to storage conversion factor. As an example, if the routing interval Δt is a 30-day month, then $C_s = 59.50 \text{ ac-ft/ft}^3/\text{s-month}$; if the routing interval is one week, $C_s = 13.99 \text{ ac-ft/ft}^3/\text{s-week}$; if the routing interval is one day, $C_s = 1.983 \text{ ac-ft/ft}^3/\text{s-day}$; and if the routing interval is one hour, $C_s = 0.08264 \text{ ac-ft/ft}^3/\text{s-hour}$.

Substituting equation (13.3.9) into equation (13.3.8) and rearranging gives

$$S_{t+\Delta t} = S_t - C_s(I - Q_p - Q_L - Q_s - E - W) \quad (13.3.10)$$

The customary U.S. unit for this equation is ac-ft. For the first iteration through the critical period, a preliminary estimate of the firm energy would be used. During the critical period the spill Q_S would normally be zero.

13.3.6 Power Rule Curve

In general *rule curves* are guidelines for reservoir operation. They are generally based on detailed sequential analysis of combinations of critical hydrologic conditions and critical demand conditions. Rule curves are developed for flood control operations and for conservation storage for irrigation, water supply, hydropower, and other purposes. Our objective here is to discuss single-purpose rule curves for power operation.

A *power rule curve* is defined as a curve, or family of curves, indicating how a reservoir is to be operated under specific conditions to obtain best or predetermined results. Figure 13.3.16 illustrates a power rule curve for the operation of a typical storage project. The general shape of a power rule curve is governed by the hydrologic and power demands. The curve defines the minimum reservoir elevation (corresponding minimum storage) that is required to generate firm power any time of the year.

Firm energy is the generation that exactly draws the reservoir level to the bottom of the power pond during the most severe drought of record. The following general steps can be taken to determine the energy output of a project in which the primary objective is to minimize firm energy (Hobbs, et al. 1996):

- Identify the critical period
- Make a preliminary estimate of the firm energy potential
- Make one or more critical SSR routings to determine the actual firm energy capability and to define operating criteria that will guide year-by-year reservoir operation
- Make an SSR routing for the total period of record to determine average annual energy
- If desired, make additional period-of-record routings using alternative operating strategies to determine which one optimizes power benefits

With a computer model for the SSR routing such as HEC-5 (U.S. Army Corps of Engineers, 1983), these operations are done automatically.

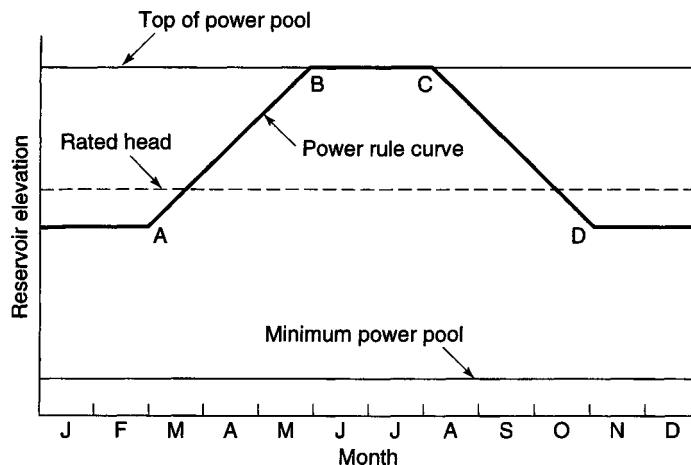


Figure 13.3.16 Rule curve for power operation of a typical storage project (from U.S. Army Corps of Engineers (1985)).

13.3.7 Multipurpose Storage Operation

Most storage projects that have power storage also have space for flood control regulation and conservation storage space for other water needs. The storage zones of a multipurpose operation are illustrated in Figure 13.3.17. A *joint-use storage zone* is one that can be used for flood regulation during part of a year and for conservation storage the remainder of the year. This is allowed in many river basins because major floods are concentrated in one season of the year. Joint-use storage allows less total reservoir storage than having separate storage zones for flood control and conservation. Figure 13.3.18 illustrates a rule curve with joint-use storage. Additional sources of information and hydroelectric and related topics can be found in Gulliver and Arndt (1991), Mays (1996, 1999), and Warnick (1989).

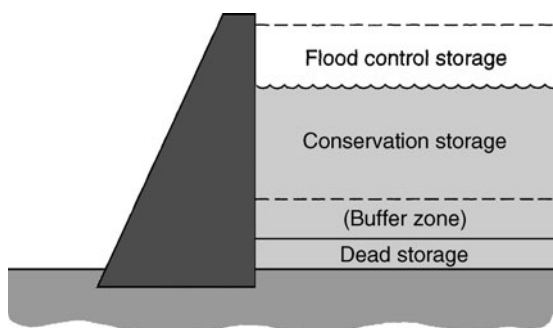


Figure 13.3.17 Storage zones (from U.S. Army Corps of Engineers (1985)).

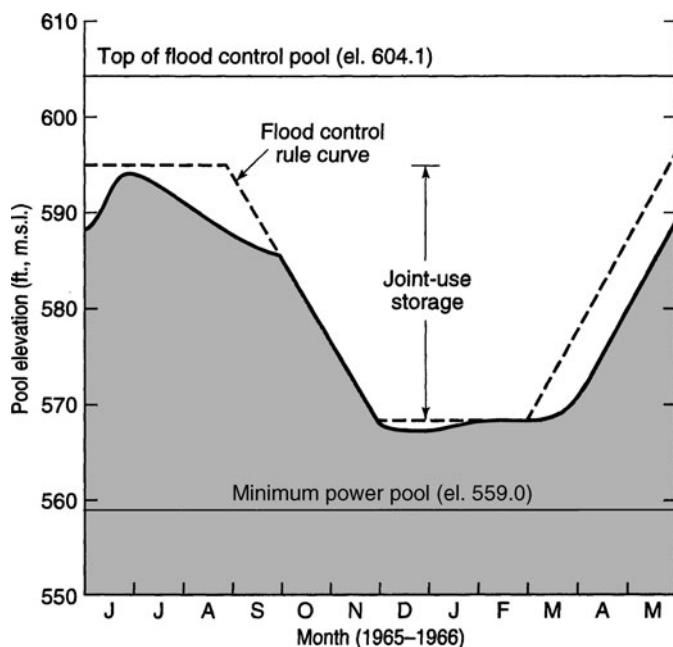


Figure 13.3.18 Regulation of a reservoir with joint-use storage through an average water year (from U.S. Army Corps of Engineers (1985)).

PROBLEMS

13.1.1 Consider the system in Figure 13.1.7a with the hydropower plant in the peaking load and determine the cost of weekly operation.

Plant symbol	Capacity (MW)	Plant factor (%)	Unit cost (mills/KWh)
CMBT-2	500	0	90
CMBT-1	500	0	80
HYDRO	1000	25	0
CYCL-2	500	15	30
CYCL-1	500	55	20
COAL-1	500	72	15
COAL-3	750	95	9
COAL-2	750	100	8
NUKE-1	1000	100	6

13.1.2 Consider the system in Figure 13.1.7b with the hydropower plant in the base load and determine the cost of weekly operation.

Plant symbol	Capacity (MW)	Plant factor (%)	Unit cost (mills/KWh)
CMBT-3	500	0	100
CMBT-2	500	0	90
CBMT-1	500	1	80
CMCY-1	500	13	60
CYCL-2	500	33	30
CYCL-1	500	48	20
COAL-1	500	62	15
COAL-3	750	85	9
HYDRO	(250)	100	0
COAL-2	750	100	8
NUKE-1	1000	100	6

13.1.3 Compare the results of problems 13.1.1 and 13.1.2. If hydropower was not used and the cost of operating an all-thermal base system for one week were \$7,256,000, what would be your conclusions?

13.2.1 An impulse turbine with a single nozzle of 300 mm diameter receives water through a 1.0-m diameter riveted-steel pipe ($k_s = 1.0$ mm) that is 300 m long. The water level in the reservoir is 300 m above the nozzle of the turbine. If the overall turbine efficiency is 85 percent and the loss coefficient of the nozzle is 0.04, what maximum power output can be expected? How much additional power is possible if a 1200 mm riveted-steel pipe is used?

13.2.2 A reaction turbine is supplied with water through a 200-cm pipe ($k_s = 1.0$ mm) that is 50 m long. The water surface in the reservoir is 30 m above the draft tube inlet, which is 4.5 m above the water level in the tailrace. If the turbine efficiency is 92 percent and the discharge is $12 \text{ m}^3/\text{s}$, what is the power output of the turbine in kilowatts? Use $f = 0.0185$.

13.3.1 Rework example 13.3.1 assuming the average head is 90 ft.

13.3.2 Rework example 13.3.2 assuming a loss of head of 5 ft.

REFERENCES

- Coleman, H. W., C. Y. Wei, and J. E. Lindell, "Hydraulic Design for Energy Generation," in *Hydraulic Design Handbook* edited by L. W. Mays, McGraw-Hill, New York, 1999.
- Federal Energy Regulatory Commission (FERC), *Hydroelectric Power Evaluation*, U.S. Department of Energy, draft, 1978.
- Gleick, P. H., "Water and Energy," in *Water in Crisis* edited by R. H. Gleick, Oxford University Press, New York, 1993.
- Greager, W. P., and J. D. Austin, *Hydroelectric Handbook*, 2nd edition, John Wiley & Sons, New York, 1950.
- Gulliver, J. S., and R. E. A. Arndt, *Hydropower Engineering Handbook*, McGraw-Hill, New York, 1991.
- Hasen, H., and G. C. Antonopoulos, "Hydroelectric Plants," in *Davis' Handbook of Applied Hydraulics* edited by V. J. Zipparo and H. Hasen, McGraw-Hill, New York, 1993.
- Hobbs, B. F., R. L. Mittelstadt, and J. R. Lund, "Energy and Water," in *Water Resources Handbook* edited by L. W. Mays, McGraw-Hill, New York, 1996.
- Linsley, R. K., J. B. Franzini, D. L. Freyberg, and G. Tchobanoglous, *Water Resources Engineering*, 4th edition, McGraw-Hill, New York, 1999.
- Mays, L. W., (editor-in-chief), *Water Resources Handbook*, McGraw-Hill, New York, 1996.
- Mays, L. W., (editor-in-chief), *Hydraulic Design Handbook*, McGraw-Hill, New York, 1999.
- Roberson, J. A., J. J. Cassidy, and M. H. Chaudhry, *Hydraulic Engineering*, 2nd Edition, John Wiley & Sons, New York, 1998.
- U.S. Army Corps of Engineers, "Feasibility Studies for Small Scale Hydropower Additions," U.S. Army Corps of Engineers, Hydrologic Engineering Center, Davis, CA, 1979.
- U.S. Army Corps of Engineers, "Application of the HEC-5 Hydropower Routines," Training Document No. 12, U.S. Army Corps of Engineers, Hydrologic Engineering Center, Davis, CA, 1983.
- U.S. Army Corps of Engineers, *Hydropower*, EM 1110-2-1701, Office of the Chief of Engineers, Department of the Army, Washington, DC, 1985.
- U.S. Department of Energy, *International Energy Annual 1990*, Energy Information, DOE/EIA-0219(90), Washington, DC, 1990.
- Warnick, C. C., *Hydropower Engineering*, Prentice-Hall, Englewood Cliffs, NJ, 1989.

This page intentionally left blank

Chapter 14

Flood Control

14.1 INTRODUCTION

Floods are natural events that have always been an integral part of the geologic history of earth. Flooding occurs (a) along rivers, streams and lakes, (b) in coastal areas, (c) on alluvial fans, (d) in ground-failure areas such as subsidence, (e) in areas influenced by structural measures, and (f) in areas that flood due to surface runoff and locally inadequate drainage. Human settlements and activities have always tended to use floodplains. Their use has frequently interfered with the natural floodplain processes, causing inconvenience and catastrophe to humans. This chapter focuses on the management of water excess (floods).

A recent example of flooding on a very large scale was the Mississippi River Basin flood of 1993 (Interagency Floodplain Management Review Committee, 1994 [commonly called the Galloway Report; Brigadier General Gerald E. Galloway was the executive director of the review committee]). Figures 7.2.9*a* and *b* illustrate, respectively, the general area of flooding streams and the areal distribution of total precipitation. Figures 14.1.1*a–h* from the Illinois State Water Survey show various flooding as a result of the Mississippi River Basin flood of 1993.



(a)

Figure 14.1.1 Pictures of the Mississippi River Basin Flood of 1993. (a) Confluence of Mississippi and Illinois Rivers. (Courtesy of the Illinois State Water Survey.); (b) Route 100 under water, Grafton, Illinois; (c) Confluence of Mississippi and Missouri Rivers; (d) Flooding due to seepage south of St. Louis, Missouri; (e) Levee break at Kaskaskia Island, Mississippi River; (f) Levee break at Miller City, Mississippi River; (g) Sand bags over a levee; (h) Flooding along the Mississippi River.



(b)



(c)



(e)



(d)



(f)



(g)

Figure 14.1.1 (Continued)



(h)

Figure 14.1.1 (Continued)

14.2 FLOODPLAIN MANAGEMENT

14.2.1 Floodplain Definition

A *floodplain* is the normally dry land area adjoining rivers, streams, lakes, bays, or oceans that is inundated during flood events. The most common causes of flooding are the overflow of streams and rivers and abnormally high tides resulting from severe storms. The floodplain can include the full width of narrow stream valleys, or broad areas along streams in wide, flat valleys. As shown in Figure 14.2.1, the channel and floodplain are both integral parts of the natural conveyance of a stream. The floodplain carries flow in excess of the channel capacity and the greater the discharge, the greater the extent of flow over the flood plain. Floodplains may be defined either as natural geologic features or from a regulatory perspective. The 100-year floodplain (see Chapter 10) is the standard most commonly used in the United States for management and regulatory purposes. Flooding concerns are not limited to riverine and coastal flooding. Also of concern are floods associated with alluvial fans, unstable channels, ice jams, mudflows, and subsidence.

Alluvial fans are characterized by a cone or fan-shaped deposit of boulders, gravel, and fine sediments that have been eroded from mountain slopes and transported by flood flows, debris flows, erosion, sediment movement and deposition, and channel migration, as illustrated in Figure 14.2.2. Alluvial fans are common throughout many parts of the world. In the United States they are common in Arizona, California, Idaho, Montana, Nevada, New Mexico, Utah, Washington, and Wyoming. Illustrated in Figure 14.2.3 is the flood insurance rate zone defined for alluvial fan systems.

14.2.2 Hydrologic and Hydraulic Analysis of Floods

Hydrologic and hydraulic analyses of floods are required for the planning, design, and management of many types of facilities, including hydrosystems within a floodplain or watershed. These analyses are needed for determining potential flood elevations and depths, areas of inundation, sizing of channels, levee heights, right of way limits, design of highway crossings and culverts, and many others. The typical requirements include (Hoggan, 1997):

1. *Floodplain information studies.* Development of information on specific flood events such as the 10-, 100-, and 500-year frequency events.
2. *Evaluation of future land-use alternatives.* Analysis of a range of flood events (different frequencies) for existing and future land uses to determine flood-hazard potential, flood damage, and environmental impact.

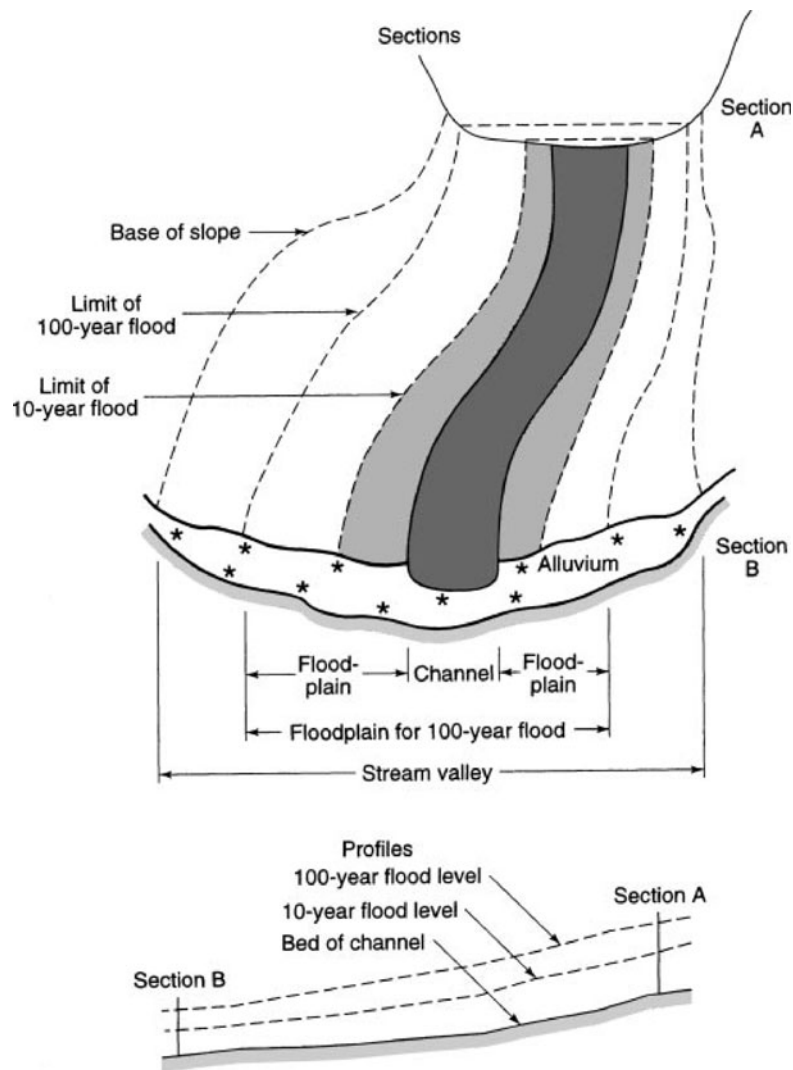


Figure 14.2.1 Typical sections and profiles in an unobstructed reach of stream valley (from Waananen et al. (1977)).

3. *Evaluation of flood-loss reduction measures.* Analysis of a range of flood events (different frequencies) to determine flood damage reduction associated with specific design flows.
4. *Design studies.* Analysis of specific flood events for sizing facilities to assure their safety against failure.
5. *Operation studies.* Evaluation of a system to determine if the demands placed upon it by specific flood events can be met.

The methods used in hydrologic and hydraulic analysis are determined by the purpose and scope of the project and the data availability. Figure 14.2.4 is a schematic of the components of a hydrologic and hydraulic analysis for floodplain studies. Hydrologic analysis for floodplains entails either a rainfall-runoff analysis or a flood-flow frequency analysis. If information from an adequate number of historical annual instantaneous peak discharges (*annual maximum series*) is available, the flood-flow frequency analysis can be performed to determine peak discharges for various return periods (as described in Chapter 10). Otherwise, a rainfall-runoff analysis must be performed using a

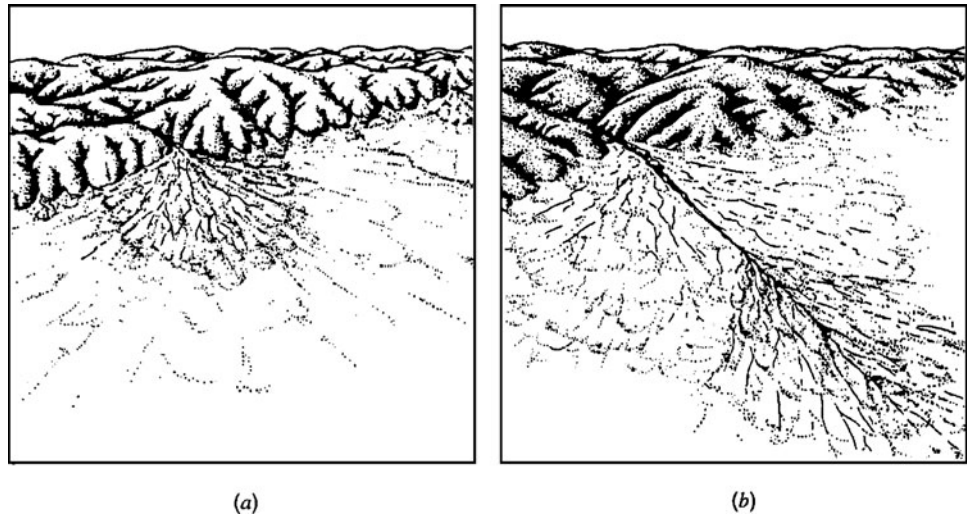


Figure 14.2.2 Two types of alluvial fans. (a) Unincised fan with the area of present deposition next to the mountain; (b) Alluvial fan with the area of present deposition downslope from the mountains due to stream-channel entrenchment at the apex of the fan (note gully extension at the toe of the fan) (from W. B. Bull (1984)).

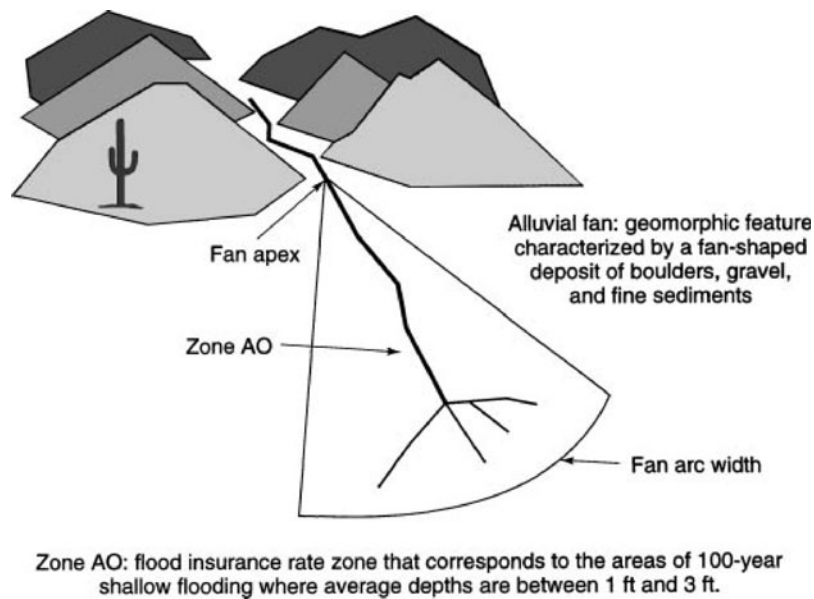


Figure 14.2.3 Alluvial fan system.

historical storm or design storm for a particular return period to develop a storm-runoff hydrograph (as described in Chapter 8).

Determination of water-surface elevations can be performed using a steady-state water-surface profile analysis (see Chapter 5) if only peak discharges are known, or one can select the peak discharges from generated storm-runoff hydrographs. Refer to Dodson (1999) for further information on floodplain analysis. For a more detailed and comprehensive analysis, an unsteady-flow analysis based upon a hydraulic-routing model (see Chapter 9) and requiring the storm-runoff

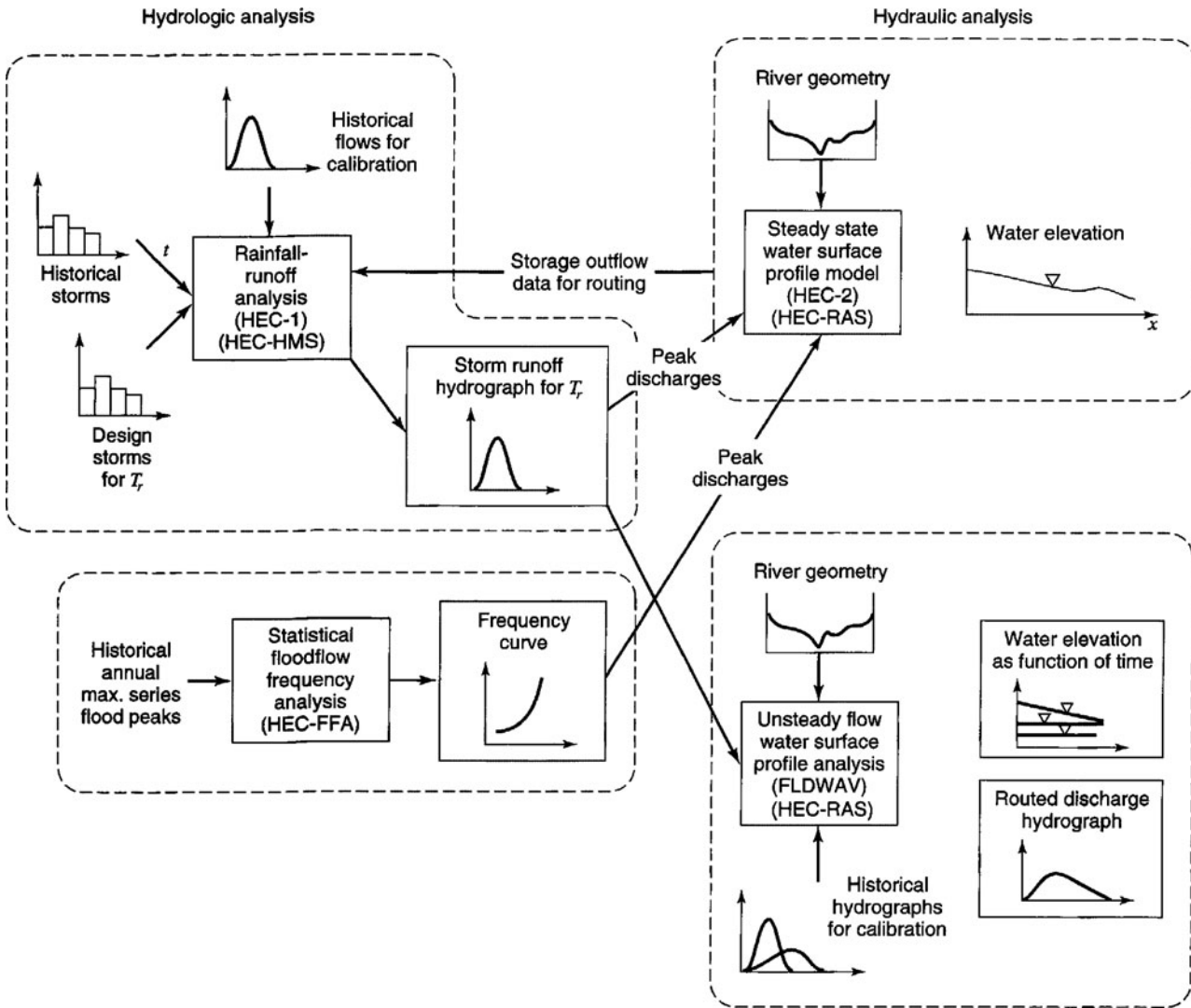


Figure 14.2.4 Components of a hydrologic-hydraulic floodplain analysis.

hydrograph can be used to define more accurately maximum water-surface elevations. The unsteady-flow analysis also provides more detailed information such as the routed-discharge hydrographs at various locations throughout a river reach.

14.2.3 Floodways and Floodway Fringes

Encroachment on floodplains, such as by artificial fill material, reduces flood-carrying capacity, increases the flood heights of streams, and increases flood hazards in areas beyond the encroachment. One aspect of floodplain management involves balancing the economic gain from floodplain development against the resulting increase in flood hazard. For purposes of the Federal Emergency Management Agency (FEMA) studies, the 100-year flood area is divided into a floodway and a floodway fringe, as shown in Figure 14.2.5. The *floodway* is the channel of a stream plus any adjacent floodplain areas that must be kept free of encroachment in order for the 100-year flood to be carried without substantial increases in flood heights. FEMA’s minimum standards allow an increase in

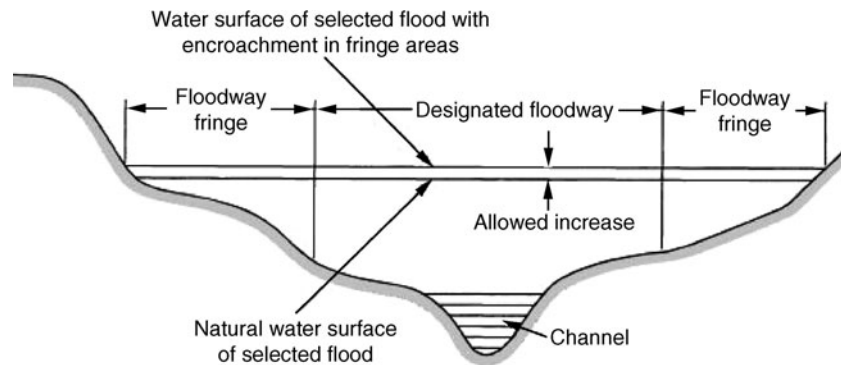


Figure 14.2.5 Definition of floodway and floodway fringe. The floodway fringe is the area between the designated floodway limit and the limit of the selected flood. The floodway limit is defined so that encroachment limited to the floodway fringe will not significantly increase flood elevation. The 100-year flood is commonly used, and a 1-ft allowable increase is standard in the United States.

flood height of 1.0 ft, provided that hazardous velocities are not produced. The *floodway fringe* is the portion of the floodplain that could be completely obstructed without increasing the water surface elevation of the 100-year flood by more than 1.0 ft at any point.

Two types of floodplain inundation maps, flood-prone area and flood-hazard maps, have been used. *Flood-prone area maps* show areas likely to be flooded by virtue of their proximity to a river, stream, bay, ocean, or other watercourse, as determined from readily available information. *Flood-hazard maps*, such as Figure 14.2.6 for Clear Creek near Houston, Texas, show the extent of inundation as determined from a study of flooding at the given location. Flood-hazard maps are commonly used in floodplain information reports and require updating when changes have occurred in the channels, on the floodplains, and in upstream areas.

14.2.4 Floodplain Management and Floodplain Regulations

According to the National Flood Insurance Program (NFIP) regulations administered by FEMA, *floodplain management* is “the operation of an overall program of corrective and preventive measures for reducing flood damage, including but not limited to emergency preparedness plans,

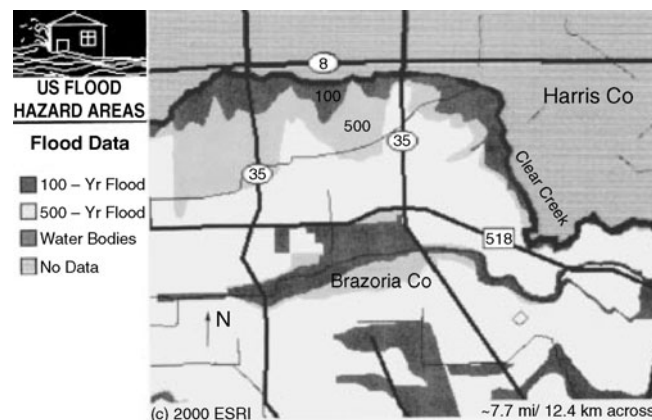


Figure 14.2.6 Floodplain map for a portion of Clear Creek in Brazoria County near Houston, Texas. Harris County is to the north and east of Clear Creek, and the flood plain of Clear Creek in Harris County is not shown.

flood control works, and floodplain management regulations.” Floodplain management regulations are the most effective method for preventing future flood damage in developing communities with known flood hazards.

Floodplain management investigates problems that have arisen in developed areas and potential problems that can be forecast due to future developments. The basic approaches to floodplain management are: (1) actions to reduce susceptibility to floods, (2) actions that modify the flood, and (3) actions that assist individuals and communities in responding to floods. *Floodplain regulation* is the centerpiece of any floodplain management program, and is particularly effective in underdeveloped areas, where the ability exists to control future development.

A key component in floodplain regulation is the definition of the *flood-hazard area* (usually defined as the 100-year floodplain) and the floodway. The floodway includes the channel of the stream and the adjacent land areas that must be reserved in order to discharge the design flood without cumulatively increasing the water surface by more than a given amount. For example, the maximum rise allowed by the National Flood Insurance Program (NFIP) is one foot, but in many situations a lesser amount may be more appropriate. An adequate floodplain management plan that eliminates development from the flood-hazard areas may be a major step in the right direction. Not allowing other obstructions such as fill and detention basins to be placed in the flood-hazard area is another step forward. A floodplain provides both a conveyance mechanism and a temporary storage area for excess water. Allowing obstructions be placed in the floodplain eliminates the temporary storage areas and in turn increases the hydraulic heads to increase flood levels both downstream and upstream of the floodplain developments.

14.2.5 National Flood Insurance Program

In 1968 the U.S. Congress created the National Flood Insurance Program (NFIP) through the passage of the National Flood Insurance Act. The Flood Disaster Protection Act of 1973 and the National Flood Insurance Reform Act of 1994 further defined the NFIP. The purpose of the NFIP is to minimize future flood loss and to allow the floodplain occupants to be responsible for flood-damage costs instead of the taxpayer. The NFIP, administered by FEMA, provides federally backed flood insurance that encourages communities to enact and enforce floodplain regulations. If a state or community does not participate in the NFIP, the following consequences occur:

1. The community will not be eligible for flood disaster relief in the event of a federally declared flood disaster.
2. Federal or federally related financial assistance for acquisition or construction purposes for structures in flood-prone areas will not be available.
3. Flood insurance will not be available.

For a state or community to be eligible for participation in the NFIP, it must agree to adopt floodplain management regulations that meet minimum standards as defined by FEMA. These minimum standards include but are not limited to:

1. Require permits for all proposed development within a flood-hazard area.
2. Assure that all necessary governmental permits have been obtained.
3. Ensure that proper materials and methods are used in new construction to protect new buildings from future floods (elevate the lowest finished floor of residential structures of flood-proof nonresidential structures above the base flood elevation).
4. Assure that all proposed development within a flood-hazard area is consistent with the need to minimize flood damage within the flood-prone area.
5. Notify adjacent communities and the state prior to the alterations or relocation of a watercourse.
6. Assure that the flood-carrying capacity within the altered or relocated portion of any watercourse is maintained.

7. Prohibit encroachments, including fill, new construction, substantial improvements, and other development within the adopted regulatory floodway unless it has been demonstrated through hydrologic and hydraulic analysis performed in accordance with standard engineering practice that the proposed encroachment would not result in any increase in flood levels within the community during the occurrence of the base flood flow.

A state is considered a “community,” and state agencies are required to comply with minimum standards just as local communities do. A state may comply with the floodplain regulations of the local community in which state land is located, or the state may establish and enforce its own floodplain regulations for state agencies.

14.2.6 Stormwater Management and Floodplain Management

Stormwater management plans are most successful when they are implemented at the start of development in an area and should be administered as part of a land-use planning process. The implementation of a stormwater management plan, in a remedial mode, to correct stream deterioration resulting from previous uncontrolled development is a much more difficult task. Stormwater detention programs can be very effective; however in some cases, they may have little effect because the flood peak caused by detention diminishes as the flood passes downstream, while the increase in total runoff caused by the development swells the total mass of the flood wave. The cumulative effect downstream of any number of detention basins would mainly be to delay the arrival of the flood crest by a few hours, and many have little or no effect on reducing the peak discharge. A partial solution to this is to provide retention over a long time period. The increases in peak flood discharges can be controlled but only through coordinated, extensive planning prior to development. Zoning to preserve undeveloped areas, particularly those in the floodplain, can be a very effective measure.

Stormwater management and floodplain management are generally separate and different programs; however, their interfaces, such as detention basins built in floodplains, are unavoidable issues. Detention basins have been placed in the floodplains of many areas of the United States. Detention basins generally should be placed out of the floodplain, particularly for small streams of relatively small drainage areas. In such cases the same storms affect the development site and the floodplain simultaneously. In other words, the time during which the detention basin is needed to store stormwater from the development is basically the same time during which the floodplain is flooded and the detention basin location would already be filled by floodwater. To the extent that the flood at the development coincides with the flooding in the floodplain, detention storage in the floodplain is ineffective. An additional factor that has decreased the effectiveness of detention basins in many areas is the large amount of fill incidental with development. The placement of effective regional detention and retention, along with improved drainage and conveyance structures and other hydraulic structures, may be required to alleviate drainage problems.

14.3 FLOOD-CONTROL ALTERNATIVES

Flooding results from conditions of hydrology and topography in floodplains such that the flows are large enough that the channel banks overflow, resulting in overbank flow that can extend over the floodplain. In large floods, the floodplain acts both as a conveyance and as a temporary storage for flood flows. The main channel is usually a defined channel that can meander through the floodplain carrying low flows. The overbank flow is usually shallow compared to the channel flow and also flows at a much lower velocity than the channel flow.

The *objective of flood control* is to reduce or to alleviate the negative consequences of flooding. Alternative measures that modify the flood runoff are usually referred to as flood-control facilities and consist of engineering structures or modifications. Construction of flood-control facilities,

Table 14.3.1 Checklist for Without-Project Conditions

Study components	✓	Issues
Layout		Review/assemble available information Conduct field reconnaissance for historic flood data and survey specification Establish local contacts
Economic studies		Assist in establishing study limits, damage reaches Determine existing and future without-project conditions discharge-frequency and associated uncertainty Determine existing and future with-project conditions stage-discharge and associated uncertainty
Performance		Determine expected capacity-exceedance probability Determine expected life-exceedance probability Evaluate existing project operations/stability for range of events and key assumptions Describe consequences of capacity exceedances Perform reliability analyses
Environmental and social		Evaluate without-project riparian impacts Evaluate without-project social impacts

Source: U.S. Army Corps of Engineers (1996a).

referred to as *structural measures*, are usually designed to consider the flood characteristics including reservoirs, diversions, levees or dikes, and channel modifications. Flood-control measures that modify the damage susceptibility of floodplains are usually referred to as *nonstructural measures* and may require minor engineering works. Nonstructural measures are designed to modify the damage potential for permanent facilities and provide for reducing potential damage during a flood event. Nonstructural measures include flood proofing, flood warning, and land-use controls. Structural measures generally require large sums of capital investment. *Floodplain management* takes an integrated view of all engineering, nonstructural, and administrative measures for managing (minimizing) losses due to flooding on a comprehensive scale.

Table 14.3.1 presents a checklist summarizing the critical requirements for *without-project condition analysis*. These represent the base condition for determining the economic value, performance, and environmental/social impacts of flood-damage-reduction measures and plans (U.S. Army Corps of Engineers, 1996a).

14.3.1 Structural Alternatives

Table 14.3.2 summarizes several flood-damage reduction measures and the parametric relationships that are modified. The basic functional relationships required to assess the value of flood-damage reduction alternatives are shown in Figure 14.3.1. *Stage-damage relationships* define the flood severity in terms of damage cost for various stages. *Stage-discharge relationships*, also referred to as *rating curves*, are modified by various flood-control alternatives. *Flood-flow frequency relationships* (described in Chapter 10) define the recurrence of nature in terms of the flood magnitudes. *Flood-control alternatives* are designed to modify the flood characteristics by altering one or more of the above relationships. The major types of flood-control structures are reservoirs, diversions, levees or dikes, and channel modifications. Each of these are discussed below, defining the resulting changes in the basic relationships.

14.3.1.1 Flood-Control Reservoir

Flood-control reservoirs are used to store flood waters for release after the flood event, reducing the magnitude of the peak discharge. Reservoirs modify the flood-flow frequency curve, which is

Table 14.3.2 Impacts of Flood-Damage-Reduction Measures

Measures	Impact of measure		
	Modifies discharge-frequency function	Modifies stage-discharge function	Modifies stage-damage function
Reservoir	Yes	Maybe, if stream and downstream channel erosion and deposition due to change in discharge	Maybe, if increased development in floodplain
Diversion	Yes	Maybe, if channel erosion and deposition due to change in discharge	Maybe, if increased development in floodplain
Channel improvement	Maybe, if channel affects timing and storage altered significantly	Yes	Not likely
Levee or floodwall	Maybe, if floodplain storage no longer available for flood flow	Yes	Yes
Floodproofing	Not likely	Not likely	Yes
Relocation	Not likely	Maybe, if flow obstructions removed	Yes
FWP plan	Not likely	Not likely	Yes
Land-use and construction regulation	Not likely	Maybe, if flow obstructions removed	Yes
Acquisition	Not likely	Maybe, if flow obstructions removed	Yes

Source: U.S. Army Corps of Engineers (1996).

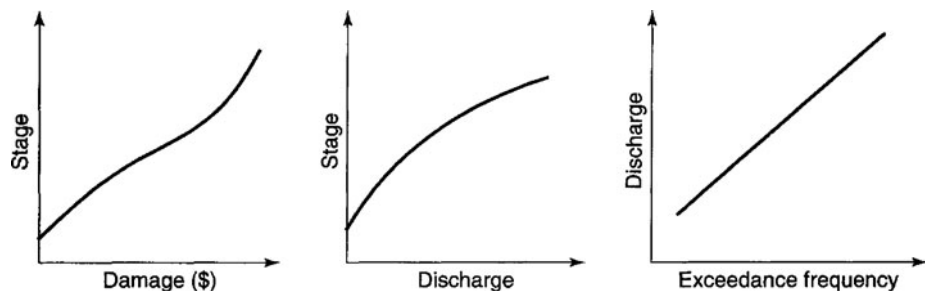


Figure 14.3.1 Flood assessment functional relationships.

lowered because of the decrease of the peak discharge of a specific event. Figure 14.3.2 illustrates the effect of flood-control reservoirs. Long-term effects of reservoir storage modify the streamflow regime and can result in channel aggradation or degradation at downstream locations, altering the rating curve.

Reservoirs reduce damage by reducing discharge directly. Table 14.3.3 is a checklist that summarizes critical requirements for reservoirs. A reservoir is well suited for damage reduction in the following cases (U.S. Army Corps of Engineers, 1996a):

1. Damageable property is spread over a large geographical area downstream from the reservoir site, with several remote damage centers and relatively small local-inflow areas between them.
2. A high degree of protection, with little residual damage, is desired.

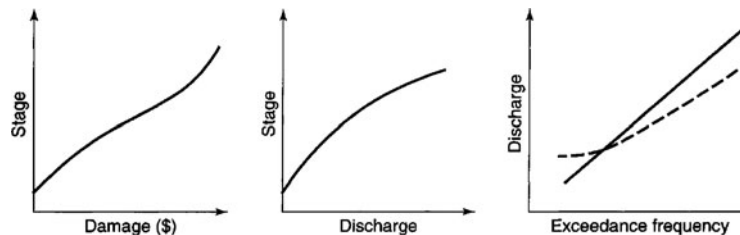


Figure 14.3.2 Effect of reservoir.

Table 14.3.3 Checklist for Reservoir

Study components	✓	Issues
Layout		Consider alternative sites based on drainage area versus capacity considerations Delineate environmentally sensitive aquatic and riparian habitat Identify damage centers, delineate developed areas, define land uses for site selection Determine opportunities for system synergism due to location
Economics		Determine with-project modifications to downstream frequency function for existing and future conditions Quantify uncertainty in frequency function Formulate and evaluate range of outlet configurations for various capacities using risk-based analysis procedures
Performance		Determine expected annual-exceedance probability Determine expected life-exceedance probability Describe operation for range of events and analyze sensitivity of critical assumptions Describe consequences of capacity exceedances Determine reliability for range of events
Design		Conduct dam-safety evaluation Formulate and evaluate preliminary spillway and outlet configurations Conduct pool sedimentation analysis Evaluate all downstream hydrologic and hydraulic impacts
Environmental and social		Formulate preliminary operation plans Evaluate with-project riparian habitat Evaluate aquatic and riparian habitat impact and identify enhancement opportunities Anticipate and identify incidental recreation opportunities

Source: U.S. Army Corps of Engineers (1996a).

3. A variety of properties, including infrastructure, structures, contents, and agricultural property, is to be protected.
4. Water impounded may be used for other purposes, including water supply, hydropower, and recreation.
5. Sufficient real estate is available for location of the reservoir at reasonable economic, environmental, and social cost.
6. The economic value of damageable property protected will justify the cost of constructing the reservoir.

14.3.1.2 Diversion

Diversion structures are used to reroute or bypass flood flows from damage centers in order to reduce the peak flows at the damage centers. Diversion structures are designed to modify (lower) the frequency curve so that the flow magnitude for a specific event is lowered at the damage center. Figure 14.3.3 illustrates the effect of diversions on the functional relationships. The stage-damage

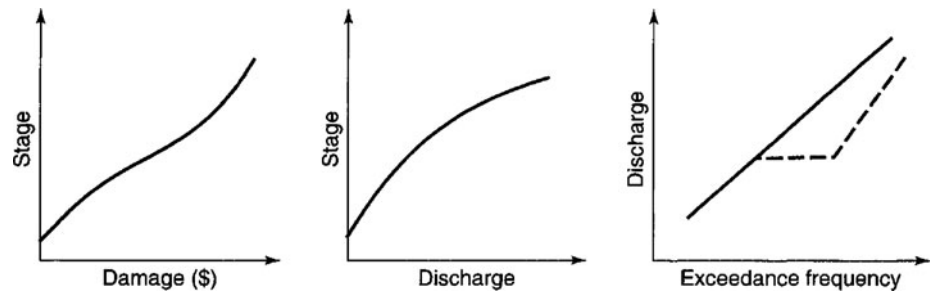


Figure 14.3.3 Effect of diversion.

and stage-discharge relationships remain the same if there are no other induced effects. Long-term effects of diversions can cause aggradation or degradation at downstream locations and result in sediment depositions in bypass channels.

A diversion is well suited for damage reduction in the following cases (U.S. Army Corps of Engineers, 1996a):

1. Damageable property is spread over a large geographical area with relatively minor local inflows for diversions removing water from the system.
2. A high degree of protection, with little residual damage, is desired.
3. A variety of property, including infrastructure, structures, contents, and agricultural property, is to be protected.
4. Sufficient real estate is available for location of the diversion channel or tunnel at reasonable cost.
5. The value of damageable property protected will economically justify the cost of the diversion.

Table 14.3.4 is a checklist that summarizes critical requirements for diversions.

Table 14.3.4 Checklist for Diversion

Study components	✓	Issues
Layout		Delineate environmentally sensitive aquatic and riparian habitat Identify damage centers, delineate developed areas, define land uses for site selection Determine right-of-way Identify infrastructure/utility-crossing conflicts
Economics		Determine with-project modifications to downstream frequency function for existing and future conditions Quantify uncertainty in frequency function Formulate and evaluate range of outlet configurations for various capacities using risk-based analysis procedures
Performance		Determine expected annual-exceedance probability Determine expected life-exceedance probability Describe operation for range of events and analyze sensitivity of critical assumptions Describe consequences of capacity exceedances Determine reliability for range of events
Design		Formulate and evaluate preliminary spillway and outlet configurations Conduct diversion channel sedimentation analysis Evaluate all downstream hydrologic and hydraulic impacts
Environmental and social		Formulate preliminary operation plans Evaluate with-project riparian habitat Evaluate aquatic and riparian habitat impact and identify enhancement opportunities

Source: U.S. Army Corps of Engineers (1996a).

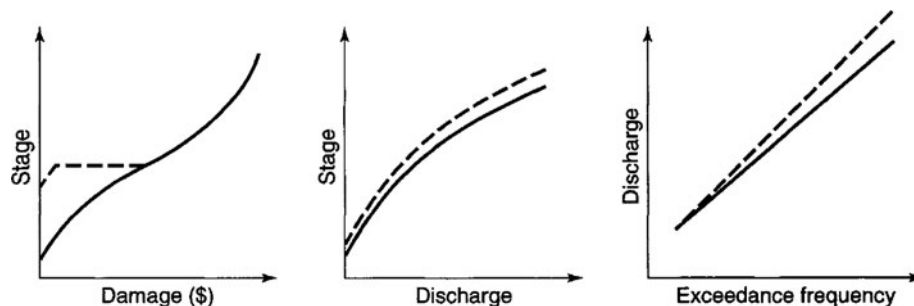


Figure 14.3.4 Effect of levee.

14.3.1.3 Levees and Floodwalls

Levees or dikes are used to keep flood flows from floodplain areas where damage can occur. Levees essentially modify all three of the functional relationships. The effect of levees is to reduce the damage in protected areas from water surface stages within the stream or main channel. This effect essentially truncates the stage-damage relationship for all stages below the design elevation of the levee, as illustrated in Figure 14.3.4. Excluding flood flows from portions of the floodplain outside the levees constricts the flow to a smaller conveyance area, resulting in an increased stage for the various discharges. This upward shift of the stage-discharge relationship is shown in Figure 14.3.4. Constricting the flow to within levees reduces the amount of natural storage of a floodwave, causing an increase in peak discharges downstream. This effect increases the discharge for various exceedance frequencies, shifting the frequency upwards, as also shown in Figure 14.3.4. Long-term effects of levees can cause aggradation or degradation of channels in downstream reaches. Even though levees have the purpose of protecting property and lives, they also bring the potential for major disasters when design discharges are exceeded and areas are inundated that had been considered safe.

Levees and floodwalls are effective damage-reduction measures in the following circumstances (U.S. Army Corps of Engineers, 1996a):

1. Damageable property is clustered geographically.
2. A high degree of protection, with little residual damage, is desired.
3. A variety of properties, including infrastructure, structures, contents, and agricultural property, is to be protected.
4. Sufficient real estate is available for location of the channel modification at reasonable economic, environmental, and social cost.
5. The economic value of damageable property protected will justify the cost of constructing the levees.

Table 14.3.5 is a checklist of the requirements for levees and floodwalls, and Table 14.3.6 is a checklist for interior areas.

14.3.1.4 Channel Modifications

Channel modifications (channel improvements) are performed to improve the conveyance characteristics of a stream channel. The improved conveyance lowers the stages for various discharges, having the effect of lowering the stage-discharge relationship, as illustrated in Figure 14.3.5. The peak discharges for flood events are passed at lower stages, decreasing the effect of natural valley storage during passage of a flood wave. This effect results in higher peak discharges downstream than would occur without the channel modifications, causing an upward shift of the frequency curve,

Table 14.3.5 Checklist for Levees and Floodwalls

Study components	✓	Issues
Layout		<p>Minimize contributing interior runoff areas (flank levees, diversion, collector system)</p> <p>Minimize area protected to reduce potential future development</p> <p>Investigate levee setback versus height tradeoffs</p> <p>Determine right-of-way available for levee or wall alignment</p> <p>Minimize openings requiring closure during flood events</p>
Economics		<p>Determine with-project modifications to stage-discharge function for all existing and future events</p> <p>Quantify uncertainty in stage-damage function</p> <p>Formulate and evaluate range of levee and interior area configurations for various capacities using risk-based analysis procedures</p>
Performance		<p>Determine expected capacity- and stage-exceedance probability</p> <p>Determine expected annual-exceedance probability</p> <p>Determine expected life-exceedance probability</p> <p>Describe operation for range of events and sensitivity analysis of critical assumptions</p> <p>Describe consequences of capacity exceedances</p>
Design		<p>Determine reliability (expected probability of exceeding target) for range of events</p> <p>Design for levee or floodwall superiority at critical features (such as pump stations, high-risk damage centers)</p> <p>Design overtopping locations and downstream end, remote from major damage centers</p> <p>Provide levee height increments to accommodate settlement, wave run-up</p> <p>Design levee exterior erosion protection</p>
Environmental and social		<p>Develop flood-warning-preparedness plan for events that exceed capacity</p> <p>Evaluate aquatic and riparian habitat impact and identify enhancement opportunities</p> <p>Anticipate and identify incidental recreation opportunities</p>

Source: U.S. Army Corps of Engineers (1996a).

Table 14.3.6 Checklist for Interior Areas

Study components	✓	Issues
Layout		<p>Define hydraulic characteristics of interior system (storm-drainage system, outlets, ponding areas, and so forth)</p> <p>Delineate environmentally sensitive aquatic and riparian habitat</p> <p>Identify damage centers, delineate developed areas, define land uses for site selection</p>
Economics		<p>Determine with-project modifications to interior stage-frequency function for all conditions</p> <p>Quantify uncertainty in frequency function</p> <p>Formulate and evaluate range of pond, pump, outlet configurations for various capacities using risk-based analysis procedures</p>
Performance		<p>Determine expected annual-exceedance probability</p> <p>Determine expected life-exceedance probability</p> <p>Describe operation for range of events and sensitivity analysis of critical assumptions</p> <p>Describe consequences of capacity exceedances</p>
Design		<p>Determine reliability (expected probability of exceeding target) for range of events</p> <p>Formulate and evaluate preliminary inlet and outlet configurations for facilities</p> <p>Formulate preliminary operation plans</p>

Source: U.S. Army Corps of Engineers (1996a).

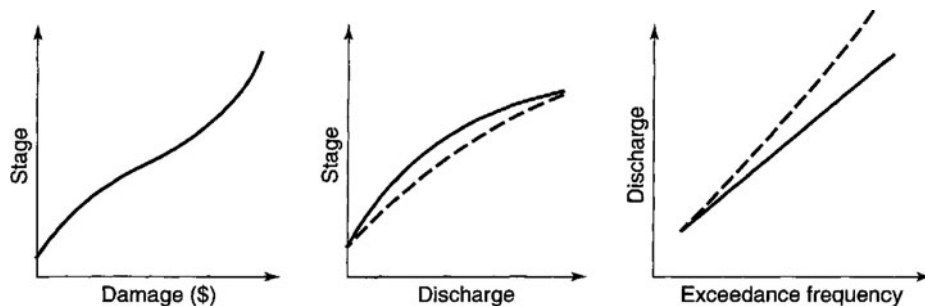


Figure 14.3.5 Effect of channel modification.

as illustrated in Figure 14.3.5. Long-term effects of channel modification can cause aggradation and degradation of downstream channel reaches. Channel modifications are usually for local protection but can be integrated with other flood-control alternatives to provide a more efficient flood-control system.

Channel modifications are effective flood-damage-reduction measures in the following cases (U.S. Army Corps of Engineers, 1996a):

1. Damageable property is locally concentrated.
2. A high degree of protection, with little residual damage, is desired.
3. A variety of properties, including infrastructure, structures, contents, and agricultural property, is to be protected.
4. Sufficient real estate is available for location of the channel modification at reasonable economic, environmental, and social cost.
5. The economic value of damageable property protected will justify the cost of constructing the channel modification.

Table 14.3.7 is a checklist of critical requirements for channel modifications.

Table 14.3.7 Checklist for Channel Modification

Study components	✓	Issues
Layout		Determine right-of-way restriction Delineate environmentally sensitive aquatic and riparian habitat Identify damage centers, delineate developed areas, define land uses for site selection Identify infrastructure/utility-crossing conflicts
Economics		Determine with-project modifications to stage-discharge function for all conditions Determine any downstream effects due to frequency discharge changes due to loss of channel storage Quantify uncertainty in stage-discharge function Formulate and evaluate range of channel configurations using risk-based analysis procedures
Performance		Determine expected annual-exceedance probability Determine expected life-exceedance probability Describe operation for range of events and analyze sensitivity of critical assumptions Describe consequences of capacity exceedances Determine reliability for range of events
Design		Account for ice and debris, erosion, deposition, sediment transport, and high velocities Evaluate straightening effects on stability Evaluate all impact of restrictions or obstructions
Environmental and social		Evaluate aquatic and riparian habitat impact and identify enhancement opportunities Anticipate and identify incidental recreation opportunities

Source: U.S. Army Corps of Engineers (1996a).

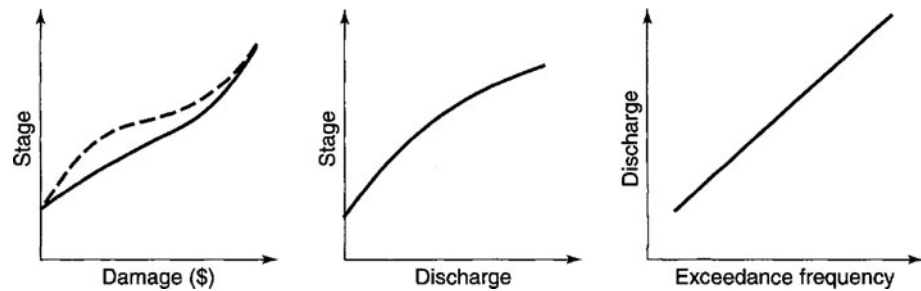


Figure 14.3.6 Effect of flood proofing.

14.3.2 Nonstructural Measures

Nonstructural measures are used to modify the damage potential of permanent structures and facilities in order to decrease the susceptibility of flooding to reduce potential damages. Nonstructural measures include flood proofing, flood warning, and various types of land-use control alternatives. These measures are characterized by their value in reducing future or potential unwise floodplain use. Of the nonstructural measures mentioned above, only flood proofing has the potential to modify present damage potential.

Flood proofing consists of a range of nonstructural measures designed to modify the damage potential of individual structures susceptible to flood damage. These measures include elevating structures, waterproofing exterior walls, and rearrangement of structural working space. Flood proofing is most desirable on new facilities, and changes only the stage-damage relation, as illustrated in Figure 14.3.6, shifting the relationship upwards.

Table 14.3.8 is a checklist for nonstructural measures that include flood proofing, relocation, and flood-warning preparedness (FWP) plans. Table 14.3.9 lists the performance requirements for flood proofing.

A *flood-warning-preparedness plan (FWP plan)* reduces flood damage by giving the public an opportunity to act before flood stages increase to damaging levels. Table 14.3.10 lists the components of an FWP system. The savings due to a FWP plan may arise from reduced inundation

Table 14.3.8 Checklist for Measures that Reduce Existing-Condition Damage Susceptibility

Study components	✓	Issues
Layout		Based on qualification of flood hazard, identify structures for which measures are appropriate
Economics		Determine with-project modifications to stage-damage function for all existing and future conditions Quantify uncertainty in stage-damage function Formulate and evaluate range of flood-proofing, relocation, and/or FWP plans, using risk-based analysis procedures
Performance		Determine expected annual-exceedance probability Determine expected life-exceedance probability Determine operation for range of events and sensitivity analysis of critical assumptions Describe consequences of capacity exceedances Determine reliability for range of events
Design		Develop, for all these measures, FWP plans
Environmental and social		Evaluate aquatic and riparian habitat impact and identify enhancement opportunities Anticipate and identify incidental recreation opportunities

Source: U.S. Army Corps of Engineers (1996a).

Table 14.3.9 Performance Requirements for Flood Proofing

Flood proofing method	Performance requirement
Window or door closure	Provide adequate forecasting and warning to permit installation of closures Identify <i>all</i> openings for closure, including fireplace cleanouts, weep holes, and so forth Ensure structural adequacy to prevent failure due to hydrostatic pressure or floating of structure Ensure watertightness to minimize and drainage to accommodate leakage Arrange adequate, ongoing public training to ensure proper operation
Small wall or levee	Requirements similar to major levee, but on a smaller scale, including: (1) providing for closure of openings in wall or levee, (2) ensuring structural stability of levee or wall, and (3) providing for proper interior damage Arrange adequate, ongoing public training to ensure proper operation Plan for emergency access to permit evacuation if protected area is isolated by rising floodwaters
Raising in-place	Protected beneath raised structure, as hazard is not eliminated Ensure structural stability of raised structure Plan for emergency access to permit evaluation if protected area is isolated by rising floodwaters

Source: U.S. Army Corps of Engineers (1996a).

Table 14.3.10 Components of a FWP System

Component	Purposes
Flood-threat-recognition subsystem	Collection of data and information; transmission of data and information; receipt of data and information; organization and display of data and information; prediction of timing and magnitude of flood events
Warning-dissemination subsystem	Determination of affected areas; identification of affected parties; preparation of warning messages; distribution of warning messages
Emergency-response subsystem	Temporary evacuation; search and rescue; mass care center operations; public-property protection; flood fight; maintenance of vital services
Post-flood-recovery subsystem	Evacuee return; debris clearance; return of services; damage assessment; provision for assistance
Continued system management	Public-awareness programs; operation, maintenance, and replacement of equipment; periodic drills; update and arrangements

Source: U.S. Army Corps of Engineers (1988b).

damage, reduced cleanup costs, reduced cost of disruption of services due to opportunities to shut off utilities and make preparations, and reduced costs due to reduction of health hazards. Furthermore, FWP plans may reduce social disruption and risk to life of floodplain occupants.

An FWP plan is a critical component of other flood-damage-reduction measures. In addition, federal Flood Plain Management Services (FPMS) staff may provide planning services in support of local agency requests for assistance in implementation of a FWP plan; this is authorized by Section 206 of the Flood Control Act of 1960.

An FWP provides lead-time notice to floodplain occupants in order to reduce potential damage. The lead time provides the opportunity to elevate contents of structures, to perform minor proofing, and to remove property susceptible to flooding. The greatest value of flood warning is to reduce or eliminate the loss of life. Flood warning requires real-time flood forecasting and communication facilities to warn inhabitants of floodplains.

Land-use controls refer to the many administrative and other actions in order to modify floodplain land use so that the uses are compatible with the potential flood hazard. These controls consist of zoning and other building ordinances, direct acquisition of land and property, building codes, flood insurance, and information programs by local, state, and federal agencies.

14.4 FLOOD DAMAGE AND NET BENEFIT ESTIMATION

14.4.1 Damage Relationships

Flood damages are usually reported as *direct damage* to property, but this is only one of five empirical categories of damages: direct damages, indirect damages, secondary damages, intangible damages, and uncertainty damages. *Indirect damages* result from lost business and services, cost of alleviating hardship, rerouting traffic, and other related damages. *Secondary damages* result from adverse effects by those who depend on output from the damaged property or hindered services. *Intangible damages* include environmental quality, social well being, and aesthetic values. *Uncertainty damages* result from the ever-present uncertainty of flooding.

Various techniques have been used to calculate direct damages. Grigg and Helweg (1975) used three categories of techniques: aggregate formulas, historical damage curves, and empirical depth-damage curves. One of the more familiar aggregate formulas is that suggested by James (1972):

$$C_D = K_D U M_S h A \quad (14.4.1)$$

where C_D is the flood damage cost for a particular flood event, K_D is the flood damage per foot of flood depth per dollar of market value of the structure, U is the fraction of floodplain in urban development, M_S is the market value of the structure inundated in dollars per developed acre, h is the average flood depth over the inundated area in feet, and A is the area flooded in acres. Eckstein (1958) presents the historical damage curve method in which the historical damages of floods are plotted against the flood stage.

The use of empirical depth-damage curves (such as shown in Figure 14.4.1) requires a property survey of the floodplain and either an individual or aggregated estimate of depth (stage) versus damage curves for structures, roads, crops, utilities, etc., that are in the floodplain. This stage damage is then related to the relationship for the stage discharge to derive the damage-discharge relationship, which is then used along with the discharge-frequency relationship to derive the damage-frequency curve, as illustrated in Figure 14.4.2.

14.4.2 Expected Damages

The *annual expected damage cost* $E(D)$ is the area under the damage-frequency curve as shown in Figure 14.4.2e, which can be expressed as

$$E(D) = \int_{q_c}^{\infty} D(q_d) f(q_d) dq_d = \int_{q_c}^{\infty} D(q_d) dF(q_d) \quad (14.4.2)$$

where q_c is the threshold discharge beyond which damage would occur, $D(q_d)$ is the flood damage for various discharges q_d , which is the damage-discharge relationship, and $f(q_d)$ and $F(q_d)$ are the probability density functions (pdf) and the cumulative distribution function (cdf), respectively, of discharge q_d . In practical applications, the evaluation of $E(D)$ by equation (14.4.2) is carried out using numerical integration because of the complexity of damage functions and probability

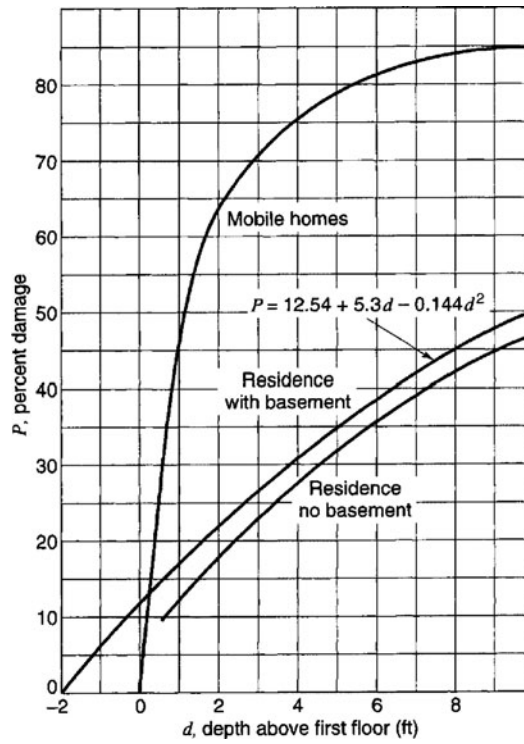


Figure 14.4.1 Percent damage, mixed residences (from Corry et al. (1980)).

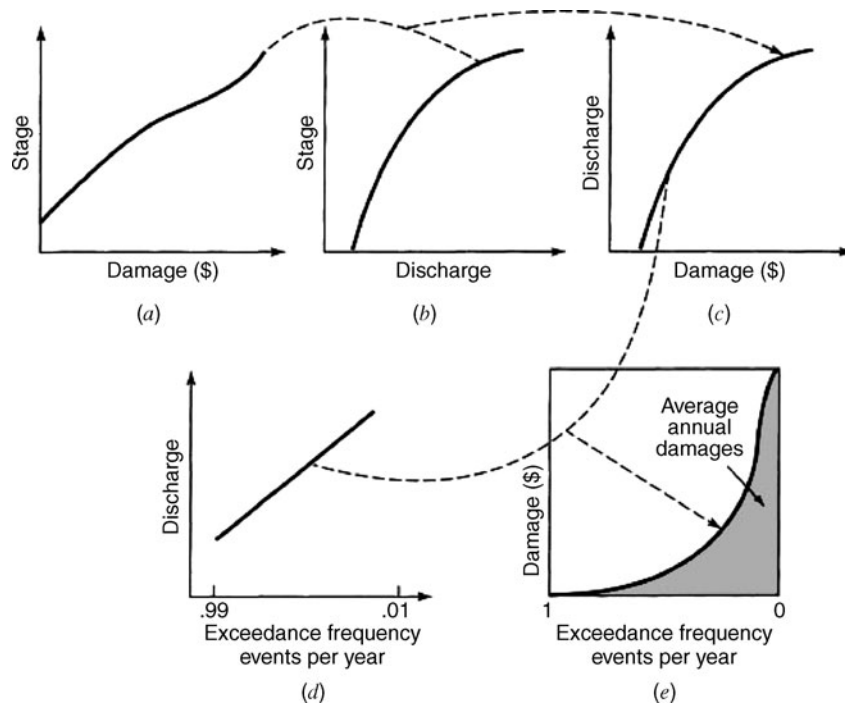


Figure 14.4.2 Computation of average annual damages. (a) Stage-damage relation; (b) Stage-discharge; (c) Discharge-damage; (d) Discharge-frequency relation; (e) Damage-frequency relation.

distribution functions. Therefore, the shaded area in Figure 14.4.2e can be approximated, numerically, by the trapezoidal rule; as an example,

$$E(D) = \sum_{j=1}^n \frac{[D(q_j) + D(q_{j+1})]}{2} [F(q_{j+1}) - F(q_j)], \text{ for } q_c = q_1 \leq q_2 \leq \dots \leq q_n < \infty \quad (14.4.3)$$

in which q_j is the discretized discharge in the interval (q_c, ∞) .

EXAMPLE 14.4.1

Use the damage-frequency relationships in Table 14.4.1 for the flood-control alternatives to rank their merits on the basis of expected flood-damage reduction.

SOLUTION

The economic merit of each flood-control alternative can be measured by the annual expected savings in flood damage of each alternative, which can be calculated as the difference between the annual expected damage at the existing condition (without flood-control measures) and the annual expected damage with a given flood-control measure under consideration. From Table 14.4.1, we determine Table 14.4.2, damage reduction associated with each flood-control measure at different return periods. From the data in Table 14.4.2, the average damage reduction for each flood-control alternative and incremental probability

Table 14.4.1 Example 14.4.1: Damage-Frequency Relationships

Exceed prob. (%)	Damage ⁰ (\$10 ⁶)	Damage ¹ (\$10 ⁶)	Damage ² (\$10 ⁶)	Damage ³ (\$10 ⁶)	Damage ⁴ (\$10 ⁶)
20	0	0	0	0	0
10	6	0	0	0	0
7	10	0	0	0	0
5	13	13	2	4	3
2	22	22	10	12	10
1	30	30	20	18	12
0.5	40	40	30	27	21
0.2	50	50	43	40	35
0.1	54	54	47	43	45
0.05	57	57	55	50	56

Note: 0—existing condition; 1—dike system; 2—upstream diversion; 3—channel modification; 4—detention basin.

Table 14.4.2 Example 14.4.1: Damage Reduction as a Function of Exceedance Probability

Exceed. prob. (%)	Damage reduction (\$10 ⁶)			
	Dike system	Upstream diversion	Channelization	Detention basin
20	0	0	0	0
10	6	6	6	6
7	10	10	10	10
5	0	9	7	10
2	0	11	9	12
1	0	10	12	18
0.5	0	10	13	19
0.2	0	7	10	15
0.1	0	5	9	9
0.05	0	2	7	1

Table 14.4.3 Example 14.4.1: Annual Expected Damage Computation

Increm. prob. (ΔF)	Damage reduction ΔD (\$10 ⁶)			
	Dike system	Upstream diversion	Channelization	Detention basin
0.1	3	3	3	3
0.03	8	8	8	8
0.02	5	9.5	8.5	10
0.03	0	10	8	11
0.01	0	10.5	10.5	15
0.005	0	10	12.5	18.5
0.003	0	8.5	11.5	17
0.001	0	6	9.5	12
0.0005	0	3.5	8	5
$\sum (\Delta D \cdot \Delta F)$	0.64	1.218	1.251	1.378

can be developed as shown in Table 14.4.3. The optimal alternative that maximizes the benefit of annual expected flood reduction is to build a detention basin upstream.

EXAMPLE 14.4.2

Columns (1)–(3) of Table 14.4.4 summarize the annual damage and annual costs for a dike system as a function of return period. Determine the return period for the dike system that maximizes the annual expected benefit.

SOLUTION

The annual total cost, shown in column (4), corresponding to different levels of production, in terms of return period, can be obtained by adding columns (2) and (3). The optimal return period associated with the least total annual expected cost is 50 years.

The same conclusion can be made by considering the annual net benefit. In this case, the annual benefit associated with different levels of protection is the saving (or reduction) in expected flood damage. For example, with a 10-year protection, the associated expected flood-damage reduction is \$0.30 M/year as compared with the existing condition; with a 50-year protection, the expected benefit is \$0.30 M + \$0.24 M + \$0.23 M + \$0.525 M = \$1.295 M/year. This information can be derived using the accumulated expected damage given in column (5). The annual expected net benefit then can be obtained by subtracting the annual cost in column (3) from column (5) and the results are listed in column (6). From column (6), the return period of 50-year is the optimal one associated with a net benefit of \$0.295 M/year.

Table 14.4.4 Example 14.4.2: Data

(1) T (yr)	(2) Annual damage (\$M/yr)	(3) Annual cost (\$M/yr)	(4) Total cost (\$M/yr)	(5) Benefit (\$M/yr)	(6) Net benefit (\$M/yr)
5	1.94475	—	1.94475	0.0	0.0
10	1.64475	0.2	1.84475	0.3	0.1
20	1.17475	0.6	1.77475	0.77	0.17
50	0.64975	1.0	1.64975	1.295	0.295
100	0.38975	1.4	1.78975	1.555	0.155
200	0.21475	1.8	2.01475	1.730	−0.07
500	0.07975	2.1	2.17975	1.865	−0.235
1,000	0.02775	2.3	2.32775	1.917	−0.383
2,000	0.00000	2.5	2.50000	1.94475	−0.5555

14.4.3 Risk-Based Analysis

Conventional risk-based design procedures for hydraulic structures consider only the inherent hydrologic uncertainty. The probability of failure of the hydraulic structure is generally evaluated by means of probability analysis as described in Chapter 10. Other aspects of hydrologic uncertainties are seldom included. Methodologies have been developed to integrate various aspects of hydrologic uncertainties into risk-based design of hydraulic structures (Mays and Tung, 1992).

Risk-based design approaches integrate the procedures of uncertainty analysis and reliability analysis in design. Such approaches consider the economic trade-offs between project costs and expected damage costs through the risk relationships. The risk-based design procedure can be incorporated into an optimization framework to determine the *optimal risk-based design*. Therefore, in an optimal risk-based design, the expected annual damage is taken into account in the objective function, in addition to the installation cost. The problem is to determine the optimal structural sizes/capacities associated with the least total expected annual cost (TEAC). Mathematically, the optimal risk-based design can be expressed as

$$\text{Min}_x TEAC = FC(x) \cdot CRF + E(D|x) \quad (14.4.4a)$$

$$\text{Subject to design specifications, } g(x) = 0 \quad (14.4.4b)$$

where FC is the total installation cost (first cost) of the structure, CRF is the capital recovery factor for conversion of cost to an annual basis, x is a vector of decision variables relating to structural sizes and/or capacities, and $E(D|x)$ is the expected annual damage cost due to structural failure. A diagram illustrating the cost computations for optimal risk-based design is shown in Figure 14.4.3.

In general, quantification of the first cost is straightforward. The thrust of risk-based design is the assessment of the annual expected damage cost. Depending on the types of uncertainty to be considered, assessment of $E(D|x)$ varies. Current practice in risk-based water-resources engineering design considers only the inherent hydrologic uncertainty due to the randomness of the hydro-logic process. The mathematical representation of the annual expected damage under this condition can be computed using equation (14.4.2).

The procedure for computations of expected annual damages illustrated in Figure 14.4.2 ignores uncertainty in the various relationships. Traditional uncertainty has been accounted for by the use of factors of safety such as large return periods or freeboard for levees. The more recent advances in risk analysis has allowed the explicit accounting of uncertainty. As a result, the U.S. Army Corps of Engineers (1996b) has adapted a policy by which flood-damage reduction studies use the risk-based analysis described in the next section.



Figure 14.4.3 Computation of expected damage cost and total cost for risk-based design.

14.5 U.S. ARMY CORPS OF ENGINEERS RISK-BASED ANALYSIS FOR FLOOD-DAMAGE REDUCTION STUDIES

14.5.1 Terminology

The U.S. Army Corps of Engineers (1996b) has developed guidance and a procedure for risk-based analysis for flood-damage reduction studies that depends on

- (a) Qualitative description of errors or uncertainty in selecting the proper hydrologic, hydraulic, and economic function to use when evaluating economic and engineering performance of flood-damage reduction measures
- (b) Qualitative description of errors or uncertainty in selecting the parameters of these functions
- (c) Conceptual techniques that determine the combined impact on plan evolution of errors in the function and their parameters

The concepts of flood risks and uncertainty made in this procedure are defined in Table 14.5.1.

A *flood-damage-reduction plan* includes measures that reduce damage by reducing discharge, reducing stage, or reducing damage susceptibility (U.S. Army Corps of Engineers, 1996b). For U.S. government projects, the objective of the plan is to solve the problem so that the solution will contribute to rational economic development (RED). A *flood-damage-reduction planning study* is conducted to determine (1) which measures to include in the plan, (2) where to locate the measures, (3) what size to make the measures, and (4) how to operate measures in order to satisfy the federal objective and constraints (U.S. Army Corps of Engineers, 1996b).

Table 14.5.1 Terminology

Term	Definition
Function uncertainty (also referred to as distribution uncertainty and model uncertainty)	Lack of complete knowledge regarding the form of a hydrologic, hydraulic, or economic function to use in a particular application. This uncertainty arises from incomplete scientific or technical understanding of the hydrologic, hydraulic, or economic process.
Parameter	A quantity in a function that determines the specific form of the relationship of known input and unknown output. An example is Manning’s roughness coefficient in energy loss calculations. The value of this parameter determines the relationship between a specified discharge rate and the unknown energy loss in a specific channel reach.
Parameter uncertainty	Uncertainty in a parameter due to limited understanding of the relationship or due to lack of accuracy with which parameters can be estimated for a selected hydrologic, hydraulic, or economic function.
Sensitivity analysis	Computation of the effect on the output of changes in input values or assumption.
Exceedance probability	The probability that a specified magnitude will be exceeded. Unless otherwise noted, this term is used herein to denote annual exceedance probability: the likelihood of exceedance in any year.
Median exceedance probability	In a sample of estimates of exceedance probability of a specified magnitude, this is the value that is exceeded by 50 percent of the estimates.
Capacity exceedance	Capacity exceedance implies exceedance of the capacity of a water conveyance, storage facility, or damage-reduction measure. This includes levee or reservoir capacity exceeded before over-topping, channel capacity exceedance, or rise of water above the level of raised structures.
Conditional probability	The probability of capacity exceedance, given the occurrence of a specified event.
Long-term risk	The probability of capacity exceedance during a specified period. For example, 30-year risk refers to the probability of one or more exceedances of the capacity of a measure during a 30-year period.

Source: U.S. Army Corps of Engineers (1996b).

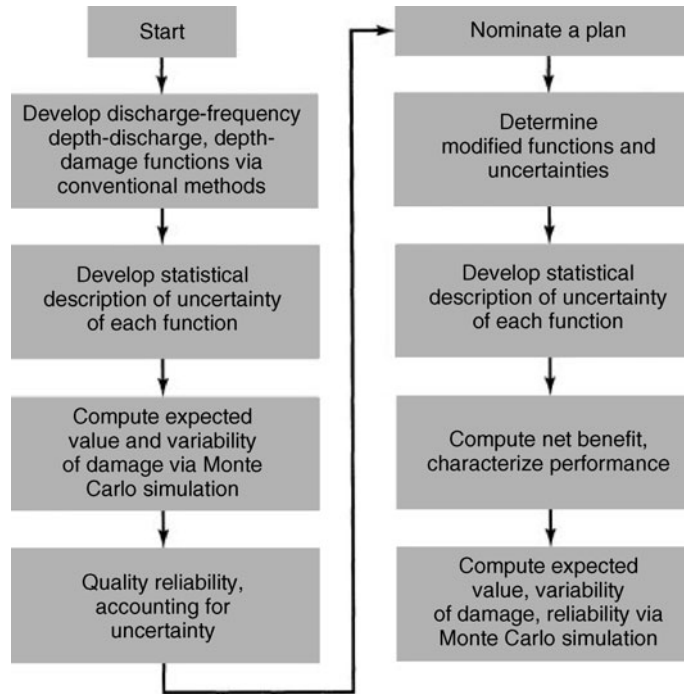


Figure 14.5.1 Risk-based analysis procedure (from U.S. Army Corps of Engineers (1996b)).

Figure 14.5.1 provides an overview of the risk-based analysis procedure that quantifies the uncertainty in the relationships of discharge frequency, storage discharge, and stage damage, and incorporates an analysis of the economic efficiency of alternatives.

The expected value $E[X]$ of inundation damage X can be calculated using equation (14.4.2), or more simply

$$E[X] = \int_{-\infty}^{\infty} xf(x)dx \quad (14.5.1)$$

where $f(x)$ is the probability density function of x .

14.5.2 Benefit Evaluation

The *net benefit* of a plan is the measure of the flood-damage-reduction plan's contribution to *national economic development (NED)*. The net benefit is computed as the sum of location benefit, intensification benefit, and flood-inundation reduction benefit, less the total cost of implementation (operating, maintenance, repairing, replacing, and rehabilitating [OMRR&R]) of the plan. The *location benefit* is the increased net income of additional floodplain development due to a plan. The *intensification benefit* is the increased net income of existing floodplain activities. The *inundation-reduction benefit* is the plan-related reduction in physical economic damage, income loss, and emergency cost.

The *economic efficiency* of a proposed flood-damage-reduction alternative is defined as

$$NB = (B_L + B_I + B_{IR}) - C \quad (14.5.2)$$

in which NB = net benefit, B_L = location benefit, B_I = intensification benefit, B_{IR} = inundation-reduction benefit, and C = total cost of implementing, operating, maintaining, repairing, replacing,

and rehabilitating the plan (the OMRR&R cost). The inundation-reduction benefit may be expressed as

$$B_{IR} = (D_{\text{without}} - D_{\text{with}}) \tag{14.5.3}$$

in which D_{without} = economic flood damage without the plan, and D_{with} = economic flood damage if the plan is implemented.

The random nature of flooding complicates determination of the inundation-reduction benefit. For example, a flood-damage-reduction plan that eliminates all inundation damage one year may be too small to eliminate all damage in an extremely wet year and much larger than required in an extremely dry year. U.S. Water Resources Council (1983) guidelines address this problem by calling for use of expected annual flood damage. Expected damage takes into account the risk of various magnitudes of flood damage each year, weighing the damage caused by each flood by the probability of occurrence. Combining equations (14.5.2) and (14.5.3) and rewriting them in terms of expected values yields:

$$NB = B_L + B_I + E[D_{\text{without}}] - E[D_{\text{with}}] - C \tag{14.5.4}$$

in which $E[]$ denotes the expected value. For urban flood damages, this generally is computed on an annual basis because significant levels of flood damage are limited to annual recurrence. For agricultural flood damages, it may be computed as the expected damage per flood, as more than one damaging flood may occur in a given year. The NED plan is then the alternative plan that yields maximum net benefit, taking into account the full range of hydrologic conditions that might occur.

The “without project” condition in equation (14.5.4) represents existing and future system conditions in the absence of a plan. It is the base condition upon which alternative plans are formulated, from which all benefits are measured, and against which all impacts are assessed (U.S. Army Corps of Engineers, 1989).

14.5.3 Uncertainty of Stage-Damage Function

The stage-damage function is a summary statement of the direct economic cost of floodwater inundation for a specified river reach (U.S. Army Corps of Engineers, 1996b). Table 14.5.2 illustrates the traditional procedure for development of a stage-damage function and Table 14.5.3 identifies some of the sources of uncertainty. From these descriptions, an aggregated description of uncertainty of the stage-damage function can be developed using the procedure in Figure 14.5.2.

Table 14.5.2 Traditional Procedure for Development of Stage-Damage Function

Step	Task
1	Identify and categorize each structure in the study area based upon its use and construction
2	Establish the first-floor elevation of each structure using topographic maps, aerial photographs, surveys, and/or hand levels
3	Estimate the value of each structure using real estate appraisals, recent sales prices, property tax assessments, replacement cost estimates, or surveys
4	Estimate the value of the contents of each structure using an estimate of the ratio of contents value to structure value for each unique structure category
5	Estimate damage to each structure due to flooding to various water depths at the structure’s site using a depth-percent damage function for the structure’s category along with the value from Step 3
6	Estimate damage to the contents of each structure due to flooding to various water depths using a depth-percent damage function for contents for the structure category along with the value from Step 4
7	Transform each structure’s depth-damage function to a stage-damage function at an index location for the floodplain using computed water-surface profiles for reference floods
8	Aggregate the estimated damages for all structures by category for common stages

Source: U.S. Army Corps of Engineers (1996b).

Table 14.5.3 Components and Sources of Uncertainty in Stage-Damage Function

Parameter/Model	Source of uncertainty
Number of structures in each category	Errors in identifying structures; errors in classifying structures
First-floor elevation of structure	Survey errors; inaccuracies in topographic maps; errors in interpolation of contour lines
Depreciated replacement value of structure	Errors in real estate appraisal; errors in estimation of replacement cost estimation-effective age; errors in estimation of depreciation; errors in estimation of market value
Structure depth-damage function	Errors in post-flood damage survey; failure to account for other critical factors: floodwater velocity; duration of flood; sediment load; building material; internal construction; condition; flood warning
Depreciated replacement value of contents	Errors in content-inventory survey; errors in estimates of ratio of content to structure value
Content depth-damage function	Errors in post-flood damage survey; failure to account for other critical factors: floodwater velocity; duration of flood; sediment load; content location; flood warning

Source: U.S. Army Corps of Engineers (1996b).

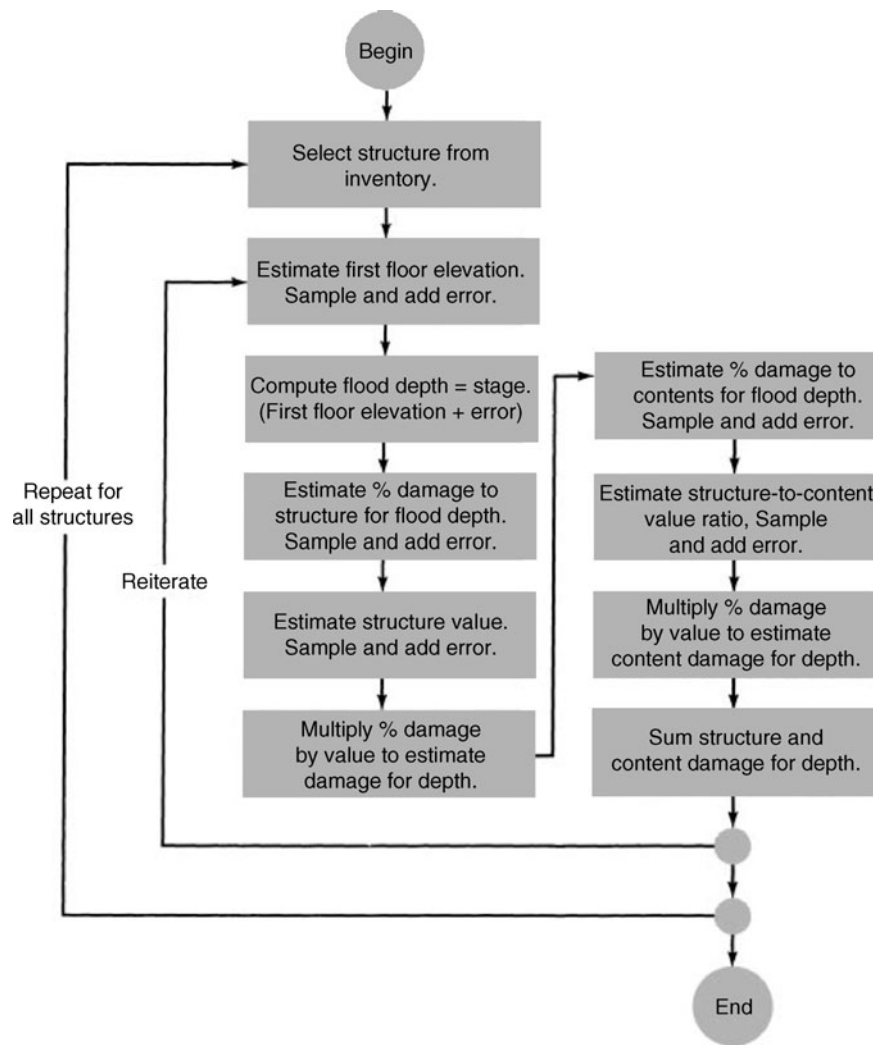


Figure 14.5.2 Development of stage-damage function with uncertainty description (from U.S. Army Corps of Engineers (1996b)).

14.6 OPERATION OF RESERVOIR SYSTEMS FOR FLOOD CONTROL

14.6.1 Flood-Control Operation Rules

Flood control is one of the general operation purposes of reservoir system operation, as discussed in Section 11.7. *Operation rules (policies)* are used to specify how water is managed throughout a system. These rules are specified in order to achieve discharge requirements and system demands that maximize the objective expressed in the form of benefits. Operation rules may be established on seasonal, monthly, or other time periods to prescribe how water is to be regulated during subsequent time periods based on the current state of the system. Even though operating rules are usually defined for each within-year period, these rules can vary over successive years, as a result for instance of changing demand.

Flood-control operating rules define the release to be made in the current time period as a function of one or more of the following: current storage in the reservoir, forecast inflow to the reservoir, current and forecast downstream flow, and current storage in and forecast flow to other reservoirs in a multiple-reservoir system. Operating rules must be defined for controlled reservoirs as a component of any plan that includes such a reservoir. Figure 11.7.6 illustrates an example of an operation rule that shows the seasonally varying storage boundaries for a multipurpose reservoir.

14.6.2 Tennessee Valley Authority (TVA) Reservoir System Operation

The Tennessee River Basin is located in a seven-state area in the southeastern United States, as illustrated in Figure 14.6.1. The drainage area is 40,900 mi² (105,930 km²). This basin is located a short distance from the Gulf of Mexico and the Caribbean Sea, which provide major sources of moisture, so that it is one of the wettest regions in the United States.

Sixty major dams are operated in an integrated multipurpose water control system by the TVA. A schematic of the system is shown in Figure 14.6.2. Of these dams, 45 are owned by the TVA in the Tennessee River Basin, another six provide flow into the TVA system but are owned and operated by others; the remaining nine dams (eight Army Corps of Engineers dams and one TVA dam) are in the Cumberland River Basin. The amount of available flood-control storage in the TVA reservoir system varies with the potential flood threat and the time of the year, as indicated in Table 14.6.1 (Miller, et al. 1996).

The typical operating rules for the TVA system reservoirs are illustrated in Figure 14.6.3. The tributary reservoir operations depend very strongly on the annual hydrologic cycle (Figure 14.6.4). The operations can be categorized into four periods: winter flood season (January 1 to March 15), fill period (March 15 to June 1), recreation season (June 1 to August 1), and drawdown season (August 1 to December 31).

During the winter flood season, reservoir levels are held below the *flood guides* (see Figure 14.6.3) to provide storage for high winter flows. During the fill period, spring rainfall is used rapidly to fill the reservoirs for the summer recreation target levels. During the fill period, an attempt is made to keep the reservoir levels between the flood guides and the *minimum operation guides* (MOGs). Summer reservoir levels are normally kept above the targeted minimum summer recreation levels until the end of July, when they are gradually lowered during the drawdown period.

Mainstream reservoir operation generally follows a similar but simpler operation rule (see Figure 14.6.3). Topography and navigation requirements allow only a few feet between winter and summer levels on the mainstream reservoir, whereas a reservoir elevation on the tributaries can fluctuate as much as 75 ft (23 m) between winter and summer. *Mosquito control fluctuations* (reservoir levels are fluctuated by 1 ft each week) are used during the late spring and summer into mainstream and reservoirs (except in Kentucky) to help control mosquitoes. The use of TVA's reservoir operating guides is unique in the United States in that most of the major reservoir systems operate within specified zones or pools, such as the U.S. Army Corps of Engineers (Miller et al. 1996).

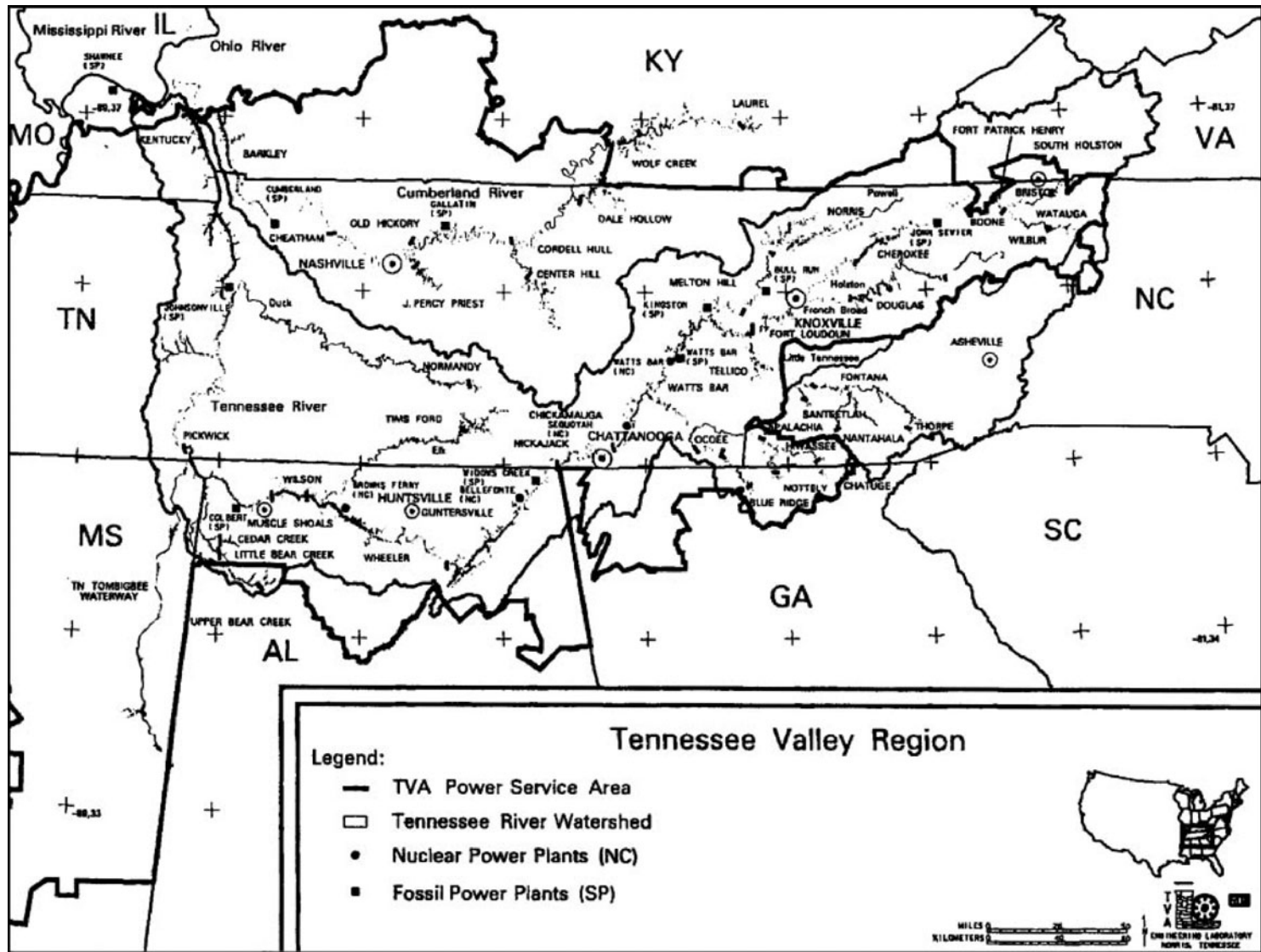


Figure 14.6.1 The Tennessee River Basin (from Miller et al. (1996)).

TENNESSEE RIVER RESERVOIR SYSTEM

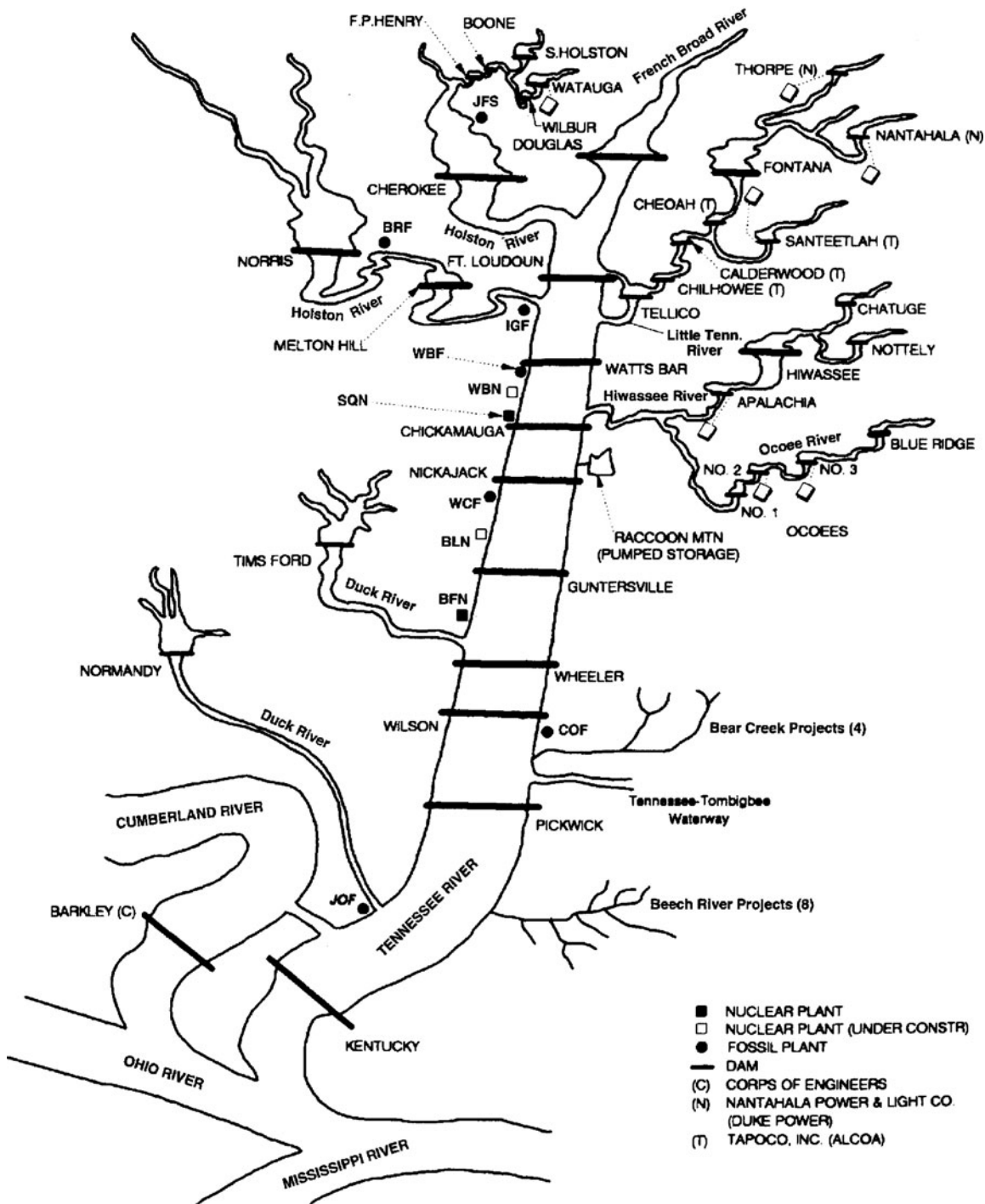


Figure 14.6.2 Schematic of the TVA water-control system (from Miller et al. (1996)).

Table 14.6.1 TVA Reservoir System Flood-Control Storage

Time of year	Detention storage (ac-ft)		
	Above chattanooga	Total system	Total system runoff (in)
January 1	6,339,780	11,330,480	5.3
March 15	5,189,750	10,030,760	4.7
June 1	1,571,580	2,137,540	1.0

Note: 1 ac-ft = 1233 m³

Source: Miller et al. (1996).

The U.S. Army Corps of Engineers HEC-5 computer program (U.S. Army Corps of Engineers, 1982) models the performance of a reservoir or a reservoir system to manage excess water. The storage in each reservoir in a system is divided into zones (see Figure 11.7.1), so that inlet storage levels are defined in each zone. Table 14.6.2 summarizes the flood-control operation rules in HEC-5. Refer to the Web site (www.hec.usace.army.mil) to obtain HEC-5 and additional information.

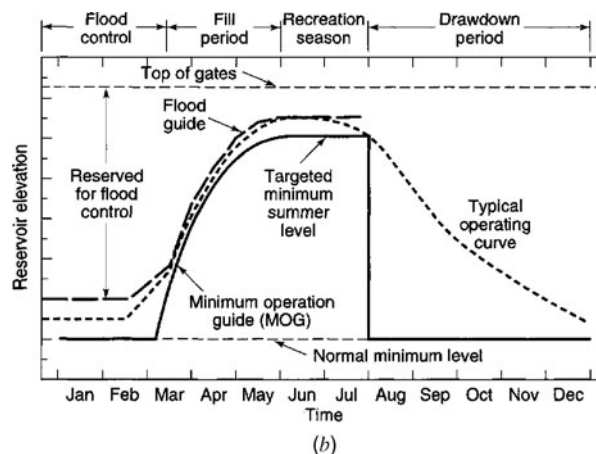
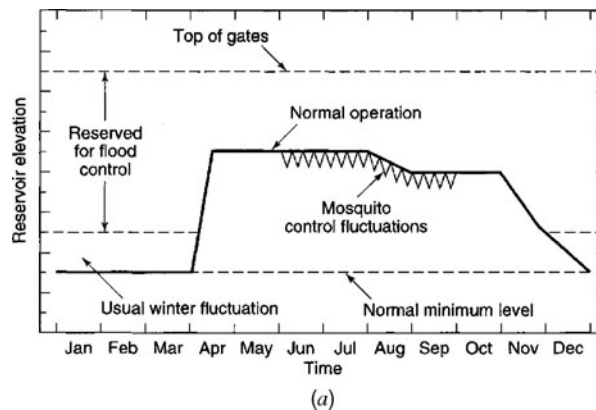


Figure 14.6.3 Typical TVA reservoir operating levels. (a) Mainstream reservoir operations; (b) Tributary reservoir operations (from Miller et al. (1996)).

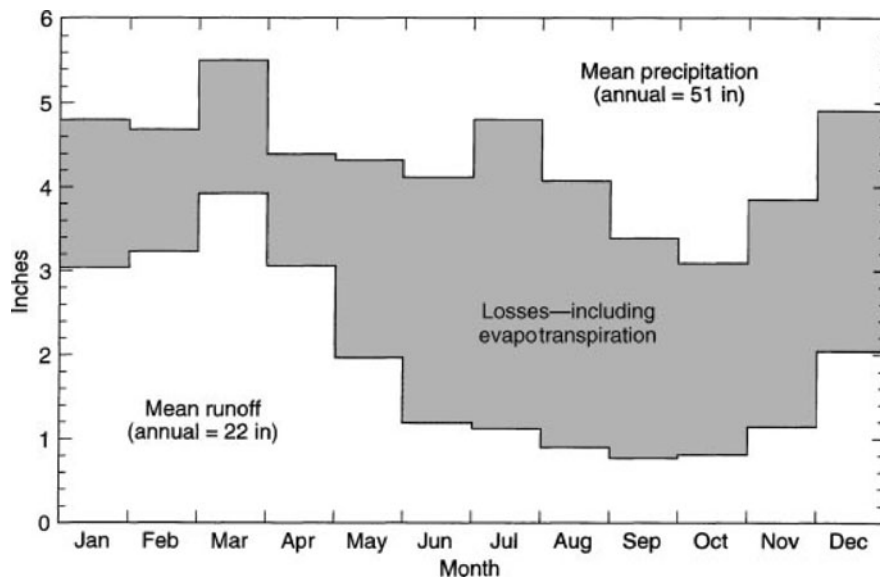


Figure 14.6.4 Tennessee River Basin mean monthly rainfall and runoff, 1894–1993 (from Miller et al. (1996)).

Table 14.6.2 HEC-5 Flood-Control Operation Rules

Constraint on release made	Condition
Release to draw storage to top of conservation pool without exceeding channel capacity at reservoir or downstream points for which reservoir is operated	Storage is between top of conservation pool and top of flood-control pool
Release equal to or greater than minimum desired flow	Storage greater than top buffer storage
Release equal to minimum desired flow	Storage between top inactive and top of buffer pool
No release	Storage below top of inactive pool
Release required to satisfy hydropower requirement	If that release is greater than controlling desired or required flows for above conditions
Release limited to user-specified rate of change	Unless reservoir is in surcharge operation
No release that will continue to flooding downstream	If flood storage available
Release to maintain downstream flow at channel capacity	If operating for flood control
Release from reservoir at greatest level	If two or more reservoirs on parallel streams operate for common downstream point
Release to bring upper reservoir to same index level as downstream reservoir	If two reservoirs in tandem

Source: Ford and Hamilton (1996).

PROBLEMS

14.2.1 Obtain the FEMA flood hazard map for your local area and identify the 100-year floodplain, the floodway, and the floodway fringe.

14.4.1 Determine the optimal design return period for a flood-control project with damage and capital costs for the following return periods:

T	1	2	5	10	15	20	25	50	100	200
Damage cost, $\$ \times 10^3$	0	40	120	280	354	426	500	600	800	1000
Capital cost, $\$/yr \times 10^3$	0	6	28	46	50	54	58	80	120	160

14.4.2 The frequency-discharge-storage-damage data for existing conditions at a particular area along a river is given in Table P14.4.2. The storage-discharge data is the rating curve, the discharge-frequency data is the frequency curve, and the storage-damage data is the storage-damage curve. Plot these three relationships.

Table P14.4.2

Exceedance probability	Q (cfs)	Stage (ft)	Damage (\$10 ⁶)
20	12,000	30	0
10	14,000	33	6
7	15,000	34	10
5	16,000	35	13
2	18,000	38	22
1	20,000	40	30
0.5	22,000	42.5	40
0.2	25,000	45	50
0.1	26,000	46	54
0.05	28,000	47	57

14.4.3 If a dike system with a capacity of 15,000 cfs were used as one alternative for the situation in problem 14.4.2, develop the damage-frequency curve for this alternative.

14.4.4 If an upstream permanent diversion that will protect up to a natural flow of 15,000 cfs is used for the situation in problem 14.4.2, develop the damage-frequency curve for this alternative.

14.4.5 If channel modifications were used for the situation in problem 14.4.2 to increase the conveyance capacity of the river up to 15,000 cfs, develop the damage-frequency curve for this alternative.

14.4.6 Referring to problems 14.4.2 and 14.4.3, determine the return period for the dike system that maximizes annual expected benefit.

14.4.7 Referring to problems 14.4.2 and 14.4.4, determine the return period for the diversion capacity with maximum expected annual benefit.

14.4.8 Referring to problems 14.4.2 and 14.4.5, determine the return period associated with the flow capacity that maximizes the expected annual net benefit in the channel modification.

14.5.1 Use the Web site for the U.S. Committee on Large Dams (www.uscold.org/~uscold/) to write a summary of the recent flood damage prevention of: (a) California's Central Valley dams; (b) Oroville Dam; and (c) Truckee River dams; and (d) Missouri River dams.

14.5.2 Write a summary of the flood control aspects of the Three Gorges Dam on the Yangtze River in China.

14.6.1 Write a history of the TVA starting with the Web address (www.TVA.gov), with particular emphasis on flood control.

REFERENCES

- Bull, W. B., "Alluvial Fans and Pediments of Southern Arizona," in *Landscapes of Arizona* edited by T. L. Smiley, et al., University Press of America, Lanham, pp. 229–252, 1984.
- Corry, M. L., J. S. Jones, and D. L. Thompson, "The Design of Encroachments of Floodplains Using Risk Analysis," Hydraulic Engineering Circular No. 17, U.S. Department of Transportation, Federal Highway Administration, Washington, DC, July 1980.
- Dodson, R., "Floodplain Hydraulics," in *Hydraulic Design Handbook* edited by L. W. Mays, McGraw-Hill, New York, 1999.
- Eckstein, O., *Water Resources Development; The Economic of Project Evaluation*, Harvard University Press, Cambridge, MA, 1958.
- Ford, D., and D. Hamilton, "Computer Models for Water-Excess Management," in *Water Resources Handbook* edited by L. W. Mays, McGraw-Hill, New York, 1996.
- Grigg, N. S., and O. J. Helweg, "State-of-the-Art of Estimating Flood Damage in Urban Areas," *Water Resources Bulletin*, vol. 11, no. 2, pp. 379–390, 1975.
- Hoggan, D. H., *Computer-Assisted Floodplain Hydrology and Hydraulics*, second edition, McGraw-Hill, New York, 1997.
- Interagency Floodplain Management Review Committee, *Sharing the Challenge: Floodplain Management into the 21st Century*, Administration Floodplain Management Task Force, Executive Office of the President, Washington, DC, June, 1994.
- James, L. D., "Role of Economics in Planning Floodplain Land Use," *Journal of the Hydraulics Division, ASCE*, vol. 98, no. HY6, pp. 981–992, 1972.
- Mays, L. W., and Y. K. Tung, *Hydrosystems Engineering and Management*, McGraw-Hill, New York, 1992.
- Meyers, Mary F., and G. F. White, "The Challenge of the Mississippi Flood," *Environment*, vol. 35, no. 10, Washington, DC, 1993.
- Miller, B. A., A. Whitelock, and R. C. Hughes, "Flood Management—The TVA Experience," *Water International, IWRA*, vol. 21, no. 3, pp. 119–130, 1996.
- U.S. Army Corps of Engineers, and Conservation System, *HEC-S Simulation of Flood Control User's Manual*, Hydrologic Engineering Center, vol. 9, Hydrologic Engineering Center, Davis, CA, 1988.
- U.S. Army Corps of Engineers, *Flood Damage Analysis Package Users Manual*, Hydrologic Engineering Center, Davis, CA, 1988a.
- U.S. Army Corps of Engineers, "National Economic Development Procedures Manual—Urban Flood Damage," Institute for Water Resources, IWR Report 88-R-2, Ft. Belvoir, VA, 1988b.
- U.S. Army Corps of Engineers, "EAD: Expected Annual Flood Damage Computation, User's Manual," CPD-30, Hydrologic Engineering Center, Davis, CA, 1989.

U.S. Army Corps of Engineers, Hydrologic Engineering Center, "Federal Perspective for Flood-Damage-Reduction Studies," *Water Resources Handbook* (edited by L. W. Mays), McGraw-Hill, New York, 1996a.

U.S. Army Corps of Engineers, *Risk-Based Analysis for Flood Damage Reduction Studies*, Engineering Manual EM 1110-2-1619, Washington, DC, 1996b.

U.S. Water Resources Council, *Economic and Environmental Principles and Guidelines for Water and Related Land Resources Implementation Studies*, U.S. Government Printing Office, Washington, DC, 1983.

Waananen, A. O., J. T. Limerinos, W. J. Kockelman, W. E. Spangle, and M. L. Blair, "Flood-Prone Areas and Land-Use Planning-Selected Examples from the San Francisco Bay Region," U.S. Geological Survey Professional Paper 942, California, 1977.

Chapter 15

Stormwater Control: Storm Sewers and Detention

15.1 STORMWATER MANAGEMENT

Stormwater management is knowledge used to understand, control, and utilize waters in their different forms within the hydrologic cycle (Wanielista and Yousef, 1993). The goal of this chapter is to provide an introduction to the various concepts and design procedures involved in stormwater management. The overall key component of stormwater management is the drainage system. Urbonas and Roesner (1993) point out the following vital functions of a drainage system:

1. It removes stormwater from the streets and permits the transportation arteries to function during bad weather; when this is done efficiently, the life expectancy of street pavement is extended.
2. The drainage system controls the rate and velocity of runoff along gutters and other surfaces in a manner that reduces the hazard to local residents and the potential for damage to pavement.
3. The drainage system conveys runoff to natural or manmade major drainage ways.
4. The system can be designed to control the mass of pollutants arriving at receiving waters.
5. Major open drainage ways and detention facilities offer opportunities for multiple use such as recreation, parks, and wildlife preserves.

Storm drainage criteria are the foundation for developing stormwater control. Table 15.1.1 provides a checklist for developing storm drainage criteria. These criteria should set limits on development, provide guidance and methods of design, provide details of key components of drainage and flood control systems, and ensure longevity, safety, aesthetics, and maintainability of the system served (Urbonas and Roesner, 1993).

Table 15.1.1 Checklist for Developing Local Storm Drainage Criteria

Governing legislation and statements of policy and procedure
Legal basis for criteria
Define what constitutes the drainage system
Benefits of the drainage system
Policy for dedication of right-of-way
Compatible multipurpose uses
Review and approval procedures
Procedures for obtaining variances or waivers of criteria

(Continued)

Table 15.1.1 (Continued)

Initial and major drainage system provisions
Definitions of initial system and major system
Where should a separate formal major drainageway begin?
Allowable flow capacities in streets for initial and major storms
Maximum and minimum velocities in pipes and channels
Maximum flow depths in channels and freeboard requirements
Data required for design, such as:
Watershed boundaries
Local rainfall and runoff data
History of flooding in the area
Defined regulatory flood plains and floodways
Existing and projected land use for project site
Existing and planned future land uses upstream
Existing and planned drainage systems off-site
Tabulation of previous studies affecting site
Conflicts with existing utilities
Design storms, intensity-duration-frequency data
Hydrologic methods and/or models
Storm sewer design criteria, including materials
Manhole details and spacing, inlet details and spacing, types of inlets, trenching, bedding, backfill, etc.
Street flow calculations and limitations
Details of major system components such as channels, drop structures, erosion checks, transitions, major culverts and pipes, bridges, bends, energy dissipators, riprap, sediment transport
Detention requirements
When and where to use detention
Design storms
Hydrologic sizing criteria and/or procedures
Safety, aesthetics, and maintainability criteria
Multipurpose uses and design details for each
Water quality criteria
Goals and objectives
Minimum capture volumes
Required or acceptable best management practices (BMP)
Technical design criteria for each BMP
Special considerations
Right-of-way dedication requirements
Use of irrigation ditches
Flood proofing and when it is accepted
Any other items reflecting local needs
List of technical references

Source: Urbonas and Roesner (1993).

15.2 STORM SYSTEMS

15.2.1 Information Needs and Design Criteria

To begin the design process of a storm sewer system, one must collect a considerable amount of information. A condensed checklist of information needs for storm sewer design is presented in Table 15.2.1. There are many sources for this information, ranging from various local government agencies to federal agencies to pipe and pump manufacturers. The designer must also obtain future development information for areas surrounding the site of interest.

Table 15.2.1 Condensed Checklist of Information Needs for Storm Sewer Design

-
- Local storm drainage criteria and design standards
 - Maps, preferably topographic, of the subbasin in which the new system is to be located
 - Detailed topographic map of the design area
 - Locations, sizes, and types of existing storm sewers and channels located upstream and downstream of design area
 - Locations, depths, and types of all existing and proposed utilities
 - Layout of design area including existing and planned street patterns and profiles, types of street cross-sections, street intersection elevations, grades of any irrigation and drainage ditches, and elevations of all other items that may post physical constraints to the new system
 - Soil borings, soil mechanical properties, and soil chemistry to help select appropriate pipe materials and strength classes
 - Seasonal water table levels
 - Intensity-duration-frequency and design storm data for the locally required design return periods
 - Pipe vendor information for the types of storm sewer pipe materials accepted by local jurisdiction
-

Source: Urbonas and Roesner (1993).

Design criteria vary from one city to another, but for the most part the following are a fairly standard set of assumptions and constraints used in the design of storm sewers (American Society of Civil Engineers and Water Pollution Control Federation, 1969, 1992):

- a. For small systems, free-surface flow exists for the design discharges; that is, the sewer system is designed for “gravity flow” so that pumping stations and pressurized sewers are not considered.
- b. The sewers are commercially available circular pipes.
- c. The design diameter is the smallest commercially available pipe that has flow capacity equal to or greater than the design discharge and satisfies all the appropriate constraints.
- d. Storm sewers must be placed at a depth that will not be susceptible to frost, will drain basements, and will allow sufficient cushioning to prevent breakage due to ground surface loading. Therefore, minimum cover depths must be specified.
- e. The sewers are joined at junctions such that the crown elevation of the upstream sewer is no lower than that of the downstream sewer.
- f. To prevent or reduce excessive deposition of solid material in the sewers, a minimum permissible flow velocity at design discharge or at barely full-pipe gravity flow is specified.
- g. To prevent the occurrence of scour and other undesirable effects of high-velocity flow, a maximum permissible flow velocity is also specified. Maximum velocities in sewers are important mainly because of the possibilities of excessive erosion on the sewer inverts.
- h. At any junction or manhole, the downstream sewer cannot be smaller than any of the upstream sewers at that junction.
- i. The sewer system is a dendritic network converging towards downstream without closed loops.

Table 15.2.2 lists the more important typical technical items and limitations to consider.

15.2.2 Rational Method Design

From an engineering viewpoint the design can be divided into two main aspects: runoff prediction and pipe sizing. The rational method, which can be traced back to the mid-nineteenth century, is still probably the most popular method used for the design of storm sewers (Yen and Akan, 1999). Although criticisms have been raised of its adequacy, and several other more advanced methods have been proposed, the rational method, because of its simplicity, is still in continued use for sewer design when high accuracy of runoff rate is not essential.

Table 15.2.2 Technical Items and Limitations to Consider in Storm Sewer Design

Velocity:	
Minimum design velocity	2–3 ft/s (0.6–0.9 m/s)
Maximum design velocity	
Rigid pipe	15–21 ft/s (4.6–6.4 m/s)
Flexible pipe	10–15 ft/s (3.0–4.6 m/s)
Maximum manhole spacing:	
(function of pipe size)	400–600 ft (122–183 m)
Minimum size of pipe	12–24 in (0.3–0.6 m)
Vertical alignment at manholes:	
Different size pipe	Match crown of pipe or 80% to 85% depth lines
Same size pipe	Minimum of 0.1–0.2 ft (0.03–0.06 m) in invert drop
Minimum depth of soil cover	12–24 in (0.3–0.6 m)
Final hydraulic design	Check design for surcharge and junction losses by using backwater analysis
Location of inlets	In street where the allowable gutter flow capacity is exceeded

Source: Urbonas and Roesner (1993).

Using the rational method, the storm runoff peak is estimated by the rational formula

$$Q = KCiA \quad (15.2.1)$$

where the peak runoff rate Q is in ft^3/s (m^3/s), K is 1.0 in U.S. customary units (0.28 for SI units), C is the runoff coefficient (Table 15.2.3), i is the average rainfall intensity in in/hr (mm/hr) from intensity-duration frequency relationships for a specific return period and duration t_c in min, and A is the area of the tributary drainage area in acres (km^2). The duration is taken as the time of concentration t_c of the drainage area.

In urban areas, the drainage area usually consists of subareas or subcatchments of substantially different surface characteristics. As a result, a composite analysis is required that must take into account the various surface characteristics. The areas of the subcatchments are denoted by A_j and the runoff coefficients for each subcatchment are denoted by C_j . Then the peak runoff is computed using the following form of the rational formula:

$$Q = Ki \sum_{j=1}^m C_j A_j \quad (15.2.2)$$

where m is the number of subcatchments drained by a sewer.

The *rainfall intensity* i is the average rainfall rate considered for a particular drainage basin or subbasin. The intensity is selected on the basis of design rainfall duration and design frequency of occurrence. The design duration is equal to the time of concentration for the drainage area under consideration. The frequency of occurrence is a statistical variable that is established by design standards or chosen by the engineer as a design parameter.

The *time of concentration* t_c used in the rational method is the time associated with the peak runoff from the watershed to the point of interest. Runoff from a watershed usually reaches a peak at the time when the entire watershed is contributing; in this case, the time of concentration is the time for a drop of water to flow from the remotest point in the watershed to the point of interest. Runoff may reach a peak prior to the time the entire watershed is contributing. A trial-and-error procedure can be used to determine the critical time of concentration. The time of concentration to any point in a storm drainage system is the sum of the inlet time t_0 and the flow time t_f in the upstream sewers connected to the catchment, that is,

$$t_c = t_0 + t_f \quad (15.2.3)$$

Table 15.2.3 Runoff Coefficients for Use in the Rational Method

Character of surface	Return period (years)						
	2	5	10	25	50	100	500
Developed							
Asphaltic	0.73	0.77	0.81	0.86	0.90	0.95	1.00
Concrete/roof	0.75	0.80	0.83	0.88	0.92	0.97	1.00
Grass areas (lawns, parks, etc.)							
<i>Poor condition</i> (grass cover less than 50% of the area)							
Flat, 0–2%	0.32	0.34	0.37	0.40	0.44	0.47	0.58
Average, 2–7%	0.37	0.40	0.43	0.46	0.49	0.53	0.61
Steep, over 7%	0.40	0.43	0.45	0.49	0.52	0.55	0.62
<i>Fair condition</i> (grass cover 50% to 75% of the area)							
Flat, 0–2%	0.25	0.28	0.30	0.34	0.37	0.41	0.53
Average, 2–7%	0.33	0.36	0.38	0.42	0.45	0.49	0.58
Steep, over 7%	0.37	0.40	0.42	0.46	0.49	0.53	0.60
<i>Good condition</i> (grass cover larger than 75% of the area)							
Flat, 0–2%	0.21	0.23	0.25	0.29	0.32	0.36	0.49
Average, 2–7%	0.29	0.32	0.35	0.39	0.42	0.46	0.56
Steep, over 7%	0.34	0.37	0.40	0.44	0.47	0.51	0.58
Undeveloped							
Cultivated land							
Flat, 0–2%	0.31	0.34	0.36	0.40	0.43	0.47	0.57
Average, 2–7%	0.35	0.38	0.41	0.44	0.48	0.51	0.60
Steep, over 7%	0.39	0.42	0.44	0.48	0.51	0.54	0.61
Pasture/range							
Flat, 0–2%	0.25	0.28	0.30	0.34	0.37	0.41	0.53
Average, 2–7%	0.33	0.36	0.38	0.42	0.45	0.49	0.58
Steep, over 7%	0.37	0.40	0.42	0.46	0.49	0.53	0.60
Forest/woodlands							
Flat, 0–2%	0.20	0.25	0.28	0.31	0.35	0.39	0.48
Average, 2–7%	0.31	0.34	0.36	0.40	0.43	0.47	0.56
Steep, over 7%	0.35	0.39	0.41	0.45	0.48	0.52	0.58

Note: The values in the table are the standards used by the City of Austin, Texas.

Source: Chow, Maidment, and Mays (1988).

where the flow time is

$$t_f = \sum \frac{L_j}{V_j} \quad (15.2.4)$$

where L_j is the length of the j th pipe along the flow path in ft (m) and V_j is the average flow velocity in the pipe in ft/s (m/s). The inlet time t_0 is the longest time of overland flow of water in a catchment to reach the storm sewer inlet draining the catchment.

In the rational method each sewer is designed individually and independently (except for the computation of sewer flow time) and the corresponding rainfall intensity i is computed repeatedly for the area drained by the sewer. For a given sewer, all the different areas drained by this sewer have the same i . Thus, as the design progresses towards the downstream sewers, the drainage area increases and usually the time of concentration increases accordingly. This increasing t_c in turn gives a decreasing i that should be applied to the entire area drained by the sewer.

Inlet times, or times of concentration for the case of no upstream sewers, can be computed using a number of methods, some of which are presented in Table 15.2.4. The longest time of concentration among the times for the various flow routes in the drainage area is the critical time of concentration used.

Table 15.2.4 Summary of Time of Concentration Formulas

Method and date	Formula for t_c (min)	Remarks
Kirpich (1940)	$t_c = 0.0078L^{0.77}S - 0.385$ $L = \text{length of channel/ditch from headwater to outlet, ft}$ $S = \text{average watershed slope, ft/ft}$	Developed from SCS data for seven rural basins in Tennessee with well-defined channel and steep slopes (3% to 10%); for overland flow on concrete or asphalt surfaces multiply t_c by 0.4; for concrete channels multiply by 0.2; no adjustments for overland flow on bare soil or flow in roadside ditches.
California Culverts Practice (1942)	$t_c = 60(11.9L^3/H)^{0.385}$ $L = \text{length of longest watercourse, mi}$ $H = \text{elevation difference between divide and outlet, ft}$	Essentially the Kirpich formula; developed from small mountainous basins in California (U.S. Bureau of Reclamation, 1973, 1987).
Izzard (1946)	$t_c = \frac{41.025(0.0007i + c)L^{0.33}}{S^{0.333}i^{0.667}}$ $i = \text{rainfall intensity, in/h}$ $c = \text{retardance coefficient}$ $L = \text{length of flow path, ft}$ $S = \text{slope of flow path, ft/ft}$	Developed in laboratory experiments by Bureau of Public Roads for overland flow on roadway and turf surfaces; values of the retardance coefficient range from 0.0070 for very smooth pavement to 0.012 for concrete pavement to 0.06 for dense turf; solution requires iteration; product i times L should be < 500.
Federal Aviation Administration (1970)	$t_c = 1.8(1.1 - C)L^{0.50}/S^{0.333}$ $C = \text{rational method runoff coefficient}$ $L = \text{length of overland flow, ft}$ $S = \text{surface slope, \%}$	Developed from airfield drainage data assembled by the Corps of Engineers; method is intended for use on airfield drainage problems, but has been used frequently for overland flow in urban basins.
Kinematic wave formulas (Morgali and Linsley (1965); Aron and Erborge (1973))	$t_c = \frac{0.94L^{0.6}n^{0.6}}{(i^{0.4}S^{0.3})}$ $L = \text{length of overland flow, ft}$ $n = \text{Manning roughness coefficient}$ $i = \text{rainfall intensity in/h}$ $S = \text{average overland slope ft/ft}$	Overland flow equation developed from kinematic wave analysis of surface runoff from developed surfaces; method requires iteration since both i (rainfall intensity) and t_c are unknown; superposition of intensity-duration-frequency curve gives direct graphical solution for t_c .
SCS lag equation (U.S. Soil Conservation Service (1975))	$t_c = \frac{100L^{0.8}[(1000/CN) - 9]^{0.7}}{1900S^{0.5}}$ $L = \text{hydraulic length of watershed (longest flow path), ft}$ $CN = \text{SCS runoff curve number}$ $S = \text{average watershed slope, \%}$	Equation developed by SCS from agricultural watershed data; it has been adapted to small urban basins under 2000 ac; found generally good where area is completely paved; for mixed areas it tends to overestimate; adjustment factors are applied to correct for channel improvement and impervious area; the equation assumes that $t_c = 1.67 \times \text{basin lag}$.
SCS average velocity charts (U.S. Soil Conservation Service 1975, 1986)	$t_c = \frac{1}{60} \sum \frac{L}{V}$ $L = \text{length of flow path, ft}$ $V = \text{average velocity in feet per second for various surfaces found using Figure 8.8.2}$	Overland flow charts in U.S. Soil Conservation Service (1986) show average velocity as function of watercourse slope and surface cover.

Source: Kibler (1982).

EXAMPLE 15.2.1

The computational procedure in the rational method is illustrated through an example design of sewers to drain a 20-ac area along Goodwin Avenue in Urbana, Illinois, as shown in Figure 15.2.1. The physical characteristics of the drainage basin are given in Table 15.2.5. The catchments are identified by the manholes they drain directly into. The sewer pipes are identified by the number of the upstream manhole of each pipe. The Manning's roughness factor n is 0.014 for all the sewers in the example (adapted from Yen, 1978).

SOLUTION

Table 15.2.6 shows the computations for the design of 12 sewer pipes, namely, all the pipes upstream of sewer 6.1. The rainfall intensity-duration relationship is developed using National Weather Service report HYDRO-35 (see Chapter 7 or Frederick, et al. 1977) and plotted in Figure 15.2.2 for the design return period of two years. The entries in Table 15.2.6 are explained as follows:

Columns (1), (2), and (3): The sewer number and its length and slope are predetermined quantities.

Column (4): Total area drained by a sewer is equal to the sum of the areas of the subcatchments drained by the sewer, e.g., for sewer 3.1, the area 8.45 acres is equal to the area drained by sewer 2.1 (7.30 ac in

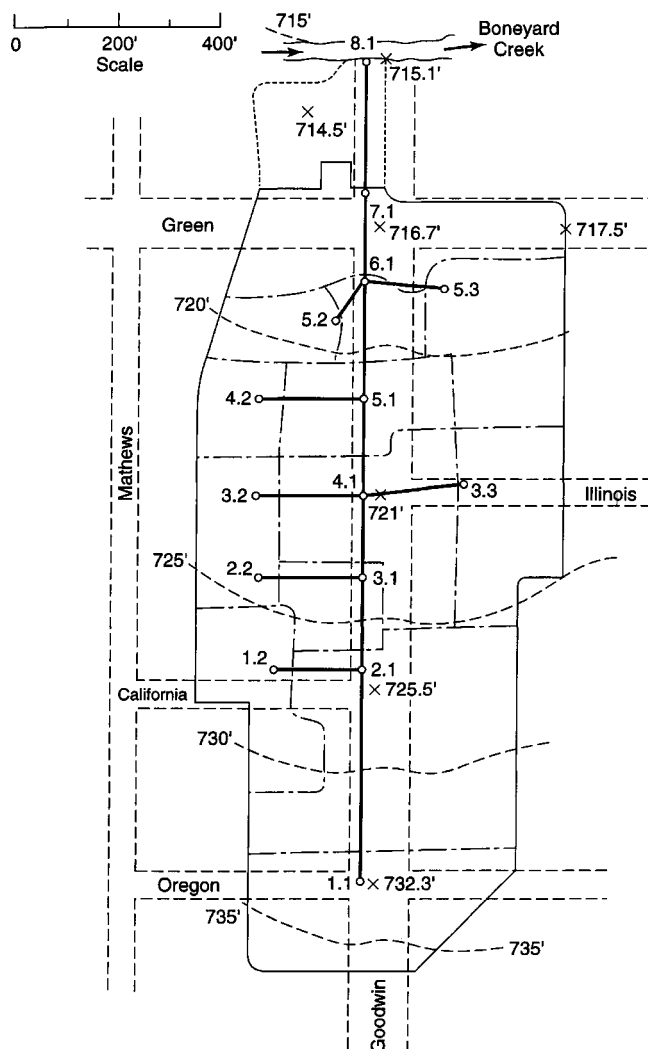


Figure 15.2.1 Goodwin Avenue drainage basin at Urbana, Illinois (from Yen (1978)).

Table 15.2.5 Characteristics of Catchments of Goodwin Avenue Drainage Basin

(1) Catchment	(2) Ground elevation at manhole (ft)	(3) Area A (ac)	(4) Runoff coefficient C	(5) Inlet time t_o (min)
1.1	731.08	2.20	0.65	11.0
1.2	725.48	1.20	0.80	9.2
2.1	724.27	3.90	0.70	13.7
2.2	723.10	0.45	0.80	5.2
3.1	722.48	0.70	0.70	8.7
3.2	723.45	0.60	0.85	5.9
3.3	721.89	1.70	0.65	11.8
4.1	720.86	2.00	0.75	9.5
4.2	719.85	0.65	0.85	6.2
5.1	721.19	1.25	0.70	10.3
5.2	719.10	0.70	0.65	11.8
5.3	722.00	1.70	0.55	17.6
6.1	718.14	0.60	0.75	7.3
7.1	715.39	2.30	0.70	14.5

Source: Yen (1978).

column (4) plus the area drained by sewer 2.2 (0.45 ac) plus the incremental area given in column (6) (0.70 ac for subcatchment 3.1).

Column (5): The identification number of the incremental subcatchments that drain directly through manhole or junction into the sewer being considered.

Column (6): Size of the incremental subcatchment identified in column (5) (Table 15.2.5).

Column (7): Value of runoff coefficient for each subcatchment (Table 15.2.5).

Column (8): Product of C and the corresponding subcatchment area.

Column (9): Summation of CA for all the areas drained by the sewer, which is equal to the sum of contributing values in column (9) and the values in column (8) for that sewer, e.g., for sewer 3.1, $5.97 = 5.12 + 0.36 + (0.49)$.

Column (10): Values of inlet time (Table 15.2.5) for the subcatchment drained (computed using methods in Table 15.2.4), i.e., the overland flow inlet time if the upstream subcatchment is no more than one sewer away from the sewer being designed (e.g., in designing sewer 3.1, 5.2 min for subcatchment 2.2 and 8.7 min for subcatchment 3.1); otherwise it is the total flow time to the entrance of the immediate upstream sewer (e.g., in designing sewer 3.1, 13.7 min for sewer 2.1).

Column (11): The sewer flow time of the immediate upstream sewer as given in column (19).

Column (12): The time of concentration t_c for each of the possible critical flow paths; $t_c =$ inlet time (column (10) + sewer flow time (column (11)) for each flow path.

Column (13): The rainfall duration t_d is assumed equal to the longest of the different times of concentration of different flow paths to arrive at the entrance of the sewer being considered; e.g., for sewer 3.1, t_d is equal to 14.1 min for sewer 2.1, which is longer than from sewer 2.2 (6.2 min) or directly from subcatchment 3.1 (8.7 min).

Column (14): The rainfall intensity i for the duration given in column (13) is based on HYDRO-35 for the two-year design return period (see Figure 15.2.2).

Column (15): Design discharge is computed by using equation (15.2.2), i.e., the product of columns (9) and (14).

Table 15.2.6 Design of Sewers by the Rational Method

(1)	(2)	(3)	(4)	(5)	(6)	(7)	(8)	(9)	(10)	(11)	(12)	(13)	(14)	(15)	(16)	(17)	(18)	(19)
Sewer	Length <i>L</i>	Slope <i>S</i> (ft)	Total area drained (ac)	Increment					Inlet time (min)	Upstream sewer flow time (min)	<i>t_c</i> (min)	<i>t_d</i> (min)	<i>i</i> (in/hr)	Design discharge <i>Q_p</i> (cfs)	Computed diameter <i>D_r</i> (ft)	Pipe size used <i>D_n</i> (ft)	Flow velocity (fps)	Sewer flow time (min)
				Catchment	Area (ac)	<i>C</i>	<i>CA</i>	ΣCA										
1.1	390	0.0200	2.20	1.1	2.20	0.65	1.43	1.43	11.0	–	11.0	11.0	4.00	5.72	1.08	1.25	4.6	1.42
1.2	183	0.0041	1.20	1.2	1.20	0.80	0.96	0.96	9.2	–	9.2	9.2	4.30	4.13	1.28	1.50	2.3	1.31
2.1	177	0.0245		2.1	3.90	0.70	2.73		13.7	–	13.7							
				1.1					11.0		12.4							
				1.2					9.2		10.5							
			7.30					5.12				13.7	3.68	18.8	1.62	1.75	7.8	0.38
2.2	200	0.0180	0.45	2.2	0.45	0.80	0.36	0.36	5.2	–	5.2	5.2	5.30	1.91	0.73	0.83	3.5	0.95
3.1	156	0.0104		3.1	0.70	0.70	0.49		8.7	–	8.7							
									13.7		14.1							
				2.2					5.2		6.2							
			8.45					5.97				14.1	3.63	21.6	2.00	2.00	6.9	0.39
3.2	210	0.0175	0.60	3.2	0.60	0.85	0.51	0.51	5.9	–	5.9	5.9	5.07	2.59	0.82	0.83	4.7	0.74
3.3	130	0.0300	1.70	3.3	1.70	0.65	1.11	1.11	11.8	–	11.8	11.8	3.90	4.32	0.90	1.00	5.5	0.39
4.1	181	0.0041		4.1	2.00	0.75	1.50		9.5	–	9.5							
									14.1		14.5							
				3.3					11.8		12.2							
			12.75					9.09				14.5	3.60	32.7	2.79	3.00	4.6	0.65
4.2	200	0.0026	0.65	4.2	0.65	0.85	0.55	0.55	6.2	–	6.2	6.2	4.98	2.75	1.20	1.25	2.2	1.49
5.1	230	0.0028		5.1	1.25	0.70	0.88		10.3	–	10.3							
									14.5		15.2							
			14.65					10.52				15.2	3.50	36.8	3.13	3.50	3.8	1.00
5.2	70	0.0250	0.70	5.2	0.70	0.65	0.46	0.46	11.8	–	11.8	11.8	3.90	1.79	0.67	0.67	5.1	0.23
5.3	130	0.0060	1.70	5.3	1.70	0.55	0.94	0.94	17.6	–	17.6	17.6	3.30	3.10	1.07	1.25	2.5	0.86

Source: Yen (1978).

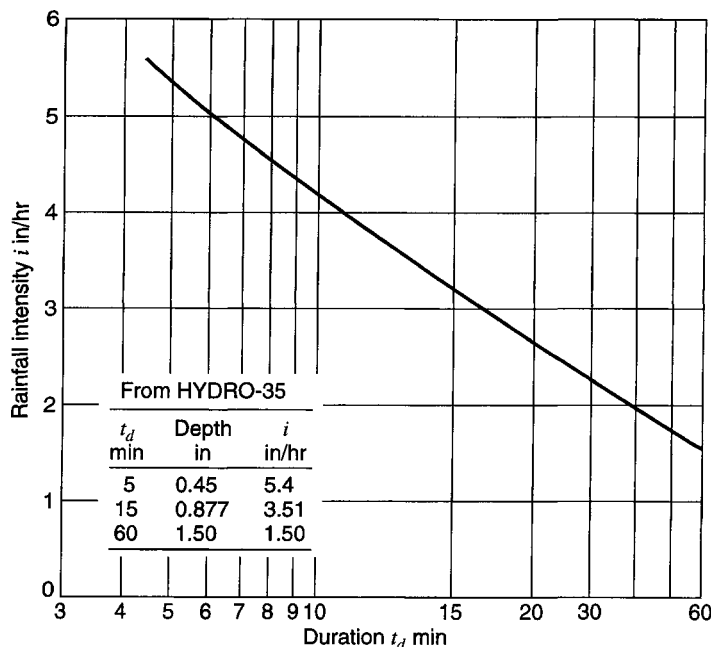


Figure 15.2.2 Variation of rainfall intensity with duration at Urbana, Illinois (from Yen (1978)).

Column (16): Required sewer diameter in feet, as computed using Manning’s formula (equation (15.2.7)); with $n = 0.014$, Q is given in column 15 and S_0 in column 3.

Column (17): The nearest commercial nominal pipe size that is not smaller than the computed size is adopted.

Column (18): Flow velocity computed by using $V = 4Q_p / (\pi D^2)$, i.e., column (15) multiplied by $4/\pi$ and divided by the square of column (17).

Column (19): Sewer flow time is computed as equal to L/V , i.e., column (2) divided by column (18) and converted into minutes.

This example demonstrates that in the rational method each sewer is designed individually and independently (except for the computation of sewer flow time) and the corresponding rainfall intensity i is computed repeatedly for the area drained by the sewer. For a given sewer, all the different areas drained by this sewer have the same i . Thus, as the design progresses towards downstream sewers, the drainage area increases and usually the time of concentration increases accordingly. This increasing t_c in turn gives a decreasing i , which should be applied to the entire area drained by the sewer. Failure to realize this variation of i is the most common mistake made in using the rational method for sewer design.

The size of a particular pipe is based upon computing the smallest available commercial pipe that can handle the peak flow rate determined using the rational formula (15.2.2). Manning’s equation (equation (5.1.23) or (5.1.25)) has been popular in the United States for sizing pipes:

$$Q = \frac{m}{n} S_f^{1/2} A R^{2/3} \tag{15.2.5}$$

where m is 1.486 for U.S. customary units (1 for SI units), S_f is the friction slope, A is the inside cross-sectional area of the pipe $\pi D^2/4$ in ft^2 (m^2), R is the hydraulic radius, $R = A/P = D/4$ in ft (m), P is the wetted perimeter (πD) in ft (m), and K is the inside pipe diameter in ft (m). By substituting in the bed slope S_0 for the friction slope (assuming uniform flow) and $A = \pi D^2/4$ and $R = D/4$ (assuming that the pipe is

flowing full under gravity, not pressurized), Manning's equation becomes

$$Q = \frac{m}{n} S_0 \left(\frac{\pi D^2}{4} \right) \left(\frac{D}{4} \right)^{2/3} = m \left(\frac{0.311}{n} \right) S_0^{1/2} D^{8/3} \quad (15.2.6)$$

Equation (15.2.6) can be solved for the diameter

$$D = \left(\frac{m_D Q n}{\sqrt{S_0}} \right)^{3/8} \quad (15.2.7)$$

where m_D is 2.16 for U.S. customary units (3.21 for SI units). Q is determined using the rational formula, and D is rounded up to the next commercial size pipe. The Darcy–Weisbach equation (4.3.13) can also be used to size pipes,

$$Q = A \left(\frac{8g}{f} R S_f \right)^{1/2} \quad (15.2.8a)$$

Equation (15.2.8a) can be solved for D using $S_f = S_0$ as

$$D = \left(\frac{0.811 f Q^2}{g S_0} \right)^{1/5} \quad (15.2.8b)$$

which is valid for any dimensionally consistent set of units.

15.2.3 Hydraulic Analysis of Designs

To analyze the hydraulic effectiveness of storm sewer design, it is necessary to analyze the hydraulic gradient. The hydraulic gradient can be used to determine if design flows can be accommodated without causing flooding at various locations or causing flows to exit the system at locations where this is not acceptable. Such analysis can be done manually or by computer. This section first discusses the form losses, then the hydraulic gradient calculations, and finally hydrograph routing.

15.2.3.1 Form Losses

During the propagation of flows through storm sewers, both open-channel flow and pressurized pipe flow can occur, depending upon the magnitude of the flows. Consequently the form loss equations for both types of flow are presented here.

Transition Losses (open-channel flow)

Contraction losses for open-channel flow are expressed as

$$H_c = 0.1 \left(\frac{V_2^2}{2g} - \frac{V_1^2}{2g} \right) \text{ for } V_2 > V_1 \quad (15.2.9)$$

where V_1 is the upstream velocity and V_2 is the downstream velocity. Expansion losses are expressed as

$$H_e = 0.2 \left(\frac{V_1^2}{2g} - \frac{V_2^2}{2g} \right) \text{ for } V_1 > V_2 \quad (15.2.10)$$

Simple size transitions through manholes with straight-through flow can be analyzed with the above two equations.

Transition losses (pressurized flow)

Contraction losses for pressurized flow are expressed as

$$H_c = K \left(\frac{V_2^2}{2g} \right) \left[1 - \frac{A_2}{A_1} \right]^2 \tag{15.2.11}$$

where $K = 0.5$ for a sudden contraction, $K = 0.1$ for a well-designed transition, A_1 is the cross-sectional area of flow at the beginning of the transition, and A_2 is the cross-sectional area of flow at the end of the transition. Expansion losses for pressurized flow are expressed as

$$H_e = K \left[\frac{(V_1 - V_2)^2}{2g} \right] \tag{15.2.12}$$

where $K = 1.0$ for a sudden expansion and $K = 0.2$ for a well-designed transition. These K values for the contractions and expansions are for approximation. For detailed analysis, Tables 15.2.7–15.2.10

Table 15.2.7 Values of K_2 for Determining Loss of Head Due to Sudden Enlargement in Pipes, from the Formula $H_2 = K_2(V_1^2/2g)$

$\frac{D_2}{D_1}$	Velocity V_1 (ft/s)												
	2	3	4	5	6	7	8	10	12	15	20	30	40
1.2	.11	.10	.10	.10	.10	.10	.10	.09	.09	.09	.09	.09	.08
1.4	.26	.26	.25	.24	.24	.24	.24	.23	.23	.22	.22	.21	.20
1.6	.40	.39	.38	.37	.37	.36	.36	.35	.35	.34	.33	.32	.32
1.8	.51	.49	.48	.47	.47	.46	.46	.45	.44	.43	.42	.41	.40
2.0	.60	.58	.56	.55	.55	.54	.53	.52	.52	.51	.50	.48	.47
2.5	.74	.72	.70	.69	.68	.67	.66	.65	.64	.63	.62	.60	.58
3.0	.83	.80	.78	.77	.76	.75	.74	.73	.72	.70	.69	.67	.65
4.0	.92	.89	.87	.85	.84	.83	.82	.80	.79	.78	.76	.74	.72
5.0	.96	.93	.91	.89	.88	.87	.86	.84	.83	.82	.80	.77	.75
10.0	1.00	.99	.96	.95	.93	.92	.91	.89	.88	.86	.84	.82	.80
∞	1.00	1.00	.98	.96	.95	.94	.93	.91	.90	.88	.86	.83	.81

D_2/D_1 = ratio of larger pipe to smaller pipe; V_1 = velocity in smaller pipe.

Source: American Iron and Steel Institute (1995).

Table 15.2.8 Values of K_2 for Determining Loss of Head Due to Gradual Enlargement in Pipes from the Formula $H_2 = K_2(V_1^2/2g)$

$\frac{D_2}{D_1}$	Angle of cone														
	2°	4°	6°	8°	10°	15°	20°	25°	30°	35°	40°	45°	50°	60°	
1.1	.01	.01	.01	.02	.03	.05	.10	.13	.16	.18	.19	.20	.21	.23	
1.2	.02	.02	.02	.03	.04	.09	.16	.21	.25	.29	.31	.33	.35	.37	
1.4	.02	.03	.03	.04	.06	.12	.23	.30	.36	.41	.44	.47	.50	.53	
1.6	.03	.03	.04	.05	.07	.14	.26	.35	.42	.47	.51	.54	.57	.61	
1.8	.03	.04	.04	.05	.07	.15	.28	.37	.44	.50	.54	.58	.61	.65	
2.0	.03	.04	.04	.05	.07	.16	.29	.38	.46	.52	.56	.60	.63	.68	
2.5	.03	.04	.04	.05	.08	.16	.30	.39	.48	.54	.58	.62	.65	.70	
3.0	.03	.04	.04	.05	.08	.16	.31	.40	.48	.55	.59	.63	.66	.71	
∞	.03	.04	.05	.06	.08	.16	.31	.40	.49	.56	.60	.64	.67	.72	

D_2/D_1 = ratio of diameter of larger pipe to diameter of smaller pipe. Angle of cone is twice the angle between the axis of the cone and its side.

Source: American Iron and Steel Institute (1995).

Table 15.2.9 Values of K_3 for Determining Loss of Head Due to Sudden Contraction from the Formula $H_2 = K_2(V_1^2/2g)$

$\frac{D_2}{D_1}$	Velocity V_2 (ft/s)												
	2	3	4	5	6	7	8	10	12	15	20	30	40
1.1	.03	.04	.04	.04	.04	.04	.04	.04	.04	.04	.05	.05	.06
1.2	.07	.07	.07	.07	.07	.07	.07	.08	.08	.08	.09	.10	.11
1.4	.17	.17	.17	.17	.17	.17	.17	.18	.18	.18	.18	.19	.20
1.6	.26	.26	.26	.26	.26	.26	.26	.26	.26	.25	.25	.25	.24
1.8	.34	.34	.34	.34	.34	.34	.33	.33	.32	.32	.31	.29	.27
2.0	.38	.38	.37	.37	.37	.37	.36	.36	.35	.34	.33	.31	.29
2.2	.40	.40	.40	.39	.39	.39	.39	.38	.37	.37	.35	.33	.30
2.5	.42	.42	.42	.41	.41	.41	.40	.40	.39	.38	.37	.34	.31
3.0	.44	.44	.44	.43	.43	.43	.42	.42	.41	.40	.39	.36	.33
4.0	.47	.46	.46	.46	.45	.45	.45	.44	.43	.42	.41	.37	.34
5.0	.48	.48	.47	.47	.47	.46	.46	.45	.45	.44	.42	.38	.35
10.0	.49	.48	.48	.48	.48	.47	.47	.46	.46	.45	.43	.40	.36
∞	.49	.49	.48	.48	.48	.47	.47	.47	.46	.45	.44	.41	.38

D_2/D_1 = ratio of larger pipe to smaller diameter; V_2 = velocity in smaller pipe.

Source: American Iron and Steel Institute (1995).

Table 15.2.10 Entrance Loss Coefficients for Corrugated Steel Pipe or Pipe-Arch

Inlet end of culvert	Coefficient K_2
Projecting from fill (no headwall)	0.9
Headwall, or headwall and wingwalls square-edge	0.5
Mitered (beveled) to conform to fill slope	0.7
End-section conforming to fill slope	0.5
Headwall, rounded edge	0.2
Beveled ring	0.25

Source: American Iron and Steel Institute (1995).

can be used in conjunction with the following form of the headloss equation:

$$H = K \left(\frac{V^2}{2g} \right) \quad (15.2.13)$$

Exit losses can be computed with the following equation:

$$H_{\text{ext}} = K_e \left(\frac{V^2}{2g} \right) \quad (15.2.14)$$

Manhole losses

In many cases manhole losses can comprise a significant percentage of the overall losses in a storm sewer system. The losses that occur at storm sewer junctions are dependent upon the flow characteristics, junction geometry, and relative sewer diameters. For a *straight-through manhole* with no change in pipe sizes, the losses can be expressed as

$$H_m = 0.05 \frac{V^2}{2g} \quad (15.2.15)$$

Losses at *terminal manholes* can be estimated using

$$H_m = \frac{V^2}{2g} \quad (15.2.16)$$

For *junction manholes* with one or more incoming laterals, the total manhole loss (pressure change) can be estimated using the following equation form:

$$H_m = K \frac{V^2}{2g} \quad (15.2.17)$$

where Figure 15.2.3 shows manhole junction types and nomenclature. Values of K for various types of manhole configurations can be found in Figures 15.2.4–15.2.8.

Bend losses

Bend losses in storm sewers can be estimated using

$$H_b = K_b \frac{V^2}{2g} \quad (15.2.18)$$

where

$$K_b = 0.25 \sqrt{\frac{\Phi}{90}} \quad (15.2.19)$$

for curved sewer segments where the angle of deflection Φ is less than 40° . For greater angles of deflection and for bends in manholes, the loss coefficient can be obtained from Figure 15.2.9.

EXAMPLE 15.2.2

Approximate the sudden expansion loss for a 400-mm sewer pipe connecting to a 450-mm sewer pipe for a design discharge of $0.3 \text{ m}^3/\text{s}$ assuming full-pipe flow.

SOLUTION

First compute the velocity of flow in each sewer pipe:

$$V_1 = \frac{Q}{A_1} = \frac{0.3 \text{ m}^3/\text{s}}{\left[\pi(400/1000)^2\right]/4} = 2.39 \text{ m/s}$$

$$V_2 = \frac{Q}{A_2} = \frac{0.3 \text{ m}^3/\text{s}}{\left[\pi(450/1000)^2\right]/4} = 1.89 \text{ m/s}$$

The expansion loss is then determined using equation (15.2.12) with $K = 1.0$:

$$H_e = (1) \left[\frac{(2.39 - 1.89)^2}{2(9.81)} \right] = 0.0127 \text{ m}$$

EXAMPLE 15.2.3

Compute the bend loss for a 30° bend in a 400-mm sewer pipe with a discharge of $0.3 \text{ m}^3/\text{s}$ assuming full-pipe flow.

SOLUTION

First compute the flow velocity in the sewer pipe:

$$V = \frac{Q}{A} = \frac{0.3}{\left[\pi(400/1000)^2\right]/4} = 2.39 \text{ m/s}$$

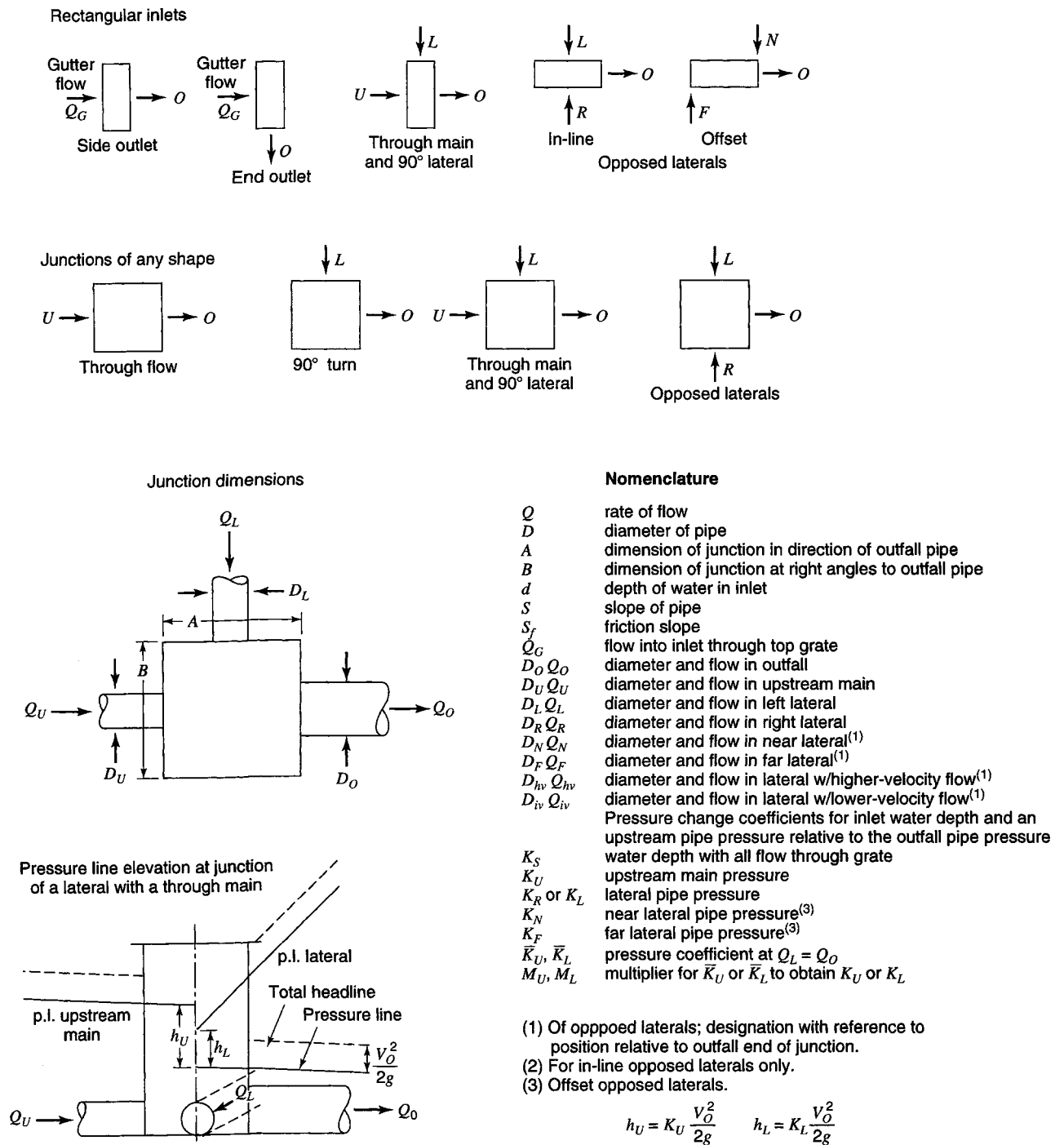
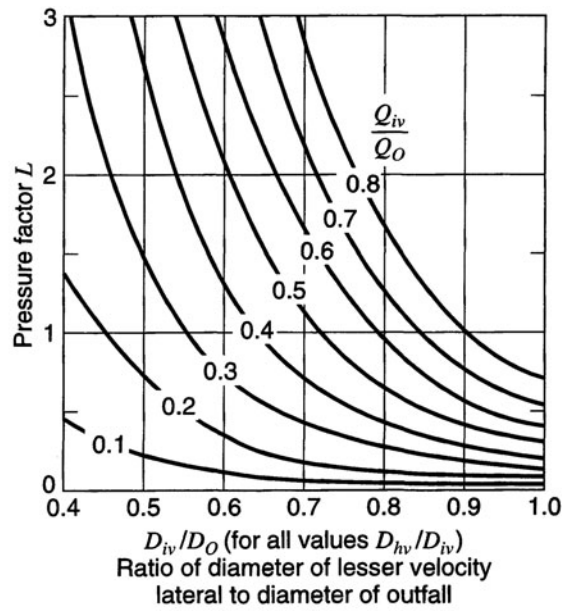
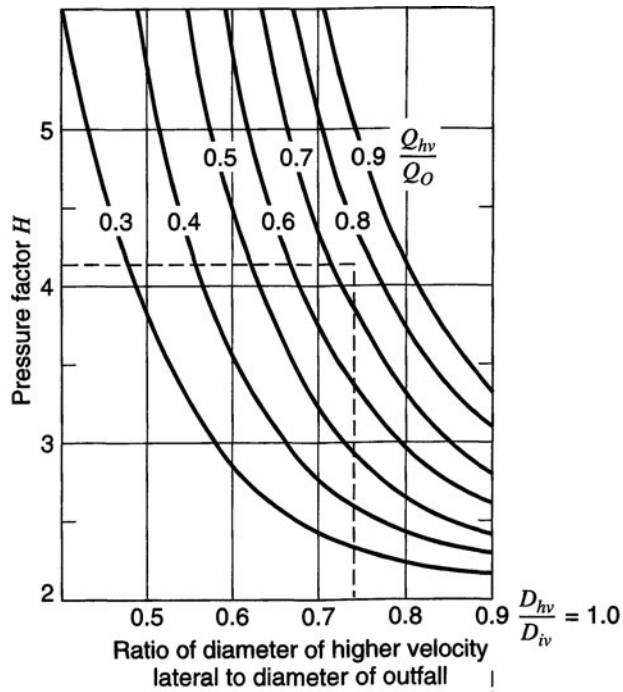


Figure 15.2.3 Manhole junction types and nomenclature (from Sangster et al. (1958)).



To find K_R or K_L for the right or left lateral pipe with flow at a lesser velocity than the other lateral, read H for the higher velocity lateral D and Q , then read L for the lower velocity lateral D and Q ; then:

$$K_R \text{ (or } K_L) = H - L$$

K_R or K_L for the lateral pipe with higher velocity flow is always 1.8

$$h_L = K_L \frac{V_o^2}{2g} \quad h_R = K_R \frac{V_o^2}{2g}$$

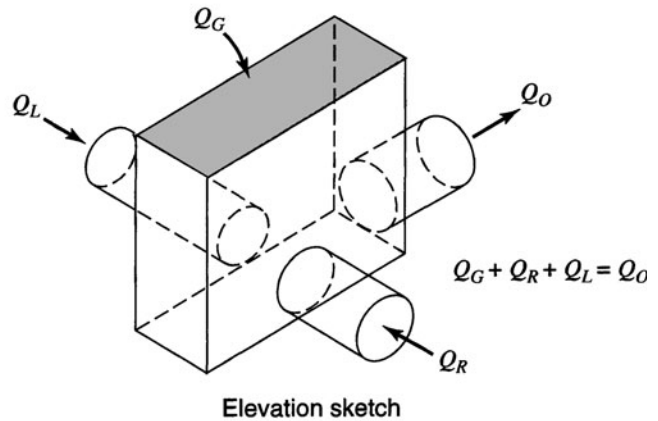
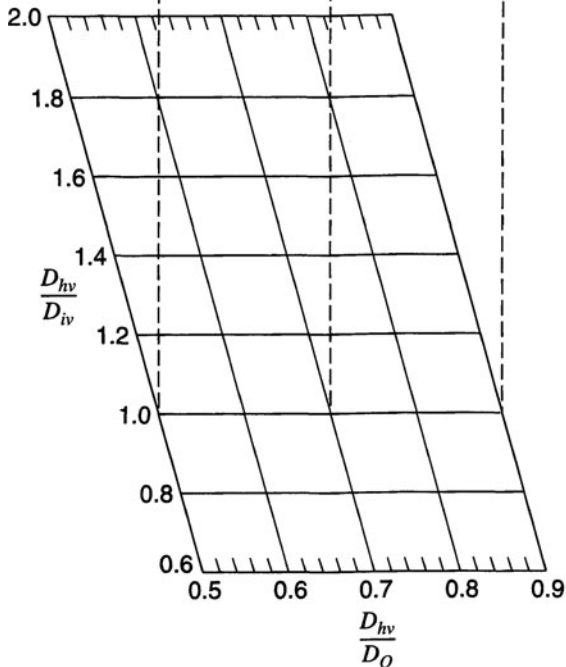


Figure 15.2.4 Rectangular manhole with in-line opposed lateral pipes each at 90° to outfall (with or without grate flow) (from Sangster et al. (1958)).

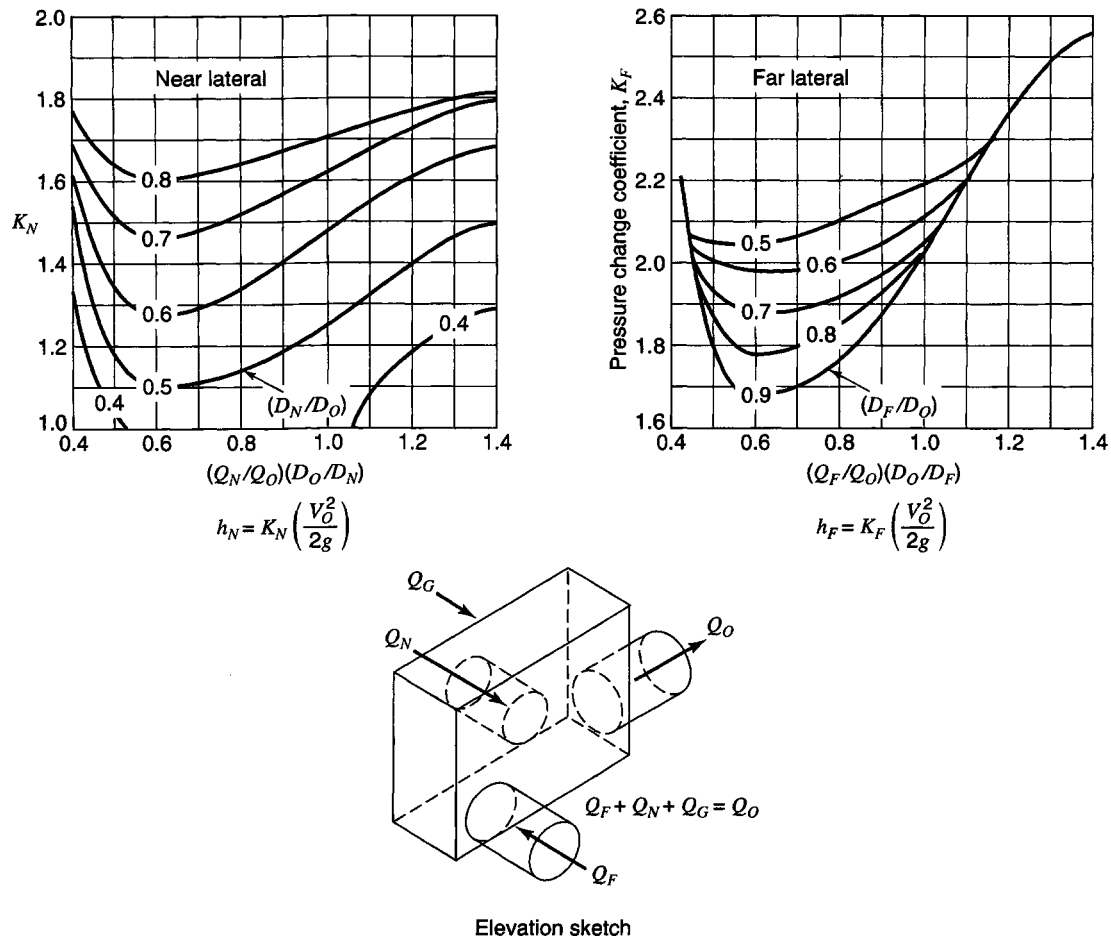


Figure 15.2.5 Rectangular manhole with offset opposed lateral pipes—each at 90° to outfall (with or without inlet flow) (from Sangster et al. (1958)).

Next compute the bend loss coefficient using equation (15.2.19):

$$K_b = 0.25 \sqrt{\frac{\Phi}{90}} = 0.25 \sqrt{\frac{30}{90}} = 0.144$$

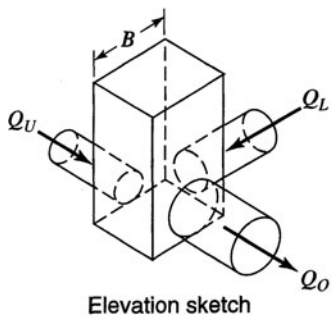
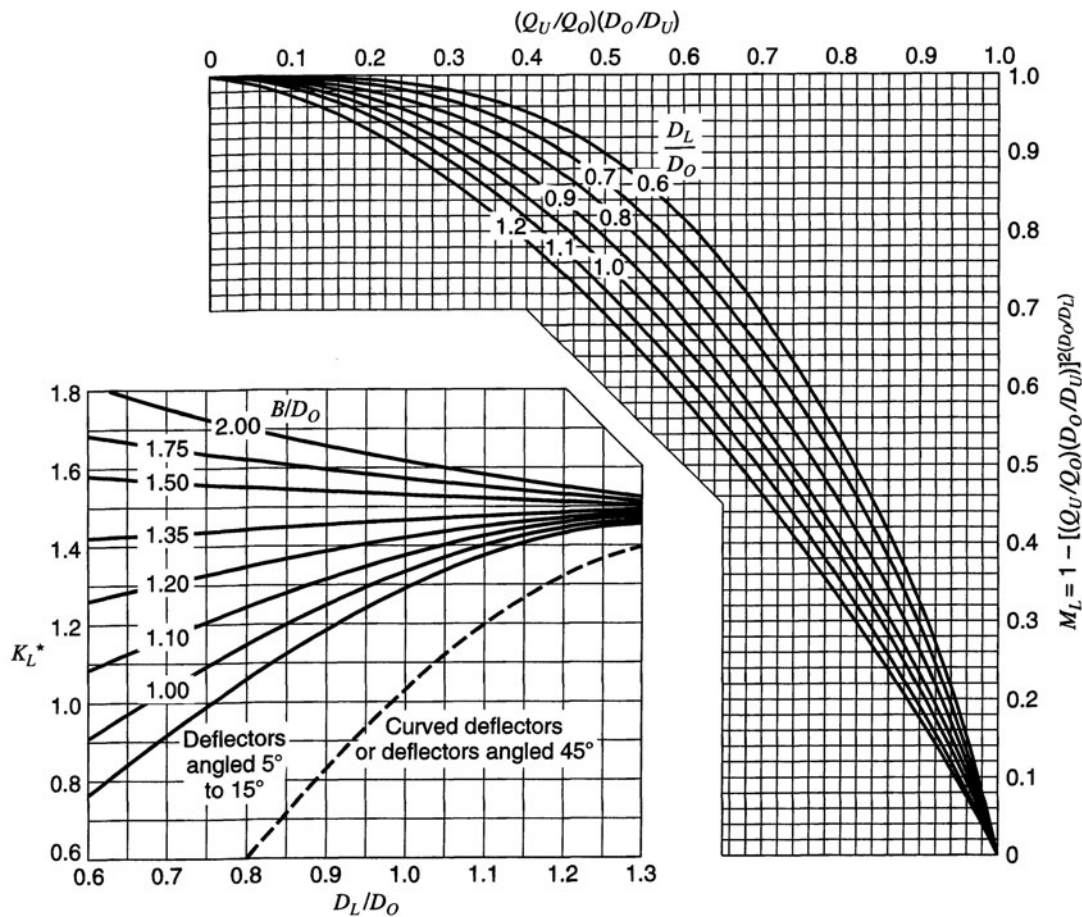
Use equation (15.2.18) to compute the bend loss:

$$H_b = K_b \frac{V^2}{2g} = 0.144 \frac{(2.39)^2}{2(9.81)} = 0.0419 \text{ m}$$

EXAMPLE 15.2.4

The hypothetical storm sewer layout shown in Figure 15.2.10 includes an existing portion and an extension of the existing system. The objective for this example is to analyze the hydraulics of manhole number 4 (MH-4). Refer to Figure 15.2.11 for details of the manhole. We have

Top of manhole elevation	476.00 ft
Bottom of manhole elevation	470.15 ft
Manhole diameter	48.0 in



To find K_L for the lateral pipe, first read \bar{K}_L^* from the lower graph. Next determine M_L . Then

$$K_L = \bar{K}_L^* \times M_L$$

Dashed curve for curved or 45° angled deflectors applies only to manholes without upstream in-line pipe.

Use this chart for round manholes also.

For rounded entrance to outfall pipe, reduce chart values of K_L^* by 0.2 for combining flow.

For $(Q_U/Q_O)^* \times (D_O/D_U) > 1$ use

$$h_L = K_L \frac{V_O^2}{2g} \text{ from Figure 15.2.8}$$

For $D_L = D_O < 0.6$ use

$$h_L = K_L \frac{V_O^2}{2g} \text{ from Figure 15.2.8}$$

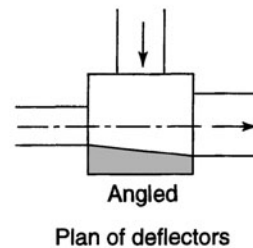
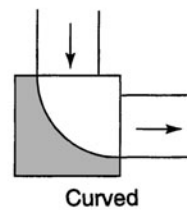
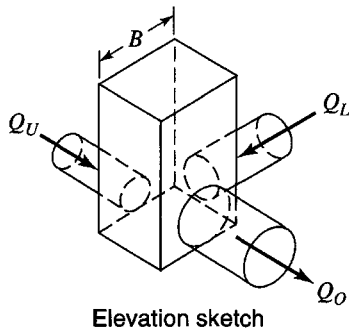
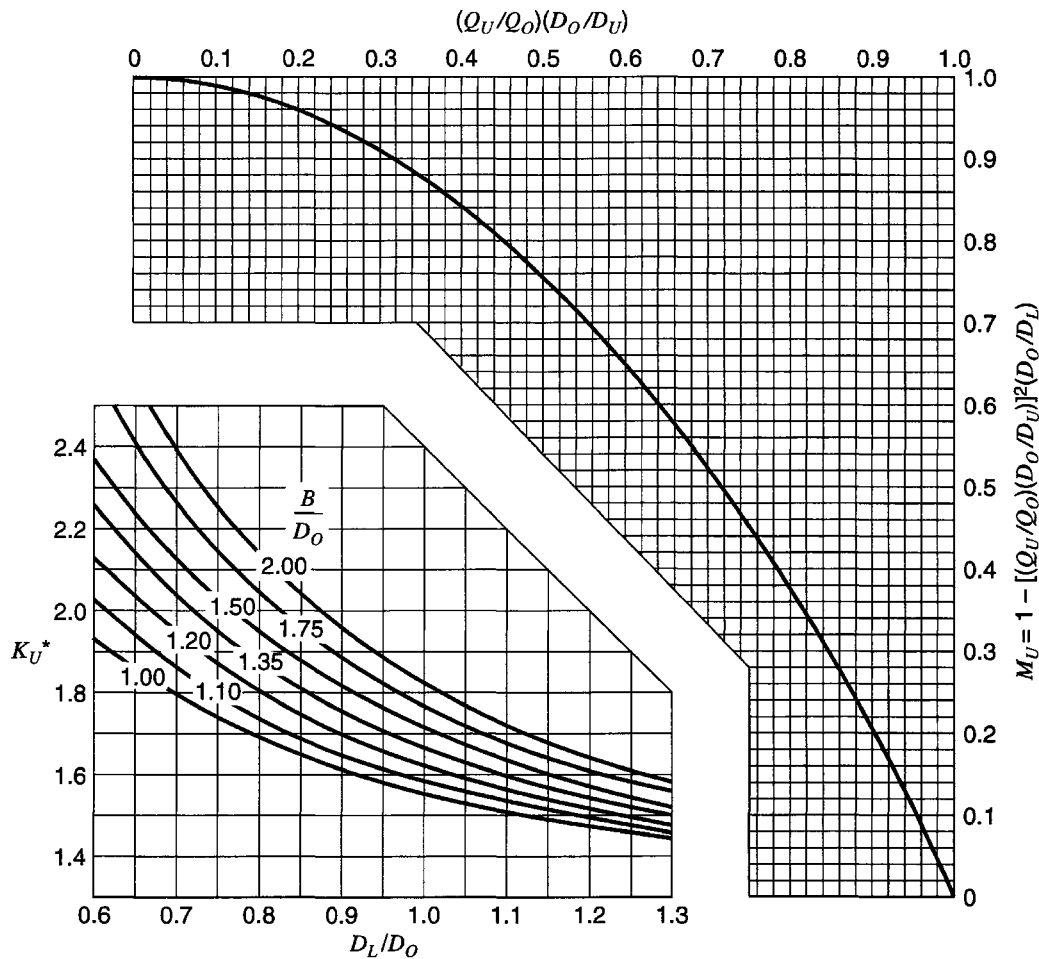


Figure 15.2.6 Manhole at 90° deflection or on through pipeline at junction of 90° lateral pipe (lateral coefficient) (from Sangster et al. (1958)).



To find K_U for the upstream main, read K_U^* from the lower graph. Next determine M_U .
Then

$$K_U = K_U^* \times M_U$$

For manholes with deflectors at 0° to 15° , read K_U^* on curve for $B/D_O = 1.0$.

Use this chart for round manholes also.

For rounded entrance to outfall pipe, reduce chart values of K_U^* by 0.2 for combining flow.

For deflectors refer to sketches on $(Q_U/Q_O) \times (D_O/D_U) > 1$ use

$$h_U = K_U \frac{V_O^2}{2g} \text{ from Figure 15.2.8}$$

For $D_L/D_O < 0.6$ use

$$h_U = K_U \frac{V_O^2}{2g} \text{ from Figure 15.2.8}$$

Figure 15.2.7 Manhole on through pipeline at junction of a 90° lateral pipe (in-line pipe coefficient) (from Sangster et al. (1958)).

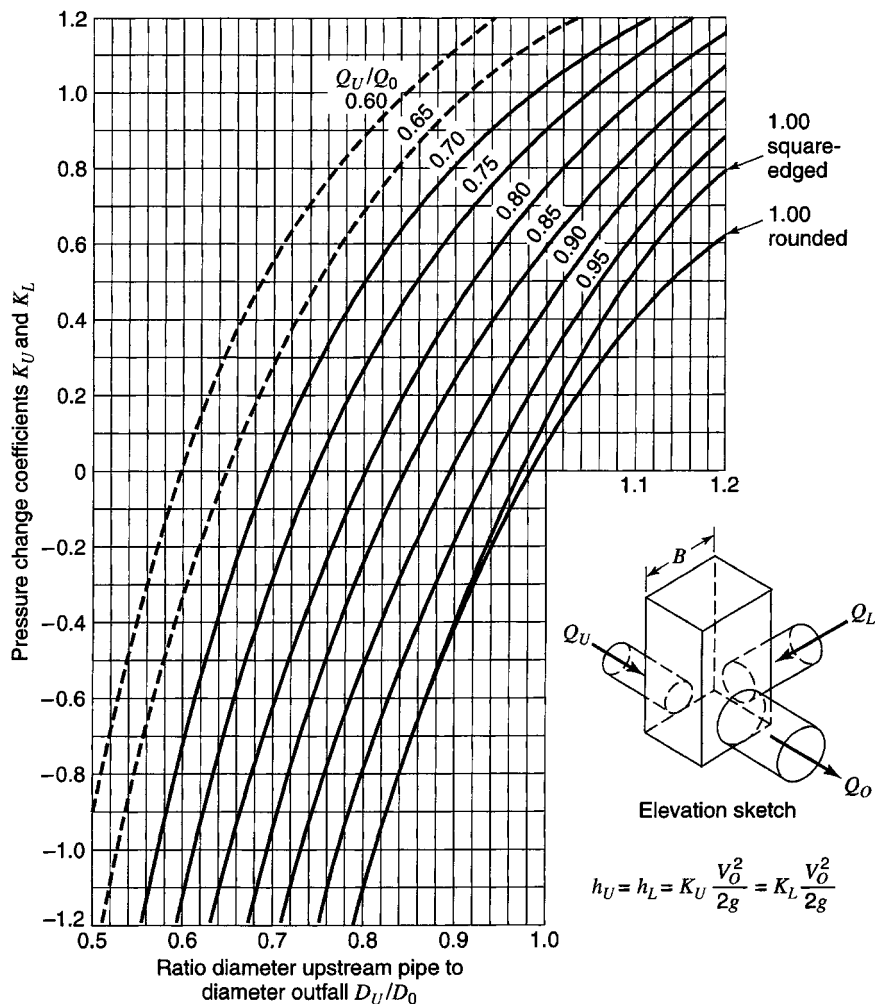


Figure 15.2.8 Manhole on through pipeline at junction of a 90° lateral pipe (for conditions outside the range of Figures 15.2.6 and 15.2.7 (from Sangster et al. (1958)).

Lateral flow, Q_L	25.0 cfs
Upstream in-line flow, Q_u	46.0 cfs
Outfall flow, Q_0	71.0 cfs
Diameter of lateral line, D_L	30.0 in
Diameter of upstream in-line, D_u	42.0 in
Diameter of outfall line, D_0	48.0 in
Elevation of outfall pipe pressure line at MH – 4	475.08 ft

SOLUTION

1. The outfall pressure line elevation at the manhole is given as 475.08 ft.
2. The velocity head at the outfall is

$$\frac{V_0^2}{2g} = \frac{1}{2g} \left(\frac{Q}{A} \right)^2 = \frac{1}{2g} \left(\frac{71}{\pi 4^2 / 4} \right) = 0.50 \text{ ft (Note: } D = 48 \text{ in} = 4 \text{ ft)}$$

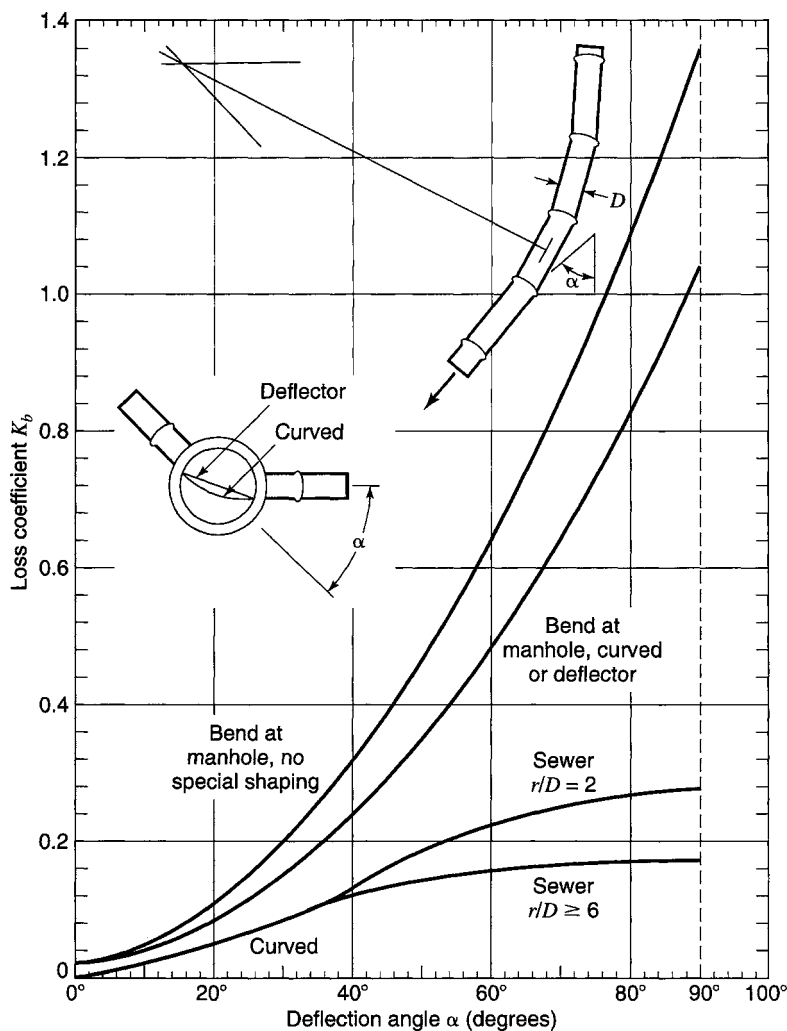


Figure 15.2.9 Sewer bend loss coefficient (from Sangster et al. (1958)).

3. Compute the ratios

$$\frac{Q_u}{Q_o} = \frac{46}{71} = 0.65, \quad \frac{D_u}{D_o} = \frac{42}{48} = 0.88, \quad \frac{D_L}{D_o} = \frac{30}{48} = 0.63$$

4. Compute $B/D_o = 48/48 = 1.0$ (where B is the manhole diameter).

5. $\left(\frac{Q_u}{Q_o}\right) \times \left(\frac{D_o}{D_u}\right) = 0.65 \times \frac{1}{0.88} = 0.74$

Consider the lateral pipe:

6. Using Figure 15.2.6, $K_L^* = 0.95$ for $D_L/D_o = 0.63$ and $B/D_o = 1.0$. For a round-edged manhole $K_L^* = K_L^* - 0.2 = 0.95 - 0.20 = 0.75$, where 0.2 is obtained from the table of reductions for K_L^* for manholes with a rounded entrance (see Table 15.2.11). When $V_o^2/2g < 1.0$ it is usually not economical to use a rounded entrance from the manhole to the outlet pipe; therefore, keep $K_L^* = 0.95$ for a square-edged entrance.
7. Determine M_L using $(Q_u/Q_o) \times (D_u/D_o) = 0.74$; $M_L = 0.61$ from Figure 15.2.6.

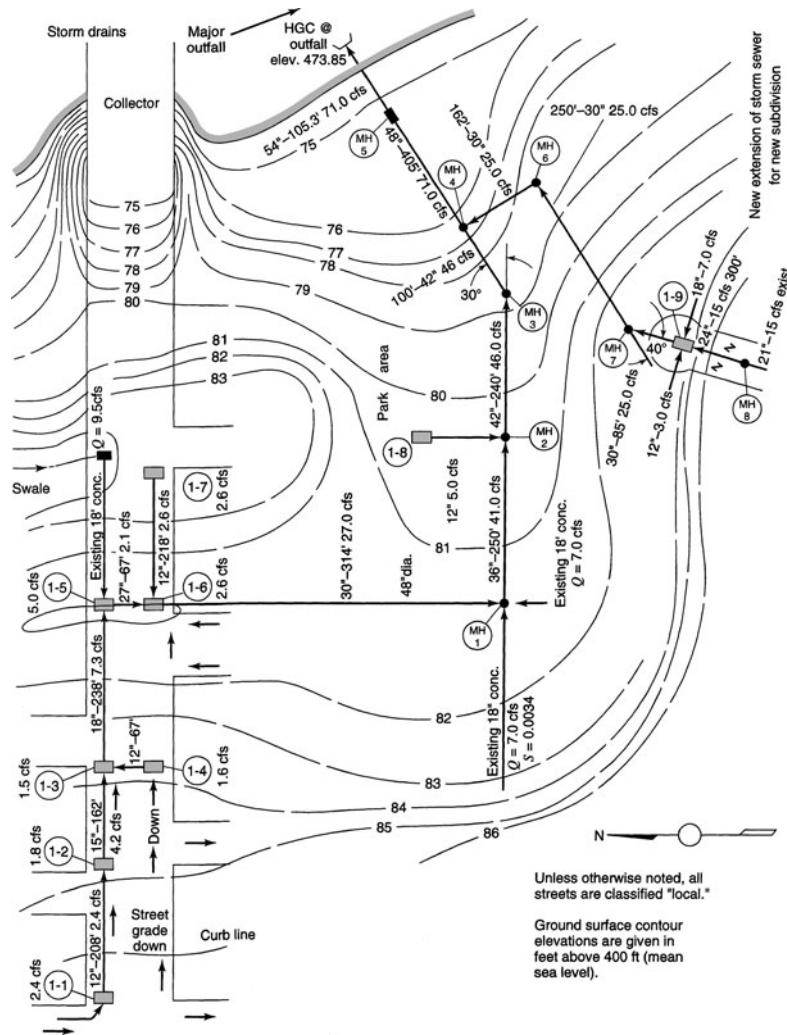
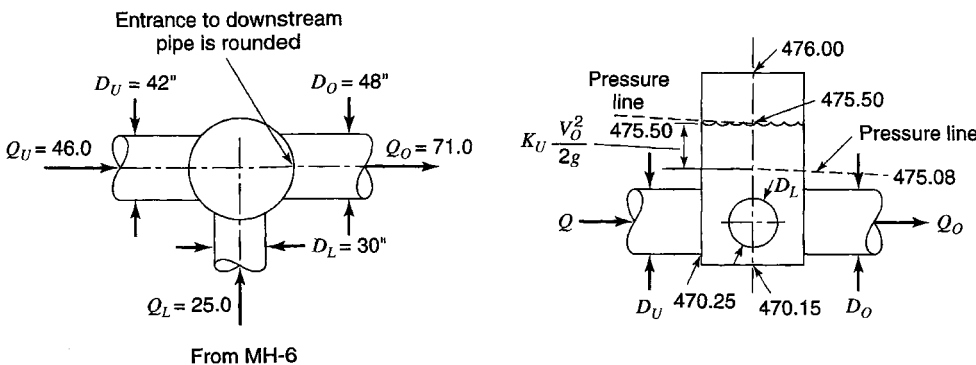


Figure 15.2.10 Storm drain design example (from Flood Control District of Maricopa County, 1992a).



From MH-6

Figure 15.2.11 Storm drain design example for manhole no. 4 (from Flood Control District of Maricopa County, 1992b).

Table 15.2.11 Reductions for K_L^* for a Manhole with Rounded Entrance Reductions for K_L

B/D_0	D_L/D_0			
	0.6	0.8	1.0	1.2
1.75	0.4	0.3	0.2	0.0
1.33	0.3	0.2	0.1	0.0
1.10	0.2	0.1	0.0	0.0

Source: Flood Control District of Maricopa County (1992b).

8. $K_L = M_L \times K_L^* = 0.61 \times 0.95 = 0.58$ (for square-edged entrance).
9. Lateral pipe pressure change = $K_L (V_0^2/2g) = 0.58 \times 0.50 = 0.29$ ft.
10. Lateral pipe pressure = $475.08 + 0.29 = 475.37$ ft.

Now consider the upstream in-line pipe:

11. From Figure 15.2.7, $K_u^* = 1.86$.
12. Because the velocity head is less than 1.0 ft/s, a rounded entrance to the outfall pipe will not be appropriate and a square-edged entrance will be used.
13. From Figure 15.2.7, $M_u = 0.45$.
14. $K_u = M_u \times K_u^* = 0.45 \times 1.86 = 0.84$.
15. $h_u = K_u \times (V_0^2/2g) = 0.84 \times 0.50 = 0.42$.
16. The in-line upstream pressure elevation is $475.08 + 0.42 = 475.50$, which is also the water surface elevation, as shown in Figure 15.2.11.

15.2.3.2 Hydraulic Gradient Calculations

Any storm sewer design must be analyzed to determine if the design flows can be accommodated without causing flows to exit the system and creating flooding conditions. Figure 15.2.12 illustrates the difference between an improper design and a proper design. Note the energy and hydraulic grade lines for the improper design as opposed to the proper design.

If the hydraulic grade line is above the pipe crown at the next upstream manhole, pressure flow calculations are indicated; if it is below the pipe crown, then open-channel flow calculations should be used at the upstream manhole. The process is repeated throughout the storm drain system. If all HGL elevations are acceptable, then the hydraulic design is adequate. If the HGL exceeds an inlet elevation, then adjustments to the trial design must be made to lower the water surface elevation. Computer programs such as HYDRA (FHWA, 1993) are recommended for the design of storm drains and include a hydraulic grade-line analysis and a pressure flow simulation.

15.2.3.3 Hydrograph Routing for Design

Hydrograph design methods consider design hydrographs as input to the upstream end of sewers and use some form of routing to propagate the inflow hydrograph to the downstream end of the sewer. The routed hydrograph is added to the surface runoff hydrograph to the manhole at the downstream junction, and the routed hydrograph for each sewer is added also. The combined hydrographs for all upstream connecting pipes plus the hydrograph for the surface runoff represents the design inflow hydrograph to the next (adjacent) downstream sewer pipe. The pipe size and sewer slope are selected by solving for the commercial size pipe that can handle the peak discharge of the inflow hydrograph and maintain a gravity flow.

A simple and rather effective hydrograph design method is the *hydrograph time lag method* (Yen, 1978), which is a hydrologic (lumped) routing method. The inflow hydrograph of a sewer is shifted without distortion by the sewer flow time t_f to produce the sewer outflow hydrograph.

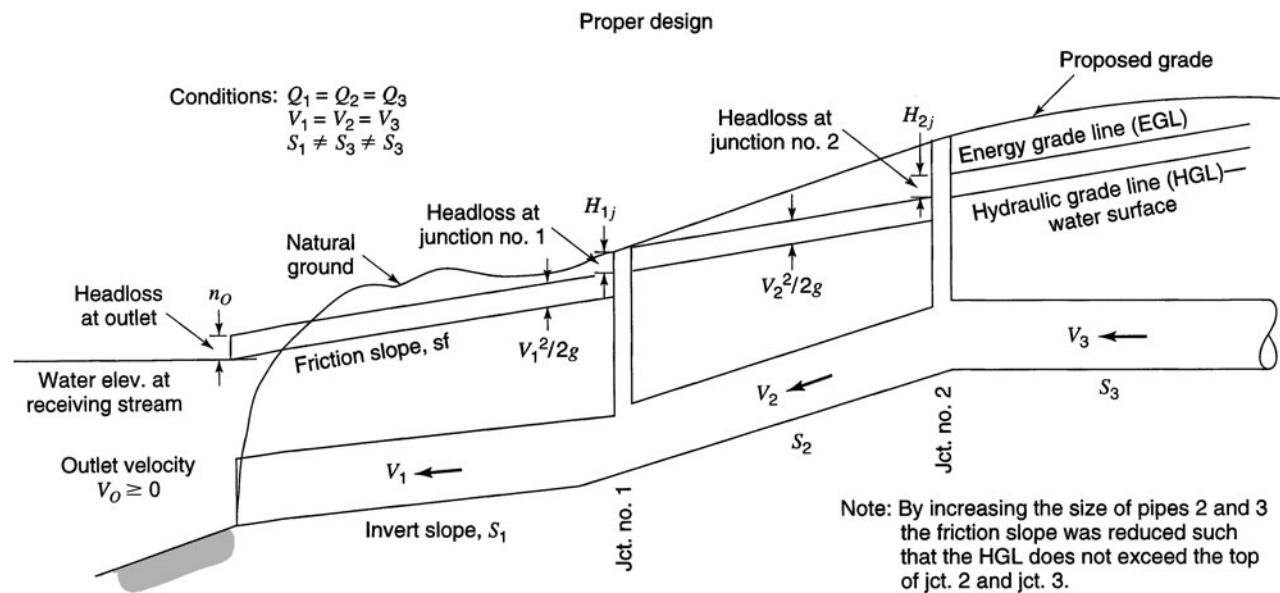
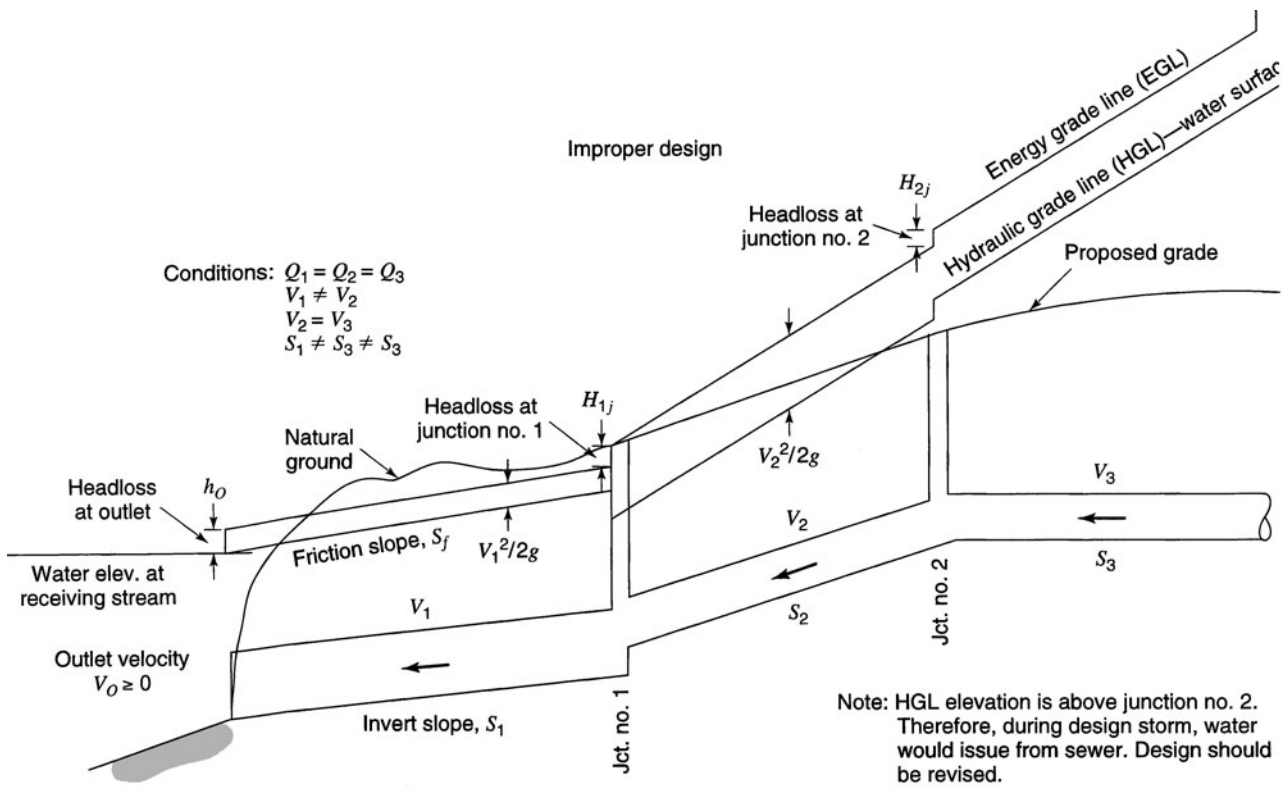


Figure 15.2.12 Use of energy losses in developing a storm drain system: energy and hydraulic grade lines for storm sewer under constant discharge (from AASHTO (1991)).

The outflow hydrographs of the upstream sewers at a manhole are added, at the corresponding times, to the direct manhole inflow hydrograph to produce the inflow hydrograph for the downstream sewer in accordance with the continuity relationship

$$\sum Q_{ij} + Q_j - Q_0 = \frac{dS}{dt} \quad (15.2.20)$$

in which Q_{ij} is the inflow from the i th upstream sewer into the junction j , Q_0 is the outflow from the junction into the downstream sewer, Q_j is the direct inflow into the manhole or junction, and S is the water stored in the junction structure or manhole. For point type junctions where there is no storage, dS/dt is 0.

The sewer flow time t_f that is used to shift the hydrograph is estimated by

$$t_f = \frac{L}{V} \quad (15.2.21)$$

in which L is the length of the sewer and V is a sewer flow velocity. The velocity could be computed, assuming a full-pipe flow, using

$$V = \frac{4Q_p}{\pi D^2} \quad (15.2.22)$$

where Q_p is the peak discharge and D is the pipe diameter. Also steady uniform flow equations such as Manning's equation or the Darcy-Weisbach equation can be used to compute the velocity.

In this method, the continuity relationship of the flow within the sewer is not directly considered. The routing of the sewer flow is done by shifting the inflow hydrograph by t_f and no consideration is given to the unsteady and nonuniform nature of the sewer flow. Shifting of hydrographs approximately accounts for the sewer flow translation time but offers no wave attenuation. However, the computational procedure through interpolation introduces numerical attenuation.

15.2.4 Storm Sewer Appurtenances

Certain appurtenances are essential to the functioning of storm sewers. These include manholes, bends, inlets, and catch basins. The discussion here briefly explains some of the common appurtenances; for additional details refer to American Society of Civil Engineers (1992).

Manholes are located at the junctions of sewer pipes and at changes of grade, size, and alignment, with street intersections being typical locations. Typical manholes for small sewers (sewer diameters less than 2 ft) are shown in Figure 15.2.13 and for intermediate sized sewers (sewer diameters greater than 2 ft) are shown in Figure 15.2.14. Manholes provide convenient access to the sewer for observation and maintenance operation. They should be designed to cause a minimum of interference with the hydraulics of the sewer. Manholes should be spaced 400 ft (120 m) or less for sewers 15 in (375 mm) or less and 500 ft (150 m) for sewers 18 to 30 in (460 to 760 mm) (Great Lakes–Upper Mississippi Board of State Sanitary Engineers, 1978). For larger sewers, spacing of up to a maximum of 600 ft (180 m) can be used.

Drop manholes (see Figure 15.2.15) are provided for sewers entering a manhole at an elevation of 24 in (0.6 m) or more above the manhole invert. These manholes are constructed with either an internal or external drop connection. For structural reasons, external connections are preferred.

Inlets are structures where stormwater enters the sewer system. Section 16.1 provides a detailed description of and design procedures for inlets.

15.2.5 Risk-Based Design of Storm Sewers

Proposed water-excess management solutions are subject—like are most solutions to engineering problems—to an element of uncertainty. The uncertainty inherent in storm sewer design

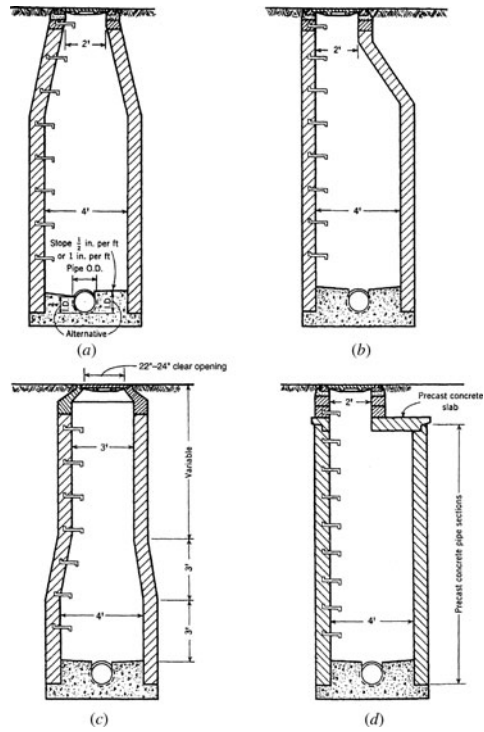


Figure 15.2.13 Typical manholes for small sewers (from ASCE (1992)).

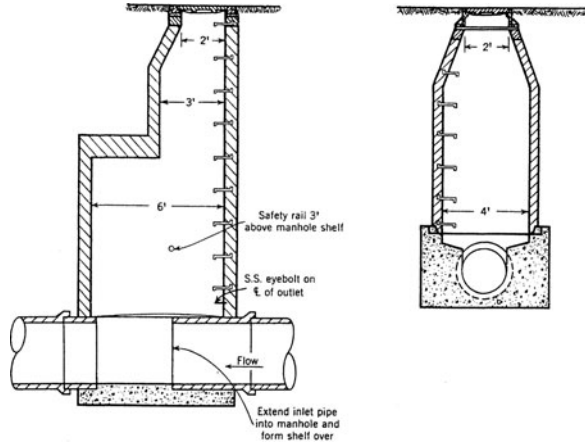


Figure 15.2.14 Two manholes for intermediate-sized sewers (from ASCE (1992)).

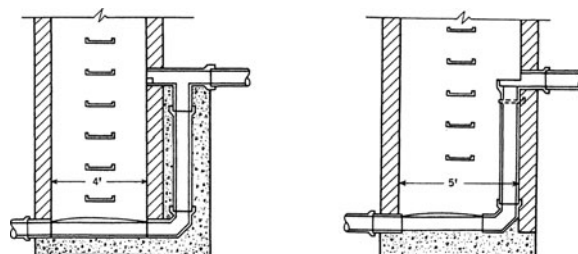


Figure 15.2.15 Drop manholes (from ASCE (1992)).

derives from both hydraulic and hydrologic aspects of the problem. Recommended references on risk-based design include Ang and Tang (1975, 1984), Chow et al. (1988), Harr (1987), Kapur and Lamberson (1977), Kececioglu (1991), Mays and Tung (1992), and Yen (1986). Also see Sections 10.6 and 10.7.

The key question is the ability of the proposed sewer design to accommodate the surface runoff generated by a storm. Although a factor of safety SF is inherent in the choice of a design frequency, the relationship between the sewer capacity Q_c and the storm runoff Q_L can also be explicitly considered: that is, $Q_c = SF \times Q_L$. Using risk/reliability analysis, a probability of failure $P(Q_L > Q_c)$ can be calculated for selected frequencies and safety factors. The corresponding risks and safety factors for each return period (recurrence interval) can be plotted to derive the risk-safety factor relationship for each return period. The procedure is as follows:

1. Select the return period T .
2. Use a rainfall-runoff model (such as the rational method) and perform an uncertainty analysis to compute the mean loading on the sewer \bar{Q}_L (the mean surface runoff) and its coefficient of variation Ω_{Q_L} , where

$$\bar{Q}_L = \bar{C}\bar{i}\bar{A} \quad (15.2.23)$$

where \bar{C} is the mean runoff coefficient, \bar{A} is the mean basin area in acres, \bar{i} is the mean rainfall intensity in in/hr, and (see derivation in Section 10.6)

$$\Omega_{Q_L}^2 = \Omega_C^2 + \Omega_i^2 + \Omega_A^2 \quad (15.2.24)$$

where Ω_C , Ω_i , and Ω_A are the coefficients of variation of C , i , A , respectively.

3. Select a pipe diameter D and compute \bar{Q}_c and Ω_{Q_c} , where \bar{Q}_c is the mean capacity of the sewer and Ω_{Q_c} is the coefficient of variation of Q_c . The mean capacity can be obtained from a modified form of the Manning equation:

$$\bar{Q}_c = \frac{0.463}{\bar{n}} D^{8/3} \bar{S}_0^{1/2} \quad (15.2.25)$$

in which \bar{n} is the mean Manning roughness coefficient, \bar{S}_0 is the mean sewer slope, and D is the sewer diameter. The coefficient of variation Ω_{Q_c} is computed using (see derivation in Section 10.6)

$$\Omega_{Q_c}^2 = \Omega_n^2 + \frac{1}{4}\Omega_{S_0}^2 + \left(\frac{8}{3}\right)^2 \Omega_D^2 \quad (15.2.26)$$

in which Ω_n , Ω_D , and Ω_{S_0} are the coefficients of variation of n , d , and S_0 , respectively.

4. Compute the risk and safety factor (see Section 10.7).
5. Repeat Step 3 for other diameters.
6. Repeat Step 2 for other rainfall duration.
7. Return to Step 1 for each return period to be considered.

EXAMPLE 15.2.5

Determine the coefficient of variation of the loading and the capacity for the following parameters. Assume a uniform distribution to define the uncertainty of each parameter.

Parameter	Mode	Range
C	0.75	0.70–0.80
i	7.5 in/hr	7.2–7.8 in/hr
A	12 ac	11.9–12.1 ac
n	0.015	0.0145–0.0155
D	5 ft	4.96–5.04 ft
S_0	0.001 ft/ft	0.0009–0.0011 ft/ft

SOLUTION

The loading Q_L is estimated using the rational equation (15.2.23), the capacity Q_C is estimated using Manning's equation (15.2.25), and the coefficients of variation of Q_L and Q_C are determined using equations (15.2.24) and (15.2.26), respectively. All the random parameters are assumed to follow a uniform distribution, so the mean and variance of each parameter are calculated using mean = $(a + b)/2$ and variance = $(b - a)^2/12$, in which a and b are the lower and upper bounds, respectively. Hence,

$$\Omega = \frac{\sqrt{\frac{(b-a)^2}{12}}}{(b+a)/2} = \left(\frac{b-a}{b+a}\right) \frac{1}{\sqrt{3}}$$

Based on the above formula, the means, variance, and coefficients of each parameter are calculated in the following table:

Parameter	Range	Mean	Variance	Ω
C	0.70–0.80	0.75	8.33×10^{-4}	3.85×10^{-2}
i (in/hr)	7.2–7.8	7.5	3.00×10^{-2}	2.31×10^{-2}
A (ac)	11.9–12.1	12.0	3.33×10^{-3}	4.81×10^{-3}
n	0.0145–0.0155	0.0150	8.33×10^{-8}	1.92×10^{-2}
D (ft)	4.96–5.04	5.00	5.33×10^{-4}	4.62×10^{-3}
S_0	0.0009–0.0011	0.0010	3.33×10^{-9}	5.77×10^{-2}

Now, the coefficients of Q_L and Q_C can be calculated as

$$\Omega_{Q_L} = \sqrt{(3.85 \times 10^{-2})^2 + (2.31 \times 10^{-2})^2 + (4.81 \times 10^{-3})^2} = 4.52 \times 10^{-2}$$

$$\Omega_{Q_C} = \sqrt{(1.92 \times 10^{-2})^2 + \left(\frac{8}{3} \times 4.62 \times 10^{-3}\right)^{-2} + \left(\frac{1}{2} \times 5.77 \times 10^{-2}\right)^{-2}} = 3.68 \times 10^{-2}$$

EXAMPLE 15.2.6

Using the results of Example 15.2.5, determine the risk of the loading exceeding the capacity of the sewer pipe. Assume the use of a safety margin ($SM = Q_C - Q_L$) that is normally distributed.

SOLUTION

The risk is defined (see Section 10.7) as Risk = $P[Q_L > Q_C] = P[SM < 0]$, in which $SM = Q_C - Q_L$. The mean and variance of SM are, respectively, $\mu_{SM} = \mu_{Q_C} - \mu_{Q_L}$ and $\sigma_{SM}^2 = \sigma_{Q_C}^2 + \sigma_{Q_L}^2$. From example 15.2.5, we have

$$\mu_{Q_L} = \bar{C}\bar{i}\bar{A} = (0.75)(7.5)(12) = 67.50 \text{ cfs}$$

$$\sigma_{Q_L} = \mu_{Q_L} \Omega_{Q_L} = (67.50)(4.52 \times 10^{-2}) = 3.05 \text{ cfs}$$

$$\mu_{Q_C} = \frac{0.463}{\bar{n}} (\bar{D})^{8/3} (\bar{S}_0)^{1/2} = \frac{0.464}{0.015} (5)^{8/3} (0.001)^{1/2} = 71.51 \text{ cfs}$$

$$\sigma_{Q_C} = \mu_{Q_C} \Omega_{Q_C} = (71.51)(3.68 \times 10^{-2}) = 2.63 \text{ cfs}$$

Therefore, $\mu_{SM} = 71.51 - 67.50 = 4.01$ and $\sigma_{SM}^2 = 3.05^2 + 2.63^2 = 16.22$. The risk then is calculated as

$$\begin{aligned} \text{Risk} = P[SM < 0] &= P\left(Z < \frac{0 - \mu_{SM}}{\sigma_{SM}}\right) \\ &= P\left(Z < \frac{-4.01}{\sqrt{16.22}}\right) = P(Z < -1.00) = 0.159 \end{aligned}$$

15.3 STORMWATER DRAINAGE CHANNELS

Stormwater-drainage channels (or flood-control channels) must behave in a stable, predictable manner to ensure that a known flow capacity will be available for a design storm event. In most cases, the design goal is a noneroding channel boundary, although, in certain cases, a dynamic channel is desired (Cotton, 1999).

Because most soils erode under a concentrated flow, either temporary or permanent channel linings are needed to achieve channel stability.

Channel linings can be classified in two broad categories: rigid or flexible. *Rigid linings* include channel pavements of concrete or asphaltic concrete and a variety of precast interlocking blocks and articulated mats. *Flexible linings* include such materials as loose stone (riprap), vegetation, manufactured mats of lightweight materials fabrics, or combinations of these materials. Rigid linings are capable of high conveyance and high-velocity flow. Rigid-lined channels are used to reduce the amount of land required for a surface drainage system. The selection of lining is a function of the design context related to the consequences of flooding, the availability of land and environmental needs (Cotton, 1999). Figures 15.3.1 and 15.3.2 show two constructed channels in Arizona, each with and without flow.



Figure 15.3.1 Views of constructed reach of Cave Creek below Cave Buttes Dam, Phoenix, Arizona. The constructed reach is straight, and cross-sections are trapezoidal in shape. The bottom and sides of the channel are composed of rounded cobbles imbedded in a matrix of cement (approximate mean diameter of the rock projections was 80 mm, about half of which seemed to be exposed to flow). Roughness elements are constant throughout the reach. The channel gradient increases from about 0.002 ft/ft at cross-section 1 to about 0.010 ft/ft at cross-section 8. The stream is ephemeral, and flow is regulated by Cave Buttes Dam (from Phillips and Ingersoll (1998)).

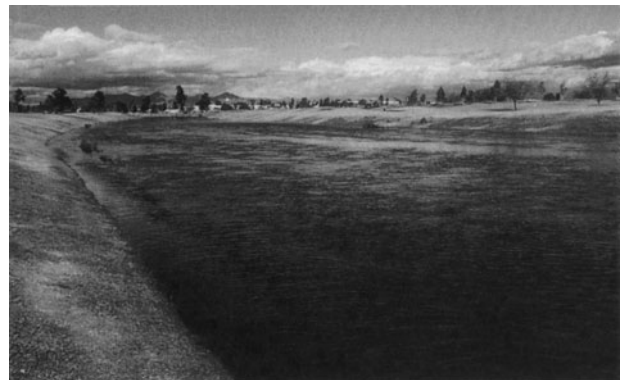


Figure 15.3.2 Views of Indian Bend Wash in Scottsdale, Arizona. The constructed channel is uniform and cross-sections are trapezoidal in shape (channel bottom is firm earth with seasonal growth of grasses and small brush) (from Phillips and Ingersoll (1998)).

15.3.1 Rigid-Lined Channels

Rigid-lined channels are nonerodible channel sides typically lined with concrete, grouted riprap, stone masonry, or asphalt. The steps in the design of such a channel are as follows:

1. Select the Manning roughness coefficient, n (see Table 15.3.1), the channel side slope z , and the channel bottom slope S_0 . The bottom slope is based upon the topography and other considerations such as alignment.
2. Compute the uniform flow section factor (see Chapter 5)

$$AR^{2/3} = \frac{Qn}{K_a S^{1/2}} \tag{15.3.1}$$

in which A is the cross-sectional area of flow, ft^2 (m^2), R is the hydraulic radius in ft (m), Q is the design discharge in ft^3/s (m^3/s), and $K_a = 1.49$ for U.S. customary units ($K_a = 1.0$ for SI units).

3. Determine the channel dimensions and flow depth for the uniform flow section factor computed in step 2. Choose the expression for the uniform flow section factor $AR^{2/3}$, as a function of depth, in Table 15.3.2 and solve for the depth using the value of $AR^{2/3}$ from equation (15.3.1). For a trapezoidal channel,

$$\left[\frac{(B_w + zy)^5 y^5}{(B_w + 2y\sqrt{1 + z^2})^2} \right]^{1/3} = AR^{2/3} \tag{15.3.2}$$

where B_w is the bottom width. By assuming several values of B_w and z , a number of combinations of section dimensions can be obtained. Final dimensions should be based upon hydraulic efficiency

Table 15.3.1 Manning’s Roughness Coefficients

Lining category	Lining type	Manning’s n		
		Depth ranges		
		0–0.5 ft (0–15 cm)	0.5–2.0 ft (15–60 cm)	>2.0 ft (>60 cm)
Rigid	Concrete	0.015	0.013	0.013
	Grouted riprap	0.040	0.030	0.028
	Stone masonry	0.042	0.032	0.030
	Soil cement	0.025	0.022	0.020
	Asphalt	0.018	0.016	0.016
Unlined	Bare soil	0.023	0.020	0.020
	Rock cut	0.045	0.035	0.025
Temporary	Woven paper net	0.016	0.015	0.015
	Jute net	0.028	0.022	0.019
	Fiberglass roving	0.028	0.021	0.019
	Straw with net	0.065	0.033	0.025
	Curled wood mat	0.066	0.035	0.028
	Synthetic mat	0.036	0.025	0.021
Gravel riprap	1 in (2.5 cm) D_{50}	0.044	0.033	0.030
	2 in (5 cm) D_{50}	0.066	0.041	0.034
Rock riprap	6 in (15 cm) D_{50}	0.104	0.069	0.035
	12 in (30 cm) D_{50}	—	0.078	0.040

Source: Chen and Cotton (1988).

and practicability. If the best hydraulically efficient section is required, select the expression for $AR^{2/3}$ from Table 15.3.3 and solve for the depth using the value of $AR^{2/3}$ from equation (15.3.1). For a trapezoidal channel,

$$\sqrt{3}\left(\frac{y^8}{4}\right)^{1/3} = AR^{2/3} \quad (15.3.3)$$

4. Check the minimum velocity to see if the water carries the silt.
5. Add an appropriate freeboard to the depth of the channel section.

EXAMPLE 15.3.1

Design a nonerodible trapezoidal channel to carry a discharge of 11.33 m³/s.

SOLUTION

1. The Manning's $n = 0.025$ slope, $S_0 = 0.0016$.
2. The uniform flow section factor is computed using equation (15.3.1):

$$AR^{2/3} = \frac{Qn}{K_a S^{1/2}} = \frac{11.33 \times 0.025}{(0.0016)^{1/2}} = 7.08$$

3. Equation (15.3.3) is used for the best hydraulic section:

$$\sqrt{3}\left(\frac{y^8}{4}\right)^{1/3} = AR^{2/3} = 7.08, \text{ solving } y = 2.02 \text{ m.}$$

Because the best hydraulic section is half of a hexagon, the side slopes are $z = \tan 30^\circ = 0.577$, z horizontal to 1 vertical. The area for a best hydraulic section is $A = \sqrt{3}y^2 = \sqrt{3}(2.02) = 7.07 \text{ m}^2 = (B_w + zy)y$, so $[B_w + (0.577)(2.02)] 2.02 = 7.07$. Solving, the bottom width is 2.33 m.

4. The velocity is $Q/A = 11.33/7.07 = 1.60 \text{ m/s}$, which is greater than the minimum permissible velocity for inducing silt deposition (if any exists).
5. A required freeboard, e.g., 1 m, can be added, so the total channel depth would be 3.02 m.

15.3.2 Flexible-Lined Channels

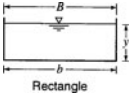
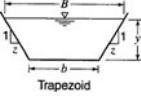
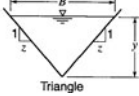
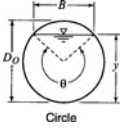
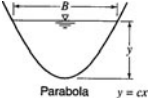
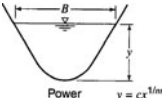
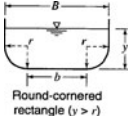
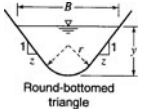
Flexible-lined channels include rock riprap and vegetative linings and are considered flexible because they can conform to change in channel slope. Flexible linings have the following advantages for stormwater conveyance: they (1) permit infiltration and exfiltration; (2) filter out contaminants; (3) provide greater energy dissipation; (4) allow flow conditions that provide better habitat opportunities for local flora and fauna, and (5) are less expensive. For a given design flow, channel geometry, and slope, the following design procedure can be used to select the appropriate flexible lining (Kouwen, et al. 1969; Bathurst, et al. 1981; Cotton, 1999; Wang and Shen, 1985; Chen and Cotton, 1988):

1. Choose a flexible lining from Table 15.3.4 and note its permissible shear stress τ_p .
2. Assume an appropriate flow depth y (for vegetative lining only; for nonvegetative lining, assume the range of flow depth and go to step 3).
3. Use Table 15.3.1 for nonvegetative lining to find the Manning n . For vegetative lining, use Table 15.3.5 to determine the appropriate retardant class. The Manning n for vegetative lining is given by the general equation

$$n = k_1/(a_c + k_2) \quad (15.3.4)$$

in which $k_1 = R^{1/6}$, where R is the hydraulic radius, ft; $k_2 = 19.97 \log(R^{1.4} S_0^{0.4})$ where S_0 is the channel longitudinal slope, ft/ft; $a_c = 15.8, 23.0, 30.2, 34.6,$ and 37.7 for retardance classes A, B, C, D, E respectively.

Table 15.3.2 Geometric Elements of Channel Cross-Sections

Cross-section	Area A	Wetted perimeter P	Hydraulic radius R	Top width B
 Rectangle	by	$b + 2y$	$\frac{by}{b + 2y}$	b
 Trapezoid	$(b + zy)y$	$b + 2y\sqrt{1 + z^2}$	$\frac{(b + zy)y}{b + 2y\sqrt{1 + z^2}}$	$b + 2zy$
 Triangle	zy^2	$2y\sqrt{1 + z^2}$	$\frac{zy}{2\sqrt{1 + z^2}}$	$2zy$
 Circle	$\frac{1}{8}(\theta - \sin\theta)D_0^2$	$\frac{1}{2}\theta D_0$	$\frac{1}{4}\left(1 - \frac{\sin\theta}{\theta}\right)D_0$	$\frac{(\sin^1/2\theta)D_0}{2\sqrt{y}(D_0 - y)}$ or $\frac{(\sin^1/2\theta)D_0}{2\sqrt{y}(D_0 - y)}$
 Parabola $y = cx$	$\frac{2}{3}By$	$B + \frac{8y^2}{3B}$	$\frac{2B^2y}{3B^2 + 8y^2}$	$\frac{3A}{2y}$
 Power $y = cx^{1/m}$	$\frac{By}{(m + 1)}$	$\frac{2y}{m}\sqrt{\frac{m^2}{c^{2m}}y^{2m-2} + 1} + \sum^{\S}$	$\frac{A}{P}$	$2\left(\frac{y}{c}\right)^m$
 Round-cornered rectangle ($y > r$)	$\left(\frac{\pi}{2} - 2\right)r^2 + (b + 2r)y$	$(\pi - 2)r + b + 2y$	$\frac{(\pi/2 - 2)r^2 + (b + 2r)y}{(\pi - 2)r + b + 2y}$	$b + 2r$
 Round-bottomed triangle	$\frac{B^2}{4z} - \frac{r^2}{z}(1 - z \cot^{-1}z)$	$\frac{B}{z}\sqrt{1 + z^2} - \frac{2r}{z}(1 - z \cot^{-1}z)$	$\frac{A}{P}$	$2\left[z(y - r) + r\sqrt{1 + z^2}\right]$

*For the section factor Z_c , the energy correction factor α or momentum correction factor β are assumed equal to unity. Otherwise, $Z_c = Q/\sqrt{g/\alpha}$ or $Z_c = Q/\sqrt{g/\beta}$.

†Satisfactory approximation for the interval $0 < x < 1$, where $x = 4y/b$. When $x > 1$, use the exact expression

$$P = (B/2)\left[\sqrt{1 + x^2} + 1/x \ln(x + \sqrt{1 + x^2})\right].$$

‡For trapezoid, approximate Y_c valid for $0.1 < Q/b^{2.5} < 0.4$; when $Q/b^{2.5} < 0.1$, use the rectangular formula.

$$\sum^{\S} = \left(1 - \frac{1}{m}\right)y \sum_{k=0}^{\infty} \frac{\left(\frac{1}{2}\right)_k \left(\frac{1}{2m-2}\right)_k \left[-\frac{m}{c^m}y^{m-1}\right]^{2k}}{\left(1 + \frac{1}{2m-2}\right)_k k!}, \text{ where } (w)_k = w(w+1)\cdots(w+k-1), k = 1, 2, \dots, (w)_{k=0} = 1.$$

Source: Yen (1996).

Hydraulic mean depth D	Uniform flow section factor $AR^{2/3} = \frac{Qn}{K_n S^{0.5}}$	Critical flow section factor* $Z_c = Q/\sqrt{g} = A_c \sqrt{D_c}$	Critical depth y_c
y	$\left[\frac{b^5 y^5}{(b+2y)^2} \right]^{1/3}$	$by^{1.5}$	$\left(\frac{Z_c}{b} \right)^{2/3}$
$\frac{(b+zy)y}{b+2zy}$	$\left[\frac{(b+zy)^5 y^5}{(b+2y\sqrt{1+z^2})^2} \right]^{1/3}$	$\frac{[(b+zy)y]^{1.5}}{\sqrt{b+2zy}}$	$0.81 \left(\frac{Z_c^4}{z^{1.5} b^{2.5}} \right)^{0.135} - \frac{b^\ddagger}{30z}$
$\frac{y}{2}$	$\left[\frac{z^5 y^8}{4(1+z^2)} \right]^{1/3}$	$\frac{\sqrt{2}}{2} zy^{2.5}$	$\left(\frac{\sqrt{2} Z_c}{z} \right)^{0.4}$
$\frac{1}{8} \left(\frac{\theta - \sin\theta}{\sin^{1/2}\theta} \right) D_0$	$\frac{1}{16} \left[\frac{(\theta - \sin\theta)^5 D_0^3}{2\theta^2} \right]^{1/3}$	$\frac{\sqrt{2}}{32} \left[\frac{(\theta - \sin\theta)^{1.5}}{(\sin^{1/2}\theta)^{0.5}} \right] D_0^{2.5}$	$\frac{1.01}{D_0^{0.26}} Z_c^{0.5^\ddagger}$ for $0.02 \leq y_c/D_0 \leq 0.85$
$\frac{2}{3}y$	$\frac{2}{3} \left[\frac{4B^7 y^5}{(3B^2 + 8y^2)^2} \right]^{1/3^\ddagger}$	$\frac{2\sqrt{6}}{9} By^{1.5}$	$0.958 (c^{0.5} Z_c)^{0.5}$
$\frac{y}{(m+1)}$	$\left[\frac{A^5}{P^2} \right]^{1/3}$	$\frac{By^{1.5}}{(m+1)^{1.5}}$	$\left[\frac{c^m}{2} (m+1)^{1.5} Z_c \right]^{1/(m+1.5)}$
$\frac{(\pi/2 - 2)r^2}{b+2r} + y$	$\left[\frac{A^5}{P^2} \right]^{1/3}$	$\frac{[(\pi/2 - 2)r^2 + (b+2r)y]^{1.5}}{\sqrt{b+2r}}$	
$\frac{A}{B}$	$\left[\frac{A^5}{P^2} \right]^{1/3}$	$A \sqrt{\frac{A}{B}}$	

4. Calculate the computed flow depth y_{comp} from the Manning equation using the value of n from step 3.
5. For vegetative lining, compare y and y_{comp} ; if they are not close enough replace y based on y_{comp} for a new y and go to step 3. For nonvegetative lining, go to step 6.
6. Compute shear stress for the design condition by

$$\tau_{\text{des}} = \gamma R S_0 \quad (15.3.5)$$

If $\tau_{\text{des}} < \tau_p$ (Table 15.3.4) the lining is acceptable. Otherwise go to step 1 and choose a different lining.

Table 15.3.3 Best Hydraulically Efficient Sections Without Freeboard

Cross-section	Area A	Wetted perimeter P	Hydraulic radius R	Top width B	Hydraulic depth D	$AR^{2/3}$
Trapezoid, half of a hexagon	$\sqrt{3}y^2$	$2\sqrt{3}y$	$\frac{1}{2}y$	$\frac{4}{3}\sqrt{3}y$	$\frac{3}{4}y$	$\sqrt{3}\left(\frac{y^8}{4}\right)^{1/3}$
Rectangle, half of a square	$2y^2$	$4y$	$\frac{1}{2}y$	$2y$	y	$(2y^8)^{1/3}$
Triangle, half of a square	y^2	$2\sqrt{2}y$	$\frac{1}{4}\sqrt{2}y$	$2y$	$\frac{1}{2}y$	$\frac{1}{2}y^{8/3}$
Semicircle	$\frac{\pi}{2}y^2$	πy	$\frac{1}{2}y$	$2y$	$\frac{\pi}{4}y$	$\frac{\pi}{2}(2y^8)^{1/3}$
Parabola, $B = 2\sqrt{2}y$	$\frac{4}{3}\sqrt{2}y^2$	$\frac{8}{3}\sqrt{2}y$	$\frac{1}{2}y$	$2\sqrt{2}y$	$\frac{2}{3}y$	$\frac{2\sqrt{2}}{3}(2y^8)^{1/3}$
Hydrostatic catenary	$1.39586y^2$	$2.9836y$	$0.46784y$	$1.917532y$	$0.72795y$	$0.84122y^{8/3}$

Source: Yen (1996).

EXAMPLE 15.3.2

Design a flexible-lined trapezoidal channel for a slope of $S_0 = 0.0016$ (same flow rate of $11.33 \text{ m}^3/\text{s}$ and slope as example 15.3.1). Use a nonvegetative lining.

SOLUTION

1. A gravel riprap (2.5 cm) D_{50} is chosen.
2. A flow depth of greater than 60 cm is assumed.
3. From Table 15.3.1, the Manning’s roughness factor is $n = 0.03$.

Table 15.3.4 Permissible Shear Stresses for Lining Materials

Lining category	Lining type	Permissible shear stress, τ_p		
		lb/ft ²	kg/m ²	
Temporary	Woven paper net	0.15	0.73	
	Jute net	0.45	2.20	
	Fiberglass roving	Single	0.60	2.93
		Double	0.85	4.15
	Straw with net	1.45	7.08	
	Curled wood mat	1.55	7.57	
	Synthetic mat	2.00	9.76	
	Vegetative	Class A	3.70	18.06
Class B		2.10	10.25	
Class C		1.00	4.88	
Class D		0.60	2.93	
Class E		0.35	1.71	
Gravel riprap	1-in	0.33	1.61	
	2-in	0.67	3.22	
Rock riprap	6-in	2.00	9.76	
	12-in	4.00	19.52	

Source: Chen and Cotton (1988).

Table 15.3.5 Classification of Vegetal Covers by Degree of Retardance

Retardance class	Cover	Condition
A	Weeping lovegrass	Excellent stand, tall (average 30 in [76 cm])
	Yellow bluestem <i>Ischaemum</i>	Excellent stand, tall (average 36 in [91 cm])
B	Kudzu	Very dense growth, uncut
	Bermuda grass	Good stand, tall [average 12 in (30 cm)]
	Native grass mixture (little bluestem, bluestem, blue gamma, and other long and short midwest grasses)	Good stand, unmowed
	Weeping lovegrasses	Good stand, (average 24 in [61 cm])
	<i>Lespedeza sericea</i>	Good stand, not woody, tall (average 19 in [48 cm])
	Alfalfa	Good stand, uncut (average 11 in [28 cm])
	Weeping lovegrass	Good stand, unmowed (average 13 in [28 cm])
	Kudzu	Dense growth, uncut
	Blue gamma	Good stand, uncut (average 13 in [28 cm])
	C	Crabgrass
Bermuda grass		Good stand, mowed (average 6 in [15 cm])
Common lespedeza		Good stand, uncut (average 11 in [28 cm])
Grass-legume mixture—summer (orchard grass, redtop, Italian ryegrass, and common lespedeza)		Good stand, uncut (6 to 8 in [15 to 20 cm])
Centipede grass		Very dense cover (average 6 in [15 cm])
Kentucky bluegrass		Good stand, headed (6 to 12 in [15 to 30 cm])
D		Bermuda grass
	Common lespedeza	Excellent stand, uncut (average 4.5 in [11 cm])
	Buffalo grass	Good stand, uncut (3 to 6 in [8 to 15 cm])
	Grass-legume mixture—fall, spring (orchard grass, redtop, Italian ryegrass, and common lespedeza)	Good stand, uncut (4 to 5 in [10 to 13 cm])
	<i>Lespedeza sericea</i>	After cutting to 2-in height (5 cm) Very good stand before cutting
E	Bermuda grass	Good stand, cut to 1.5-in height (4 cm)
	Bermuda grass	Burned stubble

Source: U.S. Soil Conservation Service (1954).

4. Compute the flow depth using Manning's equation:

$$AR^{2/3} = \frac{Qn}{K_a S^{1/2}} = \frac{11.33 \times 0.03}{(0.0016)^{1/2}} = 8.50$$

Assume a bottom width of 6 m and $z = 2$. So

$$AR^{2/3} = 8.50 = \left[\frac{(B_w + zy)^5 y^5}{(B_w + 2y\sqrt{1+z^2})^2} \right]^{1/3}$$

Solving yields $y_{\text{comp}} = 1.14$ m. Skip step 5 for nonvegetative lining and go to step 6.

5. The shear stress is computed using equation (15.3.5) with $R \approx y$, $\tau_{des} = \gamma y S_0 = (9810)(1.14 \text{ m})(0.0016) = 17.89 \text{ N/m}^2$ (1.73 kg/m^2). The allowable shear stress is $\tau = 1.61 \text{ kg/m}^2$ (from Table 15.3.4).

Because $\tau_{des} > \tau_{allowable}$, a 5-cm gravel riprap with approximately double the allowable shear stress only increases Manning's n from 0.03 to 0.034. So, returning to step 4, we find

$$AR^{2/3} = \frac{Qn}{K_a S^{1/2}} = \frac{11.33 \times 0.034}{(0.0016)^{1/2}} = 9.63$$

$$= \left[\frac{(B_w + zy)^5 y^5}{(B_w + 2y\sqrt{1+z^2})^2} \right]^{1/3} = 9.63$$

Solving yields $y \approx 1.22 \text{ m}$. The shear stress is $\tau_{des} = 1.95 \text{ kg/m}^2$ and the permissible shear stress is 3.22 kg/m^2 (Table 15.3.4).

6. Freeboard can be added.

EXAMPLE 15.3.3

Design a gravel riprap triangle-shaped channel to carry a discharge of $11.33 \text{ m}^3/\text{s}$ at a slope of 0.0016.

SOLUTION

1. Select a $D_{50} = 5.0 \text{ cm}$ gravel riprap.
2. Assume $y > 60 \text{ cm}$.
3. From Table 15.3.1, $n = 0.034$.
4. Compute flow depth:

$$AR^{2/3} = \frac{Qn}{S^{1/2}} = \frac{11.33 \times 0.034}{(0.0016)^{1/2}} = 9.63$$

Using the best hydraulic section $AR^{2/3} = 1/2y^{8/3} = 9.63$; then $y = 3.03 \text{ m}$.

5. The assumed and computed depths for the selected Manning's n are OK.
6. The design shear stress using $R = (\sqrt{2}/4)y$ is $\tau_{des} = \gamma R S_0 = 9810(\sqrt{2}/4)(3.03)(0.0016) = 16.81 \text{ N/m}^2 = 1.71 \text{ kg/m}^2 < \tau_{allowable} = 3.22$ (Table 15.3.4).
7. A freeboard can be added.

15.3.3 Manning's Roughness Factor for Vegetative Linings

Manning's roughness for vegetative linings can be determined using (Cotton, 1999)

$$n = R^{1/6} / \{g^{0.5} [a + b \log(R/k_s)]\} \tag{15.3.6}$$

where R is the hydraulic radius in meters and k_s is the effective roughness height in meters given by Kouwen and Li (1980) as

$$k_s = 0.14b \left\{ \left[(MEI/\tau_o)^{0.25} \right] / b \right\}^{1.59} \tag{15.3.7}$$

MEI is the density stiffness parameter. Below are a list of the values of the average height of vegetation and the density stiffness parameter, MEI, for the five standard retardance classifications. Class A has the highest flow resistance and class D has the lowest flow resistance.

Retardance class	Average height (h, mm)	Stiffness, MEI (N/m ²)
A	900	300.0
B	600	20.0
C	200	0.5
D	100	0.05
E	40	0.005

The MEI for green grass is expressed as $MEI = 319h^{3.3}$ in (N/m^2) and for dormant grass is $MEI = 24.5h^{2.26}$ in (N/m^2) , where h is the vegetation height (stem height) in meters (Kouwen, 1988).

The values of a and b in equation (15.3.6) are: for erect grass $a = 0.42$ and $b = 5.23$, and for flat grass $a = 0.82$ and $b = 9.90$. For grass that is submerged (bent), a and b for the Manning's roughness equation is determined using linear interpolation between the values of a and b for erect and flat grass. The criteria to determine a and b is to use $[\tau_o/\tau_{cv}]^{0.5}$, where τ_o is the total boundary shear given as $\tau_o = \gamma RS$ in N/m^2 , S is the bottom slope, and γ is the specific weight. τ_{cv} is the vegetative critical shear stress defined as

$$\tau_{cv} = \text{Minimum}[0.78 + 354MEI^2 + 40, 100MEI^4, 53MEI^{0.212}] \quad (15.3.8)$$

For erect grass, $[\tau_o/\tau_{cv}]^{0.5} \leq 1.0$, and for flat grass, $[\tau_o/\tau_{cv}]^{0.5} > 2.5$. For submerged (bent) grass, $1 < [\tau_o/\tau_{cv}]^{0.5} \leq 2.5$, and the values of a and b are determined by linear interpolation between the erect and flat values of a and b .

15.4 STORMWATER DETENTION

15.4.1 Why Detention? Effects of Urbanization

Urban stormwater management systems typically include detention and retention facilities to mitigate the negative impacts of urbanization on stormwater drainage. The effects of urbanization on stormwater runoff include increased total volumes of runoff and peak flow rates, as depicted in Figure 15.4.1. In general, major changes in flow rates in urban watershed are the result of (Chow, et al. 1988):

1. The increase in the volume of water available for runoff because of the increased impervious cover provided by parking lots, streets, and roofs, which reduce the amount of infiltration;
2. Changes in hydraulic efficiency associated with artificial channels, curbing, gutters, and storm drainage collection systems, which increase the velocity of flow and the magnitude of flood peaks.

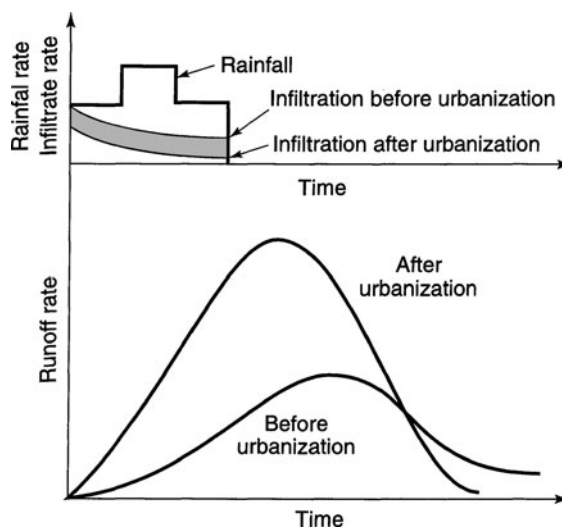


Figure 15.4.1 Effect of urbanization on stormwater runoff.

Stahre and Urbonas (1990) presented a classification of storage facilities. The major classification is *source control* or *downstream control*. Source control involves the use of smaller facilities located near the source, allowing better use of the downstream conveyance system. Downstream control uses storage facilities that are larger and consequently at fewer locations, such as at watershed outlets. Source control consists of local disposal, inlet control, and on-site detention. *Local disposal* is the use of infiltration or percolation. *Inlet control* entails detaining stormwater where the precipitation occurs (such as rooftops and parking lots). *On-site detention* typically refers to detaining stormwater from larger areas than the previous two and includes swales, ditches, dry ponds, wet ponds, concrete basins (which are typically underground), and underground piping. Wet ponds have a permanent water pool as opposed to dry ponds.

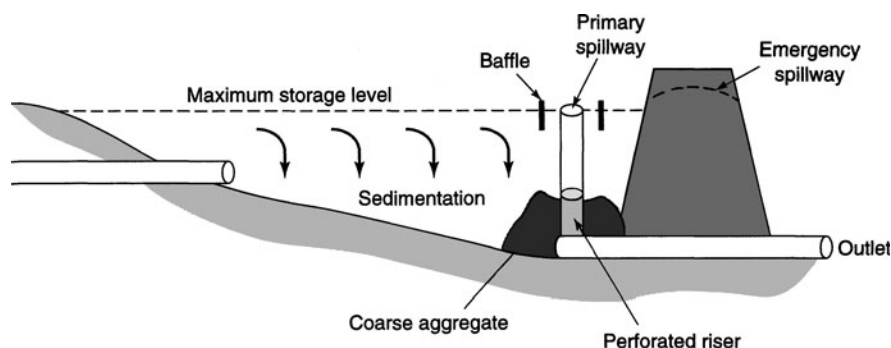
Downstream storage includes *in-line detention*, *off-line detention*, and *detention at wastewater treatment plants*. In-line detention refers to detention storage in sewer lines, tunnels, storage vaults, pipes, surface ponds, or other facilities that are connected in-line with a stormwater conveyance network. Off-line storage facilities are not in line with the stormwater conveyance system.

Detention as described in this chapter is of two major types: (1) underground or subsurface systems, and (2) surface systems. Most of this section discusses surface detention: section 15.4.3 discusses various methods for sizing detention ponds, section 15.4.4 discusses various types of detention, section 15.4.5 discusses infiltration methods, and section 15.4.6 discusses water quality aspects.

Additional references on stormwater management include Overton and Meadows (1976), Stahre and Urbonas (1990), Loganathan et al. (1996), and Whipple et al. (1983).

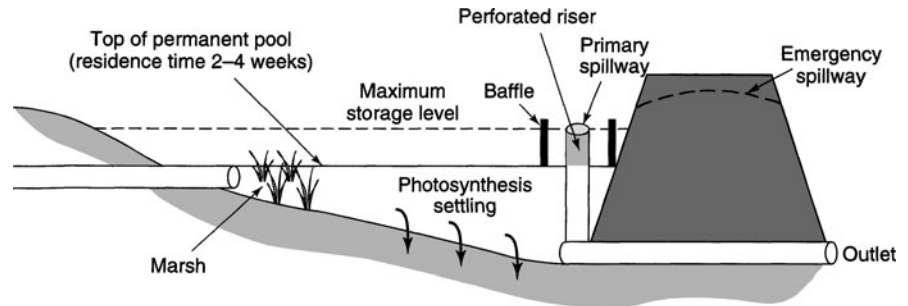
15.4.2 Types of Surface Detention

Surface detention, for purposes of this discussion, refers to *extended detention basins* (or *dry detention basins*) and *retention ponds* (or *wet detention ponds*). Dry detention ponds empty after a storm, whereas retention ponds retain the water much longer above a permanent pool of water. Dry detention is the most widely used technique in the United States and many other countries. Figure 15.4.2 illustrates an extended detention basin. Water enters the basin, is impounded behind the embankment, and is slowly discharged through a perforated riser outlet. The coarse aggregate around the perforated riser minimizes clogging by debris. Typically once a required water-quality



- Efficiency: Poor for detention times under 12 hours
Good for detention times greater than 24 hours
- Function: Settle pollutants out; soluble pollutants pass through
- Maintenance is moderate if properly designed
- Improper design can make facilities an eyesore and a mosquito-breeding mudhole
- Newer designs are incorporating a shallow marsh around outlet
Result: Better removal efficiency and no mosquito nuisance
- Regional detention facilities serving 100–200 acres can be aesthetically developed
Result: Lower maintenance costs

Figure 15.4.2 Design of an extended detention basin (from Urbonas and Roesner (1993)).



- Efficiency: Excellent if properly designed.
Can be poor if bottom goes anoxic.
- Function: Removes pollutants by settling dissolved pollutants biochemically.
- Maintenance: Relatively free after first year except for major cleanout at about 10 years.
- Aesthetic design can make pond an asset to community.
Excellent as a regional facility.

Figure 15.4.3 Design of a retention pond (from Urbonas and Roesner (1993)).

volume is filled, the remaining inflow is diverted around the basin or the pond overflows through a primary spillway. A large part of the sediment from the stormwater settles in the basin. Refer to Loganathan et al. (1996), Loganathan et al. (1985; 1989), Segarra and Loganathan (1992), and Wanielista and Yousef (1993).

Figure 15.4.3 illustrates a retention pond, which is basically a lake that can be designed to remove pollutants. The figure illustrates the basic treatment processes that occur in the retention pond. Pollutants are removed by settling. Nutrients are removed by phytoplankton growth in the water column and by shallow marsh plants around the pond perimeter.

A multipurpose detention basin for quantity and quality is illustrated in Figure 15.4.4. The outlet works are staged so that the water-quality design volume is released very slowly. The other stages (see figure) provide storage and outlet peak discharges for erosion and flood control. Whipple et al. (1987) discuss the implementation of dual purpose stormwater detention programs.

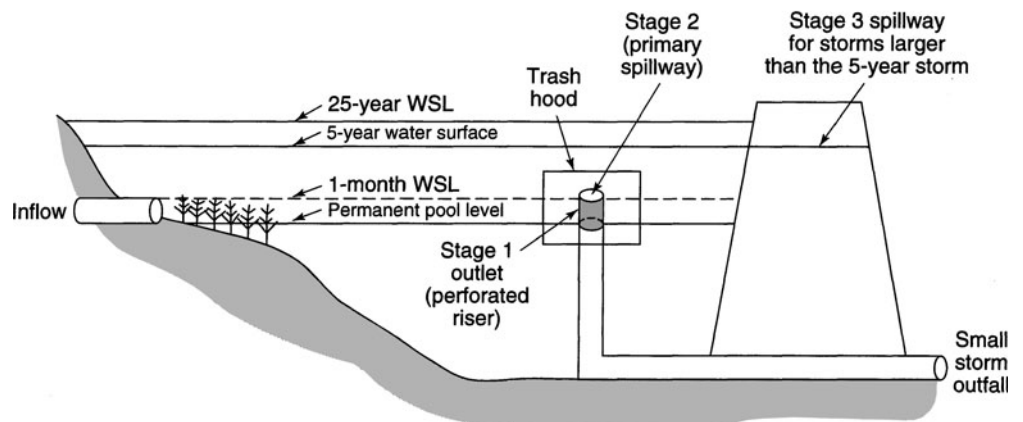


Figure 15.4.4 Conceptual design of a multipurpose pond (from Urbonas and Roesner (1993)).

15.4.3 Sizing Detention

Several simplified methods for sizing detention have been proposed in the literature (Abt and Grigg, 1978; Akan, 1989, 1990, 1993; Aron and Kibler, 1990; Donahue, et al. 1981; Kessler and Diskin, 1991; Mays and Tung, 1992; McEnroe, 1992; and Wycoff and Singh, 1976). More sophisticated procedures using optimization have also been proposed (Bennett and Mays, 1985; Mays and Bedient, 1982; Nix and Heaney, 1988; Taur, et al. 1987).

The stormwater detained during and after a storm is a function of the runoff volume, the detention basin outlet(s), and the available storage volume of the detention basin. The objective of sizing the pond is to determine the storage volume V_s , which mathematically is the time integral of the difference between the detention basin inflow and outflow hydrographs; i.e., the storage volume is

$$V_s = \int (Q_{in} - Q_{out})dt \tag{15.4.1}$$

where Q_{in} is the inflow rate and Q_{out} is the outflow rate. Figure 15.4.5 illustrates this integration showing the V_{max} .

Simple methods based upon regression equations, the rational method, or the modified rational method can be used to estimate preliminary sizes. This is followed up by iteratively routing one or more hydrographs through the preliminary sized pond to refine the size and outlet structures. The classic detention sizing procedure consists of the following steps (Urbonas and Roesner, 1993):

1. Estimate the preliminary storage volume V_s using a simplified procedure (see sections 15.4.3.1 and 15.4.3.2).
2. Use site topography to prepare a preliminary layout of a detention basin that has the desired volume and outlet configuration.
3. Determine stage-storage-outflow characteristics of the trial pond size.
4. Perform routing of input hydrographs through the pond. Steps 3 and 4 can be accomplished using computer models.
5. If the trial pond (size and outlet configuration) does not satisfy desired goals and design criteria, resize the basin and or reconfigure the outlet(s) and repeat steps 3–5 until design goals and design criteria are satisfied (optimized).

The inflow hydrographs can be generated using any of a number of rainfall-runoff models (also see Akan, 1993; Chow, et al. 1988; Kibler, 1982; and Urbonas and Roesner, 1993).

The American Association of State Highway Transportation Officials (AASHTO) (1991) recommended using triangular-shaped inflow and outflow hydrographs (see Figure 15.4.6) to determine preliminary estimates of storage volume V_s . The required storage volume is simply the cross-hatched area shown in Figure 15.4.6, which is computed using

$$V_s = 0.5t_b(Q_p - Q_A) \tag{15.4.2}$$

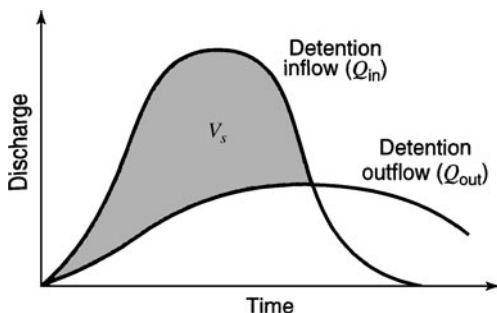


Figure 15.4.5 Detention storage volume V_s .

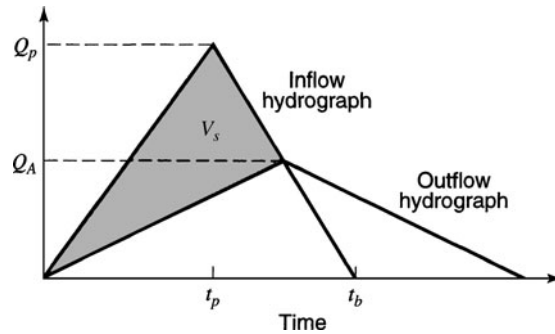


Figure 15.4.6 Inflow and outflow hydrographs for AASHTO (1991) procedure.

Any consistent units may be used in equation (15.4.2). The time to peak inflow hydrograph t_p is half of the total time base of this hydrograph.

Abt and Grigg (1978) considered a triangular inflow hydrograph and a trapezoidal outflow hydrograph to develop the following relationship to estimate the required storage volume V_s using consistent units:

$$\frac{V_s}{V_r} = \left(1 - \frac{Q_A}{Q_P}\right)^2 \quad (15.4.3)$$

where V_r is the runoff volume, Q_A is the allowable peak outflow rate, and Q_P is the peak inflow rate. This procedure assumes that the rising limbs of the inflow and outflow hydrographs coincide up to the allowable peak outflow rate (see Figure 15.4.7).

Aron and Kibler (1990) developed an approximate method considering trapezoidal inflow hydrographs. They assumed (1) that the peak outflow hydrograph falls on the recession limb of the inflow hydrograph and (2) that the rising limb of the outflow hydrograph can be approximated by a straight line (see Figure 15.4.8). The volume of storage is computed using

$$V_s = Q_P t_D - Q_A \left(\frac{t_D + t_C}{2}\right) \quad (15.4.4)$$

where t_D is the storm duration and t_C is the time of concentration of the watershed. The design-storm duration is the one that maximizes the detention storage volume V_s for a given return period. This method uses a trial-and-error procedure to find the storm duration using the local intensity-duration-frequency (IDF) relationships. The rational formula ($Q_P = CiA$) is used to compute the peak flow rate Q_P .

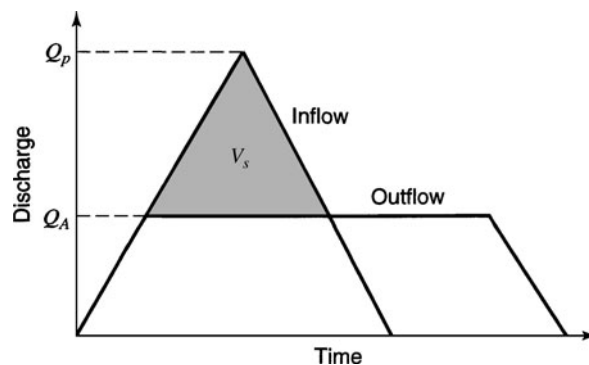


Figure 15.4.7 Inflow and outflow hydrographs for procedure by Abt and Grigg (1978).

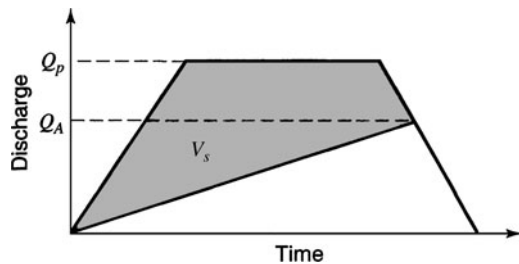


Figure 15.4.8 Inflow and outflow hydrographs for procedure by Aron and Kibler (1990).

AASHTO (1991) recommended an alternate estimate of storage volume using the regression equation developed by Wycoff and Singh (1976) as

$$\frac{V_s}{V_r} = \frac{1.29 \left(1 - \frac{Q_A}{Q_P}\right)^{0.153}}{\left(t_b/t_p\right)^{0.411}} \tag{15.4.5}$$

where V_s is the volume of storage in inches, V_r is the volume of runoff in inches, Q_A is the peak outflow in cfs, Q_P is the peak inflow in cfs, t_b is the time base of the inflow hydrograph in hours (determined as the time from the beginning of rise to a point on the recession limb where the flow is 5 percent of the peak), and t_p is the time to peak of the inflow hydrograph in hours. A preliminary estimate of the potential peak flow reduction for a selected storage volume is

$$\frac{Q_A}{Q_P} = 1 - 0.712 \left(\frac{V_s}{V_r}\right)^{1.328} \left(\frac{t_b}{t_p}\right)^{0.546} \tag{15.4.6}$$

EXAMPLE 15.4.1

The peak runoff rate for a 10-year storm of 133 ft³/s is to be limited to a peak of 40 ft³/s through the use of a detention basin. Determine a preliminary estimate of storage using the AASHTO (1991) method, equation (15.4.5); $t_p = 30$ min.

SOLUTION

First, by definition t_b = time base of inflow hydrograph in hours determined as the time from the beginning to a point on the recession limb where the flow is 5 percent of the peak. So

$$t_b = 60 - 30 \left[\frac{0.05(133)}{133} \right] = 58.5 \text{ min} = 0.98 \text{ hr}$$

Using equation (15.4.5) yields

$$\frac{V_s}{V_r} = 1.29 \frac{\left(1 - \frac{40}{133}\right)^{0.153}}{\left(\frac{0.98}{0.5}\right)^{0.411}} = \frac{1.29(0.95)}{1.32} = 0.93$$

$$\begin{aligned} V_r &= \frac{1}{2} (60 \text{ min})(133 \text{ ft}^3/\text{s}) \times 60 \text{ sec}/\text{min} \\ &= 239,400 \text{ ft}^3 = 5.50 \text{ ac-ft} \end{aligned}$$

The volume of storage is

$$V_s = V_r(0.93) = 5.50(0.93) = 5.11 \text{ ac-ft}$$

$$\text{Using equation 15.4.2, } V_s = 0.5(1 \times 3600)(133 - 40) = 16,400 \text{ ft}^3 = 3.84 \text{ ac-ft}$$

EXAMPLE 15.4.2

Solve example 15.4.1 using the Abt and Grigg (1978) method.

SOLUTION

Using equation (15.4.3) yields

$$\frac{V_s}{V_r} = \left(1 - \frac{Q_A}{Q_p}\right)^2 = (1 - 0.3)^2$$

$$V_s = 0.49V_r = 0.49(5.50) = 2.70 \text{ ac-ft}$$

The procedure adopted by the Federal Aviation Administration (FAA) (1966) is a simple mass-balance technique that is intensity-duration-frequency (IDF) based. The procedure assumes that rainfall volume accumulates with time and is a time integral of the desired IDF curve. The rainfall volume-duration curve is transformed into a runoff volume-duration curve using

$$V_{in} = K_u CiAt_D \quad (15.4.7)$$

where V_{in} is the cumulative runoff volume, $\text{ft}^3(\text{m}^3)$, K_u is 1.0 (for U.S. customary units) or 0.28 (for SI units), C is the runoff coefficient, i is the storm intensity from the IDF curve at time t_D in in/h (mm/h), A is the tributary area in acres (km^2), and t_D is the storm duration in seconds. The cumulative volume leaving the detention basin, V_{out} , is estimated by

$$V_{out} = kQ_{out}t_D \quad (15.4.8)$$

where V_{out} is in $\text{ft}^3(\text{m}^3)$, Q_{out} is the maximum outflow rate, ft^3/s (m^3/s), and k is an outflow adjustment coefficient from Figure 15.4.9 ($Q_{pin} = CiA$). The FAA procedure assumes a constant outflow rate Q_{out} , which is the rate of discharge when the detention basin is full. Because discharge increases with depth of water, the outflow adjustment factor is used. The required detention volume is computed using

$$V_{req} = \max(V_{in} - V_{out}) \quad (15.4.9)$$

which states that the required storage volume is the maximum difference between the cumulative inflow and the cumulative outflow volume.

15.4.3.1 Modified Rational Method

The *modified rational method* can be used to determine the preliminary design, which is the detention pond volume requirement for contributing drainage areas of 30 acres or less (Chow, et al. 1988). For larger contributing areas, a more detailed rainfall-runoff analysis with a detention basin flow routing procedure should be used. The modified rational method is an extension of the

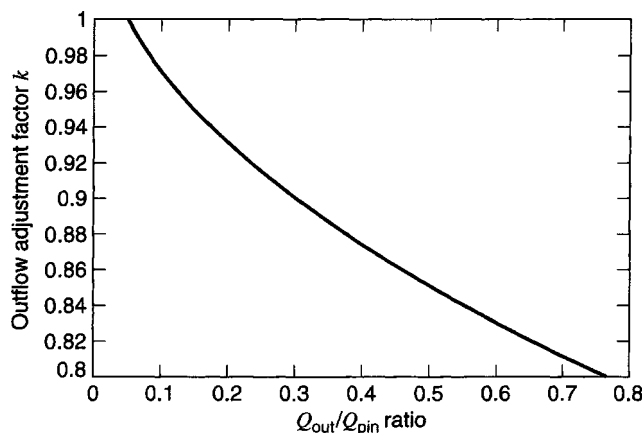


Figure 15.4.9 Outflow adjustment factor versus outflow rate/inflow peak ratio (from Urbonas and Roesner (1993)).

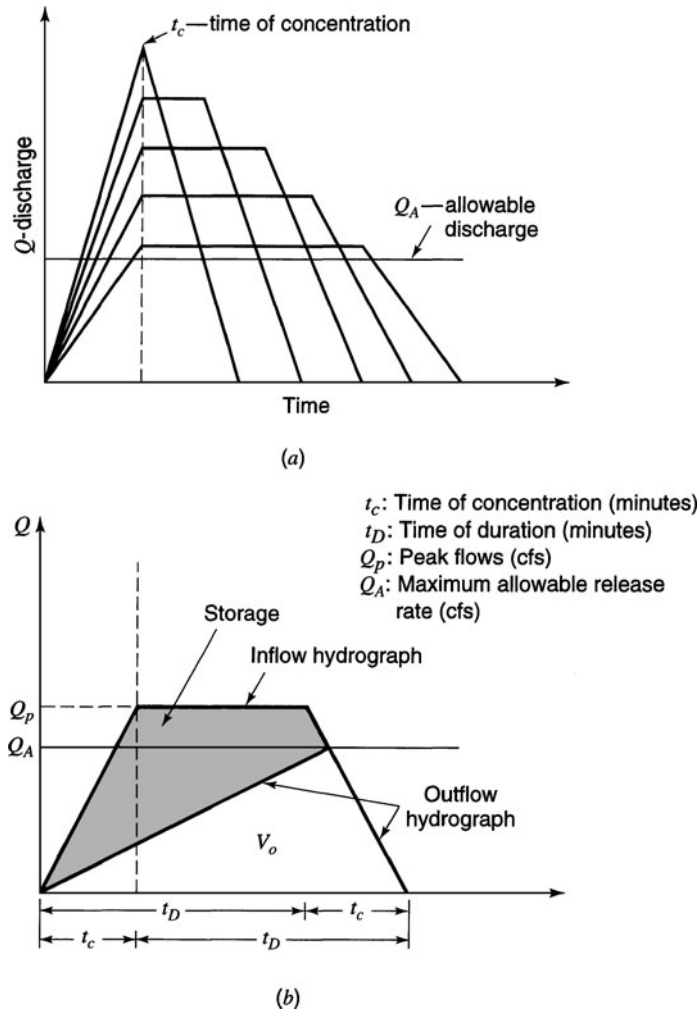


Figure 15.4.10 Modified rational method hydrographs. (a) Hydrographs for different durations; (b) Storage requirement.

rational method to develop hydrographs for storage design, rather than only peak discharges for storm sewer design. The shape of hydrographs produced by the modified rational method is either triangular or trapezoidal, constructed by setting the duration of the rising and recession limbs equal to the time of concentration t_c and computing the peak discharge assuming various durations. Figure 15.4.10a illustrates hydrographs drawn using the modified rational method.

An allowable discharge Q_A from a proposed detention basin can be the requirement that the peak discharge from the pond be equal to the peak of the runoff hydrograph for predeveloped conditions. The required detention storage V_s for each rainfall duration can be approximated as the cumulative volume of inflow minus the outflow, as shown in Figure 15.4.10b.

The assumptions of the modified rational method include:

1. The same assumptions as the rational method.
2. The period of rainfall intensity averaging is equal to the duration of the storm.
3. Because the outflow hydrograph is either triangular or trapezoidal, the effective contributing drainage area increases linearly with respect to time.

An equation for the *critical storm duration*, that is, the storm duration that provides the largest storage volume, can be determined for small watersheds based upon the modified rational method. Consider a rainfall intensity-duration equation of the general form

$$i = \frac{a}{(t_D + b)^c} \quad (15.4.10)$$

where i is the average rainfall intensity (in/hr) for the specific duration and return period, t_D is the storm duration in minutes, and a , b , and c are coefficients for a specific return period and location. Consider the trapezoidal-shaped inflow hydrograph and outflow hydrograph in Figure 15.4.10.

Using the rational formula, the peak discharge can be expressed in terms of the storm duration:

$$Q_p = C_p i A = C_p \left(\frac{a}{(t_D + b)^c} \right) A \quad (15.4.11)$$

The inflow hydrograph volume V_i in ft^3 is expressed as

$$V_i = 60(0.5)Q_p[(t_D - t_c) + (t_D + t_c)] \quad (15.4.12)$$

where t_c is the time of concentration for proposed conditions. The outflow hydrograph volume V_0 in ft^3 is expressed as

$$V_0 = 60(0.5)Q_A(t_D + t_c) \quad (15.4.13)$$

where Q_A is the allowable peak flow release in ft^3 . The storage volume V_s in ft^3 is computed using the above expressions for V_i and V_0 :

$$\begin{aligned} V_s &= V_i - V_0 = 60(0.5)Q_p[(t_D - t_c) + (t_D + t_c)] - 60(0.5)Q_A(t_D + t_c) \\ &= 60Q_p t_D - 30Q_A(t_D + t_c) \end{aligned} \quad (15.4.14)$$

The duration for the maximum detention is determined by differentiating equation (15.4.14) with respect to t_D and setting the derivative equal to zero:

$$\begin{aligned} \frac{dV_s}{dt_D} = 0 &= 60t_D + \frac{dQ_p}{dt_D} = 0 = 60t_D + 60Q_p - 30Q_A \\ &= 60t_D C_p A \frac{di}{dt_D} + 60C_p i A - 30Q_A \end{aligned} \quad (15.4.15)$$

where

$$\frac{di}{dt_D} = \frac{d}{dt_D} \left[\frac{a}{(t_D + b)^c} \right] = \frac{-ac}{(t_D + b)^{c+1}} \quad (15.4.16)$$

so

$$\frac{dV_s}{dt_D} = 0 = 60C_p A (-ac) \frac{t_D}{(t_D + b)^{c+1}} + 60C_p \left(\frac{a}{(t_D + b)^c} \right) A - 30Q_A \quad (15.4.17)$$

Simplifying results in

$$\frac{a[t_D(1-c) + b]}{(t_D + b)^{c+1}} - \frac{Q_A}{2C_p A} = 0 \quad (15.4.18)$$

t_D in equation (15.4.18) can be solved by using Newton's iteration technique (Appendix A) where the iterative equation is

$$t_{D_{i+1}} = t_{D_i} - \frac{F(t_{D_i})}{F'(t_{D_i})} \quad (15.4.19)$$

where

$$F(t_D) = \frac{a[t_D(1-c) + b]}{(t_D + b)^{c+1}} - \frac{Q_A}{2C_p A} \quad (15.4.20)$$

and

$$F'(t_{Di}) = \frac{d[F(t_{Di})]}{dt_D} = -\frac{a[t_D(1-c) + b](c+1)}{(t_D + b)^{c+2}} + \frac{a(1-c)}{(t_D + b)^{c+1}} \quad (15.4.21)$$

EXAMPLE 15.4.3

Determine the critical duration t_D and maximum detention storage for a 31.39-ac fully developed watershed with a runoff coefficient of $C_p = 0.95$. The allowable discharge is the predevelopment discharge of $Q_A = 59.08$ cfs. The time of concentration for proposed conditions is 21.2 min. The applicable rainfall intensity duration relationship is

$$i = \frac{97.86}{(t_D + 16.4)^{0.76}}$$

SOLUTION

The critical storm duration t_D can be obtained by solving equation (15.4.18) using Newton's iteration as stated in equation (15.4.19). From equation (15.4.20) we find

$$\begin{aligned} F(t_D) &= \frac{a[t_D(1-c) + b]}{(t_D + b)^{c+1}} - \frac{Q_A}{2C_p A} \\ &= \frac{a[t_D(1 - 0.76) + 16.4]}{(t_D + 16.4)^{1.76}} - \frac{59.08}{2(0.95)(31.39)} \\ &= \frac{97.86[0.24t_D + 16.4]}{(t_D + 16.4)^{1.76}} - 0.99 = \frac{23.49t_D + 1604.90}{(t_D + 16.4)^{1.76}} - 0.99 \end{aligned}$$

and from equation (15.4.21) we find

$$\begin{aligned} F'(t_D) &= -\frac{a[t_D(1-c) + b](1+c)}{(t_D + b)^{c+2}} + \frac{a(1-c)}{(t_D + b)^{c+1}} \\ &= -\frac{97.86[t_D(1 - 0.76) + 16.4](1 + 0.76)}{(t_D + 16.4)^{2.76}} + \frac{1 - 0.76}{(t_D + 16.4)^{1.76}} \\ &= -\frac{97.86(1.76)[0.24t_D + 16.4]}{(t_D + 16.4)^{2.76}} + \frac{97.86(0.24)}{(t_D + 16.4)^{1.76}} \\ &= \frac{41.34t_D + 2824.63}{(t_D + 16.4)^{1.76}} + \frac{23.49}{(t_D + 16.4)^{1.76}} \end{aligned}$$

With Newton's algorithm, the value of t_D converges to 92.0 min. Next use equation (15.4.11):

$$Q_p = C_p \left[\frac{a}{(t_D + b)^c} \right] A = 0.95 \left(\frac{97.86}{(92.0 + 16.4)^{0.76}} \right) (31.39) = 82.89 \text{ cfs}$$

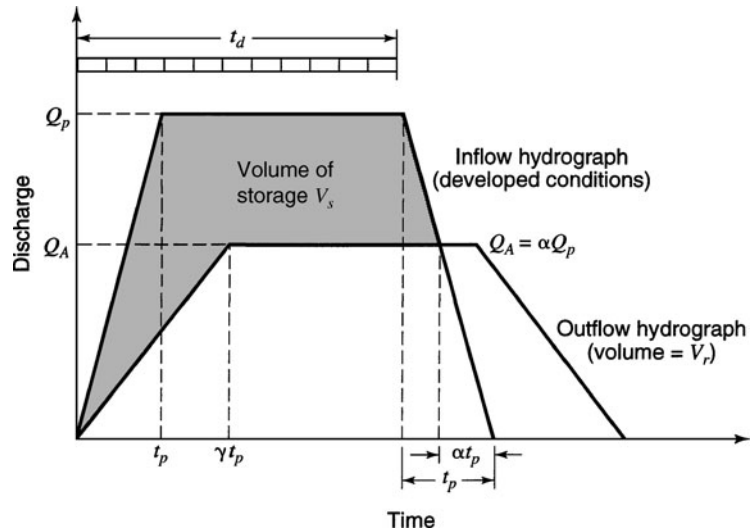


Figure 15.4.11 Inflow and outflow hydrographs for detention design. The outflow hydrograph is based on the inflow hydrograph for predeveloped conditions or on other more restrictive outflow criteria (from Donahue et al. (1981)).

Then use equation (15.4.14) to compute the detention storage:

$$\begin{aligned} V_s &= 60Q_p t_D - 30Q_A(t_D + t_c) = 60(82.89)(92.0) - 30(59.08)(92.0 + 21.2) \\ &= 256,917 \text{ ft}^3 = 5.90 \text{ ac-ft} \end{aligned}$$

Figure 15.4.11 is a representation of inflow and outflow hydrographs for a detention basin design. In this figure, α is the ratio of the peak discharge before development Q_A (or peak discharge from the detention basin that is allowable), and the peak discharge after development, Q_p :

$$\alpha = \frac{Q_A}{Q_p} \quad (15.4.22)$$

The ratio of the times to peak in the two hydrographs is γ . V_r is the volume of runoff after development. The volume of storage V_s needed in the basin is the accumulated volume of inflow minus outflow during the period when the inflow rate exceeds the outflow rate, shown shaded in the figure.

Using the geometry of the trapezoidal hydrographs, the ratio of the volume of storage to the volume of runoff V_s/V_r can be determined (Donahue, et al. 1981) as:

$$\frac{V_s}{V_r} = 1 - \alpha \left[1 + \frac{t_p}{t_D} \left(1 - \frac{\gamma + \alpha}{2} \right) \right] \quad (15.4.23)$$

where t_D is the duration of the precipitation and t_p is the time to peak of the inflow hydrograph.

Consider a rainfall intensity-duration relationship of the form

$$i = \frac{a}{t_D + b} \quad (15.4.24)$$

where i is rainfall intensity and a and b are coefficients. The volume of runoff after development is equal to the volume under the inflow hydrograph:

$$V_r = Q_p t_D \quad (15.4.25)$$

The volume of storage is determined by substituting (15.4.25) into (15.4.23) and rearranging to get

$$V_s = Q_p t_D \left\{ 1 - \alpha \left[1 + \frac{t_p}{t_D} \left(1 - \frac{\gamma + \alpha}{2} \right) \right] \right\} \quad (15.4.26)$$

$$= t_D Q_p - Q_A t_D - Q_A t_p + \frac{\gamma Q_A t_p}{2} + \frac{Q_A^2 t_p}{2} \frac{1}{Q_p} \quad (15.4.27)$$

where α has been replaced by Q_A/Q_p .

The duration that results in the maximum detention is determined by substituting $Q_p = CiA = CAa/(t_D + b)$, then differentiating (15.4.27) with respect to t_D and setting the derivative equal to zero:

$$\frac{dV_s}{dt_D} = 0 = t_D \frac{dQ_p}{dt_D} + Q_p - Q_A + \frac{Q_A^2 t_p}{2} \left[\frac{d(1/Q_p)}{dt_D} \right] = \frac{bCAa}{(t_D + b)^2} - Q_A + \frac{Q_A^2 t_p}{2CAa}$$

where it is assumed that Q_A , t_p , and γ are constants. Solving for t_D ,

$$t_D = \left(\frac{bCAa}{Q_A - \frac{Q_A^2 t_p}{2CAa}} \right)^{1/2} - b \quad (15.4.28)$$

The time to peak t_p is set equal to the time of concentration.

EXAMPLE 15.4.4

Determine the maximum storage for a detention pond on a 25-ac watershed for which the developed runoff coefficient is 0.8; the time of concentration before development is 25 min and after development 15 min. The allowable discharge is 25 cfs, and $a = 96.6$ and $b = 13.9$.

SOLUTION

The maximum storage is determined using equation (15.4.27) with allowable discharge $Q_A = 25$ cfs, $t_p = 15$ min (developed condition), $C = 0.8$ (developed condition), $a = 96.6$, and $b = 13.9$. First determine the critical duration t_D using equation (15.4.28).

$$t_D = \left[\frac{(13.9)(0.8)(25)(96.6)}{25 - \left((25)^2(15)/2(0.8)(25)(96.6) \right)} \right]^{1/2} - 13.9 = 20.59 \text{ min}$$

The peak discharge is $Q_p = CiA$. Then using equation (15.4.24) and $i = a/(t_D + b)$, with $t_D = 20.59$ min, we get

$$Q_p = CA \left(\frac{a}{t_D + b} \right) = 0.8(25) \left(\frac{96.6}{20.59 + 13.9} \right) = 56.01 \text{ cfs}$$

The maximum storage is then

$$\begin{aligned} V_s &= t_D Q_p - Q_A t_D - Q_A t_p + \frac{\gamma Q_A t_p}{2} + \frac{Q_A^2 t_p}{2} \frac{1}{Q_p} \\ V_s &= (20.59)(56.01) - (25)(20.59) - (25)(15) + \frac{(25/15)(25)(15)}{2} + \frac{(25)^2(15)}{2} \frac{1}{56.01} \\ &= 659.81 \text{ cfs}(\text{min} \times 60 \text{ s/min} = 39,588 \text{ ft}^3) \end{aligned}$$

15.4.3.2 Hydrograph Design Methods

A simple design procedure for sizing detention basins is now outlined that is useful in practice.

1. Determine the watershed characteristics and location of the detention basin.
2. Determine the design inflow hydrograph to the detention basin using a rainfall-runoff model.

3. Determine the detention storage-discharge relationship.
 - a. Determine the storage-elevation relationship.
 - b. Determine the discharge-elevation relationship for the discharge structure (culvert, spillway, etc.).
 - c. Using the above relationships, develop the storage-discharge relationship.
4. Perform the computations described in Chapter 9 or section 15.4.4 for routing the inflow hydrograph through the detention basin using hydrologic reservoir routing.
5. Once the routing computations are completed, the reduced peak can be checked to see that the reduction is adequate and also to check the delay of the peak outflow.
6. Steps 3(b) through 5 of this procedure can be repeated for various discharge structures.

15.4.4 Detention Basin Routing

The hydrograph design method presented in section 15.4.3 requires routing of a design inflow hydrograph through the detention/retention basin. The level pool routing can be accomplished using the procedure in Chapter 9. An alternative procedure is presented in this section that does not require development of the storage outflow function. This method, presented in Chow et al. (1988), is based upon the Runge–Kutta method (Carnahan, et al., 1969). It is a third-order scheme which breaks the time interval into three time increments and computes the water surface elevation and reservoir discharge for each increment.

Continuity is expressed as

$$\frac{dS}{dt} = I(t) - Q(H) \quad (15.4.29)$$

where S is the storage volume in the detention pond, $I(t)$ is the inflow into the pond as a function of time, t , and $Q(H)$ is the discharge from the pond as a function of the head or elevation H in the pond. The change in storage dS due to a change in elevation dH is

$$dS = A(H)dH \quad (15.4.30)$$

where $A(H)$ is the water surface area at elevation H . Substitution of this expression for dS into equation (15.4.29) and rearranging gives

$$\frac{dH}{dt} = \frac{I(t) - Q(H)}{A(H)} \quad (15.4.31)$$

which is an implicit differential equation.

Equation (15.4.31) is solved at each time step using three approximations of ΔH , ΔH_1 , ΔH_2 , and ΔH_3 at times t_j , $t_j + \Delta t/3$, and $t_j + 2\Delta t/3$, respectively. These approximations of ΔH are

$$\Delta H_1 = \left[\frac{I(t_j) - Q(H_j)}{A(H_j)} \right] \Delta t \quad (15.4.32)$$

$$\Delta H_2 = \left[\frac{I\left(t_j + \frac{\Delta t}{3}\right) - Q\left(H_j + \frac{\Delta H_1}{3}\right)}{A\left(H_j + \frac{\Delta H_1}{3}\right)} \right] \Delta t \quad (15.4.33)$$

$$\Delta H_3 = \left[\frac{I\left(t_j + \frac{2\Delta t}{3}\right) - Q\left(H_j + \frac{2\Delta H_2}{3}\right)}{A\left(H_j + \frac{2\Delta H_2}{3}\right)} \right] \Delta t \quad (15.4.34)$$

The value of H_{j+1} at time $t_{j+1} = t_j + \Delta t$ is

$$H_{j+1} = H_j + \Delta H \quad (15.4.35)$$

where

$$\Delta H = \frac{\Delta H_1}{4} + \frac{3\Delta H_3}{4} \tag{15.4.36}$$

This procedure requires the relationship of $Q(H)$ and $A(H)$ and the design detention pond inflow hydrograph.

EXAMPLE 15.4.5

Consider a 2-ac detention basin with vertical walls. The triangular inflow hydrograph increases linearly from zero to a peak of 540 cfs at 60 min and then decreases linearly to a zero discharge at 180 min. Route the inflow hydrograph through the detention basin using the head-discharge curve. Assuming the basin is initially empty, use the third-order Runge–Kutta method, with a 20-min time interval to determine the maximum depth.

Elevation (H , ft)	0.0	0.5	1.0	1.5	2.0	2.5	3.0
Discharge (Q , ft ³ /s)	0.0	3.0	8.0	17	30	43	60
Elevation (H , ft)	3.5	4.0	4.5	5.0	5.5	6.0	6.5
Discharge (Q , ft ³ /s)	78	97	117	137	156	173	190
Elevation (H , ft)	7.0	8.0	9.0	10	11	12	
Discharge (Q , ft ³ /s)	205	231	253	275	323	340	

SOLUTION

The function $A(H)$ relating the water surface area to the reservoir elevation is simply $A(H) = 2(43,560) \text{ ft}^2 = 87,120 \text{ ft}^2$. For all values of H , the reservoir has a base area of 2 ac and vertical sides. The routing procedure begins with determination of $I(0)$, $I(0 + 20/3)$, and $I[0 + (2/3) \times 20]$, which are determined by linear interpolation of values between 0 and $540/3 = 180$ cfs, so they are respectively 0, 60, and 120 cfs.

Next ΔH_1 is computed using equation (15.4.32) with $\Delta t = 20 \text{ min} = 1200 \text{ s}$, $A = 87,120 \text{ ft}^2$, and $I(0) = 0$ cfs. The reservoir is initially empty, so $H_1 = 0$ and $Q(H_1) = 0$, and thus $\Delta H_1 = [(0 - 0)/87,120] \times 1200 = 0$. For the next $I(0 + 20/3) = 60 \text{ ft}^3/\text{s}$, $\Delta H_2 = [(60 - 0)/87,120] \times 1200 = 0.826 \text{ ft}$, and $\Delta H_3 = [(120 - 3.507)/87,120](1200) = 1.605 \text{ ft}$, so

$$H_2 = H_1 + \frac{\Delta H_1}{4} + \frac{3}{4}\Delta H_3 = 0 + \frac{0}{4} + \frac{3}{4}(1.605) = 1.204 \text{ ft}$$

and by linear interpolation $Q(1.204) = 11.672$ cfs.

In the next iteration, $\Delta H_1 = [(180 - 11.66)/87,120](1200) = 2.319$

$$Q\left(1.204 + \frac{2.319}{3}\right) = 29.402 \text{ cfs}$$

$\Delta H_2 = [(240 - 29.402)/87,120]1200 = 2.901$, etc.

The routing computations are summarized in Table 15.4.1. The maximum depth in the pond is 12 ft.

15.4.5 Subsurface Disposal of Stormwater

Subsurface practices (infiltration practices) can be categorized as follows:

Infiltration practices:

- Swales and filter strips
- Porous pavement
- Infiltration trenches (Figure 15.4.16)
- Infiltration basins (Figure 15.4.17)

Table 15.4.1 Routing Computation for Example 15.4.5

Time (min)	Inflow (cfs)	ΔH_1 (ft)	ΔH_2 (ft)	ΔH_3 (ft)	ΔH (ft)	Depth (H) (ft)	Outflow (cfs)
0	0	—	—	—	0	0	0
20	180	0	0.826	1.605	1.203	1.204	11.66
40	360	2.319	2.901	3.237	3.008	4.137	102.48
60	540	3.506	3.699	3.921	3.818	8.152	234.34
80	450	4.247	2.992	1.982	2.549	11.124	325.11
100	360	2.029	0.864	0.061	0.553	12.087	341.48
120	270	0.479	-0.385	-1.059	-0.675	11.743	335.63
140	180	-0.370	-1.115	-1.634	-1.318	10.393	293.91
160	90	-1.047	-1.768	-2.340	-2.017	8.565	243.43
180	0	-1.627	-2.240	-2.628	-2.378	6.222	180.55

- Recharge wells (Figures 15.4.18–15.4.20)
- Underground storage (Figures 15.4.21–15.4.22)

15.4.5.1 Infiltration Practices

First the various types of infiltration practices are discussed. *Swales* are shallow vegetated trenches with nearly flat longitudinal slopes and mild side slopes. *Filter strips* are strips of land that stormwater must flow across before entering a conveyance system. These practices allow some of the runoff to infiltrate into the soil and filter the flow, removing some of the suspended solids and other pollutants attached to the solids. They also have the effect of reducing the directly connected impervious area and reducing the runoff velocity. They can be used for stormwater runoff from streets, parking lots, and roofs.

Wanielista et al. (1988) used mass balance of input and output water in swale systems to develop the following estimate of the length of a swale necessary to infiltrate all the input and rainfall excess from a specific storm event for a trapezoidal cross-sectional shape:

$$L = \frac{K\bar{Q}^{5/8}S^{3/16}}{n^{3/8}f} \quad (15.4.37)$$

where L is the length of the swale in feet (m), \bar{Q} is the average runoff flow rate, ft^3/s (m^3/s), S is the longitudinal slope, ft/ft (m/m), n is the Manning roughness coefficient for overland flow (Tables 15.4.2 and 15.4.3), f is the infiltration rate, in/h (cm/h), and K is a constant that is a function of the side slope parameter Z (1 vertical/ Z horizontal), as listed in Table 15.4.4.

Swales should be as flat as possible to maximize infiltration and to minimize resuspension of solids caused by high-flow velocities. Table 15.4.2 lists maximum or permissible velocities to reduce erosion or resuspension. The swale volume V_{swale} , for situations in which the available land is not long enough to infiltrate all the runoff, can be estimated using

$$V_{\text{swale}} = V_r - V_f \quad (15.4.38)$$

where V_{swale} is the volume of the swale (m^3), V_r is the volume of runoff (m^3), and V_f is the volume of infiltration (m^3). V_f can be derived using

$$V_f = \bar{Q}t_r \quad (15.4.39)$$

where \bar{Q} is the average infiltration flow rate in ft^3/s (m^3/s) (see equation (15.4.38)) and t_r is the runoff hydrograph time, seconds. With $\bar{Q} = [(Ln^{3/8}f)/(KS^{3/16})]^{8/5}$ from equation (15.4.37), the volume of swale is

$$V_{\text{swale}} = V_r - \left[\frac{Ln^{3/8}f}{KS^{3/10}} \right]^{8/5} t_r \quad (15.4.40)$$

Table 15.4.2 Maximum Permissible Design Velocities to Prevent Erosion and Manning’s *n* for Swales

Cover	Manning’s <i>n</i> for <i>vR</i> : ^a			Slope range (%)	Maximum permissible Velocity (ft/s)
	0.1	1.0	10		
Tufcote, Midland, and coastal Bermuda grass	0.25	0.150	0.045	{ 0.0–5.0 5.1–10.0 Over 10.0	6.0
					5.0
					4.0
Reed canary grass	0.40	0.250	0.070	{ 0.0–5.0 5.1–10.0 Over 10.0	5.0
Kentucky 31 tall fescue	0.40	0.250	0.070		4.0
Kentucky bluegrass (mowed)	0.10	0.055	0.030		3.0
Red fescue and Argentine Bahia	0.10	0.055	0.030	0.0–5.0	2.5
Annuals ^b and ryegrass	0.10	0.050	0.030	0.0–5.0	2.5

^aProduct of velocity and hydraulic radius (ft²/s).

^bAnnuals—use only as temporary protection until permanent vegetation is established.

Source: As presented in Wanielista and Yousef (1992).

Table 15.4.3 Overland Flow Manning’s *n* Values for Shallow Row (*vR* < 1.0)^a

	Recommended value	Range of values
Concrete	0.011	0.01–0.013
Asphalt	0.012	0.01–0.015
Bare sand	0.010	0.010–0.016
Graveled surface	0.012	0.012–0.030
Bare clay-loam (eroded)	0.012	0.012–0.033
Fallow (no residue)	0.05	0.006–0.16
Plow	0.06	0.02–0.10
Range (natural)	0.13	0.01–0.32
Range (clipped)	0.08	0.02–0.24
Grass (bluegrass sod)	0.45	0.39–0.63
Short grass prairie	0.15	0.10–0.20
Dense grass	0.24	0.17–0.30
Bermuda grass	0.41	0.30–0.48

^aThese values were determined specifically for overland flow conditions and are not appropriate for conventional open-channel flow calculations.

Source: As presented in Wanielista and Yousef (1993).

EXAMPLE 15.4.6

Determine the length of a swale needed to infiltrate an average runoff flow rate of 0.003 m³/s. The trapezoidal-shaped swale has a slope of 0.02, a Manning *n* = 0.05, an infiltration rate of 10 cm/h, and side slope of 1 vertical to *Z* = 5 horizontal.

SOLUTION

Equation (15.4.37) is used to determine the required length of the swale with *K* = 54,000 from Table 15.4.4 for *Z* = 5:

$$L = \frac{K\bar{Q}^{5/8}S^{3/16}}{n^{3/8}f} = \frac{54,000(0.003)^{5/8}(0.02)^{3/16}}{(0.05)^{3/8}(10)} = 211 \text{ m}$$

Table 15.4.4 Swale Length Formula Constant

Z (side slope) (1 vertical/Z horizontal)	K (SI units) ($i = \text{cm/h}$, $Q = \text{m}^3/\text{s}$)	K (U.S. units) ($i = \text{in/h}$, $Q = \text{ft}^3/\text{s}$)
1	98,100	13,650
2	85,400	11,900
3	71,200	9,900
4	61,200	8,500
5	54,000	7,500
6	48,500	6,750
7	44,300	6,150
8	40,850	5,680
9	38,000	5,255
10	35,760	4,955

Source: Wanielista and Yousef (1993).

EXAMPLE 15.4.7

For the situation in example 15.4.6, only 100 m of swale was needed. How much storage volume is required for a runoff time of 120 min?

SOLUTION

Equation (15.4.40) is solved for V_{swale} with the volume of runoff $V_r = (0.003)(60)(120) = 21.6 \text{ m}^3$:

$$V_{\text{swale}} = V_r - \left[\frac{Ln^{3/8}f}{KS^{3/10}} \right]^{8/5} t_r = 21.6 - \left[\frac{100(0.05)^{3/8}(10)}{54,000(0.02)^{3/16}} \right]^{8/5} (60)(120)$$

$$= 21.6 \text{ m}^3 - 6.5 \text{ m}^3$$

$$V_{\text{swale}} = 15.1 \text{ m}^3 \text{ of storage required}$$

Porous pavement and *modular pavement* (modular porous block pavement) can be used in parking areas to help reduce the amount of land needed for runoff quality control.

Percolation (or *infiltration*) *trenches* include both open surface type and underground (covered) trenches. Figure 15.4.12 illustrates infiltration trenches for perforated storm sewers and parking lot drainage. The perforated pipe allows distribution of stormwater along the entire length of the trench.

Perforated pipes allow the collection of sediment before it enters the aggregate backfill. Trenches are particularly suited for rights-of-way, parking lots, easements, and other areas with limited space. Their advantages are that they can be placed in narrow bands and in complex alignments. Prevention of excessive silt from entering the aggregate backfill and thus clogging the system is a major concern in design and construction. Sediment traps, filtration manholes, deep catch-basins, synthetic fibercloths, and the installation of filter bags in catch basins has proven effective (American Iron and Steel Institute, 1995).

Infiltration basins are retention facilities in which captured runoff is infiltrated into the ground. They are essentially depressions of varying size, either natural or excavated, into which stormwater is conveyed and allowed to infiltrate. Figure 15.4.13 illustrates an infiltration basin that serves the dual function of infiltration and storage. Infiltration basins are typically used in parks and urban open spaces, in highway rights-of-way, and in open spaces in freeway interchange loops. Infiltration basins are susceptible to clogging and sedimentation and can require large land areas. Standing water in these basins can create problems of security and insect breeding.

15.4.5.2 Recharge Wells

Recharge wells can be used to dispose of stormwater directly into the subsurface. Figure 15.4.14 illustrates a recharge well. Recharge wells can be used to remove standing water in areas that are difficult to drain. They can also be used in conjunction with infiltration basins to penetrate impermeable strata. Another use is as a bottomless catch basin in conventional minor system

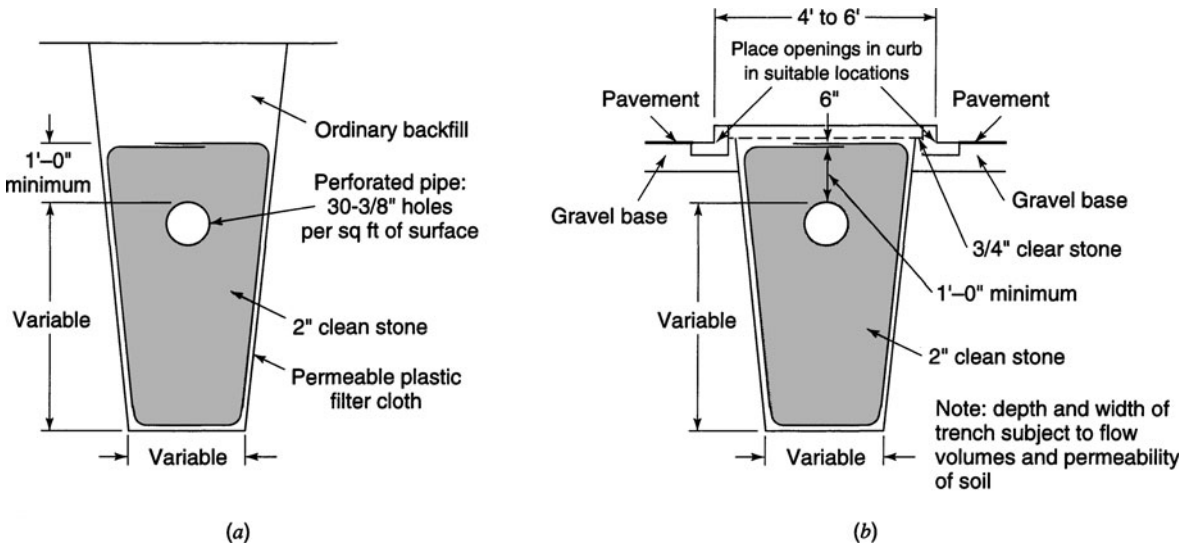


Figure 15.4.12 (a) Typical trench for perforated storm sewer; (b) Typical trench for parking lot drainage (from American Iron and Steel Institute (1995)).

design. Typically, recharge wells are used for small areas and can be combined with catch basins as illustrated in Figure 15.4.15. Figure 15.4.16 illustrates the use of a filter manhole in conjunction with a recharge well, in order to prevent excess silt entering the recharge well and causing clogging.

15.4.5.3 Underground Storage

Underground storage can be effective where surface ponds are not permitted or feasible. These storage tanks can be either *in-line*, in which the storage is incorporated directly into the sewer

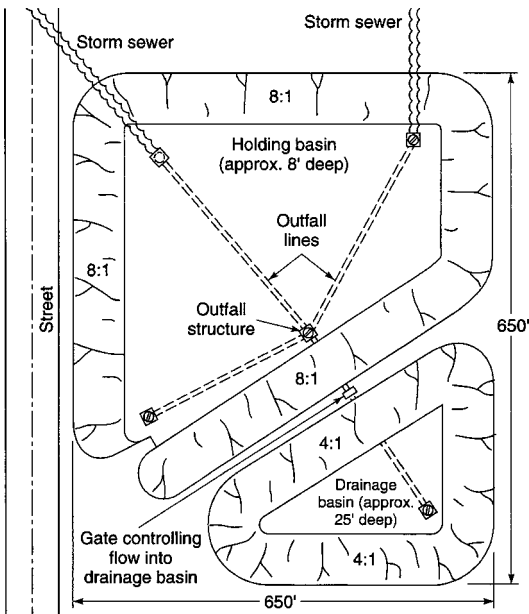


Figure 15.4.13 Infiltration basin (from American Iron and Steel Institute (1995)).

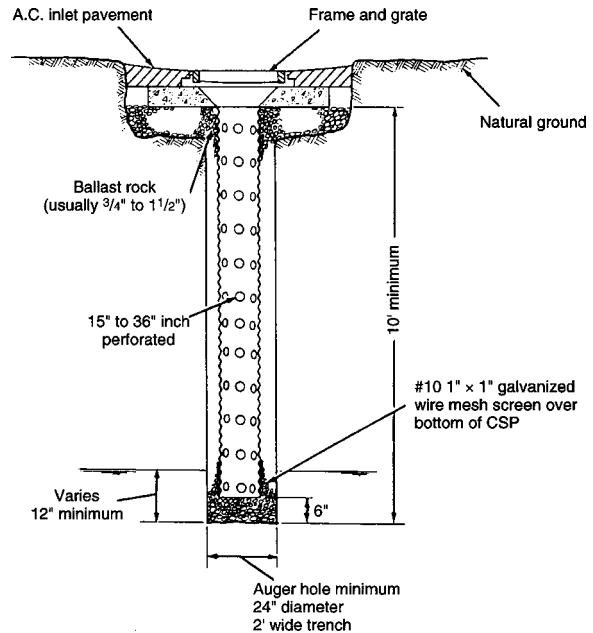


Figure 15.4.14 Recharge well (from American Iron and Steel Institute (1995)).

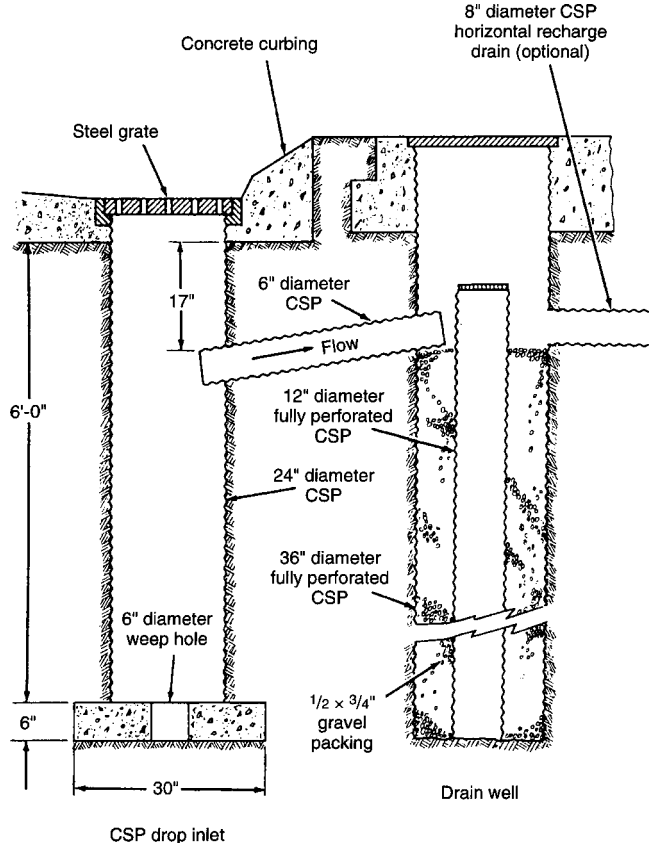


Figure 15.4.15 Typical design for combination catch basin for sand and sediment and recharge well. Catch basin would be periodically cleaned, and recharge well jetted through lower pipe to flush silt and restore permeability (from American Iron and Steel Institute (1995)).

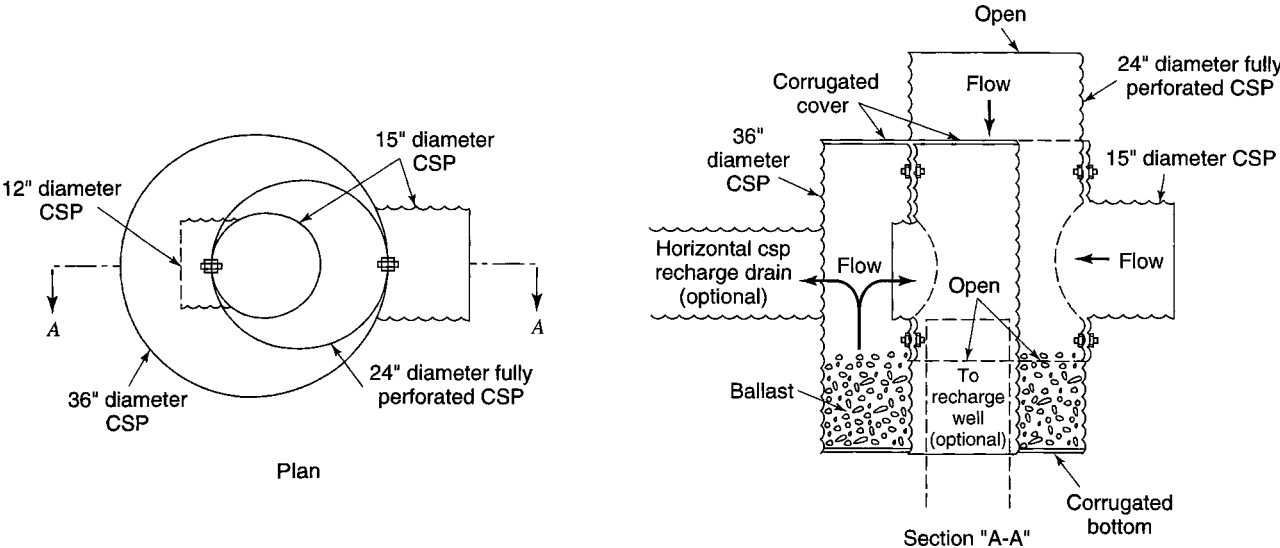


Figure 15.4.16 Typical CSP “Filter Manhole” (from American Iron and Steel Institute (1995)).

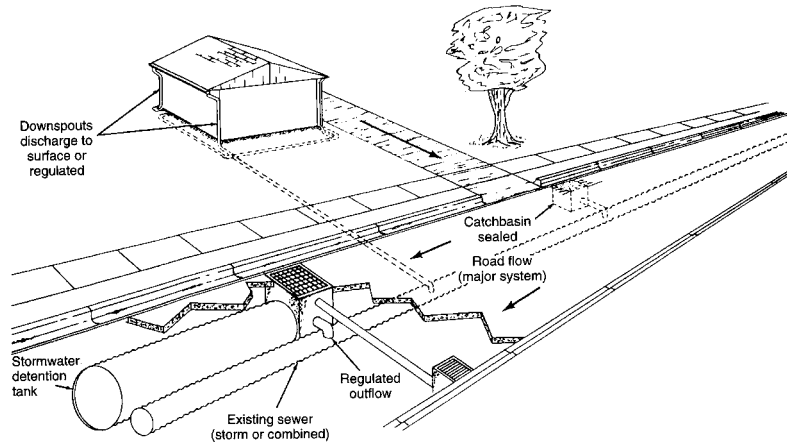


Figure 15.4.17 Inlet control system (from American Iron and Steel Institute (1995)).

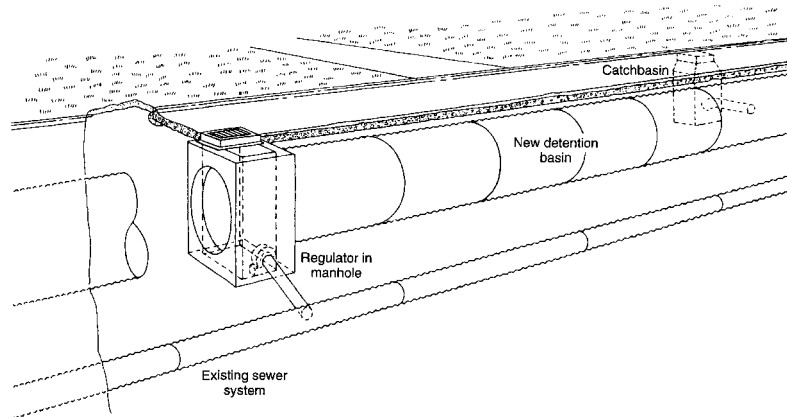


Figure 15.4.18 Typical installation of regulator for underground storage (from American Iron and Steel Institute (1995)).

system, or *off-line*, in which stormwater is collected before it enters the sewer system and then discharged to either the sewer system or an open water course at a controlled rate. When the capacity of an in-line system is exceeded, surcharging in the sewer can occur. Figure 15.4.17 illustrates an off-line underground stormwater detention tank with an inlet control system.

Figure 15.4.18 illustrates a typical installation of a regulator for underground storage. Flow regulators at inlets to storm sewers are effective in preventing storm sewer surcharging. The simplest form of a flow regulator is an orifice for which the opening has been sized for a given discharge at the maximum head. Regulators in Figure 15.4.18 are designed to handle a discharge that the sewer can handle without excessive surcharging.

PROBLEMS

15.2.1 Determine the pipe diameters for the storm sewer system in Figure P15.2.1a, which is located in Phoenix, Arizona. The rainfall-intensity-duration frequency relationship for the Phoenix

metro area is given in Figure P15.2.1b. Characteristics of the catchments are listed in Table P15.2.1. Use a return period of two years ($n = 0.014$).

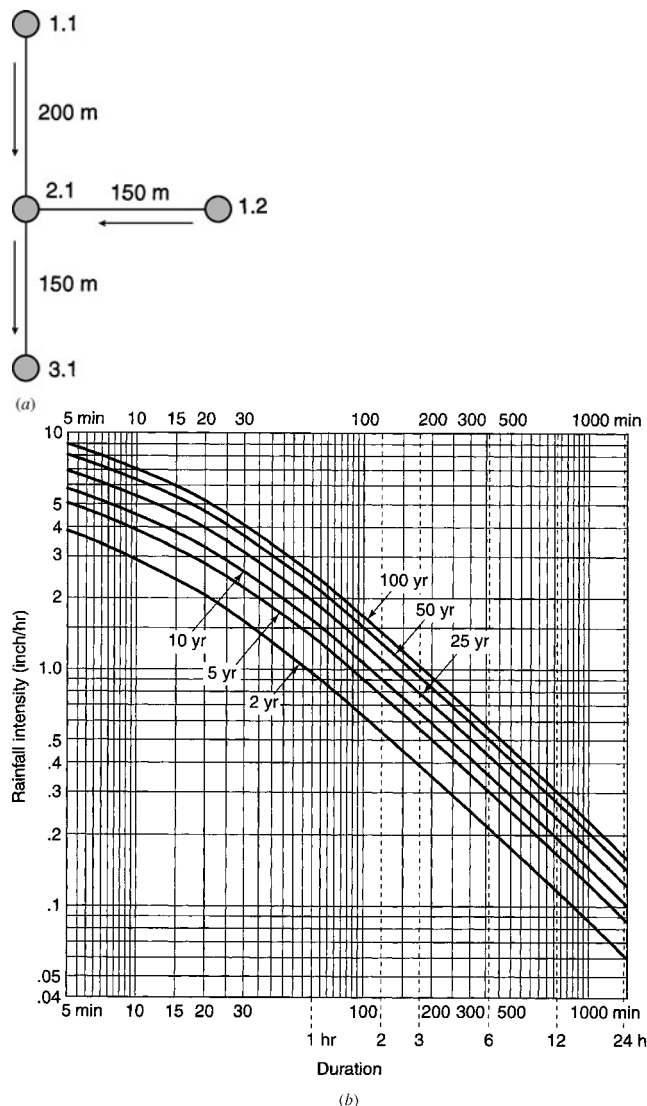


Figure P15.2.1 Rainfall intensity-duration-frequency relation (Phoenix metro area) (from Flood Control District of Maricopa County (1992a)).

Table P15.2.1 Catchment Characteristics, Problem 15.2.1

Catchment	Ground elevation (m)	Area (km ²)	Runoff coefficient	Inlet time (min)
1.1	300	0.01	0.60	25
1.2	298	0.008	0.75	20
2.1	296	0.005	0.80	15
3.1	294.5			

15.2.2 Rework problem 15.2.1 using a 10-year return period.

15.2.3 The simple storm sewer system below is to be designed using the following data. Assume the use of a 10-year frequency rainfall. The pipe is concrete with $n = 0.014$. Use Figure P15.2.1b for rainfall.

Manhole	Drainage area (ac)	Time of conc. (min)	C
1	2	15	0.5
2	3	20	0.8

Pipe	Slope (ft/ft)	Length (ft)
1–2	0.005	1000
2–3	0.006	800

15.2.4 Approximate the sudden expansion loss for a 600-mm sewer pipe connecting to a 700-mm sewer pipe for a design discharge of 0.5 m³/s.

15.2.5 Compute the bend loss for a 45° bend in a 500-mm sewer pipe with a discharge of 0.45 m³/s, assuming full-pipe flow. Assume $r/D = 2$.

15.2.6 Rework example 15.2.4 with $Q_L = 30$ cfs, $Q_u = 50$ cfs, and $Q_0 = 80$ cfs. The outfall pressure line elevation is 475.7 ft.

15.2.7 Determine the coefficient of variation of the loading and the capacity for the following parameters. Assume a uniform distribution to define the uncertainty of each parameters.

Parameter	Mode	Range
C	0.80	0.75–0.85
i	5.0 in/hr	4.5–5.5
A	10 acres	9.8–10.2
n	0.015	0.014–0.016
d	5 ft	4.98–5.02
S_0	0.0005	0.0004–0.0006

15.2.8 Rework example 15.2.5 using a triangular distribution to define the uncertainty of each parameter.

15.2.9 Using the results of problem 15.2.7, determine the risk of loading exceeding the capacity of the sewer pipe. Assume the use of a safety margin that is normally distributed.

15.2.10 Rework example 15.2.6 using a safety factor approach that is normally distributed; $SF = Q_c/Q_L$.

15.3.1 Design a nonerodible trapezoidal channel to carry a discharge of 6 m³/s. Use a Manning's $n = 0.025$ and a slope $S_0 = 0.0005$. Consider the best hydraulic section.

15.3.2 Design a concrete-lined trapezoidal channel to carry a discharge of 8 m³/s. A slope of $S_0 = 0.0001$ is to be used. Consider the best hydraulic section.

15.3.3 Design a concrete-lined rectangular channel to carry 25 ft³/s. A slope of $S_0 = 0.0001$ is to be used. Consider the best hydraulic section.

15.3.4 Design a gravel riprap-lined trapezoidal channel to carry a discharge of $11.33 \text{ m}^3/\text{s}$. Use a slope $S_0 = 0.0016$ and consider the best hydraulic section.

15.3.5 Design a gravel riprap-lined triangular channel to carry a discharge of $11.33 \text{ m}^3/\text{s}$. Use a slope $S_0 = 0.0016$ and consider the best hydraulic section.

15.3.6 Determine the value of Manning’s roughness factor for a grass-lined channel for dormant grass that has a slope of 0.015 m/m . The height of the grass is 200 mm and the hydraulic radius of the flow is 0.5 . Consider the grass to be erect.

15.3.7 Determine the value of Manning’s roughness factor for a grass-lined channel for green grass that has a slope of 0.015 m/m . The height of the grass is 200 mm and the hydraulic radius of the flow is 0.5 . Consider the grass to be erect.

15.3.8 Determine the value of Manning’s roughness factor for a grass-lined channel for dormant grass that has a slope of 0.015 m/m . The height of the grass is 200 mm and the hydraulic radius of the flow is 0.5 . Consider the grass to be flat.

15.3.9 Determine the value of Manning’s roughness factor for a grass-lined channel for green grass that has a slope of 0.015 m/m . The height of the grass is 200 mm and the hydraulic radius of the flow is 0.5 . Consider the grass to be flat.

15.3.10 Determine the value of Manning’s roughness factor for a grass-lined channel for dormant grass that has a slope of 0.0015 m/m . The height of the grass is 600 mm and the hydraulic radius of the flow is 0.5 . Compare the n -value for flat and erect grass.

15.3.11 Determine the value of Manning’s roughness factor for a grass-lined channel for green grass that has a slope of $.0015 \text{ m/m}$. The height of the grass is 600 mm and the hydraulic radius of the flow is 0.5 . Compare the n -value for flat and erect grass.

15.3.12 Design a trapezoidal channel that is to be excavated through a cohesive material (sandy clay with $< 50\%$ sand) that is very compact and has a permissible shear stress of 0.7 lb/ft^2 . The bottom slope of the excavated channel will be 0.0028 and the Manning’s roughness coefficient is 0.022 . Side slopes of the channel are $1:1$ (h:v) and the design discharge is 400 cfs .

15.3.13 Design a trapezoidal channel that is to be excavated through a noncohesive material (fine gravel) that has a permissible shear stress of 7.2 N/m^2 . The bottom slope of the excavated channel will be 0.00028 and the Manning’s roughness coefficient

is 0.025 . Side slopes of the channel are $3:1$ (h:v) and the design discharge is $11.5 \text{ m}^3/\text{s}$.

15.3.14 A trapezoidal channel is being designed using a Kentucky bluegrass lining. The bottom width of the channel is 20 ft and the bottom slope is 0.005 . Side slopes are $3:1$ (h:v). What is the maximum allowable discharge for this lining?

15.3.15 A trapezoidal channel is being designed using a grass-legume mixture lining with a stand of 4 to 5 in . The bottom width of the channel is 20 ft and the bottom slope is 0.005 . Side slopes are $3:1$ (h:v). What is the maximum allowable discharge for this lining? What would be the change in maximum allowable discharge if a grass-legume mixture lining with a stand of 6 to 8 in were used?

15.4.1 Rework example 15.4.1 with the flow peak limited to $30 \text{ ft}^3/\text{s}$.

15.4.2 Solve problem 15.4.1 using the Abt and Grigg (1978) method.

15.4.3 Solve example 15.4.3 using a runoff coefficient of $C_p = 0.85$ for a 15.24-ac watershed with $Q_A = 32.17 \text{ cfs}$.

15.4.4 Solve example 15.4.3 using a developed runoff coefficient of 0.80 .

15.4.5 Solve example 15.4.4 using a developed runoff coefficient of 0.85 .

15.4.6 Solve example 15.4.4 using a developed runoff coefficient of 0.95 .

15.4.7 Solve example 15.4.5 using the level pool routing procedure.

15.4.8 Solve example 15.4.5 using a time interval of 30 min .

15.4.9 Consider a 4047 m^2 (0.4047 ha) detention basin with vertical walls. The triangular inflow hydrograph increases linearly from zero to a peak of $10.2 \text{ m}^3/\text{s}$ at 60 min and then decreases linearly to zero at 150 min . The basin is initially empty and the discharge-elevation relationship is:

Elevation (H , m)	0.0	0.152	0.305	0.457	0.610	0.762	0.914	
Discharge (Q , m^3/s)	0.0	0.085	0.230	0.482	0.850	1.220	1.700	
Elevation (H , m)	1.067	1.219	1.524	1.830	2.134	2.438	2.743	3.048
Discharge (Q , m^3/s)	2.209	2.750	3.880	4.900	5.806	6.542	7.165	7.788

Use the Runge–Kutta method with a routing interval of 20 min to determine the detention basin discharge at the end of 20 min .

REFERENCES

Abt, S. R., and N. S. Grigg, “An Approximate Method for Sizing Retention Reservoirs,” *Water Resources Bulletin*, AWRA, vol. 14, no. 4, pp. 956–965, 1978.

Akan, A. O., “Detention Pond Sizing for Multiple Return Periods,” *Journal of Hydraulic Engineering*, vol. 115, no. 5, pp. 650–664, 1989.

Akan, A. O., “Single-Outlet Detention-Pond Analysis and Design,” *Journal of Irrigation and Drainage Engineering*, vol. 116, no. 4, pp. 527–536, 1990.

Akan, A. O., *Urban Stormwater Hydrology*, Technomic Publishing, Lancaster, PA, 1993.

American Association of State Highway and Transportation Officials (AASHTO), *Model Drainage Manual*, Washington, DC, 1991.

American Iron and Steel Institute, *Modern Sewer Design*, 3rd edition, Washington, DC, 1995.

American Society of Civil Engineers (ASCE) and Water Pollution Control Federation, *Design and Construction of Urban Stormwater*

- Management Systems*, ASCE Manual and Report of Engineering Practice no. 77, WEF Manual of Practice FD-20, New York, 1992.
- American Society of Civil Engineering (ASCE) and Water Pollution Control Federation (WPCF), *Design and Construction of Sanitary and Storm Sewers*, ASCE Manual of Practice no. 37 and WPCF Manual of Practice no. 9, 1969.
- Ang, A. H.-S., and W. H. Tang, *Probability Concepts in Engineering Planning and Design, I: Basic Principles*, John Wiley, New York, 1975.
- Ang, A. H.-S., and W. H. Tang, *Probability Concepts in Engineering Planning and Design, II: Decision, Risk, and Reliability*, John Wiley, New York, 1984.
- Aron, G., and C. E. Egborge, "A Practical Feasibility Study of Flood Peak Abatement in Urban Areas," report, U.S. Army Corps of Engineers, Sacramento District, Sacramento, CA, March 1973.
- Aron, G., and D. F. Kibler, "Pond Sizing for Rational Formula Hydrographs," *Water Resources Bulletin*, AWRA, vol. 26, no. 2, pp. 255–258, 1990.
- Bathurst, J. C., R. M. Li, and D. B. Simons, "Resistance Equation for Large-Scale Roughness," *Journal of the Hydraulics Division, ASCE*, vol. 107, no. HY12, pp. 1593–1613, 1981.
- Bennett, M. S., and L. W. Mays, "Optimal Design of Detention and Drainage Channel Systems," *Journal of the Water Resources Planning and Management Division, ASCE*, vol. III, no. 1, pp. 99–112, 1985.
- Carnahan, B., H. A. Luther, and J. O. Wilkes, *Applied Numerical Methods*, John Wiley, New York, 1969.
- Chen, Y. H., and G. K. Cotton, "Design of Roadside Channels with Flexible Linings," *Hydraulic Engineering Circular 15*, FHWA-IP-87-7, Federal Highway Administration, McLean, VA, 1988.
- Chow, V. T., D. R. Maidment, and L. W. Mays, *Applied Hydrology*, McGraw-Hill, New York, 1988.
- Cotton, G. K., "Hydraulic Design of Flood Control Channels," in *Hydraulic Design Handbook* edited by L. W. Mays, McGraw-Hill, New York, 1999.
- Donahue, J. R., R. H. McCuen, and T. R. Bondelid, "Comparison of Detention Basin Planning and Design Models," *Journal of the Water Resource Planning and Management Division, ASCE*, vol. 107, no. 2, pp. 385–400, 1981.
- Federal Aviation Administration, Department of Transportation, *Circular on Airport Drainage*, report A/C 050-5320-5B, Washington, DC, 1970.
- Federal Aviation Agency (FAA), *Airport Drainage*, Washington, DC, 1966.
- Federal Highway Administration (FHWA), "HYDRAIN—Integrated Drainage Design Computer System. Vol. III. HYDRA—Storm Drains," Structure Division, Federal Highway Administration, Washington, DC, 1993.
- Flood Control District of Maricopa County, *Drainage Design Manual for Maricopa County, Arizona*, vol. I-Hydrology, Phoenix, Arizona, 1992a.
- Flood Control District of Maricopa County, *Drainage Design Manual for Maricopa County, Arizona*, vol. II-Hydraulics, Phoenix, Arizona, 1992b.
- Frederick, R. H., V. A. Myers, and E. P. Auciello, "Five to 60-minute Precipitation Frequency for the Eastern and Central United States," NOAA Technical Memo NWS HYDRO-35, National Weather Service, Silver Spring, MD, June 1977.
- Great Lakes–Upper Mississippi River Board of State Sanitary Engineers, Ten-State Standards, "Recommended Standards for Sewage Works," Health Education Service, Albany, NY, 1978.
- Harr, M. E., *Reliability-Based Design in Civil Engineering*, McGraw-Hill, New York, 1987.
- Izzard, C. F., "Hydraulics of Runoff from Developed Surfaces," *Proc. Highway Research Board*, vol. 26, pp. 129–146, 1946.
- Kapur, K. C., and L. R. Lamberson, *Reliability in Engineering Design*, John Wiley, New York, 1977.
- Kececioglu, D., *Reliability Engineering Handbook*, vols. 1 and 2, Prentice-Hall, Englewood Cliffs, NJ, 1991.
- Kessler, A., and M. H. Diskin, "The Efficiency Function of Detention Reservoirs in Urban Drainage Systems," *Water Resources Research*, American Geophysical Union, vol. 27, no. 3, pp. 253–258, 1991.
- Kibler, D. F., *Urban Stormwater Hydrology*, Water Research Monograph 7, American Geophysical Union, Washington, DC, 1982.
- Kirpich, Z. P., "Time of Concentration of Small Agricultural Watersheds," *Civ. Eng.*, vol. 10, no. 6, p. 362, 1940.
- Kouwen, N., T. E. Unny, and H. M. Hill, "Flow Retardance in Vegetated Channels," *Journal of the Irrigation Division, ASCE*, vol. 95, no. IR2, pp. 329–342, 1969.
- Kouwen, N. and R. M. Li, "Biomechanics of Vegetated Channel Linings," *Journal of the Hydraulics Division, ASCE*, vol. 106, pp. 1085–1103, 1980.
- Kouwen, N., "Field estimation of the Biomechanical Properties of Grass," *Journal of Hydraulic Research*, vol. 26, pp. 559–568, 1988.
- Loganathan, G. V., D. F. Kibler, and T. J. Grizzard, "Urban Stormwater Management," in *Water Resources Handbook* edited by L. W. Mays, McGraw-Hill, New York, 1996.
- Loganathan, G. V., J. W. Delleur, and R. I. Segana, "Planning Detention Storage for Stormwater Management," *Journal of Water Resources Planning and Management Division, ASCE*, vol. 111, no. 4, pp. 382–398, 1985.
- Loganathan, G. V., E. W. Watkins, and D. F. Kibler, "Sizing Stormwater Detention Basins for Pollutant Removal," *Journal of Environmental Engineering, ASCE*, vol. 120, no. 6, pp. 1380–1399, 1989.
- Mays, L. W., and P. B. Bedient, "Model for Optimal Size and Location of Detention Basins," *Journal of the Water Resources Planning and Management Division, ASCE*, vol. 108, no. WR3, pp. 220–285, 1982.
- Mays, L. W., and Y. K. Tung, *Hydrosystems Engineering and Management*, McGraw-Hill, New York, 1992.
- McEnroe, B. M., "Preliminary Sizing of Detention Reservoirs to Reduce Peak Discharges," *Journal of Hydraulic Engineering, ASCE*, vol. 118, no. 11, pp. 1450–1459, 1992.
- Morgali, J. R., and R. K. Linsley, "Computer Analysis of Overland Flow," *J Hyd. Div., Am. Soc. Civ. Eng.*, vol. 91, no. HY3, pp. 81–100, May 1965.
- Nix, S. J., and J. P. Heaney, "Optimization of Stormwater Storage—Release Strategies," *Water Resources Research*, vol. 24, no. 11, pp. 1831–1838, 1988.
- Overton, D. E., and M. E. Meadows, *Stormwater Modeling*, Academic Press, New York, 1976.
- Phillips, J. V., and T. L. Ingersoll, "Verification of Roughness Coefficients for Selected Natural and Constructed Stream Channels in Arizona," U.S. Geological Survey Professional Paper 1584, U.S. Geological Survey, Denver, CO, 1998.
- Sangster, W. M., H. M. Wood, E. T. Smerdon, and H. G. Bossy, "Pressure Changes at Storm Drain Junction," *Engineering Series Bulletin*, No. 41, Engineering Experiment Station, University of Missouri, Columbia, MO, 1958.
- Segarra, R. I., and G. V. Loganathan, "Stormwater Detention Storage Design Under Random Pollutant Loading," *Journal of Water Resources Planning and Management, ASCE*, vol. 118, no. 5, pp. 475–491, 1992.
- Stahre, P., and B. R. Urbonas, *Stormwater Detention for Drainage, Water Quality and CSO Management*, Prentice Hall, Englewood Cliffs, NJ, 1990.
- Taur, C. K., G. Toth, G. E. Oswald, and L. W. Mays, "Austin Detention Basin Optimization Model," *Journal of Hydraulic Engineering, ASCE*, vol. 113, no. 7, pp. 860–878, 1987.

U.S. Bureau of Reclamation (USBR), *Design of Small Dams*, 2nd Edition, U.S. Government Printing Office, Denver, CO, 1973.

U.S. Bureau of Reclamation (USBR), *Design of Small Dams*, 3rd Edition, U.S. Government Printing Office, Denver, CO, 1987.

U.S. Soil Conservation Service, "Urban Hydrology for Small Watersheds, Tech. Release 55," Washington, DC, 1975 (updated, 1986).

U.S. Soil Conservation Service, *Handbook of Channel Design for Soil and Water Conservation, SCS-TP-61*, Stillwater, OK, 1954.

Urbonas, B. R., and L. A. Roesner, "Hydrologic Design of Urban Drainage and Flood Control," *Handbook of Hydrology* edited by D. R. Maidment, McGraw-Hill, New York, 1993.

Wang, S. Y., and H. W. Shen, "Incipient Sediment Motion and Riprap Design," *Journal of the Hydraulics Division*, ASCE, vol. 111, no. 3, pp. 521–538, 1985.

Wanielista, M. P., and Y. A. Yousef, *Stormwater Management*, Wiley Interscience, New York, 1993.

Wanielista, M. P., Y. A. Yousef, and E. Avellaneda, *Alternatives for the Treatment of Groundwater Contaminants: Infiltration Capacity of Roadside Swales*, Florida DOT, Tallahassee, Florida, #FLER-38-88, April 1988.

Whipple, W., N. S. Grigg, T. Grizzard, C. W. Randall, R. P. Shubinski, and L. S. Tucker, *Stormwater Management in Urbanizing Areas*, Prentice-Hall, Englewood Cliffs, NJ, 1983.

Whipple, W., R. Kropp, and S. Burke, "Implementing Dual Purpose Stormwater Detention Program," *Journal of Water Resources Planning and Management*, ASCE, vol. 113, no. 6, pp. 779–792, 1987.

Wycoff, R. L., and V. P. Singh, "Preliminary Hydrologic Design of Small Flood Detention Reservoirs," *Water Resources Bulletin*, AWRA, vol. 12, no. 2, pp. 337–349, 1976.

Yen, B. C., and A. O. Akan, "Hydraulic Design of Urban Drainage Systems," in *Hydraulic Design Handbook* edited by L. W. Mays, McGraw-Hill, New York, 1999.

Yen, B. C., "Hydraulics for Excess Water Management," in *Water Resources Handbook* edited by L. W. Mays, McGraw-Hill, New York, 1996.

Yen, B. C., (editor), "Storm Sewer System Design," Department of Civil Engineering, University of Illinois at Urbana-Champaign, 1978.

Yen, B. C., (editor), *Stochastic and Risk Analysis in Hydraulic Engineering*, Water Resources Publications, Littleton, CO, 1986.

Chapter 16

Stormwater Control: Street and Highway Drainage and Culverts

16.1 DRAINAGE OF STREET AND HIGHWAY PAVEMENTS

This section discusses the removal of stormwater from street and highway pavement surfaces and median areas. The removal of stormwater from streets is accomplished by collecting overland flow in gutters and intercepting the gutter flow at inlets to storm sewers. The design objective for a drainage system (for a curbed highway pavement section) is to collect runoff in the gutter and convey it to inlets in order to provide reasonable safety for traffic and pedestrians at reasonable cost. This section is based on the Federal Highway Administration's Hydraulic Engineering Circular No. 12 (Johnson and Chang, 1984). Other references are Young et al. (1993) and Young and Stein (1999).

16.1.1 Design Considerations

In the design of highway pavement drainage, two of the more significant variables are the frequency of the runoff event for design and the spread of water (*design spread*) on the pavement during the design event. The following summarizes the major considerations in the selection of design frequency and design spread:

- Classification of the highway
- Design speed of the highway
- Projected traffic volumes
- Rainfall intensities
- Capital costs
- Hazards and nuisances to pedestrian traffic
- Relative elevation of the highway and surrounding terrain

For low-volume local roads when traffic volumes and speeds are low, a two-year recurrence interval and a spread of one-half or more of the traffic lane are minimum design standards. High-speed, high-volume roads, such as freeways, are designed to minimize or eliminate spread on the traffic lanes for the design event. A 10-year frequency and a spread limited to the shoulders is common. Federal Highway Administration policy requires a 50-year frequency for underpasses and depressed sections on interstate highways. The American Association of State Highway and Transportation Officials (AASHTO, 1991) provides the design storm guidelines listed in Table 16.1.1.

Table 16.1.1 Design Storm Selection Guidelines

Roadway classification	Exceedance probability	Return period
Rural principal arterial system	2%	50-year
Rural minor arterial system	4%–2%	25–50-year
Rural collector system, major	4%	25-year
Rural collector system, minor	10%	10-year
Rural local road system	20%–10%	5–10-year
Urban principal arterial system	4%–2%	25–50-year
Urban minor arterial street system	4%	25-year
Urban collector street system	10%	10-year
Urban local street system	20%–10%	5–10-year

Note: Federal law requires interstate highways to be provided with protection from the 2 percent flood event, and facilities such as underpasses, depressed roadways, etc., where no overflow relief is available should be designed for the 2 percent event.

The rational method (discussed in Section 15.2.2) is the most commonly used method for determining discharges for highway pavement drainage. The rational formula (equation (15.2.1)) is

$$Q = KCiA \tag{15.2.1}$$

where Q is the peak discharge, ft³/s (m³/s), K is 1.0 for U.S. customary units and 0.28 for SI units, C is the dimensionless runoff coefficient, i is the average rainfall intensity, in/hr (mm/hr) for a duration equal to the time of concentration and for a design recurrence interval, and A is the drainage area (km²).

The time of concentration for inlets consists of the overland flow time and the gutter flow time. If overland flow is channeled upstream of the inlet where flow enters the gutter, then the channel flow time must also be considered. Using the work by Ragan (1971), Johnson and Chang (1984) recommend the use of the following *kinematic wave equation*

$$t_c = \frac{KL^{0.6}n^{0.6}}{i^{0.4}S^{0.3}} \tag{16.1.1}$$

where t_c is the time of concentration in seconds; L is the overland flow length in feet (m); n is Manning’s roughness coefficient, i is the rainfall intensity, in/hr (m/hr); S is the average slope of the overland flow area; and $K = 56$ (26.285). To determine the flow time in a gutter, the average velocity in the gutter must be determined.

Young et al. (1993) developed an alternative method for selecting rainfall intensity that is not dependent on rainfall frequency. Instead this method uses incipient hydroplaning that causes drivers to slow down as opposed to traffic reaction due to gutter flooding. This method selects values of vehicle speed, tire tread depth, pavement texture, and tire pressure as well as calculates the thickness of the sheet flow film at incipient hydroplaning.

EXAMPLE 16.1.1

Use the kinematic wave formula to determine the time of concentration for a small drainage area that has a length of overland flow of 150 ft (45.72 m) and an average overland slope of 0.02 ft/ft (m/m) for a rainfall rate of 3.6 in/hr (0.091 m/hr). The drainage area is a turf ($n = 0.4$).

SOLUTION

Using the kinematic wave formula (equation 16.1.1), we find

$$t_c = \frac{KL^{0.6}n^{0.6}}{i^{0.4}S^{0.3}} = \frac{56(150)^{0.6}(0.4)^{0.6}}{(3.6)^{0.4}(0.02)^{0.3}} = 1265.5 \text{ s} = 21 \text{ min}$$

Alternatively, the time of concentration using the kinematic wave equation in SI units is

$$t_c = \frac{KL^{0.6}n^{0.6}}{i^{0.4}S^{0.3}} = \frac{26.285(45.72)^{0.6}(0.4)^{0.6}}{(0.091)^{0.4}(0.02)^{0.3}} = 1267.9 \text{ s} = 21 \text{ min}$$

EXAMPLE 16.1.2

Determine the time of concentration for an overland flow length of 100 m, on a turf surface ($n = 0.4$) with an average slope of 0.02. Use a rainfall rate of 10 cm/hr.

SOLUTION

Using equation (16.1.1) with $K = 26.285$, we get

$$t_c = \frac{KL^{0.6}n^{0.6}}{i^{0.4}S^{0.3}} = (26.285) \frac{(100)^{0.6}(0.4)^{0.6}}{(0.1)^{0.4}(0.02)^{0.3}} = \frac{(26.285)(15.85)(0.577)}{(0.398)(0.309)} = 1953.8 \text{ s} = 32.56 \text{ min}$$

Alternatively, in U.S. customary units,

$$t_c = \frac{56(328)^{0.6}(0.4)^{0.6}}{(3.98)^{0.4}(0.02)^{0.3}} = 1953.8 \text{ s} = 32.56 \text{ min}$$

16.1.2 Flow in Gutters

A *pavement gutter* conveys water during a storm event by collecting overland flow along its length and concentrating the flow as channel flow. Referring to Figure 16.1.1a, the elemental gutter flow dQ through an elemental cross-section dx of the gutter is

$$dQ = V dx \left(y + \frac{dy}{2} \right) \quad (16.1.2)$$

where V is the velocity in the elemental area and y is the flow depth. Using Manning's equation, we find

$$V = \frac{1.49}{n} \left(\frac{y dx + \frac{1}{2} dy dx}{\sqrt{dx^2 + dy^2}} \right)^{2/3} S^{1/2} \quad (16.1.3)$$

where n is Manning's roughness factor, S is the longitudinal slope of the gutter, and the term $()^{2/3}$ is the hydraulic radius. The slope of the overland flow plane (or cross-slope) is S_x , so that $\sqrt{dx^2 + dy^2} = dx \sqrt{1 + S_x^2}$ where $S_x = (dy/dx) = (d/T_w)$, so that

$$V = \frac{1.49}{n} \left(\frac{y dx + \frac{1}{2} dy dx}{dx \sqrt{1 + S_x^2}} \right)^{2/3} S^{1/2} \quad (16.1.4)$$

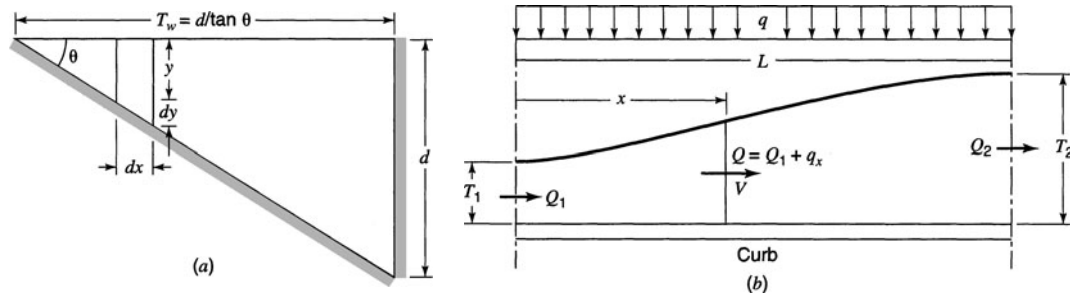


Figure 16.1.1 Pavement gutter flow. (a) Flow in triangular gutter; (b) Conceptual sketch of spatially varied gutter flow (from Johnson and Chang (1984)).

For small values of S_x , equation (16.1.4) can be approximated by

$$V = \frac{1.49}{n} \left(y + \frac{dy}{2} \right)^{2/3} S^{1/2} \quad (16.1.5)$$

Substituting equation (16.1.5) into equation (16.1.2) and assuming $\left(y + (dy/2) \right)^{5/3} = y^{5/3}$ results in

$$dQ = \frac{1.49}{n} y^{5/3} \frac{dy}{S_x} S^{1/2} \quad (16.1.6)$$

By integrating equation (16.1.6) across the cross-section of the gutter as y goes from 0 to d , the gutter flow can be expressed as

$$Q = \frac{0.56 S^{1/2}}{n S_x} d^{8/3} \quad (16.1.7)$$

The *spread* of water measured laterally from the curb is $T_w = d/\tan \theta = d/S_x$. Substituting $d = S_x T_w$ into equation (16.1.7), we can express the gutter flow in terms of the spread as

$$Q = \frac{0.56}{n} S^{1/2} S_x^{5/3} T_w^{8/3} \quad (16.1.8a)$$

or more generally as

$$Q = \left(\frac{\phi}{n} \right) S^{1/2} S_x^{5/3} T_w^{8/3} \quad (16.1.8b)$$

where ϕ is 0.56 (U.S. customary units) or 0.375 for SI units; Q is the discharge, ft^3/s (m^3/s); T_w is the top width of flow (spread) in feet (m); S_x is the cross-slope, ft/ft (m/m); and S is the longitudinal slope, ft/ft (m/m). Equation (16.1.8) neglects the resistance of the curb face, which is negligible if the cross-slope is 10 percent or less (Johnson and Chang, 1984).

Figure 16.1.1*b* is a conceptual sketch of spatially varied gutter flow. As previously mentioned, the gutter flow time can be estimated using the average velocity. An assumption is that the flow rate in the gutter varies uniformly from Q_1 at the beginning of the section to Q_2 at the inlet (refer to Figure 16.1.1*b*). Equation (16.1.8a) can be expressed as

$$Q = K_1 T_w^{8/3} \quad (16.1.9)$$

where

$$K_1 = \frac{0.56}{n} S^{1/2} S_x^{5/3} \quad (16.1.10a)$$

in U.S. customary units, or

$$K_1 = \frac{0.375}{n} S^{1/2} S_x^{5/3} \quad (16.1.10b)$$

in SI units. The velocity can be expressed as

$$V = K_2 T_w^{2/3} = \frac{1.12}{n} S^{1/2} S_x^{2/3} T_w^{2/3} \quad (16.1.11a)$$

in U.S. customary units, or

$$V = \frac{0.75}{n} S^{1/2} S_x^{2/3} T_w^{2/3} \quad (16.1.11b)$$

in SI units, where

$$K_2 = \frac{1.12}{n} S^{1/2} S_x^{2/3} \quad (16.1.12a)$$

in U.S. customary units, or

$$K_2 = \frac{0.75}{n} S^{1/2} S_x^{2/3} \quad (16.1.12b)$$

in SI units.

From equation (16.1.9), $T_w^{8/3} = (Q/K_1)$, so the velocity is

$$V = \frac{dx}{dt} = \frac{K_2}{K_1^{0.25}} Q^{0.25} \quad (16.1.13)$$

Rearranging, we get

$$\frac{dx}{Q^{0.25}} = \frac{K_2}{K_1^{0.25}} dt \quad (16.1.14)$$

The flow rate downstream of section 1 is $Q = Q_1 + q_x$ and $dQ = q dx$, which can be substituted into equation (16.1.14). Integration of this equation results in

$$t = \frac{4}{3} (Q_2^{0.75} - Q_1^{0.75}) \frac{K_1^{0.25}}{K_2 q} \quad (16.1.15)$$

The average velocity \bar{V} is then L/t , where L is the length shown in Figure 16.1.1b and

$$\bar{V} = \frac{L}{t} = \frac{3K_2 q}{4K_1^{0.25}} \left(\frac{L}{Q_2^{0.75} - Q_1^{0.75}} \right) \quad (16.1.16)$$

Substituting $L = (Q_2 - Q_1)/q$ and equation (16.1.9) into equation (16.1.16) yields

$$V = \frac{3}{4} K_2 \frac{T_2^{8/3} - T_1^{8/3}}{(T_2^2 - T_1^2)} \quad (16.1.17)$$

where T_1 is the spread at the upstream end and T_2 is the spread at the downstream end of reach of gutter.

To determine the spread at the average velocity T_w using the average velocity, let V from equation (16.1.11) equal the average velocity in equation (16.1.17); solving for T_w/T_2 gives

$$\frac{T_w}{T_2} = 0.65 \left[\frac{1 - \left(\frac{T_1}{T_2}\right)^{8/3}}{1 - \left(\frac{T_1}{T_2}\right)^2} \right]^{1.5} \quad (16.1.18)$$

This equation is used to develop the numerical relationship between T_1/T_2 and T_w/T_2 .

EXAMPLE 16.1.3

- Use equation (16.1.18) to develop the numerical relationship of T_w/T_2 for the average velocity in a reach of triangular gutter.
- Compute the time of flow in a gutter for the situation in which the spread T_1 at the upstream end is 3 ft, which results from the bypass flow from the upstream inlet, the design spread T_2 at the second inlet is 10 ft, the gutter slope is $S = 0.03$, and the cross-slope is $S_x = 0.02$. Manning's $n = 0.016$ and the inlet spacing is 200 ft.

SOLUTION

- Solving equation (16.1.18) results in the numerical relationship shown in Table 16.1.2.

Table 16.1.2 Relationship between T_1/T_2 and T_w/T_2

T_1/T_2	0	0.1	0.2	0.3	0.4	0.5	0.6	0.7	0.8	0.9	1.0
T_w/T_2	0.65	0.66	0.68	0.70	0.74	0.77	0.82	0.86	0.90	0.95	1.0

(b) From the above table, $T_1/T_2 = 3/10 = 0.3$, $T_w/T_2 = 0.7$; then $T_w = T_2(T_w/T_2) = 10(0.7) = 7$ ft. Next compute the average velocity V using equation (16.1.11):

$$V = K_2 T_w^{2/3} = \frac{1.12}{n} S^{1/2} S_x^{2/3} T_w^{2/3} = \frac{1.12}{0.016} (0.03)^{1/2} (0.02)^{2/3} (7)^{2/3} = 3.27 \text{ ft/s}$$

The time of flow is $t = L/V = 200/3.27 = 61.2 \text{ sec} = 1.0 \text{ min}$.

EXAMPLE 16.1.4

Derive the equation for the total discharge in a composite gutter section (with compound slopes) as shown in Figure 16.1.2. The distance a is referred to as the gutter depression.

SOLUTION

The depth of flow at the break in cross-section d_2 is

$$d_2 = (T_w - W)S_x$$

and the depth of flow at the curb is

$$d_1 = T_w S_x + a$$

The discharge for the outside section of gutter Q_s using equation (16.1.7) is

$$Q_s = \frac{0.56 S^{1/2}}{n S_x} d_2^{8/3} = \frac{0.56 S^{1/2} [(T_w - W)S_x]^{8/3}}{n S_x}$$

and the discharge in the inside section of gutter (next to the curb) is

$$\begin{aligned} Q_w &= \frac{0.56 S^{1/2}}{n S_w} d_1^{8/3} - \frac{0.56 S^{1/2}}{n S_w} d_2^{8/3} = \frac{0.56 S^{1/2}}{n S_w} (d_1^{8/3} - d_2^{8/3}) \\ &= \frac{0.56 S^{1/2}}{n S_w} [(T_w S_x + a)^{8/3} - [(T_w - W)S_x]^{8/3}] \end{aligned}$$

The total gutter flow (Figure 16.1.2) is

$$Q = Q_w + Q_s$$

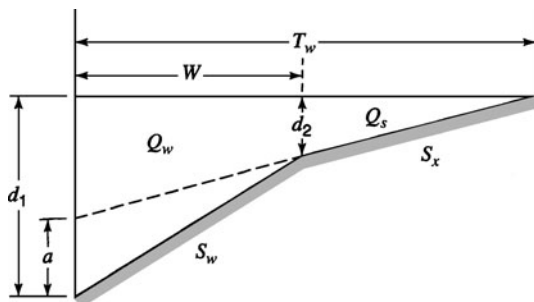


Figure 16.1.2 Flow in a composite gutter section.

EXAMPLE 16.1.5

Using the discharge relationships developed in example 16.1.4, determine the total gutter flow for a design spread of $T_w = 8$ ft, a cross-slope of $S_x = 0.025$, and $W = 2.0$ ft with a 2-in gutter depression. The gutter slope is $S = 0.01$ and Manning's n is 0.016.

SOLUTION

First compute S_w by geometry, $S_w = (d_1 - d_2)/W$, so

$$S_w = \frac{T_w S_x + a - (T_w - W)S_x}{W} = \frac{a}{W} + S_x$$

Then $S_w = [(2/12)/2] + 0.025 = 0.108$. The total discharge is

$$Q = Q_w + Q_s$$

$$Q_s = \frac{0.56 S^{1/2} [(T_w - W)S_x]^{8/3}}{n S_x} = \frac{0.56(0.01)^{1/2} [(8 - 2)0.025]^{8/3}}{0.016(0.025)} = 0.89 \text{ cfs}$$

$$\begin{aligned} Q_w &= \frac{0.56 S^{1/2}}{n S_w} \{ (T_w S_x + a)^{8/3} - [(T_w - W)S_x]^{8/3} \} \\ &= \frac{0.56(0.01)^{1/2}}{(0.016)(0.108)} \{ [(8)(0.025) + (2/12)]^{8/3} - [(8 - 2)(0.025)]^{8/3} \} \\ &= 32.41(0.0689 - 0.0064) = 2.03 \text{ cfs} \end{aligned}$$

The total gutter flow is then

$$Q = Q_w + Q_s = 2.03 + 0.89 = 2.92 \text{ cfs}$$

16.1.3 Pavement Drainage Inlets

Figure 16.1.3 illustrates the four types of pavement inlets: *grate inlets*, *curb-opening inlets*, *combination inlets*, and *slotted drain inlets*. A grate inlet consists of an opening in the gutter covered by one or more grates that are parallel with the flow. A curb-opening inlet is a vertical opening in the curb, covered by a top slab. Combination inlets typically consist of both a curb opening inlet and a grate inlet placed in a side-by-side configuration. The curb-opening may be located in part upstream of the grate. Slotted drain inlets consist of a pipe cut along the longitudinal axis with a grate of spacer bars to form slot openings.

Johnson and Chang (1984) present several types of grates that have been hydraulically tested. Only a few are presented here for comparison:

- P-1-7/8, which is a *bar grate* with bar spacing 1-7/8 in on center (Figure 16.1.4)
- P-1-7/8-4, which is a *parallel bar grate* with bar spacing 1-7/8 in on center and 3/8-in diameter lateral rods spaced at 4 in on center (Figure 16.1.4)
- CV-3-1/4-4-1/4, which is a *curved vane grate* with 3-3/4-in longitudinal bars and 4-1/4-in transverse bar spacing on center (Figure 16.1.5)
- 30-3-1/4-4, which is a 30° *tilt-bar grate* with 3-1/4 in and 4 in on center longitudinal and lateral bar spacing, respectively (Figure 16.1.6)
- *Reticuline*, which is a honeycomb pattern of lateral bars and longitudinal bearing bars (Figure 16.1.7)

16.1.4 Interception Capacity and Efficiency of Inlets on Grade

The *interception capacity* Q_i of an inlet is the flow intercepted by an inlet under a given set of conditions. On a uniform grade, the interception capacity is dependent on the overland flow, namely

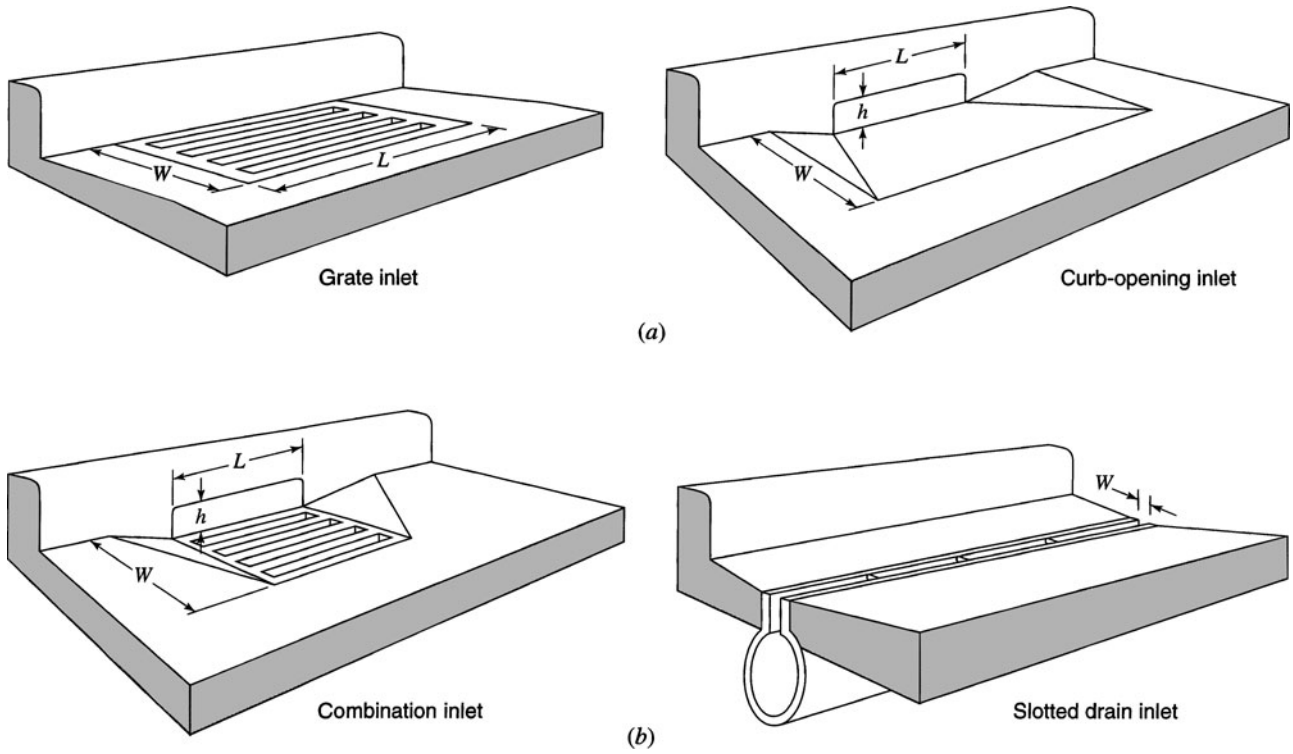


Figure 16.1.3 (a) Perspective views of grate and curb-opening inlets; (b) Perspective views of combination inlet and slotted drain inlet (from Johnson and Chang (1984)).

the cross-slope, S_x . To a lesser extent the capacity is dependent on the roughness, the gutter longitudinal slope, total gutter flow, and inlet configuration (length, width, and crossbar arrangement for grate inlets and length of inlet for curb-opening and slotted drain inlets).

The *efficiency of an inlet* is the percent of total flow that the inlet will intercept under a given set of conditions (Johnson and Chang, 1984). Efficiency is dependent upon cross-slope S_x , longitudinal slope S , interception capacity Q_i , total gutter flow Q , and minimally on pavement slope. Efficiency is expressed as

$$E = Q_i/Q \tag{16.1.19}$$

The flow that is not intercepted is the *carryover* or *bypass flow* Q_b , so that

$$Q_b = Q - Q_i \tag{16.1.20}$$

Interception capacity increases with increasing flow rate and, in general, inlet efficiency decreases with increasing flow rates.

Depth of water next to curbs is the major factor in interception capacity for both gutter inlets and curb-opening inlets. Interception capacity for grate inlets depends on the amount of water flowing over the grate, size and configuration of the grate, and velocity of flow in the gutter. Efficiency of a grate is dependent on the same factors and, in addition, on the total flow in the gutter.

Curb-opening inlet interception capacity is mostly dependent on flow depth at the curb and the curb-opening length. The use of a gutter depression at the curb opening or a depressed gutter increases the effective depth and consequently increases the inlet interception capacity and efficiency. Slotted drain inlets function as weirs, similar to curb-opening inlets. Efficiency is dependent on flow depth, inlet length, and total gutter flow. The inlet capacity of combination inlets is similar to that of grate inlets.

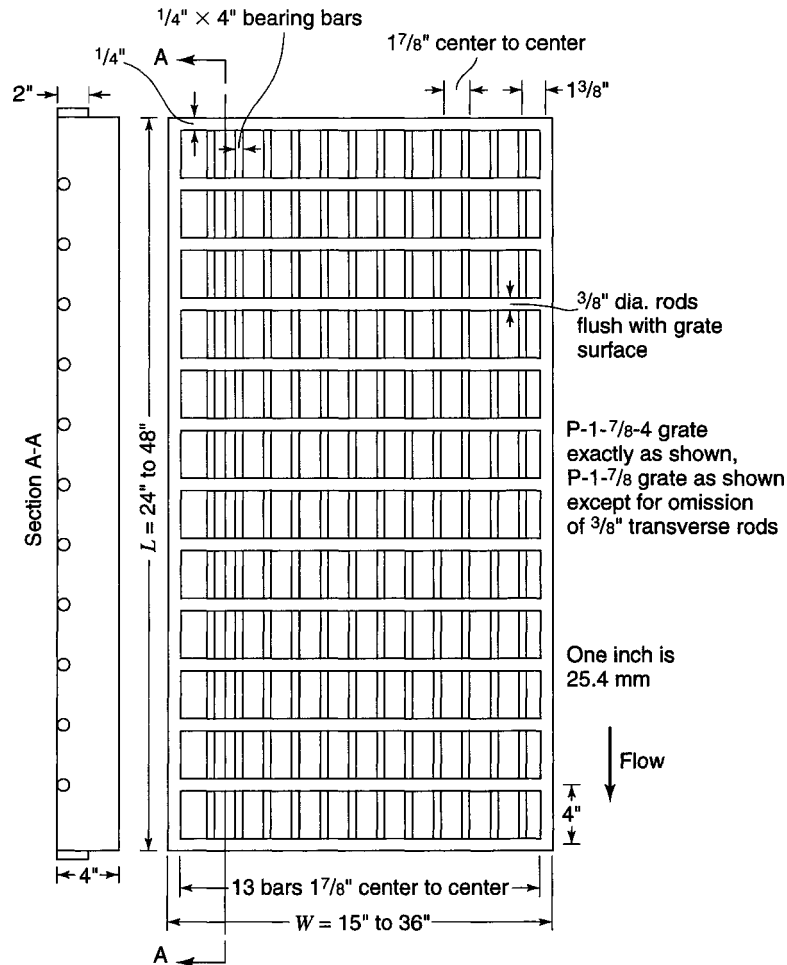


Figure 16.1.4 P-1-7/8 and P-1-7/8-4 grates (from Johnson and Chang (1984)).

16.1.4.1 Grate Inlets on Grade

This subsection addresses the hydraulic analysis of grates on a uniform grade. *Frontal flow* is the portion of flow that passes over the upstream side of a grate. *Splash-over* is the portion of the frontal flow at a grate that splashes over the grate and is not intercepted. This occurs when the flow velocity in the gutter exceeds a threshold value V_0 . *Side flow* is the portion of gutter flow that goes around the grate when the spread T_w is larger than the grate width W . *Capture efficiency* of side flow depends on the cross-slope S_x , the grate length L , and the gutter flow velocity V .

The *frontal-flow ratio* E_0 for a straight cross-slope is

$$E_0 = \frac{Q_w}{Q} = 11 - \left(1 - \frac{W}{T_w}\right)^{8/3} \quad (16.1.21)$$

where Q_w and Q have units of ft^3/s (m^3/s) and W and T_w have units of feet (m). A *side-flow ratio* is expressed as

$$E_s = \frac{Q_s}{Q} = 1 - \frac{Q_w}{Q} = 1 - E_0 \quad (16.1.22)$$

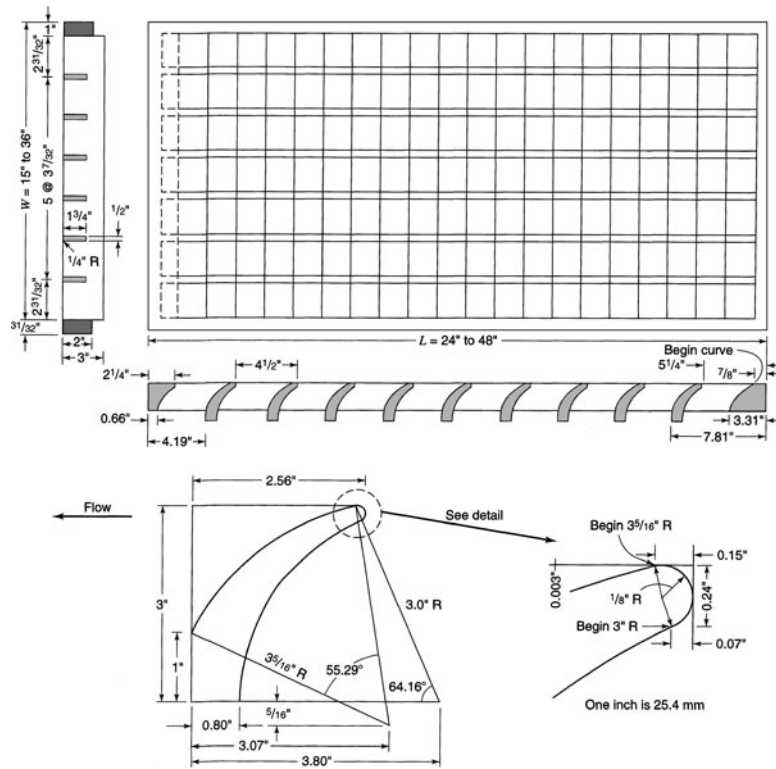


Figure 16.1.5 Curved vane grate (from Johnson and Chang (1984)).

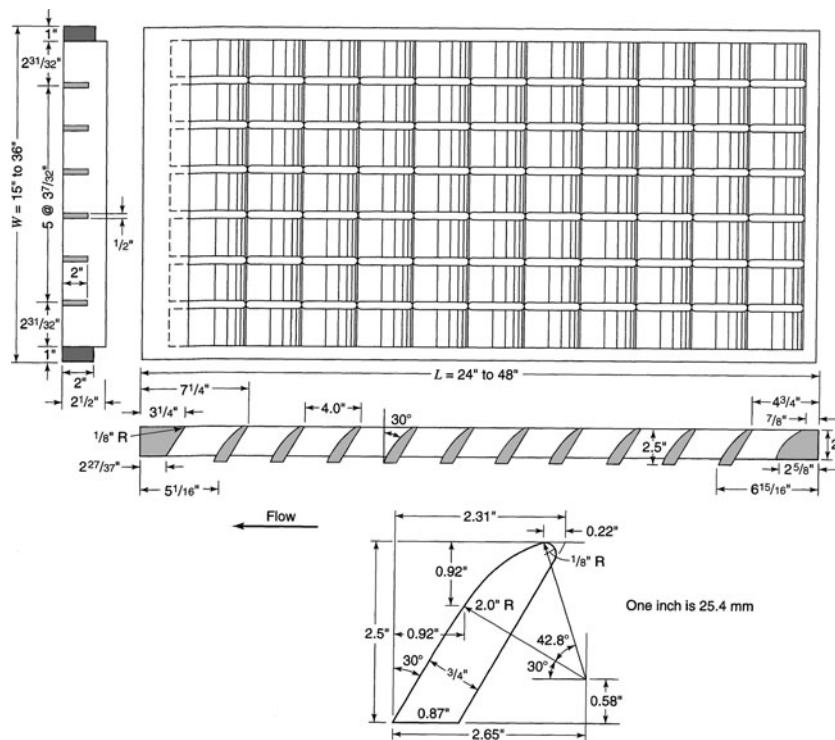


Figure 16.1.6 30° tilt-bar grate (from Johnson and Chang (1984)).

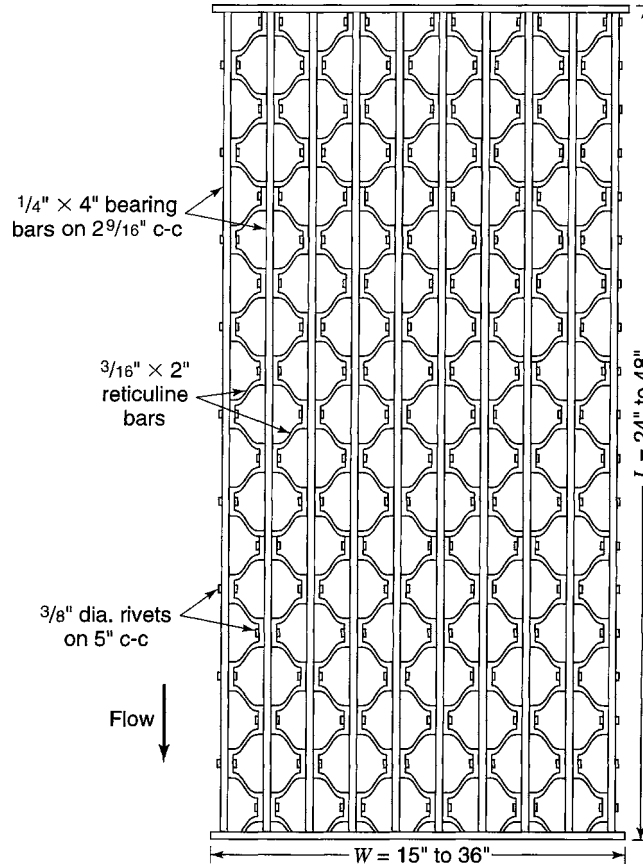


Figure 16.1.7 Reticuline grate (from Johnson and Chang (1984)).

where Q_s is the side flow, ft^3/s (m^3/s). If the gutter-flow velocity exceeds the threshold value, the *frontal-flow interception efficiency* R_f is

$$R_f = 1 - 0.09(V - V_0) \quad (16.1.23)$$

where the gutter-flow velocity is $V = Q/A_G$, A_G is the area of the gutter flow, and V_0 is the threshold gutter-flow velocity at which frontal flow skips over the grate without being captured. Figure 16.1.8 can be used to compute R_f for various types of grate inlets.

The *side-flow interception efficiency* R_s is the ratio of side flow intercepted to the total side flow, expressed as (Johnson and Chang, 1984)

$$R_s = \frac{1}{\left[1 + \frac{0.15V^{1.8}}{S_x L^{2.3}}\right]} \quad (16.1.24)$$

The *interception efficiency of a grate inlet* E is defined as

$$E = R_f E_0 + R_s E_s \quad (16.1.25)$$

or

$$E = R_f E_0 + R_s (1 - E_0) \quad (16.1.26)$$

The term $R_f E_0$ is the ratio of intercepted frontal flow to total gutter flow and $R_s E_s$ is the ratio of intercepted side flow to total side flow. $R_s E_s$ is insignificant for high velocities and short grates.

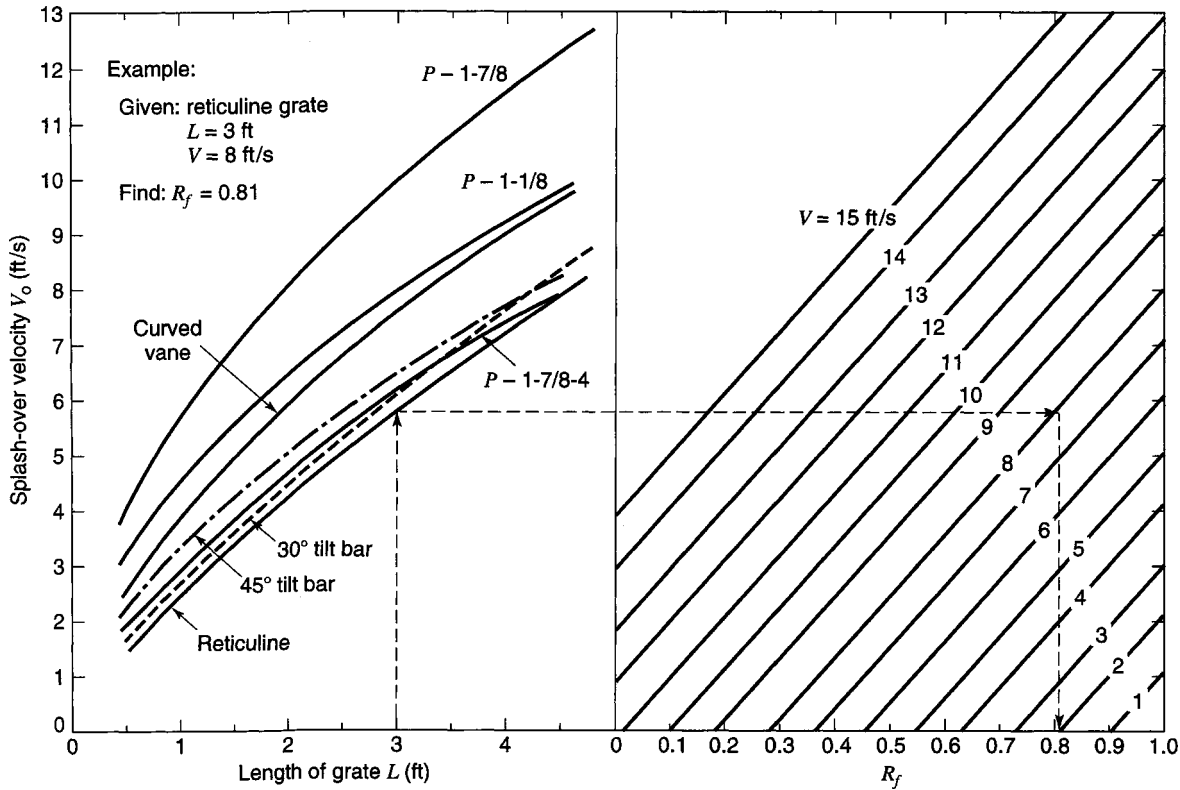


Figure 16.18 Grate inlet frontal flow-interception efficiency (from Johnson and Chang (1984)).

The interception capacity of a grate inlet (Q_i) is

$$Q_i = EQ = Q[R_f E_0 + R_s(1 - E_0)] \quad (16.1.27)$$

EXAMPLE 16.1.6

Using the data in example 16.1.5, find the interception capacity of a bar grate (P-1-7/8), $W = 2$ ft, $T_w = 8$ ft, $S = 0.01$, $S_x = 0.025$, and $Q = 2.92$ cfs. The grate is 2 ft long and 2 ft wide.

SOLUTION

Equation (16.1.27) is used to compute the interception capacity $Q_i = Q[R_f E_0 + R_s(1 - E_0)]$. Figure 16.1.8 is used to determine frontal-flow interception efficiency, R_f , for which the velocity Q/A is needed. The depths are $d_1 = T_w S_x + a = (8)(0.025) + (2/12) = 0.37$ ft and $d_2 = (T_w - W)S_x = (8 - 2)(0.025) = 0.15$ ft. The area of flow can be expressed as

$$A = \frac{1}{2}(d_1 + d_2)W + \frac{1}{2}d_2(T_w - W) = \frac{1}{2}(0.37 + 0.15)(2) + \frac{1}{2}(0.15)(8 - 2) = 0.97 \text{ ft}^2$$

The velocity is then $V = Q/A = 2.92/0.97 = 3.01$ ft/s. From Figure 16.1.8 with the grate length of 2 ft and the velocity of 3.01 ft/s, $R_f = 1.0$.

The side-flow interception efficiency R_s is computed using equation (16.1.24):

$$R_s = \frac{1}{\left[1 + \frac{0.15V^{1.8}}{S_x L^{2.3}}\right]} = \frac{1}{\left[1 + \frac{0.15(3.01)^{1.8}}{(0.025)(2)^{2.3}}\right]} = 0.10$$

The frontal-flow ratio is computed using equation (16.1.21), $E_0 = Q_w/Q$. For this problem, the grate width is 2 ft and W (the distance from curb to the break in cross-section, change in slopes) is also 2 ft. So the Q_w of 2.03 cfs from example 16.1.5 can be used; then

$$E_0 = \frac{Q_w}{Q} = \frac{2.03}{2.92} = 0.70$$

The interception capacity of the 2×2 ft bar grate inlet is then computed using equation (16.1.27) as

$$Q_i = 2.92[1 \times 0.70 + 0.10(1 - 0.70)] = 2.13 \text{ cfs}$$

16.1.4.2 Curb-Opening Inlets on Grade

These types of inlets are effective at locations where the flow at the curb is sufficient for the inlet to perform efficiently. They are relatively free of clogging and offer little interference to traffic. Curb-opening inlets do not function well on steep slopes because of the difficulty of directing flow into the inlet. Curb-opening inlets are much longer than grate inlets. This subsection provides the hydraulic analysis for curb-opening inlets on uniform grade.

The *full-interception curb-opening inlet length* L_T is the length to intercept 100 percent of the gutter flow, expressed as (Johnson and Chang, 1984)

$$L_T = \Phi Q^{0.42} S^{0.3} (nS_x)^{-0.6} \quad (16.1.28)$$

where Φ is 0.6 for U.S. customary units and 0.82 for SI units. The efficiency of curb-opening inlet lengths L that are shorter than L_T is

$$E = 1 - \left(1 - \frac{L}{L_T}\right)^{1.8} \quad (16.1.29)$$

For depressed curb-opening inlets or curb openings in depressed gutter sections, the length of inlet required for total interception can be determined using the *equivalent cross-slope* S_e , expressed as

$$S_e = S_x + S'_w E_0 \quad (16.1.30)$$

where S'_w is the cross-slope of the gutter measured from the cross-slope of the pavement S_x , so that $S'_w = a/12W$ where a is the gutter depression in inches and E_0 is the ratio of the flow in the depressed section to the total gutter flow Q_w/Q .

The curb-opening length required for total interception can be significantly reduced if the cross-slope (S_x) or equivalent cross-slope (S_e) is increased. The equivalent cross-slope can be increased by use of a continuously depressed gutter section or by a locally depressed gutter section. Equation (16.1.28) can be expressed using the equivalent cross-slope as

$$L_T = \Phi Q^{0.42} S^{0.3} (nS_e)^{-0.6} \quad (16.1.31)$$

This equation is applicable with either straight or compound cross-slopes.

EXAMPLE 16.1.7

Using the data from Example 16.1.6, determine the interception capacity of a 6-ft curb-opening inlet.

SOLUTION

Compute the full-interception curb-opening inlet length using equation (16.1.31) with $S_e = S_x + S_w E_0 = 0.025 + (0.7)(0.083) = 0.0831$:

$$\begin{aligned} L_T &= \Phi Q^{0.42} S^{0.3} (nS_x)^{-0.6} = 0.6(2.92)^{0.42} (0.01)^{0.3} [0.016 \times 0.0831]^{-0.6} \\ &= 12.57 \text{ ft} \end{aligned}$$

The efficiency is computed using equation (16.1.29):

$$E = 1 - \left(1 - \frac{L}{L_T}\right)^{1.8} = 1 - \left(1 - \frac{6.0}{12.57}\right)^{1.8} = 0.69 = 69\%$$

The interception capacity is computed using $Q_i = EQ = 0.69(2.92) = 2.01$ cfs.

16.1.4.3 Slotted Drain Inlets on Grade

Slotted drain inlets have a flow interception that is similar to curb-opening inlets because each acts as a side weir in which the flow is subjected to lateral acceleration due to the cross-slope of the pavement. For slot widths greater than 1.75 in, the length required for total interception can be computed by equation (16.1.28). Similarly, equation (16.1.29) is applicable for determining the efficiency. The use of these equations is identical to that for curb-opening inlets.

16.1.4.4 Combination Inlets on Grade

The interception capacity for combination inlets on grade (with the curb opening and grate placed side by side) is not appreciably greater than that of just a grate inlet. Interception capacity is therefore determined by neglecting the curb opening. In the case of a combination inlet with the curb opening upstream of the grate, the interception capacity is the sum of the two inlets, with the exception that the frontal flow and the interception capacity of the grate are reduced by the curb-opening interception.

EXAMPLE 16.1.8

Determine the interception capacity of a combination curb-opening grate inlet in a triangular gutter section. The curb opening is 12 ft long with 10 ft of the curb opening upstream of the grate. The grate is a 2 ft by 2 ft reticuline grate placed alongside the downstream 2 ft of curb opening, $Q = 8$ ft³/s, $S = 0.01$, $S_x = 0.025$, and $n = 0.016$.

SOLUTION

From equation (16.1.28), the full-interception curb-opening inlet length is

$$\begin{aligned} L_T &= \Phi Q^{0.42} S^{0.3} (n S_x)^{-0.6} = 0.6(8)^{0.42} (0.01)^{0.3} [0.016 \times 0.025]^{-0.6} \\ &= 39.47 \text{ ft} \end{aligned}$$

The efficiency of the curb-opening inlet (upstream of the grate) is computed using equation (16.1.29):

$$E = 1 - \left(1 - \frac{L}{L_T}\right)^{1.8} = 1 - \left(1 - \frac{10}{39.47}\right)^{1.8} = 0.41$$

The interception capacity of the curb-opening inlet is then

$$Q_i = EQ = (0.41)(8) = 3.28 \text{ cfs}$$

To compute the interception capacity of the grate inlet, equation (16.1.27) is used:

$$Q_i = Q[R_f E_0 + R_s(1 - E_0)].$$

The flow at the grate is then $Q = 8 - 3.28 = 4.72$ cfs. Using this flow rate, the spread T_w can be computed with equation (16.1.8a):

$$\begin{aligned} Q &= \frac{0.56}{n} S^{1/2} S_x^{5/3} T_w^{8/3} \\ 4.72 &= \frac{0.56}{0.016} (0.01)^{1/2} (0.025)^{5/3} T_w^{8/3} \end{aligned}$$

$$T_w = 11.22 \text{ ft}$$

Next the velocity can be computed for use in determining R_f from Figure 16.1.8, so

$$V = Q/A = \frac{Q}{\left[\frac{1}{2}T_w^2S_x\right]} = \frac{4.72}{\frac{1}{2}(11.22)^2(0.025)} = 3.00 \text{ ft/s}$$

From Figure 16.1.8, $R_f = 1.0$. The side-flow interception efficiency is computed using equation (16.1.24):

$$R_s = \frac{1}{\left[1 + \frac{0.15V^{1.8}}{S_xL^{2.3}}\right]} = \frac{1}{\left[1 + \frac{0.15(3.00)^{1.8}}{0.025(2)^{2.3}}\right]} = 0.10$$

The frontal-flow ratio is computed using equation (16.1.21):

$$E_0 = \frac{Q_w}{Q} = 1 - \left(1 - \frac{W}{T_w}\right)^{8/3} = 1 - \left(1 - \frac{2}{11.22}\right)^{8/3} = 0.41$$

The interception capacity is then

$$Q_i = Q[R_fE_0 + R_s(1 - E_0)] = 4.72[1 \times 0.41 + 0.1(1 - 0.41)] = 2.21 \text{ cfs}$$

The total interception is $Q_i = Q_{\text{grate inlet}} + Q_{\text{curb open}} = 2.21 + 3.28 = 5.49 \text{ cfs}$.

16.1.5 Interception Capacity and Efficiency of Inlets in Sag Locations

Inlets that are placed in sag locations operate as weirs under low heads and as orifices for higher heads. The transition between weir flow and orifice flow cannot be accurately defined, as the flow may fluctuate back and forth between these two controls. All runoff that enters sags must flow through the inlet. As a consequence, the efficiency of inlets in sags in passing debris is somewhat critical. Combination inlets and curb-opening inlets are recommended for sag locations, as grate inlets have clogging tendencies.

16.1.5.1 Grate Inlets in a Sag Location

The capacity of grate inlets Q_i under weir control is

$$Q_i = C_W P d^{1.5} \quad (16.1.32)$$

where C_W is the weir coefficient, 3.0 for U.S. customary units (1.66 for SI units), P is the grate perimeter disregarding bars and the curb side in ft (m), and d is the depth of water over the inlet in feet (m). The capacity of grate inlets under orifice control is

$$Q_i = C_0 A (2gd)^{0.5} \quad (16.1.33)$$

where C_0 is 0.67, A is the clear opening area of the grate, ft^2 (m^2), and g is the acceleration due to gravity, 32.16 ft/s^2 (9.81 m/s^2). Figure 16.1.9 provides a design solution for equations (16.1.32) and (16.1.33).

EXAMPLE 16.1.9

Consider a symmetrical sag vertical curve (with a curb) with equal bypass from inlets upgrade of the low point. Determine the grate size for a design Q of $6 \text{ ft}^3/\text{s}$ and the curb depth. Allow for 50 percent clogging of the grate. The design spread is $T_w = 12 \text{ ft}$, $S = 0.01$, $S_x = 0.025$, and $n = 0.015$. What happens when the flow rate is $8 \text{ ft}^3/\text{s}$?

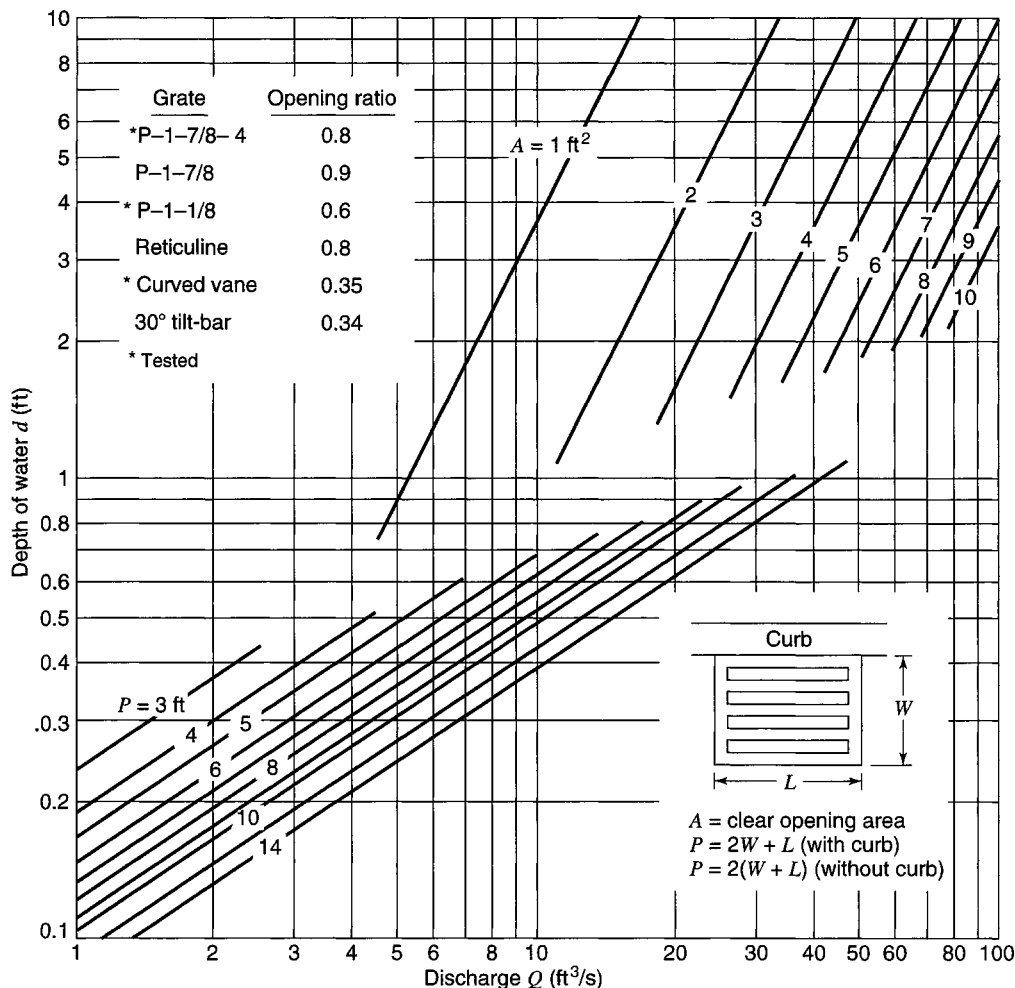


Figure 16.1.9 Grate inlet capacity in sump conditions (from Johnson and Chang (1984)).

SOLUTION

According to Figure 16.1.9, a grate must have a perimeter of 12 ft, using $d = T_w S_x = 12(0.025) = 0.3$ ft and $Q = 6 \text{ ft}^3/\text{s}$. Assuming 50 percent clogging by debris, the effective perimeter is reduced by 50 percent. Assume the use of a grate would meet the perimeter requirement with a double 2 ft \times 5 ft grate. Assuming 50 percent clogging so that the effective width of the gate is 1 ft, then the perimeter of the grate is $P = 1.0 + 1.0 + 10 = 12$ ft rather than 14 ft.

For a flow rate of $8 \text{ ft}^3/\text{s}$ and perimeter of 12 ft, the depth is 0.37 ft (from Figure 16.1.9). The spread can be computed using $S_x = (d/T_w)$, so $T_w = (d/S_x) = 0.37/0.025 = 14.8$ ft at the flow rate of $8 \text{ ft}^3/\text{s}$. The ponding will extend $14.8 - 12 = 2.8$ ft into the traffic lane.

16.1.5.2 Curb-Opening Inlets in a Sag Location

Curb-opening inlets in a sag operate as weirs to depths equal to the curb opening height and as orifices at depths greater than 1.4 times the opening height h . The transition of control occurs between 1.0 and 1.4 times the opening height h . The weir control equation for interception capacity of a depressed curb-opening inlet (Figure 16.1.10) is

$$Q_i = C_w(L + 1.8W)d^{1.5} \text{ (for } d \leq h + a/12, \text{ or } d \leq h + a \text{ for SI units)} \quad (16.1.34)$$

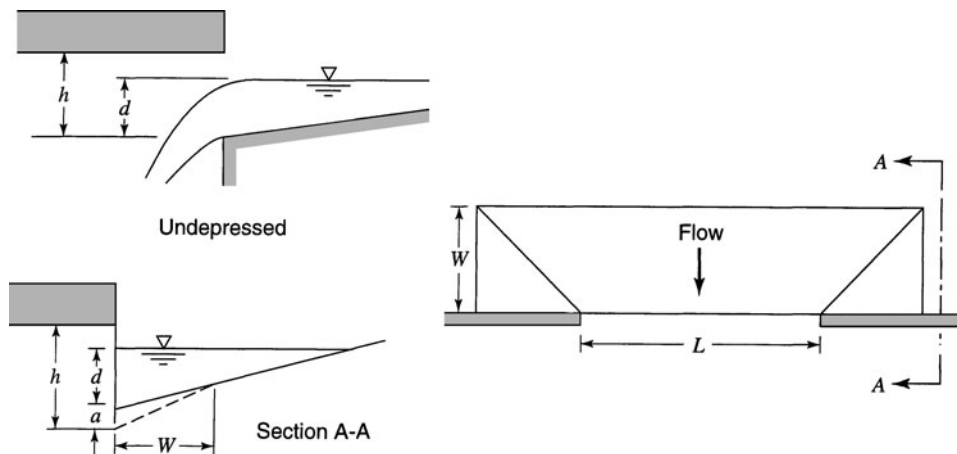


Figure 16.1.10 Depressed curb openings showing weir control in sump locations (from Johnson and Chang (1984)).

where C_W is 2.3 (or 1.25 for SI units), L is the curb-opening length in feet (m), W is the lateral width of the depression in feet (m), a is the depth of the depression in feet (m), and d is the depth at curb opening measured from the normal cross-slope $d = T_w S_x$ in feet (m). As indicated by equation (16.1.34), the limitation for use of this weir equation is that depths at the curb be less than or equal to the height of the opening plus the depth of the depression. For curb-opening inlets without any depression ($W = 0$), the weir equation is simply

$$Q_i = C_W L d^{1.5} \quad (\text{for } d \leq h) \quad (16.1.35)$$

where $C_W = 3.0$ (1.66 in SI units).

The interception capacity for orifice control ($d > 1.4h$) for both depressed and undepressed vertical curb-opening inlets is

$$Q = C_0 h L (2g d_0)^{0.5} \quad (16.1.36a)$$

$$Q = C_0 A \left[2g \left(d_i - \frac{h}{2} \right) \right]^{0.5} \quad (16.1.36b)$$

where C_0 is the weir coefficient equal to 0.67, h is the curb-opening inlet height in feet (m) (see Figure 16.1.11a), d_0 is the effective head on the center of the orifice throat in feet (m) (see Figure 16.1.11a), A is the clear area of the opening in ft^2 (m^2), h is the height of the curb-opening orifice ($T S_x + a/12$), and d_i is the depth at the lip of the curb opening in feet (m), including any gutter depression. The height h in equation (16.1.36) assumes a vertical orifice opening (see Figure 16.1.11). Other orifice throat locations change the effective depth on the orifice and the dimension $d_i - h/2$. For other than vertical faces, the orifice equation is

$$Q = C_0 h L (2g d_0)^{0.5} \quad (16.1.37)$$

where h is the orifice throat width in feet (m) and d_0 is the effective head on the center of the orifice throat in feet (m); see Figures 16.1.11b and c.

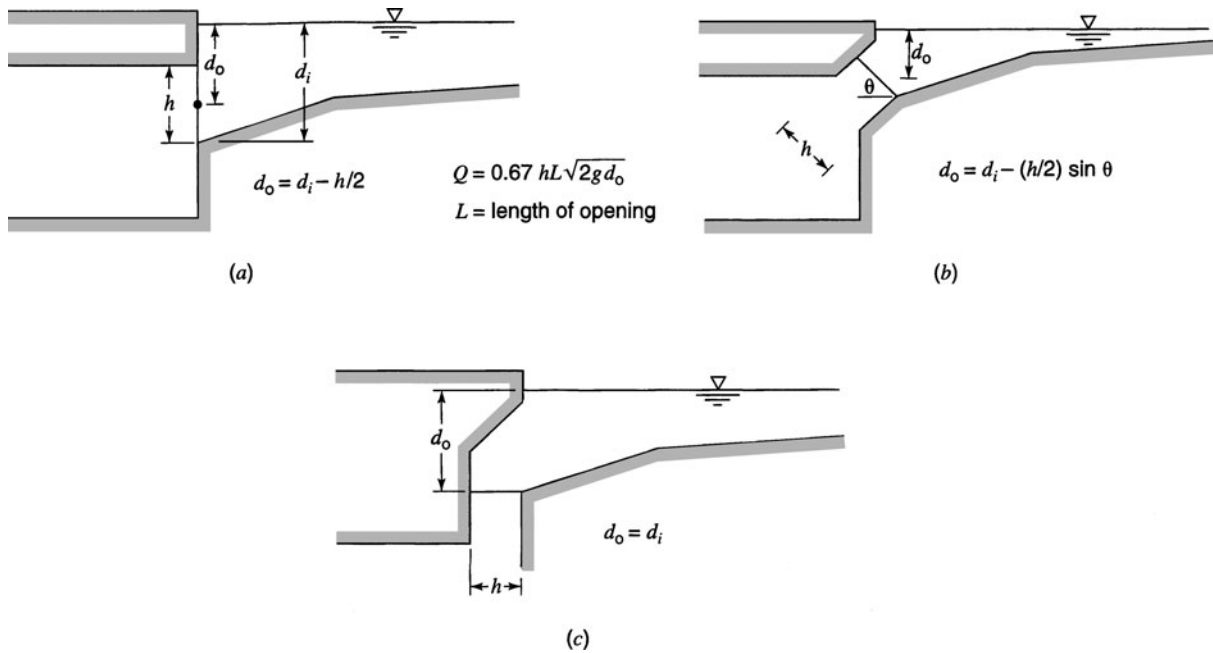


Figure 16.1.11 Curb-opening inlets. (a) Horizontal throat; (b) Inclined throat; (c) Vertical throat (from Johnson and Chang (1984)).

EXAMPLE 16.1.10

A curb-opening inlet in a sump location is to have a curb opening length of $L = 5$ ft and a height of 5 in. (a) Determine the interception capacity for an undepressed curb opening for which $S_x = 0.05$ and $T_w = 8$ ft. (b) Determine the interception capacity for a depressed curb opening with $S_x = 0.05$, $a = 2$ in, $W = 2$ ft, and $T_w = 8$ ft.

SOLUTION

- (a) The depth is $d = T_w S_x = (8)(0.05) = 0.4$ ft, for which $d < h = 5/12 = 0.42$ ft, so the flow has weir control (see Figure 16.1.10). The interception capacity is computed using equation (16.1.35), $Q_i = C_w L d^{1.5} = 3.0(5)(0.4)^{1.5} = 3.8 \text{ ft}^3/\text{s}$.
- (b) The depth is $d = T_w S_x = (8)(0.05) = 0.4$ ft, in which $d \leq (h + a)/12 = 7/12$ ft, so weir flow controls (see Figure 16.1.10) and equation (16.1.34) $Q_i = C_w(L + 1.8W)d^{1.5}$ is applicable: $Q_i = 2.3(5 + 1.8 \times 2)(0.4)^{1.5} = 5.0 \text{ ft}^3/\text{s}$. According to Johnson and Chang (1984), at $d = 0.4$ ft the depressed curb-opening inlet has about 30 percent more capacity than an inlet without depression. In a design situation, the flow rate would be known and the depth of the curb must be determined.

16.1.5.3 Slotted Drain Inlets in a Sag Location

These types of inlets (see Figure 16.1.3) operate as weirs to depths of about 0.2 ft (0.06 m) dependent upon the slot width (opening at top) and length, and operate as orifices for depths greater than about 0.4 ft (0.12 m). Transition flow occurs between these depths. The orifice control equation is

$$Q_i = 0.8LW(2gd)^{0.5} \tag{16.1.38}$$

where W is the slot width in feet (m), L is the slot length in feet (m), and d is the water depth at the slot in feet (m) for $d \geq 0.4$ ft. The interception capacity of slotted inlets for depths in the range $0.2 \leq d \leq 0.4$ ft (0.12 m) can also be approximated using the above orifice equation.

EXAMPLE 16.1.11

Determine the length of a slotted inlet that is required to limit the maximum depth at the curb to 0.3 ft for a discharge of $5 \text{ ft}^3/\text{s}$. Assuming no clogging, use a slot width of 1.75 in.

SOLUTION

Using equation (16.1.38), we find

$$Q_i = 0.8LW(2gd)^{0.5}$$

$$5 = 0.8 \frac{1.75}{12} L[2(32.2)(0.3)]^{0.5}$$

$$L = 9.75 \text{ ft} \approx 10 \text{ ft}$$

16.1.5.4 Combination Inlets in a Sag Location

For situations where hazardous ponding can occur, combination inlets in sags are advised (Johnson and Chang, 1984). Equation (16.1.32) can be used for weir flow calculations, and for complete clogging of the grate, equations (16.1.33) to (16.1.35) can be utilized. For orifice flow, equations (16.1.33) and (16.1.37) can be combined:

$$Q_i = 0.67A(2gd)^{0.5} + 0.67hL(2gd_0)^{0.5} \quad (16.1.39)$$

EXAMPLE 16.1.12

Consider a combination inlet in a sag location. The grate is a P-1-7/8, that is 2×4 ft with a curb opening of $L = 4$ ft and $h = 4$ in. The cross-slope $S_x = 0.03$ and the discharge is $Q = 5 \text{ ft}^3/\text{s}$. Determine the depth at the curb and the spread for a grate with no clogging. What would be the depth and spread if the grate were 100 percent clogged?

SOLUTION

Using Figure 16.1.9 with $P = 2 + 2 + 4 = 8$ ft and $Q = 5 \text{ ft}^3/\text{s}$, we find $d = 0.36$ ft. Alternatively, using $Q = C_w P d^{1.5}$, we get $5 = (3.0)(8.0)(d)^{1.5}$ then $d = 0.35$ ft. The spread is $T_w = d/S_x = 0.36/0.03 = 12$ ft. If the grate were 100 percent clogged, then the problem would be that of a curb-opening inlet in a sump location, so that $L = 4.0$ ft, $A = hL = (4/12)4 = 1.33 \text{ ft}^2$. Then by equation (16.1.37),

$$Q = C_0 h L (2gd_0)^{0.5} \quad \text{or} \quad 5 = 0.67(1.33) \sqrt{2(32.2)} d_0^{0.5}$$

$$d_0 = 0.5 \text{ ft}$$

$$T_w = 0.5/0.03 = 16.7 \text{ ft}$$

Interception by the curb only is a transition stage between weir and orifice flow controls.

16.1.6 Inlet Locations

Johnson and Chang (1984) recommend that inlets be located at all low points in the gutter grade, at median breaks, intersections, crosswalks, and on side streets at intersections where drainage flows onto highway pavements. Inlet locations are often dictated by street-geometrical conditions rather than the spread-of-water computations. Sheet flow on pavements is susceptible to icing so that water should be prevented from flowing across the pavement. Therefore gutter flow should be intercepted where pavement surfaces are warped, such as at cross-slope reversals and ramps. Inlets should also be placed upgrade of bridges in order to prevent flow onto bridge decks and downgrade of bridges to intercept bridge drainage. Roadside channels should be used to intercept runoff from areas draining onto pavements. Inlets should be used where open channels are not practicable.

The design spread on the pavement is the criterion for spacing inlets on continuous grades. It is possible to establish the maximum design spacing for inlets on a continuous grade for a given design if the drainage area consists only of pavement or has reasonably uniform runoff characteristics and is rectangular in shape. The assumption is that the time of concentration is the same for all inlets.

For sag locations (see Figure 16.1.12) where significant ponding can occur, such as at underpasses and sag vertical curves in depressed locations, *flanking inlets* should be placed on each side of the

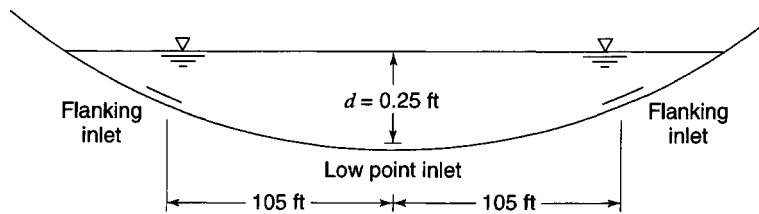


Figure 16.1.12 Example for sag locations.

Table 16.1.3 Distance to Flanking Inlets in Sag Vertical Curve Locations Using Depth-at-Curb Criteria

Speed	20	25	30	35	40	45	50	55	60		65	70
d/K	20	30	40	50	70	90	110	130	160	167	180	220
0.1	20	24	28	32	37	42	47	51	57	58	60	66
0.2	28	35	40	45	53	60	66	72	80	82	85	94
0.3	35	42	49	55	65	73	81	88	98	100	104	115
0.4	40	49	57	63	75	85	94	102	113	116	120	133
0.5	45	55	63	71	84	95	105	114	126	129	134	148
0.6	49	60	69	77	92	104	115	125	139	142	147	162
0.7	53	65	75	84	99	112	124	135	150	153	159	176
0.8	57	69	80	89	106	120	133	144	160	163	170	188

$x = (200dK)^{0.5}$, where x = distance from the low point; drainage maximum $K = 167$.

Source: Johnson and Chang (1984).

inlet and at the low point. Table 16.1.3 lists the required spacing for various depths at curb criteria and vertical curve lengths defined by $K = L/A$ where L is the length of the vertical curve and A is the algebraic difference in approach grade.

EXAMPLE 16.1.13

Consider a 32-ft pavement width on a continuous grade, $n = 0.016$, $S_x = 0.025$, $S = 0.01$, and $T_w = 8$ ft. The design rainfall intensity is 10 in/hr and $C = 0.8$. Determine the maximum design inlet spacing for a 2 ft by 2 ft curved vane grate.

SOLUTION

The discharge is expressed in terms of the maximum distance L_x where $Q = CiA$ and $A = (32 L_x / 43,560)$, so $Q = [0.8 \times 10 \times 32 L_x] / 43,560 = 0.0059L_x$ (or $0.0059 \text{ ft}^3/\text{s}/\text{ft}$). The gutter flow can be determined using equation (16.1.8a):

$$Q = \frac{0.56}{n} S^{1/2} S_x^{5/3} T_w^{8/3} = \frac{0.56}{0.016} (0.01)^{1/2} (0.025)^{5/3} (8)^{8/3} = 1.92 \text{ ft}^3/\text{s}$$

The first inlet can then be placed at L_x where $1.92 = 0.0059L_x$; then $L_x = 325$ ft.

Next the interception capacity of the grate inlet is determined using equation (16.1.26):

$$Q_i = Q[R_f E_0 + R_s(1 - E_0)]$$

where $Q = 1.92 \text{ ft}^3/\text{s}$. Figure 16.1.8 is used to compute R_f . Velocity can be computed using equation (16.1.11):

$$V = \frac{1.12}{0.016} (0.01)^{1/2} (0.025)^{2/3} (8)^{2/3} = 2.40 \text{ ft/s}$$

From Figure 16.1.8 for a curved vane grate, $R_f = 1.0$. Using equation (16.1.24) yields

$$R_s = \frac{1}{\left[1 + \frac{0.15V^{1.8}}{S_x L^{2.3}}\right]} = \frac{1}{\left[1 + \frac{0.15(2.40)^{1.8}}{0.025(2)^{2.3}}\right]} = 0.15$$

The frontal-flow ratio E_0 is computed using equation (16.1.21), $E_0 = Q_w/Q$ where $Q_w = AV$ where $V = 2.40$ ft/s, and

$$A = \frac{1}{2}[(T_w S_x) + (T_w - W)S_x]W = \frac{1}{2}[2T_w S_x - WS_x]W$$

$$= \frac{S_x W}{2}(2T_w - W) = \frac{0.025 \times 2}{2}(2 \times 8 - 2) = 0.35$$

$$Q_w = 0.35(2.40) = 0.84, E_0 = 0.84/1.92 = 0.44$$

The interception capacity is then

$$Q_i = 1.92[1 \times 0.44 + 0.15(1 - 0.44)] = 1.0 \text{ cfs}$$

The intervening drainage area between inlets should be sufficient to generate runoff equal to the interception capacity of the inlet; i.e., for each subsequent inlet, the interception is 1 cfs. Therefore, using $Q = 0.0059 L_x$, we have

$$L_x = Q/0.0059 = 1/0.0059 = 169 \text{ ft}$$

The bypass runoff at the first inlet, and consequently at all other subsequent inlets, is

$$Q_b = Q - Q_i = 1.92 - 1 = 0.92 \text{ cfs}$$

The result is that the initial inlet can be placed at 325 ft from the crest and subsequent inlets at 169-ft intervals.

EXAMPLE 16.1.14

Using the data from example 16.1.13, determine the maximum design inlet spacing for a 10-ft slotted inlet. Compare the efficiency for this inlet design and the one computed in example 16.1.13.

SOLUTION

From example 16.1.13, the gutter flow $Q = 1.92$ ft³/s, so that the full-interception curb-opening inlet length L_T is computed using equation (16.1.28) as

$$L_T = 0.6Q^{0.42}S^{0.3}(nS_x)^{-0.6}$$

$$L_T = 0.6 \times 1.92^{0.42} \times 0.01^{0.3}(0.016 \times 0.025)^{-0.6} = 21.7 \text{ ft}$$

The efficiency is computed using equation (16.1.29) as

$$E = 1 - \left(1 - \frac{L}{L_T}\right)^{1.8} = 1 - \left(1 - \frac{10}{21.7}\right)^{1.8} = 0.67$$

The interception capacity is $Q_i = EQ = 0.67(1.92) = 1.29$ ft³/s, and $Q_b = 1.92 - 1.29 = 0.63$ ft³/s. The spacing for the 10-ft inlet is then computed using $Q = 0.0059L_x$, so that $L_x = 1.29/0.0059 = 219$ ft. In example 16.1.13, the efficiency for the grate inlet design is $E = R_f E_0 + R_s(1 - E_0) = [1 \times 0.44 + 0.15(1 - 0.44)] = 0.52$ or 52 percent. For this example, the efficiency of the 10-ft inlet design is 0.67 or 67 percent. This illustrates the effects of the relative efficiencies of the different inlet configurations for the chosen design condition.

EXAMPLE 16.1.15

Consider a sag vertical curve at an underpass on a four-lane divided highway facility. Determine the location of flanking inlets that will function in relief of the inlet at the low point when the depth at the curb exceeds the design depth. The design spread is not to exceed the shoulder width of 10 ft. The cross-slope is $S_x = 0.025$ and $K = 220$ (speed = 70 mph).

SOLUTION

The depth at the curb at the design spread of 10 ft is $d = T_w S_x = 10(0.025) = 0.25$ ft. Spacing to the flanking inlet is found from Table 16.1.3 as $(94 + 115)/2 = 104.5$; use the 105-ft distance in Figure 16.1.12.

16.1.7 Median, Embankment, and Bridge Inlets

Median inlets are sometimes necessary to remove water in medians that could cause erosion. Figure 16.1.13 illustrates a median drop inlet. These drop inlets should be flush with the ditch bottom and constructed of traffic safety grates. Johnson and Chang (1984) present design charts and examples for median inlets.

Embankment inlets are commonly needed for collecting runoff from pavements to prevent erosion or to intercept water upgrade or downgrade of bridges. Figure 16.1.14 illustrates an embankment inlet and the catch basin with a down drain.

Bridge deck inlets have the same principles of inlet interception as pavement inlets. Figure 16.1.15 illustrates a grate inlet, which is about the maximum-size inlet for many bridge decks.

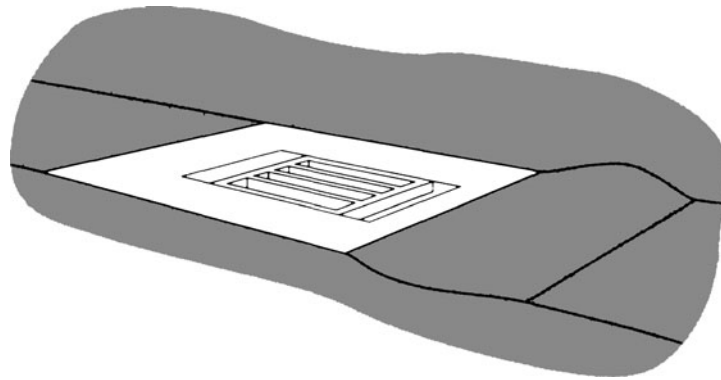


Figure 16.1.13 Median drop inlet (from Johnson and Chang (1984)).

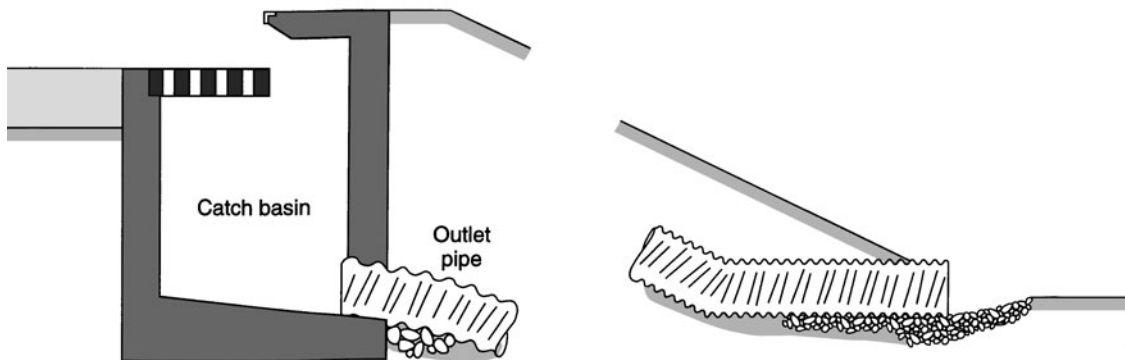
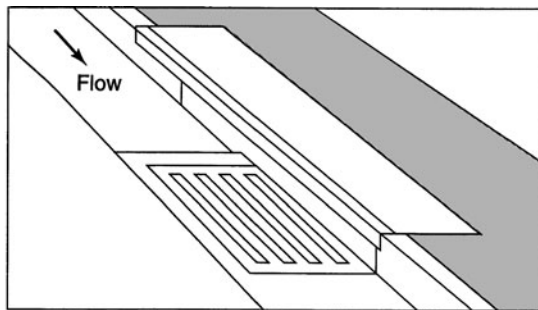


Figure 16.1.14 Embankment inlet and down drain (from Johnson and Chang (1984)).

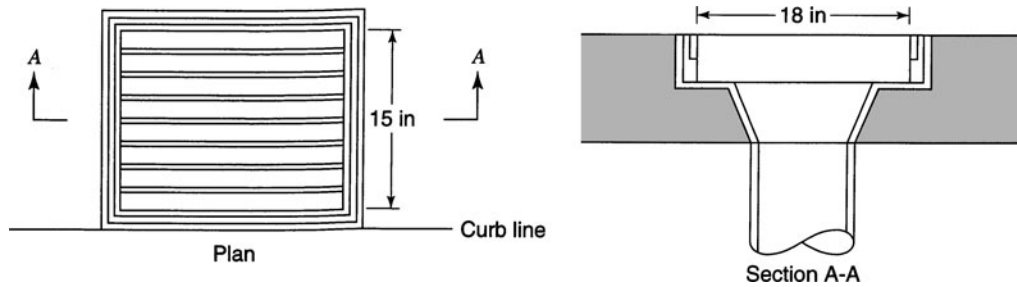


Figure 16.1.15 Bridge inlet (from Johnson and Chang (1984)).

EXAMPLE 16.1.16

Determine the interception capacity of a median drop inlet ($W = 2$ ft, $L = 2$ ft) in a median ditch (see Figure 16.1.16 for definition of parameters) with $B = 2$ ft, $z = 6$, $n = 0.03$, $Q = 10$ ft³/s, $S_x = 1/6 = 0.17$, $S = 0.03$. The grate is a P-1-7/8 grate (2 ft \times 2 ft).

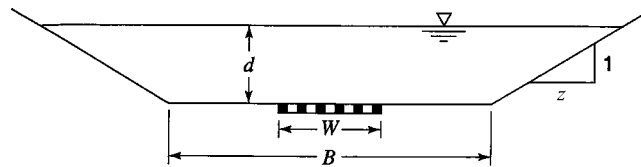


Figure 16.1.16 Median inlet in trapezoidal ditches.

SOLUTION

First determine the depth of flow in the median using Manning's equation for $B = 2$ ft, $z = 6$, $Q = 10$ ft³/s. Manning's equation can be solved for the depth of flow to yield $d = 0.61$ ft. The velocity is then computed to be 5.69 ft/s.

The frontal-flow ratio can be calculated using the following formula:

$$E_0 = \frac{W}{B + (d)(z)} = \frac{2}{2 + 0.61 \times 6} = 0.35$$

$R_f = 1.0$ from Figure 16.1.8 (for $L = 2$ ft and $V = 5.69$ ft/s) and R_s is computed using equation (16.1.24) as

$$R_s = \frac{1}{1 + \frac{0.15(5.69)^{1.8}}{(0.17)(2)^{2.3}}} = 0.20$$

The interception efficiency is then

$$E = R_f E_0 + R_s (1 - E_0) = [1 \times 0.35 + 0.20(1 - 0.35)] = 0.48$$

The interception capacity is $Q_i = EQ = 0.48 \times 10 = 4.8$ ft³/s, and $Q_b = 10 - 4.8 = 5.2$ ft³/s. A berm could be placed downstream of the grate inlet for total interception of flow in the ditch.

16.2 HYDRAULIC DESIGN OF CULVERTS

Culverts are hydraulically short closed conduits that convey streamflow through a road embankment or some other type of flow obstruction. The flow in culverts may be full flow over all its length or partly full, resulting in pressurized flow and/or open-channel flow. The characteristics of flow in culverts are very complicated because the flow is controlled by many variables, including inlet geometry, slope, size, flow rate, roughness, and approach and tailwater conditions.

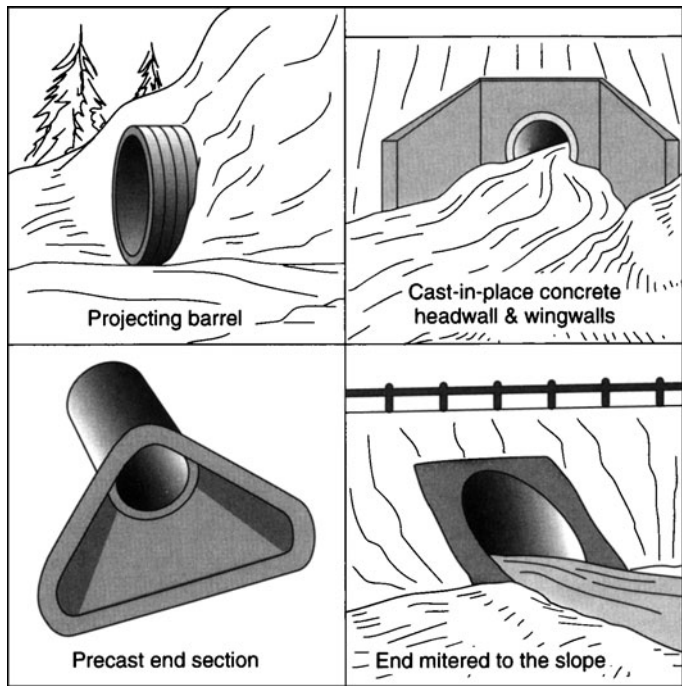


Figure 16.2.1 Four standard inlet types (schematic) (from Normann et al. (1985)).

Culverts have numerous cross-sectional shapes, including circular, box (rectangular), elliptical, pipe arch, and arch. Shape selection is typically based upon cost of construction, limitation on upstream water surface elevation, roadway embankment height, and hydraulic performance. Culverts are also made of numerous materials, depending upon structural strength, hydraulic roughness, durability, and corrosion and abrasion resistance. Concrete, corrugated aluminum, and corrugated steel are the three most common.

Various types of inlets are also used for culverts, including both prefabricated and constructed-in-place inlets. Some of the commonly used inlets are illustrated in Figure 16.2.1. Inlet design is important because the hydraulic capacity of a culvert may be improved by the appropriate inlet selection. Natural channels are usually much wider than the culvert barrel, so that the inlet is a flow contraction and can be the primary flow control.

16.2.1 Culvert Hydraulics

16.2.1.1 Types of Control

There are two basic types of flow control in culverts: *inlet control* and *outlet control*. Culverts with inlet control have high-velocity shallow flow that is supercritical, as shown in Figure 16.2.2. The control section is at the upstream end (inlet) of the culvert barrel. Culverts with outlet control have lower velocity, deeper flow that is subcritical, as shown in Figure 16.2.3. The control section is at the downstream end (outlet) of the culvert barrel. Tailwater depths are either critical depth or higher.

Figure 16.2.2 illustrates four different examples of inlet control that depend on the submergence of the inlet and outlet ends of the culvert. In Figure 16.2.2a, neither end of the culvert is submerged. Flow passes through critical depth just downstream of the culvert entrance with supercritical flow in the culvert barrel. Partly full flow occurs throughout the length of the culvert, approaching normal depth at the outlet.

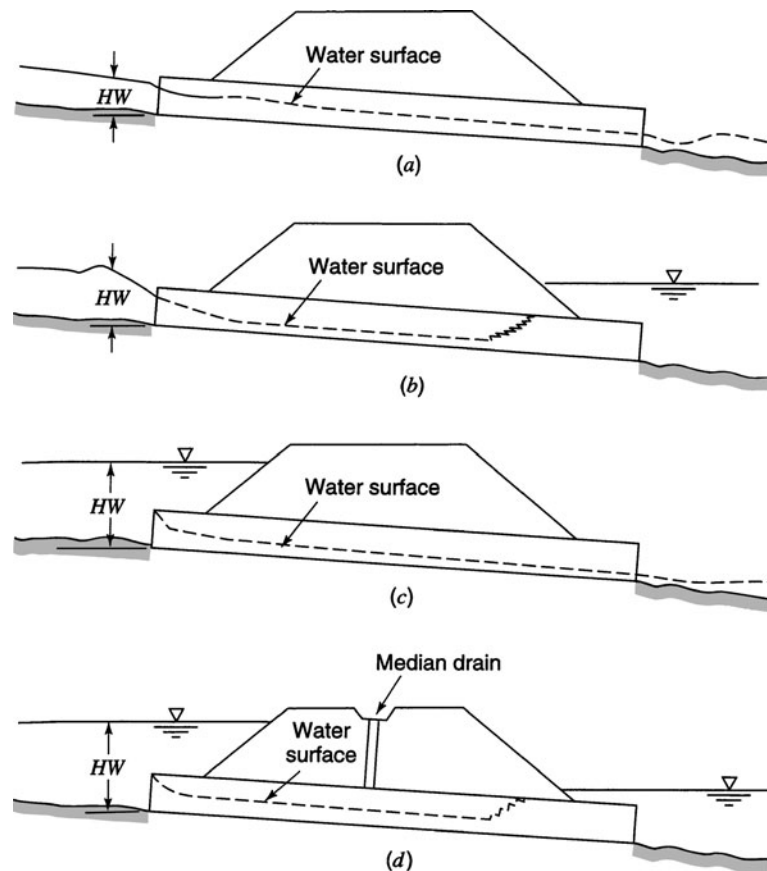


Figure 16.2.2 Types of inlet control. (a) Outlet and inlet unsubmerged; (b) Outlet submerged, inlet unsubmerged; (c) Inlet submerged and outlet unsubmerged; (d) Outlet and inlet submerged (from Normann et al. (1985)).

In Figure 16.2.2*b*, the outlet is submerged and the inlet is unsubmerged. The flow just downstream of the inlet is supercritical and a hydraulic jump occurs in the culvert barrel. In Figure 16.2.2*c*, the inlet is submerged and the outlet is unsubmerged. Supercritical flow occurs throughout the length of the culvert barrel, with critical depth occurring just downstream of the culvert entrance. Flow approaches normal depth at the downstream end. This flow condition is typical of design conditions. Figure 16.2.2*d* shows an unusual condition in which submergence occurs at both ends of the culvert with a hydraulic jump occurring in the culvert barrel. Note the median inlet, which provides ventilation of the culvert barrel.

Figure 16.2.3 illustrates five flow conditions for outlet control. Subcritical flow occurs for the partly full flow conditions. Figure 16.2.3*a* is the classic condition with both the inlet and the outlet submerged, with pressurized flow throughout the culvert. In Figure 16.2.3*b*, the outlet is submerged and the inlet is unsubmerged. In Figure 16.2.3*c*, the entrance is submerged enough that full flow occurs throughout the culvert length but the exit is unsubmerged. Figure 16.2.3*d* is a typical condition in which the entrance is submerged by the headwater and the outlet end flows freely with a low tailwater. The culvert barrel flows partly full part of the length with subcritical flow and passes through critical just upstream of the outlet. Figure 16.2.3*e* is another typical condition in which neither the inlet nor the outlet is submerged. The flow is subcritical and partly full throughout the length of the culvert barrel.

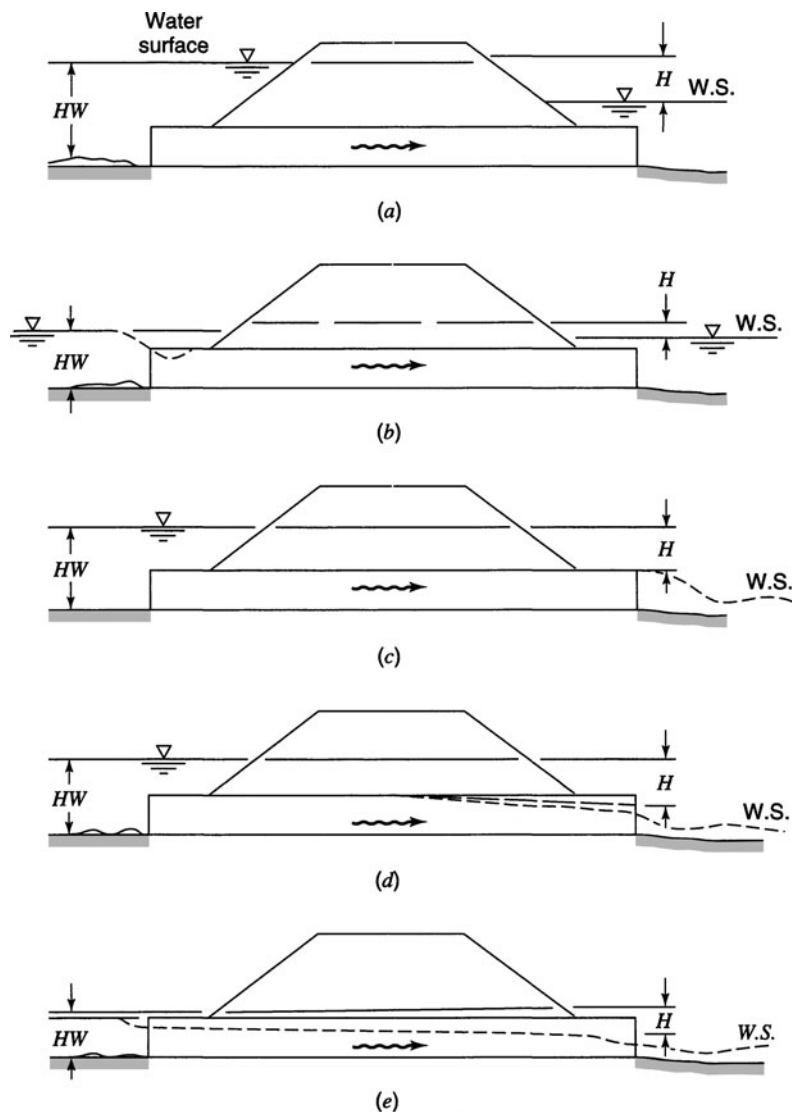


Figure 16.2.3 Types of outlet control (from Normann et al. (1985)).

16.2.1.2 Inlet-Control Design Equations

A culvert under inlet-control conditions performs as an orifice when the inlet is submerged and as a weir when it is unsubmerged. The (submerged) orifice discharge equation is computed using

$$\left[\frac{HW}{D} \right] = C \left[\frac{Q}{AD^{0.5}} \right]^2 + Y + Z \quad \text{for} \quad \left[\frac{Q}{AD^{0.5}} \right] \geq 4.0 \quad (16.2.1)$$

where HW is the headwater depth above the inlet control section invert (ft), D is the interior height of the culvert barrel (ft), Q is the discharge (ft^3/s), A is the full cross-sectional area of the culvert barrel in (ft^2), S_0 is the culvert barrel slope (ft/ft), C and Y are constants from Table 16.2.1, and Z is the slope correction factor where $Z = -0.5S_0$ in general and $Z = +0.7S_0$ for mitered inlets.

Table 16.2.1 Constants for Inlet Control Design Equations

Chart ^a no.	Shape and material	Nomograph scale	Inlet edge description	Unsubmerged			Submerged	
				Equation form ^b	<i>K</i>	<i>M</i>	<i>C</i>	<i>Y</i>
1	Circular concrete	1	Square edge w/headwall	1	0.0098	2.0	0.0398	0.67
		2	Groove and w/headwall		.0078	2.0	.0292	.74
		3	Groove and projecting		.0045	2.0	.0317	.69
2	Circular CMP	1	Headwall	1	.0078	2.0	.0379	.69
		2	Mitered to slope		.0210	1.33	.0463	.75
		3	Projecting		.0340	1.50	.0553	.54
3	Circular	A	Beveled ring, 45° bevels	1	.0018	2.50	.0300	.74
		B	Beveled ring, 33.7° bevels		.0018	2.50	.0243	.83
8	Rectangular box	1	30° to 75° wingwall flares	1	.026	1.0	.0385	.81
		2	90° and 15° wingwall flares		.061	0.75	.0400	.80
		3	0° wingwall flares		.061	0.75	.0423	.82
9	Rectangular box	1	45° wingwall flare <i>d</i> = 0.0430	2	.510	.667	.0309	.80
		2	18° to 33.7° wingwall flare <i>d</i> = 0.0830		.486	.667	.0249	.83
10	Rectangular box	1	90° headwall w/3/4" chamfers	2	.515	.667	.0375	.79
		2	90° headwall w/45° bevels		.495	.667	.0314	.82
		3	90° headwall w/33.7° bevels		.486	.667	.0252	.865
11	Rectangular box	1	3/4" chamfers; 45° skewed headwall	2	.522	.667	.0402	.73
		2	3/4" chamfers; 30° skewed headwall		.533	.667	.0425	.705
		3	3/4" chamfers; 15° skewed headwall		.545	.667	.04505	.68
			45° bevels; 10°–45° skewed headwall		.498	.667	.0327	.75
12	Rectangular box 3/4" chamfers	1	45° non-offset wing wall flares	2	.497	.667	.0339	.805
		2	18.4° non-offset wingwall flares		.493	.667	.0361	.806
		3	18.4° non-offset wingwall flares		.495	.667	.0386	.71
			30° skewed barrel					
13	Rectangular box Top bevels	1	45° wingwall flares — offset	2	.495	.667	.0302	.835
		2	33.7° wingwall flares — offset		.493	.667	.0252	.881
		3	18.4° wingwall flares — offset		.497	.667	.0227	.887
16–19	CM boxes	1	90° headwall	1	.0083	2.0	.0379	.69
		2	Thick wall projecting		.0145	1.75	.0419	.64
		3	Thin wall projecting		.0340	1.5	.0496	.57
29	Horizontal ellipse concrete	1	Square edge with headwall	1	.0100	2.0	.0398	.67
		2	Groove end with headwall		.0018	2.5	.0292	.74
		3	Groove end projecting		.0045	2.0	.0317	.69
30	Vertical ellipse concrete	1	Square edge with headwall	1	.0100	2.0	.0398	.67
		2	Groove end with headwall		.0018	2.5	.0292	.74
		3	Groove end projecting		.0095	2.0	.0317	.69
34	Pipe arch 18" corner radius CM	1	90° headwall	1	.0083	2.0	.0379	.69
		2	Mitered to slope		.0300	1.0	.0463	.75
		3	Projecting		.0340	1.5	.0496	.57
35	Pipe arch 18" corner radius CM	1	Projecting	1	.0296	1.5	.0487	.55
		2	No. bevels		.0087	2.0	.0361	.66
		3	33.7° bevels		.0030	2.0	.0264	.75
36	Pipe arch 31" corner radius CM	1	Projecting	1	.0296	1.5	.0487	.55
			No. bevels		.0087	2.0	.0361	.66
			33.7° bevels		.0030	2.0	.0264	.75

(Continued)

Table 16.2.1 (Continued)

Chart ^a no.	Shape and material	Nomograph scale	Inlet edge description	Unsubmerged			Submerged	
				Equation form ^b	<i>K</i>	<i>M</i>	<i>C</i>	<i>Y</i>
40–42	Arch CM	1	90° headwall	1	.0083	2.0	.0379	.69
		2	Mitered to slope		.0300	1.0	.0463	.75
		3	Thin wall projecting		.0340	1.5	.0496	.57
55	Circular	1	Smooth tapered inlet throat	2	.534	.555	.0196	.89
		2	Rough tapered inlet throat		.519	.64	.0289	.90
56	Elliptical Inlet face	1	Tapered inlet—beveled edges	2	.536	.622	.0368	.83
		2	Tapered inlet—square edges		.5035	.719	.0478	.80
		3	Tapered inlet—thin edge projecting		.547	.80	.0598	.75
57	Rectangular	1	Tapered inlet throat	2	.475	.667	.0179	.97
58	Rectangular concrete	1	Side tapered—less favorable edges	2	.56	.667	.0466	.85
		2	Side tapered—more favorable edges		.56	.667	.3978	.87
59	Rectangular concrete	1	Slope tapered—less favorable edges	2	.50	.667	.0466	.65
			Slope tapered—more favorable edges		.50	.667	.0378	.71

^a Chart number in Normann et al. (1985)

^b Form 1 is equation (16.2.2)

Form 2 is equation (16.2.3)

Source: Normann et al. (1985).

The (unsubmerged) weir discharge equation is (Form 1):

$$\left[\frac{HW}{D} \right] = \left[\frac{H_c}{D} \right] + K \left[\frac{Q}{AD^{0.5}} \right]^M + Z \quad \text{for} \quad \left[\frac{Q}{AD^{0.5}} \right] \leq 3.5 \quad (16.2.2)$$

where H_c is the specific head at critical depth ($H_c = d_c + V_c^2/2g$) (ft), d_c is the critical depth (ft), V_c is the critical velocity (ft/s), and K and M are constants in Table 16.2.1. A simpler equation to use for the unsubmerged condition is (Form 2):

$$\left[\frac{HW}{D} \right] = K \left[\frac{Q}{AD^{0.5}} \right]^M + Z \quad \text{for} \quad \left[\frac{Q}{AD^{0.5}} \right] \leq 3.5 \quad (16.2.3)$$

Form 2 is easier to apply and is the only documented form for some of the design inlet control nomographs in Normann et al. (1985).

Equations (16.2.1) to (16.2.3) are implemented by assuming a culvert diameter D and using it on the right-hand side of these equations and solving for $[HW/D]$. The headwater depth is then obtained by multiplying $D[HW/D]$. Typical inlet-control nomographs are presented in Figures 16.2.4 and 16.2.5.

16.2.1.3 Outlet-Control Design Equations

A culvert under outlet-control conditions has either subcritical flow or full-culvert flow, so that outlet-control flow conditions can be calculated using an energy balance. For the condition of full-culvert flow, considering entrance loss H_e , friction loss (using Manning’s equation) H_f , and exit loss H_0 , the total headloss H is

$$H = H_0 + H_e + H_f \quad (16.2.4a)$$

and in U.S. customary units is

$$H = \left[1 + K_e + \left(\frac{29n^2L}{R^{1.33}} \right) \right] \frac{V^2}{2g} \quad (16.2.4b)$$

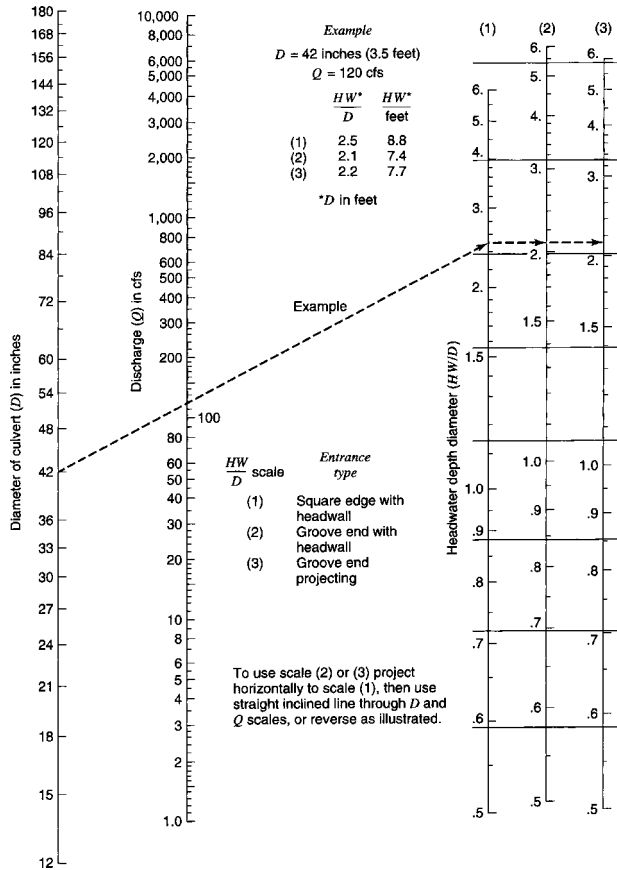


Figure 16.2.4 Headwater depth for concrete pipe culverts with inlet control (from Normann et al. (1985)).

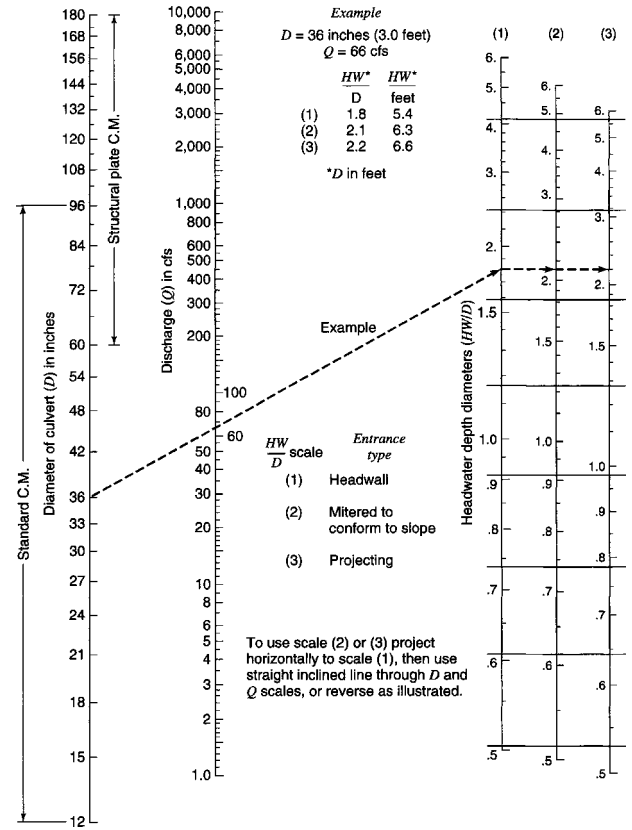


Figure 16.2.5 Headwater depth for CM pipe culverts with inlet control (from Normann et al. (1985)).

or in SI units is

$$H = \left[1 + K_e + \left(\frac{20n^2L}{R^{1.33}} \right) \right] \frac{V^2}{2g} \tag{16.2.4c}$$

where K_e is the entrance loss coefficient, n is Manning’s roughness coefficient, R is the hydraulic radius of the full-culvert barrel in feet (m), V is the velocity in ft/s (m/s), and L is the culvert length in feet (m). Other losses such as bend losses H_b , junction losses H_j , and grate losses H_g can also be added to equation (16.2.4). Table 16.2.2 lists common values of Manning’s n values for culverts. Table 16.2.3 lists entrance loss coefficients for outlet control, full or part full flow.

Figure 16.2.6 illustrates the energy and hydraulic grade lines for full flow in a culvert. Equating the total energy at section 1 (upstream) and section 2 (downstream) gives

$$HW_0 + \frac{V_u^2}{2g} = TW + \frac{V_d^2}{2g} + H_f + H_e + H_0 \tag{16.2.5}$$

where HW_0 is the headwater depth above the outlet invert and TW is the tailwater depth above the outlet invert. Neglecting the approach velocity head and the downstream velocity head (Figure 16.2.6), equation (16.2.5) reduces to

$$HW_0 = TW + H_f + H_e + H_0 \tag{16.2.6}$$

Table 16.2.2 Manning *n* Values for Culverts*

Type of conduit	Wall description	Manning <i>n</i>
Concrete pipe	Smooth walls	0.010–0.013
Concrete boxes	Smooth walls	0.012–0.015
Corrugated metal pipes and boxes, annular or helical pipe (Manning <i>n</i> varies with barrel size)	2 2/3" by 1/2" corrugations	0.022–0.027
	6" by 1" corrugations	0.022–0.025
	5" by 1" corrugations	0.025–0.026
	3" by 1" corrugations	0.027–0.028
	6" by 2" structural plate corrugations	0.033–0.035
	9" by 2 1/2" structural plate corrugations	0.033–0.037
Corrugated metal pipes, helical corrugations, full circular flow	2 2/3" by 1/2" corrugations	0.012–0.024
Spiral rib metal pipe	Smooth walls	0.012–0.013

*Note: The values indicated in this table are recommended Manning *n* design values. Actual field values for older existing pipelines may vary depending on the effects of abrasion, corrosion, deflection, and joint conditions. Concrete pipe with poor joints and deteriorated walls may have *n* values of 0.014 to 0.018. Corrugated metal pipe with joint and wall problems may also have higher *n* values, and in addition may experience shape changes that could adversely affect the general hydraulic characteristics of the pipeline.

Source: Normann et al. (1985).

Table 16.2.3 Entrance Loss Coefficients for Outlet Control, Full or Partly Full $H_e = K_e[V^2/2g]$

Type of structure and design of entrance	Coefficient K_e
<i>Pipe, concrete</i>	
Mitered to conform to fill slope	0.7
*End section conforming to fill slope	0.5
Projecting from fill, square cut end	0.5
Headwall or headwall and wingwalls	
Square-edge	0.5
Rounded (radius = 1/12D)	0.2
Socket end of pipe (groove-end)	0.2
Projecting from fill, socket end (groove-end)	0.2
Beveled edges, 33.7° or 45° bevels	0.2
Side- or slope-tapered inlet	0.2
<i>Pipe or pipe-arch, corrugated metal</i>	
Projecting from fill (no headwall)	0.9
Mitered to conform to fill slope, paved or unpaved slope	0.7
Headwall or headwall and wingwalls square-edge	0.5
*End section conforming to fill slope	0.5
Beveled edges, 33.7° or 45° bevels	0.2
Side- or slope-tapered inlet	0.2
<i>Box, reinforced concrete</i>	
Wingwalls parallel (extension of sides)	
Square-edged at crown	0.7
Wingwalls at 10° to 25° or 30° to 75° to barrel	
Square-edged at crown	0.5
Headwall parallel to embankment (no wingwalls)	
Square-edged on 3 edges	0.5
Rounded on 3 edges to radius of 1/12 barrel dimension, or beveled edges on 3 sides	0.2

(Continued)

Table 16.2.3 (Continued)

Type of structure and design of entrance	Coefficient K_e
Wingwalls at 30° to 75° to barrel	
Crown edge rounded to radius of 1/12 barrel dimension, or beveled top edge	0.2
Side- or slope-tapered inlet	0.2

*Note: "End section conforming to fill slope," made of either metal or concrete, are the sections commonly available from manufacturers. From limited hydraulic tests, they are equivalent in operation to a headwall in both *inlet* and *outlet* control. Some end sections, incorporating a *closed* taper in their design, have superior hydraulic performance. These latter sections can be designed using the information given for the beveled inlet.

Source: Normann et al. (1985).

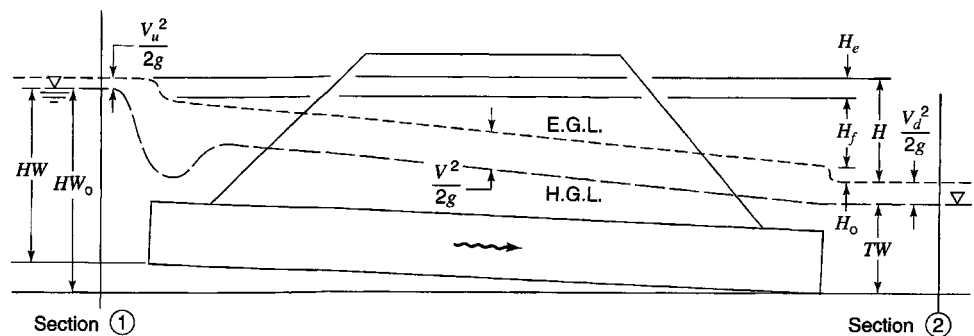


Figure 16.2.6 Full-flow energy and hydraulic grade lines (from Normann et al. (1985)).

For full flow $TW \geq D$; however, for partly full flow, the headloss should be computed from a backwater analysis. An empirical equation for the head loss H for this condition is

$$H = HW_0 - h_0 \quad (16.2.7)$$

where $h_0 = \max[TW, (D + d_c)/2]$.

The outlet-controlled headwater depth can be computed by first determining the tailwater depth from backwater computations where TW is measured above the outlet invert. By using equation (16.2.4) for full-flow conditions the headloss H is obtained. With equation (16.2.7), the *required outlet-controlled headwater elevation* HW is obtained as

$$HW = H + h_0 - LS_0 \quad (16.2.8)$$

Sample outlet-control nomographs are shown in Figures 16.2.7 and 16.2.8. Using the value of H from these nomographs, equation (16.2.8) can be implemented to compute HW_0 . For Manning's n value different from that of the outlet nomograph, a modified length L_1 is used as the length scale:

$$L_1 = L \left(\frac{n_1}{n} \right)^2 \quad (16.2.9)$$

where L is the actual culvert length, n_1 is the desired Manning's n , and n is the Manning n from the chart.

The larger of the headwater elevation, obtained from the inlet- and outlet-control calculation, is adopted as the design headwater elevation. If a design headwater elevation exceeds the permissible headwater elevation, a new culvert configuration is selected and the process is repeated. Under outlet-control conditions a larger barrel is necessary since inlet improvement may have only limited effect. In the case of very large culverts, the use of multiple culverts may be required with the new

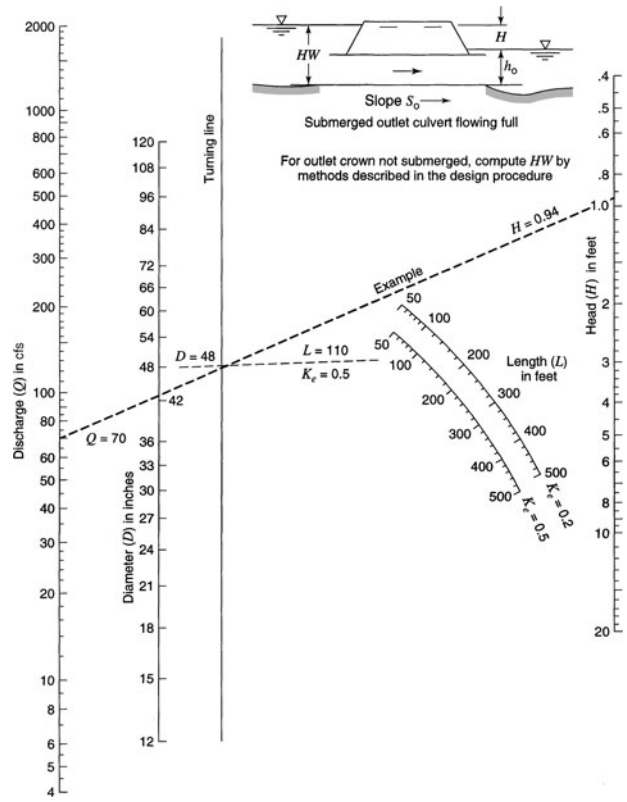


Figure 16.2.7 Head for concrete pipe culverts flowing full, $n = 0.012$ (from Normann et al. (1985)).

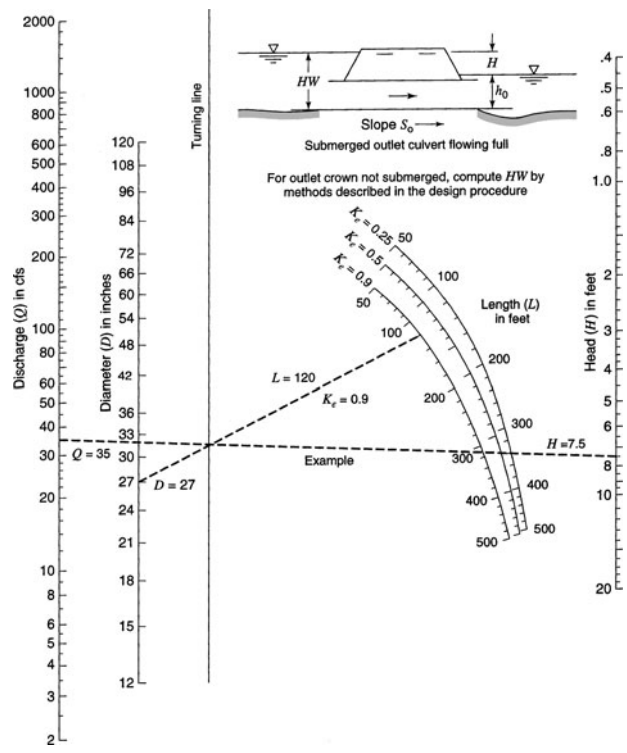


Figure 16.2.8 Head for standard CM pipe culverts flowing full, $n = 0.024$ (from Normann et al. (1985)).

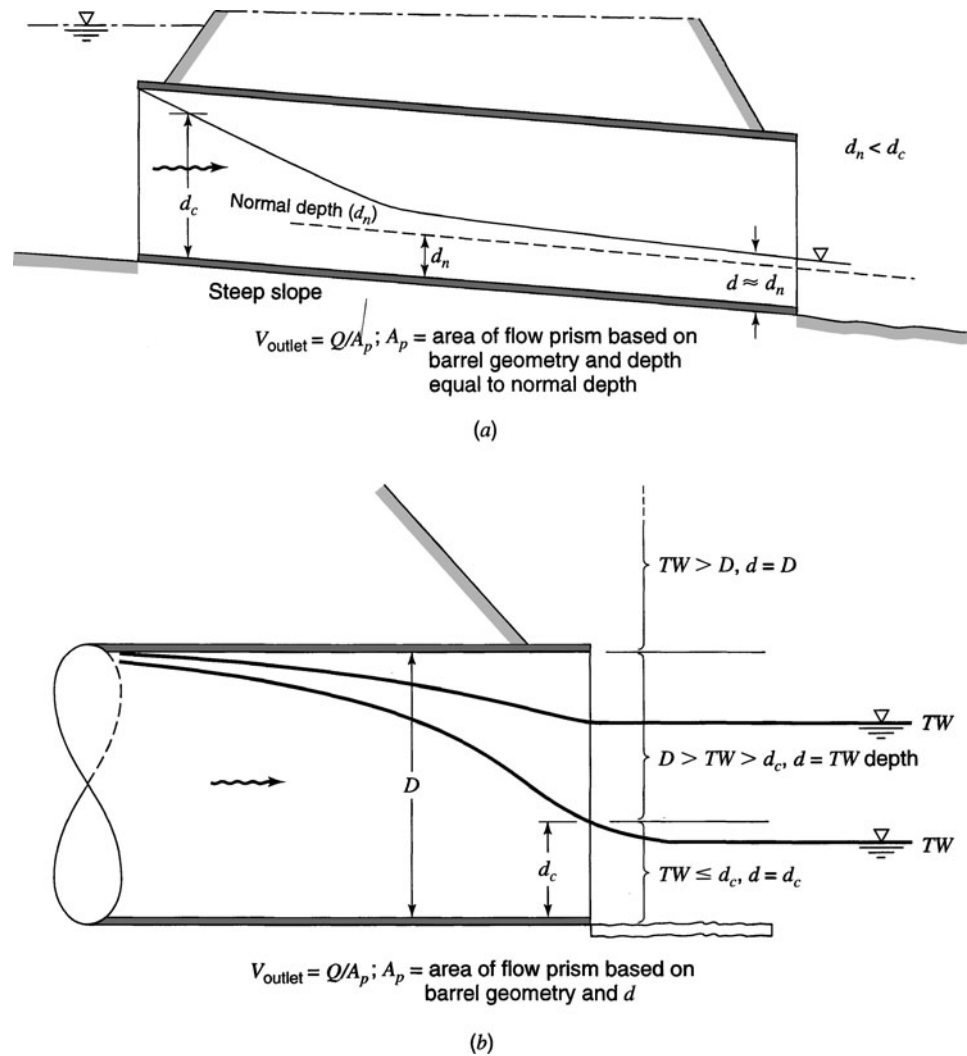


Figure 16.2.9 Outlet velocity for (a) inlet and (b) outlet control (from Normann et al. (1985)).

design discharge taken as the ratio of the original discharge to the number of culverts. Figure 16.2.9 illustrates computation of the outlet velocity under inlet control and outlet control.

EXAMPLE 16.2.1

Analyze a 6 ft × 5 ft square-edged reinforced concrete box culvert for a roadway crossing to pass a 50-year discharge of 300 ft³/s with the following site conditions (adapted from Normann et al. (1985)):

Shoulder elevation = 113.5 ft

Stream bed elevation at culvert face = 100.0 ft

Natural stream slope = 2%

Tailwater depth = 4.0 ft

Approximate culvert length = 250 ft

Maximum allowable upstream water surface (head) elevation = 110 ft (based on adjacent structures)

The inlet is not to be depressed (no fall). Refer to Figure 16.2.10 for further details.

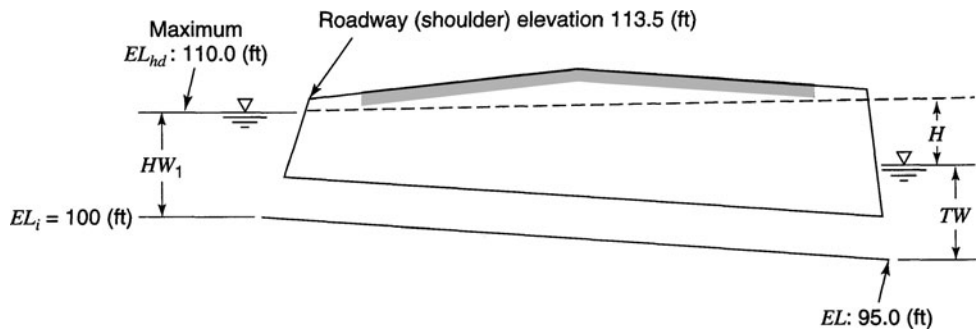


Figure 16.2.10 Details of culvert for Example 16.2.1.

SOLUTION

- Consider an outlet control and determine the headwater elevation (EL_{h0}) in steps 1–8.
- Step 1 The tailwater depth is specified as 4.0 ft, which is obtained from backwater computations or from normal depth calculations.
- Step 2 The critical depth is computed as $d_c = \sqrt[3]{\frac{(300/6)^2}{32.2}} = 4.27$ ft.
- Step 3 $\frac{d_c + D}{2} = \frac{4.27 + 5.0}{2} = 4.64$ ft.
- Step 4 $h_0 = TW$ or $(d_c + D)/2$, whichever is larger. For this problem $h_0 = 4.64$ ft.
- Step 5 Use Table 16.2.3 to obtain the entrance loss coefficient. For the square-edged entrance, $K_e = 0.5$.
- Step 6 Determine headlosses through the culvert barrel; use equation (16.2.4):

$$H = \left[1 + K_e + \left(\frac{29n^2L}{R^{1.33}} \right) \right] \frac{V^2}{2g}$$

where $A = 6 \times 5 = 30 \text{ ft}^2$, $V = 300/30 = 10 \text{ ft/s}$, $R = A/P = 30/(6 + 6 + 5 + 5) = 1.36$ ft. For concrete box culvert, take $n = 0.012$. So, $H = \left[1 + 0.5 + \left(\frac{29(0.012)^2(250)}{1.36^{1.33}} \right) \right] \frac{10^2}{2(32.2)} = 3.41$ ft. Because $TW < D$ there is only partly full flow at the exit. The headlosses would be more accurately computed from a backwater analysis.

Step 7 Determine the required outlet control head water elevation (EL_{h0}), $EL_{h0} = EL_0 + H_0 + h_0$, EL_0 is the invert elevation at the outlet (see Figure 16.2.10):

$$EL_0 = EL_i - S_0L = 100 - 0.02(250) = 95 \text{ ft}$$

Then $EL_{h0} = 95 + 3.41 + 4.64 = 103$ ft. Also the approach velocity head ($V_u^2/2g$) and the downstream velocity head can be considered in the calculation of EL_{h0} by adding $V_d^2/2g$ and subtracting $V_u^2/2g$ from the right-hand side of the above equation for EL_{h0} .

Now consider inlet control and determine headwater elevation, EL_{hi} .

Step 8 The design headwater elevation is now computed as $EL_{hi} = HW_i + EL_i$, so HW_i must be computed using equation (16.2.1), where

$$\frac{HW}{D} = C \left[\frac{Q}{AD^{0.5}} \right]^2 + Y + Z$$

and C and Y are obtained from Table 16.2.1 as $C = 0.0423$ and $Y = 0.82$ for a rectangular box culvert with 0° wingwall flares. $Z = -0.5S_0 = -0.5(0.02) = -0.01$

$$\frac{HW}{D} = 0.0423 \left[\frac{300}{30(5)^{0.5}} \right]^2 + 0.82 - 0.01 = 1.66$$

To check,

$$\left[\frac{Q}{AD^{0.5}} \right] = 4.47 > 4$$

$$HW_i = D \left[\frac{HW}{D} \right] = 5(1.66) = 8.28 \text{ ft}$$

$$EL_{hi} = 8.28 + 100 = 108.28 \text{ ft}$$

The design headwater elevation of 108.28 ft exceeds the outlet-control headwater elevation of 103 ft. Also, the headwater elevation is less than the roadway shoulder elevation of 113.5 ft.

This design is OK; however, a smaller culvert could be considered. In fact, for this problem a 5 ft × 5 ft reinforced concrete culvert with either a square-edged entrance or a 45° beveled-edge entrance will work, as shown by Normann et al. (1985).

16.2.2 Culvert Design

The hydrologic analysis for culverts involves estimation of the design flow rate based upon the climatological and watershed characteristics. Chapters 7 through 9 and 15 cover the various methods used. The previous section described the use of the hydraulic equations and nomographs for the design of culverts under inlet and outlet conditions. This section concentrates on the use of performance curves for the design process. *Performance curves* are relationships of the flow rate versus the headwater depth or elevation for different culvert designs, including the inlet configuration. Both inlet and outlet performance curves are developed.

An overall performance curve can be developed using the following procedure (Norman et al., 1985):

1. Select a range of flow rates and determine the corresponding headwater elevation for the culvert. The flow rate should cover a range of flows of interest above and below the design discharge. Both inlet and outlet control headwater are computed.
2. Combine the inlet- and outlet-control performance curves into a single curve.
3. For roadway overtopping (culvert headwater elevation > roadway crest), compute the equivalent upstream water depth above the roadway crest for each flow rate using the weir equation

$$Q_0 = C_d L (HW_r)^{1.5} \quad (16.2.10)$$

where Q_0 is the overtopping flow rate in ft^3/s (m^3/s), C_d is the discharge coefficient ($C_d = k_t C_r$, see Figure 16.2.11), L is the length of roadway crest overtopped in feet (m), and HW_r is the upstream depth measured from the roadway crest to the water surface upstream of the weir drawdown in feet (m).

4. Add the culvert flow and roadway overtopping flow for the corresponding headwater elevations to obtain the overall culvert performance curve. Figure 16.2.12 shows a culvert performance curve with roadway overtopping, showing the outlet-control portion and the inlet-control portion.

Tuncok and Mays (1999) provide a brief review of various computer models for culverts including HYDRAIN (www.fhwa.dot.gov) by the Federal Highway Administration and CAP (<http://water.usgs.gov/software/>) by the U.S. Geological Survey.

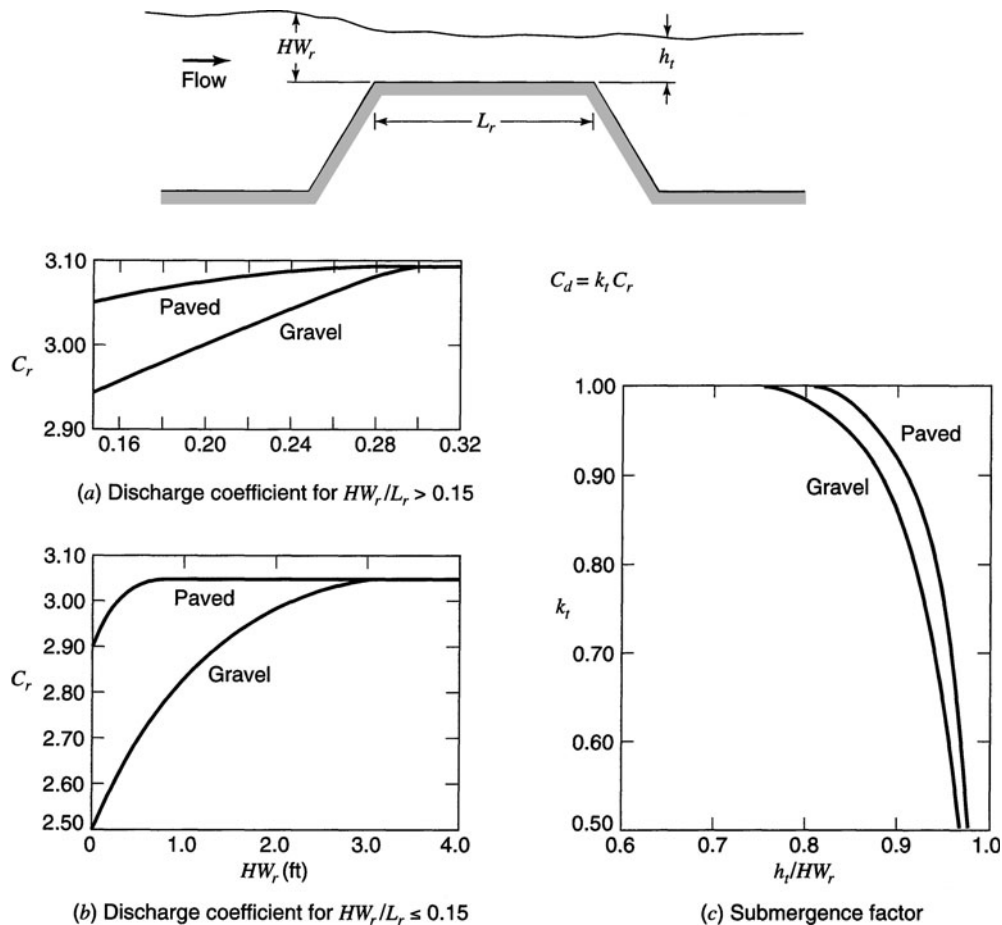


Figure 16.2.11 Discharge coefficients for roadway overtopping (from Normann et al. (1985)).

EXAMPLE 16.2.2

The objective is to develop the performance curve for an existing 7-ft × 7-ft and 200-ft long concrete box culvert on a 5 percent slope that was designed for a 50-year flood of 600 ft³/s at a design headwater elevation of 114 ft (refer to Figure 16.2.12 for further details). The roadway is a 40-ft wide gravel road that can be approximated as a broad-crested weir with center line elevation of 116 ft. The culvert inlet invert elevation is 100 ft. The tailwater depth-discharge relationship is (modified from Normann et al. (1985)):

Q (ft ³ /s)	400	600	800	1000	1200
TW (ft)	2.6	3.1	3.8	4.1	4.5

The flow width on the roadway for various elevations are:

Elevation (ft)	116.0	116.5	117.0	117.5	118.0	119.0
Flow width (ft)	0	100	150	200	250	300

SOLUTION

The same basic type of calculations performed in example 16.2.1 are followed in Table 16.2.4 for various discharges ranging from 400 ft³/s to 1000 ft³/s. From Figure 16.2.11, we find

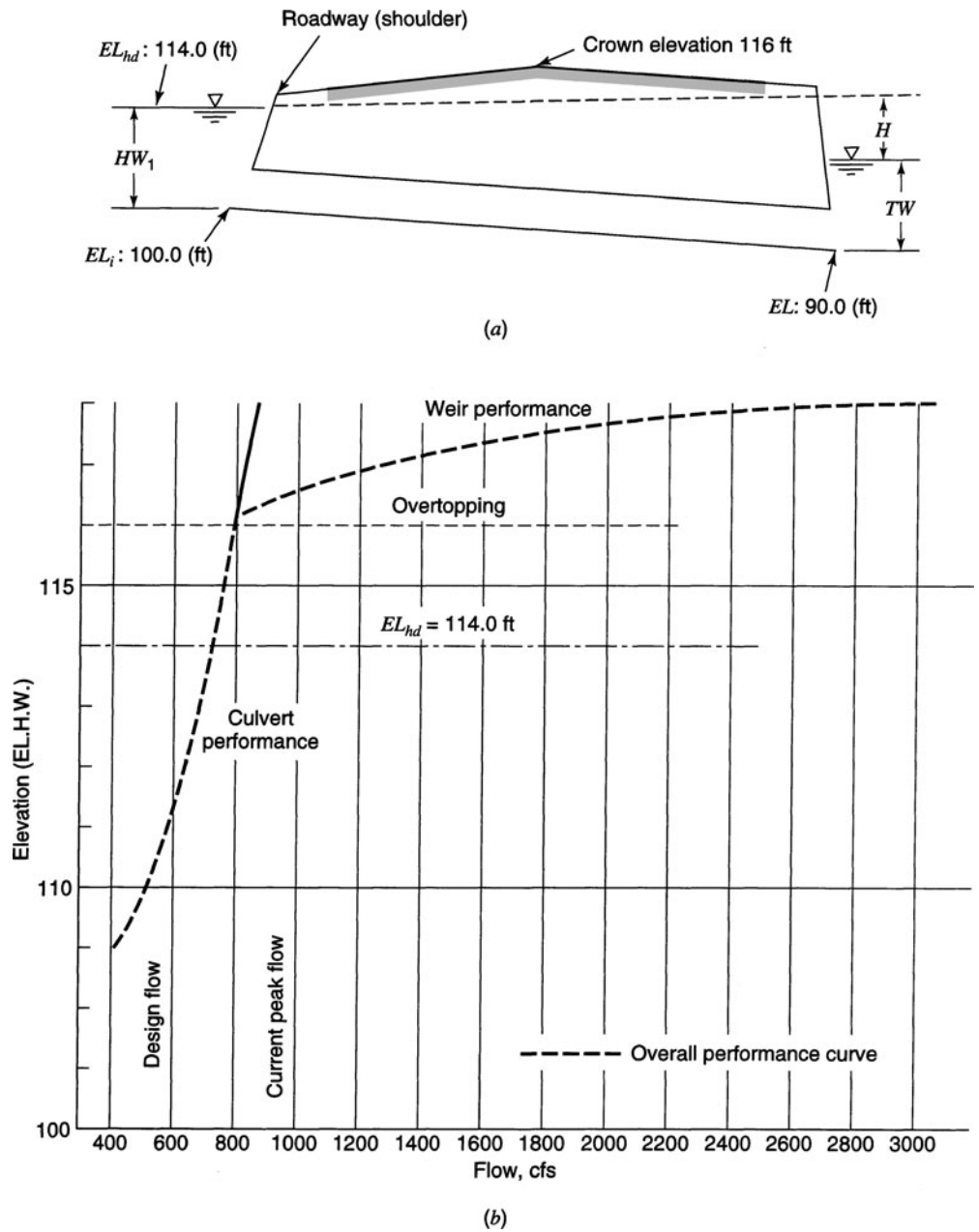


Figure 16.2.12 (a) Culvert profile; (b) Performance curve (from Johnson and Chang (1984)).

$$C_d = 2.70 @ HW_r = 0.57$$

$$Q = C_d L (HW_r)^{1.5}$$

$$C_d = 2.97 @ HW_r = 1.9$$

$$k_r = 1$$

The performance curve computations are given in Table 16.2.5. The resulting performance curve is shown in Figure 16.2.12b.

Table 16.2.4 Discharge-headwater Computations for Culvert Flow—Example 16.2.2

Headwater calculations												
Total flow Q (cfs)	Flow per barrel Q/N	Inlet control			Outlet control							Control head elevation
		HW_i/D	HW_i	EL_{hi}	TW	d_c	$\frac{d_c+D}{2}$	h_0	K_e	H	EL_{h0}	
400	400	1.15	8.1	108.1	2.6	4.6	5.8	5.8	0.5	1.95	97.8	108.1
600	600	1.65	11.6	111.6	3.1	6.1	6.6	6.6	0.5	4.4	101.0	111.6
700	700	1.95	13.7	113.7	3.5	6.8	6.9	6.9	0.5	6.0	102.9	113.7
800	800	2.35	16.5	116.5	3.8	>7	7.0	7.0	0.5	7.9	104.9	116.5
850	850	2.55	17.9	117.9	3.9	>7	7.0	7.0	0.5	9.0	106.0	117.9
1000	1000	3.21	22.5	122.5	4.1	>7	7.0	7.0	0.5	1.26	109.6	122.5

Table 16.2.5 Performance Curve Computations—Example 16.2.2

Q_c Culvert flow	EL_h	H_0	Q_0 Overtopping flow	Q Total flow
400	108.1	—	—	400
600	111.6	—	—	600
700	113.7	—	—	700
800	116.5	0.5	191	991
850	117.9	1.9	1556	2406

PROBLEMS

16.1.1 Determine the time of concentration for an overland flow length of 100 m on a turf surface ($n = 0.4$) with an average slope of 0.02 for a design frequency of 10 years in Phoenix, AZ (see Figure P15.2.1).

16.1.2 Determine the time of concentration for an overland flow length of 200 m on bare sand ($n = 0.01$) with an average slope of 0.003 m/m for a design frequency of 10 years in Phoenix, AZ (see Figure P15.2.1).

16.1.3 Determine the time of concentration for an overland flow length of 200 ft on an area ($n = 0.10$) in Colorado Springs, CO, for a design frequency of 25 years. The rainfall intensity-duration relationship for a 25-year frequency is as given below. Take the average slope of the area as 0.005 ft/ft.

Duration (min)	5	10	15	30	60
Rainfall intensity (in/hr)	7.3	5.7	4.8	3.3	2.1

16.1.4 Determine the time of concentration for an overland flow length of 400 ft on an area of bluegrass sod ($n = 0.45$) in Charlotte, NC, for a 5-year recurrence interval. The 5-year rainfall intensity-duration relationship (i in in/hr and t_D in minutes) is

$$i = \frac{57}{(t_D + 12)^{0.77}}$$

Take the average slope of the overland flow area as 0.010 ft/ft.

16.1.5 Determine the peak runoff from 500 ft of pavement (32 ft wide) that drains toward a gutter (for a 10-year frequency storm) in Phoenix, AZ. The pavement slope is 0.005, $n = 0.016$, and $C = 0.9$.

16.1.6 Rework problem 16.1.5 for a 25-year storm.

16.1.7 Determine the runoff from 600 ft of pavement (32 ft wide) that drains toward a gutter for a 25-year frequency storm in Colorado Springs, CO. The pavement slope is 0.02, $n = 0.016$, and $C = 0.9$. See problem 16.1.3 for rainfall information.

16.1.8 Compute the time of flow in a gutter for the situation in which the spread T_1 at the upstream end is 1 ft, which results from the bypass flow from the upstream inlet. The design spread T_2 at the second inlet is 5 ft, the gutter slope is $S = 0.025$, and the cross slope is $S_x = 0.02$. Manning's $n = 0.016$ and the inlet spacing is 200 ft.

16.1.9 Rework problem 16.1.8 with $T_1 = 0.5$ m, $T_2 = 1.5$ m, and the inlet spacing equals 100 m. All other information is the same as in problem 16.1.8.

16.1.10 Compute the flow rate in a gutter section with a design spread of $T_w = 8$ ft and a cross-slope of $S_x = 0.025$. The gutter slope $S = 0.01$ and Manning's n is 0.016.

16.1.11 Compute the flow rate in a gutter section with a design spread of 2.45 m and cross-slope of $S_x = 0.025$. The gutter slope $S = 0.01$ and Manning's n is 0.016.

16.1.12 Compute the flow rate in a composite gutter section with a design spread of $T_w = 8$ ft, a cross-slope of $S_x = 0.03$, $W = 2.0$ ft

with a 2-in gutter depression. The gutter slope is $S = 0.005$ and Manning's n is 0.016.

16.1.13 Compute the flow rate in a composite gutter section with a design spread of $T_w = 2.45$ m, a cross-slope of $S_x = 0.03$, $W = 0.60$ m with a 5-cm gutter depression. The gutter slope is $S = 0.005$ and Manning's n is 0.016.

16.1.14 Using the data for the composite gutter section in problem 16.1.12, find the interception capacity of a bar grate (P-1-7/8) that is 2 ft long and 2 ft wide.

16.1.15 Rework problem 16.1.14 using a parallel bar grate that is 2 ft long and 2 ft wide.

16.1.16 Rework problem 16.1.14 using a curved vane grate (CV-3-1/4-4-1/4) that is 2 ft long and 2 ft wide.

16.1.17 Using the data in problem 16.1.13, find the interception capacity of a bar grate (P-1-7/8) that is 0.6 m long and 0.6 m wide.

16.1.18 Rework problem 16.1.17 using a curved vane grate (CV-3-1/4-4-1/4) that is 0.6 m long and 0.6 m wide.

16.1.19 Using the data in problem 16.1.14, determine the interception capacity for an 8-ft curb opening.

16.1.20 Using the data in problem 16.1.16, determine the interception capacity for a 1.83-m curb opening.

16.1.21 Rework Example 16.1.6 for a 5-ft curb-opening inlet.

16.1.22 Determine the interception capacity for a 3.048-m curb-opening inlet given $S_x = 0.03$, $n = 0.016$, $S = 0.035$, and $T_w = 2.44$ m.

16.1.23 Solve problem 16.1.22 for a depressed 3.048 m curb-opening inlet with $a = 5.08$ cm and $W = 0.61$ m.

16.1.24 Determine the interception capacity for a 10-ft curb-opening inlet given $S_x = 0.03$, $n = 0.016$, $S = 0.035$, $T_w = 8$ ft.

16.1.25 Solve problem 16.1.24 for a depressed 10-ft curb-opening inlet with $a = 2$ in and $W = 2$ ft.

16.1.26 Determine the interception capacity of a combination curb opening-grate inlet on grade. The curb opening is 10 ft long and the grate is a 2 ft \times 2 ft reticulate grate placed along side the downstream 2 ft of the curb opening ($Q = 7$ ft³/s, $S = 0.04$, $S_x = 0.03$, and $n = 0.016$).

16.1.27 Compare the interception capacity of the combination inlet described in problem 16.1.26 with the interception capacity of just using the curb-opening inlet and with the interception capacity of just using the grate inlet.

16.1.28 Determine the grate size for a symmetrical sag vertical curve (with a curb) with equal bypass from inlets upgrade of the low point. Consider 50 percent clogging of the grate. The design discharge is 8 ft³/s and $Q_b = 3.6$ ft³/s. Determine the depth at the curb for a check discharge of 11 ft³/s ($Q_b = 4.4$ ft³/s). Check the spread at $s = 0.003$ on approaches to the low point ($T_w = 10$ ft, $S_x = 0.03$).

16.1.29 Compute the interception capacity of a 6-ft long and 5-in high curb opening inlet in a sag location.

- (a) First consider an undepressed curb opening ($S_x = 0.05$ and $T_w = 8$ ft).

- (b) Next consider a depressed curb opening ($S_x = 0.05$, $a = 2$ in, $W = 2$ ft, and $T_w = 8$ ft).

16.1.30 Determine the length of a slotted inlet in a sump location that is required to limit the maximum depth at a curb to 0.4 ft for a discharge of 3.0 ft³/s. Assume no clogging and use a slot width of 1.75 in.

16.1.31 Compute the interception capacity of a combination inlet in sag location. The grate is a P-1-7/8 that is 2 ft \times 6 ft with a curb opening of 12 ft and $h = 4$ in. The cross-slope $S_x = 0.03$ and the discharge is 10 ft³/s. What is the depth at the curb and the spread? Assume no clogging.

16.1.32 Consider a 26-ft pavement width on a continuous grade, $n = 0.016$, $S_x = 0.03$, $S = 0.03$, $T_w = 8$ ft, $i = 10.7$ in/hr, and $C = 0.8$. Determine the maximum inlet spacing for a 2-ft \times 2-ft curved vane inlet.

16.1.33 Consider a 7.92-m pavement width on a continuous grade, $n = 0.016$, $S_x = 0.03$, $S = 0.03$, $T_w = 2.45$ m, $i = 27.2$ mm/hr, and $C = 0.8$. Determine the maximum inlet spacing for a 0.61-m \times 0.61-m curved vane inlet.

16.1.34 Using the data from problem 16.1.32, determine the maximum design inlet spacing for a 10-ft curb opening depressed 2 in from the normal cross-slope in a 2-ft wide gutter.

16.1.35 Using the data from problem 16.1.33, determine the maximum design inlet spacing for a 3.048-m curb opening depressed 5.08 cm from the normal cross-slope in a 0.61-m wide gutter.

16.1.36 Using the data from problem 16.1.32, determine the maximum inlet spacing using a 15-ft slotted inlet.

16.1.37 Using the data from problem 16.1.33, determine the maximum inlet spacing using a 4.57-m slotted inlet.

16.1.38 Consider a sag vertical curve at an underpass on a four-lane divided highway facility. The spread at design Q is not to exceed the shoulder width of 10 ft, the cross-slope is $S_x = 0.05$, and $K = 130$.

(a) Determine the location of flanking inlets if they are to function in relief of the inlet at the low point when depth at the curb exceeds design depth.

(b) Determine the location of flanking inlets when the depth at the curb is 0.2 ft less than the depth at design spread.

16.1.39 Consider a 2 ft \times 2 ft P-1-7/8 grate that is to be placed in a flanking inlet location in a sag vertical curve that is 250 ft downgrade from the most downstream curved vane inlet in problem 16.1.32 ($Q_b = 2.37$ ft³/s, $S_x = 0.03$, $T_w = 8$ ft, $n = 0.016$, $i = 10.7$ in/hr). The slope on the curve at the inlet is $S = 0.006$. Determine the spread at the flanking inlet and at $S = 0.003$.

16.1.40 Rework example 16.1.16 to determine the interception capacity of a larger median drop inlet ($W = 2$ ft, $L = 4$ ft).

16.1.41 A curb-opening inlet in a sag location is to be designed with a curb opening length of 5 ft, curb opening height of 5 in, $S_x = 0.05$, and $T_w = 8$ ft. Compute the interception capacity for a horizontal throat, for an inclined throat (with $\theta = 45^\circ$), and for a vertical throat.

16.1.42 Compute the interception capacity for a horizontal throat, for an inclined throat (with $\theta = 45^\circ$), and a vertical throat in problem 16.1.41 using a curb opening length of 7 ft instead of 5 ft.

16.1.43 Compute the interception capacity for a horizontal throat, for an inclined throat (with $\theta = 45^\circ$), and a vertical throat in problem 16.1.41 using a curb opening height of 6 in.

16.2.1 Rework example 16.2.1 using a 5 ft \times 5 ft culvert with a square-edged entrance.

16.2.2 Rework example 16.2.1 using a 5 ft \times 5 ft culvert with a 45° beveled-edged entrance.

16.2.3 Rework example 16.2.1 for a discharge of 200 ft³/s.

16.2.4 A culvert is to be designed for a new roadway crossing for a 25-year peak discharge of 200 ft³/s. Use a circular corrugated metal pipe culvert with standard 2-2/3 by 1/2 corrugations and beveled edges. The site conditions include: elevation at culvert face = 100 ft; natural stream bed slope = 1%; tailwater for 25-year flood = 3.5 ft; approximate culvert length = 200 ft; shoulder elevation = 110 ft. Base the design headwater on the shoulder elevation with a 2-ft freeboard (elevation of 108 ft). Set the inlet invert at the natural stream bed elevation (no fall). Analyze the design.

16.2.5 Rework problem 16.2.4 using a concrete pipe with a grooved end.

16.2.6 Rework example 16.2.2 to develop the performance curve for an 8 ft \times 7 ft concrete box culvert with a square-edged entrance. All other conditions are the same as in example 16.2.2.

16.2.7 Determine if a 1.5 m \times 1.5 m square-edged reinforced concrete box culvert is adequate for a roadway crossing to pass a discharge of 8.50 m³/s. The inlet is not depressed (no fall). The site conditions are as follows:

- Shoulder elevation = 34.6 m
- Stream bed elevation at culvert face = 30.5 m
- Natural stream slope = 2%
- Tailwater depth = 1.2 m
- Approximate culvert length = 76.2 m
- Upstream water surface (head) elevation = 33.5 m

16.2.8 A culvert (8 ft \times 7 ft concrete box culvert with a square-edged entrance) is to be designed for a road crossing. Consider a 0° wingwall flare box culvert. The design discharge is 200 cfs and the following site conditions are to be considered.

- Elevation at culvert face = 100 ft
- Natural stream bed slope = 1%
- Tailwater depth (for 200 cfs) = 3.5 ft
- Approximate culvert length = 200 ft
- Shoulder elevation = 110 ft
- Base the design headwater on the shoulder elevation with a 2-ft freeboard (elevation of 108 ft). Set the inlet invert at the natural stream bed elevation (no fall). Analyze the design. What recommendations do you have for this design?

16.2.9 Develop the performance curve for two 48-in CMP culverts ($n = 0.024$) with metal end-sections. Culverts are 30 ft long and are placed on a slope of 0.0007 ft/ft. The roadway is a 20-ft wide paved crossing at an elevation of 107 ft. Consider discharges up to 400 cfs. Consider a flow width of 120 ft wide once the water overtops the roadway. Ignore tailwater effects. Upstream invert elevation = 100 ft.

16.2.10 For the culvert that you designed in problem 16.2.4, with the roadway elevation at 112 ft, develop the performance curve considering discharges up to 700 cfs. Roadway width = 40 ft.

16.2.11 Problem 16.2.8 is to be resolved using an 8 ft \times 4 ft concrete box culvert. The tailwater depth is 4.5 ft for a discharge of 200 cfs. All other information is the same.

16.2.12 Problem 16.2.8 is to be resolved using a 7 ft \times 5 ft concrete box culvert. All other information is the same.

16.2.13 Determine the dimensions of a reinforced concrete box culvert that is to be placed under a roadway, and the gradual transition needed for a 15-ft wide rectangular flood control channel at a slope of 0.0001 ft. Transition structures are used to transition flow from an open channel to a culvert and then transition flow from the downstream of the culvert back to the channel. Gradual transitions are used when the flow is subcritical throughout the culvert. Refer to Figure P16.2.13. The culvert has a length of 150 ft and is to convey a design discharge of 135 cfs. Use a Manning's n of 0.02. Straight line transitions are to be used so the expansion and contraction coefficients, C_e and C_c , are respectively, 0.5 and 0.3. Assume that section 1 defines the flood-control channel just before the contraction upstream of the culvert and section 4 defines the flood-control channel after the expansion downstream of the culvert. Sections 2 and 3 are located at the upstream and downstream ends of the culvert. The headloss in the contraction is $C_c(V_2^2/2g - V_1^2/2g)$ and the headloss in the expansion is $C_e(V_3^2/2g - V_4^2/2g)$. The transition lengths (L_T) are specified using a 4.5:1 flare so that L_T

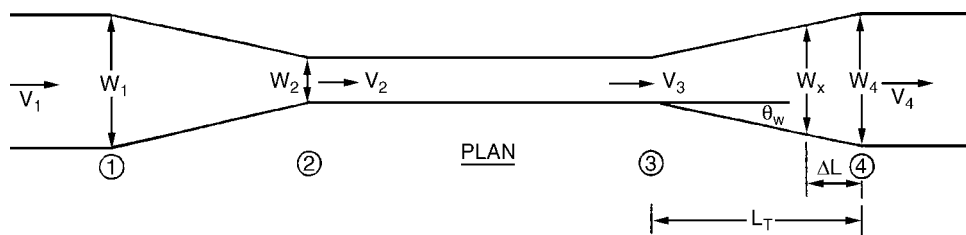


Figure P16.2.13

$= 4.5(W_4 - W_3)/2$ and $L_T = 4.5(W_1 - W_2)/2$, where W is the widths at the respective sections. Choose $y_3 \approx 1.1y_c$ to have a subcritical depth. One important aspect of the culvert and transition design is to make sure that the backwater effect ($y_1 - y_4$) does not exceed a preferred or required amount (freeboard). For the purposes of this problem, that amount is 1 ft.

16.2.14 Analyze the culvert that you design in problem 16.2.13. The streambed elevation at the upstream end of the culvert is 1000 ft above mean sea level. Will this culvert have inlet or outlet

control for the design discharge? Perform a water surface profile analysis of the culvert and transition.

16.2.15 Determine the dimensions for a culvert and gradual transition needed for a 3-m wide rectangular flood control channel at a slope of 0.001 m/m. The culvert length is 30.5 m and is to convey $8.5 \text{ m}^3/\text{s}$. Consider a freeboard ($y_1 - y_4$) ≤ 0.35 m. Refer to problem 16.2.13 for further definitions. Perform a water surface profile analysis of the culvert.

REFERENCES

American Association of State Highway and Transportation Officials (AASHTO), *Model Drainage Manual*, Washington, DC, 1991.

Johnson, F. L., and F. M. Chang, *Drainage of Highway Pavements*, Hydraulic Engineering Circular no. 12, Federal Highway Administration, McLean, VA, 1984.

Normann, J. M., R. J. Houghtalen, and W. J. Johnson, *Hydraulic Design of Highway Culverts*, Hydraulic Design Series no. 5, Report no. FHWA-IP-85-15, Federal Highway Administration, U.S. Department of Transportation, McLean, VA, 1985.

Ragan, R. M., "A Nomograph Based on Kinematic Wave Theory for Determining Time of Concentration for Overland Flow," Report no. 44, prepared by Civil Engineering Department, University

of Maryland at College Park, Maryland State Highway Administration and Federal Highway Administration, December 1971.

Tuncok, I. K., and L. W. Mays, "Hydraulic Design of Culverts and Highway Structures," in *Hydraulic Design Handbook* edited by L. W. Mays, McGraw-Hill, New York, 1999.

Young, G. K., Jr., and S. M. Stein, "Hydraulic Design of Drainage for Highways," in *Hydraulic Design Handbook* edited by L. W. Mays, McGraw-Hill, New York, 1999.

Young, G. K., Jr., S. M. Walker, and F. Chang, *Design of Bridge Deck Drainage*, Hydraulic Engineering Circular no. 21, FHWA-SA-92-010, Federal Highway Administration, U.S. Department of Transportation, Washington, DC, 1993.

This page intentionally left blank

Chapter 17

Design of Spillways and Energy Dissipation for Flood Control Storage and Conveyance Systems

This chapter is an introduction to the design of hydraulic structures (spillways and energy dissipators) for flood-control storage systems (reservoirs). A brief introduction to the development of the probable maximum flood is followed by a section on dams including types of dams, hazard classification of dams, spillway capacity criteria, safety of existing dams, and hydraulic analysis of dam failure. The major emphasis of this chapter is on the design of spillways, in particular overflow spillways, and the design of hydraulic-jump-type stilling basins and energy dissipators. The major portion of the discussion follows the U.S. Bureau of Reclamation (1987) criteria and presents the design procedures of that publication.

17.1 HYDROLOGIC CONSIDERATIONS

The purpose of this section is to briefly define the steps in determining the probable maximum flood (PMF) for the design and analysis of dams and their appurtenances. Estimated limiting values are defined in Chapter 7. The determination of the PMF involves two basic steps: (1) to synthesize a hydrograph of inflow into the reservoir and (2) to model or simulate the movement of the flood through the reservoir and past the dam. The various steps in such an analysis, all of which have been discussed in the National Research Council's (NRC's) report, *Safety of Existing Dams: Evaluation and Improvement*, Chapter 4 (1983), are generally as follows (NRC, 1985):

1. Dividing drainage area into subareas, if necessary
2. Deriving runoff model
3. Determining probable maximum precipitation (PMP) using criteria contained in the NOAA Hydrometeorological Report series (see Section 7.2.5)
4. Arranging PMP increments into a logical storm rainfall pattern called the probable maximum storm (PMS)
5. Estimating for each time interval the losses from rainfall due to such actions as surface detention and infiltration within the watershed
6. Deducting losses from rainfall to estimate rainfall excess values for each time interval
7. Applying rainfall excess values to a runoff model of each subarea of the basin

8. Adding to storm runoff hydrograph allowances for base flow of stream runoff from prior storms to obtain the synthesized flood hydrograph for each subarea
9. Routing of the flood for each subarea to points of interest
10. Routing the inflow through the reservoir storage, outlets, and spillways to obtain estimates of storage elevations, discharges at the dam, tailwater elevations, etc., that describe the passage of the flood through the reservoir. (This is essentially a process of accounting for volumes of water in inflow, storage, and outflow through the flood period. If there are several reservoirs in the watershed, the reservoir routing is repeated from the uppermost to the most downstream reservoir, in turn.)

17.2 DAMS

17.2.1 Type of Dams

Figure 17.2.1 illustrates the basic types of dams, classified on the basis of the type and materials of construction. This figure illustrates gravity dams, arch dams, buttress dams, and embankment dams. Dams can also be classified according to use or hydraulic design.

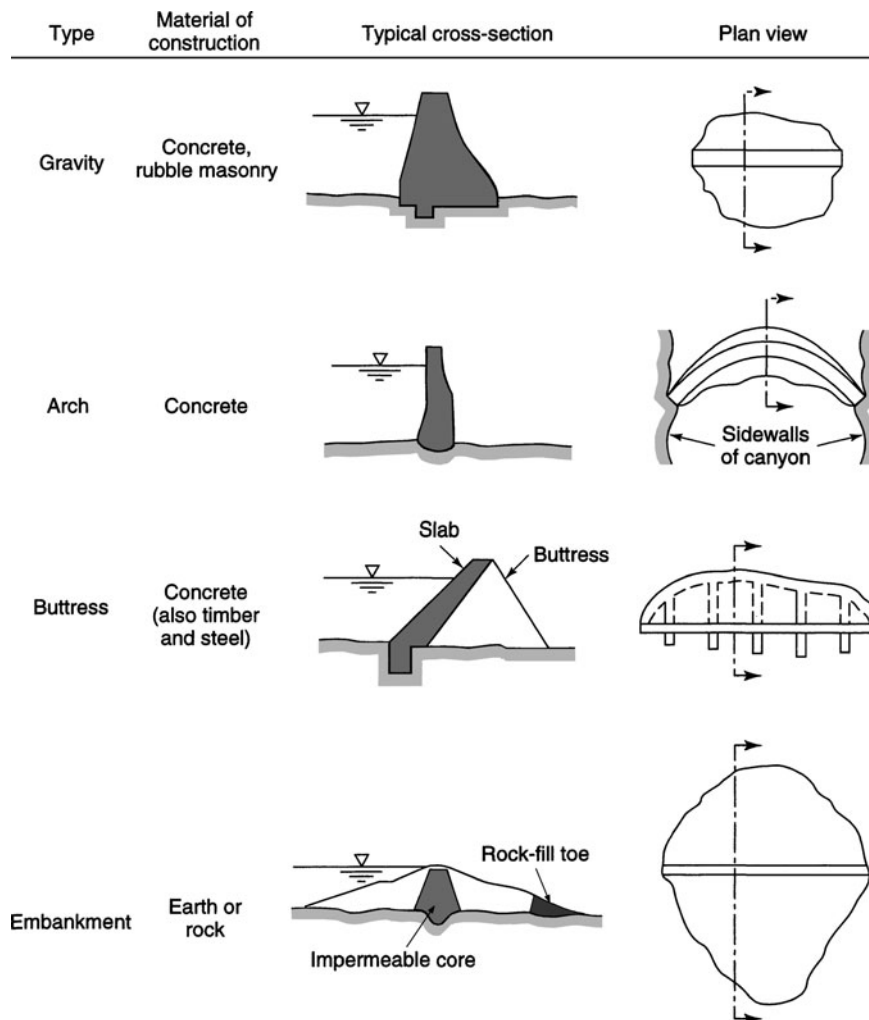


Figure 17.2.1 Basic types of dams (from Linsley et al. (1992)).

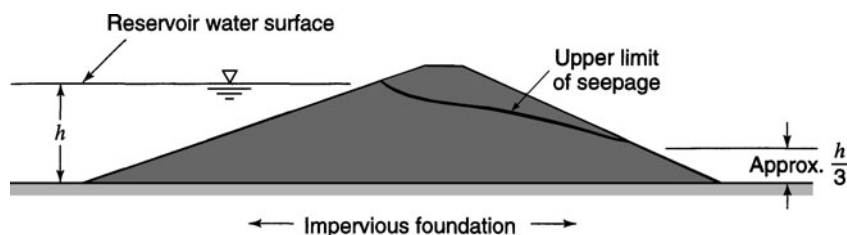


Figure 17.2.2 Seepage through a completely homogeneous dam (from U.S. Bureau of Reclamation (1987)).

The most common type of dam is embankment *earthfill dams*. Their construction is principally from required excavation using the available materials from the construction. Most new earthfill dams are roll-fill-type dams, which can be further classified as homogeneous, zoned, or diaphragm (U.S. Bureau of Reclamation, 1987). *Homogeneous dams* are composed of only one kind of material, exclusive of the slope protection. The material used must be impervious enough to provide an adequate water barrier and the slope must be relatively flat for stability. Figure 17.2.2 illustrates the seepage through a completely homogeneous dam. It is more common today to build modified homogeneous sections in which pervious materials are placed to control steeper slopes. Three methods are used: rockfill toe, horizontal drainage blanket, and inclined filter drain with a horizontal drainage blanket, as illustrated in Figure 17.2.3. Pipe drains are also used for drainage on small dams in conjunction with a horizontal drainage blanket or a pervious zone.

For *diaphragm-type earthfill dams*, the embankment is constructed of pervious materials (sand, gravel, or rock). A thin diaphragm of impermeable material is used to form a water barrier. The diaphragm may vary from a blanket on the upstream face to a central vertical core. Diaphragms may consist of earth, portland cement concrete, bituminous concrete, or other materials.

Zoned embankment-type earthfill dams have a central impervious core that is flanked by a zone of materials considerably more pervious, called *shells*. These shells enclose, support, and protect the impervious core. Figure 17.2.4 illustrates the size range of impervious cores used in zoned embankments.

The other type of embankment dam is the *rockfill dam*, which consists of rock of all sizes to provide stability and an impervious core membrane. Membranes include an upstream facing of impervious soil, a concrete slab, asphaltic concrete paving, steel plates, other impervious soil (U.S. Bureau of Reclamation, 1987). Figure 17.2.5 illustrates the typical maximum section of an earth core rockfill dam using a central core. Figure 17.2.6 illustrates a decked rockfill dam that has an asphaltic concrete membrane on the upstream face.

Concrete arch dams are used where the ratio of the width between abutments to the height is not great and where there is solid rock capable of resisting arch thrust at the abutment (foundation). Arch dams can be either single- or multiple-arch dams. *Concrete buttress dams* consist of flat deck and multiple-arch structures.

17.2.2 Hazard Classification of Dams

Many systems have been developed for the hazards classification of dams relating to hydrologic and seismic events (NRC, 1985). Most of these systems utilize dam height, volume of water impounded, and probable effects of dam failure due to the downstream. The classifications used by the U.S. Army Corps of Engineers (1982), as shown in Table 17.2.1, have been adopted by several federal and state agencies and have been adapted.

The U.S. Army Corps of Engineers' (1991) policy for *dam safety evaluation* is that "a dam failure must not present a hazard to human life. . . ." Dam safety evaluation must: (1) formulate any reservoir plan to comply with this safety requirement and (2) evaluate the impact of catastrophic

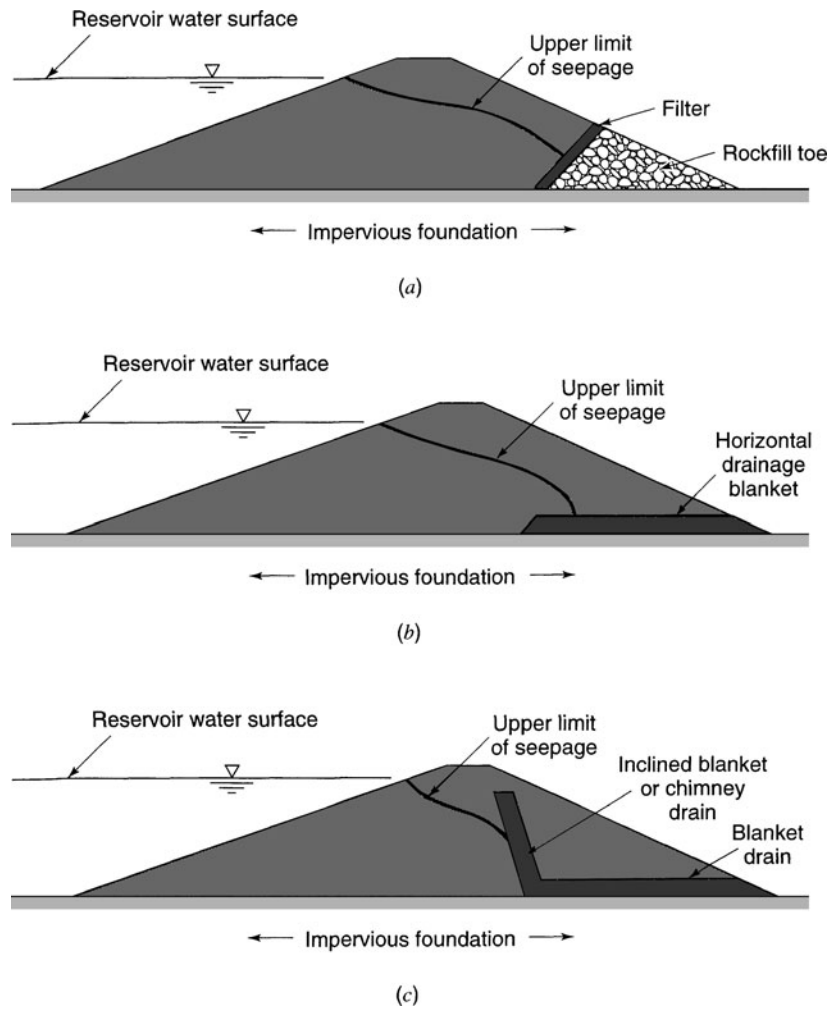


Figure 17.2.3 Seepage through modified homogeneous dams: (a) With rockfill toe; (b) With horizontal drainage blanket; (c) With chimney drain (from U.S. Bureau of Reclamation (1987)).

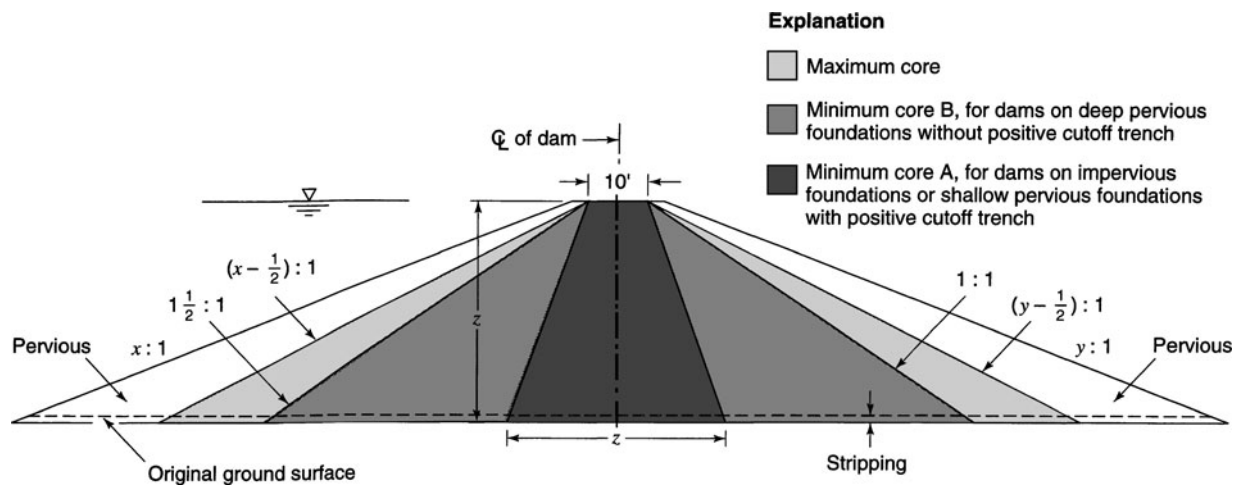


Figure 17.2.4 Size range of impervious cores used in zoned embankments (from U.S. Bureau of Reclamation (1987)).

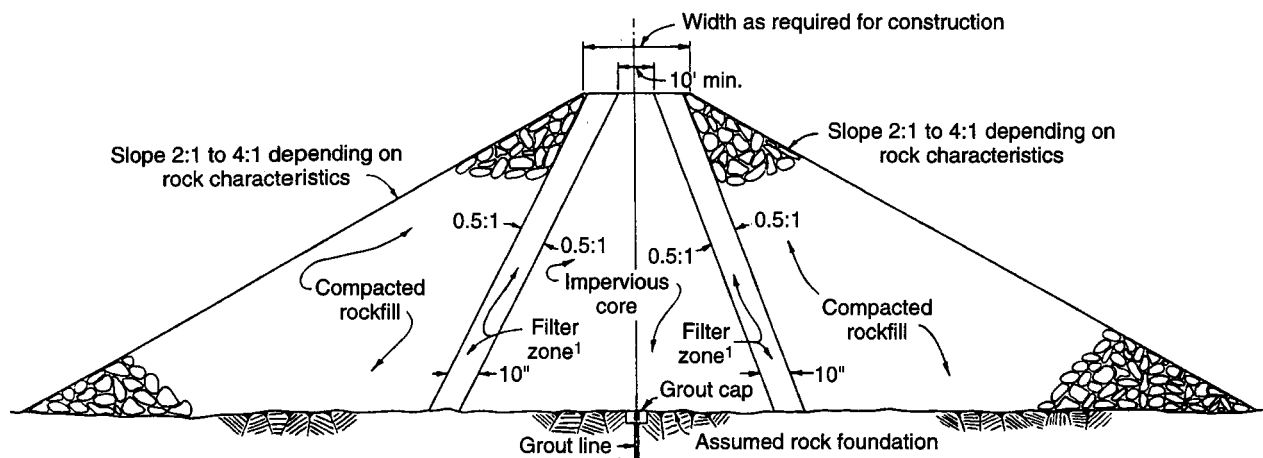


Figure 17.2.5 Typical maximum section of an earth-core rockfill dam using a central core (from U.S. Bureau of Reclamation (1987)).

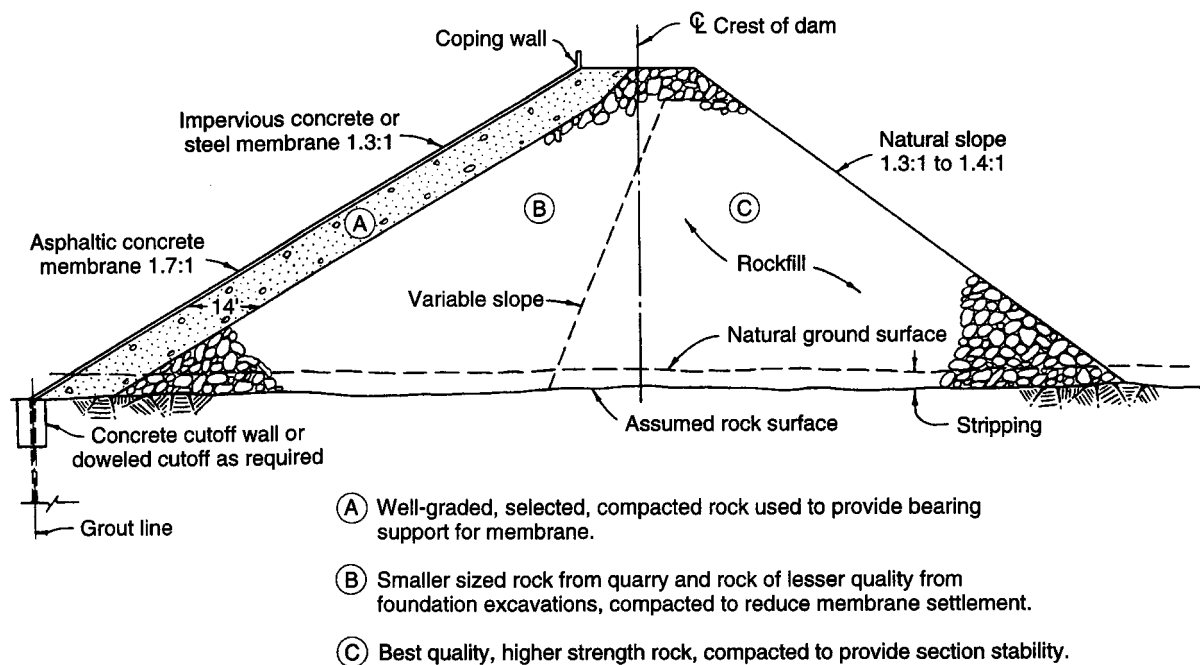


Figure 17.2.6 Typical maximum section of a decked rockfill dam (from U.S. Bureau of Reclamation (1987)).

failure of any proposed reservoir plan to confirm that their performance constraint is satisfied. The four design standards, which depend on the type of dam and risk to life, are described in Table 17.2.2. Section 17.2.4 discusses the method for failure evaluation.

17.2.3 Spillway Capacity Criteria

Table 17.2.3 compares the various spillway capacity criteria used in the United States as of 1985. These are based on the classification used for the National Dam Inspection Program. This table illustrates the diversity of criteria of various federal, state, and local government agencies,

Table 17.2.1 Terms for Classifying Hazard Potentials

Category	Impoundment (ac-ft)	Height of dam (ft)
<i>Size of dam^a</i>		
Small	50 to 1000	25 to 40
Intermediate	1000 to 50,000	40 to 100
Large	Over 50,000	over 100
Category	Loss of life (extent of development)	Economic loss
<i>Hazard potential classification</i>		
Low	None expected (no permanent structures for human habitation)	Minimal (undeveloped to occasional structures or agriculture)
Significant	Few (no urban developments and no more than a small number of inhabitable structures)	Appreciable (notable agriculture, industry, or structures)
High	More than few	Excessive (extensive community, industry, or structures)

^a Criterion that places project in largest category governs.

Source: National Research Council (1985).

Table 17.2.2 Functional Design Standards for New Dams Designed by U.S. Army Corps of Engineers

Standard 1: Design dam and spillway large enough to assure that the dam will not be overtopped by floods up to probable maximum categories.

Standard 2: Design the dam and appurtenances so that the structure can be overtopped without failing and, insofar as practicable, without suffering serious damage.

Standard 3: Design the dam and appurtenances in such a manner as to assure that breaching of the structure from overtopping would occur at a relatively gradual rate, such that the rate and magnitude of increases in flood stages downstream would be within acceptable limits, and that damage to the dam itself would be located where it could be most economically repaired.

Standard 4: Keep the dam low enough and storage impoundment small enough that no serious hazard would exist downstream in the event of breaching, and so that repairs to the dam would be relatively inexpensive and simple to accomplish.

Table 17.2.3 Comparison of Indicated Spillway Capacity Criteria in Use or Proposed by Federal Agencies

Federal agencies	Hazard class High			Hazard class Significant			Hazard class Low			
	Size of dam			Size of dam			Size of dam			
	Large	Intermediate	Small	Large	Intermediate	Small	Large	Intermediate	Small	
Ad Hoc ICODS of FCCSET	PMF	PMF	PMF	PMF	PMF	PMF	*	*	*	
Bureau of Reclamation	PMF	PMF	PMF	*	*	*	*	*	*	
FERC	PMF	PMF	PMF	PMF	PMF	PMF	*	*	*	
Forest Service			(See Corps criteria for National Dam Inspection Program)							
ICODS	PMF	PMF	PMF	*	*	*	*	*	*	
National Weather Service				(Does not establish criteria for dams)						
SCS	PMP	PMP	PMP	(P ₁₀₀ + 0.4 (PMP-P ₁₀₀))			*	*	*	

(Continued)

Table 17.2.3 Comparison of Indicated Spillway Capacity Criteria in Use or Proposed by Federal Agencies

Federal agencies	<i>Hazard class</i> High			<i>Hazard class</i> Significant			<i>Hazard class</i> Low		
	<i>Size of dam</i>			<i>Size of dam</i>			<i>Size of dam</i>		
	Large	Intermediate	Small	Large	Intermediate	Small	Large	Intermediate	Small
TVA	PMF	PMF	PMF	(TVA Max. Prob. Fld.)			*	*	*
Corps of Engineers (Corps Projects)	PMF	PMF	PMF	*	*	*	*	*	*
Corps of Engineers (National Inspection Program)	PMF	PMF	1/2 PMF to PMF	PMF	1/2 PMF to PMF	100 yr to 1/2 PMF	1/2 PMF to PMF	100 yr to 1/2 PMF	50 yr to 100 yr
Nuclear Regulatory Commission	PMF	PMF	PMF	(See Corps criteria for National Dam Inspection program.)					

Source: National Research Council (1985).

professional societies, and privately owned firms in the United States. The spillway requirements for large high-hazard dams are fairly consistent, but there are fairly widespread differences in criteria for other classes of dams. The Institution of Civil Engineers (1978) in the United Kingdom developed the standards presented in Table 17.2.4.

17.2.4 Examples of Dams and Spillways

Figures 17.2.7–17.2.11 show the Roosevelt Dam (Figure 17.2.7), Horse Mesa Dam (Figure 17.2.8), Stewart Mountain Dam (Figures 17.2.9 and 17.2.10), and Granite Reef Dam (Figure 17.2.11), all on

Table 17.2.4 Reservoir Flood and Wave Standards by Dam Category

Category	Initial reservoir condition is tolerable	Dam design flood inflow				Concurrent wind speed and minimum wave surcharge allowance
		General standard is warranted	Minimum standard if rare overtopping is tolerable	Alternative standard if economic study is warranted		
(a) Reservoir where a breach will endanger lives in a community	Spilling long-term average daily inflow	Probable maximum flood (PMF)	0.5 PMF or 10,000-year flood (take larger)	Not applicable	Winter: maximum hourly wind once in 10 years	
(b) Reservoirs where a breach: (i) may endanger lives not in a community; (ii) will result in extensive damage	Just full (i.e., no spill)	0.5 PMF or 10,000-year flood (take larger)	0.3 PMF or 1000-year flood (take larger)	Flood with probability that minimizes spillway plus damage cost, inflow not to be less than minimum standard but may exceed general standard	Summer; average annual maximum hourly wind Wave surcharge allowance not less than 0.6 m	
(c) Reservoirs where a breach will pose negligible risk to life and cause limited damage	Just full (i.e., no spill)	0.3 PMF or 1000-year flood (take larger)	0.2 PMF or 150-year flood (take larger)		Average annual maximum hourly wind; wave surcharge allowance not less than 0.4 m	

(Continued)

Table 17.2.4 (Continued)

Category	Initial reservoir condition is tolerable	Dam design flood inflow			Concurrent wind speed and minimum wave surcharge allowance
		General standard is warranted	Minimum standard if rare overtopping is tolerable	Alternative standard if economic study is warranted	
(d) Special cases where no loss of life can be foreseen as a result of a breach and very limited additional flood damage will be caused	Spilling long-term average daily flow	0.2 PMF or 150-year flood	Not applicable	Not applicable	Average annual maximum hourly wind; wave surcharge allowance not less than 0.3 m

Where reservoir control procedure requires, and discharge capacities permit, operation at or below specified levels defined throughout the year, these may be adopted providing they are specified in the certificates or reports for the dam. Where a proportion of PMF is specified, it is intended that the PMF hydrograph should be computed and then all ordinates be multiplied by 0.5, 0.3, or 0.2 as indicated.

Source: Institution of Civil Engineers (1978).

the Salt River in Arizona. These figures show releases being made during January 1993. Figures 17.2.12*a* and *b* show the intake tower and the side-channel spillways at the Hoover Dam on the Colorado River in Arizona. Figures 17.2.13 *a–e* show the Lake Vallicito Dam and parts of the spillway. Figures 17.2.14*a* and *b* show the Atatürk Dam and spillway channel located on the Euphrates River in Turkey. Figure 17.2.15 shows the Navajo Dam on the San Juan River in New Mexico showing the ungated overflow spillway. Figure 17.2.16 shows an overflow spillway on the Santa Cruz Lake Dam on the Rio Frijoles in New Mexico. Figure 17.2.17 shows the inlet (baffle



Figure 17.2.7 Roosevelt Dam on the Salt River in Arizona showing releases in January 1993. (Courtesy of the U.S. Bureau of Reclamation, photograph by J. Madrigal, Jr. (1993).)



Figure 17.2.8 Horse Mesa Dam on the Salt River in Arizona showing releases in January 1993. (Courtesy of the U.S. Bureau of Reclamation, photograph by J. Madrigal, Jr. (1993).)

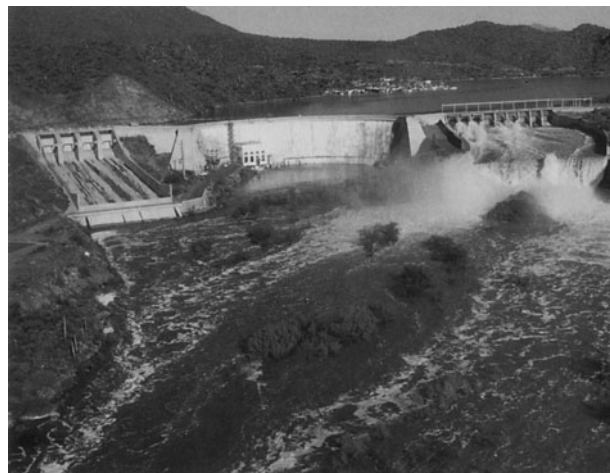
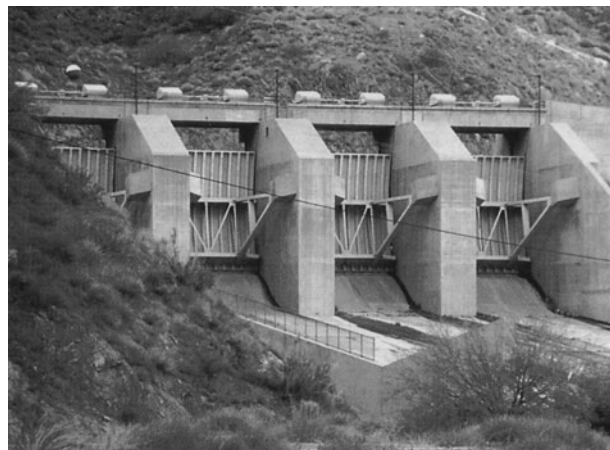


Figure 17.2.9 Stewart Mountain Dam on the Salt River in Arizona showing releases in January 1993. (Courtesy of the U.S. Bureau of Reclamation, photograph by J. Madrigal, Jr. (1993).)



(a)

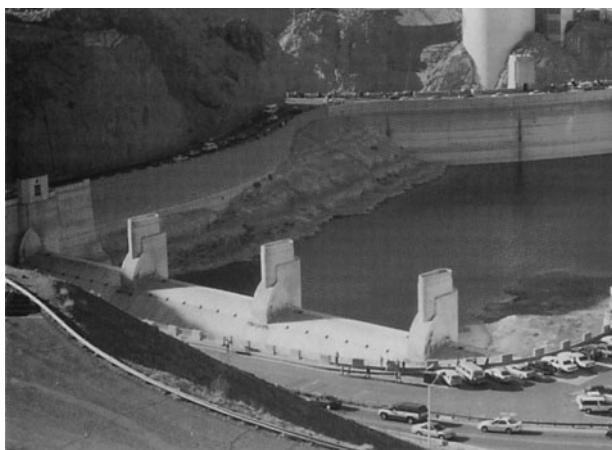


(b)

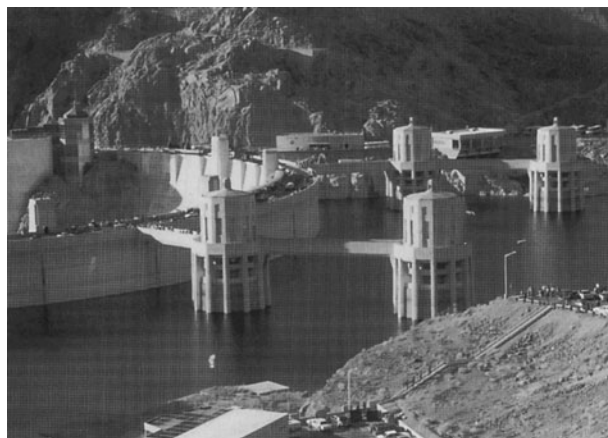
Figure 17.2.10 Stewart Mountain Dam on the Salt River in Arizona. (a), (b) Radial gates on the spillways. (Photographs by L. W. Mays.)



Figure 17.2.11 Granite Reef Dam on the Salt River in Arizona showing releases in January 1993. (Courtesy of the U.S. Bureau of Reclamation, photograph by J. Madrigal, Jr. (1993).)

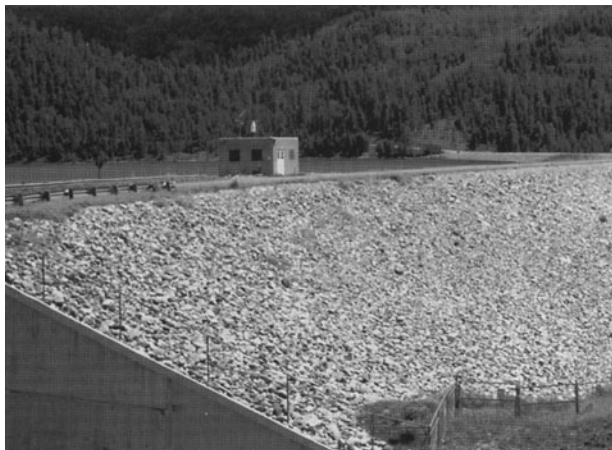


(a)



(b)

Figure 17.2.12 Hoover Dam on the Colorado River. (a) Side channel spillway with dam in background; (b) Intake towers to 30-ft diameter steel penstocks. (Photographs by L. W. Mays.)



(a)



(b)



(c)

Figure 17.2.13 Lake Vallecito Dam in Colorado. (a) Downstream side of dam; (b) Overflow spillway with radial gates; (c) Radial gates; (d) Motors and mechanisms to lift radial gates; (e) Spillway chute and downstream spillway channel. (Photographs by L. W. Mays.)



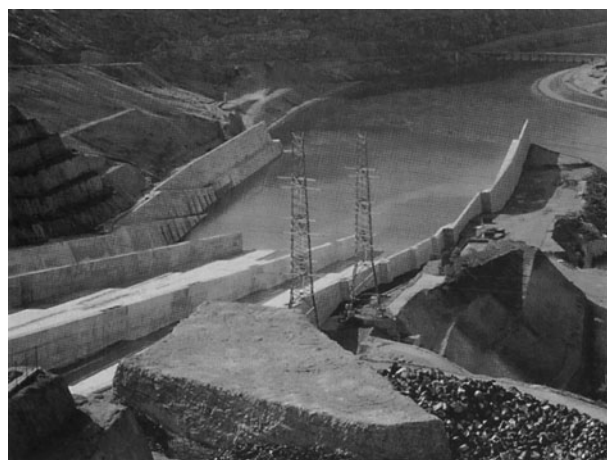
(d)



(e)

Figure 17.2.13 (Continued)

(a)



(b)

Figure 17.2.14 Atatürk Dam on Euphrates River in Turkey. (a) Dam with overflow spillway showing spillway chute; (b) Spillway chute and downstream channel. Also refer to Figures 11.4.8 and 13.2.2. (Photographs by L. W. Mays.)

apron spillway) structure and outlet structure for a detention basin in Phoenix, Arizona. Figure 17.2.18 shows a small detention basin dam and the outlet structure (culvert spillway) for a detention basin in Scottsdale, Arizona. Figure 17.2.19 shows a small dam and culvert spillway under construction in northern New Mexico. Figure 17.2.20 shows the outlet structure under construction for the New Waddell Dam on the Agua Fria River in Arizona. Also refer back to Figure 13.1.5.

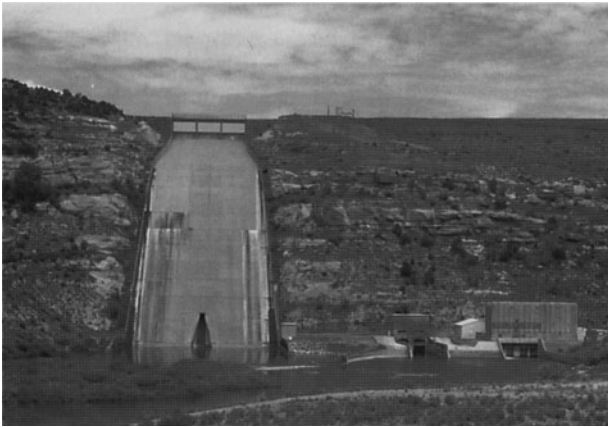


Figure 17.2.15 Navajo Dam on San Juan River in New Mexico showing ungated overflow spillway. (Photograph by L. W. Mays.)



Figure 17.2.16 Spillway on Santa Cruz Lake Dam on the Rio Frijoles in New Mexico. (Photograph by L. W. Mays.)



(a)



(b)

Figure 17.2.17 Inlet and outlet structures for a detention basin in Phoenix, Arizona. (a) Inlet structure (baffle apron spillway); (b) Outlet structure (Photographs by L. W. Mays).



Figure 17.2.18 Culvert spillway for a detention basin in Scottsdale, Arizona. (Photograph by L. W. Mays.)



Figure 17.2.19 Culvert spillway for Dulce Reservoir dam under construction in northern New Mexico. (Photograph by L. W. Mays.)

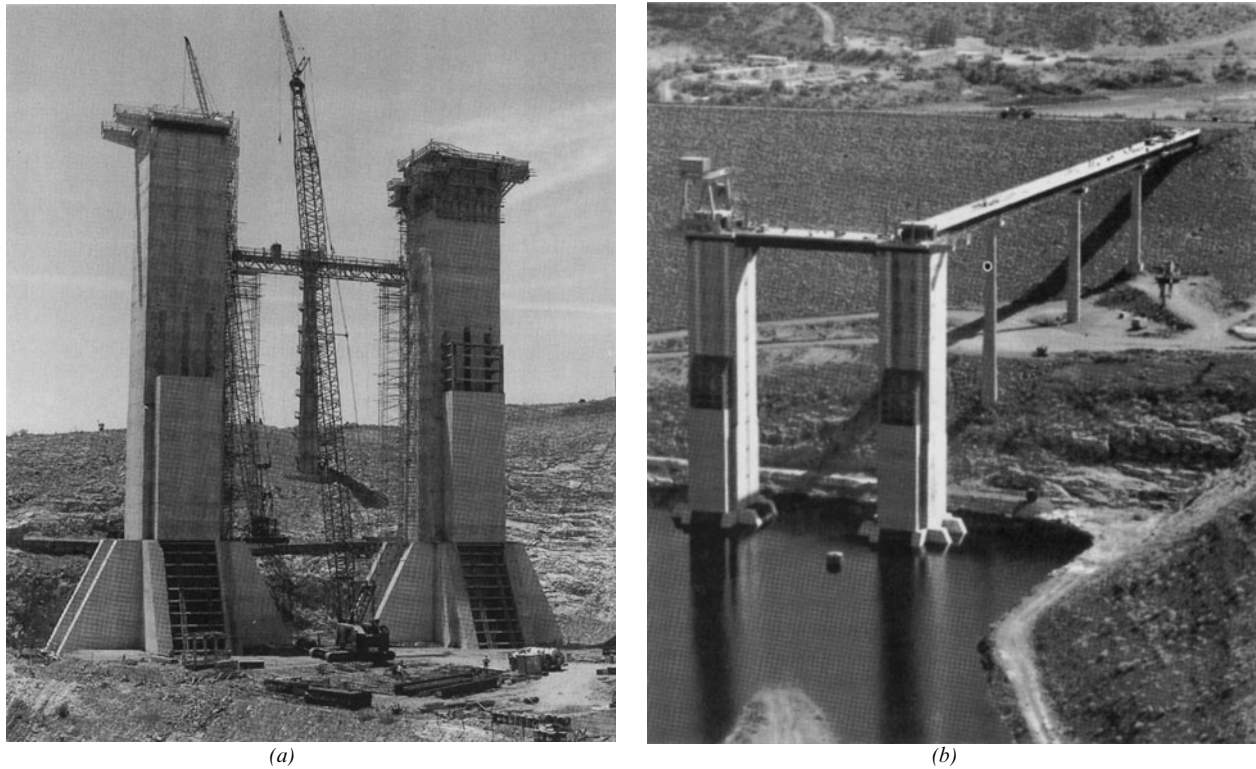


Figure 17.2.20 Photos of outlet structure at New Waddell Dam. (a) Structures under construction; (b) Prior to filling of Lake Pleasant. (Courtesy Central Arizona Project.)

17.3 SPILLWAYS

17.3.1 Functions of Spillways

The functions of spillways are “for storage and detention dams to release surplus water or flood water that cannot be contained in the allotted storage space, and for diversion dams to bypass flows exceeding those turned into the diversion system” (U.S. Bureau of Reclamation, 1987). Safe spillways are extremely important and cannot be overemphasized. Many dam failures have been caused by improperly designed spillways or by spillways of insufficient capacity. Also, spillways must be hydraulically and structurally adequate. They must be located to prevent the erosion and undermining of the downstream toe of a dam. To determine the best combination of storage capacity and spillway capacity for selected inflow design floods, hydrologic, hydraulic, design, cost, and environmental function must be considered. Spillways can be thought of as safety valves for dams.

Components of spillways include the following:

- *Entrance channels* convey water from the reservoir to the control structure
- *Control structures* regulate the outflow from the reservoir
- *Discharge channels* convey flow released through the control structure to the stream bed below the dam
- *Terminal structures* provide energy dissipation of the flow to prevent erosion and scour in the downstream stream bed
- *Outlet channels* convey the spillway flow from the terminal structure to the river channel below the dam

Spillways are typically classified according to features that pertain to control, to the discharge channel, or some other features. They are often referred to as *controlled* or *uncontrolled spillways* depending on whether they are gated or ungated, respectively. Spillway types include (U.S. Bureau of Reclamation, 1987):

- Overfall spillways (Figures 17.2.7, 17.2.8, and 17.2.16)
- Ogee (overflow) spillways (Figures 17.2.14a and 17.2.15)
- Labyrinth spillways (see U.S. Bureau of Reclamation, 1987)
- Spillway chutes (Figures 17.2.13e and 17.2.14b)
- Conduit and channel spillways (Figure 17.2.12a)
- Drop inlet (shaft or morning glory) spillways (Figures 17.2.12b and 17.2.20)
- Baffle apron drop spillways (Figure 17.2.17)
- Culvert spillways (Figure 17.2.18)
- Siphon spillways

Additional discussion of the above types of spillways is in Coleman et al. (1999).

17.3.2 Overflow and Free-Overfall (Straight Drop) Spillways

Free overfall (straight drop) spillways allow the flow to drop freely from the crest (see Figure 17.3.1). These types of spillways are characterized by the following (U.S. Bureau of Reclamation, 1987):

- Suited to a thin arch or crest that has a nearly vertical downstream face.
- Flows may be free discharge or may be supported along a narrow section of the crest.
- In many cases the crest is extended in the form of an overhanging lip to direct small discharge away from the face of the overfall section.
- The underside of the nappe is ventilated to prevent a pulsating and fluctuating jet.
- A deep plunge pool will develop at the base of the overfall as a result of scour if artificial protection is not provided.
- A hydraulic jump can form on flat aprons if the tailwater has sufficient depth.
- The major hydraulic problems with free overfall spillways are the characteristics of the control and the dissipation of flow in the downstream basin.
- Flow in the downstream basin can be dissipated by three basic approaches (U.S. Bureau of Reclamation, 1987):
 - by a hydraulic jump (see Figure 17.3.1)
 - by impact and turbulence induced by impact blocks (see Figure 17.3.1)
 - by a slotted grating dissipator installed immediately downstream from the control.

The hydraulic control of free-overfall spillways can be sharp-crested to provide a fully contracted vertical jet, broad-crested to cause a fully suppressed jet, or even shaped to increase crest efficiency. The discharge for these types of spillways is of the form (see Section 5.6)

$$Q = CLH_e^{3/2} \quad (17.3.1)$$

where Q is the discharge, C is the discharge coefficient, L is the effective length of the crest, and H_e is the actual head (total energy head) on the crest including the approach velocity head:

$$H_e = H + \frac{V_a^2}{2g} \quad (17.3.2)$$

where H is the head due to depth of water above the spillway crest and $V_a^2/2g$ is the approach velocity head.

When crest pier and abutment are shaped to cause side contraction of the flow, the effective crest length L is less than the net crest length.

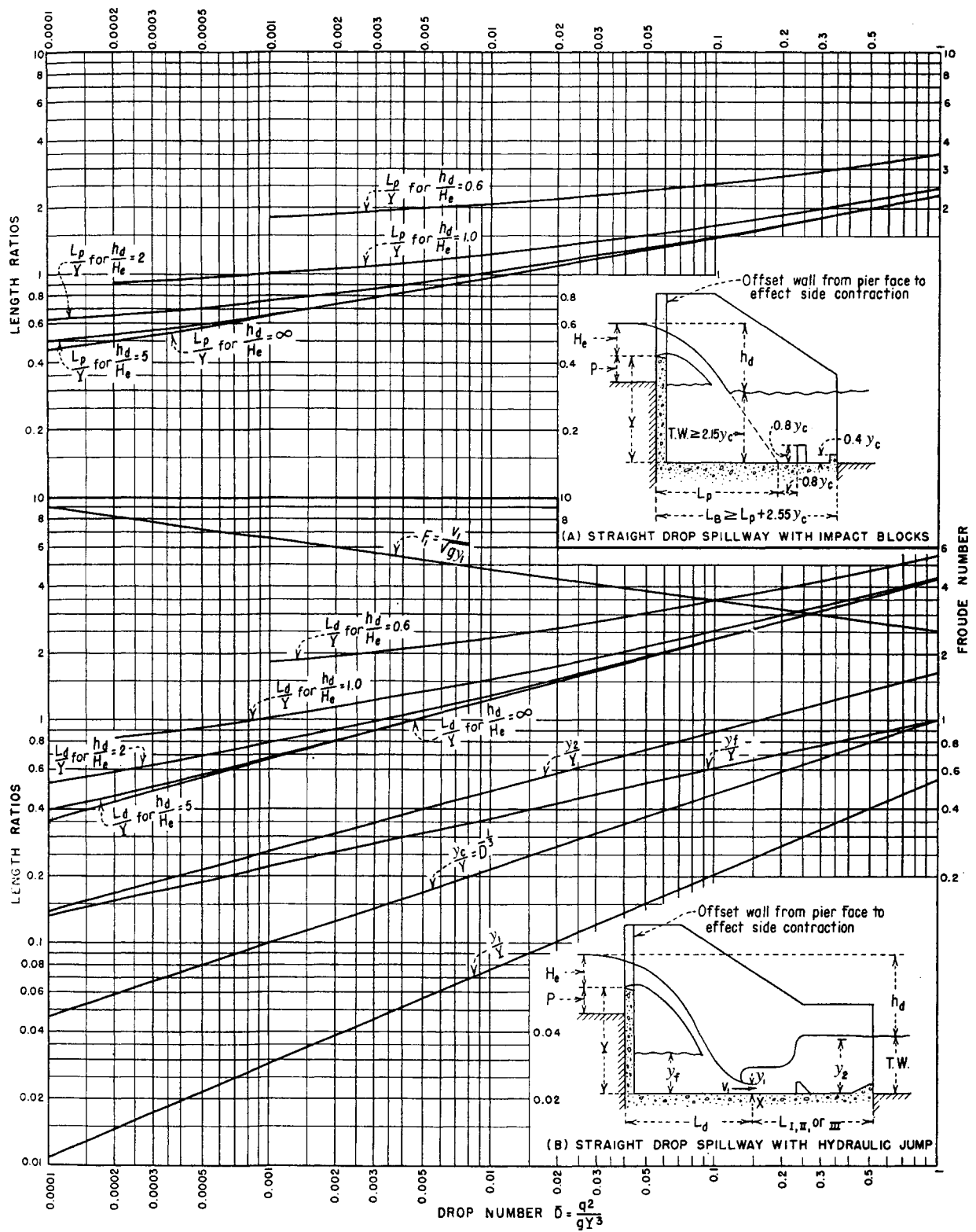


Figure 17.3.1 Hydraulic characteristics of straight drop spillways with hydraulic jump or with impact blocks (from U.S. Bureau of Reclamation (1987)).

The effective length of the crest is determined using

$$L = L' - 2(NK_p + K_a)H_e \quad (17.3.3)$$

where

L' = net length of the crest, N = number of piers, K_a = abutment contraction coefficient (approximately 0.2), and K_p = pier contraction coefficient:

- For square-nosed piers with corners rounded on a radius equal to about 0.1 of the pier thickness: $K_p = 0.02$
- For round-nosed piers: $K_p = 0.01$
- For pointed-nose piers: $K_p = 0.0$

Overflow spillways can be gated or ungated and provide for flow over an arch or arch-buttress dam, wherein the flow free-falls some distance before entering a plunge-pool energy dissipator in the tail race (see Figures 17.2.7, 17.2.8, and 17.2.16).

17.3.3 Ogee (Overflow) Spillways

Ogee (overflow) spillways have a control weir that is ogee-shaped (S-shaped in profile). These spillways can be gated (Figures 17.2.9, 17.2.10, and 17.2.11) or ungated (Figures 17.2.11 and 17.2.15) and they normally provide for flow over a gravity dam section. Flow remains in contact with the spillway surface. The upper part of the ogee spillway conforms closely to the profile of the lower nappe of a ventilated sheet falling from a sharp-crested weir (see Figure 17.3.2). This shape results in a pressure distribution on the crest that is near atmospheric for the design discharge. Discharges less than the design discharge produce pressures on the spillway face that are above atmospheric, whereas discharges greater than the design flow cause subatmospheric pressures. These subatmospheric pressures have the hydraulic effect of increasing the discharge-passing capability of the spillway, but they can also lead to cavitation for high heads, which can cause vibration and surface erosion.

Crest shapes have been studied extensively by the U. S. Bureau of Reclamation over the years. Figure 17.3.2 illustrates the suggested spillway shape for a vertical upstream face as well as values of K and n for different upstream inclinations and velocities of approach. H_0 is the design head and h_a is the approach velocity head, $h_a = V_a^2/2g$. The shape equation for the portion downstream of the apex of the crest is

$$\frac{y}{H_0} = -K \left(\frac{x}{H_0} \right)^n \quad (17.3.4)$$

where H_0 is the design head and n and K are functions of h_a/H_0 , as given in Figure 17.3.2.

The discharge over an ogee crest is described by equation (17.3.1). The discharge coefficient is influenced by a number of factors, including:

- depth of approach (Figure 17.3.3)
- heads different from design heads (Figure 17.3.4)
- upstream face slope (Figure 17.3.5)
- downstream apron interference (Figure 17.3.6)
- downstream submergence (Figure 17.3.7)

Figure 17.3.3 presents values of discharge coefficients (C_0); $C = C_0$ for the situation when $H_e = H_0$, or $H_e/H_0 = 1$ (which is for the ideal nappe shape). The discharge coefficient varies with the values of P/H , where P is the height of the spillway crest above the channel bed.

The effect of heads different from the design head on the discharge coefficient are presented in Figure 17.3.4. This figure shows the variation of the coefficient as related to values of H_e/H_0 , where

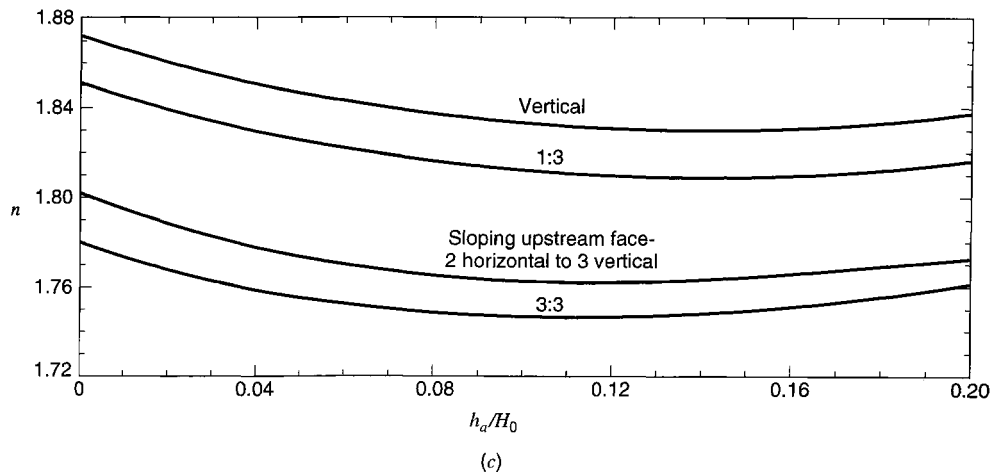
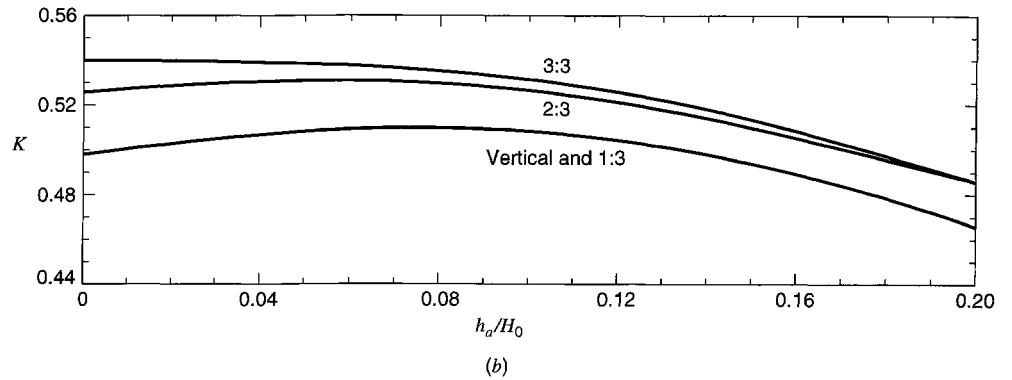
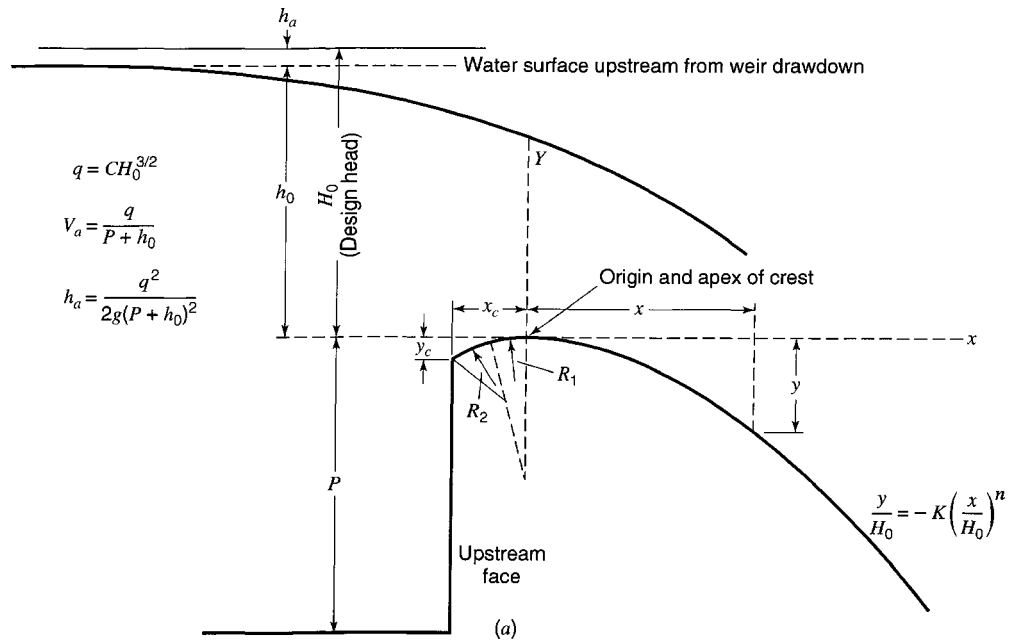


Figure 17.3.2 Factors for definition of nappe-shaped crest profiles. (a) Elements of nappe-shaped crest profiles; (b) Values of K ; (c) Values of n (from U.S. Bureau of Reclamation (1987)).

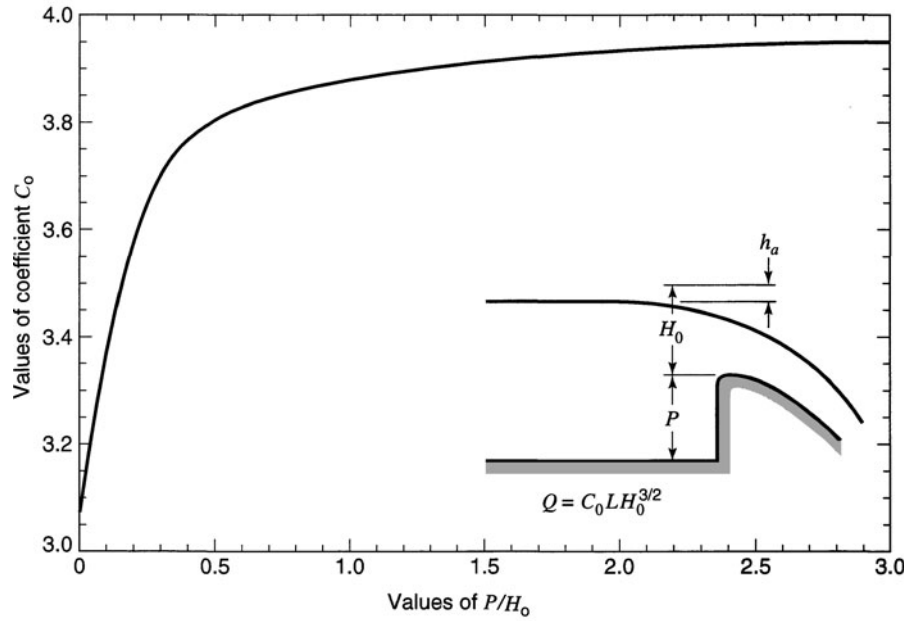


Figure 17.3.3 Discharge coefficients for vertical-faced ogee crest (from U.S. Bureau of Reclamation (1987)). To use this figure for SI units, the factor 0.552 must be multiplied times C_0 . For example if $P = 20$ m and $H_0 = 8$ m, then for $P/H_0 = 2.5$, $C_0 = (0.552)(3.945) = 2.178$ and Q would be in m^3/s for L and H_0 in meters.

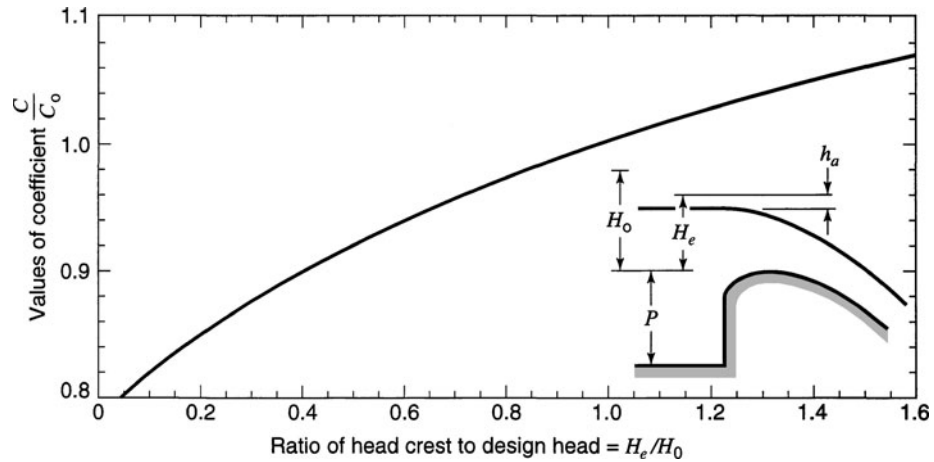


Figure 17.3.4 Discharge coefficients for other than the design head (from U.S. Bureau of Reclamation (1987)).

H_e is the actual head considered. The effect of the upstream face shape on the discharge coefficient is illustrated in Figure 17.3.5, the effect of downstream apron interference on the discharge coefficient is illustrated in Figure 17.3.6, and the effect of downstream submergence (tailwater effects) is illustrated in Figure 17.3.7.

Gate-controlled ogee crest discharge (Figures 17.2.9 and 17.2.10) is similar to discharge through an orifice, given as

$$Q = CDL\sqrt{2gH} \tag{17.3.5}$$

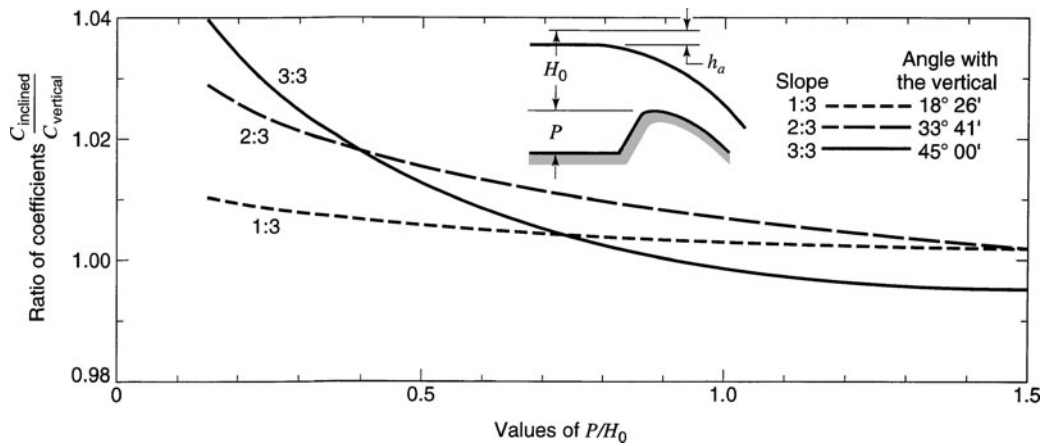


Figure 17.3.5 Discharge coefficients for ogee-shaped crest with sloping upstream face (from U.S. Bureau of Reclamation (1987)).

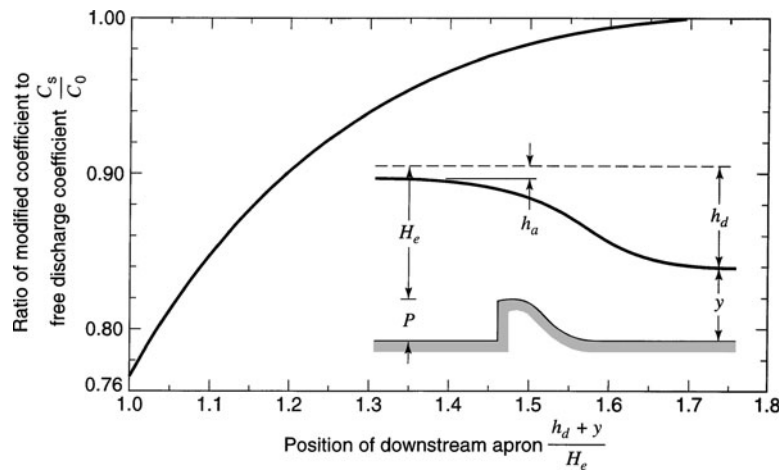


Figure 17.3.6 Ratio of discharge coefficients resulting from apron effects (from U.S. Bureau of Reclamation (1987)).

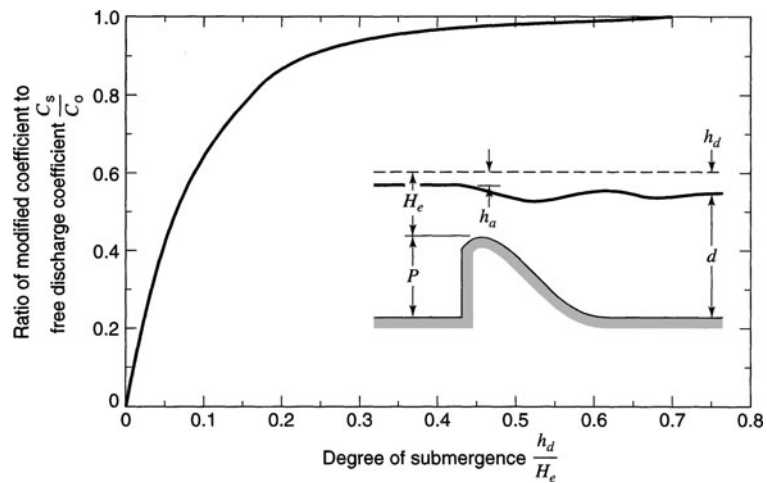


Figure 17.3.7 Ratio of discharge coefficients caused by tailwater effects (from U.S. Bureau of Reclamation (1987)).

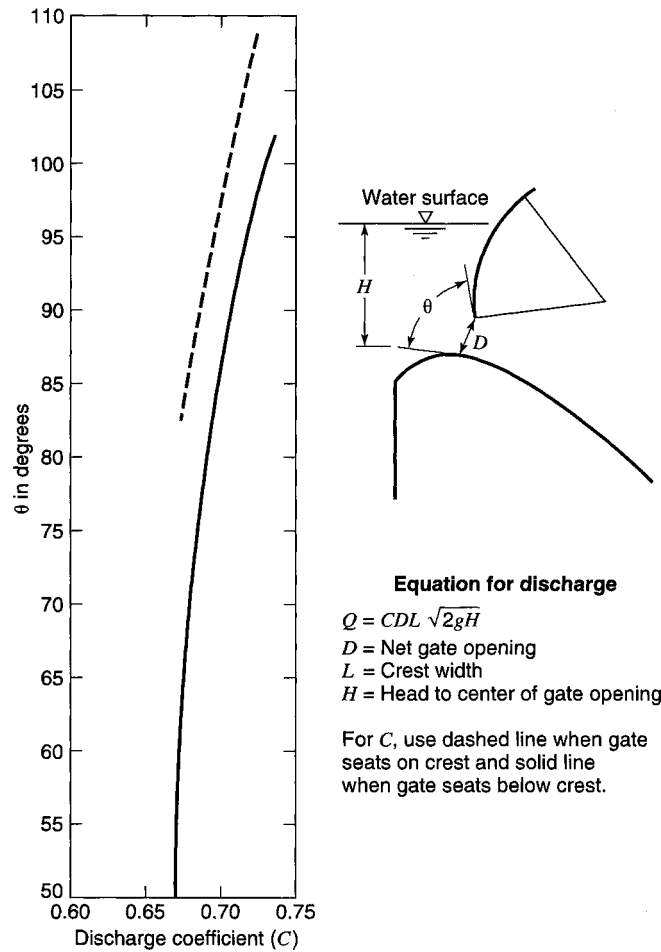


Figure 17.3.8 Discharge coefficient for flow under gates (from U.S. Bureau of Reclamation (1987)).

where C is the discharge coefficient, which is dependent upon the characteristics of the flow lines approaching and leaving the orifice, which are in turn dependent upon the crest shape and the type of gate (see Figure 17.3.8), H is the head to the center of the gate opening (including the velocity head of approach) (see Figure 17.3.8), D is the shortest distance from the gate lip to the crest curve, and L is the crest width. Figure 17.3.8 presents the variation of discharge coefficients for different angles θ . This figure can be used for leaf gates or radial gates located at the crest or downstream of the crest. θ is the angle formed by the tangent to the gate lip and the tangent to the crest curve at the nearest point of the crest curve for radial gates (U.S. Bureau of Reclamation, 1987).

Subatmospheric pressure on both uncontrolled and gate-controlled ogee crests must be given consideration in the design of these structures. For an uncontrolled ogee crest, Figure 17.3.9a illustrates the approximate force diagram of subatmospheric pressure when the design head used to define the crest shape is 75 percent of the maximum head. For a gate-controlled ogee crest, Figure 17.3.9b shows that subatmospheric pressures are equal to about one-tenth of the design head for small gate openings and the ogee is shaped to an ideal nappe profile for maximum head.

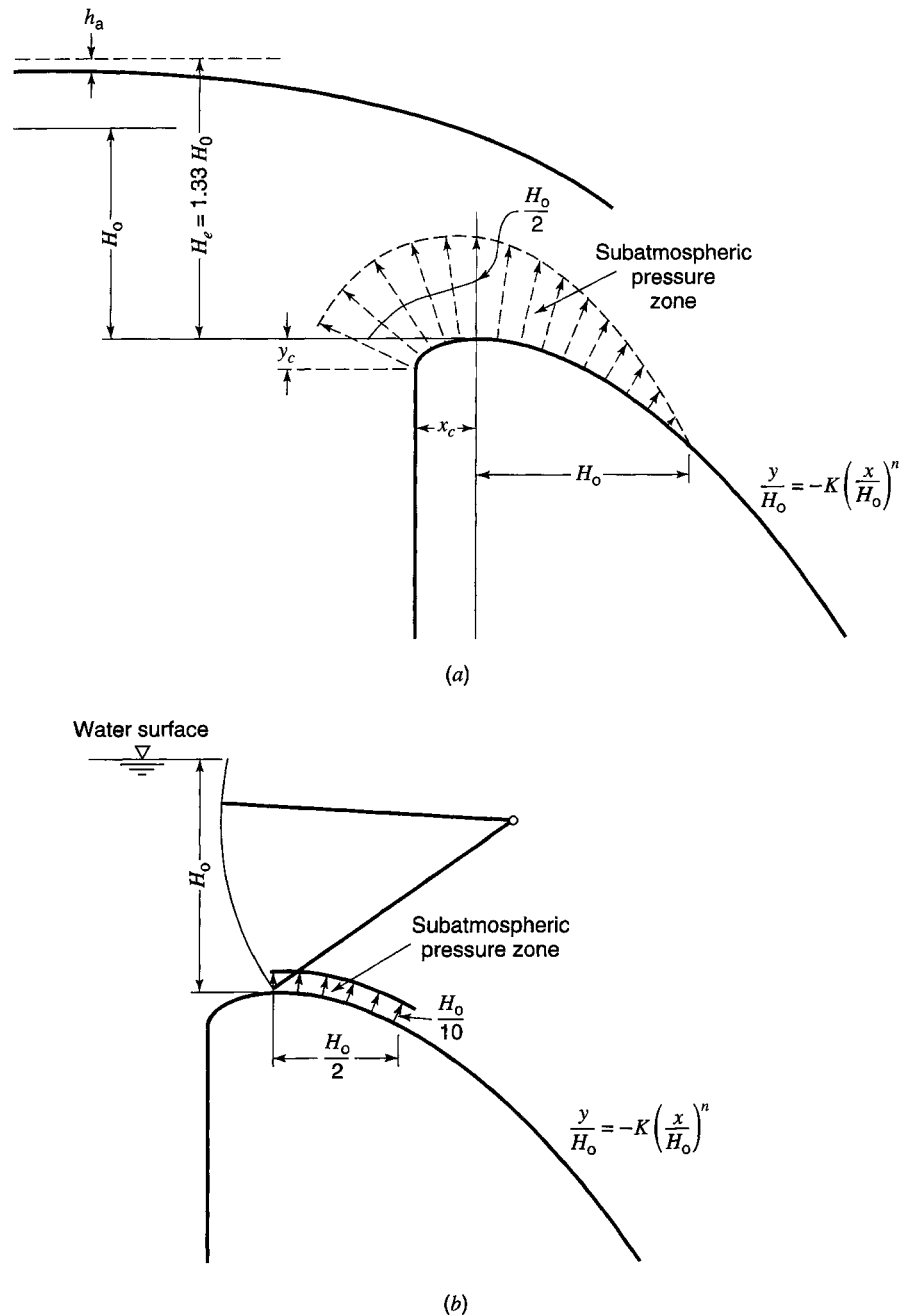


Figure 17.3.9 Subatmospheric crest pressures. (a) For $H_0/H_e = 0.75$; (b) For undershot gate flow (from U.S. Bureau of Reclamation (1987)).

EXAMPLE 17.3.1

Design an uncontrolled overflow ogee crest for a spillway to discharge 20,000 cfs. The upstream face of the crest is sloped 3:3 and a bridge is to span the crest. Bridge piers 18 in wide (pier contraction $K_p = 0.05$) with rounded noses are to be provided. The bridge spans (center to center of piers) are not to exceed 30 ft. The maximum expected head $H_e = 10$ ft. Neglect velocity of approach head. The distance from the

spillway crest to the reservoir bottom at the dam is 18 ft. The abutment coefficient $K_a = 0.10$. Your design should be based upon the design head being equal to the maximum expected head. What will be the discharges for different expected heads of up to 16 ft?

SOLUTION

The design head H_0 is selected as the maximum expected head H_e , so that $H_e/H_0 = 1.0$. The discharge coefficient C_0 is obtained from Figure 17.3.3 for $P/H_0 = 18/10 = 1.8$ (assume that the ogee is formed to the ideal nappe shape for $H_e/H_0 = 1.0$), $C_0 = 3.925$. The upstream face of the crest is sloped 3:3; therefore from Figure 17.3.5, $C_{inclined}/C_{vertical} = 0.992$ (by extrapolation). The discharge coefficient is $C = C_0(C_{inclined}/C_{vertical}) = (3.925)(0.992) = 3.894$.

The effective crest length is defined by equation (17.3.3): $L = L' - 2(NK_p + K_a)H_e$. Using the discharge equation (17.3.1), $Q = CLH_e^{3/2}$, the effective crest length L can be determined as

$$L = \frac{Q}{CH_e^{3/2}} = \frac{20,000}{(3.894)(10^{3/2})} = 162.4 \text{ ft}$$

The net length of the crest is $L' = L + 2(NK_p + K_a)H_e$ where $K_p = 0.05$ and $K_a = 0.1$. Assume four piers; then $L' = 162.4 + [2(4)(0.05) + 2(0.1)](10) = 168.4$ ft. The five span lengths not accounting for pier widths are $168.4/(4 + 1) = 33.7$ ft, which is greater than the allowable 30 ft in the problem statement. Assume five piers; then $L' = 162.4 + [2(5)(0.05) + 2(0.1)](10) = 169.4$ ft. The span length not accounting for pier widths is $169.4/(5 + 1) = 28.2$ ft < 30 ft.

Next determine the discharge-head relationship. Because the heads now considered are different from H_0 , a correction is made to C using Figure 17.3.4:

$$C = \left(\frac{C}{C_0}\right)(C_0)\left(\frac{C_{inclined}}{C_{vertical}}\right)$$

The effective crest length is $L = 169.4 - [2(5)(0.05) + 2(0.1)]H_e = 169.4 - 0.7H_e$.

The shape of the ogee crest is computed using equation (17.3.4) as $y/H_0 = -K(x/H_0)^n$, where $K = 0.54$ for $h_a/H_0 = 0$ using the 3:3 curve in Figure 17.3.2b and $n = 1.78$ using the 3:3 curve for $h_a/H_0 = 0$ in Figure 17.3.2c. Then $y/H_0 = -0.54(x/H_0)^{1.78}$. This equation is used to shape the ogee crest as shown in Figure 17.3.2. The discharges for different expected heads of up to 16 ft are given in Table 17.3.1.

Table 17.3.1 Discharge Computations for Example 17.3.1

H_e (ft)	$\frac{H_e}{H_0}$	$\frac{C}{C_0}$	C	$L = 169.4 - 0.7H_e$	$H_e^{3/2}$	Q (cfs)
1	0.1	0.820	3.193	168.7	1.000	539.
2	0.2	0.852	3.317	168.0	2.828	1576.
4	0.4	0.900	3.504	166.6	8.000	4670.
6	0.6	0.940	3.660	165.2	14.697	8886.
8	0.8	0.972	3.785	163.8	22.627	14,026.
10	1.0	1.000	3.894	162.4	31.623	19,998.
12	1.2	1.025	3.991	161.0	41.569	26,710.
14	1.4	1.050	4.088	159.6	52.383	34,177.
16	1.6	1.070	4.166	158.2	64.000	42,180.

$$\frac{C_i}{C_u} \times C_0 = 0.992 \times 3.925 = 3.894$$

For $H_e = 1$, $C = 0.820 \times 3.894 = 3.193$

Table 17.3.2 Discharge Computation for Example 17.3.2

Total head	H	D	C Fig. 17.3.8	Q (cfs) Eq. (17.3.5)	C_0 Fig. 17.3.3	H/H_0	C/C_0 Fig. 17.3.4	C	Q (cfs) Eq. (17.3.1)
5	4	2	0.68	1091					
7	6	2	0.68	1337					
9	8	2	0.68	1543					
11	10	2	0.68	1726					
13	12	2	0.68	1890					
4	4	6			3.91	0.5	0.92	3.60	1440
6	6	6			3.91	0.75	0.96	3.75	2756
10	7	6	0.68	4331					
11	8	6	0.68	4630					
13	10	6	0.68	5177					

EXAMPLE 17.3.2

A gate-controlled ogee spillway has been designed that uses Tainter gates for control. Determine the head-discharge curves for two different openings of the Tainter gate, for $D = 2$ ft and 6 ft. The heads (including the approach velocity) to the bottom of the orifice range from 4 to 13 ft. The upstream face of the crest is vertical with $P = 10$ ft and designed for $H_0 = 8$ ft, $L = 50$ ft ($\theta = 90^\circ$). The gate seats on the crest.

SOLUTION

For $D = 2$ ft, use equation (17.3.5) for all depths, where $C = 0.68$ from Figure 17.3.8, so $Q = CDL\sqrt{2gH} = (0.68)(2)(50)\sqrt{2gH} = 68\sqrt{2gH}$ where H is the head to the center of the gate opening. For $D = 6$ ft, use equation (17.3.5) for $H > 6$ ft and use equation (17.3.1) for $H \leq 6$ ft. For $H > 6$ ft, $Q = (0.68)(6)(50)\sqrt{2gH} = 204\sqrt{2gH}$. For $H \leq 6$ ft, $Q = CLH^{3/2}$, where $C_0 = 3.91$ from Figure 17.3.3 for $P/H_0 = 10/8 = 1.25$. For heads other than the design heads, Figure 17.3.4 is used to determine C/C_0 , e.g., $C/C_0 = 0.92$ for $H_e/H_0 = 0.5$, then $C = C_0(H_e/H_0) = (3.91)(0.5) = 3.60$. The computations are summarized in Table 17.3.2.

17.3.4 Side Channel Spillways

As shown in Figures 17.2.12a and 17.3.10, side channel spillways have a control weir that is alongside and approximately parallel to the upper part of the spillway discharge channel. Discharge over the crest falls into a side channel or into a conduit or tunnel. Discharge characteristics are similar to an uncontrolled overflow spillway and depend on the weir crest profile. The methods described in the previous section can be used to determine the overflow spillway discharge, and methods for water surface profile determination (Chapter 15) can be used to analyze the flow profile in the side channel.

Side channel flow characteristics are illustrated in Figure 17.3.11. When the bottom of the side channel trough is selected so that the depth below the hydraulic gradient is greater than the minimum specific energy depth, the flow will be either subcritical or supercritical depending on the critical slope or downstream control. For slopes greater than critical without downstream control, supercritical flow occurs throughout the channel (see profile B' in Figure 17.3.11a). If there is a downstream control in the channel, the flow is supercritical (see profile A' in Figure 17.3.11a). The hydraulic effects for these two profiles are illustrated in Figure 17.3.11b.

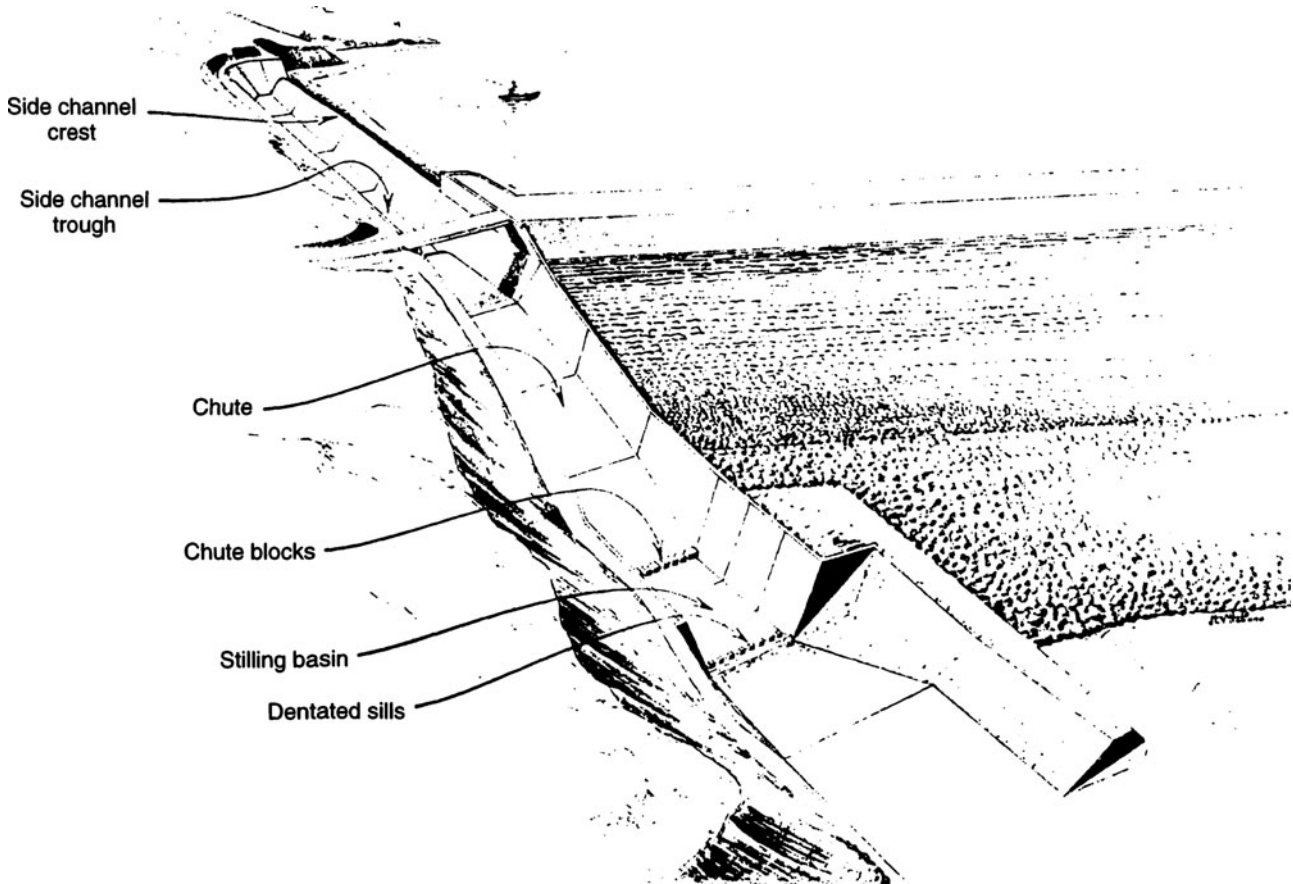


Figure 17.3.10 Typical side channel and chute spillway arrangement (from U.S. Bureau of Reclamation (1987)).

EXAMPLE 17.3.3

Analyze a side channel spillway 200 ft long to discharge for maximum of 4000 ft³/s. The spillway crest is at an elevation of 100 ft; assume a crest coefficient of 3.6.

SOLUTION

The discharge per unit length is $q = 4000/200 = 20$ ft³/s/ft. The design head is then computed using equation (17.3.1) as $H_0 = (q/C)^{2/3} = (20/3.6)^{2/3} = 3.1$ ft. Consider a trapezoidal section for the side channel trough with 0.5:1 side slopes and a bottom width of 20 ft. Consider a bottom slope of 0.01 with the upstream end of the side channel spillway having a bottom elevation of 80 ft.

A control section is placed downstream of the side channel trough with a 20-ft transition from the 0.5:1 side slope of the trough section to a rectangular section 20 ft wide at the control with no change in the bottom elevation at the control. Refer to Figure 17.3.12.

The critical depth for the flow at the control is $y_c = \sqrt[3]{q^2/g} = \sqrt[3]{(4000/20)^2/32.2} = 10.75$ ft and the velocity is $V_c = q/y_c = 200/10.75 = 18.60$ ft/s. The velocity head is $V_c^2/2g = (18.6)^2/64.4 = 5.37$ ft. The transition losses are approximated as 0.2 times the difference of the velocity heads between the ends of the transition. The energy equation can be written for the ends of the transition as (see Figure 17.3.12)

$$\frac{V^2}{2g} + y = \frac{V_c^2}{2g} + y_c + 0.2 \left(\frac{V_c^2}{2g} - \frac{V^2}{2g} \right)$$

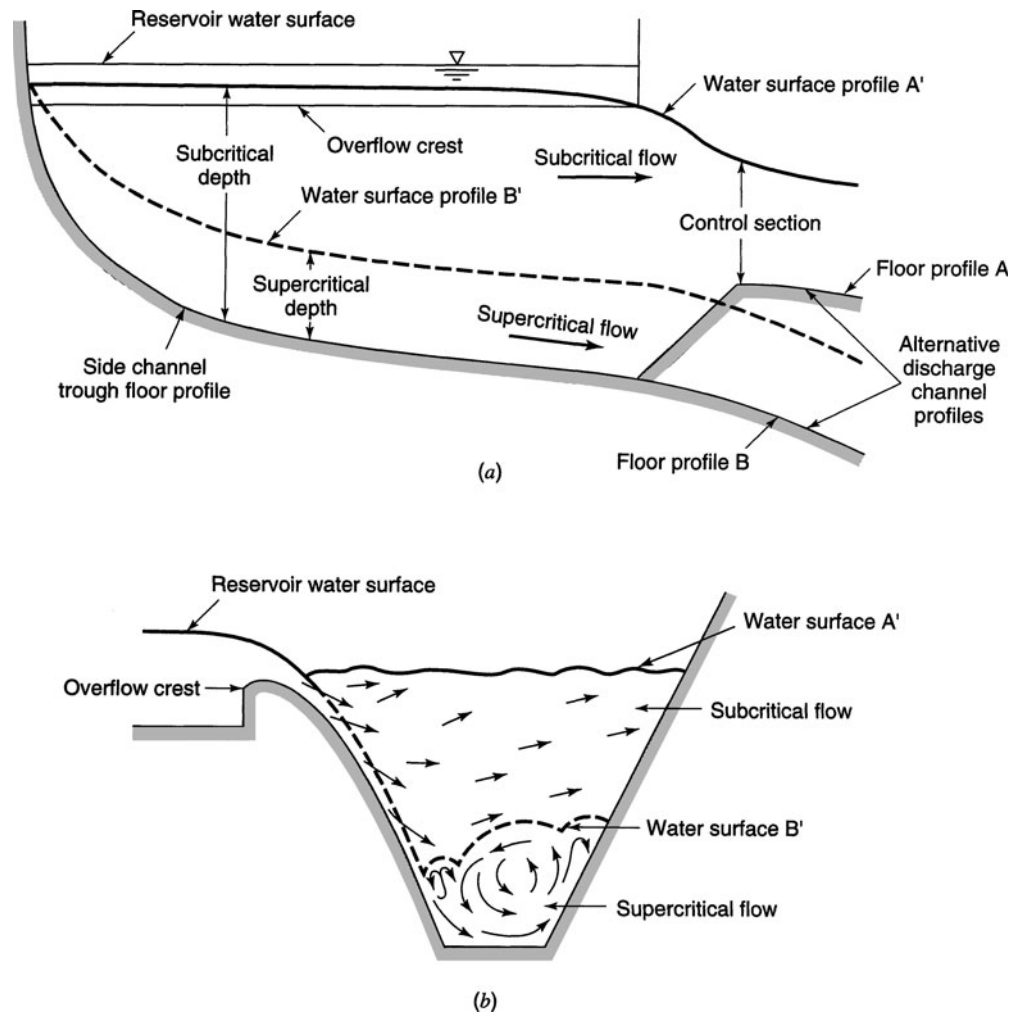


Figure 17.3.11 Side channel flow characteristics. (a) Profile; (b) Cross-section (from U.S. Bureau of Reclamation (1987)).

Substituting the known values, we find

$$\frac{V^2}{2g} + y = 5.37 + 10.75 + 0.2 \left(5.37 - \frac{V^2}{2g} \right)$$

$$1.2 \frac{V^2}{2g} + y = 17.19$$

$$V = Q/A = Q/((b + zy)y) = 4000/[(20 + 0.5y)y]$$

$$\frac{1.2}{2(32.2)} \left[\frac{4000}{[(20 + 0.5y)y]} \right]^2 + y = 17.19$$

Solving yields $y \approx 15.6$ ft; then the flow area is $A = [20 + 0.5(15.6)] 15.6 = 434 \text{ ft}^2$, $V = 4000/434 = 9.2 \text{ ft/s}$, $V^2/2g = 1.31 \text{ ft}$. The headloss through the transition is $0.2(5.37 - 1.31) = 0.81 \text{ ft}$. The maximum

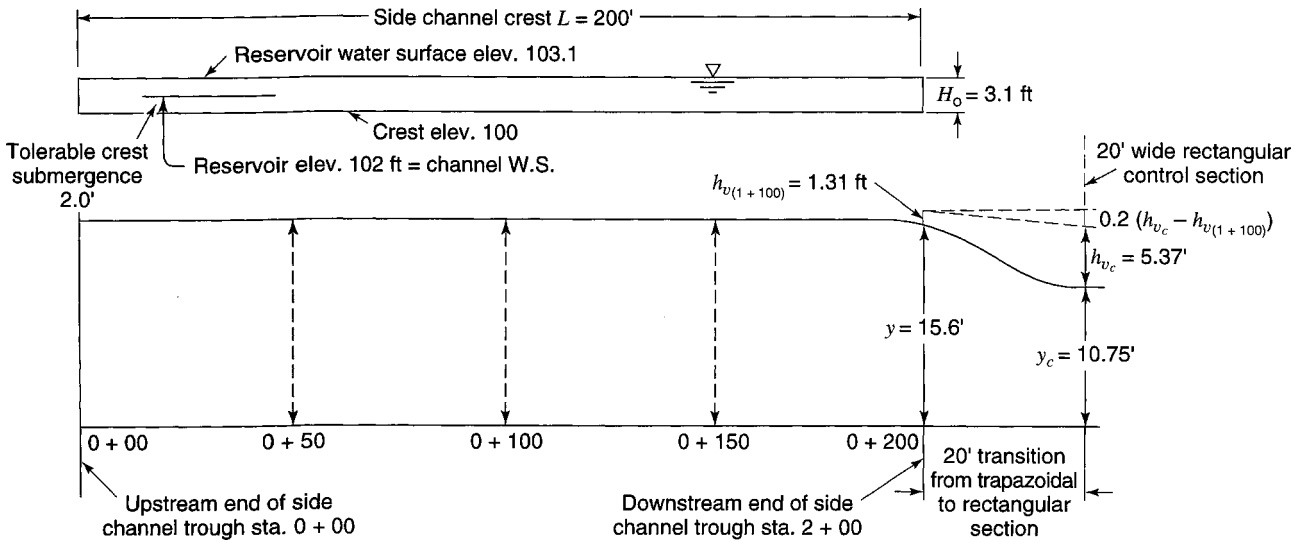


Figure 17.3.12 Example 17.3.3—Hydraulic design for side channel spillway.

bottom elevation of the side channel spillway could be placed so that there is a tolerable crest submergence of 2.0 ft. Next a water surface profile must be performed to relate the elevation to the reservoir water level.

17.3.5 Drop Inlet (Shaft or Morning Glory) Spillways

Drop inlet spillways are characterized as spillways in which the discharge enters over a horizontal lip, drops through a vertical or sloping shaft, and then discharges through a horizontal or nearly horizontal conduit or tunnel. These structures have three basic components: a control weir, a vertical transition, and a closed discharge channel. Figure 17.3.13 illustrates a typical installation of a shaft spillway for a small dam. Figure 17.3.14 illustrates a morning glory spillway, which has a funnel-shaped inlet.

There are three types of flow control in drop inlet spillways: crest control, orifice control, and full-pipe flow control. The control shifts according to the relative discharge capacities of the weir, transition, and the conduit or tunnel. The flow condition and discharge characteristics of morning glory spillways are illustrated in Figure 17.3.14. For low flows, the flow rate is governed by the relationship of weir flow $Q = f(H_e^{3/2})$, i.e., equation (17.3.1). A continuous volume of air persists throughout the spillway components.

Figure 17.3.15a illustrates the elements of a nappe-shaped profile for a circular weir. The head on the weir is measured from the crest and the length L is the circumference of the weir crest ($2\pi R_s$). The weir discharge is then

$$Q = C_0(2\pi R_s)H_0^{3/2} \quad (17.3.6)$$

The discharge coefficients for a circular crest differ from those for a straight crest because of the effect of submergence and back pressure incident to the joining of the converging flow (U.S. Bureau of Reclamation, 1987). Figure 17.3.16 presents the relationship of the circular crest coefficient C_0 to H_0/R_s for different approach depths. Figure 17.3.17 presents the circular crest coefficients for other than design head.

Weir control governs when free flow prevails for values of H_0/R_s less than approximately 0.45. As H_0/R_s increases above 0.45, the weir becomes partially submerged, and as H_0/R_s approaches 1.0 the

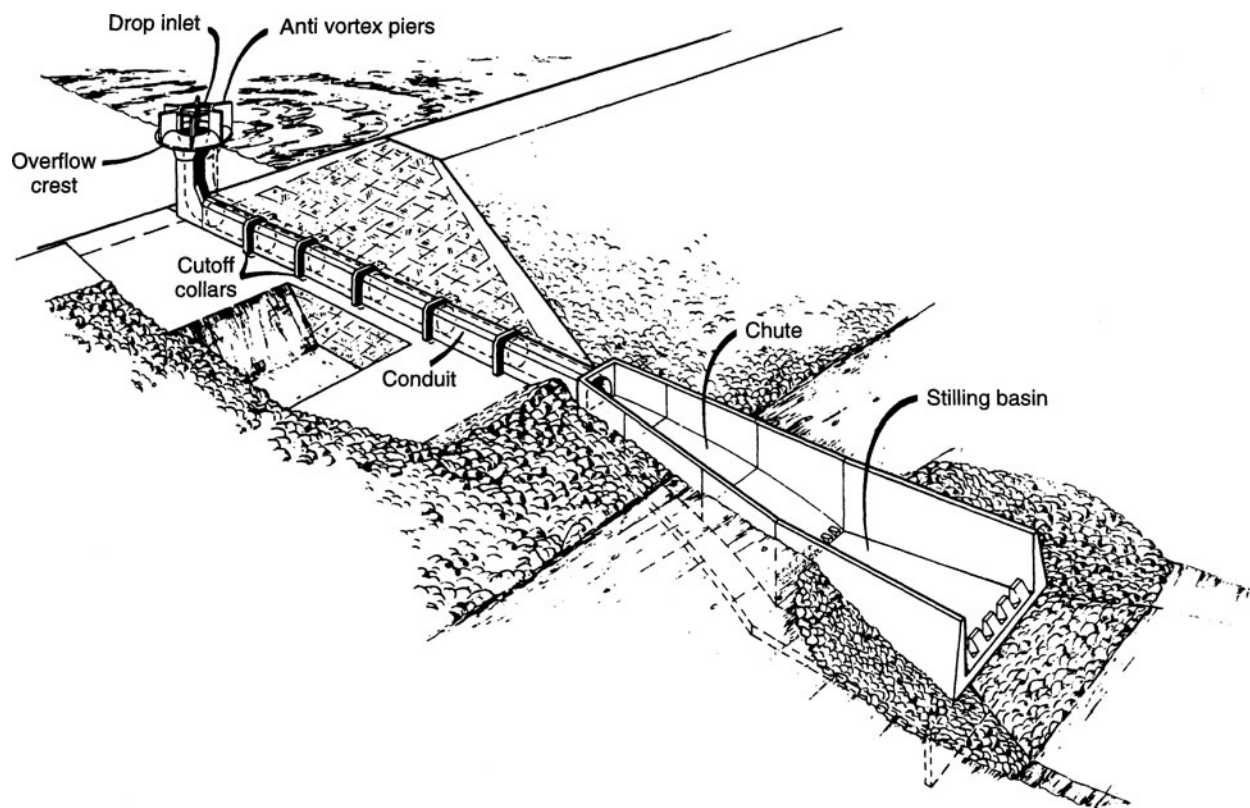


Figure 17.3.13 Drop inlet spillway for a small dam (from U.S. Bureau of Reclamation (1987)).

entrance becomes submerged when orifice flow controls $Q = f(H_a^{1/2})$. When the downstream pipe becomes full, pipe flow prevails so that relatively large increases in head produce small increases in discharge. These spillways are commonly designed so that the flow depth in the downstream tunnel is less than or equal to 75 percent of area, allowing air to enter from the downstream end and preventing subatmospheric pressure in the tunnel.

Given a design discharge and maximum expected head, the following procedure can be used to size a morning glory spillway.

Step 0. Select the crest elevation and outlet invert elevation.

Step 1. Determine the minimum radius of the crest so that subatmospheric pressure can be tolerated.

(a) Assume R_s , determine H_0/R_s , and obtain C_0 from Figure 17.3.16 for P/R_s .

(b) Compute the discharge $Q = C_0(2\pi R_s)H_0^{3/2}$ and compare with the required discharge.

Step 2. The shape of the crest can be computed using tables from the U.S. Bureau of Reclamation (1987), such as in Table 17.3.3. Use Figure 17.3.14 to obtain values of H_s/H_0 in order to compute H_s/R_s used on the tables.

Step 3. Determine transition shape for the design discharge and maximum expected head for the crest elevation. Use the following equation (U.S. Bureau of Reclamation, 1987):

$$R = 0.204 \frac{Q^{1/2}}{H_a^{1/4}} \quad (17.3.7)$$

where H_a is the distance between the water surface and the elevation being considered and R is the transition shape radius. Vary H_a to determine the relationship between throat radius and elevation. This equation assumes that the total losses through the transition are $0.1 H_a$.

DESIGN OF SMALL DAMS

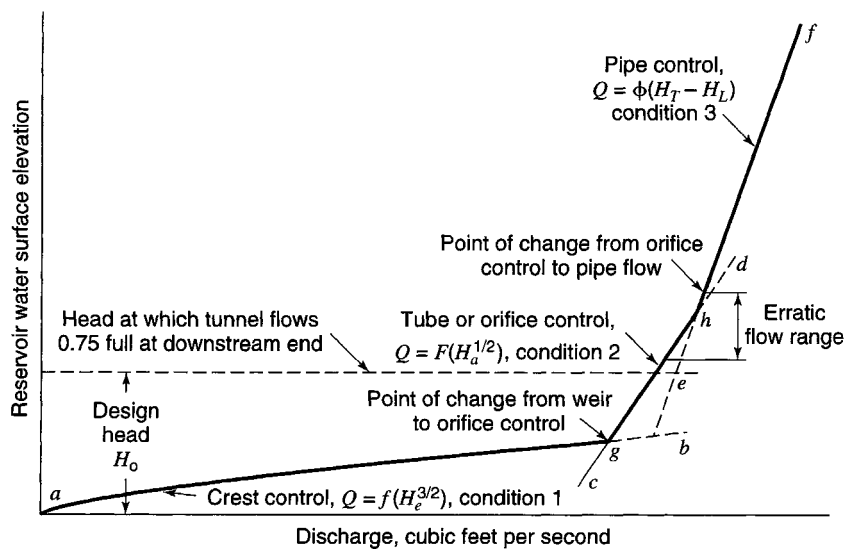
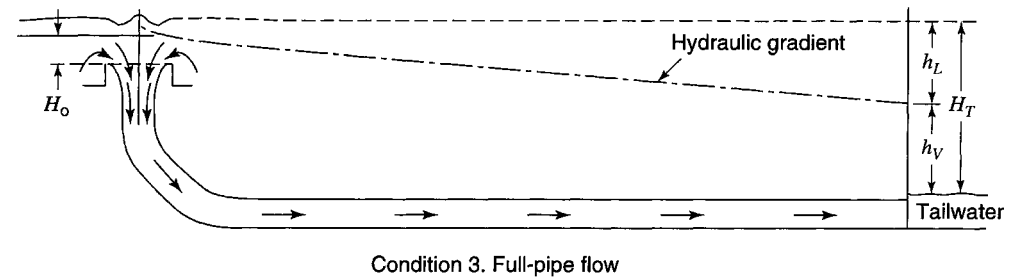
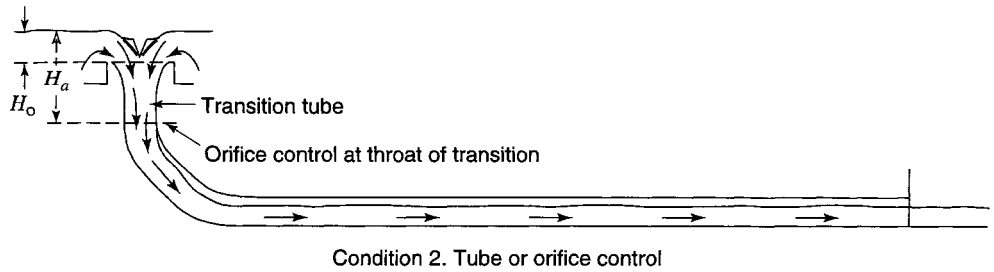
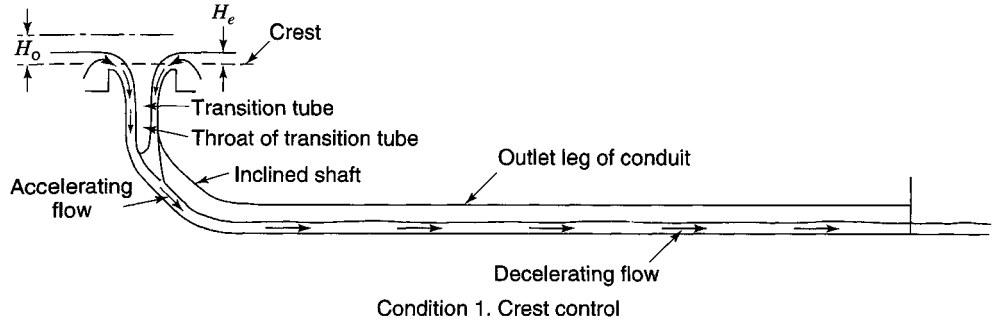


Figure 17.3.14 Nature of flow and discharge characteristics of a morning glory spillway (from U.S. Bureau of Reclamation (1987)).

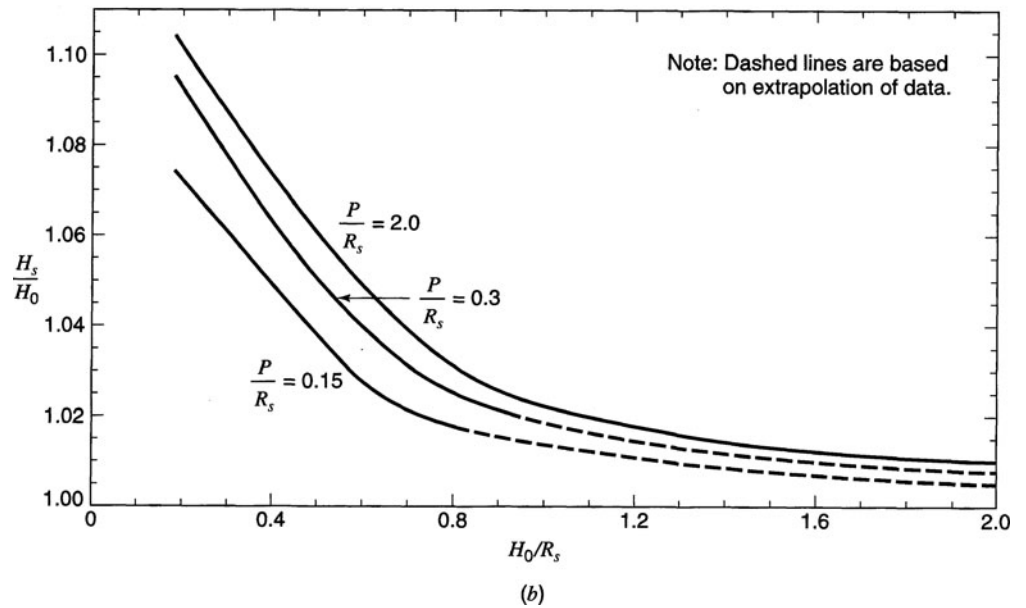
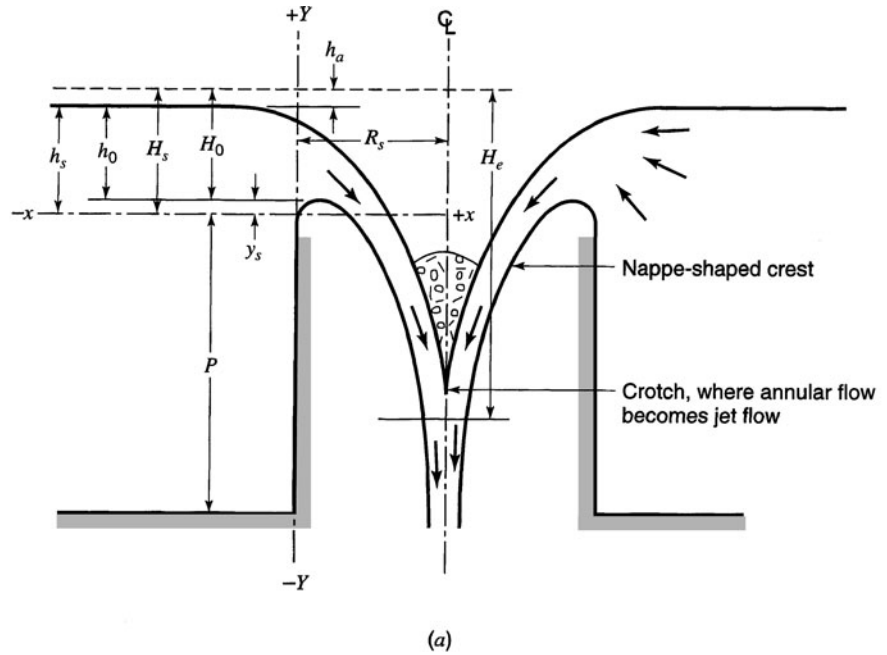


Figure 17.3.15 Circular sharp-crested weirs: (a) Elements of nappe-shaped profile for circular weir; (b) Relationship of H_s/H_0 to H_0/R_s for circular sharp-crested weirs (from U.S. Bureau of Reclamation (1987)).

Step 4. Determine the minimum conduit diameter that can pass the flow from the transition section to the conduit portal without the conduit flowing more than 75 percent at the downstream end.

- (a) Select a trial diameter and throat diameter and find the corresponding throat location.
- (b) Compute the length from the transition throat to the outlet portal.

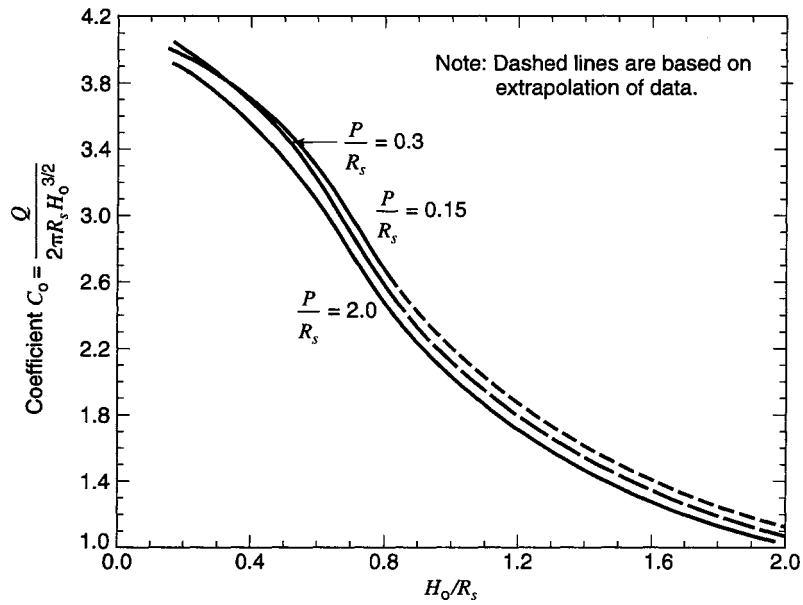


Figure 17.3.16 Relationship of circular crest coefficient C_0 to H_0/R_s for different approach depths (aerated nappe) (from U.S. Bureau of Reclamation (1987)).

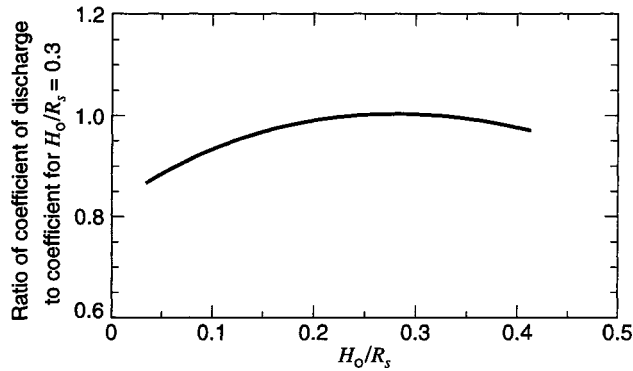


Figure 17.3.17 Circular crest discharge coefficient for other than design head (from U.S. Bureau of Reclamation (1987)).

- (c) Approximate friction losses by assuming the conduit flows 75 percent full for its entire length, using

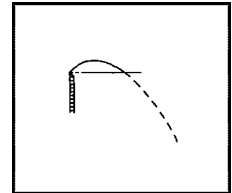
$$V = Q/(0.75A), S_f = \left(\frac{Vn}{1.49(D/2)^{2/3}} \right)^2, h_{Lf} = L \cdot S_f$$

- (d) Use the energy equation from the throat to the outlet to check elevation of invert at the outlet portal required to pass the design discharge through the selected conduit diameter. You may have to increase the conduit and repeat 4a through 4d.

Table 17.3.3 Coordinates of Lower Nappe Surface Different Values of $\frac{H_s}{R}$ when $\frac{P}{R} = 2$

[Negligible approach velocity and aerated nappe]

$\frac{H_s}{R}$	0.00	0.10*	0.20	0.25	0.30	0.35	0.40	0.45	0.50	0.60	0.80	1.00	1.20	1.50	2.00
$\frac{X}{H_s}$	$\frac{Y}{H_s}$ for portion of the surface above the weir crest														
0.000	0.000	0.000	0.000	0.000	0.000	0.000	0.000	0.000	0.000	0.000	0.000	0.000	0.000	0.000	0.000
.010	.0150	.0145	.0133	.0130	.0128	.0125	.0122	.0119	.0116	.0112	.0104	.0095	.0086	.0077	.0070
.020	.0280	.0265	.0250	.0243	.0236	.0231	.0225	.0220	.0213	.0202	.0180	.0159	.0140	.0115	.0090
.030	.0395	.0365	.0350	.0337	.0327	.0317	.0308	.0299	.0289	.0270	.0231	.0198	.0168	.0126	.0085
.040	.0490	.0450	.0435	.0417	.0403	.0389	.0377	.0363	.0351	.0324	.0268	.0220	.0176	.0117	.0050
.050	.0575	.0535	.0506	.0487	.0471	.0454	.0436	.0420	.4002	.0368	.0292	.0226	.0168	.0092	
.060	.0650	.0605	.0570	.0550	.0531	.0510	.0489	.0470	.0448	.0404	.0305	.0220	.0147	.0053	
.070	.0710	.0665	.0627	.0605	.0584	.0560	.0537	.0514	.0487	.0432	.0308	.0201	.0114	.0001	
.080	.0765	.0710	.0677	.0655	.0630	.0603	.0578	.0550	.0521	.0455	.0301	.0172	.0070		
.090	.0820	.0765	.0722	.0696	.0670	.0640	.0613	.0581	.0549	.0471	.0287	.0135	.0018		
.100	.0860	.0810	.0762	.0734	.0705	.0672	.0642	.0606	.0570	.0482	.0264	.0089			
.120	.0940	.0880	.0826	.0790	.0758	.0720	.0683	.0640	.0596	.0483	.0195				
.140	.1000	.0935	.0872	.0829	.0792	.0750	.0705	.0654	.0599	.0460	.0101				
.160	.1045	.0980	.0905	.0855	.0812	.0765	.0710	.0651	.0585	.0418					
.180	.1080	.1010	.0927	.0872	.0820	.0766	.0705	.0637	.0559	.0361					
.200	.1105	.1025	.0938	.0877	.0819	.0756	.0688	.0611	.0521	.0292					
.250	.1120	.1035	.0926	.0850	.0773	.0683	.0596	.0495	.0380	.0068					
.300	.1105	.1000	.0850	.0764	.0668	.0559	.0446	.0327	.0174						
.350	.1060	.0930	.0750	.0650	.0540	.0410	.0280	.0125							
.400	.0970	.0830	.0620	.0500	.0365	.0220	.0060								
.450	.0845	.0700	.0450	.0310	.0170	.000									
.500	.0700	.0520	.0250	.0100											
.550	.0520	.0320	.0020												
.600	.0320	.0080													
.650	.0090														



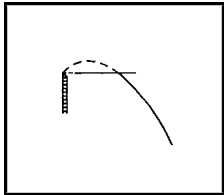
$\frac{Y}{H_s}$	$\frac{X}{H_s}$ for portion of the surface above the weir crest														
0.000	0.668	0.615	0.554	0.520	0.487	0.450	0.413	0.376	0.334	0.262	0.158	0.116	0.093	0.070	0.048
-.020	.705	.652	.592	.560	.526	.488	.452	.414	.369	.293	.185	.145	.120	.096	.074
-.040	.742	.688	.627	.596	.563	.524	.487	.448	.400	.320	.212	.165	.140	.115	.088
-.060	.777	.720	.660	.630	.596	.557	.519	.478	.428	.342	.232	.182	.155	.129	.100
-.080	.808	.752	.692	.662	.628	.589	.549	.506	.454	.363	.250	.197	.169	.140	.110
-.100	.838	.784	.722	.692	.657	.618	.577	.532	.478	.381	.266	.210	.180	.150	.118
-.150	.913	.857	.793	.762	.725	.686	.641	.589	.531	.423	.299	.238	.204	.170	.132
-.200	.978	.925	.860	.826	.790	.745	.698	.640	.575	.459	.326	.260	.224	.184	.144
-.250	1.040	.985	.919	.883	.847	.801	.750	.683	.613	.490	.348	.280	.239	.195	.153
-.300	1.100	1.043	.976	.941	.900	.852	.797	.722	.648	.518	.368	.296	.251	.206	.160
-.400	1.207	1.150	1.079	1.041	1.000	.944	.880	.791	.705	.562	.400	.322	.271	.220	.168
-.500	1.308	1.246	1.172	1.131	1.087	1.027	.951	.849	.753	.598	.427	.342	.287	.232	.173
-.600	1.397	1.335	1.250	1.215	1.167	1.102	1.012	.898	.793	.627	.449	.359	.300	.240	.179
-.800	1.563	1.500	1.422	1.369	1.312	1.231	1.112	.974	.854	.673	.482	.384	.320	.253	.184
-1.000	1.713	1.646	1.564	1.508	1.440	1.337	1.189	1.030	.899	.710	.508	.402	.332	.260	.188
-1.200	1.846	1.780	1.691	1.635	1.553	1.422	1.248	1.074	.933	.739	.528	.417	.340	.266	

(Continued)

Table 17.3.3 (Continued)

[Negligible approach velocity and aerated nappe]

$\frac{H_s}{R}$	0.00	0.10*	0.20	0.25	0.30	0.35	0.40	0.45	0.50	0.60	0.80	1.00	1.20	1.50	2.00
$\frac{Y}{H_s}$	$\frac{Y}{H_s}$ for portion of the surface above the weir crest														
-1.400	1.970	1.903	1.808	1.748	1.653	1.492	1.293	1.108	.963	.760	.542	.423	.344		
-1.600	2.085	2.020	1.918	1.855	1.742	1.548	1.330	1.133	.988	.780	.553	.430			
-1.800	2.196	2.130	2.024	1.957	1.821	1.591	1.358	1.158	1.008	.797	.563	.433			
-2.000	2.302	2.234	2.126	2.053	1.891	1.630	1.381	1.180	1.025	.810	.572				
-2.500	2.557	2.475	2.354	2.266	2.027	1.701	1.430	1.221	1.059	.838	.588				
-3.000	2.778	2.700	2.559	2.428	2.119	1.748	1.468	1.252	1.086	.853					
-3.500		2.916	2.749	2.541	2.171	1.777	1.489	1.267	1.102						
-4.000		3.114	2.914	2.620	2.201	1.796	1.500	1.280							
-4.500		3.306	3.053	2.682	2.220	1.806	1.509								
-5.000		3.488	3.178	2.734	2.227	1.811									
-5.500		3.653	3.294	2.779	2.229										
-6.000		3.820	3.405	2.812	2.232										
$\frac{H_s}{R}$	0.00	0.10	0.20	0.25	0.30	0.35	0.40	0.45	0.50	0.60	0.80	1.00	1.20	1.50	2.00



*The tabulation for $H_s/R = 0.10$ was obtained by interpolation between $H_s/R = 0$ and 0.20 .

Source: U.S. Bureau of Reclamation (1987)

EXAMPLE 17.3.4

Design an ungated drop inlet (morning glory) spillway that will operate under a maximum surcharge head of $H_0 = 10$ ft that can limit the outflow to $1500 \text{ ft}^3/\text{s}$. Determine (a) the minimum radius of the overflow crest, (b) the transition shaft radius, (c) the minimum uniform conduit diameter considering a 75 percent full flow in order to allow air to pass up the conduit from the downstream portal in order to prevent subatmospheric pressures in the conduit, and (d) develop the discharge-water surface elevation relationship. The horizontal length of the conduit is 250 ft. The crest elevation is 100 ft and outlet invert elevation is 60 ft. This example design must minimize the overflow crest radius because the intake is formed as a tower away from the abutment. Also, subatmospheric pressure along the crest can be tolerated; now the conduit portion of the spillway must not flow more than 75 percent full at the downstream end.

SOLUTION

Step 1. Assume $R_s = 5.5$ ft, then $H_0/R_s = 10/5.5 = 1.82$; assume $P/R_s \geq 2$, then $C_0 = 1.14$ (Figure 17.3.16). The discharge is computed using equation (17.3.6): $Q = 1.14(2\pi)(5.5)(10)^{3/2} = 1246 < 1500 \text{ ft}^3/\text{s}$.

Next try $R_s = 6.0$ ft, then $H_0/R_s = 1.67$; assume $P/R_s \geq 2$; then $C_0 = 1.23$ and $Q = 1466 \text{ ft}^3/\text{s}$. Next try $R_s = 6.5$ ft; then $H_0/R_s = 1.54$, and assume $P/R_s \geq 2$; then $C_0 = 1.31$ and $Q = 1692 \text{ ft}^3/\text{s}$. Select $R_s = 6.0$ ft as $1465 \text{ ft}^3/\text{s}$ is closer to the $1500 \text{ ft}^3/\text{s}$.

Step 2. The shape of the crest is computed using Table 17.3.3 with $H_0/R_s = 1.67$. From Figure 17.3.15b, $H_s/H_0 = 1.01$ for $H_0/R_s = 1.67$ and $P/R_s = 2$. Therefore, $H_s = 1.01$, $H_0 = 1.01(10) = 10.1$ ft. From Figure 17.3.15a, $y_s = H_s - H_0 = 10.1 - 10 = 0.10$ ft.

The X-Y coordinate of the crest profile for the portion above the weir crest is computed as given in the table below for $H_s/R_s = 10.1/6.0 = 1.68$:

X/H_s	Y/H_s^*	$X = \left(\frac{X}{H_s}\right)H_s$ (ft)	$Y = \left(\frac{Y}{H_s}\right)H_s$ (ft)
0.000	0.0000	0.000	0.000
0.010	0.0074	0.101	0.075
0.020	0.0106	0.202	0.107
0.030	0.0111	0.303	0.112
0.040	0.0093	0.404	0.094

$X_s = 0.303$ ft and $Y_s = 0.112$ ft are taken. The X - Y coordinates of the crest profile below the weir crest were calculated similarly:

Y/H_s	X/H_s^*	$Y = \left(\frac{Y}{H_s}\right)H_s$ (ft)	$X = \left(\frac{X}{H_s}\right)H_s$ (ft)
0.000	0.062	0.000	0.626
-0.020	0.087	-0.202	0.879
-0.040	0.105	-0.404	1.061
-0.060	0.119	-0.606	1.202
-0.080	0.129	-0.808	1.303
-0.100	0.138	-1.010	1.394
-0.150	0.156	-1.515	1.576
-0.200	0.170	-2.020	1.717
-0.250	0.181	-2.525	1.828
-0.300	0.189	-3.030	1.909
-0.400	0.201	-4.040	2.030
-0.500	0.211	-5.050	2.131
-0.600	0.218	-6.060	2.202
-0.800	0.228	-8.080	2.303
-1.000	0.234	-10.100	2.363

*Values were linearly interpolated between $H_s/R_s = 1.50$ and 2.00 .

Step 3. Determine the transition shape. The transition shape radius is computed using equation (17.3.7):

$$R = (0.204) \frac{Q^{1/2}}{H_a^{1/4}} = 0.204 \frac{(1500)^{1/2}}{H_a^{1/4}} = \frac{7.9}{H_a^{1/4}}$$

where H_a is the distance below the water surface elevation (110 ft) and the elevation being considered. The shape radius is computed for different elevations.

Elevation (ft)	100	99	98	97	96	95
H_a (ft)	10	11	12	13	14	15
R (ft)	4.44	4.34	4.24	4.16	4.08	4.01
Elevation (ft)	94	93	92	91	90	
H_a (ft)	16	17	18	19	20	
R (ft)	3.95	3.89	3.84	3.78	3.74	

Step 4. Determine minimum conduit diameter.

- (a) Consider a conduit diameter of 8 ft (or radius of 4 ft). This corresponds to $H_a = [0.204(1500)^{1/2}/4]^4 = 15.22$ ft. The throat location is $110 - 15.22 = 94.78$ ft elevation.

- (b) Assume conduit length of 250 ft from throat transition to the outlet portal.
- (c) Friction losses are approximated assuming the conduit flows 75 percent full for its entire length, so the velocity is $V = Q/(0.75A) = 1500/[0.75\pi(4)^2] = 39.8$ ft/s and $V^2/2g = 24.6$ ft. Using Manning's equation, $S_f = 0.08$ and $h_{Lf} = 20$ ft (with $n = 0.014$). For 75 percent full, $d/D = 0.702$, so $d = 0.702(8) = 5.62$ ft.
- (d) Apply the energy equation to check outlet invert elevation.

Invert elevation = throat elevation + velocity head at throat – velocity head in the conduit flowing 75 percent full – friction losses in conduit – depth at outlet

$$= 94.78 + \left(\frac{1}{1.1} (110 - 94.78) = 13.84 \right) - 24.6 - 20 - 5.62$$

$$= 58.4 \text{ ft}$$

This invert elevation is very close to the assumed invert elevation of 60 ft. A water surface profile through the conduit should be computed.

17.3.6 Baffled Chute Spillways

Figures 17.2.17a and 17.3.18 illustrate a baffled-chute spillway, which is used to lower water from one level to another in the case where a stilling basin is not desired. The baffle pier dissipates energy as water flows down the chute in order to decrease flow velocities of water entering the downstream channel. These spillways have the following advantages: (a) being economical, (b) low terminal velocities even with large elevation drops, (c) no requirements for initial tailwater depth, and (d) no effect on spillway operation due to downstream degradation. Figure 17.3.19 presents recommended

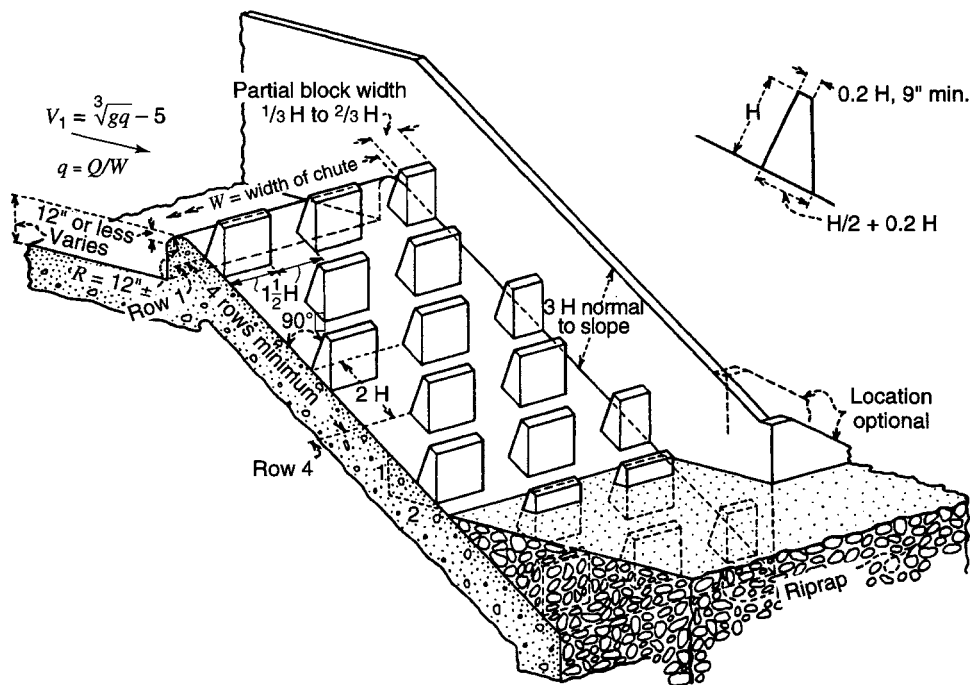


Figure 17.3.18 Basic proportions of a baffled chute spillway (from U.S. Bureau of Reclamation (1987)).

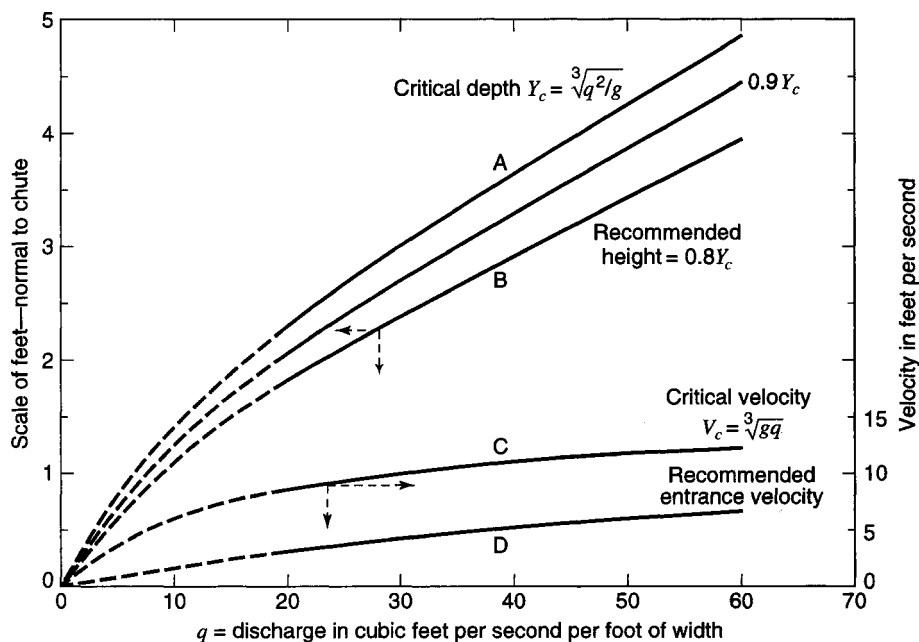


Figure 17.3.19 Recommended baffle pier heights and allowable velocities for baffled chute spillways (from U.S. Bureau of Reclamation (1987)).

baffle pier heights and allowable velocities for baffled chute spillways. Baffled chute spillways are normally constructed at slopes of 2:1 or flatter extending below the channel outlet floor, and design capacities have varied from less than 10 to over 80 cfs/ft of width (U.S. Bureau of Reclamation, 1987). USBR model studies have shown that a baffled chute spillway design can be based on a discharge of about two-thirds the maximum expected discharge.

The typical hydraulic design procedure for a baffled chute spillway is given below (adapted from U.S. Bureau of Reclamation, 1987):

1. Determine maximum expected discharge.
2. Determine unit design discharge $q = Q/W$, where W is the chute width.
3. Determine entrance velocity, ideally as $V_1 = \sqrt[3]{gq} - 5$, which is curve D in Figure 17.3.19.
4. Select a vertical offset between the approach channel flow and the chute to establish a desirable uniform entrance velocity V_1 (see Figure 17.3.18).
5. Select the baffle pier height H as $0.8d_c$ or $0.9d_c$, where d_c is the critical depth $d_c = \sqrt[3]{q^2/g}$. Refer to curve A in Figure 17.3.19.
6. Select baffle pier width and space equal to about $1.5H$, but not less than H . Figure 17.3.18 gives suggested cross-sectional dimensions of baffle piers.
7. Determine spacing between the rows of baffles as H divided by the slope. For a 2:1 slope, the row spacing is $2H$.
8. Baffle piers are typically placed with the upstream face normal to the chute flow surface. Also, vertical-faced piers can be used; these tend to produce more splash and less bed scour, but differences are minor.
9. Select at least four rows of baffle piers to establish full control of the flow. There should be at least one row of buried baffle piers with an additional row to protect against degradation.
10. Determine chute training wall heights as $3H$.
11. Place riprap consisting of 6- to 12-inch stones at the downstream ends of the training walls to prevent eddies. This riprap should be extended appreciably into the flow area.

EXAMPLE 17.3.5

Determine the dimensions for a baffled chute spillway for a maximum expected discharge of 5000 ft³/s. The spillway slope is 2:1 and the water is lowered vertically 30 ft.

SOLUTION

1. The maximum expected discharge is 5000 ft³/s.
2. Select a width of 80 ft so that the unit discharge is $q = 5000/80 = 62.5$ ft³/s/ft.
3. The entrance velocity is $V = \sqrt[3]{gq} - 5 = \sqrt[3]{32.2(62.5)} - 5 = 7.63$ ft/s. Also, from Figure 17.3.19, $V = 7.6$ ft/s.
4. A vertical offset of 1 ft is arbitrarily selected (12 in or less is recommended).
5. The critical depth is $y_c = \sqrt[3]{q^2/g} = \sqrt[3]{62.5^2/32.2} = 4.95$ ft. Choose $H = 0.8 y_c = 0.8(4.95) = 3.96$, and use $H = 4.0$ ft.
6. Referring to Figure 17.3.18, pier width is $1.5H = 6$ ft; bottom length is $H/2 + 0.2H = 2.8$ ft.
7. The longitudinal spacing of the baffle rows is $H/\text{slope} = H/0.5 = 2H = 8$ ft.
8. Use an upstream baffle face that is normal to the chute spillway.
9. At a 2:1 slope, the horizontal chute length is approximately $2(30) = 60$ ft so that the minimum chute length is $\sqrt{30^2 + 60^2} = 67$ ft. The chute length can be made 80 ft to allow for at least one buried baffle row; then 10 rows of baffles are needed.
10. The chute training wall height is $3H = 3(4) = 12$ ft.
11. Select a riprap ($D_{50} = 6$ to 12 in) and extend approximately 30 ft into the flow area.

17.3.7 Culvert Spillways

A culvert spillway (see Figure 17.2.18) usually consists of a simple culvert placed through a dam or along an abutment, usually on a uniform grade, with a vertical or inclined entrance. These spillways are circular, square, rectangular, or some other cast-in-place shapes. These spillways can discharge freely or can flow into an open channel. Culvert spillways are for elevation drops of less than 25 ft. As illustrated in Figure 17.3.20, these spillways have a variety of flow conditions depending on whether or not the inlet is submerged and whether the slope is mild or steep. The flow operation is either partial flow or full flow depending upon the condition. The hydraulics of culverts has been discussed in Chapter 15. The same design procedures discussed in Chapter 15 may be followed to analyze culvert spillway hydraulics.

17.4 HYDRAULIC-JUMP-TYPE STILLING BASINS AND ENERGY DISSIPATORS

The purpose of this section is to describe the various stilling basins and energy dissipators that are used to dissipate the energy of flow from the spillway before the discharge is returned to the downstream environment. Additional material is in Mays (1999) and Wei and Lindell (1999).

17.4.1 Types of Hydraulic Jump Basins

Using the U.S. Bureau of Reclamation (1987) classification, there are five basic hydraulic-jump-type basins that are briefly described in this section:

- Basin I Horizontal aprons
- Basin II Stilling basins for high dam and earth dam spillways and large canal structures
- Basin III Short stilling basins for canal structures, small outlet works, and small spillways
- Basin IV Stilling basins and wave suppressors for canal structures, outlet works, and diversion dams
- Basin V Stilling basins with sloping aprons

Many of the basins are based upon developing a hydraulic jump for the purpose of dissipating energy before the flow enters the downstream channel. The U.S. Bureau of Reclamation (Peterka, 1964) performed a comprehensive series of tests to determine the

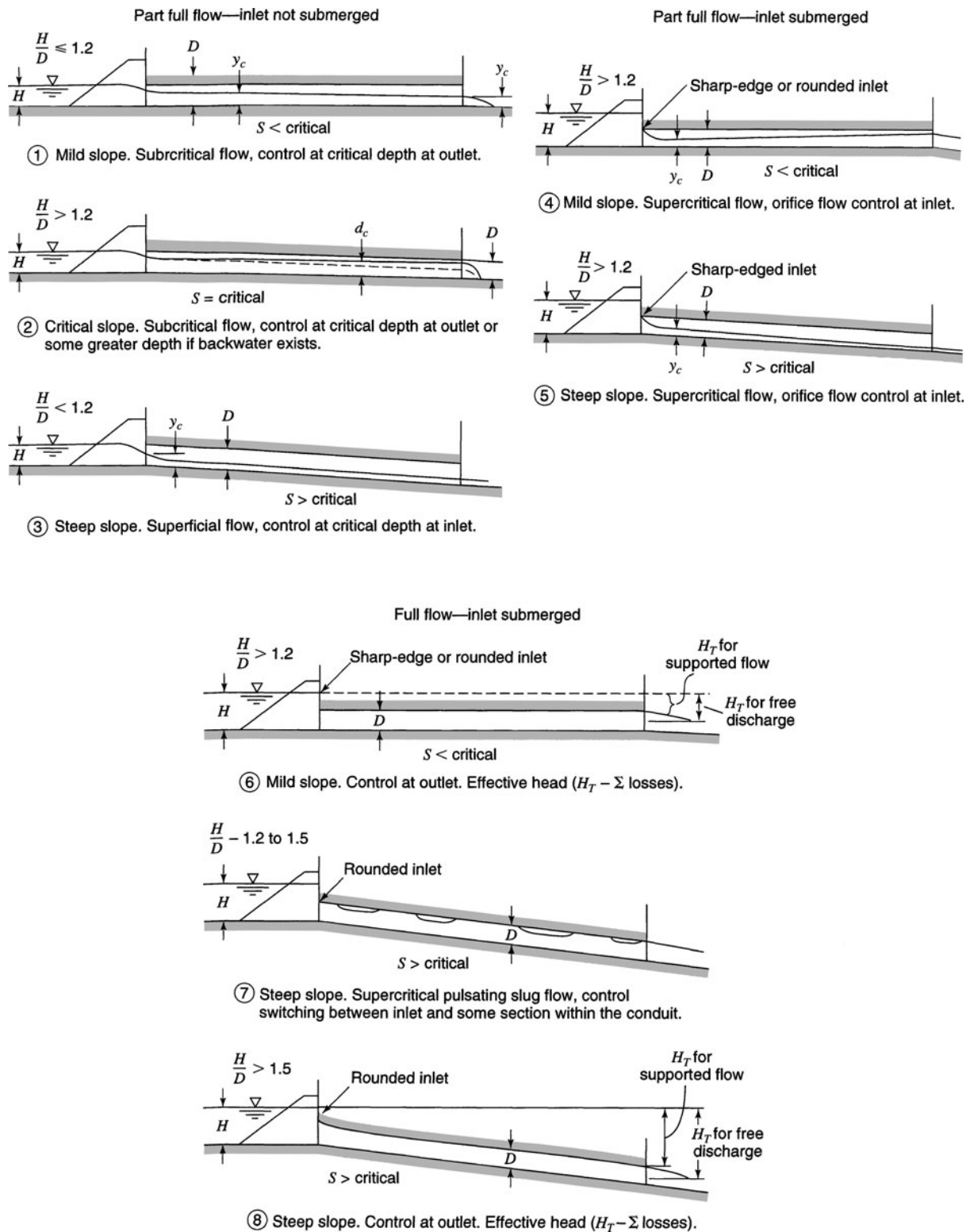


Figure 17.3.20 Typical flow conditions for culvert spillways on mild and steep slopes (from U.S. Bureau of Reclamation (1987)).

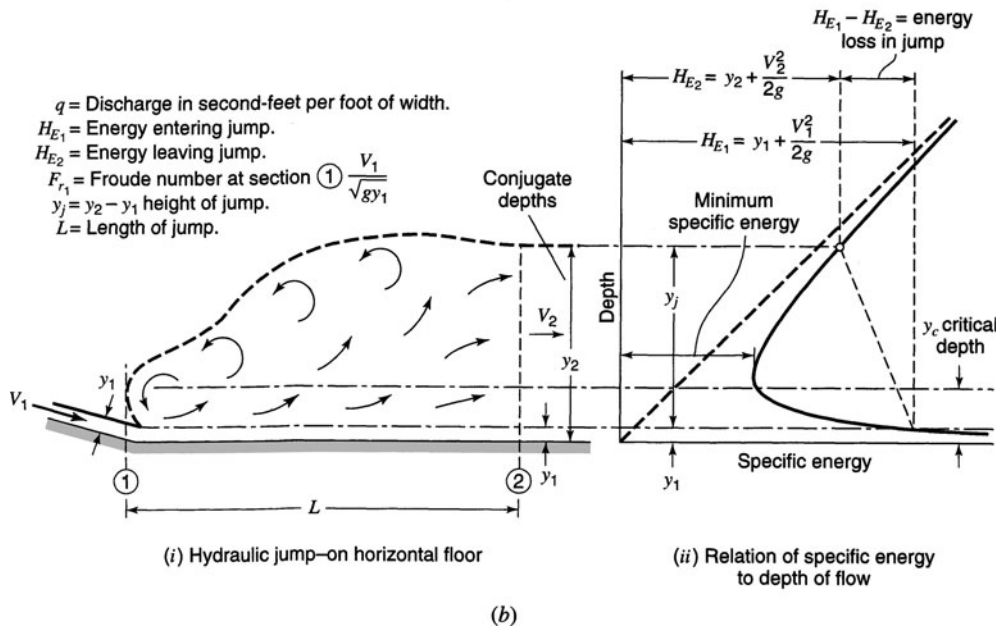
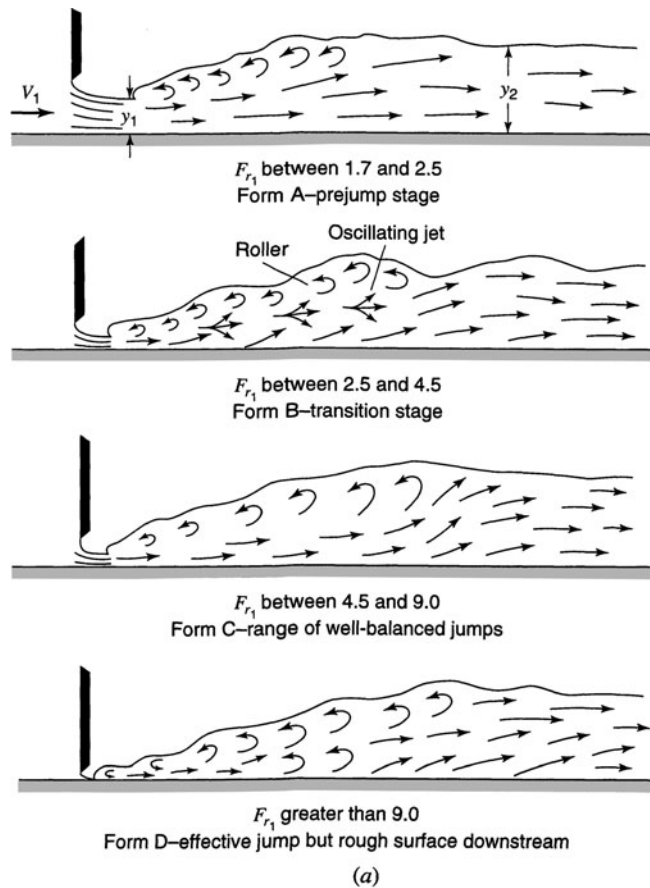


Figure 17.4.1 Hydraulic jumps on horizontal apron. (a) Characteristic forms of hydraulic jump related to the Froude number; (b) Hydraulic jump symbols and characteristics (from U.S. Bureau of Reclamation (1987)).

properties of hydraulic jumps. Figure 17.4.1 illustrates the characteristic form of the hydraulic jump related to the Froude number. For a Froude number of 1.0 for the incoming flow, the flow is critical and a jump cannot form. For Froude numbers between 1.0 to about 1.7, the incoming flow is slightly below critical depth and a jump still cannot form. For Froude numbers above 1.7, the incoming flows can produce hydraulic jumps with the characteristics shown in Figure 17.4.1.

Characteristics of the hydraulic jump and notation are shown in Figure 17.4.2. From Section 5.5, the expression for conjugate depths of a hydraulic jump can be expressed using equation (5.5.2) as

$$y_2 = -\frac{y_1}{2} + \sqrt{\frac{2V_1^2 y_1}{g} + \frac{y_1^2}{4}} \quad (17.4.1)$$

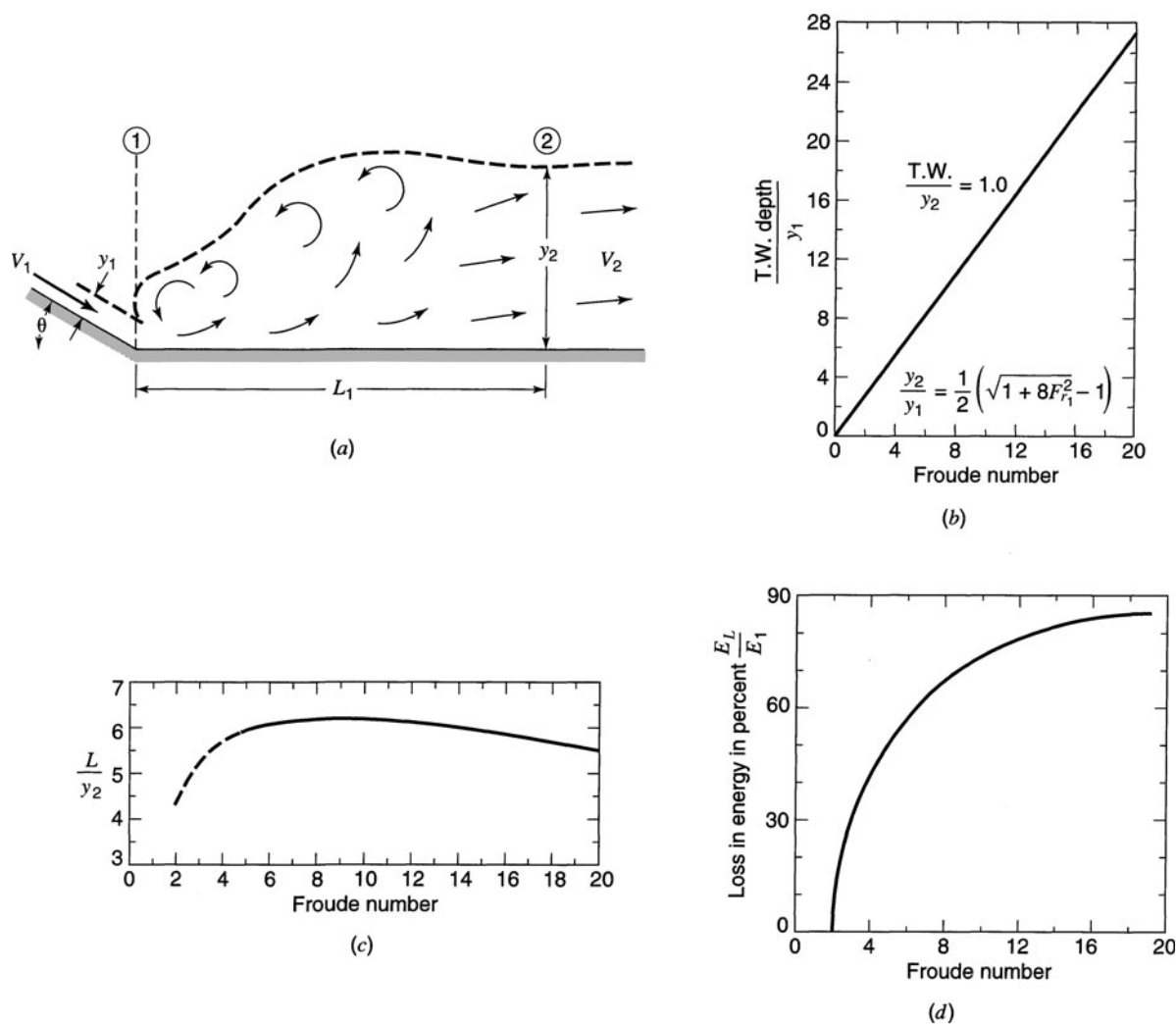


Figure 17.4.2 Type-I stilling basin. (a) Length of jump; (b) Ratio of T.W. depth to y_1 ; (c) Length of jump; (d) Loss of energy in jump (from U.S. Bureau of Reclamation (1987)).

or as

$$y_1 = -\frac{y_2}{2} + \sqrt{\frac{2V_2^2 y_2}{g} + \frac{y_2^2}{4}} \quad (17.4.2)$$

Substituting the Froude number

$$F_{r1} = \frac{V_1}{\sqrt{g y_1}} \quad (17.4.3)$$

into equation (17.4.1) results in (given in Chapter 5):

$$\frac{y_2}{y_1} = \frac{1}{2} \left(\sqrt{1 + 8F_{r1}^2} - 1 \right) \quad (5.5.4)$$

The main concern in the hydraulic design of a hydraulic-jump stilling basin is the determination of the basin width and elevation to form a stable hydraulic jump in the basin. This requires that the jump is neither swept out of the basin nor drowned as the discharge over the spillway varies. If the water depth in the stream below the basin (the tailwater depth) is lower than the conjugate depth of the jump in the basin, the jump will be swept out of the basin. This is likely to lead to erosion of the unprotected stream bed unless the basin is long enough to contain the jump. On the other hand, if the tailwater depth is higher than the conjugate jump depth, the jump moves upstream until the conjugate and tailwater depths become equal. In the process, the jump may be drowned, losing its efficiency as an energy dissipator. Although both situations are undesirable, the first can be far more serious. Therefore, the design objective is to select the basin width and elevation to match the tailwater and conjugate depths at all discharges and to contain the jump in the basin. However, this may be difficult to achieve due to limitations imposed on selection of the proper basin width and/or elevation by the topography and economy. The general practice is to sacrifice jump efficiency in order to prevent bed scour (or to avoid extremely long basins). This is done by matching the tailwater and conjugate depths only for the design discharge.

17.4.2 Basin I

For Froude numbers less than 1.7, no special stilling basin is required. Channel lengths must extend beyond the point where the depth starts to change to not less than $4y_2$. These basins do not require baffle or dissipation devices. These basins are referred to as type-I basins (U.S. Bureau of Reclamation, 1987). For Froude numbers between 1.7 and 2.5, the type-I basin also applies. Characteristics of the type-I basins are shown in Figure 17.4.2.

17.4.3 Basin II

Basins that have been used with high dam and earth dam spillways and large canal structures are type-II basins (see Figure 17.4.3). These basins contain chute blocks at the upstream end and a dentated sill near the downstream end. Baffle piers are not needed because of the relatively high velocity entering the jump. These basins are for Froude numbers above 4.5 or velocities above 50 ft/s. Relationships illustrating stilling basins proportional to minimum tailwater depths and lengths of jump, as a function of Froude number, are presented in Figure 17.4.3.

17.4.4 Basin III

Type-III basins are shorter basins than the type-II with a simpler end sill and with baffle piers downstream of the chute blocks (see Figure 17.4.4). The incoming velocity for the type-III basin

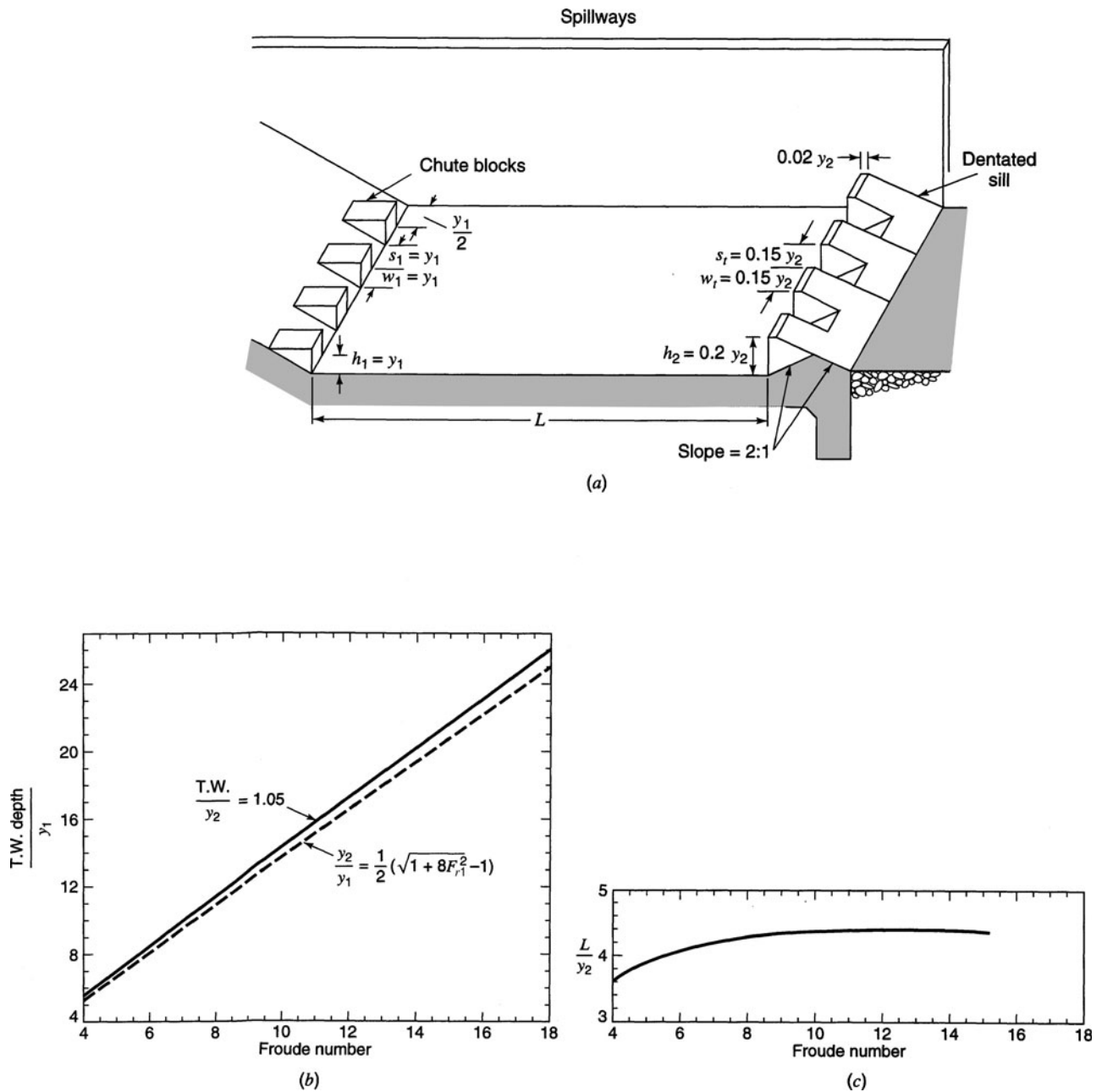


Figure 17.4.3 Stilling basin characteristics for Froude numbers above 4.5. (a) Type-II basin dimensions; (b) Minimum tailwater depths; (c) Length of jump (from U.S. Bureau of Reclamation (1987)).

must be limited to prevent the possibility of low pressures on the baffle piers that can result in cavitation. The type-III basin length is about 60 percent of the type-II basin. Type-III basins are used on small spillways, outlet works, and small canal structures where V_1 does not exceed 50 to 60 ft/sec and the Froude number $F_{r1} > 4.5$.

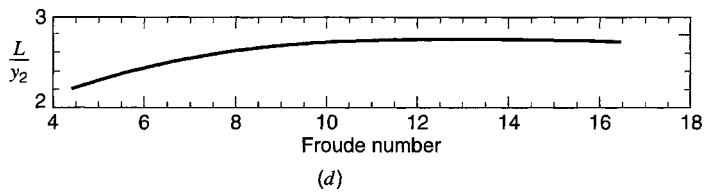
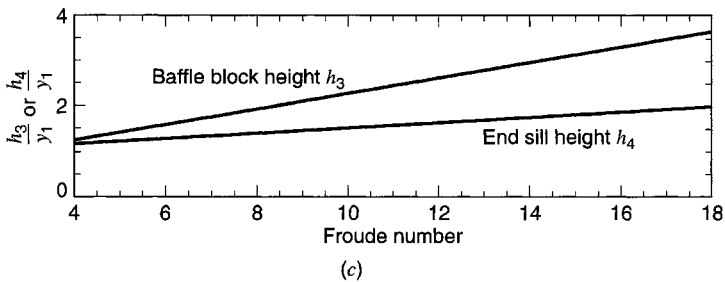
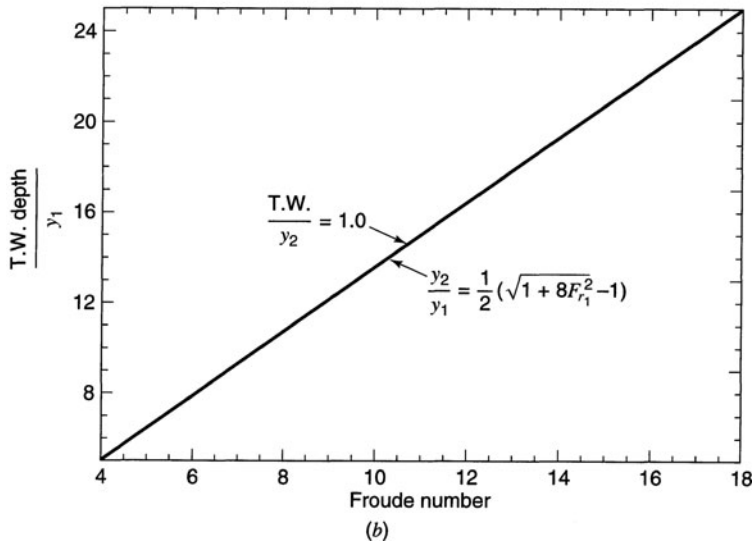
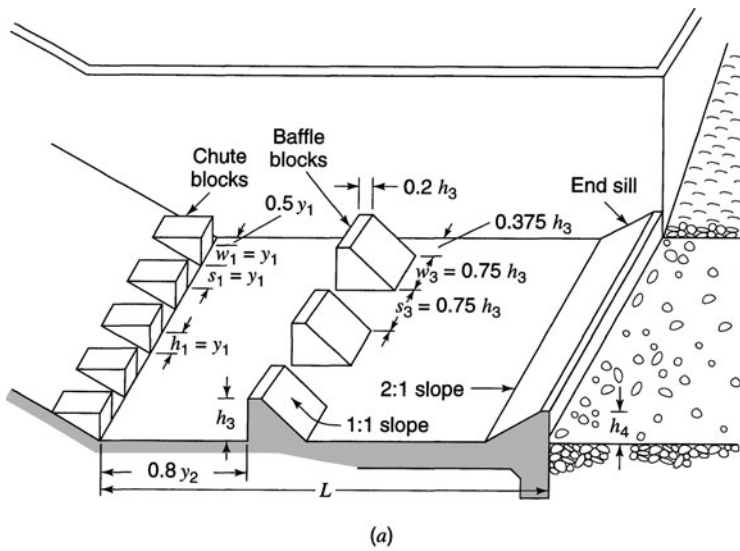


Figure 17.4.4 Stilling basin characteristics for Froude numbers above 4.5 where incoming velocity $V_1 \leq 60$ ft/s. (a) Type-III basin dimensions; (b) Minimum tailwater depths; (c) Height of baffle blocks and end sill; (d) Length of jump (from U.S. Bureau of Reclamation (1987)).

17.4.5 Basin IV

Type-IV basins are used where the Froude number is in the range of 2.5 to 4.5, which is typical of canal structures and occasionally of low dams (small spillways), small outlet works, and diversion dams. In this case the hydraulic jump is not fully developed and the main concern is the waves created in the unstable hydraulic jump. These basins reduce excessive waves created in imperfect jumps. Figure 17.4.5 illustrates the characteristics of this basin along with an alternate design and wave suppressors that may also be used in place of the type-III basin.

Figure 17.4.6 shows an alternative low Froude number stilling basin. The type-IV basin has large deflector blocks that are similar to but larger than chute blocks, and an optional solid end sill. The design shown in Figure 17.4.6 does not have chute blocks, but does have large baffle piers and a dentated end sill.

17.4.6 Basin V

Type-V basins (Figure 17.4.7) are stilling basins with sloping aprons, which are for use where structural economics make the sloping apron more desirable. They are usually used on high dam spillways. Sloping aprons need a greater tailwater depth than the horizontal (type-I) basins. Four cases are illustrated in Figure 17.4.7. Case A is a jump on the horizontal apron. Case B is also a horizontal apron but the toe of the jump forms on the slope and the jump ends on the horizontal apron. For case C, the toe of the jump is on the slope and the end of the jump is at the junction of the slope and the horizontal apron. For case D, the entire jump forms on the slope. Case B is the one usually encountered in sloping apron design (Peterka, 1964).

The expression for conjugate depths for a hydraulic jump on a sloping apron was derived by Kindsvater (1944):

$$\frac{y_2}{y_1} = \frac{1}{2 \cos \phi} \left[\sqrt{\frac{8F_{r1}^2 \cos^3 \phi}{1 - 2K \tan \phi} + 1} - 1 \right] \quad (17.4.4)$$

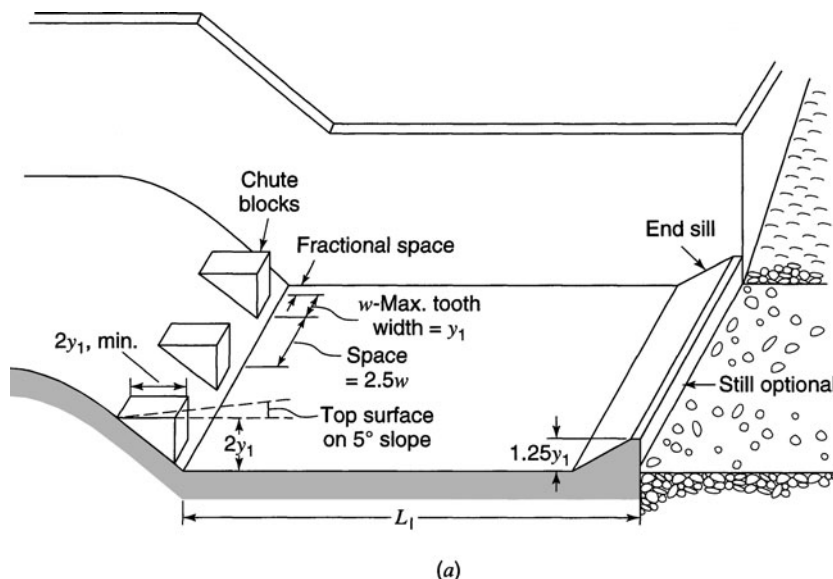


Figure 17.4.5 Stilling basin characteristics for Froude numbers between 2.5 and 4.5. (a) Type-IV basin dimensions; (b) Minimum tailwater depths; (c) Length of jump.

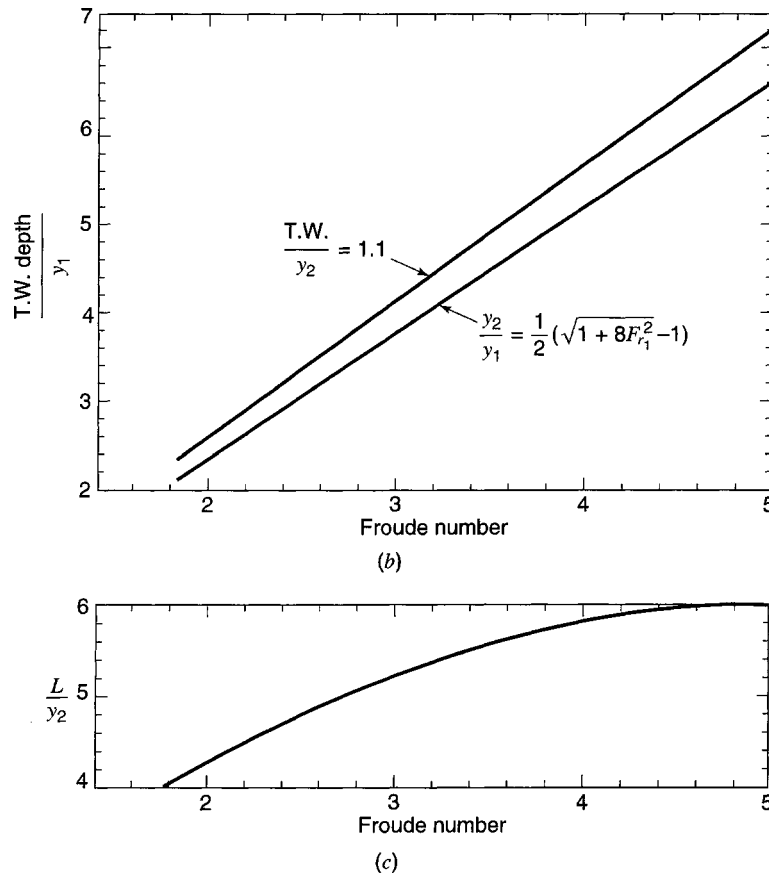


Figure 17.4.5 (Continued)

where K is a dimensionless shape factor that varies mainly with the slope of the apron and minimally with the Froude number (see Peterka (1964)). Figure 17.4.8 illustrates the variation of K with $\tan \phi$, assuming that K is independent of F_{r1} .

17.4.7 Tailwater Considerations for Stilling Basin Design

For the various terminal structures previously discussed, the tailwater conditions are a major concern in the design process. For hydraulic-jump-type basins, the basin floor level must be selected to provide a hydraulic jump elevation that conforms to tailwater elevation for various discharges in order to prevent sweepout of the jump from the basin. A *tailwater rating curve*, which is the stage-discharge relationship of the natural stream or river below a dam, must be determined using the water surface profile (backwater) determination method, as discussed in Chapter 5. Tailwater rating curves are dependent upon the natural conditions of the downstream river characteristics and are not normally changed by the spillway release characteristics.

The objective is to compare an elevation- (conjugate depth-) discharge relationship with the tailwater rating curve determined from a backwater analysis. The conjugate depth- (elevation-) discharge relationship is developed for a certain spillway basin design including the basin width and basin floor elevation. Consider conjugate depth curve 1 in Figure 17.4.9. The stilling basin elevation has been set so that at maximum spillway design capacity the tailwater rating curve and the conjugate-depth curve intersect. For smaller discharges the tailwater elevation is greater than the conjugate depth (elevation), which results in an excess tailwater that can cause a drowned jump.

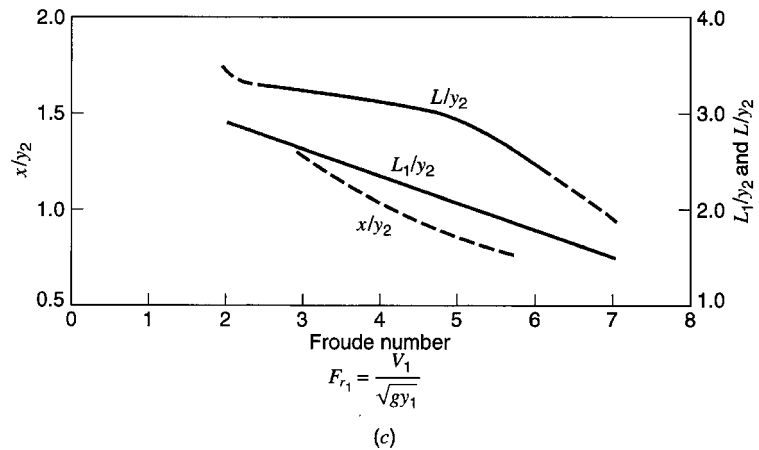
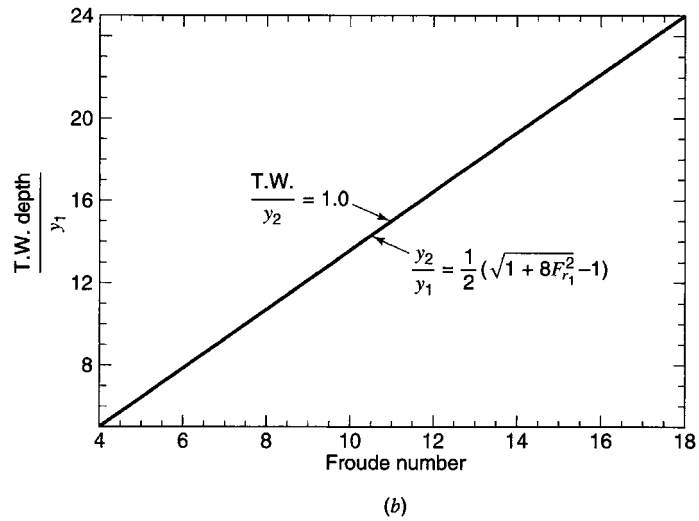
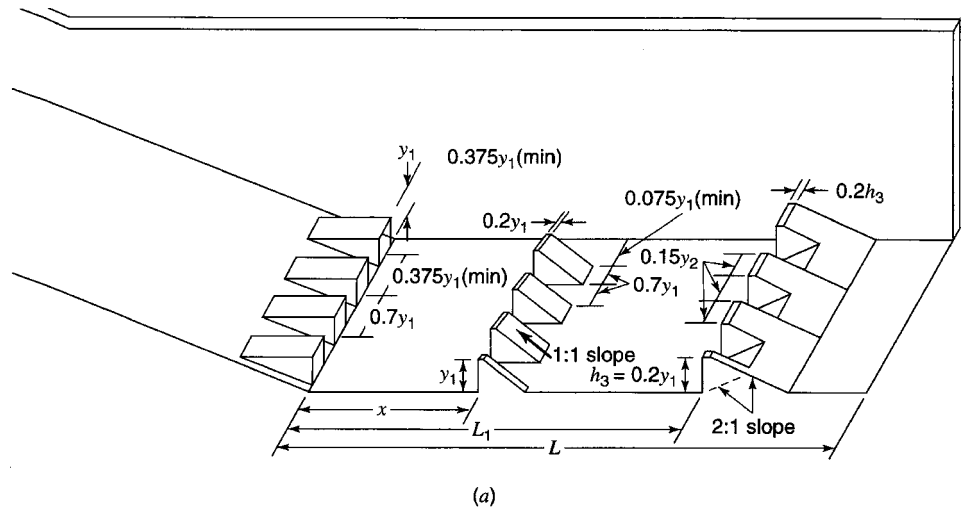


Figure 17.4.6 Characteristics for alternative low Froude number stilling basins. (a) Dimensions for alternative low Froude number basin; (b) Minimum tailwater depths; (c) Length of jump (from U.S. Bureau of Reclamation (1987)).

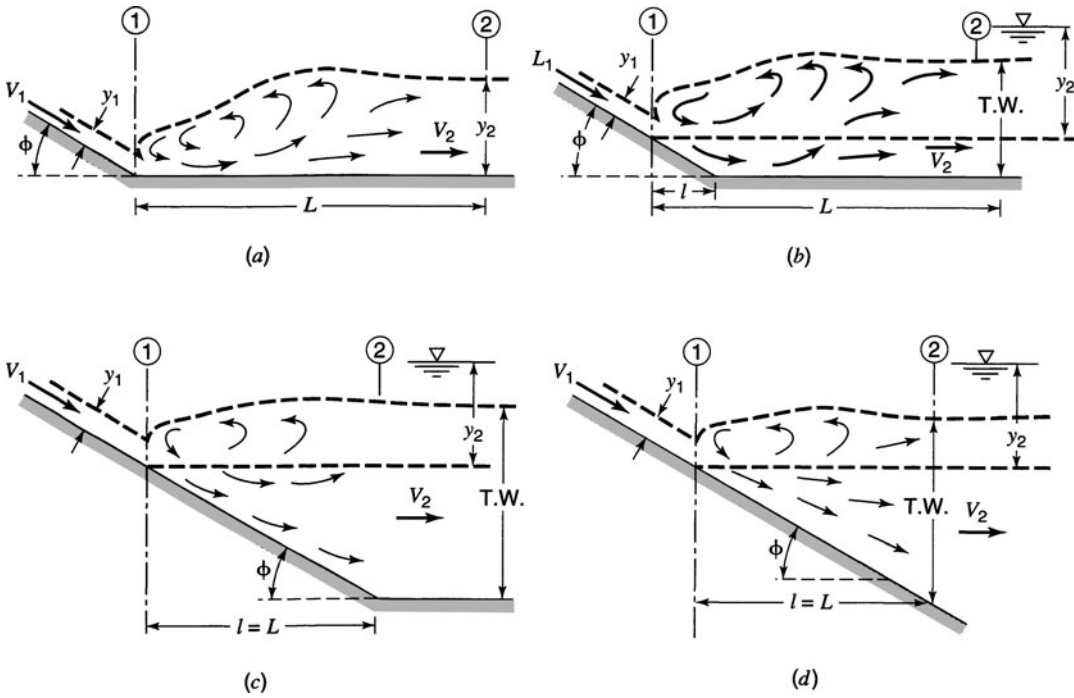


Figure 17.4.7 Sloping aprons (Basin V) (from Peterka (1964)).

Drowned jumps unfortunately do not achieve the jump-type dissipation. Curve 2 has a stilling basin elevation higher than curve 1, causing the conjugate depth (elevation) to be greater than the tailwater rating curve for the entire range of discharges. Curve 3 has a stilling basin elevation lower than that for the basin of curve 1, causing the tailwater elevation to be greater than the conjugate depth (elevation) for the entire range of discharges.

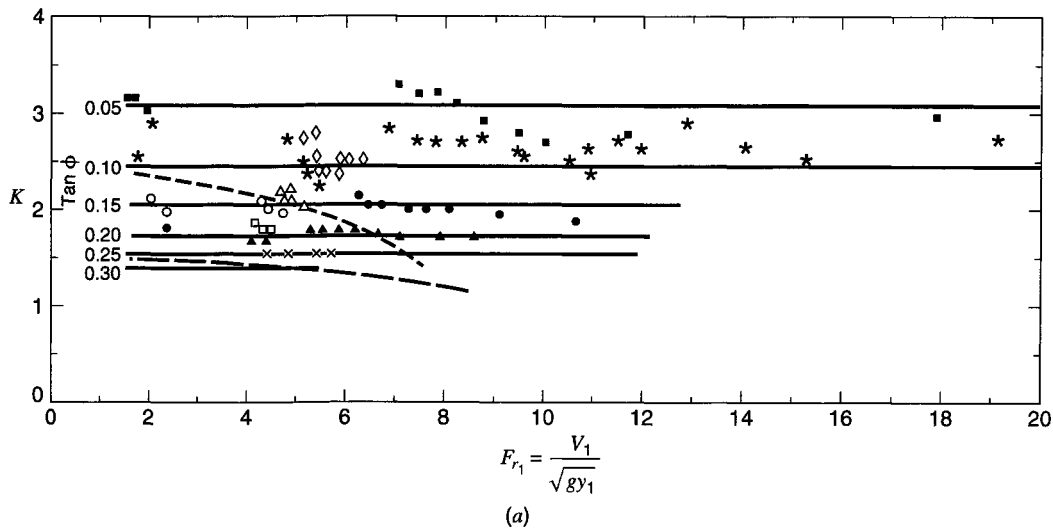


Figure 17.4.8 (a) Shape factor, K , in jump formula. K as function of F_{r1} (Basin V, Case D) (from Peterka (1964)).

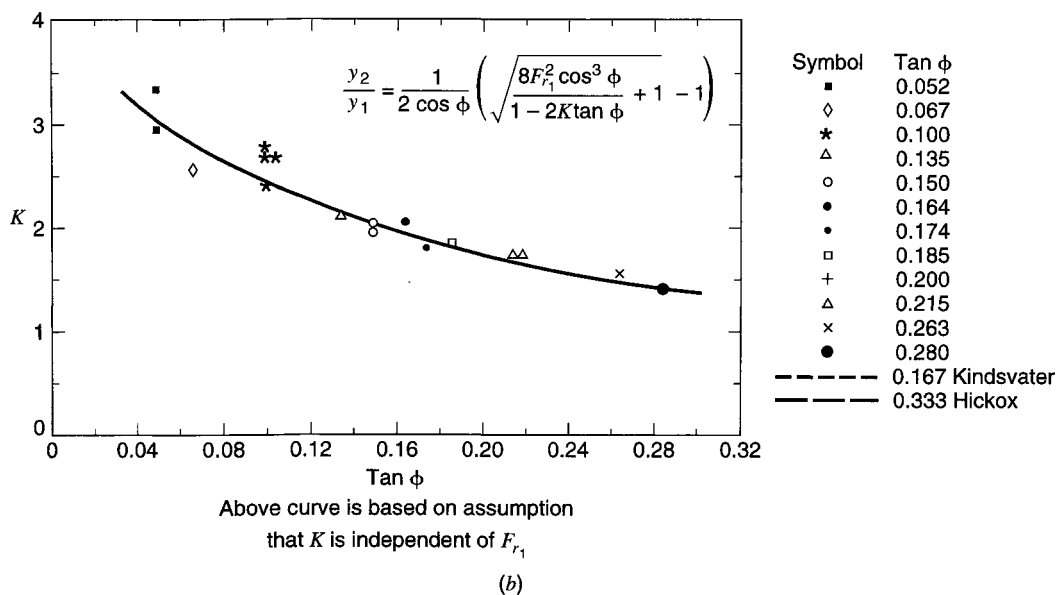


Figure 17.4.8 (b) Shape factor, K , in jump formula. K as independent of F_{r1} (Basin V, Case D) (from Peterka (1964)).

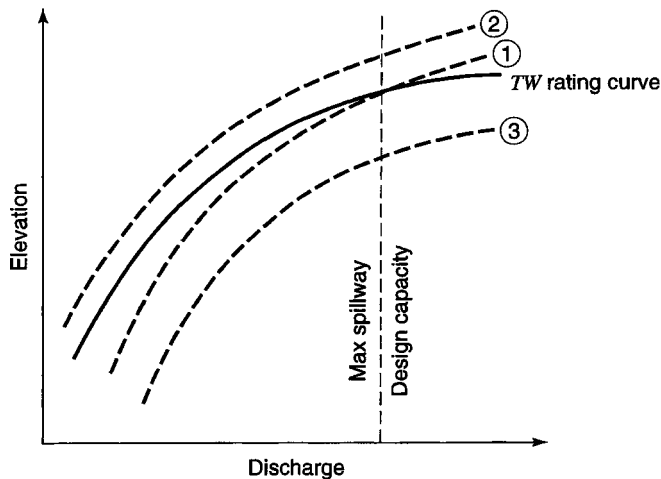


Figure 17.4.9 Relationships of conjugate depth curves to tailwater rating curve.

EXAMPLE 17.4.1

Estimate the length of the concrete apron ($S_0 = 0.001$) for a type-I stilling basin downstream from an overflow spillway (Figure 17.4.10). The spillway crest is 50 ft long and consider a discharge of 4000 cfs. Manning's roughness factor $n = 0.025$. Should a type-I basin be used for this situation, based upon the information available?

SOLUTION

The objective is to determine $\Delta x + L_j$ where L_j is the length of the jump. Flow rate is $q = 4000/50 = 80 \text{ ft}^3/\text{s/}$ unit width of spillway crest. Use the energy equation from the spillway crest to the toe (or bottom of spillway)

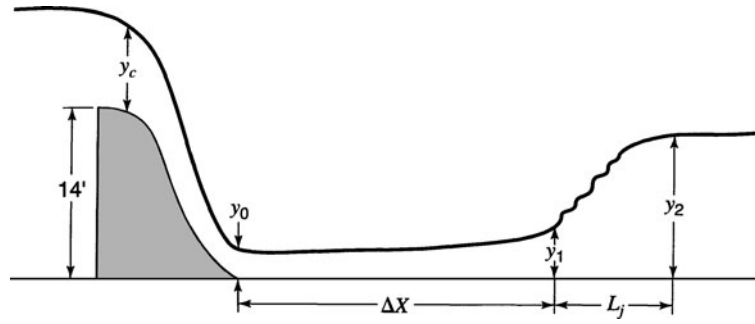


Figure 17.4.10 Example 17.4.1.

and ignore energy loss, which is conservative:

$$E_c + 14 = y_0 + \frac{V^2}{2g}$$

where the specific energy at critical flow is determined using

$$E_c = \frac{3}{2} \left(\frac{q^2}{g} \right)^{1/3} = \frac{3}{2} \left(\frac{6400}{32.2} \right)^{1/3} = 8.75 \text{ ft}$$

The energy equation is now solved for y_0 :

$$8.75 + 14 = y_0 + \left(\frac{80}{y_0} \right)^2 \frac{1}{2(32.2)}$$

$$22.75 = y_0 + \frac{99.38}{y_0^2}$$

from which $y_0 = 2.20$ ft. Next use Manning's equation to solve for y_2 , which assumes normal depth occurs after the jump:

$$Q = \frac{1.49}{n} AR^{2/3} S_0^{1/2} = \frac{1.49}{0.025} (50y_2) \left(\frac{50y_2}{50 + 2y_2} \right)^{2/3} (0.001)^{1/2} = 4000 \text{ cfs}$$

Solving by Newton's method (Appendix A) yields $y_2 = 10.98$ ft. Next compute the depth y_1 using

$$\frac{y_2}{y_1} = \frac{1}{2} \left[-1 + \sqrt{1 + \frac{8q^2}{gy_1^3}} \right] \Rightarrow \frac{10.98}{y_1} = \frac{1}{2} \left[-1 + \sqrt{1 + \frac{8(80)^2}{gy_1^3}} \right]$$

Solving, $y_1 = 2.66$ ft. Δx can now be determined using the energy equation between depths y_0 and y_1 :

$$\Delta x = \frac{\left(y_0 + \frac{V_0^2}{2g} \right) - \left(y_1 + \frac{V_1^2}{2g} \right)}{S_f - S_0}$$

$$V_0 = q/y_0 = 80/2.20 = 36.4 \text{ ft/s}$$

$$V_1 = q/y_1 = 80/2.66 = 30.1 \text{ ft/s}$$

$$V_{ave} = 33.3 \text{ ft/s}$$

The friction slope is now determined using Manning's equation:

$$S_f = \frac{n^2 V_{ave}^2}{2.22 R_{ave}^{4/3}}$$

Assuming the stilling basin is the same width as the spillway crest, the hydraulic radius R_{ave} is:

$$R_{ave} = \frac{1}{2} \left[\frac{50 \times 2.20}{50 + 2(2.20)} + \frac{50 \times 2.66}{50 + 2(2.66)} \right] = 2.21 \text{ ft}$$

The friction slope is then

$$S_f = \frac{(0.025)^2 (33.3)^2}{2.22 (2.21)^{4/3}} = 0.1087$$

and

$$\Delta x = \frac{\left(2.20 + \frac{(36.4)^2}{2g} \right) - \left(2.66 + \frac{(30.1)^2}{2g} \right)}{0.1087 - 0.001} = \frac{22.8 - 16.7}{0.1077} = 56.6 \text{ ft}$$

To compute the length of the jump L_j , Figure 17.4.2c is used. The Froude number F_{r1} is

$$F_{r1} = \frac{V_1}{\sqrt{g y_1}} = \frac{30}{\sqrt{32.2(2.66)}} = 3.25$$

From Figure 17.4.2c, for $F_{r1} = 3.25$, $L_j/y_2 = 5.4$, so $L_j = 5.4 y_2 = 5.4 (10.98) = 59.3$ ft. The length of stilling basin should be at least $(\Delta x + L_j) = 116$ ft to prevent the jump from leaving the basin. Actually, for this example, a type-III stilling basin is more appropriate because of the Froude number, $F_{r0} = 4.3$.

EXAMPLE 17.4.2

Select the type of stilling basin considering the crest length = 100 ft and the discharge = 15,000 cfs for elevations of AA equal to 0, 20, and 40 ft (refer to Figure 17.4.11).

SOLUTION

Assume a rectangular stilling basin is built.

$$q = \frac{Q}{L} = \frac{15,000}{100} = 150 \text{ cfs/ft}$$

The energy equation from spillway crest to just before the jump is

$$Z_c + E_c = Z_1 + y_1 + \frac{V_1^2}{2g}$$

$$100 + E_c = y_1 + \frac{V_1^2}{2g}$$

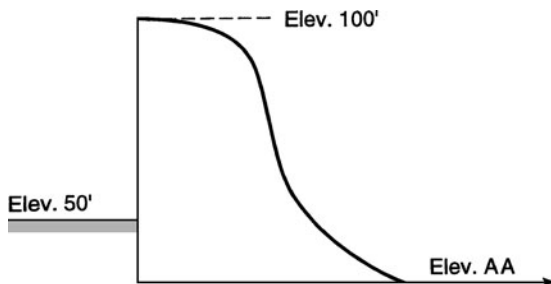


Figure 17.4.11 Example 17.4.2.

For elevation of AA = 0 ft, $Z_1 = 0$,

$$E_c = \frac{3}{2} \left(\frac{q^2}{g} \right)^{1/3} = \frac{3}{2} \left(\frac{150^2}{32.2} \right)^{1/3} = 13.31$$

$$V_1 = \frac{150}{y_1}$$

Thus

$$100 + 13.31 = y_1 + \frac{\left(\frac{150}{y_1} \right)^2}{2(32.2)}$$

which simplifies to $y_1^3 - 113.31y_1^2 + 349.38 = 0$, $y_1 = 1.77$ ft.

The Froude number at section 1 is $F_{r1} = V_1/\sqrt{gy_1} = 150/y_1\sqrt{gy_1} = 150/(1.77\sqrt{32.2 \times 1.77}) = 11.23$.

Since $F_{r1} = 11.23 > 4.5$, the type of basin can be type II or III. As a check, the incoming velocity is $V_1 = 150/1.77 = 84.7$ ft/s > 50 ft/s, so a type-II basin is recommended.

For elevation of AA = 20 ft,

$$Z_c + E_c = Z_1 + y_1 + \frac{V_1^2}{2g}$$

$$100 + 13.31 = 20 + y_1 + \frac{150^2}{2(32.2)y_1^2}$$

$$y_1^3 - 93.31y_1^2 + 349.38 = 0$$

$$y_1 = 1.96 \text{ ft}$$

The Froude number is $F_{r1} = \frac{150}{1.96\sqrt{32.2 \times 1.96}} = 9.63 > 4.5$, $V_1 = \frac{150}{1.96} = 76.5 > 50$ ft/s, so use a type-II basin.

For elevation of AA = 40 ft,

$$100 + 13.31 = 40 + y_1 + \frac{150^2}{2(32.2)y_1^2}$$

$$y_1^3 - 73.31y_1^2 + 349.38 = 0$$

$$y_1 = 2.22 \text{ ft}$$

The Froude number is $F_{r1} = \frac{150}{2.22\sqrt{32.2 \times 2.22}} = 7.99 > 4.5$,

$$V_1 = \frac{150}{2.22} = 67.57 > 50 \text{ ft/s}$$

so use a type-II basin.

EXAMPLE 17.4.3

The objective of this example is to determine the appropriate stilling basin floor elevation in order to prevent the sweepout of a hydraulic jump from the basin. The crest length is 76.6 ft and the discharge is 2,000 ft³/s (refer to Figure 17.4.12).

SOLUTION

First assume a basin floor elevation of 16.7 ft; then $Z_c = 50 - 16.7 = 33.3$ ft,
 $q = 2,000/76.6 = 26.1$ ft³/sec/ft of width; $E_c = \frac{3}{2} \sqrt[3]{q^2/g} = \frac{3}{2} \sqrt[3]{(26.1)^2/(32.2)} = 4.15$ ft.

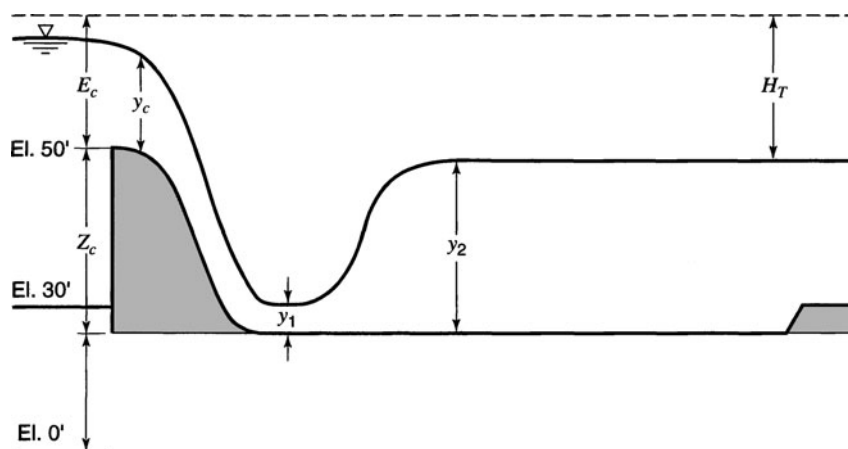


Figure 17.4.12 Example 17.4.3.

The energy equation between the crest and depth y_1 before the jump is used to compute y_1 (ignoring losses):

$$E_c + Z_c = y_1 + \frac{V_1^2}{2g} = y_1 + \frac{q^2}{2gy_1^2}$$

$$4.15 + 33.3 = y_1 + \frac{(26.1)^2}{2(32.2)y_1^2}$$

$$y_1^3 - 37.45y_1^2 + 10.59 = 0$$

Solving yields $y_1 = 0.54$ ft; then $V_1 = 26.1/0.54 = 48.8$ ft/s and the Froude number is $F_{r1} = V_1/\sqrt{gy_1} = 48.8/\sqrt{32.2(0.54)} = 11.7$. Because $F_{r1} > 4.5$ and $V_1 > 50$ ft/s, a type-II or III stilling basin would be recommended. Using Figure 17.4.3b, T.W./ $y_1 = 17$ for $F_{r1} = 11.7$ and T.W./ $y_2 = 1.05$, then T.W. = $17y_1 = 9.18$ ft and $y_2 = \text{T.W.}/1.05 = 8.8$ ft. Other stilling basin floor elevations should be considered.

EXAMPLE 17.4.4

The objective of this problem is to determine the floor elevation for the stilling basin shown in Figure 17.4.13. The results of a survey at a point on a stream at which the basin is to be built are given in Figure 17.4.14, showing the relationships of hydraulic radius and cross-sectional area of flow as a function of elevation. Manning's n is 0.030 and the average slope of the stream bed is 0.00375. The design discharge for the ogee-type spillway is to be 20,000 cfs and the spillway crest length is 100 ft at elevation 3260 ft. The approach channel floor elevation is to be at 3210 ft. The crest is to be shaped using a design head that is 85 percent of the maximum head. Note that the maximum head corresponds to design discharge. A hydraulic-jump stilling basin having the same width as the spillway crest is to be provided. Determine a suitable floor elevation for the hydraulic-jump stilling basin. Ignore the effect of abutments and piers in your design. Present a graphical comparison of computed water surface elevations in the stilling basin with tailwater elevations for all discharges up to the maximum of design discharge.

SOLUTION

To determine the floor elevation, the energy equation between cross-sections 0 and 1 along with the hydraulic jump momentum balance equation are used. The energy between cross-sections 0 and 1 (neglecting losses) is

$$3260 + E_c = Z + E_1$$

$$3260 + \frac{3}{2} \sqrt[3]{q^2/g} = Z + y_1 + \frac{V_1^2}{2g}$$

$$3260 + \frac{3}{2} \frac{\left(\frac{20,000}{100}\right)^{2/3}}{32.2^{1/3}} = Z + y_1 + \frac{(20,000)^2}{2(32.2)(100y_1)^2}$$

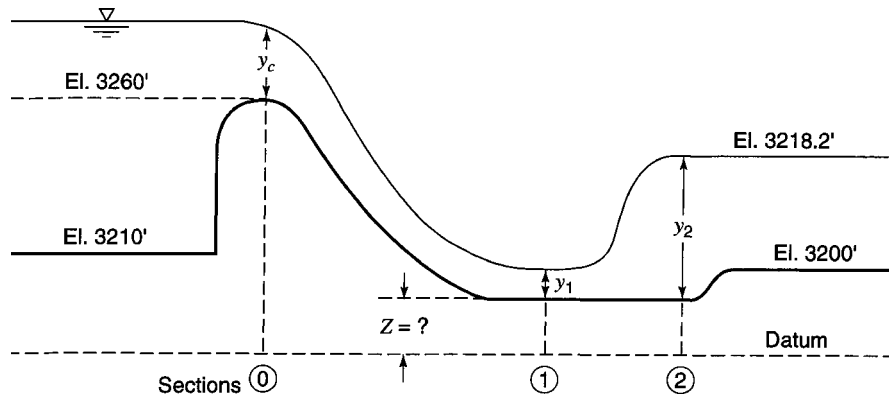


Figure 17.4.13 Example 17.4.4.

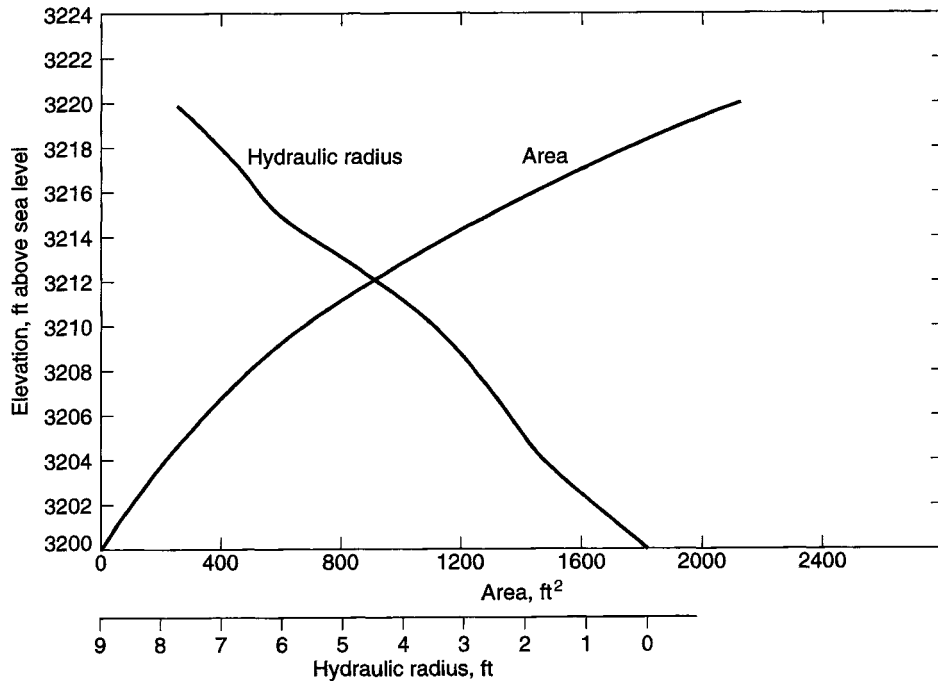


Figure 17.4.14 Information to construct tailwater rating curve for Example 17.4.4.

Solving yields $Z = 3276.1 - y_1 - \frac{621.1}{y_1^2}$. Using equation (5.5.4), we find

$$\frac{y_2}{y_1} = \frac{1}{2} \left(\sqrt{1 + 8F_{r1}^2} - 1 \right) = \frac{1}{2} \left(\sqrt{1 + \frac{8q^2}{gy_1^3}} - 1 \right)$$

$$y_2 = \frac{y_1}{2} \left(\sqrt{1 + \frac{9937.9}{y_1^3}} - 1 \right)$$

From geometry, $y_2 + Z = 3218.2$; then rearranging and substituting the above equation for y_2 gives us

$$Z = 3218.2 - y_2 = 3218.2 - \frac{y_1}{2} \left(\sqrt{1 + \frac{9937.9}{y_1^3}} - 1 \right)$$

Now the above energy and momentum equations can be combined:

$$3276.1 - y_1 - \frac{621.1}{y_1^2} = 3218.2 - \frac{y_1}{2} \left(\sqrt{1 + \frac{9937.9}{y_1^3}} - 1 \right)$$

$$\left(\frac{1242.2}{y_1^3} - \frac{115.8}{y_1} + 3 \right)^2 - \left(1 + \frac{9937.9}{y_1^3} \right) = 0$$

which can be solved to obtain $y_1 = 2.7$, and

$$Z = 3276.1 - 2.7 - \frac{621.1}{(2.7)^2} = 3188.2 \text{ ft}$$

The tailwater rating curve is developed using area–elevation and hydraulic radius–elevation relationships in Figure 17.4.14. Table 17.4.1 presents the tailwater rating curve computations where

$$K = \frac{1.49}{n} AR^{2/3}.$$

The conjugate water depths in the basin for various discharge rates may be determined by equating the energies at cross-sections 0 and 1 (neglecting any losses and setting $Z = 3188.2$ ft):

$$(50 + 21.8) + E_c = y_1 + \frac{V_1^2}{2g}$$

or

$$71.8 + \frac{3}{2} \sqrt{\frac{q^2}{g}} = y_1 + \frac{q^2}{2gy_1^2}$$

to compute y_1 for various values of q . The momentum equation (equation (5.5.4)) is then used to compute y_2 . The resulting water surface level is $y_2 + Z$. Table 17.4.2 provides the computations and

Table 17.4.1 Tailwater Rating Curve (Figure 17.4.15)

El. (ft)	A (ft ²)	R	K	Q (cfs)
3200	0	0	—	—
3204	200	1.65	13,870	849
3207	400	2.5	36,595	2241
3210	660	3.4	74,119	4535
3213	1010	4.9	144,716	8862
3215	1270	6.0	208,275	12,754
3217	1580	6.6	270,112	16,908
3220	2120	7.7	410,577	25,143

$$S = 0.00375, n = 0.03, K = \frac{1.49}{n} AR^{2/3}, Q = K\sqrt{S}.$$

Table 17.4.2 Discharge–Conjugate Depth Curves

Q (cfs)	q	y_c	E_c	$71.8 + E_c$	y_1	V_1	F_{r1}^2	y_2	El. ($y_2 + Z$)
25,000	250	12.47	18.71	90.51	3.34	74.9	52.2	32.5	3220.7
20,000	200	10.75	16.13	87.93	2.70	74.1	63.2	30.0	3218.2
15,000	150	8.87	13.31	85.11	2.05	73.2	81.2	25.1	3213.3
10,000	100	6.77	10.16	81.96	1.39	71.9	115.5	20.4	3203.6
5000	50	4.27	6.40	78.20	0.71	70.4	216.8	14.4	3202.6

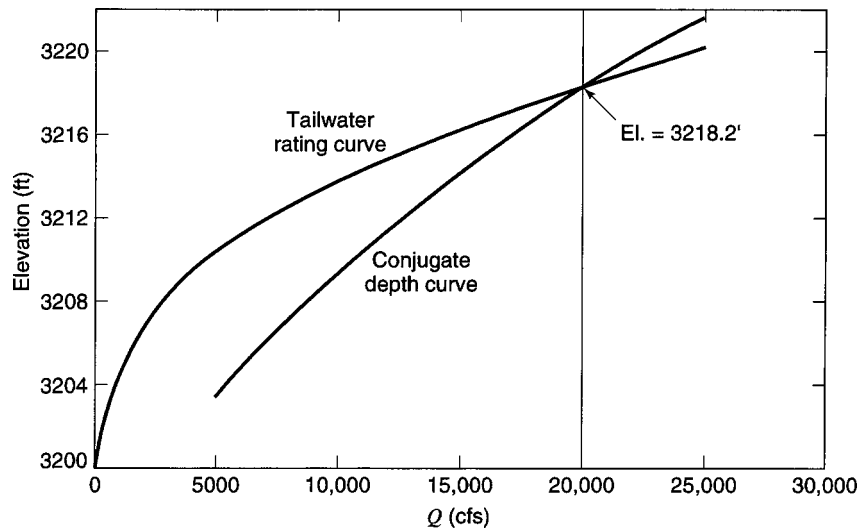


Figure 17.4.15 Tailwater rating and conjugate depth curves for Example 17.4.4.

the results are plotted on Figure 17.4.15 along with the tailwater rating curve. For discharges less than $Q_d = 20,000$ cfs, the tailwater depths are higher than the conjugate depths. Therefore the jump will move upstream and probably be drowned at the toe. This is a safe practice when we are concerned primarily with preventing the jump from sweeping downstream on the unprotected stream bed. The disadvantage would be the loss in efficiency, since the submerged jump does not dissipate as much energy.

EXAMPLE 17.4.5

Design a free-overfall spillway and hydraulic-jump basin to discharge $500 \text{ ft}^3/\text{s}$ with a drop of 12 ft from spillway crest tailwater elevation. The tailwater elevation is 108 ft and the approach channel length is 20 ft. The approach floor is level with the spillway crest, which is at elevation 120 ft. Select an energy dissipator (adapted from U.S. Bureau of Reclamation, 1987).

SOLUTION

Step 1. Select an effective length of the spillway crest as 15 ft, and use $C = 3.0$.

Step 2. The unit discharge is $q = 500/15 = 33.3 \text{ ft}^3/\text{s}$, so the design head is

$$H_e = (q/C)^{2/3} = (33.3/3.0)^{2/3} = 5 \text{ ft.}$$

The reservoir water surface level is then $120 + 5 = 125$ ft, and the drop in elevation from the reservoir level to the tailwater level is 17 ft.

Step 3. An offset of 0.5 ft is provided along each side of the weir to effect side contraction for aerating the underside of the sheet (U.S. Bureau of Reclamation, 1987). The offset is assumed square-cornered. The net crest length is then from equation (17.3.3), adding the offset, $2(0.5)$

$$L' = L + 2K_d H_e + 2(0.5) = 15 + 2(0.2)(5) + 1.0 = 18 \text{ ft}$$

Step 4. Select apron floor elevation. Referring to the notation in Figure 17.3.1, $h_d = 125 - 108 = 17$ ft. Neglecting losses and applying the energy equation at cross-sections before and after the jump, we find $h_d + y_2 = y_1 + V_1^2/2g$. Solve, for h_d in terms of y_1 , y_2 and g with y_1 expressed using equation (5.5.5) with $F_{r2}^2 = q^2/gy_2^3$.

$$h_d = \frac{2q^2}{gy_2^2 \left[\sqrt{1 + \frac{8q^2}{gy_2^3}} - 1 \right]^2} + \frac{y_2}{2} \left(\sqrt{1 + \frac{8q^2}{gy_2^3}} - 1 \right) - y_2$$

Using $h_d = 17$ ft and $q = 33.3 \text{ ft}^3/\text{s/ft}$, we find $y_2 = 8.8$ ft. The apron floor elevation would then be $108 - 8.8 = 99.2$ ft.

Step 5. The drop distance is $Y = 120 - 99.2 = 20.8$ ft, and the drop number is

$$\bar{D} = \frac{q^2}{gY^3} = \frac{(33.3)^2}{32.2(20.8)^3} = 0.0038$$

Using Figure 17.3.1 with $\bar{D} = 0.0038$ yields, the length ratio, $y_2/Y = 0.375$ and then $y_2 = 0.375(20.8) = 7.8$ ft. The elevation of the apron is adjusted to $108 - 7.8 = 100.2$ ft. The adjusted value of Y is $Y = 120 - 100.2 = 19.8$ ft, and $\bar{D} = 0.0044$.

Step 6. From Figure 17.3.1, $\bar{D} = 0.0044$ and $h_d/H_e = 17/5 = 3.4$, $L_d/Y = 1.02$ and $L_d = 20.2$ ft, $y_1/Y = 0.054$ and $y_1 = 0.054(20.8) = 1.1$ ft, and $F_{r1} = 5.3$.

Step 7. For $F_{r1} = 5.3$, $y_1 = 1.1$ ft, and $y_2 = 7.8$ ft, the Type-III basin in Figure 17.4.4 is used. From Figure 17.4.4d, for $F_r = 5.3$, $L/y_2 = 2.37$ and $L = 2.37(7.8) = 18.5$ ft. The length of the basin measured from the vertical crest is $L_d + L = 20.2 + 18.5 = 38.7$ ft.

Step 8. Baffle block heights are approximately $1.5y_1 = 1.5(1.1) = 1.65$ ft (20 in), 14 in wide and spaced at about 28 in center to center.

EXAMPLE 17.4.6

For Example 17.4.5, use an impact block basin instead of a type-III basin.

SOLUTION

Step 1. The critical depth is $y_c = \sqrt[3]{(33.3)^2/32.2} = 3.3$ ft.

Step 2. Using Figure 17.3.1 for $\bar{D} = 0.0044$ and $h_d/H_e = 3.4$, $L_p/Y = 0.85$ and $L_p = 0.85(19.8) = 17.0$ ft.

Step 3. Minimum length of the basin is $L_B = L_p + 2.55y_c = 17.0 + 2.55(3.3) = 25.4$ ft or 26 ft.

Step 4. Minimum tailwater depth is $2.15y_c = 7.1$ ft (from Figure 17.3.1a), which places the floor elevation at 100.9 ft.

Step 5. Distance from the vertical crest to the baffle blocks is $L + 0.8y_c = 17 + 0.8(3.3) = 19.6$ ft or 20 ft.

Step 6. Baffle block height is $0.8y_c = 0.8(3.3) = 2.6$ ft ≈ 3 ft and 18 in wide spaced at 3 ft center to center. The end sill is $0.4y_c = 1.5$ ft high.

Comparing this design with example 17.4.5 shows that the impact basin is considerably smaller than the hydraulic-jump basin. Impact basins should be limited to drop distances of 20 ft or less.

PROBLEMS

17.2.1 Develop a one-page write-up on the June 5, 1976 failure of the Teton Dam in Idaho, USA.

17.2.2 Develop a one-page write-up on the 1963 flood from the Vea Dam in Italy. Describe the cause of the flood wave and its downstream propagation. Also describe the type and size of the dam and the storage capacity behind the dam.

17.2.3 Briefly describe the five largest dams in the world and their spillway structures.

17.3.1 Determine the discharge through an overflow spillway with a design head of 5 m and crest length of 100 m. The distance from the spillway crest elevation to the streambed elevation is 7.5 m and is vertically faced. What is the discharge if the actual head is 4 m and 6 m?

17.3.2 Consider a 75-ft wide overflow spillway with no piers and a design head of 18 ft. The crest elevation of the spillway is 2400 ft and the streambed elevation just upstream of the spillway is 2350 ft. Neglecting approach velocity head determine the rating curve for the spillway.

17.3.3 An ungated overflow spillway has a design discharge of 40,000 cfs. The crest elevation of the spillway has been selected as 1800 ft and the upstream reservoir elevation cannot exceed 1820 ft. Just upstream of the dam the streambed elevation is 1750 ft. Compute the required length of the spillway crest.

17.3.4 Determine the rating curve for the spillway in problem 17.3.3.

17.3.5 Determine the shape of the crest for the spillway in problem 17.3.2.

17.3.6 The net length of a spillway crest is 200 ft. What would be the effective length of the crest adding two round-nosed piers for a head of 7.5 ft? Each pier is 2-ft wide. The abutment coefficient is 0.2.

17.3.7 For the situation in problem 17.3.1 two round-nosed piers, each 0.5 m wide, are being considered just in case a roadway is placed over the spillway. How would this change the effective length of the crest? What would be the discharge for the design head of 5 m and the heads 4 m and 6 m?

17.3.8 Consider a gated-controlled overflow spillway with a length of 25 ft and designed for a head of 8 ft. The gate seats on the crest with $\theta = 90^\circ$. The upstream face of the crest is vertical with the crest elevation at 1000 ft and the elevation of the streambed is 980 ft. Determine the discharge for net gate openings of 2 ft and 3 ft at the design head.

17.3.9 Determine the discharge rating curve for the following ungated overflow spillway. A bridge over the spillway will be supported on round-nosed piers 1.8 m thick, with a maximum span width of 12 m between the center line of the piers. Reservoir and flood data are as follows:

Maximum flood discharge	= 2800 m ³ /sec
Maximum flood pool elevation	= 110 m
Maximum normal pool elevation	= 100 m

Approach channel invert elevation	= 80 m
Downstream channel elevation	= 20 m
Maximum flood tailwater elevation	= 40 m

17.3.10 Determine the geometry for the spillway crest in problem 17.3.1.

17.3.11 Plot the discharge as a function of head H_1 for flow through a Tainter gate mounted atop an ogee spillway, for a gate opening of 5 ft and heads H_1 ranging from 2.0 feet to 10.0 feet. The ogee spillway is designed for a head $H_0 = 7.0$ feet, and the height of the crest above the channel bottom is 15.0 feet.

17.3.12 Design an uncontrolled overflow ogee crest for a spillway to discharge 45,000 cfs. The upstream face of the crest is vertical and a bridge is to span the crest. Bridge piers 24 in wide (pier contraction coefficient = 0.05) with rounded noses are to be provided. The abutment coefficient is 0.10. The bridge spans (center to center of piers) are not to exceed 25 ft. The maximum expected head is 10 ft. Neglect velocity of approach. The design should be based upon economic considerations such that the design head is no less than 75 percent of the maximum head. The distance from the spillway crest to the reservoir bottom at the dam is 40 ft.

17.3.13 A gate-controlled ogee spillway has been designed that uses Tainter gates for control. You have been consulted to determine the head-discharge curves for two different openings of the Tainter gate, for $D = 5$ and 10 ft. The total heads (including the approach velocity) to the bottom of the orifice range from 4 to 18 ft. The upstream face of the crest is vertical with $P = 20$ ft and designed for $H_0 = 12$ ft, $L = 100$ ft. The gate seats on the crest ($\theta = 90^\circ$).

17.3.14 An ogee overflow section is formed to the ideal nappe shape and is 100 ft long. The design head $H_0 = 8$ ft and height of crest above channel bottom = 12 ft. (a) Find the flow rate at the design head. (b) If, under unusual flood conditions, the head becomes 12 ft, find the flow rate. (c) If the head drops to 4.0 ft, find the flow rate. Take the upstream face of the overflow section as vertical and assume no downstream apron interference and downstream submergence.

17.3.15 Complete the water surface profile for the side channel spillway in Example 17.3.3 by computing the depths of flow at stations 150, 100, and 50.

17.3.16 Determine the water surface profile in a side-channel spillway (4-m wide rectangular channel) that has a bottom slope of 0.01 and a Manning's roughness coefficient of 0.016. A 30-m long overflow spillway drains into the side-channel spillway. The overflow spillway ($C = 3.8$) has a head of 1.5 m. Flow passes through critical depth at the end of the channel. What is the depth of the side-channel spillway below the crest of the overflow spillway to prevent submergence effects of the flow in the side-channel spillway?

17.3.17 Rework example 17.3.4 for a maximum surcharge head of 5 ft.

17.3.18 Rework example 17.3.4 for a maximum discharge of 2500 cfs.

17.3.19 Determine the head on the crest-discharge curve for a morning glory spillway with a crest radius of 7.0 ft, considering both crest control and throat control. The morning glory spillway was designed for a maximum surcharge head of 10 ft and to limit the outflow to 2000 cfs. Assume a coefficient of 3.75 for $H_e/R_s = 0.3$. Elevation of throat transition is 90 ft.

Crest elevation = 100 ft
 Maximum water surface elevation = 110 ft
 Throat radius = 4.5 ft
 Circular conduit diameter = 9.0 ft

Consider heads (on the crest) of 2, 3, 4, and 6 ft. Which of the elevations have crest control and which ones have throat control?

17.3.20 Rework example 17.3.5 with a discharge of 2500 ft³/s.

17.3.21 Design a baffle chute spillway for a maximum expected discharge of 5000 ft³/s.

17.4.1 A type-I stilling basin is being considered, as the energy dissipator, for an overflow spillway. Estimate the length of the concrete apron ($S_0 = 0.001$) for a design discharge of 7500 cfs. The apron elevation is 1980 ft. The spillway crest is 100 ft long at an elevation of 2000 ft. Use a Manning's roughness factor of $n = 0.025$. Should a type-I basin be used for this situation based upon the information available? If not, what type of basin should be used and show justification for your choice?

17.4.2 A U.S.B.R. type-III stilling basin (rectangular and horizontal with a uniform width of 40 ft) is used. The spillway discharges 400 cfs and the velocity of the flow at the point where water enters the basin is 30 ft/s. Compute (a) the sequent depth of the hydraulic jump, (b) the energy loss in the jump, (c) the length of the jump, (d) the specific energies before and after the jump, and (e) the ratio of the specific energy after the jump divided by the specific energy before the jump.

17.4.3 You have designed a spillway for 25 m³/s discharge. The outlet velocity is 16 m/s at a depth of 0.25 m. Select the type of stilling basin and determine the sequent depth, the length of the jump, and the energy loss through the jump.

17.4.4 Select the type of stilling basin for the following ogee spillway section (refer to Figure P17.4.4), designed for $H_0 = 10.00$ ft; crest length of spillway = 100 ft, slope = 0.001. What length L of stilling basin selected will be required? Assume $n = 0.025$.



Figure P17.4.4 Ogee spillway section for Problem 17.4.4.

17.4.5 Rework example 17.4.1 using a discharge of 2000 ft³/s.

17.4.6 Rework example 17.4.2 using a discharge of 7500 ft³/s.

17.4.7 Rework example 17.4.3 using a discharge of 10,000 ft³/s.

17.4.8 Rework example 17.4.4 using a discharge of 30,000 ft³/s.

17.4.9 You have been consulted to design a spillway and energy dissipator (hydraulic-jump-type stilling basin) for a low water dam to be placed at cross-section I of the Red Fox River (Figure 5.4.3). The discharge rating curve is given in Figure P17.4.9. A roadway will be placed across the low-water dam at an elevation of 5735 ft. You are to use a design discharge of 12,000 cfs with an overflow spillway crest elevation at 5725 ft, using a design head that is 85 percent of the maximum head. The maximum water surface elevation of the upstream impoundment (reservoir) will be 4 ft below the surface of the roadway. Upstream face of the spillway is sloped (1:3). Because of the roadway you are going to use piers for the spillway section of the road. Round-nosed bridge piers are to be used that are 24 in wide. Bridge spans (center to center of piers) are not to exceed 38 ft, or from center of pier to abutment walls are not to exceed 35 ft. Your job is to design the spillway, the energy dissipator including the type, the dimensions, and the floor elevation.

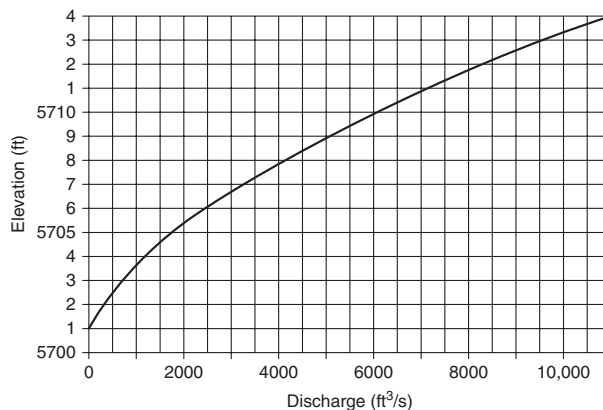


Figure P17.4.9 Discharge rating curve for cross section I (U.S. Bureau of Reclamation, 1957).

17.4.10 Compute the conjugate depth elevation curve for your design in problem 17.4.9 and graphically compare it to the discharge rating curve in Figure P17.4.9.

17.4.11 A type-I stilling basin is being considered, as the energy dissipator, for an overflow spillway. Estimate the length of the concrete apron ($S_0 = 0.001$) for a design discharge of 7,500 cfs. The spillway crest is 100 ft long at an elevation 14 ft above the basin apron. Use a Manning's roughness factor of $n = 0.025$. Should a type-I basin be used for this situation based upon the information available? If not, what type of basin should be used? Show justification for your choice.

17.4.12 Rework example 17.4.5 using a spillway crest length of 20 ft.

REFERENCES

- Coleman, H. W., C. Y. Wei, and J. E. Lindell, "Hydraulic Design of Spillways," in *Hydraulic Design Handbook* edited by L.W. Mays, McGraw-Hill, New York, 1999.
- Institution of Civil Engineers, *Floods and Reservoir Safety: An Engineering Guide*, London, 1978.
- Kindsvater, C. E., "The Hydraulic-Jump in Sloping Channels," *Transactions ASCE*, vol. 109, p. 1107, 1944.
- Linsley, R. K., J. B. Franzini, D. L. Freyberg, and G. Tchobanoglous, *Water Resources Engineering*, 4th edition, McGraw-Hill, New York, 1992.
- Mays, L. W., (editor-in-chief), *Hydraulic Design Handbook*, McGraw-Hill, New York, 1999.
- National Research Council (NRC), Committee on Safety Criteria of Existing Dams, *Safety of Existing Dams: Evaluation and Improvement*, National Academy Press, Washington, DC, 1983.
- National Research Council (NRC), Committee on Safety Criteria for Dams, *Safety of Dams: Flood and Earthquake Criteria*, National Academy Press, Washington, DC, 1985.
- Peterka, A. J., *Hydraulic Design of Spillways and Energy Dissipators*, U.S. Bureau of Reclamation, 1964. (University Press of the Pacific, 2005.)
- U.S. Army Corps of Engineers, *Report of the Chief of Engineers to the Secretary of the Army on the National Program of Inspection of Non-Federal Dams*, Washington, DC, 1982.
- U.S. Army Corps of Engineers, *Inflow Design Floods for Dams and Reservoirs*, Engineering Regulation 1110-8-2, 1991.
- U.S. Bureau of Reclamation, *Guide for Computing Water Surface Profiles*, 1957.
- U.S. Bureau of Reclamation, *Design of Small Dams*, 3rd edition, U. S. Government Printing Office, Washington, DC, 1987.
- Wei, C. Y., and J. E. Lindell, "Hydraulic Design of Stilling Basins and Energy Dissipators," in *Hydraulic Design Handbook* edited by L.W. Mays, McGraw-Hill, New York, 1999.

Chapter 18

Sedimentation and Erosion Hydraulics

18.0 INTRODUCTION

This chapter provides an introduction to the concepts of sedimentation and erosion and scour hydraulics. Sediment transport deals with the interrelationship between flowing water and sediment particles. Erosion is the displacement of soil particles caused by water or wind action. Our particular interest in this chapter is to describe the concepts related to river engineering. Many of the concepts are also of particular interest in drainage design, sand and gravel mining, watercourse stabilization, bridge scour and protection, and many others. Figures 18.0.1a–f illustrate sedimentation and scour in the Agua Fria River near Phoenix, Arizona. Figure 18.0.2 shows low flow in Chinle Wash in northern Arizona. Figure 18.0.3 shows the results of flow around a bend in a wash in northwestern New Mexico.

To quote Garcia (1999):

Since the beginning of mankind, sedimentation processes have affected water supplies, irrigation, agricultural practices, flood control, river migration, hydroelectric projects, navigation, fisheries, and aquatic habitat. In the last few years, sediment also has been found to play an important role in the transport and fate of pollutants; thus sedimentation control has become an important issue in water quality management.

Approximately 84 percent of the over 575,000 bridges in the National Bridge Inventory (NBI) are built over streams, with a large proportion of these bridges spanning alluvial streams that are continually adjusting their streambeds and stream banks. Many of these bridges will experience problems with scour and bank erosion during the life of the structure. The magnitude of these problems is on the order of average annual repair costs of approximately \$50 million for highways on the Federal aid system (Lagasse et al., 2001a, b). Bridge failure is most commonly caused by floods, with the most common cause of flood damage to bridges being the scouring of bridge foundations.

In 1985 in Pennsylvania, Virginia, and West Virginia, floods destroyed 73 bridges. During the spring floods of 1987 in New York and New England, 17 bridges were either destroyed or damaged by scour. The 1993 flood in the upper Mississippi basin caused 23 bridge failures with estimated damages of \$15 million. The failure modes included 14 from abutment scour, two from pier scour only, three from pier and abutment scour, two from lateral bank migration, one from debris load, and one from unknown scour (Richardson and Davis, 2001). In 1994, flooding in Georgia due to storm Alberto resulted in damage to over 500 state and locally owned bridges caused by scour, with approximately \$130 million in damages to the highway system.



(a)



(b)



(c)



(d)



(e)



(f)

Figure 18.0.1 (a) The Agua Fria River channel is comprised mainly of very fine sediments that have been largely transported from upstream. Looking upstream. [Location: About 0.7 mi from Gila Confluence; photograph by Carlos Carriaga: October, 1991]. (b) The Agua Fria River channel is comprised mainly of very fine sediments that have been largely transported from upstream. Looking downstream. [Location: About 0.7 mi from Gila Confluence; photograph by Carlos Carriaga: October, 1991]. (c) The concrete weir running across the Agua Fria River channel. [Location: 0.4 mi north of Buckeye Road; photograph by Carlos Carriaga: October, 1991]. (d) Downstream of the concrete weir is heavily scoured from 2 to 2.5 ft deep after four months. [Location: About 0.4 mi north of Buckeye Road; photograph by Carlos Carriaga: February 22, 1992]. (e) The Van Buren bridge crossing the Agua Fria River channel. [Location: About 0.15 mi south of Van Buren bridge; mi designation: 4.759; photograph by Carlos Carriaga: February 22, 1992]. (f) The side levee that runs from Lower Buckeye Road to Indian School Road. As shown, the in-stream power lines are also protected by levees. [Location: 0.1 mi north of McDowell Road; photograph by Carlos Carriaga: May, 1992].



Figure 18.0.2 Chinle Wash in northern Arizona. (Photograph by L. W. Mays)



Figure 18.0.3 Results of flow around a bend in a wash in northwestern New Mexico. (Photograph by L. W. Mays)

Section 18.1 describes the properties of sediments, which include parameters that are used in the sediment transport relations described in Sections 18.2 through 18.6. Section 18.7 describes watershed sediment yield; Section 18.8 describes reservoir sedimentation; Section 18.9 describes stream stability at highway structures; and Section 18.10 is a fairly detailed description of bridge scour, also including pier and abutment scour.

The discussions in Sections 18.9 and 18.10 are based upon the following U.S. Department of Transportation Federal Highway Administration Hydraulic Engineering Circulars (HEC):

HEC-18 Evaluating Scour at Bridges (Richardson and Davis, 2001)

HEC-20 Stream Stability at Highways (Lagasse et al., 2001a)

HEC-23 Bridges Scour and Stream Instability Countermeasures (Lagasse et al., 2001b)

The flow chart in Figure 18.0.4 illustrates the interrelationship between these three documents and emphasizes that they should be used as a set. Another document of interest is the River Engineering for Highway Encroachments, Hydraulic Design Series (HDS) No. 6 (Richardson et al., 2001). All four of these documents (HEC-18, HEC-20, HEC-23, and HDS-6) can be obtained on the Web at <http://www.fhwa.dot.gov/bridge/hydpub.htm>.

18.1 PROPERTIES OF SEDIMENT

18.1.1 Size and Shape

Grain size is the most important property affecting transportability of sediment. Table 18.1.1 shows the size classification of sediment particles with their corresponding units in millimeters as well as inches, used in the computer code HEC-6 developed by the U.S. Army Corps of Engineers (1991), Hydrologic Engineering Center.

Natural sediments are of irregular shape and therefore any single diameter used to characterize a certain group of grains must be chosen according to some convenient method of measurement. The usually adopted diameters are:

- a. **Triaxial diameters** (a , b , and c): These sizes represent the major, intermediate, and minor dimensions of the particle measured along mutually perpendicular axes.

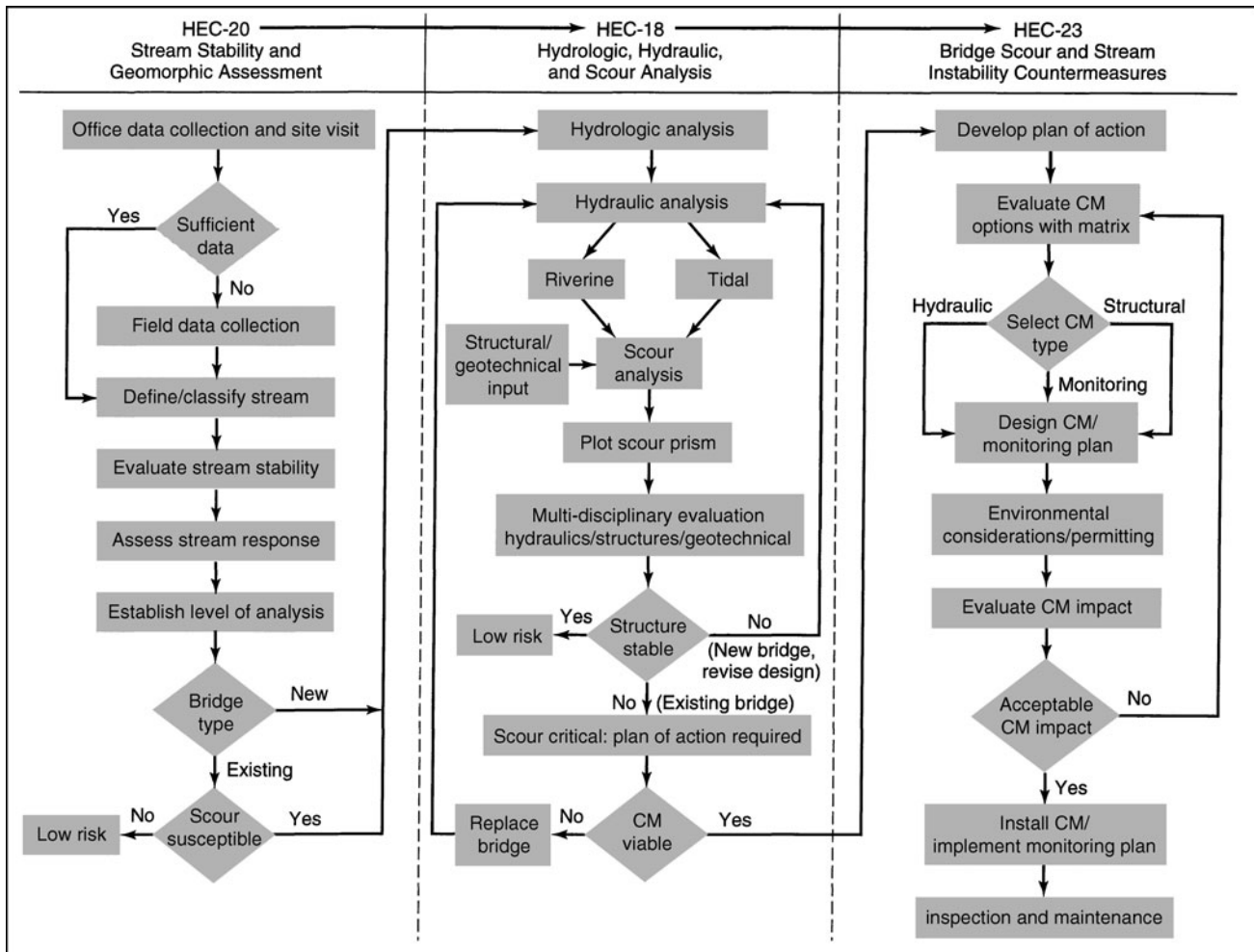


Figure 18.0.4 Flow chart for scour and stream stability analysis and evaluation (Lagasse et al., 2001a, b).

- b. Sieve diameter (D):** This size indicates the size of the sieve opening through which the particle will just pass.
- c. Sedimentation diameter (D_s):** This size represents the diameter of a sphere of the same specific weight and fall velocity as the given particle in the same sedimentation fluid with the same temperature. This is also called the *fall diameter*.
- d. Nominal diameter (D_n):** This represents the diameter of a sphere having the same volume as the given particle.
- e. Geometric mean diameter (D_g):** This is the square root of the product of the maximum and minimum size limits in a range. For example, a very coarse sand with size range of 1.00–2.00 mm has a geometric mean of 1.414 mm (i.e., $(1 \cdot 2)^{1/2}$). Table 18.1.1 lists the geometric mean diameters (D_g) that correspond to the grain size classification adopted by the U.S. Army Corps of Engineers (1991).
- f. Mean diameter (D_m):** This size is the representative grain size computed from the relation:

$$D_m = (p_1 D_1 + p_2 D_2 + \dots + p_n D_n) / (p_1 + p_2 + \dots + p_n) \quad (18.1.1)$$

where p_1, p_2, \dots, p_n are the grain size fractions associated with size classifications 1, 2, \dots , n and D_1, D_2, \dots, D_n are the average diameters for size classifications 1, 2, \dots , n .

Table 18.1.1 Scale for Size Classification of Sediment Particles (USACE, 1991)

Class name	Millimeters	Feet	PHI Value
Boulders	> 256	–	< –8
Cobbles	256–64	–	–8 to –6
Very Coarse Gravel (VCG)	64–32	.148596	–6 to –5
Coarse Gravel (CG)	32–16	.074216	–5 to –4
Medium Gravel (MG)	16–8	.037120	–4 to –3
Fine Gravel (FG)	8–4	.018560	–3 to –2
Very Fine Gravel (VFG)	4–2	.009279	–2 to –1
Very Coarse Sand (VCS)	2.0–1.0	.004639	–1 to 0
Coarse Sand (CS)	1.0–0.50	.002319	0 to +1
Medium Sand (MS)	0.50–0.25	.001160	+1 to +2
Fine Sand (FS)	0.25–0.125	.000580	+2 to +3
Very Fine Sand (VFS)	0.125–0.0625	.00288	+3 to +4
Coarse Silt	0.0625–0.031	.000144	+4 to +5
Medium Silt	0.031–0.016	.000072	+5 to +6
Fine Silt	0.016–0.008	.000036	+6 to +7
Very Fine Silt	0.008–0.004	.000018	+7 to +8
Coarse Clay	0.004–0.0020	.000009	+8 to +9
Medium Clay	0.0020–0.0010	–	+9 to +10
Fine Clay	0.0010–0.0005	–	+10 to +11
Very Fine Clay	0.0005–0.00024	–	+11 to +12
Colloids	< 0.00024	–	> +12

g. Median diameter (D_{50}): This diameter corresponds to the 50 percent finer by weight (or by volume) in the size distribution curve called the *gradation curve*. In general, D_p is used to indicate that p percent (by weight or by volume) of the sample has a diameter smaller than D_p .

18.1.2 Measurement of Size Distribution

Size determination by means of sieving can in principle be used for particles as small as 50 μm , but gives good results for particles down to 75 μm (sand fraction). Sieve sizes (openings) are made in a geometric series with every sieve being $(2)^{1/4}$ larger in size than the preceding. Taking every other sieve gives a $(2)^{1/2}$ series, whereas taking every fourth gives a ratio of 2 between adjacent sieve sizes. When the sand is fairly uniform (i.e., σ_g is fairly small), the $(2)^{1/4}$ series should be used.

18.1.3 Settling Analysis for Finer Particles

18.1.3.1 Grain Size Distribution

By means of sieving, a grain size distribution of the bed-material sample can be obtained, which generally shows a relation between percentages by weight versus grain size, called the *gradation curve*. Figure 18.1.1 shows an example of a gradation curve. The cumulative size distribution of most samples can be approximated by a log-normal distribution, so by using logarithmic probability scale, a more or less straight line is found. For an approximately log-normal distribution, the *geometric mean diameter* can be defined as:

$$D_g = (D_{84} * D_{16})^{1/2} \quad (18.1.2)$$

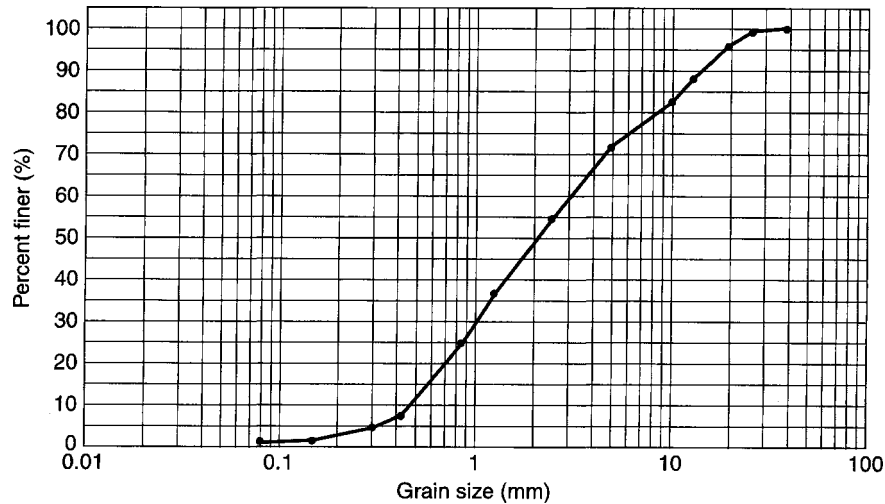


Figure 18.1.1 Gradation curve for the soil aggregates analyzed in Example 18.1.1.

where D_{84} and D_{16} are the diameters that indicate that 84 percent and 16 percent by weight of the sample has a diameter smaller than D_{84} and D_{16} , respectively. D_g for a log-normal distribution is equal to D_{50} .

The *geometric standard deviation*, σ_g , associated with D_g can be determined as follows:

$$\sigma_g = \frac{1}{2} [D_{84}/D_g + D_g/D_{16}] \quad (18.1.3)$$

For log-normal grain size distribution, the mean diameter, D_m , is determined as follows:

$$D_m = D_g \exp[0.5 \ln \sigma_g^2] \quad (18.1.4)$$

In geological literature, the diameters are often expressed in Φ -units, where $\Phi = -\log 2D_{50}$ (with D_{50} expressed in mm), $\Phi = 0$ for $D_{50} = 1$ mm, and $\Phi = 1$ for $D_{50} = 0.5$ mm.

EXAMPLE 18.1.1

Use the sieve analysis data in columns (1) and (2) of Table 18.1.2 to develop a gradation curve.

SOLUTION

Column (3) in Table 18.1.2 lists the percent of material retained. Column (4) lists the percent of material finer. For example, 1.5 in (37.5 mm) is the largest size so that 100 percent of the material is finer. The resulting gradation curve is plotted in Figure 18.1.1.

18.1.3.2 Particle Shape

In addition to the diameter of the grain particles, their shape and roundness is also important. *Shape* describes the form of the particle without reference to the sharpness of its edges, whereas *roundness* depends on the sharpness or radius of curvature of the edges. For example, a flat particle will have a smaller fall velocity than a sphere, but bed load will be more difficult to transport. Several definitions are used to characterize the shape:

- a. **Sphericity:** The ratio of the surface area of a sphere with the same volume as the particle, to the surface area of that particle.
- b. **Roundness:** The ratio of the average radius of curvature of the edges, to the radius of a circle that can be inscribed within the maximum projected area of the particle.

Table 18.1.2 Sieve Analysis Data for Example 18.1.1

(1) Sieve size (mm)	(2) Weight of material retained (lbs)	(3) % material retained	(4) % material finer
1.5" (37.5 mm)	0.00	0.00	100.00
1.0" (25.0 mm)	0.25	0.83	99.17
0.75" (19.0 mm)	1.00	3.30	95.87
0.50" (12.5 mm)	2.25	7.44	88.43
0.375" (9.5 mm)	1.75	5.78	82.65
0.25" (4.75 mm)	3.25	10.74	71.91
No. 8 (2.36 mm)	5.20	17.19	54.72
No. 16 (1.20 mm)	5.35	17.68	37.04
No. 20 (0.84 mm)	3.50	11.57	25.47
No. 40 (0.42 mm)	5.45	18.02	7.45
No. 50 (0.30 mm)	0.85	2.81	4.64
No. 100 (0.15 mm)	0.90	2.98	1.55
No. 200 (0.08 mm)	0.25	0.83	0.83
Pan	0.25	0.83	0.00
Total	30.25 lbs	100.00%	

c. Shape factor: $S.F. = c/(ab)^{1/2}$ with a, b, and c being the major, intermediate, and minor dimensions of the particle measured along mutually perpendicular axes. For spheres, $S.F. = 1$; for natural sands, $S.F. \sim 0.7$. Because sphericity and roughness are difficult to determine in practice, the shape factor does have practical application. As an example, the fall velocity of a particle can be expressed in terms of the nominal diameter, shape factor, and Reynolds number.

18.1.4 Fall Velocity

Fall velocity (or *settling velocity*) is the velocity at which a sediment particle falls through a fluid. This velocity reflects the particle size, shape, and weight, as well as the fluid characteristics. Consider a sphere of diameter D that is released at zero velocity in a quiescent fluid (water). As the fall velocity W increases, fluid resistance reduces the acceleration to an equilibrium. At equilibrium, the gravity force is in balance with the drag force and a *terminal velocity* W_T exists.

Relationships for the fall velocity can be developed using the impulse-momentum principle:

$$\sum F_y = \frac{d}{dt} \int_{CV} v_y \rho dV + \sum_{CS} v_y (\rho V \cdot A) \quad (3.5.7)$$

Referring to Figure 18.1.2, the forces are the gravity force, F_g , the buoyant force, F_B , and the resistance or drag force, F_D .

$$\sum F_y = F_g - F_D - F_B \quad (18.1.5)$$

The gravity force is expressed as

$$F_g = \left(\frac{\pi}{6} D^3\right) \gamma_s \quad (18.1.6)$$

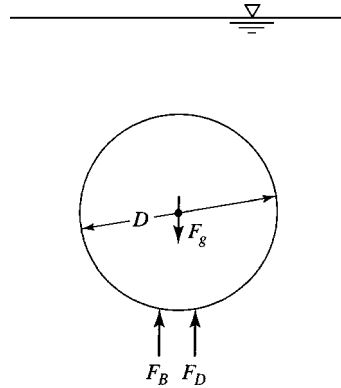


Figure 18.1.2 Fall velocity.

where $(\frac{\pi}{6}D^3)$ is the volume of the sphere and γ_s is the specific weight of the sphere. The buoyant force is due to the displaced fluid (see Section 3.6.2).

$$F_B = \frac{\pi}{6}D^3\gamma \tag{18.1.7}$$

where γ is the specific weight of water. The drag (resistance) force is

$$F_D = C_D\left(\frac{\pi}{4}D^2\right)\rho\frac{W^2}{2} \tag{18.1.8}$$

where C_D is the *drag coefficient*, which is a function of the Reynolds number for a sphere (see Figure 18.1.3). C_D is the ratio of drag per unit area $(\frac{\pi}{4}D^2)$ to the dynamic pressure

$$C_D = \left[F_D / \left(\frac{\pi}{4}D^2 \right) \right] / \left(\frac{1}{2}\rho W^2 \right).$$

The change of momentum in the control volume is $\sum_{CS} v_y(\rho V \cdot A) = 0$ and the net rate of momentum outflow is

$$\frac{d}{dt} \int_{CV} v_y \rho dV = \rho_s \left(\frac{\pi}{6}D^3 \right) \frac{dW}{dt} \tag{18.1.9}$$

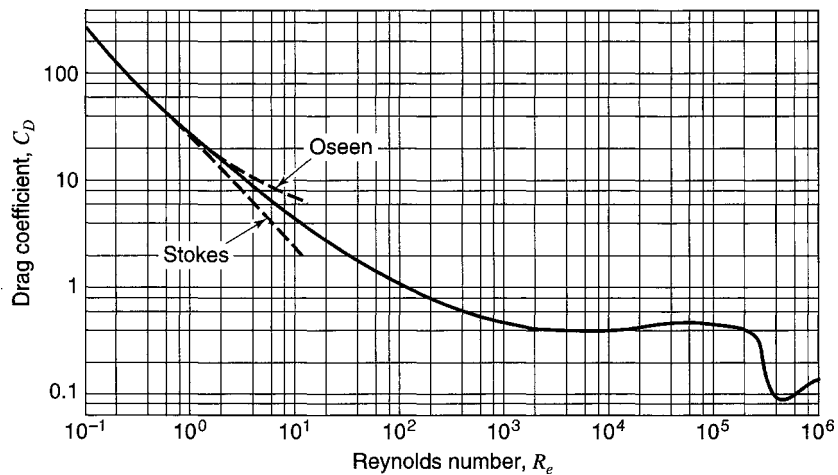


Figure 18.1.3 Drag coefficient of spheres as a function of Reynolds number (Vanoni, 1975).

The momentum equation is derived by substituting equations (18.1.5) through (18.1.9) into (3.5.7) to derive

$$\left(\frac{\pi}{6}D^3\right)\gamma_s - \left(\frac{\pi}{6}D^3\right)\gamma - C_D\left(\frac{\pi}{4}D^2\right)\rho\frac{W^2}{2} = \rho_s\left(\frac{\pi}{6}D^3\right)\frac{dW}{dt} \quad (18.1.10)$$

Because of the complex nature of the relationship between C_D and the Reynolds number, equation (18.1.10) cannot be directly integrated. The Reynolds number can be expressed as follows:

$$R_e = \frac{WD}{\nu} \quad (18.1.11)$$

For the range of $R_e < 1$, *Stokes' Law* is expressed as

$$C_D = \frac{24}{R_e} \quad (18.1.12)$$

We may then substitute equation (18.1.11) into equation (18.1.12) and use the resulting C_D in equation (18.1.8):

$$\begin{aligned} F_D &= C_D\left(\frac{\pi}{4}D^2\right)\rho\frac{W^2}{2} \\ &= \left(\frac{24}{\frac{WD}{\nu}}\right)\left(\frac{\pi}{4}D^2\right)\rho\frac{W^2}{2} \\ &= 3\pi\rho\nu WD \end{aligned} \quad (18.1.13)$$

which is referred to as *Stokes' equation*.

An equation for the fall velocity for $R_e < 1$ can be derived by substituting equation (18.1.13) to replace $C_D\left(\frac{\pi}{4}D^2\right)\rho\frac{W^2}{2}$ in equation (18.1.10), then integrating to derive

$$W = \frac{D^2g}{18\nu}\left(\frac{\rho_s}{\rho} - 1\right)\left\{1 - \exp\left[\frac{-18\nu t}{(\rho_s/\rho)D^2}\right]\right\} \quad (18.1.14)$$

When $t \rightarrow \infty$, this fall velocity is the terminal velocity:

$$W_T = \frac{D^2g}{18\nu}\left(\frac{\rho_s}{\rho} - 1\right) \quad (18.1.15a)$$

or

$$W_T = \frac{D^2g}{18\nu}\left(\frac{\rho_s - \rho}{\mu}\right) \quad (18.1.15b)$$

Figure 18.1.4 illustrates the fall velocity as a function of time for equations (18.1.14) and (18.1.15).

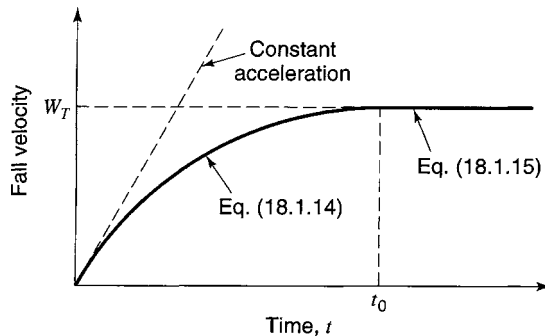


Figure 18.1.4 Velocity versus function of time.

Alternatively, we could have used equation (18.1.10) with $dW/dt = 0$ to derive the fall velocity as

$$\left(\frac{\pi}{6}D^3\right)\gamma_s - \left(\frac{\pi}{6}D^3\right)\gamma - C_D\left(\frac{\pi}{4}D^2\right)\rho\frac{W_T^2}{2} = 0 \quad (18.1.16)$$

Solving for W_T :

$$W_T = \left[\frac{4}{3}\frac{D}{C_D}\left(\frac{\rho_s}{\rho} - 1\right)g\right]^{1/2} \quad (18.1.17)$$

Sediment particles are somewhat less than spherical, and for a given diameter, based on a sieve analysis, they usually have a fall velocity a little less than that of a sphere of the same diameter. Generally speaking, Stokes' Law is applicable to gravity particles in the silt and clay-size range falling in water. Because of the very small velocity of silt and clay, they are usually not found in appreciable quantities in streambeds. They are typically referred to as *wash load* because these fine materials tend to wash on through the system.

There are actually two types of drag:

1. *form drag*, which is due to pressure differences between the front and back of the particle, and
2. *surface drag*, which is due to friction along the surface of the particle.

The two types of forces are the *inertia forces* and the *viscous forces*. Stokes' Law, which is for $Re < 1$, ignores inertia forces. The Oseen (1927) approximation for C_D is:

$$C_D = \frac{24}{Re} \left(1 + \frac{3}{16}Re\right) \quad (18.1.18)$$

and the Goldstein (1929) approximation ($Re \leq 2$) is:

$$C_D = \frac{24}{Re} \left(1 + \frac{3}{16}Re - \frac{19}{1280}Re^2 + \frac{71}{20,480}Re^3 + \dots\right) \quad (18.1.19)$$

Refer to Figure 18.1.3 for the drag coefficient as a function of Reynolds number.

When a number of particles are dispersed in a fluid, the fall velocity will differ from that of a single particle because of the mutual interference of the particles. If only a few closely spaced particles are in suspension, they will fall in a group with a velocity that is higher than that of a particle falling alone. On the other hand, if particles are dispersed throughout the fluid, the interference between neighboring particles will tend to reduce the fall velocity. Many investigators have studied the influence of the concentration on the fall velocity.

EXAMPLE 18.1.2

Given a sample of sand with mean particle size of 0.1 mm and density equal to 2.70 g/cm³, compute terminal fall velocity.

SOLUTION

Using equation (18.1.15a), where $D = 0.1 \text{ mm} = 0.0001 \text{ m}$, $\rho = 1.0$, $\rho_s = 2.7$, $\nu = 1.0 \times 10^{-6} \text{ m}^2/\text{s}$, and $g = 9.81 \text{ m/s}^2$, solve for W_T :

$$\begin{aligned} W_T &= \frac{D^2 g}{18\nu} \left(\frac{\rho_s}{\rho} - 1\right) \\ &= \frac{(0.10 \times 10^{-3})^2 \text{ m}^2 \times 9.81 \text{ m/s}^2}{18 \times 1.0 \times 10^{-6} \text{ m}^2/\text{s}} \left(\frac{2.70}{1.00} - 1\right) \\ &= 0.0093 \text{ m/s} \\ &= 9.3 \times 10^{-3} \text{ m/s} \end{aligned}$$

The fall velocity is 6.875 mm/s.

18.1.5 Density

Practically all sediments have their origin in rock material and, hence, all constituents of the parent material usually can be found in sediments. For example, fragments of the parent rock are found in boulders and gravels, quartz in sands, silicas in silt, and feldspars and micas in clays. The density of most sediment smaller than 4 mm is $2,650 \text{ kg/m}^3$ (specific gravity, $s = 2.65$). The density of clay minerals ranges from $2,500$ to $2,700 \text{ kg/m}^3$.

18.1.6 Other Important Relations

a. Relative Density, Δ

$$\Delta = (\rho_s - \rho) / \rho \quad (18.1.20)$$

where ρ_s is the density of sediment and ρ is the density of water.

b. Specific weight of submerged solid particles, γ'_s

$$\gamma'_s = (\gamma_s - \gamma) \quad (18.1.21)$$

where γ_s is the specific weight of sediment particles, lb/ft^3 , and γ is the specific weight of water, lb/ft^3 .

c. Grain Reynolds number, R_{NS}

$$R_{NS} = WD_N / \nu \quad (18.1.22)$$

where D_N is the nominal sediment diameter, ft, and W is the fall velocity associated with D_N , ft/s.

d. Sedimentation parameter

$$G = (\rho \nu^2) (\gamma'_s D_N^3) \quad (18.1.23)$$

where ν is the kinematic viscosity, ft^2/s (or m^2/s); D_N is nominal diameter of the grain, ft (or m); and γ'_s is the specific weight of the submerged sediment, lb/ft^3 (or N/m^3).

e. Porosity, n

$$n = V_v / V \quad (18.1.24)$$

where V_v is the volume of voids and V is the volume of sediment.

18.2 BED FORMS AND FLOW RESISTANCE

18.2.1 Bed Forms

Free surface flow over erodible sand beds generates a variety of different bed forms and bed configurations. The type and dimensions of a bed form depends on the properties of the flow, fluid, and bed material. Table 18.2.1 is a summary description of bed forms and configurations affecting alluvial channel roughness. Figure 18.2.1 shows bed forms arranged in increasing order of sediment transport rate. Because there is a strong relationship among the flow resistance, the bed configuration, and the rate of sediment transport, it is important to know the conditions under which different bed forms exist. Figure 18.2.2 shows bed form charts from Vanoni (1974) for flow depths up to 10 ft (3 m) and also between 100 and 600 μm . Bed forms are typically classified into a *lower regime* for subcritical flow, and an *upper regime* for supercritical flow, with a transition zone close to critical flow. The bed forms associated with these flow regimes are as follows:

1. Lower regime

- ripples
- dunes

Table 18.2.1 Summary Description of Bed Forms and Configurations Affecting Alluvial Channel Roughness [Material Taken from ASCE (1966) Task Force on Bed Forms]

Bed form or configuration (1)	Dimensions (2)	Shape (3)	Behavior and occurrence (4)
Ripples	Wavelength less than approx 1 ft; height less than approx 0.1 ft	Roughly triangular in profile, with gentle, slightly convex upstream slopes and downstream slopes nearly equal to the angle of repose. Generally short-crested and three-dimensional	Move downstream with velocity much less than that of the flow. Generally do not occur in sediments coarser than about 0.6 mm
Bars	Lengths comparable to the channel width. Height comparable to mean flow depth	Profile similar to ripples. Plan form variable	Four types of bars are distinguished: (1) Point, (2) Alternating, (3) Transverse, and (4) Tributary. Ripples may occur on upstream slopes
Dunes	Wavelength and height greater than ripples but less than bars	Similar to ripples	Upstream slopes of dunes may be covered with ripples. Dunes migrate downstream in manner similar to ripples
Transition	Vary widely	Vary widely	A configuration consisting of a heterogeneous array of bed forms, primarily low-amplitude ripples and dunes interspersed with flat regions
Flat bed	–	–	A bed surface devoid of bed forms. May not occur for some ranges of depth and sand size
Antidunes	Wave length = $2\pi v^2/g$ (approx); ^a height depends on depth and velocity of flow	Nearly sinusoidal in profile. Crest length comparable to wavelength	In phase with and strongly interact with gravity water-surface waves. May move upstream, downstream, or remain stationary, depending on properties of flow and sediment.

Reported by Kennedy (1969)

Source: Vanoni (1975).

2. Transition zone
 - bed configurations range from dunes to antidunes
3. Upper flow regions
 - plane bed with sediment movement
 - antidunes
 - breaking antidunes
 - standing waves
 - chutes and pools

Factors that affect bed forms and resistance to flow include water depth, slope, fluid density, fine material concentration, bed-material size, bed-material gradation, fall velocity of sediment particles, channel cross-sectional shape, seepage force, and others. Refer to Simons and Senturk (1977) and Yang (1996) for further discussion.

18.2.2 Sediment Transport Definitions

Table 18.2.2 provides the various sediment transport definitions. Finer materials such as silts and clays can be transported very easily once they enter a channel and are washed through with only trace amounts left in the bed. As a result, sediment transport equations do not apply. The so-called *wash*

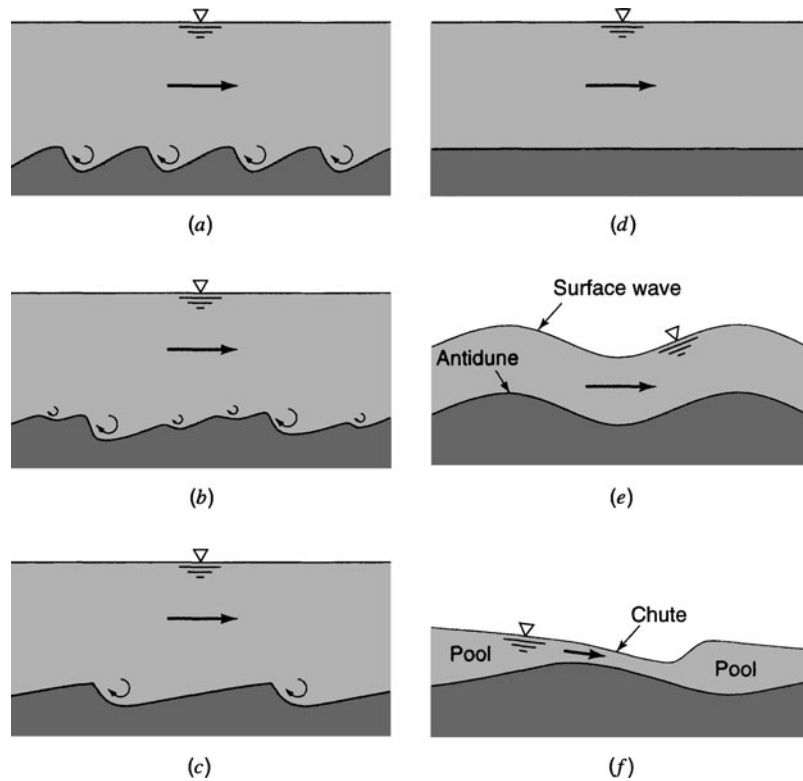


Figure 18.2.1 Bed forms arranged in increasing order of sediment transport rate. Flow increases consecutively from *a* to *f*. (*a*) Ripples; (*b*) Dunes and ripples; (*c*) Dunes; (*d*) Flat bed; (*e*) Antidune and surface waves; (*f*) Chutes and pools (from Vanoni, 1975).

load is that part of the total suspended load that is finer than the bed material. The transport of larger size materials found in the bed material is called the *bed-material load*. *Total load* is the wash load and the bed-material load combined. Under conditions when wash load is not present, bed material and total load are used interchangeably. Bed material is generally expressed on a weight of sediment per unit time tons/day in U.S. customary units (or N/s in SI units).

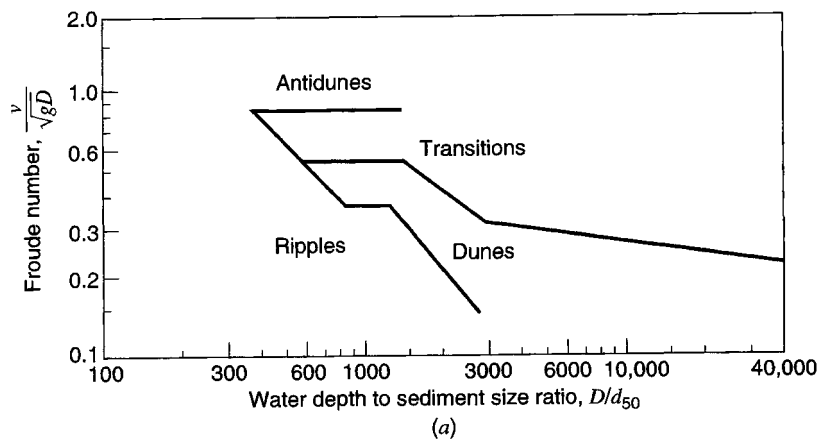


Figure 18.2.2 (*a*) Bed form chart for fine sand ($d_{50} = 100 \sim 200 \mu\text{m}$); (*b*) Bed form chart for fine to medium sand ($d_{50} = 200 \sim 300 \mu\text{m}$); (*c*) Bed form chart for medium sand ($d_{50} = 300 \sim 400 \mu\text{m}$); (*d*) Bed form chart for medium to coarse sand ($d_{50} = 400 \sim 600 \mu\text{m}$) (from Shen and Julien, 1993).

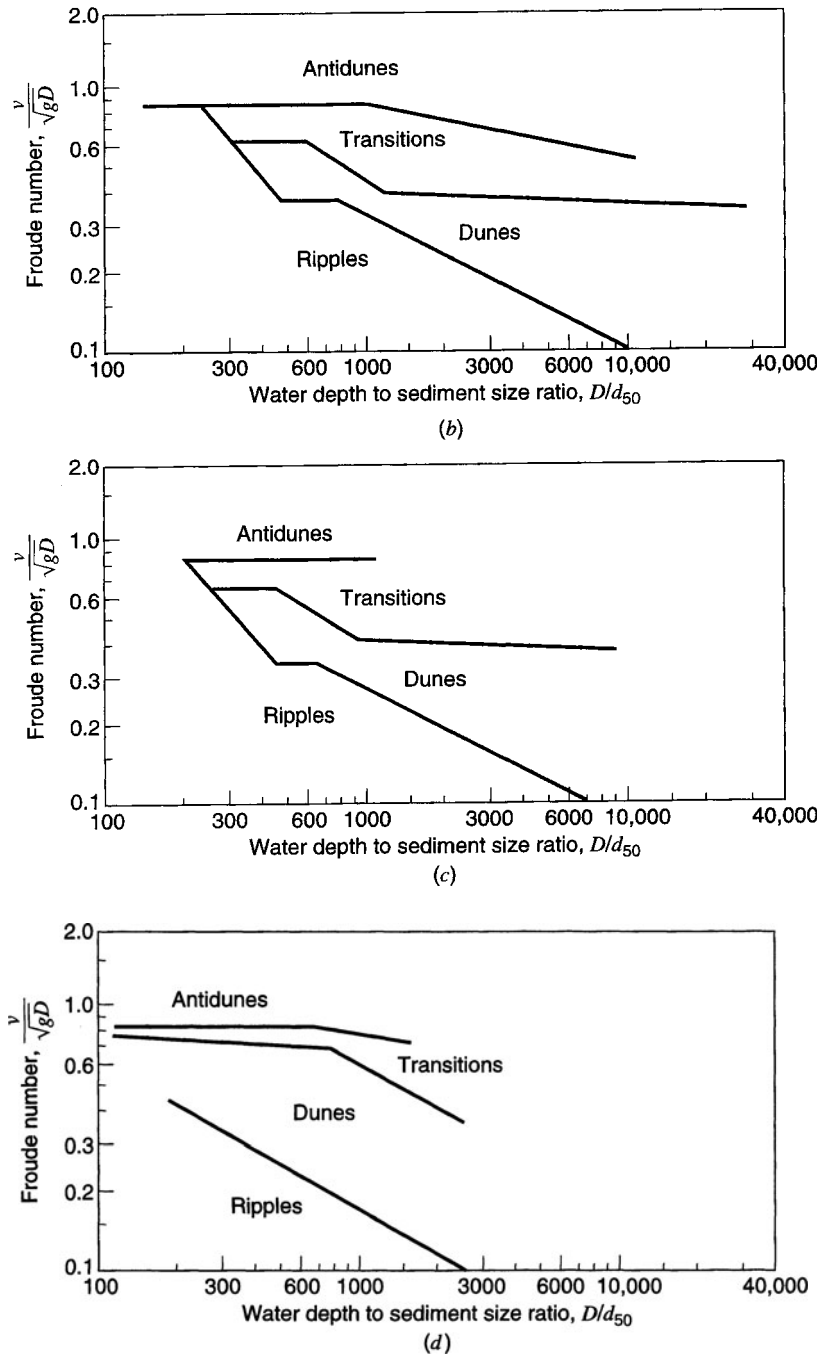


Figure 18.2.2 (Continued)

18.2.3 Flow Resistance

Flow resistance varies with different bed forms through the bed roughness, which can be described through Manning's equation as follows:

$$V = \frac{1}{n} R^{2/3} S_f^{1/2} \quad (18.2.1)$$

Table 18.2.2 Sediment Transport Definitions

Transported Sediment:	
Total sediment load	
Nontransported Sediment: Bed material (stationary sediment of the same sizes constituting the bed-material load)	
Sediment Load:	Material in suspension and/or in transport
Bed-Material Load:	Total rate at which bed material is transported by a given location on a stream (both bed load and suspended load)
Bed Load:	Material moving on or near the stream bed by rolling, sliding, and sometimes making brief excursions into the flow a few diameters above the bed (i.e., <i>jumping</i>). (Bed material that moves in continuous contact with the bed.)
Wash Load:	Part of total suspended load that is finer than bed material (wash load limited by supply not hydraulic)
Suspended Load:	Includes both suspended bed material load and wash load. Sediment that moves in suspension

where V is the average flow velocity (m/s), R is the hydraulic radius (m), and S_f is the dimensionless energy slope. Total roughness can be divided into *grain roughness* or *skin roughness* due to the existence of bed forms. A total Manning's roughness coefficient can be expressed as

$$n = n_g + n_f \quad (18.2.2)$$

where n_g is Manning's coefficient due to grain size roughness and n_f is Manning's coefficient due to form roughness. Einstein and Barbarossa (1952) were the first to separate the total flow resistance into a skin or grain resistance and a form resistance.

Several approaches have been reported in the literature for determining roughness coefficients for sediment-laden channels. See Yen (1996) and Yang (1996) for a review of these. Manning's roughness coefficients provided by Chow (1959), shown in Table 5.1.1, can be used for some bed types as indicated in the table.

Strickler's (1923) equation can be used to estimate Manning's roughness factor for streambeds and banks based on the prevailing sediment sizes on the banks and beds:

$$n = \frac{(D_{50})^{1/6}}{21} \quad (18.2.3)$$

where D_{50} is the median sediment size

$$n = \frac{(D_{50})^{1/6}}{25.6} \quad (18.2.4)$$

EXAMPLE 18.2.1

Compute the Manning's roughness factor for a streambed and banks with a median grain size of $D_{50} = 1$ mm.

SOLUTION

The Manning's roughness factor for the streambed is as follows:

$$n = \frac{(D_{50})^{1/6}}{21} = \frac{(0.001)^{1/6}}{21} = 0.015$$

The Manning's roughness factor for the stream banks is as follows:

$$n = \frac{(D_{50})^{1/6}}{25.6} = \frac{(0.001)^{1/6}}{25.6} = 0.012$$

18.3 SEDIMENT TRANSPORT

18.3.1 Incipient Motion

Incipient motion of bed particles can be considered as the critical condition between transport and no transport. Consider particle A in Figure 18.3.1 with an objective to evaluate the condition leading to the incipient motion of this particle. Assuming the particle has diameter D_s , the effective surface area is proportional to D_s^2 . The force F_x acting on the particles is considered to be a shear force due to the shear stress, τ_0 , expressed as

$$F_x = C_1 D_s^2 \tau_0 \tag{18.3.1}$$

where C_1 is a constant of proportionality and $(C_1 D_s^2)$ is the effective area.

Assume that the distance y_1 is proportional to D_s so that $y_1 = C_2 D_s$, then the *overturning moment* due to the flow is $\tau_0 C_1 D_s^2 (C_2 D_s)$. The overturning moment is balanced by the submerged weight of the particle that is proportional to $(\gamma_s - \gamma) D_s^3$. The *righting moment* can be expressed as $C_3 (\gamma_s - \gamma) D_s^3 (C_4 D_s)$, where C_3 and C_4 are constants of proportionality. The overturning moment and the righting moment are equal at the *point of incipient motion*. The shear stress associated with the point of incipient motion is the *critical shear stress*, $\tau_c = \tau_0$. Equating the overturning moment and the righting moment,

$$\tau_c C_1 D_s^2 (C_2 D_s) = C_3 (\gamma_s - \gamma) D_s^3 (C_4 D_s) \tag{18.3.2a}$$

$$\tau_c C_1 C_2 D_s^3 = (\gamma_s - \gamma) C_3 C_4 D_s^4 \tag{18.3.2b}$$

Solving for the critical shear stress

$$\tau_c = \frac{C_3 C_4}{C_1 C_2} (\gamma_s - \gamma) D_s \tag{18.3.3}$$

or

$$\tau_c = C (\gamma_s - \gamma) D_s \tag{18.3.4}$$

where $C = (C_3 C_4) / (C_1 C_2)$.

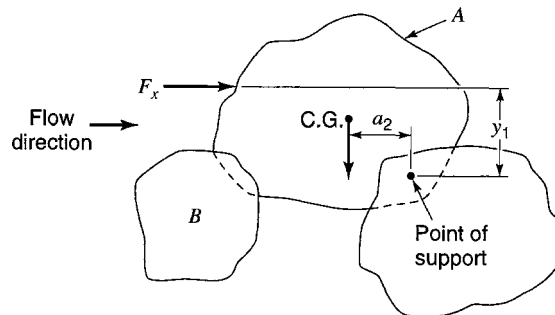


Figure 18.3.1 Incipient motion. Consider (assume) that the hydraulic force acting on the particle is due entirely to shear stress, I_0 , which acts over the surface area (portion of surface area referred to as surface area).

Dimensional analysis can be used to develop the critical shear stress more completely. A dimensionless shear stress is developed, which is

$$\frac{\tau_c}{(\gamma_s - \gamma)D_s} = \phi \left(\frac{\sqrt{\tau_c/\rho} D_s}{\nu} \right) \quad (18.3.5a)$$

$$= \phi \left(\frac{\mu_{*c} D_s}{\nu} \right) \quad (18.3.5b)$$

where $\frac{\mu_{*c} D_s}{\nu}$ is the *shear velocity Reynolds number* and

$$\mu_{*c} = \sqrt{\tau_c/\rho} \quad (18.3.6)$$

is the *critical shear velocity*. The term on the left side of equations (18.3.5a, b) is a dimensionless shear stress, τ_* ,

$$\tau_* = \frac{\tau_c}{(\gamma_s - \gamma)D_s} \quad (18.3.7)$$

The relationship between τ_* and R_{*v} developed by Shields (1936) is referred to as the *Shields diagram*, as shown in Figure 18.3.2. This diagram represents the experimental relationships implied by equations (18.3.5a, b). The Shields diagram can be used to evaluate the *critical shear stress* (the shear stress at incipient motion). To use the Shields diagram, one must first compute the following:

$$\frac{D_s}{\nu} \sqrt{0.1 \left(\frac{\gamma_s}{\gamma} - 1 \right) g D_s}$$

which can then be used to locate τ_* on the curve in the Shields diagram. With τ_* , the critical shear stress can be computed by rearranging equation (18.3.7) to

$$\tau_c = \tau_* (\gamma_s - \gamma) D_s \quad (18.3.8a)$$

$$= \tau_* (\gamma_s / \gamma - 1) \gamma D_s \quad (18.3.8b)$$

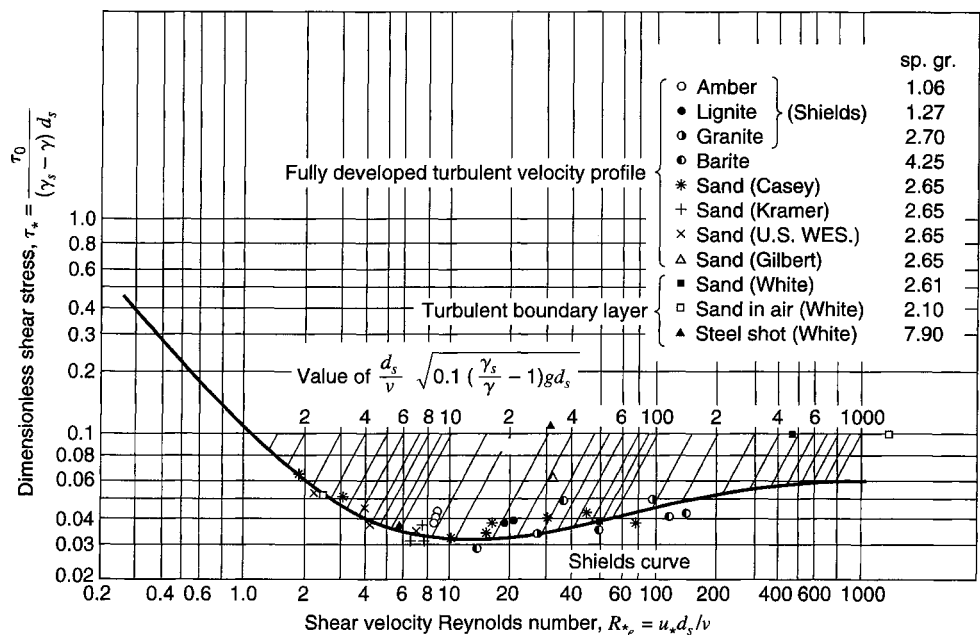


Figure 18.3.2 Shields diagram ($d_s = D_s$) (from Vanoni, 1975, p. 96).

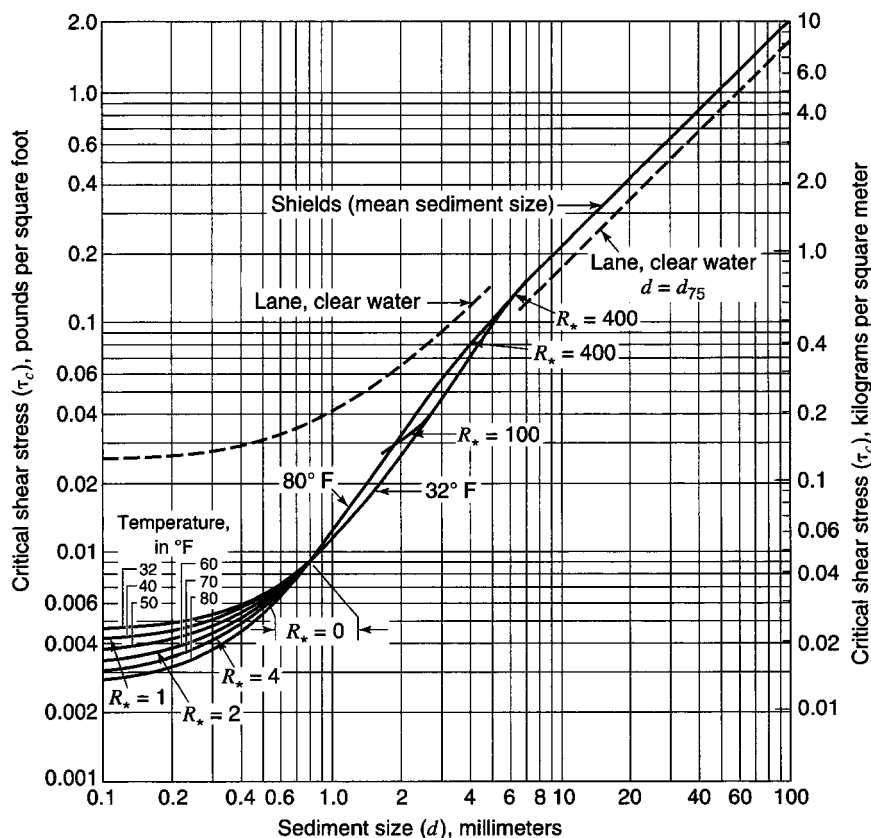


Figure 18.3.3 Critical shear stress for quartz sediment in water as function of grain size (from Vanoni, 1975).

The actual shear stress can be computed using

$$\tau_0 = \gamma RS \tag{18.3.9}$$

Then a comparison is made of τ_c and τ_0 . If τ_0 is larger than τ_c , transport is expected. Figure 18.3.3 is a rearrangement of the Shields diagram for quartz sediment in water.

EXAMPLE 18.3.1

Determine whether the critical shear stress is exceeded by the flow for the following situation. A fairly fine sand particle (with a geometric mean of 0.18×10^{-3} m) forms the bed of a wide rectangular channel with a depth of 2.5 m and a slope of 0.0001. The water is at 10°C so that $\nu = 1.308 \times 10^{-6}$ m²/s and $\gamma_s/\gamma = 2.65$.

SOLUTION

Step 1 Compute

$$\begin{aligned} & \frac{D_s}{\nu} \sqrt{0.1 \left(\frac{\gamma_s}{\gamma} - 1 \right) g D_s} \\ &= \frac{0.18 \times 10^{-3} \text{ m}}{1.308 \times 10^{-6} \text{ m}^2/\text{s}} \sqrt{0.1(2.65 - 1)9.81 \text{ m/s}^2 0.18 \times 10^{-3} \text{ m}} \\ &= 2.35 \end{aligned}$$

Step 2 Evaluate τ_* from the Shields diagram and compute the critical shear stress using equation (18.3.8b). From the Shields diagram, $\tau_* = 0.065$.

$$\begin{aligned}\tau_c &= \tau_*(\gamma_s/\gamma - 1)\gamma D_s = (0.065)(2.65 - 1)(9810)(0.18 \times 10^{-3}) \\ &= 0.8 \text{ N/m}^3\end{aligned}$$

Step 3 Compute the actual shear stress τ_0 using equation (18.3.9) where $R = y = 2.5 \text{ m}$

$$\begin{aligned}\tau_0 &= \gamma RS \\ &= 9810 \text{ N/m}^3 \times 2.5 \text{ m} \times 0.0001 \\ &= 2.45 \text{ N/m}^2\end{aligned}$$

Because the actual shear stress $\tau_0 = 2.45 \text{ N/m}^2$ is much larger than the critical shear stress $\tau_c = 0.8 \text{ N/m}^2$, transport of the fine sand particles is expected.

18.3.2 Sediment Transport Functions

Table 18.3.1 lists some of the more common sediment transport functions along with basic information on their development and use.

Table 18.3.1 Basic Information on the Development and Use of Common Sediment Transport Functions

Function Name	Type	Sediment size range (mm)	Developed from	Comments
Ackers-White	Total Load	0.04–2.5	Flume Data	Provides good description of movement for lightweight sediments in laboratory flumes and natural rivers.
Colby	Total Load	0.10–0.8	Flume and Stream Data	Temperature at 60°F. The function is recommended for sand rivers with depth less than 10 ft. Effective at velocity range of 1 to 10 ft/s. Depth range is 0.10–10 ft.
DuBoys	Bed Load	0.01–4.0	Small Flumes	The formula is not applicable for sand-bed streams that carry suspended load.
Engelund/Hansen	Total Load	Sizes in excess of 0.15 mm	Large Flume Data	Appears to satisfactorily predict sediment discharge in sand-bed rivers.
Laursen	Total Load	0.01–4.08	Flume Data	Intended to be applied only to natural sediments with specific gravity of 2.65. It is adaptable for shallow rivers with fine sand and coarse silt.
Meyer-Peter/Muller	Bed Load	0.40–30.0	Flume Data	Not valid for flows with appreciable suspended loads. The function was calibrated for coarse sands and gravels. It is recommended for rivers when the bed material is coarser than 5 mm. Depth range is from 1 to 1.2 m.
Schoklitsch	Bed Load	0.30–5.0	Small Flume Data	It is a bed load formula that should not be applied to sand-bed streams that carry considerable bed sediments in suspension.
Shields	Bed Load	1.7–2.50	Flume Data	The sediments used in the experiments were coarse and the shear velocities were low. Almost all the sediments moved were bed load.
Toffaletti	Total Load	0.062–16	Stream Data	The bed load portion may be calculated by an bed load function (for example, Schoklitsch, or Meyer-Peter and Muller). It should not be used for lightweight and coarser materials but is adaptable for large sand-bed rivers with specific gravity of 2.65.

(continued)

Table 18.3.1 (Continued)

Function Name	Type	Sediment size range (mm)	Developed from	Comments
Yang's Stream Power Function	Total Load	0.015–1.71	Stream Data	The function is effective for sediments with specific gravity of 2.65. Yang's sand formula is adaptable for sand-bed laboratory flumes and natural rivers—wash load excluded. Yang's gravel formula is for bed material between 2 and 10 mm.

18.3.3 Armoring

Armoring is the process of progressive coarsening of the bed layer by removal of fine particles until a layer is formed that becomes resistant to scour for a particular discharge. The coarse layer that remains on the surface is called the *armoring layer*. Armoring is a temporary condition because

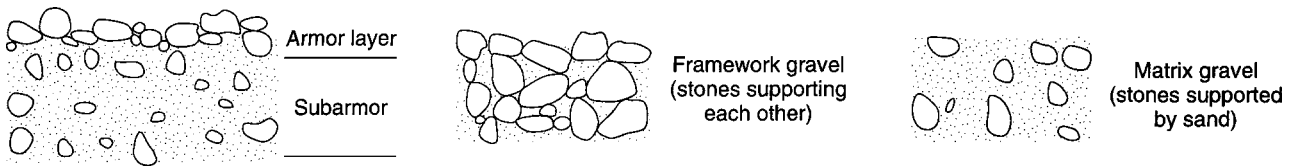


Figure 18.3.4 Patterns of gravel deposition in streambeds, cross-section view. The formation of a surface layer of *armor* or *pavement* about one grain thick protects the finer material in the underlying *subarmor* or *subpavement* zone from hydraulic transport until discharge is sufficient to mobilize the armor layer. Armor layers form frequently in gravel-bed rivers and occur when the bed contains a wide variation in grain sizes, when the supply of the finer grains is small compared to the transport energy, and when the largest grain size is transport-limited.

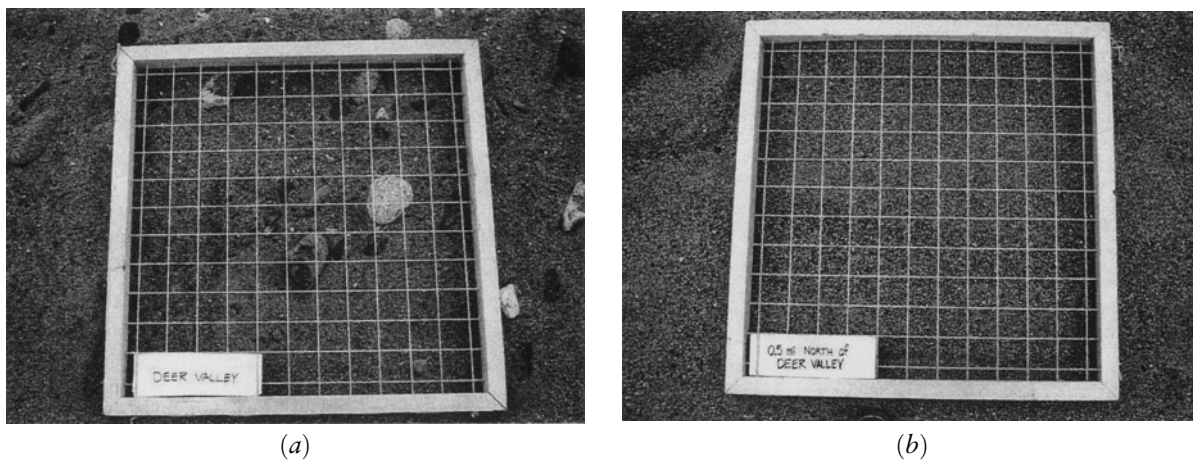
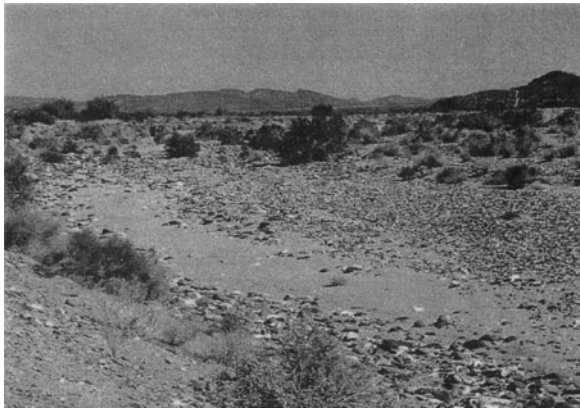
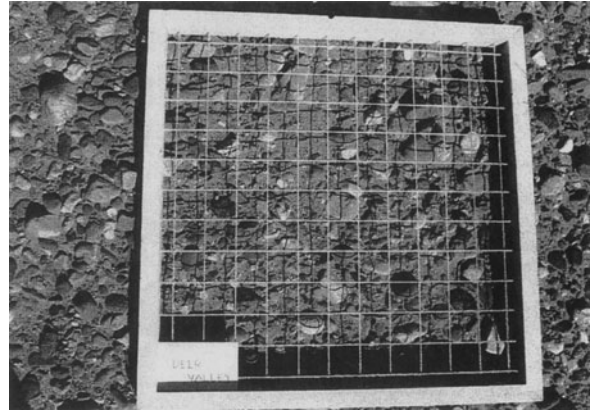


Figure 18.3.5 (a) Agua Fria River, location where the surface is not armored. [Location: Deer Valley road; mile designation: 22.32; photograph by Carlos Carriaga: January 20, 1992]; (b) Agua Fria River, the 2" × 2" grid over the surface aggregates. [Location: 0.5 mi north of Deer Valley Road; mile designation: 22.79; photograph by Carlos Carriaga: January 20, 1992]; (c) Semi-armored layer along the thalweg of the Agua Fria River. [Location: Deer Valley Road; mile designation: 22.32; photograph by Carlos Carriaga: October, 1991]; (d) The 2" × 2" grid over the semi-armored surface layer of the Agua Fria River. [Location: Deer Valley Road; mile designation: 22.32; photograph by Carlos Carriaga: October, 1991]; (e) The armored layer of the bed located at about 1.25 mi south of Highway 70 on the Agua Fria River [photograph by Carlos Carriaga: February 1, 1992]; (f) The Agua Fria River bed exhibits a range of sizes for the aggregates. [Location: 1.1 mi south of Highway 70; photograph by Carlos Carriaga: February 1, 1992]; (g) The heavily armored layer along the thalweg of the Agua Fria River. [Location: Peoria Road; mile designation: 14.38; photograph by Carlos Carriaga: October, 1991]; (h) The 2" × 2" grid over the armored layer of the Agua Fria River reach. [Location: Peoria Road; mile designation: 14.38; photograph by Carlos Carriaga: October, 1991].



(c)



(d)



(e)



(f)



(g)



(h)

Figure 18.3.5 (Continued)

larger discharges may destroy an armor layer and the layer may reform as discharges decrease. The formation of a resistant layer of relatively large particles results from removal of finer particles by erosion. Figure 18.3.4 further illustrates the concept of armoring, and Figures 18.3.5a–h show examples of different levels of armoring in the Agua Fria River near Phoenix, Arizona. Section

18.10.2.2 further discusses armoring and presents the equation by Pemberton and Lara (1984) for approximating the thickness of an armoring layer.

18.4 BED LOAD FORMULAS

As previously described, particles can be moved by the flow as bed along the streambed. This section describes several of the more commonly used bed load equations for sand-bed streams. The data in Tables 18.4.1 through 18.4.3 for the Colorado River at Taylor’s Ferry are used to apply the bed load formulas.

Table 18.4.1 Properties of the Colorado River (particularly at the site where the sediment discharge measurements were taken)

Depth range d , ft	4–12
Range in q , cfs/ft	8–35
Width, ft	350
Slope, S , ft/ft	0.000217
Temperature, °F	60
Geom. mean sed. size, mm	0.320
Geo. std. deviation	1.44
D_{35} , mm	0.287
D_{50} , mm	0.330
D_{65} , mm	0.378
D_{90} , mm	0.530
Mean size, D_m (mm)	0.396

Table 18.4.2 Size Fractions of Bed Sediment Used in Calculations (Temperature = 60°F)

Items	% by weight (i_b)		
	20.8	69.6	96
Mean size, D_{si} (mm)	0.177	0.354	0.707
(ft)	0.00058	0.00116	0.00232
Settling velocity, W_i (cm/sec)	1.9	4.8	9.6
(ft/sec)	0.063	0.158	0.314

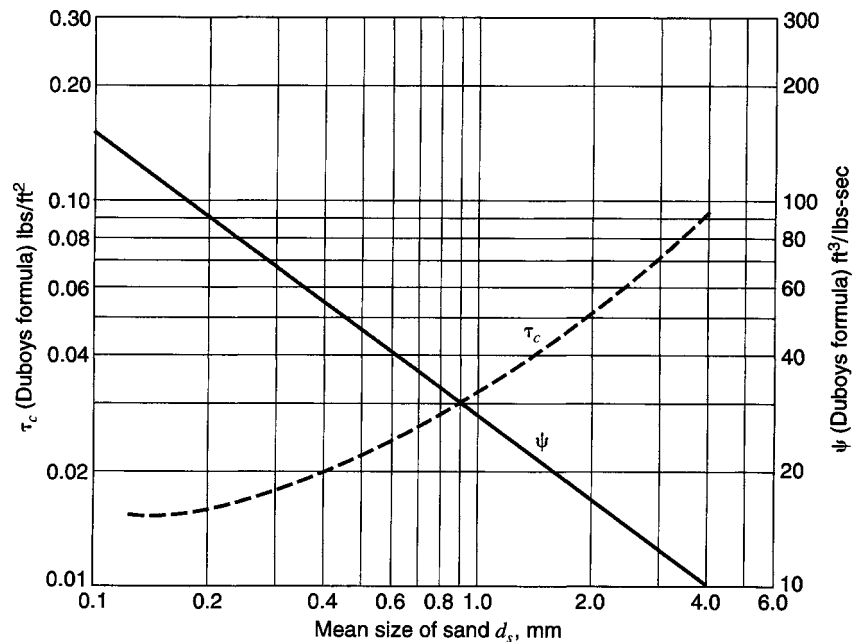
Table 18.4.3 Sieve Analysis of Bed Material from the Colorado River

Sieve opening (mm)	% finer
0.062	0.22
0.074	
0.125	1.33
0.175	
0.246	
0.250	21.4
0.351	
0.495	
0.500	88.7
0.701	
0.991	
1.000	98.0
1.400	

(Continued)

Table 18.4.3 (Continued)

Sieve opening (mm)	% finer
1.980	
2.000	99.0
3.960	
4.000	99.5

Figure 18.4.1 Graph of coefficient ψ and critical shear stress, τ_c for DuBoys formula.

18.4.1 DuBoys Formula

DuBoys (1879) developed the following formula:

$$g_s = \psi \tau_0 [\tau_0 - \tau_c] \quad (18.4.1)$$

where ψ is the coefficient depending on the mean size of bed sediment, $\text{ft}^3/\text{lb}/\text{sec}$; τ_0 is the $\gamma dS =$ bed shear stress in lb/ft^2 ; τ_c is the critical bed shear stress in lb/ft^2 ; γ is the specific weight of water in lb/ft^3 ; d is the water depth in feet; and S is the slope of the channel.

The parameters ψ and τ_c are given in Figure 18.4.1 as functions of the mean size of sand.

EXAMPLE 18.4.1

Compute the sediment discharge per unit width for the Colorado River at Taylor's Ferry for a depth of 10 ft and a flowrate of 40 cfs/ft using DuBoys formula and the data in Tables 18.4.1 through 18.4.3.

SOLUTION

For a mean size of sand, $D_s = D_m = 0.396$ mm (from Table 18.4.1), τ_c and ψ are found in Figure 18.4.1 as

$$\tau_c = 0.02 \text{ lb}/\text{ft}^2$$

$$\psi = 57 \text{ ft}^2/\text{lb}\cdot\text{s}$$

Using $S = 0.000217$ (given in Table 18.4.1), the bed shear stress is $\tau_0 = \gamma dS = 62.4(10)(0.000217) = 0.135408 \text{ lb}/\text{ft}^2$.

Substituting these values of ψ , τ_0 , τ_c in equation (18.4.1), results in

$$g_s = 57(0.135408)(0.135408 - 0.02)$$

$$g_s = 0.8907 \text{ lb/sec-ft}$$

18.4.2 Meyer-Peter and Muller Formula

Meyer-Peter and Müller (1948) developed an empirical formula for the bed load discharge in natural streams, which is expressed as

$$g_s = \left[0.368 \frac{Q_s}{Q} \left[\frac{D_{90}^{1/6}}{n_s} \right]^{3/2} d \cdot S - 0.0698 D_m \right]^{3/2} \quad (18.4.2)$$

where

- g_s = bed load discharge, lb/sec-ft width
- Q = total water discharge, ft³/s
- Q_s = that part of the water discharge apportioned to the bed in ft³/s
- D_{90} = particle size for which 90 percent of the bed mixture is finer (mm)
- D_m = effective diameter of bed-material mixture (mm)
- d = mean flow depth (ft).
- S = energy gradient (ft/ft)
- n_s = Manning's roughness value for the bed of the stream

For wide and smooth channels $Q_s/Q = 1$ and

$$n_s = \frac{1.486 d^{2/3} S^{1/2}}{V} \quad (18.4.3)$$

where V is the mean flow velocity in ft/sec.

When bank roughness is considered, the following relationships are used:

For rectangular channels:

$$n_s = n_m \left[1 + \frac{2d}{T_w} \left\{ 1 - \left[\frac{n_w}{n_m} \right]^{3/2} \right\} \right]^{2/3} \quad (18.4.4)$$

$$\frac{Q_s}{Q} = \frac{1}{1 + \frac{2d}{T_w} \left(\frac{n_w}{n_s} \right)^{2/3}} \quad (18.4.5)$$

For trapezoidal channels:

$$n_s = n_m \left[1 + \frac{2d(1+z^2)^{1/2}}{B} \left\{ 1 - \left[\frac{n_w}{n_m} \right]^{3/2} \right\} \right]^{2/3} \quad (18.4.6)$$

$$\frac{Q_s}{Q} = \frac{1}{1 + \frac{2d(1+z^2)^{1/2}}{B} \left(\frac{n_w}{n_s} \right)^{2/3}} \quad (18.4.7)$$

where

- n_w = roughness value for the channel sides
- n_m = roughness value for the total channel
- T_w = top width (ft)

- B = bottom width (ft)
 Z = channel side slope (hor/vert)
 $D_m = \sum_{i=1}^n D_{si} i_b$; n = number of size fractions
 D_{si} = mean grain diameter of the sediment in size fraction i
 i_b = fraction by weight of bed material in a given size fraction

EXAMPLE 18.4.2

Compute the sediment discharge per unit width for the Colorado River at Taylor's Ferry for a depth of 10 ft and a flow rate of 40 cfs/ft using the Meyer-Peter and Müller formula.

SOLUTION

First compute the effective diameter of bed-material mixture (mm):

$$D_m = \sum_i i_b D_{si} = 0.208(0.177) + 0.696(0.345) + 0.096(0.707) \\ = 0.351 \text{ mm}$$

Next compute the Manning's roughness factor, using equation (18.4.3):

$$n_s = \frac{1.486d^{2/3}S^{1/2}}{V} = \frac{1.486(10)^{2/3}(0.000217)^{1/2}}{4} \\ n_s = 0.0254$$

Since the river is wide, $\frac{Q_s}{Q} = 1$. The sediment discharge is computed using equation (18.4.2):

$$g_s = \left[0.368(1) \left[\frac{0.53^{1/6}}{0.254} \right]^{3/2} (10)(0.000217) - 0.0698(0.351) \right]^{3/2} \\ = 0.0545 \text{ lb/sec-ft}$$

18.4.3 Schoklitsch Formula

The Schoklitsch formula (Shulits, 1935) can be expressed as follows:

1. Unigranular material (D_{50}):

$$G_s = \frac{86.7}{\sqrt{D}} S^{3/2} (Q - T_w q_0) \quad (18.4.8)$$

where

$$q_0 = 0.00532d/S^{4/3}$$

$D \cong D_0$ (mean grain diameter) (in)

G_s = the bedload discharge (lb/s)

S = the energy gradient (ft/ft)

Q = the discharge (ft³/s)

T_w = the width (ft)

q_c = the critical discharge (ft³/s per ft of width)

(18.4.9)

2. For mixtures of different sizes (D_{si}):

$$g_s = \sum_{i=1}^n g_{s,i} = \sum_{i=1}^n i_b \frac{25}{\sqrt{D_{si}}} S^{3/2} (q - q_0) \quad (18.4.10)$$

where

$$q_0 = 0.0638D_{si}/S^{4/3}$$

- n = the number of size fractions in the bed-material mixture
 D_{si} = the mean grain diameter, ft
 $g_s = G_s/T_w$; bedload discharge, lb/sec-ft
 i_b = the fraction, by weight, of bed material in a given size fraction
 q = discharge per unit width

EXAMPLE 18.4.3

Compute the sediment discharge per unit width for the Colorado River at Taylor's Ferry for a depth of 10 ft and a flowrate of 40 cfs/ft using the Schoklitsch formula.

SOLUTION

1. From Table 18.4.2, $D_{si} = 0.177 \text{ mm} = 0.000581 \text{ ft}$

(i)

$$q_{0i} = \frac{0.0638(0.000581)}{(0.000217)^{4/3}} = 2.84 \text{ cfs/ft}$$

(ii)

$$\begin{aligned}
 g_{si} &= 0.208 \frac{(25)}{(0.000581)^{1/2}} (0.000217)^{3/2} (40 - 2.84) \\
 &= 0.0256 \text{ lb/sec-ft}
 \end{aligned}$$

2. For $D_{si} = 0.354 \text{ mm} = 0.00116 \text{ ft}$

(i)

$$q_{0i} = \frac{0.0638(0.00116)}{(0.000217)^{4/3}} = 5.6754 \text{ cfs/ft}$$

(ii)

$$\begin{aligned}
 g_{si} &= 0.696 \frac{(25)}{(0.00116)^{1/2}} (0.000217)^{3/2} (40 - 5.6754) \\
 &= 0.05606 \text{ lb/sec-ft}
 \end{aligned}$$

3. For $D_{si} = 0.707 \text{ mm} = 0.00232 \text{ ft}$

(i)

$$q_{0i} = \frac{0.0638(0.00232)}{(0.000217)^{4/3}} = 11.3509 \text{ cfs/ft}$$

(ii)

$$\begin{aligned}
 g_{si} &= 0.096 \frac{(25)}{(0.00232)^{1/2}} (0.000217)^{3/2} (40 - 11.3509) \\
 &= 0.00456 \text{ lb/sec-ft}
 \end{aligned}$$

$$\begin{aligned}
 g_s &= \sum_{i=1}^3 g_{si} = 0.0256 + 0.05616 + 0.00456 \\
 &= 0.0862 \text{ lb/sec-ft}
 \end{aligned}$$

18.5 SUSPENDED LOAD

The suspension of sediment is caused by turbulence, although other factors, such as secondary currents, obstruction, and particle impact, also play a role. In order to calculate the suspended load, the variation of sediment concentration in a vertical section of stream flow must be computed. Figure 18.5.1 illustrates the velocity distribution, the concentration distribution, and the shear stress distribution. At an equilibrium, there is a balance between the rate at which particles are falling due to gravity, $W \cdot C$, and the rate at which they are being stirred up again by turbulent eddy motion, $\epsilon_m \frac{\partial C}{\partial y}$, where W is the fall velocity of sediment particles, C is the concentration of sediment, ϵ_m is the vertical mass transfer coefficient due to eddy motion, and y is the vertical direction. At equilibrium,

$$W \cdot C + \epsilon_m \frac{\partial C}{\partial y} = 0 \quad (18.5.1)$$

which is a diffusion equation.

A solution can be developed for equation (18.5.1) by using the following fluid shear stress relationship:

$$\tau = \epsilon_m \rho \frac{du}{dy} \quad (18.5.2)$$

and a logarithmic vertical velocity distribution such as the *von Karman-Prandtl equation*:

$$\frac{u}{u_*} = \frac{2.303}{k} \log y + A \quad (18.5.3)$$

where $u_* = \sqrt{\tau_0/\rho}$ is the shear velocity, $k \approx 0.4$ for most clear water flows, and A is a constant depending on a smooth or rough boundary.

Differentiating equation (18.5.3) with respect to y gives

$$\frac{du}{dy} = \frac{u_*}{ky} \quad (18.5.4)$$

which can be substituted into equation (18.5.2) and solved for ϵ_m as follows:

$$\begin{aligned} \epsilon_m &= \frac{\tau/\rho}{du/dy} \\ &= \frac{\tau/\rho}{u_*/ky} \end{aligned} \quad (18.5.5)$$

Referring to Figure 18.5.1, the shear stress at the streambed is τ_0 ,

$$\tau_0 = \gamma R S = \gamma y_0 S \quad (18.5.6)$$

where the hydraulic radius $R = y_0$, the depth.

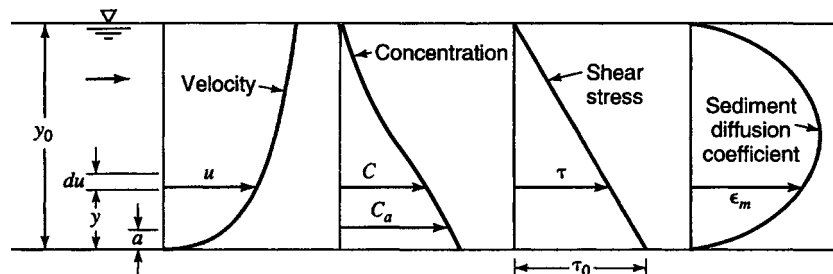


Figure 18.5.1 Definitional sketch for suspension of sediment.

At an intermediate depth y , the shear stress is

$$\tau = \gamma(y_0 - y)S \quad (18.5.7)$$

The ratio τ/τ_0 is

$$\begin{aligned} \frac{\tau}{\tau_0} &= \frac{\gamma(y_0 - y)S}{\gamma y_0 S} \\ &= \frac{(y_0 - y)}{y_0} \end{aligned} \quad (18.5.8)$$

so that

$$\tau = \tau_0 \frac{(y_0 - y)}{y_0} = \tau_0 \left(1 - \frac{y}{y_0}\right) \quad (18.5.9)$$

Equation (18.5.9) can be substituted into equation (18.5.5) to derive the vertical distribution of ϵ_m as follows:

$$\begin{aligned} \epsilon_m &= \frac{\tau_0 k y}{\rho u_*} \left(1 - \frac{y}{y_0}\right) \\ &= u_* k y \left(1 - \frac{y}{y_0}\right) \end{aligned} \quad (18.5.10)$$

Substituting equation (18.5.10) into the diffusion equation (18.5.1)

$$\begin{aligned} CW &= -\epsilon_m \frac{dC}{dy} \\ &= -u_* k y \left(1 - \frac{y}{y_0}\right) \frac{dC}{dy} \end{aligned} \quad (18.5.11)$$

Rearranging

$$\frac{dC}{C} = \frac{W y_0}{u_* k} \frac{dy}{y(y_0 - y)} \quad (18.5.12)$$

and integrating from a reference height a (see Figure 18.5.1) to any arbitrary height y gives

$$\frac{C_y}{C_a} = \left[\left(\frac{y_0 - y}{y} \right) \left(\frac{a}{y_0 - a} \right) \right]^z \quad (18.5.13)$$

Figure 18.5.2 is a verification graph of equation (18.5.13) where $z = \frac{W}{u_* k}$. This figure predicts vertical variation of sediment concentration for different values of parameter z .

The sediment discharge per unit width, g_{ss} , through an element of height dy is

$$g_{ss} = \int_a^{y_0} C_y u dy \quad (18.5.14)$$

Einstein (1950) integrated this equation using 18.5.13 for C_y and a logarithmic velocity equation.

EXAMPLE 18.5.1

Compute the sediment discharge per unit width for a depth of 10 ft, with an average velocity of 0.40 ft/sec for 8 ~ 10 ft, 0.38 ft/sec for 6 ~ 8 ft, 0.34 ft/sec for 4 ~ 6 ft, 0.30 ft/sec for 2 ~ 4 ft, and 0.15 ft/sec for 0 ~ 2 ft. $C_a = 0.10 \text{ lb/ft}^3$, $z = 0.81$.

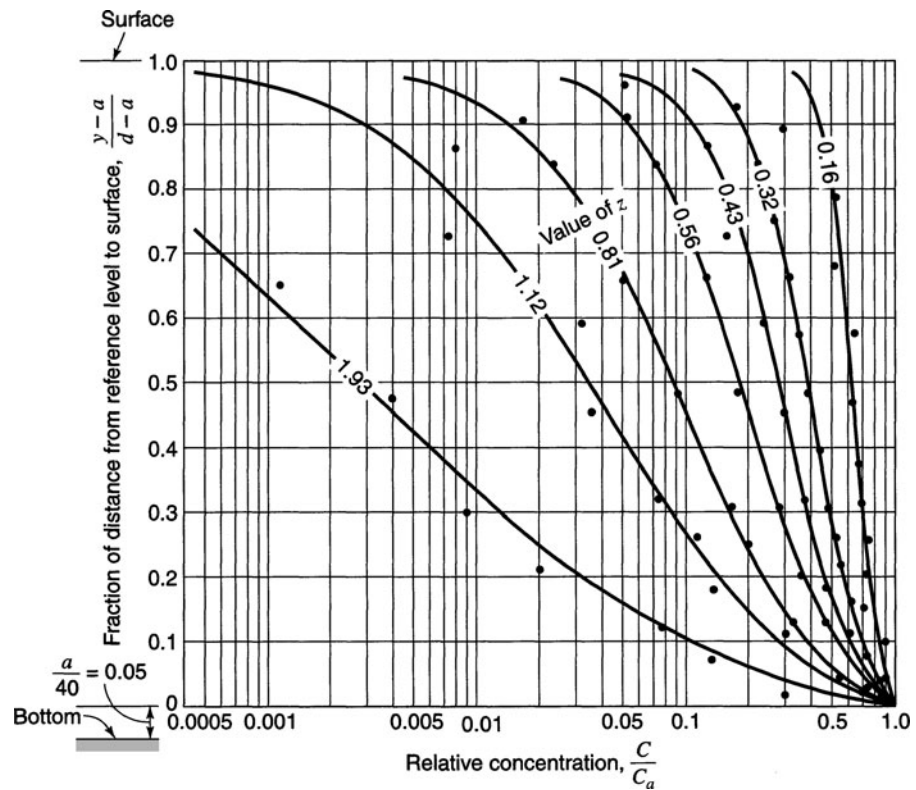


Figure 18.5.2 Vertical distribution of relative concentration C/C_a . Compared with equation (18.5.13) for wide range of stream size and z values (Vanoni, 1975).

SOLUTION

Compute C_y based on equation (18.5.13) and Figure 18.5.2:

$$C_y = 0.0015 \text{ lb/ft}^3, \text{ for } 8 \sim 10 \text{ ft}$$

$$C_y = 0.004 \text{ lb/ft}^3, \text{ for } 6 \sim 8 \text{ ft}$$

$$C_y = 0.0085 \text{ lb/ft}^3, \text{ for } 4 \sim 6 \text{ ft}$$

$$C_y = 0.016 \text{ lb/ft}^3, \text{ for } 2 \sim 4 \text{ ft}$$

$$C_y = 0.035 \text{ lb/ft}^3, \text{ for } 0 \sim 2 \text{ ft}$$

Compute g_{ss} based on equation (18.5.14):

$$\begin{aligned} g_{ss} &= \int_a^{y_0} C_y u dy = \sum_{n=1}^5 C_y u \Delta y \\ &= 0.0015 \times 0.40 \times 2 + 0.004 \times 0.38 \times 2 + 0.0085 \\ &\quad \times 0.34 \times 2 + 0.016 \times 0.30 \times 2 + 0.035 \times 0.15 \times 2 \\ &= 0.0012 + 0.00304 + 0.00578 + 0.0096 + 0.0105 \\ &= 0.03012 \text{ lb/sec-ft} \end{aligned}$$

EXAMPLE 18.5.2

A sandy channel bed with mean particle size of 0.15 mm and density equal to 2.70 g/cm³ has an elevation of 220.0 m and surface water elevation of 225.60 m. The shear stress at the streambed is 0.75 N/m². At what depth (elevation) does the relative concentration equal 0.1?

SOLUTION

Using equation (18.1.15a), where $D = 0.15 \text{ mm} = 0.00015 \text{ m}$; $\rho = 1.0$; $\rho_s = 2.7$; $\nu = 1.0 \times 10^{-6} \text{ m}^2/\text{s}$; and $g = 9.81 \text{ m/s}^2$, solve for W_T :

$$\begin{aligned} W_T &= \frac{D^2 g}{18\nu} \left(\frac{\rho_s}{\rho} - 1 \right) \\ &= \frac{(0.15 \times 10^{-3})^2 \text{ m}^2 \times 9.81 \text{ m/s}^2}{18 \times 1.0 \times 10^{-6} \text{ m}^2/\text{s}} \left(\frac{2.70}{1.00} - 1 \right) \\ &= 0.021 \text{ m/s} \end{aligned}$$

The shear velocity $u_* = \sqrt{\tau_0/\rho} = (0.75/1000)^{1/2} = 0.0274 \text{ m/s}$

$$\text{Then } z = \frac{W}{u_* k} = \frac{0.021}{0.0274 \times 0.4} = 1.92$$

From Figure 18.5.2, with $z = 1.92$ and relative concentration = 0.1, then $y/d = 0.1$, but $d = 225.60 - 220.0 = 5.6 \text{ m}$. Thus, this given relative concentration occurs when the depth is $y = \left(\frac{y}{d}\right)d = 0.56 \text{ m}$ above the bed elevation (i.e., at elevation 220.56).

18.6 TOTAL SEDIMENT LOAD (BED MATERIAL LOAD FORMULAS)

This section presents Colby’s formula, the Ackers–White formula, and Yang’s formula. These three formulas have been selected in order to illustrate total sediment load (bed material load formula).

18.6.1 Colby’s Formula

Colby (1964) recommended the diagrams in Figures 18.6.1 and 18.6.2 based on investigation of sediment transport load as a function of mean flow velocity, depth, viscosity, water temperature, and concentration of the fine sediment of the discharge of sand per foot of channel width. The bed-material discharge can be determined by Colby’s formula (Colby, 1964):

$$g_s = A(V - V_c)^B (1 + (AF - 1)CF) 0.672 \tag{18.6.1}$$

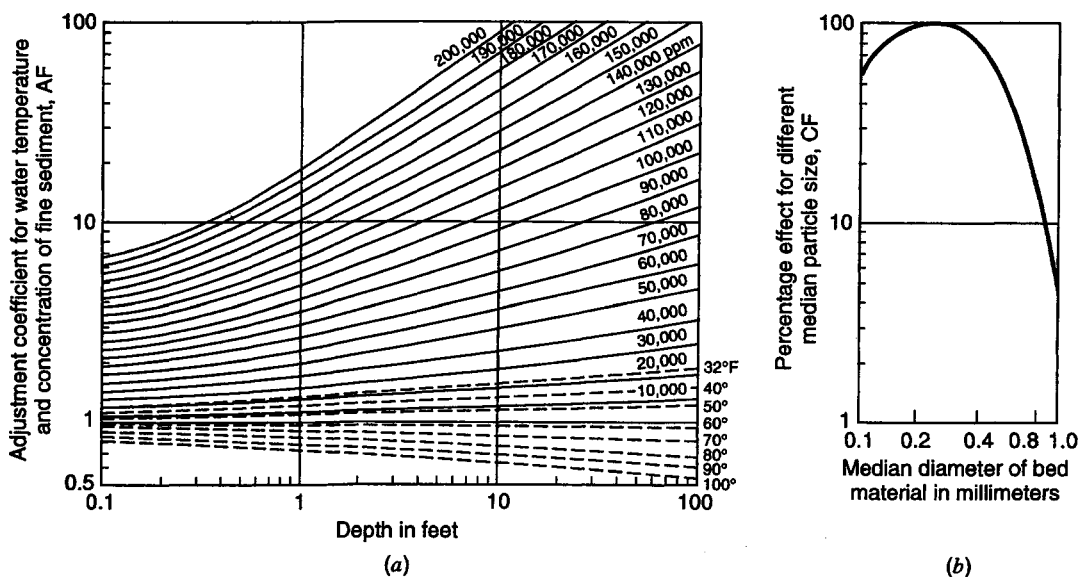


Figure 18.6.1 Approximate effect of water temperature and concentration of fine sediment on the relationship of discharge of sand to mean velocity (Colby, 1964.) Graph (a) is based on sediment sizes 0.2 to 0.3 mm. For other sediment sizes, a correction factor is needed from graph (b) (from Shen and Julien, 1993).

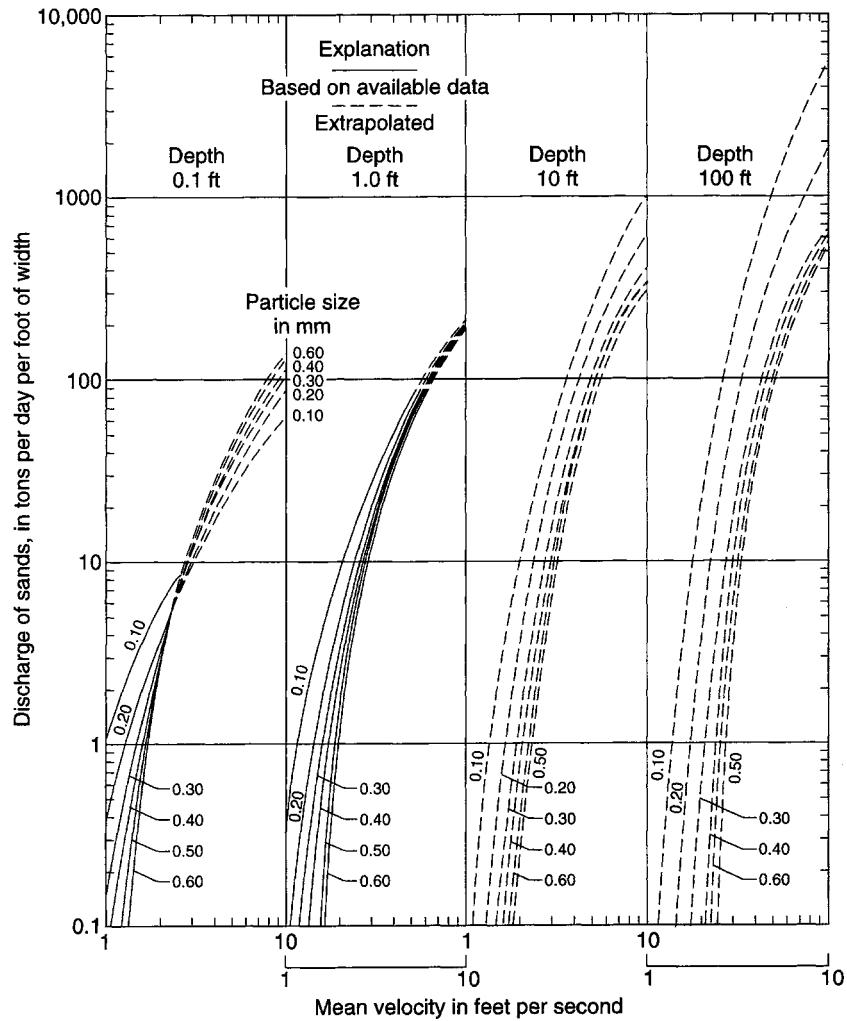


Figure 18.6.2 Relationships of discharge of sands to mean velocity for six median sizes of bed sands, four depths of flow, and a water temperature of 60°F (Colby, 1964) (from Shen and Julien, 1993).

where

A = coefficient associated with D_{50}

AF = adjustment coefficient for water temperature and concentration of fine sediment
(Figure 18.6.1a is based on sediment sizes from 0.2 to 0.3 mm. For other sizes, a correction, CF , from Figure 18.6.1b is needed.)

CF = percentage effect for different medium particle size (Figure 18.6.1b)

V = mean velocity (ft/s)

V_c = critical velocity (ft/s)

d = mean depth (ft)

D_{50} = particle size (mm) at which 50 percent of the bed material by weight is finer

B = an exponent that has the following values:

$$B = 2.5 \text{ for } (V - V_c) < 1.0 \quad (18.6.2a)$$

$$B = 1.453 D_{50}^{-0.138} \text{ for } (V - V_c) \geq 1.0 \quad (18.6.2b)$$

The following procedure is used in the evaluation of the bed-material discharge:

Step 1 Compute the critical velocity, V_c :

$$V_c = 0.4673 d^{0.1} D_{50}^{0.33} \tag{18.6.3}$$

Step 2 Determine exponent B with the value of $(V - V_c)$.

Step 3 Determine the value of A :

For $D_{50} = 0.1$ mm $A = 1.453 d^{0.61}$ (18.6.4a)

$D_{50} = 0.2$ mm $A = 1.329 d^{0.48}$ (18.6.4b)

$D_{50} = 0.3$ mm $A = 1.4 d^{0.3}$ (18.6.4c)

$D_{50} = 0.4$ mm $A = 1.26 d^{0.3}$ (18.6.4d)

$D_{50} = 0.8$ mm $A = 1.099 d^{0.3}$ (18.6.4e)

Step 4 Determine correction factor (CF) from Figure 18.6.1.

Step 5 Determine the coefficient, AF , from the correction curves in Figure 18.6.1a.

Step 6 Compute g_s using equation (18.6.1).

EXAMPLE 18.6.1

Compute the sediment discharge per unit width for the Colorado River at Taylor’s Ferry for a depth of 10 ft and a flowrate of 40 cfs/ft using Colby’s formula.

SOLUTION

Step 1 Compute V_c for a depth of 10 ft and $D_{50} = 0.33$:

$$V_c = 0.4673 d^{0.1} D_{50}^{0.33}$$

$$V_c = 0.4673(10.0)^{0.1}(0.33)^{0.33}$$

$$V_c = 0.408 \text{ ft/s}$$

Step 2 Compute B :

$$\text{Since } (V - V_c) = (4.0 - 0.408) = 3.532 \text{ ft/s}$$

$$B = 1.453(0.33)^{(-0.138)} = 1.693$$

Step 3 Compute A :

$$A = 1.4 d^{0.3} \text{ for } D_{50} = 0.3 \text{ mm}$$

$$A = 1.26 d^{0.3} \text{ for } D_{50} = 0.4 \text{ mm}$$

Since $D_{50} = 0.3$ mm, interpolation is necessary:

A	D_{50}
2.793	0.3
x	0.33
2.514	0.40

$$\frac{x - 2.793}{-0.279} = \frac{0.03}{0.1}$$

$$x = 2.7093$$

$$A = 2.7093$$

Step 4 Find $CF = 1$ using Figure 18.6.1b for $D_{50} = 0.33$ mm

Step 5 Find AF using Figure 18.6.1a for 60°F , $AF = 1$

Step 6 Compute g_s using equation (18.6.1) where $(1 + (AF - 1)CF) = 1$:

$$g_s = A(V - V_c)^B (1 + (AF - 1)CF)(0.672)$$

$$g_s = 2.7093(4 - 0.408)^{1.693}(1)(0.672)$$

$$g_s = 15.864 \text{ lb/sec-ft}$$

18.6.2 Ackers–White Formula

Ackers and White (1973) developed a general sediment discharge function in terms of three dimensionless groups: D_{gr} (size), F_{gr} (mobility), and G_{gr} (discharge). The procedure for the computation of concentration of bed-material discharge is as follows:

Step 1 Compute the dimensionless grain diameter using:

$$D_{gr} = D_{50} \left(\frac{g(S_g - 1)}{\nu^2} \right)^{1/3} \quad (18.6.5)$$

where

D_{50} = particle size, in feet, at which 50 percent of the bed material by weight is finer

g = acceleration of gravity (ft/s^2)

S_g = specific gravity of the sediment

ν = kinematic viscosity (ft^2/s)

Step 2 Determine the values of parameters A , C_A , n , and m used in equation (18.6.7) associated with the computed D_{gr} for two size ranges of bed material. For intermediate size, $1 \leq D_{gr} \leq 60$, $D_{gr} = 1$ (0.04 mm silt size) to $D_{gr} = 60$ (2.5 mm sand size):

$$n = 1.00 - 0.56 \log D_{gr}$$

$$A = \frac{0.23}{\sqrt{D_{gr}}} + 0.14$$

$$m = \frac{9.66}{D_{gr}} + 1.34$$

$$\log C_A = 2.86 \log D_{gr} - (\log D_{gr})^2 - 3.53$$

For coarse size, $D_{gr} > 60$:

$$n = 0.00$$

$$A = 0.17$$

$$m = 1.5$$

$$C_A = 0.025$$

Step 3 Compute the particle mobility, F_{gr} :

$$F_{gr} = \frac{u_*^n}{\sqrt{gD_{50}(S_g - 1)}} \left(\frac{V}{\sqrt{32} \log \left(\frac{\alpha d}{D_{50}} \right)} \right)^{1-n} \quad (18.6.6)$$

where

d = mean depth (ft)

u_* = shear velocity $(\tau_0/\rho)^{1/2}$ (ft/sec)

V = mean velocity (ft/sec)

α = coefficient in the rough turbulent equation with a value of 10

n = transition exponent depending on sediment size

Step 4 Compute the sediment transport parameter, G_{gr} :

$$G_{gr} = C_A \left[\frac{F_{gr}}{A} - 1 \right]^m \quad (18.6.7)$$

Step 5 Compute the concentration of bed-material discharge:

$$C = 10^6 \left[\frac{G_{gr} S_g D_{50} \left[\frac{V}{u_*} \right]^n}{d} \right] \quad (18.6.8)$$

where

C is the concentration of bed-material discharge, in parts per million (ppm) by weight

Step 6 Convert the concentration to appropriate units:

$$\begin{aligned} g_s &= C(\text{ppm}) \times \frac{8.34 \text{ lb}/10^6 \text{ gal}}{(1 \text{ ppm})} \times \frac{7.48 \text{ gal}}{1 \text{ ft}^3} \times q \frac{\text{cfs}}{\text{ft}} \\ &= \text{lb}/\text{sec}\text{-ft} \end{aligned}$$

EXAMPLE 18.6.2

Compute the sediment discharge per unit width for the Colorado River at Taylor's Ferry for a depth of 10 ft and a flowrate of 40 cfs/ft using the Ackers-White formula.

SOLUTION

Step 1 Compute dimensionless grain diameter, G_r :

$$D_{50} = 0.33 \text{ mm} = 0.001083 \text{ ft}$$

$$g = 32.2 \text{ ft}/\text{s}^2$$

$$S_g = 2.65$$

$$v = 1.22 \times 10^{-5} \text{ for } T = 60^\circ\text{F}$$

$$D_{gr} = 0.001083 \left[\frac{(32.2)(2.65 - 1)}{(1.22 \times 10^{-5})^2} \right]^{1/3} = 7.6825$$

Step 2 Compute A , C_A , n , and m :

$$\text{For } 1 \leq D_{gr} \leq 60$$

$$n = 1.00 - 0.56 \log D_{gr} = 0.504$$

$$A = \frac{0.23}{\sqrt{D_{gr}}} + 0.14 = 0.223$$

$$m = \frac{9.66}{D_{gr}} + 1.34 = 2.597$$

$$\log C_A = 2.86 \log(7.6825) - [\log(7.6825)]^2 - 3.53$$

$$\log C_A = -1.7816$$

$$C_A = 0.01654$$

Step 3 Compute the particle mobility using equation (18.6.6):

First compute shear velocity $u_* = (\tau_0/\rho)^{1/2}$ for $\rho = 1.94$ at 60°F . Then

$$\tau_0 = \gamma d S = 62.4(10)(0.000217) = 0.1354$$

and

$$u_* = (0.1354/1.94)^{1/2} = 0.2642 \text{ ft/s:}$$

$$F_{gr} = \frac{0.2642^{0.504}}{\sqrt{(32.2)(0.001083)(2.65 - 1)}} \left[\frac{4}{\sqrt{32} \log \left(\frac{10 \times 10}{0.001083} \right)} \right]^{0.496}$$

$$F_{gr} = \frac{0.5113}{0.2399} (0.3803) = 0.8106$$

Step 4 Compute G_{gr} using equation (18.6.7):

$$G_{gr} = C_A \left[\frac{F_{gr}}{A} - 1 \right]^m$$

$$G_{gr} = 0.01654 \left[\frac{0.8106}{0.223} - 1 \right]^{2.597} = 0.2048$$

Step 5 Compute concentration of bed-material discharge, ppm, using equation (18.6.8):

$$C = \frac{10^6 G_{gr} S_g D_{50} \left(\frac{V}{u_*} \right)^n}{d}$$

$$C = \frac{10^6 (0.2048) (2.65) (0.001083) \left(\frac{4}{0.2642} \right)^{0.504}}{10}$$

$$C = 231.2 \text{ ppm}$$

Step 6 Convert C from ppm to lb/sec-ft:

$$g_s = 231.2 \text{ ppm} \times \frac{8.34 \text{ lb}}{10^6 \text{ gal}} \times \frac{7.48 \text{ gal}}{1 \text{ ft}^3}$$

$$g_s = 0.0144 \text{ lb/ft}^3 \quad \text{or} \quad 0.5760 \text{ lb/sec-ft}$$

18.6.3 Yang's Unit Stream Power Formula

18.6.3.1 Yang's Sand Formula

Yang (1973) developed an equation for computing the concentration of bed-material discharge. This equation is for application to sand-bed streams and is based on dimensional analysis and the concept of unit stream power. Yang defined unit stream power as the rate of potential energy dissipated per unit weight of water, expressed by the product of velocity and slope.

Yang's (1973) dimensionless unit stream power for sand transport is as follows:

$$\begin{aligned} \log C = & 5.435 - 0.286 \log \frac{WD_{50}}{v} - 0.457 \log \frac{u_*}{W} \\ & + \left[1.799 - 0.409 \log \frac{WD_{50}}{v} - 0.314 \log \frac{u_*}{W} \right] \log \left[\frac{VS}{W} - \frac{V_{cr}S}{W} \right] \end{aligned} \quad (18.6.9)$$

in which the dimensionless critical velocity at incipient motion can be expressed as:

$$\frac{V_{cr}}{W} = \frac{2.5}{\log \frac{u_* D_{50}}{v} - 0.06} + 0.66 \text{ for } 1.2 < \frac{u_* D_{50}}{v} < 70 \quad (18.6.10a)$$

$$\frac{V_{cr}}{W} = 2.05 \text{ for } 70 \leq \frac{u_* D_{50}}{v} \quad (18.6.10b)$$

where

- C = concentration of bed-material discharge (ppm by weight)
- W = average fall velocity (fps) of sediment particles of diameter D_{50}
- D_{50} = particle size (ft) at which 50 percent of the bed material by weight is finer
- v = kinematic viscosity (ft^2/s)
- u_* = shear velocity (fps); $u_* = \sqrt{\tau_0/\rho}$
- V = average velocity (fps)
- S = energy slope (ft/ft)
- V_{cr} = average flow velocity (fps) at incipient motion

18.6.3.2 Yang's Gravel Formula

Yang's (1984) dimensionless unit stream power formula for gravel transport is:

$$\begin{aligned} \log C = & 6.681 - 0.633 \log \frac{WD_{50}}{v} - 4.816 \log \frac{u_*}{W} \\ & + \left[2.784 - 0.305 \log \frac{WD_{50}}{v} - 0.282 \log \frac{u_*}{W} \right] \log \left[\frac{VS}{W} - \frac{V_{cr}S}{W} \right] \end{aligned} \quad (18.6.11)$$

The dimensionless critical velocity at incipient motion is defined by equations (18.6.10a, b).

For computing the total discharge of graded material (using the gravel or sand formula), the total bed-material discharge concentration can be computed using:

$$C = \sum_{i=1}^n i_b C_i \quad (18.6.12)$$

where

- n = number of size fractions in the bed material
- i_b = fraction by weight of bed material in a given size fraction
- C_i = computed concentration in the size fraction, i (ppm)

EXAMPLE 18.6.3

Compute the sediment discharge per unit width for the Colorado River at Taylor's Ferry for a depth of 10 ft and a flowrate of 40 cfs/ft using Yang's sand formula.

SOLUTION

Step 1 Compute shear velocity, u_* :

$$\begin{aligned} D_{50} &= 0.33 \text{ mm} = 0.001083 \text{ ft} \\ \rho &= 1.94 \text{ slug/ft}^3 \text{ for } T = 60^\circ\text{F} \\ \gamma &= 68.4 \text{ lb/ft}^3 \\ u_* &= (\tau_0/\rho)^{1/2} \\ \tau_0 &= \gamma d S = 62.4(10)(0.000217) = 0.1354 \text{ lb/ft}^2 \\ u_* &= (0.1354/1.94)^{1/2} = 0.2642 \text{ ft/s} \end{aligned}$$

Step 2 Compute $\frac{u_* D_{50}}{v}$ for $v = 1.22 \times 10^{-5}$ ft²/sec at $T = 60^\circ\text{F}$

$$\frac{u_* D_{50}}{v} = \frac{0.2642(0.001083)}{(1.22 \times 10^{-6})} = 23.45$$

Step 3 Compute V_{cr}/W

Since $1.2 < \frac{u_* D_{50}}{v} < 70$,

$$\frac{V_{cr}}{W} = \frac{2.5}{\log \frac{u_* D_{50}}{v} - 0.06} + \frac{2.5}{\log(23.45) - 0.06} + 0.66 = 2.568$$

Step 4 Determine the fall velocity, W , for D_{50} by interpolation. Since $D_{50} = 0.33$ mm, interpolation is necessary:

W	D (mm)
1.9	0.177
x	0.33
4.8	0.354

$$\frac{x - 1.9}{2.9} = \frac{0.153}{0.177}$$

$$x = 4.407 \text{ cm/sec}$$

$$W = 0.1446 \text{ fps for } D_{50} = 0.33 \text{ mm}$$

Step 5 Compare V_{cr} :

$$\frac{V_{cr}}{W} = 2.568; V_{cr} = 0.3713 \text{ ft/s}$$

Step 6 Compute concentration using equation (18.6.9):

$$\begin{aligned} \log C &= 5.435 - 0.268 \log \left[\frac{0.1446(0.001083)}{1.22 \times 10^{-5}} \right] - 0.457 \left[\frac{0.2642}{0.1446} \right] \\ &+ \left[1.799 - 0.409 \log \left[\frac{0.1446(0.001038)}{1.22 \times 10^{-5}} \right] - 0.314 \log \left[\frac{0.2642}{0.1446} \right] \right] \\ &\times \log \left[\frac{(4 - 0.3713)(0.000217)}{0.1446} \right] \end{aligned}$$

$$\log C = 2.13784$$

$$C = 137.354 \text{ ppm or } 0.00857 \text{ lb/ft}^3 \text{ or } 0.343 \text{ lb/sec-ft}$$

Table 18.6.1 summarizes the resulting sediment discharge per unit width for the Colorado River at Taylor's Ferry. Figure 18.6.3 presents the sediment rating curves for the Colorado River at Taylor's Ferry using several sediment discharge formulas for the condition specified in the figure.

Table 18.6.1 Sediment Transport for a Discharge of ($q = 40$ cfs/ft width) the Functions Used

Formula	Sediment transport (lbs/sec per foot width)
Bed load	
(a) Schoklitsch Formula	0.086
(b) DuBoys Formula	0.891
(c) Meyer-Peter-Muller [English]	0.054
Meyer-Peter-Muller [Metric]	0.105

(Continued)

Table 18.6.1 (Continued)

Formula	Sediment transport (lbs/sec per foot width)
(d) Laursen formula	5.442
Total sediment load	
(a) Yang's Sand formula	0.343
(b) Tofalleti formula	3.039
(c) Ackers-White [D_{50} Option]	0.576
Ackers-White [D_{35} Option]	0.704
(d) Einstein Bed-Load Function	0.140
(e) Colby Formula [Graph]	0.718

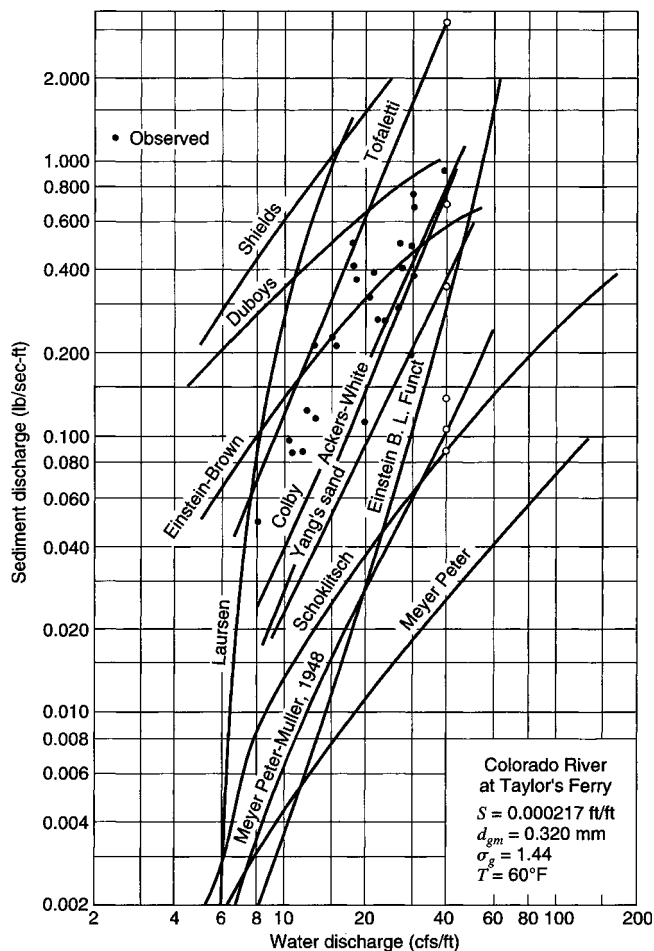


Figure 18.6.3 Sediment rating curves for the Colorado River at Taylor's Ferry according to several formulas, compared with measurements.

18.7 WATERSHED SEDIMENT YIELD

Watershed erosion is characterized by the detachment and entrainment of solid particles from the land surface. Erosion occurs under the influence of water, gravity, wind, and ice. *Water erosion* can be classified as *sheet erosion* and *channel erosion*. Sheet erosion is the detachment

caused by raindrop impact and the thawing of frozen grounds and the subsequent removal by overland flow.

The *universal soil loss equation* (USLE) was developed to predict the long-term average soil losses in runoff from field areas under specified cropping and management systems (USDA-ARS, 1961). The USLE equation is:

$$A = RKLSCD \quad (18.7.1)$$

where

- A is the computed soil loss in tons/acre
- R is the rainfall-erodibility factor (see Figure 18.7.1)
- K is the soil-erodibility factor (see Table 18.7.1)
- L is the slope-length factor normalized to a plot length of 72.6 ft
- S is the slope-steepness factor normalized to a field slope of 9 percent
- C is the cropping-management factor normalized to a tilled area with continuous fallow (see Table 18.7.2)
- D is the conservation practice factor normalized to straight-row farming up and down the slope

The value of the *rainfall erodibility factor*, R , on an annual basis is shown in Figure 18.7.1 for use in computing average annual erosion losses. R also can be computed for each storm (summed over hours) using

$$R = 0.01 \sum EI \quad (18.7.2)$$

where the summation is for the time increments of the storm and E , the kinetic energy per foot-tons per acre-inch, is given by

$$E = (916 + 331 \log I) \quad (18.7.3)$$

where I is the rainfall intensity in inches per hour.

K , the *soil-erodibility factor*, describes the inherent erodibility (intrinsic susceptibility) of a given soil to erode, expressed in tons/acre (see Table 18.7.1). The slope length-steepness factor LS is a topographic factor relating the erosion losses from a field of given slope and length when compared with soil losses of a standard plot 72.6 ft long inclined at 9 percent slope. The LS factor can be computed using:

$$LS = \left(\frac{\lambda}{72.6} \right)^m (65.41 \sin^2 \theta + 4.56 \sin \theta + 0.065) \quad (18.7.4)$$

Table 18.7.1 Soil Erodibility Factor K in tons/acre

Textural class	Organic matter content, %	
	0.5	2
Fine sand	0.16	0.14
Very fine sand	0.42	0.36
Loamy sand	0.12	0.10
Loamy very fine sand	0.44	0.38
Sandy loam	0.27	0.24
Very fine sandy loam	0.47	0.41
Silt loam	0.48	0.42
Clay loam	0.28	0.25
Silty clay loam	0.37	0.32
Silty clay	0.25	0.23

Source: From Schwab et al. (1981).

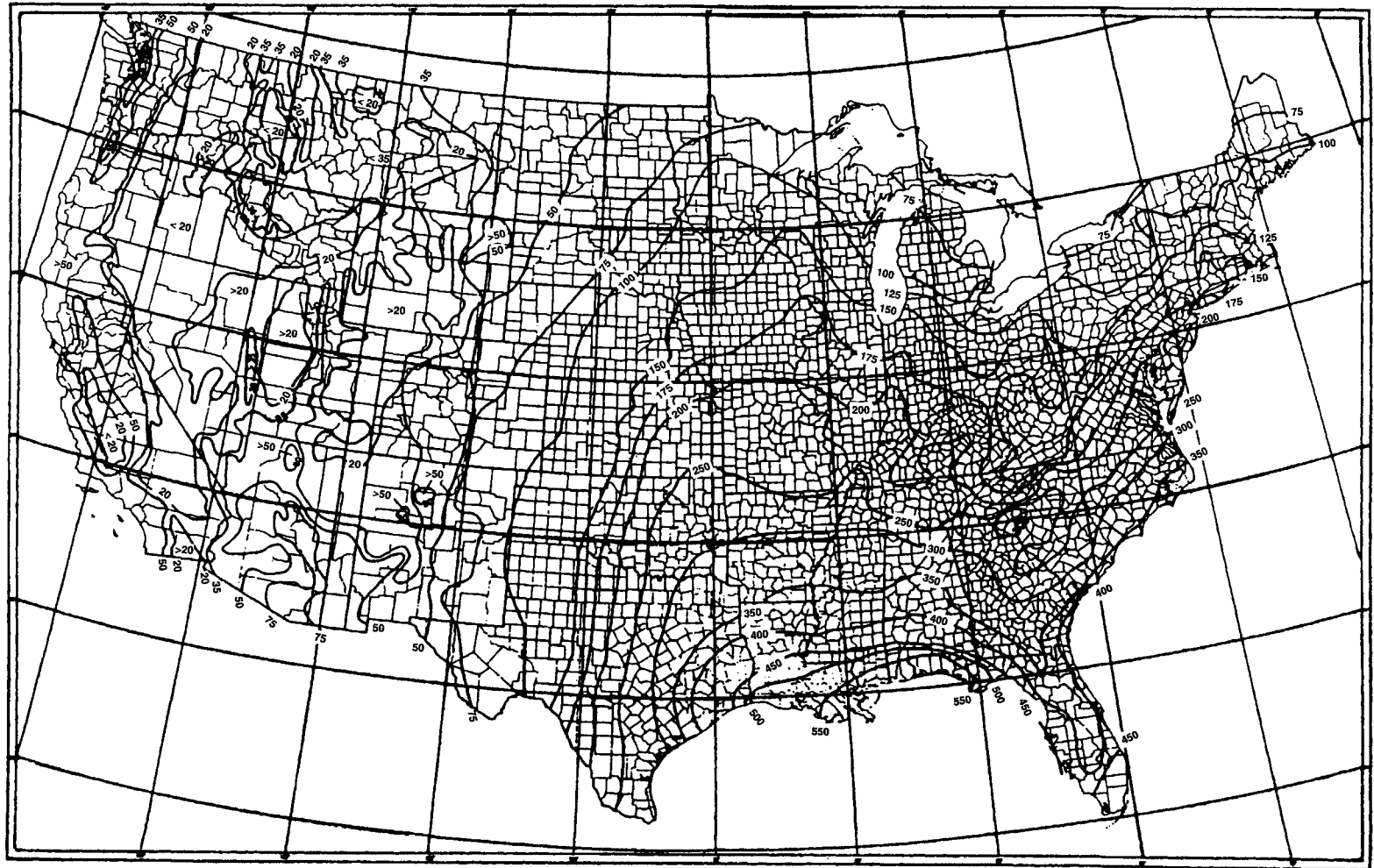


Figure 18.7.1 Average annual values of the rainfall erosion index R (Wischmeier and Smith, 1978).

Table 18.7.2 Cropping Management Factor *C*

Undisturbed forest land							
Percent of area covered by canopy of trees and undergrowth		Percent of area covered by duff at least 2 in deep			Factor <i>C</i>		
100–75		100–90			0.0001–0.001		
70–45		85–75			0.002–0.004		
40–20		70–40			0.003–0.009		

Permanent pasture, range, and idle land*							
Cover that contacts the soil surface							
Vegetative canopy		Percent ground cover					
Type and height†	Type‡	0	20	40	60	80	95 +
No appreciable canopy	G	0.45	0.20	0.10	0.042	0.013	0.003
	W	0.45	0.24	0.15	0.091	0.043	0.011
Tall weeds or short brush with average drop fall height of 20 in	G	0.17–0.36	0.10–0.17	0.06–0.09	0.032–0.038	0.011–0.013	0.003
	W	0.17–0.36	0.12–0.20	0.09–0.13	0.068–0.083	0.038–0.041	0.011
Appreciable brush or bushes, with average drop fall height of 6 1/2 ft	G	0.28–0.40	0.14–0.18	0.08–0.09	0.036–0.040	0.012–0.013	0.003
	W	0.28–0.40	0.17–0.22	0.12–0.14	0.078–0.087	0.040–0.042	0.011
Trees, but no appreciable low brush. Average drop fall height of 13 ft	G	0.36–0.42	0.17–0.19	0.09–0.10	0.039–0.041	0.012–0.013	0.003
	W	0.36–0.42	0.20–0.23	0.13–0.14	0.084–0.089	0.041–0.042	0.011

Construction slopes		
Type of mulch	Mulch rate (tons/acre)	Factor <i>C</i>
Straw	1.0–2.0	0.06–0.20
Crushed stone, 1/4–1.5 in	135	0.05
	240	0.02
	7	0.08
Wood chips	12	0.05
	25	0.02

* The listed *C* values assume that the vegetation and mulch are randomly distributed over the entire area.

† Canopy height is measured as the average fall height of water drops falling from the canopy to the ground. Canopy effect is inversely proportional to drop fall height and is negligible if fall height exceeds 33 ft.

‡ G: cover at surface is grass grass-like plants, decaying compacted duff, or litter at least 2 in deep. W: cover at surface is mostly broadleaf herbaceous plants (as weeds with little lateral-root network near the surface) or undecayed residues or both.

Source: Shen and Julien (1993).

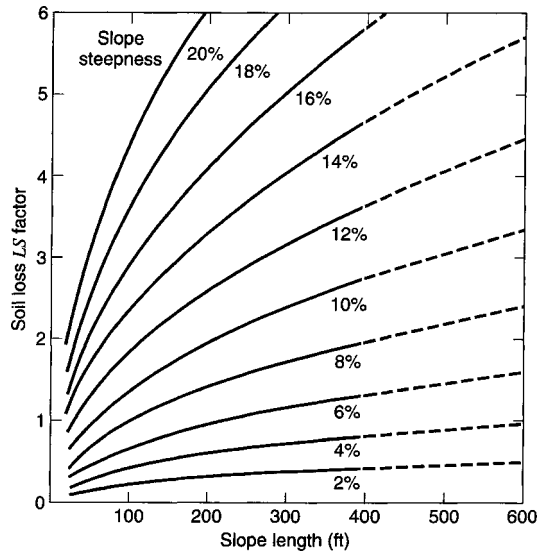


Figure 18.7.2 Topographic-effect graph used to determine *LS*-factor values for different slope-steepness–slope-length combinations (Wischmeier and Smith, 1965).

where λ is the actual slope length in feet, θ is the angle of the slope, and m is an exponent ranging from 0.5 for slopes ≥ 5 percent to 0.2 for slopes ≤ 1 percent. The graphical representation of equation (18.7.4) is presented in Figure 18.7.2.

The *cropping management factor*, C , accounts for the crop rotation, tillage method, crop residue treatment, productivity level, and other cultural practice variables (see Table 18.7.2).

EXAMPLE 18.7.1

Compute soil loss in Phoenix, Arizona for a very fine sand with 0.5 percent organic matter content. $C = 0.006$, $D = 1.5$. $S = 5$ percent, $L = 300$ ft.

SOLUTION

Use equation (18.7.1) to compute the soil loss

$$A = RKLSCD$$

where

$$\begin{aligned} R &= 50 \text{ from Figure 18.7.1} \\ K &= 0.42 \text{ from Table 18.7.1} \\ LS &= 0.928 \text{ from Figure 18.7.2} \\ C &= 0.006 \\ D &= 1.5 \\ A &= RKLSCD \\ &= 50 \times 0.42 \times 0.928 \times 0.006 \times 1.5 \\ &= 0.1754 \text{ ton/acre} \end{aligned}$$

18.8 RESERVOIR SEDIMENTATION

Accumulation of sediment in reservoirs may have the following effects (Shen and Julien, 1993):

1. reducing the useful storage volume for water in the reservoir,
2. changing the water quality near the dam,

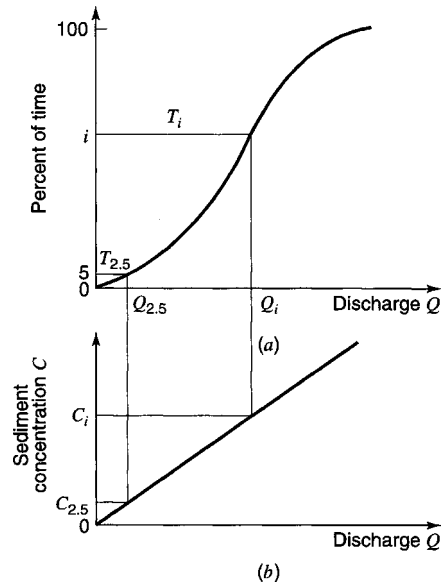


Figure 18.8.1 Flow and sediment discharge (Shen and Julien, 1993).

3. increasing flooding level upstream of the dam because of sediment aggradation,
4. influencing the stability of the stream downstream of the dam,
5. affecting stream ecology in the dam region, and
6. causing other environmental impacts by changing the water quality.

This section briefly outlines a method that can be used to estimate the potential sediment accumulation in a reservoir.

Step 1 Construct a *flow duration curve*, which is the cumulative distribution curve of stream runoff passing the dam (see Figure 18.8.1a).

Step 2 Construct a *sediment rating curve*, which relates sediment concentration to stream discharge (see Figure 18.8.1b).

Step 3 Divide the flow duration curve into equally spaced sections of percentage, Δp (e.g., 20 sections, $\Delta p = 0.05$). Read average discharge, Q_i , from the flow duration curve. Read the corresponding sediment concentration, C_i , from the sediment rating curve. Repeat for each of the sections.

Step 4 Compute the average total sediment load in weight per unit time, q_t , using

$$\begin{aligned} q_t &= \sum_i C_i Q_i \Delta p \\ &= \Delta p \sum_i C_i Q_i \end{aligned} \quad (18.8.1)$$

Step 5 Determine the percentage of sediment trapped in the reservoir, which is a function of the fall velocity of sediment and the allowable time for settling. The more important factors to determine the amount of sediment trapped include the relative size of the reservoir, the reservoir shape, the reservoir operation, and the sediment particle size. Brune (1953) developed a commonly used relation for determining sediment trapping, as illustrated in Figure 18.8.2. *Trap efficiency* is the ratio between sediment trapped in the reservoir and the total sediment entering the reservoir. Reservoir capacity is the reservoir volume at the normal operation pool level for the period considered.

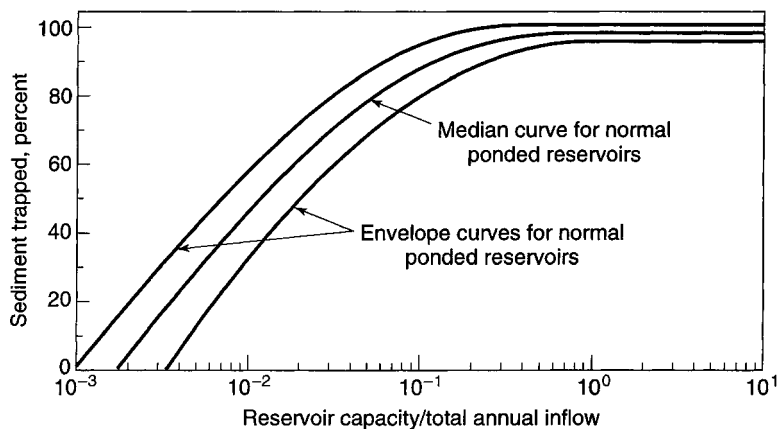


Figure 18.8.2 Sediment trap efficiency in a reservoir (after Brune, 1953) (from Shen and Julien, 1993).

The U.S. Bureau of Reclamation (1987) classifies reservoir operation according to the following:

Operation	Reservoir operation
1	Sediment always submerged or nearly submerged
2	Normally moderate to considerable reservoir drawdown
3	Reservoir normally empty
4	Riverbed sediments

The selection of the proper operation number can usually be made from the operation study prepared for the reservoir. The density of the sediment deposits is estimated using:

$$W = W_c P_c + W_m P_m + W_s P_s \tag{18.8.2}$$

where W is the unit weight in lb/ft^3 (or density in kg/m^3); P_c , P_m , and P_s are the percentages of clay, silt, and sand, respectively, of the inflowing sediment; and W_c , W_m , and W_s are the coefficients of unit weight for clay, silt, and sand, respectively, in lb/ft^3 (kg/m^3), obtained from Table 18.8.1.

Table 18.8.1 Reservoir Operation Number

Operation	Initial weight (initial mass in lb/ft^3 (kg/m^3))		
	W_c	W_m	W_s
1	26 (416)	70 (1120)	97 (1550)
2	35 (561)	71 (1140)	97 (1550)
3	40 (641)	72 (1150)	97 (1550)
4	60 (961)	73 (1170)	97 (1550)

Source: Yang (1996).

EXAMPLE 18.8.1

Determine the density of sediment deposits for a reservoir operation 2 with 23 percent clay, 40 percent silt, and 37 percent sand.

SOLUTION

$$\begin{aligned}
 W &= W_c P_c + W_m P_m + W_s P_s \\
 &= 561(0.23) + 1140(0.40) + 1550(0.37) \\
 &= 1158 \text{ kg/m}^3
 \end{aligned}$$

Table 18.8.2 *K* Values of Sand, Silt, and Clay

Reservoir operation	<i>K</i> for inch-pound units (metric units)		
	Sand	Silt	Clay
1	0	5.7 (91)	16 (256)
2	0	1.8 (29)	8.4 (135)
3	0	0 (0)	0 (0)

Source: Yang (1996).

Miller (1953) developed an approximation for the average density of sediment deposited, W_T , in T years as follows:

$$W_T = W_0 + 0.4343K \left[\frac{T}{T-1} (\ln T) - 1 \right] \quad (18.8.3)$$

where W_0 is the initial unit weight (density) derived from equation (18.8.2) and K is a constant based on the type of reservoir operation and sediment size analysis. K is expressed as:

$$K = K_c P_c + K_m P_m + K_s P_s \quad (18.8.4)$$

where K_s , K_m , and K_c are found in Table 18.8.2.

EXAMPLE 18.8.2

For data given in Example 18.8.1, determine the average density of sediments deposited after 100 years.

SOLUTION

First determine K :

$$\begin{aligned} K &= K_c P_c + K_m P_m + K_s P_s \\ &= 0(0.23) + 29(0.40) + 135(0.37) \\ &= 62 \end{aligned}$$

Determine W_{100} using equation (18.8.3):

$$\begin{aligned} W_T &= W_0 + 0.4343K \left[\frac{T}{T-1} (\ln T) - 1 \right] \\ &= 1158 + 0.4343(62) \left[\frac{100}{100-1} (\ln 100) - 1 \right] \\ &= 1256.3 \text{ kg/m}^3 \end{aligned}$$

18.9 STREAM STABILITY AT HIGHWAY STRUCTURES

18.9.1 Factors that Affect Stream Stability

The factors that affect stream stability and potentially bridge stability at highway stream crossings can be classified as geomorphic factors and hydraulic factors. FHWA Hydraulic Engineering Circular (HEC) No. 20 (Lagasse et al., 2001a) presents detailed descriptions of the various factors and how they affect stream stability. Much of the material presented in this section is adapted from HEC No. 20.

18.9.2 Basic Engineering Analysis

FHWA HEC No. 20 recommends a three-level procedure for analyzing stream stability:

Level 1 Qualitative and Other Geomorphic Analysis

Step 1 Stream characteristics

Step 2 Land use changes

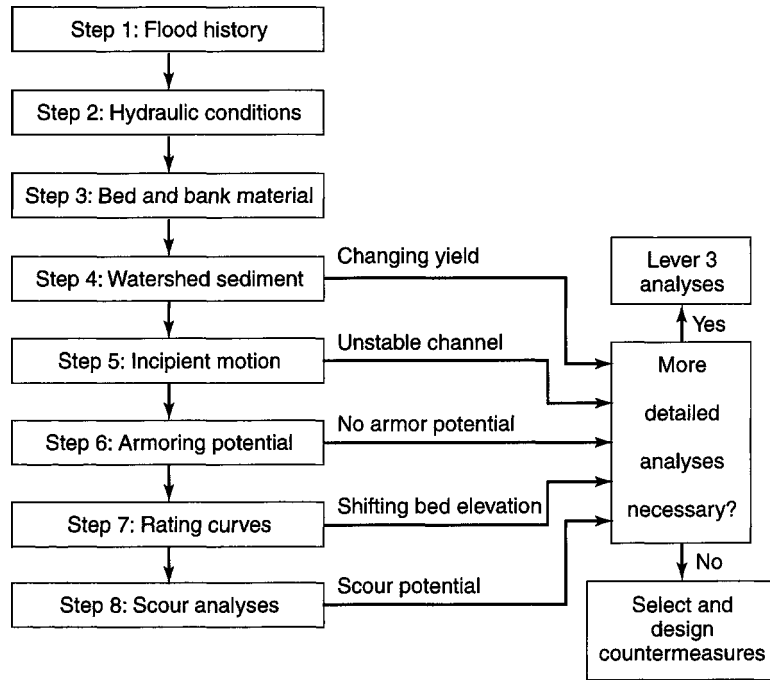


Figure 18.9.1 Flow chart for Level 2: Basic Engineering Analyses (from Lagasse et al., 2001a).

Step 3 Overall stability

Step 4 Lateral stability

Step 5 Vertical stability

Step 6 Stream response

Level 2 Basic engineering analysis (steps illustrated in Figure 18.9.1)

Level 3 Mathematical and physical model studies

The remaining discussion will focus on the steps in Level 2, basic engineering analysis. Evaluating the flood history (Step 1) is an integral step in characterizing watershed response and morphologic evaluation, particularly in arid regions. It is important to study flood records and corresponding stream responses using aerial photography or other physical information. Development of the rainfall-runoff relation is important in understanding watershed conditions and historical changes in the watershed.

To evaluate the hydraulic conditions (Step 2), it is common practice to compute water surface profiles and hydraulic conditions using a computer code. For the analysis and design of bridge crossings, the U.S. Dept. of Transportation Federal Highway Administration (1990) WSPRO computer program is recommended because the computational procedure for evaluating bridge losses is superior to other models such as the U.S. Army Corps of Engineers HEC-2 and HEC-RAS River Analysis System (see Section 5.4.3). The input structure for WSPRO was specifically developed to facilitate bridge design.

Step 3 involves performing an analysis of the bed and bank materials to determine particle size gradation and other properties and a shape, fall velocity, and so on (see Section 18.1).

Step 4 involves evaluating the watershed sediment yield using a method such as the universal soil loss equation (USLE) (see Section 18.7).

Step 5 involves performing an *incipient motion analysis* to evaluate the relative channel stability. Incipient motion was defined in Section 18.3. For most river conditions, the following equation

derived from the Shields diagram can be used (Lagasse et al., 2001a):

$$D_c = \frac{\tau}{0.047(\gamma_3 - \gamma)} \quad (18.9.1)$$

where D_c is the diameter of the sediment particle at incipient motion condition in meters; τ is the boundary shear stress in N/m^2 (pa); γ_3 and γ are the specific weights of the sediment and water, respectively in N/m^3 ; and 0.047 (for sand bed channels) is the dimensionless coefficient often referred to as Shields critical parameter.

Step 6 involves evaluating the *armoring potential*. Armoring is the natural process whereby an erosion-resistant layer of relatively large particles is formed on a streambed because of the removal of finer particles by the stream flow. An armoring layer that is sufficient to protect the bed against moderate discharges can be disrupted during high discharges and then may be restored as flows diminish. By determining the percentage of bed material equal to or larger than the armor size, D_c , computed using equation (18.9.1) for incipient motion, the depth of scour necessary to establish an armor layer can be determined using the following (Pemberton and Lara, 1984):

$$y_s = y_a \left[\frac{1}{P_c} - 1 \right] \quad (18.9.2)$$

where y_a is the thickness of the armoring layer and P_c is the decimal fraction of material coarser than the armoring size. y_a ranges from one to three times the armor size, P_c , depending on the value of D_c (Lagasse et al., 2001a). Stable armoring conditions require a minimum of the layer of armoring particles.

Step 7 involves evaluating stage-discharge rating curve shifts. Scour and fill is the most common cause of rating curve shifts. Rating curves that continually shift indicate channel instability.

Step 8 involves evaluating the scour condition at bridge crossings. Section 18.10 provides a detailed description of procedures based upon the FHWA-HEC No. 18 (Richardson and Davis, 2001). Calculation of the three components of scour (local scour, contraction scour, and aggradation/degradation) quantifies the potential instability at a bridge crossing.

Once the above steps have been completed, if a more detailed analysis is needed, Level 3 analysis is performed. In Level 3 analysis, mathematical and/or physical models are used to evaluate and assess the stream stability. If a more detailed analysis is not needed, countermeasures are selected and designed. Historically, the need for a Level 3 analysis has been for high-risk locations and for extraordinarily complex problems; however, because of the importance of stream stability to the safety and integrity of bridges, Level 3 analysis should be computed routinely according to Lagasse et al. (2001a).

18.9.3 Countermeasures (Flow Control Structure) for Stream Instability

Countermeasures are measures incorporated into a highway stream crossing system to monitor, control, inhibit, change, delay, or minimize stream and bridge stability problems or action plans for monitoring structures during and/or after flood events (Lagasse et al., 2001a). Selection of a countermeasure for a bank erosion problem depends on the erosion mechanism, stream characteristics, construction and maintenance requirements, potential for vandalism, and costs.

Of particular interest in this section are *flow control structures*, which are defined as structures, either within or outside a channel, that act as countermeasures by controlling the direction, velocity, or depth of flowing water (Richardson et al., 1990, 2001). These types of structures are also referred to as *river training works*. Figure 18.9.2 shows various types of flow control structures.

18.9.4 Spurs

Spurs are structures or embankments that are projected into streams at an angle in order to deflect flowing water away from critical zones, to prevent erosion of the banks, and to establish a more

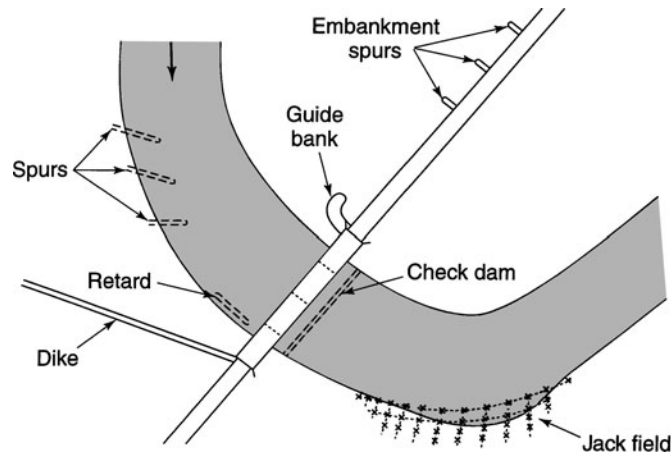


Figure 18.9.2 Placement of flow control structures relative to channel banks, crossing, and floodplain. Spurs, retards, dikes, and jack fields may be either upstream or downstream from the bridge (from Brice and Blodgett, 1978).

desirable channel alignment or width (Richardson et al., 1990, 2001). Spurs have several functions:

1. to protect highway embankments that form approaches to bridge crossings,
2. to channelize wide, poorly defined streams into well-defined channels,
3. to establish and maintain new alignments through deposition of sediments, and
4. to halt meander migration at banks.

Spurs are classified as retarder spurs, retarder/deflector spurs, and deflector spurs, based on their permeability, which is defined as the percentage of the spur surface area facing the streamflow that is open. Accordingly, *retarder spurs* are permeable and function by retarding flow velocities near stream banks. *Retarder/deflector spurs* are permeable and function by retarding flow velocities at stream banks and direct flow away from the banks. *Deflector spurs* are impermeable, basically deflecting flow currents away from banks.

18.9.5 Guide Banks (Spur Dikes)

Guide banks (spur dikes) are placed at or near the ends of approach embankments to guide the streamflow through a bridge opening. They are used to prevent erosion of the approach embankments by cutting off the flow adjacent to the embankment. By guiding flow through the opening, they transfer scour away from abutments. Guide banks reduce separation of flow at the upstream abutment face and reduce abutment scour as a result of less turbulence at the abutment face.

Figure 18.9.3 illustrates a typical guide bank plan view. Figure 18.9.4 can be used to determine guide bank length, L_s , for designs greater than 15 m and less than 75 m. Lagasse et al. (2001a) recommend 15 m as the minimum length of guide banks; if the figure indicates length larger than 75 m, the design should be set at 75 m. FHWA practice has shown that a standardized length of 46 m has performed well (Lagasse et al., 2001a). Other guidelines for design include the following:

- A minimum freeboard of 0.6 m above the design water surface elevation should be used.
- Generally, top widths of 3 to 4 m are used.
- The upstream end of the guide bank should be round-nosed.
- Side slopes should be 1V:2H or less.
- Rock riprap should be placed on the stream side face and around the end of the guide bank.
- A gravel, sand, or fabric filter may be required to protect the underlying embankment material.

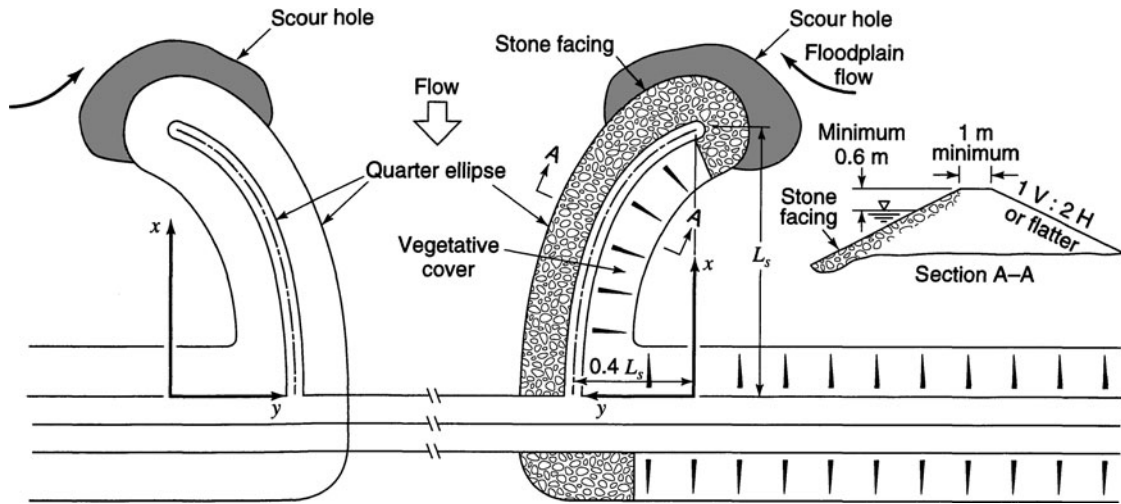


Figure 18.9.3 Typical guide bank (modified from Bradley, 1978) (as presented in Lagasse et al., 2001a).

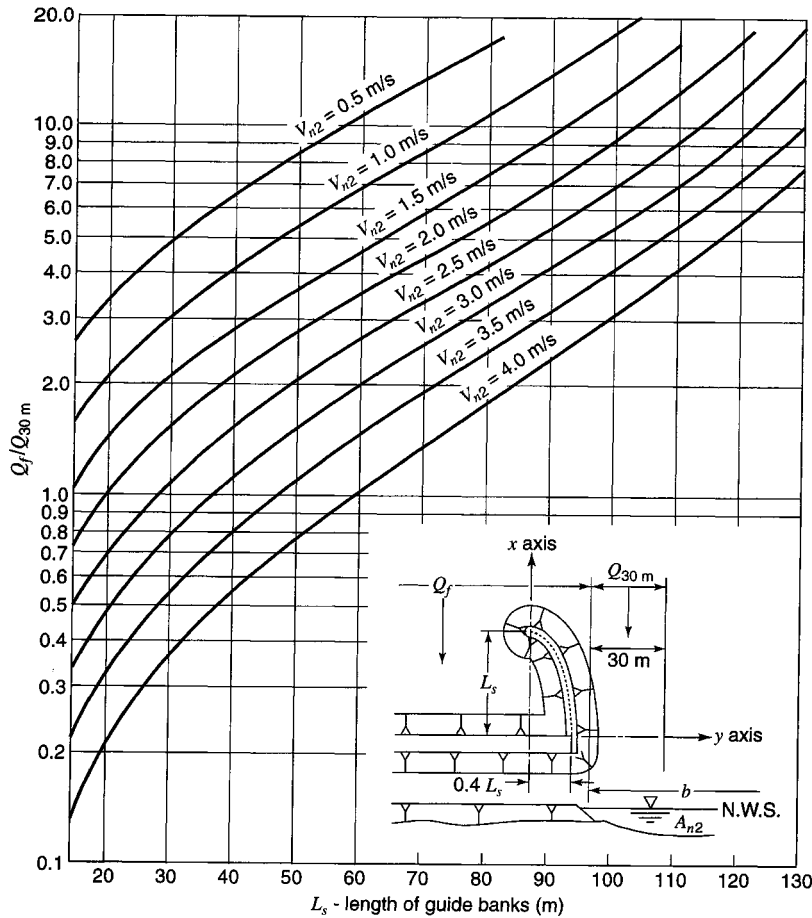


Figure 18.9.4 Nomograph to determine guide bank length (after Bradley, 1978) (as presented in Lagasse et al., 2001a).

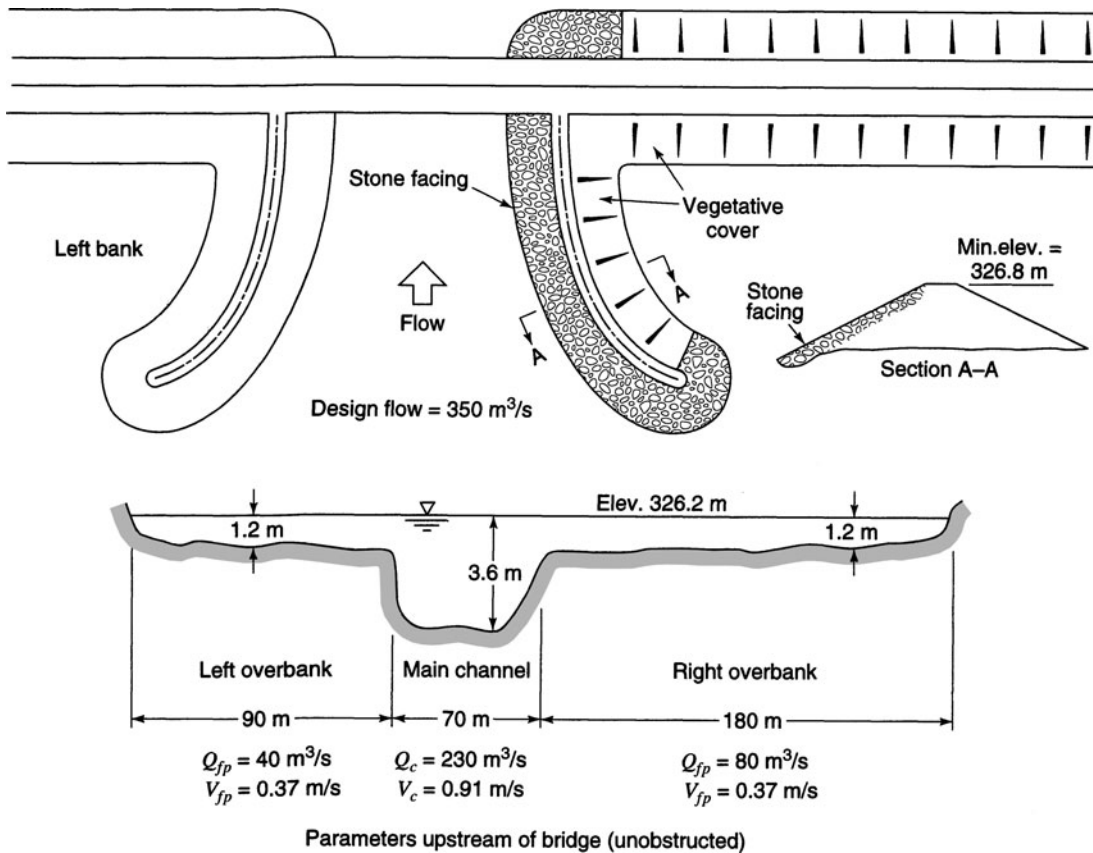


Figure 18.9.5 Example guide bank design (from Lagasse et al., 2001a).

Refer to Lagasse et al. (2001a) for more detailed design concerns.

To use Figure 18.9.4, the following parameters are needed:

- Q_f = the lateral or floodplain discharge of either floodplain intercepted by the embankment (m³/s)
- Q_{30m} = the discharge in 30 m of stream adjacent to the abutment (m³/s)
- Q = the total discharge of the stream (m³/s)
- A_{n2} = the cross-sectional flow area at the bridge opening at normal stage (m²)
- $V_{n2} = Q/A_{n2}$ = the average velocity through the bridge opening (m/s)
- Q_f/Q_{30m} = the guide bank discharge ratio

An example guide bank design is presented in Figure 18.9.5. Parameters upstream of the bridge are shown in the figure.

18.9.6 Check Dams (Channel Drop Structures)

Check dams or channel drop structures are downstream of highway crossings to arrest head cutting and to maintain stable streambed elevation in the vicinity of the bridge. They are typically constructed of rock riprap, concrete, sheet piles, gabions, or treated timber piles. Figure 18.9.6 shows a typical vertical drop structure with a free overfall.

Pemberton and Lara (1984) recommended the following equation to estimate the depth of scour downstream of a vertical drop:

$$d_s = KH_t^{0.225} q^{0.54} - d_m \quad (18.9.3)$$

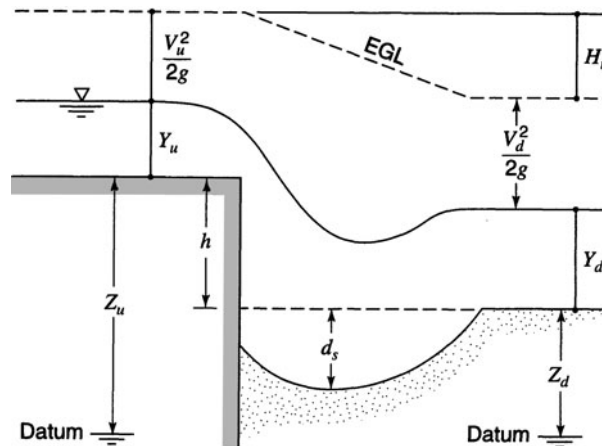


Figure 18.9.6 Schematic of a vertical drop caused by a check dam (from Lagasse et al., 2001a).

where d_s is the local scour depth for a free overfall, measured from the streambed downstream of the drop in meters; q is the discharge per unit width in $\text{m}^3/\text{s}/\text{m}$; H_t is the total drop in head, measured from the upstream to the downstream energy grade line in meters; d_m is the tail water depth in meters; and $K = 1.90$. Equation (18.9.3) is independent of grain size of the bed material and acknowledges that the bed will scour regardless of the type of material.

Based upon the energy equation,

$$H_t = \left(Y_u + \frac{V_u^2}{2g} + Z_u \right) - \left(Y_d + \frac{V_d^2}{2g} + Z_d \right) \quad (18.9.4)$$

where Y is the depth in meters; V is the velocity in m/s ; Z is the bed elevation in meters; and g is the acceleration due to gravity (9.81 m/s^2). Subscript u and d refer to upstream and downstream of the channel drop, as shown in Figure 18.9.6.

EXAMPLE 18.9.1

Determine the depth of scour for the following hydraulic parameters. Design discharge = $167 \text{ m}^3/\text{s}$; channel width = 32 m ; $Y_u = 3.22 \text{ m}$; $d_m = 2.9 \text{ m}$; $Y_d = 2.9 \text{ m}$; unit discharge (q) = $5.22 \text{ m}^3/\text{s}/\text{m}$; $V_u = 1.62 \text{ m/s}$; $V_d = 1.80 \text{ m/s}$; drop height (h) = 1.4 m .

SOLUTION

Compute H_t using equation (18.9.2):

$$\begin{aligned} H_t &= \left(3.22 + \frac{1.62^2}{2(9.81)} + 1.4 \right) - \left(2.9 + \frac{1.80^2}{2(9.81)} + 0 \right) \\ &= 1.69 \text{ m} \end{aligned}$$

Compute d_s using equation (18.9.3):

$$\begin{aligned} d_s &= 1.90(1.69)^{0.225}(5.22)^{0.54} - 2.9 \\ &= 2.3 \text{ m} \end{aligned}$$

The unsupported height of the structure is $h + d_s = 3.7 \text{ m}$.

18.10 BRIDGE SCOUR

Bridge scour is the erosion or removal of streambed or bank material from bridge foundations caused by flowing water, usually considered as long-term bed degradation caused by contraction scour and local scour. Much of the material in this section has been adapted from the FHWA, Hydraulic Engineering Circular No. 18 by Richardson and Davis (2001).

Before applying the various methods for estimating scour, it is necessary to

1. determine the fixed-bed channel hydraulics,
2. determine the long-term impact of degradation or aggradation on the bed profile,
3. if degradation occurs, adjust the fixed-bed hydraulics to reflect this change, and
4. compute the bridge hydraulics (Richardson and Davis, 2001).

The seven steps recommended in “Evaluating Scour at Bridges,” FHWA Hydraulic Engineering Circular No. 18 (Richardson and Davis, 2001) are:

1. Determine the scour analysis variables.
2. Analyze long-term bed elevation change.
3. Evaluate the scour analysis method.
4. Compute the magnitude of contraction scour.
5. Compute the magnitude of local scour of pier.
6. Compute magnitude of local scour at abutments.
7. Plot and evaluate the total scour depths.

Many of the hydraulic variables used in estimating scour can be obtained from computer models for water profile computation such as WSPRO developed by the U.S. Department of Transportation (1990).

The following definitions are from the FHWA Hydraulic Engineering Circular No. 18 by Richardson and Davis (2001).

Aggradation and degradation are long-term streambed elevation changes due to natural or man-induced causes. These changes can affect the reach of the river on which the bridge is located. Aggradation involves the deposition of material eroded from the channel or watershed upstream of the bridge, whereas degradation involves the lowering or scouring of the streambed because of a deficit in sediment supply from upstream.

Contraction scour in a natural channel or at a bridge crossing involves the removal of material from the bed and banks across all or most of the channel width. This component of scour can result from a contraction of the flow area, an increase in discharge at the bridge, or both. It can also result from a change in downstream control of the water surface elevation. The scour is the result of increased velocities and shear stress on the channel bed. Contraction of the flow by bridge approach embankments encroaching onto the floodplain and/or into the main channel is the most common cause of contraction scour. Contraction scour can be either clear-water or live-bed.

Live-bed contraction scour occurs when there is transport of bed material in the approach reach, whereas *clear-water contraction scour* occurs when there is no bed material transport in the approach reach or the bed material being transported in the upstream reach is so fine that it washes through the contracted section. Live-bed contraction scour typically occurs during the rising stage of a runoff event, whereas refilling of the scour hole occurs during the falling stage. Also, clear-water scour at low or moderate flows can change to live-bed scour at high flows. This cyclic nature creates difficulties in measuring contraction scour after a flood event.

Local scour involves removal of material from around piers, abutments, spurs, and embankments. It is caused by an acceleration of flow and resulting vortices induced by the flow obstructions. Local scour can also be either clear-water or live-bed scour. Live-bed local scour is cyclic in nature; that is, the scour hole that develops during the rising stage refills during the falling stage.

Lateral stream migration of the main channel of a stream within a floodplain may increase pier scour, erode abutments or the approach roadway, or change the total scour by changing the flow angle of attack at piers. Factors that affect lateral stream movement also affect the stability of a bridge. These factors are the geomorphology of the stream, location of the crossing on the stream, flood characteristics, and the characteristics of the bed and bank materials.

PROBLEMS

18.1.1. Given a sample of sand with D_{50} of 0.205 mm and sand density of $2,650 \text{ kg/m}^3$, with ν being $1.308 \times 10^{-6} \text{ m}^2/\text{s}$, compute fall velocity and plot the velocity with time.

18.1.2 A coarse sand has a mean particle diameter of 1.0 mm and a density of 2.70 g/cm^3 . Compute the fall velocity.

18.1.3 Water carrying a solid material such as fine silt or clay has a specific weight different from the specific weight of clear water. In other words, the suspended material and water act as if they are combined. Derive an expression for the specific weight of the mixture, γ_m , in terms of the specific weights of the solid, γ_s , and the water, γ , and the volumes of the mixture, V_m , the solid, V_s , and the water, V_w . Also express specific weight of the mixture, γ_m , in terms of γ_s , γ , and the concentration (fraction by weight) of the suspended sediment, C_s .

18.1.4 Using your results of solving Problem 18.1.3, determine the specific weight of the sediment-water mixture that was obtained during a sampling program on a river. The following are known: the concentration (fraction by weight) of the suspended sediment, $C_s = 20$ percent by weight and $\gamma_s = 2.7$ metric tons/ m^3 (1 metric ton = 1000 kg).

18.1.5 For the sieve analysis data in Table 18.1.2, determine D_{90} , D_{65} , D_{50} , and D_{35} .

18.1.6 Using the data in Table 8.1.2, assume that the particles of size finer than 0.4 mm are washed away by a flood. Compute D_{50} and D_{35} .

18.1.7 The geometric mean diameter, D_g , and the geometric mean standard deviation, σ_g , can be expressed in terms of $D_{84.1}$ and $D_{15.9}$. $D_g = (D_{84.1}D_{15.9})^{1/2}$ and $\sigma_g = (D_{84.1}/D_{15.9})^{1/2}$. For the data in Figure 18.1.1 and Table 18.1.2, determine the geometric mean diameter and the geometric mean standard deviation.

18.1.8 For the data in Figure 18.1.1, draw a straight line between the 84.1 percent finer size ($D_{84.1}$) and the 15.9 percent finer size ($D_{15.9}$). This represents the distance between plus and minus one standard deviation from the mean. In terms of the geometric mean standard deviation, σ_g , the distance is plus or minus one times $\log \sigma_g$. Intersection of the straight line with the 50 percent finer ordinate is the geometric mean sieve diameter, D_g . Intersection of the curve connecting the data points and the 50 percent finer ordinate is the median size D_{50} . Show an illustration of this analysis on Figure 18.1.1.

18.2.1 Compute the Manning's roughness factor for the streambed and banks for a $D_{50} = 2$ mm.

18.2.2 Compute the Manning's roughness factor for the streambed and banks for the stream with the sieve analysis data in Table 18.1.2.

18.3.1 A fine sand particle with a mean size of 0.25 mm forms the bed of a wide rectangular channel with a depth of 5.0 m and a slope of 0.0003. ν is $1.308 \times 10^{-6} \text{ m}^2/\text{s}$, $\gamma_s/\gamma = 2.7$. Compute the critical shear stress and the actual shear stress, and explain what will happen under this flow condition.

18.3.2 Find the critical shear stress for a medium sand with $D_{50} = 0.4$ mm and for a medium gravel with $D_{50} = 12$ mm in a wide

rectangular channel with a depth of flow of 1.0 m and bottom slope of 0.002. What will happen to the sand and gravel under these conditions?

18.3.3 For the channel in Problem 18.3.2, the depth of flow is 5.0 m. What will happen to the sand and gravel under these conditions?

18.3.4 A stream is considered as a wide rectangular channel having a slope of 0.0025. Determine the depth at which sediment motion begins for a fine gravel with $D_{50} = 5$ mm.

18.3.5 A stream is considered as a wide rectangular channel having a slope of 0.001. Determine the depth at which sediment motion begins for a fine gravel with $D_{50} = 4$ mm.

18.4.1 Using the Meyer-Peter and Muller formula, compute the sediment discharge per unit width for a rectangular channel with the following characteristics:

Water depth: 12 ft

Total flow rate: $8500 \text{ ft}^3/\text{s}$

Channel surface width: 170 ft

D_{50} and D_{90} : 2.0 mm and 2.9 mm, respectively

Gradation coefficient: 1.4

Manning's resistance coefficient for the channel bed and the channel walls is 0.04 and 0.058, respectively.

Friction slope: 0.0003 ft/ft

Effective mean diameter of sediment $D_m = 2.1$ mm

18.4.2 Compute the sediment discharge per unit width for the Colorado River at Taylor's Ferry for a depth of 8 ft and a flowrate of 32 cfs/ft width using the DuBoys formula.

18.5.1 For a certain river with total water depth of 4.30 m and mean flow velocity of 1.0 m/s, calculate and plot the vertical suspended sediment concentration profile for the D_{50} sediment size in mg/l. Given $D_{50} = 0.00026$ m, falling velocity of the sediment particle is 0.04 m/s, kinematics viscosity of a fluid is $10^{-6} \text{ m}^2/\text{s}$, and the concentration just above the bed is 666,000 mg/l.

18.6.1 Using Colby's formula, compute the sediment discharge per unit width for the rectangular channel described in Problem 18.4.1. Assume $D_{50} = 0.8$ mm.

18.6.2 Using Yang's gravel formula, calculate total bed-material discharge for a channel with total water flow = $331.39 \text{ m}^3/\text{s}$, surface water width = 150.4 m, water depth = 2.39 m, $D_{50} = 0.32$ mm, $\nu = 1.16 \times 10^{-6} \text{ m}^2/\text{s}$, particle falling velocity = 0.096 m/s, mean flow velocity = 1.05 m/s, and friction slope = 0.0003 m/m.

18.8.1 Using Table 18.8.1, determine the density of sediment deposits for a reservoir operation 1 with 33 percent clay, 40 percent silt, and 27 percent sand.

18.8.2 For data given in Problem 18.8.1 and Table 18.8.2, determine the average density of sediments deposited after 150 years.

18.9.1 Determine the unsupported height of the structure by using the following hydraulic parameters: design discharge = $210 \text{ m}^3/\text{s}$, channel width = 42 m, $Y_u = 5.2$ m, $Y_d = 4.7$ m, drop height = 1.5 m.

REFERENCES

- Ackers, P., and W. R. White, "Sediment Transport: New Approach and Analysis," *Journal of Hydraulic Engineering*, vol. 99, no. HY-11, pp. 2041-2060, 1973.
- American Society of Civil Engineers (ASCE), "Nomenclature for Bed Forms in Alluvial Channels," Task Force on Bed Forms in Alluvial Channels, John F. Kennedy, Chmn, *Journal of the Hydraulics Division*, ASCE, vol. 92, no. HY3, Proc. Paper 4823, pp. 51-64, May 1966.
- Bradley, J. N., "Hydraulics of Bridge Waterways," Hydraulic Design Series No. 1, Federal Highway Administration, U.S. Department of Transportation, Washington, D.C., 1978.
- Brady, N. S., *The Nature and Properties of Soils*, 8th edition, Macmillan, New York, 1974.
- Brice, J. C., and J. C. Blodgett, "Countermeasures for Hydraulic Problems at Bridges," vol. 1, Analysis and Assessment, FHWA/RD-78-162, Federal Highway Administration, U.S. Department of Transportation, Washington, D.C., 1978.
- Brune, G. M., "Trap Efficiency of Reservoirs," *Trans. Am. Geophys. Union*, vol. 34, no. 3, pp. 407-418, 1953.
- Chow, V. T., *Open Channel Hydraulics*, McGraw-Hill, New York, 1959.
- Colby, B., "Practical Computations of Bed Material Discharge," *Journal of Hydraulic Engineering*, vol. 90, no. HY2, pp. 217-246, 1964.
- deVries, J., "Altgermanische Religionsgeschichte," Berlin, Germany, 1970.
- DuBoys, P., "The Rhone and Streams with Movable Beds," *Annales des ponts et chaussées*, section 5, vol. 18, pp. 141-195, 1879.
- Einstein, H. A., "The Bedload Function for Bedload Transportation in Open Channel Flows," Technical Bulletin No. 1026, U.S.D.A. Soil Conservation Service, 1950.
- Einstein, H. A., and N. L. Barbarossa, "River Channel Roughness," *Trans. ASCE*, vol. 117, pp. 1121-1146, 1952.
- Exner, F. M., "Über die wechselwirkung zwischen wasser und geschiebe in flussen," *Sitzberichte der Academie der Wissenschaften*, Wien, Austria, Sec. IIA, 133:199, 1925.
- Garcia, M., "Sedimentation and Erosion Hydraulics," in *Hydraulic Design Handbook* edited by L. W. Mays, McGraw-Hill, New York, 1999.
- Goldstein, S., "The Steady Flow of Viscous Fluid Past a Fixed Spherical Obstacle at Small Reynolds' Number," *Proceedings of the Royal Society of London*, Series A, vol. 123, 1929.
- Kennedy, J. F., "The Formation of Sediment Ripples, Dunes, and Antidunes," in *Annual Review of Fluid Mechanics* edited by W. R. Sears, vol. 1, Annual Reviews, Inc., Palo Alto, California, pp. 147-168, 1969.
- Lagasse, P. F., F. Schall, F. Johnson, E. V. Richardson, and F. Chang, "Stream Stability at Highway Structure," Federal Highway Administration, U.S. Department of Transportation, Hydraulic Engineering Circular no. 20, Washington, D.C., November, 2001a.
- Lagasse, P. F., L. W. Zewenbergen, J. D. Schall, and P. E. Clapper, "Bridge Scour and Stream Instability Countermeasures," 2nd edition, Federal Highway Administration, U.S. Department of Transportation, Hydraulic Engineering Circular No. 23, FHWA NHI01-003, Washington, D.C., 2001b.
- Laurson, E. M., "Scour at Bridge Crossings," *Journal of the Hydraulics Division*, ASCE, vol. 86, no. 1142, 1960.
- Meyer-Peter, E., and R. Müller, "Formular for Bed-Load Transport," *Proceedings*, International Association for Hydraulic Structures Research, 2nd Meeting, pp. 39-64, Stockholm, Sweden, 1948.
- Miller, C. R., "Determination of the Unit Weight of Sediment for Use in Sediment Volume Computation." U.S. Bureau of Reclamation, Denver, Colorado, 1953.
- Oseen, C., *Hydrodynamik*, Chapter 10, Akademische Verlagsgesellschaft, Leipzig, Germany, 1927.
- Pemberton, E. L., and J. M. Lara, "Computing Degradation and Local Scour," Technical Guideline for Bureau of Reclamation, Engineering Research Center, Denver, Colorado, January 1984.
- Richardson, E. V., and S. R. Davis, "Evaluating Scour at Bridges," 4th edition, Hydraulic Engineering Circular No. 18, Publication No. FHWA NHI 01-001, Federal Highway Administration, U.S. Department of Transportation, Washington, D.C., 2001.
- Richardson, E. V., D. B. Simons, and P. Y. Julien, "Highways in the River Environment," FHWA-HI90-016, Federal Highway Administration, U.S. Department of Transportation, Washington, D.C., 1990.
- Richardson, E. V., D. B. Simons, and P. F. Lagasse, *River Engineering for Highway Encroachments*, Hydraulic Design Series no. 6, Publication no. FHWANHI 01-004, Federal Highway Administration, U.S. Department of Transportation, Washington, D.C., 2001.
- Schwab, G. O., R. K. Frevert, T. W. Edminster, and K. K. Barnes, *Soil and Water Conservation Engineering*, 3rd edition, Wiley, New York, 1981.
- Shen, H. W. and P. Y. Julien, "Erosion and Sediment Transport," in *Handbook of Hydrology* edited by D. R. Maidment, McGraw-Hill, New York, 1993.
- Shields, A., "Anwendung der Aechichkeits-mechanik und der turbulenz forschung auf dir Gerschiebewegung' Mitt Preussische," *Versuchanstalt für Wasserbau and Schiffbau*, Berlin, Germany, 1936.
- Shulits, S., "The Schoklitsch Bed-Load Formula," *Engineering*, London, England, June 21, 1935, pp. 644-646, and June 28, 1935, p. 687.
- Simons, D. B., and F. Sentürk, *Sediment Transport Technology*, Water Resources Publications, Littleton, Colorado, 1977.
- Strickler, A., "Beiträge zur Frage der Geschwindigkeitsformel und der Rauhigkeitszahlen für ströme, Kanäle und geschlossene Leitungen," Mitteilungen des Eidgenössischen Amtes für Wasserwirtschaft 16, Bern, Switzerland, 1923 (translated as "Contributions to the Question of a Velocity Formula and Roughness Data for Streams, Channels, and Closed Pipelines," by T. Roesgan and W. R. Brownie, Translation T-10, W. M. Keck Lab of Hydraulics and Water Resources, California Institute of Technology, Pasadena, California, January 1981).
- U.S. Army Corps of Engineers (USACE), "Scour and Deposition in River and Reservoirs, Users Manual," Hydrologic Engineering Center, Davis, California, 1991.
- U.S. Bureau of Reclamation, *Design of Small Dams*, U.S. Government Printing Office, Denver, Colorado, 1987.
- U.S. Department of Agriculture, Agricultural Research Service (USDA-ARS), "A Universal Equation for Predicting Rainfall-Erosion Losses," USDA-ARS Special Report 22-26, 1961.
- U.S. Department of Transportation, "User's Manual for WSPRO—A Computer Model for Water Surface Profile Computation," Report no. FHWA-IP-89-027, Federal Highway Administration, Washington, D.C., 1990.
- Vanoni, V. A., "Factors Determining Bed Form of Alluvial Streams," *Journal of Hydraulic Engineering*, vol. 100, no. HY3, pp. 363-378, 1974.
- Vanoni, V. A., (editor), *Sedimentation Engineering*, ASCE Manual and Reports on Engineering Practice, no. 54, ASCE, New York, 1975.
- Wischmeier, W. H., and D. D. Smith, "Predicting Rainfall Erosion Losses—A Guide to Conservation Planning," in *USDA Agriculture Handbook 537*, United States Department of Agriculture, Agricultural Research Service, December, 1978.

Wischmeier, W. H., and D. D. Smith, "Predicting Rainfall-Erosion Losses from Cropland East of the Rocky Mountains," *USDA Agriculture Handbook 282*, United States Department of Agriculture, Agricultural Research Service, May, 1965.

Yang, C. T., "Incipient Motion and Sediment Transport," *Journal of Hydraulic Engineering*, ASCE, vol. 99, no. HY10, pp. 1679–1704, 1973.

Yang, C. T., "Unit Stream Power Equation for Gravel," *Journal of Hydraulic Engineering*, ASCE, vol. 110, no. HY12, pp. 1783–1797, 1984.

Yang, C. T., *Sediment Transport: Theory of Practice*, McGraw-Hill, New York, 1996.

Yen, B. C., "Hydraulics for Water Excess Management," in *Water Resources Handbook* edited by L. W. Mays, McGraw-Hill, New York, 1996.

This page intentionally left blank

Chapter 19

Water Resources Management for Sustainability

In Chapter 2, a definition of water resources sustainability is provided along with examples of water resources unsustainability. The concept of sustainability explores the relationship among economic development, environmental quality, and social equity (Rogers et al., 2006). Then sustainable development consists of three components: economic, environmental, and social, also referred to as the triple bottom line. Many definitions, principles, criteria, and indicators have been reported (<http://www.sustainableliving.org>). Based upon the many definitions and criteria, Rogers et al., (2006) define the following three caveats to evaluate each objective of the triple bottom line:

- Economic objectives cannot be maximized without satisfying environmental and social constraints.
- Environmental benefits cannot necessarily be maximized without satisfying economic and social constraints.
- Social benefits cannot be maximized without satisfying economic and environmental constraints.

There are many factors governing sustainable development of water resources. Key ones include poverty, pollution, population, and policy. The three determinants of sustainable development are consumption, production, and distribution (Rogers et al., 2006). This chapter explores water resources management methodologies and tools for water resources sustainability. These include integrated water resources management, water-based sustainable regional development, water law and policies, nonconventional methods and traditional knowledge, water resources systems analysis, and life cycle assessment (LCA).

19.1 INTEGRATED WATER RESOURCES MANAGEMENT FOR SUSTAINABILITY

19.1.1 Principles of Integrated Water Resources Management (IWRM)

Integrated water resources management is a key component in water resources sustainability. Integrated water management may be contemplated in at least three ways (Mitchell, 1990) including: (1) the systematic consideration of the various dimensions of water: surface and groundwater, quality and quantity; (2) the implication that while water is a system it is also a component that interacts with other systems; and (3) the interrelationships between water and social and economic development. In the first thought, the concern is the acceptance that water comprises

an ecological system, which is formed by a number of interdependent components. In the second one, the interactions between water, land, and the environment, which involve both terrestrial and aquatic issues, are addressed. Finally, the concern is with the relationships between water and social and economic development, since availability or lack of water may be viewed as an opportunity for or a barrier against economic development. Each aspect of integrated management depends on and is affected by other aspects.

Integrated water resources management (IWRM) “is still an exception rather than the rule in practice” (Unver, 2007). The principles of IWRM are summarized in Table 19.1.1.

Table 19.1.1 Summary of the Principles of IWRM in Urban Areas

-
- IWRM should be applied at the catchment level.
 - It is critical to integrate water and environmental management.
 - A systems approach should be used.
 - Full participation by all stakeholders, including workers and the community.
 - Attention to social dimensions.
 - Capacity building.
 - Availability of information and the capacity to use it to make policy and predict responses.
 - Full-cost pricing complemented by targeted subsidies.
 - Central government support through the creation and maintenance of an enabling environment.
 - Adoption of the best existing technologies and practices.
 - Reliable and sustained financing.
 - Equitable allocation of water resources.
 - The recognition of water as an economic good.
 - Strengthening the role of women in water management.
-

Source: Industry Sector Report for WSSD prepared by IWA <http://www.grdc.org/uem/water/iwrm/1pager-01.html>.

19.1.2 Integrated Urban Water Management (IUWM): The Big Picture

Integrated urban water management (IUWM) is “a participatory planning and implementation process, based on sound science, which brings together stakeholders to decide how to meet society’s long-term needs for water and coastal resources while maintaining essential ecological services and economic benefits” (US AID Water Team, <http://www.grdc.org/uem/water/iwrm/1pager-1.html>).

According to the US AID Water Team, the principal components of an integrated urban water resources system include:

- *Supply optimization*, including assessments of surface and groundwater supplies, water balances, wastewater reuse, and environmental impacts of distribution and use options.
- *Demand management*, including cost-recovery policies, water use efficiency technologies, and decentralized water management authority.
- *Equitable access* to water resources through participatory and transparent management, including support for effective water users association, involvement of marginalized groups, and consideration of gender issues.
- *Improved policy, regulatory and institutional frameworks*, such as the implementation of the polluter-pays principle, water quality norms and standards, and market-based regulatory mechanisms.
- *Intersectoral approach* to decision-making, combining authority with responsibility for managing the water resource.

The following excerpt on integrated water resources management (IWRM) is from the *Industry Sector Report for World Summit on Sustainable Development (WSSD) prepared by the International Water Association (IWA)* (<http://www.grdc.org/uem/water/iwrm/index.html>).

The fundamental premise is generally accepted that IWRM should be applied at catchment level, recognizing the catchment or watershed as the basic hydrological unit of analysis and management. At implementation level, there is a growing conviction that integrated urban water management (IUWM) could be pursued as a vital component of IWRM within the specific problematic context of urban areas.

Cities are dominant features in the catchments where they occur, and successes in IUWM will make important contributions to the theory and practice of integrated catchment management (ICM) and IWRM in the broader basin context. Thus, IUWM is not seen as a goal in itself, rather a practical means to facilitate one important sub-system of the hydrological basin. IUWM must inter alia endeavour to optimise the interfacing of urban water concerns with relevant activities beyond the urban boundaries, such as rural water supply, down-stream use, and agriculture.

IUWM means that in the planning and operation of urban water management, consideration should be given to the interaction and collective impact of all water-related urban processes on issues such as human health; environmental protection; quality of receiving waters; water demand; affordability; land and water-based recreation; and stakeholder satisfaction. In addition, IUWM requires involvement by stakeholders such as those responsible for water supply and sanitation services, storm water and solid waste management, regulating authorities, householders, industrialists, labor unions, environmentalists, downstream users, and recreation groups. While local authorities are well placed to initiate and oversee IWRM/IUWM programs, planning and implementation should be driven by a combination of top-down regulatory responsibility and bottom-up user needs/obligations. Top-heavy governmental approaches are to be discouraged because they become bureaucratic and unresponsive to the concerns of water users.

A Word on Integration

Integration has many meanings in the water management context (Cabrera and Lund, 2002). Integrated water management involves many aspects of integration: *sources* (multiple water sources considered?); *variability of sources* (planning for entire range of wet to dry conditions?); *supply and demand aspects* (water supply augmentation, water supply conservation/demand management, etc. considered?); *sources and sinks* (wastewater a source, reuse potential, etc.); *scale* (user local, city, regional levels jointly considered?); *responsibility, coordination, and implementation* (water users, water supply, water treatment and delivery, wastewater collection and treatment, stormwater management, flood control management considered together by one entity?). This list is only partially complete as many other aspects are involved.

Ideally, integrated urban water management would be integrated across all these aspects; it is usually impossible to have a completely integrated urban water management. However, there remains considerable realizable potential for improving urban water management through a better “integrated” consideration of the various aspects and options. Truly integrated urban water management is practically impossible whether it is in a developed region such as the southwestern United States or in developing regions in MENA (Middle East and North Africa).

19.1.3 Water-Based Sustainable Regional Development

To quote Unver (2007), “*Water-based sustainable regional development* implies the holistic development of a region by mobilizing its water resources along with harmonious and complementary development and management in other relevant sectors and areas in a sustainable manner.” Three sets of variables: *scope* (the breadth), *scale* (the size), and *governance* (soft aspects of development) define the domain of water-based regional development. Within the scope of regional development, Unver (2007) uses water-based social and economic development. The water resources sectors include water

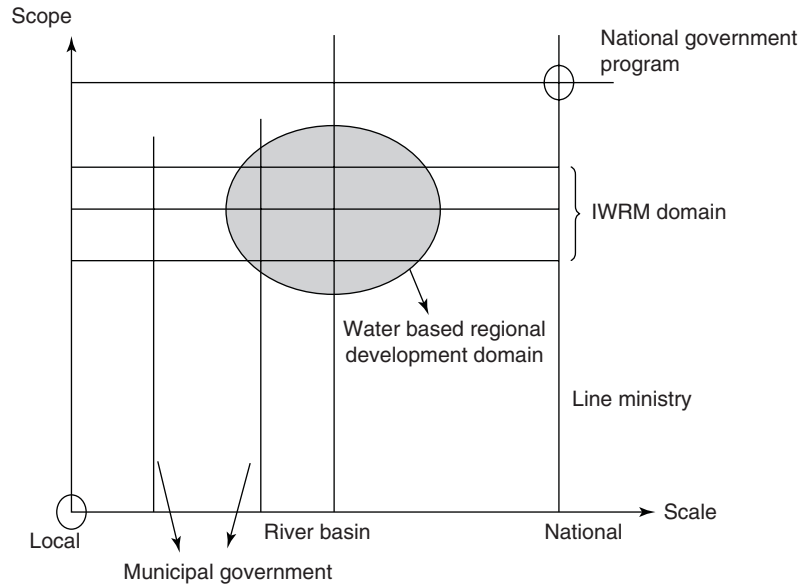


Figure 19.1.1 Water-based sustainable regional development domain. (Courtesy of Unver. (2007))

supply, irrigation, flood and drought mitigation, and hydropower, among others. Other peripheral sectors include transportation, land-use planning, trade and industry, and education. Scale ranges from local to national and intermediate zones more relevant to water-based regional development. Integrated water resources management has the river basin as the territorial jurisdiction whereas water-based regional development typically would not; however, it could. The scale could be determined by administrative division, social-cultural boundaries, geography, economy, ecology or other related factors. The governance is what would enhance the sustainability base of the regional development, comprising the public sector, the business community, and the people.

Figure 19.1.1 shows the relationships between the scope and scale for water-based sustainable regional development. A feasible scope could be similar to the IWRM but larger in that it may include sectors outside the realm of transportation such as transportation, industry, education, and others. Feasible zones include scales that could range from a portion of a municipality to the river basin to larger territorial jurisdictions. Obviously size and scope of a project would be interdependent, so that as a general rule the size and scope are interrelated.

Unver (2007) uses Turkey’s Southeastern Anatolia Project (GAP) as a contemporary example of water-based regional development in a multisectoral setting. GAP is the Turkish acronym for the project. See Section 11.4.2 for a brief description of this project. GAP was implemented as a regional, social and economic, sustainable development project, a major water development core, including agricultural, educational, transportation, environmental, manufacturing projects; and programs for poverty reduction and gender equality. A comprehensive overview of GAP is given in Biswas (1997).

19.2 WATER LAW: SURFACE AND GROUNDWATER MANAGEMENT ASPECTS

19.2.1 Water Law

Water Rights

Water management decisions are most often underlain by water laws. In the United States, water law has two basic functions: (1) the creation of supplemental private property rights in scarce resources, and (2) the imposition of public interest limitation on private use (Tarlock, 1996). For our purposes,

water law is divided into surface water law and groundwater law. Surface water law is further categorized into riparian law and appropriation law. Appropriative water rights and riparian water rights are opposite of each other. Prior appropriation is a use-based system and riparian is a land-based system of property rights.

Riparian law is based on the riparian doctrine, which states that the right to use water is considered real property, but the water itself is not property of the landowner (Wehmhoefer, 1989). Riparian rights are an incident of property ownership (Tarlock, 1996). The riparian law is the basis of water law in 31 states in the eastern United States and in numerous other countries (Cech,). Riparian doctrine has evolved into two basic principles: (1) reasonable use and (2) correlative rights. The reasonable use is a legal doctrine that allows a riparian landowner to divert and use any quantity of water so long as it does not interfere with the reasonable use of other riparian land owners. Correlative right is a legal doctrine that requires riparian landowners to share all water in a stream. This right provides a minimum, reasonable amount of water to all water users along a stream. For example, during droughts, allocations are determined so that everyone receives a proportionate share of the stream discharge.

Appropriation law states that the allocation of water rests on the proposition that the beneficial use of water is the basis, measure, and limit of the appropriative right; the first in time is prior in right. In the western United States, surface water policy generally follows this doctrine of “first in time, first in right.” In order to appropriate water, the user need only demonstrate availability of water in the source of supply, show intent to put the water to beneficial use, and give priority to more senior permit holders during times of shortage (Schmandt et al., 1988). Beneficial use of water under the law includes domestic consumption, livestock watering, irrigation, mining, power generation, municipal use, and others. The states of Arizona and New Mexico follow the appropriation law of surface water, and in California and Texas both the appropriation doctrine and the riparian doctrine coexist.

Groundwater allocation is handled quite differently and is typically divided into common law or statutory law. *Common law* doctrines include the overlaying rights doctrines of absolute ownership, reasonable use, and correlative rights. These doctrines give equal rights to all landowners overlaying an aquifer. Arizona, California, and Texas, have adopted these principles for groundwater allocation.

The above surface and groundwater laws serve as the basis for individual state water policies. The burden of developing water policies lies upon the state. This is often achieved by the state proposing a water project and securing federal funds for the construction. It is also up to the states to agree on apportionment in interstate waters; if the states can not agree, then the courts will intervene and settle the dispute by decree. The Federal government only gets involved in such disputes where federal lands and Indian reservations are concerned.

Regulation of Water Quality

Table 19.2.1 lists federal laws in the United States that regulate water quality. Most drinking water supplies in the U.S. conform to standards established by the U.S. Environmental Protection Agency. The National Primary Drinking Water Standards *Maximum Contaminant Levels* (MCLs) and the *Secondary Maximum Contaminant Levels* (SMCLs) are provided at <http://www.epa.gov/safewater>.

19.2.2 Surface Water Systems Management: Examples

Arizona Water Law

Throughout Arizona’s history, water policy has been directed at supporting the unconstrained growth of its population and major revenue-producing activities. Starting with mining, ranching, and farming, with the gradual shift to municipal and industrial uses, the water policy of the state has been directed at obtaining imported supplies. This has been an effort to

Table 19.2.1 Laws Regulating Water Quality

Federal laws in the United States that regulate the quality of water

National Environmental Policy Act of 1969 (P.L. 91–190)
 Federal Water Pollution Control Act of 1972 (P.L. 92–500)
 Clean Water Act Amendments of 1977 (P.L. 95–217)
 Safe Drinking Water Act of 1974 (P.L. 93–523) and amendments
 Resource Conservation and Recovery Act of 1976 (RCRA) (P.L. 94–580)
 Comprehensive Environmental Response, Compensation and Liability Act of 1980 (CERCLA)
 (P.L. 96–510)
 Superfund Amendments and Reauthorization Act of 1986 (SARA)
 Surface Mining Control and Reclamation Act (SMCRA) (P.L. 95–87)
 Uranium Mill Tailings Radiation and Control Act of 1978 (UMTRCA) (P.L. 95–604 as amended by
 P.L. 95–106 and P.L. 97–415)
 Toxic Substances Control Act 1988 (TOSCA) (P.L. 94–469 as amended by P.L. 97–129)
 Federal Insecticide, Fungicide and Rodenticide Act (FIFRA) (P.L. 92–516 as amended by P.L. 94–140,
 P.L. 95–396, P.L. 96–539, and P.L. 98–201)
 Oil Pollution Act (OPA) of 1990

augment what has appeared to be an insufficient and indigenous resource. In Arizona, the state's water policy and management focused more on surface water than groundwater prior to 1980, when the Groundwater Management Code was developed; thereafter, the emphasis has been on groundwater.

In regards to surface water, Arizona law defines surface water as “the waters of all sources, flowing in streams, canyons, ravines or other natural channels, or in definite underground channels, whether perennial or intermittent, flood, waste, or surplus water, and of lakes, ponds and springs on the surface.” These surface waters are subject to the “doctrine of prior appropriation” (ADWR, 1998). In Arizona, surface water rights are obtained by filing an application with the Department of Water Resources for a permit to appropriate surface water. Once the permit is issued and the water is actually put to beneficial use, proof of that use is made to the Department and a certificate of Water Right is issued to the applicant. Once a certificate is issued, the use of the water is subject to all prior appropriations.

Since water law in the state of Arizona has changed substantially over the years, Arizona is now conducting a general adjudication of water rights in certain parts of the state. Adjudications are court determinations of the status of all state law rights to surface water and all claims based upon federal law within the river systems. These adjudications will provide a comprehensive way to identify and rank the rights to the use of water in some areas. The adjudications will also quantify the water rights of the federal government and the Indian reservations within Arizona.

Texas Approach

In the state of Texas, the way to accomplish the wide range of water management duties was to develop river authorities. The term “*river authority*” implies an institution that possesses authority over a river, thereby imparting a regional character to the organization (Harper and Griffin, 1988). Some river authority boundaries are defined by watershed boundaries and some by county boundaries. Figure 19.2.1 shows the boundaries of river authorities in Texas. Some of these river authorities share jurisdiction over an entire watershed and only seven out of the 13 are the sole river authority operating in their particular basin. The duties and powers of the river authorities can be divided into those pertaining to: (1) watershed management, (2) water supply, (3) pollution control and groundwater management, (4) appurtenant development, and (5) governmental or administrative authority.

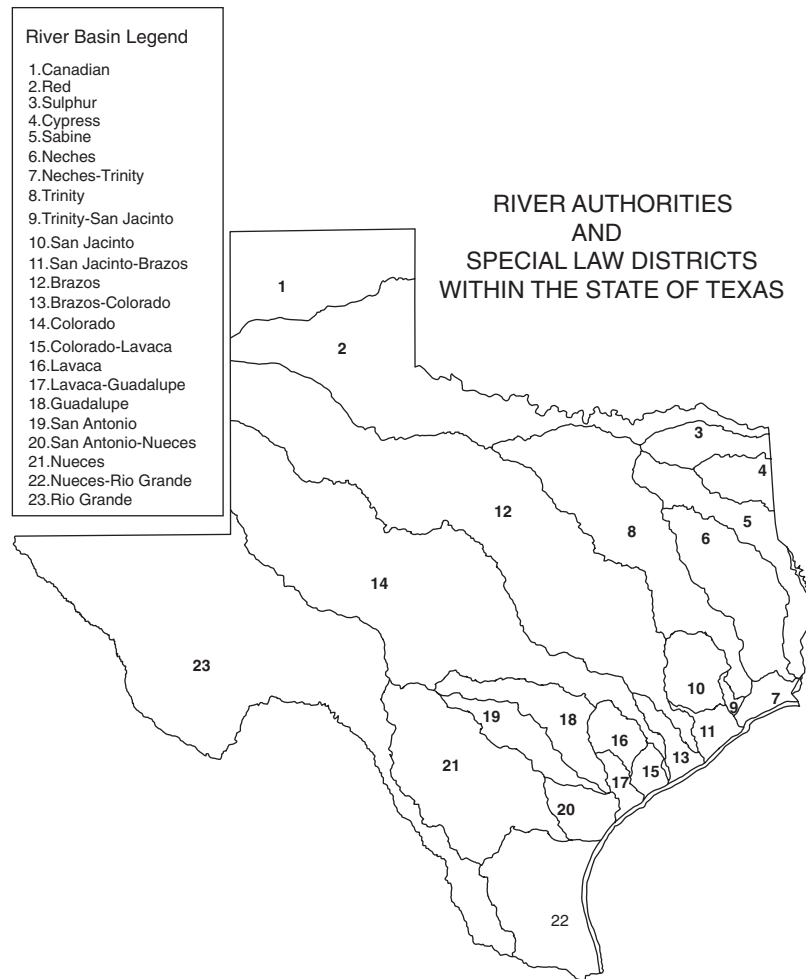


Figure 19.2.1 Texas river authorities.

The right of landowners to intercept and use *diffused surface water flows* (overland flows) on their property is superior to that of adjacent landowners and to any holder of surface water rights on streams into which the runoff might eventually flow. *Diffused surface water* is drainage over the land surface before it becomes concentrated in a stream course. Concerning stream flow, Texas is a dual-doctrine state, recognizing both the riparian doctrine and the prior appropriation doctrine. Riparian doctrine is a somewhat complex blend of Hispanic civil law and English common law principles, and the prior appropriation doctrine was adapted before the turn of the century for allocating surface water rights. This dual doctrine has caused great difficulty in coordinating the diverse private and public water rights emanating from diametrically different doctrines. Surface water rights adjudication began in 1969 to merge all unrecorded surface water rights into a permit system. This has simplified the complex management issue. In summary, private or landowner rights pertain to percolating groundwater and diffused surface water, and the state has appropriated the flow of rivers and streams.

The state of Texas is large and diverse, which insinuates that water management solutions that are appropriate for one region may not be appropriate for another. In order to implement the water policy in Texas, the state has developed a comprehensive water plan that guides surface and groundwater management. The common element underlying the State of Texas' water planning is the fact that

meeting the future water needs of the state will require a full range of management tools including Expected Water Conservation, Advanced Water Conservation, Water Reuse, Expanded Use of Existing Supplies, Reallocation of Reservoir Storage, Water Marketing, Subordination of Water Rights, Chloride Control Measures, Interbasin Transfers, and New Supply Development. Water availability, economics, environmental concerns, and public acceptance identify which management tool is best for a specific water need.

As stated above, surface water policies in Texas are governed by both the prior appropriation doctrine and the riparian doctrine, and are integrated into the water plan. Surface water in Texas is held in public trust by the state and is allocated to users through a system of water rights. The Texas Water plan delegates most of the planning authority to river authorities and water districts. Due to this type of delegation, conflicts between the various water planning entities operating in the same river basin can arise.

A large amount of Texas' water supply is from groundwater resources, which has resulted in a severe depletion of some of the major aquifers in the state. It is surprising that a state such as Texas that depends on groundwater so much has such an ill-defined groundwater plan. The Texas groundwater law is based on the "absolute ownership rule," which states that "percolating waters are the private property of the landowner" (Schmandt et al., 1988). This means that a landowner has the right to pump water from a groundwater deposit beneath his land at any rate, as long as the withdrawal does not maliciously harm his neighbor. The groundwater law excludes underground streams, where the classification of an underground stream is still a matter of debate. This lack of regulation has caused many problems in the state of Texas such as overdrafting, subsidence, and water quality issues. There have been efforts conducted by state agencies and others to develop best management techniques for regional groundwater planning.

New Mexico Approach

Similar to the state of Texas, New Mexico also allocates water rights under the legal doctrine of prior appropriation. The state is considered to be the owner of surface water and it holds it in trust for the public. The water appropriations are made through the state engineer, who administers the water law. All allocated waters are subject to appropriation with the exception of wells for domestic use, which are defined as wells that have a draw of less than 1800 gpd. All water rights are lost if the water is not used in four consecutive years. In order to settle water controversies, the following seven Interstate Stream Compacts were developed.

1. *Colorado River Compact*—signed in 1922 in Santa Fe, New Mexico, and includes the states of Arizona (AZ), California (CA), Colorado (CO), Nevada (NV), New Mexico (NM), Utah (UT), and Wyoming (WY). The compact apportions the use of the Colorado River waters to the upper and lower basins. It provides that each state, along with certain federal agencies, shall cooperate to carry out the terms of the compact.
2. *La Plata River Compact*—divides the waters of the La Plata River between CO and NM. It was signed in 1922. The state engineers of the two states shall administer the water allocations in accordance of the terms of the compact.
3. *Upper Colorado River Basin Compact*—signed in Santa Fe in 1948 by AZ, CO, NM, UT, and WY. This compact creates a commission to administer its provisions with members representing the U.S., CO, NM, UT, and WY.
4. *Rio Grande Compact*—signed in 1938 with CO, NM, and TX. It apportions the waters of the Rio Grande among the three states and provides for administration by a commission consisting of the state engineers of CO and NM. It also allows the Governor of Texas to appoint a commissioner.
5. *Costilla Creek Compact*—signed in Santa Fe in 1944 by CO and NM. It provides for an administrative commission composed of the official in each state charged with administering public water supplies.

6. *Pecos River Compact*—signed in 1948 by NM and TX. Provides for a commission to administer its provisions and concern over NM delivering the apportions of water to TX. Under this decree, New Mexico is prohibited against allowing a net shortfall in its deliveries to Texas.
7. *Canadian River Compact*—signed in Santa Fe in 1950 with NM, OK, and TX. It provides for a commission to administer its provisions with one commissioner for each state and one for the United States.

Animas-La Plata Project Compact

U.S. Supreme Court decrees govern the use of water in the Pecos and Gila River Basins in New Mexico. Unlike the state of Texas, which governs the use of groundwater by absolute ownership, New Mexico controls the use of groundwater under a system of permits, which uses the priority concept. Since most groundwater aquifers are related hydrologically to surface water, it is a concern of the state to regulate groundwater pumping as well. The state requires that applicants for groundwater wells to withdraw surface rights to offset the impacts of the pumping. This type of management coordination between surface and groundwater was developed to protect senior water rights.

19.2.3 Groundwater Systems Management: An Example

Arizona Approach

In Arizona, groundwater problems arise from the overdrafting of water from the aquifers. Groundwater overdrafts cause many problems such as increased well pumping costs and water quality issues. In areas of severe groundwater depletion, the earth's surface may also subside, causing cracks or fissures that can damage roads or building foundations. In order to manage groundwater pumping in Arizona, the Arizona Groundwater Management Code was developed in 1980 as state legislation. The Arizona Groundwater Management Code was named one of the nation's ten most innovative programs in state and local government by the Ford Foundation in 1986. This achievement came from the cooperation of Arizonans working together and compromising when necessary in order to protect the future of the state's water supply.

The Groundwater Management Code has three primary goals (ADWR, 1998):

1. control the severe overdraft currently occurring in many parts of the state;
2. provide a means to allocate the state's limited groundwater resources to most effectively meet the changing needs of the state; and
3. augment Arizona's groundwater through water supply development

In order to achieve these goals, the code set up a comprehensive management environment and established the Arizona Department of Water Resources.

There are three levels of water management that are outlined by the code. Each level is based on different groundwater conditions. The lowest level applies statewide, and includes general groundwater provisions. The next level applies to *Irrigation Non-Expansion Areas* (INAs), and the highest level applies to *Active Management Areas* (AMAs) where groundwater depletion is the highest. The boundaries that divide the INAs and AMAs are determined by groundwater basins and not by political jurisdiction. The main purpose of groundwater management is to determine who may pump groundwater and how much may be pumped. This includes identifying existing water rights and providing new ways for non-irrigation water users to initiate new withdrawals. In an AMA or INA new irrigation users are not allowed. Even with the original publicity and enthusiasm, many people now feel that the efforts under the Groundwater Management Code have been very costly with very little savings in water, making the success questionable.

19.3 SUSTAINABLE WATER SUPPLY METHODOLOGIES FOR ARID AND SEMI-ARID REGIONS

19.3.1 Overall Subsystem Components and Interactions

Conventional water supply systems include the components: water sources (groundwater and surface sources), raw water pumping and transmission, water treatment, high service pumping, and water distribution (as illustrated in Figure 12.1.2 showing the functional components of a conventional-water utility). A detailed discussion of the various components is beyond the purposes of this book.

19.3.2 Water Reclamation and Reuse

Water reclamation and reuse has become an attractive option for conserving and extending available water supplies in arid and semi-arid regions as many urban areas in these regions approach and reach the limits of their available water supplies. Water reuse can also provide urban areas an opportunity for pollution abatement when effluent discharges are replaced to sensitive surface water. Water reclamation and non-potable reuse only require conventional water and wastewater treatment technologies that are widely practiced and available in countries throughout arid and semi-arid regions of the world.

The technical issues involved in planning a water reuse system include (U.S. EPA and U.S. AID, 1992):

- The identification and characterization of potential demands for reclaimed water;
- The identification and characterization of existing sources of reclaimed water to determine their potential for reuse;
- The treatment requirements for producing safe and reliable reclaimed water that is suitable for its intended applications;
- The storage facilities required to balance seasonal fluctuations in supply with fluctuations in demand;
- The supplemental facilities required to operate a water reuse system, such as conveyance and distribution networks, operational storage facilities, and alternative disposal facilities; and
- The potential environmental impacts of implementing water reclamation.

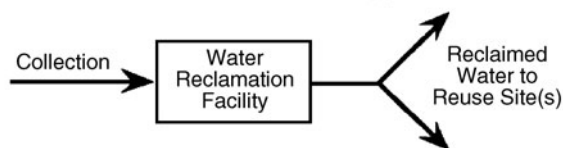
Figure 19.3.1 illustrates three alternative configurations for water reuse systems and Figure 19.3.2 shows the typical water reclamation plant process for urban reuse.

The Mediterranean region is one of the most affected water short regions of the world where improved water demand management and development of new water resources desperately is needed. In this region, wastewater in most cases is inadequately managed and treated, which in turn leads to deterioration of existing freshwater sources and even the Mediterranean Sea (Post, 2006). An EU funded project, "Efficient Management of Wastewater, Treatment and Reuse in the Mediterranean Countries," encourages reuse-oriented wastewater management in four target countries – Jordan, Palestine, Lebanon, and Turkey. Post (2006) provides an overall comparison of the different specific problems within the targeted countries. The conclusions are that because of the existing and predicted water deficits in the region, there needs to be an increase in water use efficiency and alternative water sources such as reclaimed wastewater must be considered as an option. A large effort will be required to develop a cultural acceptance as it is a key problem. There needs to be successful demonstration of wastewater treatment and reuse technologies in order to convince the people of the benefits.

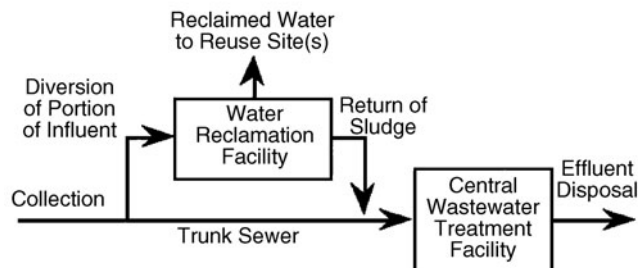
19.3.3 Managed Aquifer Recharge (MAR)

Managed aquifer recharge (MAR) has the potential to be a contributor to the UN Millenium Goals for water supply, especially in arid and semi-arid areas. MAR can be regarded as one method to manage urban water resources in conjunction with others.

A. Central Treatment Near Reuse Site(s)



B. Reclamation of Portion of Wastewater Flow



C. Reclamation of Portion of Effluent

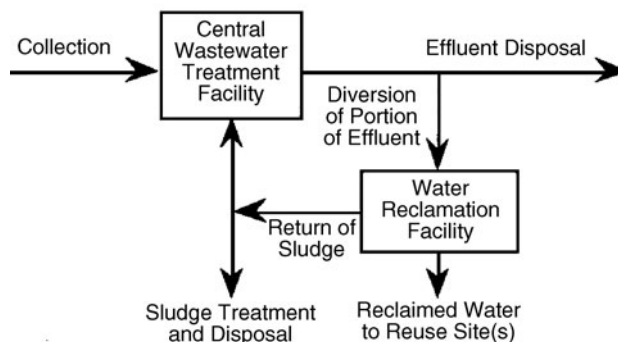


Figure 19.3.1 Configuration alternatives for water reuse systems. (A) Wastewater treatment facility located near major users of the reclaimed water for purposes of economy. (B) When trunk sewer passes through an area of significant potential reuse a portion of the flow can be diverted to a new reclamation facility to serve that area. Sludge from that facility is returned to sewer, which could be deleterious to sewer trunk and downstream treatment facility. (C) Effluent outfall passing through a potential reuse area could be tapped for some or all effluent and provide additional treatment to meet reclaimed water quality standards (from U.S. EPA and U.S. AID, 1992, 2004).

19.3.3.1 Artificial Recharge

Artificial recharge is becoming an integral part of integrated urban water management, particularly in arid and semi-arid regions, especially in the southwestern United States for sustainable water supplies. Aquifer recharge has many advantages over conventional surface water storage, especially in arid and semi-arid regions. These include negligible evaporation losses, limited vulnerability to secondary contamination by animals and/or humans, and no algae blooms resulting in decreasing surface water quality (Crook, 1998). Flow of water through the subsurface provides *soil-aquifer treatment* (SAT), along with aquifers providing seasonal and/or longer storage.

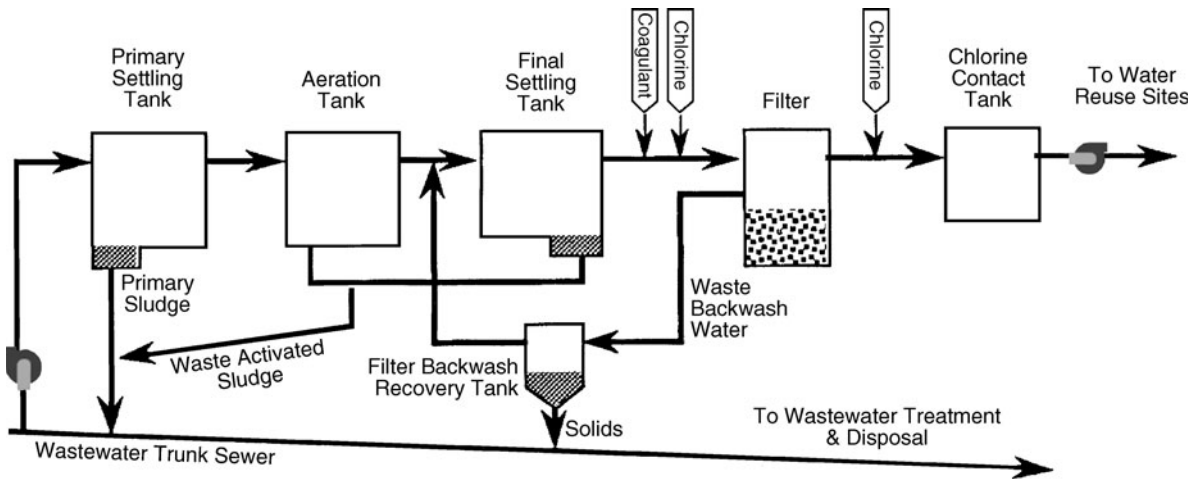


Figure 19.3.2 Typical water reclamation plant processes for urban reuse (from U.S. EPA and U.S. AID, 1992, 2004).

Groundwater recharge of reclaimed municipal wastewater is an approach to water reuse with the following purposes (Asano, 1985, 1999; Bouwer, 1998; Todd and Mays, 2005):

- To reduce, stop, or even reverse declines of groundwater levels
- To protect underground freshwater in coastal aquifers against saltwater intrusion
- To store surface water, including flood or other surplus water, and reclaimed municipal for future use.

Figure 19.3.3 illustrates the three technologies, percolation or recharge basins, vadose zone injection wells, and direct injection wells, for aquifer recharge of reclaimed municipal wastewater. Major characteristics of these technologies are summarized in Table 19.3.1. Each of the three technologies provides soil aquifer treatment (SAT) as noted in the table. The aquifer recharge basins and vadose zone injection wells provide SAT in both the vadose and saturated zones; whereas the direct injection wells provides SAT in the saturated zone in the unconfined and/or confined zones. The percolation or recharge basin is the most common and widely accepted method (Fox, 1999).

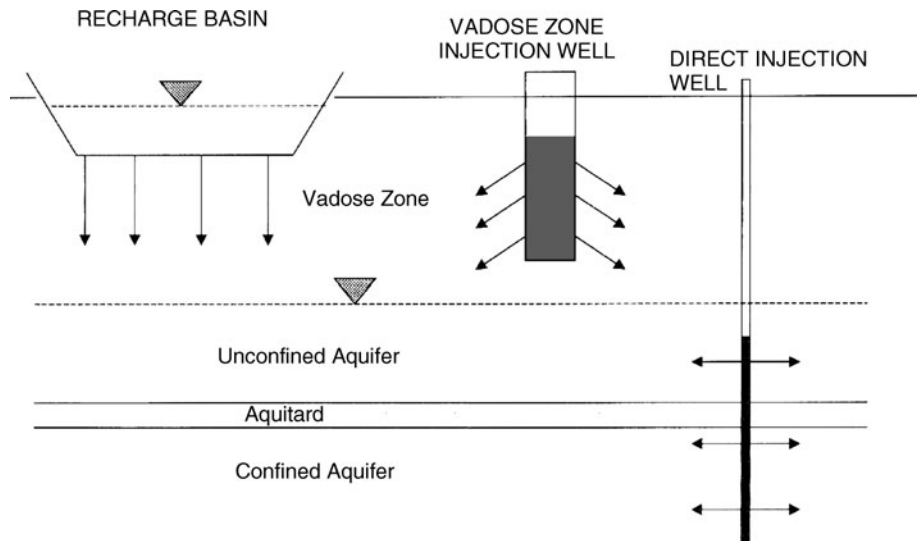


Figure 19.3.3 Methods for aquifer recharge (from Fox, 1999; U.S. EPA, 2004).

Table 19.3.1 Major Characteristics of Aquifer Recharge of Reclaimed Municipal Wastewater

	Recharge basins	Vadose zone injection wells	Direct injection wells
Aquifer type	Unconfined	Unconfined	Unconfined or confined
Pre-treatment requirements	Low technology	Removal of solids?	High technology
Estimated major capital costs (US\$)	Land and distribution system	\$25,000–75,000 per well	\$500,000–1,500,000 per well
Capacity	1000–20,000 m ³ /ha-d	1000–3000 m ³ /well-d	2000–6000 m ³ /well-d
Maintenance requirements	Drying and scraping	Drying and disinfection?	Disinfection and flow reversal
Estimated life cycle	> 100 years	5–20 years	25–50 years
Soil aquifer treatment	Vadose zone and saturated zone	Vadose zone and saturated zone	Saturated zone

Source: Fox (1999).

19.3.3.2 Recharge Basins

A *recharge basin* consists of five major components (see Figure 19.3.4): (1) the pipeline that carries the treated effluent from the wastewater treatment plant; (2) percolation (infiltration) basins where the treated effluent infiltrates into the ground; (3) the soil immediately below the infiltration basins (vadose zone); (4) the aquifer where water is stored for a long duration; and (5) the recovery well where water is pumped from the aquifer for potable or non-potable reuse.

SAT system dynamics can be described by the inputs of the system, the state of the system, and the outputs of the system. Inputs to the system include: (1) the soil type, (2) the water quality, (3) the operation of the SAT system, and (4) the environment, where each input effects the state of the system. The *state of an SAT system* includes: (1) the soil moisture profile within the vadose zone, (2)

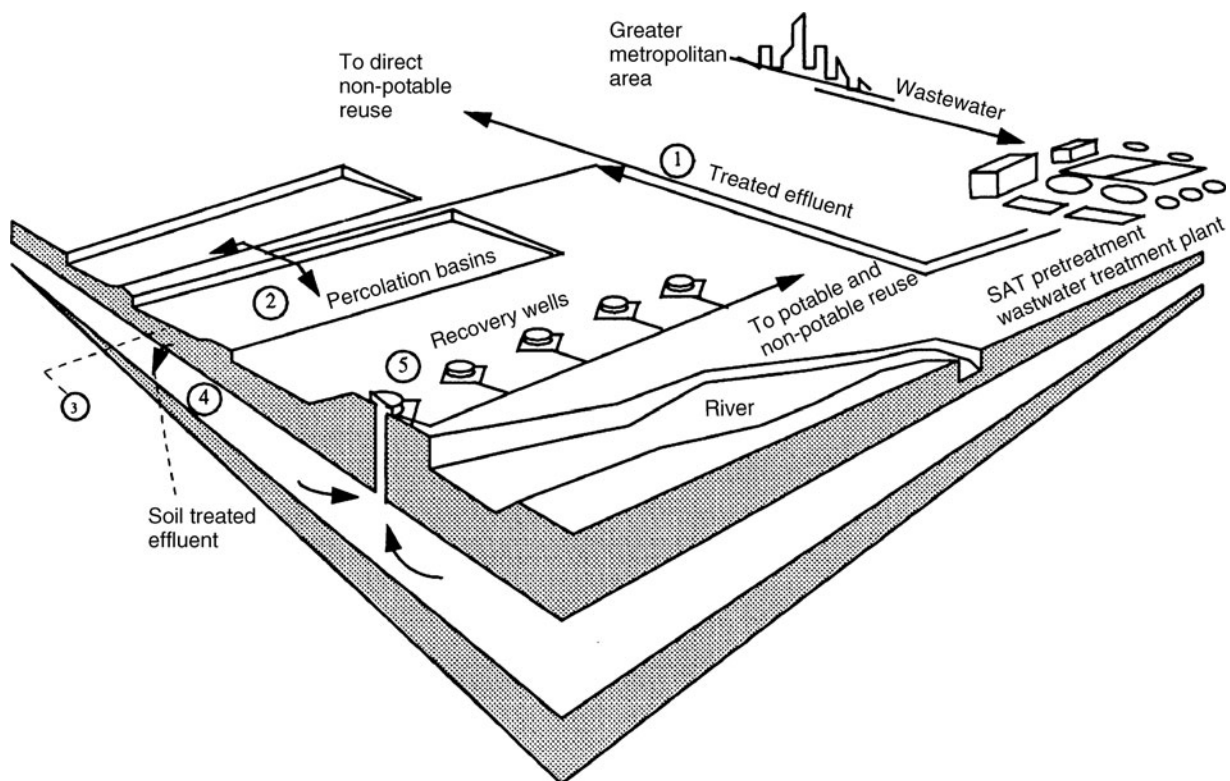


Figure 19.3.4 Recharge basin and the components (from Arizona State University et al., 1998)

the level of oxygen, (3) algal growth, and (4) soil hydraulic conductivity. The state of the system controls the residence time of water in the vadose zone and the level of microbial activity. Of particular importance is the level of oxygen, which is related to the micro-organism distribution and oxygen demanding substrates. Algal growth is related to the clogging layer formation on the soil surface and effective soil hydraulic conductivity. The soil moisture is directly affected by inputs—soil type and the environment—and indirectly by the water quality, which affects algal growth and the soil hydraulic conductivity. The oxygen in the vadose zone is affected by the soil moisture profile, the water quality of treated effluent, the operation schedule, and the algal growth. Algal growth is affected by the water quality of the treated effluent, the operation schedule, and the environment. Soil hydraulic conductivity is affected by the algal growth, the soil type, and the environment.

The critical outputs of the system are the total infiltration, the total organic carbon removal efficiency, the nitrogen removal efficiency, and the pathogen removal efficiency. The total organic carbon removal efficiency is primarily affected by the amount of oxygen in the system through the organic oxidation process. Nitrogen removal efficiency is dependent upon the amount of oxygen and the availability of organic carbon through the nitrification-denitrification process. Pathogen removal efficiency is dependent upon the soil moisture profile and the soil hydraulic conductivity through the adsorption-inactivation process.

The major purification processes occurring in the soil aquifer treatment system are: filtration, chemical precipitation/dissolution, organic biodegradation, nitrification, denitrification, disinfection, ion exchange, and adsorption/desorption. As part of a water reclamation process, soil aquifer treatment (SAT) is a key step to polishing the water. This step provides for (a) mechanical filtration of suspended particles, (b) biological processes (i.e. breakdown of organics, nitrification-denitrification), and (c) physical-chemical retention of inorganic and organic dissolved constituents (e.g. phosphorous, potassium, trace elements), from the biologically-treated waste water.

Water reuse can be one of the most important strategies for meeting water quantity objectives in arid and semi-arid regions. Local groundwater supplies can be augmented by treated wastewater that re-enters the ground via managed infiltration practices or injection wells. The infiltration of wastewater effluents to augment local aquifers is accomplished in shallow infiltration basins, usually constructed in regions with permeable soils. The treated water simply percolates through the soil mantle and unconsolidated sediments, and then the vadose zone, to reach an unconfined aquifer. Although these activities are generally not located in the vicinity of production wells, waters that are added to local aquifers in this manner mix with the native groundwater and eventually are recovered and used again.

Figures 19.3.5 through 19.3.7 show three artificial recharge systems in Arizona.



Figure 19.3.5 Pima Road recharge basin near Tucson, Arizona. (Courtesy of central Arizona Project.)

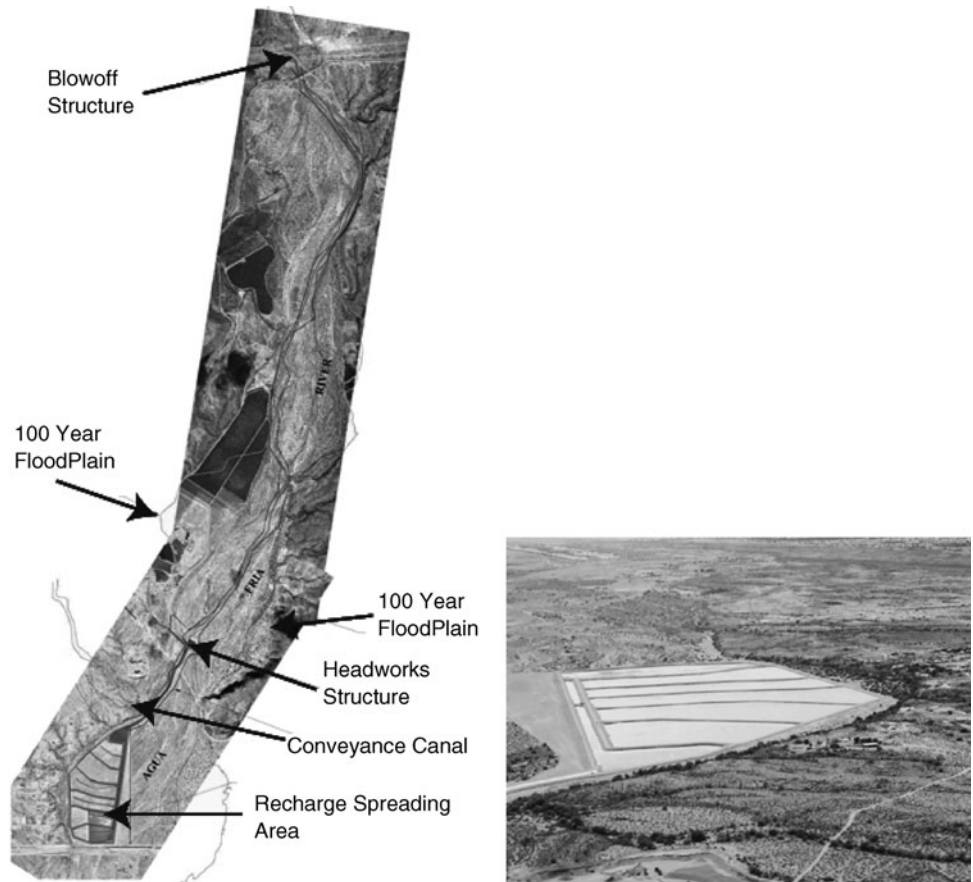


Figure 19.3.6 Agua Fria Recharge Project (AFRP) located in Agua Fria River, Peoria, Arizona. This project is located approximately 4 mi downstream of the New Waddell Dam (Lake Pleasant). The project was developed by the Central Arizona Water Conservation District (CAWCD) and in 2003 the City of Peoria purchased AFRP storage capacity for recharge to meet the demands of future growth as part of their water resources management goals. Two operational components include the 4 mi river section used for recharge and conveyance of surface water downstream, and a constructed head structure to capture surface flow in the river and a canal to convey water downstream to the spreading basins (100 ac in area). (Courtesy of central Arizona Project.)

19.3.4 Desalination

Desalination refers to any of several processes that remove the excess salt and other minerals from water in order to obtain freshwater suitable for consumption or irrigation. Desalination is an unconventional method for water supply that is gaining wider use, particularly in arid and semi-arid regions of the world. Because of water scarcity in the Middle East, desalination of ocean water is becoming more common and is growing in the US, North Africa, Spain, Australia, and China. Table 19.3.2 is a list of the number of desalination units in the MENA (Middle East and North Africa) Region as reported by the Gulf Co-operation Council (GCC).

Several Middle Eastern countries have energy reserves so great that they use desalinated water for agriculture. Saudi Arabia's desalination plants account for about 24 percent of total world capacity. Desalination meets 70 percent of Saudi Arabia's present drinking water requirement, supplying major urban and industrial centers through a network of more than 2300 mi of pipe network. The

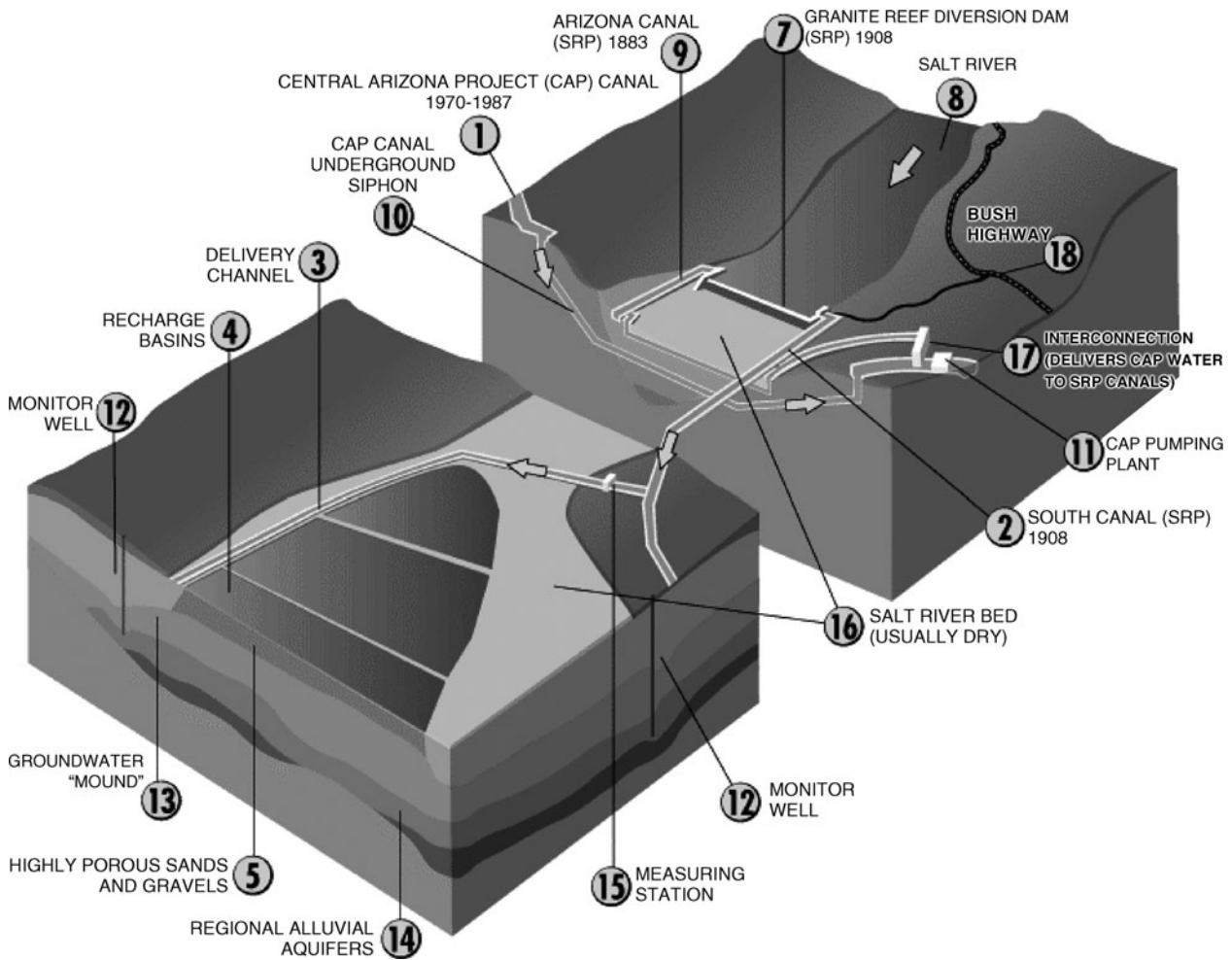


Figure 19.3.7 Granite Reef Underground Storage Project (GRUSP) operated by the Salt River Project (SRP), Arizona. This facility diverts water from the Granite Reef Diversion Dam near Phoenix, Arizona, on the Salt River to seven recharge basins totaling 217 ac for the purpose of water banking. Actual recharge is approximately 100,000 ac-ft/yr with 200,000 ac-ft/yr permitted by the state of Arizona. This was the first major recharge facility in the state of Arizona and one of the largest in the US. (Courtesy of salt river project).

world’s largest desalination plant is the Shoaiba Desalination Plant in Saudi Arabia. It uses multi-stage flash distillation, and it is capable of producing 150 million cubic meters of water per year. Several new desalination plants are planned, or under construction, which will ultimately bring the final total to almost 30 such facilities.

A new city, the Dubai World Central (DWC), is to be located in “New Dubai” in the arid United Arab Emirates. DWC will host the Dubai World Central International Airport, a Logistic City, an Aviation City, an Exhibition Center, an Enterprise Park and others, with a proposed residential population of over 988,000 and employment of over 608,000. Desalinated water will supply DWC with ultimate potable and cooling water demands, respectively, of 400,000 and 175,000 m³/day.

Table 19.3.2 Desalination Units in MENA
(Middle East and North Africa) Region

Location	Number of units	Total capacity (m ³ /d)
UAE	382	5,465,784
Bahrain	156	1,151,204
Saudi Arabia	2074	11,656,043
Oman	102	845,507
Qatar	94	1,223,000
Kuwait	178	3,129,588
GCC states total		23,471,126
Libya	431	1,620,652
Iraq	207	418,102
Egypt	230	236,865
Algeria	174	301,363
Tunisia	64	148,822
Yemen	66	132,897
Israel	n/a	149,594

Source: "The Changing Image of Desalination," Global Water Intelligence through the Middle East Desalination Research Center (MEDRC), October 2000, <http://www.medrc.org>.

Methods for Desalination

Methods for desalination include the following:

Distillation

- Multi-stage flash (see Figure 19.3.8)
- Multiple-effect (see Figure 19.3.9)
- Vapor compression (see Figure 19.3.9)
- Evaporation/condensation

Membrane processes

- Electrodialysis reversal
- Reverse osmosis (see Figure 19.3.9)
- Nanofiltration
- Forward osmosis
- Membrane distillation

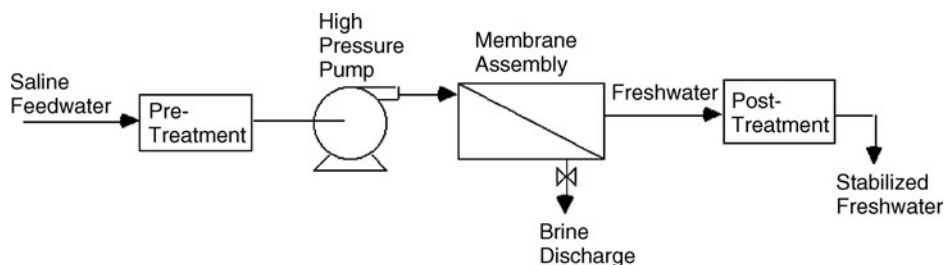
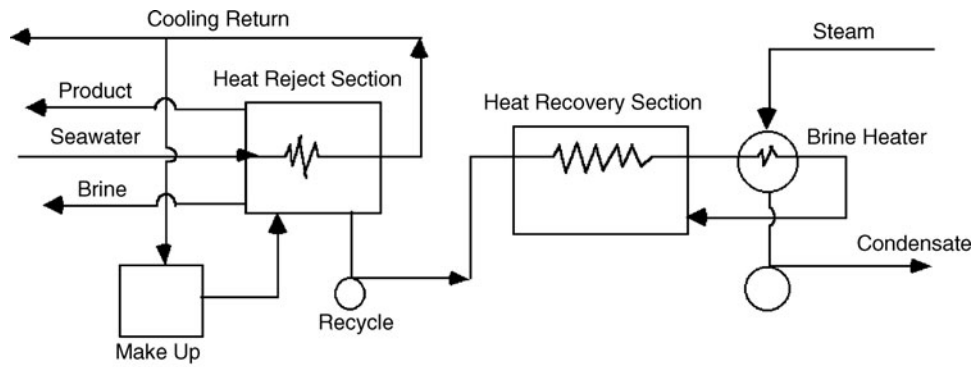
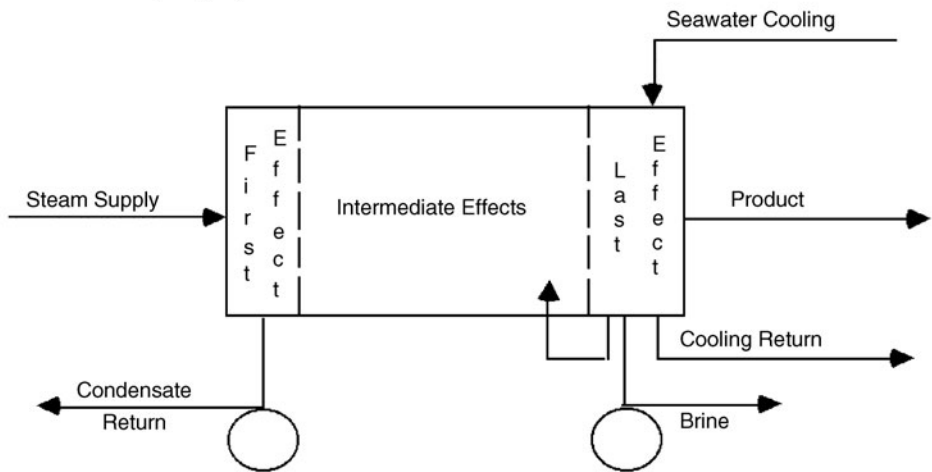


Figure 19.3.8 Flow diagram of a reverse osmosis system (from Khan, 1986). (Courtesy of USAID.)



Multi - State Flash (Recycle)



Multiple Effect

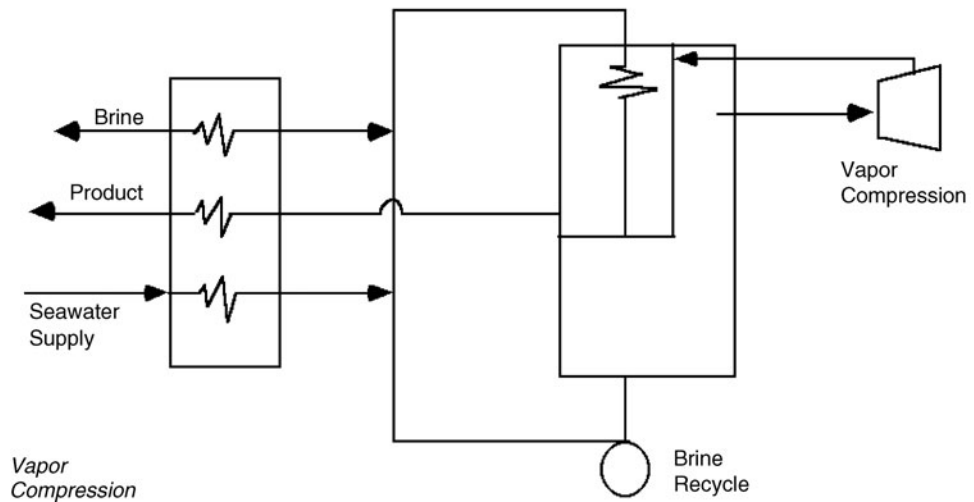


Figure 19.3.9 Common methods of distillation (Pantell, 1993).

Other methods include freezing, geothermal, solar humidification, methane hydrate crystallization, and high-grade water cycling.

The two leading methods are reverse osmosis (47.2 percent of installed capacity worldwide) and multi-stage flash (36.5 percent). (Wangnick, 2004). Electrodialysis usually is preferred for treating brackish groundwater.

19.3.5 Water Transfers

Water transfers are a common component of many urban water supply systems, particularly in arid and semi-arid regions. They are not only being used to satisfy increasing water demands but also for managing the impacts of droughts. There are many forms of water transfers that serve a number of different purposes in the planning and operation of urban water systems. Eheart and Lund (1996) define the major types as permanent transfers; contingent transfers/dry-year options (long term, intermediate term, and short term); spot market transfers; water banks; transfer of reclaimed, conserved, and surplus water; and water wheeling or water exchanges (operational wheeling, wheeling to store water, trading water of different qualities, season wheeling, and wheeling to meet environmental constraints). The major benefits and uses of transferred water include directly meet demand and reduce costs; improve system reliability; improve water quality; and satisfy environmental constraints (Eheart and Lund, 1996). Implementation of water transfers implies the need to increase integration and cooperation among diverse water users.

In arid and semi-arid regions large water transfer projects have been used as one solution to meet urban water demand because of the regional differences in water availability. The Central Arizona Project (CAP) is one project that is discussed in Chapters 2 and 9. Another transfer project is the National Water Carrier System in Israel, which is supplied mainly by Lake Kinneret. About 80 percent of all the water used in Israel comes from three principal sources: Lake Kinneret, the Coastal Aquifer, and the Western Mountain Aquifer. Two very large projects are (a) the Great Man-Made River Project (GMMRP) in Libya and (b) the newly planned south to north water transfer in China in which nearly 45 billion cubic meters of water from the Yellow, Yangtze, and other rivers will be sent north each year when the project is finished in 2050.

The GMMRP is a water conveyance system that, when completed, will transport water from aquifers in the southern part to the northern part of Libya. Approximately 80 percent of this water will be used for agricultural irrigation. Because of the extensive pumping of groundwater in the north along the coast, a substantial seawater encroachment of the coastal groundwater system has occurred. The GMMRP will pump groundwater from the aquifers of Sarir and Kufra in the southeast and Murzag in the southwestern parts of Libya. The project began in 1983 and comprises several phases, Phase I (Sarir/Sirt Tazerbo/Benghazi System) and II (Hasouna/Jefara System), serving the western part of Libya, being the two major components. The water being pumped and diverted will never be recharged so it is a nonrenewable resource. Think about how sustainable this project will be for the future.

Northern China has been the center of population, industrial and agricultural growth. As a result the region's limited water resources have been decreasing, resulting from over-exploitation of groundwater. This has resulted in the supply to urban and industrial development at the expense of agriculture, causing severe water shortages in rural areas and land subsidence. The south to north diversion routes are shown in Figure 19.3.10. Diversions for the three routes, eastern, central, and western, will be 14.8, 13.0, and 17.0 billion cubic meters per year, respectively. This project will cost three times the controversial Three Gorges Dam, China's other hydraulic mega-project.

19.3.6 Rainfall Harvesting

From the early civilizations, people in arid and semi-arid regions have relied on collecting or "harvesting" surface water from rainfalls and storing the water in human-made reservoirs or



Figure 19.3.10 Three routes of China’s South to North water diversion mega project. The project will divert 44.8 billion cubic meters of water annually from the wetter southern China to the drier north. Planned construction of the project will be completed in 2050 at an estimated cost of \$62 billion dollar (http://www.water-technology.net/projects/south_north/)

“cisterns.” Not only were cisterns used to store rainfall runoff, they were also used to store aqueduct water. Cisterns during the ancient times have ranged from construction of irregular shaped holes (tanks) dug out of sand and loose rock and then lined with plaster (stucco) to water proof them, to the construction of rather sophisticated structures such as ones built by the Romans. One of the largest is the Piscina Mirabilis in Bacoli near Naples supplied by the Augustan (Serino) aqueduct.

In the central Negev Desert in Israel, the six urban centers were (Avdat, Mamshit, Nizzana, Shivta, Rehovot, and Haluza) developed by the Nabateans in the hills during the Nabatean-Bysantine times (3–1 B.C.). Sophisticated rainwater-harvesting systems were developed as the urban water supply for the centers with populations ranging from 25,000 to 71,000 people (Broshi, 1980; Bruins,). Cisterns were dug into the rock and conduits were designed to collect the runoff from roofs, pavements, and natural catchments.

Rainfall harvesting can be used as a supplementary or even primary water source at the household or small community level (Marsalek et al., 2006). Zuhair et al. (1999) have shown that rainwater harvesting can provide a significant amount of freshwater in the Arabian Gulf States. Examples include: Kuwait (12 percent of the water demand for landscape agriculture); Muscat, Oman (27 percent of the water demand for industry); Abha, Saudi Arabia (11 percent of water demand for industry and landscape irrigation); and Ali Ain, UAE (16 percent of water demand for agriculture). Figure 19.3.11 shows the basic components of a typical rainwater harvesting system. Figure 19.3.12 shows four types of rainwater harvesting systems that are systematically distinguished according to their hydraulic properties (Nouh and Al-Shamsy, 2001).

Natural sedimentation in the storage tanks of the rainfall harvesting systems is the most effective cleansing process for roof runoff. It is important to avoid turbulent mixing in the storage tank in order

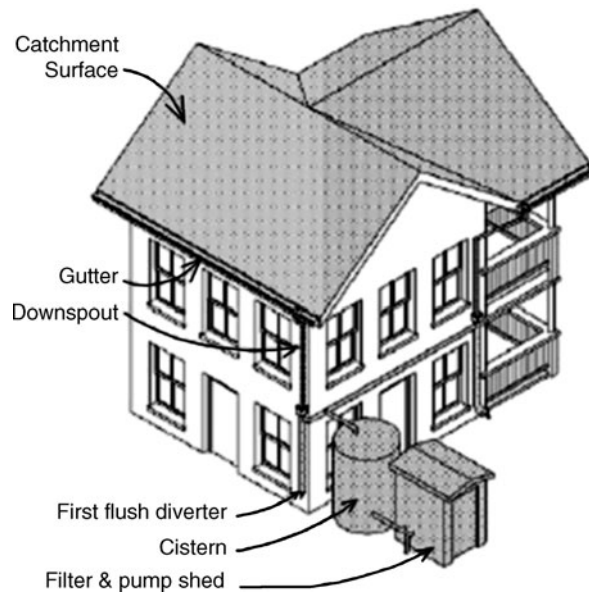


Figure 19.3.11 Components of a typical rainfall harvesting installation (TWDB, 2005).

to prevent the sediment mixing in the water column. A sieve of size 0.5 to 1.0 mm is recommended to prevent residues from entering the pump and installation (Nouh and Al-Shamsy, 2001). Other treatment such as chemical disinfection is not necessary. Hermann and Schmida (1999) made a long-term simulation of 10 years of precipitation data to identify various hydraulic factors of rainwater harvesting systems. McCann (2008) discusses the global prospects of rainwater harvesting from the viewpoint of the progression towards district and regional schemes, rather than the more traditional practice of storage on individual properties.

19.3.7 Traditional Knowledge

The United Nations organized the World Conference on the Environment and Development held in Rio de Janeiro in 1992. This conference, typically referred to as the “Earth summit” was aimed at reconciling the dramatic world environmental conditions affecting the development and welfare of people. Three conventions for climate, biodiversity, and desertification were considered from development and technology perspectives with the consideration of traditional knowledge and practices. The United Nations Convention to Combat Desertification (UNCCD) selected a Science and Technology Committee to look at the inventory and classification of traditional knowledge. This effort researched approximately 200 member countries. A definition of *traditional knowledge* was as follows:

Traditional knowledge consists of practical (instrumental) and normative knowledge concerning the ecological, socio-economic and cultural environment. Traditional knowledge originates from people and is transmitted to people by recognizable and experienced actors. It is systematic (inter-sector and holistic), experimental (empirical and practical), handed down from generation to generation and culturally enhanced. Such a kind of knowledge supports diversity and enhances and reproduces local resources.

A list of 78 techniques and practices were developed by the committee and were classified into seven topics: water management for conservation, improvement of soil fertility, protection of vegetation, fight against wind or water erosion silviculture, social organization, architecture,

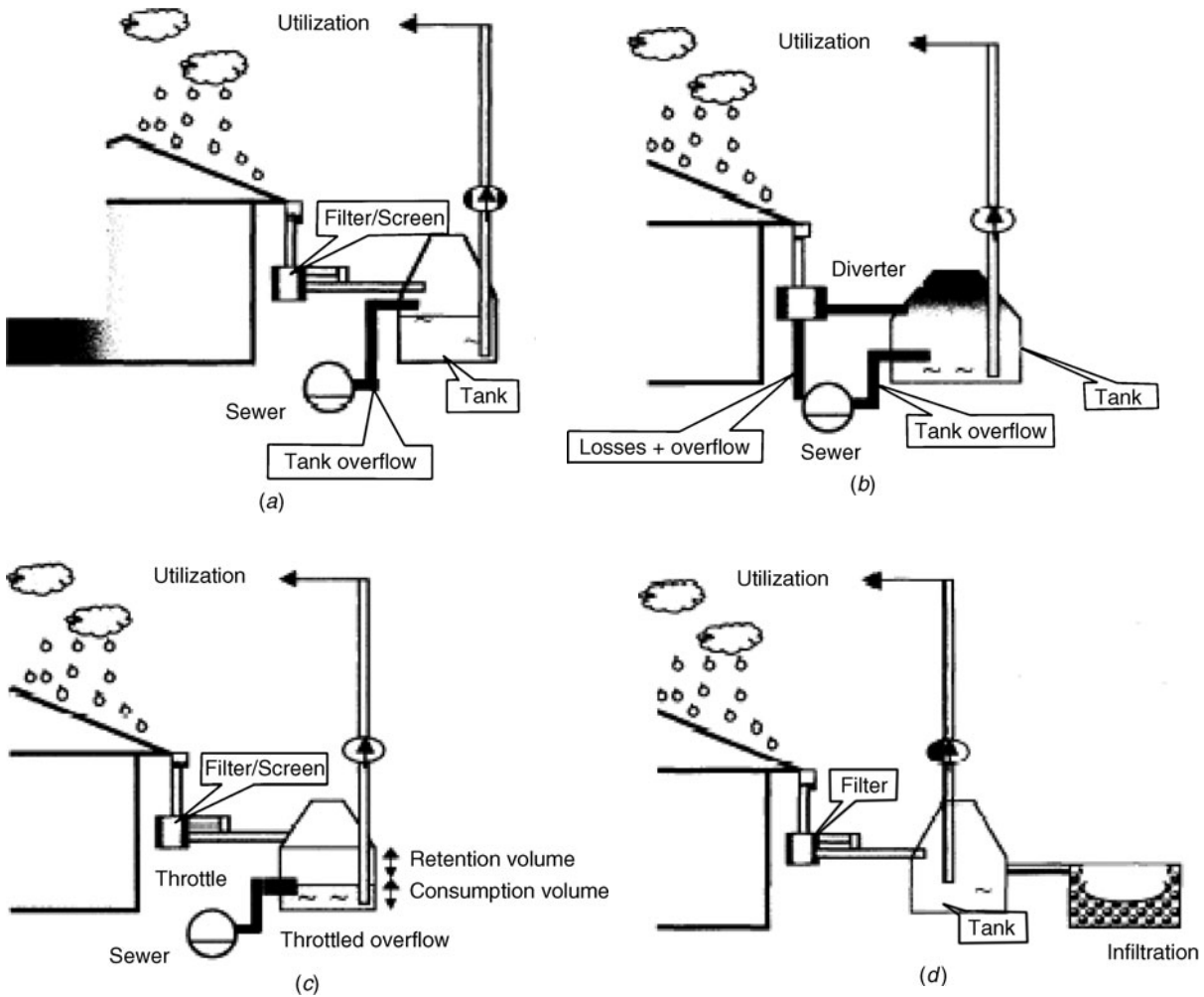


Figure 19.3.12 Types of rainwater harvesting systems (Nouh and Al-Shamsy, 2001; UNESCO, 2001). (a) Total flow type rainwater harvesting system. Runoff is confined to storage tank after passing through a filter or screen before the tank. Overflow to the drainage system only occurs when storage tank is full; (b) Diverter-type rainwater harvesting system. This type contains a branch installed in the vertical rainwater pipe either after the gutter or in the underground drainage pipe. Collected portion is separated from the gutter at the branch and the surplus is diverted to the sewer system. Branches contain a fine-meshed sieve that diverts most of the particles to the sewer; (c) Retention and throttle-type rainwater harvesting system. Storage tank provides an additional retention volume, which is emptied using the throttle to the sewer system; (d) Infiltration-type rainfall harvesting system. Local infiltration of the surplus tank overflow is possible instead of diversion to the sewer system.

and energy. Desertification was defined as “deterioration of the land in the arid, semi-arid and semi-humid dry areas due to factors including climate change and human activity.”

“Modern technology aims at an immediate efficiency through a high specialization of knowledge supported by dominant structures able to mobilize resources external to the environment” (Laureano, 2001). An example of modern technology would be to dig deep wells and pump to an extent that would harm water supplies for the future, which has been done in so many places in both the developing and developed parts of the world. Traditional knowledge would have relied on a system for harvesting meteoric water or exploiting runoff areas using the force of gravity or water catchment methods that would allow the replenishment and increasing the durability of the resource (Laureano, 2001). “Modern technological methods operate by separating and specializing, whereas traditional knowledge operates by connecting and integrating.”

19.4 WATER RESOURCES ECONOMICS

19.4.1 Engineering Economic Analysis

Engineering economic analysis is an evaluation process that can be used for comparing various water resource project alternatives and selecting the most economic one. This process requires defining feasible alternatives and then applying a discounting technique to select the best alternative. In order to perform this analysis, several basic concepts such as equivalence of kind, equivalence of time, and discounting factors must be understood.

One of the first steps in economic analysis is to find a common value unit such as monetary units. Through the use of common value units, alternatives of rather diverse kinds can be evaluated. The monetary evaluation of alternatives generally occurs over a number of years. Each monetary value must be identified by the amount and the time. The time value of money results from willingness of people to pay interest for the use of money. Consequently, money at different times cannot be directly combined or compared, but must first be made equivalent through the use of discount factors. *Discount factors* convert a monetary value at one date to an equivalent value at another date.

Discount factors are described using the notation: i is the annual interest rate; n is the number of years; P is the present amount of money; F is the future amount of money; and A is the annual amount of money. Consider an amount of money P that is to be invested for n years at i percent interest rate. The future sum F at the end of n years is determined from the following progression:

	Amount at beginning of year		Interest		Amount at end of year
First year	P	+	iP	=	$(1 + i)P$
Second year	$(1 + i)P$	+	$iP(1 + i)$	=	$(1 + i)^2P$
Third year	$(1 + i)^2P$	+	$iP(1 + i)^2$	=	$(1 + i)^3P$
	\vdots		\vdots		\vdots
	\vdots		\vdots		\vdots
i -th year	$(1 + i)^{n-1}P$	+	$iP(1 + i)^{n-1}$	=	$(1 + i)^n P$

The future sum is then

$$F = P(1 + i)^n \tag{19.4.1}$$

The *single-payment compound amount factor* is

$$F/P = (1 + i)^n = (F/P, i\%, n) \tag{19.4.2}$$

This factor defines the number of dollars that accumulate after n years for each dollar initially invested at an interest rate of i percent. The *single-payment present worth factor* $(P/F, i\%, n)$ is simply the reciprocal of the single-payment compound amount factor. Table 19.4.1 summarizes the various discount factors.

Uniform annual series factors are used for equivalence between present (P) and annual (A) monetary amounts or between future (F) and annual (A) monetary amounts. Consider the amount of money A that must be invested annually (at the end of each year) to accumulate F at the end of n years. The last value of A in the n -th year is withdrawn immediately upon deposit so it accumulates no interest. The future value F is

$$F = A + (1 + i)A + (1 + i)^2A + \dots + (1 + i)^{n-1}A \tag{19.4.3}$$

Equation (19.4.3) is multiplied by $(1 + i)$, and subtract equation (19.4.3) from the result to obtain the *uniform annual series sinking fund factor*,

$$A/F = i[(1 + i)^n - 1] = (A/F, i\%, n) \tag{19.4.4}$$

Table 19.4.1 Summary of Discounting Factors

Type of Discount Factor	Symbol	Given*	Find	Factor	
Single-Payment Factors					
Compound-amount factor	$\left(\frac{F}{P}, i\%, n\right)$	P	F	$(1 + i)^n$	
Present-worth factor	$\left(\frac{P}{F}, i\%, n\right)$	F	P	$\frac{1}{(1 + i)^n}$	
Uniform Annual Series Factors					
Sinking-fund factor	$\left(\frac{A}{F}, i\%, n\right)$	F	A	$\frac{i}{(1 + i)^n - 1}$	
Capital-recovery factor	$\left(\frac{A}{P}, i\%, n\right)$	P	A	$\frac{i(1 + i)^n}{(1 + i)^n - 1}$	
Series compound-amount factor	$\left(\frac{F}{A}, i\%, n\right)$	A	F	$\frac{(1 + i)^n - 1}{i}$	
Series present-worth factor	$\left(\frac{P}{A}, i\%, n\right)$	A	P	$\frac{(1 + i)^n - 1}{i(1 + i)^n}$	
Uniform Gradient Series Factors					
Uniform gradient series present-worth factor	$\left(\frac{P}{G}, i\%, n\right)$	G	P	$\frac{(1 + i)^{n+1} - (1 + ni + i)}{i^2(1 + i)^n}$	

The *sinking fund factor* is the number of dollars A that must be invested at the end of each of n years at i percent interest to accumulate \$1. The *series compound amount factor* (F/A) is simply the reciprocal of the sinking fund factor (Table 19.4.1), which is the number of accumulated dollars if \$1 is invested at the end of each year. The *capital-recovery factor* can be determined by simply multiplying the sinking fund factor (A/F) by the single-payment compound amount factor (Table 19.4.1),

$$(A/P, i\%, n) = (A/F)(F/P) \tag{19.4.5}$$

This factor is the number of dollars that can be withdrawn at the end of each of n years if \$1 is initially invested. The reciprocal of the capital-recovery factor is the *series present worth factor* (P/A), which is the number of dollars initially invested to withdraw \$1 at the end of each year.

A *uniform gradient series factor* is the number of dollars initially invested in order to withdraw \$1 at the end of the first year, \$2 at the end of the second year, \$3 at the end of the third year, etc.

EXAMPLE 19.4.1

A water resources project has benefits that equal \$20,000 at the end of the first year and increase on a uniform gradient series to \$100,000 at the end of the fifth year. The benefits remain constant at \$100,000 each year until the end of year 30, after which they decrease to \$0 on a uniform gradient at the end of year 40. What is the present value of these benefits using a 6-percent interest rate?

SOLUTION

The present value of the uniform gradient series for years 1 through 5 is

$$\begin{aligned} 20,000(P/G, 6\%, 5) &= 20,000(12.1411) \\ &= \$242,822 \end{aligned}$$

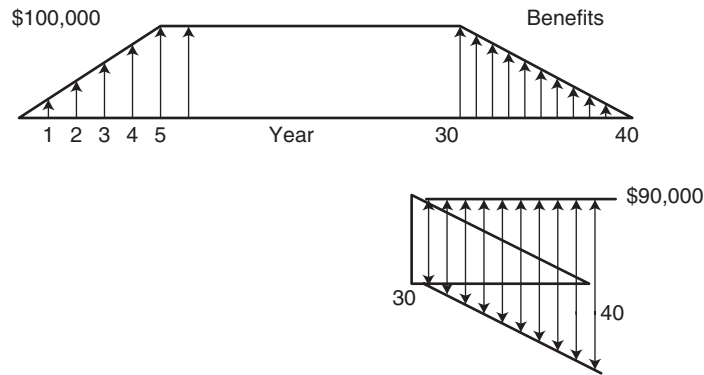


Figure 19.4.1 Cash flow diagram.

The present value of the annual series for years 6 through 30 is

$$100,000(P/A, 6\%, 25)(P/F, 6\%, 5) = 100,000(12.7834)(0.74726) = \$955,252.$$

Present value of the uniform gradient series for years 31 through 40 is modeled by a series of annual investments of \$80,000 per year for years 31 through 40, and subtracting a uniform gradient series for the same years, as shown in Figure 19.4.1. The present value is determined by applying the single-payment present-worth factor,

$$90,000(P/A, 6\%, 10)(P/F, 6\%, 30) - 10,000(P/G, 6\%, 9)(P/F, 6\%, 31) = 90,000(7.3601)(0.17411) - 10,000(31.3783)(0.16425) = \$63,793$$

The total present worth value is

$$\$242,822 + \$955,252 + \$63,793 = \$1,261,867$$

19.4.2 Benefit–Cost Analysis

Water projects extend over time, incur costs throughout the duration of the project, and yield benefits. Typically, costs are large during the initial construction and startup period, followed by only operation and maintenance costs. Benefits typically build up to a maximum over time as depicted in Figure 19.4.2. The *present value of benefits* (PVB) and *costs* (PVC) are, respectively,

$$PVB = b_0 + b_1/(1 + i) + b_2/(1 + i)^2 + \dots + b_n/(1 + i)^n \tag{19.4.6}$$

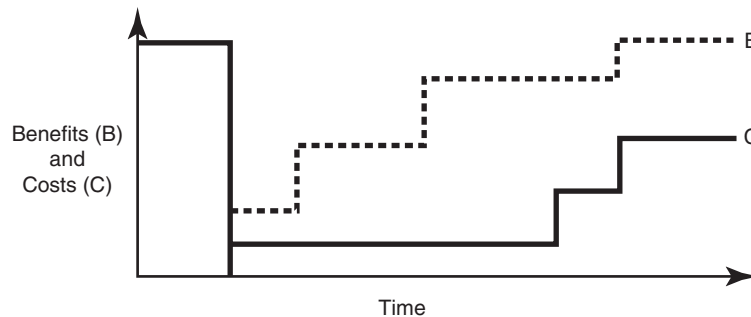


Figure 19.4.2 Benefits and costs over time.

and

$$PVC = c_0 + c_1/(1+i) + c_2/(1+i)^2 + \cdots + c_n/(1+i)^n \quad (19.4.7)$$

The present value of net benefits (PVNB) is

$$\begin{aligned} PVNB &= PVB - PVC \\ &= (b_0 - c_0) + (b_1 - c_1)/(1+i) + (b_2 - c_2)/(1+i)^2 + \cdots + (b_n - c_n)/(1+i)^n \end{aligned} \quad (19.4.8)$$

In order to carry out a benefit-cost analysis, rules for economic optimization of the project design and procedures for ranking projects are needed. Howe (1971) points out that the most important point in project planning is to consider the broadest range of alternatives. The range of alternatives selected is restricted typically by the response of the water resource agency and/or the planners. The nature of the problem to be solved may also condition the range of alternatives. Preliminary investigation of alternatives can help to rule out projects because of technical infeasibility or on the basis of costs.

Consider the selection of an optimal, single-purpose project design such as the construction of a flood-control system or a water-supply project. The optimum size can be determined by selecting the alternative such that the marginal or incremental present value of costs, ΔPVC , is equal to the marginal or incremental value of the benefits, ΔPVB ,

$$\Delta PVB = \Delta PVC$$

The marginal or incremental value of benefits and costs, for a given increase in the size of the project are

$$\Delta PVB = \Delta b_1/(1+i) + \Delta b_2/(1+i)^2 + \cdots + \Delta b_n/(1+i)^n \quad (19.4.9)$$

and

$$\Delta PVC = \Delta c_1/(1+i) + \Delta c_2/(1+i)^2 + \cdots + \Delta c_n/(1+i)^n \quad (19.4.10)$$

When selecting a set of projects, one rule for optimal selection is to maximize the present value of benefits. Another ranking criterion is to use the benefit-cost ratio (B/C), PVB/PVC ,

$$B/C = PVB/PVC \quad (19.4.11)$$

This method has the option of subtracting recurrent costs from the annual benefits or including all costs in the present value of cost. Each of these options will result in a different B/C, with higher B/Cs when netting out annual costs, if the B/C is greater than 1. The B/C ratio is frequently used to screen infeasible alternatives whose $B/C < 1$ from further consideration.

Selection of the optimum alternative is based upon the incremental benefit-cost ratios, $\Delta B/\Delta C$, whereas the B/C ratio is used for ranking alternatives. The incremental benefit-cost ratio is

$$\Delta B/\Delta C = [PVB(A_j) - PVB(A_k)]/[PVC(A_j) - PVC(A_k)] \quad (19.4.12)$$

where $PVB(A_j)$ is the present value of benefits for alternative A_j . Figure 19.4.3 is a flowchart illustrating the benefit-cost method.

EXAMPLE 19.4.2

Determine the optimal scale of development for a hydroelectric project using the benefit-cost analysis procedure. The various alternative size projects and corresponding benefits are listed in Table 19.4.2.

SOLUTION

According to Figure 19.4.3, the benefit-cost analysis procedure first computes the B/C ratios of each alternative and ranks the projects with $B/C > 1$ in order of increasing cost. Referring to Table 19.4.2, the B/C ratios for the alternatives are the incremental benefit-cost ratios given in column (8). Comparing the 50,000 and 60,000 kW alternatives, the $\Delta B/\Delta C$ is

$$\Delta B/\Delta C = 3000/2400 = 1.3$$

Note that the incremental B/C ratio is greater than one until the 100,000 and 125,000 kW projects are compared where $\Delta B/\Delta C = 0.9$. This means that the incremental benefits are not

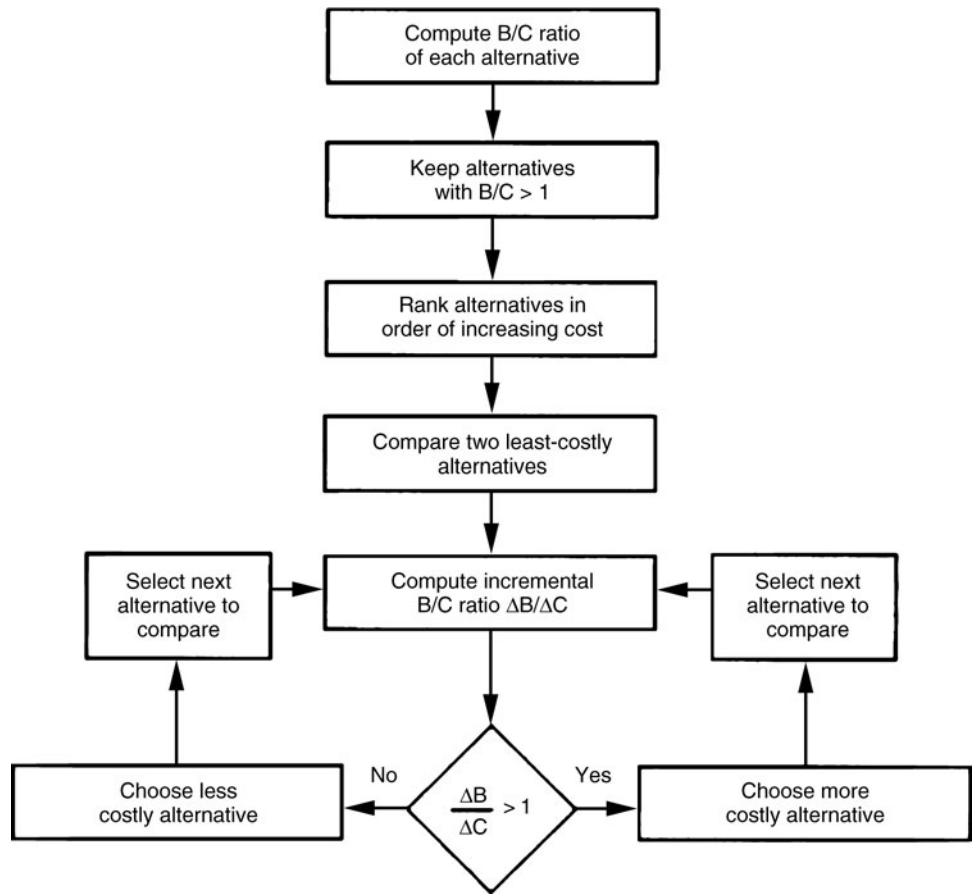


Figure 19.4.3 Flowchart for benefit-cost analysis.

Table 19.4.2 Determination of Optimum Scale of Development of a Hydroelectric Plant for Example 2.2.2

1 Scale (kW)	2 Costs C (\$000)	3 Benefits B (\$000)	4 Net benefits (\$000)	5 B/C	Incremental		8 ΔB/ΔC
					6 Costs ΔC (\$000)	7 Benefits ΔB (\$000)	
50,000	15,000	18,000	3000	1.2	—	—	—
60,000	17,400	21,000	3600	1.2	2400	3000	1.3
75,000	21,000	26,700	5700	1.3	3600	5700	1.6
90,000	23,400	29,800	6400	1.3	2400	3100	1.3
100,000*	26,000	32,700	6700	1.3	2600	2900	1.1
125,000	32,500	38,500	6000	1.2	6500	5800	0.9
150,000	37,500	42,500	5000	1.1	5000	4000	0.8
200,000	50,000	50,000	—	1.0	12,500	7500	0.6

*Optimum scale of project.
Source: Sewell et al. (1961)

longer greater than the incremental costs. The optimum scale of development is the 100,000 kW project, which has the largest net benefits.

19.4.3 Value of Water for Sustainability

We are interested in the total economic value of water. *Total economic value* includes use values and non-use values, with the basic idea to combine use values and nonuse values. Use values are concrete, such as the value we get from the production of a good, and can be broken down into separate categories; direct use, indirect use, and option values. *Direct use value* occurs when something is directly used or consumed. Indirect use values are usually measures of benefits or services. Ecosystem services can be beneficial directly or indirectly whether they are consumed or not. If water is taken out of rivers for irrigation or for municipal uses that is a direct use. Indirect use could involve aesthetic values such as the beauty of the water. Uses that involve both direct and indirect use values include water for fisheries, wildlife, and ecosystems. Estimated values and prices can be determined for such uses that are deferred, or the willingness to pay to maintain a resource.

Nonuse values include existence values and bequest values. A basic difference between option values and nonuse values is the difference in time horizons. *Bequest values*, which are nonuse values, are technically the same as option values (use values); however, the bequest values have a longer time frame, such as being held for future generations. *Existence values* (nonuse values) are pure benefits, such as the value of knowing that something exists for the value of its existence. It is the least tangible of the various types of values.

Environmental economists refer to the *total economic value of water*, which can be subdivided in different ways but usually consists of two principal components: (a) use values, including both direct *ex situ* uses such as agricultural irrigation and indirect *in situ* uses such as ecological support; and (b) non use values, which occur as a consequence of water remaining in place. Figure 19.4.4 illustrates a typical breakdown of the total economic value of water.

The use values indicated in Figure 19.4.4 are self-explanatory; however, nonuse values, which include “existence” and “bequest” values, are less intuitive. Existence values are those that an individual assigns to a resource to insure its availability for others, or for the sake of the resource itself, rather than for any direct or even indirect (e.g., ecological) benefit that it provides. *Bequest values* are those that an individual assigns out of altruism for future generations. These nonuse values are especially significant because of their obvious relation to the concept of sustainability and because they are typically the most difficult and controversial aspect of water valuation. Methods for evaluating the nonuse values of water are typically very limited. From a sustainability viewpoint, the

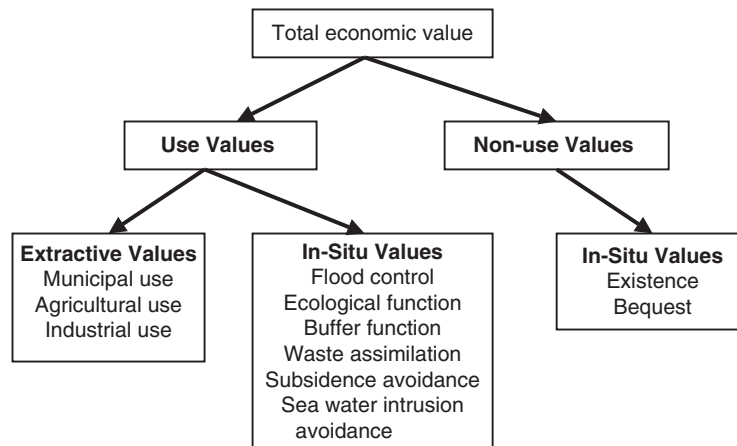


Figure 19.4.4 Total economic value of water (Rothman, 2007).

future use of water is very important, so that placing an economic value on it is very important. Rothman (2007) developed a relationship expressing the non-use value of groundwater.

19.4.4 Allocation of Water to Users

Economic Efficiency

Economic efficiency can be defined as “the organization of production and consumption such that all possibilities for increasing economic well-being have been exhausted” (Rogers et al., 2006). Economic efficiency is achieved if Pareto optimality is achieved. *Pareto optimality* is the “allocation of resources such that no further allocation is possible which would provide gains in production or consumer satisfaction to some firms or individuals without simultaneously imposing losses on others” (Rogers et al., 2006). Obviously, economic efficiency is important for water resources sustainability.

The concepts of supply and demand can be used to explain the market price of a commodity, such as water, or a service, and the total quantity of the commodity traded in the market. These concepts rely upon microeconomic theory. A consumer’s or user’s demand for a commodity depends upon its price. In Section 11.5.2, the concept of a demand function is defined. The demand curve defines the quantity of a commodity that a consumer is willing to purchase as a function of price. Figure 11.5.1 shows two demand curves, one is a typical demand curve and the second is for a situation where the same quantity is demanded no matter what the price. Demand curves are generally assumed to be negatively sloped, so that the lower the price, the greater the quantity demanded.

A *supply function* defines the quantity that a firm will produce as a function of the market price. Supply functions can be defined for (a) very short periods of time when the output level cannot vary; (b) short run during a time that the output level can vary and some inputs are fixed; and (c) long run during which all inputs are considered variable (Mays and Tung, 1992). The demand curve is the marginal benefit (MB) curve and the supply curve is the marginal cost (MC) curve.

If the supply (MC curve) and demand (MB curve) functions are plotted together (as shown in Figure 19.4.5), the location where the supply curve and the demand curve intersect (point B)

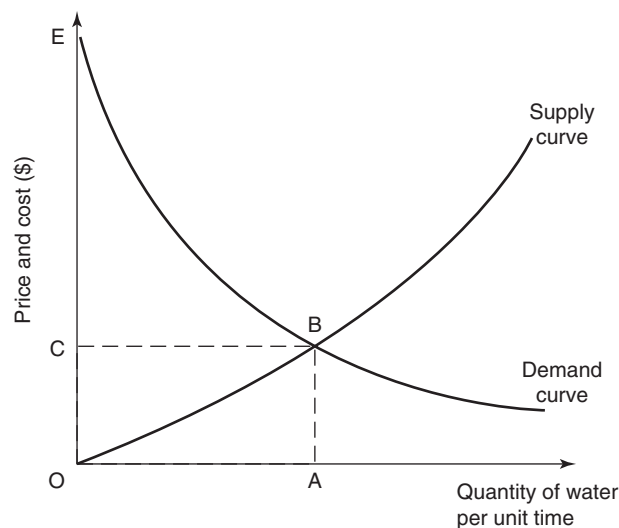


Figure 19.4.5 Optimal allocation of water as illustrated by supply, demand, and the willingness to pay for quantity of water per unit time. The optimal quantity of water to allocate to the user is A, and the optimal price per unit quantity is C. If the price is greater than C, then the consumer will underconsume, and if price is less than C, then the consumer will overconsume.

indicates the optimal allocation of resources. This location, where $MB = MC$, identifies how much should be bought, how much should be paid, and at what price. This price is the market-clearing price or equilibrium price, presuming *ceteris paribus* (all other things being equal), a free market economy. Another way to express this is to say that at point B, the *marginal willingness to pay* for an additional unit exactly equals the opportunity cost (willingness to pay for foregone alternatives) of supplying that unit (Young, 1996). Any allocation greater than A will involve use of marginal units whose worth to the user is less than the incremental cost of supply, and net total benefits will be less than maximum. Use of units of water less than A have value to the user exceeding their marginal cost, and net total benefit could be increased by allocating more units to the user.

In most parts of the world, water is underpriced, resulting in people consuming too much water. Because of this, the real challenge is how to persuade people to reduce their demand to a reasonable level, or a sustainable level for the purposes of water resources sustainability. By properly pricing water, people would consume amount A, as shown in Figure 19.4.5.

19.5 WATER RESOURCE SYSTEMS ANALYSIS

19.5.1 Application of Optimization

Optimization has a major role in water resources sustainability for the future. The major types of problems that must be solved for various types of water resources projects are (Buras, 1972):

- determining the optimal scale of development of the project,
- determining the optimal dimensions of the various components of the project, and
- determination of the optimal operation of the project.

If the solutions to these problems are denoted as X_1 , X_2 , and X_3 , then the benefit of these solutions is

$$B = f(X_1, X_2, X_3) \quad (19.5.1)$$

The objective of many water resources projects is to maximize the benefits so that the problem of developing water resources may be stated as

$$\text{Max } B = f(X_1, X_2, X_3) \quad (19.5.2)$$

subject to various types of constraints including technological constraints, economic and/or budget constraints, design constraints, operation constraints, demand constraints, and others.

What is an Optimization Problem?

An optimization problem in water resources can be formulated in a general framework in terms of decision variable \mathbf{x} , which is a vector of variables $(x_1, x_2, x_3, \dots, x_n)$ with an objective function to optimize $f(\mathbf{x})$

$$Z = \text{Maximize } f(\mathbf{x}) \text{ or Minimize } f(\mathbf{x}) \quad (19.5.3)$$

subject to constraints

$$\mathbf{g}(\mathbf{x}) = 0 \quad (19.5.4)$$

and bound constraints on the decision variables.

Every optimization problem has two essential parts: the objective function and the set of constraints. The objective function describes the performance criteria of the system. Constraints describe the system or process that is being designed, operated, or analyzed and can be of two forms:

equality constraints and inequality constraints. A *feasible solution* of the optimization problem is a set of values of the decision variables that simultaneously satisfy the constraints. The *feasible region* is the region of feasible solutions defined by the constraints. An optimal solution is a set of values of the decision variables that satisfy the constraints and provides an optimal value of the objective function.

The most common type of optimization model is the *linear programming model*, which has a linear objective function and linear constraints,

$$\text{Maximize (or Minimize)} x_0 = \sum_{j=1}^n c_j x_j \quad (19.5.5)$$

Subject to

$$\sum_{j=1}^n a_{ij} x_j = b_i \quad \text{for } i = 1, 2, 3, \dots, m \quad (19.5.6)$$

$$x_{ij} \geq 0 \quad \text{for } i = 1, 2, 3, \dots, m \text{ and } j = 1, 2, 3, \dots, n \quad (19.5.7)$$

where c_j are the objective function coefficients, a_{ij} are the technological coefficients, and b_i are the right-hand side coefficients. Linear programming (LP) problems can be solved using software based upon the simplex method.

Linear programming problems can be visualized only if two decision variables exist. Keep in mind that LP problems can have hundreds to thousands of decision variables and constraints. However, a simple two-decision variable problem can be useful in visualizing the problem. Example 19.5.1 is a simple LP with two decision variables that can be solved using Excel.

Applications in water resources

Optimization has been applied to many types of water resources engineering problems including:

Water distribution systems

Least cost design of water distribution systems

Replacement and rehabilitation of water distribution system components

Operation of water distribution systems to minimize energy costs or for water quality purposes

Surface water management

Operation policies and management of surface water reservoirs

Determination of optimal reservoir sizes

Aqueduct route optimization

Design and operation of irrigation systems

Determining fresh water flow into bays and estuaries

Water quality management

Determination of firm energy and firm yield

Groundwater management

Operation of aquifers to determine recharge and pumping

Parameter identification for aquifers

Design of aquifer reclamation systems

Determination of hydraulic containment strategies for water quality purposes

Determination of least cost dewatering systems

Conjunctive use of surface water and groundwater

Stormwater and flood-plain management systems

Design, operation, and management of flood-plain systems and components

Design of sewer systems, detention and retention basins, flood control channels

Optimal operation of detention basin systems

References on the application of optimization to water resources include Mays and Tung (1992), Mays (1997, 2005), ReVelle et al. (2003).

19.5.2 Example Applications of Optimization to Water Resources Problems

EXAMPLE 19.5.1

Consider a system composed of a manufacturing factory and a waste treatment plant owned by the manufacturer (Fiering et al., 1971). The manufacturing plant produces finished goods that sell for a unit price of \$10K. However, the finished goods cost \$3K per unit to produce. In the manufacturing process, two units of waste are generated for each unit of finished goods produced. In addition to deciding how many units of goods to produce, the plant manager must decide how much waste will be discharged without treatment so that the total net benefit to the company can be maximized and the water quality requirement of the watercourse is satisfied. The treatment plant has a maximum capacity of treating 10 units of waste with 80 percent waste removal efficiency at a treatment cost of \$0.6K per unit of waste. There is also an effluent tax imposed on the waste discharged to the receiving water body (\$2K for each unit of waste discharged). The water pollution control authority has set an upper limit of four units on the amount of waste any manufacturer may discharge. Formulate an LP model for this problem and show a graphical solution.

SOLUTION

The first step in model development is to identify the system components involved and their interconnections. In this example, the system components are the manufacturing factory, the waste treatment plant, and the water course. From the problem statement, the two decision variables to the problem are (1) the number of finished goods to be produced, x_1 ; and (2) the quantity of waste to be discharged directly into the watercourse without treatment, x_2 . From the description of the interrelationship of finished goods, waste generated, and the treatment plant efficiency, a schematic of the system under study is shown in Figure 19.5.1. The amount of waste in each branch is determined by the mass-balance principle.

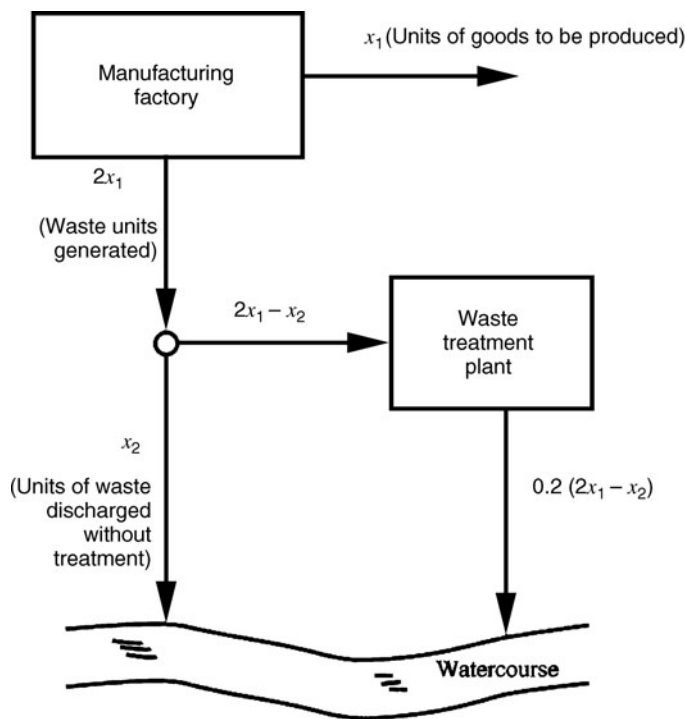


Figure 19.5.1 Schematic diagram of manufacturing-waste treatment system.

The objective of the problem is to maximize profit. Constraints arise primarily from the limitations on treatment capacity and on the allowable waste discharges set by the water pollution control authority. Now we must translate the verbal description of the problem into mathematical expressions of the objective function and constraints. Net revenue of the manufacturer is defined by four terms:

Sales of finished goods (in \$K), $10x_1$

Cost of producing goods (in \$K), $3x_1$

Cost of treating waste generated in the production process (in \$K), $0.6(2x_1 - x_2)$

Effluent tax charged on untreated waste (in \$K), $2[x_2 + 0.2(2x_1 - x_2)]$

The profit to the manufacturer is equal to total sales minus the total costs. The objective function is to Maximize $\{10x_1 - [3x_1 + 0.6(2x_1 - x_2) + 2[x_2 + 0.2(2x_1 - x_2)]]\}$ which simplifies to Maximize $[5x_1 - x_2]$, which can be expressed as

$$\text{Maximize } x_0 = [5x_1 - x_2]$$

Referring to Figure 19.5.1, the constraint on the limitation of treatment plant capacity says that the amount of waste to be treated, $2x_1 - x_2$, cannot exceed the plant capacity of 10 units of waste, expressed mathematically as

$$2x_1 - x_2 \leq 10$$

The constraint associated with the amount of total waste that can be discharged to the water course, $x_2 + 0.2(2x_1 - x_2)$, must be less than the total allowable waste units set by the water pollution control authority of four units, expressed mathematically as $x_2 + 0.2(2x_1 - x_2) \leq 4$. Simplifying the constraint is

$$0.4x_1 + 0.8x_2 \leq 4$$

In addition to the two obvious constraints above, there exists a rather subtle constraint that must be incorporated in the model. This constraint is to ensure that a positive amount of waste is treated so that $2x_1 - x_2$ must be nonnegative, so that $2x_1 - x_2 \geq 0$, which can also be written as

$$-2x_1 + x_2 \leq 0$$

Nonnegativity constraints also say that $x_1 \geq 0$ and $x_2 \geq 0$.

The final version of the mathematical statement of the LP model is

$$\text{Maximize } x_0 = [5x_1 - x_2]$$

subject to

$$2x_1 - x_2 \leq 10$$

$$0.4x_1 + 0.8x_2 \leq 4$$

$$-2x_1 + x_2 \leq 0$$

$$x_1 \geq 0 \text{ and } x_2 \geq 0$$

Because this problem has two decision variables, we can look at the problem graphically as shown in Figure 19.5.2. The feasible space for this problem is the cross-hatched area. A characteristic of LP problems is that the optimal solution will be at one of the corner points A, B, C, or D. Checking each of the corner points for this simple example, it is obvious that the optimal solution is at C where $x_1 = 6$ and $x_2 = 2$, so that the profit (maximum achievable net benefit) is $5(6) - 1(2) = \$28K$.

EXAMPLE 19.5.2

Reservoir operation

Reservoirs are built for several purposes including water supply. The water demands and the natural inflows (streamflows into a reservoir) and the water demand for municipal, industrial, and agricultural purposes are not matched in time. In other words, peak demands typically occur during seasons when reservoir inflows (rainfall and snowmelt runoff) are the least. In the case of sizing a reservoir for water supply, the record of monthly streamflows during a critical period, i.e. the period during which the inflows are minimal during a historical record of flows, must be included in the record used for the analysis.

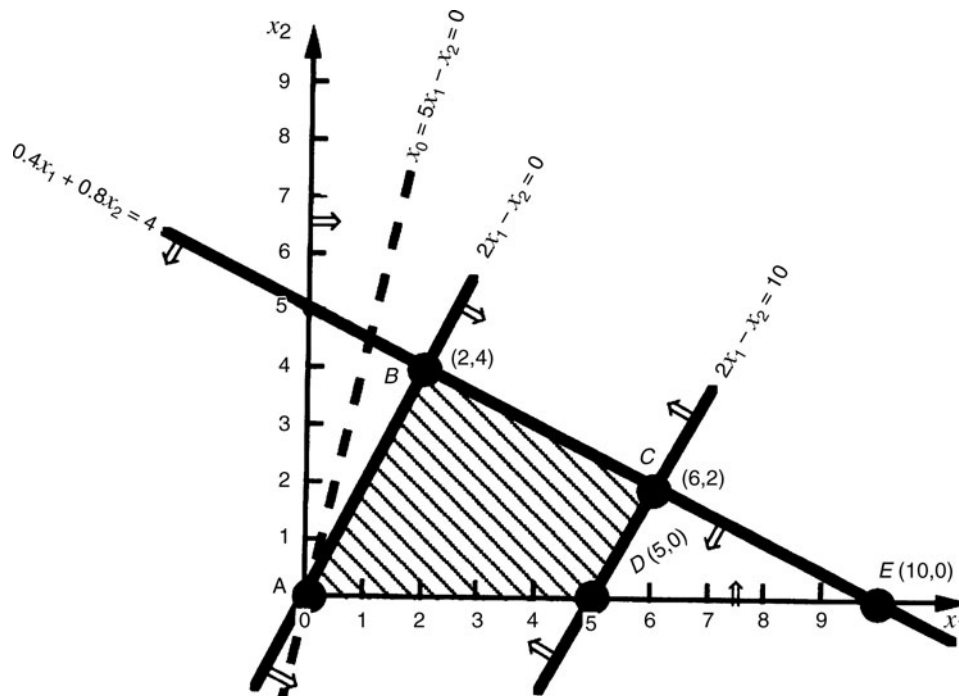


Figure 19.5.2 Feasible space of manufacturing-waste treatment example.

Our objective is to determine the active storage for a planned reservoir on the Little Weiser River near Indian Valley, Idaho, for a firm yield (firm release) of $R = 2000$ ac-ft/month (AF/month). As defined in Chapter 11, firm yield of a reservoir is the mean monthly withdrawal rate that would lower the reservoir to its minimum allowable level just once during the critical drought of record. The monthly stream flows, QT_t for $1, \dots, T$ (months), for the Little Weiser River near Indian Valley, Idaho, for the critical drought of record is for water years 1966–1970 as given in Tables 11.7.1 and 11.7.3. Precipitation on the reservoir surface, PP_t , and evaporation from the reservoir, EV_t , are listed in Table 11.7.3.

SOLUTION

In order to solve this problem, we will develop an optimization model based upon using linear programming. This model can be stated as:

Minimize active storage capacity, K_a

subject to the following constraints:

- Conservation of mass in each time period
- Reservoir capacity cannot be exceeded during any time period
- Nonnegative decision variables

Our first step is to identify the conservation of mass constraints. The monthly reservoir storage is denoted as ST_t and the spill (amount of release in excess of the specified firm release) for month t is W_t . The conservation of mass in each time period (month) is

$$ST_t - ST_{t+1} - W_t = R - QT_t - PP_t + EV_t \quad \text{for } t = 1, \dots, T$$

The second set of constraints states that the unknown reservoir capacity, K_a , cannot be exceeded during each time period, $ST_t - K_a \leq 0$, for $t = 1, \dots, T$. The constraint, $ST_T \geq ST_1$, says that storage at the end of the critical period, ST_1 , must be at least as large as the starting storage. Essentially this last constraint prevents borrowing storage to artificially inflate the amount that can be delivered steadily throughout the critical record. The decision variables are ST_t, W_t , for $t = 1, \dots, T$ and K_a must be positive.

We can now state the optimization model as

$$\text{Minimize } Z = K_a$$

subject to

$$ST_t - ST_{t+1} - W_t = 2000 - QF_t - PP_t + EV_t \quad \text{for } t = 1, \dots, T$$

$$ST_t - K_a \leq 0 \quad \text{for } t = 1, \dots, T$$

$$ST_T \geq ST_1$$

$$ST_t \text{ and } W_t \geq 0 \quad \text{for } t = 1, \dots, T$$

$$\text{and } K_a \geq 0$$

We will assume the initial storage in the reservoir is $ST_1 = K_a$ for the first month ($t = 1$). The mass balance is $ST_1 - ST_2 - W_1 = 2000 - QF_1 - PP_1 + EV_1$. From Table 11.7.3, $QF_1 = 742$ AF/month, $PP_1 = 3$ AF/month, and $EV_1 = 270$ AF/month, so the resulting mass balance constraint for month $t = 1$ is $K_a - ST_2 - W_1 = 1525$. Similarly, the mass balance for month $t = 2$ is $ST_2 - ST_3 - W_2 = 2000 - QF_2 - PP_2 + EV_2 = 1,210$. The mass balance equation is written for each of the 60 months. The second set of constraints to ensure that the monthly storage ST_t does not exceed the reservoir active capacity. The constraints are expressed as $ST_2 - K_a \leq 0, ST_3 - K_a \leq 0, \dots, ST_{60} - K_a \leq 0$. The third constraint then forces the final storage at the end of the critical period to be at least as large as the initial unknown storage, K_a . There are a total of T mass balance constraints and T storage constraints, so the total number of constraints for this LP problem is $2T = 120$ and the number of decision variables is $2T + 1 = 121$.

An alternative to this problem would be to maximize the firm yield (firm release) for a specified active storage K_a^* given as

$$\text{Maximize } Z = R$$

subject to

$$ST_t - ST_{t+1} - W_t - R = -QF_t - PP_t + EV_t \quad \text{for } t = 1, \dots, T$$

$$ST_t \leq K_a \quad \text{for } t = 1, \dots, T$$

$$ST_T \geq ST_1$$

$$ST_t \text{ and } W_t \geq 0 \quad \text{for } t = 1, \dots, T \text{ and}$$

$$R \geq 0$$

A firm yield–active storage relationship can be constructed by repeatedly solving this LP model for different values of specified active storage K_a^* . See Mays and Tung (1992) and ReVelle (1999).

19.5.3 Decision Support Systems (DSS)

Decision support systems (DSS) do not refer to a specific area of specialty, and it is not easy to give a specific definition to DSS based on their uses. Generally, DSS provide pieces of information, sometimes real-time information, that help us to make better decisions. A DSS is an interactive computer-based support system that helps decision-makers utilize data and computer programs to solve unstructured problems. DSS generally consists of three main components: (1) state representation, (2) state transition, and (3) plan evaluation (Reitsma et al., 1996). State representation consists of information about the system in such forms as databases. State transition takes place through modeling such as simulation. Plan evaluation consists of evaluation tools such as multi-criteria evaluation, visualization, and status checking. The above three components comprise the database management subsystem, model base management subsystem, and dialog generation and management subsystem, respectively.

Numerous DSSs have been developed over the years, many of which are commercially available packages that include extremely sophisticated components; however, they are deficient in the integration of various interrelations among the different social, environmental, economic, and technological dimensions of water resources (Todini et al., 2006). One model of interest is the Water Strategy Man Decision Support System (WSM DSS), which was developed by the EU-funded Water Strategy Man project (Developing Strategies for Regulating and Managing Water Resources and

Demand in Water Deficient Regions). According to Todini et al. (2006), this model was developed as a GIS-based package with the objective to emphasize the conceptual links among the various components and aspects of water resource system management, instead of merely focusing on the detailed description of the physical systems and related phenomena. Maia (2006) describes an application of the WSM DSS to evaluate the alternative water management scenarios of the Ribeiras do Algarve, Portugal in the semi-arid region of southern Portugal. This river basin includes an area of 3,837 km² and 18 municipalities.

19.6 LIFE CYCLE ASSESSMENT (LCA)

Life cycle assessment (LCA) is another tool that can be used for analyzing water resources sustainability. LCA is a quantitative procedure to assess the environmental burdens associated with the life cycle of an activity (product, process, or service) (IISD, 1996). LCA evaluates the environmental burdens associated with a product, process, or activity by identifying energy and materials used and wastes released to the environment, and to evaluate and implement opportunities to affect environmental improvements (SETAC, 1991).

Several studies have applied LCA in the field of water resources. These include applications to: life cycle assessment of rainwater use for domestic needs (Bronchi et al., 1999); life cycle assessment of water mains and sewers (Herz and Lipkow, 2002); estimate the environmental impacts from urban water systems (Lundin et al., 2000); life cycle assessment for sustainable metropolitan water systems planning (Lundie et al., 2004); and environmental life cycle assessment of water supply (Landu and Brent, 2006).

Life cycle assessment is a tool used to assess the environmental impact of products over the whole product life cycle taking into account the extraction of raw materials, energy consumption, production, and the disposal of waste. LCA is typically accomplished in four phases (see Figure 19.6.1):

- **goal definition**, which defines the aims and the scope of the study, including the definitions of functional units and system boundaries,
- **inventory**, which lists pollutant emissions and consumption of resources during the entire product life cycle, including raw material extraction, production, use, and waste treatment,
- **impact assessment**, which assesses the environmental impact,
- **interpretation**, which carries out uncertainty analyses and sensitivity studies in a looped procedure.

In a life cycle assessment study, a system delivers a product or service that performs a specified function. The study based upon LCA attempts to determine the efficiency of providing that function over the entire life cycle of the product or service. In the first phase (goal definition), the design and conduct of the LCA study must be defined based upon the purpose and objectives of the study. After the goal definition has been accomplished, the inventory phase of the LCA study requires mass balances of energy,

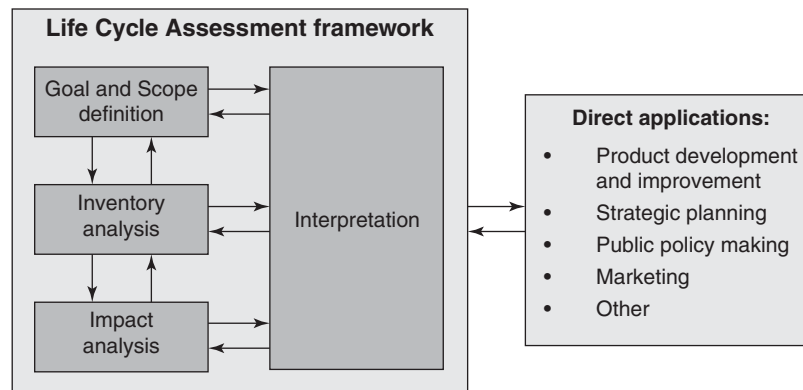


Figure 19.6.1 Standardized phases of the LCA procedure (SABS, 1998).

resources, and materials used, in addition to the wastes and pollution generated over the entire life cycle. In the impact assessment phase, the resulting inventory is then converted to a set of indicators for energy and resource efficiency, as well as for pollutant and waste loadings. It can be argued that life cycle impact assessment can be described as an indicator system (Owens, 1999). LCA studies can contribute to more sustainable uses of resources, such as water in various systems like industrial, municipal, and agricultural systems if the indicators are properly defined and applied (Owens, 2001). LCA can be used to initiate a comparison of different scenarios for a product or system, or different systems to produce a product or service. Insights can be provided on efficiencies and tradeoffs among competing issues.

Addressing the sustainable use of water resources, LCA indicators must include indicators for both water quality as well as water quantity. Owens (2001) discusses water resources in life cycle impact assessment, as water is one of many resources, wastes, and pollutants in life cycle assessment. Detailed indicators beyond the total input of water are proposed considering the essential areas of water sustainability, water quantity, and water quality. To consider water quantity, the governing principles are that water sources (as inputs to LCA) are renewable and sustainable, and the volume of water released (LCA outputs) is returned to humans or ecosystems for further use downstream. To consider water quality, the governing principle is that “the returned water is not impaired for either humans or ecosystems downstream.” Lundin et al. (1999) discuss the indicators for the assessment of temporal variations in the sustainability of sanitary systems.

The definitions proposed by Owens (2001) are based on current U.S. Geological Survey accounting definitions and may be summarized as follows:

- *Use* indicates that water resource quantities are utilized and then made available to others.
- *Consumption* indicates that the water resource quantities are denied to others.
- *Depletion* indicates that water sources are either not renewed by the hydrological cycle or cannot be sufficiently replaced at the same rates that they are used by the natural hydrological cycle.

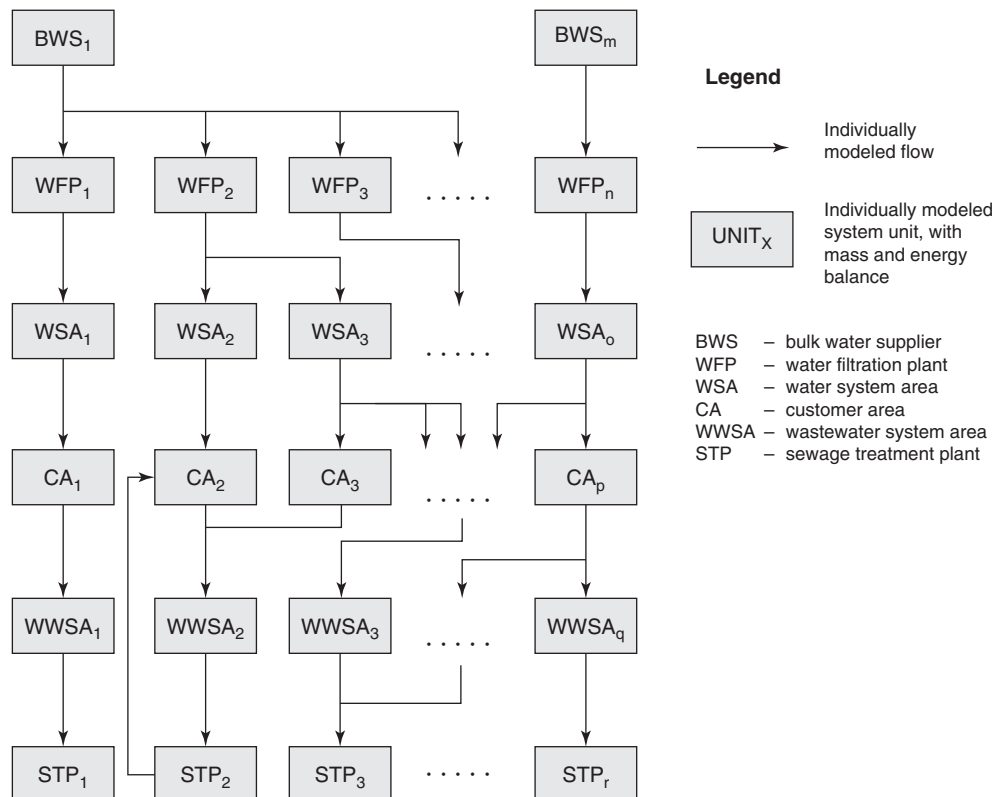


Figure 19.6.2 Schematic diagram of LCA model for Sydney Water (Lundin et al., 1999).

Lundie et al. (2004) performed life cycle assessment for sustainable metropolitan water systems planning. In particular, they developed an LCA model for a large water and wastewater system, Sydney Water, which is Australia’s largest water service provider. Figure 19.6.2 shows the schematic diagram of the LCA model for Sydney Water. Figure 19.6.3 shows the simplified flow diagram within the defined system boundaries for the Sydney Water system. Various scenarios for strategic planning were considered. These included desalination of seawater and upgrades of major coastal seawater treatment plants to secondary and tertiary treatment. The scenarios examined increased demand management, energy efficiency, energy generation, and additional energy recovery from biosolids.

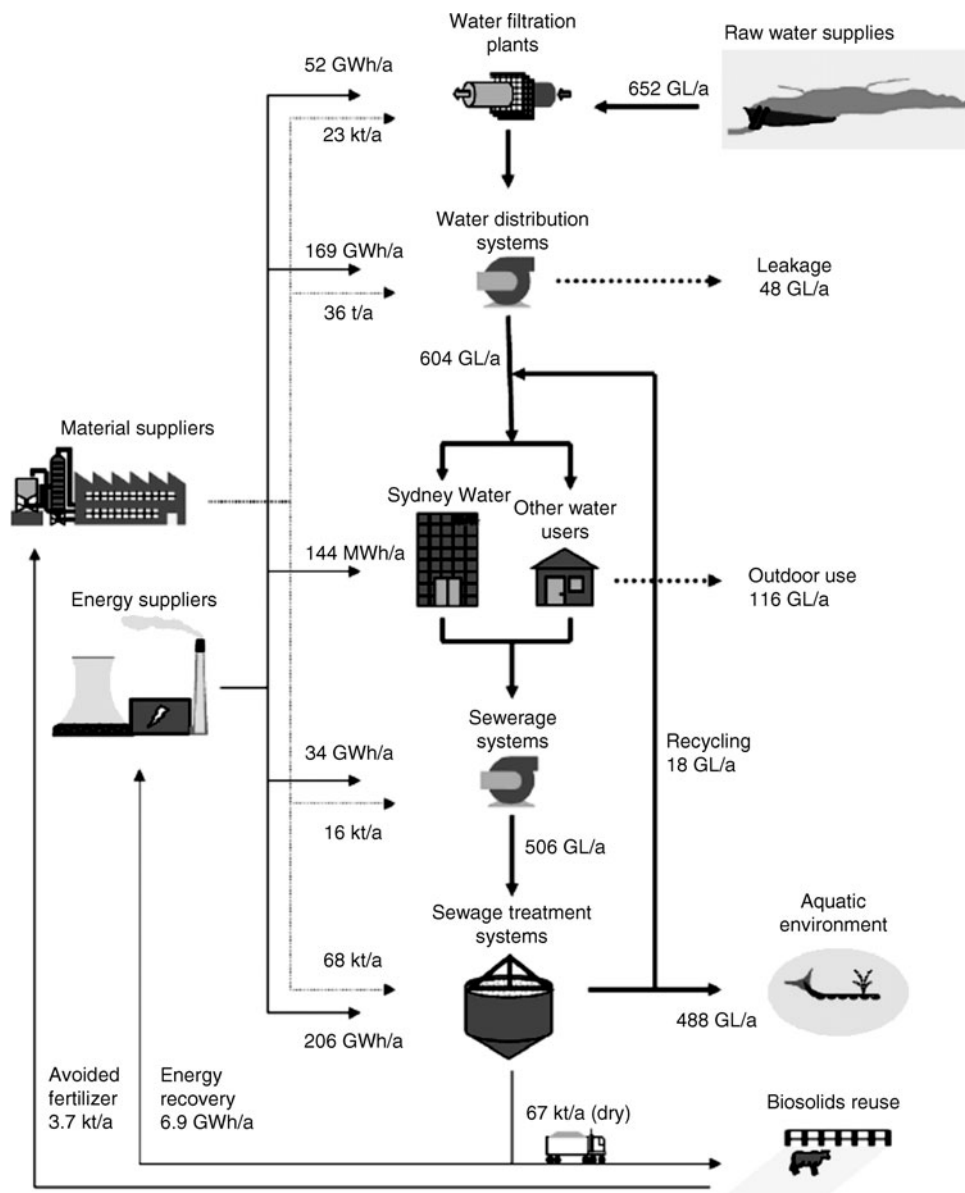


Figure 19.6.3 Simplified flow diagram within the defined system boundaries for the Sydney Water system (Lundie et al., 2004).

PROBLEMS

19.1.1 Write a short summary description of each of the principles of IWRM listed in Table 19.1.1.

19.1.2 Write a paper on how Turkey's Southeastern Anatolia Project (GAP) addresses water resources sustainability.

19.2.1 Select two states in the US and compare how the surface and groundwater policies are managed.

19.2.2 Develop a short essay on the water law policies in Spain.

19.2.3 Develop a short essay on the water law policies in a country in Africa.

19.2.4 Develop a short essay on the water law policies in a country of your choice.

19.2.5 Write a summary of the international legal water aspects of Turkey's Southeastern Anatolia Project (GAP).

19.3.1 Write an essay on the sustainability of the GMMRP.

19.3.2 Write an essay on the sustainability of the CAP.

19.3.3 Write an essay on the sustainability of the El Shalaam project in Egypt.

19.4.1 Solve Example 19.4.1 using an interest rate of 8 percent.

19.4.2 A water resources project has produced benefits of \$40,000 at the end of each of 20 years. Determine the present value of these benefits using a 6 percent interest rate. Determine the value of the benefits at the end of the 20th year.

19.4.3 A water resources project has produced benefits of \$20,000 at the end of the first year and increase on a uniform gradient series to \$100,000 at the end of the fifth year. The benefits remain constant at \$100,000 each year until the end of year 25. Determine the present value of these benefits using an interest rate of 6 percent.

19.4.4 A water resources project has produced benefits of \$10,000 at the end of the first year and an increase on a uniform gradient series to \$50,000 at the end of the fifth year. The benefits then decrease to zero on a uniform gradient series to \$0 at the end of year 10. Determine the value of these benefits in year 0 and year 25 using an interest rate of 6 percent.

19.4.5 Use the benefit–cost analysis procedure to determine the optimum scale of development for the following alternatives for a small hydroelectric facility.

Alternative (Scale)	Costs \$ × 10 ⁴	Benefits \$ × 10 ⁴
1	650	650
2	1800	2200
3	3600	4800
4	6900	9400
5	9900	14,000
6	12,700	18,000
7	15,400	19,700
8	17,400	20,900

19.4.6 Four alternative projects presented here can be used for developing a water supply for a community for the next 40 years. Assume benefits for each alternative are equal to compare and select an alternative.

Year(s)	Project I	Project II	Project III	Project IV
Construction cost × 10 ³				
0	40,000	30,000	20,000	10,000
10	0.0	0.0	0.0	10,000
20	0.0	10,000	20,000	10,000
40	0.0	0.0	0.0	10,000
Operation and maintenance costs				
0–10	100,000	110,000	120,000	120,000
10–20	120,000	110,000	130,000	120,000
20–30	140,000	120,000	140,000	130,000
30–40	160,000	140,000	150,000	130,000

19.4.7 Resolve Problem 19.4.6 using an interest rate of 5 percent.

19.5.1 Reformulate the linear programming (LP) model for Example 19.5.1 using an effluent tax of \$3K for each unit of waste discharged. Show graphically the new resulting optimal solution.

19.5.2 Reformulate the linear programming (LP) model for Example 19.5.1 using a new selling unit price of \$ 15K. Show graphically the new resulting optimal solution.

19.5.3 Reformulate the linear programming (LP) model for Example 19.5.1 using a new upper limit of five units on the amount of waste any manufacturer may discharge. Show graphically the new resulting optimal solution.

19.5.4 Use Excel to solve Example 19.5.1.

19.5.5 Use Excel to solve Example 19.5.2.

REFERENCES

- Arizona Department of Water Resources (ADWR), "Overview of Arizona's Groundwater Management Code," <http://www.adwr.state.az.us/Azwaterinfo/>, 1998.
- Arizona State University, University of Arizona, and University of Colorado, *Soil Treatability Pilot Studies to Design and Model Soil Aquifer Treatment Systems*, AWWA Research Foundation and American Water Works Association, Denver, CO, 1998.
- Asano, T., (editor), *Artificial Recharge of Groundwater*, Butterworth Publishers, Boston, MA, 1985.
- Asano, T., "Groundwater Recharge with Reclaimed Municipal Wastewater—Regulatory Perspectives," *Proceedings of the International Symposium on Efficient Water Use in Urban Areas—Innovative Ways of Finding Water for Cities*, UNEP IETC—(International Environmental Technology Centre) Report no. 9, Osaka/Shiga, Japan, pp. 173–181, 1999.
- Biswas, A. K., (editor), "Water Resources Development in a Holistic Socioeconomic Context—the Turkish Experience," *International Journal of Water Resources Development*, vol. 13, no. 4 (Special Issue), 1997.
- Bouwer, H., *Groundwater Hydrology*, McGraw-Hill, New York, 1998.
- Bronchi, V., O., Jolliet, and P. Crettaz, "Life Cycle Assessment of Rainwater Use for Domestic Needs," *Proceedings of the 2nd Inter-Regional Conference on Environment-Water: Emerging Technologies*, September 1-3, Lausanne, Switzerland, 1999.
- Broshi, M., "The Population of Western Palestine in the Roman-Byzantine Period," *Bulletin of the American Schools of Oriental Research*, vol. 236, pp. 1–10, 1980.
- Bruins, H. J., "Israel: Urban Water Infrastructure in the Desert," in *Urban Water Supply Handbook* edited by L. W. Mays, McGraw-Hill, New York, pp. 17.1–17.22, 2002.
- Buras, N., *Scientific Allocation of Water Resources*, American Elsevier Publishing Company, New York, 1972.
- Cabrera, E. and Lund, J. R., "Regional Water Management: A Long View," *Regional Water System Management: Water Conservation, Water Supply, and System Integration* edited by E. Cabrera, R. Cobacho, and J. R. Lund, A. A. Balkema Publishers, Lisse, pp. 343–346, 2002.
- Cech, T. V., *Principles of Water Resources: History, Development, Management, and Policy*, John Wiley & Sons, Inc., 2003.
- Crook, J., *Water Reclamation and Reuse Criteria*, U.S. Environmental Protection Agency, 1998.
- Eheart, J.W., and J.R. Lund, "Water-use Management: Permit and Water Transfer Systems," *Water Resources Handbook*, edited by L.W. Mays, McGraw-Hill, New York, pp. 32.1–32.34, 1996.
- Fiering, M. B., J. J. Harrington, and R. J. deLucia, *Water Resources System Analysis, Policy and Coordination Branch*, Department of Energy, Mines and Resources, Ottawa, Canada, 1971.
- Fox, P., "Advantages of Aquifer Recharge for a Sustainable Water Supply," *Proceedings of the International Symposium on Efficient Water Use in Urban Areas—Innovative Ways of Finding Water for Cities*, UNEP IETC(International Environmental Technology Centre) Report no. 9, Osaka/Shiga, Japan, pp. 163–172, 1999.
- Harper, J. K., and R. C. Griffin, *The Structure and Role of River Authorities in Texas*, *Water Resources Bulletin*, American Water Resources Association, Issue No. 6, Bethesda, Maryland, December, 1988.
- Hermann, T., and U. Schmida, "Rainwater Utilization in Germany: Efficiency, Dimensioning, Hydraulic and Environmental Aspects," *Urban Water*, vol. 1, no. 4, pp. 307–316, 1999.
- Herz, R. K. and A. Lipkow, "Life Cycle Assessment of Water Mains and Sewers," *Water Supply*, vol. 2, no. 4, pp. 51–58, 2002.
- Howe, C., *Benefit-Cost Analysis for Water System Planning*, Water Resources Monograph vol. 2, American Geophysical Union, Washington, DC, 1971.
- International Institute for Sustainable Development (IISD), *Global Green Standards—ISO 14000 and Sustainable Development*, IISD, Winnipeg, 1996.
- Khan, A. H., *Desalination Processes and Multistage Flash Distillation Practice*, Elsevier, New York, 1986.
- Landu, L., and A. C. Brent, "Environmental Life Assessment of Water Supply in South Africa: The Rosslyn Industrial Area as a Case Study," *Water SA*, vol. 32, no. 2, April 2006.
- Laureano, P., *The Water Atlas: Traditional Knowledge to Combat Desertification* (© Peatro Laureno, translated by Anna Cirella and Angela Whitehouse), 2001.
- Lundie, S., G. M. Peters, and P. C. Beavis, "Life Cycle Assessment for Sustainable Metropolitan Water Systems Planning," *Environmental Science and Technology*, vol. 38 no. 13, pp. 3465–3473, July 2004.
- Lundin, M., S. Molanders, and G. M. Morrison, "A Set of Indicators for the Assessment of Temporal Variations in the Sustainability of Sanitary Systems," *Water Science and Technology*, vol. 39 no. 5 pp. 235–242, 1999.
- Lundin, M., M. Bengtsson, and S. Molander, Life Cycle Assessment of Wastewater Systems: Influence of System Boundaries and Scale on Calculated Environmental Loads, *Environmental Science and Technology* vol. 34, pp. 180–186, 2000.
- Maia, R., "Evaluation of alternative water management scenarios: case study of Ribeiras do Algarve, Portugal," *Water Management in Arid and Semi-Arid Regions*, edited by P. Koundouri et al., Edward Elger Publishers, Cheltenham, U.K., pp. 41–104, 2006.
- Marsalek, et al., "Urban Water Cycle: Processes and Interactions," IHP-VI, Technical Publications in Hydrology no. 78, UNESCO, Paris, 2006.
- Mays, L. W., *Optimal Control for Hydrosystems*, Marcel-Dekker, Inc., New York, 1997.
- Mays, L. W., (editor), *Water Resources Systems Management Tools*, McGraw-Hill, New York, 2005.
- Mays, L. W. and Tung, Y. K., *Hydrosystems Engineering and Management*, McGraw-Hill, New York, (now available through Water Resources Publications, LLC, Highlands Ranch, CO), 1992.
- Mitchell, B., (editor), *Integrated Water Management: International Experiences and Perspectives*, Belhaven Press, London, 1990.
- McCann, B., "Global Prospects for Rainwater Harvesting," *Water 21*, pp. 12–14, December 2008.
- Nouh, M., and K. Al-Shamsy, Sustainable Solutions for Urban Drainage Problems in Arid and Semi-arid Regions, *Urban Drainage in Arid and Semi-Arid Climates*, vol. III, edited by M. Nouh, UNESCO IHP-V, Technical Documents in Hydrology, no. 40, UNESCO, Paris, pp. 106–120, 2001.
- Owens, J. W., "Why Life Cycle Impact Assessment is now Described as an Indicator System," *International Journal of Life Cycle Assessment*, vol. 4 no. 2 pp. 81–86, 1999.
- Owens, J. W., "Water Resources in Life-Cycle Impact Assessment: Considerations in Choosing Category Indicators," *Journal of Industrial Ecology*, vol. 5, no. 2, pp. 37–54, February 2001.
- Pantell, S. E., *Seawater Desalination in California*, California Coastal Commission, San Francisco, California, <http://www.coastal.ca.gov/desalrpt/dchap1.html>, 1993.
- Post, J., "Wastewater Treatment and Reuse in the Eastern Mediterranean Region," *Water 21*, IWA Publishing, London, June, pp. 36–41, 2006.

- Reitsma, R. F., et al., "Decision Support Systems (DSS) for Water Resources Management," in *Water Resources Handbook* edited by L. W. Mays, McGraw-Hill, Inc., New York, 1996.
- ReVelle, C. S., *Optimizing Reservoir Resources, Including a New Model for Reservoir Reliability*, John Wiley & Sons, Inc., New York, 1999.
- ReVelle, C. S., E. E. Whitlatch, and J. R. Wright, *Civil and Environmental Systems Engineering*, 2nd edition, Prentice Hall, NJ, 2003.
- Rogers, P. P., K. F. Jalal, and J. A. Boyd, *An Introduction to Sustainable Development*, The Continuing Education Division, Harvard University, and the Glen Educational Foundation, 2006.
- Rothman, D., "Evaluation of Water Resources Sustainability Using a Multi-objective Genetic Algorithm," Ph.D. Dissertation, Department of Civil and Environmental Engineering, Arizona State University, Tempe, AZ, May, 2007.
- Schmandt, J., E. T. Smerdon, and J. Clarkson, *State Water Policies, A Study of Six States*, Praeger, New York, 1988.
- Sewell, W. R. D., J. Davis, A. D. Scott, and D. W. Ross, *Guide to Benefit-Cost Analysis, Report*, Resources for Tomorrow, Information Canada, Ottawa, 1961.
- Society of Toxicology and Chemistry (SETAC), *Code of Practice*, 1991.
- South African Bureau of Standards (SABS), *Code of Practice: Environmental Management—Life Cycle Assessment—Principles and Framework. SABS ISO 14040: 1997*, Pretoria, 1998.
- Tarlock, A. D., "Water Law," Chapter 5 in *Water Resources Handbook* edited by L. W. Mays, McGraw-Hill, New York, 1996.
- Texas Water Development Board (TWDB), *The Texas Manual on Rainwater Harvesting*, 3rd edition, Austin, Texas, 2005.
- Todd, D. K., and Mays, L. W., *Groundwater Hydrology*, 3rd edition, John Wiley & Sons, Inc., New York, 2005.
- Todini, E., Schumann, A., Assimacopoulos, D., "The WaterStrategy-Man Decision Support System," *Water Management in Arid and Semi-Arid Regions* edited by P. Koundouri, et al., Edward Elgar Publishers, Cheltenham, pp. 13–40, 2006.
- UNESCO, IHP-V, Technical Documents in Hydrology, no. 40, vol. III, UNESCO, Paris, 2001.
- Unver, O., "Water-Based Sustainable Integrated Regional Development," in Chapter 12, *Water Resources Sustainability*, McGraw-Hill, New York, 2007.
- U.S. Environmental Protection Agency (EPA) and U.S. Agency for International Development (AID), *Guidelines for Water Reuse*, EPA/625/R-92/004, Washington, DC, September, 1992.
- U.S. Environmental Protection Agency (EPA) and U.S. Agency for International Development (AID), *Guidelines for Water Reuse*, EPA/625/R-04/108, Washington, DC, 2004.
- Wehmhoefer, R. A., Chapter 2 in *Water and the Future of the Southwest* edited by, Z. A. Smith, University of New Mexico Press, Albuquerque, NM, 1989.
- Wangnick, K., IDA Worldwide Desalting Plants Inventory Report no. 18, Wangnick Consulting GmbH, 2004.
- Young, R. A., "Water Economics," Chapter 13 in *Water Resources Handbook* edited by L. W. Mays, McGraw-Hill, Inc., New York, 1996.
- Zuhair, A., Nouh, M., El Sayed, M., "Flood Harvesting in Selected Arab States," Final Report, Institute of Water Resources, 1999.

This page intentionally left blank

Appendix A

Newton–Raphson Method

FINDING THE ROOT FOR A SINGLE NONLINEAR EQUATION

One of the most widely used methods for determining the root of a function ($f(x) = 0$) is the *Newton–Raphson equation*. Referring to Figure A.1, using an initial guess of the root as x_i , a tangent can be extended from point $[x_i, f(x_i)]$ to the x -axis. The point (value of x) where the tangent crosses the x -axis, x_{i+1} , usually represents an improved estimate of the root. The first derivative at $[x_i, f(x_i)]$ is the gradient or slope, $f'(x_i)$, expressed as

$$\left(\frac{df}{dx}\right)_i = f'(x_i) = \frac{f(x_i) - 0}{x_i - x_{i+1}} \quad (\text{A.1})$$

which can be rearranged to yield the Newton–Raphson equation.

$$x_{i+1} = x_i - \frac{f(x_i)}{f'(x_i)} \quad (\text{A.2})$$

The above derivation is simply a geometrical interpretation. See Chapra and Canale (1988) for a more rigorous mathematical derivation based on the Taylor series.

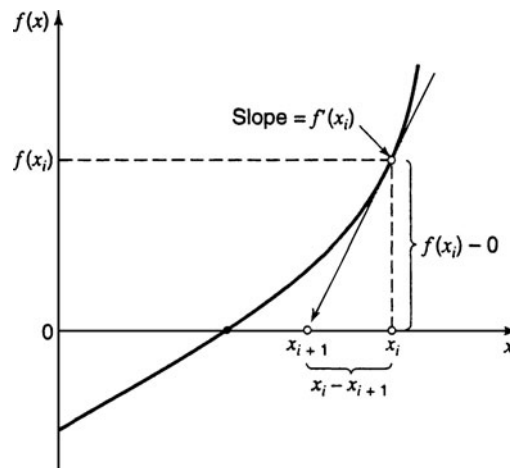


Figure A.1 Graphical depiction of the Newton–Raphson method. A tangent to the function of x_i [that is, $f'(x_i)$] is extrapolated down to the x -axis to provide an estimate of the root at x_{i+1} .

APPLICATION TO SOLVE MANNING’S EQUATION FOR NORMAL DEPTH

Given a discharge Q , the normal depth is computed using Manning’s equation (see Chapter 5).

$$Q = \frac{1.49}{n} AR^{2/3} S_0^{1/2}$$

where the cross-sectional area of flow A and the hydraulic radius R are both functions of the depth y .

Starting with an initial guess of y_i , for the normal depth, the resulting discharge is Q_i .

$$Q_i = \frac{1.49}{n} A_i R_i^{2/3} S_0^{1/2} \quad (\text{A.3})$$

To solve this problem for y given Q using the Newton–Raphson method, the nonlinear function to determine the root of is

$$f(y_i) = Q_i - Q \quad (\text{A.4})$$

The gradient, $f'(y_i)$ is

$$\frac{df}{dy_i} = \frac{dQ}{dy_i} \quad (\text{A.5})$$

because Q is a constant. Hence, assuming Manning’s n is constant,

$$\begin{aligned} f'(y_i) &= \frac{d}{dy} \left[\frac{1.49}{n} S_0^{1/2} A_i R_i^{2/3} \right] \\ &= \frac{1.49}{n} S_0^{1/2} \left(\frac{2AR^{-1/3}}{3} \frac{dR}{dy} + R^{2/3} \frac{dA}{dy} \right)_i \\ &= \frac{1.49}{n} S_0^{1/2} A_i R_i^{2/3} \left(\frac{2}{3R} \frac{dR}{dy} + \frac{1}{A} \frac{dA}{dy} \right)_i \\ &= Q_i \left(\frac{2}{3R} \frac{dR}{dy} + \frac{1}{A} \frac{dA}{dy} \right)_i \end{aligned} \quad (\text{A.6})$$

where the subscript i outside the parentheses indicates that the contents are evaluated for $y = y_i$.

The Newton–Raphson equation (A.2) in terms of the normal depth is

$$y_{i+1} = y_i - \frac{f(y_i)}{f'(y_i)} \quad (\text{A.7})$$

Substituting equation (A.4) and (A.6) into equation (A.7) gives the Newton–Raphson equation for solving Manning’s equation:

$$y_{i+1} = y_i - \frac{Q_i - Q}{Q_i \left(\frac{2}{3R} \frac{dR}{dy} + \frac{1}{A} \frac{dA}{dy} \right)_i} \quad (\text{A.8})$$

For a rectangular channel, $A = B_w y$ and $R = \frac{B_w y}{(B_w + 2y)}$ where B_w is the channel width; equation (A.8) becomes

$$y_{i+1} = y_i - \frac{1 - Q/Q_i}{\left(\frac{5B_w + 6y_i}{3y_i(B_w + 2y_i)} \right)} \quad (\text{A.9})$$

Values for the *channel shape function* $\left(\frac{2}{3R} \frac{dR}{dy} + \frac{1}{A} \frac{dA}{dy}\right)$ for other cross-sections are given in Table 5.1.2.

FINDING THE ROOTS OF A SYSTEM OF NONLINEAR EQUATIONS

The above discussion focused on the determination of the roots of a single equation. A related problem is to find the roots of simultaneous equations,

$$\begin{aligned} f_1(x_1, x_2, \dots, x_n) &= 0 \\ f_2(x_1, x_2, \dots, x_n) &= 0 \\ &\vdots \\ f_n(x_1, x_2, \dots, x_n) &= 0 \end{aligned} \quad (\text{A.10})$$

The solution of this system consists of a set of x 's that simultaneously result in all the equations equaling zero.

The Newton–Raphson method is an iterative technique for solving a system of nonlinear algebraic equations. It uses the same idea as presented above for the determination of the roots of a single equation, except that here the solution is for a vector of variables rather than for a single variable. Consider a system of equations denoted in vector form as

$$\mathbf{f}(\mathbf{x}) = 0 \quad (\text{A.11})$$

where $\mathbf{x} = (x_1, x_2, \dots, x_n)$ is the vector of unknown quantities and for iteration k , $x_k = (x_1^k, x_2^k, \dots, x_n^k)$. The nonlinear system can be linearized to

$$\mathbf{f}(\mathbf{x}^{k+1}) \approx \mathbf{f}(\mathbf{x}^k) + \mathbf{J}(\mathbf{x}^k)(\mathbf{x}^{k+1} - \mathbf{x}^k) \quad (\text{A.12})$$

where $\mathbf{J}(\mathbf{x}^k)$ is the *Jacobian*, which is a coefficient matrix made up of the first partial derivatives of $\mathbf{f}(\mathbf{x})$ evaluated at \mathbf{x}^k . The right-hand side of equation (A.12) is the nonlinear vector function of $\bar{\mathbf{x}}^k$. Basically, an iterative procedure is used to determine \mathbf{x}^{k+1} that forces the residual error $\mathbf{f}(\bar{\mathbf{x}}^{k+1})$ in equation (A.12) to zero. This can be accomplished by setting $\mathbf{f}(\bar{\mathbf{x}}^{k+1}) = 0$ and rearranging equation (A.12) to read

$$\mathbf{J}(\mathbf{x}^k)(\mathbf{x}^{k+1} - \mathbf{x}^k) = -\mathbf{f}(\mathbf{x}^k) \quad (\text{A.13})$$

This system is solved for $(\mathbf{x}^{k+1} - \mathbf{x}^k) = \Delta \mathbf{x}^k$, and the improved estimate of the solution, \mathbf{x}^{k+1} , is determined knowing $\Delta \mathbf{x}^k$. The process is repeated until $(\mathbf{x}^{k+1} - \mathbf{x}^k)$ is smaller than some specified tolerance.

Let the initial estimate for the roots be $x_1^0, x_2^0, \dots, x_n^0$ where the superscript indicates the number of the iteration—0 for the initial estimate, 1 for values obtained after one iteration, and so on. We can expand and rearrange equation (A.13) as

$$\begin{bmatrix} \frac{\partial f_1}{\partial x_1} & \frac{\partial f_1}{\partial x_2} & \dots & \frac{\partial f_1}{\partial x_i} & \dots & \frac{\partial f_1}{\partial x_n} \\ \frac{\partial f_2}{\partial x_1} & \frac{\partial f_2}{\partial x_2} & \dots & \frac{\partial f_2}{\partial x_i} & \dots & \frac{\partial f_2}{\partial x_n} \\ \dots & \dots & \dots & \dots & \dots & \dots \\ \frac{\partial f_i}{\partial x_1} & \frac{\partial f_i}{\partial x_2} & \dots & \frac{\partial f_i}{\partial x_i} & \dots & \frac{\partial f_i}{\partial x_n} \\ \dots & \dots & \dots & \dots & \dots & \dots \\ \frac{\partial f_n}{\partial x_1} & \frac{\partial f_n}{\partial x_2} & \dots & \frac{\partial f_n}{\partial x_i} & \dots & \frac{\partial f_n}{\partial x_n} \end{bmatrix}^0 \begin{bmatrix} \Delta x_1 \\ \Delta x_2 \\ \vdots \\ \Delta x_i \\ \vdots \\ \Delta x_n \end{bmatrix} = \begin{bmatrix} f_1 \\ f_2 \\ \vdots \\ f_i \\ \vdots \\ f_n \end{bmatrix}^0 \tag{A.14}$$

REFERENCE

Chapra, S. C. and R. P. Canale, *Numerical Methods for Engineers*, 2nd edition, McGraw-Hill, New York, 1988.

Index

Note: The letter “f” or “t” following page number refers to figure or table, respectively, on that page

- Absolute pressure, 60, 60f
- Abstractions, 288, 303–310
- Abutment scour, 771, 773
- Abutment shapes, 726
 - Coefficients for, 730f
- Ackers–White formula, 803–805
- Active Management Areas (AMAs), 44
- Active storage, 448
- Adiabatic lapse rate, 235
 - Dry, 235
 - Saturated, 235
- Aerodynamic method, 261, 264–265
- Aerosols, 237
- Affinity laws, 478–479
- Aggradation, 822
- Agricultural drought, 440
- Agriculture, water for, 411–427, *See also*
 - Irrigation, water for
 - Surface irrigation, 416–417
 - Water supply infrastructure, 413–415,
See also Farm infrastructure, water for
 - Brays Landing unit—Greater Wenatchee division, 414f
 - East Unit—Greater Wenatchee Division, 415f
- Agua Fria Recharge Project, 841f
- Agua Fria River channel, 772f
- Airmass lifting
 - Convective, 238
 - Frontal, 238
 - Orographic, 238
- Albedo, 263
- Allocation of water to users, 855–856
 - Economic efficiency, 855
- Alluvial fans, 579, 581, 581f
 - Fan apex, 581f
 - Fan system, 581f
 - Types of, 581f
- Anisotropy of hydraulic conductivity, 179
- Annoying, 765f–769f
- Annual-exceedance series, 377, 378f
- Annual maximum series, 377, 386f
- Annual runoff
 - By continent, 6t
 - By physiographic region, 6t
- Annual series, 377
- Antecedent moisture conditions (AMC), 303–304, 304t
- Appropriation law, 831
- Aquiclude, 175
- Aquifers, 173
 - Properties, 176–179
 - Conduit function, 176
 - Hydraulic conductivity, 176
 - Porosity, 176
 - Specific retention, 176
 - Specific yield, 176
 - Storage function, 176
 - Storativity, 176
 - Recharge, 838, 838f
 - Types, 175t, 176f
 - Confined, 175
 - Distribution, 180f
 - Unconfined, 175
- Aquifuge, 175
- Aquitard, 175
- Aral Sea, 47–48
- Archimedes’ principle, 77
- Areal average rainfall computations, 238, 246f
 - Arithmetic-mean method, 238
 - Isohyetal method, 238
 - Thiessen method, 238
- Arid regions, sustainable water supply methodologies for, 836–848
- Arithmetic-mean method, 238, 246f
- Arizona Water Law, 831–832
- Armoring, 790–792, 817
- Artesian aquifer, 141
- Artesian or pressure aquifers, 175
- Artificial recharge, 837–839
- Asbestos cement (AC) pipe (ACP), 486, 489t
- Atmosphere, zones, 235
 - Stratosphere, 235
 - Tropopause, 235
 - Troposphere, 235
- Atmospheric circulation, 234–236, 234f
 - Idealized circulation, 234f
 - Middle cell, 234
 - Polar cell, 234
 - Tropical cell, 234
- Atmospheric heat balance, 261f
- Atmospheric radiation balance, 261f
- Axial flow pumps, 475
- Baffled chute spillways, 746–748
 - Basic proportions of, 746f
 - Culvert spillways, 748
- Barrier boundaries, 207–212
- Barton Springs–Edwards aquifer, 218, 219f
- Baseflow separation, 289
- Basin irrigation, water for, 416
- Basin lag, 294
- Basins, groundwater, 179
- Bed forms, 781–782
- Bed load formulas, 792–796
 - Dubois formula, 793–794
 - Meyer-Peter and Müller formula, 794–795
 - Shoklitsch formula, 795–796
- Bed material load formulas, 783, 800–808
 - Acker’s–White formula, 803–805
 - Colby’s formula, 800–803
 - Yang’s unit stream power formula, 805–808
- Benefit–cost analysis, 851–860
 - Flowchart for, 853f
- Bequest values, 854
- Best available control technology (BACT), 407
- Best hydraulic section, 122–123, 122t
- Border-strip irrigation, water for, 416
- Boulder Canyon Project Act, 35–36
- Boundary conditions, For water surface profile computations, 147
- Boussinesq coefficient, 80, 349

- Brake power, 558
- Branching pipe system, 108–109, 496f, 498–499
- Bridge inlets, 692–693
- Bridge scour, 821–822
 - Contraction scour, 821–822
 - Clear-water, 822
 - Live-bed, 822
 - Live-bed at abutments, 822
 - Local scour (piers), 822
- Broad-crested weirs, 158, 160–161
- Brooks-Corey equation, 274
- Bubble gauges, 165, 165f
- Bubbler irrigation, 418
- Budget, hydrologic, 236–237
 - Groundwater system, 237
 - System hydrologic budget, 237
- Budgets, water, 41–47
 - Components, 42f
 - Description, 41
 - Las Vegas, Nevada
 - Predevelopment period, 43f
 - Present period, 43f
 - Nassau and Suffolk Counties, Long Island, New York, 44f
- Bulb turbines, 557
- Bulk modulus of elasticity, 59
- Buoyancy, 77–78

- Calibration, in water distribution, 525–526
- Canal building in the Salt River Valley, 3f
- CAP, *see* Culvert Analysis Program
- Capillary action, 61f
- Capital-recovery factor, 850t
- Capture efficiency, 679
- Catchments, 230
- Cavitation, 481–484, 559
 - Cavitation index, 559
 - Full cavitation, 481
 - Partial cavitation, 481
 - Thoma's cavitation constant, 482
- Center of pressure, 74
- Center-pivot irrigation systems, 417
- Central Arizona Project (CAP) system, 36, 36f, 45f, 432–433f, 550f, 845
 - Features of, 36f
 - Layout of, 36f
- Centrifugal pump, 469
- Channel drop structures, 820–821
- Channel erosion, 808
- Channel linings, 639
- Check dams, 820–821
- Check valves, 490
- Chezy coefficients, 117
- Chezy equation, 117

- Clark unit hydrograph, 295–299
- Climate change, 24–27
 - Components, 25
 - Definitions, 24–26
 - Hydrologic response, 26–27
 - In Pacific Northwest, 26
 - Realities of, 27
 - State-of-the-art climate models, limitations, 25
- Cloud seeding, 431
- Coal fuel cycle, water use for, 404t
- Coefficient of permeability, 176
- Coefficient of skew, 380–381
 - Generalized, 386
 - Map, 386
 - Sample, 386
 - Variance of sample, 386–387
 - Weighted, 386–387
- Coefficient of variance, 386
- Colby's formula, 800–803
- Colorado River Basin, 32–37
 - Annual average flow rate of, 32
 - Annual average surface air temperature for, 34f
 - Annual precipitation for, 34f
 - Basin, 32–34
 - Lower, 33f
 - Upper, 33f
 - Climate, 34–35
 - Future, 37
 - Water development of, history, 35–37
- Combined aerodynamic and energy balance method, 261
- Commercial water use, 7t
- Common law, 831
- Complete duration series, 377
- Composite hydrologic risk, 393–399
- Compound channel sections, 144f
- Compound meters, 469
- Compressibility, 59
- Computer models
 - For floodflow frequency analysis, 399–400
 - In water distribution, 525
- Computer programs
 - CAP, 705
 - EPANET, 525
 - FLDWAV, 359
 - GWSIM, 218
 - HEC-1, 277, 297, 299, 320, 350, 352–353
 - HEC-2, 148, 816
 - HEC-5, 573, 607, 608t
 - HEC-FFA, 399, 399f
 - HEC-RAS, 148–149, 816

- HSPF, 280
- HYDRAIN, 705
- KINEROS, 319–320, 350, 354
- KYPIPE, 523
- KYQUAL, 525
- MODFLOW, 220–221
- PEAKFQ, 399, 399t
- SSARR, 280, 281t
- TR-20, 320
- TR-55, 320
- WSPRO, 816
- Concrete arch dams, 715
- Concrete buttress dams, 715
- Condensation, 237
- Conduit function, aquifer, 176
- Confined aquifers, 175, 186–189, 191–194
 - Storage coefficient of, 177f
 - Well hydraulics for, 192f
- Confining beds, 173–175
 - Types, 175
 - Aquiclude, 175
 - Aquifuge, 175
 - Aquitard, 175
- Conjugate depths, 152
- Connate water, 173
- Conservation form, 347
- Conservation laws, 514–515
- Conservation reservoir simulation, 458–459
- Consolidated materials, 179
- Constriction meters, 82f
- Consumption of water, 27–32, 400
 - Consumptive use, 400t
 - Coefficient, 420
 - Definition, 28
 - For electricity production, 405t
 - Urban water supply
 - Demand-side adaptive options for, 28t
 - Supply-side for, 28t
 - Virtual water, 27–32
 - Water footprints, 27–32
- Continuity, 66–68, 268, 315, 358, 498
 - Continuity equation, 345t, 350
- Continuous-flood or paddy irrigation, water for, 416
- Continuous-move sprinkler systems, 417
- Continuous-simulation models, 320
- Contracted rectangular weirs, 159
- Contraction loss, 142
- Contraction scour, 821–822
 - Clear-water, 822
 - Live-bed, 822
- Contraction/expansion force, 348–349
- Control surface, 64, 64f

- Control valves, 490
- Control volume, 41, 46f, 64–66, 65f
 - Approach for hydrosystems, 64–66
 - Extensive properties, 64
 - Intensive properties, 64
- For evaporation from open water surface, 264
- For evaporation pan, 262
- General equation, 641
- For groundwater flow, 173
- For infiltration, 266
- For open-channel flow, 621
- For pipe flow, 63
- For porous medium flow, 182f
- For pressure wave, 531f
- For unsaturated porous medium flow, 267f
- Convective acceleration term, 344
- Convective lifting, 238
- Conventional mechanical–draft wet-cooling tower system, 408, 409f
- Converging transition, 161
- Conversion factors, 9t
- Conveyance, 141
 - Water loss, 400t
- Cooling ponds, 407
- Cooling towers, 405, 407
 - Combined wet/dry system, 410
 - Conventional mechanical-draft wet system, 409f
 - Indirect-dry cooling system, 410f
 - Mechanical-draft counter flow system, 409f
 - Mechanical-draft cross flow system, 409f
 - Natural-draft counter flow system, 409f
 - Natural-draft cross flow system, 409f
 - Series-connected wet/dry system, 411f
- Cooling water system, 406–407
 - Evaporative cooling towers, 407
 - Once-through cooling, 405t, 407, 408f
 - Pond cooling, 408f
- Co-operative Programme on Water and Climate (CPWC), 27
- Cooper-Jacob method of solution, 200–204
 - Distance-drawdown analysis, 203–204
 - Time-drawdown analysis, 200–203
- Coriolis coefficient, 78, 236
- Corrective storm 240f
- Countermeasures for stream instability, 817
- Crest stage gauges, 165
- Critical flow, 125
 - Characteristics, 132
 - Locations of, 132f
- Critical shear stress, 786–789, 793f
- Critical shear velocity, 787
- Critical storm duration, 655
- Culvert Analysis Program (CAP), 705
- Culverts, 671–711
 - Control types, 694–696
 - Inlet submerged & outlet unsubmerged, 695f
 - Inlet unsubmerged, 695f
 - Outlet and inlet unsubmerged, 695f
 - Outlet submerged, 695f
 - Design, 705–708
 - Performance curves, 705
 - Hydraulic design of, 693–708
 - Hydraulics, 694–705
 - Inlet-control design equations, 696–698
 - Outlet-control design equations, 698–705
- Cumulative distribution function (cdf), 368t
- Cumulative infiltration, 270
- Curb-opening inlet interception capacity, 678
- Current meters, 166, 166f
- Curve numbers, 307–310
 - Estimation and abstractions, 303–310
 - Antecedent moisture conditions (AMC), 303–304
- Curved vane grate, 680f
- Cyclonic storms in mid-latitude, 239f
- Dams, 714–725, *See also* Spillways
 - Arch, 714f
 - Buttress, 714f
 - Concrete arch dams, 715
 - Concrete buttress dams, 715
 - Diaphragm-type earthfill dams, 715
 - Earthfill dams, 715
 - Embankment, 714f
 - Gravity, 714f
 - Hazard classification of, 715–717
 - Dam safety evaluation, 715
 - Functional design standards, 718t
 - Terms for, 718t
 - Homogeneous dams, 715
 - Rockfill dam, 715
 - Safety of, 713
 - Evaluation matrix of appurtenant structures, 673t
- Evaluation matrix of embankment dams, 714t
- Seepage through modified homogeneous dams, 715f, 716f
- Shells, 715
- Spillway capacity criteria, 717–719
 - Types of, 714f
 - Arch dams, 715
 - Basic types, 714f
 - Buttress dams, 715
 - Concrete dams, 715
 - Embankment dams, 714, 716f
 - Zoned embankment-type, 715
- Darcy flux, 83–84, 110f
- Darcy velocity, 83
- Darcy's law, 84, 179, 180f, 268
- Darcy–Weisbach equation, 94, 474, 495, 523
- Dead storage zone, 448
- Decision support systems (DSS), 861–862
- Deconvolution, 291
- Deep sedimentary formations, 175t
- Degradation, 822
- Delta method, 390
- Demand, water, *See* Price elasticity
- Dendritic patterns, drainage, 283, 283f
- Density, 57, 781
 - Relative, 781
 - Sediments, 781
- Desalination, 431t, 841–845
 - Methods for, 843, 844f
- Design storms, 241–257
 - Areal average rainfall, computation of, 246f
 - First-quartile storms, 257f
 - Isohyetal map of total precipitation, 245f
 - Mississippi River Basin, 244f
 - NOAA–Atlas 14, 247–252
 - Rainfall-runoff analysis, 252
 - Synthetic storm hyetograph, 252
- Detention basins, 659–660, *See also* Stormwater detention
- Detention storage, 241
- Diaphragm-type earthfill dams, 715
- Diffusion equation, 183
- Diffusion wave model, 345
- Dimensions for basic mechanical properties, 9t
- Direct integration, reliability computation by, 394–397
- Direct step method, 140–141
- Direct use value, 854

- Discharge, 25
 - Discharge-area (conservation) form, 344
 - Hydrograph, 284
 - Measurement, 158–166, *See also*
 - Flumes; Weirs
 - Discrete convolution equation, 291
 - Distance-drawdown analysis, 203–204
 - Distributed event-based model, 320
 - Distributed flow routing, 344–350
 - Distributed routing, 344–350
 - Distribution of water, 463–545
 - Components, 463–470, *See also* Fittings used for water distribution; Pipes, for water distribution; Pumps for water distribution; Valves used for water distribution
 - Distribution piping, 463
 - Distribution storage, 463
 - Pumping stations, 463
 - Description, 463–470
 - Modeling, 525–527
 - Application of, 526
 - Calibration, 525–526
 - Computer models, 525
 - Water quality modeling, 526–527
 - Pipe sections or links, 464
 - Cement-lined, 465f
 - Coated steel pipe, 465f
 - Purpose, 463–470
 - Subcomponents, 464f
 - Sub-subcomponents, 464f
 - System, 464f, 475–492, *See also* System components, in water distribution
- Ditch delivery systems, 416
 - Diverging transition, 162
 - Division boxes, 416
 - Fixed proportional flow divider, 417f
 - Weir-type overflow outlets, 417f
 - Domestic water use, 7t
 - Downstream boundary condition, 147
 - Draft tubes, 552
 - Drag coefficient, 778
 - Drainage basins, 230, 230f, 283–287
 - Dendritic patterns, 283
 - Rectangular patterns, 283–284
 - And runoff, 283–287
 - Stream orders, 284f
 - Trellis on folded terrain, 283f, 284
 - Trellis on mature, dissected coastal plain, 283f
 - Drawdown, 190–191, 196
 - Drip irrigation, 418
 - Drop inlet spillways, 738–746
 - Circular sharp-crested weirs, 741f
 - Drop manholes, 635
 - Drought management, 440–447
 - Agricultural drought, 440
 - Demand reduction measures, 441t
 - Economic drought, 440
 - Emergency water supplies, 441t
 - Hydrologic drought, 440
 - Meteorological drought, 440
 - Options, 440–442
 - System improvements, 441t
 - Drought severity, 442–444
 - Palmer Drought Severity Index (PDSI), 443
 - Southern Oscillation Index (SOI), 443–444
 - Surface Water Supply Index (SWSI), 443
 - Droughts, 21–22, *See also* Drought management; Drought severity
 - Progression of, impacts, 21f
 - Types of
 - Agricultural, 440
 - Economic, 440
 - Hydrologic, 440
 - Meteorological, 440
 - U.S. drought monitor, 22f
 - Dry adiabatic lapse rate, 235
 - Dublin principles, 14
 - DuBoys formula, 793–794
 - Ductile iron pipe (DIP), 486, 488t
 - Dupuit equation, 188
 - DWOPER, 675
 - Dynamic viscosity, 59
 - Dynamic wave model, 345, 356–359
- Earthfill dams, 715
 - Ecological footprint, 28
 - Economic drought, 440
 - Economics, water resources, 849–856
 - Benefit cost analysis, 851–854
 - Capital-recovery factor, 850t
 - Discount factors, 849
 - Engineering economic analysis, 849–851
 - Series compound-amount factor, 850t
 - Series present-worth factor, 850t
 - Sinking-fund factor, 850t
 - Uniform gradient series factors, 850t
 - Value of water for sustainability, 854–855
 - Edwards (Balcones Fault Zone) aquifer, 218
 - Edwards Aquifer, Texas, 37–41
 - Annual discharge from (1986–2001), 40t
 - Annual recharge to (1980–2001), 39t
 - Flow paths of, 38f
 - Gaged basins, 39f
 - Springs, 38f
 - Ungaged areas, 39f
- Effective porosity, 273
 - Effective rainfall, 287
 - Effective saturation, 273
 - Efficiency of an inlet, 678
 - Egypt, irrigation networks in, 2, 2f
 - Elasticity, 59–60
 - Bulk modulus of elasticity, 59
 - Of demand, 436
 - Electric power plants
 - Processes and materials, 406f
 - Unit processes, 407f
 - Electrical demand, terminology
 - Base load, 547
 - Capacity demand, 547
 - Daily load shape, 547, 548f
 - Duration curve, 551f
 - Energy demand, 547
 - Intermediate load, 547
 - Load curves, 548
 - Load-duration curve, 551
 - Load factor, 548
 - Peak load, 547
 - Plant factor, 548
 - Weekly load curve, 549f
 - Electricity production, consumptive water use for, 405t
 - Basic unit processes for, 407f
 - Materials in, 406
 - Processes flows in, 406
 - Embankment dams, 692–693, 692f
 - Diaphragm-type earthfill, 715
 - Earthfill, 715
 - Homogeneous, 715
 - Rockfill, 717f
 - Zoned-embankment type earthfill, 715, 716f
 - Emissivity, 263
 - Energy balance method for, 261–264
 - Illustration of, 247f
 - Methods to compute, 225–221
 - Priestley–Taylor equation for, 266
 - Energy coefficient factor, 78, 88, 131, 143–147
 - For compound channel sections, 144
 - For pipe flow, 63
 - Energy equation, 86–87
 - For natural channel flow, 141–152
 - For open channel flow, 84–85, 84f
 - For pipe networks, 495
 - For pressurized pipe flow, 83–111

- Energy grade line (EGL), 89–90
- Energy head, 124
- Energy loss coefficients
 - For flanged fittings, 489t
 - For valves fully open, 492t
- Energy potential in hydroelectric generation, determining, 561–574, *See also* Flow duration method
 - Gross or static head, 563
 - Hydrologic data, 561
 - Multipurpose storage operation, 574
 - Net head, 563
 - Overall efficiency, 562
 - Power rule curve, 573
 - Sequential streamflow routing, 562, 572–573
 - Water power equations, 561–563
- Energy production, water for, 404–411
 - Coal fuel cycle, 404t
 - Combined wet/dry-cooling tower system, 410
 - Conventional mechanical-draft wet-cooling tower system, 408, 409f
 - Cooling ponds, 407
 - Electricity production, 405t
 - Evaporative-cooling tower systems, 407
 - Indirect dry cooling-tower system, 410f
 - Mechanical cooling towers, 408
 - Natural-draft cooling towers, 408
 - Natural-draft towers, 408
 - Natural gas fuel cycle, 404t
 - Nuclear fuel cycle, 404t
 - Oil fuel cycle, 404t
 - Synthetic fuels, 404t
 - Thermal power plant
 - Evaporative cooling towers, 407
 - Once-through cooling, 407
 - Pond cooling, 407
- Energy, flow, 68–72
 - Energy balance equation, 69
 - General energy equation for unsteady variable density flow, 69
- Energy, steady uniform flow, 113–115
- Engineering economic analysis, 849–851
 - Single-payment compound amount factor, 849, 850t
 - Single-payment present worth factor, 849
 - Uniform annual series factors, 849, 850t
 - Uniform annual series sinking fund factor, 849
- Environmental Impact Statement (EIS), 37
- Environmental restoration, 10
- Ephemeral streams, 284
- Equilibrium equation, 197f
- Equipotential lines, 185
- Erosion hydraulics, 771–823
- EROSion model, 318
- Erosion, watershed, 808
 - Channel erosion, 808
 - Sheet erosion, 808
 - Water erosion, 808
- Estimated limiting storms, 257–260
- Estimated limiting values (ELV), 257–260
 - PMF, 257, 374
 - PMP, 257, 374
 - PMS, 257
- Eulerian viewpoint of flow, 61
- Evaporation, 41–43, 260–261
 - Determining methods, 261
 - Aerodynamic method, 261, 264–265
 - Combined aerodynamic and energy balance method, 261, 265
 - Energy balance method, 261–264
 - Evaporative cooling towers, 407
 - Pans, 227f
- Evapotranspiration, 227
- Event-based models, 320
- Event-oriented models, 318
- Excess management, water, 1, 10
- Existence values, 854
- Exit (or discharge) losses, 97
- Expansion loss, 142
- Expected annual damage cost, 445
- Extended-period simulation (EPS), 524–525
- Extensive properties, 64
- External water footprint, 28
- Extreme value distribution, 385
- Extreme-value series, 377
- Fall velocity, 777–780
 - Vs. Function of time, 779f
 - Terminal velocity, 777
 - Wash load, 780
 - Form drag, 780
 - Surface drag, 780
- Farm infrastructure, water for, 415–420
- Federal Emergency Management Agency (FEMA) studies, 582
- Federal Water Pollution Control Act
 - Amendments 1972, 407
- Filter strips, 661
- Finite difference equations, 216–220
- Finite difference grid, 216–220
 - For Edwards aquifer, 219f, 220f
 - For groundwater, 173–181
- Firm capacity, 560
 - Firm energy, 560, 573
- Firm yields, 448
 - water supply, analysis for, 448–457
- First law of thermodynamics, 69
- First-order analysis of uncertainties, 390
- Fittings used for water distribution, 486–488
 - Check valve, 467f
 - Control valves, 466
 - Couplings used, 466f
 - Distribution-system storage, 466
 - Horizontal swing valve, 466
 - Joints used, 466f
 - Node, 466
 - Pressure-reducing valve (PRV), 466, 467f
 - Pressure-sustaining valves, 466
 - Two-way altitude valve, 468f
- Fixed-blade propeller turbines, 556
- Fixed-grade nodes (FGN), 514
- Fixed proportional flow divider, 417f
- FLDWAV, 359
- Flexible linings, 639, 641–646
- Flood control, 577–609, *See also* Floodplains
 - Alternatives, 585–595
 - Nonstructural measures, 586
 - Structural measures, 586–593, *See also* Nonstructural measures; Structural alternatives, flood control
 - Without-project conditions, 586t
- Flood hazard maps, 583
- Flood-prone area maps, 583
- Floodways and floodway fringes, 582–583
- Hydraulic analysis of, 579–582
 - Components of, 582f
- Hydrologic analysis of, 579–582
 - Components of, 582f
- Regulations, 583–584
- Reservoir systems for, operation, 604–608
 - Rules, 604
 - Tennessee valley authority (TVA) reservoir system operation, 604–608
- Storage, 448
- U.S. Army Corps of Engineers risk-based analysis for, 600–603

- Flood damage and net benefit estimation, 595–599
 - Damage relationships, 595
 - Direct damage, 595
 - Indirect damages, 595
 - Intangible damages, 595
 - Secondary damages, 595
 - Uncertainty damages, 595
 - Expected damages, 595–598
 - Flood-damage-reduction plan, 600
 - Flood flow frequency analysis, 385–390
 - Computer models for, 399–400
 - WRC guidelines for, 385–390, *See also* U.S. Water Resources Council (WRC) method
 - Floodplains
 - Definition, 579
 - Management, 579–585
 - National flood insurance program, 584–585
 - Regulations, 583–584
 - Flood-prone area maps, 583
 - Floods, 22–24
 - Impact to cities, 22
 - Mississippi River flooding, 23, 23f
 - Urban flood disasters, 23
 - Urban flood management in developing countries, 22
 - Floodway, 582–583, 583f
 - Floodway fringe, 582–583, 583f
 - Flow, classification, 83–85
 - Gravity (Froude number), 85t
 - Groundwater flow, 83, 84f
 - Open-channel flow, 83, 84f
 - Pipe flow, 83, 84f
 - Space, 85t
 - Time, 85t
 - Viscosity (Reynolds number), 85t
 - Flow and hydrostatic forces, 57–82, *See also* Control volume approach; Visualization of flow
 - Continuity, 66–68
 - Discharge, 63
 - Elasticity, 59–60
 - Energy, 68–72
 - Ideal fluids, 59
 - Laminar flow, 62–63
 - Mass or weight of water, properties involving, 57
 - Momentum, 72–73
 - Pressure and pressure variation, 60–61
 - Principles, 57–63
 - Real fluids, 59
 - Surface tension, 61
 - Turbulent flow, 62–63
 - Viscosity, 57–59
 - Flow classification, 85, 85t
 - Flow-control structures (for bridges), 817–818
 - Channel drop structures, 820–821
 - Check dams, 820–821
 - Dike, 818f
 - Embankment spurs, 817
 - Guide bank, 818–820, 819f
 - Jack field, 818f
 - Retard, 818f
 - Spur, 817–818
 - Flow duration method, 448, 566–571, 813
 - Adjust flow-duration curve (Step 2), 567
 - Compute average annual energy (Step 8), 568
 - Compute dependable capacity (Step 9), 568
 - Data requirements, 567
 - Define usable flow range and derive head-duration curve (Step 6), 568
 - Derive the power-duration curve (Step 7), 568
 - Determine flow losses (Step 3), 568
 - Develop flow-duration curve (Step 1), 567
 - Develop head data (Step 4), 568
 - Duration curve–energy analyses, 567
 - Flow-duration curve, 567, 567f
 - Power-duration curve, 567
 - Select plant size (Step 5), 568
 - Flow nets, 184–186
 - Equipotential lines, 185
 - Flow lines, 185
 - Hypothetical, 184f
 - Flow nozzle, 102
 - Flow profiles, 137–140
 - Flow resistance, 784–786
 - Flow routing, 335–364, *See also* Stream flow routing
 - Flow lines, 185
 - Flowlines, 151
 - Flownets, 184–186
 - For channel seepage, 186f
 - Hypothetical, 184f
 - Flowrate, 64
 - Flumes, 161–164
 - Converging transition, 161
 - Diverging transition, 162
 - Parshall flume, 162
 - Throat, 161
 - Foot-pound-second (FPS) system, 9
 - Footprints, water, 27–32
 - Composition, 29, 31t
 - Concept, 28
 - Crops contribution to, 29
 - Determining factors, 30
 - Agricultural practice, 30
 - Climate, 30
 - Consumption pattern, 30
 - Volume of consumption, 30
 - External water footprint, 28
 - Internal water footprint, 28
 - Forces in pipe flow, 101–103
 - Form losses, 97–100, 621–633
 - Due to sudden contraction, 97
 - Exit (or discharge) losses, 97
 - For gradual enlargements, 97
 - Loss coefficients for various transitions and fittings, 99t
 - Contraction, 99t
 - Expansion, 99t
 - 90° miter bend, 99t
 - Pipe entrance, 99t
 - Smooth bend, 99t
 - Threaded pipe fittings, 99t
 - Manhole losses, 623–624
 - Junction manholes, 624
 - Straight-through manhole, 623
 - Terminal manholes, 624
 - Transition losses (open-channel flow), 621
 - Transition losses (pressurized flow), 622–623
- Francis turbine, 556f
- Frequency analysis, 379–385
- Frequency factor equation, 379–380
- Freshwater resources of the world, 4–6
 - Actual water availability, dynamics, 4t
 - Water use human activity, 5t
- Friction factor, 474
- Frictional force, 347–348
- Friends Creek watershed, 231, 231f
- Frontal flow, 679
- Frontal-flow ratio, 679
- Frontal lifting, 240
- Froude number, 84, 126
- Furrow irrigation, water for, 416, 417f
- Future of water resources, 10–11
- Gauge number, 19, 20f
- Gauge pressure, 60
- Gaussian distribution, 370
- General circulation models (GCMs), 25
- General control volume equation, 66
- General energy equation for unsteady variable density flow, 69

- Geologic formation, hydraulic conductivity of, 179
- Anisotropic, 179
 - Heterogeneous, 179
 - Homogeneous, 179
 - Isotropic, 179
- Geometric functions, channel sections, 121t
- Geometric mean diameter, 775
- Global hydrologic cycle, 229
- Gradation curve, 775, 776f
- Gradually varied flow equations, 134–137
- Grain size, 775–776
- Classification scale, 775t
 - Distribution, 775–776
- Grate inlets, 677, 679–683
- Bar grates, 677, 680f
 - Curved vane grates, 677, 680f
 - Reticuline grate, 681f
 - Tilt-bar grate, 677, 680f
- Gravity (Froude number), 85t
- Gravity force, 347
- Green-Ampt method, 270–276
- Cumulative infiltration, 270, 271f
 - Infiltration parameters for, 274t
 - Rainfall infiltration rate, 271f
 - Variables in, 271f
- Ground heat flux, 263
- Groundwater changes, urbanization effect on, 19
- Pollution, 20
 - Subsurface hydrologic balance disruption, 19
- Groundwater flow, 1, 83, 84f, 173–224, *See also* Aquifers; Saturated flow; Steady-state one-dimensional flow; Steady-state well hydraulics; Transient well hydraulics
- Boundary effects, 207–215, *See also* Image well theory
 - Concepts, 173–181
 - Cooper-Jacob method of solution, 200–204
 - Groundwater basins, 179
 - Groundwater movement, 179
 - Modflow, 220–221
 - Parameters, 178t
 - Dimensions, 178t
 - Units for, 178t
 - Simulation of, 215–221
 - Finite difference equations, 216–220
 - Governing equations, 215–216
 - Specific permeability, 179
 - Subsurface water, divisions of, 174f
 - Vadose zone, 174f
 - Zone of saturation, 174f
 - Transmissivity, 179
- Groundwater Management Act, 44
- Groundwater recharge, 838
- Groundwater systems, 37–41, 179, *See also* Edwards Aquifer, Texas
- Basins, 179
 - Common units for, 178t
 - Concepts, 173–181
 - Hydrologic budget, 237
 - Hydrology, 173
 - Management, 835
 - Arizona approach, 835
 - Movement, 179–181
 - Parameters, 178t
- Gumbel (extreme value type I) distribution, 369t, 373
- Gutters, flow in, 673–677
- Pavement gutter, 673
- Hadley circulation, 236
- Hammer, water, 527
- Conditions, 529f
- Hand-move sprinklers are, 417
- Hardy Cross method, 516–522
- Harvesting systems, rainfall, 848f
- Hazen–Williams equation, 470–473, 495, 515
- Hazen–Williams roughness coefficient, 470
- Headlosses, 90–100
- Form (minor) losses, 97–100
 - From pipe friction, 94–96
 - Shear-stress distribution of flow in pipes, 90–91
 - Gravity force, 91
 - Pressure force, 91
 - Velocity distribution of flow in pipes, 92–94
- HEC-1, 277, 297, 299, 320, 346, 348–349
- HEC-2, 148, 810
- HEC-5, 573, 607–608
- HEC-6, 773
- HEC-18, 773
- HEC-20, 773
- HEC-23, 773
- HEC-FFA, 399
- HEC-RAS, 148–149, 816
- Heterogeneity, of hydraulic conductivity, 179
- Hierarchy, 231
- Histogram, 255
- Homogeneous dams, 715
- Horizontal pumps on floor above suction well, 505t
- Horizontal swing valve, 466
- Horton's equation, 276f
- Horton's stream ordering, 284
- First-order stream, 284
 - Second order, 284
- Hortonian overland flow, 314
- Household water use in United States, 403t
- HYDRAIN, 705
- Hydraulic (distributed) routing, 335, 344–350
- Continuity equation, 345–347
 - Convective acceleration term, 344
 - Diffusion wave model, 345
 - Discharge-area (conservation) form, 344
 - Dynamic wave model, 345
 - Kinematic wave model, 345
 - Local acceleration term, 344
 - Momentum equation, 344, 345t, 347–350, *See also individual entry*
 - Pressure force term, 344
 - Velocity-depth (nonconservation) form, 344
- Hydraulic analysis of designs, 621–635, *See also* Form losses
- Hydraulic gradient calculations, 633
- Hydrograph routing for design, 633–635
- Hydraulic conductivity, 268
- Anisotropy of, 179
 - Aquifer, 176
 - Heterogeneity, 179
- Hydraulic depth, 83, 125, 132
- Hydraulic grade line (HGL), 89–90
- Hydraulic gradient, 176–177, 621, 633, 735
- Hydraulic-jump-type stilling basins, 121, 122f, 748–767
- Basin I, 752
 - Basin II, 752
 - Basin III, 752–754
 - Basin IV, 755
 - Basin V, 755–756
 - Energy dissipators and, 748–767
 - On horizontal aprons, 750f
 - Stilling basin design, tailwater considerations for, 756–767
 - Type-I stilling basin, 751f
 - Types of, 748–752
- Hydraulic processes, 1–2, 57–82, *See also* Flow and hydrostatic forces; Groundwater flow; Pressurized pipe flow

- Hydraulic radius, 84
- Hydraulic risk, 393–399
- Hydraulic transients, *See* Transients, hydraulic
- Hydraulics of simple networks, 495–499
- Hydroelectric generation, water for, 547–575, *See also* Turbines
 - Capacity, 560
 - Dependable or firm capacity, 560
 - Hydraulic capacity, 560
 - Installed capacity, 560
 - Overflow capacity, 560
 - Rated capacity, 560
 - Components, 552–560
 - Elements for generation, 552–557
 - Conduit to convey water, 552
 - Means to create a head, 552
 - Power plant, 552
 - Firm energy, 560
 - Firm power, 560
 - Pondage developments, 548
 - Power system terms and definitions, 559–560
 - Pumped-storage developments, 551
 - Reregulating developments, 551
 - Run-of-river developments, 548
 - Storage developments, 551
- Hydrograph, 284
 - Components, 287–291
 - Design methods, 658–659
 - Flood hydrograph, basin characteristics effects on, 286f
- Hydrologic (lumped) routing, 335
- Hydrologic cycle, 227–229, 228f
 - With global annual average water balance, 228f
 - At global scale, 228f
- Hydrologic data series, 377
 - Annual exceedance series, 378f
 - Annual maximum series, 378f
 - Annual minimum series, 377
 - Annual series, 377
 - Complete duration series, 377
 - Extreme-value series, 377
 - Partial duration series, 377
- Hydrologic design, for water excess management, 373–379
 - Generalized design criteria, 375t
 - Airfields, 375t
 - Dams with high likelihood of considerable, 375t
 - Dams with no likelihood of loss of life, 375t
 - Dams with probable loss of life, 375t
 - Farm drainage, 375t
 - Highway bridges, 375t
 - Highway culverts, 375t
 - Intermediate, 375
 - Levees, 375t
 - Major, 375
 - Minor, 375
 - Urban drainage, 375t
 - Hydrologic design scale, 374–376, 374f
 - Hydrologic drought, 440
 - Hydrologic frequency analysis, 379–385
 - Extreme value distribution, 385
 - Frequency factor equation, 379–380
 - Log-Pearson III distribution, application, 380–385
 - K_T values for, 381t–382t
 - Hydrologic losses, 287–291
 - Hydrologic processes, 1, 227–280, *See also* Green-Ampt method; Infiltration methods; Precipitation (rainfall)
 - Atmospheric circulation, 234–236
 - Catchments, 230
 - Drainage basin, 230, 230f
 - Hadley circulation, 236
 - Hierarchy or nested hierarchy, 231
 - Hydrologic budget, 236–237
 - Hydrologic cycle, 227–229
 - Illinois River Basin, 232f
 - Infiltration, 266–277
 - Middle cell, 236
 - Ocean circulation, 234–236
 - Polar cell, 236
 - Tropical cell, 236
 - Upper Mississippi River, 233f
 - Watersheds, 230
 - Hydrologic reservoir routing, 336–339
 - Level pool routing, 336
 - Hydrologic response, 26–27
 - Groundwater sustainability and, 26
 - Influence water storage patterns, 26
 - Hydrologic risk, 376–377
 - Of failure, 376
 - Hydrologic river routing, 340–344
 - Muskingum method, 340
 - Valley storage curves, 342f
 - Hydrologic soil groups, 305–307
 - Hydrologic systems, 229–233
 - Working medium, 229
- Hydrology, description, 227
- Hydropower terms
 - Average annual energy, 548
 - Dependable capacity, 568
 - Firm capacity, 560
 - Firm energy, 560
 - Firm power, 560
- Flow duration curves, 561, 561f, 567
- Installed capacity, 548, 560
- Nameplate capacity, 560
- Net head, 563
- Overall efficiency, 562
- Overflow capacity, 560
- Rule curves, 457
- Secondary power, 560
- Sequential streamflow routing, 562, 572
 - Water power equation, 561
- Hydropower, role of, 547–552
- Hydrostatic forces, 73–77
 - On a plane surface, 74f
- Hyetographs, rainfall, 238
- Ideal fluids, 59
- Illinois River Basin, 231, 231f
- Image wells/Image well theory, 173, 173f, 174f, 207–215
 - Barrier boundary, 208–212
 - Real cone of depression, 209
 - Recharge boundary, 212–213
 - Multiple boundary systems, 214–215
- Implicit dynamic wave model, 356–359
 - Weighted four-point finite-difference approximations, 356
- Impulse turbines, 553
- In open-channel flow, 80, 131
- In pipe flow, 100–103
- Incident radiation, 263
- Incipient motion, 786–789
 - Analysis, 816
- ϕ -Index method, 276, 276f, 289–291
- Indirect dry cooling-tower system, 410f
- Industrial water use, 7t, 401t
 - Cannery, 401t
 - Chemical, 401t
 - Food and beverage, 401t
 - For municipal establishments, 402t
 - Pulp and paper, 401t
 - In the United States, 1983, 402t
- Infiltration methods, 266–277, 661–663
 - Cumulative, 271, 271f
 - Green-Ampt method of, 270–276
 - Horton's equation, 276, 276f
 - Moisture content, 267, 271
 - Moisture profile, 270
 - Moisture zones, 270, 270f
 - Ponding time, 275
 - Saturation zone, 269
 - For stormwater, *See* Subsurface disposal of stormwater
 - Transmission zone, 270

- Trenches, 663
- Unsaturated flow, 267
- Wetting front, 270
- Wetting zone, 270
- Inlets
 - Bridge inlets, 692–693
 - Combination inlets on grade, 684–685
 - Control design equations, 696–698
 - Curb-opening inlets on grade, 683–684
 - Embankment inlets, 692–693
 - Inlet locations, 689–691
 - Inlets in sag locations, interception capacity and efficiency of, 685–689
 - Curb-opening inlets in a sag location, 686–688
 - Grate inlets in, 685–686
 - Slotted drain inlets in a sag location, 688–689
 - Median inlets, 692–693
 - Slotted drain inlets on grade, 684
- Instream water use, 400t
- Intake structures, 552
- Integral momentum equation for fluid flow, 72
- Integrated water resources management (IWRM) for sustainability, 827–830
 - Demand management, 828
 - Equitable access, 828
 - Improved policy, regulatory and institutional frameworks, 828
 - Intersectoral approach, 828
 - Regional development, 829–830
 - Supply optimization, 828
- Intensity-duration frequency (IDF) relationship, 252, 612t
- Intensive properties, 64
- Intergovernmental Panel on Climate Change (IPCC), 24–25
- Intermittent streams, 284
- Internal energy, 69, 87
- Internal water footprint, 28
- Intrinsic permeability, 179
- Irrigation, water for, 7t, 411, 412t, 424–427
 - Crop water requirement, 424, 424t–425t
 - Drainway midway between supply laterals, 416f
 - Impacts of irrigation development, 426t, 427
 - Infrastructure, 411–420
 - Microirrigation, 411, 418–420
 - Sprinkler irrigation, 411, 417–418
 - Surface irrigation, 411
 - Tier arrangement, 416f
 - Total water requirement, 424
 - Trends and needs, 411
- Irrigation networks, in Egypt, 2
- Irrigation system selection and performance, 420–423
 - Application efficiency, 421
 - Characteristics, 420
 - Consumptive use coefficient, 420
 - Efficiency, 420
 - Factors affecting, 422t
 - Bubbler, 422t
 - Check back and cross furrows, 423t
 - Closely spaced borders, 422t
 - Contour bench terraces, 423t
 - Contour ditches, 423t
 - Contour levee, 423t
 - Corrugations, 423t
 - Drip, 422t
 - Graded contour furrows, 423t
 - Localized (drip, trickle, etc.), 423t
 - Microsprayer, 422t
 - Portable pipes, 423t
 - Rectangular checks, 423t
 - Sprinklers, 422t, 423T
 - Subirrigation, 423t
 - Surface, 422t
 - Widely spaced borders, 422t
 - Low-quarter distribution uniformity, 421
 - Performance, 420
 - Selection, 420
- Isohyetal maps, 238, 243, 245
- Isohyets, 238
- Isolation valves, 488
- Isotropic formation, 179
- Israel's National Water Carrier System, 433
- Iterative alternating direction implicit (IADI) procedure, 218
- Jet streams, 235
- Joint-use storage zone, 574
- Juvenile water, 173
- Karstic limestone, 175t
- Kinematic viscosity, 59
- Kinematic waves, 315
- Kinematic wave celerity, 354–355
- Kinematic wave equations, 315
- Kinematic wave model, 315, 345
 - For channels, 350–355
 - Continuity, 350
- Initial condition, 352
- KINEROS channel flow routing model, 354
- Momentum, 350
- U.S. Army Corps of Engineers, 352–353
- Upstream boundary, 352
- Kinematics, 315, 350
- Kinematic-wave overland flow runoff model, 314–320
- KINEROS channel flow routing model, 381–320, 350, 354
- Kinetic energy correction factor, 78
- Lag method, 311
- Lagrangian viewpoint of flow, 61
- Lake Decatur watershed, 232f
- Laminar flow, 62–63, 92
- Laplace equation, 184–185
- Latent heat of vaporization, 261
- Lateral stream migration, 822
- Law of times, 210
- Leaky aquifer conditions, 206–207
- Levees and floodwalls, 590
- Level basin irrigation, water for, 416
- Level pool routing, 336
- Life cycle assessment (LCA), 862–864
 - Phases, 862
 - Goal definition, 862
 - Impact assessment, 862
 - Interpretation, 862
 - Inventory, 862
- Limestone, 175t
- Linear theory method, 523–524
- Live-bed contraction, 822
- Livestock water use, 7t
- Load, 547
 - Base load, 547
 - Daily load shape, 547
 - Intermediate load, 547
 - Load curves, 548
 - Load factor, 548
 - Loading-resistance interference, 394
 - Peak load, 547
 - Plant factor, 548
- Local acceleration term, 344
- Local scour, 822
- Log-normal probability distribution, 370–373
- Log-Pearson III distribution, application, 380–385
 - K_T values for, 381t–382t
- Long-term runoff forecasting, 320

- Loop equations, 516
- Low-energy precision-application (LEPA), 418
- Managed aquifer recharge (MAR), 836–840
 - Artificial recharge, 837–839
 - Groundwater recharge, 838
 - Recharge basins, 839–840
- Manholes, 635
 - Drop manholes, 635
 - Manhole losses, 623–624
 - Junction manholes, 624
 - Straight-through manhole, 623
 - Terminal manholes, 624
- Manning's equation, 96, 120, 123, 140, 316, 318, 348, 351, 358, 390, 474, 620, 673, 784
- Manning's roughness factor/coefficients
 - Coefficients, 640f
 - Equation for vegetative linings, 646
 - For culverts, 700t
 - For form roughness, 785
 - For overland flow, 318t
 - For rigid and flexible-lined channels, 641
 - For shallow flow, 173
 - For swales, 661
 - For vegetative linings, 646–647
 - Grain roughness, 785
 - Skin roughness, 785
 - Strickler's approximation, 785
 - Total Manning's roughness, 785
- Mass balance equation, 41
- Mass-curve analysis, 452–453
- Mass density, 57
- Mass rate of flow, 63
- Maximum Contaminant Levels (MCLs), 831
- Mean velocity, 63, 144
 - Equation for compound channel section, 144, 144f
- Mechanical cooling towers, 408
- Mechanical-draft counterflow, 409f
- Mechanical-draft crossflow, 409f
- Median inlets, 692–693
- Meteorological drought, 440
- Metering, in water distribution, 469
 - Compound meters, 469
 - Multijet meters, 469
 - Proportional meters, 469
 - Turbine meters, 469
 - Ultrasonic meters, 469
- Mexico City, 48–54
 - Components, 52f
 - Mexico City Metropolitan Area (MCMA), 51
 - Social class in, water use by, 52t
 - Tula Valley, water balance of, 53f
 - Wastewater disposal drainage system of, 52f
 - Water sources for, 51f
- Meyer-Peter and Muller Formula, 794–795
- Micro-irrigation, water use for, 411, 412t, 418–420
 - Bubbler irrigation applies, 418
 - Drip irrigation, 418
 - Micro sprinklers, 418
 - Spray irrigation sprays, 418
 - Subsurface irrigation, 418
 - Trickle irrigation, 418
- Middle cell, 236
- Millennium Development Goals (MDGs), 14–15
- Mining water use, 7t
- Minor losses, 97–100
 - Coefficients for pipe flow, 98t
 - Coefficients for transitions and fittings, 99t
 - Conical diffusers, 97
 - Discharge losses, 97
 - Exit losses, 623
 - Gradual enlargements, 97, 622t
 - Sudden contractions, 97
 - Sudden enlargements, 622t
- Mississippi River flooding, 23, 23f, 233f, 577f
 - Area of flooding streams, 244f
 - Areal distribution of precipitation, 244f
- Mixed-flow pumps, 475
- MODFLOW, 220–221
- Modified rational method, 653–658
- Modular pavement, 663
- Modulus of elasticity of pipes, 533
- Moment of inertia, 74
- Momentum, 72–73, 129–131
 - Momentum correction factor, 130
 - Momentum equation for steady state open-channel flow, 130
- Momentum correction factor, 80
- Momentum equation, 116–122, 344, 345t, 347–350
 - Chezy equation, 117
 - Forces, 347
 - Contraction/expansion force, 348–349
 - Frictional force, 347–348
 - Gravity force, 347
 - Net momentum outflow, 348
 - Unbalanced pressure force, 348
- Momentum storage, 349
- Roughness coefficient, 117t–120t
- Moody diagram, 95, 95f
- Mosquito control fluctuations, 604
- Movement, groundwater, 179
- Multijet meters, 469
- Multiple boundary systems, 214–215
- Multistage pumps, 475, 477f
- Municipal establishments, water requirements for, 402t–403t
- Muskingum–Cunge model, 355–356
- Muskingum method, 340
- National Flood Insurance Program (NFIP) regulations, 583–585
 - Floodplain management, 585
 - Stormwater management, 585
- National Resources Conservation Service (NRCS), 301
- Natural channels, gradually varied flow for, 141–152
 - Contraction loss, 142
 - Energy correction factor, 143–147
 - Equations, development, 141–143
 - Expansion loss, 142
- Natural-draft cooling towers, 408
- Natural-draft counterflow, 409f
- Natural-draft crossflow, 409f
- Natural-draft towers, 408
- Natural gas fuel cycle, water use for, 404t
- Nested hierarchy, 231
- Net momentum outflow, 348
- Net positive suction head (NPSH), 481–484
 - Available net positive suction head (NPSHA), 481
 - Required net positive suction head (NPSHR), 481
- Net radiation flux, 263
- Network simulation, 514–525
 - Conservation laws, 514–515
 - Extended-period simulation (EPS), 524–525
 - Fixed-grade nodes (FGN), 514
 - Hardy Cross method, 516–522, *See also individual entry*
 - Linear theory method, 523–524
 - Loading pattern, 514
 - Network equations, 515–516
 - Primary loop, 514
- Newton's method, 273, 316, 517, 760
- Newton's second law, 72, 347, 350
- NOAA–Atlas 14, 247–252

- Nodal equation, 516
- Node, 466
- Nonconservation form, 347
- Nonequilibrium Theis solution, 207
- Nonequilibrium well pumping equation, 195–198
- Nonerodible channels, uniform flow in, 122–123
- Nonstructural measures, 593–595
 - Flood proofing, 593
 - Performance requirements for, 594t
 - Flood-warning-preparedness plan (FWP plan), 593
 - Components of, 594t
 - Land-use controls, 595
- Nonuniform flow, 62
- Nonuniform open-channel flow, 115
- Normal depth, 113
- Normal discharge, 484
- Normal probability distribution, 369t, 370
- NRCS (SCS) rainfall-runoff relation, 301–303
- NRCS (SCS) unit hydrograph procedure, 310–314
 - Peak discharge, 313–314
 - Time of concentration, 311–313
 - Time to peak, 313
- Nuclear fuel cycle, water use for, 404t

- Ocean circulation, 234–236
- Offstream water use, 400t
- Ogee (overflow) spillways, 728–735
 - Gate-controlled ogee crest discharge, 730
- Oil fuel cycle, water use for, 404t
- Once-through cooling, 407
- Open-channel delivery systems, drop structures used in, 418f
- Open-channel flow, 1, 83, 113–170, *See also* Steady uniform flow
 - Direct step method, 140–141
 - Gradually varied flow equations, 134–137
 - for natural channels, 141–152
 - Nonuniform flow, 114, 115f
 - Uniform flow, 114, 114f
 - Water surface profile classification, 137–140
- Optimization models, 457
- Orifice meter, 696
- Orographic lifting, 238
- Orographic storm, 239f
- Outliers, testing for, 387–390

- Overland flow, 285
 - Hortonian, 314
- Palmer Drought Severity Index (PDSI), 443
- Parallel axis theorem, 74
- Parallel pipe flow, 495–498
- Parallel pipe systems, 105–108
- Parshall flume, 162, 163f
- Partial-duration series, 377
- Particle shape, 751
 - Roundness, 751
 - Shape factor, 751
 - Sphericity, 751
- Pavement drainage inlet design
 - Bridge deck inlets, 692
 - Combination inlets
 - on grade, 684
 - in sag locations, 689
 - Curb-opening inlets
 - on grade, 683
 - in sag locations, 685
 - Efficiency of inlets, 677–678
 - Embankment inlets, 692
 - Equivalent cross-slopes, 683
 - Frontal-flow interception efficiency, 681
 - Frontal-flow ratio, 679
 - Full-interception curb-opening inlet length, 683
 - Grate inlets in sag locations, 685
 - Grate inlets on grade, 679
 - Interception capacity, 677–685
 - of grate inlets, 682
 - Interception efficiency, 693
 - Median drop inlets, 692, 692f
 - Side-flow interception efficiency, 681
 - Slotted drain inlets
 - on grade, 684
 - in sag locations, 688–689
- Pavement drainage inlets, 677
 - Combination inlets, 677
 - Curb-opening inlets, 677
 - Grate inlets, 677
- Peak discharge, 313–314
- PEAKFQ, 399, 399t
- Pearson type 111 distribution, 380–381
 - Frequency equation for, 385
 - K_T values for, 381t
- Pelton turbines, 553
- Penstocks convey, 552
- Perennial streams, 284
- Perforated storm sewers, 663, 664f

- Permanent, solid-set sprinklers, 417
- Permeability, 179
 - Intrinsic, 179
 - Specific, 179
- Piezometric head, 61
- Piezometric surface, 493
- Pipe flow, 1, 3, 103–109, 470–475, *See also* Pressurized pipe flow
 - Branching pipe flow, 108–109
 - Equations, 470–475
 - In simple networks, 103–109
 - Parallel pipe systems, 105–108
 - Series pipe systems, 103–105
- Pipe friction, headlosses from, 94–96
 - Darcy–Weisbach equation, 94
 - Moody diagram, 95, 95f
- Pipe sections for water distribution, 464–465, *See also under* Distribution of water
- Pipes, for water distribution, 486–488
 - Asbestos cement (AC) pipe (ACP), 486
 - Branching pipe system, 496f, 498–499
 - Ductile iron pipe (DIP), 486, 488t
 - Parallel pipe flow, 495–498
 - Polyvinyl chloride (PVC) pipe, 486, 488t
 - Reinforced concrete pressure pipe (RCP), 486
 - Series pipe flow, 495–498
- Polar cell, 236
- Pollution, groundwater, 20
- Polyvinyl chloride (PVC) pipe, 486, 488t
- Pond cooling, 407
- Pondage developments, 548
- Pore space, 173
- Porosity, 267
 - Aquifer, 176
 - Types, 177f
- Positive-displacement pumps, 475
- Potential maximum retention, 302
- Power input (bhp), 486
 - Pump efficiency, 486
 - Pump-head characteristic curve, 509
 - Pump operating envelopes, 487
 - Pump performance, curves, 485, 485f
 - Pumps in parallel, 502f
 - Rated capacity, 484
 - Shutoff head, 484
- Power rule curve, 573
- Powerhouse shelters, 552

- Precipitation (rainfall), 237–260, *See also*
 Design storms
 Convective lifting, 238
 Estimated limiting storms, 257–260
 Formation, 237–238
 Frontal lifting, 238
 Orographic lifting, 238
 Types, 237–238
 Watershed, rainfall disposal on, 240–241
 World's land areas, average annual precipitation for, 242f
- Pressure, 60–61
 Absolute pressure, 60
 Gauge pressure, 60
 Piezometric head, 61
 Pressure force, 60, 344
 Pressure head, 87
 In static fluids, 73–78
 Vacuum, 60
- Pressure-reducing valve (PRV), 466, 490
 Pressure-sustaining valves (PSV), 466, 491
- Pressurized pipe flow, 86–90, *See also*
 Headlosses
 Energy equation, 86–89
 Energy grade line (EGL), 89–90
 Hydraulic grade line (HGL), 89–90
 Venturi meter, 88
- Price elasticity, 436–440
 Price-type current meter, 166f
 Priestley–Taylor evaporation equation, 266
- Prismatic channels, 347
 With change in slope, 157
 Flow profiles in, 137t
- Probability concepts, 367–369
 Parameters used, 368
 Coefficient of skew, 368f
 Cumulative distribution function (cdf), 368t
*k*th Central moment, 368f
 Mean, average, or expected value, 368f
 Median, 368f
 Probability density function (pdf), 368f
 Probability mass function (pmf), 368f
 Quantiles, 368f
 Standard deviation, 368f
 Variance, 368f
- Probability distributions, 367, 369t, 370–373
 Exponential, 369t
 Extreme value type i, 369t, 373
- Gamma, 369t
 Log Pearson type III, 369t
 Lognormal, 369t, 370–373
 Normal, 369t
 Random variable, 367
 Sample, 367
 Sample space, 367
 Statistics used, 368
- Probable maximum flood (PMF), 257, 374
 Probable maximum precipitation (PMP), 257, 260f, 374
 Probable maximum storm (PMS), 257
- Proportional meters, 469
 Psychrometric constant, 265
- Public water
 Supply, 400t
 Use, 7t
- Pump systems analysis, 499–513
 Pump operating point, 500–503
 System design for, 503–513
 Horizontal pumps on floor above suction well, 505t
 Vertical wet well pumps, 505t
 Wet well–dry well, horizontal pumps below water level (flooded suction), 505t
 System head curves, 499–500
 System throttled by valve operation, 501f
 System with two different discharge heads, 501f
 System with varying static lift, 501f
 Well pumps, comparison, 505t–506t
- Pumps for water distribution, 463, 469, 475–486, *See also under*
 Distribution of water
 Axial flow pumps, 475
 Cavitation, 481–484
 Centrifugal pump, 469, 475
 Characteristics, 484–486
 Best efficiency point (bep), 486
 Efficiency curves, 486
 Modified head characteristic curve, 484, 485f
 Normal discharge (or head), 484
 Power input (bhp), 486
 Pump efficiency, 486
 Pump head-characteristic curve, 484
 Pump station losses, 484
 Shutoff head, 484
- Classification, 475–477
 Metering (flow measurement), 469
 Mixed-flow pumps, 475, 476f
 Multistage pumps, 475, 477f
- Net positive suction head (NPSH), 481–484
 Operating characteristics, 477–479
 Discharge coefficient, 477
 Head coefficient, 477
 Power coefficient, 477
 Positive-displacement pumps, 475
 Pumping stations, 469
 Radial flow pumps, 475, 476f
 Screw pumps, 475
 Single-stage pump, 477f
 Specific speed, 479–481
- Quality modeling, water, 526–527
- Radial flow pumps, 475
 Radiation flux, 263
 Rainfall erodibility factor, 809
 Rainfall excess, 287–291, 288f
 Rainfall harvesting, 845–847
 Rainfall hyetographs, 238, 243f
 Rainfall-runoff analysis, 252, 291
 Computer models for, 320
 Continuous-simulation models, 320
 Distributed event-based model, 320
 Event-based models, 320
 KINEROS model, 320
 Long-term runoff forecasting, 320
 Using unit hydrograph approach, 291–294
- Rainfall variability, 238–240, *See also*
 Precipitation (rainfall)
 Arithmetic–mean method, 238
 Corrective storm 240f
 Cyclonic storms in mid-latitude, 239f
 Isohyetal maps, 238
 Isohyets, 238
 Orographic storm, 239f
 Rainfall hyetographs, 238
 Thiessen method, 238
- Random variable, 367
 Rapidly varied flow, 152–157
 Hydraulic jump, 152
 Sequent depths or conjugate depths, 152
- Rating curves, 165
 Rational method design, 613–621
 For stormwater control, 613–621
 Rainfall intensity, 614
 Time of concentration, 614
- Reaction turbines, 553
 Real cone of depression, 209
 Real fluids, 59

- Recharge area, 175
 Recharge basins, 839–840
 Recharge boundaries, 208, 212–213
 Reclaimed wastewater, 400t
 Rectangular patterns, drainage, 283–284, 283f
 Recurrence interval, 379
 Regional development, sustainable water-based, 829–830
 Regional water supply systems, 432–436
 Central Arizona Project (CAP), 432, 433f–434f
 Israel's National Water Carrier System, 433
 Southeast Anatolian Project (GAP), 432–433, 435f
 Reinforced concrete pressure pipe (RCPP), 486, 489t
 Relative density, 781
 Relative roughness, 474
 Reliability computation
 By direct integration, 394–397
 Using safety margin/safety factor, 379–399
 Reservoir routing, 335–364, *See also*
 Hydraulic (distributed) routing;
 Hydrologic reservoir routing;
 Hydrologic river routing
 Reservoir sedimentation, 812–815
 Reservoir simulation, 457–459
 Conservation simulation, 458–459
 Operation rules, 457–458
 Operational decision, 457
 Optimization models, 457
 System demands, 457
 Residual moisture content, 273
 Resources management, water, 1
 Water reserves on the earth, 4t
 Retention storage, 241
 Reticuline grate, 681f
 Return period, 252
 Return water flow, 400t
 Reuse irrigation, water for, 416
 Reverse osmosis system, 843f
 Reynold's number, 63, 84t, 179, 474
 Reynolds transport theorem, 66
 Richards equation, 269
 Rigid linings, 639–641
 Rim turbine, 557
 Riparian law, 831
 Ripple method, 453
 Risk analysis, 393–399
 Composite hydrologic risk, 393–399
 Hydraulic risk, 393–399
 Reliability computation by direct integration, 394–397
 Risk-based analysis, floods, 599
 River authority, 832
 Rockfill dam, 715
 Rough pipes, 92–94
 Roughness coefficient, 117t–120t
 Closed conduits flowing partly full, 117
 Excavated or dredged, 119t
 Lined or built-up channels, 118t
 Natural streams, 119t
 Rule curves, 457, 573
 Runge–Kutta method, 659
 Runoff, *See also* Surface runoff
 Drainage basins and, 283–287
 Urban stormwater, 18–19
 Run-of-river developments, 548
 Rural water use, 7t
 Safety margin (SM)/safety factor, reliability computation using, 379–399
 Saint-Venant equations, 316, 344, 346f, 350, 356, 358
 Sample space, probability, 367
 event, 367
 Sample, probability, 367
 Sandstone, 175t
 Saturated adiabatic lapse rate, 235
 Saturated flow, 181–186
 Flow nets, 184–186
 Governing equations, 181–186
 Saturated hydraulic conductivity, 84
 Saturated zone, 270
 Saturation vapor pressure, 264
 Schoklitsch formula, 795–796
 Screw pumps, 475
 SCS rainfall distributions, 255t
 SCS unit hydrograph procedure, 310–314
 Dimensionless unit hydrograph, 310
 Mass curve, 310, 311t
 Time of concentration, 311–312
 Time to peak, 313
 Secondary losses, 97
 Secondary Maximum Contaminant Levels (SMCLs), 831
 Sedimentation, 771–823, *See also* Fall velocity; Reservoir sedimentation;
 Total sediment load; Watersheds:
 Watershed sediment yield
 Bridge scour, 821–822
 Density, 781
 DuBoys formula, 793–794
 Finer particles, settling analysis for, 775–777
 Geometric standard deviation, 776
 Grain size distribution, 775–776
 Particle shape, 776–777
 Roundness shape, 776
 Sphericity shape, 776
 Meyer-Peter and Muller formula, 794–795
 Properties of sediment, 773–781
 Geometric mean diameter (D_g), 774
 Mean diameter (D_m), 774
 Median diameter (D_{50}), 775
 Nominal diameter (D_n), 774
 Sedimentation diameter (D_s), 774
 Shape, 773–775
 Sieve diameter (D), 774
 Size, 773–775
 Triaxial diameters, 773
 Schoklitsch formula, 795–796
 Size distribution, measurement, 775
 Suspended load, 797–800
 Transport, 786–792
 Critical shear stress, 787
 Critical shear velocity, 787
 Incipient motion, 786–789
 Overturning moment, 786
 Point of incipient motion, 786
 Righting moment, 786
 Shear velocity Reynolds number, 787
 Shields diagram, 787
 Transport definitions, 782–784
 Bed-material load, 783
 Total load, 783
 Wash load, 783
 Transport functions, 789–790
 von Karman-Prandtl equation, 797
 Seepage, 227
 Self-priming centrifugals, 505t
 Self-supplied water, 400t
 Semi-arid regions, sustainable water supply methodologies for, 836–848
 Sensible heat, 263
 Sensitivity coefficients, 390
 Sequent depths, 152
 Sequential streamflow routing, 562, 572–573
 Sequent-peak analysis, 453, 455
 Series compound-amount factor, 850t
 Series pipe flow, 495–498
 Series pipe systems, 103–105
 Series present-worth factor, 850t

- Shaft work, 70, 86
- Shallow alluvium, 175t
- Sharp-crested weirs, 158
 - Flow over, 158f
- Shear stress
 - Bed shear stress, 130
 - Critical shear stress, 647, 786–788
 - Permissible, for lining materials, 644t
 - In pipe flow, 90–91
- Sheet erosion, 808
- Shells, 715
- Shields diagram, 787–788
- Shortage of water, economic aspects, 444–447
- Shortage volume, 446, 447f
- S-hydrographs, 299–301
- SI units for basic mechanical properties, 9t
- Side channel spillways, 735–738
- Side flow, 679
- Side-flow ratio, 679
- Single-stage pump, 477f
- Sinking-fund factor, 850t
- Slope-area method, 123–124
- Sluice gate, 136f
- Smooth pipe flow, 92
- Snyder's synthetic unit hydrograph, 294–295
- Soil Conservation Service (SCS), 301
- Soil-erodibility factor, 809
- Soil group classification, 304–307
- Soil moisture storage, 241
- Soil texture, 173
- Soil water diffusivity, 269
- Southeast Anatolian Project (GAP), 432–433
- Southern Oscillation Index (SOI), 443–444
- Space, 85t
- Specific discharge, 83
- Specific energy, 124–129
 - Critical flow, 125
 - Froude number, 126
 - Hydraulic depth, 125
 - Total head or energy head, 124
- Specific force, 131–133
- Specific gravity, 57
- Specific permeability, 179
- Specific retention, 176
- Specific water capacity, 269
- Specific weight, 57
- Specific yield, 176
- Spillways, 725–748, *See also* Dams; Ogee (overflow) spillways
 - Baffled chute spillways, 746–748
 - Components, 725
 - Control structures, 725
 - Discharge channels, 725
 - Entrance channels, 725
 - Outlet channels, 725
 - Terminal structures, 725
 - Conveyance systems, 713–769
 - Drop inlet spillways, 738–746
 - For flood control storage, 713–769
 - Free-overfall (straight drop) spillways, 726–728
 - Functions of, 725–726
 - Hydrologic considerations, 713–714
 - Overflow, 726–728
 - Side channel spillways, 735–738
 - Splash-over, 679
 - Spray irrigation sprays, 418
 - Springflow, 227
 - Sprinkler irrigation, water use for, 411, 417–418
 - Center-pivot irrigation systems, 417
 - Continuous-move sprinkler systems, 417
 - Hand-move sprinklers are, 417
 - Moving sprinkler-irrigation system, 419f
 - Permanent, solid-set sprinklers, 417
 - Spurs, 817–818
 - Deflector spurs, 818
 - Retarder spurs, 818
 - Spur dikes, 818
- Standard deviation, 368f
- Standard normal distribution, 370
- Standard step procedure, 147
- Static fluids, 73–78
 - Buoyancy, 77–78
 - Pressure and pressure forces in, 73–78
 - Hydrostatic forces, 73–77
- Steady flow, 62
- Steady, gradually varied flow, 134–141
- Steady-state one-dimensional flow, 186–189
 - Confined aquifer, 186–189
 - Unconfined aquifer, 187–189
- Steady-state well hydraulics, 189–195
 - Confined aquifers, 191–194
 - Flow to wells, 1891–191
 - Unconfined aquifers, 194–195
- Steady uniform flow, 113–124
 - Energy, 113–115
 - In nonerodible channels, 122–123
 - Best hydraulic sections for, 122–123
 - Slope-area method, 123–124
- Stefan–Boltzmann law, 263
- Stilling basin design, tailwater considerations for, 756–767
- Stokes' Law, 779
- Storage coefficient, 176, 177f
- Storage function, aquifer, 176
- Storage-yield studies, 448
- Storativity, aquifer, 176
- Storm
 - Movement on surface runoff, 287f
 - Shape, 287f
 - Size, 287f
 - Storm runoff hydrographs, 283–287, 290f
 - Rainfall-runoff modeling, 290f
 - Steps to define storm runoff, 290f
- Storm sewers
 - Appurtenances, 635
 - Risk-based design of, 635–639
- Stormwater, subsurface disposal, *See* Subsurface disposal of stormwater
- Stormwater control, 611–668, *See also* Hydraulic analysis of designs; Rational method design
 - Management, 611–612
 - Storm sewers and detention, 611–668
 - Storm systems, 612–639
 - Design criteria, 612–613
 - Information needs, 612–613
- Stormwater detention, 647–666
 - Detention basin routing, 659–660
 - Extended detention basins, 648
 - Hydrograph design methods, 658–659
 - Inlet control entails, 648
 - Local disposal, 648
 - Modified rational method, 653–658
 - On-site detention, 648
 - Retention ponds, 648, 649f
 - Sizing detention, 650–659
 - Source control or downstream control, 648
 - Subsurface disposal of stormwater, 660–666
 - Types, 648–649
 - Urbanization effects, 647–648
- Stormwater drainage channels, 639–647
 - Channel linings, 639
 - Flexible linings, 639, 641–646
 - Rigid linings, 639–641
- Stormwater management, 585
- Stormwater runoff, urban, 18–19
- Stratosphere, 235
- Stream flow hydrograph, 284
- Stream flow measurement, 164–166
 - Bubble gauges, 165
 - Crest stage gauges, 165
 - Current meter, 166
 - Rating curves, 165

- Velocity-area-integration method, 164–166
- Stream flow routing, 335–364
- Stream function, 184
- Stream orders, 284f
- Stream stability at highway structures, 815–821
 - Basic engineering analysis, 815–817
 - Check dams, 820–821
 - Countermeasures, 817
 - Factors affecting, 815
 - Guide banks (spur dikes), 818–820
 - Incipient motion analysis, 816
 - Spurs, 817–818
- Streamlines, 61, 184
- Streams, 284
 - Classification, 284
 - Ephemeral streams, 284
 - Horton's stream ordering, 284
 - First-order stream, 284
 - Second order, 284
 - Intermittent streams, 284
 - Perennial streams, 284
 - Separatism on idealized hydrograph, 285
 - Stream flow hydrograph, 284, 289f
- Street and highway drainage, 671–711, *See also* Gutters, flow in; Inlets
 - Capture efficiency, 679
 - Curb-opening inlet interception capacity, 678
 - Curved vane grate, 680f
 - Design considerations, 671–673
 - Efficiency of inlets on grade, 677–685
 - Frontal flow, 679
 - interception efficiency, 681
 - ratio, 679
 - Grate inlets on grade, 679–683
 - Interception capacity, 677–685
 - Interception efficiency of a grate inlet E, 681
 - Pavement drainage inlets, 677
 - Reticuline grate, 681f
 - Side flow, 679
 - interception efficiency, 681
 - ratio, 679
 - Splash-over, 679
 - 30° Tilt-bar grate, 680f
- Stress, 59
- Structural alternatives, flood control, 586–593
 - Diversion, 587t, 588–590
 - Channel modifications, 590–593
 - Checklist for, 589t
 - Interior areas, 589t
 - Levees and floodwalls, 590, 591t
 - Flood-control reservoir, 586–588
 - Stage-damage relationships, 586
 - Stage-discharge relationships, 586
- Subcritical flow, 147–148
- Subsurface disposal of stormwater, 660–666
 - Infiltration basins, 663
 - Infiltration practices, 660–663
 - Modular pavement, 663
 - Percolation trenches, 663
 - Porous pavement, 663
 - Recharge wells, 663–664
 - Underground storage, 664–666
- Subsurface flow, 227
- Subsurface irrigation, 418
- Subsurface water, divisions of, 174f
- Suction force, 268
- Suction gradient, 269
- Supercritical flow, 85
- Supply management, water, 1, 10
- Suppressed rectangular weir, 158–159
- Surface irrigation, water for, 411, 416–417
 - Basin irrigation, 416
 - Border-strip irrigation, 416
 - Continuous-flood or paddy irrigation, 416
 - Ditch delivery systems, 416
 - Furrow irrigation, 416
 - Level basin irrigation, 416
 - Reuse irrigation, 416
 - Surge-flow irrigation, 416
- Surface runoff, 227, 283–328
- Surface storage, 241
- Surface tension, 61
- Surface Water Supply Index (SWSI), 443
- Surface water supply, analysis, 448–453
 - Reservoir systems, 448
 - Active storage, 448
 - Dead storage zone, 448
 - Flood control storage, 448
 - Sequent-peak analysis, 453
- Storage, firm yield analysis for water supply, 448–457
 - Allocation zones, 449f
 - Firm yields, 448
- Surface water systems, 32–37, *See also* Colorado River Basin
 - Management, 831–835
 - Arizona water law, 831–832
 - Diffused surface water, 833
 - New Mexico approach, 834–835
 - Texas approach, 832–834
- Surge tank analysis, 539–543
 - One-way surge tank, 539f
 - Open-end surge tank or stand pipe, 539f
 - Pressure-actuated surge relief valve, 540f
 - Two-way surge tank, 539f
- Surge-flow irrigation, water for, 416
- Suspended load, 797–800
- Sustainability, water resources, 13–54, *See also* Budgets, water; Climate change; Footprints, water; Unsustainability, water resources
 - Challenges to, 16–32
 - Definition, 13–14
 - Droughts, 21–24
 - Dublin principles, 14
 - Floods, 21–24
 - Management for, 827–865, *See also* Integrated water resources management (IWRM) for sustainability
 - Traditional knowledge, 847–848
 - Millennium Development Goals (MDGs), 14–15
 - Urbanization, 15–21, *See also individual entry*
- Sustainable water use, 400
- Swales, 671
- Synthetic fuels, water use for, 404t
- Synthetic storm hyetograph, 252
- Synthetic unit hydrographs, 294–299
 - Clark unit hydrograph, 295–299
- Computing, steps, 296
 - Step 0, 296t
 - Step 1, 296t
 - Step 2, 296t
 - Step 3, 296t
 - Step 4, 296t
 - Step 5, 296t
 - Step 6, 296t
- S-hydrographs, 299–301
- Snyder's, 294–295
- System, 64
- System boundary (control surface), 64
- System components, in water distribution, 475–492, *See also* Pumps for water distribution; Pump systems analysis
 - Configuration, 492–495
 - Operation, 492–495
 - Two-pressure-zone system, 494f
- System head curves, 499–500
- System hydrologic budget, 237

- Systems of units, 8–10
 - Dimensions, 9t
 - Foot-pound-second (FPS) system, 9
 - Physical properties of water
 - In English units, 58t
 - In SI units, 58t
 - SI units, 9t
- Tailrace, 552
- Tailwater rating curve, 756
- Taylor series expansion, 390
- Tennessee River Basin, 604, 605f, 608f
- Tennessee valley authority (TVA) reservoir system operation, 604–608
- Theis's equation, *See* Nonequilibrium well pumping equation
- Thermal power plant, water use in, 408f
 - Evaporative cooling towers, 407
 - Once-through cooling, 407, 408f
 - Pond cooling, 407
- Thermoelectric power water use, 7t
- Thiem equation, 193
- Thiessen method, 238
- Thoma's cavitation constant, 482
- Thorntwaite–Holzman equation, 264
- Throat, 161
- 30° Tilt-bar grate, 680f
- Time, 85t
 - Time lag (t_L), 311
 - Time of concentration, 311–313
 - Time of redistribution, 335
 - Time of translation, 335
 - Time to equilibrium, 318
 - Time to peak, 313
- Time-drawdown analysis, 200–203
- Top width, 85, 121f
- Torque, in turbines, 559
- Total dynamic head, 479
- Total economic value of water, 854
- Total load, 783
- Total sediment load, 800–808
 - Ackers–White formula, 803–805
 - Colby's formula, 800–803
 - Yang's gravel formula, 806–808
 - Yang's unit stream power formula, 805–808
- TR-20, 320
- TR-55, 320
- Transient flow, 524
- Transient well hydraulics, 195–204
 - Confined conditions, 195–204
 - Graphical solution, 198–200
 - Nonequilibrium well pumping equation, 195–198
 - Leaky aquifer conditions, 206–207
 - Unconfined conditions, 205–206
- Transients, hydraulic, 527–543, *See also* Surge tank analysis
 - Control of, 537–543
 - Methods, 537–539
 - Upstream and downstream bypass of, 538f
 - Fundamentals of, 528–537
 - Physical description, 528–530
 - Pressure fluctuation, 530f
 - Velocity fluctuation, 530f
 - In water distribution systems, 527–528
 - Wave speed and pressure, 530–537
 - Combined modulus, 532
 - Critical time of closure, 533
 - Modulus of elasticity of pipe, 533
- Transition losses, 621–623
- Transmission zone, 270
- Transmissivity, 179
- Transpiration, 227
- Trap efficiency, 813
- Trellis on mature, dissected coastal plain, 283f
- Triangular weir, 159–160
- Triaxial diameters, 773
- Trickle irrigation, 418
 - Components of, 420f
- Tropical cell, 236
- Tropopause, 235
- Troposphere, 235
- Tubular turbines, 557
- Tucson Active Management Area (TAMA), 44, 45f
- Tucson, Arizona, water balance for, 44–47
 - Active Management Areas (AMAs), 44
 - Groundwater Management Act (GMA), 44
 - Tucson Active Management Area (TAMA), 44f
 - Water flow in, 46f
- Turbines, 552
 - Bulb turbines, 557
 - Characteristics, 563–566
 - Design head, 563–564
 - Rated discharge, 565
 - Rated head, 564
 - Fixed-blade propeller turbines, 556
 - Francis turbine, 556f
 - Hydraulics of, 557–559
 - Impulse turbines, 553, 554f
 - Reaction turbines, 553, 554f–556f
 - Rim turbine, 557
 - Selection, 566
- Tubular turbines, 557
- Turbine meters, 469
- Turbulent flow, 62–63
- U.S. army corps of engineers risk-based analysis
 - Benefit evaluation, 601–602
 - Intensification benefit, 601
 - Inundation reduction benefit, 601
 - Location benefit, 601
 - Net benefit, 601
 - For flood-damage reduction studies, 600–603
 - Flood-damage-reduction plan, 600
 - Terminology, 600–601
 - Stage-damage function, uncertainty of, 602–603
- U.S. Water Resources Council (WRC) method, 381, 385
 - For flood flow frequency analysis, 385–390
 - Outliers, testing for, 387–390
 - Procedure, 386–387
- Ultrasonic meters, 469
- Unbalanced pressure force, 348
- Uncertainties analysis, 390–393
 - First-order analysis, 390
- Unconfined aquifers, 175, 187–189, 194–195
 - Storage coefficient of, 177f
 - Well hydraulics for, 194
- Unconventional water-supply systems, characteristics, 431t
- Underground storage, 664–666
- Uniform flow, 61
- Uniform gradient series factors, 850t
- Unit hydrograph approach, rainfall-runoff analysis using, 291–294
- United Nations Children's Fund (UNICEF) report, 13
- United Nations Framework Convention on Climate Change (UNFCCC), 24
- United States
 - Household water use in, 403t
 - Water use in, 6–8, 8f
 - National Water Use Information Program (NWUI Program), 6
 - United States Geological Survey (USGS), 6
- Universal soil loss equation (USLE), 809
- Unsaturated flow, 267
 - Continuity equation for, 268
 - Unsaturated porous medium, 267f
- Unsaturated or partially saturated zone, 173

- Unsteady flow equations, 62, 344–347
 - Continuity equation, 345–347
 - Momentum equation, 347–350
- Unsustainability, water resources, 47–54
 - Aral Sea, 47–48
 - Continuous desiccation of, consequences, 47–48
 - Examples, 47–54
 - Mexico City, 48–54, *See also individual entry*
- Upland or velocity method, 311
- Upstream boundary condition, 147
- Urbanization, 15–16
 - Challenging water resources sustainability, 16–21
 - Components, 17f
 - Pathways, 17f
 - Sustainable urban stormwater runoff, 18–19
 - Urban water cycle, 16
 - Urban water systems, 16–18
 - Changes caused by, 15–16
 - Demand-side adaptive options for, 28t
 - Groundwater changes and, 19
 - Subsurface hydrologic balance disruption, 19
 - Stormwater detention affected by, 647–648
 - Supply-side for, 28t
 - Urban flood management in developing countries, 22
- Vacuum, 60
- Vadose zone (zone operation), 173, 174f
- Valves used for water distribution, 488–492
 - Check valves, 490
 - Control valves, 490
 - Flow control valves, 491
 - Isolation valves, 488
 - Pressure-reducing valves (PRV), 490
 - Pressure-sustaining valves (PSV), 491
- Vapor pressure, 265
- Vapor transfer coefficient, 265
- Velocity-area-integration method, 164–166
- Velocity-depth (nonconservation) form, 344
- Velocity distribution of flow in pipes, 78–80, 92–94
 - Laminar flow, 92
 - Turbulent flow
 - Rough pipes, 92–94
 - Smooth pipes, 93
- Velocity head, 87
- Venturi meter, 88
- Vertical turbines (V/T), 505t
- Vertical wet well pumps, 505t
- Virtual water, 27–32
- Viscosity, 57–59
 - Dynamic viscosity, 59
 - Kinematic viscosity, 59
- Viscosity (Reynolds number), 85t
- Visualization of flow, 61–62
 - Eulerian viewpoint, 61
 - Lagrangian viewpoint, 61
 - Nonuniform flow, 62
 - Steady flow, 62
 - Streamlines, 61
 - Uniform flow, 61
 - Unsteady flow, 62
- Volcanic rock, 175t
- von Karman-Prandtl equation, 797
- Wash load, 782
- Water law
 - Appropriation law, 831
 - Common law, 831
 - Groundwater management, 830–835
 - Riparian law, 831
 - Surface management, 830–835
 - Water quality regulation, 831
 - Water rights, 830
- Water power equations, 561–563
- Water resource systems analysis, 856–862
 - Optimization, 856–858
 - Groundwater management, 857
 - Stormwater and floodplain management systems, 857
 - Surface water management, 857
 - Water distribution systems, 857
- Water Resources Council (WRC), *See* U.S. Water Resources Council (WRC) method
- Water strategy Man Decision Support System (WSM DSS), 861
- Water surface profile
 - Application for, 147–152
 - Downstream boundary condition, 147
 - Standard step procedure, 147
 - Upstream boundary condition, 147
 - Classification, 137–140
- Water table, 173, 175
- Water transfers, 845
- Water use/Water-use data, 399–403, *See also* Agriculture, water for; Energy production, water for; Industrial water use
 - Definitions, 400t
 - Consumptive use, 400t
 - Conveyance loss, 400t
 - Delivery and release, 400t
 - Instream use, 400t
 - Offstream use, 400t
 - Public supply, 400t
 - Reclaimed wastewater, 400t
 - Return flow, 400t
 - Self-supplied water, 400t
 - Withdrawal, 400t
- Household water use in united states, 403t
- Sustainable water use, 400
- Uses, classification, 399–403
- Water withdrawals and uses, 399–460
- Watersheds, 230
 - Friends Creek watershed, 231, 231f
 - Lake Decatur watershed, 232f
 - Rainfall disposal on, 240–241
 - Watershed sediment yield, 808–812
 - Rainfall erodibility factor, 809
 - Soil-erodibility factor, 809
 - Universal soil loss equation (USLE), 809
- Water-use
 - Flows, 7f
 - Losses, 7f
 - Purposes of, 7t
- Wave, 315, 350
 - Wave celerity, 315, 350
- Weirs, 158–161
 - Broad-crested weirs, 158, 160–161
 - Contracted rectangular weirs, 159
 - Sharp-crested weirs, 158
 - Suppressed rectangular weir, 158–159
 - Triangular weir, 159–160
 - Weir-type overflow outlets, 417f
- Well function, 196
- Well pumps, comparison, 505t–506t
 - Self-priming centrifugals, 505t
- Vertical turbines, 505t
 - Lineshaft, 506t
 - Submersible, 506t
- Wet/dry-cooling tower system, 410
 - Mechanical-draft counterflow, 409f
 - Mechanical-draft crossflow, 409f
 - Natural-draft counterflow, 409f
 - Natural-draft crossflow, 409f
 - Series-connected, 411f
- Wet well–dry well, horizontal pumps below water level (flooded suction), 505t
- Wetness gradient, 269

- Wetting front, 270, 271
- Wetting zone, 270
- Willingness-to-pay concept, 445
- Withdrawal, water, 400t, 427–432
 - Global stocks of water, 429t
 - Groundwater withdrawals in United States, 430t
- U.S. water withdrawals (1960 to 1990), 429t
- World Commission on Environment and Development (WCED), 14
- World Summit on Sustainable Development (WSSD), 15
- Yang's gravel formula, 806–808
- Yang's sand formula, 805–806
- Yang's unit stream power formula, 805–808
- Zone of saturation, 174, 174f
- Zoned embankment-type, 715